TRANSLATION

STABILITY OF ELASTIC SYSTEMS

By

A. S. Vol'mir

FOREIGN TECHNOLOGY DIVISION

AIR FORCE SYSTEMS COMMAND

WRIGHT-PATTERSON AIR FORCE BASE

OHIO

EDITED MACHINE TRANSLATION

STABILITY OF ELASTIC SYSTEMS

BY: A. S. Vol'mir

English Pages: 1029

PREPARED BY:

TRANSLATION DIVISION
FOREIGN TECHNOLOGY DIVISION
WP-AFB, OHIO.

A. S. Vol'mir

USTOYCHIVOST' UPRUGIKH SISTEM

Gosudarstvennoye Izdatel'stvo
Fiziko-Matematicheskoy Literatury

Moskva - 1963

Pages 1-879

BLANK PAGE

TABLE OF CONTENTS

U. S. BOARD ON GEOGRAPHIC NAMES TRANSLITERATION SYSTEM

Block	Italic	Transliteration	Block	Italic	Transliteration
А а	*А а*	A, a	Р р	*Р р*	R, r
Б б	*Б б*	B, b	С с	*С с*	S, s
В в	*В в*	V, v	Т т	*Т т*	T, t
Г г	*Г г*	G, g	У у	*У у*	U, u
Д д	*Д д*	D, d	Ф ф	*Ф ф*	F, f
Е е	*Е е*	Ye, ye; E, e*	Х х	*Х х*	Kh, kh
Ж ж	*Ж ж*	Zh, zh	Ц ц	*Ц ц*	Ts, ts
З з	*З з*	Z, z	Ч ч	*Ч ч*	Ch, ch
И и	*И и*	I, i	Ш ш	*Ш ш*	Sh, sh
Й й	*Й й*	Y, y	Щ щ	*Щ щ*	Shch, shch
К к	*К к*	K, k	Ъ ъ	*Ъ ъ*	"
Л л	*Л л*	L, l	Ы ы	*Ы ы*	Y, y
М м	*М м*	M, m	Ь ь	*Ь ь*	'
Н н	*Н н*	N, n	Э э	*Э э*	E, e
О о	*О о*	O, o	Ю ю	*Ю ю*	Yu, yu
П п	*П п*	P, p	Я я	*Я я*	Ya, ya

* ye initially, after vowels, and after ъ, ь; e elsewhere. When written as ё in Russian, transliterate as yё or ё. The use of diacritical marks is preferred, but such marks may be omitted when expediency dictates.

FOLLOWING ARE THE CORRESPONDING RUSSIAN AND ENGLISH

DESIGNATIONS OF THE TRIGONOMETRIC FUNCTIONS

Russian	English
sin	sin
cos	cos
tg	tan
ctg	cot
sec	sec
cosec	csc
sh	sinh
ch	cosh
th	tanh
cth	coth
sch	sech
csch	csch
arc sin	$\sin^{-1}$
arc cos	$\cos^{-1}$
arc tg	$\tan^{-1}$
arc ctg	$\cot^{-1}$
arc sec	$\sec^{-1}$
arc cosec	$\csc^{-1}$
arc sh	$\sinh^{-1}$
arc ch	$\cosh^{-1}$
arc th	$\tanh^{-1}$
arc cth	$\coth^{-1}$
arc sch	sech^{-1}
arc csch	csch^{-1}
rot	curl
lg	log

BLANK PAGE

MT-64-335
Stability of Elastic Systems
State Publishing House of Physical and Mathematical Literature.
Moscow, 1963.
Pages: Cover-879.

PREFACE

A number of monographs, published in USSR and abroad have been devoted to the theory of stability of elastic systems. From 1935-1950 were issued books of A. N. Dinnik "Stability of elastic systems," "Buckling" and "Stability of arches." In 1936 there was published book of S. P. Timoshenko "Stability of elastic systems," translation of which was twice issued in Soviet Union. In 1939 appeared book of I. Ya. Shtayerman and A. A. Pikovskiy "Theory of stability of elastic systems."

In famous courses of the structural mechanics of ships by I. G. Bubnov (1912-1914) and P. F. Papkovich (1941), much attention is allotted calculations for stability of bars and plates. In books of V. Z. Vlasov "Thin-walled elastic bars" (First edition-1940) and "General theory of shells" (1949) are presented his research on stability of thin-walled bars and shells. A. A. Il'yushin devoted a significant place in monograph "Plasticity" (1948) to problems of stability of bars and plates beyond the limits of elasticity. Questions of stability of different structures are considered in book of C. B. Biezeno and R. Grammel "Technical dynamics" (1940) and in work "Calculations for strength in machine building" edited by S. D. Ponomarev (1952-1959). In recent years there were published monographs of

V. V. Bolotin, Kh. M. Mushtari and K. Z. Galimov, A. R. Rzhanitsyn, N. S. Streletskiy, F. Bleich, K. Kollbrunner and M. Meister, V. Pflüger and other authors, devoted to urgent regions of theory of stability and practical methods of calculation of structural members.

From many of the enumerated monographs this book differs first of all in its general orientation. Author sets himself the goal to summarize research in those sections of the theory of stability of bars, plates and shells, which have at present the greatest practical value. In book there is considered a series of new problems, appearing in recent years in connection with requirements of industry (especially aircraft construction) and construction. There are presented, in particular, theoretical and experimental data obtained by author and his colleagues on dynamic stability of elastic systems, buckling of shells "in the large" during creep, etc.

In book are given tables and graphs, which can be directly used in practical calculations. There are given certain numerical examples.

Chapters I-IV are devoted to theory of static stability of bars. Account starts with problems, known to students of course on resistance of materials; there are considered different methods of solving them. Along with widely-spread energy methods there are illuminated: method of successive approximations, method of finite differences and certain graphic methods. In subsequent chapters these methods are applied to solution of more complicated problems.

There considered different criteria of stability of bars beyond the limits of elasticity.

In Chapters VII-IX there is expounded theory of stability of rectangular and round plates. Here are presented methods of calculation of rectangular plates for stability during compression in one

and in two directions, during under shearing and combined load. Significant attention is allotted to methods of calculation of plates for stability beyond the limits of elasticity, ensuing from different theories of plasticity; there are shown methods of approximation, based on certain assumptions simplifying problem; there is given comparison of theoretical and experimental results.

Chapters X-XV pertain to stability of shells of different configuration. Here is given a series of classical solutions of problems of stability of shells in linear formulation. Furthermore, there is given concept of stability of shells "in the large," and there are given basic results obtained with respect to different particular problems by nonlinear theory. Here in part are used data presented in last sections of the author's book "Flexible plates and shells" (Gostekhizdat, 1956); certain results are new.

Chapter XVI is devoted to three-ply plates and shells. There are considered peculiarities of buckling of these structures; there are used the most acceptable hypotheses, allowing us to solve a series of practically important problems.

In Chapters V and XVII there are illuminated temperature problems. There is investigated buckling of bars, plates and shells durin creep. Chapters VI and XVIII are devoted to dynamic stability of elastic systems. In Chapter XIX there are presented certain problems of aeroelasticity, pertaining to stability of a flat and a curved panel in supersonic and hypersonic flow.

In Chapter XX are presented statistical methods in their application to problems of stability of bars, plates and shells.

Chapter XXI is devoted to general theory of stability of elastic systems and unites information, obtained by reader from preceding

sections of the book. The most attention here is allotted to more precise definition of the concept of a lower critical load, pertaining to stability "in the large". In conclusion there are enumerated certain urgent problems for subsequent research.

At the end of book is given a bibliography for the whole book and by separate sections. In bibliography are presented by far not all published works. Author sought to give primarily those sources, in which is given more detailed bibliography on various particular problems.

Formulas and figures are numbered by chapters. References to formulas within a given chapter are given without indication of chapter number.

Chapter XIII and Section 160 of Chapter XV were written at request of author by I. I. Trapezin, Chapter XVI by L. M. Kurshin. Manuscript of book was attentively read by V. I. Feodos'yev. He made a series of valuable remarks, considered in final editing of book. Separate sections of book were examined by V. V. Bolotin, I. I. vorovich, V. M. Darevskiy, B. G. Korenev, G. F. Laptev, B. P. Makarov, R. G. Surkin, and A. A. Umanskiy. Help to author on technical formulation of manuscript was rendered by I. N. Zemlyanskikh, I. G. Kil'dibekov and E. D. Skurlatov. To all these persons the author expresses deep gratitude.

A. Vol'mer.

C H A P T E R I

STABILITY OF COMPRESSED BARS IN LIMITS OF ELASTICITY

Theory, my friend, is dry,
But it nurtures the tree of life.
Goethe, "Faust."

§ 1. Basic Concepts

The concept of stability, which one will repeatedly meet in this book, every reader meets daily. Let us consider, for instance, equilibrium positions of a heavy ball, placed on a smooth surface. In Fig. 1.1 are shown equilibrium states of ball when curved surface is turned by convexity downwards (a) or upwards (b). It is easy to see

Fig. 1.1. Forms of equilibrium, a) stable, b) unstable, c) indifferent.

that these positions of ball differ among themselves according to the nature of equilibrium. If one were to slightly deflect ball from state of equilibrium, as is shown by dotted line, and leave it to itself, then in first case ball will start to vibrate about middle position, and in second it will start immediately to depart from it.

In the first of these cases equilibrium is stable, and in the second-unstable. Let us note that frequency of variations of ball with respect to stable position depends on curvature of surface, the more gentle the slope of the surface, the less the frequency.* In Fig. 1.[illegible] shown limiting case, when curved surface passes into a plane. Here any position of ball is equilibrium: such form of equilibrium call indifferent.

Fig. 1.2. Oscillations of compressed bar.

Let us turn now to problem, known from the course on strength of materials. Let us imagine a flexible elastic bar, set vertically and secured at lower end (Fig. 1.2). Let us assume that to upper end of bar is transmitted a compressing force P, directed vertically downwards.** For small forces bar will be compressed, remaining rectilinear. If we slightly bend upper end of bar (dotted line in Fig. 1.2), and then release it, the bar will vibrate relative to the vertical position. Such equilibrium position of the bar is stable. Frequency of vibrations turns out to be different here depending upon magnitude of compressing force. With growth of load, frequency will decrease. When

---

* This circumstance has meaning for dynamic criterion of stability, see §§ 16 and 197.

** Gravity of bar here is not taken into account.

force attains a certain critical value, frequency of small vibrations turns into zero, rod will be as if in neutral equilibrium*, no matter how we bend it. Bar, made of real material, already with comparatively small deflections can obtain plastic flow and will remain in deflected position, reaching rest a or b.

Let us assume that to bar is applied compressing force, exceeding critical; vertical position of bar will be, as before, equilibrium, but this equilibrium is now unstable: with any disturbance bar will bend, after which it no longer will return to vertical state. As we see, it is possible to conduct analogy between quilibrium states of compressed rod and the heavy ball in Fig. 1.1.

Let us agree subsequently to call equilibrium position of elastic bar stable, if, obtaining small deflection from this position, the bar will return to it.** Small vibrations occurring after this in real conditions quickly attenuate from action of various kinds of resisting forces.

Load, at which initial form of equilibrium ceases to be stable, is called critical. Application to bar of force, equal to critical or exceeding it, leads to buckling (bending, accomplished under action or longitudinal forces).

Stable in supercritical region now will be curved forms of equilibrium; at critical point there occurs branching (bifurcation) of equilibrium forms, characterized by exchange of stability among these forms (see § 198).

---

*Such characteristics of critical state of bar it is possible to give only in first approximation, see § 5.

**Concepts of stability and instability of elastic systems are analyzed more rigidly in §§ 197 and 201.

§ 2. Stability of a Bar. Supported by Hinge at Its Ends. Euler's Formula

We will define critical compressive load for bar with straight axis and constant cross section for its length (Fig. 1.3a). Let us assume that one end of bar 0 has a hinged fixed support, and the other end a — a hinged mobile support. We will consider that compressive force P is applied to center of gravity of the section and for whole time of loading is directed strictly vertically. We will lay out axes of coordinates as shown in Fig. 1.3.

With small forces P axis of bar remains a straight line and in bar there appear compressive stresses $\sigma=P/F$, where F is area of cross section. When, gradually increasing, force P attains critical value, then along with rectilinear form of equilibrium there should take place another, curved form, depicted in Fig. 1.3b. We assume that transition from rectilinear form to curved occurs without change of magnitude of force P, i.e., with constant length of axial line. But then point a should obtain a certain displacement Δ; it is possible to show that with small deflections Δ is proportional to square of maximum deflection of elastic line and, thus, is magnitude of the second one order of smallness. Subsequently in figures we conditionally will assume that point a in general, is not displaced in the vertical.

We will write expression for curvature of bending line of the bar:

$$\varkappa = \pm \frac{M}{EJ}. \qquad (1.1)$$

where I is moment of inertia of gross section, M is bending moment in a certain section.

General expression for curvature has the form

$$\varkappa = \mp \frac{\frac{d^2v}{dx^2}}{\left[1+\left(\frac{dv}{dx}\right)^2\right]^{3/2}}. \qquad (1.2)$$

where v is deflection is section x; $v = v(x)$.

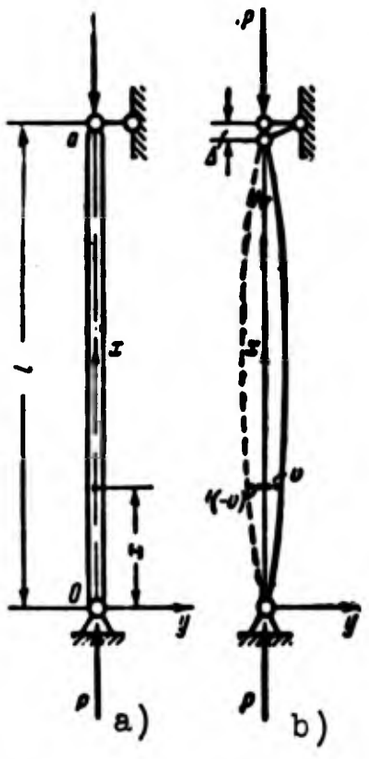

Fig. 1.3. Compressed bar, on hinges supported at ends.

We will consider here deflections <u>small</u> as compared to length of bar. Bending line will be then a <u>shallow curve</u>; considering $(dv/dx)^2 \ll 1$. It is possible here to take

$$x = \mp \frac{d^2v}{dx^2}. \qquad (1.3)$$

Bending moment in section x is equal to

$$M = \pm Pv. \qquad (1.4)$$

We obtain a differential equation for bending line in the form

$$EI\frac{d^2v}{dx^2} = -Pv. \qquad (1.5)$$

As can be seen from Fig. 1.3, during deflection of rod, corresponding to solid line, deflection is positive, and the second derivative is negative; thus, in equation of type (5) deflection and second derivative enter with <u>various signs</u>. Proceeding from this, we, independently of rule of signs for x and M, arrive at the same equation.

In courses on strength of materials subsequent solution of problem is conducted, proceeding from a second order equation of type (5). Here we will pass from (5) to a fourth-order equation. Since this will give the solution a more general nature and will allow us to extend it to other boundary conditions.

Taking EI = const, we differentiate (5) twice with respect to x;

Then we obtain,

$$EI\frac{d^4v}{dx^4} = -P\frac{d^2v}{dx^2}. \qquad (1.6)$$

This relationship can also be directly to obtained, proceeding from the known equation of an elastic line $EI(d^4v/dx^4) = q$, introducing hypothetical lateral load of intensity q. We will consider the deformed element of bar under action of compressive forces P (Fig. 1.4a); resultant of these efforts, directed along the normal, will be by Fig. 1.4b equal to $[-P(d^2v/dx^2)]dx$, and magnitude q equal to $q = -P(d^2v/dx^2)$; hence we arrive at (6).

We introduce designation

$$k^2 = \frac{P}{EI}. \qquad (1.7)$$

Then equation (6) will take the form

$$\frac{d^4v}{dx^4} + k^2\frac{d^2v}{dx^2} = 0. \qquad (1.8)$$

To uniform linear differential equation (6) there corresponds characteristic equation $s^2(s^2 + k^2) = 0$; its roots are equal to $s_1 = s_2 = 0$, $s_{3,4} = \pm ik$. Consequently, integral of equation (6) will be

$$v = A\sin kx + B\cos kx + Cx + D. \qquad (1.9)$$

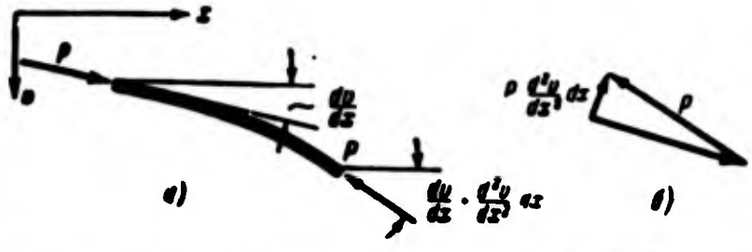

Fig. 1.4. Intensity of transverse "load", caused by compressive forces.

For resolution of problem essential is the circumstance that roots s_3 and s_4 are imaginary; this in turn is explained by the fact that in equation of type (5) magnitudes v and d^2v/dx^2 enter with different signs.

Solution (9) should satisfy boundary conditions, which in this case have the form

$$v=0,\ \frac{d^2v}{dx^2}=0 \text{ when } x=0,\ l. \tag{1.10}$$

Using these conditions, we find

$$\left.\begin{gathered} B+D=0,\ B=0, \\ A\sin kl+B\cos kl+Cl+D=0,\quad A\sin kl+B\cos kl=0. \end{gathered}\right\} \tag{1.11}$$

Hence $B = C = D = 0$. Considering $A \neq 0$, we will have

$$\sin kl=0, \tag{1.12}$$

For argument kl there are obtained values

$$kl=n\pi, \tag{1.13}$$

where n is arbitrary integer. Rejecting solution $kl = 0$ as not corresponding to initial data of problem, we find

$$k^2=\frac{n^2\pi^2}{l^2},\quad n=1,\ 2,\ 3,\ldots \tag{1.14}$$

or, by (6).

$$P=\frac{n^2\pi^2EI}{l^2}. \tag{1.15}$$

Changing number n, we obtain a consecutive series of values of force P, to which correspond different curved equilibrium forms.

By <u>critical</u> force we agreed to understand the force at which rectilinear form of equilibrium of bar ceases to be stable. Consequently, from all possible values of force it is necessary to select the least

and to take n = 1. Considering that buckling will occur in plane of least rigidity of bar, by I we will understand the minium moment of inertia of section I_{min}.

Introducing for critical force designation $P_{кр}$ we obtain:

$$P_{кр} = \frac{\pi^2 E I_{min}}{l^2}. \qquad (1.16)$$

Formula of such form was obtained by L. Euler (1.9), (1.10) and bears his name.

Let us return to equation of bending line of bar

$$v = A \sin kx = A \sin \frac{n\pi}{l} x. \qquad (1.17)$$

We obtained a sine wave having, in general, n half-waves. To critical force (when n = 1) there corresponds a sine wave with one half-wave:

$$v = A \sin \frac{\pi x}{l} = f \sin \frac{\pi x}{l}; \qquad (1.18)$$

here A = f is the maximum deflection.

Taking consecutively n = 2, 3, etc., we obtain curved forms of equilibrium in the form of a sine-wave with two, three and more half-waves within the length of tne bar. Here force P will be by four, nine, etc., times exceed critical magnitude.

There forms of equilibrium, in general, are unstable, but they can be realized if one were to pass to a new system, setting at points of inflection of the sinusoid additional hinged reinforcements.

We implied that compressive stress in bar lies within limits of action of Hooke's law, i.e., does not exceed proportional limit of the material; consequently, Euler's formula can be used only under this condition. We remind one also that we apply an approximate expression

(3) for curvature of bending line, which is appropriate only with deflections, sufficiently small as compared to length of bar. Namely for this the magnitude of maximum deflection f remained in the last analysis indefinite. In Section 5 we will show that if one were to start with "exact" equation of elastic line, the result will be different: every value of force $P > P_{kp}$ will correspond to equilibrium forms with fully definite deflections. However, in environment of point of branching of equilibrium states the bending forms of bar are arbitrarily close to rectilinear form, and therefore, in determining critical force we have a right to start from approximate expression for curvature.

From the mathematical point of view the problem considered by us constitutes problem of eigenvalues of a linear homogeneous equation of type (5). Trivial solution $v \equiv 0$ pertains to the initial, noncurved equilibrium state of bar. Nontrivial solution corresponds to so-called eigenfunctions of the problem, which in this case have form (17). The first and higher critical forces (15) are eigenvalues of parameter P, entering in fundamental equation.*

Let us give two examples of determination of critical force by Euler's formula.

Example 1.1. Section of control link to elevator in aircraft (Fig. 1.5) transmits compressive force. Link is a duralumin pipe of length L = 120 cm, esternal diameter of section d = 3.5 cm, thickness of wall t = 1 mm. To determine critical force, taking $E = 0.7 \cdot 10^6$ kg/cm^2

*For more specifics on this see book of S. M. Mikhlin "Variational methods in mathematical physics",. Gostekhizdat, M., 1957. Place of such linear solutions in general theory of stability is discussed below, in Chapter XXI.

and proportional limit of material $\sigma_{пц}$ = 2000 kg/cm².

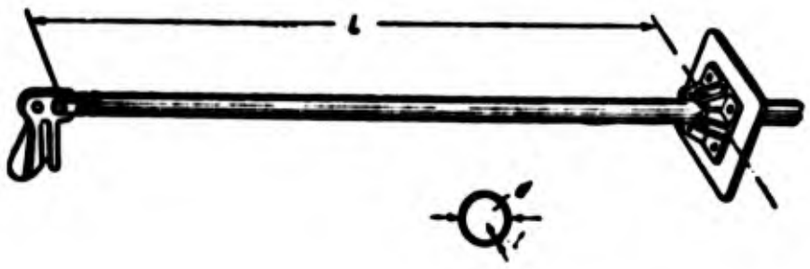

Fig. 1.5. Calculation of a section link control in aircraft.

We find moment of inertia of section. For thin pipe we take

$$I = \frac{\pi Dt}{2}\left(\frac{D}{2}\right)^2 = \frac{\pi \cdot 3{,}5 \cdot 0{,}1}{2}\left(\frac{3{,}5}{2}\right)^2 = 1{,}55 \text{ см}^4.$$

Critical force is equal to

$$P_{кр} = \frac{\pi^2 \cdot 0{,}7 \cdot 10^6 \cdot 1{,}55}{120^2} \approx 740 \text{kg}.$$

Area of section F = πDt = π·3.5·0.1 = 1.07 cm². Critical force corresponds to stress of

$$\sigma = \frac{740}{1{,}07} = 690 \text{kg/cm}^2,$$

lying below proportional limit.

Example 1.2. Roof of all-metal railroad car, consisting of sheeting and longitudinal reinforcing ribs (stringers), transmits compressing forces. Determine critical load for panel of roof, consisting of stringer and adjacent flat panel of sheeting (Fig. 1.6).

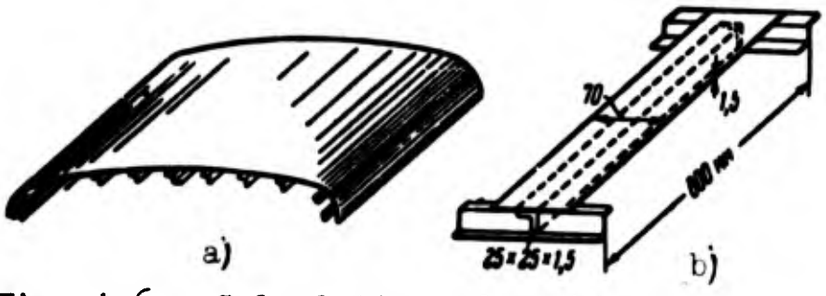

Fig. 1.6. Calculation of stability of roof of all-metal railroad car.

Stringer-angle bracket is 25 X 25 X 1.5; thickness of sheeting—1.5 mm; width of band—70mm. Material—St 3 steel, $E = 2 \cdot 10^6$ kg/cm^2. $\sigma_{nu} = 2000$ kg/cm^2. It is considered that loss of stability is possible only in direction, perpendicular to plane of sheeting. Ends of panel are assumed joined by hinge to transverse reinforcements (frames), distance between which is 800 mm.

We determine coordinate of center of gravity of section z_0:

$$z_0 = \frac{105 \cdot 0{,}75 + 37{,}5 \cdot 22{,}5 + 35{,}3 \cdot 14{,}75}{177{,}8} = 3{,}85 \text{ мм}.$$

Moment of inertia of section relative to central axis is equal to

$$I = \frac{70 \cdot 1{,}5^3}{12} + 105 \cdot 3{,}1^2 + \frac{25 \cdot 1{,}5^3}{12} + 37{,}5 \cdot 1{,}6^2 + \frac{1{,}5 \cdot 23{,}5^3}{12} + \\ + 35{,}3 \cdot 10{,}9^2 \approx 6950 \text{ мм}^4.$$

We find critical force:

$$P_{кр} = \frac{\pi^2 \cdot 2 \cdot 10^6 \cdot 0{,}695}{80^2} = 2140 \text{ kg}.$$

Corresponding stress $\sigma = 1190$ kg/cm^2 lies below σ_{nu}.

§ 3. Other Cases of Fastening of Ends

Let us consider, further, case, when one end of bar is clamped, the other is free; force P, preserving vertical direction, is applied to free end (Fig. 1.7). At loss of stability bar will acquire deflection in form depicted in Fig. 1.7.

Differential equation of bending line preserves form (8); general integral of equation as before has the form (9). We will extract boundary conditions. For the clamped end we have,

$$\left.\begin{aligned} v &= 0, \\ \frac{dv}{dx} &= 0 \end{aligned}\right\} \text{ when } x = 0. \qquad (1.9)$$

On free end bending moment should turn into zero:

$$M = -EI\frac{d^2v}{dx^2} = 0 \text{ when } x = l. \tag{1.20}$$

Fig. 1.7. Bar, clamped at one end and free at the other.

Transverse force on upper end may be expressed by force P and angle of rotation:

$$Q = P\frac{dv}{dx} \text{ when } x = l. \tag{1.21}$$

Expressing transverse force by deflection we obtain:

$$-EI\left(\frac{d^2v}{dx^2}\right)_{x=l} = P\left(\frac{dv}{dx}\right)_{x=l} \tag{1.22}$$

or

$$-\left(\frac{d^2v}{dx^2}\right)_{x=l} = k^2\left(\frac{dv}{dx}\right)_{x=l}. \tag{1.23}$$

Using written conditions we find:

$$\left.\begin{aligned} &B + D = 0, \quad Ak + C = 0, \\ &Ak^2 \sin kl + Bk^2 \cos kl = 0, \quad A = 0. \end{aligned}\right\} \tag{1.24}$$

Hence, A = C = 0, B = -D. When $B \neq 0$ we will have

$$\cos kl = 0 \tag{1.25}$$

and

$$kl = (2n+1)\frac{\pi}{2}. \quad n = 0, 1, 2, 3, \ldots \tag{1.26}$$

Reasoning just as in preceding section, we find critical magnitude of force P equal (when n = 0) to

$$P_{cr} = \frac{\pi^2 EI_{min}}{4l^2}. \tag{1.27}$$

Equation of bending line obtains the form

$$v = B(\cos kx - 1). \tag{1.28}$$

If one were to introduce designation f for displacement of free end, then we find for B = -f

$$v = f(1 - \cos kx). \tag{1.29}$$

We take now that <u>one end of bar is clamped and fixed</u>, while <u>second end is clamped in a movable support</u> (Fig. 1.8). Boundary conditions here will be:

$$v=0 \text{ when } x=0,\ l. \tag{1.30}$$

$$\frac{dv}{dx}=0 \text{ when } x=0,\ l. \tag{1.31}$$

Fig. 1.8. Bar with clamped ends.

Using (9), we obtain

$$\left.\begin{aligned} B+D=0,\ Ak+C=0,\\ A\sin kl+B\cos kl+Cl+D=0,\\ Ak\cos kl-Bk\sin kl+C=0. \end{aligned}\right\} \tag{1.32}$$

For constants A, B we obtain equation

$$\left.\begin{aligned} A(\sin kl-kl)+B(\cos kl-1)=0,\\ A(\cos kl-1)-B\sin kl=0. \end{aligned}\right\} \tag{1.33}$$

Condition of nontrivial solution ($A \neq 0$, $B \neq 0$) has the form

$$\begin{vmatrix} \sin kl-kl & \cos kl-1 \\ \cos kl-1 & -\sin kl \end{vmatrix}=0. \tag{1.34}$$

From this for kl we find equation

$$\sin\frac{kl}{2}\left(\sin\frac{kl}{2}-\frac{kl}{2}\cos\frac{kl}{2}\right)=0. \tag{1.35}$$

Equating to zero first factor, we obtain:

$$kl=2n\pi,\ n=1,\ 2,\ 3,\ldots \tag{1.36}$$

Least possible value of kl will be equal to 2π. If, however, we equate to zero the expression, standing in parentheses, then the least root will be $kl \cong 8.99$. Thus, to determine critical force we have to put

$kl = 2\pi$; then

$$P_{кр} = \frac{4\pi^2 E I_{min}}{l^2}. \tag{1.37}$$

Equation of elastic line here obtains form (when 2B = -f)

$$v = \frac{f}{2}\left(1 - \cos\frac{2\pi x}{l}\right) = f\sin^2\frac{\pi x}{l}; \tag{1.38}$$

by f, as before, we designate maximum deflection (Fig. 1.8).

Last, we turn to case where <u>lower end of bar is fixedly clamped and upper has a hinged support</u> (Fig. 1.9). Boundary conditions will be:

$$v = 0,\ \frac{dv}{dx} = 0 \quad \text{when } x = 0, \tag{1.39}$$

$$v = 0,\ \frac{d^2v}{dx^2} = 0 \text{ when } x = l. \tag{1.40}$$

Between constant expression (9) we will obtain relationship,

$$\left.\begin{aligned} B + D = 0,\quad Ak + C = 0,\\ A\sin kl + B\cos kl + Cl + D = 0,\\ A\sin kl + B\cos kl = 0. \end{aligned}\right\} \tag{1.41}$$

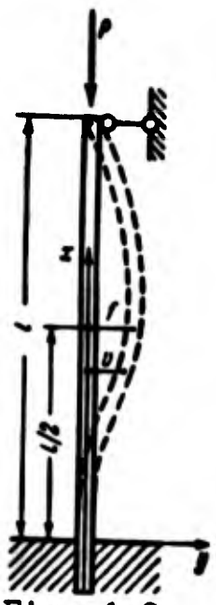

Fig. 1.9. One end of bar is clamped, other supported on hinge.

When $A \neq 0$, $-D = B = -Akl$, $C = -Ak$ we will have

$$\sin kl - kl\cos kl = 0$$

or

$$\tan kl = kl. \tag{1.42}$$

Least value of kl, satisfying this equation, will be

$$kl \approx 4.4934. \tag{1.43}$$

For critical force we find expression

$$P_{кр} \approx 20.19 \frac{EI_{min}}{l^2} \qquad (1.44)$$

or, with known approximation,

$$P_{кр} \approx \frac{2\pi^2 EI_{min}}{l^2}. \qquad (1.45)$$

Equation of elastic line will be

$$y = A[\sin kx - kx + kl(1 - \cos kx)]. \qquad (1.46)$$

In Fig. 1.10 are compared elastic lines for considered cases of fastening. Euler's formula can now be written in generalized form:

$$P_{кр} = \frac{\pi^2 EI_{min}}{l_0^2} \qquad (1.47)$$

or

$$P_{кр} = \frac{\pi^2 EI_{min}}{(\nu l)^2}. \qquad (1.48)$$

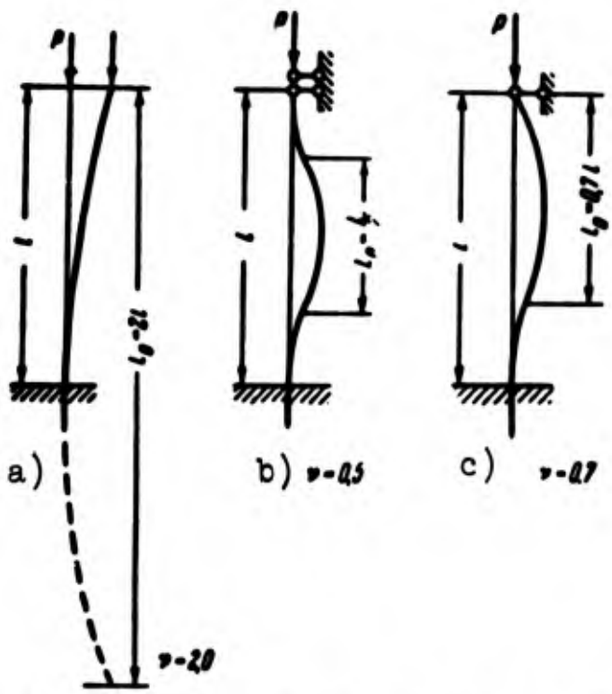

Fig. 1.10. Reduced length for different conditions of fastening.

By l_0 we understand reduced length of bar. For arbitrary boundary conditions it is possible to treat it as length of equivalent bar, having at its ends tip bearings. Magnitude $\nu = l_0/l$ we call reduction factor of length*; it is equal to ratio of length of half-wave of sine wave to real length of bar; in Fig. 1.10 half-wave of sine wave is indicated; here also are given values of ν.

Magnitude P_{kp} according to (47) corresponds to critical stress in cross section, equal to

$$\sigma_{kp} = \frac{P_{kp}}{F} = \frac{\pi^2 E I_{min}}{(\nu l)^2 F}. \tag{1.49}$$

We shall designate by l_{min} minimum radius of gyration of cross section:

$$l_{min} = \sqrt{\frac{I_{min}}{F}}; \tag{1.50}$$

then we obtain

$$\sigma_{kp} = \frac{\pi^2 E}{\lambda^2}. \tag{1.51}$$

By λ here we designate the so-called flexibility of bar:

$$\lambda = \frac{\nu l}{l_{min}}. \tag{1.52}$$

Example 1.3. Determine reduced length of column of press, subjected to compression during test of sample on extension (Fig. 1.11a). Upper end of column is clamped, but can shift together with crossarm in horizontal direction, as shown in figure.

---

*This idea was introduced by F. S. Yasinskiy [1.7]. Subsequently by "length of half-wave" is understood length of projection of curve on initial axis of bar.

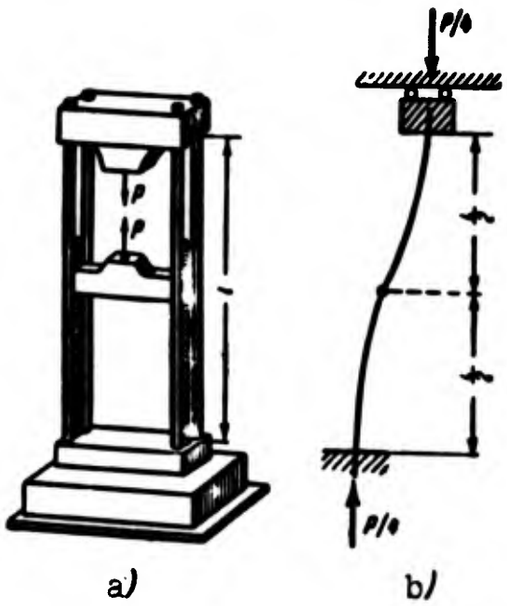

Fig. 1.11. Column of testing press as compressed bar.

Bending line has one point of inflection. Each half of column can be liken unto a bar, one end of which is clamped, and second is free (Fig. 1.10a). Consequently, reduction factor of length for half the column will be $\nu_{1/2} = 2$. For the whole column we obtain $y = 1$.

§ 4. Limits of Applicability of Euler's Formula

As we already said, Euler's formula is valid under the condition that compressive strain of bar up to moment of loss of stability obeys Hooke's law. In other words, critical stress must not exceed proportional limit for given material:

$$\sigma_{cr} \leq \sigma_{pr}. \tag{1.53}$$

or

$$\frac{\pi^2 E}{\lambda^2} \leq \sigma_{pr}. \tag{1.54}$$

Limiting "elastic" slenderness ratio of bar, i.e., least flexibility,

at which it still is possible to use Euler's formula, will be

$$\lambda_* = \pi \sqrt{\frac{E}{\sigma_{nu}}}. \tag{1.55}$$

Condition (53) acquires form

$$\lambda \geqslant \lambda_*. \tag{1.56}$$

Example 1.4. Determine limiting slenderness ratio λ for bars of steel and duralumin. We take for brand St.3 $E = 2 \cdot 10^6$ kg/cm^2 and $\sigma_{nu} = 2000$ kg/cm^2. Then $\lambda_* = \pi \sqrt{1000} \approx 100$. For duralumin we will consider $E = 7.5 \cdot 10^5$ kg/cm^2 and $\sigma_{nu} = 2000$ kg/cm^2. Here $\lambda_* = \pi \sqrt{375} \approx 60$.

§ 5. Equilibrium Forms in Supercritical Region

Till now we placed before ourselves target of determining first critical force, assuming that for compressed bar it is limiting. Actually, for elements of metallic structures achievement by load of critical magnitude is accompanied by significant deformations and, as a rule, leads to exhausting their supporting power. However, in certain cases, for instance for flexible thin bars, it is necessary to conduct calculation, proceeding from the fact that the structural element is subjected to action of loads, exceeding critical. Displacements of end sections of such a bar is usually limited, proceeding from structural considerations.

Thus, for practical purposes it is important to investigate supercritical deformation of compresses bars. Furthermore, this question has great theoretical significance, since it allows us to establish cases of inapplicability of linear equations and to definitize

the criterion of stability.*

Fig. 1.12. For exact solution of problem of supercritical deformation of a bar.

Let us consider supercritical equilibrium forms from example of bar, clamped at lower end and with free second end. We consider that to upper end is applied force P, preserving its direction (Fig. 1.12). Since here deflections no longer can be considered small as compared to length of bar, then we must use an exact expression (2) for curvature of elastic line. Assuming that stresses lie within proportional limits, we obtain nonlinear equation

$$EI\frac{\frac{d^2v}{dx^2}}{\left[1+\left(\frac{dv}{dx}\right)^2\right]^{3/2}}=-M. \tag{1.57}$$

We designate horizontal displacement of upper end by f; then bending moment in certain section at distance x from lower end is equal to

$$M=-P(f-v). \tag{1.58}$$

We introduce instead of v a new variable

$$y=v-f \tag{1.59}$$

*Equilibrium supercritical forms of compressed bar were first investigated in detail by Lagrange [1.12].

and use designation (7); then equation (57) can assume the form

$$\frac{\frac{d^2y}{dx^2}}{\left[1+\left(\frac{dy}{dx}\right)^2\right]^{3/2}}=-k^2y. \tag{1.60}$$

Boundary conditions will be

$$y=-f.\ \frac{dy}{dx}=0 \quad \text{at} \quad x=0. \tag{1.61}$$

We write first integral of equation (60):

$$\frac{1}{\left[1+\left(\frac{dy}{dx}\right)^2\right]^{1/2}}=\frac{k^2y^2}{2}+C; \tag{1.62}$$

the validity of this relationship is easy to prove by direct differentiation. Proceeding from (61), we find:

$$C=1-\frac{k^2f^2}{2}; \tag{1.63}$$

equation (62) takes form

$$\frac{1}{\sqrt{1+\left(\frac{dy}{dx}\right)^2}}=1-\frac{k^2}{2}(f^2-y^2). \tag{1.64}$$

It follows from this that

$$\frac{dy}{dx}=\frac{k\sqrt{f^2-y^2}\sqrt{1-\frac{k^2}{4}(f^2-y^2)}}{1-\frac{k^2}{2}(f^2-y^2)}. \tag{1.65}$$

Dividing variables, we obtain,

$$dx=\frac{1-\frac{k^2}{2}(f^2-y^2)}{k\sqrt{f^2-y^2}\sqrt{1-\frac{k^2}{4}(f^2-y^2)}}dy. \tag{1.66}$$

Length of element of bending line ds by Fig. 1.13 is equal to

$$ds=dx\sqrt{1+\left(\frac{dy}{dx}\right)^2}=dx\sqrt{1+\left(\frac{dy}{dx}\right)^2}. \tag{1.67}$$

Using expressions (64) and (66), we arrive at dependence

$$kds=\frac{1}{\sqrt{f^2-y^2}\sqrt{1-\frac{k^2}{4}(f^2-y^2)}}dy. \tag{1.68}$$

We introduce new variables φ and ϑ, connected with y, f and k by such relationships:

$$y^2 = f^2 \cos^2 \varphi, \quad \frac{k^2 f^2}{4} = \sin^2 \vartheta. \tag{1.69}$$

Then by (59) and (69)

$$\left.\begin{aligned} y &= \mp f \cos \varphi, \quad v = f(1 \mp \cos \varphi), \\ dy &= dv = \pm f \sin \varphi \, d\varphi. \end{aligned}\right\} \tag{1.70}$$

Relationship (68) takes form

$$k\,ds = \frac{1}{\sqrt{1 - \sin^2 \vartheta \sin^2 \varphi}} d\varphi. \tag{1.71}$$

We consider that length of axial line l is constant. Relating value $\varphi = \varphi_0$ to lower end of bar, we receive by (70):

$$\varphi_0 = -n\pi, \quad n = 0, 1, 2, \ldots \tag{1.71a}$$

On the other hand, for upper end we should have $y = 0$. Corresponding value of φ we set for definitiveness equal to $\varphi_1 = \pi/2$. Integrating left and right sides of (71) the length of the bar, we obtain:

$$kl = \int_{-n\pi}^{\pi/2} \frac{d\varphi}{\sqrt{1 - \sin^2 \vartheta \sin^2 \varphi}}. \tag{1.72}$$

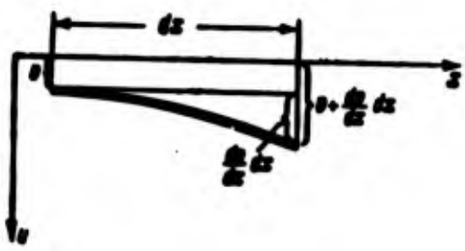

Fig. 1.13. Element of bending line of bar.

Expression of type

$$F\left(\frac{\pi}{2}, \theta\right)=\int_0^{\pi/2} \frac{d\varphi}{\sqrt{1-\sin^2\theta\sin^2\varphi}} \qquad (1.73)$$

carries name of <u>complete elliptic integral</u> of the first kind. Since lower limit of integral (72) is equal to $(-n\pi)$, then this integral will be in $(2n + 1)$ times greater than expression (73):

$$kl=(2n+1)F\left(\frac{\pi}{2}, \theta\right). \qquad (1.74)$$

Integrals of form (73) are tabulated and given in many reference books.

We return now to relationships (69); the second of them gives

$$kf=\pm 2\sin\theta. \qquad (1.75)$$

Comparing (70) and (75) and dropping one of the signs, we find:

$$kv=2\sin\theta(1-\cos\varphi). \qquad (1.76)$$

Taken together, relationships (74) and (75) allow us to establish dependence between deflection of upper end of bar f and load P. Let us assume that we know rigidity of bar EI and length l. Let us assume that we are given magnitude of load P; then by (7) there can be found k and from (74), for one or another n, we can determine parameter $. Last, by (75) we may find deflection f. Thus we determine relationship P = P (f) for every value of n.

If one were to set $ = 0, then when $k \neq 0$ we will obtain f = 0. In this limiting case expression (73) becomes $F(\pi/2, 0) = \pi/2$. Equality (74) then gives

$$P_n=\frac{\pi^2 EI}{4l^2}(2n+1)^2 \qquad (1.77)$$

or, by (26),

$$P_n=(2n+1)^2 P_{кр}. \qquad (1.78)$$

where $P_{кр}$ is first critical force. Values P_n when n = 1, 2, 3, etc., will correspond to other branching points of equilibrium states according to (26), i.e., higher critical forces. Relationships (74) and (75) can have the form

$$\sqrt{\frac{P}{P_{кр}}} = \frac{2(2n+1)}{\pi} F\left(\frac{\pi}{2}, \vartheta\right). \tag{1.79}$$

$$\frac{f}{l} = \frac{2}{2n+1} \frac{\sin\vartheta}{F\left(\frac{\pi}{2}, \vartheta\right)}. \tag{1.80}$$

Set, for instance, $P = 3P_{кр}$. Then when n = 0 from (79) we have

$$F\left(\frac{\pi}{2}, \vartheta\right) = \frac{\pi}{2}\sqrt{3} = 2.72.$$

By the table of elliptic integrals* we find $\vartheta = 74.5°$ and, further,

$$\frac{f}{l} = 2\frac{\sin 74.5°}{2,72} = \frac{2 \cdot 0,96}{2,72} \approx 0,706.$$

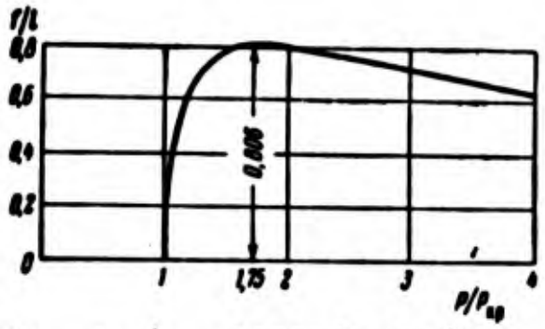

Fig. 1.14. Dependence between deflection and load in supercritical region.

In Fig. 1.14 is depicted dependence between magnitudes $P/P_{кр}$ and f/l for n = 0. With increase of load deflection of upper end in the beginning increases to value $0.806l$, and then starts to decrease.

*See, for instance, I. N. Bronstein and K. A. Semendyayev, "Reference book on mathematics," Gostekhizdat, Third edition, 1953, P. [illegible].

At limit $P \to \infty$, we should have $f \to 0$.

Analogously we may obtain dependence between load and deflection of upper end for n = 1, 2, 3, etc. Let us note that points of corresponding curves can be obtained by points of first curve (for $n = 0$), if we multiply their abscissa by $(2n + 1)^2$, and divide ordinate by $(2n + 1)$; this follows from (79) and (80). Several such curves are shown in Fig. 1.15.

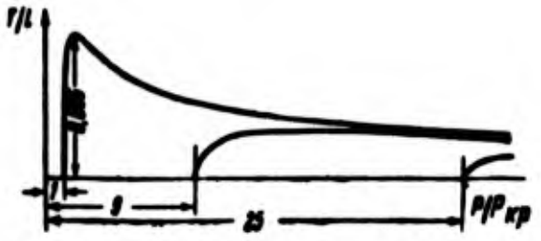

Fig. 1.15. "Deflection-load" diagrams with loads, exceeding first and higher critical forces.

Form of elastic line of bar, corresponding to some value of load, can be found, proceeding from dependence (76). As it is easy to see by (60), second derivative of y with respect to x turns into zero when y = 0, i.e., for values of deflection v, equal to f; here will lie points of inflection of elastic line. On the other hand, from (69) for these values of deflection we find $\cos\varphi = 0$ and $\varphi = -\pi(2n + 1)/2$, since upper limit for φ we took equal to $\pi/2$.

When n = 0 elastic line will not have point of inflection; when n = 1 we will obtain one point of inflection, when n = 2—two, etc. Elastic lines for cases n = 1 and n = 2 are presented in Fig. 1.16.

For values of load, differing little from first critical magnitude, it is possible to establish simple approximate dependence between P and f. We put n = 0, then by (79) and (80)

$$\sqrt{\frac{P}{P_{кр}}} = \frac{2}{\pi} F\left(\frac{\pi}{2}, \theta\right), \quad \frac{f}{l} = \frac{2\sin\theta}{F\left(\frac{\pi}{2}, \theta\right)}. \tag{1.81}$$

Expression for complete elliptic integral may be presented in the

form of a series by powers of sin ϑ:

$$F\left(\frac{\pi}{2}, \vartheta\right) = \frac{\pi}{2}\left(1 + \frac{1}{4}\sin^2\vartheta + \frac{9}{64}\sin^4\vartheta + \ldots\right). \qquad (1.82)$$

With sufficiently small ϑ, limiting ourselves to first two members of series we find,

$$\frac{P}{P_{кр}} \approx 1 + \frac{1}{2}\sin^2\vartheta. \qquad (1.83)$$

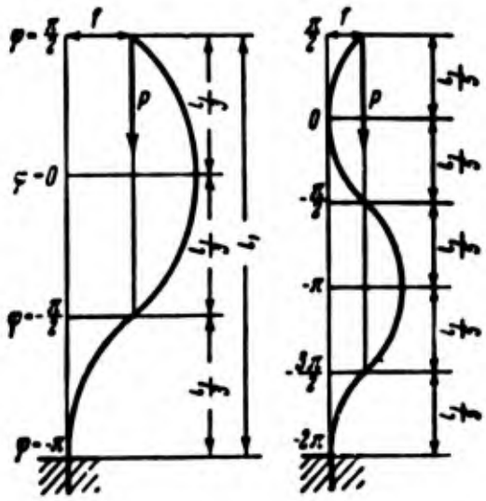

Fig. 1.16. Forms of elastic line of bar.

On the other hand, in the second of the equalities (81) it is possible to put

$$\left.\begin{aligned} F\left(\frac{\pi}{2}, \vartheta\right) &\approx \frac{\pi}{2}, \\ \sin\vartheta &= \frac{\pi}{4}\frac{f}{l}. \end{aligned}\right\} \qquad (1.84)$$

Then from (83) we obtain,

$$\frac{P}{P_{кр}} = 1 + \frac{\pi^2}{32}\left(\frac{f}{l}\right)^2. \qquad (1.85)$$

Thus, first section of curve of Fig. 1.14 it is possible with known approximation to replace by section of a square parabola. Judging by formula (85) and graphs of Fig. 1.16, in supercritical stage maximum deflection bar increases very rapidly. If load exceeds critical by only 1%, then maximum deflection should constitute already near $0.18l$. For bars in metallic structures stresses with such values of deflection usually exceed limit of proportionality. Consequently, research of supercritical deformation has sense only with respect to bars of great slenderness ratio.

§ 6. Various Criteria of Stability and Methods of Solving of Problems

Considering a compressed bar, differently secured at the ends,

we used one of the most commonly used criteria of loss of stability: we investigated, at what conditions along with initial state of equilibrium there appear adjacent, new equilibrium forms. Such approach to solution of problems of stability we will call static.

Another criterion pertains to potential energy, acquired by system, and may be called energy. We investigate transition from initial equilibrium state to a bent one and determine increase of potential strain energy, and also work of external forces. If strain energy appears larger than work of external loads, then, obviously, system will return to initial position of equilibrium; consequently, this position can be considered stable. Conversely, condition of instability is when work of external forces exceeds potential strain energy. At neutral equilibrium (in linear formulation of problem) increase of strain energy should be equal to work of external forces. If external forces are conservative, i.e., if work of them depends only on initial and final positions of points of application and does not depend on trajectories of displacement of these points, then it is possible to introduce idea of potential of external forces and total potential energy of system. Then the given criterion can be formulated in application to total energy of system, more correctly to its increase during transition from initial equilibrium state to an adjacent one.

Third, the most general way consists of research of motion of system, caused by certain small perturbations of the initial equilibrium state. Such a criterion may be called dynamic. If small perturbations cause dynamic displacements of system, lying in definite limits, then initial state is stable. To be more exact, in the presence of stability it is always possible to select such initial

perturbations, that during subsequent motion of system displacements of its points do not go beyond certain, prescribed boundaries (see § 197). If we talk about a conservative system, on which these act conservative assigned forces, and work of reactions of constraints and resisting forces is equal to zero, then such system will accomplish natural oscillations near position of equilibrium. Criterion of loss of stability here will be—as already said in Section 1—conversion into zero of frequency of natural oscillations.

Energy criterion, as it was formulated above, is, essentially static, since it pertains only to potential energy of system and allows one to analyze only different equilibrium forms. However, energy criterion can be applied also in dynamic formulation of problem, if one were to introduce into consideration kinetic energy of system and investigate change of function, including both potential and also kinetic energy.

Determining critical load, corresponding to point of branching of equilibrium states, we consider a certain ideal system. We consider, for instance, that axis of compressed bar is strictly rectilinear, that load is applied to center of gravity of section, that material is uniform, etc. In real structures such conditions, as a rule, are not realized. One can determine character of stability of ideal system, studying behavior of an imperfect system close to it and directing parameters, characterizing these imperfections, toward zero. As we will see later, influence of initial imperfections sharply increases when load nears critical magnitude calculated for corresponding ideal structure; this also serves as criterion of stability of ideal system, which it is possible to call criterion of initial imperfections.

Does above-mentioned criterion of stability of some system lead to the same result? As we will prove below, in problems pertaining to conservative systems such coincidence occurs; therefore, application of different criteria can serve to check correctness of solution of a problem. In case of nonconservative system one should use the most general dynamic criterion, since the static (or energy-static) approach can lead to erroneous results; this will be shown in one of the examples in § 21.

Defining critical load as point of bifurcation of equilibrium forms leads, as we see, to solution of a linear problem; to such problem also pertained criteria of stability enumerated by us. If, however, we investigate postcritical behavior of system, as in § 5, then problem is nonlinear. Uniqueness of nonlinear problem consists in the fact that here to the same system of loads there can correspond several different deformed states, some of which are stable, and others--unstable. Thus, for instance, in case of compressed bar with loads, slightly exceeding first critical magnitude, we obtained in § 5 two stable bending forms of bar (during bend of rod to one and to the other side) and an unstable form--rectilinear. True, during determination of point of bifurcation we also encounter a series of different equilibrium states, but from each of them it is possible directly to pass to another, neighboring one; in nonlinear system equilibrium forms can sharply differ among themselves. This it is possible to explain by example, expounded in § 1. Let us assume that heavy ball moves on surface of more complicated configuration than in § 1, and has not one but two dips (Fig. 1.17). If ball initially is in left "pit," then its behavior during deflection from stable equilibrium state A depends on

character of perturbations. If ball receives small deflection or small initial velocity, then it will experience limited vibrations near A, not exceeding the bounds of pit. If, however, ball obtains sufficiently great push, then it may jump through unstable equilibrium position B, fall in right "pit" and start to oscillate about new equilibrium state C. Probability of jump of ball from one pit to other depends on how high their dividing barrier is. For instance, in case shown in Fig. 1.17b, this probability is greater than in case of Fig. 1.17a. Since height H is proportional to potential difference of force of weight of ball, then it characterizes potential barrier, surmounting of which is necessary during jump.*

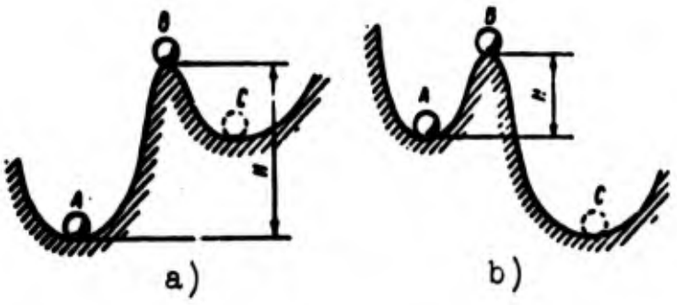

Fig. 1.17. Stability "in the large".

We will say that in position A ball is stable "in the small," i.e., with comparatively small perturbations. At the same time it can appear unstable "in the large," if perturbation exceed given limit.

Many nonlinear elastic systems, stable in the small, can be

---

*Here there is a certain analogy with concept of potential barrier in theory of the atomic nucleus.

unstable in the large. In Section 22 there will be given analysis of stability in the large of very simple elastic construction. The greatest practical value of these ideas is in theory of stability of shells (see Section 118). During research on nature of equilibrium states of nonlinear systems there are applied the same criterion, as for linear systems: static, energy and dynamic (see §§ 200 through 202).

Selecting one or another criterion, we should, further, adopt a definite method of solution of problem. If static or dynamic criterion is applied then it is possible to start from differential equations of equilibrium or motion for deflected positions and directly integrate these equations. This way is possible, however, only in the simplest problems. In more complicated cases it is necessary to use different methods of approximation of determination of critical load. Thus, for instance, differential equation of equilibrium or motion may be replaced by difference equation; depending upon number of intervals problem will be solved from greater or lesser accuracy. Another way consists of replacing the differential equation—linear or nonlinear—by an integral one, i.e., such as includes under the sign of integral functions, characterizing deflected states of system. Then for solution of problem it is possible to apply method of successive approximations, allowing one step by step to definitize character of equilibrium forms of system and, in linear problems, the magnitude of critical load. Theory of integral equations contains also a number of other ways of determining the least parameter, characterizing branching (bifurcation) of solutions; this value of the parameter corresponds to critical load interesting us (see §§ 15 and 141).

Using energy criterion, we must consider what character the deflected positions of system have and constitute expression for potential strain energy and work of external forces. In linear problems critical load is determined approximately by direct comparison of these magnitudes. Most frequently energy approach is carried out with help of Ritz' method, in which deflected position of equilibrium or motion is characterized by several independent parameters. Such approximation of deflected state is applied also in the Bubnov-Galerkin method, which may be based on energy considerations — proceeding from principle of virtual displacements—but, on the other hand, can be treated as "formal" method of approximate integration of differential equations when form of integral curve may be beforehand estimated from physical concepts.

All above-mentioned methods allowed us approximately to solve various boundary value problems of the theory of elasticity, inasmuch as together with differential equations problems must be assigned boundary conditions for displacements or efforts. There exists, however, a way—it is called below the trial-and-error method--where problem is formulated as problem with initial conditions: for instance, for bar we are given deflection and angle of rotation for one of the end sections. Boundary conditions, pertaining to second end section, are realized after trial efforts by means of varying parameter of load, entering the differential equation.

We already met one "static" method of research of stability of compressed bar—direct integration of differential equation of elastic line for deflected position. In subsequent sections we will, on the same simple example, meet other criteria of stability and methods of solution of problems.

§ 7. Application of Principle of Virtual Displacements

As we know, the most general principle allowing one to investigate equilibrium states of elastic systems is principle of virtual displacements; it pertains not only to linear, but also to nonlinear static problems; in connection with D'Alembert's principle it can also be used in dynamic problems. Therefore account of energy relationships we will begin with application of principle of virtual displacements. According to this principle equilibrium state of elastic system is characterized by the fact that sum of works of all external and internal forces in any kinematic virtual displacements of points of elastic system is equal to zero.

Let us assume that a bar of length l in a certain way secured at its ends, is subjected to action of compressive force P. We designate by δA work of internal forces during transition from given distorted form to another, close to it, and by δW--the corresponding work of compressing load. If initial form of bar is equilibrium, then this equality should be satisfied:

$$\delta A + \delta W = 0. \tag{1.86}$$

Work of internal forces may be represented by expression

$$\delta A = -\int_0^l M \delta \varkappa \, dx, \tag{1.87}$$

where by δx is designated variation of curvature of elastic line. We take for curvature value (3), since we are talking about small deflection of elastic line of bar from axis x; then

$$\delta A = \int_0^l M \delta \left(\frac{d^2v}{dx^2}\right) dx = \int_0^l M \frac{d}{dx}\left[\delta\left(\frac{dv}{dx}\right)\right] dx. \tag{1.88}$$

Integrating this expression in parts, we obtain,

$$\delta A = \left[M\delta\left(\frac{dv}{dx}\right)\right]_0^l - \left[Q\delta v\right]_0^l - \int_0^l EI\,\frac{d^4v}{dx^4}\,\delta v\,dx. \qquad (1.89a)$$

Repeated integration gives

$$\delta A = \left[M\delta\left(\frac{dv}{dx}\right)\right]_0^l - \left[\frac{dM}{dx}\,\delta v\right]_0^l + \int_0^l \frac{d^2M}{dx^2}\,\delta v\,dx.$$

Using relationships

$$\frac{dM}{dx} = Q. \quad M = -EI\,\frac{d^2v}{dx^2}. \qquad (1.89)$$

we find:

$$\delta A = \left[M\delta\left(\frac{dv}{dx}\right)\right]_0^l - \int_0^l \frac{dM}{dx}\,\frac{d}{dx}(\delta v)\,dx. \qquad (1.90)$$

Work of external load on virtual displacement will be

$$\delta W = P\delta e. \qquad (1.91)$$

whereby e we designate projection of mutual displacement of ends of bar, taking place during distortion in direction of force P; magnitude e is considered positive during approach of ends. Remember that magnitude and direction of compressing forces are considered constant. We will use relationship (67) between length of element of bending line ds and its projection dx in the direction of P:

$$ds = dx\left[1 + \left(\frac{dv}{dx}\right)^2\right]^{\frac{1}{2}}.$$

Expanding the factor with dx into a series by Newton's binomial formula and limiting ourselves to the first two members of series, we find:

$$ds = dx\left[1 + \frac{1}{2}\left(\frac{dv}{dx}\right)^2\right]. \qquad (1.92)$$

Total length of bending line, equal to length of bar before distortion, will be

$$l = l_1 + \frac{1}{2}\int_0^l \left(\frac{dv}{dx}\right)^2 dx; \qquad (1\ 93)$$

here by l_1, is designated length of projection of bending line on direction of axis x. Projection of displacement of edges turns out to be equal to

$$\Delta = l - l_1 = \frac{1}{2}\int_0^l \left(\frac{dv}{dx}\right)^2 dx. \qquad (1.94)$$

Work δW will then be

$$\delta W = \frac{1}{2} P \int_0^l \delta\left(\frac{dv}{dx}\right)^2 dx, \qquad (1.95)$$

or

$$\delta W = P\int_0^l \frac{dv}{dx}\,\delta\left(\frac{dv}{dx}\right) dx. \qquad (1.95a)$$

Partial integration gives

$$\delta W = P\left[\frac{dv}{dx}\delta v\right]_0^l - P\int_0^l \frac{d^2v}{dx^2}\,\delta v\, dx. \qquad (1.96)$$

Equation (86) obtains form

$$\left[M\delta\left(\frac{dv}{dx}\right)\right]_0^l - \left[\left(Q - P\frac{dv}{dx}\right)\delta v\right]_0^l - \int_0^l \left(EI\frac{d^4v}{dx^4} + P\frac{d^2v}{dx^2}\right)\delta v\, dx = 0. \qquad (1.97)$$

We arrived at variational equation (97), ensuing from principle of virtual displacements.

Considering that variations δv are arbitrary and that first two members in left part turn into zero, we obtain from this

differential equation (6). On the other hand, consideration members outside the integral leads to static boundary conditions of problem. Thus, in case of free end, on condition $\delta v \neq 0$ and $\delta(dv/dx) \neq 0$, we will obtain:

$$M=0. \quad Q-P\frac{dv}{dx}=0.$$

which corresponds to equalities (20) and (21).

§ 8. Energy Criterion of Stability

During research of equilibrium states of conservative systems it is possible instead of variations of work of internal and external forces to introduce variation of total potential energy of system. As we know, work of internal forces on virtual displacement is equal to variation of potential strain energy taken with the minus sign:

$$\delta A=-\delta U. \tag{1.98}$$

Comparing (88) and (89), we find,

$$\delta U=\int_0^l EI\frac{d^2v}{dx^2}\delta\left(\frac{d^2v}{dx^2}\right)dx.$$

or

$$\delta U=\frac{1}{2}\delta\int_0^l EI\left(\frac{d^2v}{dx^2}\right)^2 dx. \tag{1.99}$$

From this follows known expression for potential strain energy of bent bar:

$$U=\frac{1}{2}\int_0^l EI\left(\frac{d^2v}{dx^2}\right)^2 dx. \tag{1.100}$$

This expression can also be written in the form

$$U=\frac{1}{2}\int_0^l \frac{M^2\,dx}{EI}. \tag{1.101}$$

On the other hand, by (95) we find work of external load, produced by force P during distortion of bar;

$$W=\frac{1}{2}P\int_0^l\left(\frac{dv}{dx}\right)^2dx. \qquad (1.102)$$

Magnitude W is equal to change of potential of load taken with minus sign:

$$V=-W=-\frac{1}{2}P\int_0^l\left(\frac{dv}{dx}\right)^2dx. \qquad (1.103)$$

Sum of potential strain energy and change of potential of load constitutes total energy of elastic system $\Im$:

$$\Im=U+V=U-W. \qquad (1.104)$$

Thus, in considered case total energy is equal to

$$\Im=\frac{1}{2}EI\int_0^l\left(\frac{d^2v}{dx^2}\right)^2dx-\frac{1}{2}P\int_0^l\left(\frac{dv}{dx}\right)^2dx. \qquad (1.105)$$

During virtual deflection of bar from equilibrium position first variation of total energy should be equal to zero:

$$\delta\Im=0, \qquad (1.106)$$

which corresponds to equality (86).

It is possible to judge stability of equilibrium position by sign of second variation of total energy. If initial position is stable, then second variation is positive:

$$\delta^2\Im>0. \qquad (1.107)$$

Here energy of rectilinear form of bar will be minimum with respect to values of energy for curved forms close to it.

If second variation of energy is negative:

$$\delta^2\Im<0, \qquad (1.108)$$

then considered equilibrium form will be unstable.

To neutral equilibrium of bar there corresponds equality to zero of second variation:

$$\delta^2 \Theta = 0. \tag{1.109}$$

Let us consider case bar secured at ends by hinges, compressed by forces P at the ends. Taking for curved elastic line equation (18), we obtain from (105),

$$\Theta = \frac{\pi^4}{4} EI \frac{f^2}{l^3} - \frac{\pi^2}{4} P \frac{f^2}{l}. \tag{1.110}$$

We introduce dimensionless parameters

$$\Theta^* = \frac{2}{\pi^2} \frac{l^3}{EIh^2} \Theta, \quad \zeta = \frac{f}{h}, \tag{1.111}$$

where h is height of section of bar. Then by (110) and (16) we will have

$$\Theta^* = \frac{1}{2}\left(1 - \frac{P}{P_{кр}}\right)\zeta^2. \tag{1.112}$$

First variation of Θ^* is equal to

$$\delta\Theta^* = \left(1 - \frac{P}{P_{кр}}\right)\zeta\delta\zeta, \tag{1.113}$$

and the second variation, to

$$\delta^2\Theta^* = \left(1 - \frac{P}{P_{кр}}\right)\delta\zeta^2. \tag{1.114}$$

Any rectilinear form is equilibrium: when $\zeta = 0$ we will have $\delta\Theta^* = 0$. Stability of equilibrium depends on relationship between P and $P_{кр}$; when $P < P_{кр}$, $P > P_{кр}$ and $P = P_{кр}$ equalities (107), (108) and (109) respectively will be satisfied.

§ 9. Methods of Ritz and Timoshenko

Energy criterion serves as basis for effective methods of approximation of solution of problems of stability, briefly characterized

above. Let us consider these methods in more detail.

Assume that bending line of bar upon loss of stability may be approximately represented by the series

$$v = f_1\eta_1 + f_2\eta_2 + \dots + f_n\eta_n = \sum_{i=1}^{n} f_i\eta_i. \qquad (1.115)$$

Here by η_i we understand functions of x, satisfying geometric boundary conditions of problem, i.e., such conditions, which pertain to deflections or angles of rotation. Pot (115) in expression for total energy of system (104). Then energy will depend on parameters of deflection f_i. Variation $\delta\vartheta$ here can be presented as sum of variations, corresponding to possible changes of parameters f_i.

$$\delta\vartheta = \sum_{i=1}^{n} \frac{\partial\vartheta}{\partial f_i}\delta f_i. \qquad (1.116)$$

Since bending states considered by us are equilibrium, then variation $\delta\vartheta$ by (106) should be equal to zero:

$$\sum_{i=1}^{n} \frac{\partial\vartheta}{\partial f_i}\delta f_i = 0. \qquad (1.117)$$

But variations δf_i can be considered independent of each other; therefore equality (117) will occur, if each of factors in δf_i is equal to zero:

$$\frac{\partial\vartheta}{\partial f_i} = 0, \quad i = 1, 2, \dots, n. \qquad (1.118)$$

Judging by (105), energy should be a quadratic function of parameters f_i. Calculating derivatives with respect to f_i, we obtain linear functions of f_i. Consequently, equalities (118) constitute system of n linear algebraic homogeneous equations with respect to f_i; in coefficients with f_i there enters load P. If one were to consider $f_i \neq 0$, then condition of existence of solution of system (118) would be equality to zero of determinant, composed of coefficients in f_i:

$$\Delta = 0. \qquad (1.119)$$

Equation (119) will contain load to power n. Solving this equation, we obtain n values of P. The least of these values will approximately correspond to first critical force. Such a method of solving variational problems carries name of Ritz' method.*

Example 1.5. Determine critical force for compressed bar, clamped at one end and with other end free. We will present elastic line in first approximation in the form of a segment of a square parabola

$$v = f_2 x^2; \tag{a}$$

coordinate x is measured from clamped end. It is not difficult to prove that this expression satisfies geometric boundary conditions: deflection v and angle of rotation dv/dx turns into zero for point x = 0.

We calculate energy of system by formula (105):

$$\mathcal{Э} = \frac{1}{2} EI \int_0^l 4f_2^2 dx - \frac{P}{2} \int_0^l 4f_2^2 x^2 dx,$$

or

$$\mathcal{Э} = 2EIf_2^2 l - 2Pf_2^2 \frac{l^3}{3}. \tag{b}$$

Equating to zero derivative $\partial \mathcal{Э}/\partial f_2$, we find,

$$P_{кр} = \frac{3EI}{l^2}. \tag{c}$$

Exact solution (28) leads in that case to coefficient $\pi^2/4 = 2.47$; thus, error constitutes about 20%.

In second approximation we introduce new independent parameter f_4 and take

$$v = f_2 x^2 + f_4 x^4. \tag{d}$$

---

* W. Ritz, Über eine neue Methode zur Lösung gewisser Variationsprobleme der math. Physik, Journ. f. d. reine and angew. Math. 135, No. 1 (1908), Gesammelte Werke, Paris, 1911.

Energy will be equal to

$$\vartheta = 2EJl\left(f_2^2 + 4f_2f_4l^2 + \frac{36}{5}f_4^2l^4\right) - 2Pl^2\left(\frac{1}{3}f_2^2 + \frac{4}{5}f_2f_4l^2 + \frac{4}{7}f_4^2l^4\right). \qquad (e)$$

If we equate to zero the first derivative of ϑ with respect to f_1, and f_2, then we arrive at equations:

$$\left.\begin{aligned}\left(EJ - \frac{P}{3}l^2\right)f_2 + \left(2EJl^2 - \frac{2P}{5}l^4\right)f_4 = 0,\\ \left(EJ - \frac{P}{5}l^2\right)f_2 + \left(\frac{18}{5}EJl^2 - \frac{2P}{7}l^4\right)f_4 = 0.\end{aligned}\right\} \qquad (f)$$

If one were to take $f_2 \neq 0$ and $f_4 \neq 0$, then the determinant composed of coefficients for f_2 and f_4 should be equal to zero:

$$\begin{vmatrix} 1 - \frac{P^*}{3} & 2 - \frac{2P^*}{5} \\ 1 - \frac{P^*}{5} & \frac{18}{5} - \frac{2P^*}{7} \end{vmatrix} = 0, \qquad (g)$$

where

$$P^* = \frac{Pl^2}{EJ}. \qquad (h)$$

Expanding this determinant, we come to quadratic equation for P:

$$P^{*2} - 45P^* + 105 = 0. \qquad (i)$$

The smallest root of this equation determines critical force:

$$P_{cr} = 2{,}50\frac{EJ}{l^2}; \qquad (k)$$

here error with respect to exact value is only 1.2%.

Introducing in <u>third approximation</u> parameter f_6, we get

$$v = f_2x^2 + f_4x^4 + f_6x^6. \qquad (l)$$

Proceeding the same way, we obtain a final equation in the form

$$\begin{vmatrix} 1 - \frac{1}{3}P^* & 2 - \frac{2}{5}P^* & 3 - \frac{3}{7}P^* \\ 1 - \frac{1}{5}P^* & \frac{18}{5} - \frac{2P^*}{7} & \frac{45}{7} - \frac{P^*}{3} \\ 6 - \frac{6}{7}P^* & \frac{180}{7} - \frac{4}{3}P^* & 50 - \frac{9}{5}P^* \end{vmatrix} = 0. \qquad (m)$$

Determining smallest root of this cubic equation, we find:

$$P_{cr} = 2{,}48\frac{EJ}{l^2}. \qquad (n)$$

Error is lowered to 0.4%.

As you see, increasing the number of parameters f_i, we can come as close to an exact resolution as we wish. Let us note that in given example all approximate solutions were higher than the exact one. This is not accidental. Real bar constitutes a system with infinitely large number of degrees of freedom. Meanwhile, using the method of Ritz, we introduce only one or several modified parameters, limiting, as it were, the number of degrees of freedom of system, i.e., putting on it superfluous constraints. This leads to artificial exaggeration of rigidity of bar, so that critical load is obtained higher.

Results, obtained by first approximations according to method of Ritz, can be somewhat improved, presenting expression for energy (105) in another form. Using the second of the relationships (89), we write:

$$\Theta = \frac{1}{2}\int_0^l \frac{M^2\,dx}{EI} - \frac{1}{2}P\int_0^l \left(\frac{dv}{dx}\right)^2 dx. \qquad (1.120)$$

Bending moment M in certain section it is possible to express by compressing force P and deflection v. Then one should proceed the same means as during use of expression (105). In this case it is not necessary to calculate second derivatives of v, as was necessary before. But during approximation of bending line we usually more or less will grasp only general outline of curve, as approximate values of second derivatives strongly differ from true one. By this is explained advantage of application of expression (120) as compared to (105).

Example 1.6. We will solve example 1.5, using expression for energies (120). Bending moment in section lying distance x from

clamped end, will be equal to $[-P(v_1-v)]$, where by v_1 is designated deflection of free end. In <u>first approximation</u>, taking $v = f_2x^2$, we find: $v_1 = f_2l^2$; hence

$$M = -Pf_2(l^2-x^2). \qquad (a)$$

Energy will be equal to

$$\vartheta = \int_0^l \frac{P^2(l^2-x^2)^2 f_2^2}{EI}\,dx - P\int_0^l 4f_2^2x^2\,dx \qquad (b)$$

or

$$\vartheta = \frac{8}{15}\cdot\frac{P^2}{EI}f_2^2l^5 - P\cdot\frac{4}{3}f_2^2l^3. \qquad (c)$$

If one were now to equate to zero derivative of ϑ with respect to f_2, then, considering $f_2 \neq 0$, $P \neq 0$, we find,

$$P_{кр} = 2{,}5\frac{EI}{l^2}. \qquad (d)$$

We obtained such a result as in example 1.5 was obtained only in second approximation.

Method of Ritz in application to linear problems of stability may be used also in another form, shown by S. P. Timoshenko [0.23]. As we have seen, during neutral equilibrium we should have $\delta\vartheta = 0$, $\delta^2\vartheta = 0$. If one were to consider minute deflections of bar, then it is possible to take total energy constant: $\vartheta = \text{const}$. Let us agree that zero level will correspond to critical force, and take for $P = P_{кр}$

$$\vartheta = U - W = 0. \qquad (1.121)$$

This it is possible to explain in such a way that with buckling potential flexural strain energy U turns out to be accurately equal to work of external compressing load W. Using now expression (105), we find:

$$P_{кр} = \frac{\int_0^l EI\left(\frac{d^2v}{dx^2}\right)^2 dx}{\int_0^l \left(\frac{dv}{dx}\right)^2 dx}. \qquad (1.122)$$

It is possible also to use second expression for energy (120). We designate by m bending moment in certain section, corresponding to force $P = 1$. Then instead of (120) it is possible to write

$$\vartheta = \frac{1}{2}P^2\int_0^l \frac{m^2\,dx}{EI} - \frac{1}{2}P\int_0^l \left(\frac{dv}{dx}\right)^2 dx. \qquad (1.123)$$

Proceeding from (121), we find now

$$P_{кр} = \frac{\int_0^l \left(\frac{dv}{dx}\right)^2 dx}{\int_0^l \frac{m^2 dx}{EI}}. \qquad (1.124)$$

Let us assume that bending line of bar is approximately presented in the form of series (115). Then in numerator and denominator of fraction (122) or (124) we will obtain functions of parameters f_i. Wishing to find least value of load, we equate to zero the derivative of P with respect to f_i:

$$\frac{\partial P}{\partial f_i} = 0. \qquad i = 1, 2, \ldots, n. \qquad (1.125)$$

For linear problems we will then obtain exactly the same results as by equations (118).

§ 10. Bubnov-Galerkin Method

Another method of approximation, offered by I. G. Bubnov* and developed by B. G. Galerkin**, can be connected with variational equation of problem (97). Let us assume that bending line of bar is approximated by a series of the same form as (115), where each of the functions η_i satisfies not only geometric, and static boundary conditions of problem. We place expression (115) in equation (97). Integral members, corresponding to static boundary conditions, must then drop out. Instead of δv it is possible to substitute

---

*Review of work of Professor S. P. Timoshenko "Stability of elastic systems," in the collection: In'ta inzh putey soobshch., 31 (1913); see I. G. Bubnov, Selected Works. Sudpromgiz, 1956, 136-139.

**B. G. Galerkin, Bars and plates, Engineers Herald, No. 19 (1915), 897-908, Collected compositions, Vol. 1, Publishing House of Academy of Sciences of USSR, M., 1952, 168-195.

expression

$$\delta v = \sum_{i=1}^{n} \eta_i \delta f_i; \qquad (1.126)$$

then equation (97) will obtain form

$$\sum_{i=1}^{n} \int_0^l \left(EI \frac{d^4 v}{dx^4} + P \frac{d^2 v}{dx^2} \right) \eta_i \delta f_i \, dx = 0. \qquad (1.127)$$

But if variations of δf_i are independent and arbitrary, then there follows from this a system of n equations of type

$$\int_0^l \left(EI \frac{d^4 v}{dx^4} + P \frac{d^2 v}{dx^2} \right) \eta_i \, dx = 0, \quad i = 1, 2, \ldots, n. \qquad (1.128)$$

By v in expression in parentheses here is understood series (115). After integration we again obtain system of uniform linear algebraic equations with respect to f_i, from condition of compatibility of which (during nontrivial resolution) we find critical load. Since equations (128) of the Bubnov-Galerkin method and equations (118) of the Ritz method correspond to the same energy dependences, then results obtained by these methods must coincide.

As easily noted, in the brackets under the integral sign in (128) is found the left half of the differential equations corresponding to equation (8). The Bubnov-Galerkin method can be generalized, putting instead of these brackets other operators. Such an operator can, for instance, correspond to equation (5): then we will have

$$\int_0^l \left(EI \frac{d^2 v}{dx^2} + Pv \right) \eta_i \, dx = 0 \qquad (1.129)$$

or, in more general form,

$$\int_0^l \left(EI \frac{d^2 v}{dx^2} - M \right) \eta_i \, dx = 0. \qquad (1.130)$$

But here results of calculations no longer will, in general, coincide with the given ones, obtained according to the Ritz method. If as basis of calculations we take equation (130), then equation of chosen

elastic line should be subordinated only to geometric boundary conditions for deflection.

Example 1.7. Find critical load for rod supported by hinges at its ends, taking as initial curve the parabola

$$v = fx(l-x). \tag{a}$$

We constitute equation of type (129),

$$\int_0^l \left[-2f + \frac{P}{EI} fx(l-x)\right] x(l-x)\,dx = 0. \tag{b}$$

After integration, when $f \neq 0$, we find,

$$P = \frac{10EI}{l^3}. \tag{c}$$

§ 11. Method of Finite Differences. Elastic Hinged Chain

We return now to methods of approximation, pertaining in our classification to a static criterion of stability. We will discuss, first of all the method of finite differences.

Let us have in view equation (5). Divide total length of bar into n equal parts and designate length of every interval by s. Second derivative for certain point, dividing two neighboring intervals, it is possible to replace approximately by the so-called central difference:

$$\left(\frac{d^2v}{dx^2}\right)_i = \frac{1}{s^2}(v_{i-1} - 2v_i + v_{i+1});$$

by v_{i-1}, v_i, and v_{i+1} we understand deflections in corresponding points. To this value of second derivative corresponds bending moment from force P at the i-th point: $M = (-Pv_i)$. Then equation (5) will obtain form

$$EI\frac{1}{s^2}(v_{i-1} - 2v_i + v_{i+1}) = -Pv_i. \tag{1.131}$$

There may be (n-1) such equations; in them will enter value of deflections at end points. Thus, we obtain system of (n-1) algebraic linear equations for v_i; condition of compatibility of these equations

(during non-trivial solution) again leads to determination of critical load.

Example 1.8. Determine approximate value of critical force for compressed bar supported by hinges. Divide length of bar into four parts (Fig. 1.18).

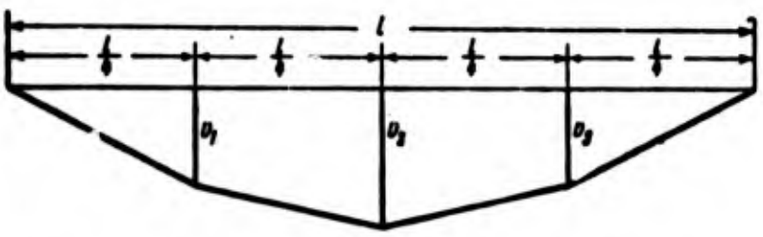

Fig. 1.18. Solution of problem in finite differences.

Constitute equation (131) for points i = 1 and i = 2, considering s = l/4;

$$EI\frac{16}{l^2}(v_0-2v_1+v_2)=-Pv_1. \qquad (a)$$

$$EI\frac{16}{l^2}(v_1-2v_2+v_3)=-Pv_2. \qquad (b)$$

For left end of point

$$v_0=0. \qquad (c)$$

Furthermore, by virtue of symmetry of elastic line

$$v_1=v_3. \qquad (d)$$

We introduce designation

$$\alpha=\frac{Pl^2}{16EI}. \qquad (e)$$

Then equations (a) and (b) will take form

$$\left.\begin{aligned}(\alpha-2)v_1+v_2&=0,\\ 2v_1+(\alpha-2)v_2&=0.\end{aligned}\right\} \qquad (f)$$

Equating to zero determinant of this system, we obtain quadratic equation for α:

$$\alpha^2-4\alpha+2=0. \qquad (g)$$

Smallest root is

$$\alpha=2-\sqrt{2}\approx 0{,}586. \qquad (h)$$

Approximate value of critical force turns out to be

$$P_{кр} = 0{,}586 \cdot 16 \frac{EI}{l^2} = 9{,}38 \frac{EI}{l^2}. \qquad (1)$$

This value deviates from exact 4.3%; in distinction from preceding examples here critical load was obtained with underestimation.

Another variant of method of finite differences, which obtained in the literature the name method of elastic hinged chain*, consists of the following. We divide length of bar into n equal parts. We designate deflections at nodes by $v_0, v_1, \ldots, v_{n-1}, v_n$. We write differential equation for bar with hinged support in the form

$$\frac{\Delta v'}{s} = -\frac{P}{EI} v,$$

where $s = l/n$, or, presenting derivative v' by a difference "taken forward,"

$$\frac{\Delta (v_{i+1} - v_i)}{s^2} = -\frac{P}{EI} v_i$$

Introducing former designation $P^* = Pl^2/EI$, we find,

$$\Delta (v_{i+1} - v_i) = -\frac{1}{n^2} P^* v_i.$$

We take for one end of the bar $v_0 = 0$, and v_1--an assigned value, not equal to zero. We determine consecutively increments of v_i, using formulas:

$$\Delta v_2 = \Delta v_1 - \frac{1}{n^2} P^* v_1.$$

$$\Delta v_3 = \Delta v_2 - \frac{1}{n^2} P^* v_2 = \Delta v_1 - \frac{1}{n^2} P^* (v_1 + v_2).$$

$$\cdots\cdots\cdots\cdots\cdots\cdots\cdots$$

$$\Delta v_{i+1} = \Delta v_1 - \frac{1}{n^2} P^* (v_1 + v_2 + \ldots + v_i).$$

Considering $\Delta v_1 = v_1$, we obtain:

$$\left.\begin{aligned} v_2 &= v_1 + \Delta v_2 = 2v_1 - \frac{1}{n^2} P^* v_1. \\ v_3 &= v_2 + \Delta v_3 = 3v_1 - \frac{1}{n^2} P^* (2v_1 + v_2). \\ &\cdots\cdots\cdots\cdots\cdots\cdots\cdots\cdots \\ v_{i+1} &= (i+1) v_1 - \frac{1}{n^2} P^* [i v_1 + (i-1) v_2 + \ldots + v_i]. \end{aligned}\right| \qquad (1.132)$$

*This method was offered by G. Hencky.

Putting here values of $v_2, \ldots, v_1$, we can express deflection of any node by v_1. Using, further, boundary condition for other end of bar, we obtain from (132) when $v_1 \neq 0$ an equation for critical load P^*.

Relationships of type (132) it is possible to explain in the following manner. Let us assume that bar is divided into n absolutely rigid sections, connected by elastic hinges. To unit angle of rotation in i-th node there corresponds moment

$$m = \frac{EI}{s} = \frac{EIn}{l}.$$

If all links had the same angle of inclination as the first link, we would obtain $v_{i+1} = (i + 1) v_1$. With mutual turn of sections in first node it is necessary to introduce "correction" to this magnitude, equal for the $(i + 1)$ th node to $P^* i v_1/n^2$. Remaining members in expression for v_{i+1} determine "corrections" from angles of turn in other nodes, up to the i-th.

Example 1.9. Determine critical force for bar with hinged supports by method of "elastic hinged chain," dividing bar into four links. We use symmetry of elastic line relative to average section: obviously, we should have $v_3 = v_1$. By the formulas (132).

$$\left.\begin{aligned} v_2 &= 2v_1 - \frac{1}{16} P^* v_1, \\ v_3 &= 3v_1 - \frac{1}{16} P^* (2v_1 + v_2). \end{aligned}\right\} \qquad (a)$$

Hence

$$v_3 = 3v_1 - \frac{1}{16} P^* \left(4v_1 - \frac{1}{16} P^* v_1\right). \qquad (b)$$

Considering $v_1 \neq 0$, we arrive at equation

$$P^{*2} - 64P^* + 512 = 0. \qquad (c)$$

Parameter of critical force turns out to be $P^* = 9.44$; error with respect to exact solution constitutes about 4.4%. Another example of application of this method will be given in § 22.

§ 12. Method of Collocation

Let us turn to method of collocation*, which occupies as if it were an intermediate position between the Bubnov-Galerkin method and the method of finite differences. Expression for deflection we approximate again with help of series (115),

$$v=\sum_{i=1}^{n} f_i\eta_i.$$

where each of the functions η_1 should correspond to all boundary conditions of the problem. Parameters f_1 are determined in such a way that after substitution of expression (115) the basic differential equation of problem is satisfied for n values of the independent variable. Points, at which the equation is satisfied, are called "points of collocation." They can be selected, in general, arbitrarily, but usually we dispose them equal distances from each other. If there is a characteristic section of sharp change of function, then it is desirable here to place points of collocation more frequently; during use of method of finite differences intervals in such a region also are "broken up."

Example 1.10. Anew we define critical force for bar, one end of which is clamped, and the other is free. Differential equation of problem we write in the form (see example 1.6)

$$EI\frac{d^2v}{dx^2}=-P(v_1-v). \qquad (a)$$

To approximating expression for v we give form

$$v=f_3x^3+f_4x^4, \qquad (b)$$

as in one variant of example 1.5. We place points of collocation

---

*Collocation is literally location, distribution. We are talking about distribution of points, at which is satisfied a certain condition.

at points $x = l/2$ and $x = l$. Putting expression (b) for these points in (a), we obtain following equations:

$$f_2 + 6f_4 = 0, \qquad (c)$$

$$\left(2 - \frac{3}{4}P^*\right)f_2 + \left(3 - \frac{15}{16}P^*\right)f_4 = 0. \qquad (d)$$

Hence

$$P^* = \frac{Pl^2}{EI} = \frac{48}{19} \approx 2{,}53. \qquad (e)$$

This result deviates from the exact one by 2.4% and is very near to what, in the same approximating expression, was obtained by us by Ritz method.

Energy methods, method of finite differences and method of collocation can be united to the respect that during their application the problem is reduced to consideration of system of algebraic equations. Such methods in mathematical physics we call direct.

§ 13. Method of Successive Approximations

During use of energy methods we had to approximate elastic line, where error of result depended on how successfully we selected expression for deflection. It is true, in example 1.3 we could approach as close as we wished to exact magnitude of critical force, but for that it was necessary every time to introduce new parameter of deflection. Character of additional component could be selected by us for any consideration. Let us now turn to consideration of method of successive approximations, in which every new approximation is wholly based on preceding and ensues from it, not being connected with intuition of the calculator.

Essence of this method is that as initial elastic line we take any curve satisfying end conditions. Absolute values of ordinates

of this curve can be selected arbitrarily, since under critical load (if one were to start from approximate differential equation of elastic line) they are determined with accuracy up to a constant factor. Further we solve problem of bend of bar under action of given system of external longitudinal forces. If we immediately selected curve correctly, then, determining bending moments and integrating differential equation of elastic line, we must obtain the same curve. If however initial curve was selected only approximately, then second curve will differ from first. In other words, new equilibrium bending form will be other than that which we selected earlier. In order to arrive at new elastic line, we must change ordinate of the former. But since with only axial compressing force bending moments are proportional to ordinates, then this is identical to change by λ times of the magnitude of external load. The circumstance that ordinates of new curve differ λ times from ordinates of initial curve indicates that external forces must be increased or to decreased λ times in order to obtain critical load. But, as a rule, in different sections of bar we will obtain different relations of ordinates. It is possible to arbitrarily determine critical load by ratio of maximum ordinates or ratio of areas, embraced by elastic line. Later we will show also method, when true value of critical load is taken "in a fork," i.e., it is conceived possible simultaneously to approach it from above and from below. From first approximation we can pass cross to second, etc. Here we will obtain series of values of λ, determining at limit true magnitude of critical load.

Method of successive approximations may be given an analytic

and graphic form.*

Example 1.11. Determine critical load for bar with hinged supports at the ends, taking as initial line a broken line, consisting of two straight sections (Fig. 1.19) with ordinate f in the middl

Equation of left half:

$$v_0 = \frac{2f}{l} x. \qquad (a)$$

Taking force P equal to one, we determine bending moment in section x when $x \leq l/2$:

$$M = Pv = \frac{2f}{l} x. \qquad (b)$$

Differential equation of elastic line (5) takes form

$$EI \frac{d^2v}{dx^2} = -\frac{2f}{l} x. \qquad (c)$$

Integrating it twice and finding constants from end conditions, we obtain equation of elastic line of first approximation,

$$EIv = -\frac{f}{l} \frac{x^3}{3} + \frac{f}{4} lx. \qquad (d)$$

Ratio of maximum ordinates of initial and obtained line gives first approximate value of critical force:

$$P^{(1)}_{sp} = \left[\frac{v_0}{v_1}\right]_{x=\frac{l}{2}} = \frac{12EI}{l^2}, \qquad (e)$$

which differs from exact magnitude by more than 20%. Then we put

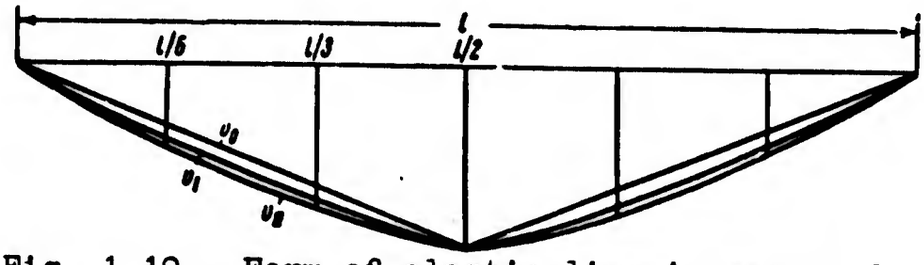

Fig. 1.19. Form of elastic line in zero and subsequent approximations.

*Graphic variant of method was offered by Vianello [1.16], and an analytic variant by F. Engesser and in another form by B. N. Gorbunov (Collection of research on theory of structures, 2, 1936, Stroyizdat.)

expression (d) in the right part of equation (c); in second approximation critical force is obtained as

$$p_{kp}^{(II)} = \left[\frac{v_1}{v_{.1}}\right]_{x=\frac{1}{2}} = \frac{10EI}{l^2}; \qquad (f)$$

error is equal here to 1.4%.

Change of form of elastic line is given in following table (maximum ordinate is taken as one):

		1/6	1/3	1/2
Initial form	0	0.33	0.67	1
First approximation	0	0.48	0.85	1
Second approximation	0	0.49	0.86	1
Exact values (by sine wave).	0	0.50	0.87	1

Initial form (v_0) is compared with forms of first two approximations (v_I and v_{II}) in Fig. 1.119.

Criterion for necessary number of approximations can be comparison of magnitude of critical force or ordinates of bending line in two successive approximations. If these values coincide with accuracy up to certain given value, then solution can be considered concluded.

As a rule, successive approximations in the form shown above lead to value of smallest critical force and in this constitute a convergent process.

Let us assume that differential equation of bending line is presented in the form of (5),

$$\frac{d^2v}{dx^2} = -\lambda v, \qquad (1.133)$$

and boundary conditions are

$$v = 0 \text{ when } x = 0, l. \qquad (1.134)$$

We expand function v_0, corresponding to elastic line of initial approximation, by natural forms of loss of stability:

$$v_0 = f_1\eta_1 + f_2\eta_2 + f_3\eta_3 + \ldots \qquad (1.135)$$

Let us remember that each of the natural forms corresponds to its own critical force--first, second, etc. For i-th natural form equation (133) takes form

$$\frac{d^2\eta_i}{dx^2} = -\lambda_i\eta_i. \qquad (1.136)$$

Taking i-th form as a diagram of moments and finding ratio of ordinates of preceding and subsequent curves, we obtain i-th critical force. Since initial curve (135) was arbitrary, then in first approximation we obtain following expansion:

$$v_1 = \frac{f_1}{\lambda_1}\eta_1 + \frac{f_2}{\lambda_2}\eta_2 + \frac{f_3}{\lambda_3}\eta_3 + \ldots \qquad (1.137)$$

Repeating this cycle n times, we come to equation

$$v_n = \frac{f_1}{\lambda_1^n}\eta_1 + \frac{f_2}{\lambda_2^n}\eta_2 + \frac{f_3}{\lambda_3^n}\eta_3 + \ldots \qquad (1.138)$$

or

$$v_n\lambda_1^n = f_1\eta_1 + f_2\left(\frac{\lambda_1}{\lambda_2}\right)^n\eta_2 + f_3\left(\frac{\lambda_1}{\lambda_3}\right)^n\eta_3 + \ldots \qquad (1.139)$$

But since second, third and subsequent critical forces always lie higher than the first, then with increase of number of cycles, the second, third, etc., members in the right part of equality (139) will constantly decrease, so that at limit we obtain,

$$v_n\lambda_1^n \to f_1\eta_1. \qquad (1.140)$$

As we see, with growth of number n approximations v_n with accuracy up to certain factor nears the first natural form.

Critical force usually is calculated, comparing maximum ordinates of elastic line in two consecutive approximations. However important peculiarity of method consists of the following. If one were to

find ratio of ordinates in two approximations for one point, then for second, etc., the true value of critical force will lie between values, determined by maximum and minimum ratios. Thus, exact magnitude of critical force can be taken "in a fork," which is narrowed for every new approximation.*

Thus, making calculation in example 1.11 for points $l/6$, $l/3$ and $l/2$, we obtain in first approximation $7.9 < P_{кр} l^2/EI < 12$, in second approximation $9.8 < P_{кр} l^2/EI < 10$, etc.

§ 14. Trial-and-Error Method

If one were to give method of successive approximations graphic form, then every new elastic line is constructed as a funicular curve with respect to preceding at arbitrary polar distance. Another variant of graphic method can be offered**, if we were given certain tentative values of critical load and we construct corresponding elastic line, varying polar distance H. Magnitude H is taken equal to

$$H = \frac{EIn}{Pml}. \qquad (1.141)$$

by n is understood the number of equal intervals, into which we divided length of bar l, 1/m is scale of drawing (Fig. 1.20). First section of funicular line we pass at arbitrary angle. Then we clarify how final point a of funicular curve is located, i.e., point of intersection of last section with horizontal line through initial point. If this final point corresponds to right end of bar, then force P taken for determination of polar distance is critical. As a rule,

---

*This property of method of successive approximations was shown by S. N. Kahn; see also book of S. P. Timoshenko [0.23], 1961 edition.

**This method was offered by Southwell.

last section of funicular line will either cross axis of bar, or lie below axial line. In first case of force quantity taken as critical is over estimated, in second--under estimated. In order to take sought value of force "in a fork," it is necessary to make "trial shots" and to make at least two constructions, as shown in Fig. 1.20.

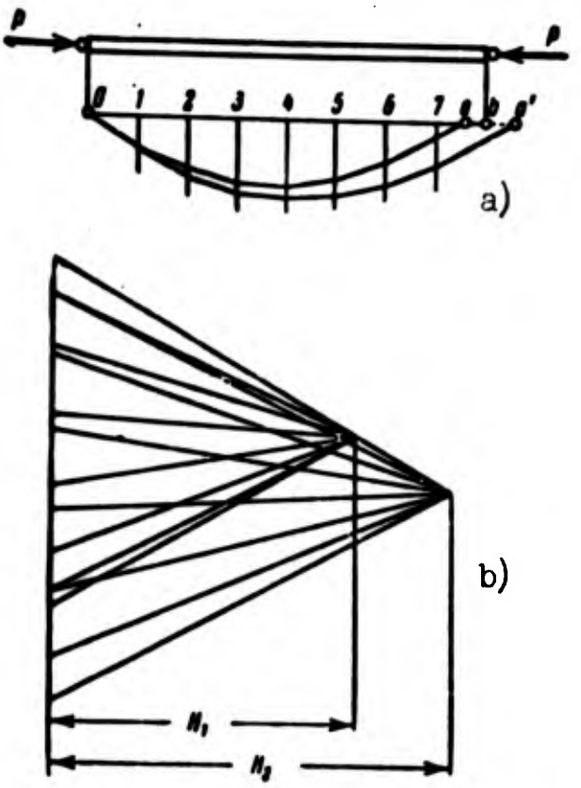

Fig. 1.20. Determining critical force by "trial-and-error method."

§ 15. Application of Integral Equations. Approximate Determination of First Critical Load

Using method of sucessive approximations, we are given some elastic line--coinciding in case of bar with articulated mount at ends with bending moments diagram from compressing forces--and we find new elastic line by means of integration; comparison of initial and newly found ordinates allowed us to determine approximate value of critical load and to establish to what form of bending line it corresponds. Proceeding this way, but from more general considerations, it is possible to constitute integral equation of the problem--

an equation including unknown function of deflection under the sign of ar integral.

Let us consider a bar, with hinged supports at its ends. We determine deflection in certain section x, using the Maxwell-Mohr formula:

$$v = \int_0^l \frac{M\bar{M}}{EI}\, d\xi. \qquad (1.142)$$

where M is bending moment in current section ξ from given forces, $\bar{M}$ is moment in that same section form unit force, applied at point with coordinate x. As can be seen from Fig. 1.21 these moments will be

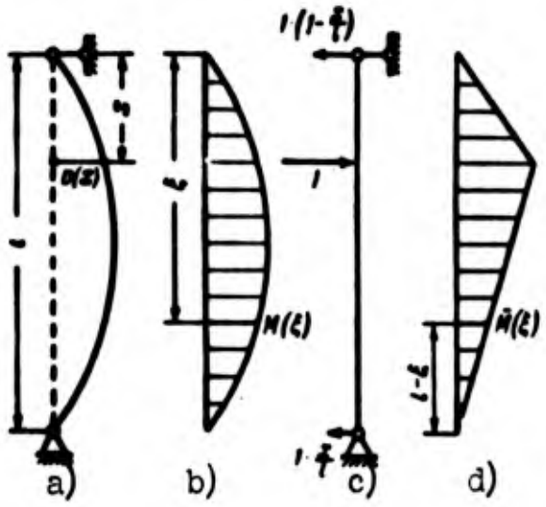

Fig. 1.21. Derivation of integral equation of problem.

(with compressing force P)

$$M = Pv(\xi),\ \bar{M} = \begin{cases} \left(1 - \frac{x}{l}\right)\xi \text{ when } \xi \leqslant x, \\ \left(1 - \frac{\xi}{l}\right)x \text{ when } x \leqslant \xi. \end{cases} \qquad (1.143)$$

We use dimensionless parameters

$$\frac{x}{l} = x_1,\ \frac{\xi}{l} = \xi_1 \qquad (1.144)$$

and present (142) in the form

$$v(x_1)=\int_0^{x_1}\frac{Pl^2}{EI}(1-x_1)\xi_1 v(\xi_1)d\xi_1+\int_{x_1}^{1}\frac{Pl^2}{EI}(1-\xi_1)x_1 v(\xi_1)d\xi_1. \qquad (1.145)$$

We will subsequently lower indices at x and ξ. We introduce designations (in dimensionless magnitudes)

$$G(x,\xi)=\begin{cases}(1-x)\xi \text{ when } \xi\leqslant x,\\ (1-\xi)x \text{ when } x\leqslant\xi.\end{cases} \qquad (1.146)$$

We consider also that in general, moment of inertia of section I and modulus E are variable by length, $I = I(\xi)$, $E = E(\xi)$, and we express them by certain given magnitudes E_0 and I_0:

$$\frac{1}{E(\xi)I(\xi)}=\frac{1}{E_0I_0}g(\xi); \qquad (1.147)$$

then expression (145) will take form

$$v(x)=\frac{Pl^2}{E_0I_0}\int_0^1 G(x,\xi)g(\xi)v(\xi)d\xi. \qquad (1.148)$$

Function $G(x,\xi)$, as it is easy to see from (146), is symmetric relative to variables x and ξ:

$$G(x,\xi)\equiv G(\xi,x). \qquad (1.149)$$

We designate

$$\lambda=\frac{Pl^2}{E_0I_0},\quad K(x,\xi)=G(x,\xi)\sqrt{g(\xi)}\sqrt{g(x)},\quad y(x)=v(x)\sqrt{g(x)}; \qquad (1.150)$$

then instead of (148) we obtain:

$$y(x)=\lambda\int_0^1 K(x,\xi)y(\xi)d\xi. \qquad (1.151)$$

Judging by (150), function $K(x,\xi)$ also turns out to be symmetric:

$$K(x,\xi)\equiv K(\xi,x). \qquad (1.152)$$

Equation (151) contains function $y(\xi)$ under the sign of the

integral, where limits of integrations are finite and are constant. If function $K(x, \xi)$ in considered interval is continuous, then equation (151) is a Fredholm uniform integral equation of the second type.* Theory of Fredholm extends also to function K, for which integral

$$S_2 = \int_0^1 \int_0^1 K^2(x, \xi)\, dx\, d\xi \qquad (1.153)$$

has a finite value. In our problem this requirement always is met. Function $K(x,\xi)$ has name of kernel, and magnitude λ is the parameter of equation. Equation (151) has, in general, trivial solution: $y(x) \equiv 0$, corresponding to rectilinear form of equilibrium of bar. Nontrivial solution $y(x)$ appears at branching points (bifurcations) of equilibrium states (see P.8); values of parameter λ corresponding to these points are called characteristic or fundamental numbers, and also singular or eigen values of parameter (see P.13), and nontrivial solutions are eigen, characteristic or fundamental functions. Characteristic numbers of equation (151) determine in our case the first and higher critical loads.

Thus, to determine first critical load it is necessary to determine smallest characteristic number of integral equation; the latter replaces differential equation of problem together with boundary conditions.

Integral equations are solved by various methods of approximation. One of the most wide-spread methods is method of successive approximations, which already was considered in § 13. Another method consists of replacing integral equation by finite system of linear

---

*See S. G. Mikhlin, Integral equations, Gostekhizdat, M., 1949.

algebraic equations, for which right side of (151) will be converted by one of the formulas of approximate integration.*

But for determination of characteristic numbers it is possible to use also the Hilbert-Schmidt** theory of symmetric integral equations. This leads to remarkable formulas, expressing first characteristic number by so-called spurs of the kernal. In first approximation it is possible to take

$$\lambda_1^2 = \frac{1}{S_2}. \qquad (1.154)$$

where S_2 is second spur of the kernel, determined by the formula (153). Such method is interesting by the fact that determination of critical load (characteristic number) as it were is separated from establishment of form of loss of stability (eigenfunction), whereas in preceding cases these problems were solved simultaneously. It is possible to show that approximate value of critical load according to (154) always lies below the true value.

Formula (153) for double integral can be transformed as follows. We divide area of integration into two equal triangles (Fig. 1.22) by line $x = \xi$: then, integrating for area of one of these triangles, we obtain:

$$S_2 = 2\int_0^1 dx \int_x^1 K^2(x, \xi)\, d\xi. \qquad (1.155)$$

Example 1.12. Determine critical load for bar with hinged supports for a constant section, if compressive forces are applied on ends. From (146) and (150) we find:

$$\varepsilon(\xi) \equiv 1, \quad \varepsilon(x) \equiv 1,$$

$$K(x, \xi) = G(x, \xi) = \begin{cases} (1-x)\,\xi & \text{when } \xi < x, \\ (1-\xi)\,x & \text{when } x < \xi. \end{cases}$$

---

*See L. V. Kantorovich and V. I. Krylov. Methods of approximation of higher analysis, 1962, P. 110.

**See above-mentioned book of S. G. Mikhlin, P. 108.

Using formula (155), we obtain:

$$S_2 = 2\int_0^1 (1-x)^2 \int_0^x \xi^2\, d\xi = \frac{2}{3}\int_0^1 (1-x)^2 x^3 = \frac{1}{90}.$$

Hence from (154)

$$\lambda = \sqrt{90}.$$

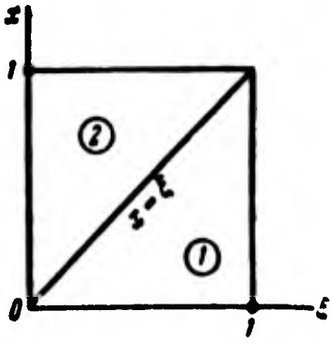

Fig. 1.22. Determination of magnitude of S with symmetric kernel.

Approximate value of critical load from (150) is equal to

$$P_{кр} = \sqrt{90}\,\frac{EI}{l^2} = 9{,}487\,\frac{EI}{l^2};$$

it turns out to be, as one should have expected, smaller than exact magnitude $P_{кр}$, and differs from it by 4.1%.

Until now we constituted integral equation, considering problem in linear formulation. If one were to take exact expression (2) for curvature of bending line, then integral equation of problem will be nonlinear. In literature on nonlinear integral equations there is considered question on admissibility of their linearization in determination of bifurcational points of problem (see § 198).

§ 16. Dynamic Criterion of Stability

We have analyzed methods, based on static and energy approaches to problem of stability of a bar. We turn now to a third, the dynamic criterion and consider free vibration of compressed bar with articulated supports at the ends.

We write differential equation of bending line of type (6):

$$EI\frac{d^4v}{dx^4} + P\frac{d^2v}{dx^2} = q. \qquad (1.156)$$

where q is intensity of lateral load. In case of vibrating motion deflection v will be a function not only of coordinate x, but also time t: $v = v(x,t)$. Therefore total derivatives with respect to x must be replaced by partial derivatives. Using D'Alembert's principle, we take as the intensity of distributed load the force of inertia of the mass of the bar, per unit length. Designating by p weight of unit length of bar, we obtain:

$$EI\frac{\partial^4 v}{\partial x^4}+P\frac{\partial^2 v}{\partial x^2}=-\frac{p}{g}\frac{\partial^2 v}{\partial t^2}. \tag{1.157}$$

where g is acceleration of force of gravity. Introducing designation $k^2 = P/EI$, we arrive at equation

$$\frac{\partial^4 v}{\partial x^4}+k^2\frac{\partial^2 v}{\partial x^2}+\frac{p}{EIg}\frac{\partial^2 v}{\partial t^2}=0. \tag{1.158}$$

We shall seek solution of equation (158) in the form of the product of two functions:

$$v(x, t)=X(x)T(t); \tag{1.159}$$

then instead of (158) we will obtain,

$$T\frac{d^4X}{dx^4}+k^2T\frac{d^2X}{dx^2}=-\frac{p}{EIg}X\frac{d^2T}{dt^2}$$

or

$$\frac{1}{X}\frac{d^4X}{dx^4}+k^2\frac{1}{X}\frac{d^2X}{dx^2}=-\frac{p}{EIg}\frac{1}{T}\frac{d^2T}{dt^2}. \tag{1.160}$$

Left part of this equation depends only on x, and right--only on t; equation can be satisfied only when left and right side are constants:

$$\frac{1}{X}\frac{d^4X}{dx^4}+k^2\frac{1}{X}\frac{d^2X}{dx^2}=\lambda, \tag{1.161}$$

$$-\frac{p}{EIg}\frac{1}{T}\frac{d^2T}{dt^2}=\lambda. \tag{1.162}$$

Th econd of these equations will be transformed to

$$\frac{d^2T}{dt^2} + \frac{EIg}{p}\lambda T = 0. \qquad (1.163)$$

Integral of this equation we present in form

$$T = A\sin(\omega t + \alpha); \qquad (1.164)$$

frequency of oscillations ω is determined by formula

$$\omega^2 = \frac{EIg}{p}\lambda. \qquad (1.165)$$

Equation (161) we rewrite in the form

$$\frac{d^4X}{dx^4} + k^2\frac{d^2X}{dx^2} - \lambda X = 0; \qquad (1.166)$$

corresponding characteristic equation will be

$$s^4 + k^2s^2 - \lambda = 0. \qquad (1.167)$$

This equation has two real roots and two imaginary ones. Introducing designations

$$s_1^2 = \frac{\sqrt{k^4 + 4\lambda} - k^2}{2}, \quad s_2^2 = \frac{\sqrt{k^4 + 4\lambda} + k^2}{2}, \qquad (1.168)$$

we write solution of equation (166) in form

$$X(x) = A\,\mathrm{ch}\,s_1x + B\sin\mathrm{h}\,s_1x + C\cos s_2x + D\sin s_2x. \qquad (1.169)$$

Expression (169), determining form of vibrations, should satisfy boundary conditions (10). First two conditions, pertaining to section $x = 0$, give: $A = C = 0$; two others lead to equalities, $B = 0$, $D \sin s_2 l = 0$. Considering $D \neq 0$, we find:

$$s_2 = \frac{n\pi}{l}, \quad n = 1, 2, 3, \ldots \qquad (1.170)$$

Hence from (168)

$$\lambda_n = \frac{n^4\pi^4}{l^4}\left(1 - \frac{k^2l^2}{n^2\pi^2}\right). \qquad (1.171)$$

Frequency n-th tone of vibrations from (165) turns out to be

$$\omega_n = \frac{n^2\pi^2}{l^2}\sqrt{\frac{EIg}{p}}\left(1 - \frac{Pl^2}{n^2\pi^2EI}\right)^{1/2}. \qquad (1.172)$$

We designate by ω_{on} frequency of n-th tone of vibrations of bar without force P:

$$\omega_{on} = \frac{n^2\pi^2}{l^2}\sqrt{\frac{EIg}{p}}. \qquad (1.173)$$

Then finally

$$\omega_n = \omega_{on}\left(1 - \frac{Pl^2}{n^2\pi^2EI}\right)^{1/2}. \qquad (1.174)$$

This formula is "key" for dynamic analysis of stability of bar. In it we find explanation of experimental data, described in § 1. Frequency of vibrations of bar with formation of one half-wave ($n = 1$) becomes equal to zero when force P attains critical value $P_э = \pi^2EI/l^2$. Thus, onset of monotonic (static) instability of bar is characterized here by transformation into zero of frequency of free vibrations.* In graph ($P/P_э$, ω^2) we obtain a straight line, intersecting axis of ordinates at point of bifurcation of equilibrium forms (Fig. 1.23). Dynamic criterion leads in this case to the same value of critical load as other criteria--static or energy. However, as was already said, such coincidence does not occur for any elastic system.

§ 17. Criterion of Initial Imperfections

Till now we considered ideal bar with straight axis, loaded with compressing force strictly on center of gravity of cross section.

---

*There is possible also case of vibrational instability; it should be considered separately (see § 21).

But real elements of structures always possess a known initial bend; compressing forces applied to them usually act with certain eccentricity; along with axial forces there can be applied various lateral loads. All these factors play role of "perturbations," affecting behavior of system. Study of "imperfect" systems is important, first of all, from practical side, since it allows us to bring calculating diagram to real structures. True, all enumerated factors are, as a rule, random; therefore to validly estimate their effect is possible only by bringing in statistical methods. Such methods will be presented later, in Chapter XX. However construction of statistical dependences requires predetermination of how the system behaves under a certain given perturbation.* Furthermore, consideration of imperfect system in a number of cases allows us to determine critical load for its ideal model: we know already that effect of different perturbations especially strongly shows near critical load.

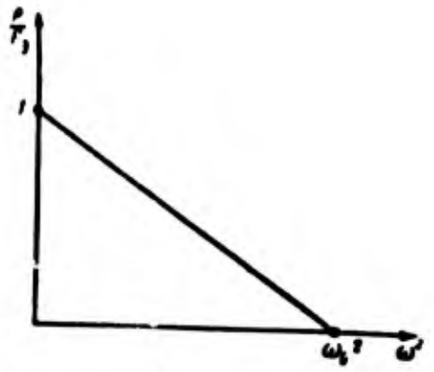

Fig. 1.23. Dependence between frequency of vibrations and compressive force.

We will consider consecutively influence of all important perturbing factors. We will start from case, when bar, supported by hinges at its edges, has initial bend

$$v_0 = v_0(x) \tag{1.175}$$

and is compressed by force P, whose direction passes through end joints. Differential equation (5) obtains the form

*For more detail see § 193.

$$EI\frac{d^2v}{dx^2} = -Pv_1. \qquad (1.176)$$

where by v we understand additional deflection, appearing in process of deformation, by v_1--total deflection:

$$v_1 = v + v_0. \qquad (1.177)$$

Introducing former designation $k^2 = P/EI$, we obtain:

$$\frac{d^2v}{dx^2} + k^2v = -k^2v_0. \qquad (1.178)$$

For instance, in initial state let bar bend by half-wave of sine wave (Fig. 124):

$$v_0 = f_0 \sin\frac{\pi x}{l}. \qquad (1.179)$$

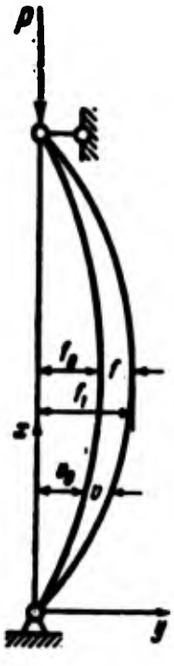

Fig. 1.24. Bar with initial bend.

The solution of equation (176), satisfying boundary conditions v = 0 when x = 0, l, will be

$$v = \frac{f_0k^2}{\frac{\pi^2}{l^2} - k^2}\sin\frac{\pi x}{l}. \qquad (1.180)$$

Additional deflection f is equal to

$$f = \frac{f_0}{\frac{P_{кр}}{P} - 1}, \qquad (1.181)$$

where by $P_{кр}$ we understand critical force (15). Total deflection $f_1 = f + f_0$ will be determined by formula

$$f_1 = \frac{f_0}{1 - \frac{P}{P_{кр}}}. \qquad (1.182)$$

Dependence between f and $P/P_{кр}$ for different initial imperfections

is depicted in Fig. 1.25; magnitudes f and f_0 are related to radius of gyration of section of bar i:

$$\frac{f}{i}=\zeta, \quad \frac{f_0}{i}=\zeta_0. \qquad (1.183)$$

Behavior of system turns out to qualitatively differ from that which was characteristic for "classical" problem of stability. Deflection appears already for small values of force P, when in case of central compression under load $P \leq P_{кр}$ bar should remain rectilinear. Speed of build-up of deflection depends on "perturbing factor"--initial deflection. For sufficiently small ζ_0 curve $P(\zeta)$ lies very close to axis of ordinates. At the same time with load, nearing critical, deflection grows quickly; function $P(\zeta)$ is <u>nonlinear</u>. When P nears $P_{кр}$, $f \to \infty$: deflection increases infinitely. Let us remember that material of bar we consider here ideally elastic and we solve the problem, proceeding from a <u>linear</u> differential equation.

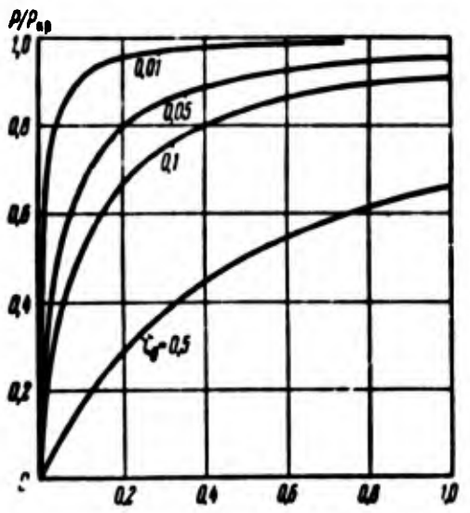

Fig. 1.25. Diagram of "additional deflection-load" for bar with initial bend.

Formula (181) may be used to determine critical force in experiments with bars with initial flaw.* We present (181) in the form

$$\frac{f}{P}P_{кр}-f=f_0. \qquad (1.181a)$$

We construct graph, placing along the axis of abscissas measured values of f, and along the axis of ordinates--values of f/P. Then on graph we must obtain a straight line, where magnitude, inverse of

*This method was offered by Southwell.

angular coefficient of straight line, will give critical force.

§ 18. Eccentric Compression. Approximate Solution

Let us consider, further, another perturbing factor--eccentricity in application of load. Let us assume that a bar, with hinged support at ends, is subjected to action of forces P, whose point of application is removed from center of gravity of section a distance e. It is assumed that arm e lies in plane of least rigidity of bar (Fig. 1.26).

Differential equation (5) will obtain here the form

$$EI\frac{d^2v}{dx^2} = -P(v+e) \tag{1.184}$$

or

$$\frac{d^2v}{dx^2} + k^2v = -k^2e. \tag{1.185}$$

General solution of corresponding homogeneous equation will be

$$v = A\cos kx + B\sin kx. \tag{1.186}$$

Here it is necessary to add particular solution v = -e; total solution obtains form

$$v = A\cos kx + B\sin kx - e. \tag{1.187}$$

Satisfying boundary conditions of problem v = 0 for x = 0, l, we find:

$$A = e, \quad B = e\tan\frac{kl}{2}. \tag{1.188}$$

Solution (187) now can be recorded in form

$$v = e\left(\cos kx + \operatorname{tg}\frac{kl}{2}\sin kx - 1\right) \tag{1.189}$$

or

$$v = e\left[\frac{\cos\left(\frac{l}{2}-x\right)}{\cos\frac{kl}{2}} - 1\right]. \tag{1.190}$$

Maximum deflection is equal, when x = 1/2, to

$$f=e\left(\frac{1}{\cos\frac{kl}{2}}-1\right)=e\left(\frac{1}{\cos\frac{\pi}{2}\sqrt{\frac{P}{P_{кр}}}}-1\right). \quad (1.191)$$

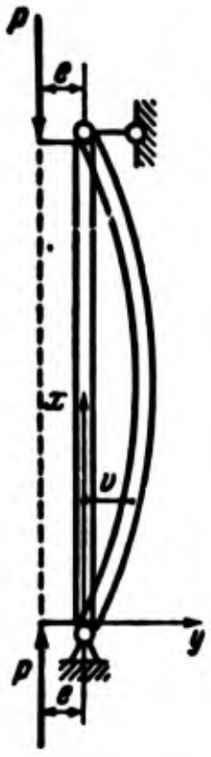

Fig. 1.26. Hinge-supported bar under action of eccentrically applied forces.

Let us note that here dependence between f and P will be nonlinear and that when $P \to P_{кр}$, $f \to \infty$.

We solve the same problem by the Bubnov-Galerkin method (see Section 10). We take equation of elastic line in the form

$$v=f\sin\frac{\pi x}{l}. \quad (1.192)$$

We constitute equation of type

$$\int_0^l\left[EI\frac{d^2v}{dx^2}+P(v+e)\right]\sin\frac{\pi x}{l}\,dx=0 \quad (1.193)$$

and place instead of v expression (192); after integration we obtain

$$f=\frac{4}{\pi}\frac{e}{\frac{P_{кр}}{P}-1}. \quad (1.194)$$

This equation has the same structure as dependence (181), pertaining to a sinusoidal initial bend.

If such type of load is experienced by bar with one end clamped and the other end free (Fig. 1.27), then equation (184) will take the form

$$EI\frac{d^2v}{dx^2}=P(e+f-v) \quad (1.195)$$

or

$$\frac{d^2v}{dx^2} + k^2v = k^2(e+f). \qquad (1.196)$$

Subordinating solution to conditions v = 0, dv/dx = 0 for x = 0, we find

$$v = (e+f)(1-\cos kx). \qquad (1.197)$$

Assuming x = l, we obtain

$$f = e\left(\frac{1}{\cos kl} - 1\right) = e\left(\frac{1}{\cos\frac{\pi}{2}\sqrt{\frac{P}{P_{кр}}}} - 1\right). \qquad (1.198)$$

Dependence between f and P turned out to be exactly the same as in case of hinge-supported ends.

Fig. 1.27. Bar with clamped end under action of eccentrically applied load.

§ 19. Eccentric Compression. Exact Solution

Let us approach the same problem of eccentric compression, proceeding from exact differential equation of elastic line, as in § 5. In Fig. 1.28 is depicted bar of length l in bent position; force P acts on arm e and preserves vertical direction. Besides, here is shown hypothetical bar of length l_1, end of which lies on line of action of force P. Obviously, with respect to this hypothetical bar it is possible to use relationship (75), connecting

maximum deflection f_1 with parameters k and ϑ (leave the plus sign).

$$kf_1 = 2\sin\vartheta. \tag{1.199}$$

We consider equilibrium positions of bar near first critical force, so that for φ_0 in (71a) we take value n = 0.

Fig. 1.28. Exact solution of problem of eccentric compression of bar.

Deflection v in certain section x is determined by (76):

$$kv = 2\sin\vartheta(1-\cos\varphi).$$

Let us assume that for upper end of bar that parameter φ has value $\varphi = \varphi_1$; then maximum deflection f will be equal to

$$kf = 2\sin\vartheta(1-\cos\varphi_1). \tag{1.200}$$

We determine, further, angle of rotation of tangent to bending line θ. We use relationship

$$\cos\theta = \frac{dx}{ds} \tag{1.201}$$

and place here values of dx and ds from (66) and (68); then we obtain

$$\cos\theta = 1 - \frac{k^2}{2}(f^2 - y^2)$$

or, by (69),

$$\cos\theta = 1 - 2\sin^2\vartheta\sin^2\varphi. \tag{1.202}$$

Angle of inclination of upper face when $x = l$ will be found then by formula

$$\cos\theta_l = 1 - 2\sin^2\vartheta\sin^2\varphi_1. \tag{1.203}$$

Considering Fig. 1.28, we write dependence between f and f_1:

$$f_1 = f + e\cos\theta_1. \tag{1.204}$$

Putting here expressions (199), (200) and (203), we find

$$ke = \frac{2\sin\vartheta\cos\varphi_1}{1-2\sin^2\vartheta\sin^2\varphi_1}. \tag{1.205}$$

Integrating expression (71) for ds, we obtain total length of bar l:

$$kl = \int_0^{\varphi_1} \frac{d\varphi}{\sqrt{1-\sin^2\vartheta\sin^2\varphi}} = F(\varphi_1, \vartheta). \tag{1.206}$$

Such an integral, in distinction from (73), carries name of <u>incomplete elliptic integral</u> of the first kind. These integrals also are tabulated.

Equations (204), (205) and (206) contain three unknowns: maximum deflection f and parameters ϑ and φ_1. Using them, it is possible for any given eccentricity e to establish dependence between load P and maximum deflection f. Such curves for e = 0.1l and e = 0.01l are depicted in Fig. 1.29 in comparison with curve, pertaining to case of central compression (e = 0). The greatest divergence between curves is obtained in region, lying near critical load; when $P > P_{кр}$, influence of eccentricity drops.

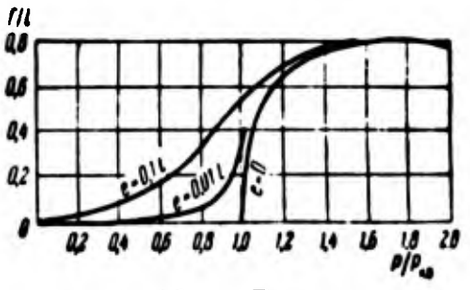

Fig. 1.29. Depencence between maximum deflection and load from exact solution of problem.

These data it is possible to compare with approximate solution. If it is considered that parameter ϑ is small for slight deflections, in (205) and (206) it is possible to disregard $\sin^2\frac{\vartheta}{2}\sin^2\varphi$ as compared to 1; then we obtain:

$$kl = F(\varphi_1, \vartheta) \approx \varphi_1. \tag{1.207}$$

$$ke \approx 2\sin\frac{\vartheta}{2}\cos\varphi_1 \approx 2\sin\frac{\vartheta}{2}\cos kl. \tag{1.208}$$

Comparing with (200), we find

$$f = e\left(\frac{1}{\cos kl} - 1\right),$$

which coincides with (198).

§ 20. Influence of Lateral Load

Let us turn to case where, along with axial force, there acts certain lateral load. Let us assume that a hinge-supported bar, compressed by force P, is subjected to action of evenly distributed load of intensity q (Fig. 1.30). Equation (5) obtains form

$$EI\frac{d^2v}{dx^2} = -Pv - \frac{ql}{2}x + \frac{qx^2}{2} \tag{1.209}$$

or, when $k^2 = P/EI$,

$$\frac{d^2v}{dx^2} + k^2v = -\frac{qk^2}{P}\left(\frac{l}{2}x - \frac{x^2}{2}\right). \tag{1.210}$$

Connecting general solution of homogeneous equation and particular solution, we find

$$k^2v = A\cos kx + B\sin kx - \frac{qk^2}{P}\left(\frac{l}{2}x - \frac{x^2}{2}\right) - \frac{q}{P}. \tag{1.211}$$

From boundary conditions we obtain

$$A=\frac{q}{P}, \quad B=\frac{q}{P}\tan\frac{kl}{2}. \tag{1.212}$$

Finally:

$$k^2v=\frac{q}{P}\left(\operatorname{tg}\frac{kl}{2}\sin kx+\cos kx-1\right)-\frac{k^2q}{P}\left(\frac{l}{2}x-\frac{x^2}{2}\right). \tag{1.213}$$

Maximum deflection is

$$f=\frac{q}{Pk^2}\left(\frac{1}{\cos\frac{kl}{2}}-1\right)-\frac{1}{P}\frac{ql^2}{8}. \tag{1.214}$$

We obtained dependence between f and P of the same type as for eccentrically compressed bar.

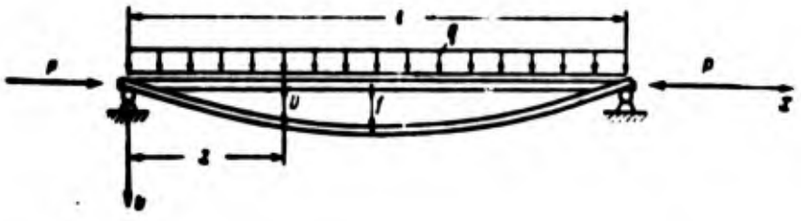

Fig. 1.30. Bar under longitudinally-lateral bending.

If, instead of distributed load there is a concentrated force Q in the middle of the span, by the same means we find equation of elastic line for one half of the bar:

$$v=\frac{Q}{2P}\left(\frac{1}{k\cos\frac{kl}{2}}\sin kx-x\right) \tag{1.215}$$

and deflection

$$f=\frac{Ql}{4P}\left(\frac{\tan\frac{kl}{2}}{\frac{kl}{2}}-1\right). \tag{1.216}$$

We solve the same problem of simultaneous action of end and lateral loads with help of Bubnov-Galerkin method. In case of evenly distributed load we write equation

$$EI\frac{d^4v}{dx^4}+P\frac{d^2v}{dx^2}=q. \qquad (1.217)$$

Introducing as approximating curve the half sine wave

$$v=f\sin\frac{\pi x}{l}, \qquad (1.218)$$

we arrive at equation

$$\int_0^l\left(EI\frac{d^4v}{dx^4}+P\frac{d^2v}{dx^2}-q\right)\sin\frac{\pi x}{l}\,dx=0. \qquad (1.219)$$

Putting (218) in place of v and integrating, we find,

$$f=\frac{\frac{4}{\pi^5}\frac{ql^4}{EI}}{1-\frac{Pl^2}{\pi^2EI}}. \qquad (1.220)$$

Numerator constitutes here approximate value of maximum deflection of bar during action of one lateral load:

$$f_0=\frac{4}{\pi^5}\frac{ql^4}{EI}; \qquad (1.221)$$

coefficient is equal to 1/76.7 instead of known value 5/384 = 1/76.8. Therefore formula (220) can be rewritten in the form

$$f=\frac{f_0}{1-\frac{P}{P_{ep}}}, \qquad (1.222)$$

which coincides in structure with (182). This simple formula may be extended to other cases of longitudinally-lateral bending. For determination of maximum normal stresses it is necessary to use formula

$$\sigma_{max}=\frac{M_{max}}{W}.$$

where W is moment of resistance of section.

Considering moments, corresponding longitudinal compressing and lateral loads, we find,

$$\sigma_{max} = \frac{P}{F} + \frac{M + Pf}{W}; \qquad (1.\ldots)$$

compressing stresses are considered here positive.

As we see, with longitudinally-lateral bending the principle of independence of action of forces is inapplicable, magnitude (...) is not equal to sum of stresses caused by longitudinal and lateral loads separately. Therefore during check of bar for "stable strength" (term of N. V. Kornoukhov) they multiply all loads by safety factor n and compare maximum stress not with permissible, but with stress, taken as limiting.

§ 21. Stability of Nonconservative System. Case of Follow-Up Force

All elastic systems considered till now pertained to conservative one: work of forces applied to them did not depend on trajectories of displacement of points of application and was determined only by initial and final position of these points. Let us turn now to one example of a nonconservative system, study of whose stability requires a special approach.*

Let us assume that one of the ends of a bar of constant section is clamped, and the second is free and that to free end is applied force P, directed, with deflection of bar, along tangent to elastic

*Similar problem was considered by M. Beck [1.8] and by K. S. Deyneko and M. Ya. Leonov [1.2]; nonconservative systems are the subject of book of V. V. Bolotin, 1961 [0.1].

line (Fig. 1.31), such a force we call follow-up. We resolve force P into two components: vertical V and horizontal H. With small angles of rotation of tangent force V it is possible to consider constant; it plays the same role as "ordinary" forces in conservative problems. Conversely, force H is specific; its magnitude essentially depends on angle of rotation of end section, and elementary work is equal to product of force by increase of deflection.

Fig. 1.31. Bar under action of follow-up force.

We apply in this problem dynamic criterion, as we did in § 15. Equation of motion of element of beam as before has form (158). Taking $v = X(x)T(t)$ and proceeding the same way, we arrive at expression (169) for form of vibrations:

$$X(x) = A\operatorname{ch} s_1 x + B\operatorname{sh} s_1 x + C\cos s_2 x + D\sin s_2 x. \qquad (1.224)$$

where s_1 and s_2, are determined by (168).

In section $x = 0$ deflection and angle of rotation turn into zero, and in section $x = l$—moment and lateral force turn into zero; consequently, boundary conditions for function $X(x)$ will be:

$$X = 0,\ \frac{dX}{dx} = 0 \text{ when } x = 0,\ \frac{d^2X}{dx^2} = 0,\ \frac{d^3X}{dx^3} = 0 \text{ when } x = l. \qquad (1.225)$$

First two conditions give

$$A+C=0, \quad s_1B+s_2D=0. \tag{1.226}$$

Remaining conditions lead to equations

$$\left.\begin{aligned}(s_1^2 \operatorname{ch} s_1 l+s_2^2 \cos s_2 l) A+s_1(s_1 \operatorname{sh} \lambda_1 l+s_2 \sin \lambda_2 l) B=0,\\ (s_1^3 \operatorname{sh} s_1 l-s_2^3 \sin s_2 l) A+s_1(s_1^2 \operatorname{ch} \lambda_1 l+s_2^2 \sin \lambda_2 l) B=0.\end{aligned}\right\} \tag{1.227}$$

Equating to zero determinant of this system, we arrive at following equation:

$$s_1^4+s_2^4+2 s_1^2 s_2^2 \operatorname{ch} s_1 l \cos s_2 l-s_1 s_2(s_1^2-s_2^2) \operatorname{sh} s_1 l \sin s_2 l=0. \tag{1.228}$$

Using expressions (168), we find

$$s_1^4+s_2^4=k^4+2\lambda^2, \quad s_1^2 s_2^2=\lambda^2, \quad s_1^2-s_2^2=-k^2. \tag{1.229}$$

Equation (228) takes now the form

$$k^4+2\lambda^2+2\lambda^2 \operatorname{ch} s_1 l \cos s_2 l+\sqrt{\lambda^2}\, k^2 \operatorname{sh} s_1 l \sin s_2 l=0. \tag{1.230}$$

Let us turn to dimensionless parameters

$$\left.\begin{aligned}K=(kl)^2=\frac{Pl^2}{EI}, \quad \Omega=\lambda^4=\frac{\rho\omega^2 l^4}{EIg},\\ \bar{s}_1=s_1 l, \quad \bar{s}_2=s_2 l;\end{aligned}\right\} \tag{1.231}$$

then we obtain dependence

$$F(K, \Omega) \equiv K^2+2\Omega+2\Omega \operatorname{ch} \bar{s}_1 \cos \bar{s}_2+\sqrt{\Omega}\, K \operatorname{sh} \bar{s}_1 \sin \bar{s}_2=0. \tag{1.232}$$

Parameter K represents compressing force, and Ω—frequency of vibrations.

In Fig. 1.32 is given graph depicting dependence between K and Ω according to equation (232).

It is interesting to compare it with analogous graph of Fig. 1.23, pertaining to conservative problem. There point of bifurcation of equilibrium states corresponded to "zero" frequency; now on axis $\Omega = 0$ we do not obtain points of bifurcation. Therefore, if one were to use only the static criterion, it is possible to arrive at the conclusion that loss of stability of bar in this case is generally impossible.

We obtain another result, using dynamic criterion, obtaining here a new interpretation. Curve (K,Ω) has the form of a loop. Points, lying on axis of abscissas, correspond two first natural frequencies of bending vibrations of bar, not bearing a compressing load. If one were to put $P = 0$, then equation (228) changes into the following:

$$\operatorname{ch} \bar{s}_1 \cos \bar{s}_2 = -1; \tag{1.233}$$

its roots, as we know, determine frequencies of free vibrations of bar with one end clamped and the other free; forms of these vibrations are shown in Fig. 1.33. When $P \neq 0$ elastic line of bar combines first and second natural forms; for left loop the first form of vibrations is predominant, for right--the second. At limit point of loop frequencies merge; to this point corresponds value K:

$$K \approx 20. \tag{1.234}$$

when $K > 20$ system will be unstable and will vibrate, being supplied with additional energy because of work of the nonconservative

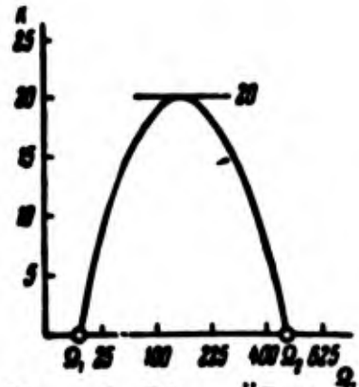

Fig. 1.32. "Loop" of frequencies of vibrations with different compressing forces.

Fig. 1.33. Forms of vibrations during action of follow-up force.

component of force P. Let us note that change of direction of force P, from condition of problem, should occur because of a certain source of energy external to system.

If we were to look for additional roots of equation (228), then we, apparently, will obtain new loops, connecting third and fourth natural frequencies, fifth and sixth, etc. However limit point for the first loop is the smallest; it determines critical load, equal approximately to

$$P_{sp} = \frac{2\pi^2 EI}{l^2}. \qquad (1.235)$$

Comparison with formula (27) shows that with <u>follow-up</u> load critical force is approximately <u>eight</u> times larger than during load of constant direction.

We considered vibrations of a bar, not taking into account influence of resisting forces. Calculation of these forces can affect magnitude of critical force and lead to its decrease.

Other examples of nonconservative problems, connected with

problems of flutter of an elastic system, will be given in Chapter XIX.

§ 22. Phenomenon of Loss of Stability "in the Large"

Let us become more specifically acquainted with phenomenon of buckling of an elastic system "in the large". An example of such system can be a compressed bar, fastened to a spring, having a nonlinear characteristic. For simplification of problem we replace elastic bar by two absolutely stiff links of length $l/2$, joined by an elastic hinge; two other ends of sections we consider freely turning (Fig. 1.34). We assume that joint A is connected to two springs AB and AC, located at certain angles to one another. Stiffness of each spring with linear characteristic we designate by k. Let us assume that initial length of every spring is r, and distance from joint A to line BC is a.

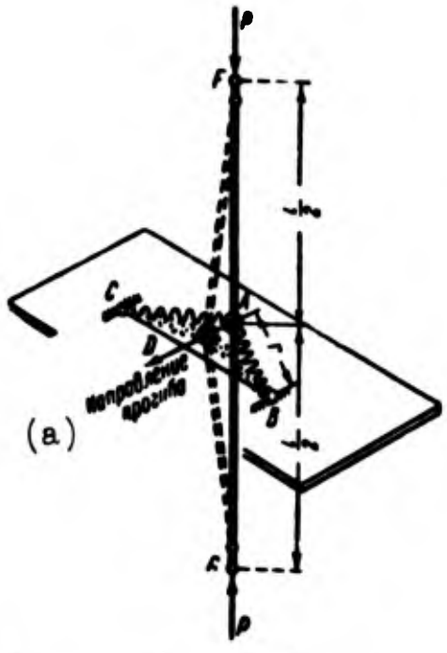

Fig. 1.34. Model illustrating phenomenon of loss of stability "in the large".
KEY: (a) Direction of deflection.

Reaction of each spring during displacement of hinge is equal to

$$S=k(r-r_1). \tag{1.236}$$

where r_1 is length of spring after deformation. Total reaction of both springs is equal to (see Fig. 1.34),

$$Q=2S\frac{a-f}{r_1}=2k\left(\frac{r}{r_1}-1\right)(a-f); \tag{1.237}$$

by f = $\overline{AD}$ is understood displacement of point A, characterizing deflection of bar. Considering triangle ABD, we find

$$r_1=r\sqrt{1-\left(\frac{2af}{r^2}-\frac{f^2}{r^2}\right)}. \tag{1.238}$$

$$Q=2k\left[\frac{1}{\left(1-\left(\frac{2af}{r^2}-\frac{f^2}{r^2}\right)\right)^{1/2}}-1\right](a-f)\approx\frac{k}{r^2}(2a^2f-3af^2+f^3). \tag{1.239}$$

Thus, with <u>linear</u> characteristic of every spring separately their total reaction changes depending upon f by <u>nonlinear</u> law.

Let us assume that bars transmit compressive load P and that there has occurred loss of stability of system. Condition of equilibrium of each link has the form

$$M=Pf-\frac{k}{4r^2}(2a^2f-3af^2+f^3)l. \tag{1.240}$$

Considering ratio f/l small, we take mutual angle of rotation in joint φ equal to 2f/(l/2) = 4f/l. Stiffness of joint C = M/φ we select from condition that in the absence of springs critical force was equal to Euler's:

$$C=\frac{P_3f}{\varphi}=\frac{P_3l}{4}. \tag{1.241}$$

With springs we have

$$Pf - \frac{kl}{4r^2}(2a^2f - 3af^2 + f^3) = \frac{P_0 l}{4}\frac{4f}{l}; \qquad (1.242)$$

hence when f ≠0

$$P = P_0 + \frac{k}{4r^2}(2a^2 - 3af + f^2)l. \qquad (1.243)$$

With loss of stability in the small it is necessary to consider f << a; then we obtain critical force equal to

$$P_0 = P_0 + \frac{ka^2l}{2r^2}. \qquad (1.244)$$

As can be seen from equation (243), with growth of f compressing force at first drops (influence of middle member in parentheses), and then starts to increase again (influence of third member). We define least value of $P = P_H$, equating to zero the derivative of P with respect to f, we find: f = 1.5 a. Hence

$$P_H = P_0 - \frac{ka^2l}{16r^2} = P_0 - \frac{9}{16}\frac{ka^2}{r}l. \qquad (1.245)$$

For all values of force P, lying between P_H and P_B, system has three equilibrium positions: one, corresponding to initial, and two displaced. Initial state becomes unstable when $P > P_B$; therefore according to the terminology, in § 6, load P_B corresponds to loss of stability in the small and may be called upper critical force. On the other hand, strongly bent equilibrium forms are possible for all values $P > P_H$; with known perturbations there is possible jump of system from initial position to bent, characterizing loss of stability in the large. Load P_H is called lower critical force.*

We introduce designations

$$\frac{P}{P_0} = \bar{P}, \quad \frac{ka^2l}{4r^3P_0} = \bar{k}, \quad \frac{f}{a} = \zeta \qquad (1.246)$$

---

*This concept is considered in more detail below, in § 201.

and rewrite equation (243) in the form

$$\bar{P}=1+\bar{k}(2-3\zeta+\zeta^3). \qquad (1.247)$$

In Fig. 1.35 is shown dependence $\bar{P}(\zeta)$ between dimensionless parameters of load and buckling, or, in other words, diagram of equilibrium states of system when $\bar{k}$ = 0.5; 1. On graph are marked points, corresponding to upper and lower critical forces. On level of load $\bar{P}_0$ we obtain, as was already said, three equilibrium states, corresponding to points a, b, c. It is possible to show that the first of them is stable, the second is--unstable and the third is also--stable. This corresponds to equilibrium positions of ball in Fig. 1.17. In the presence of known perturbation the system can jump from position a to position c.

Parameter $\bar{k}$ determines "degree of nonlinearity" of system. The higher $\bar{k}$, the greater is drop between upper and lower critical loads. Let us note that when a = 0, when springs are located on one straight line, we will have $\bar{k}$ = 0.

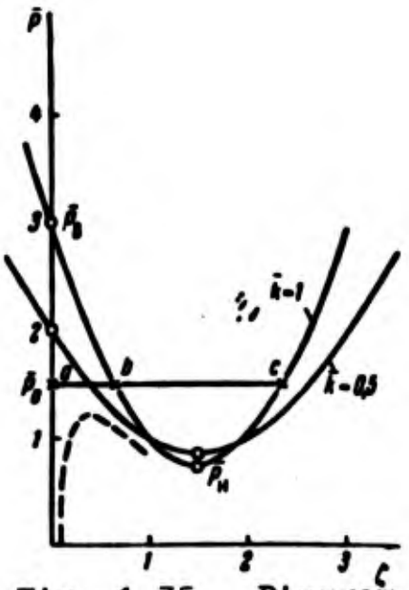

Fig. 1.35. Diagram "load-buckling".

We arrive at conclusion that for elastic systems, having "falling" characteristic $\bar{P}(\zeta)$, calculation for upper critical force, corresponding to loss of stability in the small and determined from linearized equations, is insufficient. Valid calculation of such systems is calculation for stability in the large: it may be conducted

only with help of nonlinear theory.

As the perturbation, provoking buckling of system at $P < P_B$, there can serve initial deflection of axial lines of sections from straight line FG (Fig. 1.34). Then dependence $P(\zeta)$ will have form shown in Fig. 1.35 by dotted line: as one can see, upper critical load P_B here will not be attained.

To the same conclusions leads solution of initial, more complicated problem of stability in the large of an elastic bar, fixed to a spring, having nonlinear characteristic.*

§ 23. Selection of Method of Research. Application of Digital Computers

We met different criteria of stability and methods of solution of problems. There arises the question: which of these ways of solution should we select in any case? This depends on purpose of solution of problem and character of calculating means available to calculator.

If it is necessary at least crudely to estimate magnitude of critical load for conservative system, then it is appropriately to use one of the energy methods, introducing minimum number of modified parameters; we usually start from one parameter. Result of solution here will depend on engineering intuition of calculator, allowing him more or less successfully to approximate form of loss of stability. With increase of number of independent parameters calculations are greatly hampered.

When greater accuracy of calculation is desirable (within several percents), it is expedient to apply method of successive approximations; it allows us to estimate convergence of calculations and

*Such problem was investigated by H. S. Tsien [1.15].

to establish order of error. For bar of variable stiffness analytic determination of elastic line in every new approximation is very laborious; therefore it is expedient to use graphic or graphe-analytical variants of method of successive approximations.

For studying nonconservative systems one should apply the most general criterion--the dynamic one.

All recommendations pertaining to selection of method of solution must be examined when, for calculations there are used electronic digital computers (ETsVM) or analog computers.

We shall discuss first application of digital computers. As it is known, ETsVM execute only the simplest arithmetic operations, and also logical actions and operation of control over the calculating process. Therefore selected method of calculation should reduce solution of problem to fulfillment of a sequence of very simple operations.

Further, it is necessary to ensure cyclical movement of solution of problem, i.e., multiple iteration of calculations on the same formulas with substitution in them during every iteration of the cycle of new numerical data. Last, there should be foreseen possibility of checking correctness of solution of problem on machine.

During selection of numerical method it is necessary to consider "calculating possibilities" of the applied machine.* Contemporary high-speed general-purpose digital computers execute each second from several tens or hundreds of operations (small machines, for instance "Ural-1") to several tens of thousand operations (large mach-

---

*See, for instance, A. I. Kitov and N. A. Krinitskiy, Electronic digital computers and programming, Fizmatgiz, m., 1959.

ines). Numbers, on which actions are produced, are presented in machines with high degree of accuracy--from seven to ten figures in decimal number system. Operational memory of most machines allows us to store simultaneously from 1000 to 4000 numbers or program commands, while working a lower speed additional (external) memory units possess practically infinite capacity. It is necessary also to consider that speed of introduction in machine of initial information and recovery of results is small as compared to speed of calculations.

Digital computers can be used, in principle, for solution of problems of stability by any one of above-mentioned methods. However some of them are preferable. We indicate, first of all, the method of finite differences: characteristic of it is multiple cyclical iteration of calculations by formulas having one and the same form for every interval. This method allows us easily to increase accuracy of calculation, since splitting of a step does not cause fundamental difficulties.

We saw above that during determination of critical load with help of method of finite differences we obtain system of uniform linear algebraic equations for parameters of deflection. Condition of nontrivialness of solution of this system consists of the fact that the main determinant of the system is equal to zero. Expanding the determinant, we arrive at a nonlinear algebraic equation. It is required to find least real root of equation. Such process of expansion of the determinant for finding coefficients of nonlinear equation lends itself to programming. Detecting the least root of algebraic equation also is executed on ETsVM, for instance, by one of the iterative methods.

Analogous process of calculations we will obtain during use of other direct methods--Ritz or Bubnov-Galerkin. We note, however, that application of computers for solution of problems in a trigonometric series in not fully rational, since obtaining of trigonometric functions is computer requires auxiliary calculations by special subroutines or leads to necessity of storage in memory units of bulky tables.

Very convenient for programming are indirect ways of determination of critical load. It is useful to use criterion of "initial imperfections", allowing us to introduce in equation "perturbing" members; the equation itself may be presented in finite differences. Solution of ETsVM allows us to determine equilibrium forms of bar for different initial deflections. Consecutively decreasing the parameter of perturbation, we determine critical load for an "ideal" construction.

Another variant consists in application of method of successive approximations with assignment of initial approximating function. The same method is good to apply during solution of nonlinear problems, for instance during the analysis of supercritical equilibrium forms.

Dynamic problems with initial conditions well lends itself to programming, and therefore application of the dynamic criterion for determination of critical load on ETsVM is also fully possible.

Application of ETsVM opens new prospects for different regions of mechanics and, in particular, the theory of stability of elastic systems. Those problems, which earlier were "inaccessible" in view of calculating difficulites, now turn out to be completely feasible. If in past in many cases we had to remain within limits of first or

second approximation, ETsVM now allows us to carry out practically unlimited number of approximations. At present basic attention, consequently, must be alloted to more precise definition of initial equations, so that they can as fully as possible depict properties and conditions of load of real structures.

§ 24. Use of Analog Computers

Let us turn to analog (electronic simulators) computers. Basic element of such machines is operational amplifier, schematically shown in Fig. 1.36. With help of amplifier it is possible to multiply a certain voltage by a constant number, to summarize several voltages and, last, to integrate. As operational amplifier we may use a dc amplifier (tube, semiconductor, magnetic) with sufficiently high amplification factor in combination with input impedance Z_1 and feedback impedance Z_f. Basic relationship describing mode of operational amplifier has the form

$$e_2 = -\frac{Z_f}{Z_1} e_1, \qquad (1.248)$$

where e_1--voltage fed to e_2--output voltage (Fig. 1.36a).

If we wish to multiply a certain voltage by magnitude k, then it is necessary to take relationship between input resistance and resistance feedback equal to $R_f/R_1 = k$. Passing to amplifier several voltages, it is possible to execute operation of summation (Fig. 1.36b).

If in feedback we include capacitor of capacity C, and at input we introduce ohmic resistance R, then output voltage will be proportional to integral with respect to time of input voltage (Fig. 1.36c):

$$e_2 = -\frac{1}{RC} \int e_1 \, dt. \qquad (1.249)$$

Computer includes also multiplication units (BP) and nonlinearity units (BN), which allow us to solve nonlinear problems. Multiplication units multiplies two variables entering it; with its help it is possible to form, for instance, such members, as x^2, x^4, xy, etc. Nonlinearity unit allows us to approximate given function of one argument by a piecewise-linear one. For instance, on machine MN-7 a given function can be approximated by ten linear sections. Unit of variable coefficients is used for set of given functions of time.

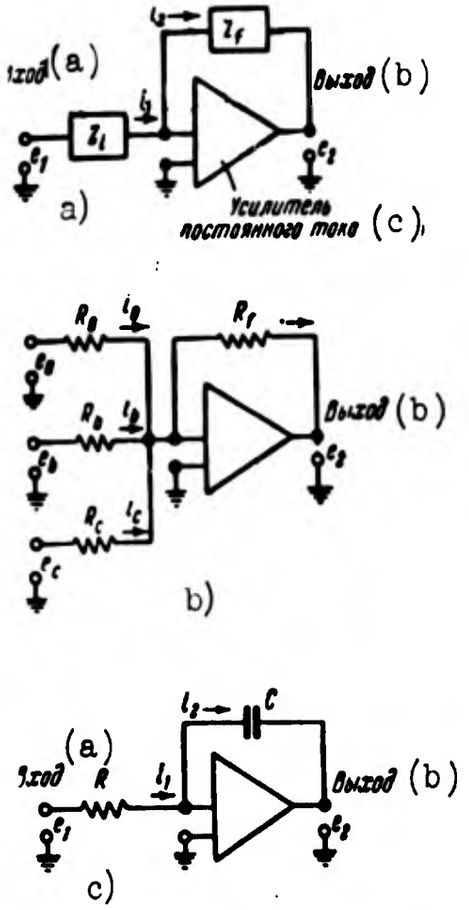

Fig. 1.36. Elements of analog computers.
KEY: (a) Input; (b) Output; (c) Dc amplifier.

Amplifiers, integrators, multiplication and nonlinearity units work on 100-volt scale; characteristic peculiarity of multiplication unit is the circumstance that it algebraically multiplies entering magnitudes and divides obtained result by 100.

For solution on computer the given system of equations usually is reduced to a system of first order equations in dimensionless magnitudes and then to machine form. For that it is necessary to know order of expected magnitudes and range of change of time (or another parameter which is an independent variable) and to conduct following linear transformation:

$$v = v_{max} v_N, \quad t = \alpha T. \tag{1.250}$$

where v_N is machine variable, v_{max} is expected maximum value of function. T is machine time in seconds, maximum value of which usually is limited to a magnitude of about 50-100 sec.

Analog computers of general type are adjusted mainly for integration of differential equations with initial conditions. Therefore for solution of problems of eigen values, for instance, determination of critical loads, it is necessary to resort to special methods. One such method is trial-and-error method, described in § 13 graphically.

As an example let us consider bar, with hinged support on ends.* Initial equation (5) we replace with two first order equations and we reduce them to dimensionless form, introducing variables $\bar{x} = x/l$, $\bar{v} = v/i$, where i is radius of gyration of section. Equations obtain form

$$\frac{d\bar{v}}{d\bar{x}} = -\bar{k}\bar{v}_1, \quad \frac{d\bar{v}_1}{d\bar{x}} = \bar{k}\bar{v}. \tag{a}$$

where $\bar{k}^2 = Pl^2/EI$. We are given parameters of compressing load $\bar{k}^2$ and take initial conditions $\bar{v} = 0$, $d\bar{v}/d\bar{x} = a$ when $\bar{x} = 0$, where magnitude a is selected arbitrarily. Integrating equation (a), we check whether condition $\bar{v} = 0$ is satisfied when $x = l$ or $\bar{x} = 1$, and repeat calculation, varying parameter $\bar{k}$. We introduce machine variables $v_N = \bar{v}/\bar{v}_{max}$ and $k_N = \bar{k}/\bar{k}_{max}$; as maximum values we take $\bar{v}_{max} = 0.2$, $k_{max} = 10$, $v_{1,max} = 0.628$. Instead of (a) we write following dependences:

$$\left.\begin{aligned} 0.2v_N &= \int (10k_N)(0.628v_{1,N})\,d\bar{x}, \\ 0.628v_{1,N} &= \int (10k_N)(0.2v_N)\,d\bar{x}. \end{aligned}\right\} \tag{b}$$

*The below-mentioned solution of problem on analog computer was carried out by E. D. Skurlatov.

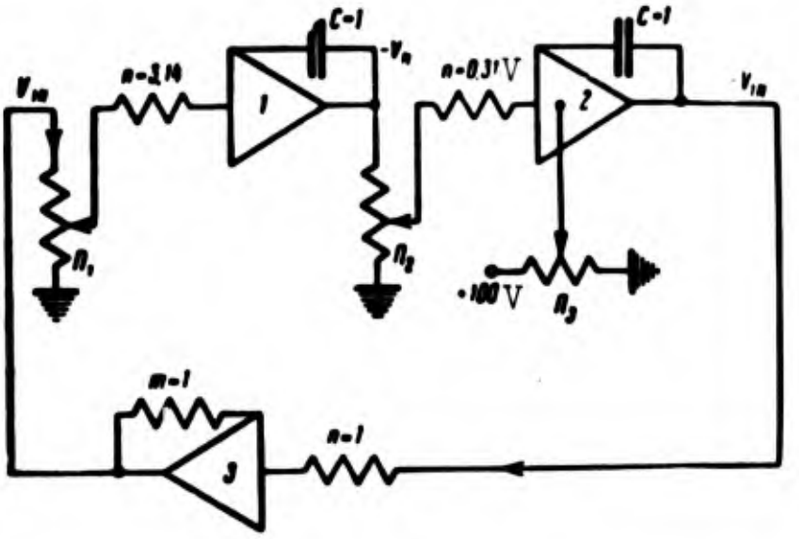

Fig. 1.37. Functional diagram for determination of critical load by trial-and-error method.

We take interval of integration (length of bar) as corresponding to 10 seconds of machine time. Functional diagram, corresponding to equations (b), is depicted in Fig. 1.37. By Π we designate spiral potentiometers; by first two (Π_1 and Π_2) we vary parameter k_N, and third (Π_3) is introduced for assignment of initial conditions. Values of conductances n in amplifiers 1 and 2 have dimension [1 Megohm], they correspond to magnitudes

$$\frac{10 \cdot 0{,}628 \cdot 0{,}1}{0{,}2} = 3{,}14,$$

$$\frac{10 \cdot 0{,}2 \cdot 0{,}1}{0{,}628} = 0{,}318,$$

amplifier 3 serves to change sign. In Fig. 1.38 are presented combined oscillograms, obtained by given circuit for different parameters $\bar{k}$; Euler's load corresponds to $\bar{k} = 3.14$. For smaller values of $\bar{k}$ we obtain solution with "undershoot": with larger--"overshoot".

This way can serve also for determination of critical loads in case of bar of <u>variable section</u>.

Another method consists of use of special unit of registration and reproduction (BRV), serving for solution of linear uniform integral equations of the Fredholm type; in given problem this equation has the form (151). Here there is applied method of successive approximations, described in Section 15. On machine are performed the following operations: formation of kernel $K(x,\xi)$, multiplication of functions $K(x, \xi)$ and $y_0(\xi)$ by (151), integration from 0 to 1 and multiplication of integral by manipulated variable λ. As a result we find function $y_1(x)$, which we anew put in the right part of equation. Unit BRV serves for memorization of intermediate solutions of integral equation proceeding from medel, and for issuing them to model for the purpose of obtaining new approximations. Unit has cathode-ray tube with afterglow; it allows us to fix form of elastic line for every approximation. Here consecutively are definitized values of critical parameter λ.

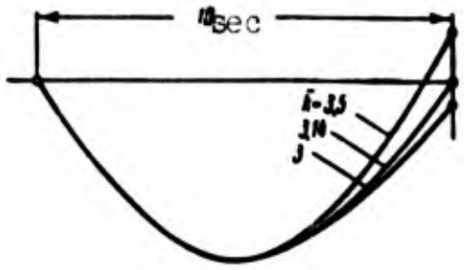

Fig. 1.38. Oscillograms, obtained in three trials.

Last, there can be composed electrical simulating circuits, not containing operational amplifiers and carrying out so-called direct simulation.* Critical loads for different structures are determined here too by means of successive approximations, as described in Section 12.

*Such circuits are described in work of Scanlan [1.14]. This direction is subject of a series of works of K. K. Keropyan, G. Ye. Pukhov and other authors.

Literature

1.1. B. G. Galerkin. Theory of buckling and experience of application of theory of buckling to multistage bars, columns with rigid connections and systems of columns. News of St. Petersburg Polytechnic Institute, 12, No. 1 (1909), 167-241, No. 2 (1909), 383-451; Collected works Vol. 1, Publishing House of Acad. of Sci. of the USSR, M., 1952, 24-124.

1.2. K. S. Deyneko and M. Ya. Leonov. Dynamic method of research of stability of a compressed bar, Applied mathematics and mechanics, 19 (1955), 738-744.

1.3. G. Yu. Dzhanelidze. On stability of a bar under action of a following force, Transactions of Leningrad Polytechic Institute, No. 192 (1958).

1.4. Yu. D. Kopeykin and M. Ya. Leonov. On one special case of loss of stability of equilibrium of a compressed bar, Applied math. and mech., 19 (1955), 736-737.

1.5. A. N. Krylov. On forms of equilibrium of vertically loaded members, News of Acad. of Sci. of USSR (1931), 963.

1.6. Ye. P. Popov. Nonlinear problems of statics of thin bars, Gostekhizdat, M., 1948.

1.7. F. S. Yasinskiy. On buckling strength, 1894; Selected works on stability of compressed bars, Gostekhizdat, 1952.

1.8. M. Beck. Die Knicklast des einseitig eingespannten, tangential gedrückten Stabes, Zeitschr. angew. Math. und Phys. 3, No. 3 (1952), 225-228.

1.9. L. Euler. Methodus inveniendi lineas curvas..., Lausanne et Geneve, 1744; Additamentum 1: De curvis elasticis. p. 267 (L. Euler, Method of finding curves possessing properties of a maximum or a minimum, M., Gostekhizdat, 1934, Appendix 1: On elastic curves).

1.10. L. Euler. Sur la force des colonnes, Mem. de l'Acad. Berlin. 13, (1757), 251-282.

1.11. F. Engesser. Ueber die Berechnung auf Knickfestigkeit beanspruchten Stäbe aus SchweiB- und GuBeisen, Z. österr. Ing. Arch. Ver., No. 45 (1893), 506-508.

1.12. L. Lagrange. Sur la figure des collonnes, Oeuvres, 2, Paris (1868), 125-170, Sur la force des ressorts plies, Oeuvres 3 (1869), 77-110.

1.13. J. Ratzersdorfer. Die Knickfestigkeit von Stäben und Stabwerken, Wien, 1936.

1.14. R. H. Scanlan. Resistance network solution of some structural problems in deflection and stability, Proc. Soc. Exp. Stress Anal. 16, No. 1 (1958), 117-128.

1.15. H. S. Tsien. Lower buckling load in the nonlinear buckling theory for thin shells, Quart. Appl. Math. 5, No. 2 (1947), 236-237.

1.16. L. Vianello. Graphische Untersuchung der Knickfestigkeit gerader Stäbe, Z. Ver. deutsch. Ing. 42 (1898), 1436-1443.

C H A P T E R II

STABILITY OF COMPRESSED BARS BEYOND THE ELASTIC LIMITS

§ 25. Experimental Dependences

Initial relationships and calculating formulas given in Chapter I are valid under the condition that critical stresses--or maximum stresses during buckling and lateral bending do not exceed limit of proportionality of the material $\sigma_{пц}$*. Meanwhile for elements of real structures in many cases this condition is not satisfied. Therefore, research of stability of bars, pertaining to nonelastic region, is of essential practical value.

Until recently most wide-spread were methods of calculation based on results of experimental research.

Data of experiments are conveniently compared with help of graph depicting dependence of critical stress $\sigma_{кр}$ on slenderness ratio λ. If experiments are done sufficiently carefully, then in elastic zone experimental points lie very tight to Euler's hyperbola, while in elasto-plastic zone they usually are greatly scattered, approximately as shown in Fig. 2.1. This is explained by the fact that in elastic

---

*Henceforth limit of proportionality of material is considered to coincide with elastic limit.

region critical stress at given slenderness ratio depends only on modulus E; variations of this magnitude for different samples, prepared from one and the same material, are insignificant. In elastoplastic region critical stresses change depending upon diagrams $\sigma(\varepsilon)$ during compression, frequently differing from each other even for samples, belonging to the same batch. Influence of perturbing factors--eccentricity of load, initial bending, residual stresses from rolling, welding, correction, etc.--in nonelastic region also turns out to be more significant than in elastic. Therefore, analysis of given experiments and composition of calculating formulas it is desirable to conduct with help of statistical methods.*

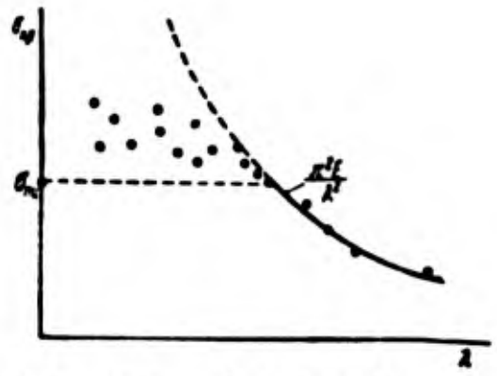

Fig. 2.1. Scattering of experimental values of critical stresses in plastic region.

Different authors offered formulas for calculation of non-elastic bending, of which the most acceptable turned out to be the following:

a) Linear formula**

$$\sigma_{кр} = a - b\lambda, \tag{2.1}$$

where a and b are parameters, depending on the material.

In determining magnitudes a and b it is desirable that there is satisfied the condition that at limiting slenderness ratio λ_* equation

---

*This was for first marked by F. S. Jasinski, applying for treatment of experimental data of Tetmaier the method of least squares [1.7].

** Formulas of this type were offered by Tetmaier [2.21] and F. S. Jasinski [1.7].

(1) gave the same result as Euler's formula. On the other hand, it would have been possible to require that when $\lambda \to 0$ magnitude $\sigma_{кр}$ approximated limiting compressive stress σ_b, so that $a = \sigma_b$. For brittle materials (for instance, duralumin) this limiting stress corresponds to temporary resistance, found during compression of samples of small length. In case of material, having diagram with clearly expressed yield surface (soft steel), critical compressive stress, as a rule, cannot exceed yield point $\sigma_т$. Therefore, for plastic materials it would be more natural to take $a = \sigma_т$. However, a basic requirement during composition of empirical formulas is their conformity to concrete data of a series of experiments on buckling for bars of different slenderness ratio.

b) Hyperbolic formula*

$$\sigma_{кр} = \frac{\sigma_0}{1 + \alpha\lambda^2}; \tag{2.2}$$

here σ_0 is a certain stress, α--empirical coefficient.

c) Parabolic formula**

$$\sigma_{кр} = a - \beta\lambda^2. \tag{2.3}$$

Constants α and β it is possible to select in such a way that parabola on graph of $\sigma_{кр}(\lambda)$ smoothly passes into Euler's hyperbola, having with it when $\lambda = \lambda_*$ a common tangent. However, the deciding thing here is conformity of formula to experimental data.

Example 2.1. During calculation of hull of ship one should

---

*A similar formula was offered by Rankine.

**This formula was offered by J. B. Johnson.

check stability of deck: in definite positions of ship with respect to ridges of waves the deck is compressed (Fig. 2.2a). To determine critical compressive stress for panel, composed of reinforcing ribs (beams) of ship located the length and strips of sheeting fixed to them, considering ends of panel supported by hinges. Loss of stability is possible only in direction, perpendicular to plane of sheeting.

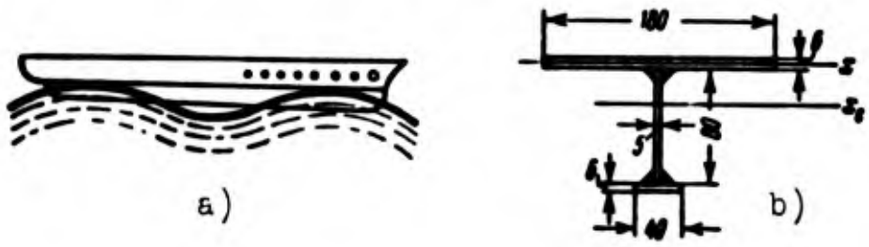

Fig. 2.2. Panel of ship deck.

Material is steel St.4. $E = 2.1 \cdot 10^6$ kg/cm^2, $\sigma_т = 2600$ kg/cm^2, $\sigma_{пц} = 2200$ kg/cm^2. When $\sigma_{кр} > \sigma_{пц}$ apply formula

$$\sigma_{кр} = 3200 - 10\lambda \ (\text{kg/cm}^2) \qquad (a)$$

on condition that $\sigma_{кр} \leq \sigma_т$. Dimensions of section of panel are shown in Fig. 2.2b (in mm), length of panel (space) is equal to 1 meter.

We determine coordinate of center of gravity of section $y_c = 1.9$ cm; area of section $F = 17.2$ cm^2. Moment of inertia of section relative to central axis x_c is $I = 190$ cm^4. We calculate radius of gyration of section and slenderness ratio:

$$i = \sqrt{\frac{190}{17,2}} = 3,32, \quad \lambda = \frac{100}{3,32} = 30.$$

Stress, calculated by formula (a), is equal to 2900 kg/cm^2 > $\sigma_т$. Therefore, we take critical stress to be equal to $\sigma_{кр} = \sigma_т$ = 2600 kg/cm^2.

§ 26. Buckling of Bar Under Constant Load

We turn to theoretical study of buckling beyond limits of elasticity. Let us assume that bar is subjected to central end compression and that dependence of stress on strain for short samples of a given material corresponds to diagram of Fig. 2.3. Section of elastic strain corresponds to segment Oa. Let us assume that during loading of sample we arrived from diagram at certain point m. If after this we unload, then on graph we will obtain a straight line mm′, approximately parallel to segment Oa; angle of inclination of this line characterizes modulus of unloading.

We will henceforth consider that modulus of unloading is equal to initial modulus E. On the other hand, with increase from point m of compressive strain we will obtain segment of diagram mm″. If additional strain is small, then it is possible to consider that ratio of increments $\Delta\sigma$ and $\Delta\varepsilon$ is determined by the so-called tangent modulus:

$$\frac{\Delta\sigma}{\Delta\varepsilon} \approx \frac{d\sigma}{d\varepsilon} = E_к. \qquad (2.4)$$

Let us consider bar subjected to central compression. Let us assume that compressive stress attained magnitude $\sigma > \sigma_{кр}$. Let us assume that with this stress occurs buckling, during which load remains constant. Then fibers, lying on concave side, will experience additional contracting strain, and those on convex--stretching (Fig. 2.4). If one were to consider bending forms, very close to rectilinear, then it is possible to take for zone of growing

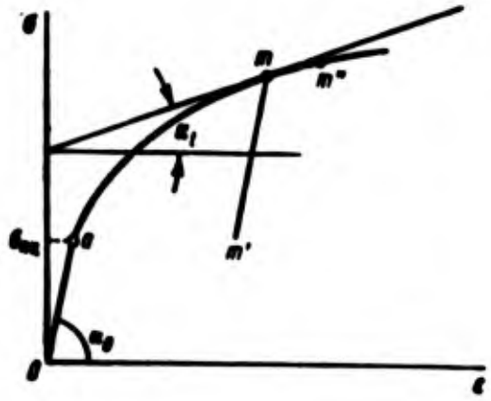

Fig. 2.3. Stress-strain diagram.

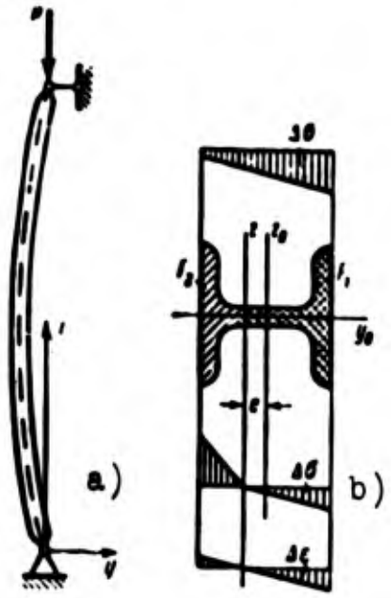

Fig. 2.4. (a) Bending line, (b) Section of bar, diagram of stresses and deformations during nonelastic buckling.

compression modulus E_K, and for zone of unloading modulus E. Neutral line z, for points of which additional stresses are equal to zero, will not pass through center of gravity of section. Such concept of "two moduli" was first offered* by F. S. Jasinski [2.14] and F. Engesser, and was subsequently developed by T. Kármán [2.15].

Let us assume that main central axes of inertia of section to be y_0 and z_0 (Fig. 2.4); we assume that buckling occurs in direction y_0. Considering that cross sections remain flat during bending of bar, and counting y from neutral line z, we obtain

$$\Delta\varepsilon = \frac{y}{\rho},$$

where ρ--is radius of curvature of elastic line. Stresses in zones

*Discussion between F. S. Jasinski and F. Engesser appearing in connection with this is illuminated in article of A. N. Mitinskiy (see book [1.7], edition 1952).

of loading and unloading will be, correspondingly,

$$\Delta\sigma_1 = E_u \frac{y}{\rho}, \quad \Delta\sigma_2 = E \frac{y}{\rho}. \tag{2.5}$$

Resultant additional forces should equal zero; therefore

$$\frac{E_u}{\rho} \int_{F_1} y\,dF + \frac{E}{\rho} \int_{F_2} y\,dF = 0$$

or

$$E_u S_1 + E S_2 = 0. \tag{2.6}$$

Here by F_1 and S_1 are designated area and static moment relative to neutral axis of that part of section in which there is loading up, and by F_2 and S_2--the part of section in which there occurs unloading. Equating sum of moments of internal forces relative to neutral line to external moment, we find

$$\frac{E_u}{\rho} \int_{F_1} y^2\,dF + \frac{E}{\rho} \int_{F_2} y^2\,dF = M,$$

or

$$\frac{1}{\rho}(E_u I_1 + E I_2) = M. \tag{2.7}$$

We designate by T the resultant or reduced modulus, equal to

$$T = \frac{E_u I_1 + E I_2}{I}, \tag{2.8}$$

where I is moment of inertia of whole section with respect to the axis passing through center of gravity. Magnitude T we call also Kármán's modulus. Equation of bending line obtains form, analogous to (1.5):

$$TI \frac{d^2v}{dx^2} = -M. \tag{2.9}$$

Assuming for case of hinged support of ends of bar M = Pv, we arrive at equation

$$TI\frac{d^2v}{dx^2}+Pv=0. \tag{2.10}$$

Magnitude T when I = const may be considered not to depend on x, so that all data, obtained in Chapter I for elastic buckling can be extended to the elasto-plastic region on the condition of replacement of E by T. To this pertain results, obtained with help of energy methods, since for any fiber of bar as before there is assumed linear dependence between increments of stresses and strains.

In generalized form expressions for critical force and critical stress will be

$$P_{кр}=\frac{\pi^2 TI}{(\nu l)^2}. \tag{2.11}$$

$$\sigma_{кр}=\frac{\pi^2 T}{\lambda^2}. \tag{2.12}$$

Coefficient ν here one should assume the same as in elastic region.

§ 27. Influence of Form of Section. Cases of I-Beam and Rectangular Sections

Judging by formulas (6) and (8), resultant modulus T should depend on form of section of bar. We calculate magnitude T for an I-beam section with thin web (Fig. 2.5) on the assumption that bending moment is perceived only by flanges of I-beam and, because of certain conditions of fastening of bar, buckling occurs in direction of axis y. We designate by h distance between centers of gravity of flanges; area of each flange is equal to half of area of section, i.e., F/2. Let us assume that distance h is divided by a neutral line when there is bend into segments h_1 (on the side loaded up and h_2 on the side of

unloading). From (6) we obtain

$$-F_1 h_1 E_к + F_2 h_2 E = 0;$$

hence

$$h_1 = h\frac{E}{E_к + E}, \quad h_2 = h\frac{E_к}{E_к + E}. \tag{2.13}$$

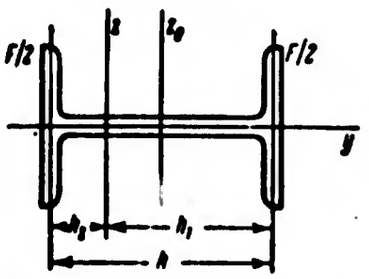

Fig. 2.5. Zones of loading and unloading in case of an I-beam section.

Moments of inertia I_1 and I_2 are equal to

$$I_1 = \frac{F}{2}h_1^2, \qquad I_2 = \frac{F}{2}h_2^2. \tag{2.14}$$

Moment of inertia of whole section relative to central axis will be

$$I = \frac{1}{4}Fh^2. \tag{2.15}$$

Formula (8) obtains form

$$T = \frac{2E_к E}{E_к + E}. \tag{2.16}$$

For elastic region $T = E_K = E$. In general the resultant modulus has a certain mean value between E and E_K. For material with a clearly expressed yield surface, within which angle $\alpha_K = 0$, magnitudes E_K and T near zero, as soon as compressive stress nears the yield point. This means that for compressed bar critical compressive stress practically cannot exceed the yield point.

In case of a rectangular section (Fig. 2.6) equation (6) takes on form

$$E_к h_1^2 - E h_2^2 = 0$$

and, consequently,

$$h_1 = h\frac{\sqrt{E}}{\sqrt{E_к}+\sqrt{E}}, \quad h_2 = h\frac{\sqrt{E_к}}{\sqrt{E_к}+\sqrt{E}}. \tag{2.17}$$

Moments of inertia will be

$$I_1 = \frac{bh_1^3}{3}, \quad I_2 = \frac{bh_2^3}{3}, \quad I = \frac{bh^3}{12}. \tag{2.18}$$

Finally

$$T = \frac{4EE_к}{(\sqrt{E_к}+\sqrt{E})^2}. \tag{2.19}$$

Deflection in magnitude T for various forms of sections are insignificant, so that in practical calculations for other forms of section it is possible to use formula (16) or (19).

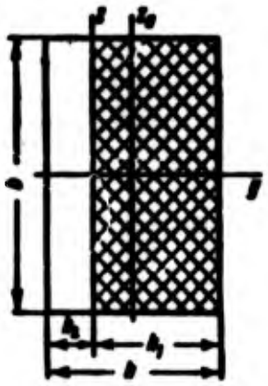

Fig. 2.6. Zones of loading and unloading in case of rectangular section.

§ 28. Construction of "Critical Stress--Slenderness Ratio Diagram".

We present formula (12) in the form

$$\lambda = \pi\sqrt{\frac{T}{\sigma_{кр}}}. \tag{2.20}$$

We are given consecutive values of $\sigma_{кр}$; knowing corresponding magnitudes of T, we find by (20) connection between $\sigma_{кр}$ and λ. But to establish dependence $T(\sigma)$ we should know diagram of $\sigma(\varepsilon)$, obtained during compression test of short samples of given material.* In Fig. 2.7 is depicted such a diagram for duralumin D16T. Elastic modulus is taken equal to $E = 7.5\cdot10^5$ kg/cm^2, limit of proportionality $\sigma_{пц} = 2\cdot10^3$ kg/cm^2. For determining $E_к$ of different points of diagram (a, b, c, etc.) we pass tangents and find

*These data for duralumin and steel St.3 were obtained by author in 1948.

the tangents of angles of their slope to axis of abscissas. Magnitudes E_K, corresponding to certain values of σ and ε, are given in Table 2.1. Here are given magnitudes of resultant modulus T and slenderness ratio $\lambda_{рез}$ calculated by formulas (16) and (20) (index "рез" indicates that value of λ corresponds to the resultant (reduced) modulus).

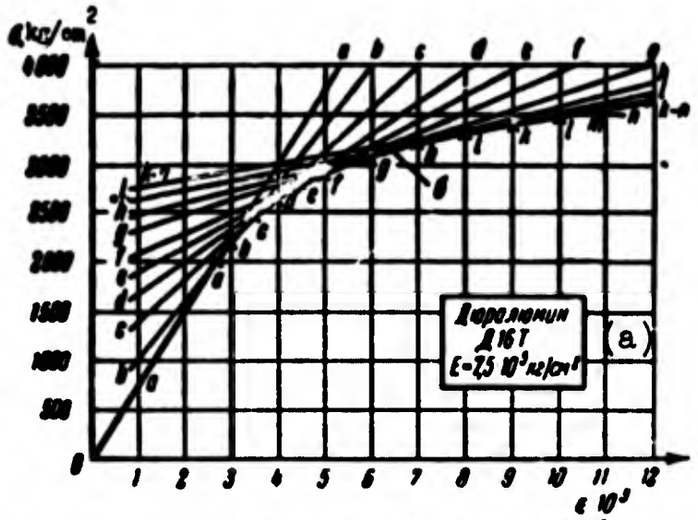

Fig. 2.7. Diagram of compression for duralumin D16T.
KEY: (a) Duralumin, D16T. E = $= 7.5 \cdot 10^5$ kg/cm^2.

Dependence $\sigma_{кр}(\lambda)$ thus obtained is presented in Fig. 2.8. For elastic

Table 2.1. Calculating Parameters for Duralumin D16T

Points on Diagram	$\varepsilon \cdot 10^3$	σ, kg/cm^2	$E_K \cdot 10^{-5}$, kg/cm^2	$T \cdot 10^{-5}$, kg/cm^2	$\lambda_{рез}$	λ_K
a	2,67	2000	7,50	7,50	60,5	60,5
b	3,0	2200	5,96	6,65	54,7	51,6
c	3,5	2460	4,34	5,50	47,0	42
d	4,0	2640	3,72	4,97	43,0	37,5
e	4,5	2780	2,55	3,81	36,8	30,2
f	5	2900	2,05	3,22	33,0	26,5
g	6	3080	1,50	2,50	28,3	22
h	7	3200	1,17	2,03	25,0	18,9
i	8	3320	0,97	1,72	22,6	17
k	9	3400	0,82	1,48	20,8	15,4
l	10	3450	0,82	1,48	20,6	15,3
m	11	3560	0,82	1,48	20,2	15,1
n	12	3640	0,82	1,48	20,0	14,9

region, where $\lambda \geq 60.5$, curve corresponds to Euler's formula.

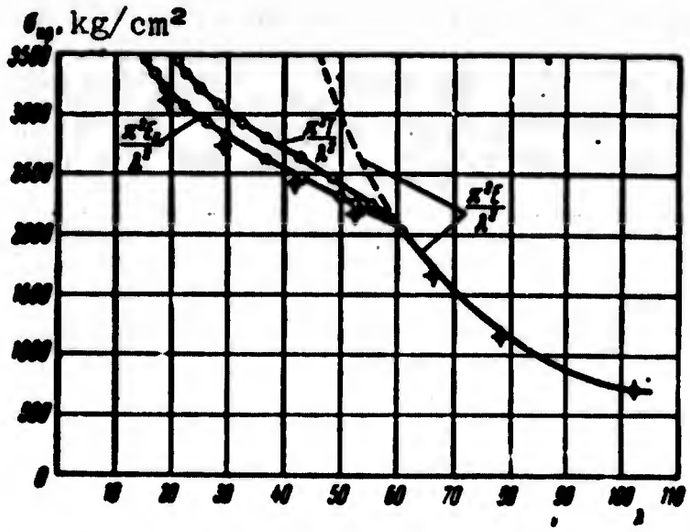

Fig. 2.8. "Critical stress--slenderness ratio" for duralumin, circles with small crosses are data of experiments.

In Table 2.2 are contained the same data for steel St. 3, corresponding to diagram $\sigma_{кр}(\lambda)$ given in Fig. 2.9.

Table 2.2 Calculating Parameters for Steel St. 3.

$\sigma \cdot 10^{0}$	σ, kg/cm²	$E_к \cdot 10^{-6}$, kg/cm²	$T \cdot 10^{-6}$, kg/cm²	$\lambda_{пц}$	$\lambda_к$
0,95	2000	2,10	2,10	102	102
1,0	2100	1,62	1,72	90	81,8
1,1	2200	0,99	1,39	79	66,6
1,2	2280	0,67	1,05	67,6	54
1,3	2340	0,46	0,85	59	44
1,4	2380	0,26	0,54	47,5	32,7
1,5	2390	0,13	0,33	37	23,1
1,6	2400	0,06	0,19	28	15,7
1,8—4,0	2400	0	0	0	0
4,5	2410	0,02	0,07	17	9,1
5	2420	0,04	0,13	23	12,7
6	2470	0,05	0,15	24,5	14,2
8	2575	0,05	0,15	24	13,8
10	2685	0,05	0,15	23,6	13,6
12	2800	0,05	0,15	23	13,5

Calculating data obtained thus it is possible to compare with results of experiments on buckling for bar of different slenderness ratio. In separate cases with very careful execution of experiments one manages to obtain points on graph of $\sigma_{кр}(\lambda)$, lying fairly close to curve $\lambda_{пез}$. However, as a rule, experimental points are located below this curve (data in Fig. 2.8). It was noticed that best result is obtain-

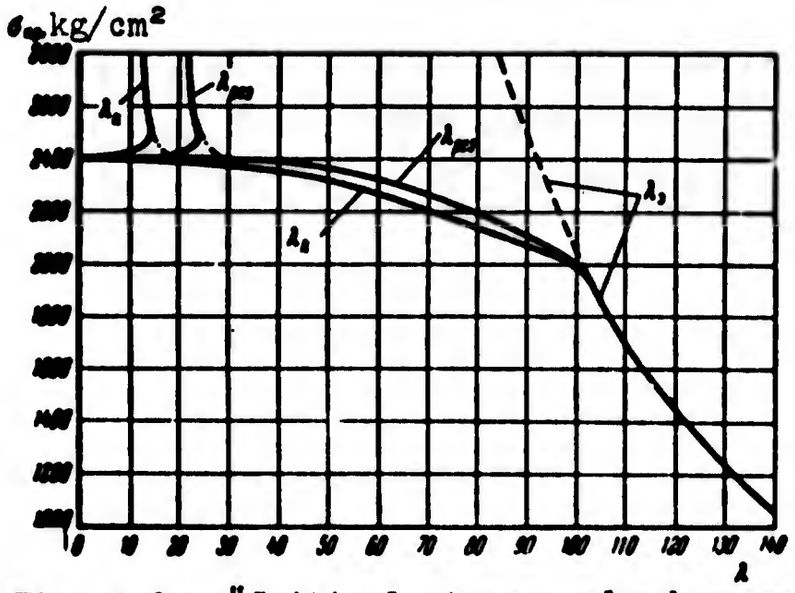

Fig. 2.9. "Critical stress--slenderness ratio" diagram for steel St. 3.

ed if in formula (12) we replace resultant modulus by tangent and take

$$\sigma_{кр} = \frac{\pi^2 E_t}{\lambda^2}. \qquad (2.21)$$

Values of slenderness ratio obtained by the formula

$$\lambda = \pi \sqrt{\frac{E_t}{\sigma_{кр}}}, \qquad (2.22)$$

we mark by index "к", they are placed in last columns of Tables 2.1 and 2.2. Corresponding curves are drawn in Fig. 2.7.

Formula (21) corresponds to initial concepts about non-elastic buckling of bars, presented in one of the articles of F. Engesser [2.11]. By this concept the effect of unloading is not considered;

it is assumed that in whole section relationship between increases of stresses and strains contains tangent modulus E_K. But if this assumption pertains to real material, then it is necessary to consider that compressive stress gets increment at all points of section, for instance, as shown in Fig. 2.4 above. In other words, it is necessary to assume that simultaneously with bend of bar there takes place increase of compressing load.* Let us consider this problem in a quasi-static formulation and investigate bent equilibrium forms of bar.

§ 29. Buckling of Bar Under Variable Load

We consider that section of bar fixed by hinge on the ends has at least one axis of symmetry y (Fig. 2.10a) and that elastic line of bar lies in plane xy.

Assume that buckling of bar began at force P_* and that during bend of bar load has an <u>increase</u>. Then in certain sections there can take place only loading up, and other sections are divided into zones loading up and unloading. We assume here as first approximation that appearance of unloading coincides with beginning of buckling.**

We designate by c distance from center of gravity of section C to extreme fibers, lying on convex side. Zones of loading up and unloading are divided by line mn, neutral at bend removed from extreme fibers by distance s; this magnitude changes. In general, with length,

---

*Such hypothesis was advanced by F. Shanley [2.19] and then Yu. N. Rabotnov [2.8] and developed by a number of other authors.

**Such formulation of problem belongs to A. Pflüger [2.17]; to him belong graphs 2.16--2.20. Solution of problem in another formulation is given by Yu. R. Lepik [8.5] and I. S. Malyutyn (and. diss., Moscow, 1958).

$s = s(x)$. Area of section F is divided by line mn into area F_1 and F_2. We assume that during buckling of bar deformation in every part of section is characterized by constant moduli--E_K during loading up and E during unloading; these moduli are determined by diagram $\sigma(\epsilon)$ and correspond to initial stress $\sigma = \sigma_* = P_*/F$ (Fig. 2.10b). In those sections where zone of unloading is absent deformation completely is determined by modulus E_K.

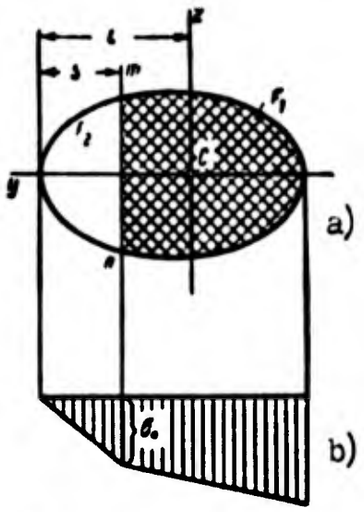

Fig. 2.10 a) Section of bar, subjected to buckling, b) diagram of stresses.

We turn to sections with mixed law of deformation and introduce designation $E/E_K = n$. We imagine a certain transformed section, in which width of all elementary lines located in zone of unloading, is increased n times (Fig. 2.11). Area of such reduced section F_e is equal to

$$F_e = F_1 + nF_2. \tag{2.23}$$

We determine distance e between centers of gravity of initial and reduced sections:

$$e = \frac{S_1 + nS_2}{F_e}; \tag{2.24}$$

by S_1 and S_2 we designate static moments of areas F_1 and F_2 relative to central axis of initial section. We designate, further, by I_e the moment of inertia of reduced section with respect to axis passing through center of gravity C_1 of this "new" section:

$$I_e = I_{1e} + nI_{2e} = \int_{F_1} y_e^2 dF + n \int_{F_2} y_e^2 dF; \qquad (2.25)$$

coordinate y_e is counted off from new central axis.

Fig. 2.11. Reduced section of bar.

We assume that load P_* obtained increment ΔP and attained magnitude P:

$$P = P_* + \Delta P. \qquad (2.26)$$

For transformed section deformation can be determined, proceeding from single modulus E_K. Additional deformation of arbitrary fiber is equal to

$$\Delta\varepsilon = \Delta\varepsilon_e - \frac{y_e}{\rho}. \qquad (2.27)$$

where $\Delta\varepsilon_e$ is deformation of fiber passing through center of gravity of reduced section, ρ is radius of curvature of bending line. Increment of stress is

$$\Delta\sigma = E_K \Delta\varepsilon_e - \frac{E_K}{\rho} y_e \qquad (2.28)$$

Additional effort in section will be applied at center of gravity of reduced section and is equal to

$$\Delta P = \int_{F_e} \Delta\sigma \, dF_e = E_K F_e \Delta\varepsilon_e; \qquad (2.29)$$

here deformation of shortening is considered positive. Let us consider, further, condition of equilibrium of part of bar shown in Fig. 2.12. In end section point of application of total force P coincides with center of gravity of initial section; in arbitrary section resultant of basic efforts is applied in that same center of gravity of

initial section, whereas resultant additional efforts turns out to be applied in new center of gravity of reduced section.

Sum of moments of forces P and P_* relative to new central axis

$$M_e = P(v+e) - P_* e. \tag{2.30}$$

or

$$M_e = Pv + \Delta P e. \tag{2.31}$$

Equating this moment to sum of moments of additional internal forces, we obtain by (28)

$$M_e = -\int_{F_e} \Delta\sigma y_e dF_e = \frac{E_x}{\rho} I_e. \tag{2.32}$$

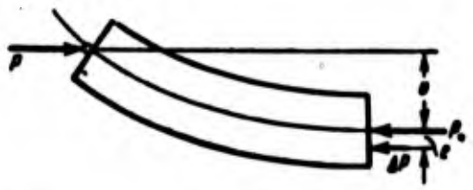

Fig. 2.12. External force and internal forces during buckling of bar.

Assuming for shallow bending line

$$\frac{1}{\rho} = -\frac{d^2v}{dx^2},$$

we arrive at equation

$$E_x I_e \frac{d^2v}{dx^2} + Pv + \Delta P e = 0. \tag{2.33}$$

In this equation magnitudes e, and I_e are functions of x. For that part of length of bar where region of unloading is absent, neutral line will pass through center of gravity of real section and, consequently, e = o, I_e = I, where I is moment of inertia of initial section relative to central axis. Equation (33) takes on these sections the form

$$E_x I \frac{d^2v_0}{dx^2} + Pv_0 = 0. \tag{2.34}$$

Boundary conditions for ends of bar have form

$$v_0 = 0, \quad \frac{d^2v_0}{dx^2} = 0 \text{ when } x = 0, l. \tag{2.35}$$

Furthermore, there must be satisfied conditions of linkage on boundary

regions, including unloading. Designating length of this region by a (Fig. 2.13), we obtain

$$v = v_0, \quad \frac{dv}{dx} = \frac{dv_0}{dx} \text{ when } x = \frac{l-a}{2}, \quad \frac{l+a}{2}. \tag{35}$$

From (34) and (35) for end sections of bar we obtain,

$$v_0 = A \sin \sqrt{\frac{P}{E_k J}}\, x. \tag{2.37}$$

For points of neutral line we have

$$0 = \Delta\varepsilon_0 - \frac{c-e-s}{\rho}; \tag{2.38}$$

hence

$$\Delta\varepsilon_0 = -(c-e-s)\frac{d^2v_0}{dx^2}. \tag{2.39}$$

Comparing this equation with (29), we find

$$\Delta P = -E_k F_0 (c-e-s)\frac{d^2v}{dx^2}. \tag{2.40}$$

Removing d^2v/dx^2 from (33) and (40), we will have

$$\frac{P}{\Delta P} v = \frac{I_0}{F_0} \frac{1}{c-e-s} - e. \tag{2.41}$$

Since on ends of bar bending moment turns into zero, from (31) it follows that

$$\Delta P e = 0 \text{ when } x = 0, \quad x = l. \tag{2.42}$$

Let us consider two limiting cases. Let us assume that region of unloading occupies the whole length of the bar, as this was assumed in Section 26. Then in end sections we should have $e \neq 0$. From this follows condition $\Delta P = 0$. Proceeding this way, we obtain formula for critical force (11), including resultant modulus T.

We assume now that region of unloading occupies only a certain part of length of bar and that end sections are deformed purely plastically. Then for $x = 0$, $x = l$ we should find $e = 0$ and, consequently, $\Delta P \neq 0$. This way leads to solution with increasing load. Let us

assume that at moment of beginning of buckling the whole rod is in pruely plastic state, so that for all sections modulus is equal to $E_к$.

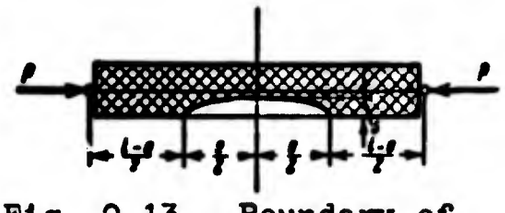

Fig. 2.13. Boundary of zone of unloading.

Zone of unloading is contracted here to extreme point of average section, so that $a \to 0$. Understanding hereafter by v deflection of average section, we obtain by (41)

$$\frac{P}{\Delta P}\Delta v = \frac{l}{Fc}. \qquad (2.43)$$

Thus, point of branching of equilibrium states, found on condition $\Delta P \neq 0$, corresponds to critical force

$$P_{эл} = \frac{\pi^2 E_э I}{l^2}. \qquad (2.44)$$

lying always below force determined from (11). From this follows formula (21), composed earlier "intuitively".

We will call the critical force $P_{кр}$, found by modulus $E_к$ <u>tangent-modular</u> in distinction from <u>reduced-modular</u> $P_{прв}$; determined with help of modulus T. The principal distinction between these ideas can be seen from Fig. 2.14. On axis of abscissas we place dimensionless parameter of deflection $\bar{v} = v/c$, on axis of ordinates we put the parameter of load $\bar{P} = P/P_{кр}$. To reduced-modular critical force there corresponds <u>indifferent</u> equilibrium, so that deflection remains indefinite; on graph we obtain a horizontal line. The branch of equilibrium states, proceeding from tangent-modular critical point, has at this point a slanting tangent. Slope of this tangent one can determine, using equation (41). Considering $s = e = 0$, $I_e = I$, $F_e = F$, we obtain

$$\left(\frac{\Delta P}{\Delta v}\right)_{\Delta v \to 0} = P_{эл}\frac{Fc}{I}. \qquad (2.45)$$

or

$$\operatorname{tg}\alpha_1=\frac{dP}{dv}=\frac{Pc^2}{I}. \tag{2.46}$$

If point of branching lies between $P_{кр}$ and $P_{рез}$, then slope of tangent will be smaller; by measure of approximation of initial force to reduced-modular load the angle of inclination approaches zero.

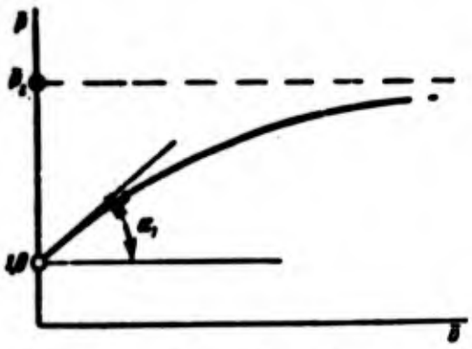

Fig. 2.14. Tangent-modular and reduced-modular load.

§ 30. Bars of I-Beam and Rectangular Sections with Variable Load.

We consider case of I-beam section with very thin web. Given section is shown in Fig. 2.15. Eccentricity of center of gravity of this section is equal, by (24), to

$$e=\frac{\frac{P}{2}\left(-\frac{h}{2}+n\frac{h}{2}\right)}{\frac{P}{2}(1+n)}=\frac{h}{2}\frac{n-1}{n+1}. \tag{2.47}$$

Area and moment of inertia of reduced section will be, by (23) and (25), equal to

$$F_e=\frac{P}{2}(1+n), \tag{2.48}$$

$$I_e=\frac{P}{2}\frac{h^2}{4}\left[\left(1+\frac{n-1}{n+1}\right)^2+ +n\left(1-\frac{n-1}{n+1}\right)^2\right]=\frac{P}{2}h^2\frac{n}{n+1}. \tag{2.49}$$

Equation (33) takes form

$$E_0 I\frac{2n}{n+1}\frac{d^2v}{dx^2}+Pv+\Delta P\frac{h}{2}\frac{n-1}{n+1}=0. \tag{2.50}$$

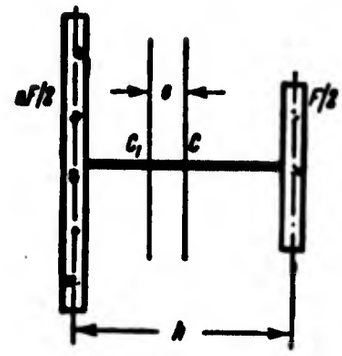

Fig. 2.15. Reduced I-section.

Instead of (40) we obtain

$$\Delta P = -\frac{E_{\text{ц}} F}{2} h\left[1 - \frac{(n+1)s}{h}\right]\frac{d^2v}{dx^2}. \tag{2.51}$$

When $\Delta P = 0$ and $d^2v/dx^2 \neq 0$ from (51) we obtain

$$\frac{s}{h} = \frac{1}{n+1},$$

which corresponds to (13). Equation (50) takes form

$$E_{\text{ц}} I \frac{2n}{n+1}\frac{d^2v}{dx^2} + Pv = 0, \tag{2.52}$$

whence we find is reduced-modular critical force:

$$P_{\text{прв}} = \frac{\pi^2 E_{\text{ц}} I}{l^2}\frac{2n}{n+1}; \tag{2.53}$$

this agrees with formula (16) for T. Tangent-modular critical force is equal to

$$P_{\text{кр}} = \frac{\pi^2 E_{\text{ц}} I}{l^2}. \tag{2.54}$$

Consequently,

$$\frac{P_{\text{прв}}}{P_{\text{кр}}} = \frac{2n}{n+1}. \tag{2.55}$$

We introduce designations

$$k_1^2 = \frac{P}{E_{\text{ц}} I}\frac{n+1}{2n}, \quad k_2^2 = \frac{P}{E_{\text{ц}} I}. \tag{2.56}$$

Equation (50) takes form

$$\frac{d^2v}{dx^2} + k_1^2 v = -\frac{\Delta P}{P}\frac{Ph}{2E_{\text{ц}} I}\frac{n-1}{2n}. \tag{2.57}$$

Integral of it will be

$$v = A_1 \sin k_1 x + B_1 \cos k_1 x - \frac{\Delta P}{P} \frac{h}{2} \frac{n-1}{n+1}. \tag{2.58}$$

We write condition of symmetry of elastic line:

$$\frac{dv}{dx} = 0 \quad \text{при} \quad x = \frac{l}{2}. \tag{2.59}$$

Using this condition, from (58) we obtain

$$A_1 = B_1 \operatorname{tg} k_1 \frac{l}{2}; \tag{2.60}$$

expression for v takes form

$$v = B_1 \frac{\cos k_1 \left(\frac{l}{2} - x\right)}{\cos k_1 \frac{l}{2}} - \frac{\Delta P}{P} \frac{h}{2} \frac{n-1}{n+1}. \tag{2.61}$$

Equation (37), pertaining to end sections, will be

$$v_0 = A_0 \sin k_2 x. \tag{2.62}$$

Conditions of linkage (36) lead to relationships,

$$\left.\begin{aligned} A_0 \sin \frac{k_2 (l-a)}{2} &= \frac{B_1 \cos \frac{k_1 a}{2}}{\cos \frac{k_1 l}{2}} - \frac{\Delta P}{P} \frac{h}{2} \frac{n-1}{n+1}, \\ A_0 k_2 \cos k_2 \frac{l-a}{2} &= B_1 k_1 \frac{\sin \frac{k_1 a}{2}}{\cos \frac{k_1 l}{2}}; \end{aligned}\right\} \tag{2.63}$$

hence

$$B_1 = -\frac{\Delta P}{P} \frac{h}{2} \frac{n-1}{n+1} \frac{\cos \frac{k_1 l}{2}}{\cos \frac{k_1 a}{2}} \frac{1}{\frac{k_1}{k_2} \operatorname{tg} \frac{k_1 a}{2} \operatorname{tg} k_2 \frac{l-a}{2} - 1}. \tag{2.64}$$

Turn to equation (51). Putting instead of v expression (61), we find

$$\Delta P = B_1 k_1^2 \frac{E_1 F}{2} h \left[1 - \frac{(n+1)s}{h}\right] \frac{\cos k_1 \left(\frac{l}{2} - x\right)}{\cos \frac{k_1 l}{2}}. \tag{2.65}$$

On boundary of zone of unloading we should have

$$s = 0 \text{ when } x = \frac{l-a}{2}; \tag{2.66}$$

using (65) and (56), we obtain

$$B_1 = \frac{\Delta P}{P} \frac{h}{2} \frac{2n}{n+1} \frac{\cos \frac{k_1 l}{2}}{\cos \frac{k_1 a}{2}}. \tag{2.67}$$

Equating expression (64) and (67), we will have

$$\frac{k_1}{k_2} \operatorname{tg} \frac{k_1 a}{2} \operatorname{tg} k_2 \frac{l-a}{2} = \frac{n+1}{2n}. \tag{2.68}$$

By (56) we will have

$$\frac{k_2}{k_1} = \sqrt{\frac{2n}{n+1}}.$$

and instead of (68) we obtain

$$\operatorname{tg} \frac{k_1 a}{2} \operatorname{tg} k_2 \frac{l-a}{2} = \sqrt{\frac{n+1}{2n}}. \tag{2.69}$$

Expression (56) can be rewritten in the form

$$k_1^2 = \frac{P}{P_{кр}} \frac{\pi^2}{l^2} \frac{n+1}{2n}, \quad k_2^2 = \frac{P}{P_{кр}} \frac{\pi^2}{l^2}. \tag{2.70}$$

Equation (69) allows us to determine length of plastic section a, if there is given, on the one hand, value of n and, on the other hand, ratio $P/P_{кр}$.

We will consider <u>ultimate cases</u>. If region of unloading is absent, we should have a = 0; hence

$$\operatorname{tg} \frac{k_2 l}{2} = \infty, \quad k_2 = \frac{\pi}{l}; \tag{2.71}$$

by (70) this gives $P = P_{кр}$. Assuming, on the other hand, that region of unloading occupies whole length of bar (a = l), we obtain

$$\operatorname{tg} \frac{k_1 l}{2} = \infty, \quad k_1 = \frac{\pi}{l}; \tag{2.72}$$

hence by (70)

$$P = P_{кр} \frac{2n}{n+1} = P_{дин}. \tag{2.73}$$

On graph of Fig. 2.16 is presented dependence between $\bar{P} = P/P_{кр}$ and a/l when n = 2; 4; and 6 for intermediate values of a/l. Dotted line shows level corresponding to force $P_{рез}$ according to (73).

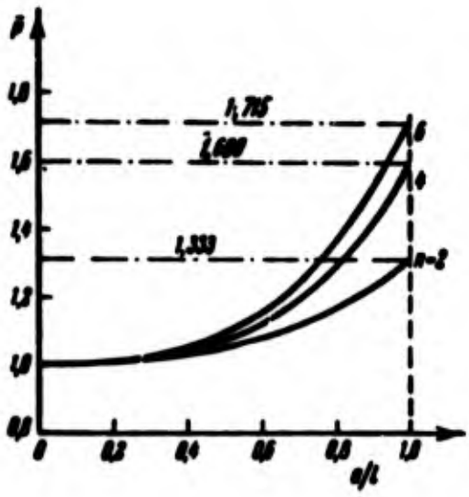

Fig. 2.16. Length of zone of unloading in case of I-beam section.

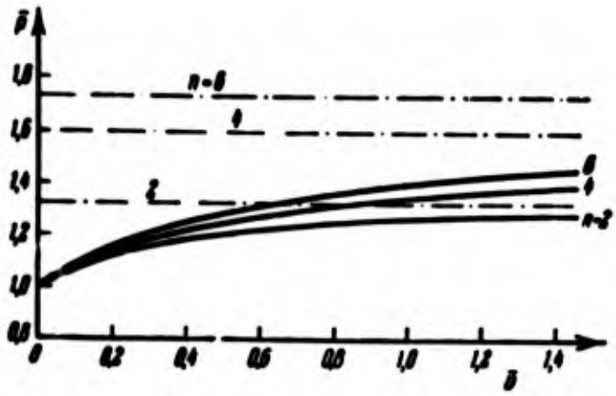

Fig. 2.17. "Load-deflection" diagram in case of I-beam section.

Using expressions (61) and (67), we find maximum deflection of bar:

$$f = v_{x=\frac{l}{2}} = \left(1 - \frac{P_{кр}}{P}\right)\frac{h}{2(n+1)}\left(\frac{2n}{\cos\frac{k_1 a}{2}} - n + 1\right). \qquad (2.74)$$

In Fig. 2.17 is shown how ratio $\bar{v} = f/(h/2)$ changes depending upon $\bar{P} = P/P_{кр}$ for different n. Slope of tangent is determined by expression

$$\frac{dP}{df} = \frac{2(n+1)}{h}\frac{P^2}{P_{кр}}\frac{1}{\frac{2n}{\cos\frac{k_1 a}{2}} - n + 1}. \qquad (2.75)$$

At point of branching we will have $P = P_{кр}$, $\bar{P} = 1$, $a = 0$; hence

$$\left(\frac{dP}{df}\right)_{P=P_{кр}} = \frac{2P_{кр}}{h}. \qquad (2.76)$$

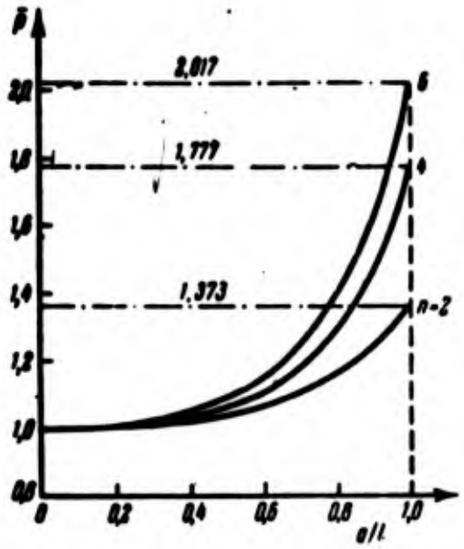

Fig. 2.18. Length of zone of unloading for bar of rectangular section.

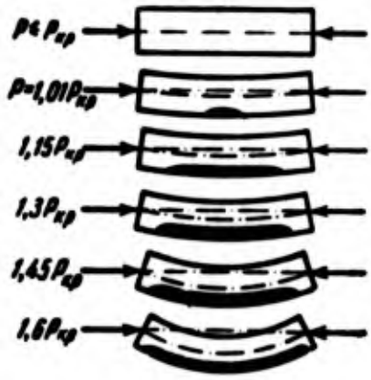

Fig. 2.19. Propagation of zone of unloading during buckling of bar.

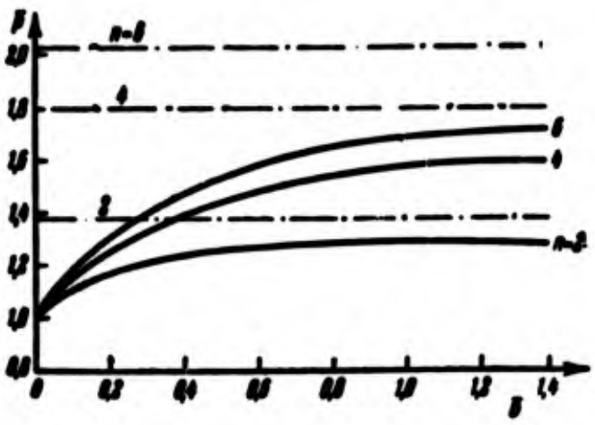

Fig. 2.20. "Load-deflection" diagram for bar of rectangular section.

In case of rectangular section calculations are significantly complicated. In Fig. 2.18 is presented final graph of dependences $\overline{P} = P/P_{кр}$ on a/l. From Fig. 2.19 one may see how deeply by section the zone of unloading spreads in different sections for one or another level of supercritical deformation; it is assumed $n = 4$. In Fig. 2.20 is given change of relative deflection $\overline{v}$ during increase of load, starting from $P_{кр}$.

§ 31. Selection of Criterion of Stability and Design Load

Problem of buckling of compressed bar beyond the limits of elasticity at first glance is simple. Really, we study deformation of bar, assuming deflections small as compared to length, i.e., in geometrically linear setting. Distributive law of strains by section is determined by hypothesis of flat sections. We can consider bar as system of longitudinally located fibers, inasmuch as state of strain is considered uniaxial. Law of stress--strain is assumed known. Nevertheless, as we see now, this problem conceals many "underwater stones".

First difficulty consists of propagation to elastoplastic region of the idea of stability. Let us assume that compressive stress in bar exceeds limit of proportionality, but critical load still is not attained; obviously, rectangular state of rod should be stable. However, if some perturbation causes distortion of bar, then in it will appear certain permanent deformations. It is possible to understand by stable in the small such equilibrium position of system which does not have neighboring distorted equilibrium forms. By critical load we must imply then such minimum force at which there are manifested neighboring equilibrium forms; but here we must exclude from consideration those forms which correspond to permanent deformations (see [21.5a, 21.11]).

Such determination can also cause objections, if one were to consider that plastic flow during load of structure constitutes, to greater or lesser measure, a process of flow, developing in time. From this point of view, talking about stability, we must compare magnitude of small perturbation changing system from considered

position, with that effect, which it will cause. If this effect, consisting in distortion of bar, is limited and small, then initial state should be considered "stable".

As a rule, we will nevertheless consider that process of plastic flow flows very slowly and that use of idea of equilibrium state of system is valid. We return, therefore, to definition of critical load as point of branching of equilibrium forms. Here we encounter a new peculiarity of non-elastic buckling: instead of fixed point of bifurcation, corresponding to first critical load in elastic region, here possible points of bifurcation fill the whole interval, lying between tangent-modular and is reduced-modular loads. At what point should there occur buckling of sample, subjected to test in laboratory, structural element in real conditions? This depends on characteristic of machine or parts of structure connected with bar. In preceding calculations ratio $\Delta P/\Delta v$ was not determined, but it can be found, if we know reaction of structural elements linked with sample given with deflection and characteristic of load, applied to structure as a whole.*

There appears question, what load--tangent-modular or reduced-modular--should be taken as design during planning? As we have seen, tangent-modular load can under known conditions correspond to point of bifurcation of equilibrium forms: it always lies below reduced-modular and better corresponds to experimental data. Therefore, we should recommend conducting practical calculations on tangent-modular

*See article of A. A. Ilyushin and V. G. Zubchaninov (Eng. Collection, Vols. 27 and 28, 1960) and Ya. G. Panovko [2.6, 1962].

load. It is true, distinction between tangent-modular and reduced-modular loads is small; therefore, as already marked by Hoff [6.13], this selection does not render essential influence on results of calculation.

Conducting calculation of tangent-modular load, we as it were, refuse to consider effect of unloading during buckling. This assumption strongly simplifies calculations, especially in more complicated problems of stability of plates and shells, and we will resort to it subsequently more than once.

Regardless of what modulus we take for calculating--T or E_K for solution of problems we can apply methods of approximation described in Chapter I. In case of bar of variable section it is necessary to consider here change of modulus T or E_K with length, depending on change of stress σ in section. But since actual critical stress usually is to be determined, calculation must be conducted by means of several trials.

§ 32. Eccentric Compression in Non-Elastic Region. Approximate Solution

Research of forms of equilibrium of bars, subjected to eccentric compression beyond the limits of elasticity, encounters new difficulties. Here it is necessary to consider diverse variants of location by section of elastic and plastic zones with different loads. Therefore, there was offered a series of approximate solutions, introducing significant simplifications already in the actual formulation of problem.*

*This problem was considered by Ros [2.18], Chwalla [2.10], Fritsche [2.12], Ježek [2.13], A. V. Gemmerling [2.3], and V. V. Pinadzhyan [2.7]. Here the account is developed according to book of Ježek [2.13].

One of essential assumptions is introduction of a model of ideally plastic material. By this is understood an imaginary material, whose diagram of compression and extension have the form shown in Fig. 2.21. It is considered that yield points during compression and extension are identical.

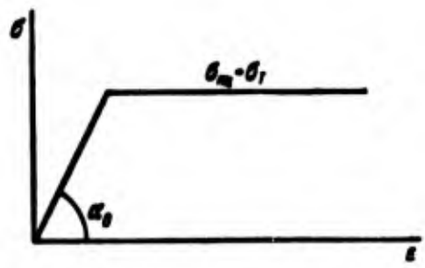

Fig. 2.21. Idealized diagram.

A second assumption is that bending line for hinge-supported bar is a half-wave of a sine wave.

In Fig. 2.22a is depicted cross section of bar, having axis of symmetry. We will consider that point A of application of force P lies on this axis and is removed from center of gravity C a distance e. Let us assume that height of section h is divided by point C into segments h_1 and h_2. We designate by f maximum deflection of the bar, counted off from line of force P. We imagine that deformations in certain part of compressed zone exceed magnitude $\varepsilon_т$, corresponding to yield point: $\varepsilon_т = \sigma_т/E$; boundary of this zone is distance ξ from edge of compressed region. Let position of neutral line be determined by segments ζ and η. Complete diagrams of distribution of strains and stresses by height of section are given in Fig. 2.22b and c.

We constitute equation of equilibrium for part of bar separated by average section. Equation of projections of forces in direction of axis of bar has the form

$$P-\left[F\sigma_т-\int_0^{h-\xi}\sigma\,dF\right]=0. \qquad (2.77)$$

Here by F is designated area of section, by σ the difference between stress at point with coordinate u and yield point $\sigma_т$:

$$\sigma = \sigma_s \frac{u}{\eta}. \tag{2.78}$$

Coordinate u is counted off from boundary of yield zone.

Equation of moments relative to line passing through ex[illegible] point of stretched zone will be

$$P(f+h_2) - \left[F\sigma_s h_2 - \int_0^{h-\xi} \sigma(h-\xi-u)\,dF\right] = 0. \tag{2.79}$$

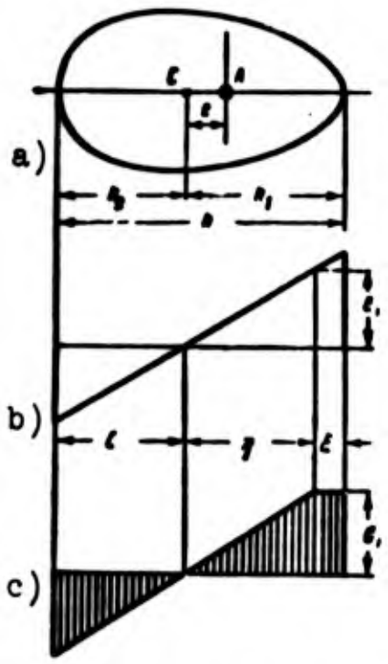

Fig. 2.22. (a) Section of bar, (b) diagram of strains and (c) diagram of stresses during eccentric compression.

We introduce designations for static moments of inertia of parts of area of section divided by boundary of yield zone:

$$S_{1\xi} = \int_0^{\xi} u_1\,dF, \quad I_{1\xi} = \int_0^{\xi} u_1^2\,dF. \tag{2.80}$$

$$S_{2\xi} = \int_0^{h-\xi} u_2\,dF, \quad I_{2\xi} = \int_0^{h-\xi} u_2^2\,dF. \tag{2.81}$$

Comparing (80) and (81), it is possible to write

$$S_{2\xi} = S_{1\xi} + F(h_1 - \xi). \tag{2.82}$$

Moment of inertia I_ξ of the whole area relative to boundary of yield zone and moment of inertia I relative to the central axis parallel to it are connected by the relationship

$$I_\xi = I_{1\xi} + I_{2\xi} = I + F(h_1 - \xi)^2. \tag{2.83}$$

We designate by $\sigma_0 = P/F$ average compressive stress in section; then from (77) ensues

$$\eta = \frac{S_{1\xi} + F(h_1 - \xi)}{F(\sigma_T - \sigma_0)} \sigma_T. \tag{2.84}$$

Using (82) and (83), from equation (79) we find,

$$f = \frac{\sigma_T}{F\sigma_0 \eta} |I - I_{1\xi} - (h_1 - \xi) S_{1\xi}|. \tag{2.85}$$

For a specific form of section equation (85) together with (84) give dependence between deflection f and average stress σ_0.

Let us consider now geometric aspect of problem. We designate by ρ radius of curvature of elastic line for average section; then

$$\frac{1}{\rho} = \frac{\sigma_T}{\eta}. \tag{2.86}$$

Using (1.3), for that section we obtain

$$-\frac{d^2v}{dx^2} \approx \frac{\sigma_T}{E\eta}. \tag{2.87}$$

Equation of bending line of bar we write in the form

$$v = e + (f - e) \sin \frac{\pi x}{l}, \tag{2.88}$$

where origin of coordinates coincides with point of application of one of forces P; when $x = l/2$ we have

$$\frac{d^2v}{dx^2} = -\frac{\pi^2}{l^2}(f - e). \tag{2.89}$$

Comparing (87) and (89), we find

$$\rho = \eta(f - e) \frac{\pi^2 E}{\sigma_T}. \tag{2.90}$$

Finally by (84) and (85) we have,

$$\rho = \frac{\pi^2 E}{F\sigma_0} \left[I - I_{1\xi} - (h_1 - \xi) S_{1\xi} - \frac{S_{1\xi} + F(h_1 - \xi)}{\sigma_T - \sigma_0} \sigma_0 e \right]. \tag{2.91}$$

We obtained relationship between average stress σ_0 and width of plastic region ξ. Analysis of it shows that magnitude σ_0 in the beginning increases, and then, after reaching a certain limit point, drops. We set ourselves the goal of finding such value ξ, at which σ_0 is the biggest, for that we equate to zero the derivative of l^2 with respect to ξ for the given σ_0; then we obtain

$$\left(h_1-\xi+\frac{\sigma_0}{\sigma_T-\sigma_0}\right)\frac{\partial S_{1\xi}}{\partial\xi}-\frac{F\sigma_0}{\sigma_T-\sigma_0}-S_{1\xi}+\frac{\partial I_{1\xi}}{\partial\xi}=0. \qquad (2.92)$$

Determining hence ξ, by (84) will find "critical" value of average stress, and by (85) the corresponding deflection.

§ 33. Eccentric Compression of Bars of Rectangular and Tee Sections

Let us consider case of rectangular section b X h. By formulas (80) when $h_1 = h/2$ we find

$$S_{1\xi}=\frac{b\xi^2}{2},\quad I_{1\xi}=\frac{b\xi^3}{3}. \qquad (2.93)$$

Put these values in (92); then we obtain value of width of plastic zone for critical value of average stress $\sigma_0 = \sigma_{кр}$:

$$\xi=2\frac{\sigma_{кр}}{\sigma_T-\sigma_{кр}}. \qquad (2.94)$$

We designate by k radius of kernel of section:

$$k=\frac{W}{F}, \qquad (2.95)$$

where W is moment of strength of section, and we introduce concept of the measure of eccentricity m:

$$m=\frac{e}{k}=\frac{eF}{W}. \qquad (2.96)$$

In this case

$$k=\frac{h}{6},\quad m=\frac{6e}{h}. \qquad (2.97)$$

Instead of (94) we have

$$\frac{\xi}{h}=\frac{m}{3}\frac{\sigma_{кр}}{\sigma_т-\sigma_{кр}}. \qquad (2.98)$$

We place this expression in equation (91): then we obtain

$$P=\frac{\pi^2 EJ}{12\sigma_{кр}}\left(1-\frac{\xi}{h}\right)^3. \qquad (2.99)$$

Slenderness ratio of bar is

$$\lambda=\frac{l}{i}=\frac{l\sqrt{12}}{h}. \qquad (2.100)$$

Equality (99) we give the form

$$\sigma_{кр}=\frac{\pi^2 E}{\lambda^2}\left(1-\frac{\xi}{h}\right)^3. \qquad (2.101)$$

Let us note that when $\xi = 0$, when there is no plastic zone, we obtain ordinary Euler's formula. Using expression (98), we obtain

$$\lambda^2=\frac{\pi^2 E}{\sigma_{кр}}\left(1-\frac{m}{3}\frac{1}{\frac{\sigma_т}{\sigma_{кр}}-1}\right)^3. \qquad (2.102)$$

We arrived at equation for $\sigma_{кр}$, allowing us to determine critical stress for given relative eccentricity. Corresponding values of η and f from (84) and (85) will be

$$\eta_{кр}=\frac{3}{2m}\left(1-\frac{\xi}{h}\right)^2\frac{\sigma_т}{\sigma_{кр}}, \qquad (2.103)$$

$$f_{кр}=\frac{mh}{18}\frac{1+\frac{\xi}{h}-2\frac{\xi^2}{h^2}}{\sqrt{\left(1-\frac{\xi}{h}\right)\frac{\xi}{h}}}. \qquad (2.104)$$

Here we must substitute the expression for ξ/h from (98). On graph of Fig. 2.23 are presented curves $\sigma_{кр}(\lambda)$, built by equation (102) for different parameters m; we assume $E = 2.1\cdot10^6$ kg/cm^2, and $\sigma_т$ = = 2400 kg/cm^2. When m = 0 we obtain horizontal line within limits $\lambda < \lambda_*$ and Euler's hyperbola $\lambda \geq \lambda_*$; here $\lambda_* = 94$. Small left section

of diagram corresponds to case of two-way yield, when plastic flows appear not only in compressed, but in stretched zone.

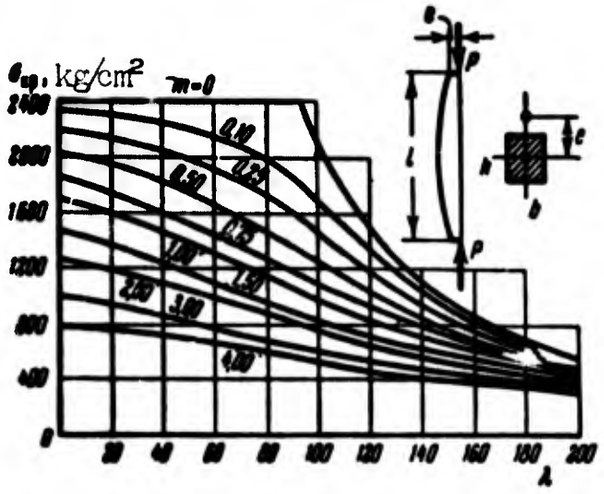

Fig. 2.23. Diagram $\sigma_{кр}(\lambda)$ in case of eccentric compression of a rectangular steel bar.

In book [2.13] are considered analogously cases of cross sections of other form. Comparison of results showed that with significant m critical stress is the smallest for bars of T-section, when point of application of force lies on axis of wall, on other side of flange (Fig. 2.24). We will discuss that case when plastic zone is only on side of compression and embraces only part of flange. Expressions for $S_{1\xi}$ and $I_{1\xi}$ will again have form (93), where by b we must understand width of shelf. Equation (92) turns out to be quadratic relative $\xi_{кр}$ and is reduced to the form

$$\xi_{кр}^2 - 2\left(h_1 + \frac{e\sigma_{кр}}{\sigma_т - \sigma_{кр}}\right)\xi_{кр} + \frac{2Fe\sigma_{кр}}{b(\sigma_т - \sigma_{кр})} = 0. \qquad (2.105)$$

We use again as designation for measure of eccentricity (96), where here $W = W_1 = I/h_1$ (see Fig. 2.22). Then least root of equation (105) can be presented in the form

$$\xi_{кр} = p - \sqrt{p^2 - q}, \qquad (2.106)$$

where

$$p = h_1 + \frac{mW_1\sigma_{кр}}{F(\sigma_т - \sigma_{кр})}, \qquad (2.107)$$

$$q = \frac{2mW_1\sigma_{кр}}{b(\sigma_т - \sigma_{кр})}. \qquad (2.108)$$

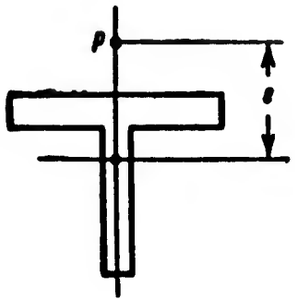

Fig. 2.24. Tee section of bar.

Comparing (106)--(108), we find

$$h_1 - \xi_{кр} = \sqrt{p^2 - q} - \frac{qb}{2F}. \quad (2.109)$$

We place expressions (106) and (109) in equation (91); then after simplifications we obtain

$$l^2 = \frac{\pi^2 EI}{F\sigma_{кр}}\left\{1 - \frac{b}{3I}\left[p^3 - (p^2 - q)^{3/2} - \frac{3}{4}\frac{bq^2}{F}\right]\right\}. \quad (2.110)$$

Hence when $\lambda = l/i$,

$$\lambda^2 = \frac{\pi^2 E}{\sigma_{кр}}\left\{1 - \frac{b}{3I}\left[p^3 - (p^2 - q)^{3/2} - \frac{3}{4}\frac{bq^2}{F}\right]\right\}. \quad (2.111)$$

We expand expression $(p^2 - q)^{3/2}$ into a series:

$$(p^2 - q)^{3/2} = p^3 - \frac{3}{2}pq + \frac{3}{8}\frac{q^2}{p} - \cdots \quad (2.112)$$

After certain transformations equation (111) will take the form

$$\lambda^2 = \frac{\pi^2 E}{\sigma_{кр}}\left[1 - \frac{m\sigma_{кр}}{\sigma_т - \sigma_{кр}} + \frac{W_1}{2bh_1^2}\left(\frac{m\sigma_{кр}}{\sigma_т - \sigma_{кр}}\right)^2 - \cdots\right]. \quad (2.113)$$

If one were to take dimensions of section from Fig. 2.25, where b = h, then coefficient containing W_1 and h_1, will be equal to 0.38. Let us note that the resolvent (102) for the case of rectangular section it is possible also to reduce to form

$$\lambda^2 = \frac{\pi^2 E}{\sigma_{кр}}\left[1 - \frac{m\sigma_{кр}}{\sigma_т - \sigma_{кр}} + \frac{1}{3}\left(\frac{m\sigma_{кр}}{\sigma_т - \sigma_{кр}}\right)^2 - \cdots\right]; \quad (2.114)$$

it differs from (113) only in coefficient in third member of series. Dependence $\sigma_{кр}(\lambda)$ by (113) for section from Fig. 2.25 is presented on graph of Fig. 2.26; here are given also sections of curves corresponding to other combinations of elastic and plastic zones of section.

V. V. Pinadzhyan [2.7] solved more complicated problem on the assumption that in diagram $\sigma(\varepsilon)$ section of plasticity is not horizontal,

but slightly slanted (Fig. 2.27). Such dependence $\sigma(\varepsilon)$ better corresponds to usual diagram for steel St. 3. Calculations showed that critical stress for such material lies 5-7% higher than in case of "ideal plasticity."

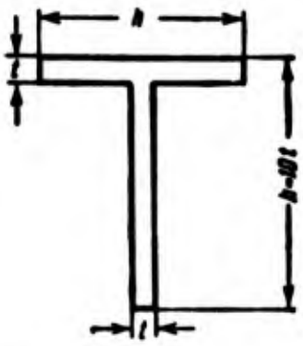

Fig. 2.25. Dimensions of tee section in numerical example.

Research of stability of elasto-plastic bars taking into account different perturbations (eccentricity of load, initial flaw) lie at basis of contemporary norms of calculation of compressed and is compresses-bent members of building constructions. This direction is illuminated in books of A. V. Gemmerling [2.3], A. A. Pikovskiy [3.7], G. Bürgermeister and H. Steup [0.16], C. Kollbrunner and M. Meister [0.19].

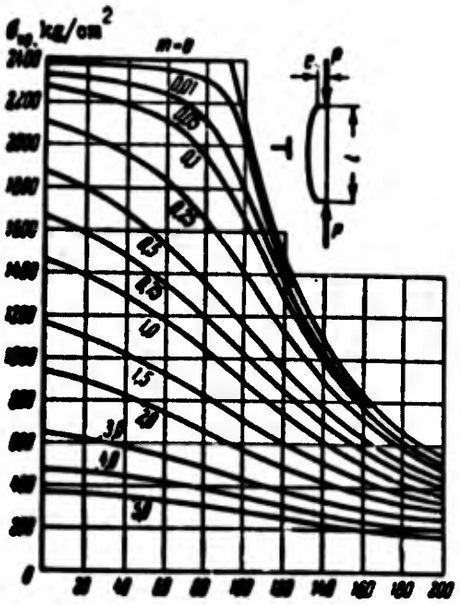

Fig. 2.26. Dependence $\sigma_{кр}(\lambda)$ in case of bar of tee section under eccentric compression.

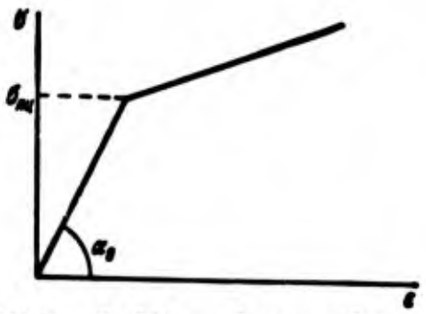

Fig. 2.27. Approximate diagram of compression for steel.

Literature

2.1. B. M. Broude. Limit states of steel beams, Gosstroyizdat, M.-L., 1953.

2.2. A. S. Vol'mir. Concerning the question of buckling beyond the elastic limit, Scientific notes of the Khar'kov Mechanics and Mathematics Inst., (1935), 137-145.

2.3. A. V. Gemmerling. On supporting power of compressed steel constructions, Transactions TsNIPS, No. 7, M. (1952).

2.4. S. D. Leytes. Stability of compressed steel bars, Gosstroyizdat, M., 1954.

2.5. S. N. Nikiforov. Stability of compressed bars of welded girders, BIZ, M.-L., 1958.

2.6. Ya. G. Panovko. On critical force for a compressed bar in the plastic region. Engineering collection, 20 (1954), On longitudinal elasto-plastic bending of bars in static indeterminable systems, News of Acad. of Sci. of USSR, Mechanics and mathematics, No. 2 (1962), 160-165.

2.7. V. V. Pinadzhyan. Certain questions of limiting state of compressed members of steel structures, Publishing House of Academy of Sciences of Armenian SSR, Yerevan, 1956.

2.8. Yu. N. Rabotnov. On equilibrium of compressed bars beyond the proportional limit, Eng. Collection. 11 (1952).

2.9. N. S. Streletskiy. Materials for course on steel constructions, Work of compressed columns, Gosstroyizdat, Moscow, 1959.

2.10. E. Chwalla. Theorie der auBermittig gedrückten Stabes aus Baustahl. Stahlbau, No. 21-23 (1934).

2.11. F. Engesser. Ueber Knickfestigkeit gerader Stäbe, Z. Arch. u. Ing. Ver. zu Hannover 35 (1889). 455: Die Knickfestigkeit gerader Stäbe, Zentralblatt der Bauverwaltung 11 (1891). 483; Ueber Knickfragen, Schweiz. Bauzeitung 26 (1895), 24.

2.12. J. Fritsche. Näherungsverfahren zur Berechnung der Tragfähigkeit auBermittig gedrückter Stäbe aus Baustahl, Stahlbau, No. 18 (1935).

2.13. K. Ježek. Die Festigkeit von Druckstaben aus Stahl. Wien, 1937.

2.14. F. Jasinski. Zu den Knickfragen, Schweiz. Bauzeitung 26 (1895), 24 (see F. S., Yasinskiy, Selected works, Gostekhizdat, M., 1952).

2.15. Th. Kármán. Untersuchungen über Knickfestigkeit. Physik. Z. (1908), 138; Mitteilungen über Forschungsarb. auf dem Gebiet d. Ing. Wesens, No. 81, Berlin (1910); J. Aeron. Sciences 14 (1947), 267.

2.16. L. Navier. Résumé de lecons, Paris, 1826.

2.17. A. Pflüger. Zur plastischen Knickung gerader Stäbe, Ing. Archiv 20, No. 5 (1952), 291-301.

2.18. M. Ros. Le stabilitè de barres comprimées par des forces excentrées, Paris, 1932.

2.19. F. R. Shanley. Inelastic column theory, J. Aeron, Sci. 13, No. 12 (1946). 678; 14, No. 5 (1947); Proc. Am. Soc. Civ. Eng. 75 (1949), 759.

2.20. F. Schleicher. Ueber die Grundlagen der Plastizitätstheorie und des plastischen Knickens, Stahlbau, No. 10 (1951), 118.

2.21. L. Tetmajer. Die Gesetze der Knickungs- und zusammengesetzten Festigkeit der technisch wichtigsten Baustoffe. Leipzig, 1907.

C H A P T E R III

MORE COMPLICATED PROBLEMS OF STABILITY OF BARS AND BAR SYSTEMS

§ 34. Bars of Variable Section. Step Change of Rigidity.

We considered till now only bars whose rigidity with length is constant. However, from the point of view of facilitating construction it is expedient to apply compressed bars of variable rigidity, with its increase in that zone, where bending moments and normal forces are the greatest. It is true, manufacture of bars of variable rigidity requires more complicated technology. But for big structures this is obviously compensated by savings of material, expended on construction. Especially convenient is application of compound bars of variable of rigidity, having two or several branches; such bars frequently are found in constructions of towers, masts, arms of hoists, etc.

Let us give solution of several problems pertaining to stability of bars of variable rigidity supported by hinges on ends. Obviously, in this case rigidity should be increased in middle section.

In Fig. 3.1, is presented a bar, consisting of three sections. Extreme sections, each of length l_1, have rigidity EI_1, and middle section is of length $a = 2l_2$, rigidity EI_2, where $I_2 > I_1$; l is total length of bar. We constitute differential equations of bending line for every section. We count off coordinate x_1 from end of bar 0, and

x_2--from point of linkage of sections. Equations will have form

$$EI_1 \frac{d^2v_1}{dx_1^2} + Pv_1 = 0. \qquad (3.1)$$

$$EI_2 \frac{d^2v_2}{dx_2^2} + Pv_2 = 0. \qquad (3.2)$$

Introducing designations

$$\frac{P}{EI_1} = k_1^2. \quad \frac{P}{EI_2} = k_2^2. \qquad (3.3)$$

We write integrals of equations (1) and (2):

$$v_1 = A \sin k_1 x_1 + B \cos k_1 x_1. \qquad (3.4)$$

$$v_2 = C \sin k_2 x_2 + D \cos k_2 x_2. \qquad (3.5)$$

Boundary conditions on ends and at point of linkage of sections will be

$$v_1 = 0 \text{ when } x_1 = 0. \qquad (3.6)$$

$$v_1 = v_2 \text{ when } x_1 = l_1 \text{ и } x_2 = 0. \qquad (3.7)$$

$$\frac{dv_1}{dx_1} = \frac{dv_2}{dx_2} \text{ when } x_1 = l_1 \text{ и } x_2 = 0. \qquad (3.8)$$

$$\frac{dv_2}{dx_2} = 0 \text{ when } x_2 = l_2. \qquad (3.9)$$

From these conditions we find

$$\left.\begin{array}{ll} B = 0, & A \sin k_1 l_1 = D. \\ Ak_1 \cos k_1 l_1 = Ck_2, & C \cos k_2 l_2 - D \sin k_2 l_2 = 0. \end{array}\right\} \qquad (3.10)$$

Comparing equations (10), we arrive at transcendental equation

$$\frac{k_1}{\operatorname{tg} k_1 l_1} = k_2 \operatorname{tg} k_2 l_2. \qquad (3.11)$$

We present critical load in the form

$$P_{кр} = K\frac{EI_2}{l^2}. \qquad (3.12)$$

In Table 3.1 are given values of factor K for certain ratios

$$\frac{a}{l} = \frac{2l_2}{l} = \lambda, \quad \frac{I_1}{I_2} = a. \qquad (3.13)$$

We will show an example of solution of this same problem by successive approximations.

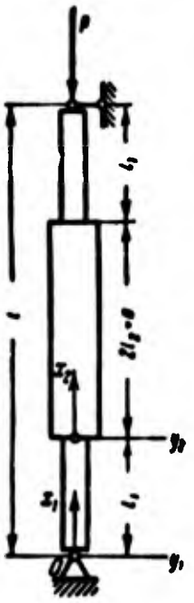

Fig. 3.1. Case of step change of section.

Example 3.1. Determine critical load for bar with step changed rigidity when $\lambda = 0.8$. We take initial equation of elastic line in the form

$$v = -\frac{4f^{(0)}}{l^2}(lx - x^2). \qquad (a)$$

Table 3.1. Values of factor K for bar with step change of rigidity.

a \ λ	0,2	0,4	0,6	0,8
0,1	1,47	2,40	4,50	8,59
0,2	2,796	4,222	6,694	9,330
0,4	5,069	6,680	8,512	9,675
0,6	6,978	8,187	9,240	9,790
0,8	8,550	9,177	9,632	9,840

Equations (1) and (2) will be rewritten then in the following form:

$$\frac{d^2v_1}{dx^2} = -4k_1\left(\frac{x}{l} - 1\right), \quad \frac{d^2v_2}{dx^2} = -4k_2\left(\frac{x}{l} - 1\right). \qquad (b)$$

Integrating these equations and using conditions (6) - (9) taking into account that x now is counted off from point 0, we find

$$v_2 = 2fk_2\left[\frac{1}{6}\left(\frac{x}{l}\right)^4 - \frac{1}{3}\left(\frac{x}{l}\right)^3 + \frac{1}{6}\frac{x}{l} + \frac{37}{6\cdot 10^4}\left(\frac{1}{a} - 1\right)\right]. \qquad (c)$$

Deflection will be

$$f^{(1)} = \frac{P_{cr}}{EI} f^{(0)}\left(\frac{193}{1875} + \frac{37}{3\cdot 10^4 a}\right). \qquad (d)$$

Critical force turns out to be equal to

$$P_{cr} = \frac{EI_2}{l^2}\,\frac{3\cdot 10^4}{3088 + \frac{37}{a}}. \qquad (e)$$

For cases given in Table 3.1, we will obtain following values of K:

a	0,1	0,2	0,4	0,6	0,8
K	8,77	9,17	9,41	9,52	9,58

Error with respect to tabular values does not exceed 5%.

§ 35. Case of Continuous Change of Rigidity by Length. Bar of Minimum Weight.

Let us turn to case where rigidity of bar continuously changes along length.* Let us consider bar supported by hinges at ends, for each half of which moment of inertia changes by exponential law:

$$I = I_2\left(\frac{x}{b}\right)^m. \qquad (3.14)$$

x is counted from point located distance b from center of bar if, for instance, the bar consists of two branches (Fig. 3.2), having rectilinear shape, and distance between branches h is equal to

$$h = h_2\frac{x}{b},$$

then moment of inertia of section, if one were to ignore natural moment of inertia of section of branch, will change by relationship (14) when m = 2.

Differential equation of elastic line will be

$$EI_2\left(\frac{x}{b}\right)^m \frac{d^2v}{dx^2} + Pv = 0; \qquad (3.15)$$

*Such problems were first solved by Lagrange; a number of cases of bars mixed rigidity was considered by A. N. Dinnik [3.1].

boundary conditions have form

$$\frac{dv}{dx}=0 \text{ when } x=b;$$
$$v=0 \text{ when } x=b-\frac{l}{2}=b_1. \qquad (3.16)$$

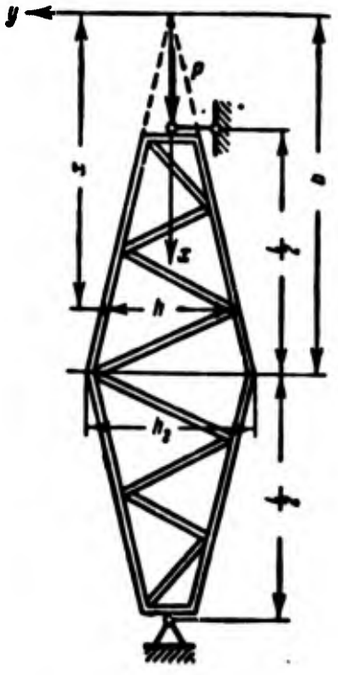

Fig. 3.2. Moment of inertia of section changes by exponential law.

We designate

$$\frac{Pb^m}{EI_b}=k^2,$$

there instead of (15) we obtain

$$\frac{d^2v}{dx^2}+k^2x^{-m}v=0. \qquad (3.17)$$

Let us consider first the case where m = 2; here besides solution of equation (17) will be

$$v=A\sqrt{x}\sin(s\ln x)+B\sqrt{x}\cos(s\ln x), \qquad (3.18)$$

where

$$s^2=k^2-\frac{1}{4}; \qquad (3.19)$$

this is easy to prove by direct differentiation. Derivative dv/dx is equal to

$$\frac{dv}{dx}=A\left[\frac{1}{2\sqrt{x}}\sin(s\ln x)+\frac{1}{\sqrt{x}}s\cos(s\ln x)\right]+$$
$$+B\left[\frac{1}{2\sqrt{x}}\cos(s\ln x)-\frac{1}{\sqrt{x}}s\sin(s\ln x)\right]. \qquad (3.20)$$

We use boundary conditions (16). From the second of these conditions

$$B=-A\operatorname{tg}(s\ln b_1).$$

First condition gives

$$A\left[\frac{1}{2}\operatorname{tg}(s\ln b)+s\right]+B\left[\frac{1}{2}-s\operatorname{tg}(s\ln b)\right]=0.$$

Hence we obtain equation for s:

$$\operatorname{tg}\left(s\ln\frac{b_1}{b}\right)=2s. \qquad (3.21)$$

Least root of this equation determines critical load:

$$P_{кр} = K_1 \frac{\pi^2 EI}{l^2}, \text{ where } K_1 = \left(s^2 + \frac{1}{4}\right)\left(\frac{l}{b}\right)^2. \qquad (3.22)$$

If $m \neq 2$, then solution of equation (17) is extracted in the following manner:

$$v = A\sqrt{x}J_{\nu}\left(2k\nu x^{\frac{1}{2\nu}}\right) + B\sqrt{x}J_{-\nu}\left(2k\nu x^{\frac{1}{2\nu}}\right), \qquad (3.23)$$

where

$\nu = \frac{1}{2-m}$ — is a fractional number.

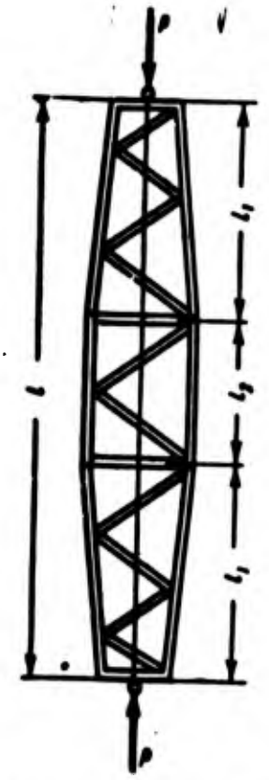

Fig. 3.3. Bar, consisting of three sections; middle section has constant cross-section.

By J_ν, is understood is Bessel's function of the first type with subscript ν. We note, that when $\nu = n + 1/2$, where n is an integer, functions J_ν and $J_{-\nu}$ can be expressed by element functions.

Let us assume, further, that bar supported by hinges consists of three sections (Fig. 3.3), where on middle section l_2 moment of inertia is constant and equal to I_2, and in extreme sections of length l_1, moment of inertia changes according to law (14). Then for middle section equation of elastic line will be written in the form (5) when $I = I_2$, and for end section in form (15). Considering conditions for end section, middle section and point of linkage of sections, we determine critical

load.

Data for calculations, pertaining to case m = 2, are shown in graph of Fig. 3.4 [0.21]. Here on axis of abscissas is placed ratio l_1/l, along the axis of ordinates--factor K_1 from formula (22) when $I = I_2$; series of curves is given for various ratios of moments of inertia I_1/I_2. Formula (22) can also be presented in the form

$$P_{кр} = \frac{\pi^2 E I_2}{(\nu l)^2}; \qquad (3.24)$$

coefficient of reduction of length is equal to $\nu = 1/\sqrt{K_1}$.

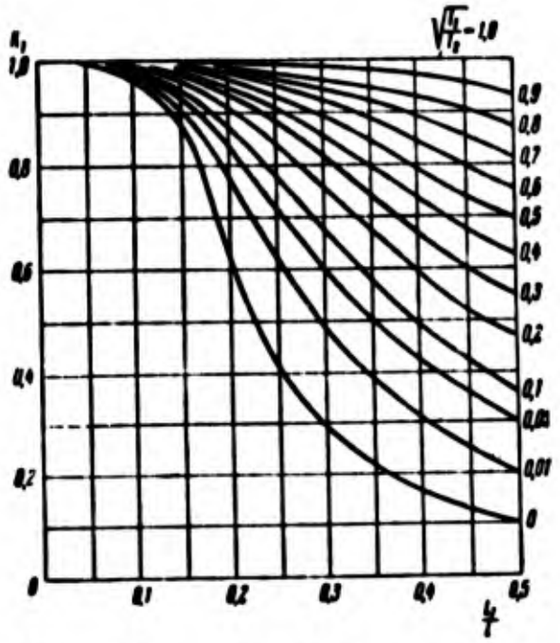

Fig. 3.4. Graph for calculation of bar of variable section.

Example 3.2. Arm AB of gantry crane (Fig. 3.5) consists of four equilateral corners 75 x 75 x 6, connected by lattice. Total length of arm is l = 17.5 m. Dimensions of section of middle part DG are constant, and under tension each of the end sections change by linear law depending upon distance to support A or B. Dimensions of sections in middle part and at supports are shown in figure. It is necessary to determine critical load when $E = 2.1 \cdot 10^6$ kg/cm^2; $\sigma_{ш}$ = 2000 kg/cm^2.

Area of cross-section of profile is equal to 8.78 cm^2, distance from axis to center of gravity of corner section in middle is 17.94 cm, at support 6.94 cm. Moment of inertia of cross-section in middle part is

$$I_2 = 4(46{,}7 + 8{,}78 \cdot 17{,}94^2) = 11\,500 \text{ см}^4,$$

at supports

$$I_1 = 4(46{,}7 + 8{,}78 \cdot 6{,}94^2) = 1900 \text{ см}^4;$$

here there is considered natural moment of inertia of profile, equal to 46.7 cm^4. Ratio $I_1/I = 0.165$, $\sqrt{I_1/I} = 0.405$. From figure we find:

$$\frac{l_1}{l} = \frac{7}{17.5} = 0.4.$$

On graph of Fig. 3.4 for these values of $\sqrt{I_1/I}$ and l_1/l we will have $K_1 \approx 0.73$. Critical load without calculation for influence of transverse force (see below, Section 43) we obtain as equal to

$$P_{кр} = \frac{0.73 \cdot \pi^2 \cdot 2.1 \cdot 10^6 \cdot 11\,500}{1750^2} = 59\,000 \text{ kg}.$$

Corresponding stress $\sigma_{кр} = 59\,000/4 \cdot 8.78 = 1570$ kg/cm^2 lies below $\sigma_{пц}$.

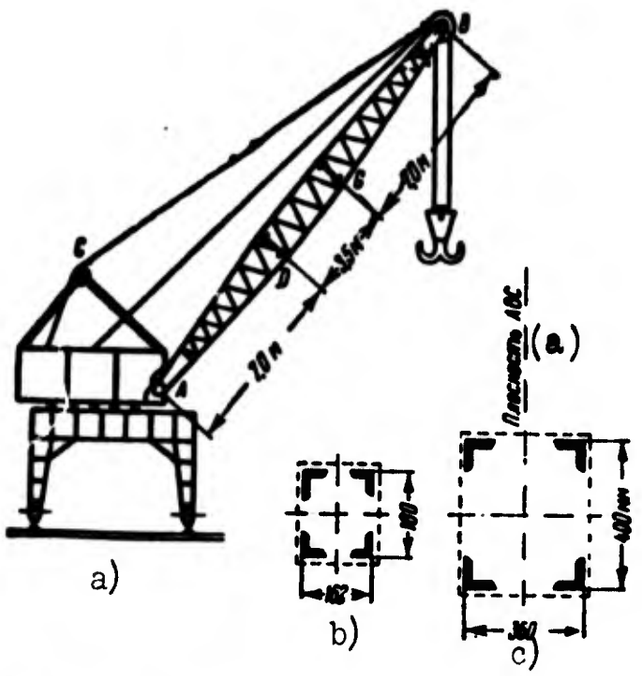

Fig. 3.5. Calculating arm of gantry crane.
KEY: (a) Plane ABC.

It is natural to pose the question: what form should a compressed bar of variable section have so that with a definite load it has minimum weight.* We give results of solution of such a problem for case where bar has solid round section and is supported by hinges at its ends. The most profitable shape of bar corresponds to the law

$$\arcsin \eta - \eta \sqrt{1 - \eta^2} = \frac{\pi x}{l}, \quad (3.25)$$

where η is ratio of current diameter to diameter of middle section, x is counted from end of bar. Form of bar is shown in Fig. 3.6; here are marked values of η in certain

*This problem was first posed by Lagrange and subsequently was investigated by Ye. L. Nikolai (Works on mechanics. Gostekhizdat, M., 1955), N. G. Chentsov [3.10], A. F. Smirnov [0.11] and other authors.

sections [1.13]. Weight of such an "ideal" bar turns out to be 13% less than weight of bar of constant section. In case of tubular section economy in weight can be significantly greater.

§ 36. Case Concentrated Force on Span

Assume that bar, supported by hinges at ends, is subjected to forces P_1, P_2 and $P_1 + P_2$ and that force P_2 is applied to certain intermediate section, located at distances l_1 and l_2 from ends (Fig. 3.7). We assume that moment of inertia of section in upper part is equal to I_1 and in the lower one, to I_2.

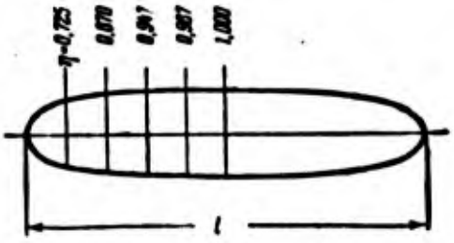

Fig. 3.6. Shape of bar of least weight.

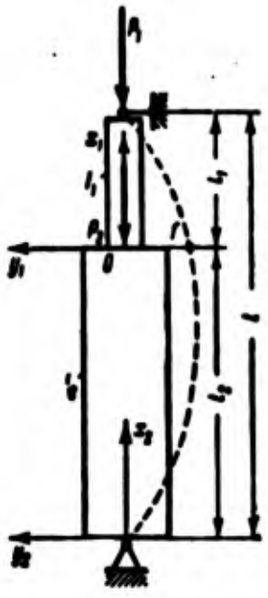

Fig. 3.7. Case of force applied in span.

We designate by f deflection of point of application of force P_2 during buckling of bar. Differential equation of elastic line for upper section will be

$$EI_1\frac{d^2v_1}{dx_1^2}=-(P_1+P_2)v_1+\frac{P_2f}{l}(x_1+l_2)-P_2(f-v_1)=$$
$$=-P_1v_1+\frac{P_2f}{l}(x_1-l_1); \qquad (3.26)$$

here is considered component of reaction of support, equal to $P_2 f/l$; coordinate x_1 is counted from 0. For lower section we obtain

$$EI_2\frac{d^2v_2}{dx_2^2}=-(P_1+P_2)v_2+\frac{P_2f}{l}x_2. \qquad (3.27)$$

We use designations

$$\frac{P_1}{EI_1}=k_1^2,\quad \frac{P_1+P_2}{EI_2}=k_2^2,\quad \frac{P_2}{EI_2}=k_3^2,\quad \frac{P_2}{EI_1}=k_4^2; \tag{3.28}$$

then equations (26) and (27) will be rewritten as follows:

$$\frac{d^2v_1}{dx_1^2}+k_1^2v_1=k_4^2\frac{f}{l}(x_1-l_1). \tag{3.29}$$

$$\frac{d^2v_2}{dx_2^2}+k_2^2v_2=k_3^2\frac{f}{l}x_2. \tag{3.30}$$

Hence

$$v_1=A_1\cos k_1x_1+B_1\sin k_1x_1+\frac{k_4^2}{k_1^2}\frac{f}{l}(x_1-l_1). \tag{3.31}$$

$$v_2=A_2\cos k_2x_2+B_2\sin k_2x_2+\frac{k_3^2}{k_2^2}\frac{f}{l}x_2. \tag{3.32}$$

Boundary conditions for ends of bar and point of linkage will be

$$\left.\begin{aligned} &v_1=0 \text{ when } x_1=l_1. \qquad v_2=0 \text{ when } x_2=0.\\ &v_1=v_2=f \text{ and } \frac{dv_1}{dx_1}=\frac{dv_2}{dx_2} \text{ when } x_1=0 \text{ и } x_2=l_2. \end{aligned}\right\} \tag{3.33}$$

Using these conditions, we find

$$A_2=0, \qquad A_1=f\left(1+\frac{k_4^2}{k_1^2}\frac{l_1}{l}\right).$$

$$B_1=-\frac{f}{\operatorname{tg}k_1l_1}\left(1+\frac{k_4^2l_1}{k_1^2l}\right), \qquad B_2=\frac{f}{\sin k_2l_2}\left(1-\frac{k_3^2l_2}{k_2^2l}\right)$$

and, last, we arrive at final equation

$$\frac{k_4^2}{k_1^2}-\frac{k_1^2l+k_4^2l_1}{k_1l\operatorname{tg}k_1l_1}=\frac{k_3^2}{k_2^2}+\frac{k_3^2l-k_3^2l_2}{k_2l\operatorname{tg}k_2l_2}. \tag{3.34}$$

For given ratio of forces and moments of inertia we find by trial and error for values of $k_1\ldots$, k_4, corresponding to least values of forces P_1 and P_2. We present critical magnitude $P_1 + P_2$ in the form

$$P_1+P_2=K\frac{EI_1}{l^2} \tag{3.35}$$

and designate

$$\frac{P_1+P_2}{P_1}=m, \quad \frac{l_2}{l_1}=n. \tag{3.36}$$

Factors K for case $l_1 = l_2$, found from equation (34), are given in Table 3.2.

Table 3.2

Factors K for case of forces, applied at ends and in the middle of span.

n \ m	1,00	1,25	1,50	1,75	2,00	3,00
1,00	9,87	10,9	11,9	12,5	13,0	14,7
1,25	8,81	9,77	10,5	11,2	11,6	—
1,50	7,90	8,86	9,53	10,1	10,7	—
1,75	7,11	8,04	8,52	9,10	9,77	—
2,00	6,40	7,30	7,90	8,43	8,97	—

Case m = 1 pertains to bar of variable section, on which there act only forces P_1 at ends. Equation (34) changes into the following:

$$\frac{k_1}{\operatorname{tg} k_1 l_1}=-\frac{k_2}{\operatorname{tg} k_2 l_2}. \tag{3.37}$$

§ 37. Influence of Distributed Longitudinal Load

Let us turn to case where longitudinal load is distributed along length of bar. One example of such a type of load is the gravity of the bar: during calculation of columns in big constructions, chimneys, etc. it is necessary to consider this. Usually in these cases one of the ends of column (top) is free, and the other (bottom) is fixed. Let us consider problem of stability of such a bar with constant section by length first under action of only gravity, and then with

joint action of forces of gravity and other loads.*

We take system of coordinates from Fig. 3.8. We designate force of gravity per unit length by p. In section x compressing force is equal to $P_x = px$, and transverse force is

$$Q = P_x \frac{dv}{dx} = px \frac{dv}{dx}. \tag{3.38}$$

Equation (2) we transform to form

$$EI \frac{d^2v}{dx^2} = -Q; \tag{3.39}$$

substituting (38), we obtain

$$EI \frac{d^2v}{dx^2} + px \frac{dv}{dx} = 0. \tag{3.40}$$

We introduce designations

$$\frac{x}{l} = \xi, \quad \frac{dv}{d\xi} = w, \quad \frac{pl^3}{EI} = a^3; \tag{3.41}$$

we arrive at equation

$$\frac{d^2w}{d\xi^2} + a^3 \xi w = 0. \tag{3.42}$$

This equation is integrated in Bessel functions**, paradiseenie has the form

$$w = A\xi^{\frac{1}{2}} J_{\frac{1}{3}}\left(\frac{2}{3} a\xi^{\frac{3}{2}}\right) + B\xi^{\frac{1}{2}} J_{-\frac{1}{3}}\left(\frac{2}{3} a\xi^{\frac{3}{2}}\right). \tag{3.43}$$

Here J(1/3) is a Bessel function of the first type. Derivative of function $J_\nu(\alpha z)$ with respect to z is

$$\frac{dJ_\nu(\alpha z)}{dz} = -\frac{\nu}{z} J_\nu(\alpha z) + \alpha J_{\nu-1}(\alpha z). \tag{3.44}$$

---

*Problem of buckling of column under action of gravity was set by Euler and subsequently considered by Greenhill [3.11], studying in connection with this also shapes of trunks of trees.

**See, for instance, E. Kamke, Handbook on ordinary differential equations, Second edition, Fizmatgiz, 1961, p. 453.

Based on this formula, we find

$$\frac{d}{dz}\left[\xi^{\frac{1}{3}}J_{\frac{1}{3}}\left(\frac{2}{3}\xi\right)^{\frac{3}{2}}\right]=aJ_{-\frac{2}{3}}\left(\frac{2}{3}a\xi^{\frac{3}{2}}\right).$$

Differentiating (43), we obtain

$$\frac{dw}{d\xi}=Aa\xi J_{-\frac{2}{3}}\left(\frac{2}{3}a\xi^{\frac{3}{2}}\right)-Ba\xi J_{\frac{2}{3}}\left(\frac{2}{3}a\xi^{\frac{3}{2}}\right).$$

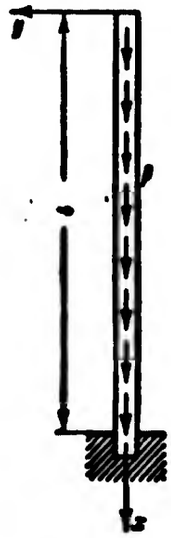

Fig. 3.8. Problem of stability of bar under the influence of gravity.

Boundary conditions of problem will be

$$M=-EI\frac{d^2v}{dx^2}=0 \text{ when } x=0,$$
$$\frac{dv}{dx}=0 \text{ when } x=l$$

or

$$\frac{dw}{d\xi}=0 \text{ when } \xi=0,\quad w=0 \text{ when } \xi=1. \quad (a)$$

As it is known, functions $J_\nu(\xi)$ turn into zero when $\xi = 0$, if subscript $\nu > 0$; if $\nu < 0$, then function $J_\nu(0) = \infty$. In our case $\nu = (1/3)$; consequently, magnitude $J_{1/3}(0) = 0$, while $J_{-2/3}(0) = \infty$. But then the first of conditions (a) may be satisfied only when $A = 0$. Considering $B \neq 0$, from second condition we find

$$J_{-\frac{1}{3}}\left(\frac{2}{3}a\right)=0. \quad (3.45)$$

Least value of argument, with which function $J_{-1/3}$ turns into zero, will be

$$\frac{2}{3}a=1.866. \quad (3.45a)$$

From (41) we find

$$p_{кр}=a^2\frac{EI}{l^3}=7.84\frac{EI}{l^3}. \quad (3.46)$$

We introduce concept of reduced load, understanding by this force $\hat{P}$, concentrated at known point and equivalent to distributed load in problem of stability. We select reduction center at free end; then

$$\frac{EJ}{l^2}=\frac{4}{\pi^2}\hat{P}=\frac{1}{7{,}84}pl$$

and finally

$$\hat{P}=\frac{1}{3{,}18}pl. \tag{3.47}$$

Consequently, reduced force is 1/3, 18th of total weight.

Let us learn solution of this problem without direct application of Bessel functions, by method of exponential series: this method is widely used in analogous problems.

We write solution of equation (42) in the form

$$w=C_0+C_1\xi+C_2\xi^2+C_3\xi^3+\ldots \tag{3.48}$$

Putting this expression in (42), we obtain

$$2C_2+2\cdot 3C_3\xi+3\cdot 4C_4\xi^2+\ldots+a^2(C_0\xi+C_1\xi^2+C_2\xi^3+\ldots)=0. \tag{3.49}$$

Comparing coefficients for identical exponents ξ, we arrive at the following relationships:

$$\left.\begin{aligned} &C_2=0,\quad 2\cdot 3C_3=-a^2C_0,\quad 3\cdot 4C_4=-a^2C_1,\\ &4\cdot 5C_5=-a^2C_3=0,\qquad 5\cdot 6C_6=-a^2C_2=a^4\frac{C_0}{2\cdot 3},\ \ldots \end{aligned}\right| \tag{3.50}$$

Thus, coefficients with subscripts 2, 5, 8, 11, etc., turn into zero: $C_{2+3n}=0$ when $n=0,\ 1,\ 2,\ \ldots$

Remaining coefficients are connected by dependences

$$C_{k+2}=-\frac{a^2}{(k+1)(k+2)}C_{k-1}.$$

It is possible to see that all these coefficients can be expressed by C_0 and C_1:

$$C_3=-\frac{a^2}{2\cdot 3}C_0,\quad C_6=\frac{a^4}{2\cdot 3\cdot 5\cdot 6}C_0,\ \ldots$$
$$C_4=-\frac{a^2}{3\cdot 4}C_1,\quad C_7=\frac{a^4}{3\cdot 4\cdot 6\cdot 7}C_1,\ \ldots$$

Expression for w takes form

$$w = C_0\left(1 - \frac{a^2}{2\cdot 3}\xi^3 + \frac{a^4}{2\cdot 3\cdot 5\cdot 6}\xi^6 - \ldots\right) + \\ + C_1\xi\left(1 - \frac{a^2}{3\cdot 4}\xi^3 + \frac{a^4}{3\cdot 4\cdot 6\cdot 7}\xi^6 - \ldots\right). \qquad (3.51)$$

Derivative with respect to ξ will be equal to

$$\frac{dw}{d\xi} = C_0\left(-\frac{a^2}{2}\xi^2 + \frac{a^4}{2\cdot 3\cdot 5}\xi^5 - \ldots\right) + \\ + C_1\left(1 - \frac{a^2}{3}\xi^3 + \frac{a^4}{3\cdot 4\cdot 6}\xi^6 - \ldots\right). \qquad (3.52)$$

Using the first of boundary conditions (a), we find $C_1 = 0$. The second of these conditions when $C_0 \neq 0$ reduces to equation

$$1 - \frac{a^2}{2\cdot 3} + \frac{a^4}{2\cdot 3\cdot 5\cdot 6} - \frac{a^6}{2\cdot 3\cdot 5\cdot 6\cdot 8\cdot 9} + \ldots = 0. \qquad (3.53)$$

which it is possible to rewrite in the form

$$1 - \frac{3}{2\cdot 4}\left(\frac{2}{3}a\right)^2 + \frac{3^2}{2\cdot 4\cdot 4\cdot 10}\left(\frac{2}{3}a\right)^4 - \frac{3^3}{2\cdot 4\cdot 4\cdot 6\cdot 10\cdot 16}\left(\frac{2}{3}a\right)^6 + \ldots = 0. \qquad (3.54)$$

In left part of this equation there is contained a series, corresponding to Bessel function $J_{-1/3}$ (2/3 a). Thus, we obtained equation, equivalent to (45); its least root is determined by (45a).

Real columns of large dimensions have, as a rule, variable section. In this case direct integration of equation of elastic line is complicated, and therefore, stability calculation must be conducted with help of approximate methods. As example, let us consider one variant of television tower planned for Moscow with height of 520 m* (Fig. 3.9a and b). In Fig. 3.9c is given diagram of longitudinal compressive force (in tons). Determination of safety factor of tower was done with help of method of successive approximations; simultaneously was established form elastic line. Ordinate v_{max} of curve of first approximation at point on top of antenna was taken equal to one.

---

*This calculation belongs to V. Khandzhi. Ordinates of diagrams c) and d) correspond to sections shown by points in Fig. 3.9a.

Further they determined bending moments from vertical forces for a series of sections. It was considered that in these sections there are elastic joints, rigidity of which (in ton--meters) corresponded to diagram of Fig. 3.9d; cut located between calculated sections was assumed absolutely rigid (Section 11). Then they determined new elastic line; comparison of resulting deflection with the initial gave possibility of finding stability factor. In Fig. 3.9e dotted line shows

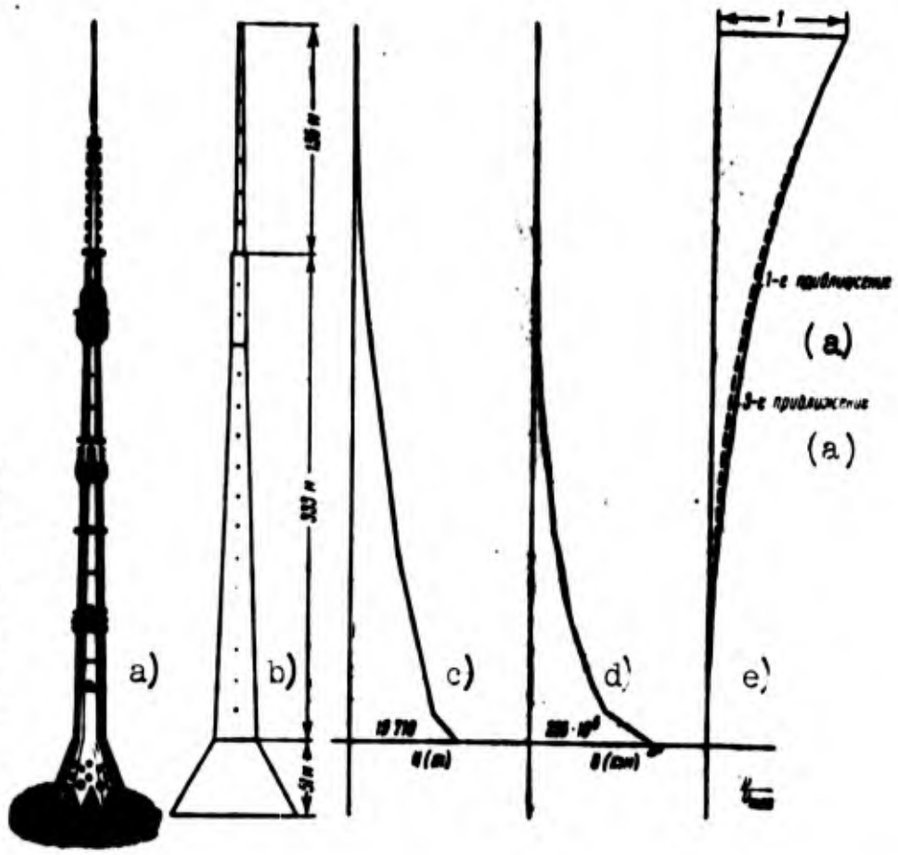

Fig. 3.9. Calculation of television tower for stability.
KEY: (a) approximations.

curve of third approximation, where deflections v anew were related to v_{max}.

§ 38. Simultaneous Action of Distributed and Concentrated Loads

Let us turn to the case where bar is subjected to action of not only of distributed load, but also concentrated force P, applied to free end (Fig. 3.10). For generality we will consider magnitude p variable: $p = p(x)$. We use the Bubnov-Galerkin method; preliminarily we derive initial equation taking into account distributed load. Let us turn to variational equation, obtained in Section 6. Expression for variation of work of internal forces we present in the form (1.88a):

$$\delta A = \left[M\delta\left(\frac{dv}{dx}\right)\right]_0^l + \int_0^l \frac{d}{dx}\left(EI\frac{d^2v}{dx^2}\right)\frac{d}{dx}(\delta v)\,dx; \qquad (3.55)$$

in distinction from Section 37 coordinate x is counted from lower end of bar.

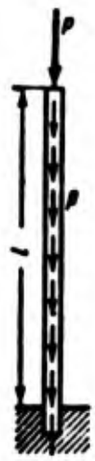

Fig. 3.10. Simultaneous action of concentrated force and gravity for bar with fixed ends.

We calculate work of distributed load, considering its intensity variable with length. On member dx there is load p dx; displacement of center of gravity of element with respect to lower end is

$$e_x = \frac{1}{2}\int_0^x \left(\frac{dv}{dx}\right)^2 dx. \qquad (3.56)$$

Total work of distributed load is equal to

$$W = \frac{1}{2}\int_0^l p\left[\int_0^x \left(\frac{dv}{du}\right)^2 du\right]dx. \qquad (3.57)$$

We introduce designations R_x, R_{l-x}, R_l for resultants of load from

0 to x, from x to l and for the whole length:

$$R_x = \int_0^x p\,du. \quad R_{l-x} = \int_x^l p\,du = R_l - R_x. \quad R_l = \int_0^l p\,dx. \tag{3.58}$$

Integrating expression (57) by parts, we obtain

$$W = \frac{1}{2}\left[R_x \int_0^x \left(\frac{dv}{du}\right)^2 du\right]_0^l - \frac{1}{2}\int_0^l R_x \left(\frac{dv}{dx}\right)^2 dx.$$

or

$$W = \frac{1}{2} R_l \int_0^l \left(\frac{dv}{dx}\right)^2 dx - \frac{1}{2}\int_0^l R_x \left(\frac{dv}{dx}\right)^2 dx. \tag{3.59}$$

Finally

$$W = \frac{1}{2}\int_0^l R_{l-x}\left(\frac{dv}{dx}\right)^2 dx. \tag{3.60}$$

Variation of δW is equal to

$$\delta W = \int_0^l R_{l-x} \frac{dv}{dx} \frac{d}{dx}(\delta v)\,dx. \tag{3.61}$$

This magnitude must be added to expression (1.95a); total variation of work of external forces will be

$$\delta W = \int_0^l (P + R_{l-x}) \frac{dv}{dx} \frac{d}{dx}(\delta v)\,dx. \tag{3.62}$$

Variational equation can, consequently, be presented in the form

$$\left[M\delta\left(\frac{dv}{dx}\right)\right]_0^l + \int_0^l \left[\frac{d}{dx}\left(EI\frac{d^2v}{dx^2}\right) + (P + R_{l-x})\frac{dv}{dx}\right]\frac{d}{dx}(\delta v)\,dx = 0; \tag{3.63}$$

rigidity EI here for generality is assumed variable. Putting instead of δv expression (1.126) and taking integral member equal to zero, we obtain fundamental equation of Bubnov-Galerkin method:

$$\int_0^l \left[\frac{d}{dx}\left(EI\frac{d^2v}{dx^2}\right) + (P + R_{l-x})\frac{dv}{dx}\right]\frac{d\eta_i}{dx}\,dx = 0. \quad i = 1, 2, \ldots, n. \tag{3.64}$$

Let us consider case where, along with concentrated force P

there must be calculated gravity of the bar $p_0 l$, where EI = const. Instead of (64) we obtain

$$\int_0^l \left\{ EI \frac{d^2v}{dx^2} + [P + p_0(l-x)] \frac{dv}{dx} \right\} \frac{d\eta_1}{dx} dx = 0. \tag{3.65}$$

Equation of elastic line is taken in a form corresponding to case of one concentrated force:

$$v = f\left(1 - \cos \frac{\pi x}{2l}\right). \tag{3.66}$$

Taking

$$\eta = 1 - \cos \frac{\pi x}{2l} \tag{3.67}$$

and substituting the last two expressions in (65), we find

$$\int_0^l \left\{ -EI \frac{\pi^3}{8l^3} \sin^2 \frac{\pi x}{2l} + \right.$$
$$\left. + [P + p_0(l-x)] \frac{\pi}{2l} \sin^2 \frac{\pi x}{2l} \right\} dx = 0. \tag{3.68}$$

Integrating, we obtain

$$EI \frac{\pi^2}{4l^2} = P + \left(\frac{1}{2} - \frac{2}{\pi^2}\right) p_0 l. \tag{3.69}$$

or

$$EI \frac{\pi^2}{4l^2} \approx P + 0.3 p_0 l. \tag{3.70}$$

Consequently, calculation for buckling can be conducted in considered case, joining to concentrated force 3/10 of gravity of bar and considering this reduced load applied to free end of bar. If load p_0 is significant, then with a total critical force equal to (70), force P can be negative, i.e., tensile. Result obtained by us well agrees with solution of problem in Bessel functions, since by (47) when P = 0 we obtained reduced load equal to $\sim 0.31 p_0 l$.

Consider the same problem on the assumption that both ends of bar are supported by hinges (Fig. 3.11). Selecting expression for v

in the form

$$v = f \sin \frac{\pi x}{l} \tag{3.71}$$

and substituting it in equation (65), we arrive at relationship

$$EI \frac{\pi^2}{l^2} = P + \frac{1}{2} p_0 l. \tag{3.72}$$

Here reduced load turns out to be equal to <u>half</u> the gravity of the bar.

Fig. 3.11. Combined action of load on bar, supported by hinges at its ends.

§ 39. Bar, Subjected to Action of Axial Force and End Couples

Let us assume that bar, supported by hinges at its ends, is subjected to joint action of axial force P and a pair, applied to end section B, moment of which is equal to M_0. We determine elastic line of bar: this will be important subsequently during research of stability of bars which lie on several supports. Considering force to be compressive (Fig. 3.12), we find bending moment in sections:

$$M = \frac{M_0}{l} x + Pv. \tag{3.73}$$

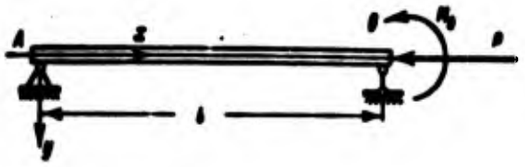

Fig. 3.12. Bending of bar under action of axial force and couple.

Differential equation of elastic line has the form

$$EI\frac{d^2v}{dx^2}+Pv=-\frac{M_0}{l}x \tag{3.74}$$

or

$$\frac{d^2v}{dx^2}+k^2v=-\frac{M_0}{EI}\frac{x}{l}. \tag{3.75}$$

Here as before $k^2 = P/EI$. Solution of equation (75) has the form

$$v=A\cos kx+B\sin kx-\frac{M_0}{EIk^2}\frac{x}{l}. \tag{3.76}$$

Considering boundary conditions v = 0 when x = 0, and x = l, we find

$$v=\frac{M_0}{EIk^2}\left(\frac{\sin kx}{\sin kl}-\frac{x}{l}\right). \tag{3.77}$$

Angle of rotation at left support will be

$$\theta_A=\left(\frac{dv}{dx}\right)_A=\frac{M_0l}{EI}\left(\frac{1}{kl\sin kl}-\frac{1}{k^2l^2}\right). \tag{3.78}$$

for right support

$$\theta_B=\left(-\frac{dv}{dx}\right)_B=\frac{M_0l}{EI}\left(\frac{1}{k^2l^2}-\frac{1}{kl\operatorname{tg}kl}\right). \tag{3.79}$$

We will use designations

$$u=kl=l\sqrt{\frac{P}{EI}}. \tag{3.80}$$

$$\varphi(u)=\frac{1}{u\sin u}-\frac{1}{u^2}. \tag{3.81}$$

$$\chi(u)=\frac{1}{u^2}-\frac{1}{u\operatorname{tg}u}. \tag{3.82}$$

then we obtain

$$\theta_A=\frac{M_0l}{EI}\varphi(u),\quad \theta_B=\frac{M_0l}{EI}\chi(u). \tag{3.83}$$

Let us assume that force P is tensile. Comparing equations (74) and (75), we conclude that in this case we can use all calculating formulas, replacing k^2 by $(-k^2)$, k by ik and u by iu, where $i=\sqrt{-1}$. Then instead of (81) and (82) we find

$$\varphi_1(u)=-\frac{1}{u\operatorname{sh}u}+\frac{1}{u^2}. \tag{3.84}$$

$$\chi_1(u)=-\frac{1}{u^2}+\frac{1}{u\operatorname{th}u}. \tag{3.85}$$

Table 3.3

Auxiliary functions

α	For compressed members		For stretched members	
	$\varphi(\alpha)$	$\chi(\alpha)$	$\varphi_1(\alpha)$	$\chi_1(\alpha)$
0	0,1667	0,3333	0,1667	0,3333
0,1	0,1669	0,3336	0,1665	0,3331
0,2	0,1674	0,3342	0,1659	0,3324
0,3	0,1684	0,3354	0,1649	0,3314
0,4	0,1698	0,3369	0,1636	0,3298
0,5	0,1717	0,3390	0,1619	0,3279
0,6	0,1739	0,3416	0,1599	0,3256
0,7	0,1767	0,3448	0,1576	0,3229
0,8	0,1800	0,3485	0,1550	0,3199
0,9	0,1839	0,3528	0,1522	0,3166
1,0	0,1884	0,3579	0,1491	0,3130
1,1	0,1936	0,3637	0,1458	0,3092
1,2	0,1997	0,3705	0,1424	0,3052
1,3	0,2066	0,3782	0,1388	0,3009
1,4	0,2146	0,3870	0,1351	0,2966
1,5	0,2239	0,3972	0,1313	0,2921
1,6	0,2346	0,4089	0,1275	0,2875
1,7	0,2472	0,4224	0,1237	0,2828
1,8	0,2618	0,4383	0,1198	0,2781
1,9	0,2792	0,4568	0,1160	0,2734
2,0	0,2999	0,4788	0, 121	0,2687
2,1	0,3249	0,5053	0,1084	0,2639
2,2	0,3556	0,5375	0,1046	0,2592
2,3	0,3940	0,5775	0,1010	0,2546
2,4	0,4433	0,6285	0.0974	0,2500
2,5	0,5084	0,6955	0,0939	0,2454
2,6	0,5982	0,7873	0,0905	0,2410
2,7	0,7294	0,9207	0,0872	0,2366
2,8	0,9386	1,1321	0,0840	0,2322
2,9	1,3224	1,5183	0,0808	0,2280
3,0	2,2509	2,4495	0,0778	0,2239
3,1	7,6539	7,8553	0,0749	0,2198
3,2	—5,4511	—5,2466	0,0721	0,2159
3,3	—2,0128	—1,8051	0,0694	0,2120
3,4	—1,2375	—1,0262	0,0669	0,2083
3,5	—0,8961	—0,6811	0,0644	0,2046
3,6	—0,7049	—0,4858	0,0620	0,2010

table continued on following page

continuation of Table 3.3

u	For compressed members		For stretched members	
	$\varphi(u)$	$\chi(u)$	$\varphi_1(u)$	$\chi_1(u)$
3,7	—0,5831	—0,3596	0,0597	0,1976
3,8	—0,4994	—0,2709	0,0575	0,1942
3,9	—0,4386	—0,2049	0,0554	0,1909
4,0	—0,3928	—0,1534	0,0533	0,1877
4,1	—0,3576	—0,1118		
4,2	—0,3299	—0,0772		
4,3	—0,3079	—0,0477		
4,4	—0,2905	—0,0217		
4,5	—0,2775	0,0015		
4,6	—0,2660	0,0227		
4,7	—0,2581	0,0426		
4,8	—0,2525	0,0617		
4,9	—0,2494	0,0804		
5,0	—0,2486	0,0992		
5,1	—0,2502	0,1185		
5,2	—0,2547	0,1390		
5,3	—0,2623	0,1613		
5,4	—0,2739	0,1864		
5,5	—0,2908	0,2157		
5,6	—0,3148	0,2513		
5,7	—0,3494	0,2967		
5,8	—0,4008	0,3583		
5,9	—0,4821	0,4492		
6,0	—0,6243	0,6005		

On p.160 , is given table for functions φ, χ, φ_1, and χ_1 for various smelled values of u.

§ 40. Bar Lying on Several Rigid Supports

In Fig. 3.13 is depicted a bar lying on three tip bearings. We will assume that in left span of length l_1 rigidity of bar is equal to E_1I_1, and in right one of length l_2 it is equal to E_2I_2 and that compressive forces P_1 and P_2 differ.

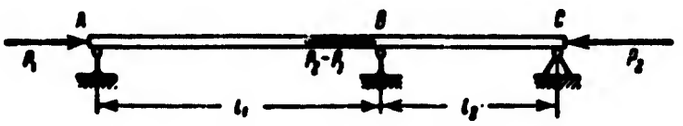

Fig. 3.13. Two-span bar.

In order to consider stability of such a bar, we use formulas obtained in Section 39.

For each span it is possible to write equation of elastic line of type (77), since influence of neighboring span is expressed in action of support moment M_0. Angle of rotation to left of support B will be

$$\theta_{B,1} = \frac{M_0 l_1}{E_1 I_1} \chi(u_1).$$

and to right of support

$$\theta_{B,2} = \frac{M_0 l_2}{E_2 I_2} \chi(u_2);$$

here we designate

$$u_1 = l_1 \sqrt{\frac{P_1}{E_1 I_1}}. \quad u_2 = l_2 \sqrt{\frac{P_2}{E_2 I_2}}. \tag{3.86}$$

Angles $\theta_{B,1}$ and $\theta_{B,2}$ must be equal in magnitude and opposite in sign; consequently, when $M_0 \neq 0$ this condition is written in the form

$$\frac{l_1}{E_1 I_1} \chi(u_1) + \frac{l_2}{E_2 I_2} \chi(u_2) = 0. \tag{3.87}$$

From equation (87) it is possible to determine critical combination of loads P_1 and P_2. Let us assume that rigidities of spans are identical: then by (87) we find

$$\frac{\chi(u_1)}{\chi(u_2)} = -\frac{l_2}{l_1}. \tag{3.88}$$

If however, lengths of spans are equal, then condition (87) cannot be satisfied; here it is necessary to set $M_0 = 0$. Hence $\chi(u_1) = \chi(u_2) = \infty$; but then we have $u = \pi$ and critical load will be determined by the ordinary Euler's formula (1.15). Equation (88) can be so interpreted that in shorter span support moment "helps" compressive forces P to bend the bar, while in longer, it "hinders" them.

If we assume that in one span (for instance, the left) force P is compressive, and in the other (right)--tensile, then instead of (87) we obtain

$$\frac{l_1}{E_1 I_1} \chi(u_1) + \frac{l_2}{E_2 I_2} \chi_1(u_2) = 0. \tag{3.89}$$

Equations (88) or (89) are solved by means of trial and error with help of Table 3.3.

Fig. 3.14. Two sections of multispan bar.

Assume now that <u>number of spans exceeds two</u>. Then it is possible to consider two neighboring spans n - 1 and n (Fig. 3.14) and again write condition $\theta_{n,1} + \theta_{n,2} = 0$; but here it is necessary to calculate influence of second support moment. For three neighboring supports we apply indices n - 1, n and n + 1. To left of middle support angle $\theta_{n,1}$ will be equal to

$$\theta_{n,1} = \frac{M_{n-1}l_{n-1}}{E_{n-1}J_{n-1}}\varphi(u_{n-1}) + \frac{M_n l_{n-1}}{E_{n-1}J_{n-1}}\chi(u_{n-1}). \tag{3.90}$$

to the right of support angle $\theta_{n,2}$ will be

$$\theta_{n,2} = \frac{M_{n+1}l_n}{E_n J_n}\varphi(u_n) + \frac{M_n l_n}{E_n J_n}\chi(u_n). \tag{3.91}$$

Equating the sum of these expressions to zero we obtain <u>equation of three moments</u>:

$$\frac{M_{n-1}l_{n-1}}{E_{n-1}J_{n-1}}\varphi(u_{n-1}) + M_n\left[\frac{l_{n-1}}{E_{n-1}J_{n-1}}\chi(u_{n-1}) + \frac{l_n}{E_n J_n}\chi(u_n)\right] + \\ + \frac{M_{n+1}l_n}{E_n J_n}\varphi(u_n) = 0. \tag{3.92}$$

Writing similar equations for every pair of spans, we obtain system of uniform three-term linear equations for moments M_1, M_2, etc. System of critical loads will be found, if we equate to zero the determinant, composed of coefficients for M_1, M_2, etc., in these equations.

Let us assume that end supports are hinged. Introducing designation

$$s = \frac{l}{EJ}, \tag{3.93}$$

we find the final equation in the form

$$\begin{vmatrix} s_0\chi(u_0) + s_1\chi(u_1) & s_1\varphi(u_1) & 0 & 0 \\ s_1\varphi(u_1) & s_1\chi(u_1) + s_2\chi(u_2) & s_2\varphi(u_2) & 0 \\ 0 & s_2\varphi(u_2) & s_2\chi(u_2) + s_3\chi(u_3) & s_3\varphi(u_3) \\ 0 & 0 & s_3\varphi(u_3) & s_3\chi(u_3) + s_4\chi(u_4) \dots \\ \dots & \dots & \dots & \dots \end{vmatrix} = 0. \tag{3.94}$$

For two-span bar determinant will consist only of one member; for three-span one it is necessary to take two first members in the first and second lines, etc.

Calculation of bar can be conducted by (87) or (89) also when in all spans or in certain of them critical stress exceeds elastic limit. In formula (86) and subsequent ones one should then introduce instead of moduli E resultant moduli T or tangents E_k. One should have in mind that magnitudes of these moduli depend on sought for critical stresses; therefore, calculation may be carried out only after several tries.

Example 3.3. Feed spindle AB of lathe-screw machine receives feed force transmitted to it from cutting tool through nut C traveling along spindle (Fig. 3.15). Spindle should be calculated for stability on the assumption that nut is in extreme right position, distance l_2, from support C, and transmits to section of screw AC, having length l_1, compressive forces P. Determine inner diameter d of spindle in two cases: 1) nut has small length and must be considered an intermediate hinged support (Fig. 3.15a); 2) length of nut is great, and screw should be considered clamped in support C (Fig. 3.51b).

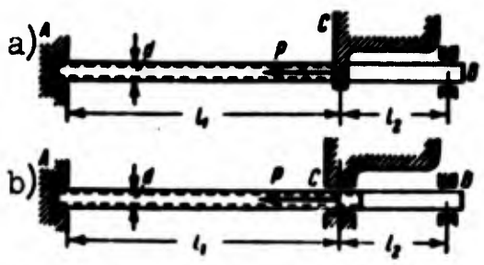

Fig. 3.15. Calculation of feed spindle of lathe-screw machine.

Ends of spindle A and B in both cases are assumed secured by hinge. Take P = 900 kg, coefficient of stability margin n = 3.5, l_1 = 150 cm, l_2 = 50 cm. Material is St. 5 steel, $E = 2.1 \cdot 10^6$ kg/cm^2, $\sigma_{cr} = 2800$ kg/cm^2. When calculating moment of inertia of section ignore influence of threading.

In first case we obtain bar with three supports; force in first section is $P_{кр}$; in second, zero. Since rigidity is constant with length, we use equation (88):

$$\frac{\chi(u_1)}{\chi(0)} = -\frac{l_2}{l_1}.$$

By Table 3.3 we find $\chi(0) = 0.333$. Consequently,

$$\chi(u_1) = -\frac{50}{150} \cdot 0{,}333 = -0{,}111.$$

To this value of χ corresponds u_1 4.1. By formula (80)

$$(k_1 l_1)^2 = u_1^2 = 16{,}81.$$

Critical force should be equal to $P_{кр} = nP = 3150$ kg. Moment of inertia of section will be

$$I = \frac{P_{кр} l_1^2}{16{,}81 E} = \frac{3150 \cdot 150^2}{16{,}81 \cdot 2{,}1 \cdot 10^6} \approx 2 \text{ см}^4;$$

hence diameter of spindle d = 26 mm, area of cross-section 5.3 cm^2. Critical stress

$$\sigma_{кр} = \frac{3150}{5{,}3} = 600 \text{ кг/см}^2$$

lies within limits of proportionality.

If we ignore influence of section CB and to consider both supports A and C hinged, then we obtain parameter u_1^2 equal to π^2; critical load would turn out to be 41% less.

In the second case spindle on section AC must be considered a bar, one end of which is secured by hinge, and the other is clamped. Parameter u_1^2 is equal to $2\pi^2$. We find I = 1.7 cm^4, d = 24 mm.

§ 41. Case of Elastic Support. Problem of Bar Set.

We considered up to now intermediate supports to be rigid. However, in practical calculations such an assumption can not always be made. We imagine, for instance, bar AB (Fig. 3.16a), compressed by forces P and connected in the middle of its length with a perpendicularly located transverse rod CD. During buckling of the first of these bars the second is an elastic support for it. In more general case instead of cross-bar it is possible to imagine a certain linear

elastic support with rigidity c (Fig. 3.16b). We determine critical force for bar AB, considering first that elastic line is symmetric relative to middle section. We designate deflection in the middle f; then components of reactions of supports will be P and cf/2. Differential equation of elastic line for half obtains form

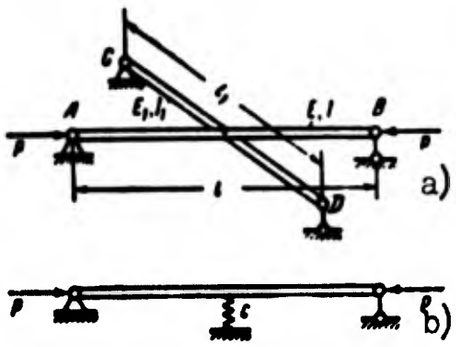

Fig. 3.16. Bar with elastic support.

$$EI\frac{d^2v}{dx^2}=-Pv+\frac{cf}{2}x; \qquad (3.95)$$

solution of it will be

$$v=A\cos kx+B\sin kx+\frac{cf}{2P}x. \qquad (3.96)$$

where $k^2 = P/EI$. We subordinate this solution to these conditions:

$$v=0 \text{ when } x=0,\ \frac{dv}{dx}=0 \text{ and } v=f \text{ when } x=\frac{l}{2}. \qquad (3.97)$$

From first two conditions we find

$$A=0,\quad B=-\frac{cf}{2Pk\cos\frac{kl}{2}},$$

and the third, when $f \neq 0$, leads to relationship

$$\operatorname{tg}\frac{kl}{2}-\frac{kl}{2}\left(1-4\frac{P}{cl}\right)=0. \qquad (3.98)$$

If however, the elastic line is antisymmetric, the middle section does not have deflection. But then each half of the bar buckles as an independent bar, supported by hinge at its ends; critical force will be

$$P_0=\frac{\pi^2EI}{(l/2)^2}. \qquad (3.99)$$

We reduce relationship (98) to dimensionless form:

$$\operatorname{tg}(\pi\sqrt{\nu})-\pi\sqrt{\nu}\left(1-\frac{2\nu}{\bar{c}}\right)=0. \qquad (3.100)$$

where

$$\nu=\frac{P}{P_0},\quad \bar{c}=\frac{cl}{2P_0}. \qquad (3.101)$$

Curve $\nu(\bar{c})$, found by (100), is depicted in Fig. 3.17.* If $\bar{c} = 0$, when there is no middle support, we will have $P = 0.25P_э$. If $c \to \infty$, then instead of (98) we obtain equation (1.42), corresponding to case of bar with one end supported by hinge and the other clamped; here $P \approx 2P_э$. But "symmetric" solution of (100) has practical value only when $P \leq P_э$, $\nu \leq 1$, which corresponds to $\bar{c} = 2$. On sloping section dependence can be approximately presented as linear:

$$\nu = \frac{1}{4} + \frac{3}{8}\bar{c}. \tag{3.102}$$

Rigidity of support $\bar{c}$, at which in problem of stability of bar this support can be considered undisplaced, is called critical. In considered case critical rigidity of support is equal to

$$\bar{c}_* = 2, \quad c_* = \frac{4\pi^2 EI}{l^3}. \tag{3.103}$$

Let us turn now to initial diagram of Fig. 3.16a, where role of elastic support is executed by bar of length l_1 and rigidity E_1I_1. Assuming that this bar is secured by hinges at its ends and that point of intersection lies in the middle of length, we find its critical rigidity from relationship

$$\frac{48E_1I_1}{l_1^3} = \frac{4\pi^2 EI}{l^3},$$

hence

$$(E_1I_1)_* = \frac{\pi^2}{12} EI\left(\frac{l_1}{l}\right)^3. \tag{3.104}$$

This problem is easy to solve with help of the energy method. We take for case of symmetric deflection

$$v = f \sin \frac{\pi x}{l}$$

and write equation of energy according to (1.121), considering potential energy of elastic support:

---

*This graph is taken from book [0.21], p. 96.

$$\frac{P}{2}\int_0^l \left(\frac{dv}{dx}\right)^2 dx = \frac{EI}{2}\int_0^l \left(\frac{d^2v}{dx^2}\right)^2 dx + \frac{cf^2}{2};$$

then finally we obtain

$$\nu = \frac{1}{4} + \frac{4}{\pi^2}\bar{c},$$

which differs little from (102).

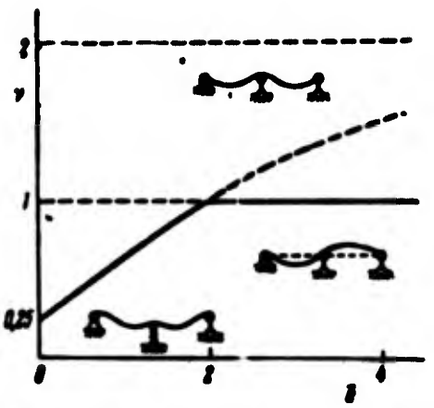

Fig. 3.17. Dependence between load and rigidity of support.

A similar study may be conducted for the more complicated system of a bar set (Fig. 3.18), composed of beams of principal direction and beams supporting them --transverse constraints. Stability problem of such a system is of practical value for many constructions, such as, for instance, coverings in hull of a ship, and was first formulated by I. G. Bubnov [0.2]. Basic goal here consisted in determining critical rigidity of transverse constraints P. F. Papkovich applied for solution of this problem the energy method [0.7], and A. M. Penkov--the method of finite differences [3.6], A. A. Kurdyumov proposed to consider closely spaced transverse constraints as a solid elastic support (see Section 42) for beams of the principal direction.*

We considered above that interaction of crossed bars is expressed only in the force, normal to the plane formed by them. In certain cases, however, it is necessary to consider that transverse constraints prevent not normal displacements, but turns of corresponding sections of the beams of the principal direction; in this case one should consider torsional rigidity of transverse constraints; furthermore, it is

*See works of A. A. Krudyumov in "Transactions of Leningrad, Shipbuilding Institute," No. 11 (1953) and in journal "Shipbuilding," No. 11-12, (1941).

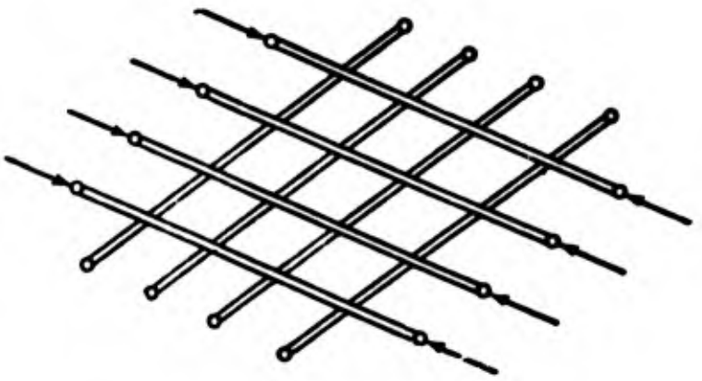

Fig. 3.18. Crossed bar set.

necessary to consider conditions of fastening of beams in each direction, differing from hinged.*

If beam of cross-set are fairly closely spaced, the set may be replaced by an anisotropic plate;** then for calculation of set we can use equations of the stability theory of plates (see Chapter VII below).

§ 42. Stability of Bar Connected with Elastic Foundation.

Imagine that bar, supported by hinges at its ends, is connected with solid elastic foundation (Fig. 3.19). Let us assume that reaction of foundation per unit length of bar is proportional to displacement:

$$R = cv, \tag{3.105}$$

dimension of coefficient c will be kg/cm^2.

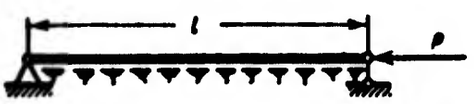

Fig. 3.19. Bar on elastic foundation.

Differential equation of elastic line we take in the form of (1.7). Substituting q = -R, we obtain

$$EI\frac{d^4v}{dx^4} + P\frac{d^2v}{dx^2} + cv = 0. \tag{3.106}$$

*Similar problems are considered with help of method of finite differences by Ye. S. Voyt in work "Study of stability of a crossed bar set" (Cond. diss., M., 1951) and by N. A. Ventsel' (Collected Works of Institute of Structural Mechanics, Academy of Sciences of Ukrainian SSR, No. 15, 1950).

**Such method was offered by L. Ya. Reznitskiy.

If one were to use designations

$$\frac{P}{EJ}=k^2, \quad \frac{c}{EJ}=r. \tag{3.107}$$

that instead of (106) we will have the following homogeneous linear equation

$$\frac{d^4v}{dx^4}+k^2\frac{d^2v}{dx^2}+rv=0. \tag{3.108}$$

Corresponding characteristic equation has the form

$$p^4+k^2p^2+r=0; \tag{3.109}$$

its roots will be

$$p^2=-\frac{k^2}{2}\pm\sqrt{\frac{k^4}{4}-r}. \tag{3.110}$$

We assume p = im, where $i=\sqrt{-1}$; then

$$m^2=\frac{k^2}{2}\mp\sqrt{\frac{k^4}{4}-r}. \tag{3.111}$$

Solution of equation (108) obtains the form

$$v=A\sin mx+B\cos mx+Cx+D. \tag{3.112}$$

Proceeding from boundary conditions (1.9), we obtain B = C = D = 0.

When A ≠ 0 we have

$$\sin ml=0; \tag{3.113}$$

hence

$$m^2=\frac{n^2\pi^2}{l^2}, \quad n=1, 2, 3, \ldots \tag{3.114}$$

Determining k^2 by (111) and using (114), we find

$$k^2=\frac{P}{EJ}=\frac{n^2\pi^2}{l^2}+\frac{rl^2}{n^2\pi^2}. \tag{3.115}$$

Bending line consists of n half sine wave:

$$v=A\sin\frac{n\pi}{l}x. \tag{3.116}$$

In distinction from freely bending bar here number of half-waves n ≠ 1; it should be determined from condition of minimum load. In Fig. 3.20 on axis of abscissas are values $\bar{r}=r(l/\pi)^4$, and along the axis of ordinates--ratio $P/P_э$, where $P_э$--is Euler's force for a bar without an elastic foundation. Taking n = 1, 2, 3, ..., we obtain series of straight lines; segments of these straight lines, shown by heavy line, are the design lines. Transition from n-th branch to (n + 1) th corresponds to magnitude r, determined from equality

$$\frac{n^2\pi^2}{l^2}+\frac{rl^2}{n^2\pi^2}=\frac{(n+1)^2\pi^2}{l^2}+\frac{rl^2}{(n+1)^2\pi^2};$$

hence

$$r = n^2(n+1)^2\frac{\pi^2}{l^2}. \qquad (3.117)$$

Corresponding values of k will be

$$k^2 = \frac{\pi^2}{l^2}[n^2+(n+1)^2]. \qquad (3.118)$$

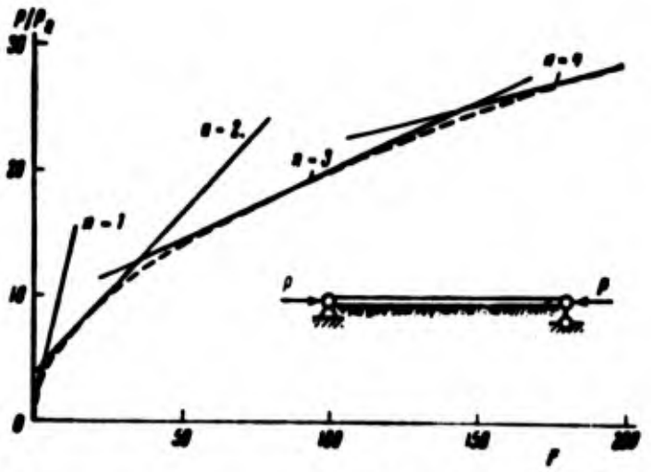

Fig. 3.20. Graph for calculation of bar on elastic foundation.

If number of half-waves n is sufficiently great, then we can write condition of minimum k^2, equating to zero the derivative of k^2 with respect to $n\pi/l$:

$$\frac{d(k^2)}{d\left(\frac{n\pi}{l}\right)} = 2\frac{n\pi}{l} - 2\frac{rl^2}{n^3\pi^3} = 0;$$

here

$$\frac{n\pi}{l} = \sqrt[4]{r}.$$

Critical load by (115) turns out to be

$$P_{cr} = 2EI\sqrt{r} = 2\sqrt{EIc}. \qquad (3.119)$$

In dimensionless magnitudes

$$\frac{P_{cr}}{P_0} = 2\sqrt{r}. \qquad (3.120)$$

Formula (120) corresponds to limiting line shown in Fig. 3.20 by dotted line.

Example 3.4. Duralumin bar, located in compressed zone of aircraft fuselage (stringer), must be calculated for stability (Fig. 3.21).

Length of stringer l = 2 m; ends rest on rigid supports; in span it is supported by closely spaced transverse constraints (ribs), lying equal distance one from the other: s = 20 cm. Ribs can be considered as beams on two supports, supported by hinges at ends, of length a = 50 cm. Moment of inertia of cross-section of stringer I = 1 cm^4, and of rib --I_1 = 0.1 cm^4; area of section of stringer F = 1.5 cm^2, E = $0.7 \cdot 10^6$ kg/cm^2, σ_{cu} = 2200 kg/cm^2. Determine critical force $P_{кр}$ for stringer and length of half-wave $l_{кр}$ at loss of stability.

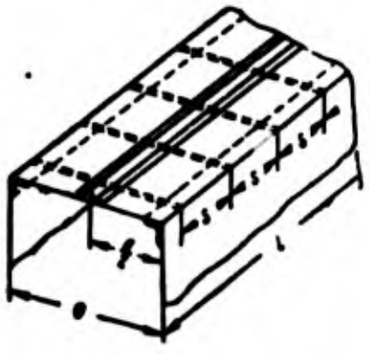

Fig. 3.21. Calculating stringer in compressed zone of aircraft fuselage.

We shall consider stringer to be a compressed beam, lying on elastic foundation. Reactive forces transmitted to stringer from ribs we consider evenly distributed along stringer. Reactive force for each rib is equal to

$$R = \frac{48EI_1}{a^3} v,$$

where v is deflection of stringer. Stiffness coefficient of elastic foundation will be

$$c = \frac{\frac{R}{v}}{s} = \frac{48EI_1}{a^3 s} = \frac{48 \cdot 0.7 \cdot 10^6 \cdot 0.1}{50^3 \cdot 20} = \frac{\text{kg/cm of deflection}}{\text{cm of length}}$$

Hence

$$\bar{r} = r\left(\frac{l}{\pi}\right)^4 = \frac{c}{EI}\left(\frac{l}{\pi}\right)^4 = \frac{1.34 \cdot 200^4}{0.7 \cdot 10^6 \cdot 1 \cdot \pi^4} = 19.5.$$

Value $\bar{r}$ = 19.5 lies between quantities $r = 1 \cdot 2^2$ and $2^2 \cdot 3^2$; consequently, at loss of stability of stringer there should form a half-wave of length $l_{кр}$ = 1 m. We find from (115) (see also graph of Fig. 3.20)

$$\frac{P_{кр}}{P_э} = n^2 + \frac{\bar{r}}{n^2} = 4 + \frac{19.5}{4} = 8.9,$$

where $P_э$ is Euler's force:

$$P_э = \frac{\pi^2 EI}{l^2} = \frac{\pi^2 \cdot 0.7 \cdot 10^6 \cdot 1}{200^2} = 173 \text{ kg}.$$

Finally $P_{кр}$ = 1540 kg; corresponding stress $\sigma_{кр} = P_{кр}/F$ = 1150 kg/cm^2 does not exceed limit of proportionality $\sigma_{пц}$.

§ 43. Influence of Transverse Force on Critical Load.

We used till now equation of bending line of bar, composed without calculation of influence of transverse force. As it is known from theory of bending of beams, this influence in case of solid section is negligible. However, for compound bars with comparatively weak lattice influence of transverse force must be taken into account.

We will explain how much magnitude of critical load changes if one were to consider influence of tangential stresses on deflection of bar. For this we use definitized differential equation of elastic line

$$\frac{d^2v}{dx^2} = -\frac{M}{EI} + \varkappa\frac{1}{GF}\frac{d^2M}{dx^2}; \tag{3.121}$$

here $\varkappa$ is numerical factor, depending on form of cross section. For case of bar with ends supported by hinges we have M = Pv; equation (121) takes form

$$\frac{d^2v}{dx^2} - \frac{\varkappa}{GF}P\frac{d^2v}{dx^2} + \frac{P}{EI}v = 0. \tag{3.122}$$

Solution of this equation, corresponding to condition v = 0 when x = 0, will be

$$v = A\sin k_1 x. \tag{3.123}$$

where

$$k_1^2 = \frac{P}{EI}\frac{1}{1-\frac{\varkappa P}{GF}}. \tag{3.124}$$

Condition v = 0 when x = l gives $k_1 = n\pi/l$. Taking n = 1 and determining P by (124), we find critical load equal to

$$P_{кр} = \frac{\pi^2 EI}{l^2}\frac{1}{1+\frac{\varkappa}{GF}\frac{\pi^2 EI}{l^2}} \tag{3.125}$$

or

$$P_{кр} = \frac{\pi^2 EI}{l^2}\frac{1}{1+2(1+\mu)\varkappa\frac{\pi^2}{\lambda^2}}, \tag{3.126}$$

where μ is Poisson's ratio, λ is slenderness ratio of the bar. Thus,

wishing to determine critical load taking into account influence of tangential stresses, we must intead of bar length substitute in Euler's formula reduced length $l_0 = \nu l$; reduction factor is

$$\nu = \sqrt{1 + 2(1+\mu)\varkappa \frac{\pi^2}{\lambda^2}}. \qquad (3.127)$$

As we shall see, value of critical force is somewhat less than that calculated by the Euler's formula. Formula (125) can be extended to elastoplastic region, replacing modulus E by resultant or tangential modulus. Putting instead of μ the greatest possible value 0.5 and considering $\varkappa$ for a rectangular section equal to 1.2, we obtain

$$\nu = \sqrt{1 + \frac{35{,}5}{\lambda^2}}. \qquad (3.128)$$

When $\lambda = 100$ reduced length will only exceed true length of bar by 0.18%. For short bars value will be larger, but for them critical stress comparatively weakly changes depending upon flexibility.

§ 44. Stability of Compound Bars.

As compressed elements of various constructions there frequently are applied bars, composed of two branches, joined by a lattice or strips.* Let us consider a bar with a lattice, consisting of diagonals, as shown in Fig. 3.22. Distance between centers of gravity of sections of branches we designate by h; length of section--by a; length diagonal - by d. We shall consider that magnitude h significantly exceeds height of section of individual branch and that moment of inertia of whole section can be approximately determined by the formula

$$I = \frac{1}{2} F_1 h^2 = \frac{1}{4} F h^2, \qquad (3.129)$$

where F_1 is area of section of branch, F is total area of section.

*The way of solving the problem used here belongs (in several variants) to F. Engesser [2.11], S. P. Timoshenko (News of Kiev Polytechnic Institute, 1908), L. Prandtl (Z. VDI, 1907) and F. Bleich [0.15]. Another direction, based on calculating model with continuous constraints of non-dilational strain was developed by A. R. Rzhanitsyn [3.8]; see also his book [0.10].

Influence of transverse force, causing strain of bars of lattice, it is possible to account for, using data from the preceding section. Initial equation (121) is derived on the assumption that the mean shear γ by section of bar is connected with transverse force by relationship

$$\gamma = \varkappa \frac{Q}{GF}. \tag{3.130}$$

For compound bars in formulas of Section 43 it is possible to place instead of w/GF ratio γ/Q, corresponding one or another type of connecting lattice. In Fig. 3.23 is depicted how configuration of section of bar changes during strain of the diagonal; the number of section by length we consider sufficiently large. Force $N_д$ in diagonal may be expressed by transverse force:

$$N_д = Q \frac{d}{h}. \tag{3.131}$$

Absolute elongation of diagonal will be

$$\lambda_д = \frac{Qd^2}{EF_д h}. \tag{3.132}$$

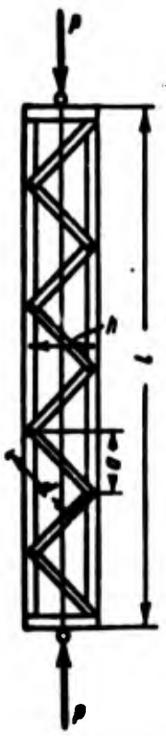

Fig. 3.22. Compound bar with lattice, consisting of diagonals.

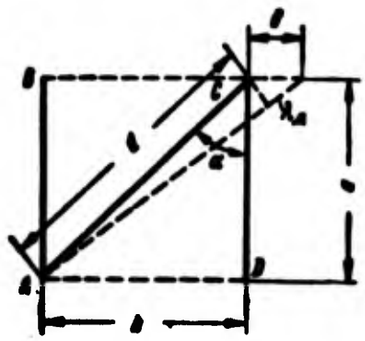

Fig. 3.23. Distortion of lattace of compound bar.

by $F_д$ we designate area of cross-section of diagonal; modulus E for bars of lattice we consider to coincide with modulus of material of

branches. Displacement δ of node C and angle of slide γ will be

$$\delta = \frac{\lambda_2}{\sin\alpha} = \frac{\lambda_2 d}{h}, \quad \gamma = \frac{\delta}{d} = \lambda_2 \frac{d}{dh}; \tag{3.133}$$

hence

$$\frac{1}{Q} = \frac{1}{EF_2} \frac{d^3}{dh^2}. \tag{3.134}$$

Putting this magnitude in place of n/GF in formula (125), we find

$$P_{кр} = \frac{\pi^2 EI}{l^2} \frac{1}{1 + \frac{1}{EF_2} \frac{d^3}{dh^2} \frac{\pi^2 EI}{l^2}}. \tag{3.135}$$

Reduction factor for length is determined here by formula

$$\nu = \sqrt{1 + \pi^2 \frac{F}{F_2} \frac{d^3}{dh^2} \frac{1}{\lambda^2}}. \tag{3.136}$$

where by λ we designate slenderness ratio of the bar:

$$\lambda = \frac{l}{i} = l\sqrt{\frac{F}{I}}.$$

If we introduce designation λ* for reduced slenderness ratio of compound bar, then we obtain

$$\lambda^* = \nu\lambda = \sqrt{\lambda^2 + \lambda_1^2}; \tag{3.137}$$

by λ_1 is understood magnitude

$$\lambda_1 = \pi\sqrt{\frac{F}{F_2} \frac{d^3}{dh^2}}. \tag{3.138}$$

When critical stress in branches exceeds elastic limit, modulus E for material of branch must be replaced by resultant modulus T or by tangent modulus E_K. Magnitude T is determined here by (2.16). However, members of lattice enter into work only during deflection of bar; therefore, for them strains should be considered elastic. Formula (138) for λ_1 takes on the form

$$\lambda_1 = \pi\sqrt{\frac{TF}{EF_2} \frac{d^3}{dh^2}} \text{ and } \lambda_1 = \pi\sqrt{\frac{E_K F}{EF_2} \frac{d^3}{dh^2}}. \tag{3.139}$$

For simplification of calculation it is possible in safety factor to take instead of (139) the former formula (138).

If lattice consists of diagonals and struts, as shown in

Fig. 3.24, it is necessary to note also strain of struts.

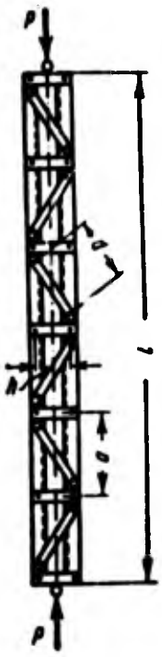

Fig. 3.24. Case of lattice, consisting of diagonals and struts.

Considering force in strut to be equal to $N_{ct} = Q$, we find angle of slide:

$$\gamma = \frac{\lambda_{ct}}{a} = \frac{Qh}{EF_{ct}a}. \qquad (3.140)$$

where λ_{ct} and F_{ct} are elongation and area of strut cross-section. Formula (135) obtains form

$$P_{kp} = \frac{\pi^2 EI}{l^2} \frac{1}{1 + \frac{1}{Eah^2}\left(\frac{d^3}{F_a} + \frac{h^3}{F_{ct}}\right)\frac{\pi^2 EI}{l^2}}. \qquad (3.141)$$

For constructions applied in practice additional member in parentheses is small as compared to member, containing d^3; therefore, in calculations it is possible here also to use the former formula (138).

For compound bar of <u>frame</u> type (Fig. 3.25) we must first of all consider strain of branches, caused by transverse force, slats in first approximation we will consider rigid. Points, dividing length of each panel in half will, obviously, be points of inflection of elastic line during local bending of branch (Fig. 3.26). Therefore, we can apply at these points transverse force Q/2 and determine deflection of branch within the semi-section:

$$\delta = \frac{Q}{2}\left(\frac{a}{2}\right)^3 \frac{1}{3EI_1}. \qquad (3.142)$$

where I_1 is moment of inertia of section of branch. Corresponding "mean" angle of rotation will be

$$\gamma = \frac{\delta}{a} = \frac{Qa^2}{24EI_1}. \qquad (3.143)$$

Fig. 3.25. Beam of frame type.

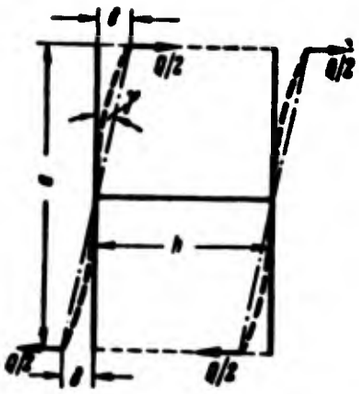

Fig. 3.26. Distortion of panel of frame type bar.

Putting ratio γ/Q in place of $\varkappa/GF$ in formula (125), we obtain

$$P_{кр} = \frac{\pi^2 EI}{l^2} \frac{1}{1 + \frac{a^2}{24EI_1} \frac{\pi^2 EI}{l^2}}. \qquad (3.144)$$

Formula (144) can be definitize, taking into account strain of slats. Middle point of slat is also point of inflection; at it one should apply transverse force for slat $Q_{пл}$, equal to $Q_{пл} = Qa/h$. Deflection of one part of slat as a beam h/2 long will be equal to

$$\delta = \frac{Qa}{h}\left(\frac{h}{2}\right)^3 \frac{1}{3EI_{пл}}, \qquad (3.145)$$

where $I_{пл}$ is moment of inertia of slat. If slats lie in two planes, as in Fig. 3.27, then by $I_{пл}$ we must understand total moment of inertia of the two slats. Angle of rotation of slat and section of branch fixed to it will be

$$\gamma_1 = \frac{2\delta}{h} = \frac{Qah}{12EI_{пл}}. \qquad (3.146)$$

Furthermore, one should consider shear of the slat. If slat is made in the form of plates, the angle of shear is equal to

$$\gamma_2 = \frac{Qa}{h} \frac{1}{GF_{пл}}, \qquad (3.147)$$

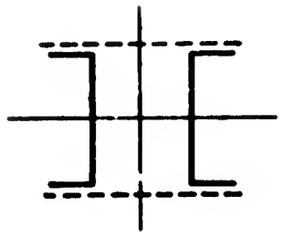

Fig. 3.27. Section of compound bar with lattice in two planes.

where $F_{пл}$ is area of section of slat (or two slats, lying in different planes). Introducing ratio $(\gamma_1 + \gamma_2)/Q$ in formula (144), we find

$$P_{кр} = \frac{\pi^2 EI}{l^2} \frac{1}{1 + \left(\frac{a^2}{24EI_1} + \frac{ah}{12EI_{пл}} + \frac{a}{GhF_{пл}}\right)\frac{\pi^2 EI}{l^2}}. \quad (3.148)$$

For usual constructions additional members, corresponding to strains of slats can be ignored. Using formula (144), again we find reduced slenderness ratio:

$$\lambda^* = \sqrt{\lambda^2 + \pi^2 \frac{Fa^2}{24I_1}}. \quad (3.149)$$

But total area of section constitutes $F = 2F_1$; ratio I_1/F_1 gives square of radius of gyration of section of branch; therefore, in second member in (149) it is possible to introduce slenderness ratio of branch λ_1 within limits of section:

$$\lambda_1 = \sqrt{\frac{Fa^2}{2I_1}}. \quad (3.150)$$

Considering approximately $\pi^2 \approx 12$, we arrive at former formula (137):

$$\lambda^* = \sqrt{\lambda^2 + \lambda_1^2} \quad (3.151)$$

with the distinction that by λ_1 is understood now the real slenderness ratio of the branch. In elastoplastic region it is possible here in safety factor to use formula (151).

Example 3.5. A disaster with a big structure (gas-holder) happened as a result of loss of stability of a compressed cross-stay, constructed from two branches of channel section, united by slats (Fig. 3.28). Total length of bar is 3600 mm. Distance between axes of slats is a = 1200 mm. Section of bar is composed of channels

No. 16b, distance of opening between which is equal to d = 28 mm. Slats are made from a strip of thickness t = 7 mm, width b = 140 mm. For material of channels and slats $E = 2.03 \cdot 10^6$ kg/cm^2, $\sigma_{пц} =$ = 2700 kg/cm^2. Find critical force: a) not considering influence of transverse force, b) taking into account transverse force.

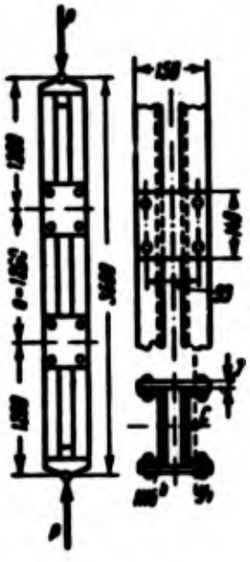

Fig. 3.28. Compressed cross-stay in structure of a gas-holder.

Moments of inertia of channel are: $I_{x_1} = 934{,}5$ cm^4, $I_{y_1} = 83{,}4$ cm^4, distance from edge to center of gravity $z_0 = 1.75$ cm; cross-sectional area $F_1 = 25.15$ cm^2, $h = d + 2z_0 = 6.3$ cm. We determine moments of inertia of the whole section:

$$I_x = 1869 \text{ cm}^4,$$
$$I_y = 2[I_{y_1} + F(1{,}4 + z_0)^2] =$$
$$= 2[83{,}4 + 25{,}15 \cdot 3{,}15^2] = 670 \text{ cm}^4.$$

Comparison of I_x and I_y shows that buckling will occur in plane of lattice. Radius of gyration

$$i_y = \sqrt{\frac{I_y}{F}} = \sqrt{\frac{670}{50{,}3}} = 3{,}64 \text{ cm}.$$

Slenderness ratio of bar as a whole is $\lambda = \frac{l}{i_y} = \frac{360}{3{,}64} = 99$. For separate branch radius of gyration is

$$i_{y_1} = \sqrt{\frac{I_{y_1}}{F_1}} = \sqrt{\frac{83{,}4}{25{,}15}} = 1{,}82 \text{ cm}.$$

Slenderness ratio within limits of the section is equal to

$$\lambda_1 = \frac{a}{i_{y_1}} = \frac{120}{1{,}82} = 66.$$

Of danger, thus, is <u>total</u> loss of stability of bar.

Euler's stress is

$$\sigma_э = \frac{\pi^2 E}{\lambda^2} = \frac{9{,}87 \cdot 2{,}03 \cdot 10^6}{99^2} = 2020 \text{ kg/cm}^2,$$

and, consequently, $\sigma_э < \sigma_{пц}$.

Critical force, calculated for bar of solid section, is equal to

$$P^0_{кр} = \sigma_э F = 2020 \cdot 50{,}3 = 101\,600 \text{ kg}. \qquad (a)$$

Taking into account influence of transverse force by the formula (148) we will have

$$P_{кр} = P^0_{кр} \frac{1}{1 + \left(\frac{a^2}{24EI_1} + \frac{ah}{12EI_{вн}} + \frac{a}{GhF_{вн}}\right)\frac{\pi^2 EI}{l^2}}. \qquad (b)$$

Considering that slats are in two planes, we find

$$I_{вн} = 2\frac{0{,}7 \cdot 14^3}{12} = 320 \text{ см}^4, \quad F_h = 2 \cdot 0{,}7 \cdot 14 = 19{,}6 \text{ см}^2.$$

By formula (b) taking G/E = 0.4, we obtain

$$P_{кр} = 101\,600 \frac{1}{1 + \frac{9{,}87}{24}\frac{670}{83{,}4}\left(\frac{120}{360}\right)^2 + \frac{9{,}87}{12}\frac{670}{320}\frac{120 \cdot 6{,}3}{360^2} + \frac{9{,}87}{0{,}4}\frac{670 \cdot 120}{19{,}6 \cdot 6{,}3 \cdot 360^2}} =$$

$$= 101\,600 \frac{1}{1 + 0{,}368 + 0{,}010 + 0{,}122} = \frac{101\,600}{1{,}5} = 67\,600 \text{ kg}. \qquad (c)$$

Weakening of bar from deformations of lattice constitutes 34%. This magnitude is not completely accurate, since formula (148) for critical forces was composed on the assumption that number of panels was comparatively great. It is clear, though, that the bar was designed unsuccessfully.

Examination of expression (c) allows us to estimate specific weight of separate members in the denominator. As we see, basic role is played by the member, which takes into account deformation of branches, but still influence of non-dilational strain of the slat is relatively great.

We find reduced slenderness ratio of the weakened bar:

$$\lambda^0 = \pi\sqrt{\frac{EF}{P_{кр}}} = \pi\sqrt{\frac{2{,}03 \cdot 10^4 \cdot 50{,}3}{67\,600}} = 121.$$

We use approximate formula (151); then we obtain

$$\lambda^0 = \sqrt{\lambda^2 + \lambda_1^2} = \sqrt{99^2 + 66^2} = 119,$$

which almost coincides with the former result, if instead of two intermediate slats we set five, i.e., halve the length of section, then we

will obtain $P_{кр} \approx 92{,}000$ kg; weakening of bar will constitute in all 9%.

§ 45. Stability of Bars Receiving Torque. Joint Action of Axial Compression and Torsion.

Long bar, subjected to action of torsional couples, can lose stability; axis of bar will form here a space besides curve. Assume that ends of bar are fixed by hinges and that the couples, whose moments are equal to $M_к$, are applied on ends of bar (Fig. 3.29), where moment vectors of couples preserve their direction along initial axis of the bar.

Moments of inertia of the bar cross-section relative to all central axes, let us assume, are identical and equal to I.

Considered system is nonconservative, since in various variants of transition of bar from initial position to bent, including pivoting of end sections around axis x, couples can accomplish various work. Consequently, given problem requires the dynamic approach, see [21.23]. However, static method leads here, as an exception, to the correct result, and we will use it.

We select basic and "local" systems of coordinates, as shown in Fig. 3.29. We designate by v and w the movement along y and z of a certain point, belonging to axial line of the bar. Determining projection moment of vector on axes y_1 and z_1, we arrive at the following differential equations:

$$\left.\begin{aligned} EI\frac{d^2v}{dx^2} &= -M_к\frac{dw}{dx}, \\ EI\frac{d^2w}{dx^2} &= M_к\frac{dv}{dx}. \end{aligned}\right| \qquad (3.152)$$

Using designation

$$k = \frac{M_к}{EI}. \qquad (3.153)$$

wi[illegible]ewrite system of equations (152) in the form

$$\left.\begin{aligned}\frac{d^2v}{dx^2}+k\frac{dw}{dx}=0,\\ \frac{d^2w}{dx^2}-k\frac{dv}{dx}=0.\end{aligned}\right\} \qquad (3.154)$$

These equations are satisfied by the following expressions for v and w:

$$\left.\begin{aligned}v=A\sin kx+B\cos kx+C,\\ w=-A\cos kx+B\sin kx+D.\end{aligned}\right\} \qquad (3.155)$$

We will use boundary conditions

$$\left.\begin{aligned}v=0 \text{ when } x=0,\ x=l,\\ w=0 \text{ when } x=0,\ x=l.\end{aligned}\right\} \qquad (3.156)$$

Conditions, pertaining to point x = 0, give

$$C=-B,\quad D=A. \qquad (3.157)$$

Other conditions lead to equations

$$\left.\begin{aligned}A\sin kl-B(1-\cos kl)=0,\\ A(1-\cos kl)+B\sin kl=0.\end{aligned}\right\} \qquad (3.158)$$

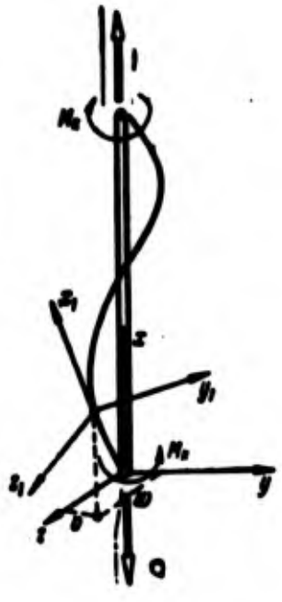

Fig. 3.29. Buckling of rod under torsion.

Considering A ≠ 0 and B ≠ 0, we equate to zero the determinant of this system; we obtain

$$\sin^2 kl+(1-\cos kl)^2=0,$$

hence

$$\cos kl=1. \qquad (3.159)$$

Least valve of kl, satisfying this equation and not equal to zero, will be

$$k=\frac{2\pi}{l}. \qquad (3.160)$$

Consequently, critical value of torque is equal to

$$M_{z,\,cp}=2\pi\frac{EI}{l}. \qquad (3.161)$$

Let us assume now that rod is subjected to <u>joint action of axial compression of force P and torsion</u> (Fig. 3.30). Equations (152) then

take the form

$$\left.\begin{aligned} EI\frac{d^2v}{dx^2} &= -M_x\frac{dw}{dx} - Pv, \\ EI\frac{d^2w}{dx^2} &= M_x\frac{dv}{dx} - Pw. \end{aligned}\right| \qquad (3.162)$$

Considering

$$\frac{M_x}{EI} = k, \quad \frac{P}{EI} = s^2, \qquad (3.163)$$

we arrive at system of equations

$$\left.\begin{aligned} \frac{d^2v}{dx^2} + k\frac{dw}{dx} + s^2v &= 0, \\ \frac{d^2w}{dx^2} - k\frac{dv}{dx} + s^2w &= 0. \end{aligned}\right| \qquad (3.164)$$

Solution of these equations we seek in the form

$$\left.\begin{aligned} v &= A\sin r_1x + B\cos r_1x + \\ &\quad + C\sin r_2x + D\cos r_2x. \\ w &= -A\cos r_1x + \\ &\quad + B\sin r_1x - C\cos r_2x + D\sin r_2x. \end{aligned}\right| \qquad (3.165)$$

Putting these expressions in (164), we find that quantities r_1 and r_2 should satisfy the same quadratic equation

$$r^2 + kr - s^2 = 0. \qquad (3.166)$$

Considering $r_1 \neq r_2$, we find

$$r_1 = -\frac{k}{2} \pm \sqrt{\frac{k^2}{4} + s^2}, \quad r_2 = -\frac{k}{2} \mp \sqrt{\frac{k^2}{4} + s^2}. \qquad (3.167)$$

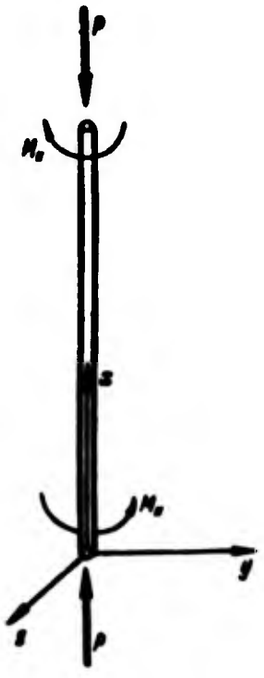

Fig. 3.30. Simultaneous action of axial force and torsional couples.

Taking into consideration boundary conditions (156) for x = 0, we have

$$B + D = 0, \quad A + C = 0. \qquad (3.168)$$

The other two conditions lead to equations

$$\left.\begin{aligned} A(\sin r_1l - \sin r_2l) + B(\cos r_1l - \cos r_2l) &= 0, \\ -A(\cos r_1l - \cos r_2l) + B(\sin r_1l - \sin r_2l) &= 0. \end{aligned}\right| \qquad (3.169)$$

Equating to zero the determinant of this system, we obtain

$$(\sin r_1l - \sin r_2l)^2 + (\cos r_1l - \cos r_2l)^2 = 0,$$

or

$$\cos(r_1 - r_2)l = 1. \qquad (3.170)$$

Least magnitude of argument, not

equal to zero, will be

$$(r_1 - r_2)l = 2\pi. \tag{3.171}$$

But by (167) we find

$$r_1 - r_2 = 2\sqrt{\frac{h^2}{4} + s^2}; \tag{3.172}$$

Consequently,

$$\frac{\pi^2}{l^2} = \frac{h^2}{4} + s^2. \tag{3.173}$$

Critical values of twisting moment and compressive force satisfy the equation:

$$\frac{\pi^2}{l^2} = \frac{1}{4}\left(\frac{M_z}{EJ}\right)^2 + \frac{P}{EJ}. \tag{3.174}$$

In particular cases of simple torsion and compression we obtain the earlier formulas (161) and (1.16). Relationship (174) may be applied also during simultaneous action of torsion and axial extension; in this case before P one should set a minus sign.

§ 46. Stability of Annular Ring and Arch.

Of large practical value is problem of stability of a closed annular ring under action of radial load, evenly distributed along circumference (Fig. 3.31). Such rings (frames) serve usually to receive radial forces, transmitted to cylindrical shell fastened to them, or as ribs, reinforcing a shell.

We designate by q the force per unit length of circumference, M, Q, and N the bending moment, transverse and axial force in section of ring, force N is considered positive during compression. We constitute equations of equilibrium of a member of length dy (Fig. 3.32), determining projection of forces in directions of the tangent and normal, and also moments about the center:

$$-\frac{dN}{dy} + \frac{Q}{R} + q_y = 0. \tag{3.175}$$

$$\frac{dQ}{dy} + \frac{N}{R} - q_z = 0. \tag{3.176}$$

$$-\frac{dM}{dy} + R\frac{dN}{dy} - Rq_y = 0; \tag{3.177}$$

coordinate y is counted along the arc, z--toward center; the R designates radius of circumference, passing through center of gravity of section q_y and q_z designate external load on corresponding directions. We assume that load q always is directed along the normal. Comparing equations (175)--(177) we obtain

$$Q=\frac{dM}{dy}. \tag{3.178}$$

$$\frac{d^2M}{dy^2}+\frac{1}{R^2}\frac{dM}{dy}+\frac{q_y}{R}-\frac{dq_z}{dy}=0 \tag{3.179}$$

Up to moment of buckling of ring axial force is equal to

$$N_0=qR. \tag{3.180}$$

Change of curvature is expressed by deflection w in the following manner:

$$\varkappa=\frac{d^2w}{dy^2}+\frac{w}{R^2}. \tag{3.181}$$

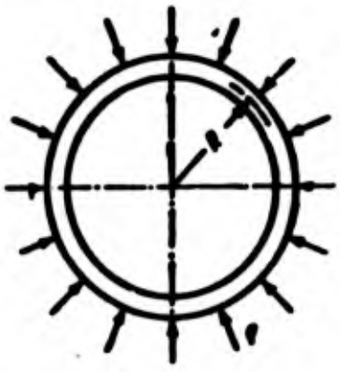

Fig. 3.31. Ring under action of radial load.

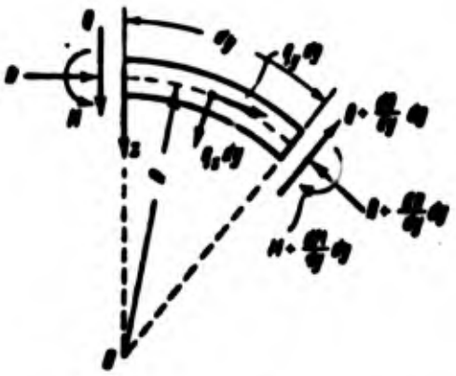

Fig. 3.32. Deriving equations of equilibrium of a member of a ring.

First member in this expression is the same as in the case of a straight beam; the second is found from Fig. 3.33 taking into account change of radius of curvature:

$$\frac{1}{R_1}-\frac{1}{R}=\frac{1}{R-w}-\frac{1}{R}\approx\frac{w}{R^2}. \tag{3.182}$$

Moment M is equal to

$$M=EI\varkappa=EI\left(\frac{d^2w}{dy^2}+\frac{w}{R^2}\right). \tag{3.183}$$

Putting this expression in (179), we obtain the following differential equation for w:

$$EI\left(\frac{d^4w}{dy^4}+\frac{2}{R^2}\frac{d^2w}{dy^2}+\frac{1}{R^4}\frac{dw}{dy}\right)=\frac{q_y}{R}-\frac{dq_z}{dy}. \qquad (3.184)$$

In problems of stability it is necessary to consider radial component of forces N, appearing during buckling of ring:

$$q_z=N_0\left(\frac{d^2w}{dy^2}+\frac{w}{R^2}\right)= \\ =qR\left(\frac{d^2w}{dy^2}+\frac{w}{R^2}\right). \qquad (3.185)$$

Considering $q_y = 0$, we find final differential equation

$$\frac{d^4w}{dy^4}+\frac{2}{R^2}\frac{d^2w}{dy^2}+\frac{1}{R^4}\frac{dw}{dy}+ \\ +\frac{qR}{EI}\left(\frac{d^2w}{dy^2}+\frac{1}{R^2}\frac{dw}{dy}\right)=0. \qquad (3.186)$$

We take for w expression

$$w=f\sin\frac{ny}{R}. \qquad (3.187)$$

where n is number of full waves, forming on the circumference. When n = 1 we obtain movement of ring as a solid body. Excluding this case, we take $n \geq 2$. Putting expression (187) in (186) and considering $f \neq 0$, we arrive at the following dependence:

$$q=(n^2-1)\frac{EI}{R^3}. \qquad (3.188)$$

Minimal critical load q_{kp} corresponds to two waves on the circumference (n = 2) and is equal to

$$q_{kp}=\frac{3EI}{R^3}. \qquad (3.189)$$

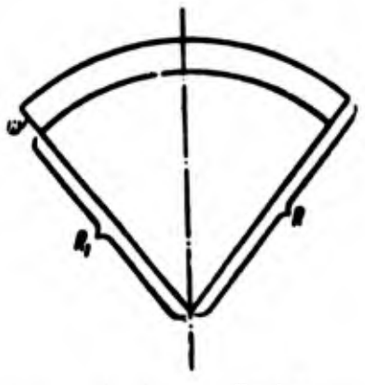

Fig. 3.33. Determination of curvature of the bending line.

We obtained the known formula for critical pressure, frequently applied in practical calculations.

Let us turn to the case of a circular arch (Fig. 3.34), subtending central angle 2α and fastened by hinges at the ends. We take expression for deflection in the form

$$w = f \sin \frac{m\pi y}{l}. \qquad (3.190)$$

where $l = 2R\alpha$ is length of center line. We place (190) in equation (186); then we obtain

$$\frac{qR}{EJ} = \frac{m^2\pi^2}{l^2} - \frac{1}{R^2}. \qquad (3.191)$$

Number of half-waves m we determine from the condition that full length of axial line remains constant. Strain of middle line is equal to

$$\epsilon_y = \frac{dv}{dy} - \frac{w}{R}. \qquad (3.192)$$

where v is displacement along arc. The second member in this expression accounts for shortening of arc according to Fig. 3.33. Considering $\epsilon_y = 0$, we find

$$\frac{dv}{dy} = \frac{w}{R}. \qquad (3.193)$$

Both ends of arch will remain fixed under condition

$$\int_0 w\,dy = 0. \qquad (3.194)$$

Least number m at which equality (194) is satisfied will be m = 2. Critical load turns out to be equal to

$$q_{кр} = \frac{EJ}{R^3}\left(\frac{\pi^2}{\alpha^2} - 1\right). \qquad (3.195)$$

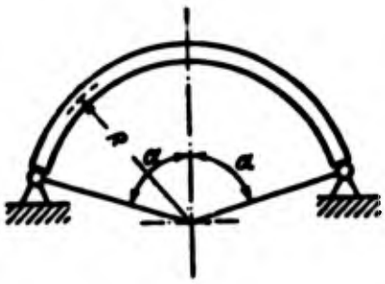

Fig. 3.34. Circular arch under action of lateral load.

Hence we can obtain formula (189) for ring, if we set $\alpha = \pi/2$; this angle corresponds to arc located between points of inflection of elastic line of the ring.

As we saw, arch fixed by hinge non-stretchable axis buckles in two half-waves. However, for shallow arch it may be that buckling occurs under smaller load, if we consider the middle line deformed. This case will be analyzed subsequently.

Here we illuminated only the simplest problem of stability of rings (frames) and arches. This region is presented in more detail

in books of A. N. Dinnik [3.1, 1946], S. P. Timoshenk [0.23], P. F. Papkovich [0.7], A. F. Smirnov [0.11], and A. Pflüger [0.21].

Literature

3.1. A. N. Dinnik. On buckling of bars of variable section, News of Donskoi Polytechnic Inst., 1 (1913), 390-404; Application of Bessel functions to problems of theory of elasticity, Selected works Vol. 2, Publishing House of Academy of Sciences of Ukrainian SSR, 1952, 73-78; Calculation of compressed columns of variable section. Engineering Herald, Nos. 1 and 2 (1929); Stability of arches, M., 1946.

3.2. B. G. Korenev. Certain problems of the theory of elasticity and thermal conduction, 1960.

3.3. Ya. I. Korotkin, A. Z. Lokshin, and N. L. Sivers. Bending and stability of bars and bar systems, Mashgiz, 1953.

3.4. Ye. L. Nikolai. Stability of rectilinear form of equilibrium of a compressed and twisted bar, Works on mechanics, Gostekhizdat, 1955.

3.5. Ya. L. Nudel'man. Methods of determining intrisic frequencies and critical forces for bar systems, Gostekhizdat, M., 1949.

3.6. A. M. Pen'kov. Stability of bar sets, Transactions of Kiev Technical Inst. of the Food Industry, No. 6 (1947).

3.7. A. A. Pikovskiy. Statics of bar systems with compressed members, Fizmatgiz, M., 1961.

3.8. A. R. Rzhanitsyn. Theory of constituent bars of building constructions, Stroyizdat, 1948.

3.9. N. K. Snitko. Stability of bar systems, Gosstroyizdat, M., 1952; Stability of compressed and is compressed-bent bar systems, 1956.

3.10. N. G. Chentsov. Columns of minimum weight, Transactions of Central Aero-Hydrodynamic Institute, No. 265 (1936).

3.11. A. Greenhill. On height ccnsistent with stability, Proc. Camb. Phil. Soc. 4 (1881), 65-75.

C H A P T E R IV

THIN-WALLED BARS. STABILITY OF PLANE FORM OF FLEXURE

§ 47. Fundamental Equations

We turn to problem of stability of a bar, consisting of thin walls and forming an unclosed (open) section. Such profiles are bars of angle, channel, cross, T (Fig. 4.1) I and Z-shaped sections (Fig. 4.2). Bar of channel section is an example of a simple profile, while a bar of I-section is an example of a branched profile. Bars of angle and cross-shaped sections form a section in the form of a beam. Peculiarity of such bars in comparison with bars of closed profile (for instance, tubular) or solid section consists of their relatively weak resistance to torsion. Therefore, we should not only study bending form of loss of stability of compressed bars, but also the form, which is accompanied by twisting of the section by joint bending strains and torsion.

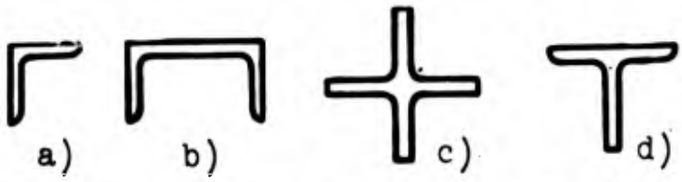

Fig. 4.1. Forms of sections of thin-walled bars.

We recall certain definitions and dependences, pertaining to general theory of thin-walled bars of open section.* During twisting of such bars--if only they do not form a section in the form of a beam--cross-section are distorted: different points of section have different displacements along axis of bar. This longitudinal displacement is called <u>distortion</u> or <u>warping</u>. If warping of sections of the bar is not carried out freely, then during torsion there are formed normal stresses, directed along axis. Normal stresses of constrained torsion are accompanied by tangential stresses, distributed evenly through the thickness of the wall (Fig. 4.3) and superimposed on tangential stresses of <u>free torsion</u>. As it is known, diagram of tangential stresses of free torsion along thickness of wall consists of two triangles; center line of section turns out to be free of stresses at points, somewhat remote from edge of section (Fig. 4.3). Tangential forces of constrained torsion form a couple; moment of this couple we designate by $\overline{\overline{M}}$. Tangential forces of free torsion give in turn a couple with moment $\overline{M}$. Adding them, we obtain total torsional moment $M_к$:

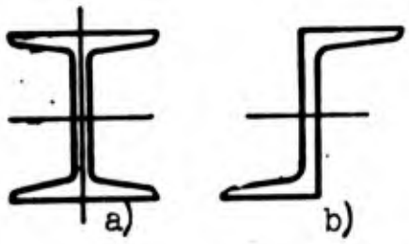

Fig. 4.2. Duralumin sections obtained by extrusion or drop forging.

$$\overline{M}+\overline{\overline{M}}=M_к. \tag{4.1}$$

Warping of any point of cross-section u may be expressed by unit angle

*This theory is presented in books of V. Z. Vlasov [4.4] (see in the same place Bibliography) and A. A. Umanskiy [4.12], see also book of G. Yu. Dzahnelidze and Ya. G. Panovko "Statics of elastic thin-walled bars," Gostekhizdat, 1948.

of torsion of bar a and the so-called sectorial area ω:

$$s = -a(x)\omega(s). \tag{4.2}$$

Magnitude a is a function of coordinate x, placed along axis of bar; section of bar is considered in its own plane to be fully rigid, unchanging. By sectorial area ω is understood twice the area formed during displacement of radius vector, where origin of radius coincides with some pole K, and end slides along center line of the section

Fig. 4.3. Tangential stresses.
a) of constrained torsion,
b) of free torsion.

(Fig. 4.4); obviously, magnitude ω will be a function of coordinates, counted off on center line. Minus sign in formula (2) corresponds to rotation of radius vector counter-clockwise. We consider that warping u changes, in general, along axis of bar; partial derivative of u with respect to x will give elongation strain of the corresponding fiber. Normal stresses of constrained torsions are equal to

$$\sigma = E\frac{\partial u}{\partial x} = -E\frac{da}{dx}\omega. \tag{4.3}$$

Unit angle of torsion in turn is equal to derivative of total angle of torsion θ with respect to length, i.e., a = dθ/dx. Consequently,

$$\sigma = -E\frac{d^2\theta}{dx^2}\omega. \tag{4.4}$$

Corresponding tangential stresses are found by equation of equilibrium

$$\frac{\partial\sigma}{\partial x} + \frac{\partial\tau}{\partial s} = 0.$$

whence

$$\tau = -\int_0^s \frac{\partial\sigma}{\partial x}\,ds = E\frac{d^2\theta}{dx^2}\int_0^s \omega\,ds. \tag{4.5}$$

We introduce designation for flux of tangential forces $q = \tau t$, where t is thickness of wall (Fig. 4.4). Magnitude t generally is variable along center line: $t = t(s)$. By (5) we find

$$q = E\frac{d^3\theta}{dx^3}\int_0^s \omega t\, ds = E\frac{d^3\theta}{dx^3}\int_0^s \omega\, dF. \tag{4.6}$$

where by $dF = t\, ds$ is implied area of member of wall of length ds. We introduce the designation

$$S_\omega = \int_0^s \omega\, dF \tag{4.7}$$

and call this magnitude, measured in cm^4, the sectorial static moment of part of the area of the section; then we obtain

Fig. 4.4. Sectorial area.

$$q = E\frac{d^3\theta}{dx^3}S_\omega. \tag{4.8}$$

Moment $\overline{M}$, formed by tangential forces of constrained torsion, we determine for axis, passing through pole K. From Fig. 4.5 it is clear that moment of elementary force q ds about the pole is equal to $q\rho\, ds$ or $q\, d\omega$, where $d\omega = \rho\, ds$ is increment of sectorial area. Total moment will be equal to

$$\overline{M} = \int_F \rho\, d\omega = E\frac{d^3\theta}{dx^3}\int_F d\omega \int_0^s \omega\, dF; \tag{4.9}$$

integral is extended to whole area of the section F. Integrating by parts, we have

$$\overline{M} = E\frac{d^3\theta}{dx^3}\left[\omega\int_F \omega\, dF - \int_F \omega^2\, dF\right]. \tag{4.10}$$

Initial position of radius vector during determination of sectorial area we shall select below from condition that full total sectorial static moment of area of section is equal to zero:

$$S_{\omega,F} = \int_F \omega\, dF = 0. \tag{4.11}$$

Sectorial moment of inertia of section is what we call the quantity

$$I_\omega = \int_F \omega^2\, dF, \tag{4.12}$$

it is measured in cm^6. Instead of (10) now we obtain

$$\overline{M} = -EI_\omega\frac{d^3\theta}{dx^3}. \tag{4.13}$$

As for moment formed by tangential forces of free torsion; it is equal to

$$\bar{M} = GI_k \alpha = GI_k \frac{d\theta}{dx}. \qquad (4.14)$$

Fig. 4.5. Determining of moment of tangential force.

here GI_k is torsional rigidity of the section, I_K is moment of inertia of section during torsion. For section consisting of n rectangles, magnitude I_K is equal to

$$I_k = \frac{1}{3} \gamma \sum_{i=1}^{n} s_i t_i^3 \qquad (4.15)$$

where s_i is length and t_i the thickness of the i-th walls; is coefficient depending on form of the cross-section, I_K is measured in cm^4.

Total torque according to (1) should be composed of (13) and (14):

$$-EI_\omega \frac{d^3\theta}{dx^3} + GI_k \frac{d\theta}{dx} = M_k. \qquad (4.16)$$

We obtained differential equation of constrained torsion for bar of open section.

Moment of tangential forces of constrained torsion $\bar{M}$ changes along the bar. We introduce new function B(x), whose first derivative is equal to $\bar{M}$:

$$\frac{dB}{dx} = \bar{M}. \qquad (4.17)$$

Magnitude B, measured in $kg \cdot cm^2$, has name of bending-twisting bimoment or simply <u>bimoment</u>. Comparing (4) and (13), we find

$$\bar{M} = \frac{d\sigma}{dx} I_\omega. \qquad (4.18)$$

Comparing now (17) and (18), we have

$$\sigma = \frac{B_\omega}{I_\omega}; \qquad (4.19)$$

it is assumed that when $\sigma = 0$ we must have $B = 0$. Thus, normal stresses of constrained torsion are proportional to the bimoment; formula (19) is built analogously to the known formula for normal stresses during bend $\sigma = My/I_z$, where y is distance of point of section from neutral axis z.

Using (13) and considering B = 0 when $d^2\theta/dx^2 = 0$, we find

$$B = -EI_\omega \frac{d^2\theta}{dx^2}. \tag{4.20}$$

Differentiating left and right side of equation (16) with respect to x, we have

$$-EI_\omega \frac{d^4\theta}{dx^4} + GI_k \frac{d^2\theta}{dx^2} = \frac{dM_k}{dx} = -m_k; \tag{4.21}$$

by m_K here is understood intensity of external torsional load; we consider this magnitude positive, if torque M_K decreases with growth of x. Proceeding from (20), we introduce in equation (21) bimoment B; then we obtain

$$\frac{d^2B}{dx^2} - \frac{GI_k}{EI_\omega} B = -m_k. \tag{4.22}$$

We arrived at a differential second order equation for bimoment.

§ 48. Centrally Compressed Bar with Section, Having Two Axes of Symmetry.

Let us consider first the case where cross-section of bar has two axes of symmetry. An example of such a bar is the I-beam section (Fig. 4.6). Let us assume that bar of length l is subjected to action of axial force P, applied in center of gravity of section.

Let us assume that during critical load along with initial form of equilibrium of rod another, a distorted form becomes possible, where distortion is obtained in all longitudinal fibers of the bar except the central one. In other works, we shall have in mind purely torsional form of loss of stability of the bar, without bending of central fiber.

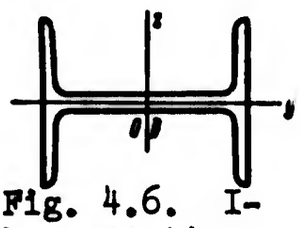

Fig. 4.6. I-beam section.

Angle of rotation of arbitrary section θ we consider positive during counter-clockwise rotation, if we look from upper end of bar (counter the direction of axis x). As initial differential equation we

take equation (22). Torsional load distributed lengthwise appears as a result of action of basic compressive stresses $\sigma = P/F$, where F is cross-section area. We isolate some fiber of the bar, parallel before deformation to axis x; in cross-section let us assume that to this fiber there corresponds member of area dF. After twisting of the bar the fiber will take the form of a curved line, located on round cylinder of radius ρ (Fig. 4.7).

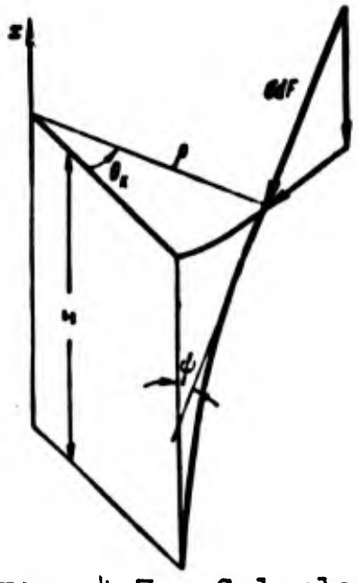

Fig. 4.7. Calculation of moment of compressive force.

We designate by ψ the small angle between tangent, passed to curved fiber at a point a distance x from lower end, and to the vertical. This angle will be, in general, variable along the length of the bar. Normal force σdF transmitted by fiber will after distortion of fiber be slanted to vertical at the same angle ψ. Horizontal projection of force will be equal to $\sigma\psi dF$. Moment, created by force σdF about axis x will be equal to product of force by arm ρ, or $\sigma\psi\rho dF$. Whole torsional moment, transmitted by compressive forces in certain section of bar, will be equal to the integral

$$\int_F \sigma\psi\rho\, dF.$$

extended to the whole area of the section. If one now were to take on adjacent section, removed from first by distance dx, then angle ψ will obtain increment $d\psi$, and torque will increase by magnitude

$$\int_F \sigma\, d\psi\, \rho\, dF.$$

Intensity of torsional load m_K we determine, dividing this magnitude by dx:

$$m_k = -\int_F \sigma \frac{d\psi}{dx} \rho\, dF. \qquad (4.23)$$

The minus sign here is taken because moment revolves clockwise about axis x, while angles θ and ψ we consider positive during rotation counter-clockwise.

Let us note that between increments of angles ψ and θ is the dependence

$$\rho d\theta = \psi dx;$$

hence

$$\psi = \rho \frac{d\theta}{dx}. \tag{4.24}$$

Substituting these magnitudes under integral sign in (23), we obtain

$$m_\kappa = - c \frac{d^3\theta}{dx^3} \int_F \rho^2 dF. \tag{4.24a}$$

or

$$m_\kappa = - cI_\rho \frac{d^3\theta}{dx^3}; \tag{4.25}$$

by I_p here is understood polar moment of inertia about the center;

$$I_\rho = \int_F \rho^2 dF. \tag{4.26}$$

But second derivative of θ with respect to x is connected by dependence (20) with bimoment B. Since we now consider <u>compressive stresses</u> positive, then by (19) and (20) we must change the sign in front of B to the opposite and set

$$EI_\omega \frac{d^3\theta}{dx^3} = B. \tag{4.27}$$

Finally, for intensity m_K we obtain expression

$$m_\kappa = - \frac{cI_\rho}{EI_\omega} B. \tag{4.28}$$

Putting this value of m_K in equation (22), we obtain

$$\frac{d^2B}{dx^2} + \left(\frac{cI_\rho}{EI_\omega} - \frac{GI_\kappa}{EI_\omega}\right) B = 0. \tag{4.29}$$

We assume that end sections of bar are free from normal stresses of constrained torsion, i.e., that <u>warping</u> of these sections is <u>carried out freely</u>. Proceeding from (19), we can formulate boundary conditions of problem in the following manner:

$$B = 0 \quad \text{when} \quad x = 0, \; x = l. \tag{4.30}$$

Considering

$$\frac{cI_\rho}{EI_\omega} - \frac{GI_\kappa}{EI_\omega} = k^2, \tag{4.31}$$

we obtain solution of equation (29) in the form

$$B = C_1 \sin kx + C_2 \cos kx. \tag{4.32}$$

From boundary conditions we find $C_2 = 0$. When $C_1 \neq 0$ we have

$$kl = n\pi, \quad n = 1, 2, 3, \ldots \tag{4.33}$$

Taking n = 1, we determine by (31) the smallest critical value of stress σ_θ:

$$\sigma_1 = \frac{\pi^2 E I_\omega}{l^2 I_\rho} + \frac{G I_k}{I_\rho}. \tag{4.34}$$

This formula is valid, obviously, only within limits of elasticity. If section consists of relatively thin walls, then second member in (34), accounting for stress of free torsion, can be disregarded as compared to first, corresponding to stresses of constrained torsion. Then we obtain formula

$$\sigma_1 \approx \frac{\pi^2 E I_\omega}{l^2 I_\rho}. \tag{4.35}$$

in structure analogous to Euler's formula.

For those cases when boundary conditions (30) are not satisfied, it is more convenient to use differential equation in form (21). Putting (25) in (21) and changing sign before σ to the opposite, we obtain

$$\frac{d^4\theta}{dx^4} + \frac{1}{E I_\omega}(\sigma I_\rho - G I_k)\frac{d^2\theta}{dx^2} = 0. \tag{4.36}$$

Let us assume, for instance, that face sections do not turn and remain flat. Proceeding from (2), we obtain boundary conditions

$$\left.\begin{aligned} \theta &= 0 \text{ when } x = 0, \ x = l. \\ \frac{d\theta}{dx} &= 0 \text{ when } x = 0, \ x = l. \end{aligned}\right\} \tag{4.37}$$

By analogy with stability problems for a bar of solid section with fixed ends (Section 3) we find

$$\sigma_1 = \frac{\pi^2 E I_\omega}{(\nu l)^2 I_\rho} + \frac{G I_k}{I_\rho}. \tag{4.38}$$

where coefficient of reduction of length ν is equal to 0.5. With one end completely fixed, and the other free we obtain in (38) $\nu = 2$; with one end fixed completely, and the other, fastened only as far as pivoting, $\nu = 0.7$.

Magnitude σ_θ one should compare with critical stresses, determined by Euler's formula for bending loss of stability in planes containing the principal axes of inertia of the section z and y:

$$\sigma_y = \frac{\pi^2 E I_y}{l^2 F}, \quad \sigma_z = \frac{\pi^2 E I_z}{l^2 F}. \tag{4.39}$$

Calculation of bar must be conducted by that one of the values of critical stress σ_θ, σ_y, or σ_z, which is the smallest.

For rolled H-beams magnitude σ_θ, as a rule, turns out to higher than σ_y or σ_z, so that check of torsional strength is unnecessary. At the same time for bars of cross-shaped section, when $I_\omega = 0$, the value of σ_θ may be smaller, than σ_x and σ_y.

§ 49. Case of Section with One Axis of Symmetry.

Assume that cross section of thin-walled bar has only one axis of symmetry, for instance axis y (Fig. 4.8). Here position of axis, about which the section turns during loss of stability, can not be predetermined, it is possible only to say that center of rotation (K) should lie on axis of symmetry.

Differential equation of constrained torsion we write in the form

$$\frac{d^2B}{dx^2} - \frac{GI_\kappa}{E\bar{I}_\omega} B = -\frac{\bar{m}_\kappa}{E\bar{I}_\omega}. \tag{4.40}$$

In distinction from (22) here above designations I_ω and m_κ are put dashes; these show that the sectorial moment of inertia and the torsional moment m_κ (and subsequently and the polar moment of inertia) are calculated about <u>axis of rotation</u>. Designations I_ω and I_p without dashes will be henceforth applied only for moments of inertia, related to center of gravity of section.

Constituting expression for $\bar{m}_\kappa$ as it was done in Section 48, we obtain equation

$$\frac{d^2B}{dx^2} + \frac{1}{E\bar{I}_\omega}(\sigma\bar{I}_\rho - GI_\kappa)B = 0. \tag{4.41}$$

We assume that face sections of the bar freely warp. Then integration of equation (41) will lead to an expression of type (34):

$$\sigma_{кр} = \frac{\pi^2 E \bar{I}_\omega}{l^2 \bar{I}_\rho} + \frac{G I_к}{\bar{I}_\rho}. \qquad (4.42)$$

We set ourselves the goal to find coordinate of center of rotation y_k, proceeding from expression (42); origin of coordinates we select at center of gravity. We assume that of all possible positions of center of rotation on axis of symmetry y we should realize such a position, for it at which <u>critical stress will be the smallest</u>. Sectorial area ω_k, calculated with the pole at some point K, is expressed by sectorial area ω, taken when pole is at center of gravity, in the following manner [taking into account (11)]:

$$\omega_k = \omega - y_k z. \qquad (4.43)$$

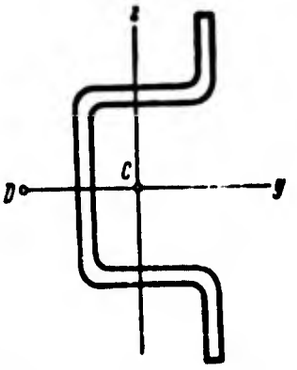

Fig. 4.8. Section with one axis of symmetry.

We place (43) in formula for sectorial moment of inertia of the section:

$$\bar{I}_\omega = \int_F \omega_k^2 \, dF; \qquad (4.44)$$

then we obtain

$$\bar{I}_\omega = \int_F \omega^2 dF - 2y_k \int_F \omega z \, dF + y_k^2 \int_F z^2 dF. \qquad (4.45)$$

First integral is equal to sectorial moment of inertia I_ω, calculated for center of gravity. For second integral we introduce designation

$$R_y = \int_F \omega z \, dF; \qquad (4.46)$$

it may be called the sectorial centrifugal moment of inertia. Finally, last integral constitutes moment of inertia of section I_y. Instead of (45) we find

$$\bar{I}_\omega = I_\omega - 2y_k R_y + y_k^2 I_y. \qquad (4.47)$$

Polar moment of inertia for point K is equal to sum of axial moments

of inertia:

$$\bar{I}_\rho = \bar{I}_{\bar{y}} + \bar{I}_{\bar{z}}; \tag{4.48}$$

axis $\bar{y}$ coincides with c y, and axis $\bar{z}$ passes through point K. We have

$$\bar{I}_{\bar{y}} = I_y, \quad \bar{I}_{\bar{z}} = I_z + y_k^2 F; \tag{4.49}$$

consequently,

$$\bar{I}_\rho = I_y + I_z + y_k^2 F = I_\rho + y_k^2 F. \tag{4.50}$$

Recall that axis y and z are principal central axes.

Thus, critical stress (42) turns out to be equal to

$$\sigma_{kp} = \frac{\frac{\pi^2 E}{l^2}(I_\omega - 2y_k R_y + y_k^2 I_y) + GI_k}{I_\rho + y_k^2 F}. \tag{4.51}$$

We introduce the following designations:

$$\sigma_\theta = \frac{\pi^2 E I_\omega}{l^2 I_\rho} + \frac{GI_k}{I_\rho}, \qquad \sigma_y = \frac{\pi^2 E I_y}{l^2 F}. \tag{4.52}$$

We already met them in the preceding section. Magnitude σ_θ it is possible to interpret as critical stress during torsional loss of stability about center of gravity of section according to (34); magnitude σ_y--as critical stress during bending loss of stability in plane zx. Furthermore, we designate

$$\rho_y = \frac{\pi^2 E R_y}{l^2 \sqrt{F I_\rho}}, \qquad \eta = y_k \sqrt{\frac{F}{I_\rho}}. \tag{4.53}$$

The first of these magnitudes, proportional to R_y, has dimension of stress. Second is dimensionless parameter for the coordinate of the center of rotation y_k.

Expression (51) can now be rewritten as follows:

$$\sigma_{kp} = \frac{\sigma_\theta - 2\rho_y \eta + \sigma_y \eta^2}{1 + \eta^2}. \tag{4.54}$$

Wishing to find minimum σ_{kp}, we equate to zero the derivative of (54) with respect to η:

$$\frac{d\sigma_{kp}}{d\eta} = (-2\rho_y + 2\sigma_y \eta)(1 + \eta^2) - 2\eta(\sigma_\theta - 2\rho_y \eta + \sigma_y \eta^2) = 0. \tag{4.55}$$

Taking into account (54), we find

$$\eta = \frac{\rho_y}{\sigma_y - \sigma_{kp}}. \tag{4.56}$$

Returning to (54), we obtain quadratic equation for $\sigma_{кр}$:

$$(\sigma_{кр}-\sigma_\theta)(\sigma_{кр}-\sigma_y)-\rho_y^2=0 \qquad (4.57)$$

or

$$\sigma_{кр}^2-\sigma_{кр}(\sigma_\theta+\sigma_y)+(\sigma_y\sigma_\theta-\rho_y^2)=0. \qquad (4.57a)$$

Of the two roots of this equation we select the smallest:

$$\sigma_{кр}=\frac{\sigma_\theta+\sigma_y}{2}-\sqrt{\left(\frac{\sigma_\theta-\sigma_y}{2}\right)^2+\rho_y^2}. \qquad (4.58)$$

Roots of equation (57) can be found by graphic construction, analogous to circle of stresses in a two-dimensional problem (Fig. 4.9). We lay off on the axis of abscissas segments AB = σ_y and AC = σ_θ, the vertical CC′ = ρ_y (upwards) and BB′ = ρ_y (downwards). Segment AF corresponds in the same scale to magnitude (58). From examination of Fig. 4.9 we conclude that critical stress $\sigma_{кр}$ for section with one axis of symmetry will be less than quantities σ_θ and σ_y.

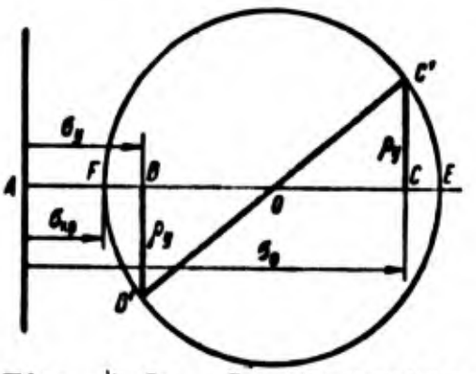

Fig. 4.9. Construction for determining parameters of critical stresses.

Along with bending--twisting form of loss of stability for a section with one axis of symmetry there is possible also pure bending loss of stability in plane xy. Corresponding critical stress σ_z is determined by (39):

$$\sigma_z=\frac{\pi^2EI_z}{l^2F}. \qquad (4.59)$$

Design critical stress is defined as the smallest of quantities (58) and (59).

With help of formulas (53) and (56) we can now determine coordinate of center of rotation:

$$y_k=\frac{\rho_y}{\sigma_y-\sigma_{кр}}\sqrt{\frac{I_p}{F}}. \qquad (4.60)$$

As we see, center of rotation does not lie at center of gravity of section. At the same time it does not coincide with the other characteristic point--center of bending of section D (Fig. 4.8). This can be shown as follows. Coordinate of center of flexure in case of thin-walled bar is equal to

$$y_D = \frac{R_y}{I_y}. \tag{4.61}$$

From (53) we find

$$\rho_y = \sigma_y y_D \sqrt{\frac{F}{I_\rho}} = \sigma_y \eta_D. \tag{4.62}$$

where

$$\eta_D = y_D \sqrt{\frac{F}{I_\rho}}. \tag{4.63}$$

formula (60) takes the form

$$y_k = \frac{y_D \sigma_y}{\sigma_y - \sigma_{кр}}. \tag{4.64}$$

Hence we conclude that, in general, $y_k \neq y_D$. Instead of (64) it is possible also to write

$$\eta = \frac{\eta_D \sigma_y}{\sigma_y - \sigma_{кр}}. \tag{4.65}$$

Example 4.1. Determine critical load for duralumin bar of length l = 1 m, subjected to compression by central force P. Section of bar has the form of a channel with folded flanges. Thickness of wall and shelves of section is equal to 1 mm, remaining dimensions (in mm) are shown in Fig. 4.10a. Assume that face sections of bar freely warp. We assume $E = 7 \cdot 10^3$ kg/mm^2, $G = 2.8 \cdot 10^3$ kg/mm^2, $\sigma_{пц} = 20$ kg/mm^2.

We determine position of center of gravity O. Distance from point O to center line of folded portions of flanges is equal to

$$e = \frac{19 \cdot 19 + 2 \cdot 19 \cdot 9{,}5}{3 \cdot 19 + 2 \cdot 13} = 8{,}7 \text{ мм}.$$

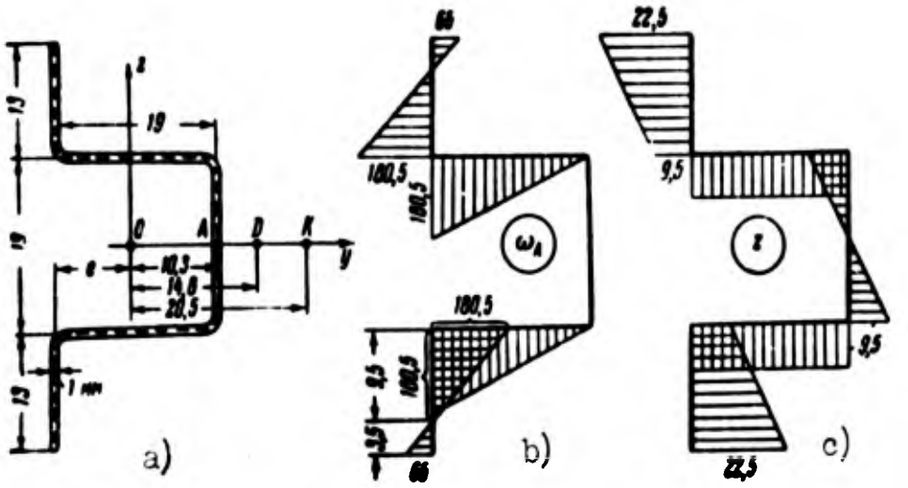

Fig. 4.10. Determining geometric characteristics of section.

We pass through center of gravity principal axes y and z of which the first coincides with axis of symmetry of the section. We calculate principal central moments of inertia, considering area of cross-section concentrated on center line of section (dotted line in Fig. 4.10):

$$I_y = \frac{1 \cdot 19^3}{12} + 2 \cdot 19 \cdot 9{,}5^2 + 2\left(\frac{13^3}{12} + 13 \cdot 16^2\right) = 11 \cdot 10^3 \text{ мм}^4,$$

$$I_z = 2\left(\frac{1 \cdot 19^3}{12} + 19 \cdot 0{,}8^2\right) + 2 \cdot 13 \cdot 8{,}7^2 + 19 \cdot 10{,}3^2 = 5{,}2 \cdot 10^3 \text{ мм}^4.$$

Polar moment of inertia relative to center of gravity is equal to

$$I_p = I_y + I_z = 16{,}2 \cdot 10^3 \text{ мм}^4.$$

Area of section is

$$F = 3 \cdot 19 + 2 \cdot 13 = 83 \text{ мм}^2.$$

Magnitude I_K we calculate by formula (15):

$$I_\kappa = \frac{1}{3}(2 \cdot 13 + 3 \cdot 19) = 28 \text{ мм}^4.$$

To determine sectorial static moment R_y when pole is at center of gravity of section. Calculations are shortened, if we first find value of $R_{y,A}$ for pole A, lying in the middle of the wall:

$$R_{y,A} = \int_F \omega_A z \, dF. \qquad \text{(a)}$$

For calculation of this integral we use the well-known Vereshchagin's rule, constructing beforehand a diagram of sectorial areas ω_A (Fig. 4.10b) and diagram of quantity z (Fig. 4.10c). Cross multiplying areas of diagram ω_A (here thickness t = 1) and ordinates of diagram

z, lying below centers of gravity of first diagram, we obtain

$$R_{y,A} = 2\left[\frac{180,5 \cdot 19}{2} 9,5 + \frac{180,5 \cdot 9,5}{2} 12,7 - \frac{66 \cdot 3,5}{2} 21,3\right] = 49,3 \cdot 10^3 \text{ мм}^4. \quad (b)$$

For transition to pole, coinciding with center of gravity, we write dependence between sectorial areas during transfer of pole along axis of symmetry:

$$\omega_A = \omega - y_0 z. \quad (c)$$

here by y_0 we designate distance between center of gravity O and previous pole A: $y_0 = 10.3$ mm. Magnitude R_y is equal to

$$R_y = \int_F \omega z \, dF = \int_F (\omega_A + y_0 z) z \, dF = R_{y,A} + y_0 I_y \quad (d)$$

or

$$R_y = 49,3 \cdot 10^3 + 10,3 \cdot 11 \cdot 10^3 = 163 \cdot 10^3 \text{ мм}^3.$$

To determine sectorial moment of inertia we proceed in this way. When pole is at point A we find

$$I_{\omega,A} = \int_F \omega_A^2 \, dF. \quad (e)$$

We multiply diagram ω_A by its ordinate and obtain

$$I_{\omega,A} = 2\left(\frac{181 \cdot 19}{2} \cdot \frac{2}{3} 181 + \frac{181 \cdot 9,5}{2} \cdot \frac{2}{3} 181 + \frac{66 \cdot 3,5}{2} \cdot \frac{2}{3} 66\right) = 633 \text{ мм}^6.$$

For shift to magnitude I_ω, related to center of gravity O, we will use formula (47), obtained during transfer of pole. Replacing in it $\overline{I}_\omega$ by $I_{\omega,A}$ and y_k by y_0, we have

$$I_\omega = I_{\omega,A} + 2y_0 R_y - y_0^2 I_y. \quad (f)$$

We find

$$I_\omega = 633 \cdot 10^3 + 2 \cdot 10,3 \cdot 163 \cdot 10^3 - (10,3)^2 \cdot 11 \cdot 10^3 = 282 \cdot 10^4 \text{ мм}^6.$$

We determine magnitude σ_y and σ_θ by (52):

$$\sigma_y = \frac{9,87 \cdot 7 \cdot 10^3 \cdot 11 \cdot 10^3}{10^6 \cdot 83} = 9,15 \text{ кг/мм}^2$$

$$\sigma_\theta = \frac{9,87 \cdot 7 \cdot 10^3 \cdot 282 \cdot 10^4}{10^6 \cdot 16,2 \cdot 10^3} + \frac{2,6 \cdot 10^3 \cdot 28}{16,2 \cdot 10^3} = 12 + 4,85 = 16,85 \text{ кг/мм}^2.$$

Further, by formula (53)

$$\rho = \frac{9,87 \cdot 7 \cdot 10^3 \cdot 163 \cdot 10^3}{10^6 \sqrt{83 \cdot 16,2 \cdot 10^3}} = 9,75 \text{ кг/мм}^2.$$

Critical stress, corresponding to bending-twisting form of loss of stability, will be according to (58),

$$\sigma_{кр} = \frac{16{,}85 + 9{,}15}{2} - \sqrt{\left(\frac{16{,}85 - 9{,}15}{2}\right)^2 + 9{,}75^2} = 2{,}52 \text{ кг/мм}^2.$$

During buckling in plane of symmetry critical stress σ_z according to (59) will be $\sigma_z = \frac{9{,}87 \cdot 7 \cdot 10^3 \cdot 5{,}2 \cdot 10^3}{10^6 \cdot 83} = 4{,}3$ кг/мм^2.

Both found quantities lie below limit of proportionality $\sigma_{пц}$ = = 20 kg/mm^2.

The design critical stress turns out to be stress $\sigma_{кр}$, lying significantly below σ_z. Critical load with length of bar l = 1 m is equal to $P_{кр} = \sigma_{кр} F = 2{,}52 \cdot 83 = 209$ кг.

We determine coordinate of center of rotation O of section from (60):

$$y_k = \frac{9{,}75}{9{,}11 - 2{,}52} \sqrt{\frac{16{,}2 \cdot 10^3}{83}} = 20{,}5 \text{ мм}.$$

We calculate also coordinate of center of flexure from (61):

$$y_D = \frac{163 \cdot 10^3}{11 \cdot 10^3} = 14{,}8 \text{ мм}.$$

As we see, center of rotation lies significantly further from point C than does the center of flexure of the section.

We shall calculate critical stress for different values of bar length. In Fig. 4.11 are depicted results of calculations for bars with length from 500 mm to 2000 mm. One of the curves ($\sigma_{кр}$) corresponds to bending-twisting loss of stability, and a second (σ_y)--buckling in plane of symmetry. For long bars, starting with l = 1580 mm, Euler's form of loss of stability becomes more dangerous. In Fig. 4.12 are compared coordinates of center of rotation of section y_k and center of flexure y_D. With growth of bar length there is observed removal of center of rotation from center of flexure.

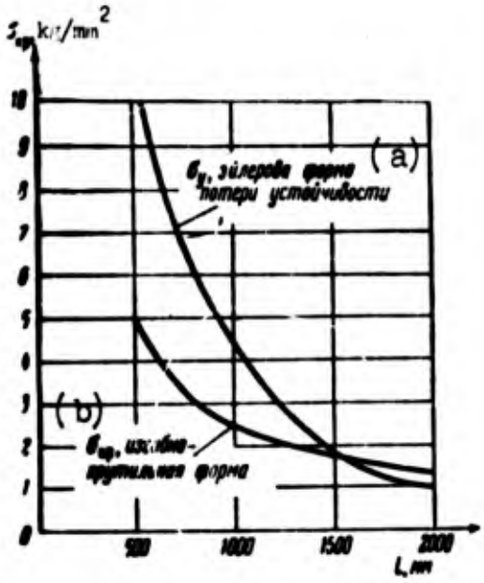

Fig. 4.11. Critical stresses depending upon length of bar.
KEY: (a) Euler's form of loss of stability;
(b) Bending-twisting form.

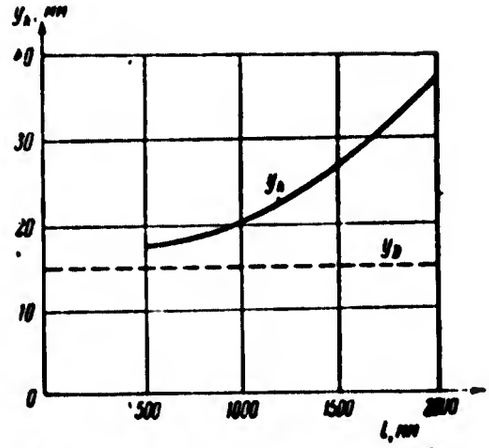

Fig. 4.12. Change of position of center of rotation depending upon length of bar.

§ 50. Bar with Asymmetric Section.

Let us turn to general case of an asymmetric section (Fig. 4.13). Let the principal central axes of inertia of section be axes y and z. Assume that bar is subjected to central compression and that its end sections are distorted. Critical stress, corresponding to bending-twisting form of loss of stability, we as before will seek in the form (42), considering position of center of rotation $K(y_k, z_k)$ unfixed. Instead of formula (43) for sectorial area at point $M(y,z)$, taking into account (11), we obtain

$$\omega_k = \omega - y_k z + z_k y; \tag{4.66}$$

here ω is sectorial area, found when pole is at center of gravity. Sectorial moment of inertia $\bar{I}_\omega$ will be according to (44),

$$\bar{I}_\omega = \int_F (\omega^2 - 2\omega y_k z + 2\omega z_k y - 2y_k z_k yz + y_k^2 z^2 + z_k^2 y^2)\, dF. \tag{4.67}$$

We introduce designation for second sectorial centrifugal moment of inertia:

$$R_y = \int_F \omega y\, dF. \tag{4.68}$$

Considering that for principal axes centrifugal moment of inertia is equal to zero,

$$I_{yz} = \int yz\, dF = 0. \tag{4.69}$$

We find

$$\bar{I}_\omega = I_\omega - 2y_k R_y + 2z_k R_z + y_k^2 I_y + z_k^2 I_z. \tag{4.70}$$

For polar moment of inertia for point K we obtain expression

$$\bar{I}_\rho = I_y + I_z + y_k^2 F + z_k^2 F = I_\rho + F(y_k^2 + z_k^2). \tag{4.71}$$

Formula (42) for critical stresses takes on form

$$\sigma_{кр} = \frac{\frac{\pi^2 E}{l^2}(I_\omega - 2y_k R_y + 2z_k R_z + y_k^2 I_y + z_k^2 I_z) + GI_k}{I_\rho + (y_k^2 + z_k^2)F}. \tag{4.72}$$

We use new designations:

$$\rho_y = \frac{\pi^2 E R_y}{l^2 \sqrt{F I_\rho}}, \quad \zeta = z_k \sqrt{\frac{F}{I_\rho}}; \tag{4.73}$$

then, taking into account (52), (53) and (59), we find

$$\sigma_{кр} = \frac{\sigma_0 - 2\rho_y \eta + 2\rho_z \zeta + \sigma_y \eta^2 + \sigma_z \zeta^2}{1 + \eta^2 + \zeta^2}. \tag{4.74}$$

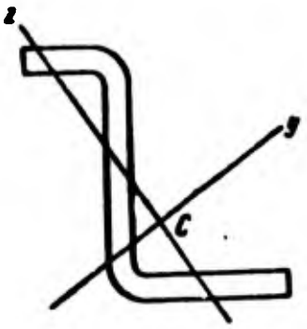

Fig. 4.13. Asymmetric section of thin-walled bar.

We equate to zero partial derivatives of $\sigma_{кр}$ with respect to η and ζ:

$$\frac{\partial \sigma_{кр}}{\partial \eta} = 0, \quad \frac{\partial \sigma_{кр}}{\partial \zeta} = 0; \tag{4.75}$$

Using (70), we obtain

$$\eta = \frac{\rho_y}{\sigma_y - \sigma_{кр}}, \quad \zeta = -\frac{\rho_z}{\sigma_z - \sigma_{кр}}. \tag{4.76}$$

Formula (74) leads now to the following cubic equation for $\sigma_{кр}$:

$$(\sigma_{кр} - \sigma_0)(\sigma_{кр} - \sigma_y)(\sigma_{кр} - \sigma_z) - \rho_y^2(\sigma_{кр} - \sigma_z) - \rho_z^2(\sigma_{кр} - \sigma_y) = 0. \tag{4.77}$$

This equation generalizes results obtained earlier. For section with two axes of symmetry $\rho_y = \rho_z = 0$; the three roots of equation (77) will be

$$(\sigma_{кр})_1 = \sigma_1, \quad (\sigma_{кр})_2 = \sigma_y, \quad (\sigma_{кр})_3 = \sigma_z. \tag{4.78}$$

which agrees with formulas (34) and (39). In the case of a section with one axis of symmetry $\rho_y \neq 0$, $\rho_z = 0$; then we obtain $(\sigma_{кр})_{1,\ 2}$ from equation (57) and $(\sigma_{кр})_3 = \sigma_z$ from (59).

Study of equation (77) shown that, whatever the relacionship between magnitudes σ_θ, σ_y, and σ_z, the smallest root will always lie below any of these magnitudes. Consequently, loss of stability of bar with asymmetric section is possible only in bending-twisting form.

§ 51. Stability of Two-Dimensional Form During Pure Bending.

Consider the case when thin-walled bar with section having one axis of symmetry is subjected to pure bending in plane of symmetry xy. Let each of the couples applied to faces have moment M (Fig. 4.14). Normal stresses in any section of bar will be distributed according to the law

$$\sigma = \frac{M}{I_z} y; \tag{4.79}$$

stresses in edge fibers σ_M will be

$$\sigma_M = \frac{M}{W_z}, \tag{4.80}$$

where W_z is resisting moment of section, pertaining to one or another edge fiber (points c or d in Fig. 4.15).

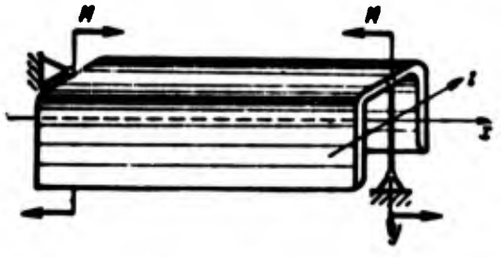

Fig. 4.14. Thin-walled bar is subjected to pure bending in plane of symmetry (supports are depicted by convention).

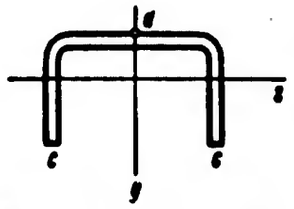

Fig. 4.15. Determination of stresses in edge fibers.

In first stage of stress elastic line of bar is plane curve, however, with known value of moment M there can occur buckling of bar in the direction of axis z, perpendicular to plane of bending. This phenomenon has the name of <u>loss of stability of plane form of bending</u>. Obviously, here any section of bar accomplishes turn around some center K, lying on axis of symmetry of section. Therefore, we can again use the differential equation of constrained torsion (40). We compose equation for intensity of torsional moment $\bar{m}_K$. From (23) and (24) we have

$$\bar{m}_z = -\frac{d^3\theta}{dx^3}\int_F \sigma\bar{\rho}^2\,dF. \tag{4.81}$$

where by $\bar{\rho}$ is understood radius vector of area dF about center of rotation. Using (79), we find

$$\bar{m}_z = -\frac{d^3\theta}{dx^3}\frac{M}{I_z}\int_F y\bar{\rho}^2\,dF. \tag{4.82}$$

We introduce designation

$$\int_F y\bar{\rho}^2\,dF = \bar{S}_y. \tag{4.83}$$

then from (27) we obtain

$$\bar{m}_z = -M\frac{\bar{S}_y}{I_z}\frac{d^3\theta}{dx^3} = -\frac{M}{E\bar{I}_\omega}\frac{\bar{S}_y}{I_z}B; \tag{4.84}$$

magnitude $\bar{I}_\omega$ should also be determined relative to center of rotation K. Equation (40) takes form

$$\frac{d^2B}{dx^2} + \left(\frac{M}{E\bar{I}_\omega}\frac{\bar{S}_y}{I_z} - \frac{GI_k}{E\bar{I}_\omega}\right)B = 0. \tag{4.85}$$

Considering that face sections freely warp, we obtain solution of equation (85) again in form (32), where

$$k^2 = \frac{M}{E\bar{I}_\omega}\frac{\bar{S}_y}{I_z} - \frac{GI_k}{E\bar{I}_\omega}. \tag{4.86}$$

Taking from (33) $kl = n\pi$ and $n = 1$, we find critical value of moment:

$$\frac{M_{cp}}{I_z} = \frac{\pi^2 E\bar{I}_\omega}{l^2\bar{S}_y} + \frac{GI_k}{\bar{S}_y}. \tag{4.87}$$

We arrived at a formula of the same structure as for critical stress during central compression according to (42), but instead of $\bar{I}_p$ there enters quantity $\bar{S}_y$. Coordinate of center of rotation we shall, as before, designate by y_k; then for $\bar{I}_\omega$ there will be preserved equation (47). We use further the relationship between radius vectors, related to center of rotation and center of gravity:

$$\bar{\rho}^2 = \bar{y}^2 + \bar{z}^2 = (y - y_k)^2 + z^2 = \rho^2 - 2y_k y + y_k^2; \tag{4.88}$$

hence by (83)

$$\bar{S}_y = \int_F (\rho^2 - 2y_k y + y_k^2)\, y\, dF = S_y - 2y_k I_z. \tag{4.89}$$

Instead of (87) we find,

$$\frac{M_{кр}}{I_s} = \frac{\frac{\pi^2 E}{l^2}(I_\omega - 2y_k R_y + y_k^2 I_y) + GI_к}{S_y - 2y_k I_z}, \tag{4.90}$$

where

$$S_y = \int_F \rho^2 y\, dF. \tag{4.91}$$

we introduce along with (53), (63) and (80) designations

$$\beta_y = \left(\frac{S_y}{2I_z} - y_D\right)\sqrt{\frac{F}{I_\rho}}, \quad s = \frac{W_z}{\sqrt{I_\rho F}}; \tag{4.92}$$

then from (90) it is possible to pass to critical value of stress in edge fiber:

$$s\sigma_M = \frac{\sigma_0 - 2\sigma_y \eta_D \eta_k + \sigma_y \eta_k^2}{2(\beta_y + \eta_D - \eta_k)}. \tag{4.93}$$

We determine position of center of rotation, equating to zero the derivative of $(s\sigma_M)$ with respect to η_k; then we obtain for $\beta_y + \eta_D - \eta_k \neq 0$

$$-2\sigma_y \eta_D + 2\sigma_y \eta_k + 2s\sigma_M = 0,$$

whence

$$\eta_k = \eta_D - s\frac{\sigma_M}{\sigma_y}. \tag{4.94}$$

We now substitute (94) in (93); for critical stress we have a quadratic equation:

$$(s\sigma_M)^2 + 2\beta_y \sigma_y (s\sigma_M) + \sigma_y^2 \eta_D^2 - \sigma_0 \sigma_y = 0; \tag{4.95}$$

its roots will be

$$\sigma_M = \sigma_y\left(-\beta_y \pm \sqrt{\beta_y^2 + \frac{\sigma_0}{\sigma_y} - r_D^2}\right). \qquad (4.96)$$

Critical magnitudes of moment turn out to be equal to

$$M = P_y\left(-r_y \pm \sqrt{r_y^2 + \frac{P_0}{P_y} r^2 - y_D^2}\right). \qquad (4.97)$$

where

$$r = \sqrt{\frac{I_\omega}{F}}, \quad r_y = \beta_y \sqrt{\frac{I_\omega}{F}} = \frac{S_y}{2I_x} - y_D, \quad P_y = \sigma_y F, \quad P_0 = \sigma_0 F. \qquad (4.98)$$

Negative sign of M refers to couples, giving to elastic line of bar buckling not downwards, as in Fig. 4.14, but upwards.

Let us turn to a particular case, when section of bar has two axes of symmetry. Then we will have $R_y = S_y = \beta_y = y_D = 0$; or critical values of σ_M and M we obtain simple formulas:

$$\sigma_{M,кр} = \frac{1}{s}\sqrt{\sigma_0 \sigma_y}, \quad M_{кр} = r\sqrt{P_0 P_y}. \qquad (4.99)$$

For section, consisting of a beam of strips, we have

$$I_\omega = 0, \quad \frac{\sigma_0}{s^2} = \frac{GI_k}{W_x^2} F;$$

consequently,

$$\sigma_{M,кр} = \frac{\pi}{W_x l}\sqrt{GI_k EI_y}, \quad M_{кр} = \frac{\pi}{l}\sqrt{GI_k EI_y}. \qquad (4.100)$$

During bending of a strip of rectangular section b X h by couples, lying in its plane, we obtain $I_K = bh^3/3$, $I_y = bh^3/12$ and

$$\sigma_{M,кр} = \pi\sqrt{GE}\,\frac{h}{l} = \frac{\pi}{\sqrt{2(1+\mu)}} E\frac{h}{l}. \qquad (4.101)$$

In case of I-beam (Fig. 4.16) sectorial moment of inertia of section may be defined by (12). For points of web sectorial area ω turns into zero. For points of flange we have: $\omega = yh/2$, where h is height of section, y is counted from center line of web, and initial radius vector coincides with this line. Consequently,

$$I_\omega = 2\frac{h^2 t_1}{4}\int_{F_1} y^2 dy = \frac{I_1 h^2}{2}; \qquad (4.102)$$

integral extends to area of flange, I_1 is moment inertia of flange

relative to axis of wall. From (52) and (92) we have

$$\frac{\sigma_0}{\delta^2}=\left(\frac{\pi^2 EI_\omega}{l^2}+GI_k\right)\frac{F}{W_0^2},\quad \sigma_y=\frac{\pi^2 EI_y}{l^2F};\tag{4.103}$$

hence

$$\sigma_{kr.sp}=\frac{1}{W_0}\frac{\pi}{l}\sqrt{EI_y GI_k}\sqrt{1+\frac{\pi^2 EI_y h^2}{2l^2 GI_k}}.\tag{4.104}$$

This formula pertains to case when bending couples lie in plane of the web.

Fig. 4.16. Calculation of sectorial area.

§ 52. Case of Eccentric Compression.

Assume that bar is subjected to eccentric compression by forces P, where point of application of force lies on axis y; this axis we shall consider axis of symmetry of the section (Fig. 4.17). With small loads here too the elastic line will appear flat. However, if force P exceeds known critical magnitude, there can occur loss of stability of plane form, so that bar will start to buckle in the direction of axis z. For finding critical value of P we will use the same method as in preceding sections. Let us assume that at moment of loss of stability section of bar revolves around point K, removed from center of gravity by y_k, and we determine this distance. Normal stresses in any section up to buckling will be equal to

$$\sigma=\frac{P}{F}+\frac{Pe}{I_z}y=\sigma_0\left(1+\frac{ey}{i_z^2}\right);\tag{4.105}$$

here $\sigma_0 = P/F$, $i_z^2 = I_z/F$ and compressive stresses as before we consider positive. Instensity of torque according to (81) is equal to

$$\bar{m}_z=-\frac{d^2\theta}{dx^2}\sigma_0\left(\int_F \bar{\rho}^2\,dF+\frac{e}{i_z^2}\int_F \bar{y}\bar{\rho}^2\,dF\right).$$

or

$$\bar{m}_x = -\frac{d^2\theta}{dx^2}\sigma_0\left(\bar{I}_\rho + \frac{e}{i_z^2}\bar{S}_y\right) = -\sigma_0\frac{\bar{I}_\rho + \frac{e}{i_z^2}\bar{S}_y}{E\bar{I}_\omega}B. \qquad (4.106)$$

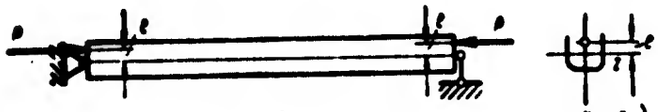

a) b)

Fig. 4.17. Thin-walled bar, subjected to eccentric compression.

Instead of (85) and (86) we obtain

$$\frac{d^2B}{dx^2} + k^2B = 0. \qquad (4.107)$$

$$k^2 = \sigma_0\frac{\bar{I}_\rho + \frac{e}{i_z^2}\bar{S}_y}{E\bar{I}_\omega} - \frac{GI_k}{E\bar{I}_\omega}. \qquad (4.108)$$

When $k = \pi/l$ we have

$$\sigma_0 = \frac{\frac{\pi^2 E\bar{I}_\omega}{l^2} + GI_k}{\bar{I}_\rho + \frac{e}{i_z^2}\bar{S}_y}. \qquad (4.109)$$

We use earlier formulas of transition (47) and (89) and introduce additionally the designation

$$\eta_e = e\sqrt{\frac{F}{I_\rho}}. \qquad (4.110)$$

Then we obtain

$$\sigma_0 = \frac{\sigma_y - \sigma_y\eta_k(2\eta_D - \eta_k)}{1 + \eta_k^2 + 2\eta_e(\beta_y + \eta_D - \eta_k)}. \qquad (4.111)$$

Equating to zero the derivative of σ_0 with respect to η_k, we find

$$\eta_k = \frac{\sigma_y\eta_D - \sigma_0\eta_e}{\sigma_y - \sigma_0} = \eta_D + \frac{\sigma_0(\eta_D - \eta_e)}{\sigma_y - \sigma_0}. \qquad (4.112)$$

In the particular case of central compression when $\eta_e = 0$ we arrive at formula (65). We place (112) in expression (111), this will lead to a quadratic equation for σ_0:

$$(\sigma_0 - \sigma_k)(\sigma_0 - \sigma_y) + 2\sigma_0(\sigma_0 - \sigma_y)\eta_e(\beta_y + \eta_D) - (\sigma_0\eta_e - \sigma_y\eta_D)^2 = 0 \qquad (4.113)$$

or

$$[1+2\eta_e(\beta_y+\eta_D)-\eta_e^2]\sigma_0^2-(\sigma_0+\sigma_y+2\sigma_y\beta_y\eta_e)\sigma_0+\sigma_0\sigma_y-\sigma_y^2\eta_D^2=0. \qquad (4.114)$$

Hence when $\eta_e = 0$ we get equations (57) and (57a).

Consider the case, when compressing force is applied in <u>center of bending</u>, of section D, so that $\eta_e = \eta_D$. Here from (112) we obtain $\eta_k = \eta_D$, if $\sigma_y \neq \sigma_0$. This means that <u>center of rotation will lie at that same point D</u>. From (113) we now find

$$\sigma_0^{(1)}=\frac{\sigma_y-\sigma_y\eta_D^2}{1+\eta_D^2+2\eta_D\beta_y}. \qquad (4.115)$$

Second root of equation (113) will be

$$\sigma_0^{(2)}=\sigma_y. \qquad (4.115a)$$

We saw that during <u>central</u> compression of bar with an asymmetric section critical stress always lies below σ_y. If, however, force is applied eccentrically and namely in center of bending, then critical stress will be exactly equal to Euler's value.

Study of equation (114) shows that for known conditions loss of plane forms of bending occurs also when force P is <u>tensile</u>. This can occur with sufficiently great eccentricity of application of load; one root of equation (114) becomes negative. Boundary values of eccentricities, at which critical force P will be tensile, are determined from that condition that the root of equation (114) is equal to $\pm\infty$. But then the coefficient in σ_0^2 should be equal to zero:

$$\eta_e^2-2\eta_e\bar{k}-1=0;$$

here dimensionless $\bar{k}$ is taken equal to

$$\bar{k}=\eta_D+\beta_y. \qquad (4.115b)$$

Two values of η_e, corresponding to equation (113), will be

$$\eta_e=\bar{k}\pm\sqrt{\bar{k}^2+1}.$$

We will find corresponding points on axis η (or y in Fig. 4.18), if we lay off from the center segment k_1, and from it in both directions segments $\sqrt{k_1^2+1}$; we assume $k_1 = \bar{k}(I_p/F)^{1/2}$. If force is applied in interval between points c and d, then its critical value can

only be compressive.

In more general case of eccentricity in two planes we find that region of compressing critical values lies inside "circle of stability,"* dimensionless radius of which will be $\sqrt{1 + \bar{k}^2 + \bar{l}^2}$, and coordinates of center equal to $\bar{k}$ and $\bar{l}$; here by $\bar{l}$ we understand quantity

$$\bar{l} = \frac{1}{2I_y}\sqrt{\frac{F}{I_p}}\int_F \rho^2 z\, dF.$$

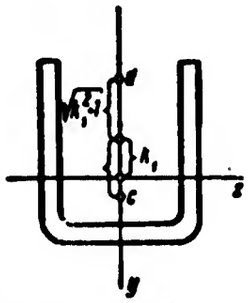

Fig. 4.18. Domain of application of compressing load during loss of stability of plane form of bending.

We considered here the problem of <u>stability</u> of a thin-walled bar under eccentric compression. In determining <u>supporting power</u> of a bar it is necessary also to start from the condition that the greatest stresses or displacements do not attain a dangerous magnitude (see [4.3], [3.7]).

<u>Example 4.2.</u> For the bar described in example 4.1 determine critical value of average stress $\sigma_0 = P/F$ for load P applied on axis of symmetry of section at different distances y_c from center of gravity C.

We determine S_y by (91):

$$S_y = \int_F \rho^2 y\, dF = \int_F y^3\, dF + \int_F x^2 y\, dF.$$

---

*Such extension of solution to case of biaxial eccentricity is absolutely <u>conditional</u>, since in this case it pertains only to a specific linear problem, see [4.3].

For the web

$$S_{y,1} = 10{,}3^2 \cdot 19 + 10{,}3 \int_{-9{,}5}^{+9{,}5} z^2\,dz =$$

$$= 20\,800 + 10{,}3\,\frac{6859}{12} = 26\,700 \text{ мм}^3.$$

For parts of flanges, parallel to axis y

$$S_{y,2} = 2 \int_{-8{,}7}^{10{,}3} y^2\,dF + 2 \int_{-8{,}7}^{10{,}3} y\,(9{,}5)^2\,dF =$$

$$= \frac{1}{2}(11\,230 - 5780) + \frac{1}{2}\,9{,}5^2\,(106 - 76) = 5420 \text{ мм}^3.$$

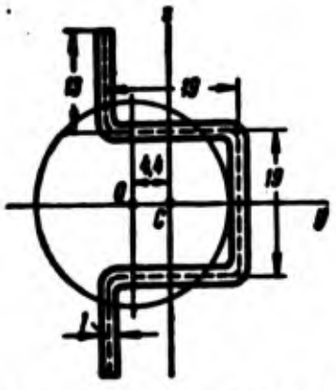

Fig. 4.19. "Circle of stability" for section with one axis of symmetry.

For bent parts of flanges

$$S_{y,3} = 2(-8{,}7)^2\,13 + (-8{,}7)\left(\frac{45^2}{12} - \frac{19^2}{12}\right) = -78\,000 \text{ мм}^3.$$

Total value of S_y will be

$$S_y = S_{y,1} + S_{y,2} + S_{y,3} = -45\,900 \text{ мм}^3.$$

Measured magnitudes k_1 and β_y by (92) and (115b) are equal to

$$k_1 = \frac{S_y}{2I_x} = -\frac{45\,900}{2 \cdot 5156} = -4{,}4 \text{ мм}, \quad \beta_y = k_1 - y_D = -4{,}4 - 14{,}8 = -19{,}2 \text{ мм}.$$

We calculate value of r:

$$r = \sqrt{\frac{I_p}{F}} = \sqrt{\frac{16\,179}{83}} = 14{,}2 \text{ мм}.$$

Radius of circle of stability will be

$$R = \sqrt{r^2 + k_1^2} = \sqrt{14{,}2^2 + 4{,}4^2} = 14{,}8 \text{ мм}.$$

In Fig. 4.19 is plotted circle of stability; its center is a distance of 4.4 mm from center of gravity of section.

Given various values of y_e (or η_e), we find critical magnitudes by equation (114). In the particular case when force is applied at center of bending of section D (see Fig. 4.10a), by (115) and (115a) we obtain

$$\sigma_0^{(1)} = \frac{16{,}85 \cdot (14{,}2)^2 - 9{,}15\,(14{,}8)^2}{14{,}2^2 + 14{,}8^2 + 2 \cdot 14{,}8\,(-19{,}2)} = -9{,}4 \text{ kg/mm}^2$$

$$\sigma_0^{(2)} = \sigma_y = 9{,}15 \text{ kg/mm}^2.$$

Design critical stress here will be $\sigma_z = 4.3$ kg/mm^2; this magnitude was found above in example 4.1.

From example 4.2 it is clear that with significant eccentricities one of the critical stresses is tensile.

§ 53. More General Equations of Bending-Twisting Deformation.

Till now we took as the pole the center of rotation of a section. In certain cases it is more convenient to select as pole the center of bending of the section. We will derive the corresponding equations, assuming that in addition to central compressive forces P on faces of bar are applied couples in planes xz and zy with moments M_y and M_z. We consider bar in a state, deflected from the base and determine intensity of "loads" corresponding to turned forces of base state. Here we first consider turns caused by distortion of the axis of centers of bending, and then turns connected with twisting around this axis. Displacements of centers of bending of different sections along axes y and z we designate by v and w. In Fig. 4.20 is shown elementary force σdF, turned in plane xz. Corresponding angles in planes xy and xz are equal to dv/dx and dw/dx. Additional projections on axes y and z of forces σdF will be $\sigma\left(\frac{dv}{dx}\right)dF$ and $\sigma\left(\frac{dw}{dx}\right)dF$; these projections give moments about center of bending equal to

$$\left[\sigma\frac{dv}{dx}(z-z_D)\,dF\right] \text{ and } \left[-\sigma\frac{dw}{dx}(y-y_D)\,dF\right];$$

by y_D and z_D we designate coordinates of center of bending.

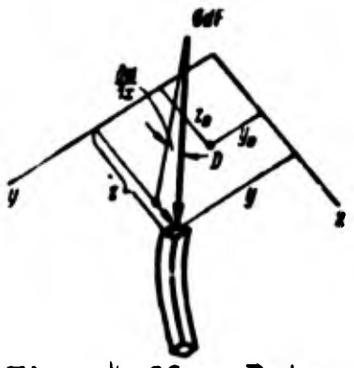

Fig. 4.20. Determination of moment of elementary force.

Per unit length of axial line there will be a load

$$q_y=-\int_F \sigma\frac{d^2v}{dx^2}\,dF,\quad q_z=-\int_F \sigma\frac{d^2w}{dx^2}\,dF \tag{4.116}$$

and a moment with intensity

$$m=\int_F \sigma\left[\frac{d^2v}{dx^2}(z-z_D)-\frac{d^2w}{dx^2}(y-y_D)\right]dF. \tag{4.117}$$

integrals pertain to the whole section.

During action of compressive central force P and moments M_y and M_z stress σ at point y, z is equal to

$$\sigma = \frac{P}{F} - \frac{M_z}{I_z} y + \frac{M_y}{I_y} z. \tag{4.118}$$

Putting this expression in (116), we find

$$q_y = -P\frac{d^2v}{dx^2}, \quad q_z = -P\frac{d^2w}{dx^2}, \tag{4.119}$$

Remaining integrals turn into zero. Moment (117) will be equal to

$$m = -(Pz_D - M_y)\frac{d^2v}{dx^2} + (Py_D + M_z)\frac{d^2w}{dx^2}. \tag{4.120}$$

We turn to turns of forces caused by twisting of the bar. Increase of component of elementary force in plane yz turned out to be equal to (p.197)

$$\sigma d\psi dF, \text{ or } \sigma d\left(\frac{d\theta}{dx}\right)\rho dF;$$

projection of it on axes y and z will be

$$\left[\sigma d\left(\frac{d\theta}{dx}\right)\rho_1 \frac{z - z_D}{\rho_1} dF\right] \text{ and } \left[-\sigma d\left(\frac{d\theta}{dx}\right)\rho_1 \frac{y - y_D}{\rho_1} dF\right],$$

by ρ_1 we understand radius vector from center of bending to element dF. Linear intensities of loads are equal to

$$q_y = \int_F \sigma \frac{d^2\theta}{dx^2}(z - z_D)\,dF, \quad q_z = -\int_F \sigma \frac{d^2\theta}{dx^2}(y - y_D)\,dF.$$

Substituting (118), we obtain,

$$q_y = -(Pz_D - M_y)\frac{d^2\theta}{dx^2}, \quad q_z = (Py_D + M_z)\frac{d^2\theta}{dx^2}. \tag{4.121}$$

We constitute differential equations for displacements v, w and angle of rotation θ.

$$\left.\begin{aligned} EI_z \frac{d^4v}{dx^4} &= q_y, \\ EI_y \frac{d^4w}{dx^4} &= q_z, \\ EI_\omega^* \frac{d^4\theta}{dx^4} - GI_k \frac{d^2\theta}{dx^2} &= m. \end{aligned}\right\} \tag{4.122}$$

Here by I_ω^* is inderstood sectorial moment of inertia about center of bending. Proceeding from formula of transition (47), we find

$$I_\omega^* = I_\omega - 2y_D R_y + 2z_D R_z + y_D^2 I_y + z_D^2 I_z.$$

But by (61) we have

$$R_y = y_D I_y, \quad R_z = -z_D I_z. \tag{4.123}$$

consequently,

$$I_\omega^\circ = I_\omega - I_y y_D^2 - I_z z_D^2. \tag{4.124}$$

Torsional moment (25) is equal to

$$m = -\frac{d^3\theta}{dx^3}\int_F \left(\frac{P}{F} - \frac{M_z}{I_z}y + \frac{M_y}{I_y}z\right)\rho_1^2\, dF. \tag{4.125}$$

or

$$m = -\frac{d^3\theta}{dx^3}\left(Pr^{\circ 2} - M_z\frac{S_y^\circ}{I_z} + M_y\frac{S_z^\circ}{I_y}\right).$$

By formula (71)

$$I_\rho^\circ = I_\rho + (y_D^2 + z_D^2)F; \tag{4.126}$$

hence

$$r^{\circ 2} = \frac{I_\rho^\circ}{F} = r^2 + y_D^2 + z_D^2. \tag{4.127}$$

Magnitudes S_y^* and S_z^* by (89) are equal to

$$S_y^\circ = S_y - 2y_D I_z, \quad S_z^\circ = S_z - 2z_D I_y. \tag{4.128}$$

Expression (125) obtains form

$$m = -\left[Pr^{\circ 2} - 2M_z\left(\frac{S_y}{2I_z} - y_D\right) + 2M_y\left(\frac{S_z}{2I_y} - z_D\right)\right]\frac{d^3\theta}{dx^3}.$$

Introducing designations of type (92)

$$\beta_y = \frac{S_y}{2I_z} - y_D, \quad \beta_z = \frac{S_z}{2I_y} - z_D,$$

we obtain

$$m = -(Pr^{\circ 2} - 2M_z\beta_y + 2M_y\beta_z)\frac{d^3\theta}{dx^3}. \tag{4.129}$$

Summarizing expressions for linear loads (119) and (121), and also for moments (120) and (129) and putting them in equations (122), we arrive at following system of differential equations:

$$\left.\begin{aligned}
&EI_z\frac{d^4v}{dx^4} + P\frac{d^2v}{dx^2} + (Pz_D - M_y)\frac{d^2\theta}{dx^2} = q_y,\\
&EI_y\frac{d^4w}{dx^4} + P\frac{d^2w}{dx^2} - (Py_D + M_z)\frac{d^2\theta}{dx^2} = q_z,\\
&EI_\omega^\circ\frac{d^4\theta}{dx^4} + (Pr^{\circ 2} - 2M_z\beta_y + 2M_y\beta_z - GI_k)\frac{d^2\theta}{dx^2} +\\
&\quad + (Pz_D - M_y)\frac{d^2v}{dx^2} - (Py_D + M_z)\frac{d^2w}{dx^2} = m.
\end{aligned}\right\} \tag{4.130}$$

Analogous equations for case of moments variable in length have a somewhat different structure ([4.4], p.369). In bifurcational problems half equations of such a type must be used with caution (see footnote on p.217).

§ 54. Stability of Plane Form of a Strip During Bending.

Let us consider the particular case of a bar of rectangular section, subjected to bending in plane xy.

We must here set $I_\omega^* = \beta_y = \beta_z = 0$. We take in (130) $P = M_y = q_z = m = 0$ and integrate twice the second of these equations, considering constant of integration equal to zero. Finally the second and third equations will take the form

$$EI_y \frac{d^2w}{dx^2} - M_z\theta = 0. \tag{4.131}$$

$$GI_k \frac{d^2\theta}{dx^2} + M_z \frac{d^2w}{dx^2} = 0. \tag{4.132}$$

Excluding from this w, we obtain one second order equation for θ:

$$\frac{d^2\theta}{dx^2} + \frac{M_z^2}{GI_kEI_y}\theta = 0. \tag{4.133}$$

During pure bending M_z = const; solution of equation has the form

$$\theta = A\sin kx + B\cos kx, \tag{4.134}$$

where

$$k = \frac{M_z}{\sqrt{GI_kEI_y}}. \tag{4.135}$$

Boundary conditions we select in the form

$$\theta = 0 \quad \text{when} \quad x = 0, \quad x = l; \tag{4.136}$$

then first critical value of k will be π/l; hence by (100)

$$M_{cr} = \frac{\pi}{l}\sqrt{GI_kEI_y}. \tag{4.137}$$

Equations (131)--(132) it is possible to use in our case and for a moment variable in length.

Assume, for instance, that right face of band is fixed, and left is free. Assume that in center of gravity of left face section there

is applied force P, directed along the vertical (Fig. 4.21). In this case $M_z = -Px$; in place of (133) we have

$$\frac{d^2\theta}{dx^2} + \frac{P^2}{GI_k EI_y} x^2\theta = 0. \tag{4.138}$$

Introducing designation

$$a = \frac{P}{\sqrt{GI_k EI_y}}, \tag{4.138a}$$

we reduce equation (138) to the form

$$\frac{d^2\theta}{dx^2} + a^2 x^{n+1}\theta = 0, \tag{4.139}$$

which we already met in Section 35 and 37. If one were to set

$$\nu = \frac{1}{n+3} \tag{4.140}$$

and consider that ν is a fractional number, the solution of equation (139) takes form (3.23):

$$\theta = A\sqrt{x}\, J_\nu\left(2a\nu x^{\frac{1}{2\nu}}\right) + B\sqrt{x}\, J_{-\nu}\left(2a\nu x^{\frac{1}{2\nu}}\right). \tag{4.141}$$

where J_ν is a Bessel function of the first type with index ν. Derivative from an expression of type (141) was already calculated by us; from (3.44) we have

$$\frac{d\theta}{dx} = Aax^{\frac{1-\nu}{2\nu}} J_{-(1-\nu)}\left(2a\nu x^{\frac{1}{2\nu}}\right) - Bax^{\frac{1-\nu}{2\nu}} J_{1-\nu}\left(2a\nu x^{\frac{1}{2\nu}}\right). \tag{4.142}$$

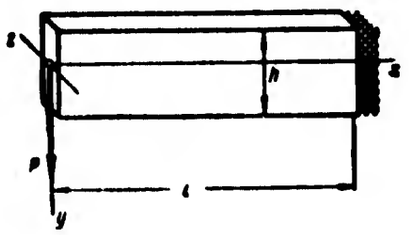

Fig. 4.21. Bending of strip by concentrated force.

In example considered by us n = 1, $\nu = 1/4$; consequently,

$$\theta = A\sqrt{x}\, J_{\frac{1}{4}}\left(\frac{a}{2}x^2\right) + B\sqrt{x}\, J_{-\frac{1}{4}}\left(\frac{a}{2}x^2\right). \tag{4.143}$$

$$\frac{d\theta}{dx} = Aax^{\frac{3}{2}} J_{-\frac{3}{4}}\left(\frac{a}{2}x^2\right) - Bax^{\frac{3}{2}} J_{\frac{3}{4}}\left(\frac{a}{2}x^2\right). \tag{4.144}$$

We shall consider that on left end torque M_K turns into zero.

From dependences (13) and (14) this magnitude, when $I_\omega = 0$, is equal to

$$M_k = \bar{M} = GI_k \frac{d\theta}{dx}. \tag{4.145}$$

Consequently, on this end we should have

$$\frac{d\theta}{dx}=0 \quad \text{when} \quad x=0. \tag{4.146}$$

On the other hand, on the fixed end the angle of torsion should be equal to zero:

$$\theta=0 \quad \text{when} \quad x=l. \tag{4.147}$$

As it is known (see Section 37), function $J_{-\frac{3}{4}}(0) = \infty$, while quantity $J_{\frac{3}{4}}(0)$ turns into zero. Therefore, condition (146) gives $A = 0$. When $B \neq 0$ from condition (147) we find

$$J_{-\frac{1}{4}}\left(\frac{\alpha}{2}l^2\right)=0. \tag{4.148}$$

Determining least root of this equation, we find critical load. In following table are given roots of equations, analogous to (148), for functions with different indices.

Table 4.1

(a) Корни	$J_{\frac{1}{4}}$	$J_{\frac{3}{4}}$	$J_{-\frac{1}{4}}$	$J_{-\frac{3}{4}}$
(b) 1-й	2,781	3,492	2,006	1,058
(c) 2-й	5,910	6,650	5,120	4,290

KEY: (a) Roots; (b) First; (c) Second.

Thus, in given problem we have

$$\frac{\alpha}{2}l^2=\frac{P}{2\sqrt{EI_xGI_\kappa}}l^2=2{,}006; \tag{4.149}$$

consequently, first critical load is equal to

$$P=\frac{4{,}01}{l^2}\sqrt{GI_\kappa EI_y}. \tag{4.150}$$

In structure dependence (150) is similar to Euler's formula.

This same problem it is possible to solve also by methods of approximation. Take, for instance, for function θ dependence

$$\theta=\theta_0(l^2-x^2). \tag{4.151}$$

satisfying boundary conditions. Equation of the Bubnov-Galerkin corresponding to (138), will be

$$\int_0^l \left(\frac{d^2\theta}{dx^2} + a^2x^2\theta\right)(l^2 - x^2)\,dx = 0. \qquad (4.152)$$

Substituting (151) and integrating, we find $a^2l^4 = 17.5$. Coefficient in formula of type (150) takes approximate value $\sqrt{17.5} = 4.18$.

Assume now that force P is applied not in center of gravity of face section, but a distance d from center (Fig. 4.22); we consider d positive if point of application of force lies above center of gravity. Then torque on left end is equal to $M_K = Pd\theta$; consequently, instead of (146) we obtain boundary condition

$$GI_k\frac{d\theta}{dx} = -Pd\theta \quad \text{when} \quad x = 0, \qquad (4.153)$$

condition (147) remains in force.

Fig. 4.22. Case, when force is applied not in center of gravity of section.

Bessel function index ν may be presented in the form of a series

$$J_\nu(x) = \frac{x^\nu}{2^\nu\Gamma(\nu)}\left[1 - \frac{x^2}{2(2\nu+2)} + \frac{x^4}{2\cdot4(2\nu+2)(2\nu+4)} - \cdots\right]; \qquad (4.154)$$

here $\Gamma(\nu)$ is a gamma-function, tables of magnitudes $\Gamma(\nu)$ are contained in reference books. From (143) we find

$$\theta = Ax^{\frac{1}{2}}\frac{\left(\frac{a}{2}x^2\right)^{\frac{1}{4}}}{2^{\frac{1}{4}}\Gamma\left(\frac{1}{4}\right)}\left[1 - \frac{\left(\frac{a}{2}x^2\right)^2}{2\cdot2,5} + \cdots\right] +$$

$$+ Bx^{\frac{1}{2}}\frac{\left(\frac{a}{2}x^2\right)^{-\frac{1}{4}}}{2^{-\frac{1}{4}}\Gamma\left(-\frac{1}{4}\right)}\left[1 - \frac{\left(\frac{a}{2}x^2\right)^2}{2\cdot1,5} + \cdots\right]$$

When $x \to 0$ we have

$$\theta(0) = B\frac{\sqrt{2}}{a^{\frac{1}{4}}\Gamma\left(-\frac{1}{4}\right)}. \tag{4.155}$$

Further, from (144)

$$\frac{d\theta}{dx} = Aax^{\frac{3}{2}}\frac{\left(\frac{ax^2}{2}\right)^{-\frac{3}{4}}}{2^{-\frac{3}{4}}\Gamma\left(-\frac{3}{4}\right)}\left[1 - \frac{\left(\frac{a}{2}x^2\right)^2}{2\cdot 0{,}5} + \ldots\right] -$$

$$- Bax^{\frac{3}{2}}\frac{\left(\frac{ax^2}{2}\right)^{\frac{3}{4}}}{2^{\frac{3}{4}}\Gamma\left(\frac{3}{4}\right)}\left[1 - \frac{\left(\frac{a}{2}x^2\right)^2}{2\cdot 3{,}5} + \ldots\right];$$

when $x \to 0$,

$$\left(\frac{d\theta}{dx}\right)_{x=0} = A\frac{2^{\frac{3}{2}}a^{\frac{1}{4}}}{\Gamma\left(-\frac{3}{4}\right)}. \tag{4.156}$$

Putting these values in (153), we obtain

$$2\Gamma\left(-\frac{1}{4}\right)GI_K A + \Gamma\left(-\frac{3}{4}\right)dP^{\frac{1}{2}}(GI_K EI_y)^{\frac{1}{4}}B = 0. \tag{4.157}$$

Second condition, i.e., (147), gives

$$J_{\frac{1}{4}}\left(\frac{a}{2}l^2\right)A + J_{-\frac{1}{4}}\left(\frac{a}{2}l^2\right)B = 0. \tag{4.158}$$

We equate to zero determinant of system of equations (157) and (158): then we will have

$$2\Gamma\left(-\frac{1}{4}\right)GI_K J_{-\frac{1}{4}}\left(\frac{a}{2}l^2\right) - \Gamma\left(-\frac{3}{4}\right)dP^{\frac{1}{2}}(GI_K EI_y)^{\frac{1}{4}}J_{\frac{1}{4}}\left(\frac{a}{2}l^2\right) = 0. \tag{4.159}$$

In Table 4.2 are given values of coefficient K in formula for critical force

$$P_{кр} = K\frac{\sqrt{GI_K EI_y}}{l^2}. \tag{4.160}$$

corresponding to equation (159); they turn out to depend on parameter $d\sqrt{EI_y}/l\ \sqrt{GI_K}$.

Table 4.2. Coefficients K for Case When Force P is Applied to Cantilever not in Center of Gravity.

(a) Над центром тяжести

$\frac{d}{l}\sqrt{\frac{EI_y}{GI_к}}$	0	0,0031	0,0887	0,164	0,238	0,322	0,425	0,568	0,791	1,224	2,485
K	4,013	4,0	3,6	3,2	2,8	2,4	2,0	1,6	1,2	0,8	0,4

(b) Под центром тяжести

$\frac{d}{l}\sqrt{\frac{EI_y}{GI_к}}$	0	0,114	0,320	0,923	∞
K	4,013	4,4	4,8	5,2	5,562

KEY: (a) Above center of gravity; (b) Below center of gravity.

Here are given also coefficients K for limiting cases, when force is transmitted through very long lever ($\frac{d}{l} \to \infty$). For small ratios d/l we may use the simple approximate formula

$$P_{кр} = 4{,}01 \frac{\sqrt{GI_к EI_y}}{l^2}\left(1 - \frac{d}{l}\sqrt{\frac{EI_y}{GI_к}}\right); \qquad (4.161)$$

this can be proved easily by Table 4.2.

Let us turn to the case when cantilever is subjected to action of load uniformly distributed along its whole length q = const. (Fig. 4.23). Here $M_z = qx^2/2$; equation (133) obtains form

$$\frac{d^2\theta}{dx^2} + \frac{q^2}{GI_к EI_y}\frac{x^4}{4}\theta = 0. \qquad (4.162)$$

If we take

$$a = \frac{q}{2\sqrt{GI_к EI_y}}, \qquad (4.163)$$

we obtain equation of type (139) for n = 3 and $\nu = 1/6$. Repeating calculations given for case of concentrated force, we arrive at equation instead of (148):

$$J_{-\frac{1}{6}}\left(\frac{a}{3}l^3\right) = 0. \qquad (4.164)$$

Least root of this equation will be 2.142; critical value of intensity of distributed load is equal to

$$q = 2a\sqrt{GI_k EI_y} = 12.85\frac{\sqrt{GI_k EI_y}}{l^3}. \qquad (4.165)$$

If load is distributed along length of beam according to triangle law $q = q_0 x/l$, we obtain equation of type (139) when

$$a = \frac{q_0}{6l\sqrt{GI_k EI_y}}. \qquad (4.166)$$

When $n = 5$ and $\nu = 1/8$ instead of (164) we have

$$J_{-\frac{1}{8}}\left(\frac{a}{4}\right) = 0. \qquad (4.167)$$

Least root of equation (167) is equal to ~2.2; therefore, values of q_0 will be

$$q_0 = 52.8\frac{\sqrt{GI_k EI_y}}{l^3}. \qquad (4.168)$$

We give values of coefficient K_1 in formula for critical maximum bending moment:

$$M_{max} = K_1\frac{\sqrt{GI_k EI_y}}{l}. \qquad (4.169)$$

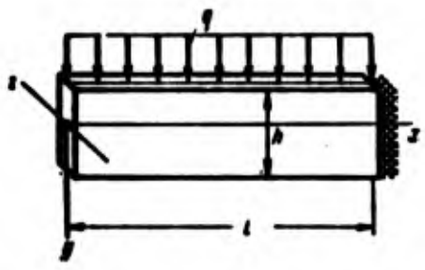

Fig. 4.23. Strip is subjected to action of uniformly distributed load.

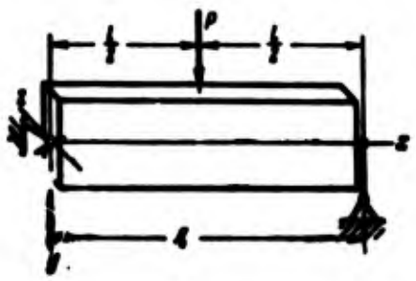

Fig. 4.24. Case of concentrated force, applied in the middle of span.

With pure bending $K_1 = \pi$; in case of concentrated force $K_1 = 4.01$, with uniformly distributed load $K_1 = 6.43$; in case of load, distributed according to triangle law $K_1 = 8.8$.

Let us turn to the case when strip supported by hinges on ends, and force P is concentrated in the middle of span (Fig. 4.24). We put origin of coordinates at left end, then moment M for left half of beam will be equal to

$$M = \frac{P}{2} x.$$

Equation (133) assumes form

$$\frac{d^2\theta}{dx^2} + \frac{P^2}{4GI_k EI_y} x^2 \theta = 0. \tag{4.170}$$

Its solution can be written in form (143), but instead of (138) it is necessary to set

$$a = \frac{P}{2\sqrt{GI_k EI_y}}. \tag{4.171}$$

We consider that support section does not turn:

$$\theta = 0 \quad \text{when} \quad x = 0. \tag{4.172}$$

On the other hand, during distortion of one half angle of rotation of average section should be maximum; so that here we should have

$$\frac{d\theta}{dx} = 0 \quad \text{when} \quad x = \frac{l}{2}. \tag{4.173}$$

Using expression (143), from first condition we find B = 0. Second condition gives

$$J_{-\frac{3}{4}}\left(\frac{al^2}{8}\right) = 0. \tag{4.174}$$

Judging by Table 4.1 (p.224), first root of this equation is equal to 1.058; consequently, critical force is equal to

$$P = 16.94 \frac{\sqrt{GI_k EI_y}}{l^2}. \tag{4.175}$$

Assume that force P is applied at point removed from center of gravity of section a distance d. Then boundary condition (172) remains, and condition (173) must be replaced by the following:

$$GI_k \frac{d\theta}{dx} = \frac{P}{2} \theta d \quad \text{when} \quad x = \frac{l}{2}. \tag{4.176}$$

Taking B = 0, we obtain from this

$$\frac{2d}{l} \sqrt{\frac{EI_y}{GI_k}} J_{\frac{1}{4}}\left(\frac{al^2}{8}\right) = J_{-\frac{3}{4}}\left(\frac{al^2}{8}\right). \tag{4.177}$$

Coefficients K in formula of type (160), obtained from equation (177), are given in Table 4.3.

Fig. 4.25. Concentrated force applied at various distances from supports.

Let us consider, finally, the case where force P is applied to strip supported by hinges various distances from face sections (Fig. 4.25). Designating these distances by m and n, we have for left half $M_z = Pnx_1/l$ and for right half $M_z = Pmx_1/l$.

Table 4.3. Coefficients K for Case, When Force P is Applied to Beam on Two Supports not at Center of Gravity

(a) Над центром тяжести

$\frac{d}{l}\sqrt{\frac{EI_y}{GI_k}}$	0	0,030	0,143	0,293	0,544	1,210
K	16,94	16,0	12,8	9,6	6,4	3,2

(b) Под центром тяжести

$\frac{d}{l}\sqrt{\frac{EI_y}{GI_k}}$	0	0,069	0,166	0,271	0,396	0,562	0,815	1,30	2,78
K	16,94	19,2	22,4	25,6	28,8	32,0	35,2	38,4	41,6

KEY: (a) Above center of gravity; (b) Under center of gravity.

We can use equation (143), considering

$$a_1 = \frac{Pn}{l\sqrt{GI_k EI_y}}, \quad a_2 = \frac{Pm}{l\sqrt{GI_k EI_y}}. \tag{4.178}$$

Boundary conditions we constitute for end sections in the form

$$\theta_1 = 0 \text{ when } x_1 = 0, \quad \theta_2 = 0 \text{ when } x_2 = 0 \tag{4.179}$$

and for point of linkage

$$\theta_1 = \theta_2 \text{ and } \frac{d\theta_1}{dx} = \frac{d\theta_2}{dx}. \tag{4.180}$$

Equation for determination of critical load will be

$$J_{\frac{1}{4}}\left(\frac{m^2 a_1}{2}\right) J_{-\frac{3}{4}}\left(\frac{n^2 a_2}{2}\right) + J_{\frac{1}{4}}\left(\frac{n^2 a_2}{2}\right) J_{-\frac{3}{4}}\left(\frac{m^2 a_1}{2}\right) = 0. \tag{4.181}$$

In Table 4.4 are given values of coefficient K for various ratios m/l, calculated by (181).

If ends of the strip are fixed, and force P is applied in the middle of span, coefficient K in formula of type (175) turns out to be equal to 26.6 and in formula of type (169)--equal to 3.54.

Table 4.4. Coefficients K for Case of Concentrated Force Applied Various Distances From Supports

$\frac{m}{l}$	0,5	0,45	0,40	0,35	0,30	0,25	0,20	0,15	0,10	0,05
K	16,94	17,15	17,82	19,04	21,01	24,10	29,11	37,88	56,01	111,6

During action of uniformly distributed load on beam supported by hinges at ends coefficient K in formula (169) is equal to 28.3/8 = = 3.54.

§ 55. Lateral Bending of Beams with Section, Having Two Axes of Symmetry.

We turn to the more general case, when bar is an arbitrary section, having two axes of symmetry; an example can be an I-beam. For

such a section the center of bending coincides with center of gravity and $\beta_y = 0$. If the beam is subjected to lateral bending in plane xy, then auxiliary equations (131) and (132) will take according to (130) the form

$$\left.\begin{aligned} EI_y \frac{d^2w}{dx^2} - M_z\theta &= q_z, \\ EI_\omega \frac{d^4\theta}{dx^4} - GI_k \frac{d^2\theta}{dx^2} - M_z \frac{d^2w}{dx^2} &= m. \end{aligned}\right\} \tag{4.182}$$

Considering $q_z = 0$, and eliminating w, we arrive at a fourth-order equation:

$$EI_\omega \frac{d^4\theta}{dx^4} - GI_k \frac{d^2\theta}{dx^2} - \frac{M_z^2}{EI_y}\theta = m. \tag{4.183}$$

If on beam there acts distributed load q, applied at distance d from center of gravity (Fig. 4.23), the intensity of moment m is equal to $(-qd\cdot\theta)$; considering dependence between q and M_z, we obtain, instead of (183),

$$EI_\omega \frac{d^4\theta}{dx^4} - GI_k \frac{d^2\theta}{dx^2} - \left(\frac{M_z^2}{EI_y} - \frac{d^2M_z}{dx^2}d\right)\theta = 0. \tag{4.184}$$

Integration of this equation may be carried out generally only by approximate methods.

Consider case of beam on two supports, to which there is applied concentrated force P at mid-span (Fig. 4.24). Then equation (184) will take form (when $0 \leq x \leq \frac{1}{2}$)

$$EI_\omega \frac{d^4\theta}{dx^4} - GI_k \frac{d^2\theta}{dx^2} - \frac{4M_{max}^2}{l^2EI_y}x^2\theta = 0; \tag{4.185}$$

here M_{max} is moment in the middle section. We consider that angle of rotation of end sections is equal to zero:

$$\theta = 0 \text{ when } x = 0, \quad x = l. \tag{4.186}$$

Furthermore, assume that bimoment in end sections turns into zero. Then we should have

$$\frac{d^2\theta}{dx^2} = 0 \text{ when } x = 0, \quad x = l. \tag{4.187}$$

We take for θ the approximate expression

$$\theta = A \sin \frac{\pi x}{l}. \tag{4.188}$$

satisfying boundary conditions. The Bubnov-Galerkin equation will be

$$\int_0^{\frac{l}{2}} \left(\frac{\pi^4}{l^4} EI_\omega + \frac{\pi^2}{l^2} GI_k - \frac{4M_{max}^2}{l^2 EI_y} x^2 \right) \sin^2 \frac{\pi x}{l} dx = 0$$

or

$$\frac{l}{4} \left(\frac{\pi^4}{l^4} EI_\omega + \frac{\pi^2}{l^2} GI_k \right) - \frac{4M_{max}^2}{l^2 EI_y} \left(\frac{l^3}{48} + \frac{l^3}{8\pi^2} \right) = 0. \tag{4.189}$$

Hence critical value M_{max} is

$$M_{max} = \frac{\frac{\pi}{l} \sqrt{GI_k EI_y}}{\sqrt{\frac{1}{3} + \frac{2}{\pi^2}}} \sqrt{1 + \frac{\pi^2}{l^2} \frac{EI_\omega}{GI_k}}. \tag{4.190}$$

For particular case, when $I_\omega = 0$, we obtain

$$M_{max} = \frac{4.28}{l} \sqrt{GI_k EI_y}. \tag{4.191}$$

In Section 54 we obtained an exact value of the coefficient in this formula, equal to 4.23. We use formula (190) in order to estimate influence of additional factor, containing I_ω. Let us note that in case of pure bending method would lead to an exact result (104):

$$M_{max} = \frac{\pi \sqrt{GI_k EI_y}}{l} \chi. \tag{4.192}$$

where by χ is understood expression

$$\chi = \sqrt{1 + \frac{\pi^2 EI_\omega}{l^2 GI_k}}. \tag{4.193}$$

This gives a basis to present calculating formula for considered case of concentrated force in form

$$M_{max} = 4.23 \frac{\sqrt{GI_k EI_y}}{l} \chi. \tag{4.194}$$

Obviously, the same factor χ may be used also in other cases of loading a beam supported by hinges. For example, under action of uniformly distributed load, applied on central lines, we will obtain

$$M_{max} = \frac{3.54}{l} \sqrt{GI_k EI_y} \chi. \tag{4.195}$$

If load is applied not in center of gravity, but on upper or lower flanges, then instead of (195) we obtain

$$M_{max} = \frac{3,54}{l}\sqrt{GI_k EI_y}\,\gamma k. \qquad (4.196)$$

The additional factor turns out to be equal to

$$k = \sqrt{1 + \frac{2,1}{\gamma^2}\frac{EI_\omega}{GI_k}} \mp \frac{1,45}{\gamma}\sqrt{\frac{EI_\omega}{GI_k}}. \qquad (4.197)$$

Minus sign pertains to case when load is transmitted to upper flange, while plus--during loading of lower flange.

In previous chapters we examined stability of bars and simple bar systems. Outside frame work of this book remains theory of stability of complex bar systems, expecially statically indeterminate frames. This region is illuminated in books of N. V. Kornoukhov [0.5], A. R. Rzhanitsyn [0.10], V. G. Chudnovskiy [0.12], A. F. Smirnov [0.11], N. K. Snitko [3.9], Ya. L. Nudel'man [3.5], I. K. Snitko (Practical methods of calculation of statically indeterminate systems, Moscow, 1960), A. A. Pikovskiy [3.7], S. A. Rogitskiy (New method of calculation for strength and stability, Sverdlovsk, 1961), R. R. Matevosyan (Transactions TsNIISK, No. 3, 1961), F. Bleich [0.15], G. Bügermeister and H. Steup [0.16].

Literature

4.1. S. A. Ambartsumyan. Concerning the question of calculation of stability of thin-walled bars, Reports of Acad. of Sci. of Armenian SSR, 17, No. 1 (1953).

4.2. V. V. Bolotin. Integral equations of constrained torsion and stability of thin-walled bars, Applied math. and mech., 17, No. 2 (1953); Spatial deformations of beams after loss of stability, Design of spatial structures, 4 (1959), 3-18; Ultimate strains of flexible pipes, Transactions of Moscow Power Engineering Inst., 19 (1956) Stability of beams united elastically, Calculations for durability, 1 (1954), 223-230.

4.3. B. M. Broude. Stability and vibrations of an elastically clamped bar, "Collection on theory of constructions," 5 (1954); Stability of slightly distorted and eccentrically loaded I-beams, Design of spatial structures, 4 (1958), 5-36; More precise solution of problem of Prandtl and Timoshenko, loc. cit., 5 (1959); Stability of bars, compressed with biaxial eccentricity, loc. cit., 31-50; Linearization of equations of stability and equilibrium of an eccentrically compressed bar, Research in theory of structures, 8 (1959), 205-221.

4.4. V. Z. Vlasov. Thin-walled elastic bars, 1st edition, 1940; 2nd ed., Fizmatgiz, M., 1959.

4.5. V. Z. Vlasov. Torsion and stability of thin-walled open sections, Stroit. prom., No. 6-7 (1938); Torsion, stability and vibration of a thin-walled bar, Applied math. and mech., 3, No. 1 (1939).

4.6. A. V. Gemmerling. Design centrifugally compressed thin-walled bars, Transactions of Laboratory of Structural Mechanics of TsNIPS, Stroyizdat (1949).

4.7. I. I. Gol'denblat. Contemporary problems of vibrations and stability of engineering constructions, Stroyizdat, 1947.

4.8. L. M. Kachanov. Stability of thin-walled bars during elasto-plastic flows, DAN SSSR, 107, No. 6 (1956), 803-806.

4.9. I. F. Obraztsov. Design of thin-walled bars for flexural strength, Transactions MAI, No. 26, Oborongiz (1953).

4.10. A. R. Rzhanitsyn. Stability of thin-walled bars beyond the elastic limit, Transactions of Laboratory of Structural Mechanics, TsNIPS, Stroyizdat (1949).

4.11. A. I. Strel'bitskaya. Supporting power of thin-walled bars with complex resistance, Applied Mechanics, Publishing House of Academy of Sciences of Ukrainian SSR, 2, No. 3 (1956).

4.12. A. A. Umanskiy. Torsion and flexure of thin-walled airplane constructions, M., 1939; Structural mechanics of aircraft, M., 1961.

4.13. Hua Hai-ch'ang and Chieh Po-min. General theory of equilibrium and stability of elastic thin-walled bars (in Chinese) Acta Phys. Sinica, No. 4 (1955).

4.14. J. Goodier. Torsional und flexural buckling of bars of thin-walled open section under compressive and bending loads. J. of the Aeron, Sci. (1942), 103-107.

4.15. R. Kappus. Drehknicken zentrisch gedrückten Stäbe mit offenem Profil in elastisch Bereich. Luftfahrtforschung 14, No. 9 (1937).

4.16. H. L. Langhaar. On torsional-flexural buckling of columns. The Journal of the Franklin Institute, No. 2 (1953), 101-112.

4.17. H. Nylander. Torsion, bending and lateral buckling of I-beams, Kgl. tekn. högskolans handl., No. 102 (1956), 140.

4.18. L. Prandtl. Kipperscheinungen, Nürenberg, 1899.

4.19. S. Timoshenko. Theory of bending, torsion and buckling of thin walled members of open cross section. The Journ. of the Franklin Institute, No. 3, 201-219; No. 4, 249-268; No. 5, 343-361 (1945).

4.20. H. Wagner. Verdrehung und Knickung von offenen Profilen, Festschrift 25-Jahre T. H. Danzig, 1929.

CHAPTER V

INFLUENCE OF TEMPERATURE. CREEP BUCKLING

§ 56. Problems of Stability of Bars, Connected with Consideration of Temperature.

Thanks to development of new regions of technology and first of all supersonic aviation recently there appeared new problems of stability of elastic systems at high temperatures. As it is known, aerodynamic heating leads to formation of nonuniform field of temperatures in constructions of aircraft. With this is connected appearance of certain stresses. Such thermal stresses are not always dangerous for strength of construction, since they are "resorbed" as deformation develops. But those structural members in which there are developed compressive stresses, may lose stability, which in a number of cases is equivalent to loss of supporting power and is impermissible.

Further, at high temperatures there appears creep of structural materials (steel, duralumin, titanium alloys, etc.), which in turn leads to loss of stability of compressed members at stresses, lying considerably below Euler's value. We note that for certain materials (plastic) creep occurs also at relatively low temperatures. Phenomenon of creep flows in time; unobtrusive deformation of compressed rod with expiration of a certain period ends in sharp buckling.

Thus, here, along with steady-state concept of critical stress, there appeared a new concept critical time. There appeared a new area of the theory of stability of elastic systems--theory of buckling during creep.

When solving problems, pertaining to unevenly heated constructions, it is necessary to examine anew criterion of stability. Existence of a nonuniform temperature field is connected with phenomenon of thermal conduction inside a body and with energy dissipation in the environment. Process of deformation during loading and buckling of a body is accompanied, furthermore, by irreversible changes of temperature field. Therefore, study of stability of unevenly heated body must, strictly speaking, be conducted, proceeding from equations of the thermodynamics of irreversible processes.*

We turn to certain particular problems.

§ 57. Influence of Temperature on Magnitude of Modulus of Elasticity. Uniform Heating of Bar with Fixed Ends.

If we examine stability of bars within limits of elastic deformations, then increase of temperature affects first of all the magnitude of the elastic modulus. In Fig. 5.1 is presented dependence of modulus E on temperature t°C for certain materials--steel ЭИ728. [EI728], ЭИ703. [EI703], ЯIТН. [YaITH], titanium alloy ВТ6 [VT6] and duralumin Д16АТ [D16AT]. As we see, with increased t° magnitude E quickly drops. Value of E for various t° one should put in design

*See work of M. Biot, published in "Aeronaut. Quarterly," 7, No. 3 (1956), "Physical Review," 97, No. 6 (1955), "Journ. of Applied Physics," 25, No. 11 (1954), and dissertation of L. A. Shapovalov [5.10].

formula. Let us note that with growth of t° values of limit of proportionality $\sigma_{пц}$ and yield point σ_t also fall.

Consider case, when bar is fastened by hinge to fixed supports at a temperature t_0°, and then is subjected to uniform heating its whole length (Fig. 5.2). With increase of temperature in bar there will appear compressive stresses, and at a centain temperature the bar will start to buckle. This case of loss of stability is interesting since it occurs without any active loads.

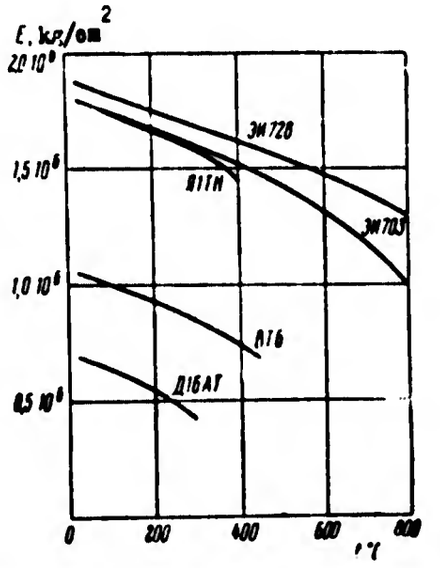

Fig. 5.1. Change of modulus E depending upon temperatures t°C for various materials.

If bar was extended freely, then its longitudinal strain at temperature t_1° would be equal to

$$\varepsilon_t = \alpha(t_1^{\circ} - t_0^{\circ}). \qquad (5.1)$$

where α is coefficient of linear expansion. In case of fixed ends there occur compressive stresses, equal to

$$\sigma_t = E\varepsilon_t = E\alpha(t_1^{\circ} - t_0^{\circ}). \qquad (5.2)$$

After quantity σ_t reaches Euler's value $\frac{\pi^2 E}{\lambda^2}$, straight-line form of equilibrium of bar will become unstable. With hinged fastening of ends of bar difference of temperatures, corresponding to critical stress, will be equal to

$$t_1^\circ - t_0^\circ = \frac{\pi^2}{\lambda^2 \alpha}. \qquad (5.3)$$

where λ is slenderness ratio of the bar. Thus, for instance, for duralumin D16AT coefficient α is $25 \cdot 10^6$. In case of bar whose slenderness ratio is $\lambda = 100$, buckling will start when difference of temperatures reach magnitude $t_1^\circ - t_0^\circ = 40^\circ$. Corresponding compressive stress constitutes about 700 kg/cm^2.

Fig. 5.2. Bar with fixed ends with variable temperature.

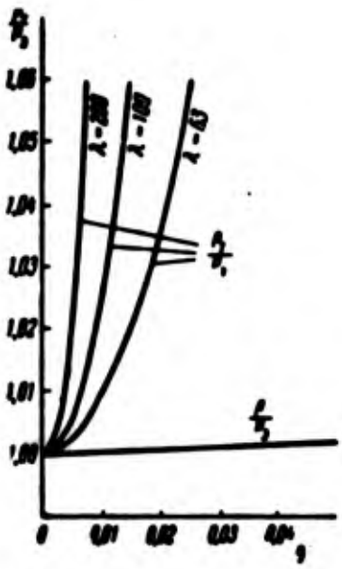

Fig. 5.3. Dependence between load and deflection after loss of stability.

If stresses in bar exceed limit of proportionality, to deformation (1) will correspond stress, equal to

$$\sigma_t = E_c \varepsilon_t \qquad (5.2')$$

where E_c is secant modulus, corresponding to temperature t_1°. Using formula for critical stress with tangential modulus E_K, we find difference of temperatures, at which buckling appears:

$$t_1^\circ - t_0^\circ = \frac{\pi^2}{\lambda^2 \alpha} \frac{E_K}{E_c}. \qquad (5.4)$$

Modulus E_K also is calculated for temperature t_1°.

Uniqueness of this problem consists in the fact that, as soon as buckling of bar starts reactions of supports, equal to compressive force in bar, will decrease; therefore, intense buckling can take place only during continuing rise in temperature.

This circumstance is illustrated by graph of Fig. 5.3.* On the axis of abscissas here is placed angle θ of slope of tangent to elastic line of bar in end section (see Fig. 5.2); along the axis of ordinates is temperature force

$$P_T = EF\alpha(t_1^\circ - t_0^\circ),$$

which must take place in a straight bar so that after distortion angle of rotation attains valve θ; magnitude P_T is related to Euler's force $P_э$. As can be seen from graph, relationship between $P_T/P_э$ and θ depends on slenderness ratio of the bar λ. For instance, when $\lambda = 100$ and $\theta = 0.015$ force P_T exceeds critical magnitude by 6%. For comparison here there is given diagram of supercritical deformation of bar with upper mobile hinge for constant temperature. For the former value of $\theta = 0.015$ compressive force P° would exceed Euler's magnitude by only 0.003%.

§ 58. Case of Nonuniform Heating.

Proceed now to case, when temperature field is not uniform.

---

*This graph was composed by V. I. Usyukin.

Let us consider centrally compressed bar of rectangular section, fixed at ends. Let us assume for example that such a piece is fixed between plates of a testing machine at temperate t_0°, after which it is subjected to heating up to a temperature, changing along one of the sides of the section (Fig. 5.4) linearly; increment of temperature equals

$$t = \frac{t_2^\circ + t_1^\circ}{2} - \frac{t_2^\circ - t_1^\circ}{2} y; \tag{5.5}$$

along each longitudinal fiber magnitude t° is constant.*

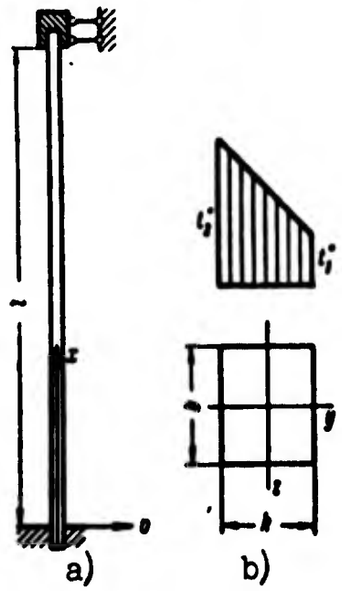

Fig. 5.4. Bar subjected to nonuniform heating.

Since ends of bar are fixed, then its axis will remain straight up to moment of buckling. Assume, further, that to bar is transmitted an increasing load; it is required to determine its critical magnitude. Such a problem is of special interest if stress in bar exceeds limit of proportionality. To each fiber of the bar there will then correspond its own diagram $\sigma(\varepsilon)$, character of which changes depending upon temperature. We consider that buckling of the bar occurs at a constant force and that therefore, the section is divided into zones of loading and unloading (Fig. 5.4b). We assume, for example, that diagram of compression of material (steel) consists of two straight lines (case of

*This problem was formulated by L. I. Balabukh and solved by L. A. Shapovalov [5.10].

"linear hardening") and what with increase of temperature there simultaneously change principal modulus E, tangential modulus on second section E_K and limit of proportionality, as shown in Fig. 5.5.

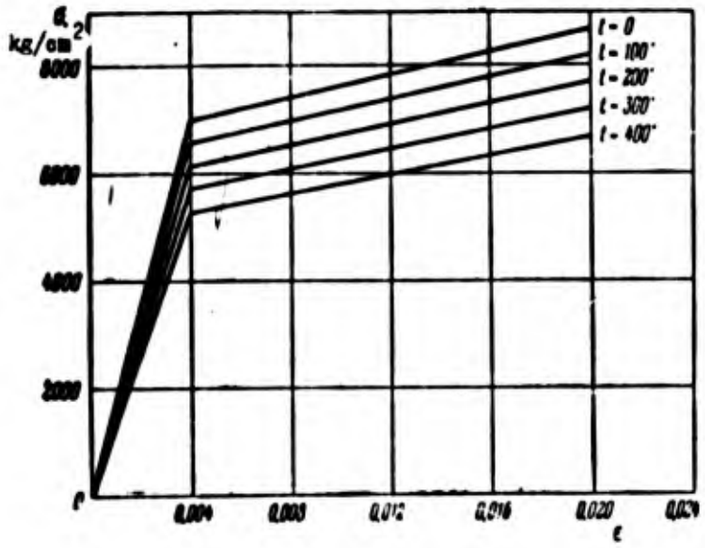

Fig. 5.5. Diagram of compression at different temperatures.

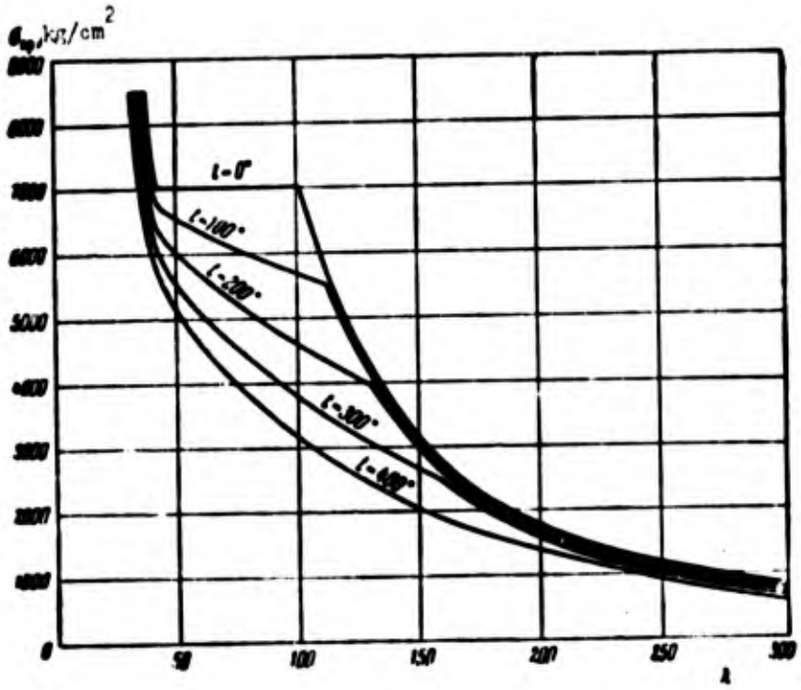

Fig. 5.6. "Critical stress--slenderness ratio" graph for nonuniform heating.

Deformation of every fiber up to loss of stability is composed of two components, one of which is caused by active load, and the

other is connected with increase of temperature:

$$\varepsilon = \varepsilon_0 + \alpha t^\circ. \tag{5.6}$$

Coefficient α we consider not dependent on temperature. Strains at moment of buckling are distributed by laws of plane sections. Proceeding from this and considering conditions equilibrium of part of the bar as this was done in Section 26, we can find resultant modulus T and construct a diagram of dependence of critical stress $\sigma_{кр}$ on slenderness ratio of the bar λ. In Fig. 5.6 is shown such a final diagram for case, when $t_1^\circ = 0$ and $t_2^\circ = t^\circ$. As we see, with growth of temperature differential critical stress sharply decreases.

§ 59. Calculation of Influence of Thermal Conduction.

Turning to thermodynamic formulation of problem of stability of compressed bar, we must definitize initial assumptions. Up to now, essentially, we assumed that initial compression and subsequent buckling of bar occur at constant temperature, i.e., isothermic. But, as it is known, any elastic or non-elastic deformation of an insulated body is accompanied by certain, albeit slight for structural materials, change of temperature. Elastic elongation of a bar is connected with a temperature drop, and shortening, with an increase. Consequently, during buckling of bar there should appear a very weak heat flow from compressed fibers to stretched ones. Behavior of the bar during buckling should depend, thus, on coefficient of thermal conductivity of the material.* If this coefficient is infinitely great, then temperature in whole volume at any moment of time is identical. If we maintain constancy of that single temperature--in

*Such dependence was established by L. A. Shapovalov [5.10]. See also book of A. Pflüger [0.21].

particular, thanks to external sources and drains of heat--that process of buckling is isothermic. Conversely, if coefficient of thermal conductivity is infinitesimal, then heat exchange between sections of compression and extension, and also between the body and the external medium does not occur, and process will be adiabatic. Such a case can occur during very fast buckling.

It is possible to show, that critical stress in both limiting cases is determined by Euler's formula, but with introduction in it different elastic moduli--isothermic E_i or adiabatic E_a. These moduli differ one from the other slightly so that, for steel we found

$$E_a \approx 1{,}004 E_i. \tag{5.7}$$

If coefficient of thermal conductivity has small, but finite value, then critical stress is determined by the isothermic modulus. Thus, from practical point of view there is no necessity to distinguish isothermal and adiabatic processes of loss of stability, but distinction between them is of significance in principle.

From this it follows that energy criterion of stability, pertaining to conservative systems, can be applied to real bar only with a certain reservation. Preferable here is the dynamic criterion, allowing us to determine region of stability of perturbed motion of the thermodynamic system.

§ 60. Buckling During Creep. Basic Information.

Let us turn to research of buckling of compressed bars during creep. By creep we understand a change in deformations of a body in time under given loads.* As was already said, for such materials as steel and duralumin, we must deal with creep only at heightened

*We leave aside the phenomenon of relaxation (change of stresses during given displacements).

temperatures. Process of uniaxial extension in conditions of heightened temperatures can be presented in the form of the graph, depicted in Fig. 5.7. Along the axis of abscissas is plotted time, along the axis of ordinates--deformation. Directly upon application of load, which in future is kept constant, there occurs elastic or elastoplastic "instantaneous" deformation, corresponding to segment OA. After this the process of creep starts, at first faster, and then slowing. On diagram we obtain curved segment AB with the name of primary or unsteady phase of creep. Subsequently, speed of creep becomes almost constant, so that diagram takes form of a straight line (Segment BC). This secondary phase of the process is called steady creep. Then on sample there appears a neck, and deformation is accelerated (Segment CD), after which, there occurs fracture. If a short sample is subjected to central compression, diagram $\varepsilon(t)$ has the same segments, corresponding to "instantaneous" deformation, primary and secondary phases of creep.

We will consider that constant compressive stress is equal to σ. Elastic deformation is equal to $\varepsilon_e = \sigma/E_{t^\circ}$, where modulus E_{t° corresponds to given temperature t°. Creep ε_c, corresponding to steady phase*, depends on time, properties of material and magnitude of applied stress. There is offered a series of approximate formulas, describing this section of the diagram, for instance:

$$\varepsilon_c = A\sigma^n t, \tag{5.8}$$

where k and n are coefficients, depending on properties of material.**

Another approximate formula has the form

$$\varepsilon_c = k\sigma^n t. \tag{5.9}$$

---

*We apply here designations for components of deformation adopted in book of L. M. Kachanov [5.3], 1960.

**Values of them are given, for instance, in "Machine Builder's Handbook," Second edition, Vol. 3, 1956, p. 290.

where A and B are constants for the material, e is the base of natural logarithms. If one were to take equations (8) or (9) and to consider here that σ does not depend on t, then velocity of change of deformation in time will be a constant magnitude:

$$\dot{\varepsilon}_c = \frac{\partial \varepsilon_c}{\partial t} = k\sigma^n. \tag{5.10}$$

or

$$\dot{\varepsilon}_c = Ae^{B\sigma}. \tag{5.11}$$

Phase of unsteady creep can be united with instantaneous plastic strain, appearing upon application of a load. This deformation is presented to be a dependence of type

$$\varepsilon_p = k_1\sigma^m. \tag{5.12}$$

including parameters of material k_1 and m; here stress σ is considered dependent on t. Since this deformation is <u>irreversible</u>, then in case of <u>unloading</u> coefficient k_1 should be considered equal to zero. Velocity of deformation for this phase is equal to

$$\dot{\varepsilon}_p = mk_1\sigma^{m-1}\frac{\partial \sigma}{\partial t} = mk_1\sigma^{m-1}\dot{\sigma}. \tag{5.13}$$

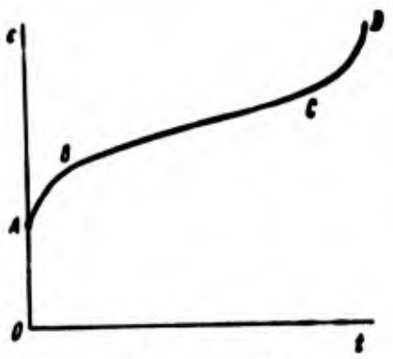

Fig. 5.7. Deformation during extension in state of creep.

In many cases we take m = 2.

If we consider all component deformations, then rate $\dot{\varepsilon}$ can be presented in the form

$$\dot{\varepsilon} = \frac{1}{E}\dot{\sigma} + r\sigma^s\dot{\sigma} + k\sigma^n; \tag{5.14}$$

here we take $r = mk_1$ and $s = m - 1$. Considering only elastic deformations and steady creep, we obtain

$$\dot{\varepsilon} = \frac{1}{E}\sigma + k\sigma^n. \tag{5.15}$$

Considering n = 1, we arrive at Maxwell's equation for velocity of flow of an elasto-viscous medium:

$$\dot{\varepsilon} = \frac{1}{E}\dot{\sigma} + \frac{\sigma}{\mu}. \tag{5.16}$$

where μ is coefficient of viscosity. Behavior of such a medium may be described by the mechanical model, presented in Fig. 5.8. It consists of a spring, whose rigidity corresponds to the modulus of the material E, and a piston; the latter moves in a cylinder with liquid. Both these elements, elastic and viscous, are connected in sequence and are loaded by a constant force, proportional to σ. Velocity of deformation of this system corresponds to formula (16).

Fig. 5.8. Mechanical model elasto-viscous medium.

To formulas of type (8) and (9) we also give form

$$\varepsilon_c = k\sigma^n t^{1/\gamma} \qquad (5.17)$$

or

$$\varepsilon_c = Ae^{B\sigma} t^{1/\gamma} \qquad (5.18)$$

when $\gamma > 1$; this gives possibility to consider simultaneously primary and secondary phases of creep.

We brought certain relationships, describing process of creep. Equations (8) and (9) or (17) and (18) connect <u>deformation of creep with stress and time</u>. In more general form this dependence is possible to present in the following form:

$$\Phi(\varepsilon_c, \sigma, t) = 0, \qquad (5.19)$$

where Φ is a certain function of magnitudes ε_c, σ and t. Equation (19) corresponds to so-called <u>theory of aging</u> in its deformation variant. Name of theory is explained by the fact that with flow of time mechanical properties of a material change, it "ages." It is possible also to offer another variant of the theory, connecting <u>velocity of change of creep</u>, ε_c, stress and time:

$$\Phi(\dot{\varepsilon}_c, \sigma, t) = 0; \qquad (5.20)$$

it can be called the variant of flow. In both equations (19) and (20) evidently there is contained time t. Deficiency of these theories consists in the fact that in describing separate sections of process of creep it is necessary to consider from what moment the parameter of time is counted off, in other words, equations are not invariant with respect to beginning of reading of time t.

Another theory of creep--the so-called theory of hardening--describes deformation by equation

$$\Phi(\varepsilon_c, \dot{\varepsilon}_c, \sigma) = 0. \tag{5.21}$$

Such an equation may, for instance, have the form

$$\dot{\varepsilon}_c \varepsilon_c^{\beta} = \alpha \sigma^{\gamma}, \tag{5.22}$$

where α, β, and γ are parameters of material.* In this equation parameter t evidently does not enter, but it allows us to establish a law of change of ε_c in time.

Experiments with compressed bars, subjected to creep, are usually conducted on special installations, in which there is automatically ensured constancy of force and temperature or change of these magnitudes according to a given law. As experiments show, process of creep of compressed bar ends in phenomenon of fast buckling with sharp increase of deflection.** Stress in bar, which is consi- ..ed constant can be significantly less than the critical stress, corresponding to the given temperature during "instantaneous" deformation.

---

*In many works instead of ε_c here there figures plastic flow, uniting creep with instantaneous plastic flow (see [5.3]). Parameters corresponding to equation (21) for duralumin D16T are given in article of N. G. Torshenov [Journal of applied mechanics and engineering physics, No. 6 (1961), pp. 158-159].

**Description of these experiments is given below in Chapter XVII. See also work [5.4].

Theoretical research in this region was conducted only during the last 10-15 years,* and it must not be considered completed. We will become aquainted with basic directions of this research.

§ 61. Criteria of Creep During Buckling.

In the literature there are offered different criteria of stability during creep. Let us consider first those which pertain to perfect structural members, for which basic equilibrium form is retained right up to moment of buckling.

One variant of a static solution of the problem consists of the following.** Assume we know the dependence between total deformation, stress and time for some theory of creep. We construct isochronous curves $\sigma(\varepsilon)$ for fixed moments of time t_0, t_1, t_2, ...(Fig. 5.9). Conditionally we assume that critical stress is determined by formula of tangential modulus for isochronous curves

$$\sigma_{кр} = \frac{\pi^2 E_к}{\lambda^2} \qquad (5.23)$$

or

$$\sigma_{кр} = \sigma_э \frac{E_к}{E}. \qquad (5.24)$$

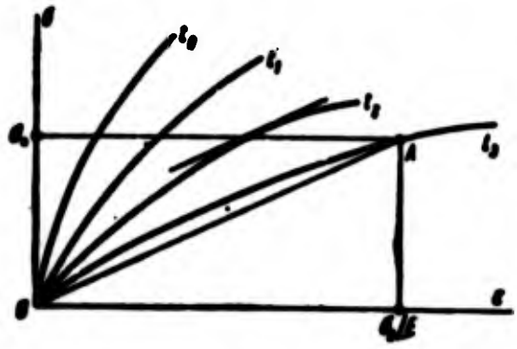

Fig. 5.9. Isochronous diagrams of compression during creep.

where $\sigma_э$ is Euler's stress, equal to π^2E/λ^2; effect of unloading here is not considered. Basic stress of compression σ_*, effective in bar, is considered given; we take $\sigma_* < \sigma_э$. After certain interval of time stress σ_* by assumption turns out to be critical: $\sigma_* = \sigma_{кр}$. Consequently, at

---

*They belong to A. R. Rzhanitsyn [5.7], [0.9]; Yu. N. Rabotnov [5.6] and [21.8a]; S. A. Shesterikov [5.11]; V. I. Rozenblyum [5.8]; Hoff [5.14], Gerard [5.13] and others.

**A similar approach was offered by Shanley [0.22].

moment of buckling the tangent modulus must become equal to

$$E_k = \frac{d\sigma}{d\varepsilon} = \frac{\sigma_*}{\varepsilon_*} E. \qquad (5.25)$$

We place on axis of abscissas of Fig. 5.9 magnitude $\varepsilon_* = \sigma_*/E$, and along the axis of ordinates σ_*. Magnitude of modulus E_K from (25) is characterized by angle α of slope of line OA. Isochronous curves intersect line σ_* at various angles. Buckling, obviously, will occur at that moment (on the Figure, t_2) when tangent to curve $\sigma(\varepsilon)$, conducted on level σ_*, becomes parallel to line OA. Period of time t_2 by this theory will be critical. Thus, the first approach to the problem corresponds to tangent-modular theory.

In second case as basic criterion we select critical deformation.* We assume that a member of a construction loses stability at a specific total deformation regardless of whether it is elastic or elastoplastic, and of what factors caused it. If one were to return to Fig. 5.9, then by this theory buckling of bar should take place at that moment (on the Figure, t_3), when isochronous curve $\sigma(\varepsilon)$ passes through point A; the latter exactly corresponds to Euler's critical deformation ε_*. Obviously, critical time in this theory will always appear larger than in tangent-modular variant. Angle α characterizes slope of secant for diagram $\sigma(\varepsilon)$; therefore, we essentially use secant modulus E_c, considering the critical stress equal to

$$\sigma_* = \frac{\pi^2 E_c}{\lambda^2}. \qquad (5.26)$$

Let us note that a formula of type (26) may be derived with help of deformation theory of plasticity in application to certain cases of elastoplastic theory of stability of plates and shells (see Chapters VII and XI).

---

*This approach proposed by Gerard [5.13].

The third criterion of stability is the dynamic one;* it comes down to research of motion of bar, occurring as the result of a certain small perturbation. We compose equation connecting deflection with time; after linearization of this equation we seek the condition, at which deflection remains bounded.

Last, the fourth approach to problem pertains to imperfect system and extends to the case of creep the criterion of initial irregularities.** Assume that axis of bar before deformation is slightly distorted or what force is applied with a certain eccentricity. Then in different sections of bar there will act from the very beginning not only axial force, but also a bending moment. In process of creep deformations will increase--both on concave, and on convex side of the bent bar. But those deformations will not be identical, since velocity of creep depends on level of stress in a given fiber. Therefore, there occurs increased curvatures of bending line which in turn is connected with increase of bending moment and stresses in individual fibers. This will lead to quick build-up of deflections, equivalent to phenomenon of buckling of the bar. Critical time it is possible here conditionally to determine, selecting a certain limiting value for deflection of the bar or for rate of growth of deflection. In certain cases we manage to find the "true" critical time, in the passage of which rate of growth of deflection becomes infinitely large.

We shall examine in more detail each of the criteria of stability.

---

*It was offered by Yu. N. Rabotnov and S. A. Shesterikov [5.6].

**Such approach was developed in works of Hoff [5.14] and other authors [5.18] and [5.22].

§ 62. Methods of Calculation by Tangent and Secant Moduli.

Let us consider first two approaches to problem of stability of a bar, using the theory of aging and taking law of creep in the form

$$\varepsilon = \frac{\sigma}{E} + k\sigma^n t. \tag{5.27}$$

We find relationship between isochronous increments ε and σ:

$$d\varepsilon = \left(\frac{1}{E} + kn\sigma^{n-1}t\right)d\sigma$$

or, by (27),

$$d\varepsilon = \left[\frac{1}{E} + \frac{n}{\sigma}\left(\varepsilon - \frac{\sigma}{E}\right)\right]d\sigma. \tag{5.28}$$

We introduce tangent modulus $E_K = d\sigma/d\varepsilon$; then relationship (28) will take the form

$$\frac{\varepsilon}{\sigma}E_K = \frac{1}{n} + \frac{E_K}{E}\left(1 - \frac{1}{n}\right). \tag{5.29}$$

Further, from (25), taking $\sigma = \sigma_*$ and $\varepsilon = \varepsilon_*$, we obtain

$$\frac{\varepsilon_* E}{\sigma_0} = \frac{1}{n} + \frac{\sigma_*}{\sigma_0}\left(1 - \frac{1}{n}\right). \tag{5.30}$$

We introduce designations

$$\frac{\varepsilon E}{\sigma_0} = \bar{\varepsilon}, \quad \frac{\sigma}{\sigma_0} = \bar{\sigma}, \tag{5.31}$$

then equation (30) takes the form

$$\bar{\varepsilon}_* = \bar{\sigma}_* + \frac{1}{n}(1 - \bar{\sigma}_*). \tag{5.32}$$

We arrived at a simple dependence between parameters of strain and stress, characterizing moment of buckling. We construct a graph of $\bar{\sigma}(\bar{\varepsilon})$ and place on the axes segments equal to 1 (Fig. 5.10), and, furthermore, axis of abscissas segment 1/n; then we obtain lines OM and KM. Passing a horizontal line on level $\bar{\sigma}_*$, we find $\bar{\varepsilon}_*$. One section of this segment--up to line OM--characterizes instantaneous deformation, equal to $\bar{\sigma}_*$, and second--creep $(1-\bar{\sigma}_*)/n$. The lower the level of stress, the greater the specific gravity creep will have.*

---

*Such a graph was offered in work [5.6].

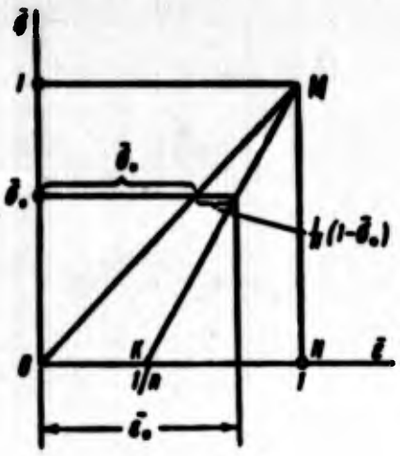

Fig. 5.10. Calculating by "tangent-modular" load.

Proceeding from (32) it is possible directly to determine "critical time" t_*. We present (27) in the form

$$\bar{\varepsilon}=\bar{\sigma}+Ek\bar{\sigma}^n t_*^{n-1}. \qquad (5.33)$$

From (32) we obtain

$$t_*=\frac{1}{nEk}\frac{1-\bar{\sigma}_0}{\bar{\sigma}_0^n\bar{\sigma}_0^{n-1}}. \qquad (5.34)$$

We take, further, the law of creep in a more general form (19) and introduce designations:

$$\frac{\partial\Phi}{\partial\sigma_c}=\nu,\quad \frac{\partial\Phi}{\partial\sigma}=\lambda. \qquad (5.35)$$

Then we find

$$\lambda d\sigma+\nu d\left(\varepsilon-\frac{\sigma}{E}\right)=0; \qquad (5.36)$$

hence, in the same way, we find

$$\frac{E_0}{E}=\bar{\sigma}_0=\frac{1}{1-E\frac{\lambda}{\nu}}. \qquad (5.37)$$

In our example we had

$$\lambda/\nu=-kn\sigma^{n-1}t; \qquad (5.38)$$

proceeding from (37), we again arrive at (34).

Formula (37) pertains, in particular, to dependence (17) with coefficient $\gamma \neq 1$. In determining critical time by a formula of type (34) we must instead of t_* place $t_*^{1/\gamma}$.

We turn to the <u>second</u> variant of solution of problem and take as the criterion of stability total deformation; then in all cases we should have

$$\varepsilon_0=\frac{\sigma_0}{E},\quad \bar{\varepsilon}_0=1. \qquad (5.39)$$

On graph of Fig. 5.10 to critical deformation will correspond vertical sections MN. From particular law (27) ensues formula for critical

time

$$t_* = \frac{1-\bar{\varepsilon}_0}{E\lambda\dot{\varepsilon}_0^{\beta}-1}. \tag{5.40}$$

Thus, period of time up to buckling by theory of critical deformation is for $\gamma = 1$ is n times more than by tangent-modular theory. When $\gamma \neq 1$ from (17) we must in (40) again replace t_* by $t_*^{1/\gamma}$.

§ 63. Dynamic Criterion.

Consider, further, perturbed motion of bar, proceeding from theory of hardening and considering from (21) $\Phi(\varepsilon_c, \dot{\varepsilon}_c, \sigma) = 0$. We introduce designations of type (35) and take here conditionally $\dot{\varepsilon}_c$ as a unvarying magnitude. Then we obtain as before

$$(E\lambda - \nu)\,d\sigma + E\nu\,d\varepsilon = 0. \tag{5.41}$$

According to law of plane sections $\delta\varepsilon = \varkappa y$, where $\varkappa$ is curvature of bending line of bar, y is distance from neutral axis to certain point of section. Integrating by area of section, we arrive at relationship

$$(E\lambda - \nu)M + EI\nu\varkappa = 0 \tag{5.42}$$

or

$$(E\lambda - \nu)\frac{\partial^2 M}{\partial x^2} + EI\nu\frac{\partial^2 v}{\partial x^2} = 0, \tag{5.43}$$

where v is deflection. Considering that "linear load" $q = \partial^2 M/\partial x^2$ corresponds to compressing forces σF and force of inertia, we find

$$-(E\lambda - \nu)\left(\sigma F\frac{\partial^2 v}{\partial x^2} + \frac{1}{g}F\frac{\partial^2 v}{\partial t^2}\right) + EI\nu\frac{\partial^4 v}{\partial x^4} = 0. \tag{5.44}$$

We take for hinge-supported bar

$$v = \tau(t)\sin\frac{\pi x}{l}, \tag{5.45}$$

then we have

$$(\nu - E\lambda)\dot{\tau} + \frac{\pi^2 g}{\gamma}\left[E\lambda\sigma + \nu(\sigma_0 - \sigma)\right]\tau = 0. \tag{5.46}$$

Frequency of vibrations turns into zero when

$$\frac{E\lambda\sigma + \nu(\sigma_0 - \sigma)}{\nu - E\lambda} = 0,$$

hence

$$\bar{\dot{\varepsilon}}_0 = \frac{1}{1 - E\frac{\lambda}{\nu}}. \tag{5.47}$$

which in form coincides with (37).

We use for example the dependence

$$\Phi = \dot{\varepsilon}_c \dot{\varepsilon}_0 - k\varepsilon^{q/A} = 0. \tag{5.48}$$

We find

$$\lambda = -\frac{k}{A}\varepsilon^{q/A}, \quad \nu = \frac{qk}{\dot{\varepsilon}_c}\varepsilon^{q/A}. \tag{5.49}$$

From this according to (47)

$$\bar{\dot{\varepsilon}}_0 = \frac{1}{1 + \frac{E\dot{\varepsilon}_c}{Aq}}. \tag{5.50}$$

Critical value of dimensionless creep will be

$$\bar{\dot{\varepsilon}}_c = \frac{Aq}{\dot{\varepsilon}_0}\frac{1 - \bar{\dot{\varepsilon}}_0}{\bar{\dot{\varepsilon}}_0}. \tag{5.51}$$

From this we can draw the conclusion that dynamic approach in application to theory of hardening leads again to the tangent-modular criterion. Let us note that the derivation given here contained essentially the same calculations as in Section 16, but for an elasto-plastic problem, without calculation for effect of unloading.

In article of Yu. N. Rabotnov and S. A. Shesterikov [5.6] was another, more founded treatment of the dynamic criterion, although the final dependences had the same form. These authors considered first $\dot{\varepsilon}_c$ a variable and obtained instead of (46) a third-order equation for τ. In a later work [21.8a] Yu. N. Rabotnov offered another variant of derivation of analogous dependences--a quasi-static variant.

Let us assume that at a certain moment of the creep process the bar is transferred into an adjacent bent position and is left to itself. If characteristic deflection v after that starts to decrease, then critical state was not attained. With growth of deflection the

critical state we consider surpassed. Consequently, stability may be judged sign of velocity $\dot{v}$. In that same case, if bar is given an initial lateral velocity $\dot{v}$, then one should judge stability by sign of acceleration $\ddot{v}$. A discussion of criteria of stability during creep is contained also in works of G. V. Ivanov [21.5a] and L. M. Kurshin [5.5].

§ 64. Criterion of Initial Imperfections.

We assume that before loading, a bar has a certain initial flaw (Fig. 5.11)

$$v_0 = v_0(x). \tag{5.52}$$

We apply to bar a central compressing load, lying below Euler's force $P_э$; then deflection of different sections immediately increases. Designating by v(x) <u>additional deflection</u>, we find bending moment in an arbitrary section:

$$M = P(v + v_0). \tag{5.53}$$

Differential equation (1.178) we rewrite in the form

$$\frac{d^2v}{dx^2} + \frac{P}{EJ}v = -\frac{P}{EJ}v_0. \tag{5.54}$$

We expand function $v_0(x)$ into a series with respect to sines:

$$v_0(x) = \sum_{i=1}^{s} a_i \sin\frac{i\pi x}{l}. \tag{5.55}$$

limiting ourselves to the first s members of series. Solution of equation (13) we will seek in the form

$$v(x) = \sum_{i=1}^{s} b_i \sin\frac{i\pi x}{l}. \tag{5.56}$$

Substituting these last expressions in (54), we find

$$b_i = \frac{a_i}{\frac{P_э^{(i)}}{P} - 1}, \tag{5.57}$$

where $P_э^{(i)}$ is the i-th Euler's force:

$$P_э^{(i)} = \frac{i^2\pi^2 EJ}{l^2}. \tag{5.58}$$

Fig. 5.11. Compressed bar with initial deflection, experiencing creep.

Stresses at a certain point of the cross-section will be

$$\sigma = \frac{P}{F} - \frac{P(v+v_0)y}{I}, \qquad (5.59)$$

where by y we designate distance to central axis; compressive stresses are considered positive. Then there is accomplished the first "plastic" step of deformation of the bar.* Let us assume that dependence between creep and time is given in the form

$$\varepsilon_c = \varepsilon_c(\sigma, t). \qquad (5.60)$$

We take interval of time equal to Δt and calculate $\Delta\varepsilon_c$ for different points of cross-sections; in practice it is necessary to limit ourselves to a certain number of points (for instance, five or seven) in several sections along the bar (three or five); stress at these points are determined beforehand by (59). Together with plastic deformations there occurs elastic ones, connected with increases of stresses by the relationship

$$\Delta\sigma = E\,\Delta\varepsilon_e. \qquad (5.61)$$

Total changes of deformations in a given fiber are equal to

$$\Delta\varepsilon_1 = \Delta\varepsilon_c + \Delta\varepsilon_e; \qquad (5.62)$$

they must satisfy the law of plane sections. If we designate increase of deformation of a fiber passing through centers of gravity of sections by $\Delta\varepsilon^0$, and changes of curvature by $\Delta\varkappa$, then increment of

---

*The method of calculation "step by step" given here was offered by Lin [5.20].

deformation of an arbitrary fiber, removed from center of gravity a distance y, will be

$$\Delta\varepsilon_1 = \Delta\varepsilon^0 - \Delta\varkappa y. \tag{5.63}$$

Instead of (61) we have

$$\Delta\sigma = E(\Delta\varepsilon^0 - \Delta\varkappa y - \Delta\varepsilon_c). \tag{5.64}$$

We compose expressions for changes of axial force and bending moment in arbitrary section:

$$\Delta P = \int_F \Delta\sigma\, dF = E\Delta\varepsilon^0 F - E\int_F \varepsilon_c\, dF. \tag{5.65}$$

$$\Delta M = -\int_F \Delta\sigma y\, dF = EI\Delta\varkappa + E\int_F \varepsilon_c y\, dF. \tag{5.66}$$

Since static moment relative to central axis is equal to zero, then in composing (65) and (66) the corresponding expressions drop out; by I is understood moment of inertia of a section relative to central axis.

Hypothetically axial force is considered constant, so that $\Delta P = 0$; hence we obtain

$$\Delta\varepsilon^0 = -\frac{1}{F}\int_F \varepsilon_c\, dF. \tag{5.67}$$

We compose differential equation for function of increment of deflection $\Delta v(x)$. Change of curvature equally

$$\Delta\varkappa = -\frac{d^2\Delta v}{dx^2}. \tag{5.68}$$

on the other hand, we have

$$\Delta M = P\Delta v. \tag{5.69}$$

Thus, from (66) we obtain

$$\frac{d^2\Delta v}{dx^2} + \frac{P}{EI}\Delta v = -\frac{1}{EI}\left(-\frac{E}{P}\int_F \varepsilon_c y\, dF\right). \tag{5.70}$$

Equation (70) has the same structure as (54); for integration of it we apply the previous method. We expand the expression in

parentheses with measurements in cm, into a trigonometric series:

$$-\frac{E}{P}\int_F \varepsilon_c y\,dF=\sum_{i=1}^{\infty}\Delta a_i \sin\frac{i\pi x}{l}. \tag{5.71}$$

Presenting solution of equation (70) in the form

$$\Delta w=\sum_{i=1}^{\infty}\Delta b_i \sin\frac{i\pi x}{l}, \tag{5.72}$$

we find, as before,

$$\Delta b_i=\frac{\Delta a_i}{\frac{P^{(i)}}{P}-1}. \tag{5.73}$$

Thus, we determine increments of coefficients b_i in expansion (56) for function of deflection v; knowing them, we find the new elastic line. Deflection after the first step will increase

$$\Delta f=\sum_{i=1}^{\infty}\Delta b_i \sin\frac{i\pi}{2}=\Delta b_1-\Delta b_3+\Delta b_5-\dots \tag{5.74}$$

Using (72), we determine change of curvature in each of the considered sections:

$$\Delta\varkappa=-\frac{d^2\Delta w}{dx^2}=\sum_{i=1}^{\infty}\Delta b_i\frac{i^2\pi^2}{l^2}\sin\frac{i\pi x}{l}. \tag{5.75}$$

Change of deformation of fiber, at distance y from center of gravity, we calculate by (63), and increase of stress--by (64). New total stresses will be equal to

$$\sigma_1=\sigma+\Delta\sigma. \tag{5.76}$$

Passing to second step, we consider the next segment of time Δt; by (60) we determine change of plastic deformations $\Delta\varepsilon_c$, corresponding to stresses σ_1, etc. Continuing this process, we find dependence between deflection of bar and time. Directly after application of load stresses are distributed in the section by linear law (59). However, by measure of development of plastic strains the diagram of stresses in any section will all the more depart from straight line.

Example 5.1. Duralumin bar of length $l = 21.4$ cm of rectangular cross-section ($b = 2$ cm, $h = 0.8$ cm) with hinge-supported ends is subjected to action of central compressive force $P = 500$ kg at a temperature of 300°C. Axial line is bent before application of load according to the half-wave of a sinusoid:

$$v = 0{,}01 \sin \frac{\pi x}{l} \text{ cm.} \qquad \text{(a)}$$

When $t° = 300°C$ we consider modulus $E = 4 \cdot 10^5$ kg/cm^2. To determine dependence of deflection of time, taking into account elastic deformations and steady creep, for given temperature we present the law of creep in the form

$$\varepsilon_c = 5 \cdot 10^{-13} \sigma^3 t, \qquad \text{(b)}$$

where σ is measured in kg/cm^2, and t in hours.

Radius of gyration of section is equal to

$$i = \frac{0{,}8}{\sqrt{12}} = 0{,}232 \text{ cm.}$$

Slenderness ratio of bar constitutes

$$\lambda = \frac{l}{i} = \frac{21{,}4}{0{,}232} = 92.$$

Euler's stress is equal to

$$\sigma_0 = \frac{\pi^2 \cdot 4 \cdot 10^5}{92^2} = 470 \text{ kg/cm}^2;$$

to it corresponds load

$$P_0^{(1)} = \sigma_0 F = 470 \cdot 1{,}6 = 750 \text{ kg.}$$

We divide length of bar l into six equal parts, and the height of section h into four equal parts. We determine stresses at each of the five points with coordinates

$$y = \frac{h}{2}; \frac{h}{4}; 0; \left(-\frac{h}{4}\right); \left(-\frac{h}{2}\right).$$

By formula (57) we find additional deflection:

$$b_1 = \frac{a_1}{\frac{P_0^{(1)}}{P} - 1} = \frac{0{,}01}{\frac{750}{500} - 1} = 0{,}02 \text{ cm.}$$

Total deflection $f = 0.03$ cm. Stresses are determined by (59):

$$\sigma = \frac{P}{F}\left[1 + \frac{y(a_1 + b_1)}{i^2} \sin \frac{\pi x}{l}\right].$$

or

$$\sigma = 310\left(1 + 0{,}56\, y \sin\frac{\pi x}{l}\right). \qquad (c)$$

Values of σ obtained by (c) are written in first line of Table 5.1.

First interval of time we select equal to 30 minutes. We find plastic deformations $\Delta\varepsilon_c$ by (b), substituting $t = 0.5$ and value of stresses (c). Quantities $\Delta\varepsilon_c \cdot 10^5$ are given in second line of table. Further, we find elongation of axial line by (67), using in every case Simpson's rule:

$$\frac{1}{F}\int_F \varepsilon_c\, dF = \frac{1}{12}\left(\varepsilon_{\frac{h}{2}} + 4\varepsilon_{\frac{h}{4}} + 2\varepsilon_0 + 4\varepsilon_{-\frac{h}{4}} + \varepsilon_{-\frac{h}{2}}\right). \qquad (d)$$

indices $\frac{h}{2}$, $\frac{h}{4}$, etc., correspond to coordinates of points of section. Values of $\Delta\varepsilon_c$ are put in third line of table.

We determine integral (71) for considered sections, using the same formula:

$$-\frac{E}{P}\int_F \varepsilon_c y\, dF = -\frac{4\cdot 10^5 \cdot 2 \cdot 0{,}8}{500 \cdot 12}\left(\varepsilon_{\frac{h}{2}}\frac{h}{2} + 4\varepsilon_{\frac{h}{4}}\frac{h}{4} - 4\varepsilon_{-\frac{h}{4}}\frac{h}{4} - \varepsilon_{-\frac{h}{2}}\frac{h}{2}\right). \qquad (e)$$

or

$$-\frac{E}{P}\int_F \varepsilon_c y\, dF = -86\left(\frac{1}{2}\varepsilon_{\frac{h}{2}} + \varepsilon_{\frac{h}{4}} - \varepsilon_{-\frac{h}{4}} - \frac{1}{2}\varepsilon_{-\frac{h}{2}}\right). \qquad (f)$$

By expression (f) there is obtained the following line of the table. Using these data, we must determine coefficients of trigonometric series (71) Δa_i for i, changing from 1 to 6. Since function is symmetric relative to point $x = l/2$, then magnitudes Δa_i with even indices are equal to zero. Thus, we have

$$-\frac{E}{P}\int_F \varepsilon_c y\, dF = \Delta a_1 \sin\frac{\pi x}{l} + \Delta a_3 \sin\frac{3\pi x}{l} + \Delta a_5 \sin\frac{5\pi x}{l}. \qquad (g)$$

Let us note that for all points of end sections $\sigma = \text{const} = P/F$. But then in these sections we also have $\varepsilon_c = \text{const}$, so that integral of (71) turns into zero. Finally for points 0, 1, ..., 6, removed $l/6$

from one another, we obtain the following values of function (multiplied by 10^5): $y = y_6 = 0,\ y_1 = y_5 = 360,\ y_2 = y_4 = 760,\ y_3 = 900.$

Supplementing interval $0 \leq x \leq l$ by section $l \leq x \leq 2l$, we have the following six points with ordinates $y_7 = y_{11} = -y_1, y_8 = y_{10} = -y_2$, and $y_9 = -y_3$. We find coefficients Δa_i by the Bessel formulas (when number of section is to equal 12, by length $2l$)

$$6\,\Delta a_i = \sum_0^{11} y_i \sin \frac{in\pi}{6}. \tag{h}$$

In our case we obtain

$$\left.\begin{aligned} \Delta a_1 &= \frac{1}{6}\left(4y_1 \sin\frac{\pi}{6} + 4y_2 \sin\frac{\pi}{3} + 2y_3\right), \\ \Delta a_2 &= \frac{1}{6}(4y_1 - 2y_3), \\ \Delta a_3 &= \frac{1}{6}\left(4y_1 \sin\frac{\pi}{6} - 4y_2 \sin\frac{\pi}{3} + 2y_3\right). \end{aligned}\right| \tag{i}$$

Substituting values of ordinates, we have

Now from (73) one can determine increment Δb_1:

$$\Delta b_1 = \frac{\Delta a_1}{\frac{P_0^{(1)}}{P} - 1} = \frac{855 \cdot 10^{-5}}{\frac{750}{500} - 1} = 1710 \cdot 10^{-5}\ \text{см},$$

$$\Delta b_2 = \frac{\Delta a_2}{\frac{P_0^{(2)}}{P} - 1} = -\frac{60 \cdot 10^{-5}}{\frac{9 \cdot 750}{500} - 1} = -5 \cdot 10^{-5}\ \text{см},$$

$$\Delta b_3 = \frac{\Delta a_3}{\frac{P_0^{(3)}}{P} - 1} = -\frac{3{,}3 \cdot 10^{-5}}{\frac{25 \cdot 750}{500} - 1} = -0{,}5 \cdot 10^{-5}\ \text{см}.$$

Change of curvature in every section we determine using formula (75). Thus, for instance, for section $x = l/6$ we have

$$\Delta x = \left(\Delta b_1 \frac{\pi^2}{l^2} \sin\frac{\pi}{6} + \Delta b_2 \frac{9\pi^2}{l^2} \sin\frac{\pi}{2} + \Delta b_3 \frac{25\pi^2}{l^2} \sin\frac{5\pi}{6}\right) =$$
$$= \frac{\pi^2}{21{,}4^2}(0{,}5\,\Delta b_1 + 9\,\Delta b_2 + 12{,}5\,\Delta b_3) = 17{,}5 \cdot 10^{-5}.$$

Table 5.1

Section	$x=\frac{l}{6}$					$x=\frac{l}{3}$					$x=\frac{l}{2}$				
Coordinates	$\frac{h}{2}$	$\frac{h}{4}$	0	$-\frac{h}{4}$	$-\frac{h}{2}$	$\frac{h}{2}$	$\frac{h}{4}$	0	$-\frac{h}{4}$	$-\frac{h}{2}$	$\frac{h}{2}$	$\frac{h}{4}$	0	$-\frac{h}{4}$	$-\frac{h}{2}$
σ, kg/cm^2	275	293	310	328	348	250	280	310	340	372	240	276	310	348	380
$\Delta\varepsilon_c \cdot 10^5$	5,20	6,30	7,45	8,80	10,5	3,90	5,50	7,45	9,85	12,9	3,45	5,25	7,45	10,5	13,8
$\Delta\varepsilon^0 \cdot 10^5$			7,60					7,75					7,90		
$\left(-\frac{E}{P}\int_F y\,\Delta\varepsilon_c\,dF\right)\cdot 10^5$			360					760					900		
$\Delta\varkappa \cdot 10^5$			17,4					32,3					37,5		
$\Delta\varepsilon_c \cdot 10^5$	0,80	4,10	7,60	11,1	14,6	−5,25	1,25	7,75	14,3	20,7	−7,1	0,4	7,9	15,4	22,9
$\Delta\varepsilon_e \cdot 10^5$	−4,6	−2,2	0,15	2,3	4,1	−9,15	−4,25	0,3	4,45	9,8	−10,6	−4,85	0,45	4,9	9,1
$\Delta\sigma$, kg/cm^2	−18,5	−8,8	0,6	9,2	16,4	−36,6	−9	1,2	17,8	39	−42	−19,5	1,7	19,5	36,4
σ_1, kg/cm^2	256	284	311	337	364	213	217	311	358	411	198	256	312	368	416

In the same manner we calculate values of $\Delta\varkappa$ for sections $x = l/3$, and $x = l/2$; they are written in Table 5.2. Knowing $\Delta\varkappa$, from (23) we can find total deformations ε_1 in each of the considered points. Thus, for instance, for point with coordinates $x = l/6$, $y = h/2$ we get

$$\Delta\varepsilon_1 \cdot 10^5 = 7{,}6 - 17{,}4 \cdot 0{,}4 = 0{,}6.$$

In Table 5.2 are placed increments of total and elastic deformations $\Delta\varepsilon_e = \Delta\varepsilon_1 - \Delta\varepsilon_c$ for every point. Here also are given increments of stresses $\Delta\sigma = E\,\Delta\varepsilon_e$ and total stresses, taking place toward the end of the 30th minute: $\sigma_1 = \sigma + \Delta\sigma$. Deflection has increment of $\Delta b_1 = 1710 \cdot 10^5$ cm and, consequently, constitutes

$$f_1 = f + \Delta b_1 = 0{,}0471\ \text{cm}.$$

Table 5.2

Coordinates y	$\frac{h}{2}$	$\frac{h}{4}$	0	$-\frac{h}{4}$	$-\frac{h}{2}$
Integral 0--30 min					
σ, kg/cm^2	240	276	310	348	380
$\Delta\varepsilon_c \cdot 10^6$	3,45	5,25	7,45	10,5	13,8
$\Delta\varepsilon^0 \cdot 10^6$			7,90		
$\left(-\frac{E}{P}\int_F y\,\Delta\varepsilon_c\,dF\right)\cdot 10^6$			900		
$\Delta\varepsilon \cdot 10^6$			39		
$\Delta\varepsilon_c \cdot 10^6$	—7,6	0,15	7,90	15,7	23,4
$\Delta\varepsilon_g \cdot 10^6$	—10,1	—4,4	0,45	5,2	9,6
$\Delta\sigma$, kg/cm^2	—40	—16	1,8	21	38
f_1, cm			0,048		
Integral 30--60 min					
σ_1, kg/cm^2	200	260	312	369	418
$\Delta\varepsilon_c \cdot 10^6$	2,0	4,4	7,56	12,6	18,3
$\Delta\varepsilon^0 \cdot 10^6$			8,80		
$\left(-\frac{E}{P}\int_F y\,\Delta\varepsilon_c\,dF\right)\cdot 10^6$			1570		
$\Delta\varepsilon \cdot 10^6$			68		
$\Delta\varepsilon_c \cdot 10^6$	—18,2	—4,7	8,8	22,3	35,8
$\Delta\varepsilon_g \cdot 10^6$	—20,2	—9,1	1,24	9,7	17,5
$\Delta\sigma$, kg/cm^2	—81	—36	5,0	39	70
f_2, cm			0,079		
Integral 60--90 min					
σ, kg/cm^2	119	224	317	408	488
$\Delta\varepsilon_c \cdot 10^6$	0,42	2,8	8	17	29
$\Delta\varepsilon^0 \cdot 10^6$			10,6		
$\left(-\frac{E}{P}\int_F y\,\Delta\varepsilon_c\,dF\right)\cdot 10^6$			2740		
$\Delta\varepsilon \cdot 10^6$			118		
$\Delta\varepsilon_c \cdot 10^6$	—36,4	—12,9	10,6	34,1	57,6
$\Delta\varepsilon_g \cdot 10^6$	—36,8	—15,7	2,6	17,1	28,6
$\Delta\sigma$, kg/cm^2	—147	—63	10	68	114
f_3, cm			0,134		

table continued on following page

continuation of Table 5.2.

Coordinates y	$\frac{h}{2}$	$\frac{h}{4}$	0	$-\frac{h}{4}$	$-\frac{h}{2}$
Integral 90--120 min					
σ_c, kg/cm^2	−28	161	327	476	602
$\Delta\varepsilon_c \cdot 10^5$	−0,005	1,04	8,75	27	54,5
$\Delta\varepsilon^0 \cdot 10^5$	16,0				
$\left(-\frac{E}{P}\int_F y\,\Delta\varepsilon_c\,dF\right)\cdot 10^5$	5120				
$\Delta\varkappa \cdot 10^5$	220				
$\Delta\varepsilon_c \cdot 10^5$	−72	−28	16	60	104
$\Delta\varepsilon_g \cdot 10^5$	−72	−29	7	33	50
$\Delta\sigma_c$, kg/cm^2	−284	−126	28	132	200
f_0, cm	0,236				
Integral 120--150 min					
σ_c, kg/cm^2	−312	35	355	608	802
$\Delta\varepsilon_c \cdot 10^5$	−7,6	0,01	11,2	56	129
$\Delta\varepsilon^0 \cdot 10^5$	32				
$\left(-\frac{E}{P}\int_F y\,\Delta\varepsilon_c\,dF\right)\cdot 10^5$	11 600				
$\Delta\varkappa \cdot 10^5$	500				
$\Delta\varepsilon_c \cdot 10^5$	−168	−68	32	132	232
$\Delta\varepsilon_g \cdot 10^5$	−160	−68	21	76	103
$\Delta\sigma_g$, kg/cm^2	−640	−272	84	304	412
f_g, cm	0,468				
σ_g, kg/cm^2	−952	−237	439	912	1214

Judging by Table 5.1, in this case, where initial bending line of bar was a half-wave, it is possible to assume that the newly obtained elastic line is a half-sine wave. In other words we could conduct calculation only for average section, considering $\Delta a_1 \neq 0$ and $\Delta a_3 = \Delta a_5 = 0$; then magnitude Δa_1 is by the formula

$$\Delta a_1 = -\frac{E}{P}\int_F y\,\Delta\varepsilon_c\,dF, \qquad (k)$$

where integral pertains namely to the <u>average</u> section. This gives in our example $\Delta a_1 = 900 \cdot 10^{-5}$. Hence

$$\Delta\delta_1 = \frac{900\cdot 10^{-5}}{\frac{750}{500}-1} = 1800\cdot 10^{-5}\ \text{см}.$$

Change of curvature in section $x = l/2$ now will be

$$\Delta\varkappa = \frac{\pi^2}{l^2}\Delta\delta_1 = 39\cdot 10^{-5}$$

instead of earlier obtained magnitude $37.5\cdot 10^{-5}$. New values of strains and stresses for average sections are presented in Table 5.2. As we see, the assumption we made is wholly acceptable. Therefore, we continue calculations for following intervals of time: from 30-th minute to 60-th, from 60-th to 90-th, etc., considering that elastic line remains a half-wave of a sinusoid. Results of calculations are given in the same Table 5.2.

In Fig. 5.12 is depicted change of deflection in time. Magnitude f grows quickly; it is possible to consider that in the course of 150 minutes supporting power of bar will be exhausted. Diagrams of distribution of stresses by height of average sections are presented in Fig. 5.13. As we see, irregularity of distribution of stresses is intensified on each step. Thus, the given criterion leads to a value of critical time, approximately equal to

$$t_* = 2{,}5 \text{ hours}.$$

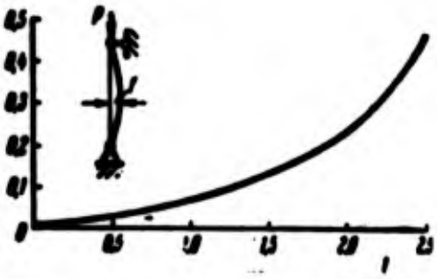

Fig. 5.12. Change of deflection during creep (f--in cm, t--in hours).

We determine critical time for the same example, considering bar as not having initial flaw and using first two criteria of buckling. Basic parameters are equal to

$$\sigma_0 = 470\ \text{kg/cm}^2,\ \bar{\sigma} = \frac{500}{16 \cdot 470} = 0{,}67,\ k = 5 \cdot 10^{-12},\ n = 3,\ E = 4 \cdot 10^5\ \text{kg/cm}^2$$

where t is measured in hours.

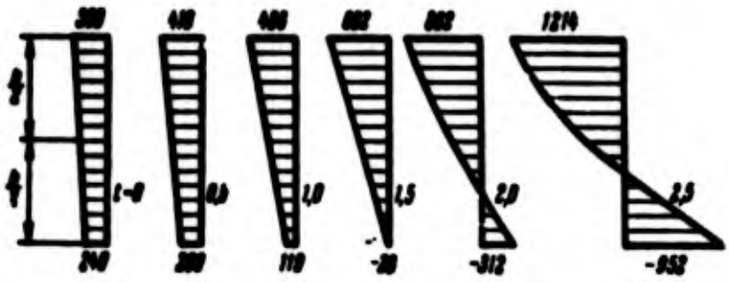

Fig. 5.13. Distribution diagrams of stresses at different moments of time.

We use tangent-modular theory. By formula (34) we find

$$t_* = \frac{1}{3} \frac{1 - 0{,}67}{4 \cdot 10^5 \cdot 5 \cdot 10^{-12} \cdot 0{,}67^3 \cdot 470^2} = 0{,}83\ \text{hr}$$

If, further, we use theory of critical deformation, then by (40) we obtain $t_* = 2{,}5$ hr

Coincidence with value found for bar with initial flaw is, of course, accidental.

§ 65. Formulas for Critical Time in Case of an H-Beam Section.

The problem considered by us may be solved by other means for an "idealized" H-beam,* consisting of two identical flanges joined by a thin web of height h (Fig. 5.14). Moment of inertia of section we consider equal to

$$I \approx 2\frac{F}{2}\left(\frac{h}{2}\right)^2 = \frac{Fh^2}{4}. \tag{5.77}$$

radius of gyration is equal to i = h/2.

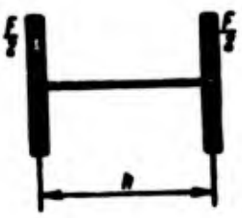

Fig. 5.14. Cross-section of H-beam with a thin web.

We consider section of bar at distance x from left end. In Fig. 5.15 is depicted one of its parts in bent position. We designate by σ_1 the stress in flange on concave side and by σ_2 the stress in the flange lying on the convex side. Condition of equilibrium in projections on axis x gives

$$(\sigma_1 + \sigma_2)\frac{F}{2} = P. \tag{5.78}$$

where P is compressive force, taken by us as constant. Determining moments relative to the central line of section (Fig. 5.15) we find

$$(\sigma_1 - \sigma_2)\frac{Fh}{4} = M = Pv. \tag{5.79}$$

where M is bending moment, equal to the product of force by deflection v. In the section by v is understood <u>total</u> deflection in section x. Comparing (77) and (79), we find

---

*The solution given here and in the following section, belongs to N. Hoff [5.14].

$$\left.\begin{aligned}\sigma_1 &= \frac{P}{F}\left(1+\frac{2v}{h}\right),\\ \sigma_2 &= \frac{P}{F}\left(1-\frac{2v}{h}\right).\end{aligned}\right| \qquad (5.80)$$

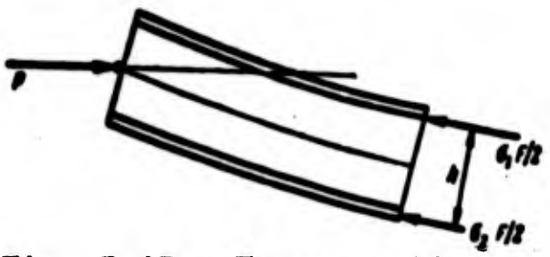

Fig. 5.15. Forces acting on a cut-off part of compressed bar.

We take dependence (14) between velocity of deformation and stress, eliminating first instantaneous plastic deformations and the primary phase of creep. Then we have

$$\dot{\varepsilon} = \frac{1}{E}\dot{\sigma} + k\sigma^n; \qquad (5.81)$$

exponent n we consider odd. For flange on concave side we obtain (for P = const):

$$\dot{\varepsilon}_1 = \frac{2P}{EFh}\frac{\partial v}{\partial t} + k\left(\frac{P}{F}\right)^n\left(1+\frac{2v}{h}\right)^n; \qquad (5.82)$$

for other flange,

$$\dot{\varepsilon}_2 = -\frac{2P}{EFh}\frac{\partial v}{\partial t} + k\left(\frac{P}{F}\right)^n\left(1-\frac{2v}{h}\right)^n. \qquad (5.83)$$

We express curvature of bending line of bar by deformations of fibers belonging to the flanges:

$$\varkappa = \frac{\varepsilon_1-\varepsilon_2}{h}. \qquad (5.84)$$

Considering dependence

$$\varkappa = -\frac{\partial^2 v}{\partial x^2}, \qquad (5.85)$$

we find

$$\frac{\partial^2 v}{\partial x^2} = \frac{\varepsilon_2-\varepsilon_1}{h}. \qquad (5.86)$$

Differentiating left and right sides with respect to t and substituting (82), (83), we obtain

$$\frac{\partial^3 v}{\partial x^2\,\partial t} = -\frac{4P}{EFh^2}\frac{\partial v}{\partial t} + k\left(\frac{P}{F}\right)^n\frac{1}{h}\left[\left(1-\frac{2v}{h}\right)^n-\left(1+\frac{2v}{h}\right)^n\right]. \qquad (5.87)$$

Subsequently we take n = 3. After simple transformations taking into account (87) we arrive at the basic differential equation of the problem:

$$\frac{\partial^2 v}{\partial x^2 \partial t} + \frac{P}{EI}\frac{\partial v}{\partial t} + 4k\left(\frac{P}{F}\right)^3 \frac{1}{h}\left(3\frac{v}{h} + 4\frac{v^3}{h^3}\right) = 0. \tag{5.88}$$

This equation is nonlinear. Assume that ends of bar are supported by hinge and that bending line is a half sine wave:

$$v = f(t)\sin\frac{\pi x}{l}. \tag{5.89}$$

We place (89) in equation (88) and integrate it according to the Bubnov-Galerkin method; we obtain

$$\int_0^l \left[-\frac{df}{dt}\frac{\pi^2}{l^2}\sin\frac{\pi x}{l} + \frac{P}{EI}\frac{df}{dt}\sin\frac{\pi x}{l} + 4k\left(\frac{P}{F}\right)^3\frac{1}{h}\left(3\frac{f}{h}\sin\frac{\pi x}{l} + 4\frac{f^3}{h^3}\sin^3\frac{\pi x}{l}\right)\right]\sin\frac{\pi x}{l}\,dx = 0. \tag{5.90}$$

We calculate integral

$$\int_0^l \sin^4\frac{\pi x}{l}\,dx = \frac{3}{8}l; \tag{5.91}$$

then instead of (90) we have

$$\frac{df}{dt}\left(\frac{\pi^2 EI}{l^2} - P\right) - 12k\left(\frac{P}{F}\right)^3\frac{EI}{h}\left(\frac{f}{h} + \frac{f^3}{h^3}\right) = 0. \tag{5.92}$$

Substituting in place of I expression (77) and dividing by F, we obtain the following differential equation with respect to f:

$$(\sigma_э - \sigma)\frac{df}{dt} = 3k\sigma^3 Eh\left(\frac{f}{h} + \frac{f^3}{h^3}\right). \tag{5.93}$$

where $\sigma_э$, as before, is Euler's stress. Here is introduced sign of total derivative, since deflection f depends only on time.

Introducing dimensionless parameter of deflection $\zeta = f/h$, we obtain

$$dt = \frac{\sigma_э - \sigma}{3k\sigma^3 E}\frac{d\zeta}{\zeta + \zeta^3}. \tag{5.94}$$

We consider that at moment of time t = 0 relative deflection is equal to $\zeta = \zeta_0 = f_0/h$. Integrating equation (94) for the interval of time from 0 to t, we find

$$t = \frac{\sigma_э - \sigma}{3Ek\sigma^3}\int_{\zeta_0}^{\zeta}\frac{d\zeta}{\zeta(1+\zeta^2)}. \tag{5.95}$$

As is easily proved by direct differentiation, the integral entering here is equal to

$$\int \frac{d\zeta}{\zeta(1+\zeta^3)} = \frac{1}{3} \ln \frac{\zeta^3}{1+\zeta^3}. \tag{5.96}$$

Expression for t takes the form

$$t = \frac{\sigma_0 - \sigma}{6Ek\sigma^3} \ln \frac{\zeta^3}{\zeta_0^3} \frac{1+\zeta_0^3}{1+\zeta^3}. \tag{5.97}$$

Such is the interval of time, necessary so that deflection of bar increases from value ζ_0 to ζ. We determine time t, at which deflection will become infinitely great, and consider it <u>critical</u>. Considering in (97) $\zeta \to \infty$, we find

$$t_* = \frac{\sigma_0 - \sigma}{6Ek\sigma^3} \ln \frac{1+\zeta_0^3}{\zeta_0^3}. \tag{5.98}$$

This expression can be simplified, if we consider that initial deflection is small as compared to height of section ($\zeta_0^2 \ll 1$); then we have

$$t_* = \frac{\sigma - \sigma_0}{6Ek\sigma^3} \ln \zeta_0^3. \tag{5.99}$$

We will obtain another result if characteristic of creep of material is linear, i.e., if the exponent in (81) is equal to one. Considering n = 1 in dependence (87), we arrive at the linear differential equation

$$\frac{\partial^3 v}{\partial x^2 \partial t} + \frac{P}{EI} \frac{\partial v}{\partial t} + k \frac{P}{I} v = 0. \tag{5.100}$$

Taking v in form (89), we obtain

$$(P_* - P) \frac{df}{dt} = kEPf. \tag{5.101}$$

so that rate of growth of f is proportional to the actual magnitude f. Integration of (101) gives

$$t = \frac{\sigma_0 - \sigma}{kE\sigma} \ln \frac{f}{f_0}. \tag{5.102}$$

From formula (102) it follows that infinitely great deflection may be accomplished in a infinitely great time. Therefore, in this case there must be introduced another criterion for determining critical

time.

Example 5.2. Determine critical interval of time for bar of H-beam section with section area $F = 1.6$ cm^2, compressed by force $P = 500$ kg, so that $\sigma = 310$ kg/cm^2. Height of section h we select in such a way that radius of gyration of H-beam section is equal to radius of gyration of a rectangular section of the bar considered in example 5.1: $h = 2 \cdot 0.23 = 0.46$ cm. Then slenderness ratio of the bar remains the same: $\lambda = 92$; Euler's stress will be $\sigma_э = 470$ kg/cm^2. As before we take $f_0 = 0.01$ cm, $n = 3$, $E = 4 \cdot 10^5$ kg/cm^2, $k = 5 \cdot 10^{-12}$. We have $f_0 \ll h$; by formula (99) we find

$$t_* = \frac{310 - 470}{6 \cdot 4 \cdot 10^5 \cdot 5 \cdot 10^{-12} \cdot 310^3} \ln\left(\frac{1}{46^2}\right) = 3{,}4 \text{ hr.}$$

We arrived at a result, close to that which was found by the numerical method in example 5.1; here magnitude t_* had to be larger, since we applied a somewhat different criterion of buckling. Formulas (98) and (99) for "estimating" calculations can be applied to bars of any form of section, considering the slenderness ratio of hypothetical bar of H-beam section of equal to the slenderness ratio of the considered bar.

We recall that for corresponding "ideal" bar we found by tangent-modular theory $t_* = 0.83$ hr. and by theory of critical deformation $t_* = 2.5$ hrs.

We turn to a more general case, where instantaneous deformations, appearing after application of load or upon subsequent growth of stresses, is not purely elastic. Initial dependence (81) should, consequently, be supplemented by term $r\sigma^s\dot{\sigma}$, appearing in equation (14). As we already said, introduction of this term also gives possibility of taking into account the phase of unsteady creep. We assume here

that exponent s is odd. The new term should be introduced with a plus sign when there occurs an increase of compressive stress, i.e., when $\sigma > 0$ and $\sigma > 0$, with a minus sign with growth of tensile stresses. During unloading instantaneous plastic deformations will be absent, so that for process of unloading it is necessary to take $r = 0$.

If a bar of H-beam section has a slight distortion before application of load, then one may assume that on the first stage of loading in both flanges there will take place compressive stresses, where on the concave side they will increase (additional load), and on convex--decrease (unloading). We take for $\dot{\varepsilon}_1$ the additional term

$$r\sigma^s \frac{\partial \sigma}{\partial t} = r\left(\frac{P}{F}\right)^{s+1}\left(1+\frac{2v}{h}\right)^s \frac{2}{h}\frac{\partial v}{\partial t}; \tag{5.103}$$

this expression must be introduced in (82); value $\dot{\varepsilon}_2$ by (83) will remain without changes. Equation (87) will now take the form

$$\frac{\partial^2 v}{\partial x^2 \partial t} = -\frac{4P}{EFh^2}\frac{\partial v}{\partial t} + k\left(\frac{P}{F}\right)^n \frac{1}{h}\left[\left(1-\frac{2v}{h}\right)^n - \left(1+\frac{2v}{h}\right)^n\right] - r\left(\frac{P}{F}\right)^{s+1}\left(1+\frac{2v}{h}\right)^s \frac{2}{h}\frac{\partial v}{\partial t}. \tag{5.104}$$

We assume in subsequent calculations that $n = 3$ and $s = 1$; values correspond to data of experiments on certain steels, and also aluminum alloys. Curve $\varepsilon(\sigma)$ will be represented in this case the quadratic parabola

$$\varepsilon = \frac{\sigma}{E} - m\sigma^2. \tag{5.105}$$

We take $v(t, x)$ from (89); then the left part of equation (90) should be supplemented by expression

$$\int_0^l \frac{2r}{h^2}\left(\frac{P}{F}\right)^2\left(\frac{\partial f}{\partial t}\sin^2\frac{\pi x}{l} + \frac{2}{h} f \frac{\partial f}{\partial t}\sin^3\frac{\pi x}{l}\right)dx. \tag{5.106}$$

Calculating integral

$$\int_0^l \sin^3\frac{\pi x}{l}\,dx = \frac{4l}{3\pi}, \tag{5.107}$$

we obtain instead of (92) equation

$$\left[\frac{\pi^2 EI}{l^2}-P-2r\left(\frac{P}{F}\right)^3\frac{EI}{h^2}\right]\frac{df}{dt}-$$
$$-\frac{32}{3\pi}r\left(\frac{P}{F}\right)^3 EIf\frac{df}{dt}\frac{1}{h^2}-12k\left(\frac{P}{F}\right)^3\frac{EI}{h}\left(\frac{f}{h}+\frac{f^3}{h^3}\right)=0 \qquad (5.108)$$

or

$$\left(e_0-e-\frac{1}{2}r\sigma^2 E\right)\frac{d\zeta}{dt}-\frac{8}{3\pi}r\sigma^2 E\zeta\frac{d\zeta}{dt}=3k\sigma^3 E(\zeta+\zeta^3). \qquad (5.109)$$

We introduce designations

$$\frac{1}{2}r\sigma^2 E=\lambda,\quad 3k\sigma^3 E=\nu \qquad (5.110)$$

and reduce (109) to the form

$$dt=\frac{e_0-e-\lambda}{\nu}\frac{d\zeta}{\zeta+\zeta^3}-\frac{16}{3\pi}\frac{\lambda}{\nu}\frac{d\zeta}{1+\zeta^2}. \qquad (5.111)$$

We find the integral

$$\int_{\zeta_0}^{\zeta}\frac{d\zeta}{1+\zeta^2}=\operatorname{arctg}\zeta-\operatorname{arctg}\zeta_0=\operatorname{arctg}\frac{\zeta-\zeta_0}{1+\zeta\zeta_0}. \qquad (5.112)$$

Instead of (96) we now obtain a new expression for t:

$$t=\frac{e_0-e-\lambda}{2\nu}\ln\frac{\zeta^2}{\zeta_0^2}\frac{1+\zeta_0^2}{1+\zeta^2}-\frac{16}{3\pi}\frac{\lambda}{\nu}\operatorname{arctg}\frac{\zeta-\zeta_0}{1+\zeta\zeta_0}. \qquad (5.113)$$

Judging by equation (113), effect of elastic deformation and primary phase of creep is reduced here to decrease of time, necessary for achieving a given value of ζ.

Velocity of lateral displacement $d\zeta/dt$ becomes infinitely large if the coefficient for it in the left part of equation (109) turns into zero:

$$e_0-e-\lambda-\frac{16}{3\pi}\lambda\zeta=0. \qquad (5.114)$$

From this we find "critical" value of relative deflection:

$$\zeta_*=\frac{3\pi}{16\lambda}(e_0-e-\lambda). \qquad (5.115)$$

Substituting expression (115) in (113), we find <u>critical interval of time</u> t_*. If we take $\lambda = 0$, i.e., assume that instantaneous plastic deformations are absent, then (115) gives $\zeta_* \to \infty$, and formula for

critical interval of time (113) will change into formula (99) of the preceding section.

We assumed here that stresses on convex side of bent bar were compressive. In reality, as we saw in example 5.1, they can pass into tensile. Then instead of unloading on convex side we obtained loading up; in expression (83) for $\dot{\varepsilon}_2$ it will be necessary to introduce complementary term considering instantaneous plastic deformations. As can be seen from formulas (80), magnitude σ_2 changes sign when $2v = h$. In mid-section stress will change sign when $f = h/2$ or when $\zeta = 0.5$. Thus, all the preceding relationships are valid, strictly speaking, only for $\zeta \leq 0.5$. If we use calculating formulas (113) and (115) for $\zeta > 0.5$, we obtain somewhat overstated values of t_*. In one of works [5.14] there is offered an analogous formula, giving very understated value for t_*; it is derived on the assumption that at all points of flange, lying on convex side, instantaneous plastic tensile strains appear simultaneously.

Example 5.3. Determine critical interval of time for the bar described in example 5.2, taking $n = 3$, $s = 1$, $E = 4 \cdot 10^5$ kg/cm^2, $k = 5 \cdot 10^{-12}$, $r = 3 \cdot 10^{-10}$. With such value of r dependence $\sigma(\varepsilon)$ has the form (stress is expressed in kg/cm^2)

$$10^3\varepsilon = 2{,}5\sigma - 1{,}5 \cdot 10^{-4}\sigma^3. \qquad (a)$$

Magnitudes λ and ν constitute, according to (110),

$$\lambda = \frac{1}{2} 3 \cdot 10^{-10} \cdot 310^2 \cdot 4 \cdot 10^5 = 5{,}8, \quad \nu = 3 \cdot 5 \cdot 10^{-12} \cdot 310^3 \cdot 4 \cdot 10^5 = 179. \qquad (b)$$

By the formula (115) critical value of dimensionless deflection will be

$$\zeta_* = \frac{3\pi}{16 \cdot 5{,}8} (470 - 310 - 5{,}8) = 15{,}6. \qquad (c)$$

We obtained $\zeta_* > 0.5$. We use formula (113) too, in order to find approximate value of critical interval of time; we find

$$t_* = \frac{470 - 310 - 5{,}8}{2 \cdot 179} \ln \frac{15{,}6^2}{\left(\frac{1}{46}\right)^2} \frac{1 + \left(\frac{1}{46}\right)^2}{1 + 15{,}6^2} -$$

$$- \frac{16}{3\pi} - \frac{5{,}8}{179} \operatorname{arctg} \frac{15{,}6 - \frac{1}{46}}{1 + \frac{15{,}6}{46}} = 3{,}3 + 0{,}1 = 3{,}4 \text{ hr}. \qquad (d)$$

The result turned out in this case to be the same as in example 5.2, when instantaneous plastic deformations were not taken into account. This is explained by the fact that instantaneous plastic deformations for a given value of σ are small as compared to elastic deformations: the second term in expression (a) for ε constitutes only about 2% as compared to the first.

§ 66. Comparison of Different Criteria of Buckling.

We have become acquainted with various approaches to problem of stability of a bar during creep. Each of them has its advantages and disadvantages.

The criterion of tangent modulus is in accordance to known measure with general theory of stability of compressed bars during plastic deformations. Calculating formulas are simple in structure and allow us to use various theories and laws of creep. At the same time derivation of basic dependences of this criterion contains certain assumptions, requiring additional analysis. It may be that law of creep, describing general process of change of deformation in time well, should not be extended to isochronous deformations which are the result of small perturbations; this especially pertains to deformations in the direction of unloading.

Criterion of critical deformation is ultimately simple from the point of view of practical application. However, as we already said,

it does not correspond to theory of elastoplastic buckling of bars and does not have, essentially, definite foundation, being a sort of "conjecture." Values of critical time, according to this theory, turn out several times greater than from the preceding one. It is necessary at the same time to note that existing, not numerous, experimental data fairly well agree with criterion of critical deformation.*

The dynamic criterion, which could serve for appraisal of all other methods, is developed at present time only in application to theory of hardening. Here it leads practically to the same results as the "tangent-modular" approach. It is desirable to find uncontradictory ways of application of this criterion to dependences of the theory of aging.

Finally, the criterion of initial imperfections is completely based on known relationships of theory of bending of bars and from the point of view of logic of calculation is fully justified. However, initial data--character and maximum of initial deflection--depend on many circumstances, which are difficult to account for during designing. It is possible to recommend use of approximate formulas for maximum of initial deflection in dependence of slenderness ratio of the bar (see Chapter XX) and to apply the static approach to the problem. It is necessary to note also that calculations, necessary for solution of problem by numerical method, "step by step," are comparatively labor-consuming. True, they easily yield to programming for execution on digital computers; in this case there is no necessity

---

*This is attested to by results of experimental research of A. P. Kuznetsov [5.4].

to seek analytical dependences, approximating process of creep; it is possible to directly use tabular data or diagrams obtained experimentally.

In conclusion we should recommend for "estimating" calculation use of the theory of tangent modulus or critical deformation, remembering that the first gives, as a rule, understated values of critical time and determines virtual initial moment of buckling. For more founded determination of resource of a real bar one should apply criterion of initial imperfections. It is exceedingly important to accumulate experimental data in comparison with results of calculations.

Another trend in theory of stability during creep, important primarily for calculation of concrete and reinforced concrete structures, is connected with use of the so-called theory of inheritance, representing a connection between total deformation, stress and time with the help of the Boltzmann-Volterra equation; it expresses influence on the process of creep of unit "impulses," acting in moments of time, preceding the given (see books of A. R. Rzhanitsyn [0.9], N. Kh. Arutyunyan "Certain questions of theory of creep," Moscow, 1952 and L. M. Kachanov [5.3]). This trend is developed by G. S. Grigoryan (Transactions of Yerevan conference on theory of shells, 1962).

Literature

5.1. L. B. Bunatyan. Stability of thin-walled bars taking into account creep of material, News of Acad. of Sci. of Armenian SSR, Physico-mathematical series, natural and engineering sciences, 6, No. 2 (1953), 43-53.

5.2. V. F. Vorob'yev. Stability of rods in state of creep, Journal of applied mechanics and technical, physics, No. 6 (1961), 135-144.

5.3. L. M. Kachanov. Certain questions of theory of creep, Gostekhizdat, 1948; Theory of creep, Fizmatgiz, 1960.

5.4. A. P. Kuznetsov. Stability of compressed bars, made of duralumin, in conditions of creep, Journal of applied mech. and tech. physics, No. 6 (1961), 160-162.

5.5. L. M. Kurshin. Stability of bars under conditions of creep, Journal of applied mech. and tech. physics, No. 6 (1961), 128-134; No. 2 (1962).

5.6. Yu. N. Rabotnov and S. A. Shesterikov. Stability of bars and plates in state of creep, applied math. and mech., 21. No.3 (1957). 406-412; Journ. of Mech. and Phys. Solids, 6 (1957), 27.

5.7. A. R. Rzhanitsyn. Processes of deformation of constructions of viscoelastic elements, DAN SSSR 52 No. 1 (1946), 25-28.

5.8. V. I. Rozenblyum. Stability of a compressed bar in the state of creep, Eng. Collection, 18 (1954), 99-104.

5.9. M. R. Fel'dman. Buckling of a bar taking into account plastic after-effect, News of Acad. of Sci. of Armenian SSR, physical and mathematical series, natural and engineering sciences, 9, No. 1 (1956), 75-86.

5.10. L. A. Shapovalov. Influence of uneven heating on stability of a compressed bar, Applied math. and mech., 22, No. 1 (1958), 119-123; Equations of thermoelasticity and stability during action of external forces and thermal stresses, cand. diss., M., 1960.

5.11. S. A. Shesterikov. Concerning the question of stability during creep, cand. diss., Moscow State University, 1957; Criterion of stability of a bar during creep, Applied math. and mech., No. 3 (1959).

5.12. R. L. Carlson. Time-dependent tangent modulus applied to column creep buckling, J. Appl. Mech. 23, No. 3 (1956), 390.

5.13. G. Gerard. Note on creep buckling of columns, J. Aeron. Sci. 19, No. 10 (1954), 714; A creep buckling hypothesis, J. Aeron. Sci. 23, No. 9 (1956), 879-882, 887; J. Aerospace Sci., 29 No. 6 (1962).

5.14. N. J. Hoff. Creep buckling, Aeron, Quarterly, 7, No. 1 (1956), 1-20 (see coll. of translations "Mechanics," IL, No. 6, (1956); Buckling at high temperature, J. of the Royal Aer. Soc, 61, No. 563 (1957), 756-774 (see coll. "Mechanics," IL, No. 5, 1958, 65-100); A survey of the theories of creep buckling, Stanford U. Division of Aeronaut. Engineering Research, No. 80, 1958 (coll. "Mechanics," IL, No. 1, 1960, 63-96).

5.15. L. W. Hu and N. H. Triner. Bending creep and its applications to beam columns, J. Appl. Mech. 23, No. 1 (1956), 35-42.

5.16. J. A. Hult. Critical time in creep buckling, J. Appl. Mech., 22, No. 3 (1955), 432.

5.17. J. Kempner. Creep bending and buckling of non-linearly visco-elastic columns. NACA Techn. Note 3137, 1954.

5.18. J. Kempner and V. Pohl. On the non-existence of a finite critical time for linear visco-elastic columns, J. Aeron. Sci. 20 (1953).

5.19. C. Libove. Creep buckling of columns, J. Aeron. Sci. 19, No. 7 (1952), 459-467; Creep buckling analysis of rectangular section columns, NACA Techn. Note No. 2956, 1953.

5.20. T. H. Lin. Creep stresses and deflections of columns, J. Appl. Mech. 23, No. 2 (1956), 214-218; Creep deflections and stresses of beam-columns. J. Appl. Mech. 25, No. 1 (1958), 75.

5.21. J. Marin. Creep buckling in columns, J. Appl. Physics 18, No. 1 (1947), 103-109.

5.22. F. K. Odquist. Infleunce of primary buckling on column buckling, J. Appl. Mech. 21, No. 3 (1954), 295; Trans. Roy. Inst. Techn., No. 66, Stockholm (1953).

5.23. S. A. Patel and J. Kempner. Effect of higher-harmonic deflection components on the creep buckling of columns, Aeronaut. Quarterly 8, No. 3 (1957), 215-225.

5.24. D. Rosenthal and H. W. Baer. An elementary theory of creep buckling of columns, Proc. of the 1st U. S. Congr. of Appl. Mech., 1951.

5.25. F. B. Veubeke. Creep buckling, "High temperature effects in aircraft structures," 1958.

CHAPTER VI

STABILITY OF BARS UNDER DYNAMIC LOAD

§ 67. Classification of Dynamic Problems.

All problems, which we considered up till now, were *static* and pertained to stability of *equilibrium forms*. It is true, during research of stability of bars in plastic region or in the state of creep there appeared processes occurring *in time*, but they were considered so *slow* that forces of inertia of elements of a body could be ignored. We turn now to *dynamic* problems, in which it is necessary to consider *acceleration* of elements of a body.

One such problem consists of studying behavior of a compressed bar under *quick loading*. If rate of growth of compressive force is sufficiently great, then elements of the bar do not succeed in shifting in a direction, normal to axis of the bar. Thanks to this, compressive force can attain the first critical magnitude and even significantly exceed it, before deflections attain noticeable values. Inasmuch as in such a dynamic process compressive force can pass not only the first, but also higher critical values, here one should expect appearance of higher forms of loss of stability. This peculiarity of the process of fast loading is important, since it is connected with substantial increase of supporting power of a bar stream. Similarly to how this was in the problem about creep, we here will be interested in

critical time, in the course of which stresses or displacements attain limiting values, determined from conditions of use of the structure.

In solving problems pertaining to behavior of a bar under fast loading, we will use Alembert's principle; in the equation of "equilibrium" of an element of a bar we will introduce forces of inertia. Subsequently we consider, as a rule, only forces of inertia which correspond to transverse displacements (deflections) of elements of a bar. It is easy to verify that such a solution is valid only for comparatively fast, but not impact loading.

Assume that the compressive load applied in impulses is received by one end of the bar. Elements of the bar adjoining this end will experience elastic deformation, which begins to spread along the bar with a velocity, which coincides with the velocity of sound in the material of the bar, equal to

$$V=\sqrt{\frac{Eg}{\gamma}}. \tag{6.1}$$

where γ is the specific gravity of the material. For steel and duralumin this magnitude is $V = 5 \cdot 10^5$ cm/sec.

We assume that time interval necessary for propagation of elastic wave the length of the bar is small as compared to the "critical time" of interest to us. Then it is possible to consider transverse displacements as relatively slow and conditionally consider that compressive force at every moment of time has in all sections of the bar the same value, transmitted the length as if instantaneously.

Otherwise we should pose the problem of stability of a bar in case of a strictly impact load, transmitted to the bar during a very short time interval. Here the essence of problem consists in tracing process of transmission of forces along length of bar. In other words,

in this case it is necessary additionally to consider force of inertia of elements of the bar, corresponding to longitudinal displacements.

Along with problems of fast or impact loading, consisting in single application of force, of great value also is the problem in which compressive force is a periodic function of time. Transverse vibrations of the bar in this case are called parametric. They have unique features, distinguishing them from usual constrained vibrations. Depending upon character of parametric vibrations the bar may be dynamically stable or unstable. The term dynamic stability in the literature frequently is connected specifically with behavior of a structure under action of a periodic force. Subsequently, we will sometimes apply this term in a more general treatment, extending it to the case of impulse application of load.

An intermediate position is occupied by cases where load is changed not periodically, but by a specific given program either when its change is in part given, and in part depends on behavior of the elastic system itself.

Research pertaining to stability of elastic systems under dynamic load has drawn attention to itself mainly in connection with requirements of contemporary aircraft technology and machine building. Parametric vibrations dangerous for constructions were observed also in suspension bridges.

In given chapter we consider problems of dynamic stability of bars, round rings, and high beams. Speaking of stability during fast loading, we will, as a rule, investigate systems which have initial deflections from ideal form and determine development of these deflections in time. In the preceding chapter we already said that

such an approach gives the possibility to determine supporting power of real constructions, always having various initial defects in manufacturing, transporting, and assembly. True, for a unit construction initial imperfections have, as rule, a random character; therefore, during development of practical methods of calculation it is necessary to use statistical methods and data on possible scattering of initial perturbations.

§ 68. Dynamic Loading of a Bar. Initial Equation

We start from problem of a bar fixed by hinges at its ends and subjected to compression by force P, variable in time t; $P = P(t)$. We assume that the bar has an initial deflection; other perturbing factors, for instance eccentricity in application of load, will be as if replaced by equivalent distortion of the bar.

We designate initial deflection by $v_0 = v_0(x)$, total and additional deflections (Fig. 6.1) will be functions of the coordinate and time $v_1(x, t)$ and $v(x, t)$ respectively.

The differential equation of the bending line of the bar has the form

$$EI \frac{\partial^4 (v_1 - v_0)}{\partial x^4} = -P \frac{\partial^2 v_1}{\partial x^2} - \frac{1}{g} F \frac{\partial^2 v}{\partial t^2}, \qquad (6.2)$$

where I and F are the moment of inertia and the cross-sectional area of the bar. In the left side there appears the derivative of the additional (elastic) deflection $v = v_1 - v_0$. In the right side force is multiplied by the derivative of total deflection; from Fig. 6.1 it is evident that during calculation of bending moment force P should be multiplied by v_1. The last member constitutes the force of inertia per unit length of the bar; here there can appear either a

function of v_1 or of v.

We set ourselves the goal of determining the nature of motion of elements of the bar under various laws of change of compressive force in time. As was already said, compressive force in all sections of bars is considered equal to P.*

Equation (2) is written on the assumption that deflections v_1 and v_0 are very small with respect to length of the bar. In considering deflections comparable with length, one should compose a nonlinear equation, using an exact expression for curvature of elastic line.

Function $v_0(x, t)$ can generally be expanded into a Fourier series of forms of static loss of stability or of forms of vibrations; in the case of a bar these forms are identical. Depending upon circumstances of bending of greatest significance may be the form of initial deflection with a definite number of half-waves m. Therefore, subsequently, we will take for v_0 and v_1 the expressions

$$v_0 = f_0 \sin \frac{m\pi x}{l}, \quad v_1 = f_1 \sin \frac{m\pi x}{l}, \qquad m = 1, 2, 3, \ldots \tag{6.3}$$

Maximum initial deflection f_0 we consider given; maximum of total deflection f_1 is a function of time: $f_1 = f_1(t)$. We place expression (3) in equation (2); then we obtain

$$m^4(f_1 - f_0) - \frac{P}{P_e} m^2 f_1 = -\frac{1}{Eg} \frac{l^4 F}{\pi^4 I} \frac{d^2 f_1}{dt^2}, \quad \text{when} \quad P_e = \frac{\pi^2 EI}{l^2}. \tag{6.4}$$

If we consider $P \equiv 0$, we obtain from this an equation of free transverse vibrations of a bar with initial deflection:

---

*A similar problem was formulated by I. M. Rabinovich in 1947.

$$\frac{d^2f_1}{dt^2}+\frac{Eg}{\gamma}\frac{\pi^4Im^4}{l^4F}(f_1-f_0)=0. \tag{6.5}$$

Fig. 6.1. Bar with initial deflection receiving dynamic load.

Frequency of m-th normal vibration is

$$k_m=m^2\frac{\pi^2}{l^2}\sqrt{\frac{EIg}{\gamma F}}. \tag{6.6}$$

Frequency of fundamental tone of vibrations we designate by k (without index); it is equal to

$$k=\frac{\pi^2}{l^2}\sqrt{\frac{Eg}{\gamma}\frac{I}{F}}=P_э^*\frac{V}{i}. \tag{6.7}$$

Here by $P_э^*$ is understood dimensionless parameter of Euler's load (equal to corresponding deformation), by i, the radius of gyration of section, namely:

$$P_э^*=\frac{P_э}{EF}=\frac{\pi^2}{\lambda^2},\quad \lambda=\frac{l}{i},\quad i=\sqrt{\frac{I}{F}}; \tag{6.8}$$

magnitude V is expressed by formula (1).

Considering in (4) inertial member equal to zero, we find total maximum deflection of a bar, having before loading by force P an initial distortion of m half-waves and receiving additional deflection of the same form:

$$f_1=\frac{f_0}{1-\frac{P}{m^2P_э}}. \tag{6.9}$$

We introduce dimensionless parameter of time

$$t_1=kt=\frac{2\pi}{T}t, \tag{6.10}$$

where T is period of fundamental tone of vibrations; then initial equation (4) takes the form

$$\frac{d^2 f_1}{dt_1^2} + m^2\left(m^2 - \frac{P}{P_0}\right) f_1 = m^4 f_0. \tag{6.11}$$

We use this equation to solve a number of particular problems.

§ 69. Case of Sudden Application of Load.

Let us assume that a bar is subjected to action of suddenly applied force P, which then remains constant.*

Such formulation of a problem does not fully agree with the assumptions made above. We considered that velocity of build-up of compressive force is within known limits, for which it is possible to ignore inertia of longitudinal displacements; meanwhile in given problem we assume that in initial moment of time compressive force the whole length of the bar will increase instantly to quantity P. However study of this very simple case is important from the viewpoint of method.

We use equation (11), taking the following initial conditions:

$$f_1 = f_0. \quad \frac{df_1}{dt_1} = 0 \text{ when } t_1 = 0. \tag{6.12}$$

Let us consider case, when $P/P_3 < m^2$; then instead of (11) we obtain

$$\frac{d^2 f_1}{dt_1^2} + \omega^2 f_1 = m^4 f_0, \tag{6.13}$$

where

$$\omega^2 = m^2\left(m^2 - \frac{P}{P_0}\right). \tag{6.14}$$

The integral of this equation will be

$$f_1 = A \sin \omega t_1 + B \cos \omega t_1 + \frac{m^4}{\omega^2} f_0. \tag{6.15}$$

Using conditions (12), we find

---

*In the formulation offered here this problem was first investigated by M. A. Lavrentyev and A. Yu. Ishlinskiy [6.4] in 1949.

$$f_1 = \left(\frac{1}{1 - \frac{P}{m^2 P_э}} - \frac{1}{\frac{m^2 P_э}{P} - 1} \cos \omega t_в \right) f_0. \tag{6.16}$$

We arrived at equation of free vibrations of bar near position of equilibrium, characterized by maximum deflection (9).

Vibrations become impossible when $P/P_э \geq m^2$. When $P/P_э = m^2$ we obtain

$$\frac{d^2 f_1}{dt_в^2} = m^4 f_0. \tag{6.17}$$

whence

$$f_1 = f_0 \left(1 + \frac{m^4}{2} t_в^2 \right). \tag{6.18}$$

When $P/P_э > m^2$ equation (11) takes the form

$$\frac{d^2 f_1}{dt_в^2} - \Omega^2 f_1 = m^4 f_0. \tag{6.19}$$

where

$$\Omega^2 = m^2 \left(\frac{P}{P_э} - m^2 \right). \tag{6.20}$$

Solution of equation (19) will be

$$f_1 = \left(\frac{1}{1 - \frac{m^2 P_э}{P}} \operatorname{ch} \Omega t_в - \frac{1}{\frac{P}{P_э m^2} - 1} \right) f_0. \tag{6.21}$$

Thus, when $P/P_э \geq m^2$, maximum deflection increases in time without limit. As soon as load reaches Euler's critical value $P_э$, there will start to develop a form with one half-wave ($m = 1$). When $P = 4P_э$, there is possible build-up of maximum deflection for forms with one, two half-waves ($m = 1,2$) etc. Rate of growth of deflection is determined by magnitude Ω^2. If with sufficiently large number m we consider it continuously changing, then the condition of a maximum for Ω^2 will have the form

$$\frac{d\Omega^2}{dm^2} = 0 \quad \text{when} \quad \frac{P}{P_э} - 2m^2 = 0. \tag{6.22}$$

Consequently, maximum of Ω^2 occurs at value m,* equal to

$$m^* = \sqrt{\frac{P}{2P_э}}. \tag{6.23}$$

or at m,* equal to the integer the nearest to $\sqrt{\frac{P}{2P_0}}$.

Meanwhile static highest equilibrium form of bar has number, equal to

$$\eta=\sqrt{\frac{P}{P_0}} \tag{6.24}$$

or the nearest magnitude to this.

As we see, the highest rate of build-up will belong not to those forms, which correspond to number η, but to forms with the smallest number, equal approximately to 0.7η. Let us assume, e.g., that to bar there suddenly is applied force $P = 9P_0$. Then we have $\eta = 3$; with greatest intensity will grow form of deflection with two half-waves ($m^* = 2$); when $P = 16P_0$ we have $m^* = 3$, etc. This conclusion is of essential importance for the following sections.

We considered that initial elastic line may be presented by a Fourier series and that all component harmonics are equally possible. If however, character of initial deflection is completely definite, then comparison of different variants of distortion of bar loses meaning. We note, however, that form of deflection, developed in accordance with initial deflection, can, as a result of small perturbations appearing already in process of motion, change into another form, with predominance of the harmonic, characteristic for the given velocity of the load.

§ 70. Load, Quickly Increasing in Time.

Let us consider further the case when force P increases in proportion to time: $P = ctF$, magnitude c, measured in $kg/cm^2 \cdot sec$, characterizes rate of change of compressive stress.*

---

*This problem is analyzed by the author [6.2a].

We introduce a new parameter of time

$$t^* = \frac{P}{P_0} = \frac{cFt}{P_0}; \tag{6.25}$$

it is connected with quantity t_k (10) by

$$\frac{P_0}{cF} t^* = \frac{1}{P_0^2 V} t_k. \tag{6.26}$$

We use dimensionless parameter of rate of change of stress

$$S^* = P_0^{*2} \left(\frac{\pi VE}{cl}\right)^2; \tag{6.27}$$

then we obtain

$$t_k = \sqrt{S^*}\, t^*. \tag{6.28}$$

Equation (11) takes on the form

$$\frac{1}{S^*} \frac{d^2 f_1}{dt^{*2}} - m^2 (t^* - m^2) f_1 = m^4 f_0. \tag{6.29}$$

We divide each member by radius of gyration of section i and designate:

$$\zeta = \frac{f_1}{i}, \quad \zeta_0 = \frac{f_0}{i}, \tag{6.30}$$

then we will obtain

$$\frac{1}{S^*} \frac{d^2 \zeta}{dt^{*2}} - m^2 (t^* - m^2) \zeta = m^4 \zeta_0. \tag{6.31}$$

Equation (31) may be integrated in Bessel functions (see Section 72). Furthermore, integration of equation (31) and more complicated equations of such a type can be accomplished numerically, and also with help of analog and digital computers.

In Fig. 6.2 are presented results of calculations conducted by numerical method of Adams for case S* = 0.1, ζ_0 = 0.001. On the axis of abscissas is placed parameter t*, equal to ratio of variable of compressive force to Euler's load, and on axis of ordinates--dimensionless maximum deflection ζ. Different curves correspond to values of m = 1, 2, 3. As we see, sharp increase of deflection occurs first of all during bending of bar in two half-waves (m = 2); to the right lie curves for m = 1 and m = 3. Judging by curve for m = 2,

deflections start to increase sharply only at a force seven times exceeding Euler's load. Deflection, equal to radius of gyration of section, is attained at load $P = 9.6P_э$.

If we use formula (9), then it is possible to determine dependence of ζ on $P/P_э$ for static loading for various m. To the left of all here lies curve m = 1, depicted in Fig. 6.2 by the dotted line. Deflection $\zeta = 1$ is attained when $P/P_э \approx 1$.

It is interesting to note that load $P \approx 9P_э$ corresponds to static form of loss of stability with three half-waves, while dynamic process occurs with two half-waves; explanation of this was given above, in Section 69.

Thus, here as a criterion determining critical time and at the same time critical load we took the condition that maximum deflection must not exceed radius of gyration of section. This criterion is, of course, arbitrary; it is possible to start from limiting value of maximum stress or the greatest deformations, etc.

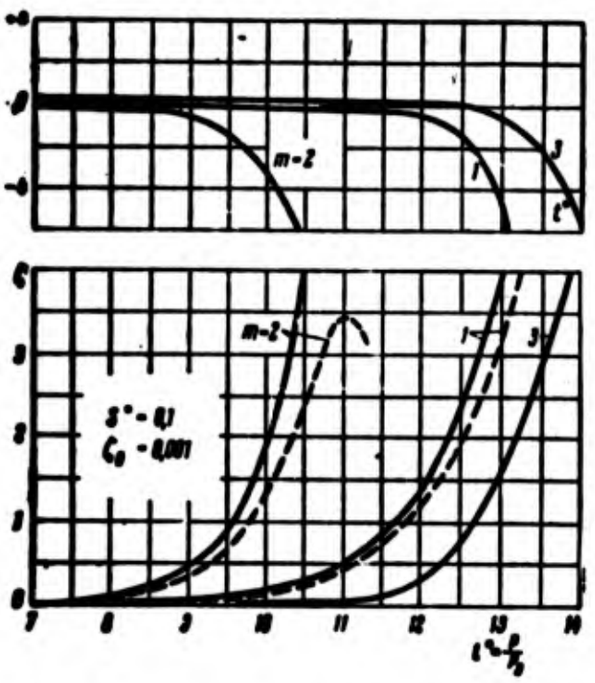

Fig. 6.2. Change of maximum deflection in time for different numbers of half-waves.

§ 71. Study of Energy of the System.

We make a comparison of different forms of dynamic loss of stability from the energy point of view. Kinetic energy of bar is equal to

$$T=\frac{1}{2g}\int_0^l\left(\frac{\partial v_1}{\partial t}\right)^2 dx. \tag{6.32}$$

Substituting expression (3), we find

$$T=\frac{1}{2g}\left(\frac{df_1}{dt}\right)^2\frac{l}{2}. \tag{6.33}$$

We use dimensionless parameter

$$\dot{T}=\frac{4l^2}{\pi^2 EJl^2}T \tag{6.34}$$

and introduce parameter of time from (25); then we have

$$T^*=\frac{1}{S^2}\left(\frac{d\zeta}{d\tau}\right)^2. \tag{6.35}$$

Potential strain energy is composed of energy of bending and compression:

$$U=\frac{EJ}{2}\int_0^l\left[\frac{\partial^2(v_1-v_0)}{\partial x^2}\right]^2 dx+\frac{P^2l}{2EF}. \tag{6.36}$$

In order to calculate potential of load, we determine convergence of ends of the bar Δ. Initial distance between joints is equal to

$$l_0=l-\frac{1}{2}\int_0^l\left(\frac{\partial v_0}{\partial x}\right)^2 dx. \tag{6.37}$$

and final distance

$$l_1=l-\frac{Pl}{EF}-\frac{1}{2}\int_0^l\left(\frac{\partial v_1}{\partial x}\right)^2 dx. \tag{6.38}$$

where l is length of bar in rectilinear state. Convergence of edges is equal to

$$\Delta=l_0-l_1=\frac{Pl}{EF}+\frac{1}{2}\int_0^l\left[\left(\frac{\partial v_1}{\partial x}\right)^2-\left(\frac{\partial v_0}{\partial x}\right)^2\right]dx. \tag{6.39}$$

Using (3), we find

$$\Delta=\frac{Pl}{EF}+\frac{1}{4l}m^2\pi^2(f_1^2-f_0^2). \tag{6.40}$$

Potential of load will have form

$$V = -P\Delta = -\frac{P^2 l}{EF} - \frac{P}{4l} m^2\pi^2 (f_1^2 - f_0^2). \tag{6.41}$$

Total potential energy is equal to

$$\Im = U + V = \frac{EI}{4} \frac{m^4\pi^4}{l^3} (f_1 - f_0)^2 - \frac{P^2 l}{2EF} - \frac{P}{4l} m^2\pi^2 (f_1^2 - f_0^2). \tag{6.42}$$

Hence in dimensionless magnitudes

$$\Im^* = \frac{4l^3}{\pi^4 EIl^2} \Im = m^4 (\zeta - \zeta_0)^2 - m^2 l^* (\zeta^2 - \zeta_0^2) - 2l^{*2}. \tag{6.43}$$

We determine dimensionless function of Lagrange

$$L^* = T^* - \Im^* = \frac{1}{S^2} \dot{\zeta}^2 - m^4 (\zeta - \zeta_0)^2 + m^2 l^* (\zeta^2 - \zeta_0^2) + 2l^{*2}. \tag{6.44}$$

where $\dot{\zeta} = \frac{d\zeta}{dt}$, and compose Lagrange's equation

$$\frac{d}{dt^*} \frac{\partial L^*}{\partial \dot{\zeta}} - \frac{\partial L}{\partial \zeta} = 0; \tag{6.45}$$

then we arrive at fundamental equation (31).

We find, further, total energy of the system

$$\Pi^* = T^* + \Im^* = \frac{1}{S^2} \dot{\zeta}^2 + m^4 (\zeta - \zeta_0)^2 - m^2 l^* (\zeta^2 - \zeta_0^2) - 2l^{*2}. \tag{6.46}$$

The system considered is not conservative--a given force evidently depends on time--and therefore, total energy does not remain constant here.

We introduce designation

$$\Pi_1^* = \Pi^* + 2l^{*2}. \tag{6.47}$$

In Fig. 6.2 above is depicted dependence $\Pi_1^*(t^*)$ for different values of m. Judging by the graph, at any moment of time the level of total energy corresponding to m = 2 is lower than energy level for m = 1 or m = 3. Evidently, the form of loss of stability with two half-waves is the most probable for the given value of S*.

Graphs, analogous to Fig. 6.2, were constructed for different values of S*; there were found curves, corresponding to such a value of m, for which increase of deflections is the most intensive. In

Fig. 6.3 is given combined graph of functions $\zeta(t^*)$ for $\zeta_0 = 0.001$ for consecutively increasing velocities of load c; remember that parameter S* is reciprocal to c^2. Value m for each curve is indicated.

From graph it is clear that for relatively small initial maximum

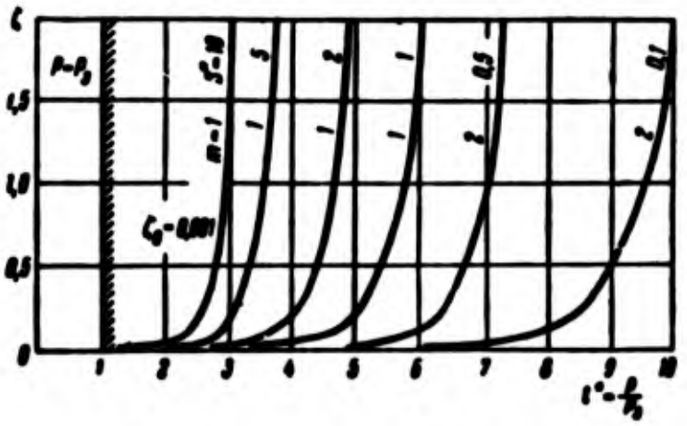

Fig. 6.3. Diagram of "deflection-load" for various velocities of load.

deflection and great velocity of load the force received by the bar can exceed Euler's load by many times. Deflections are developed chiefly with a certain specific form of elastic line, depending on rate of build-up of compressive force; the higher this velocity, the greater the number of half-waves will be formed along the bar.

§ 72. Solution in Bessel Functions.

We already said that the considered problem may be solved exactly without application of numerical methods. Let us turn to this means of solution.

We present equation (31) in the form

$$\frac{d^2\zeta}{dt^{*2}} - S^*m^2(t^* - m^2)\zeta = S^*m^4\zeta_0. \qquad (6.48)$$

We use substitution

$$t^* = m^2 - z(S^*m^2)^{-\frac{1}{3}} \qquad (6.49)$$

and introduce new variable z. Considering relationships

$$S^2m^2(m^2-t^2)=(S^2m^2)^{\frac{3}{2}}z, \tag{6.50}$$

$$(dt^2)^2=(dz)^2(S^2m^2)^{-\frac{2}{3}}, \tag{6.51}$$

we obtain

$$\frac{d^2\zeta}{dz^2}+z\zeta=A\zeta, \tag{6.52}$$

where

$$A=\sqrt[3]{S^2m^2}. \tag{6.53}$$

Let us consider first the case when

$$t^2<m^2,\quad z>0. \tag{6.54}$$

These relationships are valid for the first stage of motion, when compressive load does not exceed the m-th static Euler force:

$$P<m^2P_*. \tag{6.55}$$

General solution of equation (52) may be presented in the form

$$\zeta=C_1\zeta_1+C_2\zeta_2+\zeta_3. \tag{6.56}$$

By ζ and ζ_2 we understand linearly independent solutions of homogeneous equation

$$\frac{d^2\zeta}{dz^2}+z\zeta=0, \tag{6.57}$$

generators of a so-called fundamental system of solution; under ζ_3 is implied a particular solution of the initial equation.

We already met an equation of type (57) in Section 37; as we saw, it has solutions.*

$$\zeta_1=z^{\frac{1}{2}}J_{\frac{1}{3}}\left(\frac{2}{3}z^{\frac{3}{2}}\right),\quad \zeta_2=z^{\frac{1}{2}}J_{-\frac{1}{3}}\left(\frac{2}{3}z^{\frac{3}{2}}\right), \tag{6.58}$$

where $J_{\frac{1}{3}}$ and $J_{-\frac{1}{3}}$ are Bessel functions of the first type with indices

*See (indicated on p. 150) book of E. Kamke, p. 453.

$\frac{1}{3}$ and $\frac{1}{3}$.

Particular solution ζ_3 can be written in the form

$$\zeta_3 = \frac{A\zeta_0}{W}\left(\zeta_2 \int \zeta_1 dz - \zeta_1 \int \zeta_2 dz\right), \tag{6.59}$$

where W is the Wronskian,

$$W = \begin{vmatrix} \zeta_1 & \zeta_2 \\ \frac{d\zeta_1}{dz} & \frac{d\zeta_2}{dz} \end{vmatrix}. \tag{6.60}$$

We calculate derivatives of functions ζ_1 and ζ_2:

$$\frac{d\zeta_2}{dz} = \frac{1}{2} z^{-\frac{1}{2}} J_{-\frac{1}{3}}\left(\frac{2}{3} z^{\frac{3}{2}}\right) + z \frac{d}{dz} J_{-\frac{1}{3}}\left(\frac{2}{3} z^{\frac{3}{2}}\right). \tag{6.61}$$

$$\frac{d\zeta_1}{dz} = \frac{1}{2} z^{-\frac{1}{2}} J_{\frac{1}{3}}\left(\frac{2}{3} z^{\frac{3}{2}}\right) + z \frac{d}{dz} J_{\frac{1}{3}}\left(\frac{2}{3} z^{\frac{3}{2}}\right). \tag{6.62}$$

Putting these expressions in (60), we obtain

$$W = z^{\frac{3}{2}}\left\{J_{\frac{1}{3}}\left(\frac{2}{3} z^{\frac{3}{2}}\right) \frac{d}{dz}\left[J_{-\frac{1}{3}}\left(\frac{2}{3} z^{\frac{3}{2}}\right)\right] - J_{-\frac{1}{3}}\left(\frac{2}{3} z^{\frac{3}{2}}\right) \frac{d}{dz}\left[J_{\frac{1}{3}}\left(\frac{2}{3} z^{\frac{3}{2}}\right)\right]\right\}. \tag{6.63}$$

Expression (63) may be presented by gamma-functions with the help of a formula of type

$$W_0 = J_\nu(z) J'_{-\nu}(z) - J_{-\nu}(z) J'_\nu(z) = -\frac{1}{z}\left[\frac{1}{\Gamma(\nu+1)\Gamma(-\nu)} - \frac{1}{\Gamma(\nu)\Gamma(-\nu+1)}\right]. \tag{6.64}$$

In our case

$$W = \frac{3}{2}\left[\frac{1}{\Gamma\left(\frac{4}{3}\right)\Gamma\left(-\frac{1}{3}\right)} - \frac{1}{\Gamma\left(\frac{1}{3}\right)\Gamma\left(\frac{2}{3}\right)}\right]. \tag{6.65}$$

We use known relationships for a gamma-function*

$$\Gamma(z+1) = z\Gamma(z), \quad \Gamma(z)\Gamma(1-z) = \frac{\pi}{\sin \pi z}, \tag{6.66}$$

---

*See, e.g., N. N. Lebedev, Special functions and their application, Gostekhizdat, Moscow, 1958, p. 13.

then we find,

$$\Gamma\left(\frac{4}{3}\right)\Gamma\left(-\frac{1}{3}\right)=-\Gamma\left(\frac{1}{3}\right)\Gamma\left(\frac{2}{3}\right) \tag{6.67}$$

and further,

$$W=-\frac{3}{\Gamma\left(\frac{1}{3}\right)\Gamma\left(-\frac{1}{3}\right)}=-\frac{\sin\frac{\pi}{3}}{\frac{\pi}{3}}. \tag{6.68}$$

Finally we have

$$W=-\frac{3\sqrt{3}}{2\pi}. \tag{6.69}$$

Integrating* in (59), we substitute resulting expression for ζ_3 in solution of (56); constants C_1 and C_2 must be determined from initial conditions

$$\zeta=\zeta_0,\ \frac{d\zeta}{dt^*}=0 \text{ when } t^*=0 \text{ и } z=(S^*m^2)^{\frac{1}{3}}. \tag{6.70}$$

Functions (56) change periodically, so that motion of system during the first stage has an oscillatory character. Change of ζ occurs with amplitude of the order of ζ_0; therefore, on graph in Fig. 6.3, composed for $\zeta_0 = 0.001$, oscillations are unnoticeable.

During growth of parameter of time t* quantity z decreases. Determining ζ and $\frac{d\zeta}{dz}$ for z = 0, we obtain initial data for the next, the second stage of motion. Equation (52) for the second stage takes form

$$\frac{d^2\zeta}{d\bar{z}^2}-\bar{z}\zeta=A\zeta_0 \tag{6.71}$$

where

$$\bar{z}=-z=(t^*-m^2)(S^*m^2)^{\frac{1}{3}}. \tag{6.72}$$

Solution of equation (71) we write in the form

$$\zeta=\bar{C}_1\bar{\zeta}_1+\bar{C}_2\bar{\zeta}_2+\bar{\zeta}_3. \tag{6.73}$$

---

*Detailed calculations for this particular example are given by N. Hoff [6.12]. Another law of change of load is considered by a similar method by B. A. Olisov.

Solutions of homogeneous equation

$$\frac{d^4\bar{\zeta}}{d\bar{x}^4} - \bar{\zeta} = 0 \tag{6.74}$$

will be*

$$\bar{\zeta}_1 = \bar{x}^{\frac{1}{2}} I_{\frac{1}{3}}\left(\frac{2}{3}\bar{x}^{\frac{3}{2}}\right), \quad \bar{\zeta}_2 = \bar{x}^{\frac{1}{2}} I_{-\frac{1}{3}}\left(\frac{2}{3}\bar{x}^{\frac{3}{2}}\right), \tag{6.75}$$

where $I_{\frac{1}{3}}$ and $I_{-\frac{1}{3}}$ are modified Bessel functions of the first type. These functions change monotonically, amplitude of deflection when $t^* > m^2$ will increase without limit. We already came to this result in Section 70, using the numerical method. Particular solution for $\bar{\zeta}_3$ is determined by a formula of type (59); the Wronskian, as before, is expressed by formula (68).

§ 73. Experiments in Longitudinal Impact.

Peculiarities of phenomenon of dynamic loss of stability marked above are detected also in experiments. In work [6.5] there are described interesting experiments on wooden bars subjected to impact loading by a falling load. There was applied high-speed filming of consecutive configurations of the bar (from 2200 to 2700 frames per second); furthermore, there was conducted oscillographing of deformations at separate points.

Judging by these data, the whole process of deformation of the test piece was divided into several phases. During the first period, which in one experiment constituted about 1/500 sec, the whole piece experienced compression. During the second period, of approximately the same duration, through the test piece passed a reflected wave, and there appeared transverse vibrations. Here in different test pieces,

---

*See above-indicated book of E. Kamke, p. 453.

depending upon the slenderness ratio, there appeared different numbers of half-waves along the length, whereas the load per unit area of section remained identical. During the third period, constituting 1/250 sec, there occurred a change of the form of loss of stability with transition to one half-wave. Finally, the fourth period (1/10 sec) consisted of damped vibrations of the piece in one half-wave. In Fig. 6.4 are depicted different configurations of bars of two types, and in Fig. 6.5--three frames of the filmstrip, reflecting dynamic loss of stability with three half-waves.

Fig. 6.4. Distortion of bars during dynamic loading.
KEY: (а) Test pieces of ....

Thus, in theory we described above only one of the phases of bending of a bar upon impact; we did not investigate preliminary phase of propagation of deformation along the bar, and we did reflect transition from large number of half-waves to a smaller number in the final phase.

Judging by data of experiments, work of falling load, expended in process of buckling of bar, can be for more flexible rods higher than for rigid ones, since in case of a flexible bar there will be formed a larger number of half-waves.

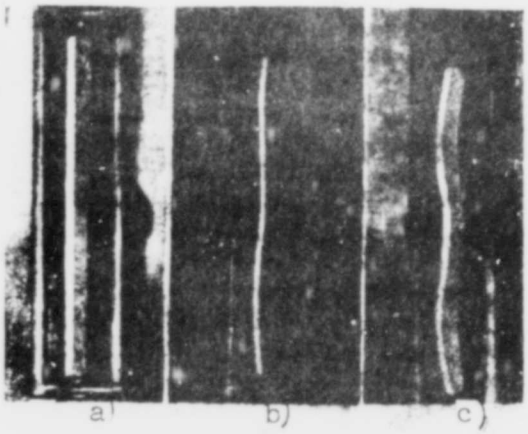

Fig. 6.5. Buckling of bar in three half-waves.

§ 74. Case of Given Law of Convergence of Bar Ends.

Let us turn to another case, when given variable is not compressive force P, but mutual displacement of bar ends Δ. Such case is characteristic for loading of a bar by a "rigid" testing machine.* If one cross-bar of the machine is moved by an electric motor through reducing gear, then one may assume that mutual convergence of ends of bar increases in proportion to time. Using force-measuring machine, we determine dependence between load and mutual displacement of ends of the test piece.

We designate velocity of mutual displacement of bar by s cm/sec and take

$$\Delta = st. \tag{6.76}$$

By (40) we obtain

$$\frac{Pl}{EF} = st - \frac{1}{4l}\pi^2(f_1^2 - f_0^2). \tag{6.77}$$

We introduce new parameter of time

$$t_0 = \frac{st}{lP_0^2}. \tag{6.78}$$

Dividing both parts of equation (77) by lP_0^2, we have

$$\frac{P}{P_0} = t_0 - \frac{\pi^2}{4}(\zeta^2 - \zeta_0^2). \tag{6.79}$$

Comparing expressions (25), (26), and (78), we find

$$t = \frac{lP_0^2}{s}t_0 = t_0\frac{l}{P_0^2 V}; \tag{6.80}$$

hence

$$t_0 = t\frac{P_0^2 Vl}{ls}. \tag{6.81}$$

We place expressions (79) and (81) in equation (31), then we arrive at the following fundamental equation:

---

*This case was considered in a number of works of Hoff and other authors [6.12], [6.13] under the condition that along the bar there forms one half-wave.

$$\frac{1}{S_*}\frac{d^2\zeta}{dt_*^2}+m^2\left[(m^2-t_*)\zeta+\frac{m^2}{4}(\zeta^2-\zeta_0^2)\zeta\right]=m^2\zeta_0; \tag{6.82}$$

here by S_* is designated parameter

$$S_*=P_*^2\left(\frac{\pi V}{s}\right)^2=\left(\frac{V}{s}\right)^2\frac{\pi^2}{\lambda^2}. \tag{6.83}$$

Let us note that magnitude S_* depends on ratio of velocity of mutual displacement of bar ends s to velocity of sound in the material. According to the basic assumption adopted above this ratio should be small.

We set inertial member in equation (82) equal to zero; then we obtain dependence $\zeta(t_*)$, corresponding to <u>static loading</u>:

$$\left[m^2-t_*+\frac{m^2}{4}(\zeta^2-\zeta_0^2)\right]\zeta=m^2\zeta_0. \tag{6.84}$$

Value $t_* = 1$ corresponds according to (78) to Euler's deformation. We note that, in distinction from case of a preset load (Section 70), here magnitude of ζ when $t_* = 1$ and $m = 1$ does not become infinitely great. Maximum deflection remains finite for any finite parameter t_*, inasmuch as in this case convergence of ends of the bar are fixed.

If one were to set $\zeta_0 = 0$, then we obtain

$$\zeta=0 \quad \text{or} \quad \frac{m^2}{4}\zeta^2=t_*-m^2. \tag{6.85}$$

When $t_* < m^2$ we have $\zeta = 0$, and when $t_* > m^2$ there are possible three values of ζ: one will be $\zeta = 0$, and the two others are determined by the second equation of (85).

Behavior of the bar during <u>dynamic loading</u> is described by equation (82). It was integrated numerically* [6.13]; results when $m = 1$ and $\zeta_0 = 0.001$ are represented in Fig. 6.6.

---

*In articles [6.13] are presented other methods of integration of equation (82), for $m = 1$.

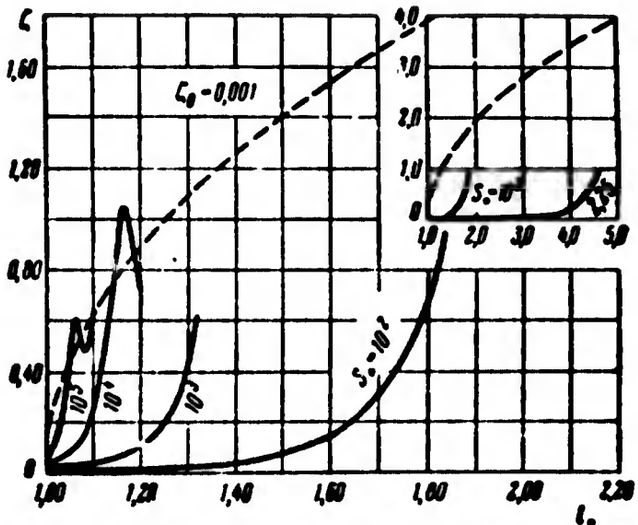

Fig. 6.6. Case, when there is given the law of convergence of bar ends in time.

Solid lines here give dependence $\zeta(t_*)$ for different values of parameter S_*. Let us remember that by t_* is understood ratio of variable convergence of ends of the bar to shortening of the straight bar with a Euler load equal to $(lP_э^*)$. Dotted line shows static curve of (84). General character of curves $\zeta(t_*)$ on first section — up to moment of sharp growth of ζ — is the same as in Fig. 6.3. Growth of deflections occurs at a value of Δ, significantly exceeding Euler's magnitude $lP_э^*$. "Pulling" of deflections appears stronger the higher the velocity s. Subsequently, dependence $\zeta(t_*)$ corresponds to vibrations of bar near position of static equilibrium.

Using equation (79), it is possible, further, to determine dependence of load P on parameter of time. Curves $(P/P_э, t_*)$ are given in Fig. 6.7. As one can see from the graph, at great velocity Euler's load turns out to be strongly exceeded. Maxima of ratio $P/P_э$, taking place in process of load, are presented in Fig. 6.8 depending upon parameter S_* and initial maximum deflection ζ_0. Fig. 6.7 pertains to case when there will be formed one half-wave $(m = 1)$. However, when

$S_* = 0.1$ of predominant significance is the form of buckling for $m = 2$; this one may be seen from Fig. 6.2, in which to considered type of load pertain dotted lines; designations S* and t* must in this case be replaced by S_* and t_* by (83) and (78).

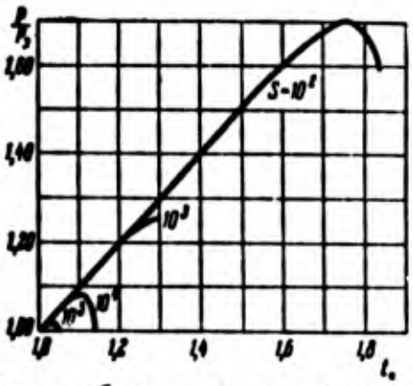

Fig. 6.7. Dependence between load received by a bar and time.

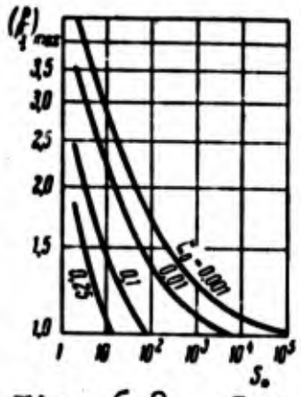

Fig. 6.8. Supporting power of bar for various initial maximum deflections.

The leading edge of the wave when $m = 2$ lies significantly to the left of where it does when $m = 1$.

The case of a preset law of convergence of bar ends is an example of loading in which magnitude of compressive force depends on behavior of the test piece, on its deformation.

§ 75. Behavior of a Bar During Action of Impulsive Load.

We considered previously that load – constant or variable, predetermined or set by deformation of a bar – acts during the whole considered period; we were interested in "critical" time interval after which supporting power of the bar is considered exhausted.

For practical calculations also of interest is the case of load of explosive type, which in the beginning increases and then drops by a definite law. As the simplest example let us consider behavior of a bar under the condition that to it there is <u>suddenly</u> applied compressive force P, remaining constant for a short time interval τ and then <u>disappearing</u>. We consider the form of initial deflection as

before coincides with the form of additional deflection.

Behavior of the bar in period τ is described by equation (13) when $P < P_э$ and equation (19) when $P > P_э$; variable t_k by (10) changes from 0 to $k\tau = 2\pi\tau/T$, where T is the period of vibrations in absence of compressive force.

For section $0 < t_k < k\tau$ equation of motion will be

$$f_1 = C_1 \cos k_1 t_k + C_2 \sin k_1 t_k + \frac{m^4}{k_1^2} f_0 \quad \text{when} \quad P < P_э, \tag{6.86}$$

or

$$f_1 = C_1 \operatorname{ch} k_1 t_k + C_2 \operatorname{sh} k_2 t_k + \frac{m^4}{k_2^2} f_0 \quad \text{when} \quad P > P_э; \tag{6.87}$$

constants C_1 and C_2 are determined from initial conditions. For the subsequent period differential equation has form

$$\frac{d^4 f_1}{dt_k^4} + m^4 f_1 = m^4; \tag{6.88}$$

solution of it we write in the form

$$f_1 = C_3 \cos m^2 t_k + C_4 \sin m^2 t_k + f_0. \tag{6.89}$$

Constants C_3 and C_4 we find, equating values and deflections when $t_k = k\tau$.

As we see, in second case deflection, in general, has a maximum value at a moment of time, not coinciding with moment of cessation of action of force P. Subsequently, there occur vibrations relative to initial bending line.

§ 76. Case of Pulsating Load. Approximate Solution.

Let us turn to case where impulses are repeated one after another and bar is subjected to action of periodic load, equal P in single time intervals and dropping to zero in other intervals (Fig. 6.9). We designate by θ the frequency of application of force P and by $\tau = \frac{\pi}{\theta}$ — the half-period of change of force. The first two intervals we already studied in Section 56. The new condition consists of the

fact that length of time $t_k > k\tau$ is limited and is completed at moment $t_k = 2k\tau$ by a new application of force P.

It is important to explain what will be the character of vibrations of the bar, caused by such a pulsating load. If vibrations attenuate, then initial form of bar can be called dynamically stable. With vibrations growing from one impulse to the next the initial form is dynamically unstable. In intermediate case, when vibrations of the bar are periodic or close to periodic, initial form can be considered dynamically indifferent. Let us note that in the differential equation of motion of the bar (13) load enters not as an disturbing force, but as a parameter determining rigidity of the system. Therefore, vibrations appearing with periodic change of force P, are called parametric vibrations.

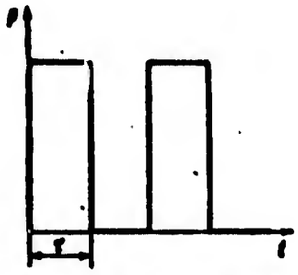

Fig. 6.9. Law of change of load in time.

In order to investigate character of motion of a bar it is sufficient to trace change of deflections and velocities during one full period 2τ. Obviously, when $P > P_3$ deflections caused by repeated load always will grow. Therefore, we consider case $P \leq P_3$.

For half-period equation (13) will take form

$$\frac{d^2 f_1}{dt_k^2} + \omega^2 f_1 = 0. \tag{6.90}$$

where

$$\omega^2 = 1 - \frac{P}{P_3}. \tag{6.91}$$

Hence

$$f_1 = A_1 \cos \omega t_k + B_1 \sin \omega t_k. \tag{6.92}$$

For second half-period we will have $\omega^2 = 1$ and, consequently,

$$f_1 = A_2 \cos t_k + B_2 \sin t_k. \tag{6.93}$$

Assume that when $t_k = 0$ initial deflection constitutes f_0 and the derivative with respect to t_k will be $\dot{f}_0$, where initial velocity will be $v_0 = \dot{f}_0 k$. Then by (92)

$$A_1 = f_0. \quad B_1 = \frac{1}{\omega} \dot{f}_0. \tag{6.94}$$

At the end of full period parameter t_k by (10) is equal to $t_k = 2k\tau_1 = \frac{2\pi k}{\theta}$. We assume* that deflection and velocity change toward the end of period the same number of times s:

$$f_1 = sf_0. \quad \frac{df_1}{dt_k} = s\dot{f}_0. \tag{6.95}$$

Then by (93) we have

$$\left.\begin{aligned} A_2 \cos \frac{2\pi k}{\theta} + B_2 \sin \frac{2\pi k}{\theta} &= sf_0. \\ -A_2 \sin \frac{2\pi k}{\theta} + B_2 \cos \frac{2\pi k}{\theta} &= s\dot{f}_0. \end{aligned}\right\} \tag{6.96}$$

From this

$$\left.\begin{aligned} A_2 &= sf_0 \cos \frac{2\pi k}{\theta} - s\dot{f}_0 \sin \frac{2\pi k}{\theta}. \\ B_2 &= sf_0 \sin \frac{2\pi k}{\theta} + s\dot{f}_0 \cos \frac{2\pi k}{\theta}. \end{aligned}\right\} \tag{6.97}$$

At the end of first half-period, when $t_k = \pi k/\theta$, deflection and velocity, calculated by (92) or (93), must be the same; this condition leads to equalities

$$\left.\begin{aligned} A_1 \cos \frac{\pi\omega k}{\theta} + B_1 \sin \frac{\pi\omega k}{\theta} &= A_2 \cos \frac{\pi k}{\theta} + B_2 \sin \frac{\pi k}{\theta}. \\ \omega\left(-A_1 \sin \frac{\pi\omega k}{\theta} + B_1 \sin \frac{\pi\omega k}{\theta}\right) &= -A_2 \sin \frac{\pi k}{\theta} + B_2 \cos \frac{\pi k}{\theta}. \end{aligned}\right\} \tag{6.98}$$

Putting in (98) expressions (94) and (97), we arrive at the following equations:

$$\left.\begin{aligned} (a - \omega b) f_0 + \left(c + \frac{d}{\omega}\right) \dot{f}_0 &= 0. \\ (c + \omega d) f_0 - \left(a - \frac{b}{\omega}\right) \dot{f}_0 &= 0. \end{aligned}\right\} \tag{6.99}$$

---

*Such solution of problem is adopted in book of Den-Hartog [6.10].

where

$$\left.\begin{aligned} a &= s\cos\frac{2\pi k}{\theta} - \cos\frac{\pi\omega k}{\theta}\cos\frac{\pi k}{\theta}, \quad b = \sin\frac{\pi\omega k}{\theta}\sin\frac{\pi k}{\theta}, \\ c &= s\sin\frac{2\pi k}{\theta} - \cos\frac{\pi\omega k}{\theta}\sin\frac{\pi k}{\theta}, \quad d = \sin\frac{\pi\omega k}{\theta}\cos\frac{\pi k}{\theta}. \end{aligned}\right\} \tag{6.100}$$

If we take $f_0 \neq 0$ and $\dot{f}_0 \neq 0$, then determinant of system (99) should be equal to zero:

$$\begin{vmatrix} a-\omega b & c+\frac{d}{\omega} \\ -(c+\omega d) & a-\frac{b}{\omega} \end{vmatrix} = 0. \tag{6.101}$$

Expanding this determinant, we, arrive at equation

$$a^2+b^2+c^2+d^2+\left(\omega+\frac{1}{\omega}\right)(cd-ab)=0. \tag{6.102}$$

By (100) we find

$$\left.\begin{aligned} a^2+b^2+c^2+d^2 &= s^2-2s\cos\frac{\omega\pi k}{\theta}\cos\frac{\pi k}{\theta}+1, \\ cd-ab &= s\sin\frac{\omega\pi k}{\theta}\sin\frac{\pi k}{\theta}. \end{aligned}\right\} \tag{6.103}$$

Equation (102) takes form

$$s^2-2ns+1=0, \tag{6.104}$$

where

$$n=\cos\frac{\pi\omega k}{\theta}\cos\frac{\pi k}{\theta}-\frac{1}{2}\left(\omega+\frac{1}{\omega}\right)\sin\frac{\pi\omega k}{\theta}\sin\frac{\pi k}{\theta}. \tag{6.105}$$

Coefficient s is equal to

$$s=n\pm\sqrt{n^2-1}. \tag{6.106}$$

If magnitude n^2 is less than 1, for s we obtain a complex expression. Obviously, initial assumption of simultaneous growth of deflection f_0 and velocity $\dot{f}_0$ by s times in this case is not satisfied. However, real part s turns out to be a proper fraction; vibration of the bar will not grow; so initial form of motion of bar must be considered stable.

Conversely, when $n^2 > 1$ coefficient s will be larger than 1, so that vibrations toward end of each period will be intensified; consequently, initial form will appear unstable.

Intermediate case $n^2 = 1$ corresponds as if to indifferent form

of motion. Thus, equality

$$n = \cos\frac{\pi\omega k}{\theta}\cos\frac{\pi k}{\theta} - \frac{1}{2}\left(\omega + \frac{1}{\omega}\right)\sin\frac{\pi\omega k}{\theta}\sin\frac{\pi k}{\theta} = \pm 1 \qquad (6.107)$$

determines boundary, separating zone of stable motion from zone of instability. Let us note that when $n < 1$ deflection and velocity change sign at the end of the period with respect to the beginning of the same period, but when $n > 1$ we preserve the sign.

Assume that magnitude of pulsating load is minute in comparison with Euler's load: $P \ll P_э$; then it is possible to consider that $\omega \to 1$. Condition (107) takes form

$$\cos\frac{2\pi k}{\theta} = \mp 1. \qquad (6.108)$$

From this we obtain the following two series of values for k/θ:

$$\left.\begin{aligned} \frac{k}{\theta} &= \frac{1}{2}, \frac{3}{2}, \frac{5}{2}, \ldots \text{ when } k = -1, \\ \frac{k}{\theta} &= 1, 2, 3, \ldots \text{ when } k = 1. \end{aligned}\right\} \qquad (6.109)$$

The first zone of instability occurs <u>at a frequency of pulsating load θ</u>, <u>twice</u> the frequency of free vibrations of the bar k. This is possible to explain in the following manner. Assume that force P is <u>applied</u> to bar in those intervals of time, when, distorting, it moves from mid-position to an extreme; since point of application of force will shift downwards, then force will accomplish positive work. In those same intervals of time, when bar straightens, shifting to mid-position, force P <u>is removed</u>, so that work will not be accomplished. In the full period of vibrations of a bar force will be applied twice which corresponds to value $\theta/k = 2$. Work of force P will, thus, continuously increase, and this should be accompanied by growing vibrations of the bar.

Let us consider a second limiting case, when force P is close to Euler's: $P \to P_э$ and $\omega \to 0$. Relationship (107) is rewritten in

the form

$$n = \lim_{\omega \to 0} \left[\cos \frac{\pi \omega k}{\theta} \cos \frac{\pi k}{\theta} - \left(\frac{\omega}{2} \sin \frac{\pi \omega k}{\theta} - \frac{\pi k}{2\theta} \frac{\sin \frac{\pi \omega k}{\theta}}{\frac{\pi \omega k}{\theta}} \right) \sin \frac{\pi k}{\theta} \right] = \pm 1$$

or

$$n = \cos \frac{\pi k}{\theta} - \frac{\pi k}{2\theta} \sin \frac{\pi k}{\theta} = \pm 1. \qquad (6.110)$$

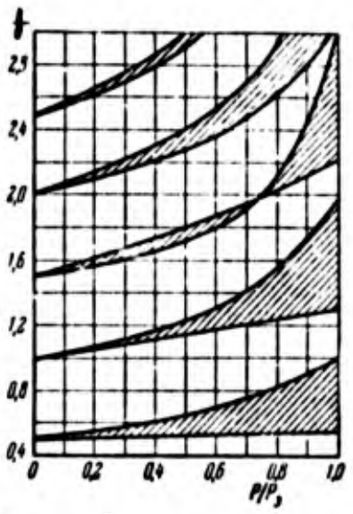

Fig. 6.10. Regions of instability during parametric vibrations.

We find first two roots of equation (110). The first of them corresponds to ratio $k/\theta = 0.548$; we have

$$n = -0.157 - \frac{1}{2} 0.548\pi \cdot 0.988 \approx -1.$$

Second root corresponds to $k/\theta = 1$; here again $n = -1$.

Results of calculations for other values of ω are shown in Fig. 6.10.* For all values of k/θ included inside the hachured regions magnitude n will either be less than (-1), which occurs in the first, third, etc., zones, or larger than (+1)— in second, fourth, etc., zones. In points of boundary lines we have $n = \pm 1$.

Thus, for $\omega \neq 0$ we obtain a range of values k/θ for which there is dynamic instability. We must explain that we did not take into account resisting forces, influencing vibrating process. When accounting for these forces zones of instability turn out to be somewhat different (see Section 77).

Let us present our results in another form. Let us refer frequency of pulsating load θ to frequency of free vibrations Ω of the

*A similar graph is given in work of V. M. Makushin [6.6], p. 65.

bar with mean value of force P, equal to P/2. As it is easy to see, we get

$$\Omega = k\sqrt{1-\frac{P}{2P_0}} = k\sqrt{\frac{1+\omega^2}{2}}. \qquad (6.111)$$

On the other hand, we introduce parameter load

$$\nu = \frac{\frac{P}{2P_0}}{1-\frac{P}{2P_0}}, \qquad (6.112)$$

characterizing ratio between variable part of load and its mean value. In coordinates $(\nu, \frac{\theta}{2\Omega})$ first region of instability has the form shown in Fig. 6.11. Boundaries of region constitute lines, close to straight lines.

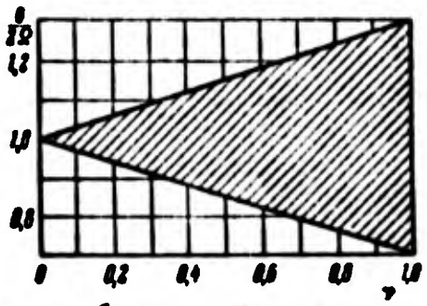

Fig. 6.11. First zone of instability.

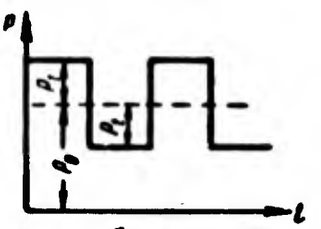

Fig. 6.12. Character of change of load.

Analogous investigation can be conducted for case when pulsating load changes by the same law for a certain mean value of P_0, and its variable part is equal to P_t (Fig. 6.12), where $P_0 + P_t \leq P_*$. Frequencies of vibrations of the bar for two intervals of period of variation of the force will be

$$p_1 = k\sqrt{1-\frac{P_0+P_t}{P_*}}, \quad p_2 = k\sqrt{1-\frac{P_0-P_t}{P_*}}. \qquad (6.113)$$

Condition (107) assumes the form

$$n = \cos\frac{\pi p_1}{\theta}\cos\frac{\pi p_2}{\theta} - \frac{1}{2}\left(\frac{p_1}{p_2}+\frac{p_2}{p_1}\right)\sin\frac{\pi p_1}{\theta}\sin\frac{\pi p_2}{\theta} = \pm 1; \qquad (6.114)$$

from this we determine boundary lines of zones of instability. As

it is easy to see, for above discussed example we must take

$$p_1 = k\omega, \quad p_2 = k.$$

Parameters Ω and ν in general are equal to

$$\Omega = k\sqrt{1-\frac{P_0}{P_3}}, \quad \nu = \frac{\frac{P_1}{P_3}}{1-\frac{P_0}{P_3}}; \tag{6.115}$$

§ 77. Load, Changing by Harmonic Law. Parametric Vibrations

We investigated behavior of a bar during stepped periodic change of compressive force. It is natural to pass from here to the case when the magnitude of load follows a harmonic law (Fig. 6.13):

$$P = P_0 + P_1 \cos \theta t \tag{6.116}$$

or

$$P = P_0 + P_1 \cos \frac{\theta}{k} t_k. \tag{6.117}$$

where t_K is determined as before by (10).

Equation (11) when $f_0 = 0$ and $m = 1$ has form

$$\frac{d^2 f}{dt_k^2} + \left(1 - \frac{P_0}{P_3} - \frac{P_1}{P_3} \cos \frac{\theta}{k} t_k\right) f = 0. \tag{6.118}$$

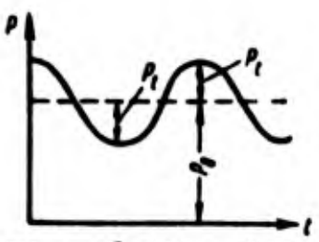

Fig. 6.13. Load changes by harmonic law.

We use designations (115) and introduce new parameter of time

$$t_1 = \sqrt{1-\frac{P_0}{P_3}}\, t_k = \frac{\Omega}{k} t_k = \Omega t, \tag{6.119}$$

then instead of (118) we obtain

$$\frac{d^2 f}{dt_1^2} + \left(1 - \nu \cos \frac{\theta t_1}{\Omega}\right) f = 0. \tag{6.120}$$

Equation of such type has the name of Mathieu equation; it is encountered in astronomy and in certain problems of mathematical physics. Detailed investigation showed that for ratios θ/Ω lying inside certain definite regions, solution of the equation becomes unstable.

In other words, with variation of compressive force by (116) we obtain certain regions of dynamic instability, as it was in example of Section 76; deflections and velocities grow during each period of variation of load. It is natural to expect that, here too, the phenomenon of parametric resonance for small P will appear near values of Ω/θ equal to

$$\frac{\Omega}{\theta}=\frac{1}{2}.\ 1.\ \frac{3}{2}.\ 2.\ldots \tag{6.121}$$

Boundaries of regions of instability again are determined from the condition that dynamic form of bar is as if indifferent; vibrations must be maintained, not intensified or weakened. We set ourselves the target to determine approximately the boundaries of the first region of instability, lying near value $\theta = 2\Omega$. Considering that motion of bar should be periodic, we take as first approximation the expression for f in the form*

$$f=A_1\cos\frac{\theta t_1}{2\Omega}+B_1\sin\frac{\theta t_1}{2\Omega}. \tag{6.122}$$

Substituting (122) in equation (120), we have

$$A_1\left(1-\frac{\theta^2}{4\Omega^2}-\nu\cos\frac{\theta t_2}{2\Omega}\right)+B_1\left(1-\frac{\theta^2}{4\Omega^2}-\nu\cos\frac{\theta t_2}{\Omega}\right)\sin\frac{\theta t_2}{2\Omega}=0. \tag{6.123}$$

Considering relationship

$$\left.\begin{aligned}\cos\frac{\theta t_1}{\Omega}\cos\frac{\theta t_1}{2\Omega}&=\frac{1}{2}\left(\cos\frac{\theta t_1}{2\Omega}+\cos\frac{3\theta t_1}{2\Omega}\right).\\ \cos\frac{\theta t_1}{\Omega}\sin\frac{\theta t_1}{2\Omega}&=\frac{1}{2}\left(-\sin\frac{\theta t_1}{2\Omega}+\sin\frac{3\theta t_1}{2\Omega}\right)\end{aligned}\right\} \tag{6.124}$$

and discarding members with tripled frequency, we obtain

$$A_1\left(1-\frac{\theta^2}{4\Omega^2}-\frac{\nu}{2}\right)\cos\frac{\theta t_1}{2\Omega}+B_1\left(1-\frac{\theta^2}{4\Omega^2}+\frac{\nu}{2}\right)\sin\frac{\theta t_1}{2\Omega}=0. \tag{6.125}$$

Considering $A_1 \neq 0$ and $B_1 \neq 0$, we equate of zero the expressions in parentheses; then we find

$$\frac{\theta}{2\Omega}=\sqrt{1-\frac{\nu}{2}}.\quad \frac{\theta}{2\Omega}=\sqrt{1+\frac{\nu}{2}}. \tag{6.126}$$

---

*This method of solving the Mathieu equation was given by Rayleigh [6.17].

In Fig. 6.14 are depicted lower and upper boundaries of first region of instability, constructed by (126). This graph is very close to the graph of Fig. 6.11.

Definitized solution of problem can be obtained, taking the expression for f in the form of the series

$$f=\sum_n\left(A_n\cos\frac{n\theta t_1}{2\Omega}+B_n\sin\frac{n\theta t_1}{2\Omega}\right) \tag{6.127}$$

and retaining new members of the series in supplement to A_1 and B_1. Detailed study shows [6.2] that, for values $\nu \leq 0.6$, correction to formulas (126) lies within 1%.

To expressions (126) it is possible to give another form, expanding the right side by the formula of Newton's binomial theorem. In first approximation we obtain*

$$\frac{\theta}{2\Omega}=1-\frac{\nu}{4},\quad \frac{\theta}{2\Omega}=1+\frac{\nu}{4}. \tag{6.128}$$

Formulas (126) correspond in Fig. 6.14 to dotted lines.

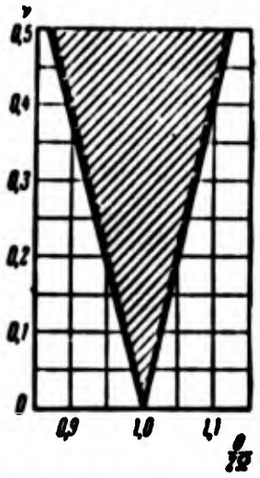

Fig. 6.14. Comparison of exact and approximate solutions.

In deriving the formulas we ignored resisting force to vibrations. In order to estimate influence of these forces, we consider them proportional to velocity and write the initial equation in fuller form:

$$\frac{d^2f}{dt^2}+2\varepsilon\frac{df}{dt}+k^2\left(1-\frac{P_0}{P_*}-\frac{P_1}{P_*}\cos\omega t\right)f=0. \tag{6.129}$$

Passing to variable t_1 of (119),

*These formulas were offered by N. M. Belyayev [6.1].

we obtain, instead of (120),

$$\frac{d^2f}{dt_1^2}+2\frac{\varepsilon}{\Omega}\frac{df}{dt_1}+\left(1-\nu\cos\frac{\theta t_1}{\Omega}\right)f=0. \tag{6.130}$$

We use again solution (122), then equation (130) will have the form

$$\left[A_1\left(1-\frac{\theta^2}{4\Omega^2}-\frac{\nu}{2}\right)+B_1\frac{\theta\varepsilon}{\Omega^2}\right]\cos\frac{\theta t_1}{2\Omega}+$$

$$+\left[B_1\left(1-\frac{\theta^2}{4\Omega^2}+\frac{\nu}{2}\right)-A_1\frac{\theta\varepsilon}{\Omega^2}\right]\sin\frac{\theta t_1}{2\Omega}=0. \tag{6.131}$$

Equating to zero the expressions in brackets, we obtain two equations for A_1 and B_1; conditions $A_1 \neq 0$ and $B_1 \neq 0$ lead to equation

$$\begin{vmatrix} 1-\frac{\theta^2}{4\Omega^2}-\frac{\nu}{2} & \frac{\theta\varepsilon}{\Omega^2} \\ -\frac{\theta\varepsilon}{\Omega^2} & 1-\frac{\theta^2}{4\Omega^2}+\frac{\nu}{2} \end{vmatrix}=0 \tag{6.132}$$

or

$$\frac{\theta^4}{16\Omega^4}-2\frac{\theta^2}{4\Omega^2}\left(1-\frac{2\varepsilon^2}{\Omega^2}\right)+1-\frac{\nu^2}{4}=0. \tag{6.133}$$

Considering magnitude ε/Ω small and discarding members of higher order of smallness, we present solution of equation (133) in the form

$$\frac{\theta}{2\Omega}=\sqrt{1\mp\sqrt{\frac{\nu^2}{4}-\frac{4\varepsilon^2}{\Omega^2}}}. \tag{6.134}$$

For $\varepsilon = 0$ we obtain former formulas (126). If however, $\varepsilon \neq 0$, then boundaries of regions of instability shift somewhat. Thus, for example, for $\nu = 0$ we do not obtain here that point on axis $\theta/2\Omega$, from which curves of Fig. 6.14 branched out. Real values of $\theta/2\Omega$ occur on the condition that

$$\nu \geqslant \frac{4\varepsilon}{\Omega}. \tag{6.135}$$

New outlines of first region of instability are shown in Fig. 6.15 by the solid line. They differ little from boundaries of the same region when $\varepsilon = 0$, shown on graph by the dotted line.

Significantly great is the influence of resistance on outlines of second and subsequent regions of instability. They strongly move away from axis of abscissas of Fig. 6.15, so that instability can

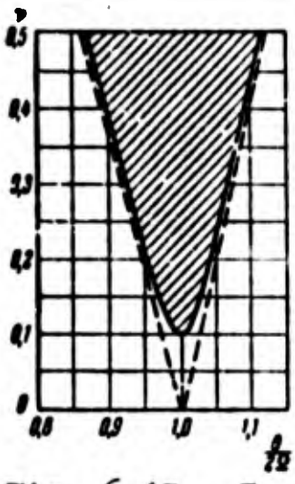

Fig. 6.15. Influence of damping on boundaries of first retion of instability.

appear only at a significant magnitude of parameter ν. Therefore, of practical value for designing real structures is basically, determination of the first region. More detailed account of theory of dynamic stability is beyond the scope of this book. Those interested in this theory can turn to special literature and, primarily, the book of V. V. Bolotin, 1956 [0.1].

§ 78. Stability of Compressed Ring with Dynamic Loading.

We have met different directions of theory of dynamic stability of a compressed bar. Let us now turn to dynamic problems pertaining to other structures. We shall investigate first of all behavior of a circular closed ring with rapid loading by radial forces (Fig. 3.31). This problem is of interest for calculation of frames in reinforced shells subjected to dynamic application of external pressure.

We preserve former approach to solution of problem and assume the ring has certain initial deflections w_0 from circular form. We use basic dependences derived for an "ideal" ring in Section 46 and supplement them, taking into account initial deflection. By w subsequently, we will understand <u>total</u> deflection.

Equations of equilibrium (3.175) – (3.177) remain in force; however, derivatives with respect to y must be replaced by partial derivatives. Variation of curvature $\varkappa$ by (3.181) now will be determined by expression

$$\varkappa = \frac{\partial^2(w - w_0)}{\partial y^2} + \frac{w - w_0}{R^2}. \tag{6.136}$$

bending moment M in an arbitrary section is equal to

$$M = EI\left[\frac{\partial^2(w - w_0)}{\partial y^2} + \frac{w - w_0}{R^2}\right]. \tag{6.137}$$

Using (3.179), we obtain instead of (3.184) a differential equation for w in such a form:

$$EI\left[\frac{\partial^6(w - w_0)}{\partial y^6} + \frac{2}{R^2}\frac{\partial^4(w - w_0)}{\partial y^4} + \frac{1}{R^4}\frac{\partial^2(w - w_0)}{\partial y^2}\right] = \frac{q_y}{R} - \frac{\partial q_z}{\partial y}. \tag{6.138}$$

In dynamic problems we must take into account component forces of inertia

$$q_z' = -\frac{\gamma F}{g}\frac{\partial^2 w}{\partial t^2}, \quad q_y' = -\frac{\gamma F}{g}\frac{\partial^2 v}{\partial t^2}; \tag{6.139}$$

here v is displacement along the arc, F is area of section, γ is specific weight of the material.

We write expression for deformation along the arc:

$$\varepsilon_y = \frac{\partial(v - v_0)}{\partial y} - \frac{w - w_0}{R}. \tag{6.140}$$

and assume as before that the axis of the ring is inextensible: $\varepsilon_y = 0$; then we have

$$\frac{\partial(v - v_0)}{\partial y} = \frac{w - w_0}{R}. \tag{6.141}$$

Using (138) – (141), we arrive at the following final differential equation:

$$EI\left[\frac{\partial^6(w - w_0)}{\partial y^6} + \frac{2}{R^2}\frac{\partial^4(w - w_0)}{\partial y^4} + \frac{1}{R^4}\frac{\partial^2(w - w_0)}{\partial y^2}\right] + qR\left(\frac{\partial^4 w}{\partial y^4} + \frac{1}{R^2}\frac{\partial^2 w}{\partial y^2}\right) + \frac{\gamma F}{g}\left(\frac{\partial^4 w}{\partial y^2 \partial t^2} - \frac{1}{R^2}\frac{\partial^2 w}{\partial t^2}\right) = 0. \tag{6.142}$$

We take for w and w_0 expressions

$$w = f \sin\frac{ny}{R}, \quad w_0 = f_0 \sin\frac{ny}{R}. \tag{6.143}$$

Considering $n \geq 2$, we obtain

$$(f - f_0)n^2(n^2 - 1)^2 - f\frac{qR^3}{EI}n^2(n^2 - 1) + \frac{\gamma F R^4}{EIg}\frac{d^2 f}{dt^2}(n^2 + 1) = 0. \tag{6.144}$$

Introducing expression (3.188) for static critical pressure q_*,

we present (144) in the form

$$\frac{d^2f}{dt^2}+\alpha\frac{n^2(n^2-1)}{n^2+1}\left(n^2-1-3\frac{q}{q_0}\right)f=\alpha\frac{n^2(n^2-1)^2}{n^2+1}f_0; \tag{6.145}$$

here is introduced designation

$$\alpha=\frac{Elg}{\gamma FR^4}. \tag{6.146}$$

Let us assume first that ring is subjected to sudden loading.* When $q < q_0$, we obtain vibrations near position of static equilibrium. When $q > q_0$, deflection will start to increase without limit. Reasoning in this way, as in Section 70, we find form with the greatest rate of growth. We shall consider $n \gg 1$; then in equation (145) it is possible to disregard 1 as compared to n^2, and it will take the form

$$\frac{d^2f}{dt^2}-k_2^2f=\alpha n^4f_0, \tag{6.147}$$

where

$$k_2^2=\alpha n^2\left(3\frac{q}{q_0}-n^2\right). \tag{6.148}$$

Equating to zero the derivative dk_2^2/dn, we find the value of n:

$$n^0=\frac{1}{\sqrt{2}}\sqrt{\frac{3q}{q_0}}. \tag{6.149}$$

We obtained the same result as in Section 70: most vigorously increases that form of loss of stability, whose number is approximately 0.7 of the number of static form, corresponding to the given level of load.

Assume, further, that pressure increases in time by the law $q = ct$. Then equation (145) will be rewritten in form

$$\frac{1}{\alpha}\frac{d^2f}{dt^2}+\frac{n^2(n^2-1)}{n^2+1}\left(n^2-1-3\frac{ct}{q_0}\right)f=\frac{n^2(n^2-1)^2}{n^2+1}f_0. \tag{6.150}$$

We use parameters

$$t_2=\frac{q}{q_0}=\frac{ct}{q_0},\quad S=\alpha\frac{q_0^2}{c^2}=\alpha_0^3\left(\frac{VEF}{cR^2}\right)^2; \tag{6.151}$$

---

*This problem was investigated by M. A. Lavrentyev and A. Yu. Ishlinskiy (see footnote on p. 288).

by V as before is implied velocity of sound; by $\varepsilon_3 = q_3 R/EF$ the arc deformation corresponding to pressure q_3. Equation (150) obtains form

$$\frac{1}{S}\frac{d^2f}{dt_2^2} - n^2(t_2 - n^2)f = n^1 f_0. \tag{6.152}$$

When $n \gg 1$ equation (152) changes to the following:

$$\frac{1}{S}\frac{d^2f}{dt_2^2} + \frac{n^2(n^2-1)}{n^2+1}(n^2 - 1 - t_2)f = \frac{n^2(n^2-1)^2}{n^2+1} f_0. \tag{6.153}$$

This equation in structure coincides with equation (31) pertaining to case of bar. Therefore, when $n \geq 4$ it is possible in case of ring to use all results obtained for bars on the condition we determine t_2 and S by formulas (151).

§ 79. Lateral Distortion of a Strip During Dynamic Application of Moment.

Let us turn to the problem of lateral buckling of a narrow strip, loaded by a couple in its plane. In Fig. 6.16 is depicted an element of the strip in deformed state. Assume that axes of coordinates x, y, and z, passed in some section of the strip (Fig. 6.16a) acquire after deformation directions ξ, η, and ζ (Fig. 6.16b). We designate by w total deflection of center of gravity of strip along axis z and by θ the total angle of rotation of the section in plane yz.

Equations of equilibrium of the element in projections on axis ζ and in moments about axes y and z have form

$$\frac{\partial Q_\eta}{\partial x} + q_\zeta = 0. \tag{6.154}$$

$$\frac{\partial M_\eta}{\partial x} - Q_\eta + m_\eta = 0. \tag{6.155}$$

$$\frac{\partial M_\xi}{\partial x} + m_\xi = 0. \tag{6.156}$$

where M_η and M_ξ are bending moments; Q_η is transverse force; q_ζ is intensity of load along axis ζ, m_η; m_ξ is components of moment load.

Magnitudes q_ξ, m_η, and m_ξ are expressed through moment of the applied couple M and inertial loads:

$$q_\xi = -\frac{\gamma F}{g}\frac{\partial^2 w}{\partial t^2}, \tag{6.157}$$

$$m_\xi = -J\frac{\partial^2 \beta}{\partial t^2} - M\frac{\partial^2 w}{\partial x^2}, \tag{6.158}$$

$$m_\eta = M\frac{\partial \beta}{\partial x}; \tag{6.159}$$

here F is area of section of strip; J is moment of inertia of mass of the beam per unit length.

Bending moments can be expressed by total displacements w and β and their initial values, w_0 and β_0:

$$M_\eta = EI_y\frac{\partial^2 (w - w_0)}{\partial x^2}. \tag{6.160}$$

$$M_\xi = GI_\kappa\frac{\partial (\theta - \theta_0)}{\partial x}; \tag{6.161}$$

by I_y is understood moment of inertia of section with respect to axis y: by GI_K, torsional rigidity.

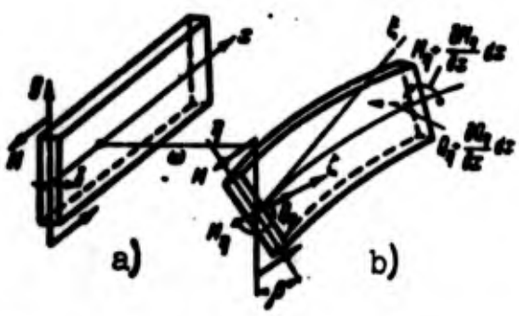

Fig. 6.16. Lateral distortion of a strip during dynamic loading.

Comparing the relationships written above, we arrive at the following equations:

$$EI_y\frac{\partial^4 (w - w_0)}{\partial x^4} + M\frac{\partial^2 \theta}{\partial x^2} + \frac{\gamma F}{g}\frac{\partial^2 w}{\partial t^2} = 0. \tag{6.162}$$

$$GI_\kappa\frac{\partial^2 (\theta - \theta_0)}{\partial x^2} - M\frac{\partial^2 w}{\partial x^2} - J\frac{\partial^2 \theta}{\partial t^2} = 0. \tag{6.163}$$

If we take $w_0 = \theta_0 = 0$ and exclude inertial members, we obtain static equations (4.131) and (4.132), derived in a different manner in Chapter IV.

Assuming that torey ends of the strip are supported by hinges, and considering the fundamental form of buckling, we set

$$\left.\begin{aligned} w &= f\sin\frac{\pi x}{l}, \quad w_0 = f_0\sin\frac{\pi x}{l}, \\ \theta &= \varphi\sin\frac{\pi x}{l}, \quad \theta_0 = \varphi_0\sin\frac{\pi x}{l}; \end{aligned}\right\} \tag{6.164}$$

then equations (162) and (163) assume form

$$\frac{\gamma F}{g}\frac{d^2f}{dt^2} + EI_y\frac{\pi^4}{l^4}(f - f_0) = 0. \tag{6.165}$$

$$J\frac{d^2\varphi}{dt^2} + GI_k\frac{\pi^2}{l^2}(\varphi - \varphi_0) - M\frac{\pi^2}{l^2}f = 0. \tag{6.166}$$

Considering inertial members equal to zero and considering $\varphi_0 = f_0 = 0$, we find from this the static critical load:

$$M_0 = \frac{\pi}{l}\sqrt{EI_y GI_k} = \sqrt{P_3 GI_k}. \tag{6.167}$$

where by $P_э$, as before, we designate Euler's force; this formula coincides with (4.100).

On the other hand, taking $M = 0$, we determine fundamental frequencies $\omega_и$ and $\omega_к$ of flexural and torsional vibrations.

$$\omega_и = \frac{\pi^2}{l^2}\sqrt{\frac{EIg}{F\gamma}}, \quad \omega_к = \frac{\pi}{l}\sqrt{\frac{GI_k}{J}}. \tag{6.168}$$

Using these designations, we give to equations (162) and (163) their final form,

$$\left.\begin{aligned} \frac{1}{\omega_и^2}\frac{d^2f}{dt^2} - \frac{M}{M_0}\frac{M_0}{P_э}\varphi + f &= f_0. \\ \frac{1}{\omega_к^2}\frac{d^2\varphi}{dt^2} - \frac{M}{M_0}\frac{P_э}{M_0}f + \varphi &= \varphi_0. \end{aligned}\right\} \tag{6.169}$$

Let us assume that moment of applied couple varies in time according to the law $M = M(t)$. Integrating equations (169), it is possible then to determine magnitudes t and β as a function of time.

Let us consider a case, similar to that which was investigated in Section 69, when a strip is subjected to <u>sudden</u> loading by moment $M > M_э$, keeping constant magnitude during period τ and then <u>dropping to zero</u>.* Initial conditions we take as the following;

---

*This problem was investigated by Davidson [6.9].

$$f=f_0,\quad \varphi=\varphi_0,\quad \frac{df}{dt}=0,\quad \frac{d\varphi}{dt}=0 \text{ when } t=0. \tag{6.170}$$

Excluding f from (169), we obtain equation for φ:

$$\frac{d^4\varphi}{dt^4}+(\omega_1^2+\omega_2^2)\frac{d^2\varphi}{dt^2}+\omega_1^2\omega_2^2\left(1-\frac{M^2}{M_0^2}\right)\varphi=\omega_1^2\omega_2^2\left(\varphi_0+f_0\frac{MP_0}{M_0^2}\right). \tag{6.171}$$

Integral of this equation we write in form

$$\frac{\varphi}{\varphi_0}=\frac{M^2}{M^2-M_0^2}(A\operatorname{ch}\omega_1 t+B\operatorname{sh}\omega_1 t+C\cos\omega_2 t+D\sin\omega_2 t)- \\ -\left(\frac{M_0^2}{M^2}+\frac{P_0 f_0}{M\varphi_0}\right). \tag{6.172}$$

where

$$\left.\begin{aligned} 2\omega_1^2&=\omega_1^2+\omega_2^2+\sqrt{(\omega_2^2-\omega_1^2)+4\omega_1^2\omega_2^2\frac{M^2}{M_0^2}}\,,\\ \omega_1^2-\omega_2^2&=\omega_1^2+\omega_2^2. \end{aligned}\right\} \tag{6.173}$$

Taking into consideration initial conditions, we find

$$A+C=1+\frac{P_0 f_0}{M\varphi_0},\quad B=D=0, \tag{6.174}$$

$$A\omega_1^2-C\omega_2^2=\frac{P_0}{M_0^2}\frac{M^2-M_0^2}{M}\frac{f_0}{\varphi_0}\omega_2^2. \tag{6.175}$$

Considering relationship

$$\omega_2^2\omega_2^2\left(1-\frac{M^2}{M_0^2}\right)=-\omega_1^2\omega_2^2, \tag{6.176}$$

ensuing from consideration of equations (173), we arrive at the following expression for φ:

$$\frac{\varphi}{i\varphi_0}=\frac{M^2}{M^2-M_0^2}\left\{\frac{\omega_2^2\operatorname{ch}\omega_1 t+\omega_1^2\cos\omega_2 t}{\omega_2^2+\omega_1^2}-\frac{M_0^2}{M^2}+\right. \\ \left.+\frac{P_0 f_0}{M_0\varphi_0}\left[\frac{\omega_2^2\left(1+\frac{\omega_1^2}{\omega_2^2}\right)\operatorname{ch}\omega_1 t+\omega_1^2\left(1-\frac{\omega_2^2}{\omega_2^2}\right)\cos\omega_2 t}{\omega_2^2+\omega_1^2}-1\right]\right\}. \tag{6.177}$$

A similar expression can be written for f. Dependence of type (177) has the peculiarity as compared to analogous relationship (87) for a compressed bar that, along with exponential components it contains a harmonic component. In Fig. 6.17 is shown magnitudes φ/φ_0 (solid lines) and f/f_0 (dotted lines) vary in time under the condition

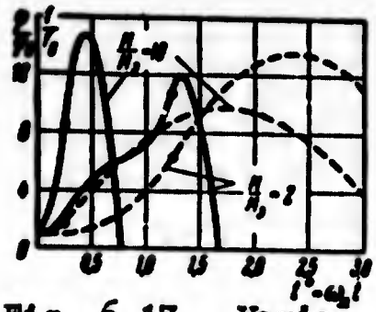

Fig. 6.17. Variation of parameters of deflection of a strip in time.

that applied moment constitutes $M = 2M_*$ and $M = 10M_*$, and that ratio $\omega_н/\omega_к$ is equal to 0.2; furthermore, we take $P_* f_0/M_* \varphi_0 = 1$. On axis of abscissas is placed magnitude $t^* = \omega_н t$; to period of flexural vibrations $T_н$ corresponds the value $t^* = 2\pi$. Time of action of load in one case is selected equal to $t^* = 0.25$; in another it corresponds to period of torsional vibrations and is equal to $t^* = 1.25$. Circles show moments when load is removed. As we see, for the given relationship of frequencies of vibrations, angle of torsion grows and then drops with significantly more intensity than deflection.

Literature on stability of a bar during dynamic loading is given below (p.324); we note also works of L. N. Vorob'yev (Trans. Novocherkassk Polytechnic Inst., 21/35, 1949), I. A. Burnashev (News of Acad. of Sci. of Uzbek SSR, No. 11, 1951), Sh. S. Mazitov (News of Acad. of Sci. Tadzhik SSR, No. 16, 1956), Ye. Prokopovich, S. Reutu and F. Dinke (Jour. Applied Mech., Acad. of Sci., Romanian Republic, 1957), O. I. Katsitadze (Cand. dissertation, Tbilisi, 1958), S. Sevin (J. Appl. Mech., No. 1, 1960), A. I. Oseled'ko (Trans. Voronezh Engineering Inst., No. 4, 1958), U. R. Upmanis (Problems of dynamics and strength, Nos. 7 and 9, Riga, 1961).

Literature

6.1. N. M. Belyayev. Stability of prismatic bars under action of variables longitudinal forces, Coll. "Engineering constructions and structural mechanics," Publishing House "Put'," 1924.

6.2. V. V. Bolotin. Transverse vibrations of bars caused evoked by periodic forces, "Transverse vibrations and critical velocities," 1, Publishing House of Academy of Sciences of USSR (1951), 46-77; On parametrically excited vibrations of elastic arches, DAN SSSR, 83, No. 4 (1952), 537-539; Determining amplitudes of transverse vibrations. "Transverse vibrations and critical velocities," Publishing House of Academy of Sciences of USSR, 2 (1953), 45-64; Parametric excitation of transverse vibrations, loc. cit., 5-44; Dynamic stability of plane form of bending, Eng. Collection, 14 (1953), 109-122; Interaction of forced and parametrically excited vibrations, News of Acad. of Sci. of USSR, OTN, No. 4 (1954).

6.2a. A. S. Vol'mir. Stability of compressed bars during dynamic loading, Structural, mechanics and design of structures, No. 1 (1960), 6-9.

6.3. I. I. Gol'denblat. Contemporary problems of vibrations and stability of engineering constructions, Stroyizdat, M., 1947; Dynamic stability of constructions, Stroyizdat, M., 1948.

6.4. M. A. Lavrentyev and A. Yu. Ishlinskiy. Dynamic forms of loss of stability of elastic systems, DAN SSSR, 65, No. 6 (1949).

6.5. M. Ye. Kagan and N. D. Genya. Experimental research of work of wooden bars on a longitudinal shock, News of Higher Educational Institutions, Construction and architecture, No. 3 (1961), 33-38.

6.6. V. M. Makushin. Transactions of Moscow Higher Technical School named after Bauman, Department of strengths of materials, 3 (1947).

6.7. V. N. Chelomey. Dynamic stability of elements of aviation constructions, Aeroflot Press, 1938.

6.8. J. P. Chawla. Numerical analysis of the process of buckling of elastic and inelastic columns, Proc. of the 1st U. S. Congr. of Applied Mech., 1952, 435-440.

6.9. J. F. Davidson. Impact buckling of deep beams in pure bending, Quarterly Journ. of Mech. and Appl. Math. 8, No. 1 (1955), 81-87 (see "Mechanics," IL, No. 2 (36), 1956, 133-139).

6.10. Den Hartog. Theory of vibrations, 1940 (in translation, Gostekhizdat, 1942).

6.11. N. J. Hoff. The process of the buckling of elastic columns, Rep. No. 163, Polit. Inst. of Brookline, 1949; Dynamic criteria of buckling, Research Eng. Struct. Supplement, Butterworths Publ., 1949; The dynamics of the buckling of elastic columns, J. Appl. Mech., No. 1 (1951), 68-74 (see Coll. of translations "Mechanics," IL, No. 3, 1952).

6.12. N. J. Hoff. Buckling and stability, J. of the Royal Aeron. Soc. 58, No. 1 (1954) (translation, IL, 1955).

6.13. N. J. Hoff, S. Nardo, and B. Erickson. The maximum load supported by an elastic column in a rapid compression test, Proc. of the 1st U. S. Nat. Congress of Appl. Mech., 1952, 419-423; An experimental investigation of the process of buckling of columns, Roc. of the Soc. for Exper. Stress analysis 9, No. 1 (1951), 201-208.

6.14. S. Kaliski. Statecznosc udarowa preta, Biuletyn Wojckowei Akademj technicznej, Warszawa, 1955.

6.15. C. Koning and J. Taub. Stossartige Knickbeanspruchung schlanker Stäbe in elastischen Bereich, Luftfahrtforschung 10, No. 2 (1933), 55-64.

6.16. S. Lubkin and J. J. Stoker. Stability of columns and springs under periodically varying forces, Quart. of Appl. Math. 1, No. 3 (1943).

6.17. Rayleigh. The theory of sound, Vol. 1, London, 1926 (in translation Gostekhizdat, 1940, pp. 311-313).

6.18. J. S. Rinehart and J. Pearson. Behavior of metal under impulsive loads, 1953 (in translation, IL, 1958).

6.19. V. L. Salerno, F. Bauer, and I. Sheng. The behavior of a simply supported column under constant or varying end load. Proc. of the 1st U. S. Nat. Congr. of Appl. Mech., 1952, 425-434.

6.20. J. Taub. Stossartige Knickbeanspruchung schlauker Stäbe im elastischen Bereich, Luftfahrtforschung 10, No. 2 (1933), 65-85.

CHAPTER VII

STABILITY OF RECTANGULAR PLATES WITHIN ELASTIC LIMITS

§ 80. Basic Dependences of the Theory of Rigid Plates.

Plates of rectangular form enter in composition of various structures – aircraft wings, bottoms, decks and sides of a ship, walls of all-metal railroad car, etc. – usually in the form of panels of plating, fastened to system of reinforcing ribs. The shell is subjected in these structures to action of one or another "local" transverse load, e.g., aerodynamic pressure, and besides receives "fundamental" forces together with other structural members – from general bending of the aircraft wing, the ship hull or the railroad car. In many cases these fundamental forces prevail; they cause compression, flexure or shear of the plate in its plane and lead, in certain conditions, to buckling of plates (Fig. 7.1); therefore, calculation of plates for stability constitutes an inseparable part of general calculation of a structure. Plates reinforced on longitudinal edges, after loss of stability, can carry an increasing load. For certain structures it is considered fully permissible that the plating has relatively shallow dents, with this condition, however, that members reinforcing it remain sufficiently rigid. Consequently, designer should be interested not only in the actual phenomenon of loss of

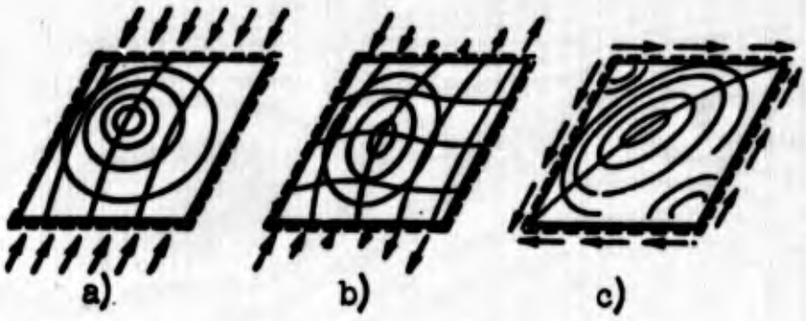

Fig. 7.1. Buckling of a plate during compression, flexure and shear.

stability of plates, but also their postcritical behavior. Webs of high beams, and also elements of different thin wall bars and beams also constitute rectangular plates, subject to buckling; consequently, here too, calculation for stability is of paramount importance.

In determining critical loads while investigating equilibrium states adjacent to initial ones, it is possible to consider that stresses in middle surface of a plate, appearing in process of buckling, are small as compared to stresses of free bending; deflections of plate are also considered small as compared to thickness. In this case it is possible to use the theory of rigid plates, disregarding stresses in the middle surface of the plate. If, however, we are investigating postcritical behavior of a plate, then we must start from more general theory of flexible plates, considering simultaneously stresses in middle surface and flexural stresses.*

We shall recount first the most important propositions of the theory of rigid plates. Consider a rectangular plate with sides a and b and of thickness h (Fig. 7.2). Let coordinate plane xy coincides with middle plane of the plate; axis x will be, as a rule, passed along the long side a, axis y — along the short side b. We designate

*For more detail on this see book [0.3], p. 13.

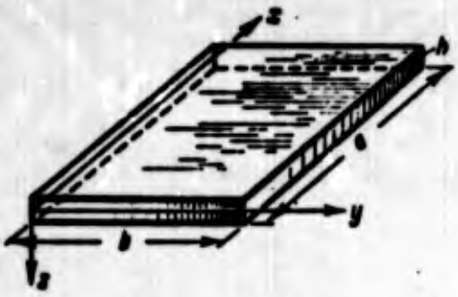

Fig. 7.2. System of coordinates during consideration of a rectangular plate.

displacements of points of middle surface along axes x, y and z by u, v, and w.

We dissect middle surface of bent plate by a plane, parallel to plane xz (Fig. 7.3). Since deflections are small, then in cross-section we will obtain a shallow curve. Angle of inclination θ_x of the tangent to the curve is equal to

$$\theta_x = \frac{\partial w}{\partial x}. \tag{7.1}$$

analogously for cross-section, parallel to plane yz,

$$\theta_y = \frac{\partial w}{\partial y}. \tag{7.2}$$

Curvature of the section we consider positive if the bulge is directed toward positive direction of axis z. Then <u>curvature</u> in sections parallel to planes xz and yz will be equal to

$$\varkappa_x = -\frac{\partial \theta_x}{\partial x}, \quad \varkappa_y = -\frac{\partial \theta_y}{\partial y}. \tag{7.3}$$

or

$$\varkappa_x = -\frac{\partial^2 w}{\partial x^2}, \quad \varkappa_y = -\frac{\partial^2 w}{\partial y^2}. \tag{7.4}$$

With variation of y angle θ_x generally also changes; referring increase of angle θ_x to increase of coordinate y (or increase of θ_y to increase of x), we find <u>torsion</u> of middle surface:

$$\chi = -\frac{\partial \theta_x}{\partial y} = -\frac{\partial \theta_y}{\partial x}. \tag{7.5}$$

or

$$\chi = -\frac{\partial^2 w}{\partial x \partial y}. \tag{7.6}$$

If we are talking about rigid plates, the middle surface is considered <u>free from deformations</u> accompanying bending. For arbitrary

Fig. 7.3. Cross-section of deflection surface of plate.

layer of the plate, lying at distance z from middle surface, deformations of elongation $\varepsilon_{x,и}$ and $\varepsilon_{y,и}$ are equal to

$$\varepsilon_{x,и} = z\varkappa_x, \quad \varepsilon_{y,и} = z\varkappa_y; \tag{7.7}$$

deformation of non-dilational strain will be

$$\gamma_и = 2z\chi. \tag{7.8}$$

To these deformations correspond normal stresses σ_x and σ_y and tangential stresses τ (Fig. 7.4). Using Hooke's law and disregarding stresses σ_z, we obtain

$$\sigma_{x,и} = \frac{E}{1-\mu^2}(\varepsilon_x + \mu\varepsilon_y), \quad \sigma_{y,и} = \frac{E}{1-\mu^2}(\varepsilon_y + \mu\varepsilon_x), \quad \tau_и = \frac{E}{2(1+\mu)}\gamma. \tag{7.9}$$

or

$$\sigma_{x,и} = \frac{Ez}{1-\mu^2}(\varkappa_x + \mu\varkappa_y), \quad \sigma_{y,и} = \frac{Ez}{1-\mu^2}(\varkappa_y + \mu\varkappa_x), \quad \tau_и = \frac{Ez}{1+\mu}\chi. \tag{7.10}$$

Fig. 7.4. Normal and tangential stresses during flexure.
KEY: (a) Middle plane.

In sections of the plate, parallel to axes x and y, we select strips of a length, equal to one. Forces σ_x and σ_y form bending moments per unit length of the section:

$$M_x = \int_{-\frac{h}{2}}^{\frac{h}{2}} \sigma_{x,и}\, z\, dz, \quad M_y = \int_{-\frac{h}{2}}^{\frac{h}{2}} \sigma_{y,и}\, z\, dz,$$

or

$$M_x = D(\varkappa_x + \mu\varkappa_y), \quad M_y = D(\varkappa_y + \mu\varkappa_x), \tag{7.11}$$

where D is cylindrical rigidity of the plate:

$$D = \frac{Eh^3}{12(1-\mu^2)}. \tag{7.12}$$

Tangential forces τ form a torsional moment per unit length of section of

$$H = \int_{-\frac{h}{2}}^{\frac{h}{2}} \tau z\, dz, \tag{7.13}$$

or

$$H = D(1-\mu)\chi. \tag{7.14}$$

We introduce, then, designations Q_x and Q_y for transverse forces in sections xz and yz, also per unit length.

Let us assume that plate is subjected to action of transverse load of intensity q. In Fig. 7.5 is shown element of plate dxdy with effective forces acting on it. Double arrows designate moment vectors. If in the section with coordinate x there acts moment $M_x dy$, then in the neighboring section, having coordinate x + dx, there will act moment $\left(M_x + \frac{\partial M_x}{\partial x} dx\right) dy$. Analogous increases are received by remaining components of moments and transverse forces. We compose equations of equilibrium of the element in projections on axis z and in moments relative to axes x and y. After simple transformations these equations acquire the form

$$\frac{\partial Q_x}{\partial x} + \frac{\partial Q_y}{\partial y} = -q. \tag{7.15}$$

$$\frac{\partial M_x}{\partial x} + \frac{\partial H}{\partial y} - Q_x = 0. \tag{7.16}$$

$$\frac{\partial H}{\partial x} + \frac{\partial M_y}{\partial y} - Q_y = 0. \tag{7.17}$$

Hence

$$\frac{\partial^2 M_x}{\partial x^2} + 2\frac{\partial^2 H}{\partial x\,\partial y} + \frac{\partial^2 M_y}{\partial y^2} = -q. \tag{7.18}$$

Using expressions for moments and curvatures, we arrive at known differential equation of bending of a rigid plate,

$$D\left(\frac{\partial^4 w}{\partial x^4} + 2\frac{\partial^4 w}{\partial x^2 \partial y^2} + \frac{\partial^4 w}{\partial y^4}\right) = q \tag{7.19}$$

or

$$D\nabla^4 w = q. \tag{7.20}$$

where

$$\nabla^4 w = \nabla^2 \nabla^2 w, \quad \nabla^2 = \frac{\partial^2}{\partial x^2} + \frac{\partial^2}{\partial y^2}$$

is a two-dimensional Laplace operator.

In "classical" problems of stability external transverse load is not considered; initial state of strain is considered momentless. But together with this in consideration of "neighboring" bent states of a plate it is necessary to consider projections of turned internal forces on axis of fixed system of coordinates. In Fig. 7.6 is shown plate element dxdy after bending with normal forces σ_x and σ_y and tangential forces τ acting on it.

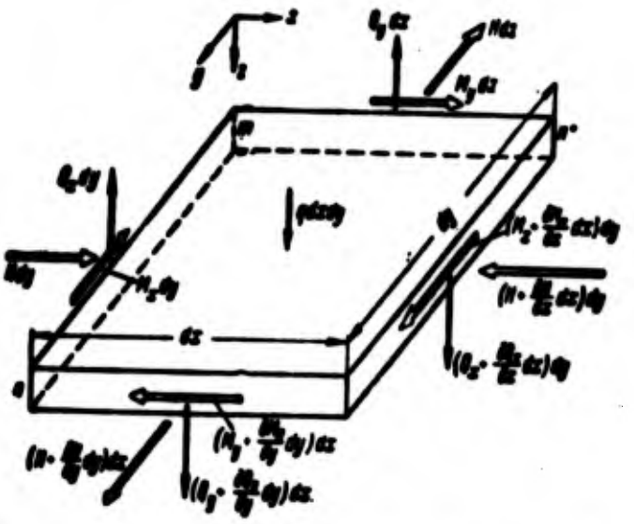

Fig. 7.5. Forces applied to deformed element of plate.

Stresses σ_x and σ_y are considered positive during compression; tangential stresses we take as positive, if they are directed as shown in Fig. 7.6; non-dilational strain corresponding to them increases angle between faces of the element, located closer to the origin of coordinates. We determine resultant forces $\sigma_x h\,dy$. Left edge of element turns on axis y and angle $\frac{\partial w}{\partial x}$, and the right edge, an angle $\frac{\partial w}{\partial x} + \frac{\partial^2 w}{\partial x^2}\,dx$ (Fig. 7.7). Total projection of forces $\sigma_x h\,dy$ on axis z, equal, with accuracy up to smallness of higher order, to their resultant, will be (axes of coordinates in Fig. 7.7 and 7.8 differ from

those in Fig. 7.6):

$$\sigma_x h \frac{\partial w}{\partial x} dy - \sigma_x h \left(\frac{\partial w}{\partial x} + \frac{\partial^2 w}{\partial x^2} dx \right) dy = - \sigma_x h \frac{\partial^2 w}{\partial x^2} dx\, dy. \tag{7.21}$$

Fig. 7.6. Forces in middle surface.

Analogous expression for forces σ_y has the form

$$- \sigma_y h \frac{\partial^2 w}{\partial y^2} dy\, dx. \tag{7.21a}$$

We then find resultant of tangential forces τh, also obtaining new directions. If one of the edges parallel to y turns about axis x at angle $\frac{\partial w}{\partial y}$, and second, the closest to the reader (Fig. 7.8), at angle $\frac{\partial w}{\partial y} + \frac{\partial^2 w}{\partial x \partial y} dx$, then forces τh dy will give a total projection equal to

$$- \tau h \frac{\partial^2 w}{\partial x \partial y} dx\, dy. \tag{7.22}$$

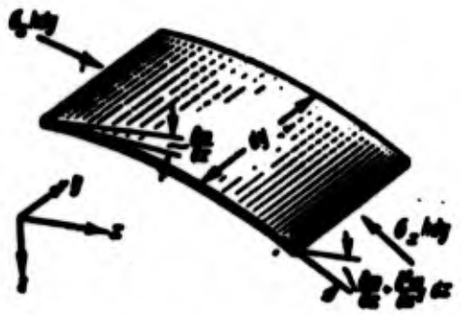

Fig. 7.7. Determination of resultant turned forces of compression.

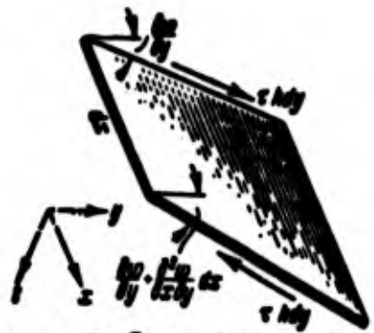

Fig. 7.8. Determination of resultant turned forces of shear.

Left edge turns about axis y and angle $\frac{\partial w}{\partial x}$, and the right – at angle $\frac{\partial w}{\partial x} + \frac{\partial^2 w}{\partial x \partial y} dy$. Total projection of forces τh dx will also be equal to

$$- \tau h \frac{\partial^2 w}{\partial x \partial y} dx\, dy. \tag{7.22a}$$

We find sum of projections of "turned" forces and divide it by dx dy; this magnitude must be introduced in left part of equation (15); for

q = 0 it has form

$$\frac{\partial Q_x}{\partial x}+\frac{\partial Q_y}{\partial y}-\sigma_x h\frac{\partial^2 w}{\partial x^2}-\sigma_y h\frac{\partial^2 w}{\partial y^2}-2\tau h\frac{\partial^2 w}{\partial x\,\partial y}=0. \tag{7.23}$$

Hence

$$\frac{\partial Q_x}{\partial x}+\frac{\partial Q_y}{\partial y}=\left(\sigma_x\frac{\partial^2 w}{\partial x^2}+\sigma_y\frac{\partial^2 w}{\partial y^2}+2\tau\frac{\partial^2 w}{\partial x\,\partial y}\right)h. \tag{7.24}$$

We compare this equation with (15); as it is easy to see, the expression in parentheses can be treated as the intensity of <u>hypothetical lateral load</u>

$$q^*=-\left(\sigma_x\frac{\partial^2 w}{\partial x^2}+\sigma_y\frac{\partial^2 w}{\partial y^2}+2\tau\frac{\partial^2 w}{\partial x\,\partial y}\right)h=(\sigma_x\varkappa_x+\sigma_y\varkappa_y+2\tau\chi)h. \tag{7.25}$$

Finally equation (20) take the form (for q = 0)

$$\frac{D}{h}\nabla^4 w+\left(\sigma_x\frac{\partial^2 w}{\partial x^2}+2\tau\frac{\partial^2 w}{\partial x\,\partial y}+\sigma_y\frac{\partial^2 w}{\partial y^2}\right)=0. \tag{7.26}$$

Integrating operation (26) we should satisfy boundary conditions. Consider some variants of these conditions.

1. <u>One of the edges</u>, for instance edge x = 0, is <u>supported by hinges</u>.

Such an assumption can be made if plate is connected with a reinforcing rib, having low torsional rigidity (thin rod of open section), or if fastening of the plate to rib is carried out by a narrow strip (one row of rivets, spot welding) (Fig. 7.9a). Then boundary conditions have form

$$w=0. \tag{7.27}$$

$$M=-D\left(\frac{\partial^2 w}{\partial x^2}+\mu\frac{\partial^2 w}{\partial y^2}\right)=0. \tag{7.28}$$

If condition (27) is satisfied, then along edge x = 0 obviously $\frac{\partial^2 w}{\partial y^2}\equiv 0$; consequently, condition (28) will be written in the form

$$\frac{\partial^2 w}{\partial x^2}=0. \tag{7.29}$$

2. <u>Edge x = 0 is clamped</u>. Such an assumption corresponds to case of plate, strongly linked (for instance with help of two-row rivet seam) with a rib, sufficiently rigid to torsion (Fig. 7.9b). Boundary conditions will be

$$w=0. \tag{7.30}$$

$$\frac{\partial w}{\partial x}=0. \tag{7.31}$$

3. Plate fastened on edge x = 0 to elastic rib, having flexural rigidity EI. One of the conditions of linkage consist of equality of deflections:

$$w_1=(w)_{x=0}; \tag{7.32}$$

by w_1 we designate deflection of rib. Second condition expresses equality of linear force, transmitted from plate to rib, to reaction of the rib. It is possible to show (see [0.3], p. 40) that linear reactive force, normal to surface of plate, will be, for the considered edge,

$$R_x=Q_x+\frac{\partial H}{\partial y}, \tag{7.33}$$

or

$$R_x=-D\left[\frac{\partial^3 w}{\partial x^3}+(2-\mu)\frac{\partial^3 w}{\partial x\,\partial y^2}\right]. \tag{7.34}$$

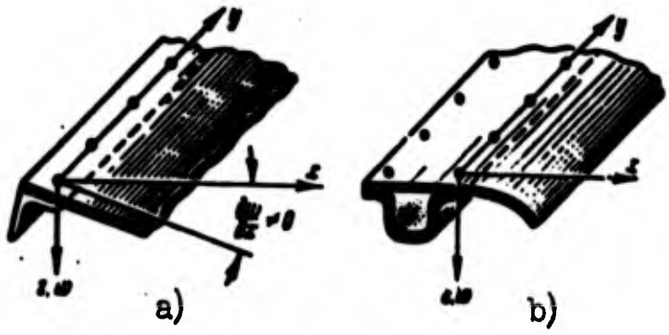

Fig. 7.9. Boundary conditions:
a) hinged fastening, b) clamping.

Second boundary condition takes the form

$$EI\frac{\partial^4 w_1}{\partial x^4}=-D\left[\frac{\partial^3 w}{\partial x^3}+(2-\mu)\frac{\partial^3 w}{\partial x\,\partial y^2}\right]_{x=0}. \tag{7.35}$$

4. Edge x = 0 is free. Then we should have

$$\left.\begin{aligned} M_x&=0,\\ R_x&=0. \end{aligned}\right\} \tag{7.36}$$

or

$$\frac{\partial^2 w}{\partial x^2}+\mu\frac{\partial^2 w}{\partial y^2}=0. \tag{7.37}$$

$$\frac{\partial^2 w}{\partial x^2}+(2-\mu)\frac{\partial^3 w}{\partial x\,\partial y^2}=0. \tag{7.38}$$

We determine <u>work of internal forces</u> on virtual displacement of plate. If curvature $\varkappa_x$ receives increase $\delta\varkappa_x$, then work of moment $M_x dy$ on the length of element dx, will be equal to $(-M_x \delta\varkappa_x dx\,dy)$. Calculating in this way work of remaining forces and integrating with respect to area of plate F = ab, we obtain

$$\delta A=-\int\int_F (M_x\delta\varkappa_x+M_y\delta\varkappa_y+2H\delta\chi)\,dx\,dy.$$

Increase of <u>potential energy</u> is equal to $\delta U = -\delta A$; using expressions for moments and curvatures, we find

$$\delta U=D\int\int_F\left[\left(\frac{\partial^2 w}{\partial x^2}+\mu\frac{\partial^2 w}{\partial y^2}\right)\delta\left(\frac{\partial^2 w}{\partial x^2}\right)+\left(\frac{\partial^2 w}{\partial y^2}+\mu\frac{\partial^2 w}{\partial x^2}\right)\delta\left(\frac{\partial^2 w}{\partial y^2}\right)+\right.$$
$$\left.+2(1-\mu)\frac{\partial^2 w}{\partial x\,\partial y}\delta\left(\frac{\partial^2 w}{\partial x\,\partial y}\right)\right]dx\,dy.$$

or

$$\delta U=\frac{1}{2}D\delta\int\int_F\left\{\left(\frac{\partial^2 w}{\partial x^2}+\frac{\partial^2 w}{\partial y^2}\right)^2-2(1-\mu)\left[\frac{\partial^2 w}{\partial x^2}\frac{\partial^2 w}{\partial y^2}-\left(\frac{\partial^2 w}{\partial x\,\partial y}\right)^2\right]\right\}dx\,dy.$$

Total energy of bending is equal to

$$U=\frac{1}{2}D\int\int_F\left[(\nabla^2 w)^2-(1-\mu)L(w,w)\right]dx\,dy; \tag{7.39}$$

by L(w,w) is understood the expression

$$L(w,w)=2\left[\frac{\partial^2 w}{\partial x^2}\frac{\partial^2 w}{\partial y^2}-\left(\frac{\partial^2 w}{\partial x\,\partial y}\right)^2\right]. \tag{7.40}$$

We calculate, further, <u>work of external forces</u>, accomplished during buckling of the plate. Assume that plate is subjected to action of forces σ_x, σ_y, and τ, applied in middle plane. We designate by u and v displacements of a certain point of the middle plane along axes x and y. We find mutual displacement of the edges of the plate, to which forces σ_x are applied. We select element AB of a fiber, parallel to axis x (Fig. 7.10). Assume that displacement of point A along axes x and z will be u and w, and of point B - $u + \frac{\partial u}{\partial x}dx$ and $w + \frac{\partial w}{\partial x}dx$: new positions of points we designate by A_1 and B_1. Length ds_1 of element after deformation will be

$$ds_1=\left[\left(dx+\frac{\partial u}{\partial x}dx\right)^2+\left(\frac{\partial w}{\partial x}dx\right)^2\right]^{\frac{1}{2}}.$$

or

$$ds_1=dx\left[1+2\frac{\partial u}{\partial x}+\left(\frac{\partial u}{\partial x}\right)^2+\left(\frac{\partial w}{\partial x}\right)^2\right]^{\frac{1}{2}}.$$

Expanding this expression into a series and limiting ourselves to first members of expansion, we obtain

$$ds_1=\left[1+\frac{\partial u}{\partial x}+\frac{1}{2}\left(\frac{\partial u}{\partial x}\right)^2+\frac{1}{2}\left(\frac{\partial w}{\partial x}\right)^2\right]dx.$$

We consider case, when plate is buckled from its own plane; therefore, magnitude $(\frac{\partial u}{\partial x})^2$ can be disregarded as compared to $(\frac{\partial w}{\partial x})^2$. Finally, we find

$$\varepsilon_x=\frac{\partial u}{\partial x}+\frac{1}{2}\left(\frac{\partial w}{\partial x}\right)^2. \tag{7.41}$$

By analogy we write expressions for elongation of the element parallel to axis y:

$$\varepsilon_y=\frac{\partial v}{\partial y}+\frac{1}{2}\left(\frac{\partial w}{\partial y}\right)^2. \tag{7.42}$$

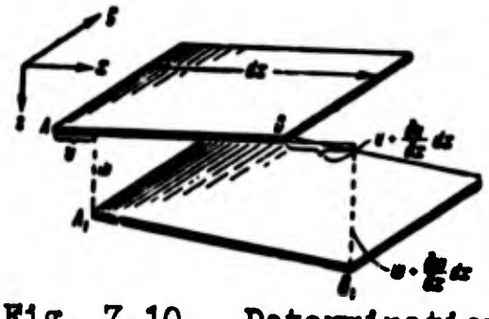

Fig. 7.10. Determination of work of compressive forces during buckling of a plate.

But for hard plates deformations in middle surface ε_x and ε_y must be considered equal to zero. Consequently, we should have

$$\left.\begin{aligned}\frac{\partial u}{\partial x}&=-\frac{1}{2}\left(\frac{\partial w}{\partial x}\right)^2,\\ \frac{\partial v}{\partial y}&=-\frac{1}{2}\left(\frac{\partial w}{\partial y}\right)^2.\end{aligned}\right\} \tag{7.43}$$

Mutual displacement of points, belonging to edges x = 0 and x = a, referred to dimension a, are equal to

$$e_x=-\frac{1}{a}\int_0^a\frac{\partial u}{\partial x}dx=\frac{1}{2a}\int_0^a\left(\frac{\partial w}{\partial x}\right)^2dx; \tag{7.44}$$

magnitude e_x we consider positive during convergence of edges. We shall assume that in process of buckling forces σ_x remain constant. Then their work will be equal to

$$W_1=\sigma_x e_x hb=\frac{1}{2}\int_0^b\sigma_x h\left[\int_0^a\left(\frac{\partial w}{\partial x}\right)^2dx\right]dy; \tag{7.45}$$

magnitude σ_x is left under the integral sign, since, in general, forces σ_x vary along dimension b. Analogously mutual displacement of edges y = 0 and y = b will be

$$e_y = -\frac{1}{b}\int_0^b \frac{\partial v}{\partial y}\,dy = \frac{1}{2b}\int_0^b \left(\frac{\partial w}{\partial y}\right)^2 dy. \tag{7.46}$$

and work of forces σ_y will be

$$W_2 = \frac{1}{2}\int_0^a \sigma_y h\left[\int_0^b \left(\frac{\partial w}{\partial y}\right)^2 dy\right]dx. \tag{7.47}$$

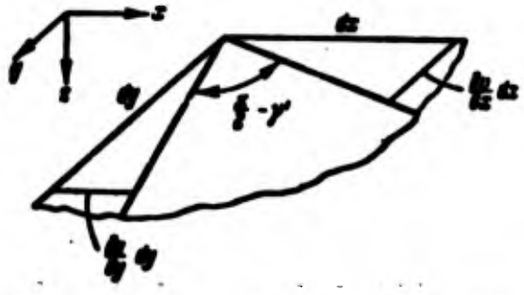

Fig. 7.11. Shear deformation in middle of surface.

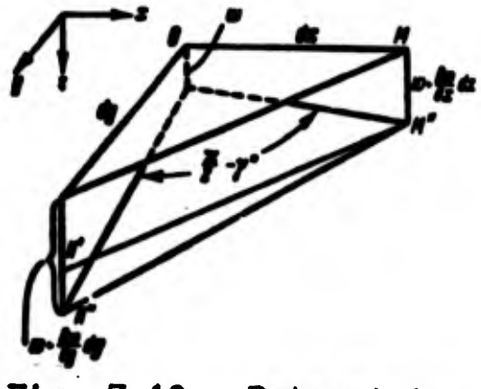

Fig. 7.12. Determining work of shear forces.

We pass to determination of work of <u>tangential</u> forces τh. We find shear deformation γ' of element dx dy, corresponding to displacements u and v. As can be seen from Fig. 7.11, it is equal to

$$\gamma' = \frac{\partial u}{\partial y} + \frac{\partial v}{\partial x}. \tag{a}$$

On Fig. 7.12 is shown, how triangle OMN with sides dx and dy is distorted during shear deformation γ'', caused by displacements w. Examining the figure, we find

$$\overline{M''N''} = \left[(dx)^2 + \left(\frac{\partial w}{\partial x}\,dx\right)^2 + (dy)^2 + \left(\frac{\partial w}{\partial y}\,dy\right)^2 - 2\sqrt{(dx)^2 + \left(\frac{\partial w}{\partial x}\,dx\right)^2}\sqrt{(dy)^2 + \left(\frac{\partial w}{\partial y}\,dy\right)^2}\cos\left(\frac{\pi}{2} - \gamma''\right)\right]^{\frac{1}{2}} \tag{b}$$

or, approximately,

$$\overline{M''N''}=\left\{(dx)^2\left[1+\left(\frac{\partial w}{\partial x}\right)^2\right]+(dy)^2\left[1+\left(\frac{\partial w}{\partial y}\right)^2\right]-2\gamma''\,dx\,dy\right\}^{\frac{1}{2}}. \tag{b'}$$

On the other hand, from examination of triangle N'N"M" we find

$$\overline{M''N''}=\left[(dx)^2+(dy)^2+\left(\frac{\partial w}{\partial y}dy-\frac{\partial w}{\partial x}dx\right)^2\right]^{\frac{1}{2}}. \tag{c}$$

Comparison of expressions (b') and (c) gives

$$\gamma''=\frac{\partial w}{\partial x}\frac{\partial w}{\partial y}. \tag{d}$$

Total shear deformation will be

$$\gamma=\frac{\partial u}{\partial y}+\frac{\partial v}{\partial x}+\frac{\partial w}{\partial x}\frac{\partial w}{\partial y}. \tag{7.48}$$

Considering for hard plates $\gamma = 0$, we find $\gamma' = -\gamma''$, or

$$\gamma'=-\frac{\partial w}{\partial x}\frac{\partial w}{\partial y}. \tag{7.49}$$

We assume that tangential forces τ are <u>constant</u> along plate edges a and b. To them there corresponds "integral" distortion of the plate

$$g=\int_0^a\int_0^b\frac{\partial w}{\partial x}\frac{\partial w}{\partial y}\,dx\,dy. \tag{7.50}$$

Work of forces τh will be

$$W_3=\tau hg=\tau h\int_0^a\int_0^b\frac{\partial w}{\partial x}\frac{\partial w}{\partial y}\,dx\,dy. \tag{7.51}$$

Final expression for work of external forces has form

$$W=\frac{h}{2}\left\{\int_0^b\sigma_x\left[\int_0^a\left(\frac{\partial w}{\partial x}\right)^2dx\right]dy+\right.$$
$$\left.+\int_0^a\sigma_y\left[\int_0^b\left(\frac{\partial w}{\partial y}\right)^2dy\right]dx\right\}+\tau h\int_0^a\int_0^b\frac{\partial w}{\partial x}\frac{\partial w}{\partial y}\,dx\,dy. \tag{7.52}$$

Total energy of system is equal to

$$\Im=U-W. \tag{7.53}$$

We use the expressions for U and W (given above) when solving problems of stability of plates by the energy method.

§ 81. Flexible Plates.

Let us give dependences pertaining to <u>flexible</u> plates; as was already said, we need them during the study of behavior of plates in post critical region. We write expressions for deformations in middle surfaces, which were just now derived:

$$\left.\begin{aligned} \varepsilon_x &= \frac{\partial u}{\partial x} + \frac{1}{2}\left(\frac{\partial w}{\partial x}\right)^2, \\ \varepsilon_y &= \frac{\partial v}{\partial y} + \frac{1}{2}\left(\frac{\partial w}{\partial y}\right)^2, \\ \gamma &= \frac{\partial u}{\partial y} + \frac{\partial v}{\partial x} + \frac{\partial w}{\partial x}\frac{\partial w}{\partial y}. \end{aligned}\right\} \tag{7.54}$$

We consider positive, here, deformations of <u>elongation</u>. Note that right sides of all these expressions contain the same functions u, v, and w; consequently, magnitudes ε_x, ε_y, and γ are not independent. The <u>equation of compatibility or continuity of deformations</u> connecting them has the form

$$\frac{\partial^2 \varepsilon_x}{\partial y^2} + \frac{\partial^2 \varepsilon_y}{\partial x^2} - \frac{\partial^2 \gamma}{\partial x\, \partial y} = \left(\frac{\partial^2 w}{\partial x\, \partial y}\right)^2 - \frac{\partial^2 w}{\partial x^2}\frac{\partial^2 w}{\partial y^2} \tag{7.55}$$

or, if one we use operator L,

$$\frac{\partial^2 \varepsilon_x}{\partial y^2} + \frac{\partial^2 \varepsilon_y}{\partial x^2} - \frac{\partial^2 \gamma}{\partial x\, \partial y} = -\frac{1}{2} L(w, w). \tag{7.56}$$

The validity of relationship (56) is easily proved by direct differentiation. From the physical point of view it signifies that adjacent element of the plate can not be deformed independently, as if isolated, since in this case between them there will appear a void and there will be disturbed the continuity of the material. Deformations ε_x, ε_y, and γ are connected with stresses in the middle surface σ_x, σ_y, and τ by expressions

$$\varepsilon_x = \frac{\sigma_x}{E} - \mu\frac{\sigma_y}{E}, \quad \varepsilon_y = \frac{\sigma_y}{E} - \mu\frac{\sigma_x}{E}, \quad \gamma = \frac{2(1+\mu)}{E}\tau \tag{7.57}$$

or

$$\sigma_x = \frac{E}{1-\mu^2}(\varepsilon_x + \mu\varepsilon_y), \quad \sigma_y = \frac{E}{1-\mu^2}(\varepsilon_y + \mu\varepsilon_x), \quad \tau = \frac{E}{2(1+\mu)}\gamma. \tag{7.58}$$

These stresses must satisfy equations of equilibrium.

In Fig. 7.13 are depicted forces acting on edges dx and dy. Directions of forces shown in the figure are taken as positive. Projecting all forces on axes x and y, we find

$$\left.\begin{aligned}\frac{\partial \sigma_x}{\partial x}+\frac{\partial \tau}{\partial y}=0,\\ \frac{\partial \tau}{\partial x}+\frac{\partial \sigma_y}{\partial y}=0.\end{aligned}\right\} \tag{7.59}$$

Equations (59) will automatically be satisfied if we express σ_x, σ_y, and τ by a function of stresses Φ in the following manner:

$$\sigma_x=\frac{\partial^2\Phi}{\partial y^2},\quad \sigma_y=\frac{\partial^2\Phi}{\partial x^2},\quad \tau=-\frac{\partial^2\Phi}{\partial x\,\partial y}. \tag{7.60}$$

We turn now to equation of equilibrium in projections on axis z. Here element of plate should be considered in deformed state. But this was already done by us earlier. Therefore, we can use equations (23) and (26); we need only to change before σ_x, σ_y, and τ the sign to its opposite, since in deriving these equations we considered directions of forces to be positive. Finally equation (26) takes form

$$\frac{D}{h}\nabla^4 w=\sigma_x\frac{\partial^2 w}{\partial x^2}+\sigma_y\frac{\partial^2 w}{\partial y^2}+ +2\tau\frac{\partial^2 w}{\partial x\,\partial y}. \tag{7.61}$$

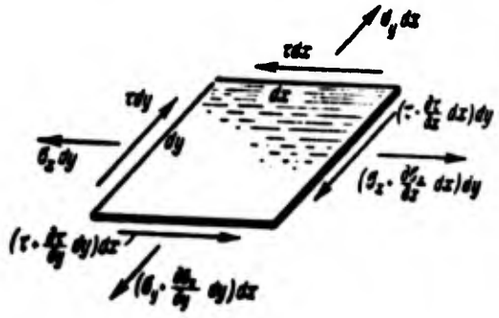

Fig. 7.13. Forces in middle surface of flexible plate.

We express stresses σ_x, σ_y, and τ by function Φ according to (60) and introduce operator $L(w,\Phi)$:

$$L(w,\Phi)=\frac{\partial^2 w}{\partial x^2}\frac{\partial^2\Phi}{\partial y^2}+\frac{\partial^2 w}{\partial y^2}\frac{\partial^2\Phi}{\partial x^2}-2\frac{\partial^2 w}{\partial x\,\partial y}\frac{\partial^2\Phi}{\partial x\,\partial y}; \tag{7.62}$$

then equation of equilibrium (61) will take form

$$\frac{D}{h}\nabla^4 w=L(w,\Phi). \tag{7.63}$$

If, we then place in equation of

compatibility of deformations (56) the expressions (54) for ε_x, ε_y, and γ then it will take form

$$\frac{1}{E}\nabla^4\Phi = -\frac{1}{2}L(w, w). \tag{7.64}$$

Let us note that operators L(w,Φ) from (62) and L(w,w) from (40) have the same structure.

Equations (63) and (64), connecting function Φ of stresses in the middle surface and deflection function w, are basic in theory of flexible plates. When integrating these equations we must satisfy certain boundary conditions. Conditions depending on deflection of plate have the same form as for hard plates. As for conditions pertaining to deformation in middle surface, they are formulated in the following manner.

1. Points of edge x = C freely shift along axes x and y. Then here stresses σ_x and τ:

$$\sigma_x = \frac{\partial^2\Phi}{\partial y^2} = 0, \quad \tau = -\frac{\partial^2\Phi}{\partial x\,\partial y} = 0. \tag{7.65}$$

2. Points of edge x = 0 remain motionless; then for x = 0 we should have

$$u = 0, \quad v = 0.$$

3. Edges of plate remain rectilinear. If we consider that one of the edges, for instance x = 0, is motionless, it turns out that mutual displacement of edges x = 0 and x = a should have a fixed value. Designating by e_x the relative approach of edges,

$$e_x = \frac{1}{a}(u_{x=a} - u_{x=0}).$$

from (54) we obtain

$$\frac{1}{a}\int_0^a \left[\varepsilon_x - \frac{1}{2}\left(\frac{\partial w}{\partial x}\right)^2\right]dx = \text{const} \tag{7.66}$$

or

$$\int_0^a \left[\frac{\partial^2\Phi}{\partial y^2} - \mu\frac{\partial^2\Phi}{\partial x^2} - \frac{E}{2}\left(\frac{\partial w}{\partial x}\right)^2\right]dx = \text{const}. \tag{7.67}$$

As P. F. Papkovich showed,* the condition can be simplified if we consider that bending surface is symmetric with respect to axes of symmetry of the plate, or, in other words, if functions w and Φ have the same values at symmetric points. Then condition (67) changes into the following:

$$\frac{\partial^2\Phi}{\partial x^2}=0 \text{ when } x=a. \tag{7.67a}$$

Potential energy of deformation of a flexible plate consists of two components: flexural energy U_1 and strain energy in middle surface U_2. The first of these quantities is determined as before by formula (26). Energy U_2 is equal to

$$U_2=\frac{1}{2}h\int_F\int(\sigma_x\varepsilon_x+\sigma_y\varepsilon_y+\tau\gamma)\,dx\,dy,$$

or, by formulas (57),

$$U_2=\frac{1}{2}\frac{h}{E}\int_F\int[\sigma_x^2+\sigma_y^2-2\mu\sigma_x\sigma_y+2(1+\mu)\tau^2]\,dx\,dy.$$

Introducing function of stresses Φ, we obtain

$$U_2=\frac{h}{2E}\int_F\int\left\{\left(\frac{\partial^2\Phi}{\partial x^2}+\frac{\partial^2\Phi}{\partial y^2}\right)^2-\right.$$
$$\left.-2(1+\mu)\left[\frac{\partial^2\Phi}{\partial x^2}\frac{\partial^2\Phi}{\partial y^2}-\left(\frac{\partial^2\Phi}{\partial x\,\partial y}\right)^2\right]\right\}dx\,dy. \tag{7.68}$$

or

$$U_2=\frac{h}{2E}\int_F\int[(\nabla^2\Phi)^2-(1+\mu)L(\Phi,\Phi)]\,dx\,dy. \tag{7.69}$$

Let us turn to various particular problems of stability and post critical deformation of plates.**

§ 82. Stability of Plate Supported by Hinge Compressed in One Direction.

Buckling of plates in aircraft and ship structures most frequently is caused by action of compressive forces, located in plane of the

---

*See book [0.7], p. 899.

**Survey of research in this region is given in book of Kollbrunner and Meister [0.19], 1958; from this book are taken some of the graphs given later on.

plate. Since width of a plate which is a panel of an aircraft wing, deck of a vessel, etc., is usually small as compared to dimensions of the structure, then in many cases compressive forces can be considered evenly distributed the width of the plate. Therefore, the problem of stability of plates during uniform compression is that "classical" problem, which attracts to itself the greatest attention; its solution* is the point of departure for formulation and study of other, more complicated problems.

Let us consider first a plate, elongated along axis x($a \gg b$) and compressed along long side by forces σ_x (Fig. 7.14). Let us assume that plate is secured by hinge on long edges; boundary conditions on short edges in this case are nonessential.

Equation (26) obtains form

$$\frac{D}{h}\nabla^4 w + \sigma_x \frac{\partial^2 w}{\partial x^2} = 0. \tag{7.70}$$

Boundary conditions have form

$$\frac{\partial^2 w}{\partial y^2} = 0 \quad \text{when} \quad y = 0, b. \tag{7.71}$$

We write the solution satisfying these conditions in the form

$$w = f \sin \frac{\pi x}{l} \sin \frac{n\pi y}{b}. \tag{7.72}$$

We consider that along short side there form n half-waves. Since for elongated plate it is possible to consider that wave formation is carried out in the direction x freely, then by l we designate length of half-wave in this direction.

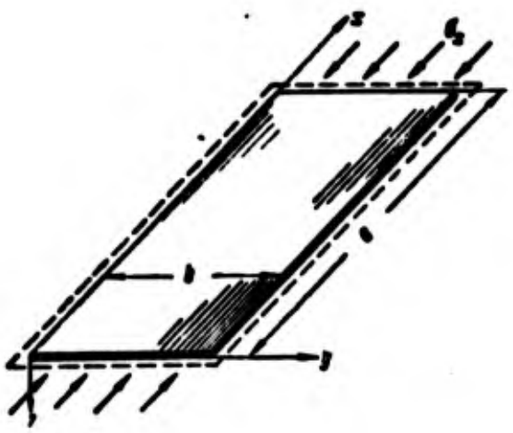

Substituting (72) in (70), we obtain

$$\frac{D\pi^2}{h}\left(\frac{1}{l^2} + \frac{n^2}{b^2}\right)^2 - \sigma_x \frac{1}{l^2} = 0. \tag{7.73}$$

*This problem was first solved by Bryan [7.14] in 1888 by the energy method. Equation of type (70) was composed by Navier already in 1823.

Hence

$$\sigma_x = \left(\frac{b}{l} + \frac{n^2 l}{b}\right)^2 \frac{D\pi^2}{hb^2}. \tag{7.74}$$

In order to find <u>critical stress</u>, it is necessary to set n = 1. Considering, further, stress σ_x as a function of variable l/b and wishing to find the minimum for σ_x, we equate the derivative to zero:

$$\frac{d\sigma}{d\left(\frac{l}{b}\right)} = 0. \tag{7.75}$$

From this we find

$$l = b. \tag{7.76}$$

Thus, bending surface of elongated plate consists, in the given case, of <u>square</u> sections of dimensions b x b; within each section in directions x and y there will form one half-wave of a sine wave. For adjacent sections convexity of the sine-wave is directed in the opposite direction, as shown in Fig. 7.15.

Putting (76) in (74), we find critical stress equal to

$$\sigma_{kp} = 4\frac{\pi^2 D}{b^2 h} \tag{7.77}$$

or

$$\sigma_{kp} = \frac{\pi^2}{3(1-\mu^2)} E\left(\frac{h}{b}\right)^2. \tag{7.78}$$

Taking $\mu \approx 0.3$, we obtain

$$\sigma_{kp} \approx 3.6E\left(\frac{h}{b}\right)^2. \tag{7.79}$$

This formula is valid only when critical stress lies within elastic limit.

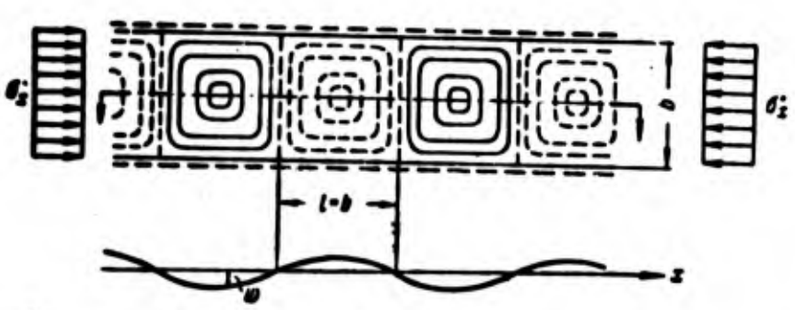

Fig. 7.15. Wave formation of elongated hinge-supported plate.

We assume, further, that <u>sides of the plate are comparable in size</u>. Taking previous boundary conditions (71), we select solution of equation (70) in the form

$$w = f \sin \frac{m\pi x}{l} \sin \frac{n\pi y}{b}, \tag{7.80}$$

where m, n is number of half-waves in directions x and y. After substituting this expression in (70), we have

$$\sigma_x = \frac{D\pi^2}{\delta b^2}\left(\frac{mb}{a} + \frac{n^2 a}{mb}\right)^2. \tag{7.81}$$

Here we must set n = 1. Considering that m is sufficiently great, we find that the minimum of expression (81) is at

$$m = \frac{a}{b}. \tag{7.82}$$

Putting (82) in (81), we find that critical stress, as before, is determined by expressions (77) – (79). This result is easily anticipated: we, as it were, cut off from elongated plate (according to Fig. 7.15) as many squares as times that the width of the plate fits into the length.

Expressions (77) – (79) are exact when ratio a/b is an integer. If, however, the number is not an integer, then we must, as before, take n = 1, and from the two nearest values of m take that which gives expression (81) the least magnitude. Transition from m to m + 1 half-waves will take place when

$$\frac{\left(\frac{m^2}{a^2} + \frac{1}{b^2}\right)^2}{\frac{m^2}{a^2}} = \frac{\left[\frac{(m+1)^2}{a^2} + \frac{1}{b^2}\right]^2}{\frac{(m+1)^2}{a^2}},$$

hence

$$\frac{a}{b} = \sqrt{m(m+1)}. \tag{7.83}$$

For instance, when $a/b < \sqrt{2}$ we have m = 1, and when $a/b > \sqrt{2}$, m = 2. When $a/b = \sqrt{2}$ equally possible is formation of one and two half-waves.

We introduce designation

$$K = \left(\frac{mb}{a} + \frac{a}{mb}\right)^2. \tag{7.84}$$

Then expression for critical stress can be presented in the form

$$\sigma_{кр} = K\frac{\pi^2 D}{b^2 h}. \qquad (7.85)$$

In Table 7.1 and the graph given in Fig. 7.16 are values of K, calculated by formula (84).

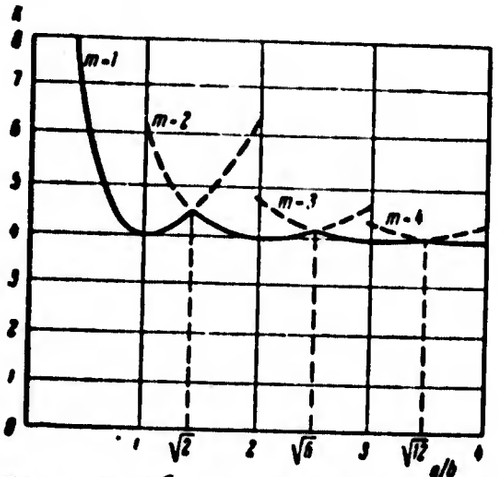

Fig. 7.16. Coefficient K for various numbers of half-waves.

If plate width b is great as compared to length a, we must take m = n = 1; formula (85) is more conveniently given the form

$$\sigma_{кр} = K_1\frac{\pi^2 D}{a^2 h}, \qquad (7.86)$$

where

$$K_1 = 1 + \left(\frac{a}{b}\right)^2. \qquad (7.87)$$

With sufficiently large value of b/a it is possible to ignore second member in expression (87), or, in other words, consider longitudinal edges free. Then we obtain $K_1 = 1$; expression (86) will have form

$$\sigma_{кр} = \frac{\pi^2 D}{a^2 h} = \frac{\pi^2 E h^2}{3(1-\mu^2)a^2}. \qquad (7.88)$$

Plate here turns into a bar of rectangular section 1 x h, hinge-supported on its ends; expression (88) differs from ordinary Euler's formula only by the fact that modulus is replaced by "reduced" modulus $E(1 - \mu^2)$.

Table 7.1. Values of Coefficients K for a Plate Fastened by Hinge on all Edges.

$\frac{a}{b}$	0,2	0,3	0,4	0,5	0,6	0,7	0,8	0,9
K	27,0	13,2	8,41	6,25	5,14	4,53	4,20	4,04
$\frac{a}{b}$	1,0	1,1	1,2	1,3	1,4	1,5	1,6	1,7
K	4,00	4,04	4,13	4,28	4,47	4,34	4,20	4,06
$\frac{a}{b}$	1,8	1,9	from 2 to ∞					
K	4,05	4,01	~4,00					

§ 83. Case of Clamped Longitudinal Edges.

Let us turn to case where loaded edges of the plate are secured by hinge, and unloaded ones are rigidly clamped. By the example of this practically important problem we will meet method of solution which is frequently applied in theory of stability of plates. Place axes of coordinates as in Fig. 7.14. We present integral of equation (70) in the form

$$w = Y(y)\sin\frac{m\pi x}{a}, \tag{7.89}$$

where Y(y) is the searched for function depending only on y. Obviously, expression (89) satisfies boundary conditions for edges x = 0 and x = a. Putting (89) in (70) and cancelling $\sin(m\pi x/a)$, we obtain

$$\frac{d^4Y}{dy^4} - 2\left(\frac{m\pi}{a}\right)^2\frac{d^2Y}{dy^2} + \left[\left(\frac{m\pi}{a}\right)^2 - \frac{\sigma_x h}{D}\right]\left(\frac{m\pi}{a}\right)^2 Y = 0. \tag{7.90}$$

From equation (70) in partial derivatives we shifted, thus, to an ordinary differential equation for function Y; this is the basic step. Integration of equation (90) in this case does not present difficulties; in more complicated problems it may be carried out by various methods of approximation, for instance, the Bubnov-Galerkin method.

Turning to equation (90), we introduce designation

$$\frac{m\pi}{a}=\lambda \tag{7.91}$$

and compose the characteristic equation

$$k^4-2\lambda^2k^2+\left(\lambda^2-\frac{\sigma_x h}{D}\right)\lambda^2=0; \tag{7.92}$$

its roots will be

$$k_{1,2}=\sqrt{\lambda\left(\lambda+\sqrt{\frac{\sigma_x h}{D}}\right)},\quad k_{3,4}=\sqrt{\lambda\left(\lambda-\sqrt{\frac{\sigma_x h}{D}}\right)}. \tag{7.93}$$

As we saw, in limiting case of plate with free longitudinal sides critical stress is determined by formula (88); with fastening of longitudinal sides we should have

$$\sigma_x>\lambda^2D/h. \tag{7.94}$$

Consequently, roots k_3 are <u>imaginary</u>. Considering

$$\alpha=\sqrt{\lambda\left(\lambda+\sqrt{\frac{\sigma_x h}{D}}\right)},\quad \beta=\sqrt{\lambda\left(\sqrt{\frac{\sigma_x h}{D}}-\lambda\right)}. \tag{7.95}$$

we get integral of equation (90) in the form

$$Y(y)=C_1\operatorname{ch}\alpha y+C_2\operatorname{sh}\alpha y+C_3\cos\beta y+C_4\sin\beta y. \tag{7.96}$$

Boundary conditions have form

$$Y=0,\quad \frac{dY}{dy}=0 \quad \text{when} \quad y=0,\quad y=b. \tag{7.97}$$

Using these conditions, we find

$$C_1+C_3=0,\quad \alpha C_2+\beta C_4=0 \tag{7.98}$$

and, further,

$$C_1(\operatorname{ch}\alpha b-\cos\beta b)+C_2\left(\operatorname{sh}\alpha b-\frac{\alpha}{\beta}\sin\beta b\right)=0; \tag{7.99}$$

$$C_1\left(\operatorname{sh}\alpha b+\frac{\beta}{\alpha}\sin\beta b\right)+C_2(\operatorname{ch}\alpha b-\cos\beta b)=0. \tag{7.100}$$

System of equations (99) and (100) has solutions, different from zero, on the condition that

$$\begin{vmatrix} \operatorname{ch}\alpha b-\cos\beta b & \operatorname{sh}\alpha b-\frac{\alpha}{\beta}\sin\beta b \\ \operatorname{sh}\alpha b+\frac{\beta}{\alpha}\sin\beta b & \operatorname{ch}\alpha b-\cos\beta b \end{vmatrix}=0; \tag{7.101}$$

from this we obtain

$$(\operatorname{ch}\alpha b-\cos\beta b)^2-\left(\operatorname{sh}\alpha b+\frac{\beta}{\alpha}\sin\beta b\right)\left(\operatorname{sh}\alpha b-\frac{\alpha}{\beta}\sin\beta b\right)=0. \tag{7.102}$$

From (95) we have

$$\alpha^2+\beta^2=2\lambda\sqrt{\frac{\sigma_x h}{D}},\quad \alpha^2-\beta^2=2\lambda^2. \tag{7.103}$$

Using equations (102) and (103), we determine critical stress.

Problem is simplified if we take into account the symmetry of elastic surface of plate with respect to axis x'(Fig. 7.17). Expression (96) will be rewritten in the form

$$Y(y) = A\operatorname{ch}\alpha y + C\cos\beta y. \tag{7.104}$$

Boundary conditions will be

$$Y = 0, \quad \frac{dY}{dy} = 0 \quad \text{when} \quad y = \frac{b}{2}. \tag{7.105}$$

Instead of equations (100) we obtain the following ones:

$$\left.\begin{aligned} A\operatorname{ch}\frac{\alpha b}{2} + C\cos\frac{\beta b}{2} &= 0, \\ A\alpha\operatorname{sh}\frac{\alpha b}{2} - C\beta\sin\frac{\beta b}{2} &= 0. \end{aligned}\right\} \tag{7.106}$$

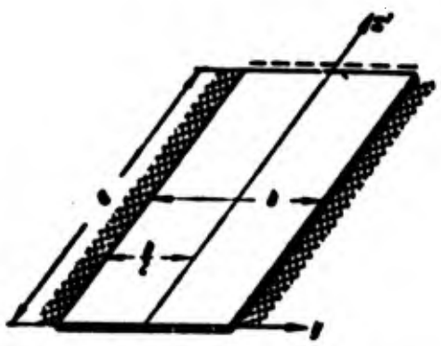

Fig. 7.17. Plate with clamped longitudinal edges.

Equating to zero the determinant of system (106), we find

$$\alpha\operatorname{th}\frac{\alpha b}{2} + \beta\operatorname{tg}\frac{\beta b}{2} = 0. \tag{7.107}$$

Following Hartmann [0.18], we introduce designations

$$\xi = \frac{\alpha b}{2}, \quad \eta = \frac{\beta b}{2}. \tag{7.108}$$

Then instead of (107), we have

$$-\xi\operatorname{th}\xi = \eta\operatorname{tg}\eta. \tag{7.109}$$

Equation (103) has form

$$\sigma_x = \frac{D}{h}\frac{4}{\pi^2 b^2}\left(\frac{a}{mb}\right)^2(\xi^2+\eta^2)^2. \tag{7.110}$$

$$\xi^2 - \eta^2 = \frac{1}{2}\left(\frac{mb\pi}{a}\right)^2. \tag{7.111}$$

We determine magnitudes ξ and η from equations (109) and (111) and by (110) we find critical value of σ_x. In Fig. 7.18 along the axis of abscissas are placed values of ξ, and on axis of ordinates η. Curves $\eta(\xi)$ from equation (109) cross axis of ordinates at points $\eta = \pi, 2\pi, 3\pi, \ldots$, and are located one above the other. Magnitude σ_x from (110) is proportional to $(\xi^2 + \eta^2)^2$, consequently, we must select a curve having the least ordinates; it is depicted in Fig. 7.18

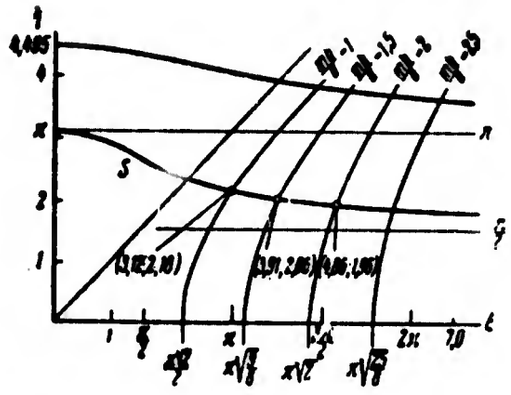

Fig. 7.18. Determining critical stress in case of clamped edges.

and is designated by S. Here too are given hyperbolic curves corresponding to equation (111) for different values mb/a. Points of intersection of these curves with line S determine the sought magnitudes of ξ and η; they are given in parentheses. We present critical stress by formula (85); coefficient K will be equal to

$$K = \frac{4}{\pi^4}\left(\frac{a}{mb}\right)^2(\xi^2+\eta^2)^2. \qquad (7.112)$$

For a/mb = 1 we obtain K = 8.67; for a/mb = 0.67, K = 7.00; for a/mb = = 0.5, K = 7.80. More detailed study shows that stress is the least when a/mb = 0.662, where K = 6.97.

Table 7.2. Values of Coefficient K in Case of Hinged Support of Loaded Edges and Clamping of Unloaded Edges.

a/b	0,4	0,5	0,6	0,7	0,8	0,9	1,0
K	9,44	7,69	7,05	7,00	7,29	7,83	7,69

In Table 7.2 are given values of K for different ratios a/b. In case a >> b bending surface of plate consists of hollows, length of which l = a/m constitutes approximately 2/3 the width b (Fig. 7.19).

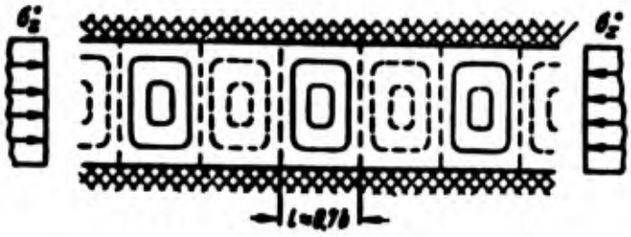

Fig. 7.19. Wave formation of elongated plate, clamped on long edges.

We apply for solution of this problem the Ritz method. Boundary conditions of problem are satisfied if we select expression, for deflection in the form

$$w = f \sin \frac{m\pi x}{a} \sin^2 \frac{\pi y}{b}. \tag{7.113}$$

We compose expression for potential energy of flexure by the formula (39):

$$U = \frac{\pi^4}{32} Df^2 \left(\frac{3m^4 b}{a^3} + \frac{8m^2}{ab} + \frac{16a}{b^3} \right). \tag{7.114}$$

Work of external forces is equal, by (45), to

$$W = \frac{1}{2} \sigma_x h \int_0^a \int_0^b \left(\frac{\partial w}{\partial x} \right)^2 dx\, dy. \tag{7.115}$$

or

$$W = \frac{3}{64} \sigma_x h f^2 m^2 \pi^2 \frac{b}{a}. \tag{7.116}$$

Equating expressions (114) and (116), we find

$$\sigma_x = \frac{\pi^2 D}{b^2 h} \left(\frac{1}{\lambda^2} + \frac{8}{3} + \frac{16}{3} \lambda^2 \right). \tag{7.117}$$

where $\lambda = a/mb$. If we consider $a \gg b$, then we find minimum value of σ_x from condition

$$\frac{d\sigma_x}{d\lambda} = 0, \tag{7.118}$$

whence

$$\lambda^2 = \frac{\sqrt{3}}{4}, \quad \lambda = 0{,}658 \tag{7.119}$$

and

$$\sigma_{кр} = 7{,}3 \frac{\pi^2 D}{b^2 h}. \tag{7.120}$$

Let us note that value of λ was close to that found above (0.662); value of critical stress was higher by exactly 4%.

We considered case when longitudinal edges of plate do not turn. Critical stress as compared to case of hinges support here significantly increases: the minimum value of $\sigma_{кр}$ increases 7/4 times. This circumstance must be considered during designing. It is possible to satisfy conditions of total clamping, as already was said, by fastening the plate by a two-row rivet seam.

At the same time reinforcing ribs must have sufficient torsional rigidity: their section, jointly with section of the adjacent section of sheeting, should have a closed profile, as shown in Fig. 7.9b.

If it is necessary to make a definitized calculation taking into account actual torsional rigidity of ribs, then it is necessary to turn to the problem of stability of a plate with elastically clamped longitudinal edges.* Results of solution of this problem are shown in Fig. 7.20. Each series of curves pertains to a definite value of coefficient α, equal to $\alpha = \frac{bD}{GI_к}$,

where b is the width of the plate, $GI_к$ is torsional rigidity of longitudinal ribs. When $\alpha = \infty$ and $\alpha = 0$ we obtain limiting cases, correspondingly, of hinged support and rigid clamping.

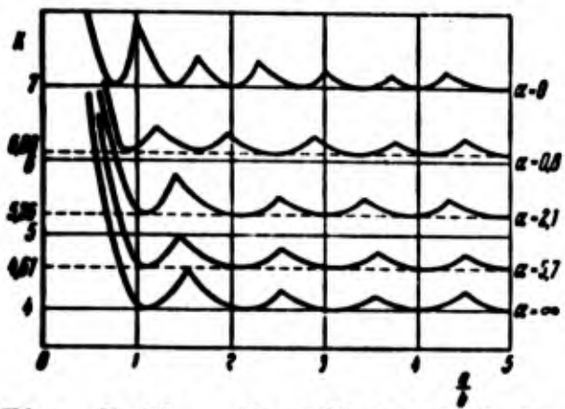

Fig. 7.20. Coefficient K for plate with elastically clamped edges.

*This problem was investigated by E. Lundquist and E. Stowell in [NACA Rep. No. 733, 1942].

Example 7.1. Determine critical stress and form of buckling for panel of skin of upper part of an aircraft wing, fastened in hinged manner with rigid ribs and compressed along lone sides* (Fig. 7.21a). Dimensions of panel: a = 200 mm, b = 120 mm, h = 2 mm. How will magnitude of critical stress change, if we consider that plate is clamped on longitudinal edges, and consider torsional rigidity of the ribs? Ribs are prepared from pressed angle sections (Fig. 7.21b). Material of skin and ribs is duralumin; $E = 0.72 \cdot 10^6$ kg/cm^2, $\mu = 0.34$.

Cylindrical rigidity of the plate is equal to

$$D = \frac{0{,}72 \cdot 10^6 \cdot 0{,}2^3}{12(1-0{,}34^2)} =$$

ratio of sides a/b = 1.67. $= 545$ kg·cm;

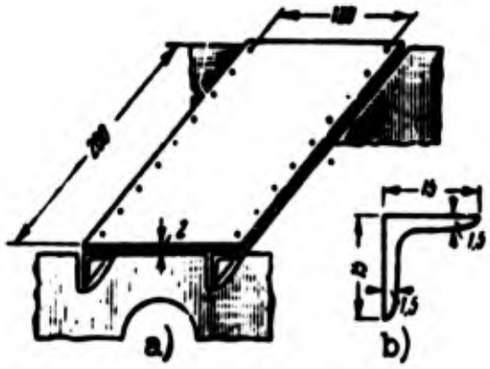

Fig. 7.21. Panel of aircraft wing.

For case of hinged fastening from the table 7.1 we have K ≈ 4.12. Critical stress will be

$$\sigma_{cr} = K\frac{\pi^2 D}{b^2 h} = 4{,}12\frac{\pi^2 \cdot 545}{12^2 \cdot 0{,}2} = 775 \text{ kg/cm}^2.$$

Turning to second case, we calculate torsional rigidity of a rib:

$$GI_k \approx \frac{E}{2(1+\mu)}\frac{1}{3}\sum sh^3 = \frac{0{,}72 \cdot 10^6}{2(1+0{,}34)}\frac{2}{3}1{,}5 \cdot 0{,}2^3 = 0{,}27 \cdot 10^6 \cdot 0{,}008.$$

Coefficient α is equal to

$$\alpha = \frac{bD}{GI_k} = \frac{12 \cdot 545}{0{,}27 \cdot 10^6 \cdot 0{,}008} = 2{,}9.$$

---

*Examples 7.1 – 7.3 were composed by Yu. P. Grigor'yev.

From graph of Fig. 7.20 we find

$$K = 5.2, \quad \sigma_{кр} = 5.2 \cdot \frac{\pi^2 \cdot 545}{12^2 \cdot 0.2} = 970 \text{ кг/см}^2.$$

Thus, with elastic clamping on longitudinal edges critical stress will be increased by 25%.

§ 84. Plate with Free Edge. Summary of Calculating Data

Let us consider combinations of boundary conditions, when one of the edges of the plate is free.

1. Loaded edges fixed by hinge; one of unloaded edges is fixed by hinge, and the second is free. Such boundary conditions take place, for instance, for each of the flanges of an equilateral angle, compressed along its axis (Fig. 7.22a). For longitudinal edges the relationships of paragraphs 1 and 4 of Section 80 take form

$$w = 0, \quad \frac{\partial^2 w}{\partial y^2} + \mu \frac{\partial^2 w}{\partial x^2} = 0 \quad \text{when } y = 0. \tag{7.121}$$

$$\frac{\partial^2 w}{\partial y^2} + \mu \frac{\partial^2 w}{\partial x^2} = 0, \quad \frac{\partial^3 w}{\partial y^3} + (2 - \mu) \frac{\partial^3 w}{\partial x^2 \partial y} = 0 \quad \text{when } y = b. \tag{7.122}$$

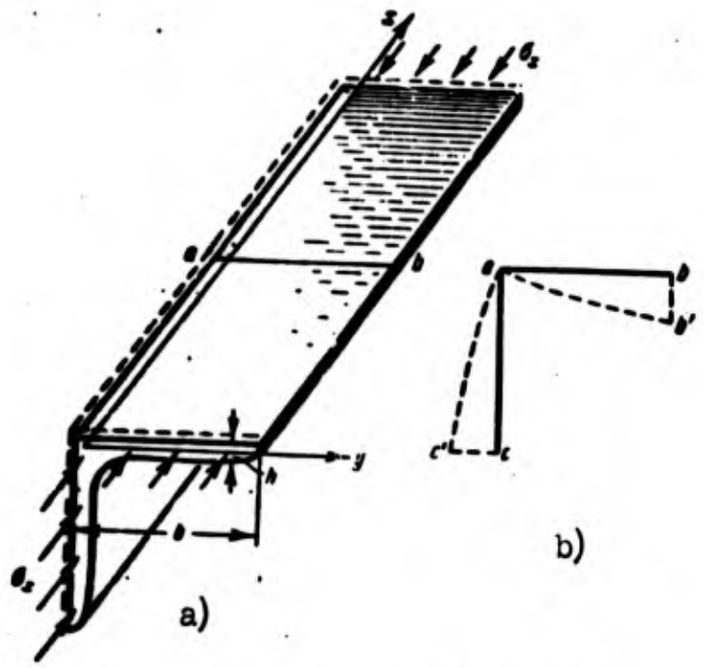

Fig. 7.22. Buckling of a plate, one of whose sides is free.

Presenting w, as before, in form (89), we find for Y expression (96). Conditions (121) give

$$C_1+C_3=0. \tag{7.123}$$

$$C_1\alpha^2-C_3\beta^2-\mu\frac{m^2\pi^2}{a^2}(C_1+C_3)=0. \tag{7.124}$$

whence $C_1 = C_3 = 0$. From conditions (122), then, we obtain

$$\left.\begin{aligned} C_2\left(\alpha^2-\mu\frac{m^2\pi^2}{a^2}\right)\operatorname{sh}\alpha b-C_4\left(\alpha^2+\mu\frac{m^2\pi^2}{a^2}\right)\sin\beta b=0,\\ C_2\alpha\left[\alpha^2-(2-\mu)\frac{m^2\pi^2}{a^2}\right]\operatorname{ch}\alpha b-C_4\beta\left[\beta^2+(2-\mu)\frac{m^2\pi^2}{a^2}\right]\cos\beta b=0.\end{aligned}\right\} \tag{7.125}$$

Equating to zero the determinant of this system, we arrive at equation

$$\frac{\beta^2-\mu\frac{m^2\pi^2}{a^2}}{\beta^2+\mu\frac{m^2\pi^2}{a^2}}=\frac{\alpha\operatorname{tg}\beta b}{\beta\operatorname{th}\alpha b}. \tag{7.126}$$

Study of this equation shows that for any values a/b the least value of σ_x corresponds to m = 1, so that in longitudinal direction there always forms only one half-wave (Fig. 7.22b). Values of coefficient K in final expression (85) are given in Table 7.3 (for μ = = 0.25).

Table 7.3. Values of Coefficient K When One of Unloaded Edges is Secured by Hinge, and Other is Free.

a/b	0,6	0,8	1,0	1,2	1,4	1,6	1,8	2,0	3,0	∞
K	3,65	2,15	1,44	1,14	0,95	0,84	0,76	0,70	0,56	0,456

Let us turn to the energy method. We present w in the form

$$w=fy\sin\frac{m\pi x}{a}, \tag{7.127}$$

Considering each section, x = const, of the middle surface a straight line. Flexural energy U is equal to [See formulas (39) – (45)]

$$U=\frac{D}{2}f^2\frac{m^2\pi^2}{a^2}\left[\frac{m^2\pi^2}{6a^2}+(1-\mu)\right]ab. \tag{7.128}$$

work of external forces is

$$W = \frac{\sigma_x h}{2} f^2 \frac{m^2\pi^2}{a^2} \frac{ab^3}{6}. \tag{7.129}$$

Equating these expressions, we find

$$\sigma_x = \frac{D}{b^2 h}\left[m^2\pi^2 \frac{b^2}{a^2} + 6(1-\mu)\right]. \tag{7.130}$$

Obviously, here we must take m = 1. For $\mu = 0.3$ coefficient K turns out to be equal to

$$K = 1.03\left(\frac{b}{a}\right)^2 + 0.427. \tag{7.131}$$

This formula gives values of K very close to those in Table 7.3.

2. <u>One of the unloaded edges is clamped, the other is free</u>. In this case conditions (121) take the form

$$w = 0, \quad \frac{\partial w}{\partial y} = 0 \text{ when } y = 0, \tag{7.132}$$

conditions (122) remain as before. From (132) there follows

$$C_3 = -C_1, \quad C_4 = -\frac{\alpha}{\beta} C_2. \tag{7.133}$$

From (122) we find

$$\begin{aligned} &C_1\alpha^2 \operatorname{ch}\alpha b + C_2\alpha^2 \operatorname{sh}\alpha b + C_1\beta^2 \cos\beta b + C_2\alpha\beta \sin\beta b - \\ &-\mu\frac{m^2\pi^2}{a^2}\left(C_1 \operatorname{ch}\alpha b + C_2 \operatorname{sh}\alpha b - C_1\cos\beta b - \frac{\alpha}{\beta} C_2 \sin\beta b\right) = 0, \end{aligned} \tag{7.134}$$

$$\begin{aligned} &C_1\alpha^3 \operatorname{sh}\alpha b + C_2\alpha^3 \operatorname{ch}\alpha b - C_1\beta^3 \sin\beta b + C_2\alpha\beta^2 \cos\beta b + \\ &+(2-\mu)\frac{m^2\pi^2}{a^2}(C_1\alpha \operatorname{sh}\alpha b - C_2\alpha \operatorname{ch}\alpha b + \\ &+C_1\beta \sin\beta b - C_2\alpha\cos\beta b) = 0. \end{aligned} \tag{7.135}$$

Equating the determinant of this system to zero, we obtain the equation

$$2\gamma\delta + (\gamma^2 + \delta^2)\operatorname{ch}\alpha b \cos\beta b = \frac{\alpha^2\gamma^2 - \beta^2\delta^2}{\alpha\beta} \operatorname{sh}\alpha b \sin\beta b, \tag{7.136}$$

where

$$\left.\begin{aligned} \gamma &= \alpha^2 - (2-\mu)\frac{m^2\pi^2}{a^2}, \\ \delta &= \beta^2 + (2-\mu)\frac{m^2\pi^2}{a^2}. \end{aligned}\right\} \tag{7.137}$$

Analysis of equation (136) shows that when a >> b the deflection surface is divided into half-waves of length 1.64b. Values of coefficient K for different ratios a/b are given in Table 7.4($\mu = 0.25$).

Table 7.4. Values of Coefficient K When One of Unloaded Edges is Clamped and Other is Free.

a/b	0,8	1,0	1,2	1,4	1,6	1,8	2,0	3,0	∞
K	2,70	1,70	1,47	1,36	1,33	1,34	1,38	1,36	1,33

Solution of this problem by energy method is possible, considering

$$w = f \sin\frac{\pi x}{a} \sin^2\frac{\pi y}{2b}. \qquad (7.138)$$

Expression for K takes the form

$$K = 1{,}04\left(\frac{mb}{a}\right)^2 + 0{,}139\left(\frac{a}{mb}\right)^2 + 0{,}684. \qquad (7.139)$$

When a >> b minimum value of K corresponds to a/mb = 1.64 and is equal to K = 1.43. Error compared to exact solution constitutes about 8%.

In Fig. 7.23 are given values of K depending on ratio a/b for cases discussed above, and also for those cases when loaded edges are clamped, and unloaded ones are secured by hinge or are clamped.*

We give also a summary of values of minimum critical stresses; along with quantities K in Table 7.5 are placed values of coefficient k in a formula convenient for practical calculations:

$$\sigma_{cr} = k\left(\frac{100\delta}{b}\right)^2. \qquad (7.140)$$

in application to steel (we take $E = 2.1 \cdot 10^6$ kg/cm^2, $\mu = 0.3$) and duralumin ($E = 0.7 \cdot 10^6$ kg/cm^2, $\mu = 0.3$).

*Certain divergences in values of K shown in Table 7.5 and previous tables and graphs is explained by variation in magnitudes μ and by the fact that the problems were solved in various approximations.

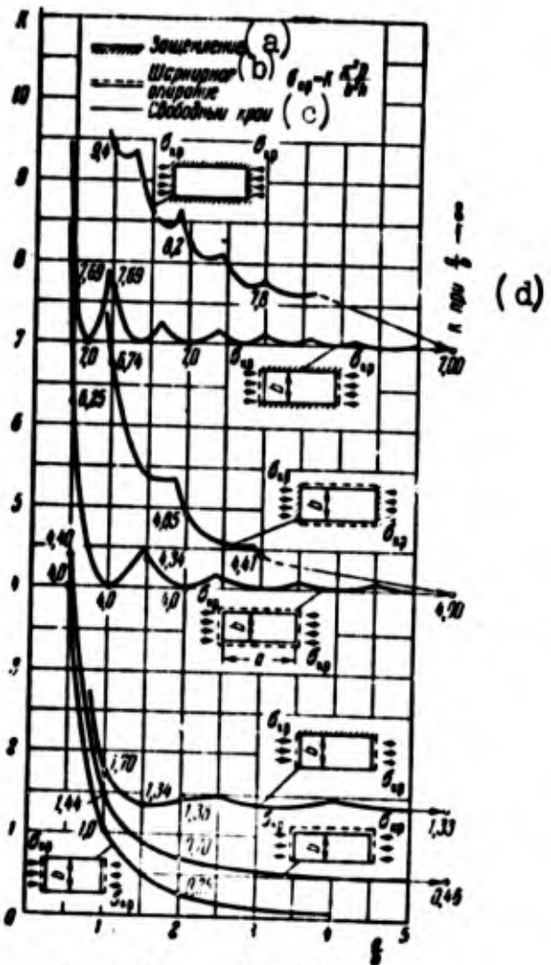

Fig. 7.23. Coefficient K for different conditions of fastening of plate, compressed in one direction.
KEY: (a) Clamping; (b) Hinged joint; (c) Free edge; (d) When.

Table 7.5. Minimum Critical Stresses During Compression in One Direction.

Boundary conditions for unloaded edges	K $\mu = 0.3$	k in kg/cm²	
		Steel	Duralumin
Hinged support	4.00	760	253
Clamping	6.97	1320	440
One of edges is supported by hinges, the other is free	0.425	80.5	26.8
One is clamped, the other is free	1.28	243	80.8

§ 85. Stability of Plates Under Shearing Strain.

The second classical problem of theory of stability of plates pertains to case of shearing strain (Fig. 7.24). In such a state of strain is the panel of a box-like (caisson) structure, transmitting a torque. Another example is thin webs of beams, receiving transverse force, on the condition that normal stresses in the web can be ignored.

Determination of critical forces for a plate during shearing strain is a more difficult problem than in the case of uniform compression, since dents, forming upon loss of stability, have unique form, greatly varying depending upon ratio of sides of the plate.

We consider here, first of all, case of an elongated plate ($a \gg b$) supported by hinge on long edges and give approximate solution of the problem. Experiments show [7.22] that during buckling of such a plate there form shallow folds, close to rectilinear. Therefore, the deflection surface can be presented by the expression

$$w = f \sin \frac{\pi y}{b} \sin \frac{\pi}{l}(x - ky). \tag{7.141}$$

Deflection here turns into zero on longitudinal edges of plate and, furthermore, on "nodal" lines $y = kx$, whose slope is characterized by parameter k; magnitude l represents here distance between nodal lines.

Potential energy, according to (39), turns out to be equal to

$$U = D\frac{\pi^4}{4lb}\left[\left(\frac{l}{b}\right)^2 + 6k^2 + 2 + \left(\frac{b}{l}\right)^2(1+k^2)^2\right]f^2; \tag{7.142}$$

work of external forces, according to (15), will be

$$W = \tau\frac{\pi^2 kb}{4}kf^2. \tag{7.143}$$

Equating these quantities, we find

$$\tau = \frac{\pi^2 D}{2kb^2k}\left[6k^2 + 2 + \left(\frac{l}{b}\right)^2 + \left(\frac{b}{l}\right)^2(1+k^2)^2\right]. \tag{7.144}$$

We determine parameters k and l from the conditions that τ takes the least value when

$$\frac{\partial \tau}{\partial k}=0, \quad \frac{\partial \tau}{\partial l}=0; \tag{7.145}$$

from this

$$k=\frac{1}{\sqrt{2}}, \quad l=1{,}22b. \tag{7.146}$$

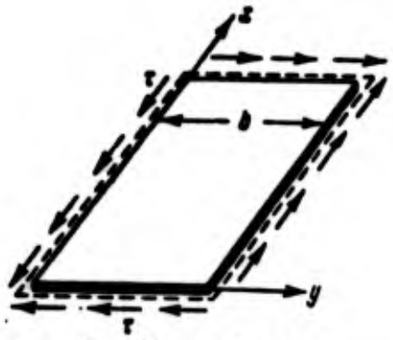

Fig. 7.24. Plate subjected to shearing strain.

Thus, angle of inclination of nodal lines to axis is equal, approximately, to 35°. Putting (146) in expression (144), we determine coefficient K in the formula

$$\tau_{кр}=K\frac{\pi^2 D}{b^2 h}; \tag{7.147}$$

it turns out equal to $K = 4\sqrt{2} = 5.64$. Solution of the problem in closed form* leads to exact value K = 5.34; thus, error of approximate solution is about 6%. The form of the horizontal of the deflection surface and bending lines in sections normal to axis x, corresponding to exact solution, is shown in Fig. 7.25; the distance between "nodal" lines is $l = 1.25b$.

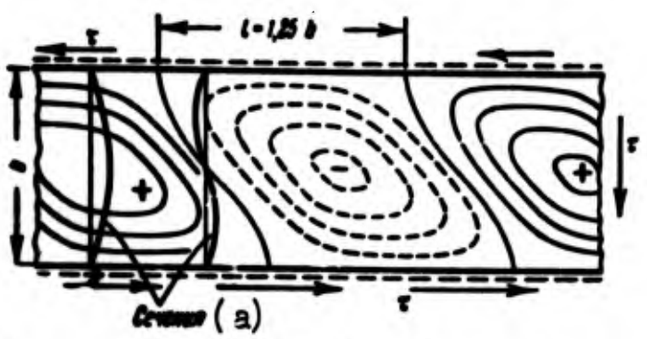

Fig. 7.25. Wave formation of elongated plate with hinge-supported edges under shearing strain.
KEY: (a) Cross-sections.

*It was obtained by Southwell and Skan in Proc. Roy. Soc. London, Ser. A 105 (1924), 582.

In case of a plate rigidly clamped on long edges of a plate coefficient K reaches magnitudes of 8.98; thus, effect of "rigid fixing" of edges turns out to be approximately the same as during compression. Deflection surface for this case is depicted in Fig. 7.26; nodal lines here also grow closer, and distance between them is lowered to $l = 0.8b$.

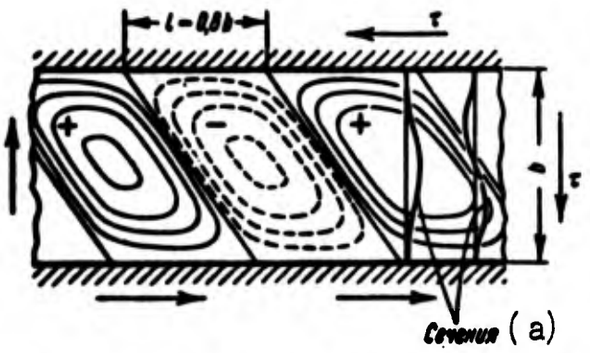

Fig. 7.26. Wave formation of an elongated plate with clamped edges under shearing strain.
KEY: (a) Cross-sections.

Let us turn to problem of buckling of a plate with a finite ratio of sides; its solution turned out to be especially complicated. We use the Ritz method, approximating the expression for deflection by the series

$$w = \sum_{m=1}^{\infty}\sum_{n=1}^{\infty} A_{mn} \sin\frac{m\pi x}{a} \sin\frac{n\pi y}{b}. \qquad (7.148)$$

We calculate energy of bending from (39), taking into account the relationships

$$\int_0^a \sin\frac{m\pi x}{a} \sin\frac{l\pi x}{a}\,dx = \begin{cases} \frac{a}{2} & \text{when } m = l, \\ 0 & \text{when } m \neq l; \end{cases} \qquad (7.149)$$

then we obtain

$$U = \frac{D}{2}\pi^4 \frac{ab}{4} \sum_m \sum_n A_{mn}^2 \left(\frac{m^2}{a^2} + \frac{n^2}{b^2}\right)^2. \qquad (7.150)$$

Further we determine work of external forces by (51); taking into account the relationships

$$\int_0^a \sin\frac{l\pi x}{a} \cos\frac{m\pi x}{a}\,dx\,dy = \begin{cases} \frac{2a}{\pi}\frac{l}{l^2-m^2} & \text{for odd sum } l+m, \\ 0 & \text{for even sum } +m. \end{cases} \qquad (7.151)$$

we get

$$W = 4\tau h \sum_m \sum_n \sum_i \sum_j A_{mn} A_{ij} \frac{mnij}{(i^2 - m^2)(j^2 - n^2)}; \tag{7.152}$$

here we must take into account only those combinations of indices $m + i$ and $n + j$ which simultaneously are odd.

Conditions of the extremum of energy

$$\frac{\partial \Theta}{\partial A_{mn}} = \frac{\partial (U - W)}{\partial A_{mn}} = 0 \tag{7.153}$$

take the form

$$\pi^4 D \frac{ab}{4} A_{mn} \left(\frac{m^2}{a^2} + \frac{n^2}{b^2}\right)^2 - 8\tau h \sum_i \sum_j A_{ij} \frac{mnij}{(m^2 - i^2)(n^2 - j^2)} = 0. \tag{7.154}$$

sums $m + i$ and $n + j$ must be odd.

In the first approximation we take the following combinations of indices:

m, n	i, j
1; 1	2; 2
2; 2	1; 1

System (154) is reduced to two equations:

$$\pi^4 D \frac{ab}{4} A_{11} \left(\frac{1}{a^2} + \frac{1}{b^2}\right)^2 - \frac{32}{9} \tau h A_{22} = 0. \tag{7.155}$$

$$\frac{32}{9} \tau h A_{11} - 4\pi^4 D ab A_{22} \left(\frac{1}{a^2} + \frac{1}{b^2}\right)^2 = 0. \tag{7.156}$$

We introduce the designations

$$\alpha = \frac{a}{b}, \quad \lambda = \frac{\pi^4 D}{32 \tau b^2 h}; \tag{7.157}$$

then equations (155) and (156) will take the following form:

$$\frac{\lambda}{\alpha^2} (1 + \alpha^2)^2 A_{11} + \frac{4}{9} A_{22} = 0, \tag{7.158}$$

$$\frac{4}{9} A_{11} + \frac{16\lambda}{\alpha^2} (1 + \alpha^2)^2 A_{22} = 0. \tag{7.159}$$

We equated the determinant of the system to zero:

$$\begin{vmatrix} \frac{\lambda}{\alpha^2}(1+\alpha^2)^2 & \frac{4}{9} \\ \frac{4}{9} & \frac{16\lambda}{\alpha^2}(1+\alpha^2)^2 \end{vmatrix} = 0, \tag{7.160}$$

from this

$$\lambda = \pm \frac{\alpha^2}{9(1+\alpha^2)^2}. \tag{7.161}$$

Critical stress $\tau_{кр}$ will be equal to

$$\tau_{кр} = \frac{9\pi^4 D (1+\alpha^2)^2}{32 \alpha^2 b^2 h}. \tag{7.162}$$

For square plate we obtain

$$\tau_{кр} = 11.1 \frac{\pi^2 D}{b^2 h}. \tag{7.163}$$

Then from (158) there can be found relationship between A_{11} and A_{22}; when a = b we have $A_{22} = 0.25A_{11}$.

In the second approximation we take such combinations of indices:

m, n	i, j
1,1; 1,3; 3,1; 3,3	2,2
2,2	1,1; 1,3; 3,1; 3,3

The determinant of system (149) has the form

$$\begin{vmatrix} \frac{\lambda}{a^2}(1+a^2)^2 & \frac{4}{9} & 0 & 0 & 0 \\ \frac{4}{9} & \frac{16\lambda}{a^2}(1+a^2)^2 & -\frac{4}{5} & -\frac{4}{5} & \frac{36}{25} \\ 0 & -\frac{4}{5} & \frac{\lambda}{a^2}(1+9a^2)^2 & 0 & 0 \\ 0 & -\frac{4}{5} & 0 & \frac{\lambda}{a^2}(9+a^2)^2 & 0 \\ 0 & \frac{36}{25} & 0 & 0 & \frac{81\lambda}{a^2}(1+a^2)^2 \end{vmatrix} = 0. \tag{7.164}$$

In all directions except one there is contained here only two members. Thanks to this the equation, obtained after expanding the determinant, can be reduced by λ^3. As a result we find

$$\lambda = \pm \frac{a^2}{9(1+a^2)^2} s. \tag{7.165}$$

where

$$s = \sqrt{1 + \frac{81}{625} + \frac{81}{25}\frac{(1+a^2)^2}{(1+9a^2)^2} + \frac{81}{25}\frac{(1+a^2)^2}{(9+a^2)^2}}; \tag{7.166}$$

to this there corresponds critical stress

$$\tau_{kp} = \frac{9\pi^2 D(1+a^2)^2}{32a^3b^3hs}. \tag{7.167}$$

Correction factor with respect to value of first approximation (161) is equal to s. For square plate it constitutes s = 1.18; therefore, in second approximation instead of (163) we obtain

$$\tau_{kp} = 9.4\frac{\pi^2 D}{b^2 h}. \tag{7.163a}$$

We investigated only that case when sum of indices m + n is even. In general a determinant of type (164) is the product of two determinants, one of which contains even m + n, and the other contains odd. In case $1 < \alpha < 2.5$ the least value comes from determinant with <u>even</u>

m + n; for larger α we must alternately consider the first and second determinants.*

As a result critical stress $\tau_{кр}$ can, as before, be presented in the form

$$\tau_{кр} = K\frac{\pi^2 D}{b^2 h}. \qquad (7.168)$$

Definitized values of coefficient K are given in Table 7.6.

Table 7.6. Coefficients K in Case of Hinge-Supported Plate Under Shearing Strain.

a/b	1,0	1,1	1,2	1,3	1,4	1,6	1,8	2,0	3,0	5,0	∞
K	9,34	8,47	7,97	7,57	7,30	6,90	6,64	6,47	6,04	5,71	5,34

For determination of K it is possible also to use approximate formula (α ≥ 1)

$$K = 5{,}34 + \frac{4}{\alpha^2}. \qquad (7.169)$$

For limiting values α = 1 and α = ∞ this formula gives magnitudes K, coinciding with those given in Table 7.6. In Fig. 7.27 is shown the form of the deflection surface of the plate for α = 0.5 and α = 1.0.

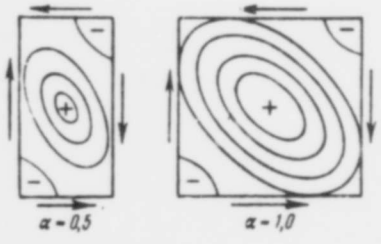

Fig. 7.27. Wave formation of plate with ratio of sides 0.5 and 1 during shearing strain.

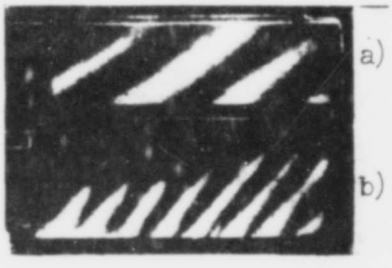

Fig. 7.28. Buckling of surface of reinforced plate with shearing strain: a) at moment of loss of stability, b) during post critical deformation.

*This study was made by Seydel [7.19], Hartmann [0.18] and by H. Stein, J. Neff, [NACA TN 1222, 1947].

If plate is clamped on all edges, then formula (169) takes form ($\alpha \geq 1$)

$$K = 8.98 + \frac{5.6}{\alpha^2}. \qquad (7.170)$$

In conclusion we give photograph of elongated plate, reinforced on edges, at moment of loss of stability (Fig. 7.28a) and during significant exceeding of critical magnitude by shearing forces (Fig. 7.28b).

Combined graph for determining K depending on a/b is given in Fig. 7.29. Here are given design curves not only for the boundary conditions considered above, but also for cases when two edges of the plate (long or short) are clamped and the other two are fastened by hinge.

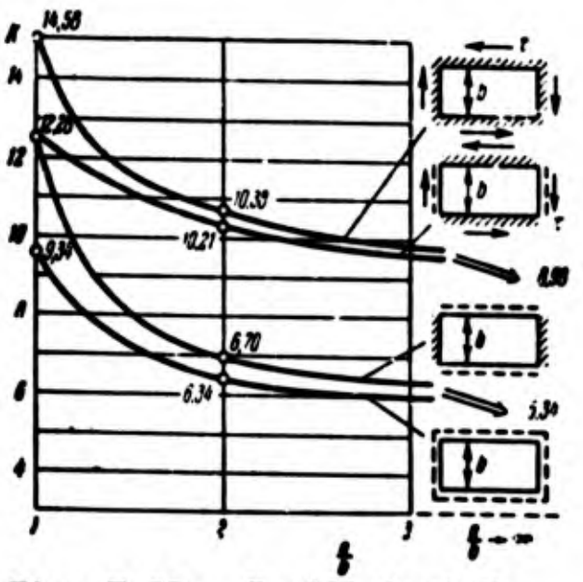

Fig. 7.29. Coefficient K for different conditions of fastening of plate, subjected to shearing strain.

Example 7.2. Reinforced cylindrical shell (Fig. 7.30) experiences action of a torsional moment M_K = 5000 kg m. Struts are located a distance a = 250 mm from one another. Determine maximum spacing b of stringers from the condition that critical shearing stress in skin attains proportional limit $\tau_{пц}$ = 2000 kg/cm^2; thickness of skin

h = 2 mm. Check for stability of vertical walls of longerons, whose thickness is equal to h = 4 mm. Consider that panels of the skin are rigidly clamped on the edges, fastened to strips of longerons, and secured by hinges on the other two edges. The material is duralumin, $E = 7.2 \cdot 10^5$ kg/cm^2, $\mu = 0.32$.

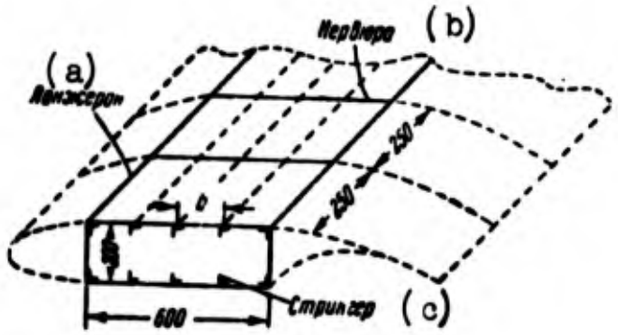

Fig. 7.30. Calculation for stability during shearing strain of shell of aircraft wing type. KEY: (a) Longeron; (b) Strut; (c) Stringer.

We assume that torsional moment is transmitted by central section of the shell, having dimensions 600 x 200 mm. Linear tangential force by Bredt's formula is equal to

$$T = \frac{5 \cdot 10^6}{2 \cdot 20 \cdot 60} = 208 \text{ kg cm}^2.$$

Stress in skin will be

$$\tau_{об} = \frac{T}{h_{об}} = \frac{208}{0{,}2} = 1040 \text{ kg/cm}^2.$$

Spacing of stringers we find from the condition

$$K \frac{\pi^2 \cdot 0{,}72 \cdot 10^6 \cdot 0{,}2^2}{12(1-0{,}32^2)\,b^2} = 1040;$$

hence $b^2/K = 25$. Since K depends on ratio a/b, when a = 260 mm solution must be sought by trial-and-error, given value of b and estimating by graph of Fig. 7.29 the corresponding magnitude of K. Finally, we obtain

$$K \approx 6{,}7, \quad a = 130 \text{ мм}.$$

Stresses in the wall of the longeron are

$$\tau_{ст} = \frac{T}{h_{ст}} = \frac{208}{0{,}4} = 520 \text{ kg/cm}^2.$$

Wall of longeron we consider to be a plate clamped on strips and supported by hinge on adjacent struts. When a/b = 26/20 = 1.3 on graph of Fig. 7.29 K ≈ 11.6. Critical stress equals

$$\tau_{кр} = 11{,}6\frac{\pi^2 \cdot 0{,}72 \cdot 10^6 \cdot 0{,}4^2}{12(1-0{,}32^2)20^2} = 3060 \text{ кг/см}^2.$$

Since magnitude $\tau_{кр}$ exceeds $\tau_{пц}$, then it should be definitized by formulas, derived by taking into account plastic deformations. In any case it is obvious that stability of wall of longeron is ensured.

§ 86. Nonuniform Compression. Pure Bending.

We turn to the case when on two edges of a plate there are distributed normal forces, variable by the linear law* (Fig. 7.31):

$$\sigma_x = \sigma_0\left(1-\alpha\frac{y}{b}\right). \qquad (7.171)$$

When α = 0 we obtain case of uniform compression; when α = 1 we have a case of compressive forces, distributed by the law of the triangle. If α > 1, then a certain part of the plate will experience tension. When α = 2 we arrive at case of pure bending. Thus, here are united different forms of loading of panels of sheeting and thin walls, consisting of eccentric compression and flexure.

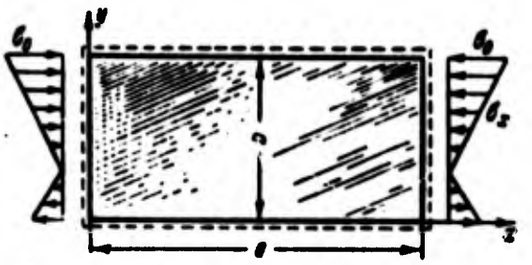

Fig. 7.31. Plate under action of normal forces, distributed by linear law.

We consider that all edges of the plate are fastened by hinge and use the same method of solution as in Section 85. We approximate

*This problem was studied by I. G. Bubnov [0.2] and S. P. Timoshenko [0.23].

deflection, as before, by the series

$$w = \sum_{m=1}^{\infty}\sum_{n=1}^{\infty} A_{mn} \sin\frac{m\pi x}{a} \sin\frac{n\pi y}{b}. \tag{7.172}$$

Energy of bending strain will be equal to

$$U = \frac{D}{2}\frac{ab\pi^4}{2}\sum_m\sum_n A_{mn}^2\left(\frac{m^2}{a^2}+\frac{n^2}{b^2}\right)^2. \tag{7.173}$$

Work of external forces will be

$$W = \frac{1}{2}\int_0^a\int_0^b \sigma_0 h\left(1-\alpha\frac{y}{b}\right)\left(\frac{\partial w}{\partial x}\right)^2 dx\,dy. \tag{7.174}$$

Taking into account relationships

$$\int_0^b y \sin\frac{i\pi y}{b}\sin\frac{j\pi y}{b}\,dy = \begin{cases} -\frac{16b^2}{\pi}\frac{ij}{(i^2-j^2)^2}, & \text{if } i\pm j \text{ is odd,} \\ 0, & \text{if } i\pm j \text{ is even,} \\ \frac{b^2}{4}, & \text{if } i=j. \end{cases} \tag{7.175}$$

we find

$$W = \frac{\sigma_0 h}{2}\left\{\frac{ab}{4}\sum_m\sum_n A_{mn}^2\frac{m^2\pi^2}{a^2} - \right.$$
$$\left. -\frac{a\alpha}{2b}\sum_m\frac{m^2\pi^2}{a^2}\left[\frac{b^2}{4}\sum_n A_{mn}^2 - \frac{8b^2}{\pi^2}\sum_n\sum_i\frac{A_{mn}A_{mi}ni}{(n^2-i^2)^2}\right]\right\} \tag{7.176}$$

when n $\pm$ i is odd.

Equations

$$\frac{\partial(U-W)}{\partial A_{mn}} = 0$$

take the form

$$DA_{mn}\pi^4\left(\frac{m^2}{a^2}+\frac{n^2}{b^2}\right)^2 -$$
$$-\sigma_{xp}h\left\{A_{mn}\frac{m^2\pi^2}{a^2} - \frac{\alpha m^2\pi^2}{2a^2}\left[A_{mn} - \frac{16}{\pi^2}\sum_{i=1}^{\infty}\frac{A_{mi}ni}{(n^2-i^2)^2}\right]\right\}. \tag{7.177}$$

In first approximation we assume that $A_{11} \neq 0$, and all remaining coefficients are equal to zero; then we arrive at the unique equation

$$D\pi^2\left(\frac{1}{a^2}+\frac{1}{b^2}\right)^2 - \sigma_0 h\frac{1}{a^2}\left(1-\frac{\alpha}{2}\right) = 0,$$

from which

$$\sigma_{0,\,xp} = \frac{\pi^2 D}{b^2 h}\left(\frac{b}{a}+\frac{a}{b}\right)^2\frac{1}{1-\frac{\alpha}{2}}. \tag{7.178}$$

This solution has meaning only for small α. Considering consecutively systems of two, three, etc., equations of type (177), we find definitized values of critical stresses. We present critical value σ_0 in

the form

$$\sigma_{0,\,cp} = K\frac{\pi^2 D}{b^2 h}. \qquad (7.179)$$

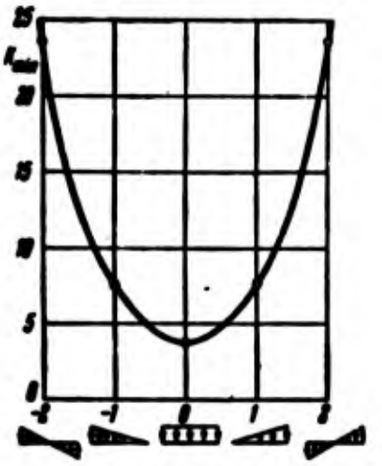

Fig. 7.32. Coefficient K in different cases of loading.

Definitized values of K for various cases of loading are presented in Table 7.7; in distinction from previous cases a is not always the large side of the plate.

In the case of pure bending minimum value K is obtained for a/b = = 2/3. In Fig. 7.32, are compared smallest values of K for certain forms of loading with hinge-supported edges of plate. As we see,

Table 7.7. Coefficients K for Case of Non-uniformly Distributed Normal Forces.

ψ \ a/b	0,4	0,5	0,6	0,667	0,75	0,8	0,9	1,0	1,5
2	29,1	25,6	24,1	23,9	24,1	24,4	25,6	25,6	24,3
4/3	18,7		12,9		11,5	11,2		11,0	11,5
1	15,1		9,7		8,4	8,1		7,8	8,4
4/5	13,3		8,3		7,1	6,9		6,6	7,1
2/3	10,8		7,1		6,1	6,0		5,8	6,1

coefficient K, for the largest bending stress turns out to be approximately 6 times greater than during uniform compression.

§ 87. Combined Loading.

We determined critical stresses during compression (extension) in one direction and shearing strain. In many structures, however, plates experience simultaneously different types of forces. One example is skin of an aircraft wing; bending of wing causes appearance of compressive (tensile) stresses in skin, torsion causes shearing strains. Let us consider different forms of combined loads.

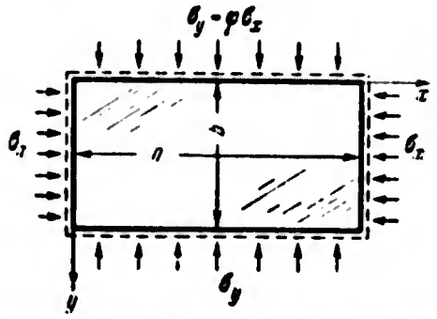

Fig. 7.33. Plate is compressed simultaneously in two directions.

1. Compression in two directions. Let us assume that a plate fastened by hinge on all edges is compressed simultaneously by forces σ_x and σ_y, evenly distributed along corresponding sides* (Fig. 7.33).

Equation (26) obtains form

$$\frac{D}{h}\nabla^4 w + \sigma_x \frac{\partial^2 w}{\partial x^2} + \sigma_y \frac{\partial^2 w}{\partial y^2} = 0. \quad (7.180)$$

We write solution in the form

$$w = A_{mn} \sin \frac{m\pi x}{a} \sin \frac{n\pi y}{b}. \quad (7.181)$$

Substituting in (180), we obtain

$$D\left[\left(\frac{m}{a}\right)^2 + \left(\frac{n}{b}\right)^2\right]^2 = \frac{h}{\pi^2}\left[\sigma_x \left(\frac{m}{a}\right)^2 + \sigma_y \left(\frac{n}{b}\right)^2\right]. \quad (7.182)$$

We introduce the designations

$$\alpha = \frac{a}{b}, \quad \varphi = \frac{\sigma_y}{\sigma_x} \quad (7.183)$$

and express critical stresses in the following manner:

$$\sigma_{x,\text{кр}} = K_x \frac{\pi^2 D}{b^2 h},$$

$$\sigma_{y,\text{кр}} = K_y \frac{\pi^2 D}{b^2 h} = \varphi \sigma_{x,\text{кр}}; \quad (7.184)$$

*This problem was first considered by Bryan [7.14].

then from (182) we find

$$K_x=\frac{\left[\left(\frac{m}{a}\right)^2+n^2\right]^2}{\left(\frac{m}{a}\right)^2+\varphi n^2}. \tag{7.185}$$

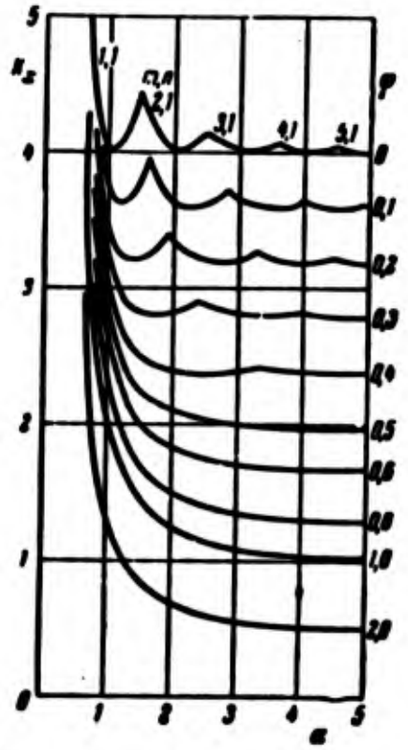

Fig. 7.34. Critical stresses for a plate compressed in two directions.

In Fig. 7.34 there are given minimum values of K_x depending on α for various φ; for individual branches there are shown indices m and n. For a square plate we obtain always m = n = 1; here

$$K_x=\frac{4}{1+\varphi},\qquad K_y=\frac{4\varphi}{1+\varphi}. \tag{7.186}$$

hence

$$K_x+K_y=4. \tag{7.187}$$

2. Uniform compression (tension) in one direction and shearing. Let us turn to case of joint action of compressive or tensile forces σ in one direction and tangential forces τ (Fig. 7.35). Edges of plate we take secured by hinge.

For a very long plate deflection may be approximated by an expression analogous to (141):

$$w=f\sin\frac{\pi y}{b}\sin\frac{\pi}{l}(x-ky). \tag{7.188}$$

Potential energy of bending, as before, is determined by equality (142). Supplementing (143), we obtain for work of external forces a new expression:

$$W=\left(\frac{\sigma h\pi^2 b}{8l}+\frac{\tau h\pi^2 kb}{4l}\right)f^2. \tag{7.189}$$

Comparing (142) and (189), we find

$$\sigma+2\tau k=\frac{D\pi^2}{hb^2}\left[\left(\frac{l}{b}\right)^2+6k^2+2+\left(\frac{b}{l}\right)^2(1+k^2)^2\right]. \tag{7.190}$$

The expression in parentheses takes a minimum value for a length the half-wave of

$$l = b\sqrt{1+k^2}. \tag{7.191}$$

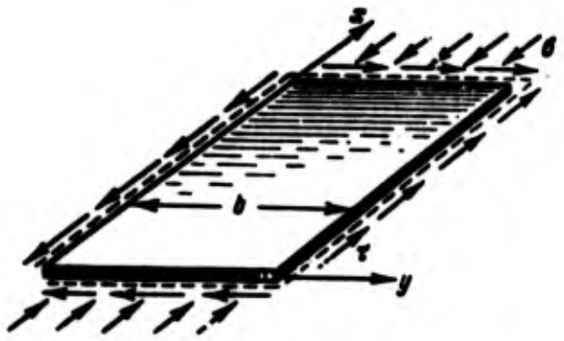

Fig. 7.35. Simultaneous action of compression in one direction and shear.

Thus, system of critical stresses satisfies equation

$$\sigma_{кр} + 2\tau_{кр}k = \frac{D\pi^2}{hb^2}(4+8k^2). \tag{7.192}$$

With separate action of compression and shear we have

$$\sigma_{0,кр} = 4\frac{\pi^2 D}{b^2 h}, \quad \tau_{0,кр} = 4\sqrt{2}\frac{\pi^2 D}{b^2 h}. \tag{7.193}$$

Equation (192) takes form

$$\frac{\sigma_{кр}}{\sigma_{0,кр}} + 2\sqrt{2}\frac{\tau_{кр}}{\tau_{0,кр}}k = 1 + 2k^2. \tag{7.194}$$

Let us assume that ratio $\tau_{кр}/\tau_{0,кр}$ is given; then minimal value $\sigma_{кр}$ corresponds to the angle of inclination of nodal lines, determined as follows:

$$k = \frac{1}{\sqrt{2}}\frac{\tau_{кр}}{\tau_{0,кр}}. \tag{7.195}$$

For simple compression k = 0; with shear $k = 1/\sqrt{2}$, with combined load k has an intermediate value. Putting (195) in (194), we find the relationship

$$\frac{\sigma_{кр}}{\sigma_{0,кр}} + \left(\frac{\tau_{кр}}{\tau_{0,кр}}\right)^2 = 1. \tag{7.196}$$

As one would expect, variation of direction of tangential forces (change of sign of τ) does not affect magnitude of critical stress.

Equation (196) may be used also in the case when forces σ are tensile; the sign before σ must be changed here to its opposite. Critical tangential stress here will be larger than during simple shearing strain.

In the case of a plate with a finite ratio of sides it is possible to use the same equation (196). Definitized solution of problem was obtained by approximating deflection by expression (141). If we maintain during solution five parameters A_{mn}, then we arrive at

the following results. We introduce designations

$$\sigma_{кр} = K_\sigma \frac{\pi^2 D}{b^2 h}, \quad \tau_{кр} = K_\tau \frac{\pi^2 D}{b^2 h}. \tag{7.197}$$

Values of K_σ and K_τ for different ratios $\alpha = a/b$ are given in Table 7.8. Minus sign before K_σ corresponds to tensile forces.*

Table 7.8. Coefficients K_σ and K_τ in Case of Combined Action of Compression and Shear.

$\alpha = 1$	K_σ	−1,0	0	1,0	2,0	3,0	3,6	4,0
	K_τ	10,57	9,42	8,15	6,67	4,72	3,02	0
$\alpha = 1,6$	K_σ	−2,0	0	2,0	2,83	3,6	3,9	4,2
	K_τ	8,46	7,0	5,31	4,46	2,95	2,09	0,06
$\alpha = 3,2$	K_σ	−1,0	0	1,7	2,5	3,0	3,7	4,017
	K_τ	7,45	6,75	5,4	4,66	4,14	3,29	2,19

In the graph of Fig. 7.36 is given dependence $\sigma_{кр}/\sigma_{0,\ кр}$ and $\tau_{кр}/\tau_{0,\ кр}$ for different ratios b/a, definitized as compared to (196).

3. Compression in two directions and shear. Assume that elongated plate, supported by hinge on its edges, is subjected to action of compressive (tensile) forces along the long side σ_x, along the short side σ_y, and also tangential forces τ. Using the same method as in the previous case, we arrive at the following dependence between critical stresses:

$$\left(\frac{\tau_{кр}}{\tau_{0,\ кр}}\right)^2 = \left[\frac{1}{2}\left(1 + \sqrt{1 - 4\frac{\sigma_{y,\ кр}}{\tau}}\right) - \frac{\sigma_{x,\ кр}}{\sigma_{0,\ кр}}\right] \times \left[\frac{1}{4}\left(3 + \sqrt{1 - 4\frac{\sigma_{y,\ кр}}{\sigma}}\right) - \frac{\sigma_{y,\ кр}}{2\sigma_{0,\ кр}}\right]; \tag{7.198}$$

by $\tau_{0,\ кр}$ and $\sigma_{0,\ кр}$ we understand critical stresses during separate action of shear and compression in direction x; by σ we understand

*Slight divergence between magnitudes K_τ for $K_\sigma = 0$ in Table 7.8 and 7.6, is explained by the fact that problem is solved in a different approximation.

magnitude

$$\sigma = \frac{\pi^2 D}{b^2 h}. \qquad (7.199)$$

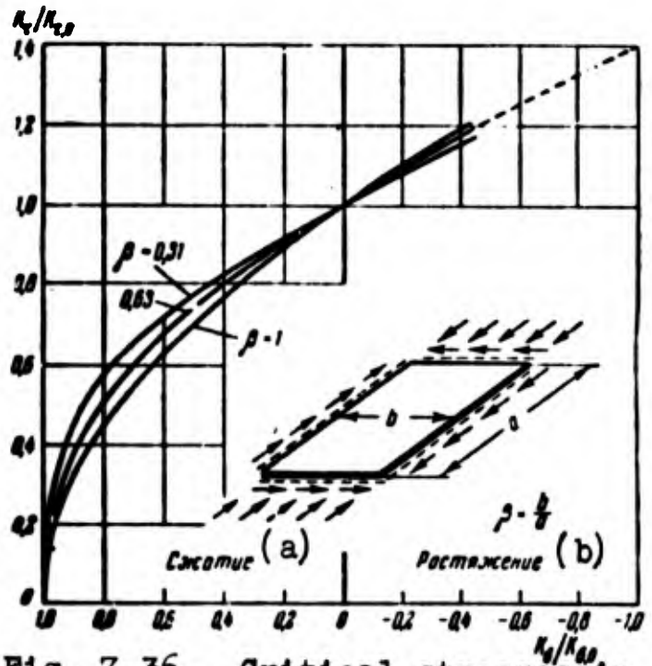

Fig. 7.36. Critical stresses in case of joint action of compression and shear.
KEY: (a) Compression; (b) Tension.

4. Pure bending and shearing. Consider, further, a hinge-supported plate under action of normal forces on two edges, and uniformly

$$\sigma = \sigma_1\left(1 - \frac{2y}{b}\right). \qquad (7.200)$$

distributed shearing forces τ. Critical stresses are expressed by relationships

$$\sigma_{1,\,кр} = K_\sigma \frac{\pi^2 D}{b^2 h},$$

$$\tau_{кр} = K_\tau \frac{\pi^2 D}{b^2 h}. \qquad (7.201)$$

We designate value of coefficients K_σ and K_τ during separate action of bending and shearing by $K_{\sigma,\,0}$ and $K_{\tau,\,0}$. Quantities K_σ and K_τ can be determined from the approximate relationship

$$\left(\frac{K_\sigma}{K_{\sigma,0}}\right)^2 + \left(\frac{K_\tau}{K_{\tau,0}}\right)^2 = 1. \qquad (7.202)$$

Definitized values of K_σ and K_τ for different ratios of sides of plate $\alpha = a/b$ are given in Table 7.9 and on graph of Fig. 7.37.

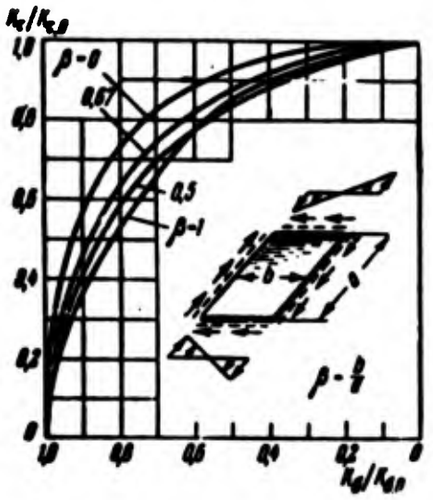

Fig. 7.37. Critical stresses in the case of joint action of flexure and shearing.

Table 7.9. Coefficients K_σ and K_τ During Joint Action of Bending and Shearing.

$\alpha=1$		$\alpha=\frac{1}{2}$		$\alpha=\frac{1}{3}$		$\alpha=\frac{1}{4}$	
K_τ	K_σ	K_τ	K_σ	K_τ	K_σ	K_τ	K_σ
0	25,6	0	24,5	0	23,9	0	26,6
2	24,6	4	22,8	4	23,05	4	25,4
4	22,2	8	17,7	8	20,35	8	24,3
6	18,4	10	13,25	12	15,23	12	22,55
8	12,4	11	10,01	14	11,04	16	19,94
9	6,85	12	4,61	15	8,0	20	16,13
9,42	0	12,26	0	16,09	0	24	10,26
						26	5,44
						26,9	0

§ 88. Post Critical Deformation of Plate During Compression.

We previously determined stress at which the plane form of plate ceases to be stable. However, if plate is fastened at edges with sufficiently rigid ribs, then its supporting power at moment loss of stability is not exhausted; the plate is capable even after this to carry an <u>increasing</u> load. Therefore, in order to judge the supporting power of a plate, it is necessary to study its post-critical behavior.

As we have seen, at moment of buckling of a plate in it there appear only flexural stresses; in calculating potential strain energy it was possible to limit ourselves to determinating energy, corresponding to flexural stresses. In the post-critical stage, when deflections become comparable with thickness of the plate stresses in the middle surface start to play an important role. At every point of the plate stresses will be composed of stresses of free bending stresses in middle surface; with development the buckles of the role of the latter increases.

Stresses in the middle surface appear because of two circumstances. On the one hand, during large deflections of a nonreinforced plate its edges are distorted noticeably, as is shown in Fig. 7.38a; here it is assumed that edge fibers remain in initial plane of the plate. But when plate is furnished with hard ribs, they resist distortion of edge strips. During buckling of edges there are formed additional forces, compressive near angles and tensile in middle section (Fig. 7.38b); here there is accumulated additional potential energy. On the other hand, buckling of a plate occurs in such a way that middle surface turns into a nondeveloping surface; this causes new stresses, depending on character of distortion of the plate at this or that point. As we shall see later, influence on plate behavior of the first factor — rigidity of reinforcing ribs — is significantly greater than the effect connected with wave formation of the middle surface.

A characteristic peculiarity of post-critical deformation of a plate consists of variation of form of dents; if at moment of loss of stability of an elongated plate the dents are square, then the length

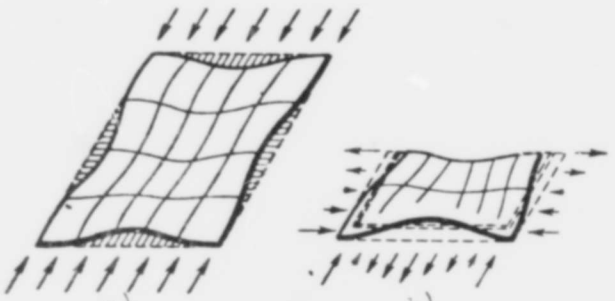

Fig. 7.38. Forces in middle surface during buckling of a plate.

of them decreases, where transition from one number of waves to another is usually accompanied by knocks. In Fig. 7.39 is shown form of wave formation of plate for moment when stress in reinforcing ribs by 40 times exceeds critical stress for the plate.*

Let us consider first post-critical deformation of plate, fastened by hinge at edges with rigid ribs and compressed in one direction. We assume that reinforcing ribs remain rectilinear, but that points of the plate can slip freely along the ribs. Consider a section of the plate, perpendicular to the direction of compression. If before loss of stability of plate compressive stresses are distributed evenly by wide, then after buckling they increase more intensely at the edges; in the middle section stresses differ little from critical value (Fig. 7.40a).

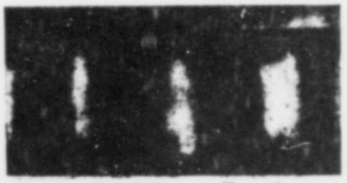

Fig. 7.39. Post-critical wave formation of plate during compression.

We designate by σ_0 stress in an edge fiber of plate, located in middle surface, and by σ, the average stress by width:

$$\sigma = \frac{1}{b}\int_0^b \sigma_x\, dy. \qquad (7.203)$$

*According to R. Lahde and H. Wagner, Luftfahrtorschung, 13, No. 7 (1936).

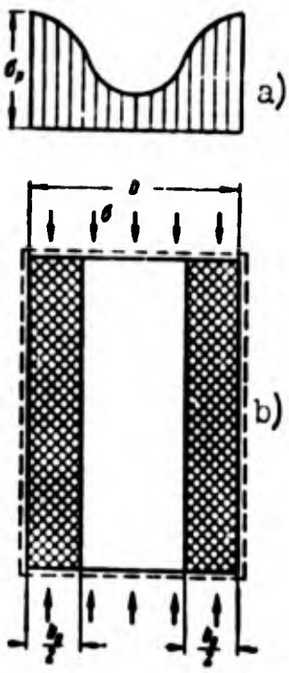

Fig. 7.40. Distribution of stresses during post-critical deformation of a plate.

Total compressing force transmitted by plate is equal to $P = bh\sigma$. We express it by edge stress:

$$P = \varphi bh\sigma_p. \qquad (7.204)$$

introducing the so-called reduction factor φ. This factor is equal to

$$\varphi = \frac{\sigma}{\sigma_p}. \qquad (7.205)$$

It is possible conditionally to assume that working parts of plate are only the strips adjacent to edges, as shown in Fig. 7.40b; total width of these two strips we will call reduced width and designate it by $b_0 = b_{пр}$; then we have

$$\varphi = \frac{b_{пр}}{b}. \qquad (7.206)$$

If we know how reduction factor changes with growth of σ_p, then we can determine resistance of plate to compressing force on every stage of loading. In turn, magnitude σ_p is connected with deformation of reinforcing ribs. Depending upon conditions of deformation of ribs we must take

$$\sigma_p = \frac{E_p \varepsilon_p}{1-\mu^2} \text{ when } \sigma_p = E_p \varepsilon_p. \qquad (7.207)$$

where E_p is elastic modulus of material; ε_p is deformation of shortening of ribs. Determining reduction factors allows us to establish role which plate plays as a member of some structure, for instance, the body of an aircraft of the hull of a ship.

Let us give derivation of a simple approximate formula for the reduction factor, not pretending to take into account all circumstances of post-critical deformation of a plate.* We separate working extreme

*This derivation belongs to Kármán, Sechler and Donnell [7.16].

bands of the plate and mentally join them together; then we obtain a plate of width $b_{пр}$. We consider that stresses σ_p in a plate thus reduced are such that plate is on the verge of buckling; in other words, we assume that magnitude σ_p is equal to critical stress for a plate of width $b_{пр}$:

$$\sigma_p = K\frac{\pi^2 D}{b_{пр}^2 h}. \tag{7.208}$$

On the other hand, at moment of buckling of initial plate critical stress is equal to

$$\sigma_{кр} = K\frac{\pi^2 D}{b^2 h}. \tag{7.209}$$

Comparing (208) and (209), we find

$$\varphi = \sqrt{\frac{\sigma_{кр}}{\sigma_p}} = \sqrt{\frac{1}{n^*}}. \tag{7.210}$$

Here by n* we designate ratio of stress in an edge fiber to critical stress:

$$n^* = \frac{\sigma_p}{\sigma_{кр}}; \tag{7.211}$$

this magnitude characterizes level of development of post-critical deformation. We note that when $n^* \to \infty$ reduction factor approaches zero. In all our reasonings we assume that stresses in plate and ribs lie within the elastic limit.

Approximate formula (210) frequently is applied in practical calculations. Below we give a more strict solution of the problem of post-critical behavior of a plate.

§ 89. Application of Theory of Flexible Plates.

After buckling of a plate its deflections can not be considered small in comparison with its thickness. Therefore, during study of post-critical deformation it is necessary to start from general equations of theory of flexible plates (63) and (64). We assume that all edges of the plate remain rectilinear and that longitudinal edges

during bending of the plate move freely relative to one another; furthermore, we shall consider that points which belong to edges of the plate freely slide along the reinforcing ribs. This last assumption does not correspond, as a rule, to real conditions of fastening of plates to ribs, but significantly facilitates calculations. A more strict solution [7.11], belonging to G. G. Rostovtsev, showed that error introduced by this assumption for such "integral" characteristics as the reduction factor is small.

Solution of system of nonlinear equations (63) and (64) for given boundary conditions is satisfied by various methods of approximation. Most frequently they use the following method.

We select approximate expression for deflection w in the form of the series

$$w=\sum_{m=1}^{\infty}\sum_{n=1}^{\infty}A_{mn}\sin\frac{m\pi x}{a}\sin\frac{n\pi y}{b}. \tag{7.212}$$

We place this expression in the right part of equation (64); then we obtain a linear differential equation for function Φ. Its integral has the form

$$\Phi=\sum_{p=0}^{\infty}\sum_{q=0}^{\infty}B_{pq}\cos\frac{p\pi x}{a}\cos\frac{q\pi y}{b}-\frac{\sigma y^2}{2}. \tag{7.213}$$

From this by (60) we find stresses σ_x, σ_y, and τ. Coefficients B_{pq} are expressed by A_{mn}; by σ is understood average compressive stress by width of plate.

Total compressive force in any section of the plate parallel to y will be

$$P=\int_0^b h\sigma_x\,dy=\sigma bh; \tag{7.214}$$

Let us note that this magnitude does not depend on coordinates and, thus, remains constant the whole length of the plate.

We determine, then, mutual displacement of points of the plate, with coordinates (x, 0) and (x, b), by (54)

$$u=\int_0^x\left[\varepsilon_x-\frac{1}{2}\left(\frac{\partial w}{\partial x}\right)^2\right]dx. \tag{7.215}$$

Deformation ε_x by (57) and (60) is equal to

$$\varepsilon_x = \frac{1}{E}\left(\frac{\partial^2\Phi}{\partial y^2} - \mu\frac{\partial^2\Phi}{\partial x^2}\right). \tag{7.216}$$

Substituting (212) and (213), we obtain

$$u = -\frac{\alpha x}{E} - \frac{\pi^2}{8a}\sum_{m=1}^{\infty}\sum_{n=1}^{\infty} m^2 A_{mn}^2. \tag{7.217}$$

Analogously we find mutual displacement of points with coordinates (0, y) and (a, y):

$$v = \int_0^b \left[\varepsilon_y - \frac{1}{2}\left(\frac{\partial w}{\partial y}\right)^2\right] dy. \tag{7.218}$$

or

$$v = \mu\frac{\alpha b}{E} - \frac{\pi^2}{8b}\sum_{m=1}^{\infty}\sum_{n=1}^{\infty} n^2 A_{mn}^2. \tag{7.219}$$

As we see, magnitudes u and v do not depend on the coordinates; consequently, the condition of rectilinearity of edges is satisfied.

Using expressions for w and Φ, we approximately integrate equation (63). For this we can apply the method of Ritz or Bubnov-Galerkin.* Here are found coefficients A_{mn} and B_{pq}, determining deflection and stresses in the middle surface. Then by formula (205) we calculate reduction factor.

Consider for simplicity a square plate with side b and assume in the first approximation that $A_{11} \neq 0$ and all remaining coefficients equal zero. In other words, we consider that the plate is distorted in <u>one half-wave</u> on axes x and y. Then for expression (213) we obtain

$$B_{20} = B_{02} = \frac{EA_{11}^2}{32}, \tag{7.220}$$

other coefficients turn into zero. As it is easy to see, parameter A_{11} is the maximum deflection of the plate; therefore, we designate further $A_{11} = f$. By (217) we find

---

*Such a way of solving a problem was developed in studies of P. F. Papkovich, the first of which pertains to 1920. P. A. Sokolov and other authors; for a survey of these works see [0.3], p. 390.

$$\varepsilon = -\frac{\sigma}{E} - \frac{\pi^2 f^2}{8a^2}. \qquad (7.221)$$

Mutual approach of loaded edges, referred to side of plate, will be

$$\varepsilon_x = \frac{\sigma}{E} + \frac{\pi^2}{8}\left(\frac{f}{a}\right)^2. \qquad (7.222)$$

We assume that this magnitude corresponds to deformation of longitudinal rib and what elastic moduli of plate and ribs are identical ($E_p = E$); from (207) stress σ_p turns out to be equal to

$$\sigma_p = \sigma + E\frac{\pi^2}{8}\left(\frac{f}{a}\right)^2. \qquad (7.223)$$

factor $1/(1 - \mu^2)$ here is omitted.

Applying for integration of equation (63) the Bubnov-Galerkin method, we write the relationship

$$\int_0^a \int_0^b X \sin\frac{\pi x}{a} \sin\frac{\pi y}{b}\, dx\, dy = 0, \qquad (7.224)$$

where

$$X = \frac{D}{h}\nabla^4 w - L(w, \Phi). \qquad (7.225)$$

Substituting values of w and Φ and calculating, we arrive at the following dependence:

$$\sigma f - \frac{4\pi^2 D}{b^2 h} f - E\frac{\pi^2}{8b^2} f^3 = 0. \qquad (7.226)$$

We take $f \neq 0$ and consider that in second member there appears critical stress $\sigma_{кр}$; then we find

$$\sigma = \sigma_{кр} + E\frac{\pi^2}{8}\left(\frac{f}{b}\right)^2. \qquad (7.227)$$

Comparing formulas (223) and (227), we obtain

$$\sigma = \frac{1}{2}(\sigma_{кр} + \sigma_p). \qquad (7.228)$$

Reduction factor according to (205) appears equal to*

$$\varphi = 0.5 + \frac{0.5}{n^*}. \qquad (7.229)$$

where by n^*, as before, there is understood ratio (211). This dependence differs from Kármán's formula (210) already by the fact that

---

*This formula was shown by Marguerre [7.18].

when $n^* \to \infty$ the reduction factor nears a value of 0.5, and not zero; in general quantity φ is significantly higher than it is by (210).

Definitized solutions can be constructed by increasing the number of variable parameters A_{mn}. In book [0.3] are calculations, taking into account two parameters, A_{11} and A_{31} (first index is number of half-waves in direction x, the second – along y); it turned out that values of reduction factors lies somewhat lower than according to data of the first approximation.

In Marguerre's [7.18] there also were calculations with retention of coefficients A_{11}, A_{13}, and A_{31}. As a result there was obtained the following approximate formula for reduction factor:

$$\varphi = \sqrt[6]{\frac{1}{n^*}}; \qquad (7.230)$$

obviously, it also gives higher values for φ than Kármán's formula (210).

Further in work of Levy [7.17] are contained data, obtained with preservation of coefficients A_{11}, A_{13}, A_{33}, and A_{51}. The dependence found here, $\varphi(n^*)$, is depicted in Fig. 7.41 in comparison with formulas (210) and (230). Levy's curve, on first glance, may be considered the most justified. However, solution of S. A. Alekseyev [7.1], carried out with help of method of successive approximations, led to other results. It appears, in those calculations, which were previously carried out by the Ritz method; they dropped coefficients pertaining to even numbers of half-waves (for instance, A_{21}). Besides, as was shown by S. A. Alekseyev, curve m = 2 (m is number of half-waves by length) gives in a definite region of variation of n^* smaller values φ than neighboring curves m = 1 and m = 3. Therefore, Levy's solution gave for $n^* > 3.5$ exaggerated values of reduction factor.

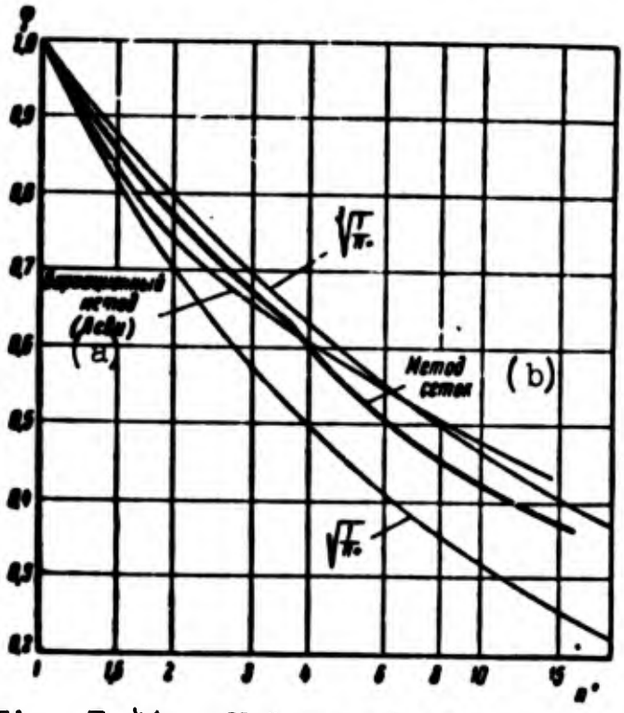

Fig. 7.41. Values of reduction factors from results of different solutions.
KEY: (a) Variational method (Levy); (b) Method of nets.

Simple experiments, in which there is realized compression of a reinforced plate within the elastic limit, confirm this conclusion. With insignificant exceeding of critical stress the square plate bulges in such a manner along its length there will form one half-wave. Further loading of the plate leads, as we already saw, to a knock in the process of which there appear two half-waves, subsequently there are formed three half-waves, etc.

§ 90. Solution of Problem by Digital Computer.

Application of the Ritz or Bubnov-Galerkin method to problem of post-critical behavior of a plate leads to solution of system of cubic equations of type (226) for parameters of deflection. With a significant number of retained parameters calculations are very laborious. Complicated calculations must be carried out also when using the

method of successive approximations. Therefore, solution of this problem should be executed by digital computers. The calculating process connected with application of the Ritz method or the method of successive approximations, yields, in general, to programming. However, most convenient here is application of the method of finite differences or method of collocation. Below we expound solution of a problem about post-critical behavior of a plate, conducted by method of finite differences.*

We introduce in fundamental equations (63) and (64) the dimensionless magnitudes

$$\left.\begin{aligned} &\bar{x}=\frac{x}{a},\quad \bar{y}=\frac{y}{b},\quad \lambda=\frac{a}{b},\quad \bar{w}=\frac{w}{h},\quad \nu=\frac{1}{12(1-\mu^2)},\\ &\bar{\Phi}=\frac{\Phi}{Eh^2},\quad \bar{\sigma}_x=\frac{\sigma_x}{E}\left(\frac{b}{h}\right)^2,\quad \bar{\sigma}_y=\frac{\sigma_y}{E}\left(\frac{a}{h}\right)^2,\quad \bar{\tau}=\frac{\tau}{E}\frac{ab}{h^2}. \end{aligned}\right\} \qquad (7.231)$$

then these equations will take the form

$$\nu\left(\frac{1}{\lambda^2}\frac{\partial^4\bar{w}}{\partial\bar{x}^4}+2\frac{\partial^4\bar{w}}{\partial\bar{x}^2\partial\bar{y}^2}+\lambda^2\frac{\partial^4\bar{w}}{\partial\bar{y}^4}\right)=\bar{L}(\bar{w},\ \bar{\Phi}), \qquad (7.232)$$

$$\frac{1}{\lambda^2}\frac{\partial^4\bar{\Phi}}{\partial\bar{x}^4}+2\frac{\partial^4\bar{\Phi}}{\partial\bar{x}^2\partial\bar{y}^2}+\lambda^2\frac{\partial^4\bar{\Phi}}{\partial\bar{y}^4}=-\frac{1}{2}\bar{L}(\bar{w},\ \bar{w}); \qquad (7.233)$$

operators $\bar{L}$ include derivatives with respect to $\bar{x}$ and $\bar{y}$. Stresses in middle surfaces are equal to

$$\bar{\sigma}_x=\frac{\partial^2\bar{\Phi}}{\partial\bar{y}^2},\quad \bar{\sigma}_y=\frac{\partial^2\bar{\Phi}}{\partial\bar{x}^2},\quad \bar{\tau}=-\frac{\partial^2\bar{\Phi}}{\partial\bar{x}\partial\bar{y}}. \qquad (7.234)$$

The flexural stresses greatest in thickness will be

$$\bar{\sigma}_{x,u}=\frac{1}{2(1-\mu^2)}\left(\frac{1}{\lambda^2}\frac{\partial^2\bar{w}}{\partial\bar{x}^2}+\mu\frac{\partial^2\bar{w}}{\partial\bar{y}^2}\right). \qquad (7.235)$$

$$\bar{\sigma}_{y,u}=\frac{1}{2(1-\mu^2)}\left(\frac{1}{\lambda^2}\frac{\partial^2\bar{w}}{\partial\bar{y}^2}+\mu\frac{\partial^2\bar{w}}{\partial\bar{x}^2}\right). \qquad (7.236)$$

$$\bar{\tau}_u=\frac{1}{2(1+\mu)}\frac{\partial^2\bar{w}}{\partial\bar{x}\partial\bar{y}}. \qquad (7.237)$$

Let us note that in dimensionless variables $\bar{x}$ and $\bar{y}$ the rectangular region with any ratio of sides λ is depicted in a square region

---

*This solution belongs to A. Yu. Birkgan.

with a side equal to one. System of equations (232) and (233) we present in finite differences. We use a square net and divide each side into m equal parts. Step of net will be c = 1/m. We also introduce extra-contour nodes at distance c and 2c from the edges (Fig. 7.42).

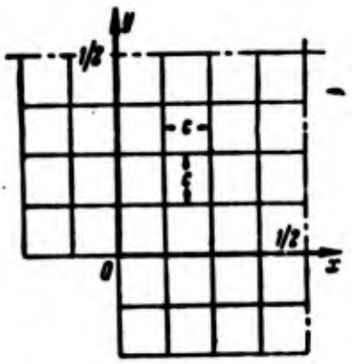

Fig. 7.42. For application of net method.

We investigate, as before, the case of a plate, secured by hinges on all sides and loaded by forces σ, evenly distributed on the edges x = 0 and x = 1. Obviously, the deflection surface will be symmetric relative to line y = 1/2 and symmetric or skew relative to line x = 1/2; therefore, it is sufficient to consider 1/4 of the plate.

To shift to finite differences we apply central operators, having error of the square of the step (the dashes above w and Φ are henceforth dropped):

$$\left.\begin{aligned}\frac{\partial^2 w}{\partial x^2}&=\frac{1}{c^2}(w_1-2w_0+w_2).\\ \frac{\partial^2 w}{\partial y^2}&=\frac{1}{c^2}(w_3-2w_0+w_4).\\ \frac{\partial^2 w}{\partial x\,\partial y}&=\frac{1}{4c^2}(w_5-w_6+w_7-w_8).\end{aligned}\right\} \tag{7.238}$$

$$\left.\begin{aligned}\frac{\partial^4 w}{\partial x^4}&=\frac{1}{c^4}(w_9-4w_1+6w_0-4w_3+w_{11}).\\ \frac{\partial^4 w}{\partial y^4}&=\frac{1}{c^4}(w_{10}-4w_2+6w_0-4w_4+w_{12}).\\ \frac{\partial^4 w}{\partial x^2\,\partial y^2}&=\frac{1}{c^4}[4w_0-2(w_1+w_2+w_3+w_4)+w_5+w_6+w_7+w_8].\end{aligned}\right\} \tag{7.239}$$

Numbering of nodes in the calculating cell is given in Fig. 7.43. We compose analogous formulas for stress function Φ. Putting difference operators in equations (232) and (233), we find value of deflection and stress function in the instantaneous node which is the "center"

of the calculating cell (when $\lambda = 1$)

$$w_0 = \{(w_1 + w_3)(\Phi_2 - 2\Phi_0 + \Phi_4 + 8\nu) + \\ + (w_2 + w_4)(\Phi_1 - 2\Phi_0 + \Phi_3 + 8\nu) - \\ - \tfrac{1}{8}(w_5 + w_7)(\Phi_5 - \Phi_6 + \Phi_7 - \Phi_8 + 16\nu) - \\ - (w_6 + w_8)(\Phi_5 - \Phi_6 + \Phi_7 - \Phi_8 - 16\nu) - \\ - \nu(w_9 + w_{10} + w_{11} + w_{12})\} : 2(\Phi_1 + \Phi_2 + \Phi_3 + \Phi_4 - 4\Phi_0 + 10\nu). \qquad (7.240)$$

$$\Phi_0 = \tfrac{1}{20}\{8(\Phi_1 + \Phi_2 + \Phi_3 + \Phi_4) - 2(\Phi_5 + \Phi_6 + \Phi_7 + \Phi_8) - \\ - (\Phi_9 + \Phi_{10} + \Phi_{11} + \Phi_{12}) + \tfrac{1}{16}(w_5 - w_6 + w_7 - w_8)^2 - \\ - (w_1 - 2w_0 + w_3)(w_2 - 2w_0 + w_4)\}. \qquad (7.241)$$

We compose as many nonlinear algebraic equations of type (240) as values of deflection necessary to be found in internal nodes of the net region. The stress function is definite at internal and boundary nodes; at corner point $x = 0$ and $y = 0$, it is assumed that $\Phi = 0$.

Magnitudes of w and Φ at extra-contour nodes are expressed in terms of values at internal nodes by boundary conditions. We assume that edges of the plate are supported by hinge and that displacements of points of each edge in the plane of the plate are not constrained; then boundary conditions for edges $x = 0$ and $x = 1$ have the form

$$w = 0, \quad \frac{\partial^2 w}{\partial x^2} = 0, \quad \frac{\partial^2 \Phi}{\partial y^2} = -a, \\ \frac{\partial^2 \Phi}{\partial x \partial y} = 0. \qquad (7.242)$$

To these conditions there corresponds an <u>odd</u> continuation of function w and an <u>even</u> continuation of function Φ beyond the contour of the plate; at points on the contour $w = 0$. If we consider these relationships, then values of w and Φ at nodes lying on straight lines $x = 1 + c$, $x = 1 + 2c$, $y = 1 + c$, $y = 1 + 2c$ will not be additional unknowns.

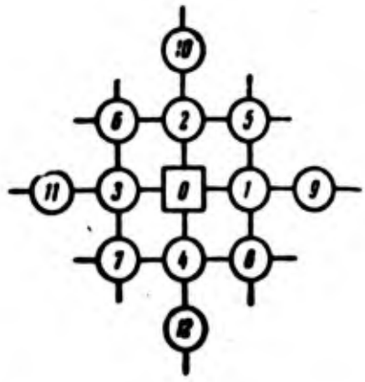

Fig. 7.43. Calculating cell.

Solution of system of differential equations (240) and (241) can be sought by successive approximations by the following scheme. We are given at nodes of the net region an initial (zero) approximation of functions w and Φ. Selecting the direction of advancing around the net (for instance, from node x = c, y = 0 along line y = const with transition between lines in the direction of increase of y), we put the taken values of $w^{(0)}$ and $\Phi^{(0)}$ into equation (241). The first approximation $\Phi^{(1)}$ and the zero approximation of functions of the remaining twelve neighboring points we use to determine the stress function at the node x = 2c, y = 0, etc. Finding $\Phi^{(1)}$ in the first line, we pass to line y = c. At internal nodes of net calculations start with application of formula (240), where the found value of deflection is used for calculating the function of stresses at that same point. One approximation is finished if values of functions at all nodes of the region, including extra-contour nodes, are calculated. With the selected order of advance operating formulas have the form

$$w_0^{(\nu+1)} = \varphi\left(w^{(\nu)}_{1,2,5,6,9,10},\ w^{(\nu+1)}_{3,4,7,8,11,12},\ \Phi^{(\nu)}_{0,1,2,5,6},\ \Phi^{(\nu+1)}_{3,4,7},\ \mu,\ c\right),$$

$$\Phi_0^{(\nu+1)} = \psi\left(w^{(\nu)}_{1,2,5,6},\ w^{(\nu+1)}_{0,3,4,7,8},\ \Phi^{(\nu)}_{1,2,5,6,9,10},\ \Phi^{(\nu+1)}_{3,4,7,8,11,12},\ c\right),$$

where ν is the number of the approximation. Values, pertaining to the $(\nu + 1)$th approximation, we use to accelerate the iterative process.

Iterations are repeated until we obtain solution of the system of differential equations with the necessary degree of accuracy. Error of the solution is approximately proportional to the square of

the step. Calculating for different values of the step, for instance, 1/6, 1/8, or 1/12, one can estimate error of solution with any step. Test calculations showed that error in determining deflection and stresses at various points of a square plate constitutes about 1.5–2.5% with a step c = 1/12 and 3–5% at step c = 1/8.

Described method was used to study post-critical deformation of a plate on the assumption that its edges are secured by hinge and remain rectilinear and that points of each edge are freely displaced along it. To this case there correspond, as we saw, the boundary conditions

$$w=0,\quad \frac{\partial^2 w}{\partial x^2}=0,\quad \frac{\partial^2 \Phi}{\partial x\,\partial y}=0,\quad \frac{\partial^2 \Phi}{\partial x^2}=0 \qquad (7.243)$$

for edges x = 0, x = 1.

It is necessary to remember that solution of system of principal equations of a flexible plate in post-critical region is many-valued. It is important to compose such a plan of the calculation process so that solutions pertaining to stable forms of equilibrium of plate at the given load were not lost. It is expedient, e.g., to construct process of calculation, proceeding from forms of buckling of the plate with one, two, three, etc., half-waves in direction of compression (m = 1, 2, 3, ...) and with one half-wave (n = 1) in the perpendicular direction. These forms correspond to first eigenvalues of the linear problem of stability of the plate:

$$\sigma_*=\frac{\pi^2(m^2+n^2)^2}{12(1-\mu^2)m^2}.$$

Let us give results of calculations, carried out on the digital computer "Arrow" with step c = 1/8. In Fig. 7.44 is depicted dependence between load σ and deflection in center of plate (for m = 1 and 3) or in center of half the plate (for m = 2). For case m = 3 deflection is laid off with reverse sign. As can be seen from the graph, on first stage of post-critical deformation, at $3.62 < \sigma < 5.65$, there

is only one equilibrium form of plate with one half-wave in the direction of compression. With growth of compressive load in center part of the plate there gradually is developed a hollow, directed in the opposite direction to the "principal" deflection. Therefore, growth of maximum deflection is delayed: at $\sigma > 16$ maximum deflection

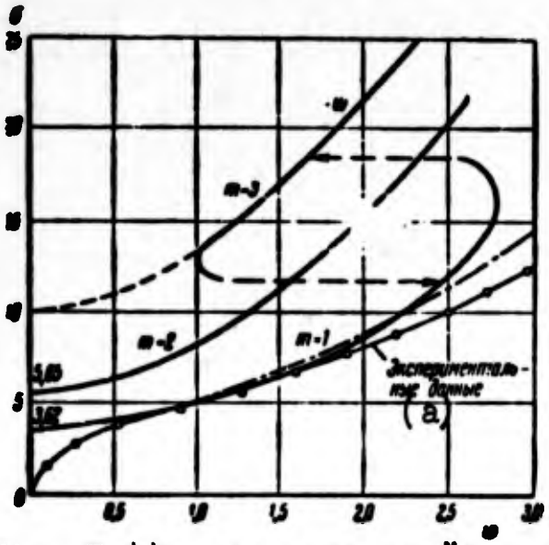

Fig. 7.44. Dependence "force of compression — deflection" according to computing on digital machine.
KEY: (a) Experimental data.

begins to decrease. Finally, at $\sigma = 18.5$ the first form becomes unstable, at least in the "computing sense": the iterative process converges here already to the form of buckling with three half-waves. Proceeding along the branch of the solution for $m = 3$ downward, we can not reach the third eigenvalue (dotted part of curve $m = 3$ is conducted hypothetically); at $\sigma < 12$ we again arrive at a form of bending by one half-wave. It is possible to consider that two branches of stable equilibrium forms are connected by a branch of an unstable state of the plate.

With a load, exceeding second eigenvalue $\sigma = 5.65$, we obtain also branch of antisymmetric forms of buckling ($m = 2$); this confirms the

the conclusion of S. A. Alekseyev.

In Fig. 7.44, there are also plotted the experimental points of Yamaki [7.23]; they agree well with results of computing by method of nets for $w < 2$.

In Fig. 7.45 is presented dependence between load, referred to first critical value, and mutual displacement of loaded edges, also referred to critical magnitude; here too are presented results of calculations of Yamaki. Proceeding from these data, one can determine reduction factor; its values are given in Fig. 7.41. As we see, introduction into consideration of the antisymmetric form allowed us to definitize magnitude φ as compared to the solution of Levy. Characteristically, in contrast to previous solutions, we obtain here several branches according to different "generating" forms of buckling of the plate.

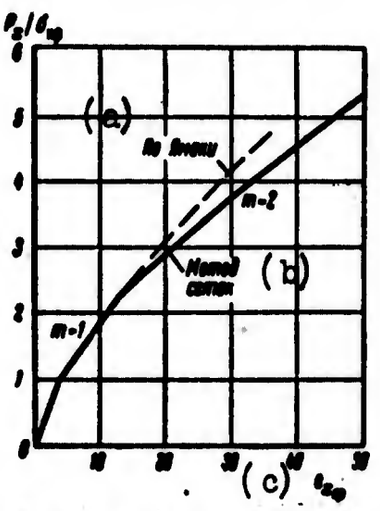

Fig. 7.45. Dependence "effort of compression — nearing of edges."
KEY: (a) Per Yamaki; (b) Net method; (c) e_x average.

§ 91. Case of Distorted Edges.

All the preceding calculation pertained to case where edges of plate remain rectilinear, or, in other words, when reinforcing ribs are sufficiently hard. To find the significance of this condition, consider the same problem for a square plate (a = b) on the assumption that hinged-fastened edges freely bend, remaining in the plane of the support contour.*

Here stress σ_x and σ_y in middle surface for points of the edges must be such that

$$\left.\begin{aligned} \sigma_x &= -\sigma \text{ when } x=0,\ b; \\ \sigma_y &= 0 \quad \text{when } y=0,\ b. \end{aligned}\right\} \tag{7.244}$$

We shall consider, furthermore, that tangential stresses are equal to zero "on an average" along each edge of the plate:

$$\frac{1}{b}\int_0^b \tau\, dy = 0 \quad \text{when} \quad x=0,\ b. \quad y=0,\ b. \tag{7.245}$$

We select a method of solution of the problem, differing from that adopted in Section 89; we apply the Bubnov-Galerkin method not only with respect to equation of equilibrium (63), as before, but also to equation of compatibility of deformations (64).**

In first approximation we take for functions w and Φ expressions

$$w = f \sin\frac{\pi x}{b}\sin\frac{\pi y}{b}, \quad \Phi = B\sin\frac{\pi x}{a}\sin\frac{\pi y}{b} - \frac{\sigma y^2}{2}. \tag{7.246}$$

As it is easy to see, all these boundary conditions will hereby be satisfied.

We compose equations

$$\int_0^b\int_0^b X \sin\frac{\pi x}{b}\sin\frac{\pi y}{b}\,dx\,dy = 0, \quad \int_0^b\int_0^b Y \sin\frac{\pi x}{b}\sin\frac{\pi y}{b}\,dx\,dy = 0. \tag{7.247}$$

---

*This problem was investigated by P. Ya. Polubarinova-Kochina (Applied Math. and Mech. 3, No. 1 (1936), pp. 16-22), applying for its solution an original method which received the name "of perturbation calculation."

**This way was offered by V. Z. Vlasov [10.3] and is applied in works of M. A. Koltunov [7.6] and other authors.

where by X is designated, as before, expression (225), and by Y there is understood according to (64) expression

$$Y=\frac{1}{E}\nabla^4\Phi+\frac{1}{2}L(w,w). \qquad (7.248)$$

Substituting (246) in (247) and considering $f \neq 0$, we arrive at the following relationships:

$$c=\frac{4\pi^2 D}{b^2 h}-\frac{32}{3}\frac{B}{b^2}, \quad B=-\frac{4}{3\pi^2}Ef^2. \qquad (7.249)$$

Hence

$$c=c_{cl}+\frac{128}{9\pi^2}E\left(\frac{f}{b}\right)^2. \qquad (7.250)$$

We compare this formula with (227); the coefficient in the second member, equal here approximately to 1.44, with rectilinear edges was equal to 1.23.* Comparison of these magnitudes must be made with caution, since they are obtained by different methods. It is desirable to continue the solution given here and to find definitized results, as was done for the other problem by M. A. Koltunov (see p.769).

§ 92. Data for Practical Calculations.

We have met certain methods of solution of problem of post-critical behavior of a plate, leading to various calculating graphs and formulas. Which of them should be recommended for practical calculations?

Comparison of results obtained for cases of rectilinear and distorted edges shows that the effectiveness of sheeting after loss of stability in great measure is determined by rigidity of reinforcing ribs. If the ribs are markedly rigid and the sheeting is divided into

---

*In work of P. Ya. Polubarinova-Kochina (op. cit., p.392) with that same structure of formula there was obtained a somewhat different coefficient, equal to 1.804.

a series of adjacent panels, reduction factors should be determined by the curve of Fig. 7.41, obtained with the help of the method of nets; this solution should, obviously, be considered the most reliable.

Solutions of Levy and Marguerre give for this region of variation of n^* (which is covered by graph of Fig. 7.41) values of φ close to curve of the method of nets.

However, in case of relatively weak reinforcing ribs and if panel is isolated, so that there is no sureness that condition of rectilinearity of edges will be carried out, it is necessary to use Kármán's formula (210):

$$\varphi=\sqrt{\frac{T}{n^*}}=\sqrt{\frac{\sigma_{kp}}{\sigma_p}}. \tag{7.210a}$$

giving usually values of φ in the safety factor. Substituting the minimum value of σ_{kp} by (97), we obtain

$$\varphi=1.9\sqrt{\frac{E}{\sigma_p}}\frac{h}{b}. \tag{7.210b}$$

Reduced width then is equal to

$$b_{np}=1.9h\sqrt{\frac{E}{\sigma_p}}. \tag{7.210c}$$

When one of the loaded sides is secured by hinge, and the other is free, we recommend a formula, close to (229):

$$\varphi=0.44+0.56\frac{\sigma_{kp}}{\sigma_p}. \tag{7.210d}$$

All these methods of calculation pertain to elastic region.

§ 93. Anisotropic Plates.

Study of stability of plates possessing different mechanical properties in different directions attracted attention to itself initially in connection with application in structures of such a material

as plywood, possessing marked anisotropy.* At present this region obtained special urgency thanks to rapid introduction of glass plastics, which are also anisotropic. This is stresses in the name of one form of plastic – "SVAM" which signifies, "fiberglass anisotropic material." Furthermore, certain plates can be considered as "structurally anisotropic" (see Section 94).

Let us consider orthotropic plates, whose elastic properties are characterized by four independent magnitudes: elastic moduli E_1 and E_2 for two mutually perpendicular main directions x and y, shear modulus G and Poisson's ratio μ_1, corresponding to transverse deformation along axis y. A second factor μ_2, corresponding to transverse deformation in direction x, is connected to μ_1 by the relationship

$$\mu_2 = \frac{E_2}{E_1}\mu_1. \tag{7.251}$$

Equations of Hooke's law take the form

$$\left.\begin{aligned} \varepsilon_x &= \frac{\sigma_x}{E_1} - \mu_2\frac{\sigma_y}{E_2}, \\ \varepsilon_y &= \frac{\sigma_y}{E_2} - \mu_1\frac{\sigma_x}{E_1}, \\ \gamma &= \frac{\tau}{G}. \end{aligned}\right\} \tag{7.252}$$

or

$$\left.\begin{aligned} \sigma_x &= \frac{E_1}{1-\mu_1\mu_2}(\varepsilon_x + \mu_2\varepsilon_y), \\ \sigma_y &= \frac{E_2}{1-\mu_1\mu_2}(\varepsilon_y + \mu_1\varepsilon_x), \\ \tau &= G\gamma. \end{aligned}\right\} \tag{7.253}$$

We introduce designations for flexural rigidity in the principle directions

$$D_1 = \frac{E_1h^3}{12(1-\mu_1\mu_2)}, \quad D_2 = \frac{E_2h^3}{12(1-\mu_1\mu_2)} \tag{7.254}$$

and for torsional rigidity

$$D_3 = \frac{1}{12}Gh^3; \tag{7.255}$$

*Basic work in this region belong to M. T. Huber, Teoria sprezystosci, Warsaw, 1950 and S. G. Lekhnitskiy, Anisotropic plates, Gostekhizdat, M., 1947.

then instead of (11) we obtain the following expressions for bending and torsional moments:

$$M_x = D_1(\varkappa_x + \mu_2\varkappa_y), \quad M_y = D_2(\varkappa_y + \mu_1\varkappa_x), \quad H = 2D_k\chi. \tag{7.256}$$

From equations of equilibrium of a member of the plate (16) and (17) we find

$$Q_x = \frac{\partial}{\partial x}(D_1\varkappa_x + D_3\varkappa_y), \quad Q_y = \frac{\partial}{\partial y}(D_2\varkappa_y + D_3\varkappa_x); \tag{7.257}$$

by D there is understood <u>reduced rigidity</u>:

$$D_3 = D_1\mu_2 + 2D_k = \frac{1}{2}(D_1\mu_2 + D_2\mu_1 + 4D_k). \tag{7.258}$$

For an orthotropic plate equation (23) takes the form

$$D_1\frac{\partial^4 w}{\partial x^4} + 2D_3\frac{\partial^4 w}{\partial x^2\partial y^2} + D_2\frac{\partial^4 w}{\partial y^4} + \\ + h\left(\sigma_x\frac{\partial^2 w}{\partial x^2} + \sigma_y\frac{\partial^2 w}{\partial y^2} + 2\tau\frac{\partial^2 w}{\partial x\,\partial y}\right) = 0, \tag{7.259}$$

which corresponds to equation (26).

Equations (63) and (64), relating to <u>flexible</u> plates, must be replaced by the following ones [0.3]:

$$D_1\frac{\partial^4 w}{\partial x^4} + 2D_3\frac{\partial^4 w}{\partial x^2\partial y^2} + D_2\frac{\partial^4 w}{\partial y^4} = hL(w, \Phi), \tag{7.260}$$

$$\delta_2\frac{\partial^4 \Phi}{\partial x^4} + 2\delta_3\frac{\partial^4 \Phi}{\partial x^2\partial y^2} + \delta_1\frac{\partial^4 \Phi}{\partial y^4} = -\frac{1}{2}L(w, w), \tag{7.261}$$

where

$$\delta_1 = \frac{1}{E_1}, \quad \delta_2 = \frac{1}{E_2}, \quad 2\delta_3 = \frac{1}{G} - \frac{\mu_1}{E_1} - \frac{\mu_2}{E_2}. \tag{7.262}$$

We investigate stability of an orthotropic plate, fixed by hinge at its edges and compressed in one direction; coordinate axes we plot as in Fig. 7.14. Boundary conditions have the form:

$$w = 0, \quad \frac{\partial^2 w}{\partial x^2} + \mu_2\frac{\partial^2 w}{\partial y^2} = 0 \quad \text{when} \quad x = 0, \quad x = a,$$

$$w = 0, \quad \frac{\partial^2 w}{\partial y^2} + \mu_1\frac{\partial^2 w}{\partial x^2} = 0 \quad \text{when} \quad y = 0, \quad y = b.$$

Taking for w the former expression (80) and considering in equation (259) $\sigma_y = \tau = 0$, we obtain

$$\sigma_x = \frac{\pi^2\sqrt{D_1D_2}}{b^2}\left[\sqrt{\frac{D_1}{D_2}}\left(\frac{mb}{a}\right)^2 + \frac{2D_k}{\sqrt{D_1D_2}}n^2 + \sqrt{\frac{D_2}{D_1}}\left(\frac{a}{mb}\right)^2\right]. \tag{7.263}$$

Obviously, in this expression we must set n = 1. Critical stress σ_{kp} we determine, varying the number of half-waves m. For a plate, <u>elongated</u> along axis x(a >> b), we have

$$\sigma_{kp} = \frac{2\pi^2\sqrt{D_1D_2}}{b^2}\left(1 + \frac{D_3}{\sqrt{D_1D_2}}\right). \tag{7.264}$$

Considering D_1, D_2, and D_3 equal to D, we arrive at the former formula (77) for an isotropic plate. For a plate with a finite ratio of sides we must assume

$$m=1 \text{ when } 0<\frac{a}{b}<\sqrt[4]{4\frac{D_1}{D_2}}.$$

$$m=2 \text{ when } \sqrt[4]{4\frac{D_1}{D_2}}<\frac{a}{b}<\sqrt[4]{36\frac{D_1}{D_2}}.$$

$$m=3 \text{ when } \sqrt[4]{36\frac{D_1}{D_2}}<\frac{a}{b}<\sqrt[4]{144\frac{D_1}{D_2}} \text{ etc.}$$

Let us note that number of half-waves formed in the direction of compression essentially depends on ratio of rigidities D_1/D_2. A plate with low rigidity D_1 will buckle, all things equal, in a larger number of half-waves than an isotropic plate.

§ 94. Reinforced Plates.

Plates, in construction of an airplane fuselage, a ship hull, an all-metal railroad car, etc., as a rule, are reinforced by reinforcing ribs. In practical calculations it is necessary to determine critical load not only for a strip of the plate lying between ribs, but also for the reinforced plate as a whole. Here there are possible two approaches to the problem. The first of them consists in considering the reduced anisotropy of the plate with rigidity of ribs "spread" along the section. If the plate has only longitudinal ribs, as shown in Fig. 7.46, then rigidities of the equivalent anisotropic plate can be considered equal to

$$D_1=\frac{EI}{l}+\frac{Eh^3}{12(1-\mu^2)}, \quad D_2=D_3=\frac{Eh^3}{12(1-\mu^2)}, \tag{7.265}$$

where I is the moment of inertia of a section of the rib with respect to the axis passing through the center of gravity of the section, l is the distance between ribs. Obvious, this way of calculation is applicable if the ribs are located sufficiently close together: magnitude $1/n$, where n is the number of ribs in the whole width of the plate, should be small as compared to unity [7.5]. Torsional rigidity of ribs in formulas (265) is ignored.

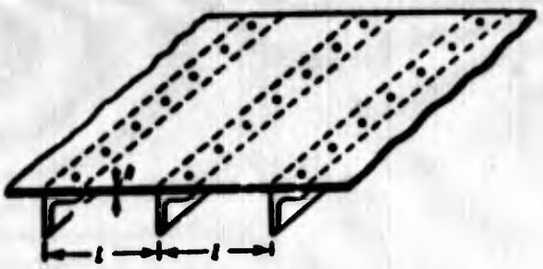

Fig. 7.46. Determination of reduced rigidity of a reinforced plate.

Another approach consists of studying the plate with discretely placed ribs. Let us consider as an example the problem of stability of a plate, fixed by hinge at its edges and reinforced by one longitudinal rib, located in the middle of the span* (Fig. 7.47. We will take into account only the flexural rigidity of rib in the plane perpendicular to the plane of the plate. We write differential equation (70) in application to one of the halves of the plate. Its integral we present in the form (89):

$$w = Y(y)\sin\frac{m\pi x}{a}, \tag{7.266}$$

then we arrive at equation (90) for function Y(y). Its solution has the form (96):

$$Y(y) = C_1 \operatorname{ch}\alpha y + C_2 \operatorname{sh}\alpha y + C_3\cos\beta y + C_4\sin\beta y; \tag{7.267}$$

α and β are determined by expressions (95). Boundary conditions for edge y = b/2 will be

$$w = 0,\quad \frac{\partial^2 w}{\partial y^2} = 0 \quad \text{when} \quad y = \frac{b}{2}. \tag{7.268}$$

If it is considered that plate buckles together with the rib, then, obviously, the deflection surface should symmetric to line y = 0; this leads to the condition

$$\frac{\partial w}{\partial y} = 0 \quad \text{when} \quad y = 0. \tag{7.269}$$

Further, to rib there will be transmitted the difference of reactive forces from two strips of the plate, determined by a formula of type (34):

$$R_y = -D\left[\frac{\partial^3 w}{\partial y^3} + (2-\mu)\frac{\partial^3 w}{\partial x^2 \partial y}\right]. \tag{7.270}$$

---

*This problem was considered by S. P. Timoshenko (Izv. In-ta. inzh. putey soobshch., St. Petersburg, 1915). (R. Barbre' Ingenieur-Archiv, 1937, p. 117). Graphs of Figs. 7.45 and 7.50 were taken from book [0.19].

As it is easy to see, when composing difference of forces one must take into account only first members in the brackets. If it is considered that rib together with plate is subjected to action of compressive stress σ_x, then for bending line of rib we obtain the following equation:

$$\left(EI\frac{\partial^4 w}{\partial x^4}+F\sigma_x\frac{\partial^2 w}{\partial x^2}+2D\frac{\partial^2 w}{\partial y^2}\right)_{y=0}=0; \qquad (7.271)$$

here I and F are the moment of inertia and area of the rib cross-section.

We use parameters

$$\alpha=\frac{a}{b},\quad \gamma=\frac{EI}{Db},\quad \delta=\frac{F}{bh}. \qquad (7.272)$$

Magnitudes δ and γ characterize relationship between rigidities and areas of sections of the rib and plate. Introducing in conditions (268) – (272) expression (266), we obtain system of equations for C_1, ..., C_4. Equating to zero the determinant of this system, we arrive at the following equation:

$$\left(\frac{1}{\beta\alpha}\operatorname{th}\frac{\beta\alpha}{2}-\frac{1}{\beta\beta}\operatorname{tg}\frac{\beta\beta}{2}\right)\left(\frac{\gamma m^2}{\alpha^2}-K\delta\right)\frac{m^2\pi^2}{\alpha^2}-4\frac{m}{\alpha}\sqrt{K}=0. \qquad (7.273)$$

By K here is implied ratio of critical stress to Euler's stress, determined for a plate with free edges:

$$K=\frac{\sigma_{kp}}{\sigma_0}=\frac{\alpha b^2 h}{\pi^2 D}. \qquad (7.274)$$

Equation (273) is solved by trial-and-error. Results for cases $\delta = 0$ and $\delta = 0.2$ presented in Fig. 7.48. To each pair of values of γ and δ there corresponds a series of curves, constructed for different numbers of half-waves m. Curves $\gamma = 0$ and $\delta = 0$ correspond on unreinforced plate and reproduce the graph of Fig. 7.15. It is interesting to note that for $\gamma = 0$ and $\delta = 0.2$ we obtain values of K lying lower than for a smooth plate. In this case, obviously, the rib no longer is a reinforcing member, and is itself supported by the plate.

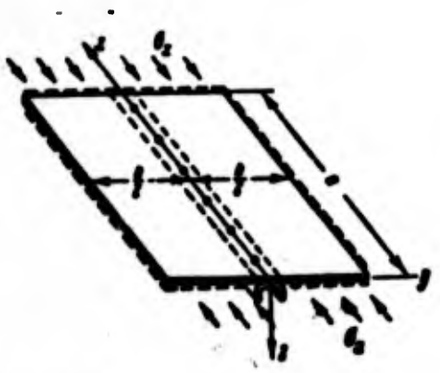

Fig. 7.47. Plate reinforced by one longitudinal rib.

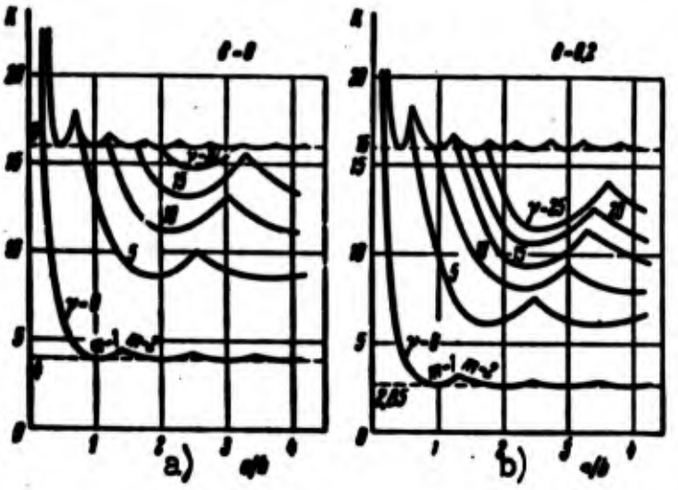

Fig. 7.48. Data for calculation of reinforced plates.

Gradually increasing rigidity of the rib, it is possible to arrive at a point where critical stress of local buckling of each half of the plate (Fig. 7.49a) is less than critical stress of total loss of stability for the plate together with the rib (Fig. 7.49b).

Curves of local loss of stability bound in Fig. 7.48 a series of curves characterizing total losses of stability; when a > b minimum value of K is close to 16. By analogy with the problem of stability of a bar on elastic supports we shall call critical or equivalent that rigidity of a rib, at which it can be considered absolutely hard. The equivalent rigidity of a rib $\gamma_{экв}$ is determined, obviously, by point of intersection of curves pertaining to total and local loss of stability on graphs of the type of Fig. 7.48. For instance, when $\delta = 0.2$ and $a/b = 1$ we find $\gamma_{экв} \approx 10$. In Fig. 7.50 are given values of $\gamma_{экв}$ depending upon parameters α and δ according to (272). Since critical stresses of total and local loss of stability depend on the number of half-waves of the deflection surface, the curves of Fig. 7.50 have "dips." Practically these curves smooth off after the first maximum, as was shown by the dotted lines.

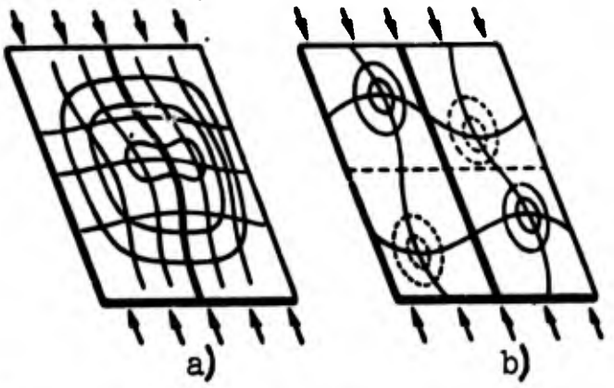

Fig. 7.49. Various forms of stability of a reinforced plate.

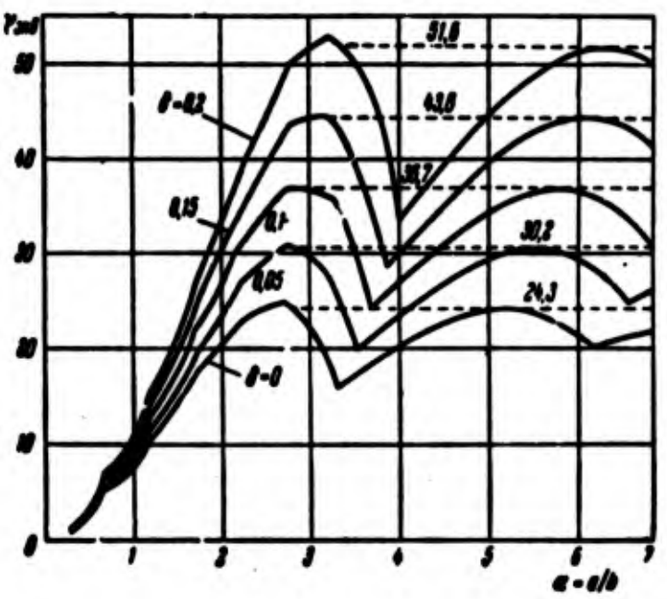

Fig. 7.50. Equivalent rigidity of ribs.

We analyzed a very simple example of a plate joined to one elastic longitudinal rib. Let us assume now that the plate is reinforced by a system of longitudinal and transverse ribs. Then the method of solution of the problem, which we used, turned out to be very complicated: it is necessary to constitute conditions of linkage of plate and ribs on many lines. If the system is "regular," e.g., if distance between ribs is identical, and their rigidities are equal, then for solution of the problem it is possible to use the method of finite

differences. In general for research of the stability of a combined system they frequently use the energy method, joining to strain energy of the plate flexural energy of the ribs and also taking into account work of external forces applied to the ribs.* As a result there were obtained for application to various structures tables and graphs for determination of critical forces and equivalently rigidity of ribs.**

§ 95. Supporting Power of Reinforced Panels Under Compression.

We considered various approaches to calculation of reinforced plates for total and local stability. How do we determine optimal relationship between rigidities of a plate and its reinforcing members? How do we determine supporting power of a combined structure? These questions inevitably arise in design work.

For some structures from the conditions of utilization local buckling of sheeting between ribs is considered impermissible. Then the criterion of least weight of the structure will be equality of critical stresses, pertaining to local stability of the individual panel of the plate and to general stability of the structure.

However, in many cases local loss of stability of sheeting is permissible. E.g., passenger of an aircraft, watching deformation of the wing, may be convinced that the skin of the compressed zone of the wing obtains hollows, located between stringers and wing ribs (Fig. 7.51).*** Influence of repeated knocks of skin on fatigue of

---

*This method was applied to reinforced plates by S. P. Timoshenko [6.13], solving a series of concrete problems; subsequently it was used by P. F. Papkovich [0.7], A. V. Karmishin [7.5] and other authors.

**See, e.g., "Designer's Reference Book (calculating-theoretical), edited by A. A. Umanskiy, Stroyizdat, M., 1960.

***Photographs of Fig. 7.51, 7.53 and 7.57 – 7.59 are taken from book of (H. Hertel, Leichtbau, Springer-Verlag, 1960).

the structure should be considered specially.

Process of deformation of a reinforced plate under gradual loading by compressive forces consists of the following. If plate is sufficiently thin, then local buckling of it sets in at comparatively

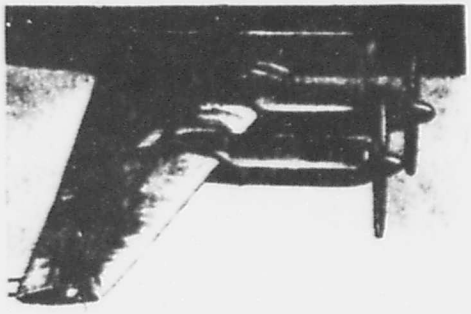

Fig. 7.51. Buckling of skin in compressed zone of an aircraft wing.

low compressive stresses (Fig. 7.52.)

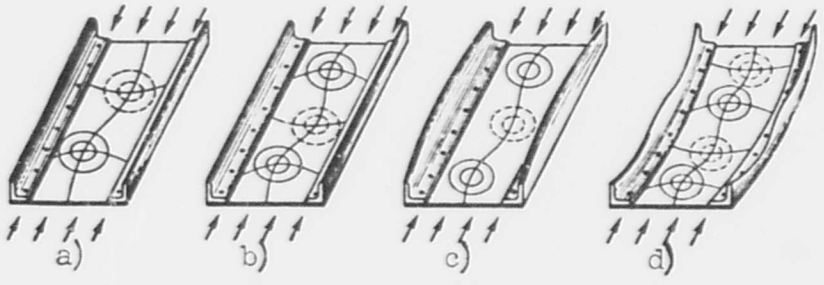

Fig. 7.52. Consecutive stages of buckling of a plate reinforced by thin-walled ribs.

Subsequently the hollows deepen; here from time to time there occurs a change in the number of hollows, frequently accompanied by knocks. When skin is divided into panels of different width, for instance with reinforcement by U-shape ribs, then in a later stage there occurs loss of stability of "narrow" panels (Fig. 7.53). If the reinforcing

rib is thin-walled, then the following stage consists of local loss of stability of members of the rib — wall or flanges. At separate stages of loading in the skin and webs of reinforcing sections there appear plastic flows. Finally, there appears total loss of stability or the structure; it buckles as a whole, like a compressed bar or a plate secured on its edges; together with this the sheeting and walls of sections are additionally bent. At this instant the supporting power of the structure is exhausted.

Fig. 7.53. Buckling of different strips of a compressed reinforced panel.

Thus, determination of supporting power of a structure is reduced to calculation of it for total stability, where sheeting, and in separate cases the walls of reinforcing sections must be considered taking into account reduction factors. Since reduction factors depend on magnitude of compressive stress in the ribs, the calculation is made by successive approximations: given tentative values of maximum load, they find reduction factors, determine load, anew, etc. In examining total stability reduction factors for sheeting and walls of a section are usually assumed the same as in the case of "static" compression,* i.e., by data of Section 92.

Example 7.3. Determine supporting power for panel of width B = = 450 mm, thickness h = 1 mm (Fig. 7.54a), reinforced by four stringers and compressed lengthwise. Section of stringer is shown in Fig. 7.54b, by C is understood center of gravity. Material of skin and stringers is

*A more strict approach to problem requires determining reduction factors taking into account the fact that compressed edges of the plate shift relative to one another (See [0.3], p. 155).

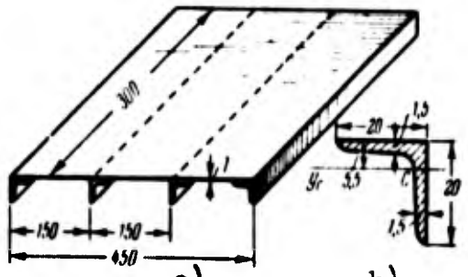

a) b)

Fig. 7.54. Calculation of supporting power of panel, reinforced by four stringers.

duralumin: $E = 0.72 \cdot 10^6$ kg/cm^2, $\mu = 0.32$, $\sigma_{пц} = 2800$ kg/cm^2. Calculate thickness of sheeting on the assumption that two intermediate stringers are removed, and the supporting power remained as before. Compare weight of new panel with weight of the initial one.

We assume, first, that supporting power is determined by local loss of stability of the free flange of the stringer. Considering this flange as a plate for which one of the loaded edges is clamped, and the other is free, we find critical stress by Fig. 7.23, equal to

$$\sigma_{стр} = \frac{0{,}46\pi^2 D}{b^2 h} = \frac{0{,}46 \cdot \pi^2 \cdot 0{,}72 \cdot 10^6 \cdot 0{,}15^3}{12(1-0{,}32^2)\,20^2} = 1680 \text{ kg/cm}^2.$$

[стр = stringer]

We calculate reduction factor for sheeting (with this stress in the rib) by (210b):

$$\varphi = 1{,}9\frac{0{,}1}{15}\sqrt{\frac{0{,}72 \cdot 10^6}{1680}} = 0{,}262.$$

Supporting power of panel is equal to

$$P = 1680(4 \cdot 0{,}584 + 0{,}262 \cdot 0{,}1 \cdot 45) = 1680 \cdot 3{,}52 = 5900 \text{ kg}.$$

We determine critical load for total loss of stability, considering panel as a compressed bar. We arbitrarily consider area of the sheeting with the former reduction factor 0.261, and section of stringer – with a factor of 1. We calculate coordinate of center of gravity of reduced section $y_{ц.т}$, counting from axis y_C, passing through center of gravity of the angles (Fig. 7.55):

$$y_{ц.т} = \frac{0{,}1 \cdot 45 \cdot 0{,}262 \cdot 0{,}6}{3{,}52} = 0{,}2 \text{ см}.$$

Moment of inertia of reduced section is equal to

$$I = 4 \cdot (0{,}222 + 0{,}584 \cdot 0{,}2^2) + 0{,}1 \cdot 45 \cdot 0{,}262 \cdot 0{,}4^2 + \frac{45 \cdot 0{,}262 \cdot 0{,}1^3}{12} = 1{,}17 \text{ см}^4.$$

Fig. 7.55. Determining reduction factors.

Tentative value of critical Euler force appears equal to

$$P_э = \frac{\pi^2 \cdot 0{,}72 \cdot 10^6 \cdot 1{,}17}{45^2} = 9250 \text{ kg},$$

and corresponding stress will be

$$\sigma_э = \frac{9250}{3{,}52} = 2600 \text{ kg/cm}^2 < \sigma_{пр}.$$

Thus, breaking load corresponds to <u>total loss of stability</u> of the structure. In order to definitize magnitude $P_э$, one should find new reduction factors for sheeting, proceeding from stress σ_p = = 2600 kg/cm^2, and then make a new approximation (see next example).

Let us consider then the case when two intermediate stringers are removed, and let us assume that supporting power is determined by local stability of the stringer, so that stress σ_p is equal to 1680 kg/cm^2. We find thickness of sheeting h_1 from condition that load constitutes P = 5900 kg:

$$5900 = 1680\,(2 \cdot 0{,}584 + \varphi_1 \delta_1 \cdot 45); \qquad \text{(a)}$$

reduction factor φ_1 for sheeting is equal to

$$\varphi_1 = 1{,}9\,\frac{\delta_1}{45}\sqrt{\frac{0{,}72 \cdot 10^6}{1680}} = 0{,}875\delta_1.$$

Putting this value φ_1 in (a), we arrive at equation

$$3{,}5 = 1{,}168 + 39{,}3\delta_1^2.$$

Hence h_1 = 0.224 cm. We select a standard thickness h_1 = 0.25 cm. Determining, as in preceding case, the Euler force for the panel as a whole, we find $P_э$ = 6450 kg.

Weight of initial and new panels are related as the area of their sections:

$$\frac{G_1}{G_2} = \frac{4 \cdot 0{,}584 + 0{,}1 \cdot 45}{2 \cdot 0{,}584 + 0{,}25 \cdot 45} = 0{,}55.$$

Thus, with identical supporting power a panel with thin sheeting and four stringers appears approximately half as heavy as a panel with thick sheeting and two stringers.

Example 7.4. Calculate supporting power under compression for the duralumin panel depicted in Fig. 7.56a. Section of longitudinal ribs is shown in Fig. 7.56b; area of section $F = 0.684$ cm^2, moment of inertia about central axis $I = 0.204$ cm^4. Assume $E = 0.72 \cdot 10^6$ kg/cm^2, $\mu = 0.32$, $\sigma_{пц} = 2800$ kg/cm^2. How much would we increase maximum load, if length of panel is decreased to $l = 150$ mm?

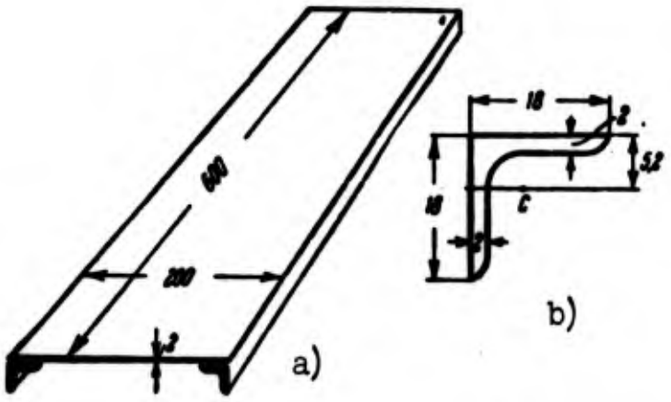

Fig. 7.56. Calculation of panel, reinforced by two stringers.

We shall determine the load corresponding to local loss of stability of the free wall of the stringer:

$$\sigma_{кр} = \frac{0{,}46 \cdot \pi^2 \cdot 0{,}72 \cdot 10^6 \cdot 0{,}2^2}{12(1-0{,}32^2)\,18^2} = 3680 \text{ kg/cm}^2.$$

This magnitude exceeds the limit of proportionality of the material; therefore, it must be definitized, proceeding from theory of stability of plates in plastic region (see Chapter VIII). We take as maximum stress $\sigma_{пц} = 2800$ kg/cm^2. Reduction factor for sheeting is equal to

$$\varphi = 1{,}9\,\frac{0{,}2}{20}\sqrt{\frac{0{,}72 \cdot 10^6}{2800}} = 0{,}3,$$

here the load will be

$$P = 2800\,(2 \cdot 0{,}684 + 0{,}2 \cdot 20 \cdot 0{,}3) = 7200 \text{ kg}.$$

Let us consider, further, total stability of the panel, taking for sheeting as the initial one the same reduction factor $\varphi = 0.3$, and for flange of stringer $\varphi = 1$. Center of gravity of reduced section will be found a distance from center of gravity of section of

stringer equal to

$$y_{\text{ц. т}} = \frac{0{,}2 \cdot 20 \cdot 0{,}3 \cdot 0{,}62}{2{,}57} \approx 0{,}3 \text{ см}.$$

Moment of inertia of reduced section is equal (see calculation in preceding example) to I = 0.66 cm^4. Critical force for panels of various length is

$$P^{(1)} = \frac{\pi^2 \cdot 0{,}72 \cdot 10^6 \cdot 0{,}66}{60^2} = 1300 \text{ kg} \quad P^{(2)} = 16 P_9^{(1)} = 20\,800 \text{ kg}.$$

For the first panel local loss of stability of the flange of the stringer, obviously, is excluded. In following approximation we take stress σ_p equal to

$$\sigma_p = \frac{1300}{2{,}57} = 500 \text{ kg/см}^2;$$

then reduction factor per (210b) will be φ = 0.72 and P = 2130 kg. Again we calculate coordinate of center of gravity of the reduced section, $y_{\text{ц. т}}$ = 0.42 cm, and find moment of inertia of section, I = = 0.77 cm^4. Euler's force is equal to P = 1520 kg. This value nevertheless strongly differs from the preceding one (2130 kg; therefore, we must make one more approximation, taking

$$\sigma_{\text{ср}} = \frac{1520}{4{,}25} = 360 \text{ kg/см}^2,$$

then φ = 0.85, P = 1720 kg. New coordinate of center of gravity $y_{\text{ц. т}}$ = 0.44 cm; here i = 0.792 cm^4. Value of critical force is P = = 1570 kg, which differs from the initial by 9%. Stopping with this approximation, we finally find the supporting power of the panel, equal to P ≈ 1600 kg.

Supporting power of second panel must be definitized, taking into account local loss of stability of flange of stringer. Taking conditionally for this panel as limiting load P = 7200 kg, we arrive at conclusion that shortening of the panel led to increase of supporting power of 7200/1600 = 4.5 times.

§ 96. Supporting Power of Compressed Thin-Walled Bars.

In Chapter IV we found that total loss of stability for a compressed thin-walled bar occurs in torsional-flexural or flexural form; here it was assumed that section of bar preserves its shape. Now we can consider a new circumstance – local loss of stability of walls of a section, where each wall here cannot buckle separately, but only jointly with others. This phenomenon leads to distortion of the shape of the section; it either precedes total loss of stability, or occurs after it, depending upon relationship between dimensions of the cross-section and length of the section.

Let us consider the case of a bar of channel section. With sufficiently great length of the bar most dangerous is the flexural or torsional-flexural form of loss of stability. If width of flange b is comparable with width of web a, the section loses stability in torsional-flexural form; at $b \ll a$, in flexural form. In Fig. 7.57a and b there is shown case of flexural loss of stability; in course of buckling there can additionally occur local buckling if the flanges are on the concave side (Fig. 7.57a).

For shorter bars at first there occurs local buckling of flanges and wall (Fig. 7.58a), and then torsion of section (Fig. 7.58b). Last, in case of short bar to local buckling will be dangerous (Fig. 7.59a and b).

Study of local buckling of a channel section is conducted taking into account simultaneous bending of flanges and wall* on the assumption that angles of the section remain straight. For each of these

---

*It was made by Kimm, Luftfahrtforschung, No. 5 (1941).

a) b)
Fig. 7.57. Flexural form of loss of stability of thin-walled bar.

a) b)
Fig. 7.58. Buckling of thin-walled bar, accompanied with torsion.

a) b)
Fig. 7.59. Local buckling of walls of bar.

members we write differential equations of flexure type (70), and also conditions of linkage. Results of calculations for a channel with constant web thickness are shown* in Fig. 7.60. Critical compressive stress is presented by formula

$$\sigma_{кр} = kE\left(\frac{h}{b}\right)^2.$$

Along the axis of abscissas in Fig. 7.60 is plotted ratio b/a; on axis of ordinates, values of k. Above is located the zone of local instability. Here too are given curves determining onset of flexural or torsional-flexural instability; the following magnitude serves as parameter

$$m = \frac{a}{b}\frac{a}{l}\frac{b}{h} = \frac{a^2}{lh}.$$

As one should have been led to expect, for low values m total loss of stability is dangerous. Zone of torsional-flexural instability is isolated.

---

*They belong to Winckler (by book of Hertel, op. cit., p.402).

Graph of Fig. 7.60 only lets us determine initial critical state. Important is determination of supporting power for that case when flexural or torsional-flexural instability sets in after local buckling (Fig. 7.58). Solution of this problem is difficult: "reinforcing ribs," which here are the angles of the section, do not remain straight as it is assumed in Section 89, but are twisted together with the whole section. One approach offered for the problem* consists in keeping the critical force, corresponding to local loss of stability, constant in magnitude and direction, remaining applied to center of gravity of the section. Further increase of load corresponds to supercritical force, which is balanced by additional compressive stresses, where resistivity of bar to action of these supercritical stresses is determined by the least (tangential) modulus, differing for each fiber. This important problem awaits more complete solution.

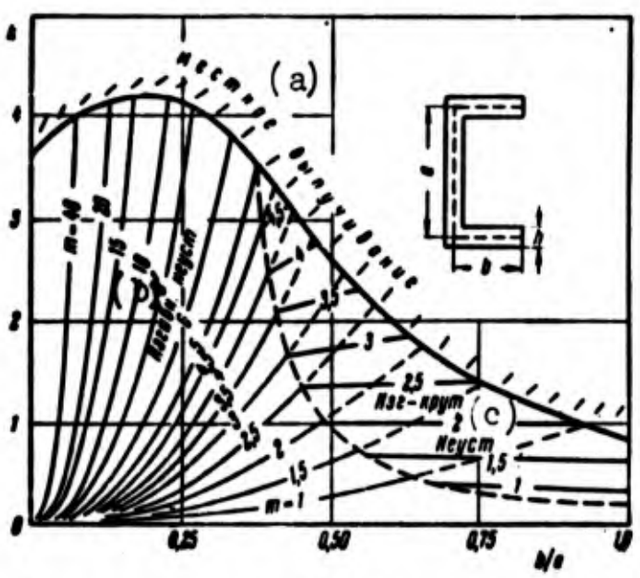

Fig. 7.60. Different variants of buckling of a channel section. KEY: (a) Local buckling; (b) Flexural instability; (c) Torsional-flexural instability.

*Problem is formulated by A. A. Umanskiy and was solved by B. I. Ivaniem.

§ 97. Post-Critical Behavior of Plate with Shear. Diagonally Stretched Field.

We previously considered post-critical deformation of a plate only during compression in one direction. However during calculation of certain structures it is necessary to take into account behavior of a plate after loss of stability due to shear. This pertains, for instance, to some panels of the wing or fuselage of an aircraft, and also to the webs of tall beams.

Thus as in case of compression, here there are two approaches to the problem. One consists in use of a model, allowing us to describe character of buckling of the plate during significant exceeding of tangential stresses of critical magnitude. The other approach consists in solving the problem on the basis of nonlinear theory of flexible plates. We shall first examine the first way.

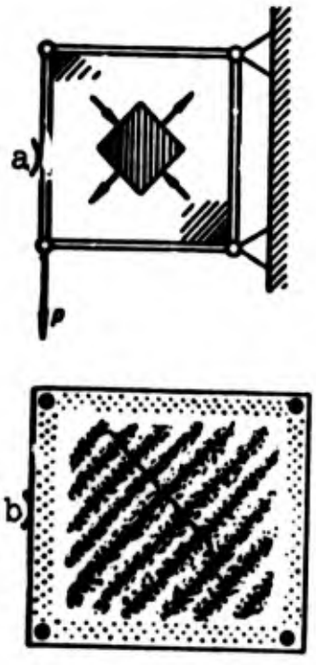

Fig. 7.61. Corrugation of a plate during shear.

We recall that during non-dilatational strain axes of principal stresses form with edges an angle equal to 45°, and one of the principal stresses is tensile, and the other, compressive. At loss of stability there occurs a sort of corrugation of the plate in the direction of principal compressive stress (Fig. 7.61). If edges of the plate remain in initial plane, then, here too, buckling leads to formation of stresses in the middle surface. Case of shear is interesting because the fibers of the plate, parallel to the folds, can

support very significant tensile forces, transmitted to longitudinal ribs. Reaction from longitudinal ribs are received in turn by transverse members: the latter are compressed. Thus, there is created a system of skew tensile forces, balanced by reactions of transverse ribs (struts). Such a model, simplifying true distribution of stresses in middle surface and flexural stresses, has the name of a diagonally stretched field.*

We shall in the first approximation consider that direction of folds coincides with direction of the principal tensile stress and that the principle compressive stress is equal to zero. In other words, we consider that plate is incapable of transmitting any forces normal to the corrugations.

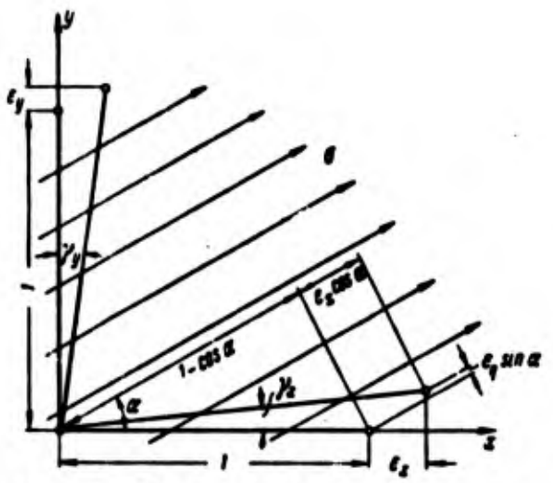

Fig. 7.62. Deformations in case of diagonally stretched field.

We designate: τ is shear stress in sections parallel to coordinate axes; σ is principal tensile stress; α is angle of inclination of vector of σ to longitudinal edges; ε and ε_q are deformations in

*The theory of a diagonally stretched field of developed by Wagner [7.22].

direction σ and perpendicularly to it.

We take $\varepsilon = \sigma/E$. Magnitude ε_q is composed of elastic deformation $(-\mu\sigma/E)$ and approach of points of plate, caused by formation of folds.

Let us consider deformation of a square with a side equal to one (Fig. 7.62). Deformations in directions x and y are equal to

$$\left.\begin{aligned} \varepsilon_x &= \varepsilon\cos^2\alpha + \varepsilon_q \sin^2\alpha, \\ \varepsilon_y &= \varepsilon\sin^2\alpha + \varepsilon_q \cos^2\alpha. \end{aligned}\right\} \tag{7.275}$$

Lines, parallel to the x and y axes during deformation will turn at angles γ_x and γ_y, equal to

$$\gamma_x = \gamma_y = (\varepsilon - \varepsilon_q)\sin\alpha\cos\alpha. \tag{7.276}$$

Deformation of shear will be

$$\gamma = \gamma_x + \gamma_y = (\varepsilon - \varepsilon_q)\sin 2\alpha. \tag{7.277}$$

Using these relationships, we find

$$\operatorname{tg} 2\alpha = \frac{\gamma}{\varepsilon_x - \varepsilon_y}, \tag{7.278}$$

$$\varepsilon = \frac{\varepsilon_x + \varepsilon_y}{2} + \frac{1}{2}\sqrt{(\varepsilon_x - \varepsilon_y)^2 + \gamma^2}. \tag{7.279}$$

$$\varepsilon_q = \frac{\varepsilon_x + \varepsilon_y}{2} - \frac{1}{2}\sqrt{(\varepsilon_x - \varepsilon_y)^2 + \gamma^2}. \tag{7.280}$$

These equations allow us to determine angle of inclination of folds and angle of slide, if we are given deformation of reinforcing ribs and deformation in the direction of the principal tensile stress:

$$\operatorname{tg}^2\alpha = \frac{\varepsilon - \varepsilon_x}{\varepsilon - \varepsilon_y}, \tag{7.281}$$

$$\gamma = 2\sqrt{(\varepsilon - \varepsilon_x)(\varepsilon - \varepsilon_y)}. \tag{7.282}$$

The last expression can also be presented in the form

$$\gamma = 2(\varepsilon - \varepsilon_x)\operatorname{ctg}\alpha. \tag{7.283}$$

We note the relationship

$$\varepsilon + \varepsilon_q = \varepsilon_x + \varepsilon_y. \tag{7.284}$$

Stress of slide τ is expressed through principal tensile stress in the following manner:

$$\tau = \frac{\sigma}{2} \sin 2\alpha. \tag{7.285}$$

Let us consider the case where reinforcing ribs can be considered undeformed, so that $\varepsilon_x = \varepsilon_y = 0$. Then from (281) we obtain:

$$\operatorname{tg}^2 \alpha = 1. \tag{7.286}$$

Thus, angle of inclination of folds will be equal to 45°. Further we find

$$\varepsilon = \frac{\sigma}{2}, \quad \gamma = 2\frac{\sigma}{E}. \tag{7.287}$$

From this

$$\tau = 0{,}25E\gamma. \tag{7.288}$$

Introducing idea of reduced modulus G_1, characterizing rigidity of plate after loss of stability, we have

$$G_1 = \frac{\tau}{\gamma} = 0{,}25E. \tag{7.289}$$

With respect to initial shear modulus G magnitude G_1 will constitute

$$G_1 = \frac{G(1+\mu)}{2} \tag{7.290}$$

or, for $\mu = 0.3$,

$$G_1 = 0{,}65G. \tag{7.291}$$

Thus, with undeformed reinforcing ribs rigidity of plate to shear drops after loss of stability by 35%; in case of deformed ribs this lowering will be greater.

§ 98. Study of Post-Critical Shear by Theory of Flexible Plates.

Model of diagonally stretched field is appropriate only with sufficiently well-developed post-critical deformation of the plate. If critical stress of shear is exceeded insignificantly, study should be based on the theory of flexible plates.

Let us consider a square plate with a side b, hinge-supported at the edges, subjected to action of shearing forces s on all edges. It

is assumed that edges can be distorted in plane of the support contour. We use equations (232) and (233); boundary conditions for edges $x = 0$ and $x = 1$ we take in the form

$$w=0, \quad \frac{\partial^2 w}{\partial x^2}=0, \quad \frac{\partial^2 \Phi}{\partial y^2}=0, \quad \frac{\partial^2 \Phi}{\partial x\,\partial y}=s. \tag{7.292}$$

We present basic equations and conditions (292) in finite differences, as this was described in Section 90. Below are presented results of the solution of the problem,* carried out on digital computer "ural-2," with step of net $c = 1/8$. Contour of net domain constitutes edges $x = 0$, $y = 0$ and diagonal $y = 1 - x$. Extra-contour points lay on lines $x = -c$ and $y = -c$. We considered that the plate is bent symmetrical to diagonal $y = 1 - x$.

In Fig. 7.63 solid lines depict dependence between parameter of load $\bar{s}$, equal to

$$\bar{s}=\frac{s}{E}\left(\frac{b}{h}\right)^2,$$

and deflection $\bar{w}$ at points A(1/2, 1/2) and B(3/4, 1/4), where magnitude $\bar{w}_B$ is plotted with reverse sign. Critical stress constitutes by (161) $\bar{s}_{kp} = 9.4$. Dotted lines present given solutions of the same problem by Bubnov-Galerkin method (see [0.3], p. 157) with introduction of two manipulated variables. As we see, error of such a solution appears significant.**

In Fig. 7.64 are plotted horizontals of deflection surfaces, pertaining to various values of $\bar{w}$ for $\bar{s} = 12$ and $\bar{s} = 50$. Critical stress was exceded in first case by 1.25 times, and in second, by 5.3 times.

---

*It was conducted by A. Yu. Birkgan.

**Let us note that in solution by Bubnov-Galerkin method boundary conditions (292), pertaining to function Φ, a satisfied only "on the average."

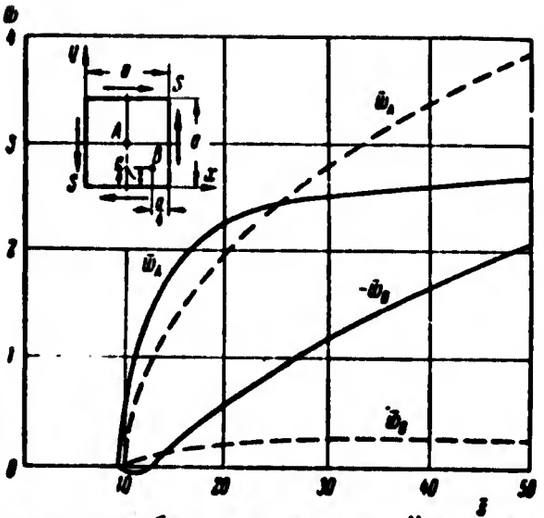

Fig. 7.63. Diagram "deflection – shear force" after loss of stability.

Judging by Fig. 7.51, with relatively large exceeding of critical stress in the middle part of the plate there form closely spaced folds, similar to those which correspond to model of a diagonally stretched field.

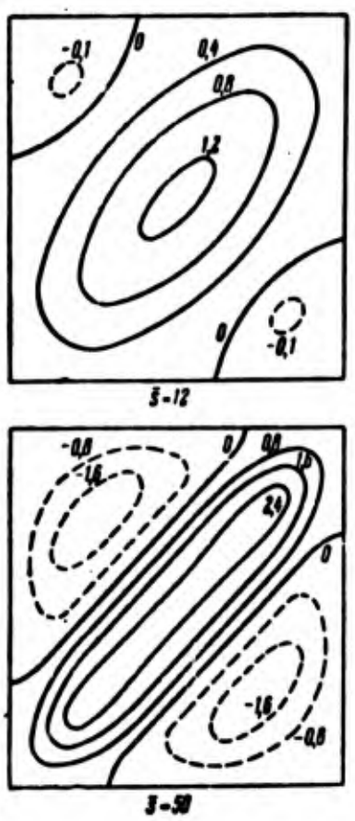

Fig. 7.64. Buckling of square plate during shear.

Literature

7.1. S. A. Alekseyev. Postcritical work of flexible elastic plates, Applied Math. and Mech., 20, No. 6 (1956), 673-679.

7.2. V. P. Belkin. Work of elements of deck covering after loss of stability, Sudpromgiz, L., 1956.

7.3. B. M. Broude. Stability of plates in elements of steel constructions, Mashstroyizdat, M., 1949.

7.4. A. S. Kalmanok. Structural mechanics of plates, Mashstroyizdat, 1950.

7.5. A. V. Karmishin. Stability of freely supported rectangular plates, reinforced by ribs, under action of uniform load, Eng. Collection of Acad. of Sci. of USSR, 24 (1956).

7.6. M. A. Koltunov. Postbuckling behavior of a plate, Herald of Moscow State University, No. 10 (1953); No. 6 (1962), 43-50.

7.7. A. S. Lokshin. Designing plates, reinforced by stiff ribs, Applied math. and mech., 2, No. 2 (1935).

7.8. S. N. Nikiforov. Compressed rectangular plate with longitudinal edges freely distorted in its plane, Scientific notes of Moscow State of University, 117, Mechanics, No. 1 (1946).

7.9. P. M. Ogibalov. Flexure, stability and vibration of plates, Moscow State University Press, 1958.

7.10. P. F. Papkovich. Concerning the question of buckling of flat plates, compressible by forces exceeding their Euler load, Naval collection, Nos. 8-9 (1920).

7.11. G. G. Rostovtsev. Longitudinally-transverse bending of a flexible rectangular plate, Eng. collection, 8 (1950), 83-104.

7.12. P. A. Sokolov. Stresses in a compressed plate after loss of stability, Transactions of NISS, No. 7 (1932).

7.13. S. P. Timoshenko. Stability of plates, reinforced by elastic ribs, Press of Institute for Engineering Ways of Communication, 1915.

7.14. G. H. Bryan. On the stability of a plane plate under thrusts in its own plane, Proc. of the London Math. Soc. 22 (1891).

7.15. H. L. Cox. Buckling of thin plates in compression, Rep. and Memor., Nos. 1553, 1554 (1933).

7.16. Th. Kármán, E. E. Sechler, and L. H. Donnell. The strength of thin plates in compression, Trans. ASME 54 (1932), 53-57.

7.17. S. Levy. Bending of rectangular plates with large deflections, NACA Rep. No. 737 (1942).

7.18. K. Marguerre. Die mittragende Breite des gedrückten Plattenstreifens, Luftfahrtforschung 14, No. 3 (1937) (translation ed. by A. A. Umanskiy, Oborongiz, Moscow, 1938).

7.19. E. Seydel. Ueber das Ausbeulen von rechteckigen isotropen oder orthogonal anisotropen Platten bei Schubbeanspruchung, Ing. Archiv 4 (1933), 169.

7.20. R. V. Southwell and S. W. Skan. On the stability under shearing forces of a flat elastic strip, Proc. of Royal Society, A105 (1924), 582.

7.21. E. Trefftz. Die Bestimmung der Knicklast gedrückter rechteckiger Platten, Z. für angew. Math. u. Phys. 15 (1935).

7.22. H. Wagner, Ebene Blechwandträger mit sehr dünner Stegblech, Zeitschr. f. Flugtechnik and Motorluftschiffahrt 20, No. 8-12 (1922), 200 (translation in collection edited by A. A. Umanskiy and P. M. Znamenskiy, Publishing House of Central Aero-Hydrodynamic Institute, 1937, 58-117).

7.23. N. Yamaki. Postbuckling behaviour of rectangular plates with small initial curvature loaded in edge compression, J. Appl. Mech 26 (1959), 407-414; 28 (1960), 335-342; Experiments on the post-buckling behaviour of square plates loaded in edge compression, J. Appl. Mech. 29 (1961), 238-244.

CHAPTER VIII

STABILITY OF RECTANGULAR PLATES BEYOND THE ELASTIC LIMIT

§ 99. Application of Theories of Plasticity to Problems of Stability of Plates

Formulas for calculation of plates for stability, derived for the elastic region, are applicable only for relatively small thickness of plate. Let us consider, for instance, an elongated hinge-supported plate compressed in one direction. Critical stress $\sigma_{кр}$ for such a plate is determined by formula (7.79), valid under the condition that magnitude $\sigma_{кр}$ does not exceed the proportional limit of the material, $\sigma_{кр} \leq \sigma_{пц}$. Ratio of width of plate to thickness should constitute

$$\frac{b}{h} \geqslant \sqrt{3{,}6\frac{E}{\sigma_{пц}}} \approx 1{,}9\sqrt{\frac{E}{\sigma_{пц}}}.$$

Maximum value b/h turns out to be equal for soft steels to about 60, and for duralumin, 36.

Meanwhile in real structures we frequently meet a plate, for which ratio b/h lies below the shown limit. This pertains, in particular, to aircraft structures: in heavy aircraft in connection with new aerodynamic requirements the thickness of the skin recently significantly increased. Therefore, research of stability of plates during plastic flows is very important; it is necessary also for structures of glass plastics, proportional limit of these materials is

comparatively low.

In Chapter II it was shown that, the problem of stability of a bar in the elastoplastic region is complicated, if we determine the relationship between zones of loading and unloading in a section of the bar depending upon conditions of application of external forces. All the more difficult is research of buckling of plate; in each layer of the plate there will form, not uniaxial, as in the case of a bar, but a plane stress.

At present there are two approaches to solution of the problem of stability of plates during plastic deformations. One of them consists in considering the plate anisotropic, i.e., not having that cylindrical rigidity which is determined for the elastic region, but different rigidities for flexure in two directions and for torsion. Relationship between rigidities depends on how much the proportional limit is exceeded by some "fundamental" (subcritical) forces.

For instance, in case of uniaxial compression instead of differential equation (7.70)*

$$D\left(\frac{\partial^4 w}{\partial x^4}+2\frac{\partial^4 w}{\partial x^2\partial y^2}+\frac{\partial^4 w}{\partial y^4}\right)=-\sigma_x h\frac{\partial^2 w}{\partial x^2} \qquad (a)$$

we propose to take as the basis the following:

$$D\left(\lambda\frac{\partial^4 w}{\partial x^4}+2\lambda^*\frac{\partial^4 w}{\partial x^2\partial y^2}+\frac{\partial^4 w}{\partial y^4}\right)=-\sigma_x h\frac{\partial^2 w}{\partial x^2}. \qquad (b)$$

Coefficient of decrease of rigidity λ in direction x some authors consider equal to $\lambda = T/E$, where T is resultant modulus for a bar of rectangular section, and others – $\lambda = E_K/E$, where E_K is the tangential modulus. Coefficient of torsional rigidity is taken within limits

---

*Such an approach is contained in books of S. P. Timoshenko [0.23], F. Bleich and J. Geckeler, and also in a number of works of Kollbrunner (see [0.19]).

$\lambda < \lambda^* < 1$; most frequently we consider $\lambda^* = \sqrt{\lambda}$. Here it is assumed that plastic properties of material must be manifested mainly in direction of fundamental stress σ_x, whose magnitude exceeds proportional limit. Regarding direction y, then here material is considered "fresh" and as having an elastic modulus. For torsional rigidity there is taken a certain intermediate characteristic. This approach allows us to obtain without exceptional difficulties calculating formulas for critical stresses, but it must be considered only approximate. We know well that in complex state of strain plastic properties of a material at every given point of a solid depend on certain total characteristics, in which stress and deformation in the direction of a given axis enter only as certain components. These characteristics are determined by theories of plasticity. Therefore, valid research of buckling of plates in the elastoplastic region can be conducted only with the help of some theory of plasticity; this is the second approach to solution of the problem. Application of theories of plasticity leads in the end to differential equations close in form to equations of type (b) for anisotropic plates, but anisotropy factors here no longer are selected by intuition.

The most valuable results in this region were obtained, starting in 1944, with help of the theory of small elastoplastic deformations.* This theory** connects magnitude of principal shearing strains with corresponding tangential stresses. Use of theory of deformations is equivalent to considering a plate in the plastic stage as a nonlinearly elastic body. Advantage of this theory is the comparative simplicity

---

*First research of this problem belongs to A. A. Ilyushin [8.1 and 8.2].

**Below, for short, it is called theory of deformations.

of initial dependences. All the same, in problems of buckling of plates the theory of deformations should be used with caution, since, strictly speaking, it pertains only to case of simple loading, when all components of the tensor of deformations change proportionally to one parameter and, consequently, directions of principal axes of deformation remain constant. But this assumption is fulfilled only in process of loading of the plate up to moment of buckling. With loss of stability of the plate at different points there appear additional flexural strains, and principal axes of deformation change direction. True, one may assume that with weak distortion of the plate additional deformations are small as compared to the principal strains, and therefore, loading is close to being simple.

The natural desire to be liberated from limitations of deformation theory led to the appearance of research in stability of plates, based on the theory of flow: this theory establishes relationship between stresses and increases of plastic deformations, i.e., rates of change of deformations, whereas preceding theory operated with complete deformations.

We will acquaint ourselves with the application to different problems of stability of plates of both the theory of deformations and also the theory of flow and compare results of calculations with experimental data.

We must not forget that term "stability" is applied to a structure, experiencing elastoplastic deformation, in a conditional sense. Really, here any small perturbation causes irreversible deformations of the structure. Removed from position of stable equilibrium, a structure will accomplish damped vibrations already near some new bent position, characterized by a residual bend. Therefore, here there

remain in force those stipulations which were made in Section 31 (p.126) with respect to determination of stability. We will consider state of plate stable in the small, if are absent neighboring "non-trivial" equilibrium form.

Effect of chain stresses, by which plate is able to receive an increasing load after buckling, extends also to elastoplastic region. Problem of post-critical behavior of plates during plastic deformations is very complicated. We shall learn the possible approaches to its solution in Chapter XII; furthermore, in Section 111 we shall present an approximate method for determining of reduction factors.

§ 100. Theory of Deformations. Initial Dependences

We turn first of all to theory of deformations and give certain basic dependences.

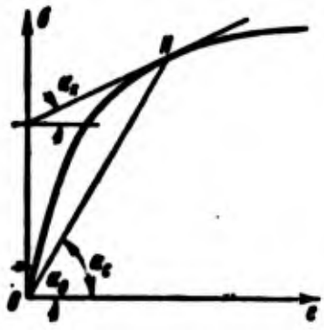

Fig. 8.1. Determining secant and tangential moduli.

We start diagram of $\sigma(\varepsilon)$, obtained for uniaxial extension of samples of a given material (Fig. 8.1). Tangent of angle of inclination α_0 of initial section of diagram corresponds to modulus of elasticity E. We pass at a certain point N a tangent to curve $\sigma(\varepsilon)$; the tangent of angle α_K between this tangent and the axis of abscissas determines the tangent modulus E_K^0:*

$$E_k^0 = \frac{d\sigma}{d\varepsilon}. \qquad (8.1)$$

*Index "0" designates that magnitude E_K corresponds to uniaxial stress.

We join point N with origin O; the tangent of the angle of inclination of the obtained line to axis of abscissas corresponds to the so-called secant modulus E_c^0, which, like the principle modulus E, is equal to ratio of σ to ε:

$$E_c^0 = \frac{\sigma}{\varepsilon}. \tag{8.2}$$

Magnitudes E_c^0 and E_K^0 are functions of ε.

Regarding Poisson's ratio μ, in the elastic region, as we know, for steel and duralumin it lies between 0.25 and 0.33. With appearance of plastic deformations magnitude μ rapidly increases, approaching a limiting value $\mu = 0.5$. Taking $\mu = 0.5$ we consider material incompressible: a small cube of such material, subjected to compression from all sides, will not experience change of volume.

In order to determine dependence $\sigma(\varepsilon)$ in case of uniaxial compression, we test short samples, where thin plates are connected in packs. Subsequently, we will assume that within limits comparatively small deformations of diagram $\sigma(\varepsilon)$, corresponding to uniaxial compression and extension, are identical.

In case of complex state of strain there are introduced the concepts of intense stresses σ_i and intensity of deformations ε_i:

$$\sigma_i = \frac{1}{\sqrt{2}} \sqrt{(\sigma_x - \sigma_y)^2 + (\sigma_y - \sigma_z)^2 + (\sigma_z - \sigma_x)^2 + 6(\tau_{xy}^2 + \tau_{yz}^2 + \tau_{zx}^2)}. \tag{8.3}$$

$$\varepsilon_i = \frac{\sqrt{2}}{3} \sqrt{(\varepsilon_x - \varepsilon_y)^2 + (\varepsilon_y - \varepsilon_z)^2 + (\varepsilon_z - \varepsilon_x)^2 + \frac{3}{2}(\gamma_{xy}^2 + \gamma_{yz}^2 + \gamma_{zx}^2)}; \tag{8.4}$$

here σ_x, σ_y, and σ_z are normal stresses in coordinate planes passing through the given points; τ_{xy}, τ_{yz}, and τ_{zx} are tangential stresses; ε_x, ε_y, and ε_z are elongation strains; γ_{xy}, γ_{yz}, and γ_{zx} are shear strains.

Let us assume that the intensity of deformations at a given point increases and we have condition of "simple loading." Then magnitudes

σ_i and ε_i are interconnected, regardless of form of stress, by dependence

$$\sigma_i = E_c \varepsilon_i. \tag{8.5}$$

By E_c here is understood secant modulus in diagram $\sigma_i(\varepsilon_i)$; the connection of it with modulus E_c^0, corresponding to uniaxial extension, will be determined later.

Components of deformations are connected in turn with components of stresses by the following relationships:

$$\left.\begin{aligned} \varepsilon_x - \frac{1}{3}\theta &= \frac{3}{2E_c}(\sigma_x - S), \\ \varepsilon_y - \frac{1}{3}\theta &= \frac{3}{2E_c}(\sigma_y - S), \\ \gamma_{xy} &= \frac{3}{E_c}\tau_{xy}. \end{aligned}\right\} \tag{8.6}$$

Analogous expressions can be written for the remaining components. By θ in (6) is understood dilatational deformation:

$$\theta = \varepsilon_x + \varepsilon_y + \varepsilon_z. \tag{8.7}$$

By S we mean "average" normal stress:

$$S = \frac{\sigma_x + \sigma_y + \sigma_z}{3}. \tag{8.8}$$

Quantities θ and S are connected by dependence

$$\theta = \frac{3(1-2\mu)}{E} S. \tag{8.9}$$

For incompressible material we must take $\theta = 0$. During deformation of a relatively thin plate in each of its layers, parallel to the middle plane, there is plane stress; on known assumptions of theory of plates it is possible to assume

$$\varepsilon_z = 0, \quad \gamma_{yz} = \gamma_{zx} = 0. \tag{8.10}$$

Expression for intensity of stresses (3) obtains the form

$$\sigma_i = \sqrt{\sigma_x^2 - \sigma_x\sigma_y + \sigma_y^2 + 3\tau^2}. \tag{8.11}$$

Magnitude S will be equal to

$$S = \frac{\sigma_x + \sigma_y}{3}. \tag{8.12}$$

Here, and subsequently, there are introduced designations $\tau_{xy} = \tau$, $\gamma_{xy} = \gamma$.

Using (9), we write relationship (6) in form

$$\left.\begin{aligned} \varepsilon_x &= \frac{3}{2E_c}\sigma_x - \left(\frac{3}{2E_c} - \frac{1-2\mu}{E}\right)S, \\ \varepsilon_y &= \frac{3}{2E_c}\sigma_y - \left(\frac{3}{2E_c} - \frac{1-2\mu}{E}\right)S, \\ \gamma &= \frac{3}{E_c}\tau. \end{aligned}\right\} \tag{8.13}$$

In expressions (13) it is possible to separate components of elastic and plastic deformation, if we assume*

$$\frac{1}{G_c} = \frac{1}{G} + \frac{1}{G_{пл}}. \tag{8.14}$$

Here, by G is understood shearing modulus within elastic limit; by G_c – secant shearing modulus, by $G_{пл}$ – shearing modulus for intrinsic plastic deformations. Magnitude G is connected with modulus E by the known dependence

$$G = \frac{E}{2(1+\mu)}. \tag{8.15}$$

For G_c and $G_{пл}$ it is possible to write analogous relationships, taking $\mu = 0.5$:

$$G_c = \frac{E_c}{3}, \quad G_{пл} = \frac{E_{пл}}{3}. \tag{8.16}$$

Instead of (14) it is possible to write relationship

$$\frac{1}{E_c} = \frac{2(1+\mu)}{3E} + \frac{1}{E_{пл}}. \tag{8.17}$$

Introducing (17) and (12) in expressions (13), we obtain

$$\left.\begin{aligned} \varepsilon_x &= \frac{1}{E}(\sigma_x - \mu\sigma_y) + \frac{3}{2E_{пл}}(\sigma_x - S), \\ \varepsilon_y &= \frac{1}{E}(\sigma_y - \mu\sigma_x) + \frac{3}{2E_{пл}}(\sigma_y - S), \\ \gamma &= \frac{2(1+\mu)}{E}\tau + \frac{3}{E_{пл}}\tau. \end{aligned}\right\} \tag{8.18}$$

First member in each of these expressions corresponds to elastic deformation, and second, to purely plastic deformation.

---

*See book of L. M. Kachanov [8.3], p. 41.

Let us assume that we know diagram $\sigma(\varepsilon)$, pertaining to uniaxial extension or compression. Then by (18) and (2), considering $\sigma_x = \sigma$, $\sigma_y = 0$, we have

$$\varepsilon = \frac{\sigma}{E_c^0} = \frac{\sigma}{E} + \frac{3}{2E_{пл}}\left(\sigma - \frac{\sigma}{3}\right);$$

hence

$$\frac{1}{E_{пл}} = \frac{1}{E_c^0} - \frac{1}{E}. \tag{8.19}$$

Dependence (19) allows us to find value of $E_{пл}$ by the diagram obtained for uniaxial extension or compression. Using relationship (17), we have, further,

$$\frac{1}{E_c} = \frac{1}{E_c^0} - \frac{1-2\mu}{3E}. \tag{8.20}$$

In case of incompressible material we always have $E_c^0 = E_c$. In other words, $\mu = 0.5$, we obtain diagram of $\sigma_i(\varepsilon_i)$ coinciding with diagram of $\sigma(\varepsilon)$.

If we write expression for intensity of deformations (4) in applications to plane stress and set $\mu = 0.5$, then it will take the form

$$\varepsilon_i = \frac{2}{\sqrt{3}}\sqrt{\varepsilon_x^2 + \varepsilon_x\varepsilon_y + \varepsilon_y^2 + \frac{1}{4}\gamma^2}. \tag{8.21}$$

Let us assume, further, that at given point of the body there is <u>unloading</u>, expressed in <u>decrease</u> of ε_i; then in known limits of change of intensity stresses and deformations will be connected by Hooke's law:

$$\Delta\sigma_i = E\,\Delta\varepsilon_i. \tag{8.22}$$

where E is fundamental modulus of extension-compression for the given material.

§ 101. Basic Differential Equation in Case of Incompressible Material

We shall apply the derived dependences to problems of stability of plates on the assumption that the material is <u>incompressible</u>. We consider that at certain point of plate up to moment of loss of

stability stresses have value σ_x, σ_y, and τ, corresponding deformations are equal to ε_x, ε_y, and γ and that subcritical loading was simple.

Taking in relationships (6) $\theta = 0$ and using (12), we obtain

$$\left.\begin{aligned} \varepsilon_x &= \frac{1}{E_c}\left(\sigma_x - \frac{1}{2}\sigma_y\right), \\ \varepsilon_y &= \frac{1}{E_c}\left(\sigma_y - \frac{1}{2}\sigma_x\right), \\ \gamma &= \frac{3}{E_c}\tau. \end{aligned}\right\} \tag{8.23}$$

We introduce designations

$$s_x = \sigma_x - \frac{1}{2}\sigma_y, \quad s_y = \sigma_y - \frac{1}{2}\sigma_x; \tag{8.24}$$

then we have

$$\varepsilon_x = \frac{s_x}{E_c}, \quad \varepsilon_y = \frac{s_y}{E_c}, \quad \gamma = \frac{3\tau}{E_c}. \tag{8.25}$$

Using relationship (5), we obtain

$$\frac{\varepsilon_x}{\varepsilon_i} = \frac{s_x}{\sigma_i}, \quad \frac{\varepsilon_y}{\varepsilon_i} = \frac{s_y}{\sigma_i}, \quad \frac{\gamma}{\varepsilon_i} = \frac{3\tau}{\sigma_i}. \tag{8.26}$$

At moment of loss of stability the plate takes a bent equilibrium position, infinitely close to the initial. We determine variations $\delta\sigma_x$, $\delta\sigma_y$, and $\delta\tau$ of stresses, occurring during buckling of the plate. Proceeding from (23), we find

$$\left.\begin{aligned} \sigma_x &= \frac{4}{3}E_c\left(\varepsilon_x + \frac{1}{2}\varepsilon_y\right), \\ \sigma_y &= \frac{4}{3}E_c\left(\varepsilon_y + \frac{1}{2}\varepsilon_x\right), \\ \tau &= \frac{1}{3}E_c\gamma. \end{aligned}\right\} \tag{8.27}$$

We calculate variations of these magnitudes, remembering that modulus E_c is variable and depends on ε_i:

$$\left.\begin{aligned} \delta\sigma_x &= \frac{4}{3}E_c\left(\delta\varepsilon_x + \frac{1}{2}\delta\varepsilon_y\right) + \frac{4}{3}\left(\varepsilon_x + \frac{1}{2}\varepsilon_y\right)\frac{dE_c}{d\varepsilon_i}\delta\varepsilon_i, \\ \delta\sigma_y &= \frac{4}{3}E_c\left(\delta\varepsilon_y + \frac{1}{2}\delta\varepsilon_x\right) + \frac{4}{3}\left(\varepsilon_y + \frac{1}{2}\varepsilon_x\right)\frac{dE_c}{d\varepsilon_i}\delta\varepsilon_i, \\ \delta\tau &= \frac{1}{3}E_c\delta\gamma + \frac{1}{3}\gamma\frac{dE_c}{d\varepsilon_i}\delta\varepsilon_i. \end{aligned}\right\} \tag{8.28}$$

By analogy with (1) we introduce concept of tangent modulus for diagram $\sigma_i(\varepsilon_i)$:

$$E_u = \frac{d\sigma_i}{d\varepsilon_i}. \tag{8.29}$$

From (5) we have

$$E_c = \frac{\sigma_i}{\varepsilon_i}; \tag{8.30}$$

differentiating, we find

$$\frac{dE_c}{d\varepsilon_i} = \frac{1}{\varepsilon_i}\frac{d\sigma_i}{d\varepsilon_i} - \frac{\sigma_i}{\varepsilon_i^2} = \frac{1}{\varepsilon_i}(E_u - E_c). \tag{8.31}$$

Dependences (28) taking into account (31) take the form

$$\left.\begin{aligned} \delta\sigma_x &= \frac{4}{3}E_c\left(\delta\varepsilon_x + \frac{1}{2}\delta\varepsilon_y\right) - (E_c - E_u)\frac{\sigma_x}{\sigma_i}\delta\varepsilon_i. \\ \delta\sigma_y &= \frac{4}{3}E_c\left(\delta\varepsilon_y + \frac{1}{2}\delta\varepsilon_x\right) - (E_c - E_u)\frac{\sigma_y}{\sigma_i}\delta\varepsilon_i. \\ \delta\tau &= \frac{1}{3}E_c\delta\gamma - (E_c - E_u)\frac{\tau}{\sigma_i}\delta\varepsilon_i. \end{aligned}\right\} \tag{8.32}$$

Variations of components s_x, s_y by (24) are equal to

$$\delta s_x = \delta\sigma_x - \frac{1}{2}\delta\sigma_y, \qquad \delta s_y = \delta\sigma_y - \frac{1}{2}\delta\sigma_x. \tag{8.33}$$

Using (32), we obtain

$$\left.\begin{aligned} \delta s_x &= E_c\delta\varepsilon_x - (E_c - E_u)\frac{s_x}{\sigma_i}\delta\varepsilon_i. \\ \delta s_y &= E_c\delta\varepsilon_y - (E_c - E_u)\frac{s_y}{\sigma_i}\delta\varepsilon_i. \\ \delta\tau &= \frac{1}{3}E_c\delta\gamma - (E_c - E_u)\frac{\tau}{\sigma_i}\delta\varepsilon_i. \end{aligned}\right\} \tag{8.34}$$

We determine variations of intensity of deformations ε_i. Using (21), we obtain

$$\delta\varepsilon_i = \frac{2(\varepsilon_x\delta\varepsilon_x + \varepsilon_y\delta\varepsilon_y) + \varepsilon_y\delta\varepsilon_x + \varepsilon_x\delta\varepsilon_y + \frac{1}{2}\gamma\delta\gamma}{\sqrt{3}\frac{\sqrt{3}}{2}\varepsilon_i}.$$

After multiplication by σ_i we find

$$\sigma_i\delta\varepsilon_i = \frac{4}{3}E_c\left[\left(\varepsilon_x + \frac{1}{2}\varepsilon_y\right)\delta\varepsilon_x + \left(\varepsilon_y + \frac{1}{2}\varepsilon_x\right)\delta\varepsilon_y + \frac{1}{4}\gamma\delta\gamma\right].$$

Substitution of relationships (27) yields

$$\sigma_i\delta\varepsilon_i = \sigma_x\delta\varepsilon_x + \sigma_y\delta\varepsilon_y + \tau\delta\gamma. \tag{8.35}$$

Expression (35) may be given an energy meaning: it is equal to work of forces applied to an element of a body on virtual displacement.

Let us assume that during loading of a plate up to loss of stability intensity of stresses at all points exceeded proportional limit.

At moment of buckling to fundamental stresses will be added flexural stresses. Plate is divided by thickness into two zones: in one there will occur loading, and in the other, unloading (Fig. 8.2). Using hypothesis of straight normals, we express variations of deformations at an arbitrary point of a plate by variations of deformation in the middle surface $\delta\varepsilon_x$, $\delta\varepsilon_y$, and $\delta\gamma$ and by variation of curvatures $\varkappa_x$, $\varkappa_y$, χ:

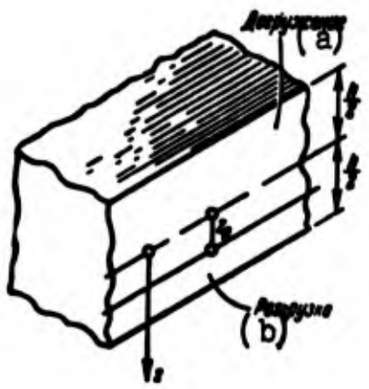

Fig. 8.2. Zones of loading and unloading during buckling of plate. KEY: (a) Loading; (b) Unloading.

$$\delta\varepsilon_x^z = \delta\varepsilon_x + z\varkappa_x, \qquad \delta\varepsilon_y^z = \delta\varepsilon_y + z\varkappa_y,$$
$$\delta\gamma^z = \delta\gamma + 2z\chi. \tag{8.36}$$

As earlier, by z is understood coordinate, counted from middle surface along a normal to it.

We determine position of that neutral point of the normal, which lies on boundary of zones of loading and unloading. Obviously, variation of $\delta\varepsilon_1$ at this point should be equal to zero. Proceeding from (35), we find

$$\sigma_x \delta\varepsilon_x^z + \sigma_y \delta\varepsilon_y^z + \tau\delta\gamma^z = 0. \tag{8.37}$$

Substituting value (36) and designating by z_0 the coordinate of the neutral point, we have

$$\sigma_x(\delta\varepsilon_x + \varkappa_x z_0) + \sigma_y(\delta\varepsilon_y + \varkappa_y z_0) + \tau(\delta\gamma + 2\chi z_0) = 0. \tag{8.38}$$

Hence

$$z_0 = -\frac{\sigma_x \delta\varepsilon_x + \sigma_y \delta\varepsilon_y + \tau\delta\gamma}{\sigma_x \varkappa_x + \sigma_y \varkappa_y + 2\tau\chi}. \tag{8.39}$$

We introduce designations

$$\Pi(\sigma, \varepsilon) = \sigma_x \delta\varepsilon_x + \sigma_y \delta\varepsilon_y + \tau\delta\gamma. \tag{8.40}$$

$$\Pi(\sigma, \varkappa) = \sigma_x \varkappa_x + \sigma_y \varkappa_y + 2\tau\chi; \tag{8.41}$$

then we have

$$z_0 = -\frac{\Pi(\sigma, \varepsilon)}{\Pi(\sigma, z)}. \tag{8.42}$$

Variation of $\delta\varepsilon_1^z$ for arbitrary point with coordinate z turns out to be, by (35), equal to

$$\delta\sigma_i^z = \frac{\sigma_x(\delta\varepsilon_x + z\varkappa_x) + \sigma_y(\delta\varepsilon_y + z\varkappa_y) + \tau(\delta\gamma + 2z\chi)}{\sigma_i}. \tag{8.43}$$

Using (42), we find

$$\delta\sigma_i^z = -\frac{\Pi(\sigma, z)(z_0 - z)}{\sigma_i}. \tag{8.44}$$

Let us turn to <u>zone of loading</u>: we assume that it embraces layer of plate between points $z = -\frac{h}{2}$ and $z = z_0$. Here variations of magnitudes s_x^z and $\delta\varepsilon_x^z$ are connected by the first of relationships (34):

$$\delta s_x^z = E_c\,\delta\varepsilon_x^z - (E_c - E_K)\frac{s_x}{\sigma_i}\delta\sigma_i^z. \tag{8.45}$$

Using (36) and (44), we obtain

$$\delta s_x^z = E_c(\delta\varepsilon_x + z\varkappa_x) + (E_c - E_K)\frac{s_x(z_0 - z)\Pi(\sigma, z)}{\sigma_i^2}. \tag{8.46}$$

By analogy we have

$$\delta s_y^z = E_c(\delta\varepsilon_y + z\varkappa_y) + (E_c - E_K)\frac{s_y(z_0 - z)\Pi(\sigma, z)}{\sigma_i^2}. \tag{8.47}$$

$$\delta\tau^z = \frac{1}{3}E_c(\delta\gamma + 2z\chi) + (E_c - E_K)\frac{\tau(z_0 - z)\Pi(\sigma, z)}{\sigma_i^2}. \tag{8.48}$$

For <u>zone of unloading</u>, lying between points $z = z_0$ and $z = \frac{h}{2}$, it is necessary to set $E_c = E_K = E$; then we find

$$\left.\begin{aligned} \delta s_x^z &= E(\delta\varepsilon_x + z\varkappa_x), \\ \delta s_y^z &= E(\delta\varepsilon_y + z\varkappa_y), \\ \delta\tau^z &= \tfrac{1}{3}E(\delta\gamma + 2z\chi). \end{aligned}\right\} \tag{8.49}$$

We designate by δN_x, δN_y, and δT variation of resultant forces per unit length of the section of the plate:

$$\delta N_x = \int_{-\frac{h}{2}}^{\frac{h}{2}} \delta\sigma_x^z\,dz, \quad \delta N_y = \int_{-\frac{h}{2}}^{\frac{h}{2}} \delta\sigma_y^z\,dz, \quad \delta T = \int_{-\frac{h}{2}}^{\frac{h}{2}} \tau^z\,dz. \tag{8.50}$$

We introduce auxiliary quantities

$$\delta R_x = \delta N_x - \frac{1}{2}\delta N_y = \int_{-\frac{h}{2}}^{\frac{h}{2}} \delta s_x^z\,dz, \quad \delta R_y = \delta N_y - \frac{1}{2}\delta N_x = \int_{-\frac{h}{2}}^{\frac{h}{2}} \delta s_y^z\,dz. \tag{8.51}$$

By (46) and (49) we have

$$\delta R_x = \int_{z_0}^{\frac{h}{2}} E(\delta\varepsilon_x + z\varkappa_x)\,dz + \int_{-\frac{h}{2}}^{z_0} E_c(\delta\varepsilon_x + z\varkappa_x)\,dz + \\ + \int_{-\frac{h}{2}}^{z_0} \frac{(E_c - E_u)\,s_x\,\Pi(\sigma, \varkappa)}{\sigma_i^2}(z_0 - z)\,dz; \tag{8.52}$$

hence

$$\delta R_x = \left[(E + E_c)\frac{h}{2} - (E - E_c)z_0\right]\delta\varepsilon_x + \\ + \frac{1}{2}(E - E_c)\left(\frac{h^2}{4} - z_0^2\right)\varkappa_x + (E_c - E_u)\frac{\Pi(\sigma, \varkappa)\,s_x}{2\sigma_i^2}\left(\frac{h}{2} + z_0\right)^2. \tag{8.53}$$

In an analogous manner we find

$$\delta R_y = \left[(E + E_c)\frac{h}{2} - (E - E_c)z_0\right]\delta\varepsilon_y + \\ + \frac{1}{2}(E - E_c)\left(\frac{h^2}{4} - z_0^2\right)\varkappa_y + (E_c - E_u)\frac{\Pi(\sigma, \varkappa)\,s_y}{2\sigma_i^2}\left(\frac{h}{2} + z_0\right)^2. \tag{8.54}$$

$$\delta T = \frac{1}{3}\left[(E + E_c)\frac{h}{2} - (E - E_c)z_0\right]\delta\gamma + \frac{1}{3}(E - E_c)\left(\frac{h^2}{4} - z_0^2\right)\chi + \\ + (E_c - E_u)\frac{\Pi(\sigma, \varkappa)\,\tau}{2\sigma_i^2}\left(\frac{h}{2} + z_0\right)^2. \tag{8.55}$$

We assume here that process of loss of stability occurs with constant external forces. We extend this assumption to variations of internal resultant forces and assume*

$$\delta R_x = \delta R_y = \delta T = 0. \tag{8.56}$$

We multiply expressions (53)–(55) correspondingly by σ_x, σ_y, and 3τ and we add these products. Considering relationship

$$s_x\sigma_x + s_y\sigma_y + 3\tau^2 = \sigma_i^2 \tag{8.57}$$

and using designations (40) and (41), we obtain

$$\left[(E + E_c)\frac{h}{2} - (E - E_c)z_0\right]\Pi(\sigma, \varepsilon) + \frac{1}{2}(E - E_c)\left(\frac{h^2}{4} - z_0^2\right)\Pi(\sigma, \varkappa) + \\ + (E_c - E_u)\frac{\Pi(\sigma, \varkappa)}{2}\left(\frac{h}{2} + z_0\right)^2 = 0.$$

Division by $\Pi(\sigma, \varkappa)$ taking into account (42) gives

$$-\left[(E + E_c)\frac{h}{2} - (E - E_c)z_0\right]z_0 + \frac{1}{2}(E - E_c)\left(\frac{h^2}{4} - z_0^2\right) + \\ + \frac{E_c - E_u}{2}\left(\frac{h}{2} + z_0\right)^2 = 0. \tag{8.58}$$

---

*More exact solution of problem, in which variations of internal forces are not considered equal to zero, was given by A. A. Ilyushin [8.2] and Yu. R. Lepik [8.5].

or

$$E\left(\frac{h}{2}-z_0\right)^2-E_c\left(\frac{h}{2}+z_0\right)^2=0. \tag{8.59}$$

If we were to designate by h_1 thickness of zone of additional loading, and by h_2, the thickness of zone of unloading, then we have

$$Eh_2^2-E_ch_1^2=0. \quad h_2=\frac{h}{2}-z_0. \quad h_1=\frac{h}{2}+z_0. \tag{8.60}$$

We obtained precisely the same relationship between h_1 and h_2 as in case of compressed bar of rectangular section using theory of two moduli (see Section 27). From (60) we find

$$h_1=h\frac{\sqrt{E}}{\sqrt{E_c}+\sqrt{E}}. \quad h_2=h\frac{\sqrt{E_c}}{\sqrt{E_c}+\sqrt{E}}. \tag{8.61}$$

Coordinate z_0 is equal to

$$z_0=\frac{h}{2}\frac{\sqrt{E}-\sqrt{E_c}}{\sqrt{E}+\sqrt{E_c}}. \tag{8.62}$$

We determine, further, flexural and torsional moments happening per unit length of the section:

$$M_x=\int_{-\frac{h}{2}}^{\frac{h}{2}}\sigma_x^1z\,dz. \quad M_y=\int_{-\frac{h}{2}}^{\frac{h}{2}}\sigma_y^1z\,dz. \quad H=\int_{-\frac{h}{2}}^{\frac{h}{2}}\tau^1z\,dz. \tag{8.63}$$

We introduce additional designations

$$\mathfrak{M}_x=M_x-\frac{1}{2}M_y=\int_{-\frac{h}{2}}^{\frac{h}{2}}s_x^1z\,dz. \quad \mathfrak{M}_y=M_y-\frac{1}{2}M_x=\int_{-\frac{h}{2}}^{\frac{h}{2}}s_y^1z\,dz. \tag{8.64}$$

Substituting expressions (46) and (49), we find

$$\mathfrak{M}_x=\int_{z_0}^{\frac{h}{2}}E(\delta\varepsilon_x+z\varkappa_x)z\,dz+\int_{-\frac{h}{2}}^{z_0}E_c(\delta\varepsilon_x+z\varkappa_x)z\,dz+$$
$$+\int_{-\frac{h}{2}}^{z_0}\frac{(E_c-E_c)s_x\Pi(\sigma,\varkappa)}{\sigma_i^2}(z_0-z)z\,dz. \tag{8.65}$$

Integrating, we have

$$\mathfrak{M}_x=\frac{1}{2}(E-E_c)\left(\frac{h^2}{4}-z_0^2\right)\delta\varepsilon_x+\frac{1}{3}\left[(E+E_c)\frac{h^3}{8}-\right.$$
$$\left.-(E-E_c)z_0^3\right]\varkappa_x-\frac{1}{24}(E_c-E_c)\frac{\Pi(\sigma,\varkappa)s_x}{\sigma_i^2}(h^3-4z_0^3+3z_0h^2). \tag{8.66}$$

For $\mu = 0.5$ cylindrical rigidity of plate within elastic limit will be equal to

$$D' = \left[\frac{Eh^3}{12(1-\mu^2)}\right]_{\mu=0.5} = \frac{Eh^3}{9}. \tag{8.67}$$

Introducing designations

$$\varphi_c = \frac{E_c}{E}, \quad \varphi_u = \frac{E_u}{E}, \tag{8.68}$$

we rewrite (66) in the form

$$\mathfrak{M}_x = D'\left\{3\left[\frac{1}{8}(1+\varphi_c) - (1-\varphi_c)\left(\frac{z_0}{h}\right)^3\right]\varkappa_x + \right.$$
$$\left. + \frac{9}{2h}(1-\varphi_c)\left(\frac{1}{4} - \frac{z_0^2}{h^2}\right)\delta\varepsilon_x - \frac{3}{8}(\varphi_c - \varphi_u)\frac{\Pi(s,z)\,s_x}{\sigma_i^2}\left(1 - 4\frac{z_0^2}{h^2} + 3\frac{z_0}{h}\right)\right\}. \tag{8.69}$$

We express magnitude $\mathfrak{M}_x$ by curvatures. For that we determine $\delta\varepsilon_x$, using (53) and (56):

$$\delta\varepsilon_x = -\frac{1}{2}\frac{(1-\varphi_c)\left(\frac{h^2}{4} - z_0^2\right)\varkappa_x}{(1+\varphi_c)\frac{h}{2} - (1-\varphi_c)z_0} - \frac{1}{2}\frac{(\varphi_c - \varphi_u)\,\Pi(s,z)\,s_x\left(\frac{h}{2} + z_0\right)^2}{\left[(1+\varphi_c)\frac{h}{2} - (1-\varphi_c)z_0\right]\sigma_i^2}. \tag{8.70}$$

Putting this value in (69), we find

$$\mathfrak{M}_x = D'\left(\left\{3\left[\frac{1}{8}(1+\varphi_c) - (1-\varphi_c)\bar{z}_0^3\right] - \right.\right.$$
$$\left. - \frac{9}{4}\frac{(1-\varphi_c)^2\left(\frac{1}{4} - \bar{z}_0^2\right)^2}{\frac{1}{2}(1+\varphi_c) - (1-\varphi_c)\bar{z}_0}\right\}\varkappa_x - \frac{3}{8}(\varphi_c - \varphi_u)\left[(1 - 4\bar{z}_0^3 + 3\bar{z}_0) + \right.$$
$$\left.\left. + \frac{6(1-\varphi_c)\left(\frac{1}{2} + \bar{z}_0\right)^2\left(\frac{1}{4} - \bar{z}_0^2\right)}{\frac{1}{2}(1+\varphi_c) - (1-\varphi_c)\bar{z}_0}\right]\frac{\Pi(s,z)\,s_x}{\sigma_i^2}\right); \tag{8.71}$$

here there is introduced the designation

$$\bar{z}_0 = \frac{z_0}{h}. \tag{8.72}$$

We present (71) in the form

$$\mathfrak{M}_x = \frac{3}{4}D'\left[(1-r)\varkappa_x - (1-s)\frac{\Pi(s,z)\,s_x}{\sigma_i^2}\right], \tag{8.73}$$

where

$$r = \frac{1}{2}(1-\varphi_c)\left[(1 + 8\bar{z}_0^3) + \frac{3}{4}\frac{(1-\varphi_c)(1-4\bar{z}_0^2)^2}{(1+\varphi_c) - 2(1-\varphi_c)\bar{z}_0}\right]. \tag{8.74}$$

$$s = 1 - \frac{1}{2}(\varphi_c - \varphi_u)\left[1 - 4\bar{z}_0^3 + 3\bar{z}_0 + \frac{3}{4}\frac{(1-\varphi_c)(1+2\bar{z}_0)^2(1-4\bar{z}_0^2)}{(1+\varphi_c) - (1-\varphi_c)2\bar{z}_0}\right]. \tag{8.75}$$

In an analogous manner we obtain

$$\mathfrak{M}_y = \frac{3}{4} D' \left[(1-r) \varkappa_y - (1-s) \frac{\Pi(\sigma, \varkappa) s_y}{\sigma_i^2} \right]. \tag{8.76}$$

$$H = \frac{3}{4} D' \left[\frac{2}{3} (1-r) \chi - (1-s) \frac{\Pi(\sigma, \varkappa) \tau}{\sigma_i^2} \right]. \tag{8.77}$$

From (64) we have

$$M_x = \frac{4}{3} \left(\mathfrak{M}_x + \frac{1}{2} \mathfrak{M}_y \right). \qquad M_y = \frac{4}{3} \left(\mathfrak{M}_y + \frac{1}{2} \mathfrak{M}_x \right). \tag{8.78}$$

Hence

$$\left.\begin{aligned} M_x &= D' \left[(1-r) \left(\varkappa_x + \frac{1}{2} \varkappa_y \right) - \frac{3}{4} (1-s) \frac{\Pi(\sigma, \varkappa) \sigma_x}{\sigma_i^2} \right], \\ M_y &= D' \left[(1-r) \left(\varkappa_y + \frac{1}{2} \varkappa_x \right) - \frac{3}{4} (1-s) \frac{\Pi(\sigma, \varkappa) \sigma_y}{\sigma_i^2} \right]. \end{aligned}\right\} \tag{8.79}$$

We express curvatures and torsion of the bending surface by deflection:

$$\varkappa_x = -\frac{\partial^2 w}{\partial x^2}. \qquad \varkappa_y = -\frac{\partial^2 w}{\partial y^2}. \qquad \chi = -\frac{\partial^2 w}{\partial x \partial y}. \tag{8.80}$$

Then expressions (79) and (77), taking into account (41), will take the form

$$M_x = -D' \left[(1-r) \left(\frac{\partial^2 w}{\partial x^2} + \frac{1}{2} \frac{\partial^2 w}{\partial y^2} \right) - \frac{3}{4} (1-s) \frac{\sigma_x}{\sigma_i^2} \Pi(\sigma, w) \right]. \tag{8.81}$$

$$M_y = -D' \left[(1-r) \left(\frac{\partial^2 w}{\partial y^2} + \frac{1}{2} \frac{\partial^2 w}{\partial x^2} \right) - \frac{3}{4} (1-s) \frac{\sigma_y}{\sigma_i^2} \Pi(\sigma, w) \right]. \tag{8.82}$$

$$H = -D' \left[\frac{1}{2} (1-r) \frac{\partial^2 w}{\partial x \partial y} - \frac{3}{4} (1-s) \frac{\tau}{\sigma_i^2} \Pi(\sigma, w) \right], \tag{8.83}$$

where

$$\Pi(\sigma, w) = \sigma_x \frac{\partial^2 w}{\partial x^2} + \sigma_y \frac{\partial^2 w}{\partial y^2} + 2\tau \frac{\partial^2 w}{\partial x \partial y}. \tag{8.83a}$$

Considering small deflections of the plate and using relationships (7.16), (7.17), and (7.156), we write equation of equilibrium of the member

$$\frac{\partial^2 M_x}{\partial x^2} + 2 \frac{\partial^2 H}{\partial x \partial y} + \frac{\partial^2 M_y}{\partial y^2} + h \Pi(\sigma, w) = 0. \tag{8.84}$$

Here stresses σ_x and σ_y are considered positive during compression. Substituting here expression (81)–(83), we arrive at the following

differential equation for deflection:*

$$\left(1-\frac{3}{4}\frac{1-s}{1-r}\frac{\sigma_x^2}{\sigma_i^2}\right)\frac{\partial^4 w}{\partial x^4}+2\left[1-\frac{3}{4}\frac{1-s}{1-r}\frac{\sigma_x\sigma_y+2\tau^2}{\sigma_i^2}\right]\frac{\partial^4 w}{\partial x^2\partial y^2}+$$
$$+\left(1-\frac{3}{4}\frac{1-s}{1-r}\frac{\sigma_y^2}{\sigma_i^2}\right)\frac{\partial^4 w}{\partial y^4}-3\frac{1-s}{1-r}\frac{\tau}{\sigma_i^2}\left(\sigma_x\frac{\partial^4 w}{\partial x^3\partial y}+\sigma_y\frac{\partial^4 w}{\partial x\partial y^3}\right)+$$
$$+\frac{h}{(1-r)D'}\Pi(\sigma, w)=0. \qquad (8.85)$$

Equation (85) together with boundary conditions is the initial one during solution of different particular problems. If we put $\varphi_c = \varphi_k = 1$, then we have r = 0, s = 1; then instead of (85) we obtain known equation, pertaining to stability of plates within elastic limit; if in it we consider $\mu = 0.5$,

$$D'\nabla^4 w+h\Pi(\sigma, w)=0. \qquad (8.86)$$

We note certain relationships, facilitating calculation of parameters r and s. As we have seen, coordinate (62) of the layer, dividing zone of loading and unloading is the same as in problem of stability of a bar of rectangular section. We introduce dimensionless magnitude, corresponding to resultant modulus T in this problem:

$$t=\frac{T}{E}=\frac{4E_k}{(\sqrt{E}+\sqrt{E_k})^2}=\frac{4\varphi_k}{(1+\sqrt{\varphi_k})^2}; \qquad (8.87)$$

consequently,

$$1-\sqrt{t}=\frac{1-\sqrt{\varphi_k}}{1+\sqrt{\varphi_k}}. \qquad (8.88)$$

From (62) we have

$$\bar{z}_0=\frac{1}{2}\frac{1-\sqrt{\varphi_k}}{1+\sqrt{\varphi_k}}, \qquad (8.89)$$

hence

$$(1-2\bar{z}_0)^2=t. \qquad (8.90)$$

---

*This equation was first derived by A. A. Il'yushin [8.1 and 8.2]. In his works are contained also the solution of a series of particular problems for plates, compressed in one and in two directions.

$$1-4\bar{z}_0^2=2\sqrt{t}\left(1-\frac{\sqrt{t}}{2}\right). \tag{8.91}$$

$$1+8\bar{z}_0^3=2\left(1-\frac{\sqrt{t}}{2}\right)\left[\left(1-\frac{\sqrt{t}}{2}\right)^2+\frac{3}{4}t\right]. \tag{8.92}$$

Using these dependences, we reduce expression (74) to form

$$r=(1-\varphi_c)\left(1-\frac{\sqrt{t}}{2}\right)\left[\left(1-\frac{\sqrt{t}}{2}\right)^2+\frac{3}{4}\frac{t}{\frac{\sqrt{t}}{2}+\varphi_c\left(1-\frac{\sqrt{t}}{2}\right)}\right]. \tag{8.93}$$

We turn to expression (75). We present it in the form

$$s=(1-2\bar{z}_0)^2+4\bar{z}_0(1-\bar{z}_0)-\frac{1}{2}(\varphi_c-\varphi_\kappa)\left[(1+2\bar{z}_0)^2(1-\bar{z}_0)+\right.$$
$$\left.+\frac{3}{4}\frac{(1-\varphi_c)(1+2\bar{z}_0)^2(1-4\bar{z}_0^2)}{(1+\varphi_c)-(1-\varphi_c)2\bar{z}_0}\right]. \tag{8.94}$$

From (89) we have

$$\varphi_\kappa=\left(\frac{1-2\bar{z}_0}{1+2\bar{z}_0}\right)^2. \tag{8.95}$$

Using, furthermore, relationship (90), we obtain

$$s=t+\frac{1}{2}(1-\varphi_c)(1-\bar{z}_0)(1+2\bar{z}_0)^2-$$
$$-\frac{3}{8}\frac{[(1+2\bar{z}_0)^2-\varphi_c(1-2\bar{z}_0)^2](1-\varphi_c)(1-4\bar{z}_0^2)}{(1+\varphi_c)+(1-\varphi_c)2\bar{z}_0}. \tag{8.96}$$

or

$$s=t+\frac{1}{2}(1-\varphi_c)\left[(1+8\bar{z}_0^3)-3\bar{z}_0(1-4\bar{z}_0^2)-\right.$$
$$\left.-\frac{3}{8}\frac{[(1+2\bar{z}_0)^2-\varphi_c(1-2\bar{z}_0)^2](1-\varphi_c)(1-4\bar{z}_0^2)}{(1+\varphi_c)+(1-\varphi_c)2\bar{z}_0}\right]. \tag{8.97}$$

Uniting the last two members contained in parentheses and comparing obtained expression with (74), we arrive at the following simple relationship:

$$s=t+r. \tag{8.98}$$

Having for given material of plate values of secant and resultant moduli, one can determine parameters r by (93) and s by (98); such calculations are made in Section 110 for duralumin and steel.

§ 102. Application of Variational Methods

We compose the expression for work of forces M_x, M_y, and H on virtual displacements, at which curvatures receive increments $\delta\varkappa_x$, $\delta\varkappa_y$, and $\delta\chi$. To the section of the plate with dimensions along axes x and y equal to one, there will correspond specific work

$$\delta A^\circ = -(M_x \delta\varkappa_x + M_y \delta\varkappa_y + 2H\delta\chi). \tag{8.99}$$

Considering relationship (77) and (79), we find

$$\delta A^\circ = -D'\left\{(1-r)\left[\left(\varkappa_x + \frac{1}{2}\varkappa_y\right)\delta\varkappa_x + \left(\varkappa_y + \frac{1}{2}\varkappa_x\right)\delta\varkappa_y + \chi\delta\chi\right] - \right.$$
$$\left. - \frac{3}{4}(1-s)\frac{\Pi(\varkappa, \sigma)(\sigma_x\delta\varkappa_x + \sigma_y\delta\varkappa_y + 2\tau\delta\chi)}{\sigma_i^2}\right\}. \tag{8.100}$$

Expression (100) can be presented in the form of complete variation:*

$$\delta A^\circ = -D'\delta\frac{1}{2}\left\{(1-r)(\varkappa_x^2 + \varkappa_x\varkappa_y + \varkappa_y^2 + \chi^2) - \right.$$
$$\left. - \frac{3}{4}(1-s)\frac{[\Pi(\varkappa, \sigma)]^2}{\sigma_i^2}\right\}. \tag{8.101}$$

We introduce concept of potential strain energy, variation of which is equal to

$$\delta U^\circ = -\delta A^\circ. \tag{8.102}$$

Such a step is valid: as was already said, the theory of small elastoplastic deformations, can be considered as the theory of a nonlinearly elastic body. Further we find

$$U^\circ = \frac{D'}{2}\left\{(1-r)(\varkappa_x^2 + \varkappa_x\varkappa_y + \varkappa_y^2 + \chi^2) - \frac{3}{4}(1-s)\frac{[\Pi(\varkappa, \sigma)]^2}{\sigma_i^2}\right\}. \tag{8.103}$$

Moments will be equal to partial derivatives of potential energy:

$$M_x = \frac{\partial U^\circ}{\partial\varkappa_x}, \quad M_y = \frac{\partial U^\circ}{\partial\varkappa_y}, \quad 2H = \frac{\partial U^\circ}{\partial\chi}; \tag{8.104}$$

this corresponds to known Lagrange theorem.

Total potential energy will be

$$U = \int_F\int U^\circ\, dx\, dy. \tag{8.105}$$

---

*Stresses σ_x, σ_y, and τ are considered unvaried.

We determine work of external forces with small distortion of the plate, considering forces $\sigma_x h$ and $\sigma_y h$ evenly distributed along corresponding edges of the plate. From (7.52) we find

$$W=\frac{h}{2}\int_F\int\left[\sigma_x\left(\frac{\partial w}{\partial x}\right)^2+\sigma_y\left(\frac{\partial w}{\partial y}\right)^2+2\tau\frac{\partial w}{\partial x}\frac{\partial w}{\partial y}\right]dx\,dy. \tag{8.106}$$

If we consider transition from initial equilibrium form to bent form as virtual displacement of plate, then we should have

$$\delta A+\delta W=0 \tag{8.107}$$

or

$$\delta(U-W)=\delta\vartheta=0. \tag{8.108}$$

where $\vartheta = U - W$ increment of total energy of system during buckling of the plate.

Using variational equation (108), it is possible to interpret from energy point of view application of the Bubnov-Galerkin method for approximate integration of initial equation (85). On the other hand, when considering loss of stability "in the small" every possible equilibrium form of the plate must be considered indifferent; in process of transition from initial to bent form total energy should remain constant. In other words, work of external forces during buckling of plate should be equal to potential energy, corresponding to internal efforts appearing during bending. Proceeding from this condition, it is possible to apply for approximate solution of problems of stability of plate the Ritz-Timoshenko method (see Section 9).

§ 103. Solution of Particular Problems

Consider, for example, the case of a plate supported by hinges at its ends, compressed in direction x (see Fig. 7.14). In equation (85) one should put

$$\sigma_1=\sigma_x=\sigma,\quad \sigma_y=\tau=0. \tag{8.109}$$

As a result, using (98), we obtain

$$\left(1-\frac{3}{4}\frac{1-t-r}{1-r}\right)\frac{\partial^4 w}{\partial x^4}+2\frac{\partial^4 w}{\partial x^2\partial y^2}+\frac{\partial^4 w}{\partial y^4}+\frac{h\sigma}{(1-r)D'}\frac{\partial^2 w}{\partial x^2}=0. \tag{8.110}$$

We take the solution in the form

$$w=f\sin\frac{m\pi x}{a}\sin\frac{n\pi y}{b}; \tag{8.111}$$

after substitution in (110) we have,

$$\left(\frac{1}{4}+\frac{3}{4}\frac{t}{1-r}\right)\frac{m^4}{a^4}+2\frac{m^2n^2}{a^2b^2}+\frac{n^4}{b^4}-\frac{h\sigma}{(1-r)D'}\frac{m^2}{a^2\pi^2}=0; \tag{8.112}$$

hence

$$\sigma=\frac{\pi^2D'}{b^2h}(1-r)\left[\left(\frac{1}{4}+\frac{3}{4}\frac{t}{1-r}\right)\left(\frac{bm}{a}\right)^2+2n^2+n^4\left(\frac{a}{bm}\right)^2\right]. \tag{8.113}$$

Critical stress will be defined as minimum of expression (113). Here it is first necessary to put n = 1; consequently, the plate should bulge, forming one half-wave along side b. Considering a/bm = λ, we write, further, condition of minimum σ in the form

$$\frac{\partial\sigma}{\partial\lambda}=0; \tag{8.114}$$

this gives

$$\lambda=\sqrt[4]{\frac{1}{4}+\frac{3}{4}\frac{t}{1-r}}. \tag{8.115}$$

Critical stress turns out to be equal to

$$\sigma_{cp}=K\frac{\pi^2D'}{b^2h}. \tag{8.116}$$

where

$$K=2(1-r)\left(\sqrt{\frac{1}{4}+\frac{3}{4}\frac{t}{1-r}}+1\right). \tag{8.117}$$

Formula (117) pertains to an elongated plate, for which wave-formation along side a is free. For a value of a, comparable to b, one should find the number of half-waves m, giving coefficient K the least value.

Let us assume that for a square plate to minimum K there corresponds m = 1; then magnitude K in formula (116) according to (113) is

equal to

$$K=\left(3{,}25+\frac{3}{4}\frac{t}{1-r}\right)(1-r)=\frac{13(1-r)+3t}{4}. \qquad (8.118)$$

In limiting case of an elastic problem it is necessary to set $r = 0$ and $t = 1$; then formulas (117) and (118) will lead to known value $K = 4$. If diagram $\sigma_i(\varepsilon_i)$ corresponding to given material, has a yield surface, then for points of this surface we have by (93) $r = 1 - \varphi_c$, and $t = 0$; instead of (117) we obtain $K = 3\varphi_c$, and instead of (118) $K = \frac{13}{4}\varphi_c$.

In case of elongated plate expression for critical stress can then be presented in the form

$$\sigma_{kp}=3\frac{\pi^2 D_c'}{b^2 h}; \qquad (8.119)$$

here by D_c' is designated, by analogy with (67), cylindrical rigidity, corresponding to the secant modulus, when $\mu = 0.5$:

$$D_c'=\left[\frac{E_c h^3}{12(1-\mu^2)}\right]_{\mu=0,5}=\frac{E_c h^3}{9}. \qquad (8.120)$$

Let us remember that when $t \to 0$ supporting power of compressed bars always was exhausted. In theory of stability of plates we arrive at a different result: for points of the yield surface magnitude $\sigma_{kp} \neq 0$. In other words, transition of "threshold" of yield surface is not necessarily accompanied by buckling of the plate.* This is explained by the fact that with buckling of the plate, in distinction from case of bar, there will be formed a plane stress. Judging by formulas (32), here there can take place increments of σ_x, σ_y, and τ also when the material is in a state of yielding (when $E_c \neq 0$, $E_k = 0$). Let us assume that magnitudes σ_x, σ_y, and τ obtained

*This conclusion pertains to an "infinitely slow" process of loading. If we consider the dynamic effect taking place in an elastic testing machine upon reaching the yield surface, then state of the plate can nevertheless appear unstable.

increments, while magnitude of intensity of stresses (11) remains constant. Then we should have

$$(\sigma_x+\delta\sigma_x)^2-(\sigma_x+\delta\sigma_x)(\sigma_y+\delta\sigma_y)+(\sigma_y+\delta\sigma_y)^2+3(\tau+\delta\tau)^2=$$
$$=\sigma_x^2-\sigma_x\sigma_y+\sigma_y^2+3\tau^2;$$

disregarding small members of higher order, we have

$$\sigma_x(2\delta\sigma_x-\delta\sigma_y)+$$
$$+\sigma_y(\delta\sigma_x-2\delta\sigma_y)+3\tau\delta\tau=0. \qquad (8.121)$$

Assuming here that $\sigma_y = \tau = 0$, we obtain

$$2\delta\sigma_x=\delta\sigma_y. \qquad (8.122)$$

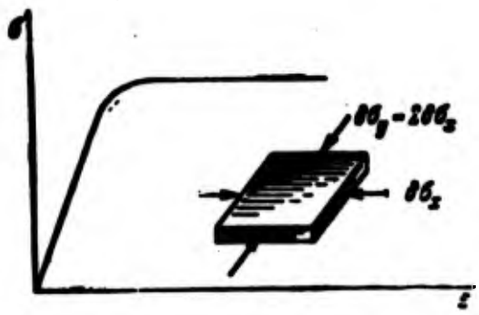

Fig. 8.3. On case of buckling of plate during stress, equal to yield point.

Namely such a relationship should exist in the considered problem between $\delta\sigma_x$ and $\delta\sigma_y$ for points of diagram $\sigma(\varepsilon)$, lying on yield surface (Fig. 8.3).

We considered here only one particular problem of stability of a compressed plate with hinge-fastened edges. A series of problems, pertaining to other forms of loading and other boundary conditions is investigated with the help of the same initial relationships by B. M. Broude [7.3], S. M. Popov [8.6], and Yu. R. Lepik [8.5].

§ 104. Deriving the Fundamental Equation Ignoring the Effect of Unloading

Theory of stability of plates, stated above, in the particular case of compressed bar is reduced to theory of "two moduli." Judging by (61), thickness of plate is divided into zones of loading and unloading in the same way as we divide height of rectangular section of bar during buckling. It is natural to try to extend to plates another approach, in which effect of unloading is not considered. In application to bars this concept corresponds, as we saw in Chapter II, to the case when compressing force increases in process of buckling.

Thus, we shall consider that relationships between increments of stresses and deformations are the same in zones of loading and unloading. Then, obviously, the "neutral" surface dividing these zones will coincide with middle surface of the plate. Consequently, variations of deformations for points of middle surface will be equal to zero during buckling of the plate. We use relationships of type (46) between variations of stresses and deformations, found above for the zone of loading:

$$\delta\sigma_x^z = E_c\delta\varepsilon_x^z - (E_c - E_u)\frac{s_x}{\sigma_i}\delta\varepsilon_i^z. \tag{8.123}$$

$$\delta\sigma_y^z = E_c\delta\varepsilon_y^z - (E_c - E_u)\frac{s_y}{\sigma_i}\delta\varepsilon_i^z. \tag{8.124}$$

$$\delta\tau^z = \frac{1}{3}E_c\delta\gamma^z - (E_c - E_u)\frac{\tau}{\sigma_i}\delta\varepsilon_i^z. \tag{8.125}$$

Considering $\delta\varepsilon_x = \delta\varepsilon_y = \delta\gamma = 0$, by (36) we obtain

$$\delta\varepsilon_x^z = z\varkappa_x,\quad \delta\varepsilon_y^z = z\varkappa_y,\quad \delta\gamma^z = 2z\chi. \tag{8.126}$$

Variation of intensity of deformations (42) is equal to

$$\delta\varepsilon_i^z = \frac{(s_x\varkappa_x + s_y\varkappa_y + 2\tau\chi)z}{\sigma_i} = \frac{\Pi(\sigma, \varkappa)}{\sigma_i}z. \tag{8.127}$$

Expressions (46)–(48) are replaced by the following:

$$\delta\sigma_x^z = \left[E_c\varkappa_x - (E_c - E_u)\frac{s_x\Pi(\sigma, \varkappa)}{\sigma_i^2}\right]z. \tag{8.128}$$

$$\delta s_y^z = \left[E_c \varkappa_y - (E_c - E_u) \frac{s_y \Pi(\sigma, \varkappa)}{\sigma_i^2} \right] z, \tag{8.129}$$

$$\delta \tau^z = \left[\frac{2}{3} E_c \chi - (E_c - E_u) \frac{\tau \Pi(\sigma, \varkappa)}{\sigma_i^2} \right] z. \tag{8.130}$$

As we can see, condition (56) is fulfilled: variations of resultant forces δR_x, δR_y, and δT turn out to be equal to zero. Magnitude $\mathfrak{M}_x$ will be equal to

$$\mathfrak{M}_x = \int_{-\frac{h}{2}}^{\frac{h}{2}} \delta s_x^z z \, dz = \left[E_c \varkappa_x - (E_c - E_u) \frac{s_x \Pi(\sigma, \varkappa)}{\sigma_i^2} \right] \frac{h^3}{12}. \tag{8.131}$$

Introducing value of cylindrical rigidity (67), we obtain

$$\mathfrak{M}_x = \frac{3}{4} D' \left[\varphi_c \varkappa_x - (\varphi_c - \varphi_u) \frac{s_x \Pi(\sigma, \varkappa)}{\sigma_i^2} \right]. \tag{8.132}$$

In the same manner we find

$$\mathfrak{M}_y = \frac{3}{4} D' \left[\varphi_c \varkappa_y - (\varphi_c - \varphi_u) \frac{s_y \Pi(\sigma, \varkappa)}{\sigma_i^2} \right]. \tag{8.133}$$

$$H = \frac{3}{4} D' \left[\frac{2}{3} \varphi_c \chi - (\varphi_c - \varphi_u) \frac{\tau \Pi(\sigma, \varkappa)}{\sigma_i^2} \right]. \tag{8.134}$$

Bending moments by (78) are equal to

$$M_y = D' \left[\varphi_c \left(\varkappa_y + \frac{1}{2} \varkappa_x \right) - \frac{3}{4} (\varphi_c - \varphi_u) \frac{\sigma_y \Pi(\sigma, \varkappa)}{\sigma_i^2} \right]. \tag{8.135}$$

$$M_x = D' \left[\varphi_c \left(\varkappa_x + \frac{1}{2} \varkappa_y \right) - \frac{3}{4} (\varphi_c - \varphi_u) \frac{\sigma_x \Pi(\sigma, \varkappa)}{\sigma_i^2} \right]. \tag{8.136}$$

Using expressions (80) for curvatures, we have

$$M_x = - D' \left[\varphi_c \left(\frac{\partial^2 w}{\partial x^2} + \frac{1}{2} \frac{\partial^2 w}{\partial y^2} \right) - \frac{3}{4} (\varphi_c - \varphi_u) \frac{\sigma_x}{\sigma_i^2} \Pi(\sigma, w) \right]. \tag{8.137}$$

$$M_y = - D' \left[\varphi_c \left(\frac{\partial^2 w}{\partial y^2} + \frac{1}{2} \frac{\partial^2 w}{\partial x^2} \right) - \frac{3}{4} (\varphi_c - \varphi_u) \frac{\sigma_y}{\sigma_i^2} \Pi(\sigma, w) \right]. \tag{8.138}$$

$$H = - D' \left[\frac{1}{2} \varphi_c \frac{\partial^2 w}{\partial x \partial y} - \frac{3}{4} (\varphi_c - \varphi_u) \frac{\tau}{\sigma_i^2} \Pi(\sigma, w) \right]. \tag{8.139}$$

equation of equilibrium (84) takes form*

$$\left[1-\frac{3}{4}\left(1-\frac{\varphi_к}{\varphi_c}\right)\frac{\sigma_x^2}{\sigma_i^2}\right]\frac{\partial^4 w}{\partial x^4}+2\left[1-\frac{3}{4}\left(1-\frac{\varphi_к}{\varphi_c}\right)\frac{\sigma_x\sigma_y+2\tau^2}{\sigma_i^2}\right]\frac{\partial^4 w}{\partial x^2\partial y^2}+$$
$$+\left[1-\frac{3}{4}\left(1-\frac{\varphi_к}{\varphi_c}\right)\frac{\sigma_y^2}{\sigma_i^2}\right]\frac{\partial^4 w}{\partial y^4}-3\left(1-\frac{\varphi_к}{\varphi_c}\right)\frac{\tau}{\sigma_i^2}\left(\sigma_x\frac{\partial^4 w}{\partial x^3\partial y}+\right.$$
$$\left.+\sigma_y\frac{\partial^4 w}{\partial x\partial y^3}\right)+\frac{h}{D_c'}\Pi(\sigma, w)=0. \tag{8.140}$$

Here is introduced cylindrical rigidity (129), corresponding to the secant modulus.

All relationships – from (132) to (140) – we could directly obtain from dependences of Section 101 considering $z_0=\frac{h}{2}$, $\bar{z}_0=\frac{1}{2}$. Really, with such a value of z_0 the whole thickness of the plate turns out to be enveloped by the zone of loading. Parameters r and s by (74) and (75) will be equal to

$$r=1-\varphi_c,\quad s=1-(\varphi_c-\varphi_к). \tag{8.141}$$

In examining an elastic problem it is necessary to consider

$$\varphi_к=\varphi_c=1,\quad D_c'=D'.$$

Variational equation (113) and the energy criterion remain in force also during solution of a problem ignoring unloading: only expression for specific energy U* will change; instead of (103) we obtain

$$U^*=\frac{D'}{2}\left\{\varphi_c\left(\chi_x^2+\chi_x\chi_y+\chi_y^2+\chi^2\right)-\frac{3}{4}\left(\varphi_c-\varphi_к\right)\frac{[\Pi(\chi, \sigma)]^2}{\sigma_i^2}\right\}. \tag{8.142}$$

§ 105. Buckling of Compressed Plate

We start from the new differential equation (140). In case of compression of plate in one direction it takes form

$$\left(\frac{1}{4}+\frac{3}{4}\frac{\varphi_к}{\varphi_c}\right)\frac{\partial^4 w}{\partial x^4}+2\frac{\partial^4 w}{\partial x^2\partial y^2}+\frac{\partial^4 w}{\partial y^4}+\frac{h\sigma}{D_c'}\frac{\partial^2 w}{\partial x^2}=0. \tag{8.143}$$

*This equation was obtained by Stowell [8.16]. He also solved a series of particular problems for plates, compressed in one direction.

Let us consider different conditions of fastening.

1. <u>All edges of plate are supported by hinge</u>. Taking w as before in the form (111), we obtain

$$\sigma=\frac{\pi^2 D_c'}{b^2 h}\left[\left(\frac{1}{4}+\frac{3}{4}\frac{\varphi_\kappa}{\varphi_c}\right)\frac{1}{\lambda^2}+2n^2+\lambda^2 n^4\right]. \qquad (8.144)$$

where $\lambda = a/bm$. We take $n = 1$ and write condition (114) for an elongated plate; then we find

$$\lambda=\sqrt[4]{\frac{1}{4}+\frac{3}{4}\frac{\varphi_\kappa}{\varphi_c}}. \qquad (8.145)$$

Judging by (145) in elastoplastic region <u>waves are shortened in direction of compression</u>, and more intensely the less ration φ_K/φ_C. This is natural; relative rigidity of plate along x with development of plastic deformations drops.

Coefficient K in formula (116) obtains the value

$$K=2\varphi_c\left(\sqrt{\frac{1}{4}+\frac{3}{4}\frac{\varphi_\kappa}{\varphi_c}}+1\right). \qquad (8.146)$$

In case of a <u>square</u> plate, if we take $m = 1$, we obtain

$$K=3{,}25\varphi_c+0{,}75\varphi_\kappa. \qquad (8.146a)$$

With strongly developed plastic deformation it is possible to put $\varphi_K = \varphi_C$; then instead of (146) and (146a), we obtain

$$\sigma_{кр}=4\frac{\pi^2 D_c'}{b^2 h}; \qquad (8.147)$$

thus, critical stress will be determined by the "secant modulus." For points of the yield surface when $\varphi_K = 0$ in the case of an elongated plate we have

$$\sigma_{кр}=3\frac{\pi^2 D_c'}{b^2 h}.$$

which coincides with (124). Length of half-waves here constitutes by (145) about 0.7 of the width of the plate. As one should have expected, value of K found without calculation of effect of unloading, lies, as a rule, lower than that taking into account unloading.

We introduce a designation for the "reduced" factor

$$\varphi_{пр}=\frac{1}{2}\varphi_c\sqrt{1+3\frac{\varphi_т}{\varphi_c}}. \tag{8.148}$$

and rewrite formula (116) for an elongated plate in the form

$$\sigma_{кр}=2\frac{\pi^2D'}{b^2h}(\varphi_{пр}+\varphi_c). \tag{8.116a}$$

For elastic region $\varphi_{пр} = \varphi_c = 1$. During calculation of D' we take $\mu = 0.5$. Therefore (116a) does not pass into known formula (7.77). This transition will be carried out below, in Section 107; here conditionally we take $D' = D$ and designate critical stress for elastic region by $\sigma_{кр.э}$; then instead of (116a) we obtain

$$\sigma_{кр}=\eta\sigma_{кр.э}. \tag{8.149}$$

where by η is understood correction factor for the elastoplastic region:

$$\eta=0.5(\varphi_c+\varphi_{пр}). \tag{8.150}$$

For square plate from (147)

$$\eta=0.81\varphi_c+0.19\varphi_т. \tag{8.150a}$$

Let us consider, further, a plate, <u>compressed along short side</u>, where $a \ll b$, $\lambda^2 \ll 1$; then

$$\sigma_{кр}=\frac{\pi^2D'}{4b^2h}(\varphi_c+3\varphi_т).$$

Relating this magnitude to value $\sigma_{кр.э}$ and taking $D' = D$ we arrive at the correction factor for the case of "cylindrical buckling" of the plate in the form

$$\eta=0.25\varphi_c+0.75\varphi_т. \tag{8.150b}$$

Let us remember that since we do not consider effect of unloading, then in limiting case of <u>compressed bar</u> we should have

$$\eta=\varphi_т. \tag{8.150c}$$

2. <u>Loaded edges of plates are secured by hinge, and unloaded edges are pinched (Fig. 7.17)</u>. We shall use the energy method of solving the problem. With uniaxial compression expression (142) for

U* will take the form

$$U^* = \frac{D'}{2}\left[\varphi_c(\varkappa_x^2 + \varkappa_x\varkappa_y + \varkappa_y^2 + \chi^2) - \frac{3}{4}(\varphi_c - \varphi_\kappa)\varkappa_x^2\right]. \qquad (8.151)$$

hence

$$U = \frac{D'_c}{2}\int_F\int\left[\left(\frac{1}{4} + \frac{3}{4}\frac{\varphi_\kappa}{\varphi_c}\right)\left(\frac{\partial^2 w}{\partial x^2}\right)^2 + \frac{\partial^2 w}{\partial x^2}\frac{\partial^2 w}{\partial y^2} + \right.$$

$$\left. + \left(\frac{\partial^2 w}{\partial y^2}\right)^2 + \left(\frac{\partial^2 w}{\partial x\,\partial y}\right)^2\right] dx\,dy. \qquad (8.151a)$$

Work of external forces according to (106) will be

$$W = \frac{h}{2}\int_F\int \sigma_x\left(\frac{\partial w}{\partial x}\right)^2 dx\,dy. \qquad (8.152)$$

Using (108) and considering $\sigma_x = \sigma$, we find

$$\sigma = \frac{D'_c\int_F\int\left[\left(\frac{1}{4} + \frac{3}{4}\frac{\varphi_\kappa}{\varphi_c}\right)\left(\frac{\partial^2 w}{\partial x^2}\right)^2 + \frac{\partial^2 w}{\partial x^2}\frac{\partial^2 w}{\partial y^2} + \left(\frac{\partial^2 w}{\partial y^2}\right)^2 + \left(\frac{\partial^2 w}{\partial x\,\partial y}\right)^2\right] dx\,dy}{h\int_F\int\left(\frac{\partial w}{\partial x}\right)^2 dx\,dy}. \qquad (8.153)$$

Expression for deflection we write in the form

$$w = f\sin\frac{m\pi x}{a}\sin^2\frac{n\pi y}{b}. \qquad (8.154)$$

After substitution of this expression in (153) and integration we find

$$\sigma = \frac{\pi^2 D'_c}{b^2 h}\left[\left(\frac{1}{4} + \frac{3}{4}\frac{\varphi_\kappa}{\varphi_c}\right)\frac{m^2 b^2}{a^2} + \frac{8n^2}{3} + \frac{16}{3}\frac{a^2 n^4}{b^2 m^2}\right].$$

Magnitude σ will be as before, minimum when n = 1. We assume that plate is elongated and loaded edges are free. Considering $\frac{a}{bm} = \lambda$, we obtain

$$\sigma = \frac{\pi^2 D'_c}{b^2 h}\left[\left(\frac{1}{4} + \frac{3}{4}\frac{\varphi_\kappa}{\varphi_c}\right)\frac{1}{\lambda^2} + \frac{8}{3} + \frac{16}{3}\lambda^2\right]. \qquad (8.155)$$

Condition (114) leads to relationship

$$\lambda = \frac{1}{2}\sqrt[4]{\frac{3}{4} + \frac{9}{4}\frac{\varphi_\kappa}{\varphi_c}},$$

and then

$$\sigma_{kp} = 8\frac{\pi^2 D'_c}{b^2 h}\left(\frac{1}{3} + \frac{1}{2}\sqrt{\frac{1}{3} + \frac{\varphi_\kappa}{\varphi_c}}\right). \qquad (8.156)$$

For $\varphi_K = \varphi_c = 1$ and $D' = D$ we arrive at formulas of Section 83 for the elastic region,

$$\lambda_0 = \frac{\sqrt[4]{3}}{2}, \quad \sigma_{кр.0} = \frac{8(\sqrt{3}+1)}{3}\frac{\pi^2 D}{b^2 h}.$$

Correction factor η for $D' = D$ obtains value

$$\eta = \frac{\varphi_c + \sqrt{3}\varphi_{кр}}{\sqrt{3}+1},$$

or

$$\eta \approx 0.36\varphi_c + 0.64\varphi_{кр}. \tag{8.157}$$

3. Loaded edges are supported by hinge, and one unloaded edge is secured by hinge while the other is free. In this case we take such an expression for w:

$$w = f\frac{y}{b}\sin\frac{m\pi x}{a}; \tag{8.158}$$

axes of coordinates are located, as shown in Fig. 7.22. From formula (153) we obtain

$$\sigma = \frac{D'_c\left[\left(\frac{1}{4}+\frac{3}{4}\frac{\varphi_K}{\varphi_c}\right)\frac{\pi^2 b m^4}{6a^3}+\frac{\pi^2 m^2}{2ab}\right]}{h\frac{\pi^2 b m^2}{6a}}. \tag{8.159}$$

Expression (159) will be a minimum when $m = 1$; just as in the elastic problem, here along axis x there will be formed one half-wave; consequently,

$$\sigma_{кр} = \frac{\pi^2 D'_c}{b^2 h}\left[\left(\frac{1}{4}+\frac{3}{4}\frac{\varphi_K}{\varphi_c}\right)\left(\frac{b}{a}\right)^2+\frac{3}{\pi^2}\right]. \tag{8.160}$$

In case of elongated plate when $b \ll a$

$$\sigma_{кр} = \frac{3D'_c}{b^2 h} = \frac{1}{3}E_c\left(\frac{h}{b}\right)^2. \tag{8.160a}$$

Correction factor turns out to be, for $D' = D$, equal to

$$\eta = \varphi_c. \tag{8.161}$$

Critical stress turned out to be here proportional to secant modulus. This allows us significantly to facilitate practical calculations. For ratio b/h we find critical deformation:

$$\varepsilon_{кр} = \frac{1}{3}\left(\frac{h}{b}\right)^2. \tag{8.162}$$

and by diagram $\sigma(\varepsilon)$ for given material – corresponding value of secant modulus E_c, we then have

$$\sigma_{кр} = E_c \varepsilon_{кр}.$$

Gerard proposed [8.10] to use this method for determining critical stresses with other boundary conditions; in a formula of type (162) he recommends we put, instead of coefficient 1/3, such coefficient k which ensues from the solution of the elastic problem; for example in the case of an elongated plate with hinge-secured edges, k = 3.6.

As we have seen, such calculation by secant modulus, frequently met in the literature, ensues from theory of deformations in case of uniaxial compression only in one particular case. In all other problems this method must be considered approximate, where error in its use may be sizable.

4. Loaded edges are supported by hinge, one of unloaded edges is clamped and the other is free. Using the same method as in paragraph 3, we find the following final expression for correction factor η when $D' = D$:

$$\eta = 0{,}43\varphi_c + 0{,}57\varphi_{кр}. \qquad (8.163)$$

Value of η for duralumin and steel plates are given below in Section 110.

§ 106. Buckling of Plate During Shearing

Let us turn to case of square plate with side a, subject to action of tangential stresses τ on all edges (see Fig. 7.24). From (11) we find

$$\sigma_1 = \sqrt{3}\tau. \qquad (8.164)$$

Equation (140) obtains the form

$$\frac{\partial^4 w}{\partial x^4} + \left(1 + \frac{\varphi_1}{\varphi_c}\right)\frac{\partial^4 w}{\partial x^2 \partial y^2} + \frac{\partial^4 w}{\partial y^4} + \frac{2h}{D_c'}\tau\frac{\partial^2 w}{\partial x \partial y} = 0 \qquad (8.165)$$

or

$$X \equiv \nabla^4 w - \psi \frac{\partial^4 w}{\partial x^2 \partial y^2} + \frac{2h}{D_c'} \tau \frac{\partial^2 w}{\partial x \partial y} = 0. \tag{8.166}$$

Here we assume

$$\psi = 1 - \frac{\tau_x}{\tau_c}. \tag{8.167}$$

Expression for deflection we take in the form of (7.148):

$$w = \sum_m \sum_n f_{mn} \sin \frac{m\pi x}{a} \sin \frac{n\pi y}{a}. \tag{8.168}$$

We write equation of Bubnov-Galerkin method:

$$\int_p \int X \sin \frac{i\pi x}{a} \sin \frac{j\pi y}{a} dx\, dy = 0. \tag{8.169}$$

Taking into account relationships (7.151), we obtain

$$f_{mn} \frac{\pi^4}{a^4} \left[\frac{(m^2+n^2)^2}{4} - \lambda_{mn} \right] - \sum_i \sum_j f_{ij} 8a^2 \frac{mnij}{(m^2-i^2)(n^2-j^2)} = 0. \tag{8.170}$$

We introduce designations

$$\tau^0 = \frac{\tau a^2}{E_c h^2}, \quad p^0 = \frac{\pi^2}{3(1-\mu^2)}. \tag{8.171}$$

Proceeding the same as in Section 85, we consider first combinations of indices: (1, 1), (2, 2) and (2, 2), (1, 1); then we obtain a system of equations for f_{11} and f_{22}. We equate to zero the determinate of the system:

$$\begin{vmatrix} (4-\psi)p^0 & -\frac{4}{9}\frac{128}{\pi^2}\tau^0 \\ -\frac{1}{9}\frac{128}{\pi^2}\tau^0 & (16-4\psi)p^0 \end{vmatrix} = 0. \tag{8.172}$$

Parameter τ^*_{kp}, corresponding to critical shearing stress, turns out to be, in the first approximation, equal to

$$\tau^0_{kp.1} = \frac{9\pi^2}{32} p^0 \left(1 - \frac{\psi}{4}\right); \tag{8.173}$$

hence

$$\tau_{kp.1} = 12.1 \left(1 - \frac{\psi}{4}\right) E_c \left(\frac{h}{a}\right)^2. \tag{8.173a}$$

We select as the second approximation the following indices m and n: (1, 1), (1, 3), (3, 1), (3, 3), and i, j – (2, 2) and then change their places. This will lead to an equation, generalizing the former

equation (7.164) for the elastoplastic region:

$$\begin{vmatrix} (4-\psi)p^* & -\frac{4}{9}\frac{128}{\pi^2}\tau^* & 0 & 0 & 0 \\ -\frac{1}{9}\frac{128}{\pi^2}\tau^* & (16-4\psi)p^* & \frac{1}{5}\frac{128}{\pi^2}\tau^* & \frac{1}{5}\frac{128}{\pi^2}\tau^* & -\frac{9}{25}\frac{128}{\pi^2}\tau^* \\ 0 & -\frac{4}{5}\frac{128}{\pi^2}\tau^* & (33-3\psi)p^* & 0 & 0 \\ 0 & -\frac{4}{15}\frac{128}{\pi^2}\tau^* & 0 & (33-3\psi)p^* & 0 \\ 0 & -\frac{4}{15}\frac{128}{\pi^2}\tau^* & 0 & 0 & (36-9\psi)p^* \end{vmatrix} = 0. \tag{8.174}$$

Determining from this $\tau^*_{кр,2}$ of the second approximation and comparing this magnitude with $\tau^*_{кр,1}$, we obtain

$$\tau^*_{кр,2} = \frac{\tau^*_{кр,1}}{\sqrt{1+\frac{81}{25}\left[\frac{2(4-\psi)}{100-9\psi}+\frac{1}{25}\right]}}. \tag{8.175}$$

In Section 85 one could see that magnitude in the denominator, for $\psi = 0$ is equal to 1.18. Extending this value to case $\psi = 0$, we obtain

$$\tau^*_{кр} = 10{,}2E_c\left(1-\frac{\psi}{4}\right)\left(\frac{h}{a}\right)^2. \tag{8.176}$$

or

$$\tau^*_{кр} = 10{,}2E(0{,}75\varphi_c + 0{,}25\varphi_u)\left(\frac{h}{a}\right)^2. \tag{8.177}$$

Correction factor turns out to be equal to

$$\eta = 0{,}75\varphi_c + 0{,}25\varphi_u. \tag{8.178}$$

This value of η we take conditionally also for plates with arbitrary ratio of sides. Let us note that Gerard recommends in case of shear that we make calculations by secant modulus [8.10] and take $\eta = \varphi_c$.

§ 107. Generalization of Theory of Deformations to Case of Compressible Material

Preceding solutions of problem of elastoplastic stability of plates have the deficiency that for all points of diagram $\sigma_1(\varepsilon_1)$ Poisson's ratio was considered equal to 0.5. Therefore, the fundamental

differential equations (85) or (140), do not lead in the particular case of purely elastic deformation to known equation of classical theory of plates; this also pertains to separate calculating formulas.

In order to obtain definitized solution for a material, compressible in elastic region, we shall use the more complete dependences of Section 100 between deformations and stresses.* We shall limit ourselves here to case of uniaxial stress up to loss of stability ($\sigma_y = \tau = 0$) and will not consider effect of unloading.

We use relationships

$$\sigma_x - S = \sigma_x - \frac{\sigma_x + \sigma_y}{3} = \frac{2}{3} s_x, \quad \sigma_y - S = \frac{2}{3} s_y. \tag{8.179}$$

then expressions (18) for deformations can be rewritten in the following form:

$$\varepsilon_x = \frac{1}{E}(\sigma_x - \mu\sigma_y) + \frac{1}{E_{ш.}} s_x. \tag{8.180}$$

$$\varepsilon_y = \frac{1}{E}(\sigma_y - \mu\sigma_x) + \frac{1}{E_{ш.}} s_y. \tag{8.181}$$

$$\gamma = \left[\frac{2(1+\mu)}{E} + \frac{3}{E_{ш.}}\right]\tau. \tag{8.182}$$

We express variation of magnitudes ε_x, ε_y, and γ by variations of stresses in this general form:

$$\left.\begin{aligned} \delta\varepsilon_x &= A_{11}\delta\sigma_x + A_{12}\delta\sigma_y + A_{13}\delta\tau, \\ \delta\varepsilon_y &= A_{21}\delta\sigma_x + A_{22}\delta\sigma_y + A_{23}\delta\tau, \\ \delta\gamma &= A_{31}\delta\sigma_x + A_{32}\delta\sigma_y + A_{33}\delta\tau. \end{aligned}\right\} \tag{8.183}$$

Coefficients A_{11}, A_{12},... are equal to the corresponding derivatives:

$$A_{11} = \frac{\partial\varepsilon_x}{\partial\sigma_x}, \quad A_{12} = \frac{\partial\varepsilon_x}{\partial\sigma_y}, \quad A_{13} = \frac{\partial\varepsilon_x}{\partial\tau} \text{ and etc.} \tag{8.184}$$

Considering expressions (182), immediately we find

$$A_{13} = A_{23} = A_{31} = A_{32} = 0. \tag{8.185}$$

---

*Such a solution was first given by L. A. Tolokonnikov [8.8]. Another way of solution, presented below, was offered for case $\sigma_y = \tau = 0$ by Bijlaard [8.9], and in more general form, by A. P. Prusakov [16.12]. The last two authors considered problem without calculation of effect of unloading.

We determine the remaining coefficients. Using equality (180), we obtain

$$A_{11}=\frac{\partial \varepsilon_x}{\partial \sigma_x}=\frac{1}{E}+\frac{1}{E_{пл}}\frac{\partial s_x}{\partial \sigma_x}+s_x\frac{\partial}{\partial \sigma_x}\left(\frac{1}{E_{пл}}\right). \tag{8.186}$$

Derivative of s_x is equal to

$$\frac{\partial s_x}{\partial \sigma_x}=1. \tag{8.187}$$

We find derivative of $1/E_{пл}$. Proceeding from relationship (17), we have

$$\frac{\partial}{\partial \sigma_x}\left(\frac{1}{E_{пл}}\right)=\frac{\partial}{\partial \sigma_x}\left(\frac{1}{E_c}\right). \tag{8.188}$$

We write this expression in the form

$$\frac{\partial}{\partial \sigma_x}\left(\frac{1}{E_c}\right)=\frac{d}{d\sigma_i}\left(\frac{s_i}{\sigma_i}\right)\frac{\partial \sigma_i}{\partial \sigma_x}. \tag{8.189}$$

We find

$$\frac{d}{d\sigma_i}\left(\frac{s_i}{\sigma_i}\right)=\left(\frac{d s_i}{d\sigma_i}\sigma_i-s_i\right)\frac{1}{\sigma_i^2}=\left(\frac{1}{E_к}-\frac{1}{E_c}\right)\frac{1}{\sigma_i} \tag{8.190}$$

and, further,

$$\frac{\partial \sigma_i}{\partial \sigma_x}=\frac{\partial}{\partial \sigma_x}\sqrt{\sigma_x^2-\sigma_x\sigma_y+\sigma_y^2+3\tau^2}=\frac{2\sigma_x-\sigma_y}{2\sigma_i}=\frac{s_x}{\sigma_i}. \tag{8.191}$$

Finally

$$\frac{\partial}{\partial \sigma_x}\left(\frac{1}{E_c}\right)=\left(\frac{1}{E_к}-\frac{1}{E_c}\right)\frac{s_x}{\sigma_i^2}. \tag{8.192}$$

Expression (186) obtains the form

$$A_{11}=\frac{1}{E}+\frac{1}{E_{пл}}+\left(\frac{1}{E_к}-\frac{1}{E_c}\right)\frac{s_x^2}{\sigma_i^2}. \tag{8.193}$$

Analogously we calculate the remaining coefficients:

$$A_{12}=A_{21}=-\frac{\mu}{E}-\frac{1}{2E_{пл}}+\left(\frac{1}{E_к}-\frac{1}{E_c}\right)\frac{s_x s_y}{\sigma_i^2}. \tag{8.194}$$

$$A_{22}=\frac{1}{E}+\frac{1}{E_{пл}}+\left(\frac{1}{E_к}-\frac{1}{E_c}\right)\frac{s_y^2}{\sigma_i^2}. \tag{8.195}$$

Considering the fundamental stress uniaxial, we take

$$s_x=\sigma_x,\quad s_y=-\frac{\sigma_x}{2},\quad \sigma_i=\sigma_x; \tag{8.196}$$

then we obtain

$$\left.\begin{aligned} A_{11} &= \frac{1}{E} + \frac{1}{E_{ш}} + \frac{1}{E_{к}} - \frac{1}{E_{с}}. \\ A_{12} = A_{21} &= -\frac{\mu}{E} - \frac{1}{2E_{ш}} - \frac{1}{2}\left(\frac{1}{E_{к}} - \frac{1}{E_{с}}\right). \\ A_{22} &= \frac{1}{E} + \frac{1}{E_{ш}} + \frac{1}{4}\left(\frac{1}{E_{к}} - \frac{1}{E_{с}}\right). \end{aligned}\right\} \qquad (8.197)$$

We use relationship (17); then expression (197) can be reduced to the form

$$A_{11} = \frac{1}{E_{к}} + \frac{1-2\mu}{3E}. \qquad (8.198)$$

$$A_{12} = A_{21} = -\frac{1}{2E_{к}} + \frac{1-2\mu}{3E}. \qquad (8.199)$$

$$A_{22} = \frac{3}{4}\frac{1}{E_{с}} + \frac{1}{4}\frac{1}{E_{к}} + \frac{1-2\mu}{3E}. \qquad (8.200)$$

Coefficient A_{33} we find directly from (182); using (17), we have

$$A_{33} = \frac{3}{E_{с}}. \qquad (8.201)$$

We express variations of stresses by variations of deformations; in general form we have

$$\left.\begin{aligned} \delta\sigma_x &= a_{11}\delta\varepsilon_x + a_{12}\delta\varepsilon_y + a_{13}\delta\gamma. \\ \delta\sigma_y &= a_{21}\delta\varepsilon_x + a_{22}\delta\varepsilon_y + a_{23}\delta\gamma. \\ \delta\tau &= a_{31}\delta\varepsilon_x + a_{32}\delta\varepsilon_y + a_{33}\delta\gamma. \end{aligned}\right\} \qquad (8.202)$$

We must find the matrix of coefficients a_{11}, a_{12}, ..., the inverse of matrix of magnitudes A_{11}, A_{12}, ... As it is easy to see, in this case

$$a_{13} = a_{23} = a_{31} = a_{32} = 0. \qquad (8.203)$$

Remaining coefficients are equal to

$$a_{11} = \frac{A_{22}}{\Delta}, \quad a_{12} = a_{21} = -\frac{A_{12}}{\Delta}, \quad a_{22} = \frac{A_{11}}{\Delta}, \quad a_{33} = \frac{1}{A_{33}}. \qquad (8.204)$$

By Δ here is implied determinant, composed from coefficients A_{11}, ..., A_{22}:

$$\Delta = \begin{vmatrix} A_{11} & A_{12} \\ A_{21} & A_{22} \end{vmatrix}. \qquad (8.205)$$

Substituting expressions (198)–(200), after simplifications we find

$$\Delta = \frac{3}{4E_{с}E_{к}} + \frac{1-2\mu}{E}\left(\frac{1}{4E_{с}} + \frac{3}{4E_{к}}\right). \qquad (8.206)$$

Let us turn to dimensionless magnitudes:

$$\bar{a}_{11}=\frac{a_{11}}{E},\quad \bar{a}_{12}=\frac{a_{12}}{E},\quad \ldots,\quad \bar{\Delta}=\frac{\Delta}{E^2}; \tag{8.207}$$

then we obtain

$$\bar{a}_{11}=\frac{1}{\bar{\Delta}}\left(\frac{3}{4\varphi_c}+\frac{1}{4\varphi_u}+\frac{1-2\mu}{3}\right),\quad \bar{a}_{22}=\frac{1}{\bar{\Delta}}\left(\frac{1}{\varphi_u}+\frac{1-2\mu}{3}\right). \tag{8.208}$$

$$\bar{a}_{12}=\bar{a}_{21}=\frac{1}{\bar{\Delta}}\left(\frac{1}{2\varphi_u}-\frac{1-2\mu}{3}\right),\quad \bar{a}_{33}=\frac{\varphi_c}{3}, \tag{8.209}$$

where

$$\bar{\Delta}=\frac{3}{4\varphi_c\varphi_u}+(1-2\mu)\left(\frac{1}{4\varphi_c}+\frac{3}{4\varphi_u}\right). \tag{8.210}$$

If we ignore effect of unloading during buckling of plate, then for all points of the thickness relationships (202) will be valid. Bending and torsional moments will be equal to

$$M_x=\int_{-\frac{h}{2}}^{\frac{h}{2}}\delta\sigma_x z\,dz,\quad M_y=\int_{-\frac{h}{2}}^{\frac{h}{2}}\delta\sigma_y z\,dz,\quad H=\int_{-\frac{h}{2}}^{\frac{h}{2}}\delta\tau z\,dz. \tag{8.211}$$

Increments of bending strains we will express by curvatures:

$$\delta\varepsilon_x=z\varkappa_x,\quad \delta\varepsilon_y=z\varkappa_y,\quad \delta\gamma=2z\chi; \tag{8.212}$$

then we obtain

$$\left.\begin{aligned}&\frac{12M_x}{Eh^3}=\bar{a}_{11}\varkappa_x+\bar{a}_{12}\varkappa_y,\quad \frac{12M_y}{Eh^3}=\bar{a}_{21}\varkappa_x+\bar{a}_{22}\varkappa_y.\\&\frac{12H}{Eh^3}=2\bar{a}_{33}\chi.\end{aligned}\right\} \tag{8.213}$$

If we use expressions (80) for curvatures, then equation of equilibrium (84) obtains the form

$$\bar{a}_{11}\frac{\partial^4 w}{\partial x^4}+2(\bar{a}_{12}+2\bar{a}_{33})\frac{\partial^4 w}{\partial x^2\partial y^2}+\bar{a}_{22}\frac{\partial^4 w}{\partial y^4}+\frac{12}{Eh^2}\sigma\frac{\partial^2 w}{\partial x^2}=0. \tag{8.214}$$

Before last member we take a plus sign, since stress is considered positive during compression.

Differential equation (214) is valid both for purely elastic, and also for elastoplastic region, Poisson's ratio μ may be selected in

accordance with given experiments for considered material. In limiting case of elastic deformation it is necessary to use dependence (20). Considering for uniaxial extension or compression $E_c^0 = E$, we obtain

$$\frac{1}{E_c} = \frac{1}{E}\left(1 - \frac{1-2\mu}{3}\right) = \frac{2(1+\mu)}{3E}. \tag{8.215}$$

We will have an analogous formula for magnitude, the reciprocal of the tangent modulus in diagram $\sigma_1(\varepsilon_1)$:

$$\frac{1}{E_\kappa} = \frac{2(1+\mu)}{3E}; \tag{8.216}$$

hence

$$\frac{1}{\varphi_c} = \frac{1}{\varphi_\kappa} = \frac{2(1+\mu)}{3}. \tag{8.217}$$

Formula (210) obtains the form

$$\bar{\Delta} = 1 - \mu^2. \tag{8.218}$$

Instead of (208) and (209) we find,

$$\bar{a}_{11} = \bar{a}_{22} = \frac{1}{1-\mu^2}, \quad \bar{a}_{12} = \bar{a}_{21} = \frac{\mu}{1-\mu^2}, \quad \bar{a}_{33} = \frac{1}{2(1+\mu)}. \tag{8.219}$$

Using these values, instead of (214), we obtain known equation (7.70) pertaining to elastic region.

If we were to consider material incompressible and put $\mu = 0.5$, we have

$$\bar{\Delta} = \frac{3}{4\varphi_c\varphi_\kappa}, \quad \bar{a}_{11} = \varphi_\kappa + \frac{1}{3}\varphi_c, \quad \bar{a}_{12} = \frac{2}{3}\varphi_c, \quad \bar{a}_{22} = \frac{4}{3}\varphi_c, \quad \bar{a}_{33} = \frac{\varphi_c}{3}, \tag{8.220}$$

and then equation (214) acquires the form

$$\left(\frac{1}{4} + \frac{3}{4}\frac{\varphi_\kappa}{\varphi_c}\right)\frac{\partial^4 w}{\partial x^4} + 2\frac{\partial^4 w}{\partial x^2 \partial y^2} + \frac{\partial^4 w}{\partial y^4} + \frac{\sigma}{Eh^2\varphi_c}\frac{\partial^2 w}{\partial x^2} = 0. \tag{8.221}$$

which coincides with the equation (143) obtained above.

We shall consider case of <u>elongated hinge-supported plate, compressed in one direction.</u> We take for deflection expression (111) and substitute it in equation (214); considering $n = 1$, we have

$$\sigma = \frac{\pi^2 E h^2}{12b^2}\left[\bar{a}_{11}\frac{1}{\lambda^2} + 2(\bar{a}_{12} + 2\bar{a}_{33}) + \bar{a}_{22}\lambda^2\right], \quad \lambda = \frac{a}{bm}. \tag{8.222}$$

Condition (114) gives

$$\lambda=\sqrt[4]{\frac{\bar{a}_{11}}{\bar{a}_{22}}}.$$

Critical stress turns out to be equal to

$$\sigma_{xp}=\frac{\pi^2Eh^2}{6b^2}(\sqrt{\bar{a}_{11}\bar{a}_{22}}+\bar{a}_{12}+2\bar{a}_{33}). \tag{8.223}$$

If we use values of coefficients (219), for elastic region we obtain known formula

$$\sigma_{xp}=\frac{\pi^2Eh^2}{3(1-\mu^2)b^2}=\frac{4\pi^2D}{b^2h}. \tag{8.224}$$

Substituting in (223) the expression (220), we arrive at former formula (146), pertaining to incompressible material.

We turn to case of square hinge-supported plate. Taking (222) $m = n = 1$, we find critical stress equal to

$$\sigma_{xp}=\frac{\pi^2Eh^2}{12b^2}[\bar{a}_{11}+\bar{a}_{22}+2(\bar{a}_{12}+2\bar{a}_{33})]. \tag{8.225}$$

In elastic region we obtain formula, coinciding with (224). For $\mu = 0.5$ we again arrive at expression (146a).

§ 108. Application of Flow Theory

We apply to solution of problems of stability of plates another theory of plasticity – flow theory, directly connecting increase of deformations and stresses with components of stresses.* Let us remember basic dependences (5) and (6) of theory of elastoplastic deformations included total values of deformations.

We consider that increments of deformations have elastic and plastic components. We assume that both these components are determined for incompressible material where $\mu = 0.5$. Elastic components

*Flow theory was applied to problems of stability of plates by Handelman and Prager [8.12], Pearson [8.14], and L. M. Kachanov [8.3].

in case of plane stress are equal to

$$\left.\begin{aligned}\delta\varepsilon'_x &= \frac{1}{E}\left(\delta\sigma_x - \frac{1}{2}\delta\sigma_y\right) = \frac{1}{E}\delta s_x,\\ \delta\varepsilon'_y &= \frac{1}{E}\left(\delta\sigma_y - \frac{1}{2}\delta\sigma_x\right) = \frac{1}{E}\delta s_y,\\ \delta\gamma' &= \frac{1}{G}\delta\tau = \frac{3}{E}\delta\tau.\end{aligned}\right\} \tag{8.226}$$

Plastic components according to the flow theory are determined in the following manner [8.3]:

$$\left.\begin{aligned}\delta\varepsilon''_x &= \theta\left(\sigma_x - \frac{1}{2}\sigma_y\right) = \theta s_x,\\ \delta\varepsilon''_y &= \theta\left(\sigma_y - \frac{1}{2}\sigma_x\right) = \theta s_y,\\ \delta\gamma'' &= 3\theta\tau.\end{aligned}\right\} \tag{8.227}$$

In case of uniaxial extension total increment of deformation will be

$$\delta\varepsilon_x = \frac{1}{E}\delta\sigma_x + \theta\sigma_x. \tag{8.228}$$

hence

$$\theta = \frac{1}{\sigma_x}\left(\delta\varepsilon_x - \frac{1}{E}\delta\sigma_x\right) = \frac{\delta\sigma_x}{\sigma_x}\left(\frac{\delta\varepsilon_x}{\delta\sigma_x} - \frac{1}{E}\right). \tag{8.229}$$

Using former designation for tangent modulus

$$E_\tau^0 = \frac{d\sigma_x}{d\varepsilon_x} = E\eta, \tag{8.230}$$

we obtain

$$\theta = \frac{1}{E}\frac{\delta\sigma_x}{\sigma_x}\left(\frac{1}{\eta} - 1\right). \tag{8.231}$$

We shall subsequently designate

$$\psi = \frac{1}{\eta} - 1. \tag{8.232}$$

Relationship (231) is generalized to case of complex stress in such a way that instead of σ_x here is introduced intensity of stresses σ_i; then we have

$$\theta = \frac{1}{E}\frac{\delta\sigma_i}{\sigma_i}\psi. \tag{8.233}$$

Finally increments of deformations turn out to be equal to

$$\left.\begin{aligned}\delta\varepsilon_x &= \frac{1}{E}\left(\delta\sigma_x + \psi\frac{\delta\sigma_i}{\sigma_i}s_x\right).\\ \delta\varepsilon_y &= \frac{1}{E}\left(\delta\sigma_y + \psi\frac{\delta\sigma_i}{\sigma_i}s_y\right).\end{aligned}\right\} \tag{8.234}$$

$$\delta\gamma = \frac{3}{E}\left(\delta\tau + \psi\frac{\delta\sigma_i}{\sigma_i}\tau\right). \tag{8.235}$$

Finding variation from intensity of stresses, we have

$$\delta\sigma_i = \frac{s_x \delta s_x + s_y \delta s_y + 3\tau\delta\tau}{\sigma_i}. \tag{8.236}$$

Using (236) we rewrite expressions (234) and (235) in the form of (183); as coefficients here there serve magnitudes

$$\left.\begin{aligned} &A_{11} = \frac{1}{E}(1+\psi\bar{s}_x^2),\ A_{22} = \frac{1}{E}(1+\psi\bar{s}_y^2),\ A_{33} = \frac{3}{E}(1+3\psi\bar{\tau}^2),\\ &A_{12} = A_{21} = \frac{1}{E}\left(-\frac{1}{2}+\psi\bar{s}_x\bar{s}_y\right),\\ &A_{13} = A_{31} = \frac{3}{E}\psi\bar{s}_x\bar{\tau},\ A_{23} = A_{32} = \frac{3}{E}\psi\bar{s}_y\bar{\tau}; \end{aligned}\right| \tag{8.237}$$

by $\bar{s}_x$, $\bar{s}_y$, and $\bar{\tau}$ are understood dimensionless parameters

$$\bar{s}_x = \frac{s_x}{\sigma_i},\quad \bar{s}_y = \frac{s_y}{\sigma_i},\quad \bar{\tau} = \frac{\tau}{\sigma_i}. \tag{8.238}$$

We determine increments of stresses by formulas (202). Coefficients a_{11}, a_{12}, ... here too form a matrix, the reverse of the matrix of coefficients A_{11}, A_{12}, ... We designate by Δ the basic determinant of system (183):

$$\Delta = \begin{vmatrix} A_{11} & A_{12} & A_{13} \\ A_{21} & A_{22} & A_{23} \\ A_{31} & A_{32} & A_{33} \end{vmatrix}. \tag{8.239}$$

Calculating this determinant, we find

$$\begin{aligned} E^3\Delta = &(1+\psi\bar{s}_x^2)\left[3(1+\psi\bar{s}_y^2)(1+3\psi\bar{\tau}^2) - 9\psi^2\bar{s}_y\bar{\tau}^2\right] + \\ &+\left(-\frac{1}{2}+\psi\bar{s}_x\bar{s}_y\right)\left[9\psi^2(\bar{s}_x\bar{s}_y\bar{\tau}^2) - 3(1+3\psi\bar{\tau}^2)\left(-\frac{1}{2}+\psi\bar{s}_x\bar{s}_y\right)\right] + \\ &+3\psi\bar{s}_x\bar{\tau}\left[\left(-\frac{1}{2}+\psi\bar{s}_x\bar{s}_y\right)3\psi\bar{s}_y\bar{\tau} - (1+\psi\bar{s}_y^2)3\psi\bar{s}_x\bar{\tau}\right]. \end{aligned} \tag{8.240}$$

Taking into account relationship

$$\bar{s}_x^2 + \bar{s}_y^2 + \bar{s}_x\bar{s}_y + \frac{9}{4}\bar{\tau}^2 = \frac{3}{4\sigma_i^2}(\sigma_x^2 + \sigma_y^2 - \sigma_x\sigma_y + 3\tau^2) = \frac{3}{4}. \tag{8.241}$$

after simplifications we have

$$E^3\Delta = \frac{9}{4}(1+\psi) = \frac{9}{4\varphi_2}. \tag{8.242}$$

Coefficient a_{11} turns out to be equal to

$$a_{11} = \frac{\begin{vmatrix} A_{22} & A_{23} \\ A_{32} & A_{33} \end{vmatrix}}{\Delta/E} = \frac{4E\varphi_2}{3}\left[1+\psi(\bar{s}_y^2 + 3\bar{\tau}^2)\right]. \tag{8.243}$$

Analogously we find the remaining coefficients. Finally we obtain

$$
\left.
\begin{aligned}
a_{11} &= \frac{4E}{3(1+\psi)}\left[1+\psi(\bar{s}_y^2+3\bar{\tau}^2)\right].\\
a_{22} &= \frac{4E}{3(1+\psi)}\left[1+\psi(\bar{s}_x^2+3\bar{\tau}^2)\right].\\
a_{12} = a_{21} &= \frac{4E}{3(1+\psi)}\left[\frac{1}{2}+\psi\left(\frac{3}{2}\bar{\tau}^2-\bar{s}_x\bar{s}_y\right)\right].\\
a_{33} &= \frac{4E}{3(1+\psi)}\left[\frac{1}{4}+\frac{\psi}{3}(\bar{s}_x^2+\bar{s}_y^2+\bar{s}_x\bar{s}_y)\right].\\
a_{13} = a_{31} &= -\frac{4E\psi}{3(1+\psi)}\bar{\tau}\left(\frac{1}{2}\bar{s}_y+\bar{s}_x\right).\\
a_{23} = a_{32} &= -\frac{4E\psi}{3(1+\psi)}\bar{\tau}\left(\frac{1}{2}\bar{s}_x+\bar{s}_y\right).
\end{aligned}
\right\}
\tag{8.244}
$$

We shall solve the problem <u>without calculation of effect of unloading</u>. Then for all points through the thickness of the plate one should take relationships (202).

We express increments of deformations by curvatures according to (212) and give expressions for moments the following form:

$$
\left.
\begin{aligned}
\frac{12M_x}{h^3} &= a_{11}\varkappa_x+a_{12}\varkappa_y+2a_{13}\chi.\\
\frac{12M_y}{h^3} &= a_{21}\varkappa_x+a_{22}\varkappa_y+2a_{23}\chi.\\
\frac{12H}{h^3} &= a_{31}\varkappa_x+a_{32}\varkappa_y+2a_{33}\chi.
\end{aligned}
\right\}
\tag{8.245}
$$

We express curvatures by deflection as per formulas (80). Putting expression (245) in equation of equilibrium (84), we obtain the following differential equation for deflection:

$$
\begin{aligned}
&\left[\varphi_2+(1-\varphi_2)(\bar{s}_y^2+3\bar{\tau}^2)\right]\frac{\partial^4 w}{\partial x^4}+2\left\{\varphi_2+(1-\varphi_2)\left[\frac{2}{3}(\bar{s}_x^2+\bar{s}_y^2)-\right.\right.\\
&\left.\left.-\frac{1}{3}\bar{s}_x\bar{s}_y+\frac{1}{2}\bar{\tau}^2\right]\right\}\frac{\partial^4 w}{\partial x^2\partial y^2}+\left[\varphi_2+(1-\varphi_2)(\bar{s}_x^2+3\bar{\tau}^2)\right]\frac{\partial^4 w}{\partial y^4}-\\
&-4(1-\varphi_2)\bar{\tau}\left[\left(\frac{1}{2}\bar{s}_y+\bar{s}_x\right)\frac{\partial^4 w}{\partial x^3\partial y}+\left(\frac{1}{2}\bar{s}_x+\bar{s}_y\right)\frac{\partial^4 w}{\partial x\,\partial y^3}\right]+\\
&+\frac{h}{D}\Pi(\sigma, w)=0.
\end{aligned}
\tag{8.246}
$$

Equation (246), is the initial one during solution of particular problems.

We turn, as an example, to problem of compression of a hinge-supported plate in direction x by forces σ; then

$$
s_x=\sigma,\quad s_y=-\frac{\sigma}{2},\quad \tau=0.
\tag{8.247}
$$

Instead of (246), we obtain

$$\left(\frac{1}{4}+\frac{3}{4}\varphi_c\right)\frac{\partial^4 w}{\partial x^4}+2\frac{\partial^4 w}{\partial x^2\partial y^2}+\frac{\partial^4 w}{\partial y^4}+\frac{h}{D'}\sigma\frac{\partial^2 w}{\partial x^2}=0. \tag{8.248}$$

Equation (248) has the same structure as equation (143) in the theory of deformations; they coincide if in equation (143) we set $\varphi_c = 1$, $D'_c = D'$, i.e., if instead of secant modulus we place modulus E. Therefore, we can use with this replacement all formulas of Section 105. It is clear that flow theory leads to higher values of critical stress than theory of deformations; the difference will be sharper the lower modulus E_c as compared to E. With weakly developed plastic flows both theories give close results.

§ 109. Influence of Compressibility of Material According to Flow Theory

In Section 108 it was assumed that material is incompressible both in the elastic and also in the plastic region. Let us assume now that components of elastic deformations are connected with stresses by Hooke's law in its ordinary form, i.e., we consider material compressible. Instead of relationship (226), we obtain

$$\left.\begin{aligned}\delta\varepsilon'_x&=\frac{1}{E}(\delta\sigma_x-\mu\,\delta\sigma_y),\\ \delta\varepsilon'_y&=\frac{1}{E}(\delta\sigma_y-\mu\,\delta\sigma_x),\\ \delta\gamma'&=\frac{2(1+\mu)}{E}\delta\tau.\end{aligned}\right\} \tag{8.249}$$

Components of plastic deformation, as before, are determined by formulas (227).

We consider case where initial stress is uniaxial: $\sigma_1 = \sigma_x = \sigma$, $\sigma_y = \tau = 0$. Variation of $\delta\sigma_1$ from (236) is equal to

$$\delta\sigma_1=\delta\sigma_x-\frac{1}{2}\delta\sigma_y. \tag{8.250}$$

Total increments of deformations turn out to be, taking into account (233), equal to

$$\left.\begin{aligned}\delta\varepsilon_x &= \frac{1}{E}\left[(1+\psi)\delta\sigma_x - \left(\mu+\frac{1}{2}\psi\right)\delta\sigma_y\right].\\ \delta\varepsilon_y &= \frac{1}{E}\left[-\left(\mu+\frac{1}{2}\psi\right)\delta\sigma_x + \left(1+\frac{1}{4}\psi\right)\delta\sigma_y\right].\\ \delta\gamma &= \frac{2}{E}(1+\mu)\delta\tau.\end{aligned}\right\} \tag{8.251}$$

Determining, from this, increments of stresses, we obtain

$$\left.\begin{aligned}\delta\sigma_x &= \frac{E}{\Delta_1}\left[\left(1+\frac{\psi}{4}\right)\delta\varepsilon_x + \left(\mu+\frac{\psi}{2}\right)\delta\varepsilon_y\right].\\ \delta\sigma_y &= \frac{E}{\Delta_1}\left[\left(\mu+\frac{\psi}{2}\right)\delta\varepsilon_x + (1+\psi)\delta\varepsilon_y\right].\\ \delta\tau &= \frac{E}{2(1+\mu)}\delta\gamma.\end{aligned}\right\} \tag{8.252}$$

where

$$\Delta_1 = 1-\mu^2+\frac{5-4\mu}{4}\psi. \tag{8.253}$$

In general formulas (202) we should, consequently, set

$$\left.\begin{aligned}&a_{11} = \frac{E}{\Delta_1}\left(1+\frac{\psi}{4}\right).\quad a_{22} = \frac{E}{\Delta_1}(1+\psi).\quad a_{12} = a_{21} = \frac{E}{\Delta_1}\left(\mu+\frac{\psi}{2}\right).\\ &a_{13} = a_{23} = a_{13} = a_{31} = 0.\quad a_{33} = \frac{E}{2(1+\mu)}\end{aligned}\right\} \tag{8.254}$$

Differential equation of type (204) acquires the form

$$\left(1+\frac{\psi}{4}\right)\frac{\partial^4 w}{\partial x^4} + 2\left(\mu+\frac{\psi}{2}+\frac{\Delta_1}{1+\mu}\right)\frac{\partial^4 w}{\partial x^2\partial y^2} + (1+\mu)\frac{\partial^4 w}{\partial y^4} + \\ + \frac{h}{D\Delta_1(1-\mu^2)}\sigma\frac{\partial^2 w}{\partial x^2} = 0. \tag{8.255}$$

where D is determined from (7.12). Using formulas (253) and (232), after simple transformations, we reduce equation (255) to form

$$\frac{(1+3\eta_x)(1-\mu^2)}{(5-4\mu)-(1-2\mu)^2\eta_x}\frac{\partial^4 w}{\partial x^4} + \\ + 2\frac{2(1+\mu)(1+\eta_x)+(5-4\mu)(1-\eta_x)}{(5-4\mu)-(1-2\mu)^2\eta_x}(1-\mu)\frac{\partial^4 w}{\partial x^2\partial y^2} + \\ + \frac{4(1-\mu^2)}{(5-4\mu)-(1-2\mu)^2\eta_x}\frac{\partial^4 w}{\partial y^4} + \frac{h\sigma}{D}\frac{\partial^2 w}{\partial x^2} = 0. \tag{8.256}$$

In the particular case $\mu = 0.5$ equation (256) will obtain its former form (246) if we take $\sigma_y = \tau = 0$.

We use equation (256) for case of square plate. We will take expression (111) for deflection, considering $m = n = 1$. Then we obtain for critical stress formula (116) with replacement of D' by D,

where coefficient K will be equal to

$$K=\frac{(9+7\varphi_K)(1-\mu^2)+2(1-\mu)(5-4\mu)(1-\varphi_K)}{(5-4\mu)-(1-2\mu)^2\varphi_K}. \qquad (8.257)$$

If we take $\varphi_K = 1$, then we arrive at magnitude K = 4, corresponding to the solution of the problem for the elastic region.

§ 110. Comparison of Calculating Formulas for Duralumin and Steel

The above-mentioned formula for critical stresses can be applied, if we know dependence $\sigma(\varepsilon)$ during uniaxial compression and extension. From this dependence it is possible to pass to relationship between σ_i and ε_i; as was shown in Section 100 diagrams $\sigma(\varepsilon)$ and $\sigma_i(\varepsilon_i)$ will coincide if we take $\mu = 0.5$.

We use the above-mentioned (Section 28) approximate diagram $\sigma(\varepsilon)$ for duralumin D16T (p.111) and we supplement Table 2.1 with values of t, r, and μ (see Table 8.1). Below there is given Table 8.2, also augmented, for steel (St. 3).

Table 8.1. Calculating parameters for duralumin D16T

$\cdot 10^{3}$	σ_* kg/cm^2	$E_c \cdot 10^{-5}$, kg/cm^2	$E_K \cdot 10^{-5}$, kg/cm^2	$T \cdot 10^{-5}$ kg/cm^2	φ_c	φ_K	t	r	μ
2,67	2000	7,50	7,50	7,50	1	1	1	0	0,320
3,0	2200	7,33	5,96	6,65	0,98	0,79	0,88	0,01	0,320
3,5	2460	7,03	4,34	5,50	0,94	0,58	0,73	0,03	0,322
4,0	2640	6,55	3,72	4,97	0,87	0,50	0,66	0,067	0,323
4,5	2780	6,18	2,55	3,81	0,82	0,34	0,51	0,10	0,326
5,0	2900	5,80	2,05	3,22	0,77	0,27	0,43	0,13	0,330
6,0	3080	5,13	1,50	2,50	0,68	0,20	0,33	0,19	0,338
7,0	3200	4,57	1,17	2,03	0,61	0,16	0,27	0,24	0,344
8,0	3320	4,15	0,97	1,72	0,55	0,13	0,23	0,29	0,350
9,0	3400	3,78	0,82	1,48	0,49	0,11	0,20	0,33	0,352
10,0	3450	3,48	0,82	1,48	0,46	0,11	0,20	0,35	0,356
11,0	3560	3,24	0,82	1,48	0,43	0,11	0,20	0,38	0,358
12,0	3640	3,03	0,82	1,48	0,40	0,11	0,20	0,40	0,360

Proceeding from these data, we compare value of critical stresses obtained by diverse variants of the theory of deformations and flow theory.

In Figs. 8.4 and 8.5 there is depicted dependence between critical stress $\sigma_{кр}$ and ratio b/h for elongated plate, subject to compression in one direction and hinge-secured on all edges. Fig. 8.4 pertains to duralumin D16T. Solid curves correspond to theory of deformations; one curve is obtained by formula (117) for incompressible material taking into account effect of unloading, the second, by formula (146) for incompressible material without calculation of unloading, the third, by formula (223) for compressible material without calculation for effect of unloading. Dotted curve corresponds to flow theory, it is constructed by formula (257) for $\mu = 0.5$ without calculation of effect of unloading.

Analogous curves, shown in Fig. 8.5 pertain to steel (St. 3). Horizontal sections of curves correspond to yield surface. If we conduct calculation by formula (146), then on section of hardening, strictly speaking, we obtain for every value of b/h two different magnitudes $\sigma_{кр}$; curve $\sigma_{кр}(b/h)$ has a loop here. Dot-dash section smooths transition from one branch of curve to the other.*

Experimental data available in literature pertain to duralumin plates with elastically clamped edges [8.16]. If we use coefficients of fastening of edges, taken from solution of elastic problem, then they can be conditionally reduced to case of hinge-secured edges. Experimental points found this way are shown in Fig. 8.4; material of

---

*About use for practical calculations of those sections of curves which lie above the yield point, see Section 111.

Table 8.2. Calculating parameters for Steel St. 3

$\varepsilon \cdot 10^3$	σ, kg/cm^2	$E_c \cdot 10^{-6}$, kg/cm^2	$E_u \cdot 10^{-6}$, kg/cm^2	$T \cdot 10^{-6}$, kg/cm^2	ν_c	ν_u	f	r	p
0,95	2000	2,10	2,10	2,10	1	1	1	0	0,270
1,0	2100	2,08	1,42	1,72	0,99	0,68	0,82	0,005	0,272
1,1	2200	2,00	0,99	1,39	0,95	0,47	0,66	0,025	0,274
1,2	2280	1,90	0,67	1,05	0,90	0,32	0,50	0,052	0,280
1,3	2340	1,80	0,46	0,85	0,86	0,22	0,41	0,075	0,285
1,4	2380	1,70	0,26	0,54	0,81	0,12	0,26	0,11	0,290
1,5	2390	1,60	0,13	0,33	0,76	0,062	0,16	0,15	0,295
1,6	2400	1,50	0,06	0,19	0,71	0,029	0,094	0,19	0,304
1,8	2400	1,33	0	0	0,63	0	0	0,33	0,318
2,0	2400	1,20	0	0	0,57	0	0	0,43	0,330
2,5	2400	0,96	0	0	0,46	0	0	0,54	0,358
3,0	2400	0,80	0	0	0,38	0	0	0,62	0,375
3,5	2400	0,69	0	0	0,33	0	0	0,68	0,390
4,0	2400	0,60	0	0	0,25	0	0	0,71	0,400
4,5	2410	0,54	0,02	0,07	0,26	0,010	0,033	0,61	0,405
5,0	2420	0,48	0,04	0,13	0,23	0,019	0,062	0,60	0,408
6,0	2470	0,41	0,05	0 15	0,20	0,024	0,071	0,63	0,414
7,0	2520	0,36	0,05	0,15	0,17	0,024	0,071	0,65	0,417
8,0	2575	0,32	0,05	0,15	0,15	0,024	0,071	0,68	0,420
9,0	2630	0,29	0,05	0,15	0,14	0,024	0,071	0,70	0,424
10,0	2685	0,27	0,05	0,15	0,13	0,024	0,071	0,71	0,426
11,0	2740	0,25	0,05	0,15	0,12	0,024	0,071	0,73	0,428
12,0	2800	0,23	0,05	0,15	0,11	0,024	0,071	0,74	0,430

tested pieces is near in mechanical properties to duralumin D16T. As we see, these points lie near curves obtained according to the theory of deformations, but without calculation of unloading.

In Fig. 8.6 there also are compared calculating data with experimental data for duralumin compressed plates, but in another interpretation.* Along the axis of abscissas are plotted deformations $\varepsilon_{кр}$, and along the axis of ordinates, stresses $\sigma_{кр}$. In Figure is plotted curve $\sigma_{кр}(\varepsilon_{кр})$, pertaining to uniaxial compression, and here too are curves, constructed by deformation theory, taking into account and ignoring effect of unloading, and according to flow theory. Experimental points are located, as before, near the curve pertaining to theory of deformations.

*See work of Pride and Heimerl, NACA Tech. Note No. 1817, 1949.

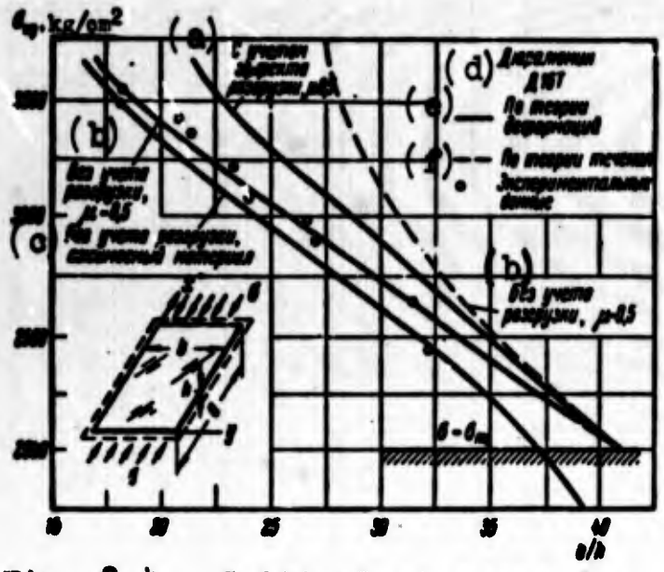

Fig. 8.4. Critical stresses for duralumin plates according to the theory of deformations and according to flow theory in comparison with experimental data.
KEY: (a) Accounting for effect of unloading; (b) Ignoring unloading; (c) Ignoring unloading, compressible material; (d) Duralumin D16T; (e) By deformation theory; (f) By flow theory.

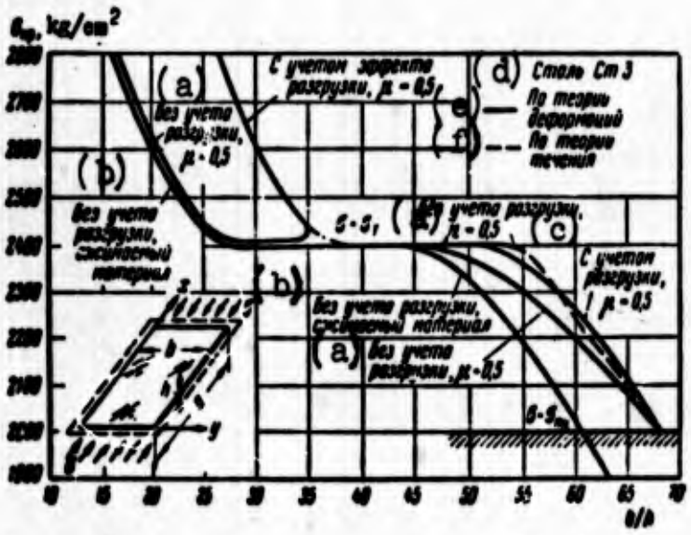

Fig. 8.5. Critical stresses for steel plates according to the theory of deformations and according to flow theory.
KEY: (a) Ignoring unloading; (b) Ignoring unloading, compressible material; (c) Accounting unloading effect; (d) Steel St. 3; (e) Deformation theory; (f) Flow theory.

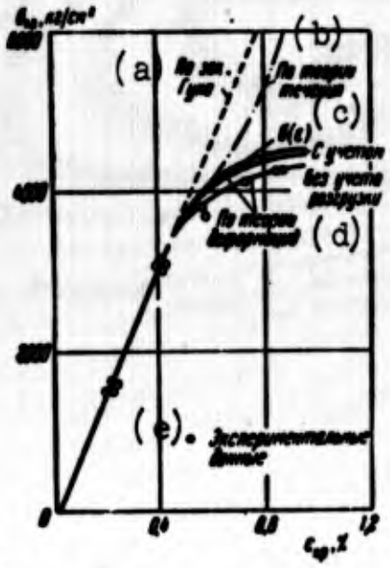

Fig. 8.6. Comparison of calculating and experimental data. KEY: (a) By Hooke's law; (b) By flow theory; (c) Accounting for and ignoring unloading; (d) By deformation theory; (e) Experimental data.

Judging by Figs. 8.4 and 8.6, flow theory leads to values of critical stresses, lying significantly higher than experimental data. Consequently, in development of practical methods of calculation of plates for stability at present it is necessary to give preference to theory of deformations. Possibly, flow theory can be effectively used during research of behavior of plates with initial imperfections. Let us note that conditions of simple loading in this case will not be satisfied during the whole process of deformation of the plate.

§ 111. Data for Practical Calculations

We arrived at the conclusion that henceforth until we accumulate more extensive experimental material for practical calculations it is expedient to use theory of deformations in its simplified variant which does not consider effect of unloading. Here calculated critical stresses will, as a rule, lie with respect to real values in the safety factor, as during calculation of compressed bars by tangent-modular load. Necessary calculating formulas are given in Sections 105 and 106. For determination of critical stress one should calculate its value by known formulas and graphs pertaining to the elastic region, and then multiply by correction factor η; we assume approximately that $D' = D$.

In Fig. 8.7 is given summary of formulas for correction factor, pertaining in case of compression to elongated plates; however, in practical calculations they can also be used for plates with different ratios of sides.

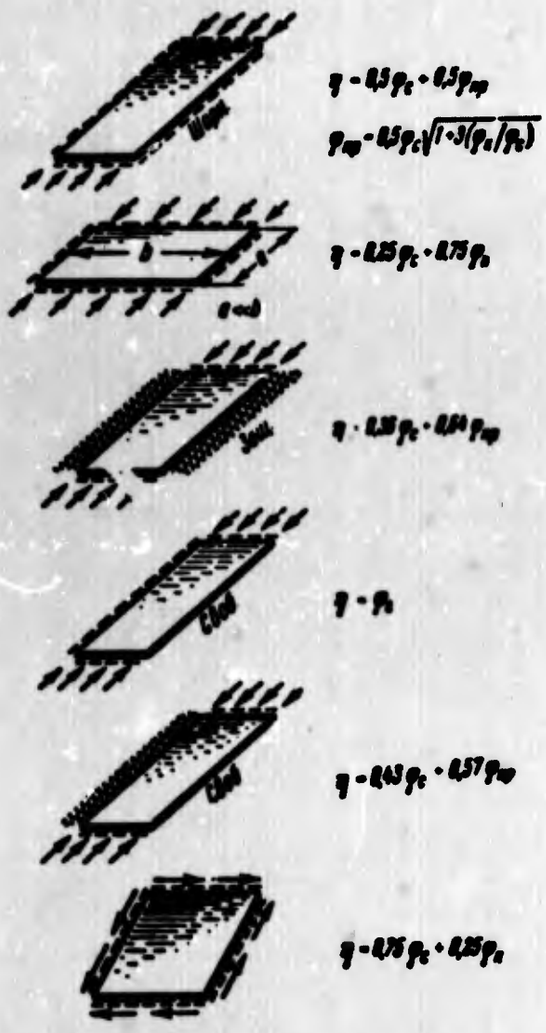

Fig. 8.7. Correction factors for calculation of compressed plates under different conditions.

In Figs. 8.8 and 8.9 is depicted dependence $\sigma_{kp}(b/h)$ for duralumin and steel plates compressed in one direction, found by these formulas for various conditions of fastening.

Sections of curves lying in Fig. 8.9 above the yield point are shown by dotted line; for material with clearly expressed yield surface one should, apparently, consider the yield point the upper boundary for critical stresses. Although theories of plasticity lead to another result here, we do not consider, as was already said in Section 103, unique "instability" of process of plastic flow and sensitivity of structure, experiencing this process, to any kind to perturbations. Possibly, the plate will appear in state practically to cross the threshold of the yield surface if it is fastened on edges with sufficiently hard ribs, made of another material.

We give approximate method, allowing us to determine reduction factors for compressed plate after loss of stability in the case when

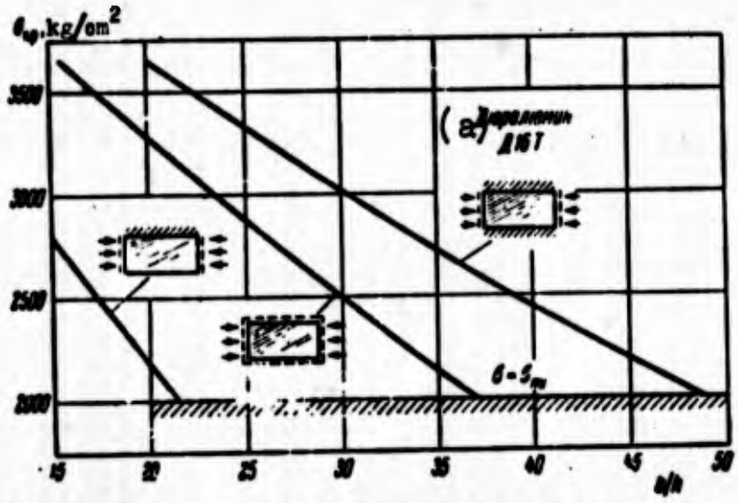

Fig. 8.8. Critical stresses for duralumin plates by approximate formulas.
KEY: (a) Duralumin D16T.

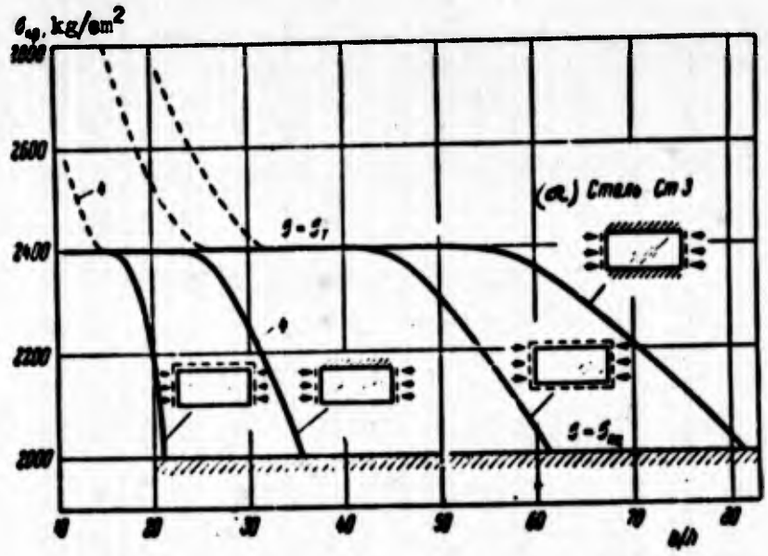

Fig. 8.9. Critical stresses for steel plates by approximate formulas.
KEY: (a) Steel St. 3.

stresses in strips of the plate, adjacent to longitudinal edges, lie beyond the elastic limit* and if reinforcing ribs remain rectilinear.**

*See (G. Gerard, Jour. of Aeron. Sciences 10 (1946), 518–523) and [0.3], p. 144.

**For more detail on this see Chapter XII.

Let us assume that deformation changes along width of plate in the same way as in the elastic region. Then by measure of development of plastic deformations irregularity of distribution of stresses should smooth out — just as in known problem of concentration of stresses around apertures. This circumstance can be accounted for by applying the formula for reduction factors already known by us and substituting, instead of critical stress and stress in extreme fibers, their true values — independently of whether they are within or beyond the elastic limit.

Literature

8.1. A. A. Il'yushin. Stability of plates and shells beyond the elastic limit, Applied Math. and Mech., 8, No. 5, 337-360.

8.2. A. A. Il'yushin. Plasticity, Gostekhizdat, 1948.

8.3. L. M. Kachanov. Principles of the theory of plasticity, Gostekhizdat, 1956, 165-173.

8.4. V. D. Klyushnikov. Stability of plates beyond the elastic limit, News of Acad. of Sci. of USSR, OTN, No. 7 (1957), 41-56.

8.5. Yu. R. Lepik. One possibility for solving the problem of stability of elasto-plastic plates in exact formulation, News of Acad. of Sci. of USSR, STN, No. 8 (1957), 13-19; Stability of elasto-plastic plate, compressed in one direction. Applied Math. and Mech., 21, No. 5 (1957), 722-724; Stability of rectangular elasto-plastic plate, unevenly compressed in one direction, Eng. Collection, 18, (1954), 161-164; Certain questions of equilibrium of elasto-plastic plates and bars, Doct. diss., Moscow State U., 1957.

8.6. S. M. Popov. Stability of freely supported plates beyond the elastic limit, Eng. Collection, 9 (1951); Extension of method of softening of boundary conditions to stability beyond the elastic limit of rectangular plates, Applied Math. and Mech., 15, No. 1 (1951); Stability beyond the elastic limit of plates during eccentric extension or compression, Eng. Collection, 18 (1954), 165-173.

8.7. A. P. Prusakov. Stability and free vibrations of sandwich plates with light filler, Doct. diss., Dnieperpetrovsk, 1955.

8.8. L. A. Tolokonnikov. Influence of compressibility of matter on elasto-plastic stability of plates and shells, Herald of Moscow State University, No. 6 (1949), 35-44; Concerning the question about stability of round plates, compressed by evenly distributed pressure on its edge, Scientific notes of Rostov State University, 18, No. 3 (1953).

8.9. P. Bijlaard. Theory of plastic stability, Proc. Kon. Ned. Akad. d. Wet. 41, No. 5 (1948) (translation in collection "Theory of plasticity," IL, 1948, 392-404); Theory and tests on the plastic stability of plates and shells, J. Aeron. Sci., 16, No. 9 (1949), 529-541.

8.10. G. Gerard. Secant modulus method for determining plate instability above the proportional limit, J. Aeron. Sci. 13, No. 1 (1946), 38-41, 48; Critical shear stress of plates above the proportional limit; J. Appl. Mech., No. 3 (1948), 7-11; Effective width of elastically supported flat plates, J. Aeron. Sci. 13, No. 10 (1946), 518-524.

8.11. G. J. Heimerl. Determination of plate compression strength, NACA Techn. Note No. 1480, 1947.

8.12. G. H. Handelman and W. Prager. Plastic buckling of a rectangular plate under edge thrusts, NACA Techn. Note No. 1530, 1948.

8.13. H. G. Hopkins. The plastic instability of plates, Quart. of Appl. Math. 11, No. 2 (1953).

8.14. C. E. Pearson. Bifurcation criterion and plastic buckling of plates and shells, J. Aeron. Sci. 17, No. 7 (1950), 417-424, 455 (see coll. "Mechanics," IL, No. 5, 1951).

8.15. R. A. Preide and G. J. Heimerl. Plastic buckling of simply supported compression plates, NACA Techn. Note No. 1817, 1949.

8.16. E. Z. Stowell. A unified theory of plastic buckling of columns and plates, NACA Techn. Note No. 1556, 1948.

8.17. E. H. Shuette. Buckling of curved sheet in compression and its relation to the secant modulus, J. Aeron. Sci. 15, No. 1 (1948), 18-22.

C H A P T E R IX

CIRCULAR PLATES

§ 112. Basic Dependences for Rigid and Flexible Plates

Circular plates in measuring instruments usually serve as sensors (membranes), reacting to change of transverse pressure. In certain cases, during changes of temperature, in process of assembly, etc., a "membrane" is subjected to action of radial compressive forces on the part of supporting device; this can lead to buckling of the membrane. In structures of elementary particle accelerators there are plates which are irradiated by a neutron flux; here there occurs deformation of the plates, connected with the thermal effect, nuclear transformations and change of crystal lattice [9.6], and here there can occur loss of stability of the plate.

Buckling is observed also when plates are not connected on boundary by a rigid ring and receive only transverse pressure. With large deflections of the plate near the boundary there will form compressed zone, which is the focus of the loss of stability.

In general during loss of stability of a plate there can form a series of shallow hollows of different direction both along a radius, and also on the circumference. Such asymmetric buckling occurs, e.g., in the case of a plate, experiencing large deflections, or a plate,

reinforced by ribs. However, of greatest practical value are cases of axisymmetric buckling, when middle plane of plate becomes the surface of revolution (Fig. 9.1); we first of all shall consider such particular problems.

We shall recall preliminarily certain dependences of theory of circular plates, pertaining to small deflections, for an asymmetric deflection surface. We use a cylindrical system of coordinates, the principal plane of which coincides with the middle plane of the plate (Fig. 9.2). Length of radius-vector we designate by r, polar angle — φ. We can apply all relationships of theory of rectangular plates known by us, passing to the new system of coordinates. Transition formulas can be obtained by merging x axis of the rectangular system with radius-vector r, as shown in Fig. 9.2. Derivatives of a certain function Z with respect to x and y are expressed through derivatives of Z with respect to r and φ in the following manner:

$$\frac{\partial Z}{\partial x}=\frac{\partial Z}{\partial r},\quad \frac{\partial Z}{\partial y}=\frac{1}{r}\frac{\partial Z}{\partial \varphi}. \tag{9.1}$$

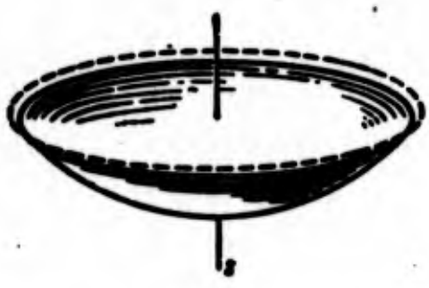

Fig. 9.1. Axisymmetric buckling of circular plate.

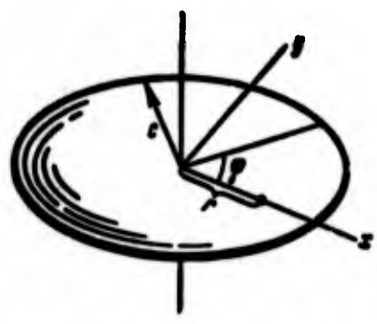

Fig. 9.2. System of coordinates in examining circular plates.

$$\frac{\partial^2 Z}{\partial x^2}=\frac{\partial^2 Z}{\partial r^2},\quad \frac{\partial^2 Z}{\partial x\,\partial y}=\frac{\partial}{\partial r}\left(\frac{1}{r}\frac{\partial Z}{\partial \varphi}\right),\quad \frac{\partial^2 Z}{\partial y^2}=\frac{1}{r}\frac{\partial Z}{\partial r}+\frac{1}{r^2}\frac{\partial^2 Z}{\partial \varphi^2}. \tag{9.2}$$

Operator $\nabla^2 Z$ turns out to be equal to

$$\nabla^2 Z = \frac{\partial^2 Z}{\partial x^2} + \frac{\partial^2 Z}{\partial y^2} = \frac{\partial^2 Z}{\partial r^2} + \frac{1}{r}\frac{\partial Z}{\partial r} + \frac{1}{r^2}\frac{\partial^2 Z}{\partial \varphi^2} =$$

$$= \frac{1}{r}\frac{d}{dr}\left(r\frac{dZ}{dr}\right) + \frac{1}{r^2}\frac{\partial^2 Z}{\partial \varphi^2}. \qquad (9.3)$$

We find by (2) curvatures of deflection surface in the section along the diameter and in perpendicular direction:

$$\varkappa_r = -\frac{\partial^2 w}{\partial r^2}, \quad \varkappa_\varphi = -\frac{1}{r}\frac{\partial w}{\partial r} - \frac{1}{r^2}\frac{\partial^2 w}{\partial \varphi^2}. \qquad (9.4)$$

Torsion of surface will be equal to

$$\chi = -\frac{\partial}{\partial r}\left(\frac{1}{r}\frac{\partial w}{\partial \varphi}\right). \qquad (9.5)$$

Bending and torsional moments are determined by the former relationships,

$$M_r = D(\varkappa_r + \mu\varkappa_\varphi), \quad M_\varphi = D(\varkappa_\varphi + \mu\varkappa_r), \quad H = D(1-\mu)\chi. \qquad (9.6)$$

We determine transverse force in arc section Q_r. If we start from condition of equilibrium of a member of the plate, cut by two radial and two arc sections (Fig. 9.3), then we obtain

$$Q_r = \frac{\partial M_r}{\partial r} + \frac{M_r - M_\varphi}{r} + \frac{\partial H}{r\partial \varphi}. \qquad (9.7)$$

As compared to case of rectangular plate new here is the second member: it should be introduced, since moments M_r and $M_r + \frac{\partial M_r}{\partial r}dr$ act on arcs of different length, and vector-moments M_φ and $M_\varphi + \frac{\partial M_\varphi}{\partial \varphi}d\varphi$ form with each other angle $d\varphi$.

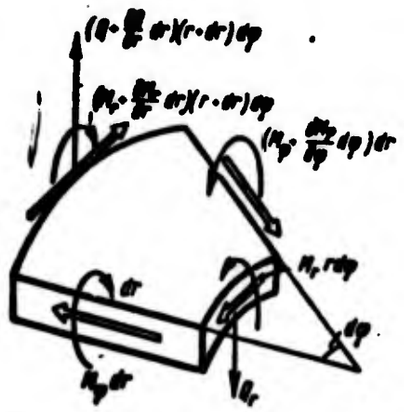

Fig. 9.3. Moments and transverse forces.

Transverse reactive force R_r per unit length of boundary and transmitted to support device, is composed of transverse force and the derivative of the torque (see [0.3], p. 41):

$$R_r = Q_r + \frac{\partial H}{r\partial \varphi}. \qquad (9.8)$$

Assume that the plate is subjected to action of forces σ_r and τ in the middle surface (Fig. 9.4); tensile forces we consider positive. Differential equation of bending of the plate (7.26) will be rewritten in the form

$$\frac{D}{h}\nabla^4 w = \Pi_1(\sigma, w), \tag{9.9}$$

where

$$\Pi_1(\sigma, w) = \sigma_r \frac{\partial^2 w}{\partial r^2} + \sigma_\varphi\left(\frac{1}{r}\frac{\partial w}{\partial r} + \frac{1}{r^2}\frac{\partial^2 w}{\partial \varphi^2}\right) + 2\tau\frac{\partial}{\partial r}\left(\frac{1}{r}\frac{\partial w}{\partial \varphi}\right). \tag{9.10}$$

Fig. 9.4. Stresses in middle surface.

Principal stresses in the middle surface can be expressed as a function of stresses Φ by formulas of type (7.60), if we use relationships

$$\sigma_r = \frac{1}{r}\frac{\partial \Phi}{\partial r} + \frac{1}{r^2}\frac{\partial^2 \Phi}{\partial \varphi^2}, \quad \sigma_\varphi = \frac{\partial^2 \Phi}{\partial r^2},$$

$$\tau = -\frac{\partial}{\partial r}\left(\frac{1}{r}\frac{\partial \Phi}{\partial \varphi}\right). \tag{9.11}$$

Boundary conditions of boundary of plate in case of rigid clamping have the form

$$w = 0, \quad \theta = 0 \text{ when } \frac{\partial w}{\partial r} = 0. \tag{9.12}$$

With hinged support they will be

$$w = 0, \quad M_r = 0 \text{ when } \frac{\partial^2 w}{\partial r^2} + \frac{\mu}{r}\frac{\partial w}{\partial r} + \mu\frac{\partial^2 w}{r^2 \partial \varphi^2} = 0. \tag{9.13}$$

For axisymmetric problems all relationships are significantly simplified; any function of Z will depend only on r, so that, instead of partial derivatives with respect to r we will obtain total derivatives. Formulas of transition (1)–(3) obtain the form

$$\frac{\partial Z}{\partial x} = \frac{dZ}{dr}, \quad \frac{\partial Z}{\partial y} = 0, \tag{9.14}$$

$$\frac{\partial^2 Z}{\partial x^2} = \frac{\partial^2 Z}{\partial r^2}, \quad \frac{\partial^2 Z}{\partial x \partial y} = 0, \quad \frac{\partial^2 Z}{\partial y^2} = \frac{1}{r}\frac{dZ}{dr}, \tag{9.15}$$

$$\nabla^2 Z = \frac{d^2 Z}{dr^2} + \frac{1}{r}\frac{dZ}{dr} = \frac{1}{r}\frac{d}{dr}\left(r\frac{dZ}{dr}\right). \tag{9.16}$$

Curvatures and torsion of deflection surface will be equal to

$$\varkappa_r = -\frac{d^2w}{dr^2}, \quad \varkappa_\varphi = -\frac{1}{r}\frac{\partial w}{\partial r}, \quad \chi = 0. \tag{9.17}$$

Using (16) and considering $Z = \nabla^2 w$, we rewrite equation (9) in the form

$$\frac{D}{h}\frac{1}{r}\frac{d}{dr}\left[r\frac{d}{dr}(\nabla^2 w)\right] = \sigma_r\frac{d^2w}{dr^2} + \sigma_\varphi\frac{1}{r}\frac{dw}{dr}. \tag{9.18}$$

Expressions (11) take the form

$$\sigma_r = \frac{1}{r}\frac{d\Phi}{dr}, \quad \sigma_\varphi = \frac{d^2\Phi}{dr^2}, \quad \tau = 0. \tag{9.19}$$

From this follows the dependence between radial and arc stresses:

$$\sigma_\varphi = \frac{d}{dr}(r\sigma_r). \tag{9.20}$$

Right side of equation (18) can, consequently, be presented in the form

$$\frac{1}{r}\frac{d}{dr}\left(r\sigma_r\frac{dw}{dr}\right);$$

hence instead of (18) we obtain,

$$D\frac{d}{dr}\left[r\frac{d}{dr}(\nabla^2 w)\right] = h\frac{d}{dr}\left(r\sigma_r\frac{dw}{dr}\right). \tag{9.21}$$

We find the first integral of this equation:

$$D\frac{d}{dr}(\nabla^2 w) = h\sigma_r\frac{dw}{dr} + \frac{C_0}{r}. \tag{9.22}$$

Obviously, constant C_0 should turn into zero, if region of integration contains point r = 0, i.e., if plate does not have a center aperture.

We introduce designation θ for <u>angle of rotation of the normal</u> to the middle surface (Fig. 9.5):

$$\theta = -\frac{dw}{dr}. \tag{9.23}$$

The minus sign is explained by the fact that, as one may see from Fig. 9.5, reading of angle θ occurs in direction, opposite rotation from axis r to axis z or w. Instead of (17) we obtain

$$\varkappa_r = \frac{d\theta}{dr}, \quad \varkappa_\varphi = \frac{\theta}{r}; \tag{9.24}$$

bending moments are equal to

$$\left.\begin{aligned} M_r &= D\left(\frac{d\theta}{dr}+\mu\frac{\theta}{r}\right),\\ M_\varphi &= D\left(\frac{\theta}{r}+\mu\frac{d\theta}{dr}\right). \end{aligned}\right\} \qquad (9.25)$$

Expression for $\nabla^2 w$ according to (16) obtains form

$$\nabla^2 w = -\left(\frac{d\theta}{dr}+\frac{\theta}{r}\right). \qquad (9.26)$$

therefore for a <u>continuous plate</u>, instead of (22), we have

$$D\left(\frac{d^2\theta}{dr^2}+\frac{1}{r}\frac{d\theta}{dr}-\frac{\theta}{r^2}\right)=k\sigma_{r,0}. \qquad (9.27)$$

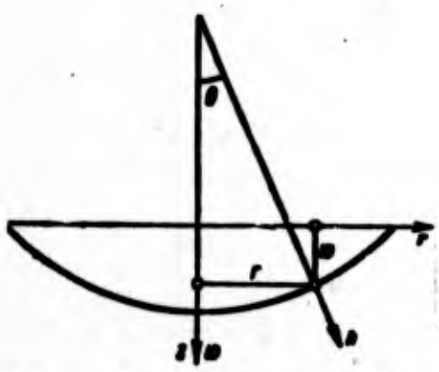

Fig. 9.5. Deflection during axisymmetric buckling.

This equation will be the initial one during solution of particular problems.

Equations of <u>nonlinear</u> theory of flexible plates, as before, have form (7.63) and (7.64); operator $L(w, \Phi)$ here is equal to

$$L(w,\Phi)=\frac{\partial^2 w}{\partial r^2}\left(\frac{1}{r}\frac{\partial\Phi}{\partial r}+\frac{1}{r^2}\frac{\partial^2\Phi}{\partial\varphi^2}\right)+ \\ +\left(\frac{1}{r}\frac{\partial w}{\partial r}+\frac{1}{r^2}\frac{\partial^2 w}{\partial\varphi^2}\right)\frac{\partial^2\Phi}{\partial r^2}-2\frac{\partial}{\partial r}\left(\frac{1}{r}\frac{\partial\Phi}{\partial\varphi}\right)\frac{\partial}{\partial r}\left(\frac{1}{r}\frac{\partial w}{\partial\varphi}\right); \qquad (9.28)$$

by replacement of Φ by w we find $L(w,w)$. With <u>axial symmetry</u> we have

$$L(w,\Phi)=\frac{1}{r}\frac{d}{dr}\left(\frac{dw}{dr}\frac{d\Phi}{dr}\right),\quad L(w,w)=\frac{1}{r}\frac{d}{dr}\left(\frac{dw}{dr}\right)^2. \qquad (9.29)$$

We find the first integral of equations (7.63) and (7.64) analogously to the way this was done for equation (21):

$$D\frac{d}{dr}(\nabla^2 w)=\frac{h}{r}\frac{d\Phi}{dr}\frac{dw}{dr}. \qquad (9.30)$$

$$\frac{d}{dr}(\nabla^2\Phi)=-\frac{E}{2r}\left(\frac{dw}{dr}\right)^2; \qquad (9.31)$$

here we take $q = 0$.

When using the <u>Bubnov-Galerkin method</u> in problems pertaining to circular plates it is necessary to observe caution. If we are talking about <u>axisymmetric problems</u>, then we naturally start from those relationships which are the first integral of the initial equations.

However, here there can be obtained different results depending upon structure of the integrand in the solved equation.

Let us consider for example a linear problem. Let us assume that deflection is approximated by the series

$$w=\sum A_i\eta_i(r). \tag{9.32}$$

We introduce the designation

$$X=D\left(\frac{d^2\theta}{dr^2}+\frac{1}{r}\frac{d\theta}{dr}-\frac{\theta}{r^2}\right)-hc_r\theta, \tag{9.33}$$

then the equation of the Bubnov-Galerkin method, corresponding to (22), is best recorded in the form

$$\int_F X\frac{d\eta_i}{dr}r\,dr=0; \tag{9.34}$$

integral is extended to area of plate F. It is possible to show (see [0.3], p. 183) that (34) corresponds to a variational equation, composed by the principle of virtual displacements.

In the literature there frequently is used an equation of type

$$\int_F X\eta_i\,dr=0, \tag{9.35}$$

which leads to somewhat different final dependences.

An analogous remark pertains to nonlinear equations (30) and (31).

Let us turn to solution of separate problems; we start with the determination of critical forces during axisymmetric buckling of a plate; then we turn to an asymmetric problem and, in conclusion, consider post-critical deformation of plates.

§ 113. Plate Clamped at Boundary Under Action of Radial Compression

We investigate stability of a circular plate of radius c, clamped on its boundary and under the action of radial compressive forces p, evenly distributed along the edge (Fig. 9.6). We consider that points of the edge can freely be displaced in the plane of the plate and that

the deflection surface is axisymmetric.*

Fig. 9.6. Plate, clamped on its edge, under action of radial compression.

Taking $\sigma_r = -p$, instead of (22), we obtain

$$D\left(\frac{d^2\theta}{dr^2}+\frac{1}{r}\frac{d\theta}{dr}-\frac{\theta}{r^2}\right)+hp\theta=0. \quad (9.36)$$

or

$$r^2\frac{d^2\theta}{dr^2}+r\frac{d\theta}{dr}+\left(\frac{hp}{D}r^2-1\right)\theta=0. \quad (9.37)$$

We designate

$$\frac{hp}{D}=\alpha^2;\ \ s=r\alpha. \quad (9.38)$$

Introducing in equation (37) instead of r variable u, we arrive at equation

$$s^2\frac{d^2\theta}{ds^2}+s\frac{d\theta}{ds}+(s^2-1)\theta=0. \quad (9.39)$$

constituting a Bessel equation. Integral of it has the form

$$\theta=C_1J_1(s)+C_2Y_1(s). \quad (9.40)$$

where $J_1(u)$ is a Bessel function of the first kind with index 1; $Y_1(u)$ is a Bessel function of the second kind with index 1.

Function $Y_1(u)$ when $u = 0$ becomes infinitely large; since angle of rotation θ in the center, in general, is limited (here it is equal to zero), one should set $C_2 = 0$; therefore

$$\theta=C_1J_1(s). \quad (9.41)$$

The second of boundary conditions (12) takes the form

$$\theta=0 \text{ when } r=c. \quad (9.42)$$

Considering $C_1 \neq 0$, from (16) we find

$$J_1(\alpha c)=0. \quad (9.43)$$

Function $J_1(u)$ is expressed by the series

$$J_1(s)=\frac{s}{2}\left[1-\frac{1}{1\cdot2}\left(\frac{s}{2}\right)^2+\frac{1}{1\cdot2\cdot2\cdot3}\left(\frac{s}{2}\right)^4-\dots\right]. \quad (9.44)$$

Equation (18) is satisfied for the following values of $u = \alpha c$ (if we exclude $u = 0$):

*This problem was first considered by Bryan [7.14] in 1891.

$$\alpha_1 c = 3.83, \quad \alpha_2 c = 7.02, \quad \alpha_3 c = 10.2, \ldots \tag{9.45}$$

Using the first of these roots, we find by (38) critical stress:

$$p_{кр} = \frac{\alpha_1^2 D}{c^2 h},$$

or

$$p_{кр} = K \frac{D}{c^2 h} \tag{9.46}$$

when

$$K = 14.68. \tag{9.47}$$

Critical forces of higher order during axisymmetric buckling correspond to roots α_2, α_3, and etc.

We determine deflection surface of the plate after buckling. Integrating (41), we find

$$w = -\frac{1}{a} C_1 \int J_1(u)\,du = \frac{1}{a} C_1 J_0(u) + C_0. \tag{9.48}$$

where $J_0(u)$ is a Bessel function with index zero:

$$J_0(u) = 1 - \left(\frac{u}{2}\right)^2 + \frac{1}{(1\cdot 2)^2}\left(\frac{u}{2}\right)^4 - \frac{1}{(1\cdot 2\cdot 3)^2}\left(\frac{u}{2}\right)^6 + \ldots \tag{9.49}$$

Constant C_0 we express through C_1, proceeding from first boundary condition (10):

$$w = 0 \quad \text{when} \quad u = ac. \tag{9.50}$$

We use for solution of the same problem by the Bubnov-Galerkin method. We present deflection surface by expression

$$w = f\left(1 - \frac{r^2}{c^2}\right)^2, \tag{9.51}$$

satisfying conditions (37) and (45); it corresponds to solution of a problem of small deflections of a plate under action of evenly distributed lateral load. We find

$$\theta = -\frac{dw}{dr} = \frac{4f}{c}\left(\frac{r}{c} - \frac{r^3}{c^3}\right). \tag{9.52}$$

We write the equation of Bubnov-Galerkin in the form of (34):

$$\int_0^c X\left(\frac{r}{c} - \frac{r^3}{c^3}\right) r\,dr = 0. \tag{9.53}$$

We find expression for X by (33):

$$X = -32Df\frac{r}{c^4} + 4hp\frac{f}{c}\left(\frac{r}{c} - \frac{r^3}{c^3}\right). \tag{9.54}$$

and use designation

$$\frac{r}{c}=\rho; \tag{9.55}$$

then, instead of (53), we obtain

$$\int_0^1 [32Df\rho-4hpfc^2(\rho-\rho^3)](\rho-\rho^3)\rho\,d\rho=0. \tag{9.56}$$

Calculations give

$$\frac{8}{3}Df-\frac{1}{6}fphc^2=0. \tag{9.57}$$

Hence for f ≠ 0

$$p_{кр}=\frac{16D}{hc^2},\quad K=16; \tag{9.58}$$

deviation from exact value of (47) constitutes about 9%.

§ 114. Case of Hinged Fastening on the Edge

We shall solve the same problem as in Section 113, but on the assumption that plate is secured by hinge on its edge (Fig. 9.7).* The second of boundary conditions (13) has the form

$$\frac{d\theta}{dr}+\mu\frac{\theta}{r}=0 \quad \text{when} \quad r=c. \tag{9.59}$$

Let us give the formula of differentiation:

$$\frac{dJ_1(u)}{du}=J_0(u)-\frac{J_1(u)}{u}. \tag{9.60}$$

Substituting (41) in (59), we obtain

$$J_0(\alpha c)-\frac{1-\mu}{\alpha c}J_1(\alpha c)=0. \tag{9.61}$$

Using tables of functions $J_0(u)$ and $J_1(u)$, one can determine roots of equation (61); the first of them turn out to be equal (for $\mu = 0.3$) to

$$\alpha_1 c=2.05,\quad \alpha_2 c=5.39,\quad \alpha_3 c=8.57. \tag{9.62}$$

In expression for critical stress coefficient K turns out to be equal to

$$K=4.2. \tag{9.63}$$

---

*First research of this problem belongs to A. N. Dinnik [9.4]; in his works there is also contained solution of a series of more complicated problems, e.g., for stability of a plate lying on an elastic support.

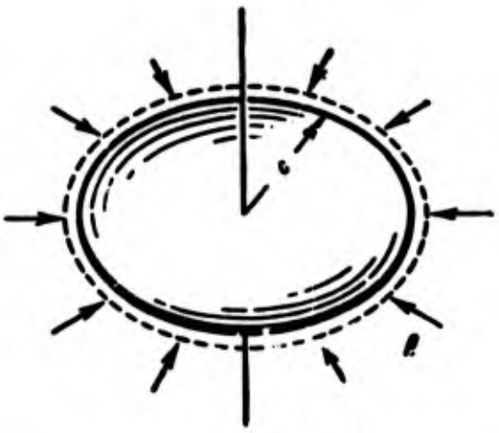

Fig. 9.7. Plate, supported by hinge on its edge, under action of radial compression.

This value is close to the critical stress for hinge-supported square plate with side 2c, compressed in two directions by forces p: in this case we obtained

$$K=\frac{\pi^2}{2}\approx 4.93.$$

We turn to approximate solution of the problem according to the Bubnov-Galerkin method. The approximating expression for w we select, as before, the same as in the case of small deflections of the plate with a lateral load:

$$w=fa\left(\frac{1}{a}-2\frac{r^2}{c^2}+b\frac{r^4}{c^4}\right). \tag{9.64}$$

where

$$a=\frac{3+\mu}{5+\mu},\quad b=\frac{1+\mu}{3+\mu}. \tag{9.65}$$

Instead of equation (56), we obtain

$$\int_0^1 [32\,Dabf\rho-4hpfc^2a(\rho-b\rho^3)](\rho-b\rho^3)\rho\,d\rho=0. \tag{9.66}$$

After calculations we find

$$\frac{8}{3}Dab(3-2b)f-\frac{p(6-8b+3b^2)}{6}hc^2af=0. \tag{9.67}$$

Magnitude K is equal to

$$K=\frac{16b(3-2b)}{6-8b+3b^2}. \tag{9.68}$$

For $\mu = 0.3$ we have

$$a=0.623,\quad b=0.394. \tag{9.69}$$

Hence

$$K=4.21. \tag{9.70}$$

which almost coincides with the exact solution.

Let us note that calculations for case of a clamped plate ensue from those given here, if we set a = b = 1. Critical stress for clamped plate is approximately 3.5 times as great as for a hinge-

supported one.

§ 115. Asymmetric Buckling of a Plate

Till now we assumed that the deflection surface of a plate during buckling is axisymmetric. Let us consider now the case when deflection changes not only along the radius, but also along the arc.*

First we will consider the former problem, when the plate is subjected to action of radial compression. Taking

$$\sigma_r = \sigma_\varphi = -p \tag{9.71}$$

and using former designations (38) and (16), we reduce equation (9) to form

$$\nabla^4 w + \alpha^2 \nabla^2 w = 0. \tag{9.72}$$

We obtained an analogous equation in Chapter VII in the case of a rectangular plate, compressed in two directions (p.370).

We write the integral of equation (72) in the form

$$w = [C_1 J_m(\alpha r) + C_2 r^m] \sin m\varphi. \tag{9.73}$$

where $J_m(\alpha r) = J_m(u)$ is a Bessel function with indices m = 1, 2, 3, ... Let us note that expression $r^m \sin m\varphi$ is the integral of equation $\nabla^2 w = 0$.

We assume that the plate is clamped on its edge. Boundary conditions (12) lead to the following equations:

$$\left.\begin{aligned} C_1 \left[\frac{dJ_m}{d(\alpha r)}\right]_{r=c} + C_2 m (\alpha c)^{m-1} = 0, \\ C_1 J_m(\alpha c) + C_2 (\alpha c)^m = 0. \end{aligned}\right\} \tag{9.74}$$

We equated the determinant of system (74) to zero; then we obtain

$$\left[\frac{dJ_m}{d(\alpha r)}\right]_{r=c} \alpha c - m J_m = 0. \tag{9.75}$$

---

*This problem was considered by Bryan [7.14] and Nadai [9.13]. Survey of research on stability of circular plates and solution of certain new problems are contained in works of V. M. Makushin [9.5]. Case, when plate is clamped on one part of its circumference, and on other is supported by hinge, was considered by V. Novatskiy and Z. Olesyak [9.7].

We use the differentiation formula

$$\frac{dJ_m(u)}{du} = \frac{m}{u} J_m - J_{m+1}; \tag{9.76}$$

then equation (75) will change into the following:

$$J_{m+1}(ac) = 0. \tag{9.77}$$

Finding roots of this equation for different m = 1, 2, 3, ..., we determine critical stresses.

Fig. 9.8. Asymmetric buckling of circular plate.

In Fig. 9.8 there is shown the character of buckling of plate for different values of m. Number of nodal diameters is equal to m; number of nodal circumferences also depends on α. E.g., when m = 1 first root of equation (77) corresponds to coefficient K = 26.4, buckled surface is shown in Fig. 9.9a. Second root corresponds to K = 70.6, here there appears one nodal circumference (Fig. 9.9b).

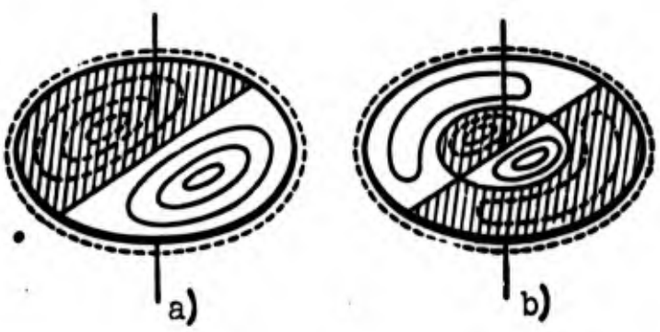

Fig. 9.9. Wave formation of a plate, a) with one nodal diameter, b) with one nodal diameter and one nodal circumference.

As we see, to asymmetric buckling there correspond higher eigenvalues of the problem than for axisymmetric buckling; therefore, asymmetry can take place only in case of a reinforced plate.

As we already said, asymmetric buckling of a circular plate can appear in other cases, when load is transverse* (Fig. 9.10). We assume that points of the edge of the plate freely are displaced in radial direction. With sufficiently large deflections in the edge there appear significant compressive stresses, and this leads to loss of stability. A peculiarity of this problem consists of the fact that the principal stress, preceding buckling, is characterized by presence of variables forces in middle surface and of moments and that the plate obtained a preliminarily distortion. Therefore here it is necessary to use fundamental equations of the theory of flexible plates, considering the influence of initial deflection w_0 and functions of initial stresses in the middle surface Φ_0. Dependence between

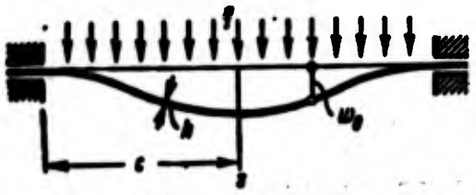

Fig. 9.10. Flexible plate under action of lateral load.

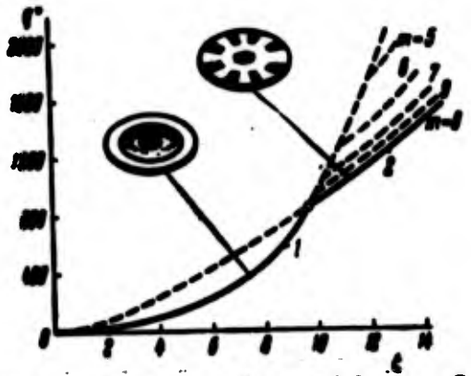

Fig. 9.11. Formation of asymmetric forms of buckling.

parameters of intensity of pressure $q^* = \frac{qc^4}{Eh^4}$ and maximum deflection of the plate $\zeta = \frac{f}{h}$, found in article [9.8], is depicted in Fig. 9.11.

During the study of symmetric forms we obtain a relationship of type (see [0.3], p. 186)

$$q^* = A\zeta^3 + B\zeta; \qquad (a)$$

it corresponds to curve 1. Research of asymmetric forms when $m \neq 0$ leads to the same equations, but with different coefficients A and B.

*This problem was first investigated by D. Yu. Panov and V. I. Feodos'yev [9.8]; see also work of Bodner [9.9].

Curve 2 corresponds to a number of nodal diameters, equal to m = 8; curves for the nearest values m = 7, 9, etc., lie above line 2.

At point of intersection of curves 1 and 2, corresponding to $q^* = 880$ and $\zeta = 9.6$, there should occur loss of stability of axisymmetric form of deflection; here there appear eight hollows along the circumference. After that simultaneously there will increase deflection at center of plate and maximum deflection of "local hollows." Subsequently, obviously, there will set in a new change of form of wave-formation, with subsequent growth of the number of "local hollows."

§ 116. Annular Plates

In many structures there are annular plates, in various ways secured by their edges. Such an annular plate is, for instance, the wall of a circular frame of the fuselage of an aircraft, or of a submarine. Annular plates are also met in instrument-making. Let us consider the stability of an annular plate (Fig. 9.12), if its inner and outer edges, whose radii are equal to a and b, there act forces of identical intensity,*

$$p_1 = p_2 = p.$$

If we limit ourselves to the case of <u>axial symmetry</u> of the deflection surface, then it is possible to start from equation (22) taking into account member C_0/r; then instead of (40) we obtain

$$0 = C_1 J_1(\alpha r) + C_2 Y_1(\alpha r) + \frac{C_3}{r}. \qquad (9.78)$$

---

*Stability of annular plates was investigated initially by W. R. Dean, Proc. Royal Soc. London, Ser. A 106 (1924) and A. S. Lokshin (Comptes rendus (1924). Resolution of the given problem was given for axisymmetric case by V. M. Makushin [9.5], and in more general form by Yamaki [9.14]. Graph of Fig. 9.13 was given in [9.14].

Hence

$$w=\frac{1}{a}[C_1J_0(ar)+C_2Y_0(ar)]+C_3\ln r+C_4. \qquad (9.79)$$

But it is possible to assume that for an annular plate, reinforced on the inner edge, the decisive case will be the asymmetric case, and therefore, it is necessary to investigate the more general equation (72). Supplementing (73), we find

$$w=[C_1'J_m(ar)+C_2'Y_m(ar)+C_3'r^m+C_4'r^{-m}]\sin m\varphi. \qquad (9.80)$$

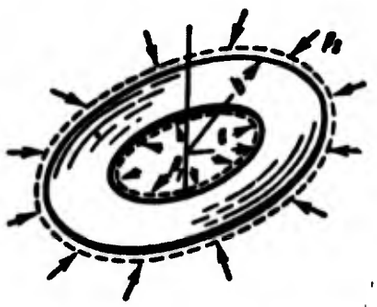

Fig. 9.12. Annular plate under action of radial compression.

Expressions (79) or (80) must satisfy boundary conditions on inner and outer edges. Conditions, corresponding to clamped and hinged support, have form (12) and (13). We shall analyze the practically important case where one of the edges of the plate (for instance, the inner one) can be displaced in direction of the axis of the plate, but here does not turn. Then here we should have

$$\frac{\partial w}{\partial r}=0,\quad R_r=0. \qquad (9.81)$$

If we substitute in expressions (8) and (7) values of curvatures, then after certain transformations it is possible to reduce the second of conditions (81) to form

$$\frac{\partial}{\partial r}\left(\frac{\partial^2 w}{\partial r^2}+\frac{1}{r}\frac{\partial w}{\partial r}+\frac{1}{r^2}\frac{\partial^2 w}{\partial\varphi^2}\right)+\frac{1-\mu}{r}\frac{\partial}{\partial\varphi}\left[\frac{\partial}{\partial r}\left(\frac{1}{r}\frac{\partial w}{\partial\varphi}\right)\right]=0. \qquad (9.82)$$

Subordinating (79) or (80) to boundary conditions, we arrive at a system of equations for C_1, ..., C_4; equating the determinant of the system to zero, we find critical value of p.

In Fig. 9.13 are represented results of calculations* for different cases of fastening: a — clamping on both edges, b — hinged support on both edges, c — clamping on outer edge and free displacement without rotation on the inner, d — hinged fastening on outer edge and the same free displacement on the inner. Along the axis of abscissas is plotted ratio a/b, and along the axis of ordinates, the value of $\sqrt{K}$, where K is the coefficient in formula

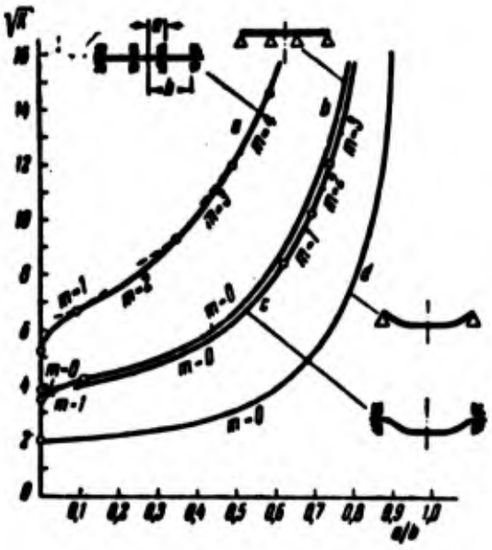

Fig. 9.13. Calculating graph for case of annular plate with different conditions of fastening.

$$p_{кр} = K\frac{D}{b^2 h}. \qquad (9.83)$$

On the graph is shown the number m of nodal diameters, which corresponds to the least stress for a given a/b. At the $\frac{a}{b} \to 0$, under the boundary conditions a and b, we obviously arrive at the case of a solid plate with reinforced center; the deflection surface will form here one nodal diameter, as in Fig. 9.9a. However, when $\frac{a}{b} > 0.1$ the plates buckle differently: a clamped plate has bigger hollows on its circumference the narrower it is, while a hinge-supported is bent axisymmetrically (m = 0).

With boundary conditions c and d and $\frac{a}{b} \to 0$ we arrive at the ordinary case of a solid plate with a freely displaced center; therefore, here there will be m = 0, and critical stresses will be determined by formulas (47) and (63).

With growth of a/b the forms of deflection surface are different:

---

*For $\mu = 0.3$, we assume that h is small as compared to (b − a).

a hinge-supported plate in all cases is bent axisymmetrically. In the other limiting case $\frac{a}{b} \to 1$ we obtain the same critical stress as if an elongated rectangular plate of width b – a was compressed in two directions by forces p and would have analogous boundary conditions on the long edges.

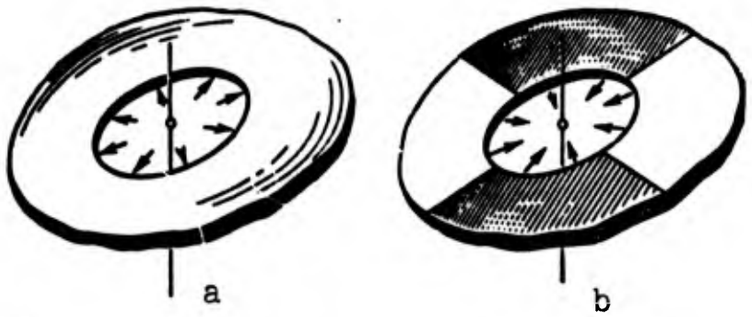

Fig. 9.14. Annular plate, loaded on inner edge.

In the literature there are also considered cases where annular plate is subjected to action of radial forces only on the inner [9.11] or outer edge [9.12]. In these problems "fundamental" forces σ_r and σ_φ will change along the radius. If on inner edge there are applied compressive forces, then stresses σ_r will be compressive at all points of the plate, and σ_φ will be tensile; if however, there are applied tensile forces, then the converse is true. Interesting is the case of loading on the inner edge when b >> a. In case of compression (Fig. 9.14a) critical value of p is equal (under the condition that inner edge does not turn) to

$$p_{kp} = \frac{D}{a^2}. \tag{9.84}$$

and with tensile forces regardless of conditions of fastening (Fig. 9.14b)

$$-p_{kp} = \frac{3D}{a^2}. \tag{9.85}$$

i.e., three times larger than during compression. In case of

compression the plate bends axisymmetrically, and during extension – with two nodal diameters.

§ 117. Postcritical Behavior of a Circular Plate

A circular plate is able to support an increasing load after loss of stability just as a rectangular plate. As we saw, a solid plate, in one way or another secured on its edge* and subjected to action of radial compression, buckles in axisymmetric form. Naturally, in the initial stage of postcritical deformation axial symmetry of the deflection surface is preserved. However, with further growth of the load there occurs formation of more shallow waves and symmetry is disturbed. The greater the load, even greater should become the number of waves on the circumference. Solution of this problem pertained till now, as a rule, to axisymmetric forms of bending of a plate.**

Let us consider a hinge-supported plate of radius c with freely displaced edges, compressed by forces p. For study of the postcritical region during axisymmetric buckling we have to turn to general equations (30) and (31), pertaining to flexible plates. We take for w the former approximating expression (64). Putting it in the right part of equation (31), we find

$$\frac{d}{dr}(\nabla^2\Phi)=\frac{d}{dr}\left[\frac{1}{r}\frac{d}{dr}\left(r\frac{d\Phi}{dr}\right)\right]=-\frac{8Ef^2c^2}{c^4}\left(\frac{r}{c}-2b\frac{r^3}{c^3}+b^2\frac{r^5}{c^5}\right) \qquad (9.86)$$

and, hence,

$$\frac{d\Phi}{dr}=\frac{Ef^2c^2}{6c^2}(6-4b+b^2)r+C_1\frac{r}{2}+\frac{C_2}{r}. \qquad (9.87)$$

Constants C_1 and C_2 we find from condition of limitedness of $\frac{d\Phi}{dr}$ at the center of the plate ($C_2 = 0$) and condition

---

*It is assumed that points of the edge freely shift in radial direction.

**It was given by Friedrichs and Stoker in 1939 [9.10], by E. I. Grigolyuk [9.3], applying Bubnov-Galerkin by I. I. Vorovich [9.1] and Bodner [9.9].

$$(\sigma_r)_{r=c} = \left(\frac{1}{r}\frac{d\Phi}{dr}\right)_{r=c} = -p. \tag{9.88}$$

Then finally

$$\frac{d\Phi}{dr} = \frac{Ef^2a^2}{6c}\left[(6-4b+b^2)\frac{r}{c} - 6\frac{r^3}{c^3} + 4b\frac{r^5}{c^5} - b^2\frac{r^7}{c^7}\right] - pr. \tag{9.89}$$

We use the Bubnov-Galerkin method and write equation (34); magnitudes X and $\frac{d\eta}{dr}$ by (30) and (32) will be equal to

$$X = D\frac{d}{dr}(\nabla^2 w) - \frac{h}{r}\frac{d\Phi}{dr}\frac{dw}{dr}, \quad \frac{d\eta}{dr} = \frac{r}{c} - \frac{br^3}{c^3}. \tag{9.90}$$

After integration we arrive at equation

$$\frac{8}{3}Db(3-2b)f - \frac{1}{6}p(6-8b+3b^2)hc^2f + \\ + \frac{1}{252}Eha^2f^3(84-168b+140b^2-56b^3+9b^4) = 0. \tag{9.91}$$

Dropping the nonlinear member, we find critical stress $p_{кр}$ by (70). We determine dependence between load and maximum deflection, introducing dimensionless parameters

$$p^* = \frac{p}{E}\left(\frac{c}{h}\right)^2, \quad n^* = \frac{p^*}{p^*_{кр}}, \quad \zeta = \frac{f}{h}, \tag{9.92}$$

will find

$$p^*_{кр} = 0.385. \tag{9.93}$$

Magnitude n* shows, in by how many times the boundary stresses p exceed critical value, here p plays the same role as stress in edge fibers σ_p for rectangular plates.

Taking a and b according to (69) for $\mu = 0.3$, we find from (91), when $f \neq 0$,

$$n^* \approx 1 + 0.16\zeta^2. \tag{9.94}$$

Hence

$$\frac{\zeta}{\sqrt{n^*}} = 1.96\sqrt{1 - \frac{1}{n^*}}. \tag{9.95}$$

If we assume that critical force is greatly exceeded, so that 1/n* is negligible as compared to 1, and at the same time deformations remain

elastic, then we obtain

$$\zeta \approx 1.96 \sqrt{n^*}. \tag{9.96}$$

Dependence (95) is depicted in Fig. 9.15 by the dotted line. As we have seen, in case of clamped plate the solution remains in force, but we must take a = b = 1. Then (91) obtains form

$$\frac{8}{3} Df - phc^2 f + \frac{1}{28} Ehf^3 = 0. \tag{9.97}$$

Substituting value of p_{kp} from (58), we obtain, when $f \neq 0$,

$$n^* = 1 + 0.16\zeta^2; \tag{9.98}$$

hence

$$\frac{\zeta}{\sqrt{n^*}} = 2.5 \sqrt{1 - \frac{1}{n^*}}. \tag{9.99}$$

When $1/n^* \to 0$ we obtain $\zeta/\sqrt{n^*} \to 2.5$.

Effect of clamping of the plate on its edge is manifested most strongly at moment of buckling, with growth of deflections it weakens. Therefore, with an identical degree of exceeding critical stress the maximum deflection of a clamped plate is somewhat greater than for a hinge-supported one.

In works [9.9] and [9.10] this problem was solved by perturbation calculation.* As parameter we select magnitude $\varepsilon = \sqrt{n^* - 1}$, equal to zero at moment of buckling. Magnitudes $\frac{1}{r}\frac{d\Phi}{dr}$ and $\frac{1}{r}\frac{dw}{dr}$ are expanded in a series by powers of this parameter, and then are put in fundamental equations (30) and (31). Equating coefficients for identical powers of ε, we arrive at a system of linear differential equations for functions, comprising the series. The problem is reduced to consecutive solution of these equations. Obviously, this method is applicable for a relatively small magnitude ε.

*This method was offered earlier for analogous problem by P. Ya. Polubarinova-Kochina, op. cit., p.392.

Another approach to the problem [9.10] consists of application of the method of power series.* Functions $\frac{1}{r}\frac{d\Phi}{dr}$ and $\frac{1}{r}\frac{dw}{dr}$ are expanded in series by powers of r; the first member of the series determines value of these functions at center of plate, when r = 0.

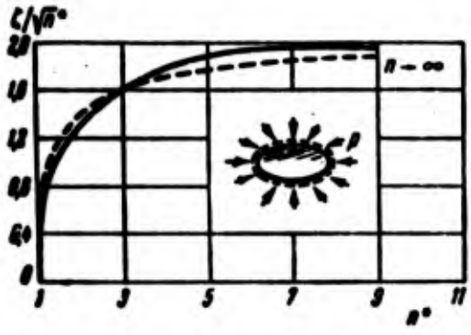

Fig. 9.15. Diagram of postcritical deformation of a circular plate.

Using boundary conditions, we reduce the problem to solution of a system of transcendental equations.

In Fig. 9.15 are presented results of calculations according to method of series for case of hinged support (solid line); it lies comparatively close to the curve obtained by the Bubnov-Galerkin method. In Fig. 9.16 is depicted law of distribution σ_φ along radius for different n*. As we see, for n* = 14.7 in whole central zone of plate, occupying about 0.7c, there are <u>tensile</u> stresses. Compressive stresses are concentrated in "boundary zone," at edge of the plate. Here the central part of plate becomes almost flat, as is depicted in Fig. 9.17 for n* = 14.7. At the limit this central part embraces the whole plate, as is shown in Fig. 9.17 by dotted line. Comparison of data, pertaining to stress $\sigma_ц$

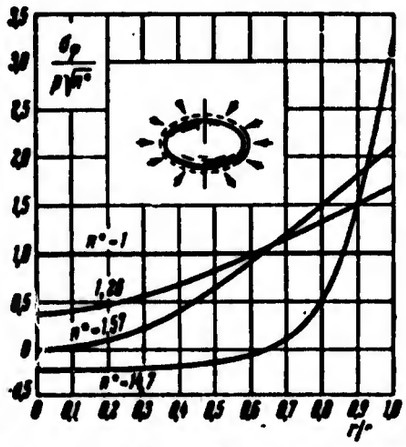

Fig. 9.16. Arc stresses during postcritical deformation of a plate.

---

*Method of series was applied Way in solving the problem of large deflections of a circular plate during action of lateral load.

in center of plate for hinge-supported and clamped plates, is given in Fig. 9.18. Dot-dash line pertains to solution according to Bubnov-Galerkin method.

Fig. 9.17. Deflection surface of circular plate at different stages of postcritical deformation.

Thus, with significant n* functions Φ and w sharply change only at the actual edge of the plate. This allows us to simplify the initial equations and to use asymptotic solution of the problem of edge effect, as is the case in the theory of shells [10.6] and in examining of boundary layer in aerodynamics. Such asymptotic solution of the problem led to the following results. For hinge-supported plate when $n^* \to \infty$ we obtain

$$\zeta = 2\sqrt{n^*}. \qquad (9.100)$$

which is very close to (96). Stresses in center for $n^* \to \infty$ are close to values shown in Fig. 9.18.

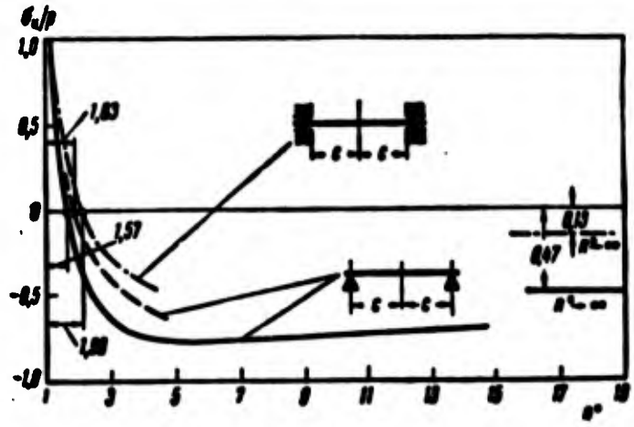

Fig. 9.18. Stresses in center of hinge-supported and clamped plates during postcritical deformation.

All these data pertain to <u>axisymmetric</u> buckling. At a certain value of n*, approximately equal to n* = 15 for hinge-supported plate,

in frontier zone there should occur "secondary" buckling; the axisymmetric bent state of the plate becomes unstable. Study of this phenomenon constitutes an interesting problem.

Literature

9.1. I. I. Vorovich. Behavior of a circular plate after loss of stability, Scientific notes of Rostov State University 32, No. 4 (1955), 55-60.

9.2. B. G. Gazizov. Concerning the question of stability of an annular plate, News of Kazan' Branch of Academy of Sciences of USSR, 12 (1958), 155-164.

9.3. E. I. Grigolyuk. Concerning the question of behavior of circular plates after loss of stability, Herald of engineering and technology., No. 3 (1949).

9.4. A. N. Dinnik. Stability of a compressed round plate, News of Kiev Polytechnic Institute (1911); Application of Bessel functions to problems of the theory of elasticity, 1913; Selected works, Vol. 2, Publishing House of Academy of Sciences of Ukrainian SSR, Kiev, 1955, 62-72.

9.5. V. M. Makushin. Critical values of intensity of radial compressive forces for round thin plates, "Strength analysis," calculations on 4 (1959), 270-298; 5 (1960), 236-248; and 6 (1960), 171-181.

9.6. Yu. I. Remnev. Stability of a round plate during irradiation, Scientific report of the higher school, of physics and mathematics, No. 3 (1959), 145-147.

9.7. V. Novatskiy and Z. Olesyak. Vibrations, stability and bending of a circular plate on a circumference, clamped completely and partially supported, Bulletin of Polish Academy of Sciences, Dept. 4, 4, No. 4 (1956).

9.8. D. Yu. Panov and V. I. Feodosyev. Equilibrium and loss of stability of shallow shells during large deflections, Applied math. and mech., 12, No. 4 (1948), 384-406, 13; No. 1 (1949), 116.

9.9. S. R. Bodner. The postbuckling behaviour of a clamped circular plate, Quart. Appl. Math. 12, No. 4 (1955), 397-401.

9.10. K. Friedrichs and J. Stoker. The non-linear boundary value problem of the buckled plate, Proc. of the Nat. Acad. of Sci. 25 (1939), 535-540; Amer. J. Math. 63 (1941), 839-888; Buckling of the circular plate beyond the critical thrust, J. Appl. Mech. 9, No. 1 (1942), 7-14.

9.11. E. H. Mansfield. On the buckling of an annular plate, Quart. Journ. of Mech. and Appl. Math. 13 No. 1 (1960), 16-23.

9.12. E. Meissner. Ueber das Knicken kreisförmiger Scheiben, Schweiz. Bauzeitung 101 (1933), 87-89.

9.13. A. Nadai. Ueber das Ausbeulen von kreisförmigen Platten, Zeitschr. VDJ, No. 9 (1915), 10.

9.14. N. Yamaki. Buckling of a thin annular plate under uniform compression, J. Appl. Mech. 25 (1958), 267-273.

CHAPTER X

GENERAL INFORMATION ON SHELLS

§ 118. Distinctive Features of Problems of Stability of Shells

Let us turn to problems pertaining to stability of shells. These problems are of special interest for many regions of new technology and also for all those "settled" regions, in which there occurs introduction of light structures and new materials. Calculations for stability of shells of different form, smooth and reinforced, isotropic and anisotropic, deformed within and beyond the elastic limit, we constantly encounter primarily during designing of aircraft and their motors. About half a century ago I. G. Bubnov noted that the hull of a ship almost wholly consists of plates. Now we can say that the structure of an aircraft consists mainly of shells. Curved panels of the skin in these structures constitute shallow shells; at the same time, the body of an aircraft as a whole can be considered a reinforced shell. Demands of aviation technology primarily explain the intense development of the theory of stability of shells in recent times. Calculations of shells for stability have essential value in designing of above surface and underwater ships, steam locomotives and railroad cars, pipelines, tanks, domes and coverings in engineering constructions, etc.

Behavior of shells during loss of stability essentially differs from behavior of bars and plates. Buckling of shells, as a rule, is accompanied by appearance not only of flexural stresses, but also secondary stresses in the middle surface (chain stresses), while for bars and plates we could consider only flexural stress.* A certain part of the potential of external load is "expended" in case of shell on increase of flexural energy, and the other part is spent on change of energy of the middle surface. Relationship between these magnitudes depends on what configuration the shell takes during buckling.

We imagine a bar, a plate, and a shell as a system with one degree of freedom and consider diagrams of dependence between load P and parameter of deflection f characteristic for them in problems of stability (Fig. 10.1). We consider that deflection remain small as compared with dimensions of the structure, but they can be comparable with height of the section of the bar or thickness of the plate and shell. Segment OA pertains in all cases to initial equilibrium states, which here are considered zero-moment and segments AD and AC refer to bent, moment equilibrium states.

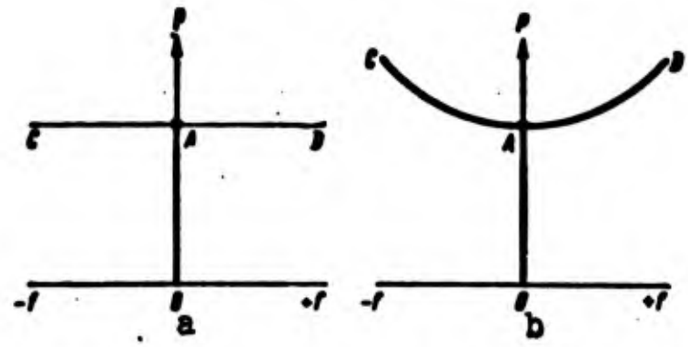

Fig. 10.1. "Load-deflection" diagrams for bar and plate.

*As we saw, during research of postcritical deformation of plates there also are considered stresses of both types.

In case of a bar diagram P(f) has the form of a horizontal line (Fig. 10.1a), which corresponds to "indifferent" equilibrium. For the plate we obtain a curve of postcritical stable states, symmetric with respect to the axis of ordinates (Fig. 10.1b); it is obvious that for an ideally flat plate, as for an ideally straight bar, both directions of deflection, (+f) and (-f), are equal. Meanwhile in case of a shell the branch of bent equilibrium forms CABD turns out to be asymmetric, as is shown in Fig. 10.2.

Such uniqueness in behavior of a shell is possible to explain by the example of arch-strip ACB, shown in Fig. 10.3 and secured at edges A and B. If we were to give the arch additional deflection (-f) from center of curvature, as is shown by dotted line, fibers of the middle layer must stretch. Conversely, with deflection (+f) toward the center of curvature (solid thin line) middle fibers shorten. When arch obtains outline AC'B, mirror image of the initial stresses in the middle layer are equal to zero. Only during further bending by (dot-dash line) will middle fibers be stretched. For a shell, the connection between forces of extension and compression in the middle surface are more complicated than in the case of an arch, since problem is two-dimensional. But the general tendency remains the same, the shell "prefers" to buckle inward, toward the center of curvature.* This is shown in Fig. 10.4 with example of a cylindrical panel, compressed along the generatrix.

We return to Fig. 10.2; here deflection toward the center of curvature is plotted along the axis of abscissas to the right, and

---

*Here we have in mind shells, for which centers of curvature of all normal sections lie on one side of the middle surface (see § 119.)

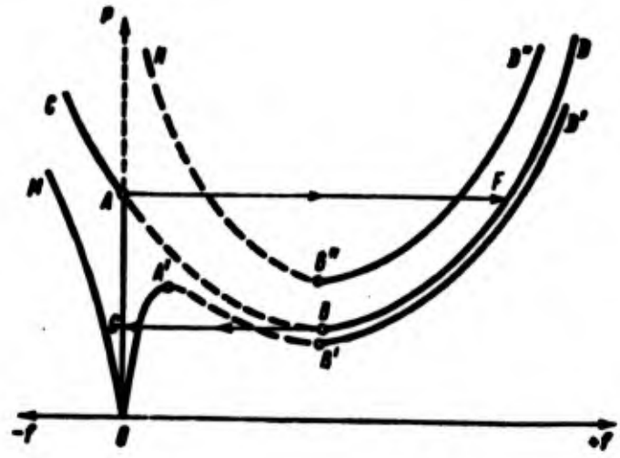

Fig. 10.2. Characteristic "load-deflection" diagrams for a shell of ideal form and with initial deflection.

and from the center, to the left. Asymmetry of the diagram of equilibrium states is connected with the fact that branch ABF of the diagram lies below the point of branching (bifurcation) A. On section AB equilibrium forms are unstable, and on section BF they are stable. Sections AC and FD correspond stable states. But we already obtained a similar diagram in Chapter I (p. 89) for a compressed bar with a nonlinear elastic support. By analogy with this problem in the theory of stability of shells there are applied the concepts of upper and lower critical loads.* By upper critical load P_B we shall, as before, understand the greatest load, below which initial equilibrium state is stable in the small, i.e., with respect to neighboring equilibrium states. In reference to the model which is described by diagram OABD,

Fig. 10.3. Clicking an arch-strip.

*These concepts were first introduced by Kármán and Tsien Hsüeh-seng [11.35] in 1939; they are considered in more detail in § 201.

the upper critical force corresponds to the point of bifurcation of equilibrium states. By lower critical load P_H we will understand the load below which the initial state is the only stable state;* with loads, lying below P_H, there is ensured stability of the shell not only in the small, but in the large.

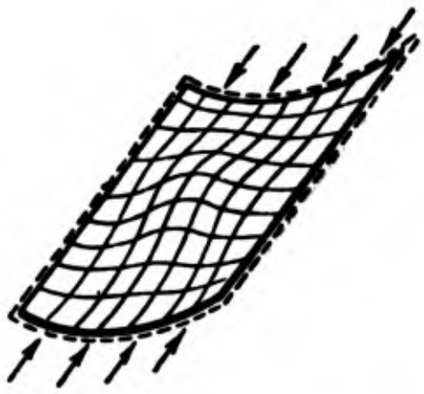

Fig. 10.4. Cylindrical panel "prefers" to buckle toward the center of curvature.

Let us assume that the initial form of the shell is ideal (there are no initial deflections), and load is static and occurs in such a way that state of strain is strictly momentless; then the load applied to the shell should increase to the upper critical value P_B after which the shell will accomplish a jump (knock) from equilibrium position A to position F, after which load anew will start to increase,** but now on branch FD. The reverse process consists of drop of the load along line DB, "exhaust" of shell along line BG, and then in new lowering of load from G to O. Consequently, the jump during unloading occurs at a level below critical force P_H. Regarding equilibrium states, corresponding to line AC, they usually are not realized, since to them there corresponds a higher energy level.

Real shells always have, however, various initial imperfections

---

*We recall that here we consider deflections comparable to the thickness of the shell; they can exceed thickness a few times, even by 10–20 times, but still they must remain small as compared to radii of curvature. Therefore, e.g., the case of total crushing of a rubber ball does not enter into the framework of this theory.

**Here it is assumed that load in process of knock is kept constant. Other variants of change of load are considered below, in §§ 127 and 129.

of form. For such shells the initial state, as a rule, no longer can be considered momentless, so that the branch of equilibrium states with a growing load no longer will coincide with axis of ordinates. In many cases diagram P(f) as in Fig. 10.2 here too consists of stable branches OA' and B'D' and unstable A'B'. Transition from one stable state to another also should be in a jump — on level A'. Loads, corresponding to points A' and B', will be, by analogy with the preceding case, called upper and lower critical loads P_B and P_H. We assumed that initial deflection is aimed in that same direction as the additional one, chiefly toward the center of curvature. If initial deflection is directed away from center of curvature, then initial branch OM will go to the left of the axis of ordinates. Other possible equilibrium forms are characterized by sections NB'' and B''D''. Here also there is (although not in all cases) a jump from branch OM to branch B''D'': the energy level for points of the second of these branches can be significantly lower than for corresponding points of the first branch.

As we see, initial imperfections of form and other perturbations are manifested in the case of a shell quite differently than for plate; they lead to great lowering of the upper critical load. Therefore, experimental data pertaining to critical loads for shells are usually characterized by significant scattering.* Actual buckling of shells in practice in many cases is accompanied by a sharp knock. From this follows the conclusion that in practical calculations one should consider both the upper, and also, particularly, the lower

---

*With the exception of such laboratory tests in which special attention is turned to techniques of manufacture of shells and load conditions.

critical loads. Operational load should constitute a certain fraction of the upper critical magnitude and at the same time, as a rule, must not exceed the lower critical value. True, for certain structures the second requirement can not be satisfied, if, e.g., the lower critical load is close to zero or even is negative, i.e., has an opposite direction as compared to the principal state. In all cases most justified will be calculation directly considering influence of initial irregularities of form and other perturbing factors. If we talk about a large number of identical structural members, then the most natural approach here is the statistical (see Chapter XX).

In one way or another, practical calculations of shells for stability must be conducted taking into account behavior of shells during large deflections. If for bars and plates it was possible to separate determination of points of bifurcation and research of the postcritical region, here this is in most cases impossible.* Therefore, subsequently we shall, as a rule, consider in a parallel manner the same problem, approaching it from the point of view of stability in the small and in the large. In the first case it is necessary to start from linear theory of hard shells, in the second, from nonlinear theory of flexible shells.

We turn to the basic propositions of linear and nonlinear theory.

§ 119. Certain Information from Surface Theory

If we approach shells from the geometric point of view, then they are characterized, first of all, by the shape of the middle surface. Therefore, in deriving basic dependences pertaining to the

*As we shall see later, in certain problems the lower critical load turns out to be very close to the upper; then necessity of separate calculation for stability in the large may disappear.

shell, it is necessary to use many concepts of general surface theory.*

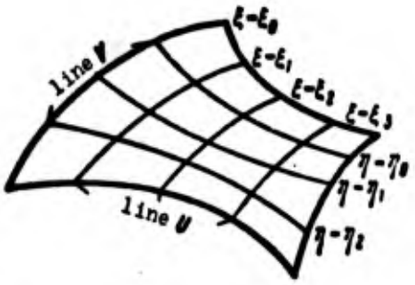

Fig. 10.5. Net of coordinate lines on a surface.

We consider the section of a surface, shown in Fig. 10.5, and select on it a system (family) of lines U in such a way that each of them corresponds to a definite value of a certain parameter ξ: $\xi = \xi_0$, $\xi = \xi_1$, $\xi = \xi_2$, etc. Further, we select a new system of lines V, each of which would correspond to a certain value of a second parameter η: $\eta = \eta_0$, $\eta = \eta_1$, $\eta = \eta_2$, etc., and in such a manner that lines V intersect all lines U. We satisfy the requirement that through any point of the surface there passes one and only one line of each family; the net of lines selected thus, is called regular. If lines of systems U and V cross at right angles (i.e., the angle between tangents to these lines is equal to a right angle), then the net is called orthogonal.

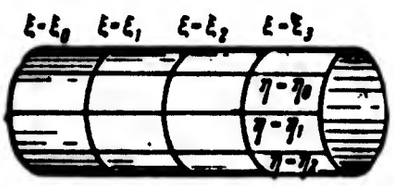

Fig. 10.6. Coordinate lines on a cylindrical surface.

Concrete meaning of parameters ξ and η may be different. For example in Fig. 10.6 there are depicted coordinate lines on a section of a cylindrical surface, where lines U coincide with generatrices and lines V lie in cross sections of the cylinder. As parameters ξ and η here it is possible to select directly lengths of segments laid off along the lines. In Fig. 10.7 is shown a section of a spherical surface.

---

*See, e.g., courses of differential geometry of M. Ya. Vygodskiy (Moscow, 1949), A. V. Pogorelov (Khar'kov, 1961), P. K. Rashevskiy (Moscow, 1956), and S. P. Finikov (Moscow, 1961).

Here it is convenient to use geographic coordinates and as parameters ξ and η to select the angle of latitude α and the longitude β. Let us note that in this example pole A

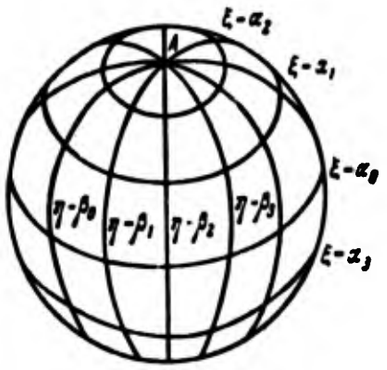

Fig. 10.7. Geographic coordinates on a sphere.

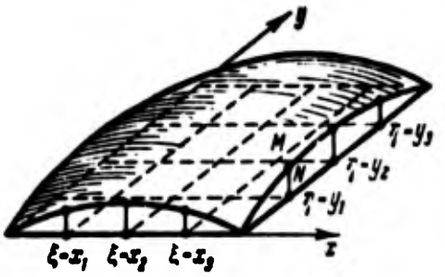

Fig. 10.8. Coordinate lines, characterizing shallow surface.

is a singular point, since for it the requirement of regularity of the coordinate is not satisfied.

In case of a shallow surface M, close to plane N, parameters can be the cartesian coordinates of the corresponding points of the plane (Fig. 10.8) or polar coordinates of these points.

No matter how parameters ξ and η are selected, position of every point of the surface is determined by their values; they are curvilinear coordinates of points of the surface; coordinate ξ is counted off along lines $\eta = \eta_0$, $\eta = \eta_1$, ..., and coordinate η, along lines $\xi = \xi_0$, $\xi = \xi_1$, ... The actual lines of families U and V carry the name of coordinate lines.

If we designate by r the radius-vector of a point of the surface relative to an arbitrary origin O (Fig. 10.9), then r will be an unambiguous vector function of curvilinear coordinates ξ and η:

$$r = r(\xi, \eta). \qquad (10.1)$$

We pass vectors r and $r + \Delta r$, corresponding to two adjacent points M and M' of line η = const. Relating increment of the function Δr

to increment of the parameter $\Delta\xi$ and considering $\Delta\xi \to 0$, we obtain at the limit a partial derivative of r with respect to ξ:

$$\lim\left(\frac{\Delta r}{\Delta \xi}\right)_{\Delta\xi\to 0}=\frac{\partial r}{\partial \xi}.$$

The sense of vector $\frac{\partial r}{\partial \xi}$ coincides with the sense of the tangent y to line ξ at the given point; therefore, it has the name <u>coordinate vector</u>. A second coordinate vector

Fig. 10.9. Radius-vector of a point of a surface as a function of curvilinear coordinates.

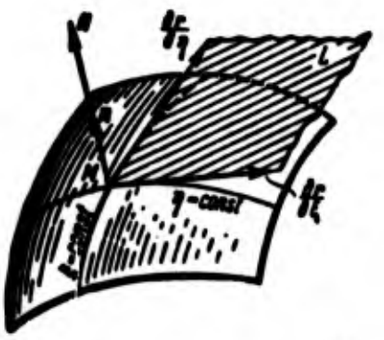

Fig. 10.10. Coordinate vectors at point M of a surface.

$\frac{\partial r}{\partial \eta}$ is directed along the tangent to line η (Fig. 10.10).

Plane L, passed through vectors $\frac{\partial r}{\partial \xi}$ and $\frac{\partial r}{\partial \eta}$ is a <u>plane tangent to the surface</u> at point M. The line, perpendicular to plane L is a <u>normal to the surface</u>; sense of the normal is determined by the vector product of vectors $\frac{\partial r}{\partial \xi}$ and $\frac{\partial r}{\partial \eta}$:

$$N=\frac{\partial r}{\partial \xi}\times\frac{\partial r}{\partial \eta}.$$

Unit vector of the normal is equal to

$$n=\frac{\frac{\partial r}{\partial \xi}\times\frac{\partial r}{\partial \eta}}{\left|\frac{\partial r}{\partial \xi}\times\frac{\partial r}{\partial \eta}\right|}; \qquad (10.2)$$

In the denominator here is the absolute value of N. Vector n should not, of course, depend on selection parameters ξ and η. If

coordinate lines form angle α, then, using the definition of a scalar product, we obtain

$$\cos\alpha = \frac{\frac{\partial r}{\partial \xi}\frac{\partial r}{\partial \eta}}{\left|\frac{\partial r}{\partial \xi}\right|\left|\frac{\partial r}{\partial \eta}\right|} = \frac{a_{12}}{\sqrt{a_{11}a_{22}}}; \tag{10.3}$$

here there are introduced designations

$$a_{11} = \left(\frac{\partial r}{\partial \xi}\right)^2, \quad a_{12} = \frac{\partial r}{\partial \xi}\frac{\partial r}{\partial \eta}, \quad a_{22} = \left(\frac{\partial r}{\partial \eta}\right)^2. \tag{10.4}$$

Using (3), we find

$$\sin\alpha = \frac{\omega}{\sqrt{a_{11}a_{22}}}, \tag{10.5}$$

where

$$\omega = \sqrt{a_{11}a_{22} - a_{12}^2}. \tag{10.6}$$

Proceeding from definition of vector product, we reduce (2) to form

$$n = \frac{\frac{\partial r}{\partial \xi} \times \frac{\partial r}{\partial \eta}}{\omega}. \tag{10.7}$$

We set ourselves the target of investigating the surface near a certain point M (Fig. 10.11). In <u>first approximation</u> an infinitesimal section of the surface can be replaced by an infinitesimal section of the tangent plant. We use this in order to determine the differential ds of the arc, passing through point M. Direction of arc will be fixed, if we are given ratio of corresponding differentials of curvilinear coordinates $d\eta : d\xi$ (when $d\xi \neq 0$). By dr we shall mean the differential radius-vector r during displacement from point M on the tangent to the given arc. Square ds can be calculated by composing the scalar product

$$ds^2 = dr \cdot dr = dr^2.$$

Total differential dr is equal to

$$dr = \frac{\partial r}{\partial \xi} d\xi + \frac{\partial r}{\partial \eta} d\eta; \tag{10.8}$$

hence

$$ds^2 = a_{11} d\xi^2 + 2a_{12} d\xi\, d\eta + a_{22} d\eta^2. \tag{10.9}$$

Expression (9) carries name of <u>first quadratic form of surface</u>, and magnitudes a_{11}, a_{12}, a_{22} from (4) are <u>coefficients of first quadratic form</u>. These coefficients depend on curvilinear coordinates for point M, but do not depend on their differentials; consequently, for the given point of a surface magnitudes a_{11}, a_{12}, and a_{22} are determined unambiguously. Knowing the first quadratic form of the surface, one can find the angle between any lines, passing through this point (i.e., angle of the tangent to these lines); as an example we give formula (3), allowing us to find the angle between coordinate lines. Integrating the expression for ds along certain curve it is possible to calculate total length of an arc of the curve.

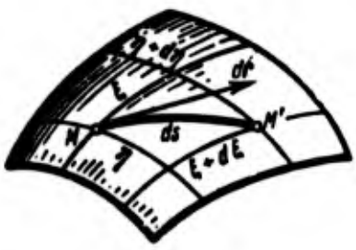

Fig. 10.11. Studying the surface near point M in the first approximation.

Since during research of buckling of shells it is important to determine lengthening and sliding of the middle surface, i.e., change of lengths of arcs and angles between arcs, then, obviously, the first quadratic form of the middle surface of the shell should play an essential role in such research. We note, besides, that with help of the first quadratic form it is possible to calculate areas of various sections of the surface.

We shall henceforth designate the first quadratic form by I:

$$I = a_{11}\,d\xi^2 + 2a_{12}\,d\xi\,d\eta + a_{22}\,d\eta^2. \qquad (10.9a)$$

For an orthogonal coordinate net we have from (3) $a_{12} = 0$; here

$$I = a_{11}\,d\xi^2 + a_{22}\,d\eta^2. \qquad (10.10)$$

If radius-vector r is expressed in cartesian coordinates x, y, and z, then by (4) we obtain

$$\left.\begin{aligned} a_{11} &= \left(\frac{\partial x}{\partial \xi}\right)^2 + \left(\frac{\partial y}{\partial \xi}\right)^2 + \left(\frac{\partial z}{\partial \xi}\right)^2. \\ a_{12} &= \frac{\partial x}{\partial \xi}\frac{\partial x}{\partial \eta} + \frac{\partial y}{\partial \xi}\frac{\partial y}{\partial \eta} + \frac{\partial z}{\partial \xi}\frac{\partial z}{\partial \eta}. \\ a_{22} &= \left(\frac{\partial x}{\partial \eta}\right)^2 + \left(\frac{\partial y}{\partial \eta}\right)^2 + \left(\frac{\partial z}{\partial \eta}\right)^2. \end{aligned}\right\} \qquad (10.11)$$

Then we investigate the surface in the second approximation and explain how the surface deviates from the tangent plane in the environment of the point of tangency. We pass through M an arbitrary line l, lying on the surface, and tangent m to this line (Fig. 10.12). We imagine a plane passing through the tangent to line l and a certain point N, lying on the line near point of tangency M. We trace change of position of this plane, driving length of arc $\overset{\smile}{MN}$ to zero; at the limit we obtain a so-called osculating plane S. If curve l lies in one plane, then this plane would be osculating for all points of the curve. The normal to the curve, lying in the osculating plane, is

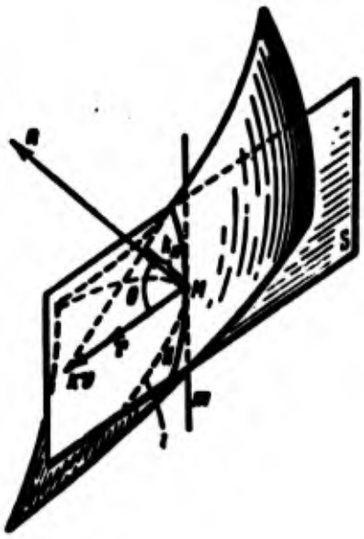

Fig. 10.12. Study of a surface near point M in the second approximation.

called the principal normal. Unit vector of the principal normal we designate by ν; it is shown in Fig. 10.12. If r is the radius-vector of point M, and s is length of the arc, measured along the line, then the unit vector of the tangent will be $\frac{dr}{ds}$. Derivative of this vector with respect to s, equal to $\frac{d^2r}{ds^2}$, determines degree of curvature k and is called vector of curvature; it is directed along the unit vector of the principal normal ν, similarly to normal acceleration during motion of a point on a curve. Thus, we arrive at the known formula of Frenet:

$$\frac{d^2r}{ds^2} = k\nu. \qquad (10.12)$$

We project the vector of curvature of line l on the normal to the surface, as shown in Fig. 10.12; then we find the so-called normal curvature of line k_n. For determination of k_n we take the scalar product of vector $k\nu$ by the unit vector of the normal to surface n; then we find

$$k_n = k\nu n, \text{ when } k_n = \frac{d^2r}{ds^2} n. \qquad (10.13)$$

If we designate by θ the angle between senses ν and n, we have $\nu n = \cos\theta$ and, consequently,

$$k_n = k\cos\theta. \qquad (10.14)$$

This dependence allows us to determine curvature k of any slanted section of the surface with respect to normal curvature k_n (Meusnier's theorem).

We select as the parameter determining the position of a point on curve l length of arc s; then curvilinear coordinates of the point will be functions of s, i.e., $\xi = \xi(s)$, $\eta = \eta(s)$. From (8) we obtain

$$\frac{dr}{ds} = \frac{\partial r}{\partial \xi}\frac{d\xi}{ds} + \frac{\partial r}{\partial \eta}\frac{d\eta}{ds}. \qquad (10.15)$$

Differentiating this expression anew with respect to s, we find

$$\frac{d^2r}{ds^2}=\frac{\partial r}{\partial \xi}\frac{d^2\xi}{ds^2}+\frac{\partial r}{\partial \eta}\frac{d^2\eta}{ds^2}+\frac{\partial^2 r}{\partial \xi^2}\left(\frac{d\xi}{ds}\right)^2+2\frac{\partial^2 r}{\partial \xi\,\partial \eta}\left(\frac{d\xi}{ds}\right)\left(\frac{d\eta}{ds}\right)+\frac{\partial^2 r}{\partial \eta^2}\left(\frac{d\eta}{ds}\right)^2. \qquad (10.16)$$

We write the scalar product (13), considering that each of coordinate vectors $\frac{\partial r}{\partial \xi}$ and $\frac{\partial r}{\partial \eta}$ is orthogonal to the unit vector of normal n; then we have

$$k_n=b_{11}\left(\frac{d\xi}{ds}\right)^2+2b_{12}\frac{d\xi}{ds}\frac{d\eta}{ds}+b_{22}\left(\frac{d\eta}{ds}\right)^2. \qquad (10.17)$$

where

$$b_{11}=n\frac{\partial^2 r}{\partial \xi^2},\quad b_{12}=n\frac{\partial^2 r}{\partial \xi\,\partial \eta},\quad b_{22}=n\frac{\partial^2 r}{\partial \eta^2}. \qquad (10.18)$$

Expression (17) can be rewritten in the form

$$k_n=\frac{II}{I}=\frac{b_{11}d\xi^2+2b_{12}d\xi\,d\eta+b_{22}d\eta^2}{a_{11}d\xi^2+2a_{12}d\xi\,d\eta+a_{22}d\eta^2}; \qquad (10.19)$$

by II here is understood the expression, constructed analogously to (9a) and carrying the name of <u>second quadratic form of surface</u>:

$$II=b_{11}d\xi^2+2b_{12}d\xi\,d\eta+b_{22}d\eta^2. \qquad (10.20)$$

Magnitudes b_{11}, b_{12}, and b_{22} carry name <u>coefficients of the second quadratic form</u>. Judging by formulas (18)–(20), for all lines on the surface, having a common tangent, i.e., characterized by the same relationship $d\eta:d\xi$, the normal curvature k_n will be the same. Consequently, magnitude k_n gives a summary idea of the curvature of the surface in the selected direction; it can be called the <u>normal curvature of the surface</u>.

If in (19) we set $d\eta = 0$, and then $d\xi = 0$, we will obtain accordingly $k_{11} = b_{11}/a_{11}$, $k_{22} = b_{22}/a_{22}$. Thus, coefficients of second quadratic form b_{11} and b_{22} characterize normal curvature of lines η = const and ξ = const. As for coefficient b_{12}, it corresponds to parameter of torsion of the surface. Introducing (7) to (18) we

present scalar-vector products in the form,

$$b_{11}=\frac{1}{\omega}\left(\frac{\partial^2 r}{\partial\xi^2}\frac{\partial r}{\partial\xi}\frac{\partial r}{\partial\eta}\right),\quad b_{12}=\frac{1}{\omega}\left(\frac{\partial^2 r}{\partial\xi\partial\eta}\frac{\partial r}{\partial\xi}\frac{\partial r}{\partial\eta}\right),$$
$$b_{22}=\frac{1}{\omega}\left(\frac{\partial^2 r}{\partial\eta^2}\frac{\partial r}{\partial\xi}\frac{\partial r}{\partial\eta}\right).$$

where ω is determined by (6).

If we express r in cartesian coordinates x, y, and z, then for b_{11} it is possible to constitute the determinant

$$b_{11}=\frac{1}{\omega}\begin{vmatrix}\frac{\partial^2 x}{\partial\xi^2} & \frac{\partial^2 y}{\partial\xi^2} & \frac{\partial^2 z}{\partial\xi^2}\\ \frac{\partial x}{\partial\xi} & \frac{\partial y}{\partial\xi} & \frac{\partial z}{\partial\xi}\\ \frac{\partial x}{\partial\eta} & \frac{\partial y}{\partial\eta} & \frac{\partial z}{\partial\eta}\end{vmatrix}. \qquad (10.21)$$

Analogous determinants can be constituted for b_{12} and b_{22}.

We approach determination of the second quadratic form from another point of view. Taking, as before, the length of the arc of curves s as the parameter, we write relationship

$$\frac{dr}{ds}n=0.$$

Differentiating this product with respect to s, we obtain

$$\frac{d^2 r}{ds^2}n+\frac{dr}{ds}\frac{dn}{ds}=0.$$

Comparing this dependence with (13) and (19), we find

$$\mathrm{II}=-dr\cdot dn.$$

Thus, second quadratic form depends on how intensely the orientation of the unit vector to normal n changes in environment of the given point.

Comparing information pertaining to the first and second quadratic forms of surface, it is possible to say that form I characterizes length of arcs, angles between curves and areas of regions on the surface, while form II allows us to determine normal curvatures of the surface. It is possible to show that forms I and II, taken

together, completely determine the outline of the surface with accuracy up to its position in space.

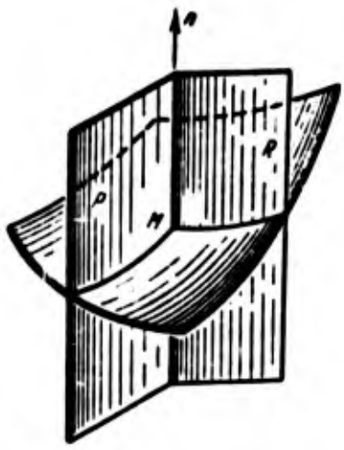

Fig. 10.13. Normal section of a surface.

Let us turn to the study of different normal sections of a surface, conducted at any point M of the surface (Fig. 10.13), i.e., sections, containing a normal to the surface n. If we fix the direction of the tangent, through which a certain section P passes, then curvature of the surface k_n in the corresponding direction; vectors ν and n constitute for a normal section angle 0 or π. We trace change of k_n during rotation of the section around the normal to surface during transition, e.g., from plane P to plane R. Such rotation is equivalent to change of ratio $d\eta : d\xi$ for fixed η and ξ. For a smooth surface this ratio changes continuously and at the same time periodically; consequently, curvature k_n should take for specific positions of the section maximum and minimum values. We shall find these values; for this we rewrite (19) in the form

$$b_{11}d\xi^2 + 2b_{12}d\xi d\eta + b_{22}d\eta^2 - k_n(a_{11}d\xi^2 + 2a_{12}d\xi d\eta + a_{22}d\eta^2) = 0. \qquad (10.22)$$

We assume in the beginning that differential $d\eta$ is constant; differentiating (22) with respect to $d\xi$ and equating the derivative to zero, we obtain

$$b_{11}d\xi + b_{12}d\eta - k_n(a_{11}d\xi + a_{12}d\eta) = 0.$$

Analogously, considering differential $d\xi$ constant, we find

$$b_{12}d\xi + b_{22}d\eta - k_n(a_{12}d\xi + a_{22}d\eta) = 0.$$

We exclude from this ratio $d\eta : d\xi$; then we arrive at a quadratic equation for k_n:

$$(a_{11}a_{22}-a_{12}^2)k_n^2-(a_{11}b_{22}+a_{22}b_{11}-2a_{12}b_{12})k_n+(b_{11}b_{22}-b_{12}^2)=0. \qquad (10.23)$$

From this we find two extreme values of k_n, which are called the principal curvatures of the surface in the given point; corresponding directions, determined by ratio $d\eta : d\xi$ by (22), carry name of principal directions. We consider that curvature $k_{n,\xi}$ corresponds to line $\eta = \text{const}$, and $k_{n,\eta}$ to line $\xi = \text{const}$; then from (22) we obtain, considering in turn $d\eta = 0$ and $d\xi = 0$,

$$b_{12}-a_{12}k_{n,\xi}=0, \quad b_{12}-a_{12}k_{n,\eta}=0.$$

Taking $k_{n,\xi} \neq k_{n,\eta}$, we find for principal directions $b_{12} = 0$, and $a_{12} = 0$. It follows from this that principal directions are mutually perpendicular. Subsequently we designate principal curvatures by k_1 and k_2.

We pass lines on the surface in such a manner that at every point tangents to them go along the principal directions. Such curves are called lines of curvature; they are convenient to select as coordinate curves.

We determine the product and half-sum of the principal curvatures, proceeding from equation (23):

$$\Gamma = k_1k_2 = \frac{b_{11}b_{22}-b_{12}^2}{a_{11}a_{22}-a_{12}^2}. \qquad (10.24)$$

$$K = \frac{k_1+k_2}{2} = -\frac{2a_{12}b_{12}-a_{11}b_{22}-a_{22}b_{11}}{2(a_{11}a_{22}-a_{12}^2)}. \qquad (10.25)$$

The first of these magnitudes is called the Gaussian curvature of the surface at the given point, and the second, the mean curvature.

As an example we calculate coefficients of first and second quadratic forms and Gaussian curvature for the surface, given by equation $z = f(x, y)$. We take x and y as curvilinear coordinates: $x = \xi$, $y = \eta$; then from (11) and (6)

$$a_{11}=1+\left(\frac{\partial z}{\partial x}\right)^2,\quad a_{12}=\frac{\partial z}{\partial x}\frac{\partial z}{\partial y},\quad a_{22}=1+\left(\frac{\partial z}{\partial y}\right)^2,$$
$$\omega^2=1+\left(\frac{\partial z}{\partial x}\right)^2+\left(\frac{\partial z}{\partial y}\right)^2 \qquad (10.26)$$

and, further, by formulas of type (21)

$$b_{11}=\frac{1}{\omega}\frac{\partial^2 z}{\partial x^2},\quad b_{12}=\frac{1}{\omega}\frac{\partial^2 z}{\partial x\,\partial y},\quad b_{22}=\frac{1}{\omega}\frac{\partial^2 z}{\partial y^2}. \qquad (10.27)$$

Let us note that for <u>shallow</u> shell when $\left(\frac{\partial z}{\partial x}\right)^2 \ll 1$, $\left(\frac{\partial z}{\partial y}\right)^2 \ll 1$ we can take $\omega \approx 1$; then coefficients b_{ij} will be expressed just as curvature and torsion of the deflection surface of a plate. Gaussian curvature, according to (24), will be

$$\Gamma=\frac{1}{\omega^4}\left[\frac{\partial^2 z}{\partial x^2}\frac{\partial^2 z}{\partial y^2}-\left(\frac{\partial^2 z}{\partial x\,\partial y}\right)^2\right]. \qquad (10.28)$$

It is interesting to note that for a shallow shell for $\omega \approx 1$ we obtain the expression which appeared in one of the fundamental equations of the theory of flexible plates. Comparing (7.40) and (28), we find

$$\frac{1}{2}L(w, w)=\Gamma. \qquad (10.29)$$

Thus, chain stresses, forming during large deflections of a plate, are directly connected with Gaussian curvature of the deflection surface.

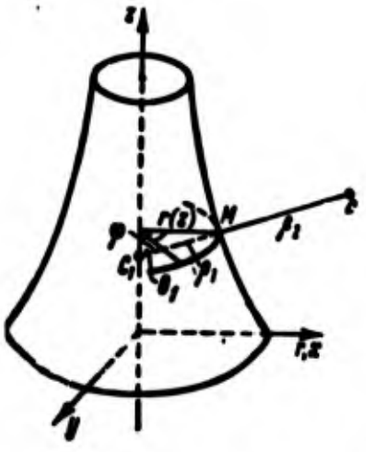

Fig. 10.14. Centers of curvature C_1 and C_2 in case of a surface of revolution.

Let us consider, further, a <u>surface of revolution</u> (Fig. 10.14), given by equations

$$\left.\begin{aligned} x&=r(z)\cos\varphi,\\ y&=r(z)\sin\varphi,\quad z=z.\end{aligned}\right\} \qquad (10.30)$$

By r is understood radius of the parallel circle in section z; by φ — the angle of rotation of the meridional plane. As parameters we take $\xi = \varphi$, $\eta = z$. By formulas (11), (6), and (21) we find

$$\left.\begin{aligned} a_{22}&=1+r'^2, \quad a_{12}=0, \quad a_{11}=r^2, \quad \omega=r\sqrt{1+r'^2}.\\ b_{22}&=\frac{r''}{\sqrt{1+r'^2}}, \quad b_{12}=0, \quad b_{11}=-\frac{r}{\sqrt{1+r'^2}}; \end{aligned}\right| \qquad (10.31)$$

by r' and r'' are designated derivatives of r with respect to z, characterizing outline of the meridian. Gaussian curvature is equal, by (24), to

$$\Gamma=-\frac{r''}{r(1+r'^2)^2}. \qquad (10.32)$$

If convexity of the meridian is turned toward axis z, as depicted in Fig. 10.14, then we have $r'' > 0$; such a shell has a negative Gaussian curvature. In Fig. 10.14 there are shown centers of curvature C_2 and C_1 of normal sections, one of which coincides with the plane of the meridian, and the second is perpendicular to this plane.

Let us note that curvature of the parallel circle 1/r should be according to Meusnier's theorem (14) equal to $(1/\rho_1 \sin\theta_1)$, where ρ_1 is principle radius MC_1 of curvature of the section. It follows from this that center of curvature C_1 is the intersection point of the normal to the surface with the axis of symmetry; as it is easy to see, the corresponding curvature is equal to

$$k_1=\frac{1}{\rho_1}=-\frac{1}{r\sqrt{1+r'^2}}.$$

The second principal curvature is equal to

$$k_2=\frac{1}{\rho_2}=\frac{r''}{(1+r'^2)^{3/2}}.$$

The concept of Gaussian curvature is fundamental in the theory of surfaces. Transforming expression (24) for Γ, it is possible to show that Gaussian curvature depends only on coefficients of the first quadratic form and their derivatives. Together with other magnitudes, depending on form factors I, Gaussian curvature pertains to

the so-called inner geometry of the surface.

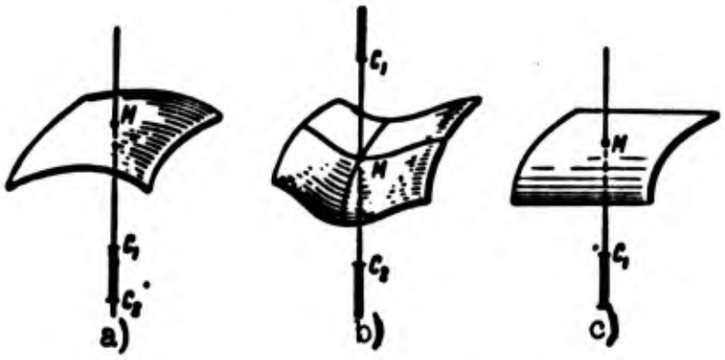

Fig. 10.15. Location of centers of curvature C_1 and C_2 for (a) elliptic, (b) hyperbolic and (c) parabolic points of a surface.

By the sign of Gaussian curvature it is possible to judge the form of the surface in the neighborhood of a given point. If $\Gamma > 0$, then, as one may see from (24), curvatures k_1 and k_2 have identical sign. This means that centers of curvature C_1 and C_2 in principal directions are on the same side of the surface; as shown in Fig. 10.15a, centers of curvature of all other normal sections will lie on segment C_1C_2. Point M of the surface, for which centers of curvature are disposed thus, is called elliptic. Conversely, when $\Gamma < 0$ centers C_1 and C_2 lie, as we saw, on opposite sides of the surface (Fig. 10.15b); centers of curvature of remaining normal sections are on outer regions of segment C_1C_2; corresponding point of the surface carries name of hyperbolic. Finally, in case $\Gamma = 0$ the point is called parabolic. Here one of the principal curvatures turns into zero; centers of curvature lie on one side of C_1, and C_2 is at infinity. This pertains, for instance, to point M in Fig. 10.15c, belonging to a cylindrical surface.

In Fig. 10.16 is depicted a surface of revolution; at points of the upper part we have $\Gamma < 0$, as in Fig. 10.14; at points of the lower

part $\Gamma > 0$: these parts are divided by a parabolic line, for whose points $\Gamma = 0$.

Examples of surfaces, at all points of which Gaussian curvature is positive, can be a sphere or an ellipsoid. Negative Gaussian curvature, and thereby constant for all points, belongs to so-called pseudosphere: here $k_1 = -k_2 =$ = const. Cylindrical and conical surfaces have zero Gaussian curvature.

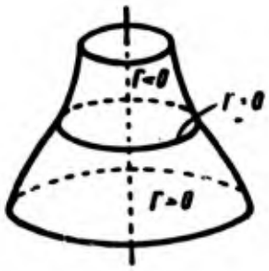

Fig. 10.16. Surface of revolution with sections, having various Gaussian curvature.

Gaussian curvature plays a special role in the theory of bending of surfaces. By bending is understood very transformation of a surface in which lengths of any curves on the surface remain constant; at the same time angles between intersecting curves are also preserved. Such transformation we call also isometric. Surface during bending must be like an absolutely flexible inextensible shell, which can change its form without folds and breaks.*

During isometric transformation the first quadratic form, equal to square of the length of a linear member, should remain constant, and then Gaussian curvature will be preserved. Consequently, isometric surfaces have at corresponding points identical Gaussian curvature.** It is interesting to note that during bending of the surface all

---

*Simple displacement of the surface in space here is excluded.

**This remarkable theorem was proven by Gauss in 1816. Talking of isometric transformation, Guss presented a surface namely as a "flexible, but inextensible body, one of whose measurements is assumed to be disappearing" ("General study of curved surfaces" translation 1887, p. 34).

three form factors II change, but in such a way that the discriminant of this form, equal to $b_{11}b_{22}-b_{12}^2$ and contained in expression (24), remains constant. Example of isometric surfaces are surfaces developable on a plane; all of them have zero Gaussian curvature.

We till now did not place conditions so that bending of a surface was a continuous process. Therefore, it is possible to say, that transition of a convex segment with secured edge (Fig. 10.17) from position 1 to position 2, the specular reflection of the first, is bending,* but it occurs in the large. If however we talk about infinitesimal deformation, then it can be realized only for limited class of surfaces. Such bending turns out to be impossible for any convex continuous closed surface (for instance, a complete sphere). In other words, such a convex surface is rigid in the small.** On the other hand for surfaces of zero and negative Gaussian curvature infinitesimal deformation, in general, is possible. This can be illustrated by the simple example of the bar system, shown in Fig. 10.18. If bars are inextensible, then infinitesimal displacements of the center hinge in the first case (Fig. a) are excluded, and in the second (Fig. b), when bars are stretched in one line, can be realized.

All these conclusions, contained in theory of surfaces, as we shall see below, have direct relation to problems of stability of shells in the small and in the large. If shell is infinitely thin,

---

*Compare deformation of arch-strip in Fig. 10.3.

**Survey of research in qualitative problems of the theory of deformation of surfaces was published by N. V. Efimov (Successes of mathematical sciences, 3, No. 2 (1948), 47–158); a series of relevant general theorems was obtained by A. V. Pogorelov (see for instance, his work "Certain results in geometry as a whole," Khar'kov 1961).

then its deformation could have been characterized completely by the

Fig. 10.17. Clicking of a convex segment.

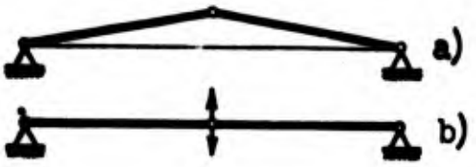

Fig. 10.18. Bar systems, a) "invariable" and b) "variable" in the small.

theory of surfaces. However in real shells any change of form, even if it is accompanied by isometric transformation of the middle surface, causes the appearance of flexural strains, unevenly distributed in the thickness. Therefore, we will use the above-mentioned dependences in studying deformation of the middle surface, but we should at the same time consider deformation of natural bending of the shell. In other words, we must, as it were, unite theory of absolutely flexible shells with theory of rigid plates.

§ 120. Three-Dimensional Linear Problem in Curvilinear Coordinates

During study of small deflections of a shell, causing deformation of mixed type, we start from general linear relationships of a three-dimensional problem of theory of elasticity. We introduce three curvilinear coordinates ξ, η, and ζ which will determine the position of an arbitrary point of space just as two parameters ξ and η characterized position of any point of a surface.

Lengths of arcs, counted off along coordinate lines, are equal to

$$ds_1 = H_1 d\xi. \quad ds_2 = H_2 d\eta. \quad ds_3 = H_3 d\zeta. \tag{10.33}$$

Magnitudes H_1, H_2, and H_3, each of which is a certain function of ξ, η, and ζ are called Lamé coefficients; they correspond to the

to the coefficients of the first quadratic form a_{11} and a_{22} in theory of surfaces. We assume from the very beginning the system of coordinates is orthogonal; then square of a linear member, as the first quadratic form of three-dimensional space, will be*

$$ds^2 = H_1^2 d\xi^2 + \\ + H_2^2 d\eta^2 + H_3^2 d\zeta^2. \qquad (10.34)$$

Henceforth coordinates ξ and η we shall attach to middle surface of the shell, and coordinate ζ let us agree to count off along the normal, but here will make calculations in common form.

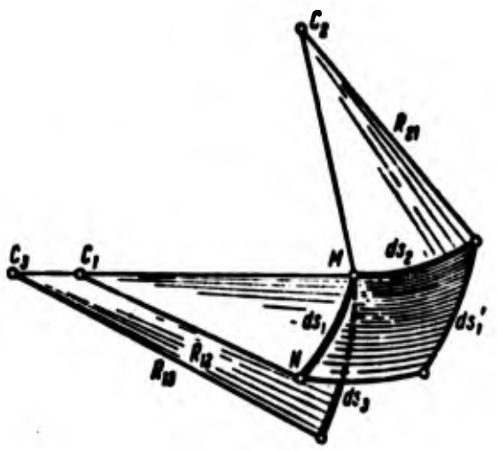

Fig. 10.19. Arcs of curvilinear coordinates in case of three-dimensional problem.

In Fig. 10.19 is depicted a member of a surface, containing arcs ds_1 and ds_2. We designate by C_1 and C_2 centers of curvature of these arcs in a plane, normal to arc ds_3, and by R_{12} and R_{21}, the corresponding radii of curvature. With change of coordinate η by $d\eta$ the length of arc ds_1 obtains an increment: the new length will be

$$ds_1' = \left(H_1 + \frac{\partial H_1}{\partial \eta} d\eta\right) d\xi.$$

Obviously, we should have

$$\frac{ds_1}{R_{12}} = \frac{ds_1'}{R_{12} + ds_2};$$

from this we find curvature of arc ds_1:

$$\frac{1}{R_{12}} = \frac{ds_1' - ds_1}{ds_1 ds_2}.$$

---

*Lamé parameters must satisfy six conditions of continuity of three-dimensional space, see [10.3], p. 193.

or

$$\frac{1}{R_{12}} = \frac{1}{H_1 H_2} \frac{\partial H_1}{\partial \eta}. \qquad (10.35)$$

Analogously curvature of arc ds_2 will be

$$\frac{1}{R_{21}} = \frac{1}{H_2 H_1} \frac{\partial H_2}{\partial \xi}. \qquad (10.36)$$

If we now consider a member of the surface formed by arcs ds_1 and ds_2, then in this way we find curvature of arc ds_1 in a plane, normal to ds_2:

$$\frac{1}{R_{13}} = \frac{1}{H_1 H_3} \frac{\partial H_1}{\partial \zeta}. \qquad (10.37)$$

Proceeding similarly, one can determine curvature of arc ds_2 in a plane, normal to ds_1, and curvature of arc ds_3 in planes, normal to ds_1 and ds_2.

Let us assume that during deformation of an elastic body point M belonging to it receives displacement along coordinate lines ξ, η, and ζ, equal accordingly to u, v, and w. We determine deformation of elongation which arcs ds_1, ds_2, and ds_3 receive, and also shifts in planes, formed by different arcs.

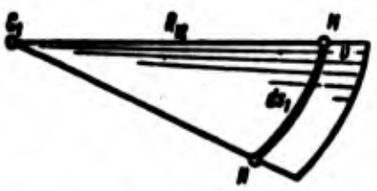

Fig. 10.20. Determination of deformation caused by displacements v.

Deformation of elongation of arc ds_1 is equal to

$$\varepsilon_\xi = \frac{\partial u}{H_1 \partial \xi} + \frac{v}{R_{12}} + \frac{w}{R_{13}}. \qquad (10.38)$$

First component corresponds to increment u during transition from point M to adjacent point N (Fig. 10.20); if u depends only on s_1, then we would have $\varepsilon_\xi = \frac{\partial u}{\partial s_1}$. If all points of arc $ds_1 = R_{12}\, d\theta_{12}$ received shift v (Fig. 10.20), then

radius of curvature R_{12} would be increased by v. Here arc ds_1 obtains length $(R_{12} + v)\,d\theta_{12}$, and unit deformation will be

$$\frac{(R_{12}+v)\,d\theta_{12}-R_{12}\,d\theta_{12}}{R_{12}\,d\theta_{12}}=\frac{v}{R_{12}}.$$

This gives the second component in expression (38). Analogous reasoning pertains to displacement w which gives the third component. We substitute in (38) expressions (35) and (37) for $1/R_{12}$ and $1/R_{13}$, then we find

$$\varepsilon_\xi=\frac{1}{H_1}\frac{\partial u}{\partial \xi}+\frac{1}{H_1H_2}\frac{\partial H_1}{\partial \eta}v+\frac{1}{H_1H_3}\frac{\partial H_1}{\partial \zeta}w. \qquad (10.39)$$

Shear deformation in a plane, tangent to arcs ds_1 and ds_2, equal to change of the right angle between these arcs, will be

$$\gamma_{\xi\eta}=\frac{1}{H_2}\frac{\partial u}{\partial \eta}+\frac{1}{H_1}\frac{\partial v}{\partial \xi}-\frac{u}{R_{12}}-\frac{v}{R_{21}}; \qquad (10.40)$$

plus sign here, as usual, corresponds to decrease of angle between the arcs. First two components correspond to rotation of arcs ds_1 and ds_2, caused by displacement of points L and N with respect to point M (Fig. 10.21), and have the same form as for a member of a plate (see p. 336). We assume, further, that all points of arc ds_2 receive displacement v (Fig. 10.22); then angle between ds_1 and ds_2 should increase by v/R_{21}; but if points of arc ds_1 are displaced by u, then angle will be increased by u/R_{12}. This gives the third and fourth components in (40). We substitute here expressions (35) and (36); then we have

$$\gamma_{\xi\eta}=\frac{1}{H_2}\frac{\partial u}{\partial \eta}-\frac{1}{H_1H_2}\frac{\partial H_2}{\partial \xi}v+\frac{1}{H_1}\frac{\partial v}{\partial \xi}-\frac{1}{H_1H_2}\frac{\partial H_1}{\partial \eta}u. \qquad (10.41)$$

or

$$\gamma_{\xi\eta}=\frac{H_1}{H_2}\frac{\partial}{\partial \eta}\left(\frac{u}{H_1}\right)+\frac{H_2}{H_1}\frac{\partial}{\partial \xi}\left(\frac{v}{H_2}\right). \qquad (10.41a)$$

Fig. 10.21. Determination of deformations caused by rotations of members.

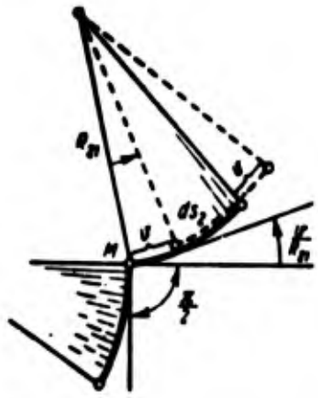

Fig. 10.22. Determination of additional deformations from rotations.

Analogous calculations allow us to obtain the expression for other components of deformation. Finally deformations of elongation are these:

$$\left.\begin{aligned} \varepsilon_1 &= \frac{1}{H_1}\frac{\partial u}{\partial \xi} + \frac{1}{H_1 H_2}\frac{\partial H_1}{\partial \eta} v + \frac{1}{H_1 H_2}\frac{\partial H_1}{\partial \zeta} w, \\ \varepsilon_2 &= \frac{1}{H_2}\frac{\partial v}{\partial \eta} + \frac{1}{H_2 H_3}\frac{\partial H_2}{\partial \zeta} w + \frac{1}{H_1 H_2}\frac{\partial H_2}{\partial \xi} u, \\ \varepsilon_3 &= \frac{1}{H_3}\frac{\partial w}{\partial \zeta} + \frac{1}{H_3 H_1}\frac{\partial H_3}{\partial \xi} u + \frac{1}{H_2 H_3}\frac{\partial H_3}{\partial \eta} v. \end{aligned}\right\} \qquad (10.42)$$

and shear deformations:

$$\left.\begin{aligned} \gamma_{12} &= \frac{H_1}{H_2}\frac{\partial}{\partial \eta}\left(\frac{u}{H_1}\right) + \frac{H_2}{H_1}\frac{\partial}{\partial \xi}\left(\frac{v}{H_2}\right), \\ \gamma_{23} &= \frac{H_2}{H_3}\frac{\partial}{\partial \zeta}\left(\frac{v}{H_2}\right) + \frac{H_3}{H_2}\frac{\partial}{\partial \eta}\left(\frac{w}{H_3}\right), \\ \gamma_{31} &= \frac{H_3}{H_1}\frac{\partial}{\partial \xi}\left(\frac{w}{H_3}\right) + \frac{H_1}{H_3}\frac{\partial}{\partial \zeta}\left(\frac{u}{H_1}\right). \end{aligned}\right\} \qquad (10.43)$$

We use these expressions for construction of theory of thin shells. Let us remember that all derived dependences pertain only to small displacements; therefore, they can be applied only if deflections of shell are small as compared to its thickness.

§ 121. Shell of Small Deflection. Dependence Between Deformations and Displacements.

At the basis of the theory of flexure of thin shells lies the hypothesis of straight normals, according to which points belonging

to a normal to the middle surface up to deformation, remain and after deformation lie on a straight line normal to the middle surface. Strictly speaking, in process of deformation of a shell rectilinearity of normals is somewhat disturbed; this is connected with shifts in sections normal to the middle surface. Therefore, hypothesis of straight normals, essentially, is reduced to the assumption that shifts in normal sections are small as compared to angles of rotation of normals and that, therefore, shifts can, as a rule, be taken equal to zero.*

We relate middle surface to lines of curvature and plot along these lines coordinates ξ and η (Fig. 10.23). Such a net of lines is orthogonal; coefficients of the first quadratic form of the middle surface we designate as follows: $a_{11} = A_1^2$, $a_{22} = A_2^2$, where $a_{12} = 0$. Magnitudes A_1 and A_2 are equivalent to Lame's coefficients: $A_1 = H_1$, $A_2 = H_2$. Line ζ we combine with the normal to the middle surface and we take $H_3 = 1$. We introduce, further, designations R_1 and R_2 for radii of curvature of normal sections of middle surface, correspondingly, along lines ξ and η.

Let us consider a layer of the shell a distance of $\zeta = z$ from the middle surface; here $(-\frac{h}{2}) \leqslant z \leqslant \frac{h}{2}$, where h is thickness of the shell. Positive direction z and w we arbitrarily lay out toward the center of curvature.** Since length of arcs are proportional to distances to center of curvature, then coefficients A_1^z and A_2^z for given

---

*See V. V. Novozhilov, Theory of thin shells [10.11].

**This pertains to elliptic and parabolic points of the middle surface.

layer will be

$$\left.\begin{aligned} A_1^z &= A_1\left(1-\frac{z}{R_1}\right).\\ A_2^z &= A_2\left(1-\frac{z}{R_2}\right). \end{aligned}\right\} \qquad (10.44)$$

Derivatives of them with respect to z are equal to

$$\left.\begin{aligned} \frac{\partial A_1^z}{\partial z} &= -\frac{A_1}{R_1}.\\ \frac{\partial A_2^z}{\partial z} &= -\frac{A_2}{R_2}. \end{aligned}\right\} \qquad (10.45)$$

After we have calculated derivatives, in (44) we take $z \ll R_1$, $z \ll R_2$ and, consequently, $A_1^z \approx A_1$, $A_2^z \approx A_2$; derivatives (45) will be the same for any point of the normal.

Fig. 10.23. Member of a shell formed by lines of curvature of the middle surface.

According to hypotheses of straight normals we must take $\gamma_{\eta\zeta} = \gamma_{\zeta\xi} = 0$. Developing expressions (43) for $\gamma_{\eta\zeta}$ and $\gamma_{\zeta\xi}$ by type (41) and considering $A_3 = 1$, we obtain

$$\left.\begin{aligned} \frac{\partial u^z}{\partial z}-\frac{u^z}{A_1}\frac{\partial A_1}{\partial z}+\frac{1}{A_1}\frac{\partial w^z}{\partial \xi} &= 0.\\ \frac{\partial v^z}{\partial z}-\frac{v^z}{A_2}\frac{\partial A_2}{\partial z}+\frac{1}{A_2}\frac{\partial w^z}{\partial \eta} &= 0. \end{aligned}\right\} \qquad (10.46)$$

where u^z, v^z, and w^z are displacements of an arbitrary point of the normal. For points of a straight member, normal to the middle surface, derivatives $\frac{\partial u^z}{\partial z}$ and $\frac{\partial v^z}{\partial z}$ should keep constant values, equal to

$$\frac{\partial u^z}{\partial z}=\frac{\partial u}{\partial z}=\frac{u^z-u}{z}, \quad \frac{\partial v^z}{\partial z}=\frac{\partial v}{\partial z}=\frac{v^z-v}{z}. \qquad (10.47)$$

But, on the other hand, taking $z = 0$ in (46) and using (45), we obtain

$$\frac{\partial u}{\partial z}=-\frac{u}{R_1}-\frac{1}{A_1}\frac{\partial w}{\partial \xi}, \quad \frac{\partial v}{\partial z}=-\frac{v}{R_2}-\frac{1}{A_2}\frac{\partial w}{\partial \eta}. \tag{10.48}$$

Comparing (47) and (48), we find

$$u^z=u-z\left(\frac{u}{R_1}+\frac{1}{A_1}\frac{\partial w}{\partial \xi}\right), \quad v^z=v-z\left(\frac{v}{R_2}+\frac{1}{A_2}\frac{\partial w}{\partial \eta}\right). \tag{10.49}$$

We designate deformations of elongation along lines of curvature by ε_1 and ε_2 and deformation of shearing by γ; if we take in general expressions (42) and (43) $H_1 = A_1$, $H_2 = A_2$, $H_3 = 1$, $w^z = w$, then for any z we have

$$\left.\begin{aligned}
\varepsilon_1^z&=\frac{1}{A_1}\frac{\partial u^z}{\partial \xi}+\frac{1}{A_1A_2}\frac{\partial A_1}{\partial \eta}v^z+\frac{1}{A_1}\frac{\partial A_1}{\partial z}w,\\
\varepsilon_2^z&=\frac{1}{A_2}\frac{\partial v^z}{\partial \eta}+\frac{1}{A_1A_2}\frac{\partial A_2}{\partial \xi}u^z+\frac{1}{A_2}\frac{\partial A_2}{\partial z}w,\\
\gamma^z&=\frac{A_1}{A_2}\frac{\partial}{\partial \eta}\left(\frac{u^z}{A_1}\right)+\frac{A_2}{A_1}\frac{\partial}{\partial \xi}\left(\frac{v^z}{A_2}\right).
\end{aligned}\right| \tag{10.50}$$

Using (49), it is possible now to present deformations in the form*

$$\varepsilon_1^z=\varepsilon_1+z\varkappa_1, \quad \varepsilon_2^z=\varepsilon_2+z\varkappa_2, \quad \gamma^z=\gamma+2z\chi. \tag{10.51}$$

By ε_1, ε_2, and γ here are understood deformations in the middle surface:

$$\left.\begin{aligned}
\varepsilon_1&=\frac{1}{A_1}\frac{\partial u}{\partial \xi}+\frac{1}{A_1A_2}\frac{\partial A_1}{\partial \eta}v-\frac{w}{R_1},\\
\varepsilon_2&=\frac{1}{A_2}\frac{\partial v}{\partial \eta}+\frac{1}{A_1A_2}\frac{\partial A_2}{\partial \xi}u-\frac{w}{R_2},\\
\gamma&=\frac{A_1}{A_2}\frac{\partial}{\partial \eta}\left(\frac{u}{A_1}\right)+\frac{A_2}{A_1}\frac{\partial}{\partial \xi}\left(\frac{v}{A_2}\right).
\end{aligned}\right| \tag{10.52}$$

by $\varkappa_1$ and $\varkappa_2$ we mean changes of curvatures and by χ, "torsion" of the middle surface;

---

*Expressions of type (52) and (53) were obtained in different ways by many authors: detailed analysis of them is given in books of V. Z. Vlasov [10.3], A. L. Gol'denveyzer [10.6], and V. V. Novozhilov [10.11]. Derivation given here belongs to E. Reissner [10.21]. The first five expressions (52) and (53) coincide for all these authors; the sixth expression – for torsion – has several variants, slightly differing from each other.

$$\left.\begin{aligned}
\varkappa_1 &= -\frac{1}{A_1}\frac{\partial}{\partial\xi}\left(\frac{u}{R_1}+\frac{1}{A_1}\frac{\partial w}{\partial\xi}\right)-\frac{1}{A_1A_2}\left(\frac{v}{R_2}+\frac{1}{A_2}\frac{\partial w}{\partial\eta}\right)\frac{\partial A_1}{\partial\eta},\\
\varkappa_2 &= -\frac{1}{A_2}\frac{\partial}{\partial\eta}\left(\frac{v}{R_2}+\frac{1}{A_2}\frac{\partial w}{\partial\eta}\right)-\frac{1}{A_1A_2}\left(\frac{u}{R_1}+\frac{1}{A_1}\frac{\partial w}{\partial\xi}\right)\frac{\partial A_2}{\partial\xi},\\
\chi &= -\frac{1}{2}\left[\frac{A_2}{A_1}\frac{\partial}{\partial\xi}\left(\frac{v}{A_2R_2}+\frac{1}{A_2^2}\frac{\partial w}{\partial\eta}\right)+\frac{A_1}{A_2}\frac{\partial}{\partial\eta}\left(\frac{u}{A_1R_1}+\frac{1}{A_1^2}\frac{\partial w}{\partial\xi}\right)\right].
\end{aligned}\right\} \qquad (10.53)$$

Taking in (53) $A_1 = A_2 = 1$ and $R_1 = R_2 = \infty$, we arrive at the former expressions for curvature and torsion of a plate:

$$\varkappa_1 = -\frac{\partial^2 w}{\partial\xi^2},\quad \varkappa_2 = -\frac{\partial^2 w}{\partial\eta^2},\quad \chi = -\frac{\partial^2 w}{\partial\xi\partial\eta}.$$

Let us note that six magnitudes – deformations in middle surface and changes of curvatures – are expressed in three functions of displacements u, v, and w. Obviously, these six magnitudes are not independent; for them it is possible to write three compatible equations. We give one of these equations:*

$$\frac{1}{A_1A_2}\left\{\frac{\partial}{\partial\xi}\frac{1}{A_1}\left[A_2\frac{\partial\varepsilon_2}{\partial\xi}+\frac{\partial A_2}{\partial\xi}(\varepsilon_2-\varepsilon_1)-\frac{A_1}{2}\frac{\partial\gamma}{\partial\eta}-\frac{\partial A_1}{\partial\eta}\gamma\right]+\right.$$
$$\left.+\frac{\partial}{\partial\eta}\frac{1}{A_2}\left[A_1\frac{\partial\varepsilon_1}{\partial\eta}+\frac{\partial A_1}{\partial\eta}(\varepsilon_1-\varepsilon_2)-\frac{A_2}{2}\frac{\partial\gamma}{\partial\xi}-\frac{\partial A_2}{\partial\xi}\gamma\right]\right\}-\frac{\varkappa_1}{R_2}-\frac{\varkappa_2}{R_1}=0. \qquad (10.54)$$

This equation can be checked by direct substitution of expressions for deformations ε_1, ε_2, and γ and parameters of change of curvature $\varkappa_1$, $\varkappa_2$; here it is necessary to use the following relationships, known from theory of surfaces** (formulas of Petersona-Codazzi and Gauss):

$$\frac{\partial}{\partial\xi}\left(\frac{A_2}{R_2}\right)=\frac{1}{R_1}\frac{\partial A_2}{\partial\xi},\quad \frac{\partial}{\partial\eta}\left(\frac{A_1}{R_1}\right)=\frac{1}{R_2}\frac{\partial A_1}{\partial\eta}. \qquad (10.55)$$

$$\frac{1}{R_1R_2}=-\frac{1}{A_1A_2}\left[\frac{\partial}{\partial\xi}\left(\frac{1}{A_1}\frac{\partial A_2}{\partial\xi}\right)+\frac{\partial}{\partial\eta}\left(\frac{1}{A_2}\frac{\partial A_1}{\partial\eta}\right)\right]. \qquad (10.56)$$

Dependences (55) and (56), written here for principal directions, express, essentially, the connection between coefficients of first

---

*See book of A. L. Gol'denveyzer [10.6], p. 58. Two other equations are given below, on p 541 .

**See P. K. Rashevskiy, Course of differential geometry, 1956, p. 350 .

and second quadratic form of middle surface. Formula (56) indicates that Gaussian curvature, equal to $1/R_1R_2$, only depends on the coefficients of the first quadratic form and their derivatives; we already spoke of this in § 119.

In the particular case where A_1 and A_2 are constant and can be taken as equal $A_1 = A_2 = 1$, the equation of compatibility (54) changes into the following

$$\frac{\partial^2 \varepsilon_2}{\partial \xi^2} + \frac{\partial^2 \varepsilon_1}{\partial \eta^2} - \frac{\partial^2 \gamma}{\partial \xi \partial \eta} = -\frac{1}{R_2}\frac{\partial^2 w}{\partial \xi^2} - \frac{1}{R_1}\frac{\partial^2 w}{\partial \eta^2}. \qquad (10.54a)$$

As we shall see later, in many problems pertaining to stability of shells it is possible to simplify expression (53) for parameters of change of curvature and torsion, considering shifts "en masse" of the material, u and v small as compared to deflection w; then we obtain

$$\left.\begin{aligned} \varkappa_1 &= -\frac{1}{A_1}\frac{\partial}{\partial \xi}\left(\frac{1}{A_1}\frac{\partial w}{\partial \xi}\right) - \frac{1}{A_1 A_2^2}\frac{\partial w}{\partial \eta}\frac{\partial A_1}{\partial \eta}, \\ \varkappa_2 &= -\frac{1}{A_2}\frac{\partial}{\partial \eta}\left(\frac{1}{A_2}\frac{\partial w}{\partial \eta}\right) - \frac{1}{A_1^2 A_2}\frac{\partial w}{\partial \xi}\frac{\partial A_2}{\partial \xi}, \\ \chi &= -\frac{1}{2}\left[\frac{A_2}{A_1}\frac{\partial}{\partial \xi}\left(\frac{1}{A_2^2}\frac{\partial w}{\partial \eta}\right) + \frac{A_1}{A_2}\frac{\partial}{\partial \eta}\left(\frac{1}{A_1^2}\frac{\partial w}{\partial \xi}\right)\right]. \end{aligned}\right\} \qquad (10.57)$$

Let us turn to study of the stress of a shell.

§ 122. Forces and Moments. Equations of Equilibrium of a Member of a Shell

We pass normal sections of a shell along lines of curvature. We designate by σ_1, σ_2, and τ stresses in the middle surface in these sections, and by σ_1^z, σ_2^z, and τ^z stresses in a certain layer at distance z from the middle surface.

Normal and tangential forces per unit length of arc of line η, we designate by N_1 and T_{12} (Fig. 10.24); they will be equal to

$$N_1=\frac{1}{A_2 d\eta}\int_{-h/2}^{h/2}\sigma_1^z A_2^z d\eta dz,\quad T_{12}=\frac{1}{A_2 d\eta}\int_{-h/2}^{h/2}\tau^z A_2^z d\eta dz.$$

These expressions are composed taking into account the fact that length of arc $A_2 d\eta$ in middle layer is not equal to length of arc $(A_2^z d\eta)$ of an arbitrary layer. Substituting here value A_2^z from (44), we obtain

$$N_1=\int_{-h/2}^{h/2}\sigma_1^z\left(1-\frac{z}{R_2}\right)dz,\quad T_{12}=\int_{-h/2}^{h/2}\tau^z\left(1-\frac{z}{R_2}\right)dz. \qquad (10.58)$$

By analogy we find forces in section along line ξ:

$$N_2=\int_{-h/2}^{h/2}\sigma_2^z\left(1-\frac{z}{R_1}\right)dz,\quad T_{21}=\int_{-h/2}^{h/2}\tau^z\left(1-\frac{z}{R_1}\right)dz. \qquad (10.59)$$

In the common case where $R_1 \neq R_2$, tangential forces T_{12} and T_{21} turn out to be different. If we consider, however, that for thin shells $z \ll R_1$ and $z \ll R_2$, it is possible in expressions (58) and (59) to take $1 - z/R_2 \approx 1$, $1 - z/R_1 \approx 1$; then we obtain $T_{12} = T_{21}$ as in the case of a plate. We write, further, expressions for bending and torsional moments (Fig. 10.25):

$$M_1=\int_{-h/2}^{h/2}\sigma_1^z\left(1-\frac{z}{R_2}\right)z\,dz,\quad H_{12}=\int_{-h/2}^{h/2}\tau^z\left(1-\frac{z}{R_2}\right)z\,dz. \qquad (10.60)$$

$$M_2=\int_{-h/2}^{h/2}\sigma_2^z\left(1-\frac{z}{R_1}\right)z\,dz,\quad H_{21}=\int_{-h/2}^{h/2}\tau^z\left(1-\frac{z}{R_1}\right)z\,dz. \qquad (10.61)$$

And here it is possible approximately to take $H_{12} = H_{21}$. Let transverse forces in sections along η and ξ be Q_1 and Q_2; external load per unit along lines ξ, η, and z we designate by q_1, q_2, and q_z.

We compose equation of equilibrium of a member of the shell,

cut by sections along lines of curvature.* Lengths of arcs in middle surface, laid out along ξ and η are equal to $A_1 d\xi$ and $A_2 d\eta$ and lengths of adjacent arcs are $(A_1 + \frac{\partial A_1}{\partial \eta} d\eta) d\xi$ and $(A_2 + \frac{\partial A_2}{\partial \xi} d\xi) d\eta$. Equation of equilibrium in projections on tangent to line ξ has the form

$$\begin{aligned} &-N_1 A_2 d\eta + \left(N_1 + \frac{\partial N_1}{\partial \xi} d\xi\right)\left(A_2 + \frac{\partial A_2}{\partial \xi} d\xi\right) d\eta - \\ &- T_{21} A_1 d\xi + \left(T_{21} + \frac{\partial T_{21}}{\partial \eta} d\eta\right)\left(A_1 + \frac{\partial A_1}{\partial \eta} d\eta\right) d\xi - \\ &- N_2 \frac{\partial A_2}{\partial \xi} d\xi d\eta + T_{12} \frac{\partial A_1}{\partial \eta} d\xi d\eta - \\ &- Q_1 \frac{A_1 A_2}{R_1} d\xi d\eta + q_z A_1 A_2 d\xi d\eta = 0. \end{aligned} \tag{10.62}$$

Here members, depending on N_2 and T_{12} appear as a result of change of lengths of arcs with variable A_1 and A_2. From Fig. 10.26a

Fig. 10.24. Positive directions of forces in middle surface.

Fig. 10.25. Positive directions of moments, transverse forces and lateral load.

one may see that small "angle of rotation" β of arc $(A_1 + \frac{\partial A_1}{\partial \eta}) d\xi$ is equal to difference of segments $(A_2 + \frac{\partial A_2}{\partial \xi} d\xi) d\eta$ and $A_2 d\eta$, divided by arc length:

---

*Account given here is constructed by Wang Chi-The (see [21.21], p. 366).

$$\beta = \frac{\frac{\partial A_2}{\partial \xi} d\xi\, d\eta}{\left(A_1 + \frac{\partial A_1}{\partial \eta} d\eta\right) d\xi}.$$

Angle α is equal (Fig. 10.26b) to

$$\alpha = \frac{\frac{\partial A_1}{\partial \eta} d\eta\, d\xi}{\left(A_2 + \frac{\partial A_2}{\partial \xi} d\xi\right) d\eta}.$$

Multiplying force $\left(N_2 + \frac{\partial N_2}{\partial \eta} d\eta\right)\left(A_1 + \frac{\partial A_1}{\partial \eta} d\eta\right) d\xi$ by angle β and correspondingly force $\left(T_{12} + \frac{\partial T_{12}}{\partial \xi} d\xi\right)\left(A_2 + \frac{\partial A_2}{\partial \xi} d\xi\right) d\eta$ by angle α and rejecting small quantities of higher order, we arrive at the expressions appearing in (62). Then, we note that the section, in which transverse force $\left(Q_1 + \frac{\partial Q_1}{\partial \xi} d\xi\right)\left(A_2 + \frac{\partial A_2}{\partial \xi} d\xi\right) d\eta$ acts, is inclined to the section with force $Q_1 A_2 d\eta$ at an angle $d\gamma$, equal to $d\gamma = A_1 d\xi / R_1$ (Fig. 10.27); from this we find projection of the first of these forces, written in (62). Projection of external load on an element is equal to $q_x A_1 A_2 d\xi d\eta$; the last member of the equation corresponds to this magnitude.

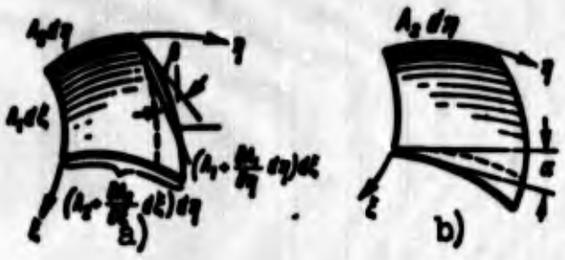

Fig. 10.26. Derivation of equations of equilibrium of a member of a shell. System of coordinates here differs from that taken in Fig. 10.24.

Disregarding in (62) small quantities of higher order and presenting members depending on N_1 and T_{12} in the form

$$\left(\frac{\partial N_1}{\partial \xi} A_2 + N_1 \frac{\partial A_2}{\partial \xi}\right) d\xi\, d\eta = \frac{\partial (A_2 N_1)}{\partial \xi} d\xi\, d\eta,$$

$$\left(\frac{\partial T_{21}}{\partial \eta} A_1 + T_{21} \frac{\partial A_1}{\partial \eta}\right) d\xi\, d\eta = \frac{\partial (A_1 T_{21})}{\partial \eta} d\xi\, d\eta,$$

we arrive at the following equation:

$$\frac{\partial(A_2N_1)}{\partial\xi}+\frac{\partial(A_1T_{21})}{\partial\eta}-N_2\frac{\partial A_2}{\partial\xi}+$$
$$+T_{12}\frac{\partial A_1}{\partial\eta}-Q_1\frac{A_1A_2}{R_1}+q_1A_1A_2=0. \qquad (10.63)$$

In this way we obtain equation of equilibrium in projections on the tangent to line η:

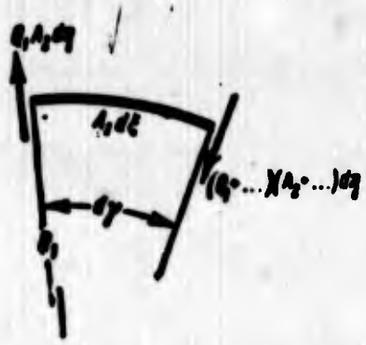

Fig. 10.27. Determination of resultant transverse forces.

$$\frac{\partial(A_1N_2)}{\partial\eta}+\frac{\partial(A_2T_{12})}{\partial\xi}-N_1\frac{\partial A_1}{\partial\eta}+$$
$$+T_{21}\frac{\partial A_2}{\partial\xi}-Q_2\frac{A_1A_2}{R_2}+q_2A_1A_2=0. \qquad (10.64)$$

Projecting then, all forces on the direction of the normal, we find

$$\frac{\partial(A_2Q_1)}{\partial\xi}+\frac{\partial(A_1Q_2)}{\partial\eta}+N_1\frac{A_1A_2}{R_1}+$$
$$+N_2\frac{A_1A_2}{R_2}+q_zA_1A_2=0. \qquad (10.65)$$

Here, members depending on N_1 and N_2 appear thanks to the fact that corresponding forces act at angles $A_1d\xi/R_1$ and $A_2d\eta/R_2$ with respect to one another.

Projecting moment-vectors shown in Fig. 10.25 and finding moment of transverse force, we obtain equation of moments for tangent to line η:

$$M_1A_2d\eta-\left(M_1+\frac{\partial M_1}{\partial\xi}d\xi\right)\left(A_2+\frac{\partial A_2}{\partial\xi}d\xi\right)d\eta+$$
$$+H_{21}A_1d\xi-\left(H_{21}+\frac{\partial H_{21}}{\partial\eta}d\eta\right)\left(A_1+\frac{\partial A_1}{\partial\eta}d\eta\right)d\xi+$$
$$+M_2d\xi\frac{\partial A_2}{\partial\xi}d\eta-H_{12}\frac{\partial A_1}{\partial\eta}d\eta d\xi+$$
$$+\left(Q_1+\frac{\partial Q_1}{\partial\xi}d\xi\right)\left(A_2+\frac{\partial A_2}{\partial\xi}d\xi\right)d\eta A_1d\xi=0.$$

Members depending on M_2 and H_{12} are calculated taking into account angles of rotation α and β analogously to how this was done above for N_1 and T_{12}; small quantities of higher order are rejected. After simple transformations we arrive at equation

$$\frac{\partial(A_2M_1)}{\partial\xi}+\frac{\partial(A_1H_{21})}{\partial\eta}-M_2\frac{\partial A_2}{\partial\xi}+H_{12}\frac{\partial A_1}{\partial\eta}-Q_1A_1A_2=0. \qquad (10.66)$$

Equation of moments for the tangent to ξ takes form

$$\frac{\partial(A_2H_{12})}{\partial\xi}+\frac{\partial(A_1M_2)}{\partial\eta}-M_1\frac{\partial A_1}{\partial\eta}+H_{21}\frac{\partial A_2}{\partial\xi}-Q_2A_1A_2=0. \qquad (10.67)$$

It remains to compose equation of moments with respect to axis z, directed along normal at point (ξ, η); it has the form

$$\left(T_{12}+\frac{\partial T_{12}}{\partial\xi}d\xi\right)\left(A_2+\frac{\partial A_2}{\partial\xi}d\xi\right)d\eta\,A_1\,d\xi-$$
$$-\left(T_{21}+\frac{\partial T_{21}}{\partial\eta}d\eta\right)\left(A_1+\frac{\partial A_1}{\partial\eta}d\eta\right)d\xi\,A_2d\eta-$$
$$-H_{12}\frac{A_1A_2}{R_1}d\xi d\eta+H_{21}\frac{A_1A_2}{R_2}d\xi d\eta=0$$

or

$$T_{12}-T_{21}-\frac{H_{12}}{R_1}+\frac{H_{21}}{R_2}=0. \qquad (10.68)$$

We introduce in sixth equation of equilibrium (68) initial expressions (58)–(61) for magnitudes in it; then it turns out that it is satisfied identically. If however we take approximately $T_{12} = T_{21}$ and $H_{12} = H_{21}$, then when $R_1 \neq R_2$ sixth equation will not be satisfied; it is possible to show, however, that error here introduced, as a rule, is of the same order as error of other relationships of the theory of shells.

Let us turn to relationships between forces and deformations, and also moments and changes of curvatures, corresponding to Hooke's law. We take for some layer of the shell, a distance of z from middle surface, dependences of the same type as for a plate:

$$\sigma_1^z=\frac{E}{1-\mu^2}(\varepsilon_1^z+\mu\varepsilon_2^z),\quad \sigma_2^z=\frac{E}{1-\mu^2}(\varepsilon_2^z+\mu\varepsilon_1^z),\quad \tau^z=\frac{E}{2(1+\mu)}\gamma^z. \qquad (10.69)$$

Expressions (69) correspond to generalized plane stress of a layer of a shell; in other words, it is considered that stress σ_z does not affect stresses σ_1 and σ_2.

We introduce (69) in expressions for forces (58) and (59) and use relationships (51); then, considering $z \ll R_1$ and $z \ll R_2$, we obtain

$$\left.\begin{aligned} N_1 &= \frac{Eh}{1-\mu^2}(\varepsilon_1+\mu\varepsilon_2),\quad N_2 = \frac{Eh}{1-\mu^2}(\varepsilon_2+\mu\varepsilon_1),\\ T_{12} &= T_{21} = T = \frac{Eh}{2(1+\mu)}\tau. \end{aligned}\right\} \qquad (10.70)$$

Analogously we find expression for moments:

$$\left.\begin{aligned} M_1 &= D(\varkappa_1+\mu\varkappa_2),\quad M_2 = D(\varkappa_2+\mu\varkappa_1),\\ H_{12} &= H_{21} = H = D(1-\mu)\chi. \end{aligned}\right\} \qquad (10.71)$$

We obtained precisely the same relationship as in the theory of plates; they are enticing in their simplicity. But we still marked certain contradictions, to which this simplification leads; there appear other difficulties, for instance, in examining potential energy of deformation of a shell. These contradictions can be eliminated, taking conditionally as expressions for T_{12} and T_{21} the following:*

$$T_{12} = \frac{Eh}{2(1+\mu)}\left(\tau - \frac{h^2}{6R_2}\chi\right),\quad T_{21} = \frac{Eh}{2(1+\mu)}\left(\tau - \frac{h^2}{6R_1}\chi\right). \qquad (10.72)$$

Putting (72) in (68), we prove that the sixth equation of equilibrium now is satisfied identically. Thus, in this variant of theory of shells, as before, we have $H_{12} = H_{21} = H$, but tangent forces T_{12} and T_{21} are different.

At our disposal now are 6 dependences (52) and (53), connecting deformations with displacements, 5 equations of equilibrium and 8 relationships of Hooke's law. Unknowns are the 3 displacements u, v, and w, 4 forces in the middle surface, 4 moments, 2 transverse forces, 3 deformations in the middle surface and 3 parameters of curvature. Total number of equations (19) corresponds to number of unknowns.

---

*These expressions were offered by L. I. Balabukh and V. V. Novozhilov, see [10.11], p. 47.

Solving the equations, we must satisfy boundary conditions for a concrete problem.

Ways of solution of equations can be selected differently depending on what quantities are selected as the basic unknowns — displacements or forces and moments. Subsequently we will also frequently use mixed method, as in the theory of flexible plates; basic unknowns will be deflection and the function of forces in the middle surface.

§ 123. Simplified Variant of Fundamental Equations of Linear Theory of Shells

As we have seen, structure of initial equations of general theory of shells even for region of small deflections is comparatively complex; therefore, solution of concrete problems presents significant difficulties. Fortunately, for many problems of stability of shells, of the greatest practical value, fundamental equations can be greatly simplified. This pertains to those cases, when buckling of shells is accompanied by appearance of comparatively small waves, i.e., waves whose dimensions, at least in one direction, are small as compared to radii of curvature of middle surface or dimensions of the shell. Here within each hollow the shell can be considered shallow. This allows us to apply in such problems of stability of shells of arbitrary outline the devices of the theory of shallow shells.*

In constructing a theory of shallow shells one may assume that internal geometry of middle surface independently of its Gaussian curvature is on a certain section the same as the geometry of a

*This theory was developed for circular cylindrical shells by Donnell [10.16], and for a shell of arbitrary outline, by V. Z. Vlasov [10.3], A. L. Gol'denveyzer [10.6], Kh. M. Mushtari [10.9], V. V. Novozhilov [10.11] and [10.12], Yu. N. Rabotnov [10.13], and S. Feynberg [10.14].

plane.* In other words, first quadratic form of a surface is considered the same as for a plane:

$$I = A_1^2 d\xi^2 + A_2^2 d\eta^2.$$

But then dependence (56) of Gaussian curvature on coefficients of first quadratic form is disrupted, and we must set

$$\frac{\partial}{\partial \xi}\left(\frac{1}{A_1}\frac{\partial A_2}{\partial \xi}\right) + \frac{\partial}{\partial \eta}\left(\frac{1}{A_2}\frac{\partial A_1}{\partial \eta}\right) \approx 0. \qquad (10.73)$$

Another criterion consists in that the functions, through which displacements, deformations, and stresses are expressed, change comparatively fast at least along one coordinate, so that during differentiation on a given coordinate the function significantly increases.

At the same time it is necessary to consider that displacements u and v along lines of curvature of middle surfaces are small as compared to deflections w. This allows us to use simplified expressions (57) for changes of curvature.

Further, the sixth equation of equilibrium is not taken into account; relationships of elasticity obtain form (70) and (71), where $T_{12} = T_{21} = T$ and $H_{12} = H_{21} = H$. Regarding first two equations of equilibrium (63) and (64), in them it turns out to be possible to disregard members, which depend on transverse forces; these equations change into the following:

$$\frac{\partial (A_2 N_1)}{\partial \xi} + \frac{\partial (A_1 T)}{\partial \eta} - N_2 \frac{\partial A_2}{\partial \xi} + T \frac{\partial A_1}{\partial \eta} = 0. \qquad (10.74a)$$

$$\frac{\partial (A_1 N_2)}{\partial \eta} + \frac{\partial (A_2 T)}{\partial \xi} - N_1 \frac{\partial A_1}{\partial \eta} + T \frac{\partial A_2}{\partial \xi} = 0. \qquad (10.74b)$$

---

*This assumption was first formulated by V. Z. Vlasov ([10.3], p. 303); see also article of S. A. Ambartsumyan, Applied Math. and Mech., 11 (1947).

Equations (74) will be identically satisfied, if we introduce the function of efforts in middle surface φ by formulas

$$\left.\begin{aligned} N_1 &= \frac{1}{A_2}\frac{\partial}{\partial\eta}\left(\frac{1}{A_2}\frac{\partial\varphi}{\partial\eta}\right)+\frac{1}{A_1^2A_2}\frac{\partial A_2}{\partial\xi}\frac{\partial\varphi}{\partial\xi}, \\ N_2 &= \frac{1}{A_1}\frac{\partial}{\partial\xi}\left(\frac{1}{A_1}\frac{\partial\varphi}{\partial\xi}\right)+\frac{1}{A_1A_2^2}\frac{\partial A_1}{\partial\eta}\frac{\partial\varphi}{\partial\eta}, \\ T &= -\frac{1}{2}\left[\frac{A_2}{A_1}\frac{\partial}{\partial\xi}\left(\frac{1}{A_2^2}\frac{\partial\varphi}{\partial\eta}\right)+\frac{A_1}{A_2}\frac{\partial}{\partial\eta}\left(\frac{1}{A_1^2}\frac{\partial\varphi}{\partial\xi}\right)\right]= \\ &= -\frac{1}{A_1A_2}\left(\frac{\partial^2\varphi}{\partial\xi\partial\eta}-\frac{1}{A_1}\frac{\partial A_1}{\partial\eta}\frac{\partial\varphi}{\partial\xi}-\frac{1}{A_2}\frac{\partial A_2}{\partial\xi}\frac{\partial\varphi}{\partial\eta}\right). \end{aligned}\right\} \qquad (10.75)$$

Magnitude φ is analogous to function of stresses in middle surface Φ, which appears in theory of flexible plates. If we set $A_1 = A_2 = 1$, and introduce coordinates x and y, then we have, e.g.;

$$N_1 = h\sigma_x = h\frac{\partial^2\Phi}{\partial y^2},$$

so that $\varphi = \Phi h$.

Let us note that forces N_1, N_2, and T are expressed according to (75) by function φ in the same way (with accuracy up to that of the sign), while curvatures $\varkappa_2$, $\varkappa_1$, and χ are expressed by function of deflection w by (57). Obviously, curvatures have to satisfy relationships, analogous to equations of equilibrium (74):

$$\left.\begin{aligned} \frac{\partial(A_2\varkappa_2)}{\partial\xi}-\frac{\partial(A_1\chi)}{\partial\eta}-\varkappa_1\frac{\partial A_2}{\partial\xi}-\chi\frac{\partial A_1}{\partial\eta}=0, \\ \frac{\partial(A_1\varkappa_1)}{\partial\eta}-\frac{\partial(A_2\chi)}{\partial\xi}-\varkappa_2\frac{\partial A_1}{\partial\eta}-\chi\frac{\partial A_2}{\partial\xi}=0. \end{aligned}\right\} \qquad (10.76)$$

These dependences constitute a simplified variant of two additional equations of compatibility, mentioned in § 121 (p. 532).

We find, further, transverse forces Q_1 and Q_2 from equations of equilibrium (66) and (67):

$$\left.\begin{aligned} Q_1 &= \frac{1}{A_1A_2}\left[\frac{\partial(A_2M_1)}{\partial\xi}+\frac{\partial(A_1H)}{\partial\eta}-M_2\frac{\partial A_2}{\partial\xi}+H\frac{\partial A_1}{\partial\eta}\right], \\ Q_2 &= \frac{1}{A_1A_2}\left[\frac{\partial(A_1M_2)}{\partial\eta}+\frac{\partial(A_2H)}{\partial\xi}-M_1\frac{\partial A_1}{\partial\eta}+H\frac{\partial A_2}{\partial\xi}\right]. \end{aligned}\right\} \qquad (10.77)$$

We will use relationships of elasticity (71). If we consider relationship (76), then we obtain here

$$Q_1 = D\frac{1}{A_1}\frac{\partial(\varkappa_1+\varkappa_2)}{\partial\xi},\quad Q_2 = D\frac{1}{A_2}\frac{\partial(\varkappa_1+\varkappa_2)}{\partial\eta}. \tag{10.78}$$

On the other hand, by (57) we find

$$\varkappa_1+\varkappa_2 = -\left[\frac{1}{A_1}\frac{\partial}{\partial\xi}\left(\frac{1}{A_1}\frac{\partial w}{\partial\xi}\right)+\frac{1}{A_1^2A_2}\frac{\partial A_2}{\partial\xi}\frac{\partial w}{\partial\xi}+\right.$$
$$\left.+\frac{1}{A_2}\frac{\partial}{\partial\eta}\left(\frac{1}{A_2}\frac{\partial w}{\partial\eta}\right)+\frac{1}{A_1A_2^2}\frac{\partial A_1}{\partial\eta}\frac{\partial w}{\partial\eta}\right]. \tag{10.79}$$

or

$$\varkappa_1+\varkappa_2 = -\nabla^2 w; \tag{10.80}$$

here by ∇^2 is understood the Laplacian operator in curvilinear coordinates:

$$\nabla^2 = \frac{1}{A_1A_2}\left[\frac{\partial}{\partial\xi}\left(\frac{A_2}{A_1}\frac{\partial}{\partial\xi}\right)+\frac{\partial}{\partial\eta}\left(\frac{A_1}{A_2}\frac{\partial}{\partial\eta}\right)\right]. \tag{10.81}$$

Operator ∇^2 in Cartesian coordinates we obtain when $A_1 = A_2 = 1$.

Finally we find the following expressions for transverse forces:

$$Q_1 = -D\frac{1}{A_1}\frac{\partial(\nabla^2 w)}{\partial\xi},\quad Q_2 = -D\frac{1}{A_2}\frac{\partial(\nabla^2 w)}{\partial\eta}; \tag{10.82}$$

similar expressions we obtained in theory of plates.

We introduce (82) into remaining equation of equilibrium (65) and express forces N_1 and N_2 through function φ by (75); then we arrive at equation

$$D\nabla^4 w = \nabla_k^2\varphi + q; \tag{10.83}$$

here is introduced a new operator [10.3]:

$$\nabla_k^2 = \frac{1}{A_1A_2}\left[\frac{\partial}{\partial\xi}\left(\frac{1}{R_2}\frac{A_2}{A_1}\frac{\partial}{\partial\xi}\right)+\frac{\partial}{\partial\eta}\left(\frac{1}{R_1}\frac{A_1}{A_2}\frac{\partial}{\partial\eta}\right)\right]. \tag{10.84}$$

which is distinguished from ∇^2 by coefficients $1/R_2$ and $1/R_1$, accounting for curvature of the shell.

We use, further, equation of compatibility of deformations (54).

If we introduce in it expressions for deformations from (70)

$$\varepsilon_1=\frac{1}{Eh}(N_1-\mu N_2),\quad \varepsilon_2=\frac{1}{Eh}(N_2-\mu N_1),\quad \gamma=\frac{2(1+\mu)}{Eh}T. \tag{10.85}$$

and, further, expression N_1, N_2, and T through function of forces according to (75), and change of curvatures, by w according to (57), then we arrive at the following equation,

$$\frac{1}{Eh}\nabla^4\varphi=-\nabla_k^2 w. \tag{10.86}$$

Thus, we obtained a system of symmetrically constructed linear equations of fourth order for the function of deflection w and function of force φ: when q = 0 this system takes form

$$\left.\begin{aligned} D\nabla^4 w&=\nabla_k^2\varphi,\\ \frac{1}{Eh}\nabla^4\varphi&=-\nabla_k^2 w. \end{aligned}\right\} \tag{10.87}$$

In the particular case when $A_1 = A_2 = 1$, if we introduce x and y instead of ξ and η, we obtain

$$\nabla^2=\frac{\partial^2}{\partial x^2}+\frac{\partial^2}{\partial y^2},\quad \nabla_k^2=\frac{1}{R_2}\frac{\partial^2}{\partial x^2}+\frac{1}{R_1}\frac{\partial^2}{\partial y^2}. \tag{10.88}$$

However, in problems of stability the first of equations (87) must be supplemented by members, considering fundamental forces in the shell. If the fundamental state is momentless, then it is necessary to consider subcritical forces in the middle surface; in general it is necessary also to consider flexural forces. Let us consider case of <u>momentless fundamental state</u>; here it is possible to introduce in equation (83) hypothetical lateral load $q_z = q$, equal to sum of additional projections of fundamental forces p_x and p_y, in a direction of a normal to the deflection surface:

$$q=h(p_x\varkappa_1+p_y\varkappa_2+2s\tau)=h\Pi(p,\varkappa). \tag{10.89}$$

Here we consider positive forces facilitating increase of parameters of curvature; in application to p_x and p_y we take forces of compression as positive. When $A_1 = A_2 = 1$ we obtain

$$q = -h\left(p_x\frac{\partial^2 w}{\partial x^2} + p_y\frac{\partial^2 w}{\partial y^2} + 2s\frac{\partial^2 w}{\partial x\,\partial y}\right) = -h\Pi(p, w). \qquad (10.89a)$$

We apply to the first of equations (87) operator ∇^4, and to second, operator ∇_k^2; then system (87) can be reduced to one resolving equation of eighth order:

$$\frac{D}{Eh}\nabla^8 w + \nabla_k^2\nabla_k^2 w = 0 \qquad (10.90)$$

or

$$\frac{h^2}{12(1-\mu^2)}\nabla^8 w + \nabla_k^2\nabla_k^2 w = 0. \qquad (10.90a)$$

In problems of stability equation (90) must be supplemented by member $\nabla^4 q$; it will obtain according to (89a) form

$$\frac{D}{Eh}\nabla^8 w + \nabla_k^2\nabla_k^2 w - \frac{1}{E}\nabla^4\Pi(p, w) = 0; \qquad (10.91)$$

here parameters of change of curvature must be expressed by w according to (57). When $A_1 = A_2 = 1$ we have

$$\frac{D}{Eh}\nabla^8 w + \nabla_k^2\nabla_k^2 w + \frac{1}{E}\nabla^4\Pi(p, w) = 0. \qquad (10.91a)$$

Henceforth we shall use equations of type (91) during solution of many particular problems. When there is applied energy method, we must find potential strain energy of the shell, composed of energy of deformation in middle surface and energy of flexure. The first of these components is calculated by a formula analogous that which was given in Chapter VII for flexible plates (see p. 342):

$$U_c = \frac{h}{2E}\int_\sigma\int[(\sigma_1+\sigma_2)^2 - 2(1+\mu)(\sigma_1\sigma_2 - \tau^2)]\,A_1A_2\,d\xi\,d\eta; \qquad (10.92)$$

integral is extended to middle surface of shell. Using relationships of type (70), we express U_c by deformations:

$$U_\varepsilon = \frac{Eh}{2(1-\mu^2)} \int_F \int \left[(\varepsilon_1+\varepsilon_2)^2 - 2(1-\mu)\left(\varepsilon_1\varepsilon_2 - \frac{\gamma^2}{4}\right)\right] A_1 A_2 \, d\xi \, d\eta. \qquad (10.93)$$

Energy of flexure is determined, as before, by a formula of type (7.39):

$$U_\kappa = \frac{D}{2} \int_F \int |(\varkappa_1+\varkappa_2)^2 - 2(1-\mu)(\varkappa_1\varkappa_2 - \chi^2)| \, A_1 A_2 \, d\xi \, d\eta. \qquad (10.94)$$

For a <u>shallow shell</u> it is possible to introduce here functions of stresses and deflection; then we obtain

$$\left.\begin{aligned} U_\varepsilon &= \frac{h}{2E} \int_F \int |(\nabla^2\Phi)^2 - (1+\mu) L(\Phi, \Phi)| \, dx \, dy. \\ U_\kappa &= \frac{D}{2} \int_F \int |(\nabla^2 w)^2 - (1-\mu) L(w, w)| \, dx \, dy. \end{aligned}\right\} \qquad (10.95)$$

Let us turn to the fundamental relationships of the theory of flexible shells.

§ 124. Shells of Large Deflection

Linear theory of shells gives possibility to investigate stability in the small. But total solution of a problem, including approach to it in the large can be given, as we know, only from the positions of nonlinear theory. We give fundamental relationships pertaining to a shell of large deflection.*

We start from simplified variant, in which shell is considered shallow, at least within limits of an individual hollow. We assume, therefore, $A_1 = A_2 = 1$, and we plot along lines of curvature coordinates x and y. Initial curvatures of middle surface we designate by

---

*These relationships were derived in more general form by Chien Wei-Zang [10.15], N. A. Alumyae [10.1], Kh. M. Mushtari and K. Z. Galimov [10.10].

$k_1 = 1/R_1$ and $k_2 = 1/R_2$ and we take them for a given section of shell as constant.

Expressions for deformations in middle surface for linear problem have form (52):

$$\varepsilon_x = \frac{\partial u}{\partial x} - k_1 w, \quad \varepsilon_y = \frac{\partial v}{\partial y} - k_2 w, \quad \gamma = \frac{\partial u}{\partial y} + \frac{\partial v}{\partial x}. \tag{10.96}$$

Supplementing them with the same nonlinear members as in the theory of flexible plates, we obtain

$$\varepsilon_x = \frac{\partial u}{\partial x} - k_1 w + \frac{1}{2}\left(\frac{\partial w}{\partial x}\right)^2, \tag{10.97}$$

$$\varepsilon_y = \frac{\partial v}{\partial y} - k_2 w + \frac{1}{2}\left(\frac{\partial w}{\partial y}\right)^2, \tag{10.98}$$

$$\gamma = \frac{\partial u}{\partial y} + \frac{\partial v}{\partial x} + \frac{\partial w}{\partial x}\frac{\partial w}{\partial y}. \tag{10.99}$$

Equation of compatibility of deformations (54a) takes form

$$\frac{\partial^2 \varepsilon_x}{\partial y^2} + \frac{\partial^2 \varepsilon_y}{\partial x^2} - \frac{\partial^2 \gamma}{\partial x \partial y} = -\frac{1}{2} L(w, w) - \nabla_k^2 w; \tag{10.100}$$

by L(w, w) here is understood former operator (7.40), and by ∇_k^2, the simplified operator (84):

$$\nabla_k^2 = k_2 \frac{\partial^2}{\partial x^2} + k_1 \frac{\partial^2}{\partial y^2}. \tag{10.101}$$

Formulas (57) for changes of curvatures change into the following,

$$\varkappa_1 = -\frac{\partial^2 w}{\partial x^2}, \quad \varkappa_2 = -\frac{\partial^2 w}{\partial y^2}, \quad \chi = -\frac{\partial^2 w}{\partial x \partial y}; \tag{10.102}$$

new nonlinear members here will not be introduced. Thus, parameters $\varkappa$ and χ will be the same as in the case of a plate.

Relationships of Hooke's law (70) and (71) also remain as before. First two equations of equilibrium (74a) and (74b) take form

$$\frac{\partial \sigma_x}{\partial x} + \frac{\partial \tau}{\partial y} = 0, \quad \frac{\partial \tau}{\partial x} + \frac{\partial \sigma_y}{\partial y} = 0; \tag{10.103}$$

here we assume $\sigma_x = N_1/h$, $\sigma_y = N_2/h$.

Third equation of equilibrium (65) we will rewrite in the form

$$\frac{\partial Q_1}{\partial x}+\frac{\partial Q_2}{\partial y}+(\sigma_x k_x+\sigma_y k_y)h+q=0; \qquad (10.104)$$

it should be augmented by members depending on changes of curvatures, as in the case of a flexible plate, and obtains form

$$\frac{\partial Q_1}{\partial x}+\frac{\partial Q_2}{\partial y}+\left[\sigma_x\left(k_x+\frac{\partial^2 w}{\partial x^2}\right)+\sigma_y\left(k_y+\frac{\partial^2 w}{\partial y^2}\right)\right]h+ \\ +2\tau h\frac{\partial^2 w}{\partial x\,\partial y}+q=0. \qquad (10.105)$$

where $\tau = T/h$.

Transverse forces according to (82) will be

$$Q_1=-D\frac{\partial(\nabla^2 w)}{\partial x},\quad Q_2=-D\frac{\partial(\nabla^2 w)}{\partial y}. \qquad (10.106)$$

Introducing these expressions in (105), we arrive at the following equation:

$$D\nabla^2\nabla^2 w=\sigma_x h\left(k_x+\frac{\partial^2 w}{\partial x^2}\right)+\sigma_y h\left(k_y+\frac{\partial^2 w}{\partial y^2}\right)+2\tau h\frac{\partial^2 w}{\partial x\,\partial y}+q. \qquad (10.107)$$

Introducing in equation of compatibility of deformations (100) stresses according to relationships of elasticity of type (85), we obtain

$$\frac{1}{E}\left[\frac{\partial^2\sigma_x}{\partial y^2}-2\frac{\partial^2\tau}{\partial x\,\partial y}+\frac{\partial^2\sigma_y}{\partial y^2}-\mu\left(\frac{\partial^2\sigma_x}{\partial y^2}+2\frac{\partial^2\tau}{\partial x\,\partial y}+\frac{\partial^2\sigma_y}{\partial x^2}\right)\right]= \\ =-\frac{1}{2}L(w,w)-\nabla_k^2 w. \qquad (10.108)$$

We now use the function of stresses $\Phi = \varphi/h$ and express σ_x, σ_y, and τ in (107) and (108) by Φ by known formulas (7.60); then we arrive at the final equations (for $q = 0$):

$$\left.\begin{aligned}\frac{D}{h}\nabla^4 w&=L(w,\Phi)+\nabla_k^2\Phi,\\ \frac{1}{E}\nabla^4\Phi&=-\frac{1}{2}L(w,w)-\nabla_k^2 w.\end{aligned}\right| \qquad (10.109)$$

These equations generalize system (87) for case of shell of large deflection. On the other hand, assuming here that members, containing operator ∇_k^2 are equal to zero, we obtain equations (7.63)

and (7.64), pertaining to flexible plates. As we have seen, the first of equations (109) expresses condition of equilibrium of the member of the shell, and the second, the condition of compatibility of deformations.

Let us assume now that shell has before loading certain deflections from ideal form, or, in other words, <u>initial deflections</u> $w_0(x, y)$. Then expressions for deformations (97)–(99) obtain form

$$\left.\begin{aligned} \varepsilon_x &= \frac{\partial u}{\partial x} - k_x(w - w_0) + \frac{1}{2}\left(\frac{\partial w}{\partial x}\right)^2 - \frac{1}{2}\left(\frac{\partial w_0}{\partial x}\right)^2, \\ \varepsilon_y &= \frac{\partial v}{\partial y} - k_y(w - w_0) + \frac{1}{2}\left(\frac{\partial w}{\partial y}\right)^2 - \frac{1}{2}\left(\frac{\partial w_0}{\partial y}\right)^2, \\ \gamma &= \frac{\partial u}{\partial y} + \frac{\partial v}{\partial x} + \frac{\partial w}{\partial x}\frac{\partial w}{\partial y} - \frac{\partial w_0}{\partial x}\frac{\partial w_0}{\partial y}; \end{aligned}\right\} \qquad (10.110)$$

by w here is understood total deflection. Repeating derivation of fundamental equations, we obtain, instead of (109),

$$\left.\begin{aligned} \frac{D}{h}\nabla^4(w - w_0) &= L(w, \Phi) + \nabla_k^2\Phi, \\ \frac{1}{E}\nabla^4\Phi &= -\frac{1}{2}[L(w, w) - L(w_0, w_0)] - \nabla_k^2(w - w_0). \end{aligned}\right\} \qquad (10.111)$$

We now pass to concrete problems of stability in the small and in the large of shells of different outline. We start with circular cylindrical shells.

Literature

10.1. N. A. Alumyae. Equilibrium of thin-walled elastic shells in postcritical stage, Tartu, 1948; Applied math. and mech., 13, No. 1 (1949); On concept of basic relationships of nonlinear theory of shells, Applied math. and mech., 20, No. 1 (1956), 136-139.

10.2. S. A. Ambartsumyan. Theory of anisotropic shells, Fizmatgiz, M., 1961.

10.3. V. Z. Vlasov. Basic differential equations of general theory of elastic shells, Applied math. and mech., 8, No. 2 (1944).

10.4. V. Z. Vlasov. General theory of shells and its application in engineering, Gostekhizdat, M., 1949.

10.5. A. L. Gol'denveyzer. Supplement and correction to theory of thin shells of Lyav, Coll. "Plates and shells," Gosstroyizdat, 1939; Equations of the theory of shells in shifts and functions of stresses, Applied math. and mech., 21, No. 6 (1957), 801-814; Asymptotic properties of values in problems of the theory of thin elastic shells, Applied math. and mech., 25, No. 4 (1961), 729-741.

10.6. A. L. Gol'denveyzer. Theory of elastic thin shells, Gostekhizdat, M., 1953.

10.7. N. A. Kil'chevskiy. Generalization of contemproary theory of shells, Applied math. and mech., 2, No. 4 (1939).

10.8. A. I. Lur'ye. Statics of thin-walled elastic shells, Gostekhizdat, 1947.

10.9. Kh. M. Mushtari. Certain generalizations of the theory of thin shells with application to problem of stability of elastic equilibrium, News of physics and mathematics society at Kazan' State University (1938), 71-97; Applied math. and mech., 2, No. 4 (1939); Elastic equilibrium of a thin shell with initial anomalies in the form of the middle surface, loc. cit., 15, No. 6 (1951).

10.10. Kh. M. Mushtari and K. Z. Galimov. Nonlinear theory of elastic shells, Tatknigoizdat, Kazan', 1957.

10.11. V. V. Novozhilov. Theory of thin shells, Oborongiz, 1941; Sudpromgiz, 1951.

10.12. V. V. Novozhilov. General theory of stability of thin shells, DAN SSSR, 32, No. 5 (1941).

10.13. Yu. N. Rabotnov.Fundamental equations of theory of shells, DAN SSSR, 47, No. 2 (1945); Equations of boundary zone in theory of shells, loc. cit., 47, No. 5 (1945); Local stability of shells, loc. cit., 52, No. 2 (1946).

10.14. S. Feynberg. Concerning the question of construction of approximate theory of thin-walled shells of arbitrary outline, coll. "Research in the theory of constructions," Gostroyizdat, 1939.

10.15. Wei-Zang Chien. The intrinsic theory of thin shells and plates, Quart. of Appl. Math. 1, No. 4 (1944), 297-327; 2, No. 1, 43-59, No. 2, 120-135 (1945).

10.16. L. Donnell. A discussion of thin shell theory, Proc. 5th congr. for Appl. Mech., 1939.

10.17. Y. C. Fung and E. E. Sechler. Instability of thin elastic shells, "Structural Mechanics," Pergamon-Press (1960), 115-168.

10.18. W. Flügge. Statik und Dynamik der Schalen, 2. Auflage, Springer-Verlag, 1957 (translation: Statics and dynamics of shells, Gosstroyizdat, M., 1961).

10.19. A. Love. Mathematical theory of elasticity. 1927.

10.20. K. Marguerre. Zur theorie der gerkrümmten Platte grosser Formänderung, Jahrbuch 1939 der deutschen Luftfahrtforschung, 413-418.

10.21. E. Reissner. A new derivation of the equations for the deformation of elastic shells, Am. Journ. of Math. 63, No. 1 (1941), 177-184; On some problems in shell theory. "Structural Mechanics," Pergamon-Press (1960), 74-114.

10.22. J. L. Synge and W. Z. Chien. The intrinsic theory of elastic shells and plates, Th. Karman Ann. Volume (1941), 103-120.

CHAPTER XI

STABILITY OF CYLINDRICAL SHELLS WITHIN ELASTIC LIMIT

§ 125. Fundamental Equations for Shell of Circular Outline

In studies of stability of shells greatest attention has been paid to circular cylindrical shells. Shells of such outline correspond, as a rule, to requirements of minimum weight of construction and simplicity of manufacture; therefore, they are widely applied in different regions of technology. Cylindrical shells enter into construction of aircraft and motors, submarines, tanks, pipelines, etc.

Buckling of cylindrical shells can occur when they are subjected to axial compression, transverse pressure, torsion, bending, where these loads are met separately or in various combinations. Subsequently we will consider in order problems of stability of shells with these forms of loading.

First of all we shall give basic relationships of linear theory of circular cylindrical shells of constant thickness h. We designate radius of curvature of middle surface by R. As parameters determining position of any point of middle surface we select coordinates x and y, plotted correspondingly along the generatrix and along the arc (Fig. 11.1). Displacements along these lines and on the normal as before we designate by u, v, and w; we consider deflections w positive,

if they are directed toward center of curvature.

First quadratic form of middle surface here will be

$$I = dx^2 + dy^2. \tag{11.1}$$

Consequently, we must assume in designations of preceding chapter that $a_{11} = A_1 = 1$, $a_{22} = A_2 = 1$, $a_{12} = 0$ and, further $\xi = x$, $\eta = y$. Furthermore, we must put $R_1 = \infty$, $R_2 = R$. Since coefficients A_1 and A_2 here are constant, all relationships of theory of shells are greatly simplified.

Fig. 11.1. Coordinate lines for examining cylindrical shell.

Expressions (10.52) for deformations in middle surface obtain form

$$\varepsilon_x = \frac{\partial u}{\partial x}, \quad \varepsilon_y = \frac{\partial v}{\partial y} - \frac{w}{R}, \quad \gamma = \frac{\partial u}{\partial y} + \frac{\partial v}{\partial x}; \tag{11.2}$$

parameters of change of curvature by (10.53) will be

$$\varkappa_x = -\frac{\partial^2 w}{\partial x^2}, \quad \varkappa_y = -\frac{1}{R}\frac{\partial v}{\partial y} - \frac{\partial^2 w}{\partial y^2}, \quad \chi = -\frac{1}{2R}\frac{\partial v}{\partial x} - \frac{\partial^2 w}{\partial x\,\partial y}. \tag{11.3}$$

Let us note that for parameter $\varkappa_y$ in literature there is also applied another expression:

$$\varkappa_y = -\frac{w}{R^2} - \frac{\partial^2 w}{\partial y^2}; \tag{11.4}$$

it can be obtained from (3), if we take condition of "inextensionality" of the middle surface in direction of arc: $\varepsilon_y = 0$, then we have*

$$\frac{\partial v}{\partial y} = \frac{w}{R}. \tag{11.5}$$

Subsequently in examining isotropic shells we introduce in basic relationships not forces N_x, N_y, and T but directly the stresses

---

*In variant of fundamental relationships taken by V. Z. Vlasov [10.3], expression (4) is not connected with condition of inextensionality.

in the middle surface $\sigma_x = N_x/h$, $\sigma_y = N_y/h$, and $\tau = T/h$. Equations of equilibrium (10.63)–(10.65) in projections on axis x, tangent to line y, and axis z are rewritten in the form

$$\left.\begin{aligned} &\frac{\partial \sigma_x}{\partial x}+\frac{\partial \tau}{\partial y}+\frac{1}{h}q_x=0, \quad \frac{\partial \tau}{\partial x}+\frac{\partial \sigma_y}{\partial y}-\frac{Q_y}{Rh}+\frac{1}{h}q_y=0,\\ &\frac{\partial Q_x}{\partial x}+\frac{\partial Q_y}{\partial y}+\frac{hz_y}{R}+q_z=0. \end{aligned}\right\} \tag{11.6}$$

Equations of moments (10.66)–(10.68) obtain form

$$\frac{\partial M_x}{\partial x}+\frac{\partial H}{\partial y}-Q_x=0, \quad \frac{\partial H}{\partial x}+\frac{\partial M_y}{\partial y}-Q_y=0. \tag{11.7}$$

We find Q_x and Q_y from (7) and substitute (6); then we obtain

$$\left.\begin{aligned} &\frac{\partial \sigma_x}{\partial x}+\frac{\partial \tau}{\partial y}+\frac{1}{h}q_x=0, \quad \frac{\partial \tau}{\partial x}+\frac{\partial \sigma_y}{\partial y}-\frac{1}{Rh}\left(\frac{\partial H}{\partial x}+\frac{\partial M_y}{\partial y}\right)+\frac{1}{h}q_y=0,\\ &\frac{\partial^2 M_x}{\partial x^2}+2\frac{\partial^2 H}{\partial x\,\partial y}+\frac{\partial^2 M_y}{\partial y^2}+\frac{h\sigma_y}{R}+q_z=0. \end{aligned}\right\} \tag{11.8}$$

Sixth equation of equilibrium (10.68) we shall not consider.

We determine, further, stress in middle surface by (10.70) and (2),

$$\left.\begin{aligned} \varepsilon_x&=\frac{E}{1-\mu^2}\left[\frac{\partial u}{\partial x}+\mu\left(\frac{\partial v}{\partial y}-\frac{w}{R}\right)\right],\\ \varepsilon_y&=\frac{E}{1-\mu^2}\left[\frac{\partial v}{\partial y}-\frac{w}{R}+\mu\frac{\partial u}{\partial x}\right],\\ \tau&=\frac{E}{2(1+\mu)}\left(\frac{\partial u}{\partial y}+\frac{\partial v}{\partial x}\right). \end{aligned}\right\} \tag{11.9}$$

and moments by (10.71) and (3):

$$\left.\begin{aligned} M_x&=-D\left[\frac{\partial^2 w}{\partial x^2}+\mu\left(\frac{1}{R}\frac{\partial v}{\partial y}+\frac{\partial^2 w}{\partial y^2}\right)\right],\\ M_y&=-D\left[\frac{\partial^2 w}{\partial y^2}+\frac{1}{R}\frac{\partial v}{\partial y}+\mu\frac{\partial^2 w}{\partial x^2}\right],\\ H&=-D(1-\mu)\left(\frac{1}{2R}\frac{\partial v}{\partial x}+\frac{\partial^2 w}{\partial x\,\partial y}\right). \end{aligned}\right\} \tag{11.10}$$

We introduce expressions (9) and (10) in conditions of equilibrium

(8); then we arrive at following equations:

$$\left.\begin{aligned}
&\frac{\partial^2 u}{\partial x^2}+\frac{1-\mu}{2}\frac{\partial^2 u}{\partial y^2}+\frac{1+\mu}{2}\frac{\partial^2 v}{\partial x\,\partial y}-\frac{\mu}{R}\frac{\partial w}{\partial x}+\frac{1-\mu^2}{Eh}q_x=0,\\
&\frac{\partial^2 v}{\partial y^2}+\frac{1-\mu}{2}\frac{\partial^2 v}{\partial x^2}+\frac{h^2}{12R^2}\left(\frac{\partial^2 v}{\partial y^2}+\frac{1-\mu}{2}\frac{\partial^2 v}{\partial x^2}\right)+\\
&+\frac{1+\mu}{2}\frac{\partial^2 u}{\partial x\,\partial y}-\frac{1}{R}\frac{\partial w}{\partial y}+\frac{h^2}{12R}\left(\frac{\partial^3 w}{\partial x^2\,\partial y}+\frac{\partial^3 w}{\partial y^3}\right)+\frac{1-\mu^2}{Eh}q_y=0,\\
&\frac{h^2}{12}\nabla^4 w+\frac{w}{R^2}-\frac{\mu}{R}\frac{\partial u}{\partial x}-\frac{1}{R}\frac{\partial v}{\partial y}+\\
&+\frac{h^2}{12R}\left(\frac{\partial^3 v}{\partial x^2\,\partial y}+\frac{\partial^3 v}{\partial y^3}\right)-\frac{1-\mu^2}{Eh}q_z=0.
\end{aligned}\right\} \qquad (11.11)$$

where $\nabla^4=\nabla^2\nabla^2$ is double Laplacian operator according to (7.20a).

We obtained one of variants of equations of theory of cylindrical shells in shifts.* We rewrite these equations in the form of a table of operators relation with respect to u, v, and w (load members are omitted).

Table 11.1. Differential Operators of Fundamental Equations.

$\frac{\partial^2}{\partial x^2}+\frac{1-\mu}{2}\frac{\partial^2}{\partial y^2}$	$\frac{1+\mu}{2}\frac{\partial^2}{\partial x\,\partial y}$	$-\frac{\mu}{R}\frac{\partial}{\partial x}$
$\frac{1+\mu}{2}\frac{\partial^2}{\partial x\,\partial y}$	$\left(\frac{\partial}{\partial y^2}+\frac{1-\mu}{2}\frac{\partial^2}{\partial x^2}\right)\times\left(1+\frac{h^2}{12R^2}\right)$	$-\frac{1}{R}\frac{\partial}{\partial y}+\frac{h^2}{12R}\left(\frac{\partial^3}{\partial x^2\,\partial y}+\frac{\partial^3}{\partial y^3}\right)$
$-\frac{\mu}{R}\frac{\partial}{\partial x}$	$-\frac{1}{R}\frac{\partial}{\partial y}+\frac{h^2}{12R}\left(\frac{\partial^3}{\partial x^2\,\partial y}+\frac{\partial^3}{\partial y^3}\right)$	$\frac{h^2}{12}\nabla^4+\frac{1}{R^2}$

Let us note that nondiagonal members of this table are built symmetrically. V. Z. Vlasov considers [10.3] that this property is

*See book of Wang Chi-the [21.21] p. 395.

in accordance with energy principles of theory of elasticity and, in particular, with theorem of reciprocity of works.

We turn now to simplified variant of linear theory of shells, presented in § 123. New expressions for change of curvature according to (10.57) have form

$$\varkappa_x = -\frac{\partial^2 w}{\partial x^2}, \quad \varkappa_y = -\frac{\partial^2 w}{\partial y^2}, \quad \chi = -\frac{\partial^2 w}{\partial x \partial y}. \tag{11.12}$$

As it is easy to see, final expressions for deformations (2) and parameters of curvature (12) coincide with the same expressions in theory of plates; an exception is formula for ε_y, including here an additional member $(-w/R)$. First two equations of equilibrium (8) obtain form

$$\left.\begin{aligned} \frac{\partial \sigma_x}{\partial x} + \frac{\partial \tau}{\partial y} + \frac{1}{h} q_x = 0, \\ \frac{\partial \tau}{\partial x} + \frac{\partial \sigma_y}{\partial y} + \frac{1}{h} q_y = 0; \end{aligned}\right\} \tag{11.8a}$$

they are analogous to corresponding equations for a member of a plate. This permits us to introduce function of stresses Φ from (10.75)

$$\sigma_x = \frac{\partial^2 \Phi}{\partial y^2}, \quad \sigma_y = \frac{\partial^2 \Phi}{\partial x^2}, \quad \tau = -\frac{\partial^2 \Phi}{\partial x \partial y}. \tag{11.13}$$

Equation of compatibility deformations (10.54a) obtains form

$$\frac{\partial^2 \varepsilon_x}{\partial y^2} + \frac{\partial^2 \varepsilon_y}{\partial x^2} - \frac{\partial^2 \gamma}{\partial x \partial y} = -\frac{1}{R} \frac{\partial^2 w}{\partial x^2}. \tag{11.14}$$

Proceeding further on the path described in § 123, we arrive at final equations (10.83) and (10.86). Considering from (10.84)

$$\nabla_k^2 = \frac{1}{R} \frac{\partial^2 w}{\partial x^2},$$

we find

$$\frac{D}{h} \nabla^4 w = \frac{1}{R} \frac{\partial^2 \Phi}{\partial x^2} + \frac{q_z}{h}. \tag{11.15}$$

$$\frac{1}{E}\nabla^4\Phi = -\frac{1}{R}\frac{\partial^2 w}{\partial x^2}. \qquad (11.16)$$

We obtained known system of equations of mixed type for deflection w and functions of stresses Φ, lying at base of much research. During solution of problems of stability of shells, in equation (15) it is necessary to place instead of q_z/h magnitude $\Pi(\sigma, \varkappa)$ from (10.89); in complete form the equation will be

$$\frac{D}{h}\nabla^4 w = \frac{1}{R}\frac{\partial^2 \Phi}{\partial x^2} - p_x\frac{\partial^2 w}{\partial x^2} - p_y\frac{\partial^2 w}{\partial y^2} - 2s\frac{\partial^2 w}{\partial x\,\partial y}. \qquad (11.15a)$$

Further, equations (15a) and (16) can be reduced to one resolving equation of form (10.91a). If stresses p_x, p_y, and s do not depend on coordinates, we obtain

$$\frac{D}{h}\nabla^8 w + \frac{E}{R^2}\frac{\partial^4 w}{\partial x^4} + p_x\nabla^4\left(\frac{\partial^2 w}{\partial x^2}\right) + p_y\nabla^4\left(\frac{\partial^2 w}{\partial y^2}\right) + 2s\nabla^4\left(\frac{\partial^2 w}{\partial x\,\partial y}\right) = 0. \qquad (11.17)$$

Simplified variant of theory of cylindrical shells can be presented also in the form of equations in displacements. In Table 11.1 it is possible here to reject members with second and third derivatives, coefficients in which contain h^2; then we arrive at following Table 11.2:*

Table 11.2. Differential Operators of Simplified Equations.

•	•	•
$\frac{\partial^2}{\partial x^2} + \frac{1-\mu}{2}\frac{\partial^2}{\partial y^2}$	$\frac{1+\mu}{2}\frac{\partial^2}{\partial x\,\partial y}$	$-\frac{\mu}{R}\frac{\partial}{\partial x}$
$\frac{1+\mu}{2}\frac{\partial^2}{\partial x\,\partial y}$	$\frac{\partial^2}{\partial y^2} + \frac{1-\mu}{2}\frac{\partial^2}{\partial x^2}$	$-\frac{1}{R}\frac{\partial}{\partial y}$
$-\frac{\mu}{R}\frac{\partial}{\partial x}$	$-\frac{1}{R}\frac{\partial}{\partial y}$	$\frac{h^2}{12}\nabla^4 + \frac{1}{R^2}$

*These equations were given by V. Z. Vlasov (see [10.3], p. 316) and Donnell [11.30].

These operators also possess complete symmetry. Equations given in Table 11.2 it is possible to transform. Differentiating second equation with respect to x and y, we find

$$\frac{1+\mu}{2}\frac{\partial^4 u}{\partial x^3 \partial y^2}+\frac{\partial^4 v}{\partial x \partial y^3}+\frac{1-\mu}{2}\frac{\partial^4 v}{\partial x^3 \partial y}-\frac{1}{R}\frac{\partial^3 w}{\partial x \partial y^2}=0.$$

Using the first equation, we determine derivatives of v involved here; then we arrive at equation

$$\nabla^4 u=\mu\frac{\partial^3 w}{\partial x^3}-\frac{\partial^3 w}{\partial x \partial y^2}. \qquad (11.17a)$$

Analogous equation for v has the form

$$\nabla^4 v=(2+\mu)\frac{\partial^3 w}{\partial x^2 \partial y}+\frac{\partial^3 w}{\partial y^3}. \qquad (11.17b)$$

These two relationships supplement equation (17) for w.

We gave variant of simplified equations, pertaining to case when dimension of hollow is small as compared to dimensions of shell at least in one direction. For instance, if shell received axisymmetric (annular) hollows, then length of them should be small with respect to total length of shell. If, however, to the contrary, the hollow occupies whole length of shell, then number n of waves along circumference should satisfy condition $n^2 \gg 1$. In practice simplified equations can be applied when $n \geqslant 4$; this condition is met in various cases of loading of a shell, if ration L/R is not too great. At the same time, this ratio should not be excessively small: in zones of shell, adjacent to faces, are local stresses will have great effect. Thus, in application to problems of stability, simplified equations from Table 11.2 are valid for shells of average length; this term is frequently encountered in the literature. More detailed analysis shows that parameters of shells of average length must satisfy the condition (from V. M. Darevskiy)

$$\frac{1}{\sqrt{12(1-\mu^2)}}\frac{h}{R} \ll \left(\frac{L}{\pi R}\right)^2. \qquad (11.18)$$

$$\sqrt{12(1-\mu^2)}\frac{R}{h} \gg \left(\frac{L}{\pi R}\right)^2. \qquad (11.18a)$$

We shall attempt to establish more definite limits for L/R, writing instead of (18) and (18a) the following inequalities:

$$\sqrt{\frac{\pi}{\sqrt{12(1-\mu^2)}}\frac{h}{R}} < \frac{L}{R} < \sqrt{\frac{\sqrt{12(1-\mu^2)}}{\pi}\frac{R}{h}} \qquad (11.18b)$$

or

$$\sqrt{\frac{h}{R}} < \frac{L}{R} < \sqrt{\frac{R}{h}}. \qquad (11.18c)$$

Later we will definitize these relationships from example of problem of axial compression of shell.

Let us consider another variant of simplification of fundamental equations, pertaining to case of weakly expressed wave formation the length of the shell. This variant consists in taking middle surface as inextensional in arc direction ($\varepsilon_y = 0$) and considering, furthermore, that there are no shifts in middle surface ($\gamma = 0$). Further, it is possible to set transverse forces and bending moments in axial direction, and also torques equal to zero: $Q_x = M_x = H = 0$, and take into account only forces Q_y and M_y. Such theory of shells obtained the name of <u>semimembrane</u>.* Here condition (5) is met; therefore, for $\varkappa_y$ we obtain expression (4):

$$\varepsilon_x = \frac{\partial u}{\partial x}, \quad \varkappa_y = -\left(\frac{\partial^2 w}{\partial y^2} + \frac{w}{R^2}\right), \quad \frac{\partial v}{\partial y} = \frac{w}{R}, \quad \frac{\partial u}{\partial y} = -\frac{\partial v}{\partial x}.$$

---

*This theory, application of which is especially appropriate for reinforced (orthotropic) shells, was developed by V. Z. Vlasov [10.3]. Equations (23) belong to him.

From this follows relationship

$$\frac{\partial^2 \varepsilon_y}{\partial y^2} = -\frac{1}{R}\frac{\partial^2 w}{\partial x^2}.$$

Comparing it with expression for $\varkappa_y$, we arrive at following <u>equation of compatibility of deformations</u>:

$$R\frac{\partial^2 \varepsilon_x}{\partial y^2} + \frac{1}{R}\frac{\partial^2 \varepsilon_x}{\partial y^2} = \frac{\partial^2 \varkappa_y}{\partial x^2}. \tag{11.19}$$

Equations (8) obtain form

$$\frac{\partial \sigma_x}{\partial x} + \frac{\partial \tau}{\partial y} + \frac{1}{h} q_x = 0, \quad \frac{\partial \tau}{\partial x} + \frac{\partial \sigma_y}{\partial y} - \frac{1}{Rh}\frac{\partial M_y}{\partial y} + \frac{1}{h} q_y = 0,$$

$$\frac{\partial^2 M_y}{\partial y^2} + \frac{h}{R}\sigma_y + q_z = 0.$$

Uniting them, we obtain <u>equation of equilibrium</u>

$$R\frac{\partial^4 M_y}{\partial y^4} + \frac{1}{R}\frac{\partial^2 M_y}{\partial y^2} + h\frac{\partial^2 \varepsilon_x}{\partial x^2} = P. \tag{11.20}$$

where

$$P = -\frac{\partial q_x}{\partial x} + \frac{\partial q_y}{\partial y} - R\frac{\partial^2 q_z}{\partial y^2}. \tag{11.20a}$$

Relationships of Hooke's law we write in the form

$$\sigma_x = \frac{E}{1-\mu^2}\varepsilon_x \approx E\varepsilon_x, \qquad M_y = \frac{Eh^3}{12(1-\mu^2)}\varkappa_y = D\varkappa_y. \tag{11.21}$$

We introduce variables $\alpha = x/R$ and $\beta = y/R$ and use operator

$$\Omega = \frac{\partial^4}{\partial \beta^4} + \frac{\partial^2}{\partial \beta^2}; \tag{11.22}$$

then equations (19) and (20) will take form

$$\Omega\sigma_x - \frac{12R}{h^3}\frac{\partial^2 M_y}{\partial \alpha^2} = 0, \quad Rh\frac{\partial^2 \varepsilon_x}{\partial \alpha^2} + \Omega M_y = R^2 P'. \tag{11.23}$$

where

$$P' = -\frac{\partial q_x}{\partial \alpha} + \frac{\partial q_y}{\partial \beta} - \frac{\partial^2 q_z}{\partial \beta^2}. \tag{11.24}$$

Excluding σ_x and substituting M_y from (21), we arrive, after the

exclusion (for problems of stability) of operator $(\partial^2/\partial\beta^2 + 1)$, at equation

$$D\nabla\nabla w + Eh\frac{\partial^4 w}{\partial x^4} = -R^4\frac{\partial^2 P^*}{\partial\beta^2}. \qquad (11.25)$$

This equation should be used when investigating stability of shells of average and especially great length with that character of wave formation about which we talked above.

Let us note that equation (19) directly connects change of curvature $\varkappa_y$, characterizing distortion of cross section contour, with deformation ε_x, determining distortion of section in direction of generatrix, i.e., warping of section. Stresses σ_x, appearing with such warping, form in cross section a system of forces, which in Chapter IV we called a bimoment. Thus, the given variant of theory of shells is intimately connected with theory of thin-walled bars.

To the above mentioned equations we shall turn subsequently during solution of linear problems. In nonlinear problems we shall use equations of the theory of flexible shells, given in § 124, considering $k_1 = 0$, $k_2 = 1/R$. Final equations (10.109) obtain form*

$$\frac{D}{h}\nabla^4 w = L(w, \Phi) + \frac{1}{R}\frac{\partial^2\Phi}{\partial x^2}. \qquad (11.26)$$

$$\frac{1}{E}\nabla^4\Phi = -\frac{1}{2}L(w, w) - \frac{1}{R}\frac{\partial^2 w}{\partial x^2}. \qquad (11.27)$$

Additional resolving equation of type (17) will be

$$\frac{D}{h}\nabla^8 w + \frac{E}{R^2}\frac{\partial^4 w}{\partial x^4} - \nabla^4 L(w, \Phi) + \frac{E}{2R}\frac{\partial^2}{\partial x^2}L(w, w) = 0. \qquad (11.28)$$

---

*These equations were first composed by Kármán and Tsien Hsüeh-sêng [11.35]. Equation (28) was obtained by Chien Wei-Zang [10.15].

During study of shells with initial deflection we must use equations (10.111); they change into the following (when q = 0):

$$\left.\begin{aligned}\frac{D}{h}\nabla^4(w-w_0)&=L(w,\Phi)+\frac{1}{R}\frac{\partial^2\Phi}{\partial x^2},\\ \frac{1}{E}\nabla^4\Phi&=-\frac{1}{2}[L(w,w)-L(w_0,w_0)]-\frac{1}{R}\frac{\partial^2(w-w_0)}{\partial x^2}.\end{aligned}\right\} \qquad (11.29)$$

If with the help of equations (26)–(29) we investigate postcritical deformation of shell, then derivatives of Φ with respect for formulas (13) determine total stresses and include, thus, critical forces.

Integrating above-mentioned linear (or nonlinear) equations, we must satisfy boundary conditions. We find what these conditions will be for face sections of closed shell.* With <u>hinged support</u> or <u>clamping</u> of shell on edges x = 0, x = L should be, correspondingly,

$$w=0,\ \frac{\partial^2 w}{\partial x^2}=0 \quad \text{or} \quad w=0,\ \frac{\partial w}{\partial x}=0.$$

Further, it is necessary to formulate conditions, concerning displacements u and v and also forces in the middle surface. If point of edges are freely displaced along generatrix and along the arc, at these points we have $\sigma_x = 0$, $\tau = 0$. In the other limiting case of unshifting edges it is necessary to set u = 0, v = 0. One of the important properties of a shell as an elastic construction consists of the fact that the effect of influences, concentrated in a certain zone, expressed, in formation of moments and transverse forces in sections of shell, during removal of section from this zone is essentially damped.** This circumstance must be considered during study of influence of boundary conditions in concrete problems.

---

*For boundary conditions for open shell (cylindrical panel) see § 139.

**An exception is the case, when influences occur along asymptotic lines, i.e., lines of zero normal curvature. See books [10.6], [10.8], and [10.2].

§ 126. Compression of Closed Shell Along Generatrix. Linear Problem

We turn first of all to problem of stability of closed circular cylindrical shell, subjected to compression along generatrix by forces p, evenly distributed along arc edges (Fig. 11.2). This case of loading is of great practical interest. For instance, the body of an aircraft is subjected on the section of acceleration to action of compressive forces, transmitted from motor. Certain other problems, including the problem of stability of shells during bending, lead, as we will see, to application of results, pertaining to case of central compression. At the same time, circular shell, compressed along generatrix, is a unique standard, serving for comparison of theoretical and experimental data and for a check of different approches in theory of stability of shells.

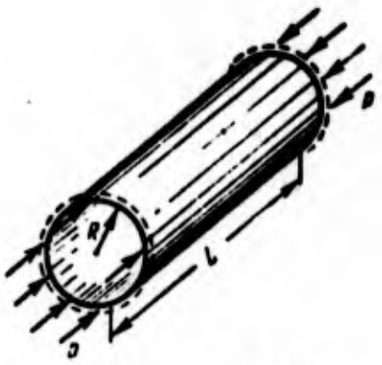

Fig. 11.2. Shell, compressed along generatrix.

Experiments and observations of real constructions shows that character of buckling of compressed shells in practice is not quite such as it is depicted, if one were to originate from linear theory. Critical stresses in experiments are obtained here in three or four times as small as would follow from research of stability of a shell in the small. A more complete solution of this problem may be realized by nonlinear theory of shells. Thus, this classical problem which is, at first sight, elementary, conceals in itself unexpected difficulties; till now they have not been completely surmounted.

We start from consideration of stability of a shell in the small.* We consider that a shell of length L is supported by hinge on faces. We shall use differential equation (17); it takes, in this case, the form

$$\frac{D}{h}\nabla^4 w + \frac{E}{R^2}\frac{\partial^4 w}{\partial x^4} + p\nabla^4\left(\frac{\partial^2 w}{\partial x^2}\right) = 0. \qquad (11.30)$$

Boundary conditions for w will be

$$w = 0,\ \frac{\partial^2 w}{\partial x^2} = 0 \text{ when } x = 0,\ L.$$

Certain conditions, pertaining to displacements u and v we will not set.

As the first variant of solution we assume that deflection surface of shell after buckling is axisymmetric, i.e., that cross section remain circular. Then w will depend only on x and equation (30) changes into the following:

$$\frac{D}{h}\frac{d^4 w}{dx^4} + p\frac{d^2 w}{dx^2} + \frac{E}{R^2}\frac{d^2 w}{dx^2} = 0. \qquad (11.30a)$$

We take for w expression

$$w = f \sin\frac{m\pi x}{L}. \qquad (11.31)$$

satisfying boundary conditions; here m is number of half-waves of deflection surface along length. Obviously, with such character of buckling every longitudinal line is in the same conditions as a compressed bar on an elastic foundation (see Chapter III), such a "foundation" here are the arc fibers.

Putting (31) in equation (30a), we find

$$p = \frac{D}{h}\frac{\pi^2}{R^2} + \frac{E}{\pi^2}. \qquad (11.32)$$

---

*Solution of this problem, belonging to R. Lorentz [11.45] and S. P. Timoshenko [11.23], was given in 1908–1914.

where $\lambda = m\pi R/L = \pi R/l_x$. We determine minimum value of p, equating to zero the derivative of p with respect to λ; here we consider $m \gg 1$. Then we obtain

$$\lambda = \sqrt[4]{12(1-\mu^2)}\sqrt{\frac{R}{h}}, \qquad (11.32a)$$

We designate by p_B the upper critical value of stress, corresponding to point of bifurcation for linear problem; the preceding relationships give

$$p_B = \frac{1}{\sqrt{3(1-\mu^2)}} E\frac{h}{R}. \qquad (11.33)$$

When $\mu = 0.3$, we have

$$p_B = 0.605E\frac{h}{R}. \qquad (11.34)$$

Formula (33) is fundamental in theory of stability of shell. It shows that ratio of upper critical compression stress to elastic modulus of material is of the same order as ratio of thickness of shell to radius of curvature of middle surface.

Judging by (32a), length of half-wave l_x is equal to

$$l_x = \frac{\pi}{\sqrt[4]{12(1-\mu^2)}}\sqrt{Rh}. \qquad (11.35)$$

so that its magnitude is about $\sqrt{Rh}$.

In case of very short shell, if $(L/R)^2 \ll 1$, it is necessary to set $m = 1$, and differentiation expression (32) with respect to λ becomes uneven. But then λ will be great, so that the second member in (32) can be disregarded as compared to the first; hence

$$p_{кр} = \frac{\pi^2 D}{hL^2}. \qquad (11.32b)$$

[cyr. кр may be "crit"]

We obtained the formula of Euler for a strip cut from shell in direction of generatrix.

We turn now to more general variant of solution of problem and assume that deflection surface is not axisymmetric; then it is necessary to originate from differential equation (30). We take for w an expression, also satisfying boundary conditions:

$$w = f \sin \frac{m\pi x}{L} \sin \frac{ny}{R}, \tag{11.36}$$

where m is number of half-waves on generatrix, n is number of full waves on circumference.

Putting (36) in equation (30), we find

$$\frac{D}{h}\left(\frac{m^2\pi^2}{L^2} + \frac{n^2}{R^2}\right)^2 + \frac{E}{R^2}\frac{m^4\pi^4}{L^4} - p\left(\frac{m^2\pi^2}{L^2} + \frac{n^2}{R^2}\right)^2 \frac{m^2\pi^2}{L^2} = 0. \tag{11.37}$$

We introduce dimensionless parameters

$$\hat{p} = \frac{pR}{Eh}, \quad \beta = \frac{m\pi R}{nL}, \quad \eta = \frac{n^2 h}{R}. \tag{11.38}$$

Let us note that quantities β and η it is possible to express through lengths of half-waves of deflection surface along arc ($l_y = \pi R/n$) and on generatrix ($l_x = L/m$):

$$\beta = \frac{l_y}{l_x}, \quad \eta = \frac{\pi^2 Rh}{l_y^2}. \tag{11.38a}$$

Thus, parameter β characterizes outline of hollow, and η, the length of half-wave l_y. From (37) we find

$$\hat{p} = \frac{1}{12(1-\mu^2)} \frac{(1+\beta^2)^2}{\beta^2}\eta + \frac{\beta^2}{(1+\beta^2)^2\eta}. \tag{11.39}$$

Considering numbers m and n sufficiently large, we find minimum $\hat{p}$ from condition

$$\frac{\partial \hat{p}}{\partial \eta} = 0,$$

where

$$\rho = \frac{(1+\beta^2)^2}{\beta^2}\eta;$$

this gives

$$\rho = \sqrt{12(1-\mu^2)}.$$

Upper critical value of parameter $\hat{p}$ is equal to

$$\hat{p}_* = \frac{1}{\sqrt{3(1-\mu^2)}} \approx 0.605. \tag{11.40}$$

Corresponding stress p_B is determined by formula, exactly coinciding with (33).

In the frames of given solution it is impossible to establish simply the form of wave formation of a shell; quantities η and ψ need only to satisfy condition

$$\eta\left(\psi + \frac{1}{\psi}\right)^2 = \sqrt{12(1-\mu^2)} \approx 3.3. \tag{11.41}$$

If we assume that waves are <u>square</u> ($\psi = 1$), we obtain $\eta = 0.825$; hence

$$p_* \approx 0.91\sqrt{\frac{R}{h}}. \tag{11.42}$$

[Trans. Ed. Note: B = upper]

Consequently, loss of stability of shell in the small with formation of hollows, located in checkerboard order, occurs at the same critical stress as in case of axisymmetric buckling, where number of waves along arc is about $\sqrt{R/h}$. We will see subsequently, that this conclusion pertains only to isotropic shells.

Analogous results can be obtained, proceeding from equations about displacements, from Table 11.2. Here it is necessary to set

$$\left.\begin{aligned} u &= A\cos\frac{m\pi x}{L}\sin\frac{ny}{R}, \\ v &= B\sin\frac{m\pi x}{L}\cos\frac{ny}{R}, \\ w &= C\sin\frac{m\pi x}{L}\sin\frac{ny}{R} \end{aligned}\right\} \tag{11.43}$$

and to introduce in third equation of a load member

$$\frac{1-\mu^2}{E}p\frac{\partial^2 w}{\partial x^2}=\varphi\frac{\partial^2 w}{\partial x^2},\ \text{where}\ \varphi=\frac{(1-\mu^2)p}{E};$$

then we arrive at system of algebraic linear equations for A, B, and C. We equate to zero the determinant composed from coefficients with these magnitudes:

$$\begin{vmatrix} \lambda^2+\frac{1-\mu}{2}n^2 & \frac{n(1+\mu)}{2}\lambda & \mu\lambda \\ \frac{n(1+\mu)}{2}\lambda & n^2+\frac{1-\mu}{2}\lambda^2 & n \\ \mu\lambda & n & \varepsilon(n^2+\lambda^2)^2+1-\lambda^2\varphi \end{vmatrix}=0. \qquad (11.44)$$

where, as before, $\lambda = m\pi R/L = \frac{1}{2}n$ and $\varepsilon = h^2/12R^2$. Then we find φ:

$$\varphi=\varepsilon\frac{(n^2+\lambda^2)^2}{\lambda^2}+\frac{(1-\mu^2)\lambda^2}{(n^2+\lambda^2)^2};$$

this corresponds to expression (39) for $\hat{p}$.

All above mentioned formulas pertain to case $n^2 \gg 1$; in <u>more general solution</u> of problem we must originate from system of equations according to Table 11.1. If we use expressions (43) for u, v, and w, we arrive at following equation:*

$$\begin{vmatrix} \lambda^2+\frac{1-\mu}{2}n^2 & \frac{1+\mu}{2}\lambda n & \mu\lambda \\ \frac{1+\mu}{2}\lambda n & (1+\varepsilon)n^2+\frac{(1-\mu)(1+\varepsilon)\lambda^2}{2}-\lambda^2\varphi & n[1+\varepsilon n(n^2+\lambda^2)] \\ \mu\lambda & n[1+\varepsilon n(n^2+\lambda^2)] & \varepsilon(n^2+\lambda^2)^2+1-\lambda^2\varphi \end{vmatrix}=0. \qquad (11.44a)$$

Determining from this φ and $\hat{p}$ depending upon relative length of shell and number of waves, we arrive at results depicted in Fig. 11.3.**

---

*See book of Wang Chi-The [21.21], p. 396.

**Graph of Fig. 11.3 is built for $\mu = 1/6$ and $R/h = 100$; see book of Flügge [10.18], p. 248. Sections, lying between curves $n = 2$, $n = 1$, etc., are obtained by parallel shift of branches, lying to the left; they correspond to other forms of wave formation.

Here along the axis of abscissas are plotted (on sections a and b of Fig. 11.3) different quantities:

$$\omega_1 = \frac{\sqrt[4]{12(1-\mu^2)}}{\pi} \frac{L}{R}\sqrt{\frac{R}{h}}, \quad \omega_2 = \frac{1}{\pi\sqrt[4]{12(1-\mu^2)}} \frac{L}{R}\sqrt{\frac{h}{R}}.$$

and along the axis of ordinates, quantity $k\hat{p}$, where $k = \sqrt{1 - \mu^2}$. Obviously, Fig. 11.3a pertains to short shell, b, to a long one. Descending line in left angle of Fig. a corresponds to equation (32b); every strip of shell bulges, as a plate. Further we obtain a horizontal line on level $1/\sqrt{3} = 0.577$, which corresponds to expression (33). Numbers n here are so big that change during transition from n to (n - 1) is imperceptible. However, in the right part of diagram, for relatively long shells, transition from one integer n to another becomes perceptible. In the figure are depicted only lower parts of curves for various n, lying between points of their intersection. As we see, when $n > 4$ values of $\hat{p}_B$ lie close to value of (33). However, when $n = 3$, and especially, when $n = 2$ minimum of $\hat{p}_B$ dips sharply. Last, on the right curve $n = 2$ is limited by line $n = 1$; this line corresponds to Euler's form of loss of stability of shell as a bar; really, when $n = 1$ any section of pipe shifts, as a rigid whole.

Radius of gyration of circular section of thin pipe is equal to $i = R/\sqrt{2}$; Euler's stress is equal to $\sigma_э = \pi^2 ER^2/2L^2$, where

$$\hat{p} = \frac{\pi^2 R^2}{2L^2 k}.$$

Thus, here we pass from <u>local</u> loss of stability to <u>general</u>. Consideration of Fig. 11.3 allows us to determine range of values of L/R, for which it is possible to consider formula (33) valid. On the left it is bounded by value $\omega_1 \approx 0.8$, on the right, by value

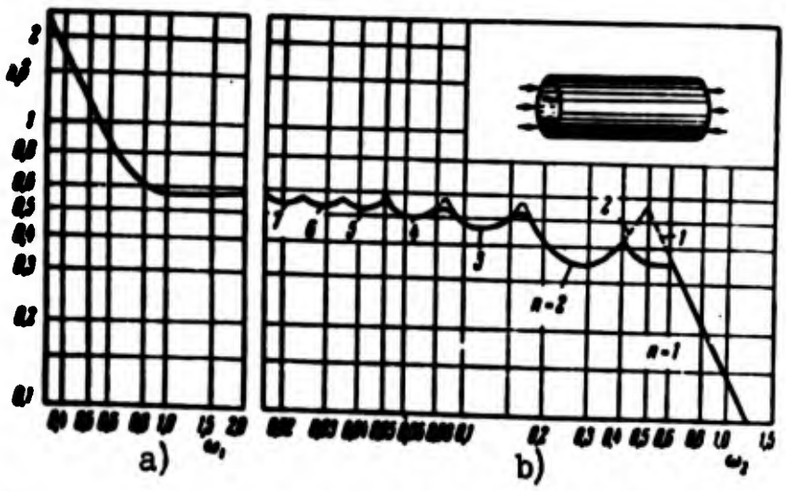

Fig. 11.3. Values of upper-critical stress in case of compression along generatrix.

$\omega_2 \approx 0.1$. Here ratio L/R lies within

$$1.38\sqrt{\frac{h}{R}} < \frac{L}{R} < 0.57\sqrt{\frac{R}{h}}.$$

which approximately corresponds to (18b). For instance, when R/h = = 100 we find $0.14 < L/R < 5.7$. As we see, limits of applicability of theory of shells of average length are comparatively great and embrace a significant part of range of values of L/R encountered in practice.

Let us consider now more specifically cases n = 2 and n = 3, when shell buckles with formation of long waves. In § 125 there was prepared for that the apparatus of semimembrane theory of shells. We shall use equation (25). Here it is necessary to take displacements v and w as mutually comparable and in (24) set $q_x = 0$, $q_y = -ph\frac{\partial^2 v}{\partial x^2}$, $q_z = -ph\frac{\partial^2 w}{\partial x^2}$; then

$$-P' = \frac{\partial}{\partial\varphi}\left(ph\frac{\partial^2 w}{R^2\partial\alpha^2}\right) - \frac{\partial^2}{\partial\beta^2}\left(ph\frac{\partial^2 w}{R^2\partial\alpha^2}\right).$$

But from initial relationships (p. 559) it follows that $\frac{\partial v}{\partial \beta} = w$; therefore,

$$-P' = p\frac{h}{R^2}\frac{\partial^2}{\partial \alpha^2}\left(w - \frac{\partial^2 w}{\partial \beta^2}\right).$$

Considering $w = W(\alpha) \sin n\beta$, we bring (25) to form*

$$EhR^2\frac{d^4W}{d\alpha^4} + \frac{Eh^3}{12(1-\mu^2)}n^4(n^2-1)^2W = -phR^2n^2(n^2+1)\frac{d^2W}{d\alpha^2}. \qquad (11.25a)$$

Taking $W = f \sin m\pi R\alpha/L$, we obtain:

$$p = \frac{E}{n^2+1}\left[\frac{\lambda^2}{n^2} + \frac{\varepsilon n^2(n^2-1)^2}{\lambda^2(1-\mu^2)}\right].$$

where, as before, $\varepsilon = h^2/12R^2$. Minimizing p with respect to λ, we find $\lambda^2 = \varepsilon^{1/2}n^2(n^2 - 1)/(1 - \mu^2)^{1/2}$; hence

$$\hat{p}_B = \frac{1}{\sqrt{3(1-\mu^2)}}\frac{n^2-1}{n^2+1}$$

or, for $\mu = 0.3$,

$$\hat{p}_B \approx 0.605\frac{n^2-1}{n^2+1}. \qquad (11.45)$$

This remarkable formula can be obtained also from general equation (44a), disregarding certain members. Very interesting is the limiting case n = 2, when minimum of $\hat{p}_B$ goes far downwards; from (45) we find $\hat{p}_B = 0.363$. Thus, here $\hat{p}_B$ constitutes 0.6 of "classical" value. When n = 3 this ratio is equal to 0.8. When $n^2 \gg 1$ we again obtain $\hat{p}_B \approx 0.605$.

Thus, for very long shells we must obtain lowering of critical stress as compared to (33).

---

*Equation of type (25a) is derived for reinforced shell by another method by K. D. Turkin [11.24].

§ 127. Nonlinear Problem

As we have seen, to upper critical stress (33) there corresponds a form of deflection surface according to (31) with axisymmetric buckling and according to (36) without symmetry. These two variants are depicted in Fig. 11.4a and b. However character of buckling of real shells of average length will agree with neither one of these variants. Instead of hollows of right-angle outline, arranged in checkerboard order and turned alternately toward center and from center of curvature (Fig. 11.4b), in reality there are formed diamond-shaped hollows, similar to edge of a crystal, as it is shown in Fig. 11.4c. These hollows, depth of which already in original moment is comparable with thickness of shell, usually appear in process of a sharply expressed knock. In most cases hollows constitute two or three adjacent belts. However, in separate experiments with carefully made test pieces we managed to obtain grid of diamond-shaped deepenings on the whole surface of shell or on a large part of it. Thus, here absolutely clearly there is realized loss of stability of shell in the large. From this follows the necessity of solution of problem from tenets of nonlinear theory; it was first given by Kármán and Tsien Hsüch-sêng [11.27]. These authors used the same method as is usually applied in theory of flexible plates (see Chapter VII). It consists of selection of approximating expression for deflection w, containing several modified parameters, and substitution of this expression in the right part of equation (27). Integration of this equation determines function of stresses. Further we calculate energy of system; varying energy with respect to Φ parameters of deflection, we find diagram of equilibrium states of shell. Problem is complicated by the fact that

in process of buckling number and dimensions of hollows are variable; therefore, diagram of equilibrium forms constitutes an envelope of a certain series of curves, corresponding to one or another numbers of waves. In works of other authors, published in the last two decades, there were offered definitized variants of solving the problem. In certain works instead of the Ritz method there was used the Bubnov-Galerkin method in application to equation (26).

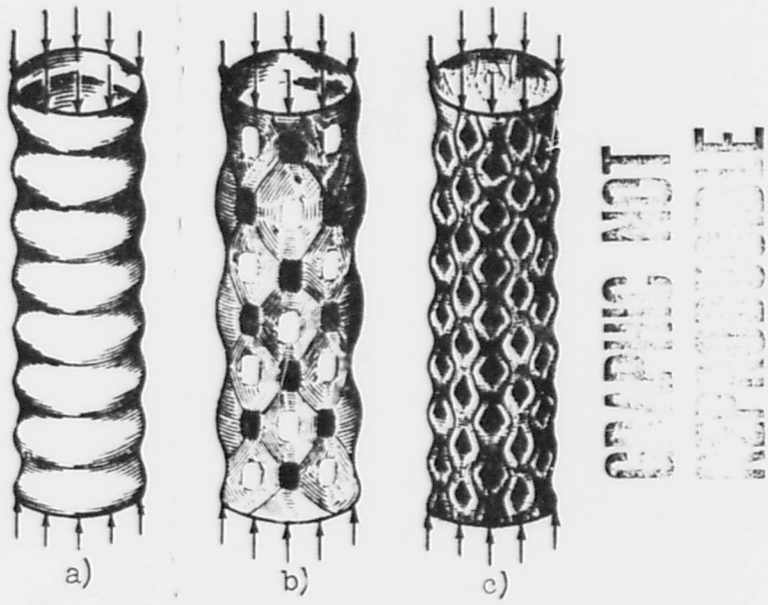

Fig. 11.4. Different forms of buckling of shell; a) axisymmetric, b) "checkerboard," c) diamond-shaped.

We shall give one of the simplest variants of solution of problem by Ritz method.* We select expression for w in the form

$$w = f_1 \sin \frac{m\pi x}{L} \sin \frac{ny}{R} + f_2 \sin^2 \frac{m\pi x}{L} + f_0. \qquad (11.46)$$

*This solution belongs to P. G. Burdin.

The first of these members is taken proceeding from solution of problem of stability in the small and coincides with (36). Second member reflects as symmetry of deflection relative to middle surface, with dominant direction toward center of curvature. If, summarizing first two members, we construct lines of equal deflection, they will give outline of hollows, recalling Fig. 11.4c. Last, third member in (46) corresponds to radial displacements of points on face sections for x = 0, L. This member does not depend on y; it is considered that during buckling of shell face sections remain circular.

We introduce designation

$$r = \frac{mnR}{L} = n\beta \tag{11.47}$$

for ratio of length of semi-circumference to length of half-wave along generatrix; instead of (46), we obtain

$$w = f_1 \sin\frac{rx}{R}\sin\frac{ny}{R} + f_2\sin^2\frac{rx}{R} + f_0. \tag{11.48}$$

Putting (48) in the right part of equation (27), we find

$$\frac{1}{E}\nabla^4\Phi = f_1^2\frac{r^2n^2}{2R^4}\left(\cos\frac{2rx}{R}+\cos\frac{2ny}{R}\right)+ \\ + f_1f_2\frac{r^2n^2}{R^4}\left(\sin\frac{3rx}{R}\sin\frac{ny}{R}-\sin\frac{rx}{R}\sin\frac{ny}{R}\right)+ \\ + f_1\frac{r^2}{R^2}\sin\frac{rx}{R}\sin\frac{ny}{R}-2f_2\frac{r^2}{R^2}\cos\frac{2rx}{R}. \tag{11.49}$$

Integral of this equation will be

$$\frac{1}{E}\Phi = f_1^2\cdot\frac{r^2n^2}{2}\left(\frac{1}{16n^4}\cos\frac{2ny}{R}+\frac{1}{16r^4}\cos\frac{2rx}{R}\right)+ \\ + f_1f_2r^2n^2\left[\frac{1}{(3r,\,n)}\sin\frac{3rx}{R}\sin\frac{ny}{R}-\frac{1}{(r,\,n)}\sin\frac{rx}{R}\sin\frac{ny}{R}\right]+ \\ + f_1\frac{r^2R}{(r,\,n)}\sin\frac{rx}{R}\sin\frac{ny}{R}-f_2\frac{R}{8r^2}\cos\frac{2rx}{R}-\frac{py^2}{2E}; \tag{11.49a}$$

here under p is understood <u>mean</u> value of compressive forces in face section; there is introduced designation

$$(ar,\ bn)=[(ar)^2+(bn)^2]^2. \tag{11.50}$$

Knowing functions Φ and w one can determine stresses and deformations in middle surface, and also displacements u and v. Special attention should be paid to seeing that these functions satisfy condition of periodicity or closure. This pertains, first of all, to displacement v; increase of v with change of y by $2\pi R$ should be equal to zero:

$$\int_0^{2\pi R}\frac{\partial v}{\partial y}dy=0. \tag{11.51}$$

Using relationships (10.98) and (13), we find

$$\varepsilon_2=\frac{\partial v}{\partial y}+\frac{1}{2}\left(\frac{\partial w}{\partial y}\right)^2-\frac{w}{R}. \tag{11.52}$$

$$\varepsilon_2=\frac{1}{E}\left(\frac{\partial^2\Phi}{\partial x^2}-\mu\frac{\partial^2\Phi}{\partial y^2}\right). \tag{11.53}$$

hence instead of (51), we obtain

$$\int_0^{2\pi R}\left[\frac{1}{E}\left(\frac{\partial^2\Phi}{\partial x^2}-\mu\frac{\partial^2\Phi}{\partial y^2}\right)-\frac{1}{2}\left(\frac{\partial w}{\partial y}\right)^2+\frac{w}{R}\right]dy=0. \tag{11.54}$$

Substituting (48) and (49a), we find

$$\frac{f_0}{R}=-\mu\frac{p}{E}+f_1\frac{n^2}{8R^2}-\frac{f_1}{2R}. \tag{11.55}$$

We determine, further, total energy of system:

$$\vartheta=U_c+U_u-W. \tag{11.56}$$

where U_c is potential strain energy of middle surface, U_H is potential energy of bending, W is work of external forces. First two magnitudes we find by formulas (10.95). For calculation of work of forces p we find mean value of approach of points belonging to faces of shell:

$$\Delta=-\int_0^L \frac{\partial u}{\partial x}\,dx=-\int_0^L\left[\frac{1}{E}\frac{\partial^2\Phi}{\partial y^2}-\frac{\mu}{E}\frac{\partial^2\Phi}{\partial x^2}-\frac{1}{2}\left(\frac{\partial w}{\partial x}\right)^2\right]dx; \tag{11.57}$$

then

$$W=-\frac{h}{E}\int_0^L\int_0^{2\pi R}\left(\frac{\partial^2\Phi}{\partial y^2}\right)_{x=0,\,L}\left[\frac{\partial^2\Phi}{\partial y^2}-\mu\frac{\partial^2\Phi}{\partial x^2}-\frac{E}{2}\left(\frac{\partial w}{\partial x}\right)^2\right]dx. \tag{11.58}$$

Finally

$$\begin{aligned}\Theta=&\frac{D\pi L}{4R^2}\left[f_1^2(r,n)+8f_2^2r^4\right]+\frac{E\pi Lh}{4R^2}\left\{\frac{1}{32}f_1^4(r^4+n^4)+\right.\\&+f_1^2f_2^2\,(rn)^4\left[\frac{1}{(3r,n)}+\frac{1}{(r,n)}\right]+R^2f_1^2\frac{r^4}{(r,n)}+\frac{R^2}{2}f_2^2-\\&\left.-\frac{R}{4}f_1^2f_2n^2\left[1+\frac{8r^4}{(r,n)}\right]\right\}-\frac{\pi LhR}{E}p^2-2\pi LhRp\left(f_1^2\frac{r^2}{8R^2}+f_2^2\frac{r^2}{4R^2}\right).\end{aligned} \tag{11.59}$$

Solving problem in <u>first approximation</u>, we vary energy with respect to two parameters:

$$\frac{\partial\Theta}{\partial f_1}=0,\quad \frac{\partial\Theta}{\partial f_2}=0. \tag{11.60}$$

We introduce designations supplementing (38):

$$\zeta_1=\frac{f_1}{h},\quad \zeta_2=\frac{f_2}{h},\quad \psi=\frac{f_2}{f_1}; \tag{11.61}$$

then equation (60) will take form

$$\begin{aligned}&\frac{\eta(1+\vartheta^4)}{16\vartheta^2}\zeta_1^2+\eta\vartheta^2\left(\frac{1}{s_1^2}+\frac{1}{s_2^2}\right)\zeta_2^2+\frac{\vartheta^2}{s_1s_2}+\\&\qquad+\frac{\eta\zeta_1^2}{12(1-\mu^2)\vartheta^2}-\frac{1}{4\vartheta^2}\left(1+\frac{8\vartheta^4}{s_1^2}\right)\zeta_2=\hat{p}.\end{aligned} \tag{11.62}$$

$$\zeta_1^2=\frac{\left[\frac{1}{4\vartheta^2\eta}+\frac{\eta\vartheta^2}{3(1-\mu^2)}-\hat{p}\right]\zeta_2}{\frac{1}{16\vartheta^2}\left(1+\frac{8\vartheta^4}{s_1^2}\right)-\frac{\eta\vartheta^2}{2}\left(\frac{1}{s_1^2}+\frac{1}{s_2^2}\right)\zeta_2}. \tag{11.63}$$

where

$$s_1=1+\vartheta^2,\quad s_2=1+9\vartheta^2.$$

Substituting ζ_1^2 from (63) in (62), we arrive at equation connecting $\hat{p}$ and ζ_2, and considering $\zeta_2 = 0$, we arrive at former formula (39) for $\hat{p}$, obtained by linear theory. Selecting, further, definite values of $ and η we construct curves $\hat{p}(\zeta_2)$. In Figs. 11.5 and 11.6 there are shown two series of such curves for $ = 0.5 and $ = 0.6; calculations were also given for 12 other values of $, lying within limits $0.3 < $ < 2.4$. Dotted lines are envelopes of curves, corresponding to different values of η. In comparing all variants it turned out that least magnitude of $\hat{p}$ – lower critical stress – corresponds to parameters $ = 0.6, $\eta = 0.19$, $\zeta_1 = 7.2$, $\zeta_2 = 3.04$ and is equal to $\hat{p}_н = 0.124$.

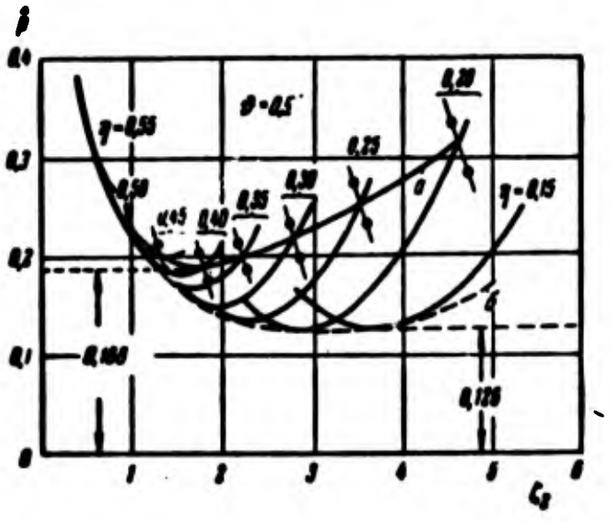

Fig. 11.5. Equilibrium forms of shell at $ = $l_y/l_x = 0.5$, to research in first and second approximations.

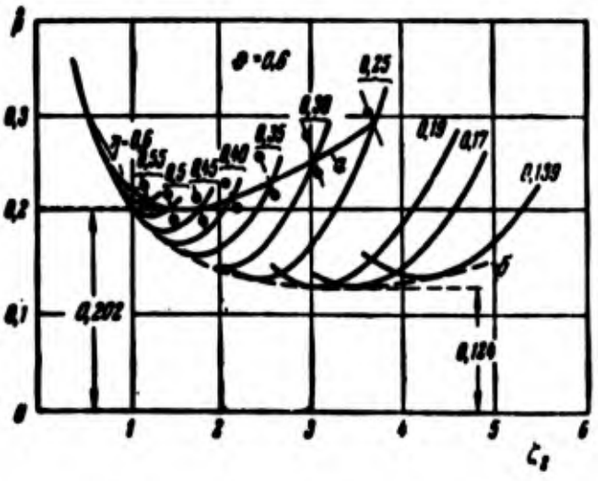

Fig. 11.6. Equilibrium forms of shell when $ = $l_y/l_x = 0.6$.

In second approximation we vary energy of system additionally for n and constitute equation

$$\frac{\partial \Theta}{\partial n} = 0; \qquad (11.64)$$

it takes form

$$\frac{\eta s_1}{6(1-\mu^2)\vartheta^3}+\frac{\eta}{16\vartheta^2}\zeta_1^2-\frac{2\vartheta^2}{(1+\vartheta^2)^3\eta}+$$
$$+2\eta\vartheta^4\left(\frac{1}{s_1^3}+\frac{9}{s_2^3}\right)\zeta_2^2-\frac{1}{4\vartheta^2}\left[1-\frac{8\vartheta^4(1-\vartheta^2)}{(1+\vartheta^2)^3}\right]\zeta_2=0. \qquad (11.65)$$

Combining equation (65) with (62) and (63), we find new dependence $\hat{p}(\zeta_2)$. Corresponding curves for different η and Ψ are shown in Figs. 11.5 and 11.6 by dotted lines. Connecting anew resulting points of intersection, we find new envelope (solid line). In Fig. 11.7 are compared envelopes for different Ψ. Least value of $\hat{p}$ occurs when $\Psi = 0.48$, $\eta = 0.4$, $\zeta_1 = 3.45$, $\zeta_2 = 1.9$ and is equal to $\hat{p}_H = 0.186$. Thus, in second approximation lower critical stress turned out to be equal to

$$p_* = 0.186\frac{h}{R}. \qquad (11.66)$$

which constitutes approximately 30% of upper value (34).

Obtained data allow us to construct diagram of dependence of parameter of load from magnitude $\hat{e}$, characterizing mutual approach of faces of shell: $\hat{e} = \Delta R/Lh$. By formula (57) we find

$$\hat{e}=\hat{p}+\frac{\eta\vartheta^2}{8}\left(\zeta_1^2+\frac{1}{2}\zeta_2^2\right). \qquad (11.67)$$

When $\zeta_1 = \zeta_2 = 0$, we obtain straight line $\hat{e} = \hat{p}$, depicted in Fig. 11.8; it corresponds to initial equilibrium state. Point of bifurcation A corresponds to $\hat{p}_B = 0.605$. Here, there branches off curve ABC of bending forms, points of which correspond to different Ψ and η; values of Ψ are shown in the figure. As we see, transition from unstable forms to stable and further development of postcritical deformations is connected with growth of parameter Ψ; judging by (38a), this means that hollows are drawn along arc. We must assume that on section AB parameter Ψ sharply drops, and near point B starts to increase gradually.

Thus, postcritical diagram $\hat{p}(\hat{e})$ consists of "falling" branch, corresponding to unstable equilibrium states, and "ascending" branch of stable states. We considered that process of transition from some equilibrium forms to others is static. But since unstable equilibrium states are not realized, then shell should pass from initial form to bent stable form dynamically, by a knock.

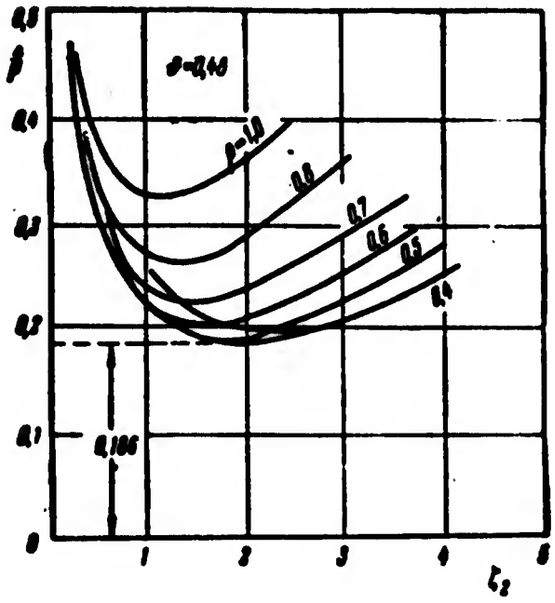

Fig. 11.7. Equilibrium forms of shell when $\$ = l_y/l_x =$ $= 0.48$. The lower critical stress corresponds to $\hat{p} =$ $= 0.186$.

In § 118 we talked only about such a case, when knock occurs with constant external load. But this case comparatively rarely is realized in practice. If shell was located vertically and was subjected to compression by load of definite weight, then requirement $\hat{p} = \text{const}$ could be realized; however such experiments are difficult to conduct. During compression of shell in testing machine it is possible also to create fixed load, but for that the machine had to be supplied with special attachment, including gas "cushion," during knock of shell gas contained in this "cushion" (for instance, air or nitrogen*) expands, keeping pressure to constant. Other limiting

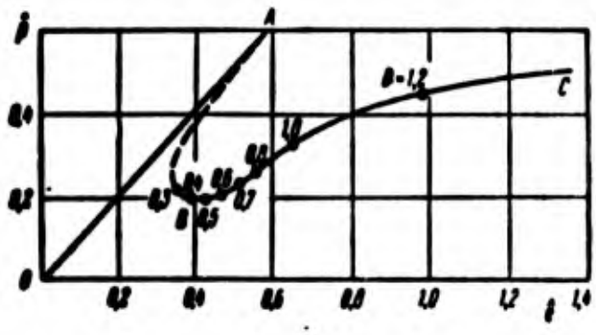

Fig. 11.8. Diagram "compressive force — approach of edges."

*To avoid explosion it is better to use nitrogen.

case consists that in process of knock there is fixed general deformation of shell $\hat{e}$. Such requirement $\hat{e}$ = const may be realized only under conditions very rigid testing machine, distance between plates of which remains unchanged during knock. Usually, however, construction of testing machine is elastic, so that during sharply increasing deformacion of shell there simultaneously is lowered load applied to it. This is possible to illustrate by Fig. 11.9: compressed spring A, simulating elastic part of loading device of machine, is unloaded during knock of shell. In real constructions, members connected with shell usually also are elastic. Character of knock in two limiting cases and in the presence of elastic linkage is depicted in Fig. 11.10. Reverse knock should occur on dotted lines. In one way or the other, diagram of equilibrium states is limited from below by load $\hat{p}_H$; therefore, as already said in § 118, for practical calculations it is of great interest.

Fig. 11.9. Shell in testing machine.

We turn to other solutions of problem of stability of compressed cylindrical shell in the large. In book [0.3] in detail there is presented variant of solution of problem, belonging to V. L. Agamirov, with selection of approximating expression for w in form

$$w = f_1 \sin\frac{m\pi x}{l}\sin\frac{ny}{R} + f_2 \sin^2\frac{m\pi x}{l}\sin^2\frac{ny}{R} + f_0. \qquad (11.68)$$

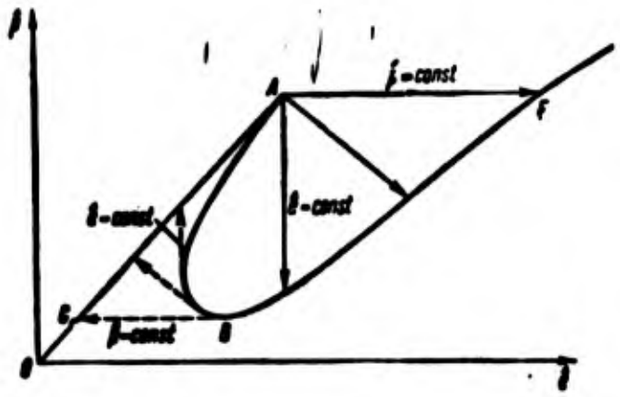

Fig. 11.10. Different variants of knock of shell.

differing from (48) in the second member. Magnitude $\hat{p}_H$ turned out to be in first approximation equal (with variation of energy with respect to two parameters) to 0.284, and in second (with four varied parameters) equal to 0.334, corresponding to value $\$ = 0.59$. Comparison with preceding variant shows how the insignificant, one would think, change of structure of second member in (48) influences results of solution: value $\hat{p}_H$ increased approximately by factor of two. This pertains also to other nonlinear problems of stability of shells. Similarly to the way real shell sharply react to small perturbations, which leads to large scattering of critical stresses (see § 129), results of solution of corresponding problems according to Ritz method strongly change even with insignificant change of approximating expression for deflection.

In initial solution of Kármán and Tsien Hsüeh-sêng [11.27] second member of expression (48) was selected in the form $f_2(\cos\frac{2m\pi x}{L} + \cos\frac{2ny}{R})$, and there was obtained for square waves ($\$ = 1$) $\hat{p}_H = 0.194$. Later Michielson [11.46] found, in definitized solution, $\hat{p}_H = 0.195$. Kempner [11.38] introduced in place of second member the expression $(f_2\cos\frac{2m\pi x}{L} + f_3\cos\frac{2ny}{R})$ and conducted variation for five parameters (f_1, f_2, f_3, $\$$ and η); as a result he obtained $\hat{p}_H = 0.182$ for $\$ = 0.36$.

Thus, available solutions according to Ritz method* lead to values of $\hat{p}_H$, lying from 0.182 to 0.334.

In all the above-mentioned solutions parameter $\hat{p}_H$ did not depend on ratio R/h; this ensued from structure of initial relationships. However S. A. Alekseyev [11.2], using method of successive approximations, arrived at another conclusion, consisting in the fact that magnitude $\hat{p}_H$ decreases with growth of R/h.

Such uncertainty of values of $\hat{p}_H$ found till now anew testifies to great sensitivity of results of approximate solution to method of calculation. In further research a large role should be played by application of digital computers (see § 139).

§ 128. Geometric Approach to Problem

Selecting approximating expression for deflection, we sought to reflect inclination of shell to bulge in rhombic form. We come now to phenomenon of knocking of shell from geometric point of view, and we shall endeavor more specifically to study character of wave formation appearing as the result of knocking. If shell continued, after loss of stability, to bulge in the same symmetric form** (31) or (36), which is reflected by linear theory, then this would be connected with expenditure of significant work on deformation of middle surface. As was already said in § 118, shell in many cases "prefers" to bulge inward, and therefore, here middle surface does not receive significant tensile-compressive deformations. Therefore, it is expedient

---

*See also work of Ye. D. Golitsinskaya [11.6] and N. N. Leont'yev [11.13].

**By symmetry here there is conditionally understood equality maximum deflection toward and from center of curvature.

to consider such a limiting case of wave formation of shell, in which there is no additional strain energy in middle surface in general.* But as we know from § 118, besides here the deflection surface should be isometric to initial surface of circular cylinder. In other words, Gaussian curvature at every point of new surface should remain equal to zero.

Such geometric curving is not continuous and is realized in process of knocking of shell.

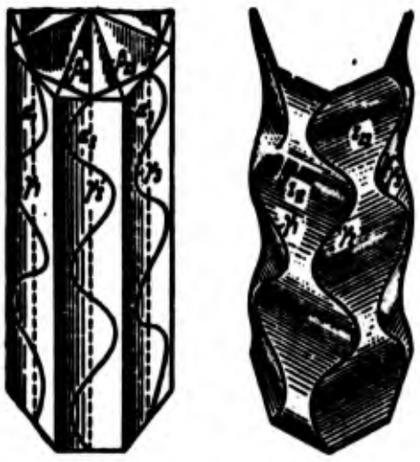

a) b).

Fig. 11.11. Construction of surface, isometric to cylinder.

In order to obtain desired surface, isometric to circular cylinder, we proceed in the following manner. Let there be given a regular prism with even number of faces, as depicted in Fig. 11.11. We draw on one of lateral faces α_1 a certain smooth curve γ_1, simply projecting on axis of prism; in figure this curve is depicted for an example in the form of a sinusoid, zero points of which pass through center line of face. Then we draw on neighboring face α_2 curve γ_2, the mirror image of γ_1 relative to plane β_{12} passing through axis of prism and rib δ_{12}. We repeat the same construction for the following faces; then we obtain curves γ_3, γ_4, etc.

---

*Detailed research in this region was done by A. V. Pogorelov [11.19] and [11.20]. Below there is expounded a method of construction of isometric surfaces offered by him. See also article of Kirste [11.38].

We now construct cylindrical surface Z_{12} in such a way that it passes through curves γ_1 and γ_2 and so that its generatrices are perpendicular to plane β_{12} (Fig. 11.11b). By this means we make surfaces Z_{23}, Z_{34}, etc. Tubular surface, consisting of Z_{12}, Z_{23}, etc., is the sought one. This is easily shown.

Really, it is obvious that at points, not belonging to curves γ_1, γ_2, ..., newly formed surface has zero Gaussian curvature, so that it is isometric to initial one. But also at points of curves γ_1, γ_2, ..., isometry is preserved, since, if we reflect cylindrical surface Z_{23} specularly in plane of face α_2, then the obtained surface Z^*_{23} will be a continuation of surface Z_{12}.

In cross section of newly formed tubular surface we will obtain closed curve. It is possible to show that length of this line by the same in all sections independently of form of lines γ_1, γ_2, ...; it is equal to perimeter of regular polygon (see Fig. 11.11a), vertices of which coincide with middles of sides in section of initial prism. We shall consider length of this line equal to $2\pi R$, where R is radius of curvature of isometric cylindrical surface. We note also that length of line of intersection of tubular surface with plane, passing through axis of prism and any rib, is equal to height of cylinder.

Consequently, obtained tubular surface is isometric to circular cylinder of radius R. Since this conclusion does not depend on form of curve γ, then such a construction is essentially universal.

With development of postcritical deformation of shell the form of deflection surface should change; this is possible to depict, increasing amplitude of sinusoid in Fig. 11.12a. If we now replace

sinusoid by rectilinear segments with smoothed sections at places of linkages, then at the limit we obtain surface depicted in Fig. 11.12b. We arrived at those characteristic of "crystal edges" about which we talked in § 127. Thus, geometric approach to problem allows us to investigate character of surface of shell after knocking qualitatively. It is possible to try to use obtained isometric model also for quantitative appraisal of lower critical stress.

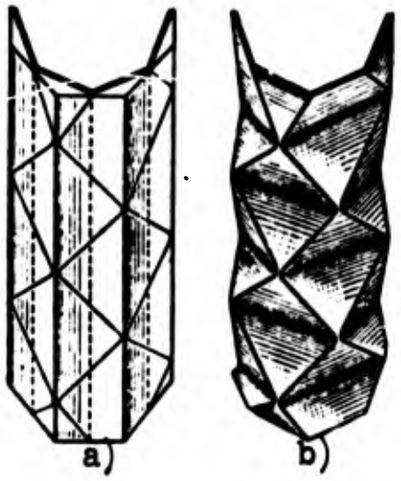

Fig. 11.12. Surface isometric to cylinder, with "crystal edges."

As soon as we will disregard deformations in middle surfaces, nonlinear members in fundamental equations connected with them disappear. Potential strain energy of shell during buckling will consist only of energy of bending.

We meet first the method of approximation of **Kirstein** [11.39], consisting of isolation of curvilinear strips from shell in longitudinal direction. We consider stability of such strip of radius R, length l_x and width l_y, compressed along length, taking into account "elastic foundation," formed thanks to supporting influence of arc strips (see example 3.4, p. 171).

Cross-section of two neighboring strips is shown in Fig. 11.13. Moment of inertia of line is taken approximately equal to $I = l_y^5 h/720R^2$. Considering that in transverse direction strip is bent in a sinusoid $w = f \sin(\pi y/l_y)$, we determine reaction of elastic

foundation per unit deflection:

$$r=\frac{1}{f}\int_0^{l_y} D\frac{d^4w}{dy^4}\,dy=\int_0^{l_y} D\frac{\pi^4}{l_y^4}\sin\frac{\pi y}{l_y}\,dy=\frac{2\pi^2 D}{l_y^2}.$$

Determining critical stress $p_{кр}$ by formula of type (3.115), we find

$$\hat{p}_{кр}=\frac{\pi^2 lR}{l_x^2 l_y h^2}+r\frac{l_x^2 R}{\pi^2 l_y h^2}=\frac{\pi^2 R}{6(1-\mu^2)h}\left(\frac{l_y^4}{120R^2 l_x^2}+\frac{h^2 l_x^2}{\pi l_y^4}\right).$$

Minimizing $\hat{p}_{кр}$, we obtain

$$\frac{l_y^4}{l_x^2}=\sqrt{\frac{120}{\pi}}Rh,\quad \hat{p}_{кр}=\frac{\pi^2}{3(1-\mu^2)\sqrt{120\pi}}\approx 0{,}187. \qquad (11.69)$$

The first of these equalities gives, in designations of § 126, $\Phi = 0.75\sqrt{\eta}$. It is interesting to note that such elementary approach leads to magnitude of $\hat{p}_{кр}$ very close to lower critical stress of § 127; even relationship between Φ and η corresponds to data of above-mentioned variant of solution according to Ritz method.

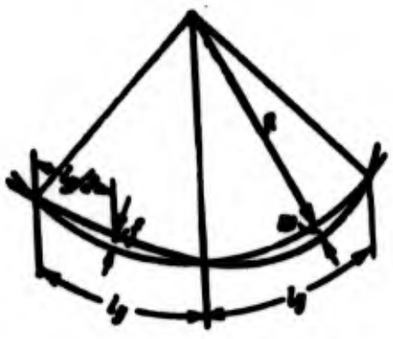

Fig. 11.13. Approximate determination of lower critical stress.

In work of A. V. Pogorelov ([11.19], Parts 1 and 2) is given determination of $\hat{p}_{кр}$ with help of energy method, proceeding from above-described presentation of deflection surface. Potential energy of bending is calculated separately for smooth sections of surface and for zones, adjacent to ridges on boundaries of hollows. In one variant of solution it was assumed that hollows are square, and lines γ were represented by rectilinear segments, joined by arcs of parabolas. Lower critical load for

elastic shell was determined from condition of "joining" of ridges of neighboring hollows, and was obtained $\hat{p}_H = 0.138$. If however lines γ are selected in the form of arcs of sinusoids, then upon different assumptions about initial state of strain of shell we will have $\hat{p}_H = 0.15$ and $\hat{p}_H = 0.18$.

§ 129. Results of Experiments. Data for Practical Calculations

We turn to experimental data pertaining to magnitude of critical stress and character of wave formation. These data are contradictory, since they strongly depend on initial incorrectnesses in form of shell and conditions of loading.

Let us consider first of all results of tests of metal shells, prepared with great care, as a rule, by machining of lathe by a special template, with minimum deflections of thickness of wall and radius of curvature from given values.*

In similar tests up to knock we managed to observe – best of all by distortion of light bands on surface of test piece – formation hardly noticeable rectangular hollows of a type which corresponds to buckling in the small in Fig. 11.4b. Such preliminary hollows turn out to be approximately "square;" dimensions of them along generatrix and along arc are close. Then there occurs sharp knock, after which on piece there appear hollows of rhombic type as in Fig. 11.4c, and here diagonals of hollow are approximately equal. Load, recorded by manometer of machine, sharply drops during knock. If, however, we continue to load test piece, then force of compression is slightly increased, and hollows extend along arc. Unfortunately, during tests of steel or duralumin piece we usually cannot conduct experiment in pure form, since in zones, adjacent to ridges of hollows, there are formed plastic deformations. If equilibrium forms of shell were changed statically, according to diagram $\hat{p}(\hat{e})$ Fig. 11.10, then initial hollows, corresponding to point A in Fig. 11.14, should have

---

*Such tests were conducted by L. R. Ispravnikov, V. L. Agamirov, and other authors: see [0.3], pp. 320-325.

been strongly stretched along generatrix, as shown for point B, and only then gradually change form, extending along the arc. But in real dynamic process, the shell, apparently, "skips" intermediate equilibrium forms, so that on diagram of Fig. 11.14 we arrive directly at point C with "square" hollows. Parameter of stress, at which knock occurs, for such pieces constitutes $\hat{p}_{кр} \approx 0.23$–$0.35$. As we see, even with very thorough carrying out of experiment critical stress constitutes only about half of upper value $\hat{p}_{в}$.

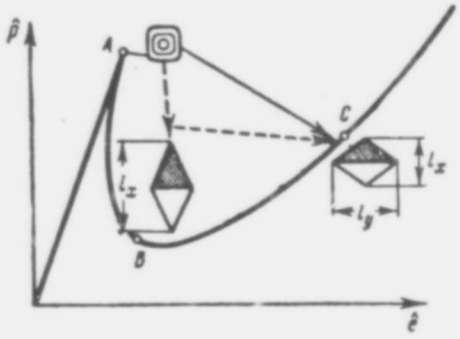

Fig. 11.14. Forms of hollow with diverse variants of knock.

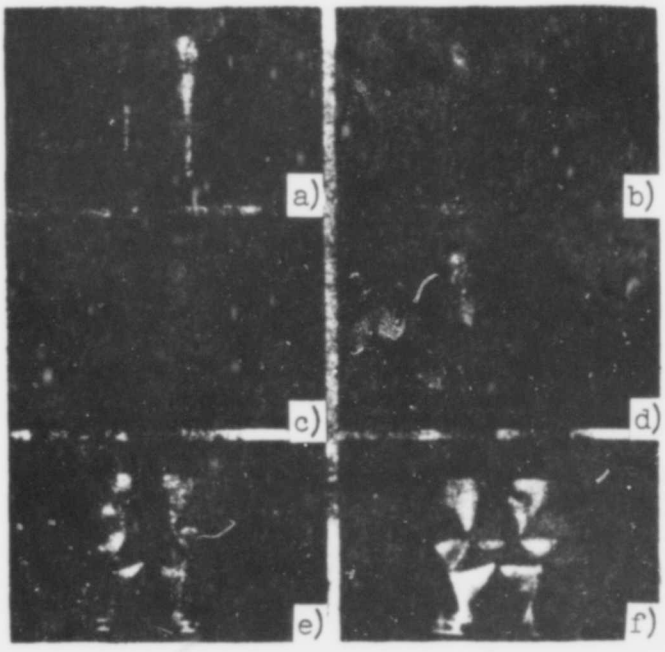

Fig. 11.15. Consecutive stages of formation of diamond-shaped dents.

During tests of shells, prepared crudely, e.g., from folded flat sheet, it is usually possible to note already at small loads formation of single hollows in places, where there are various perturbations, initial deflection or concentration of stresses. Subsequently, there occurs a series of knocks, leading to appearance of new hollows.

Such process is shown in photograph of Fig. 11.15, pertaining to steel shell ($L/R = 1.4$, $R/h = 1870$).* Finally there will be formed the same system of rhombic hollows as in case of carefully prepared samples.

In Fig. 11.16 is shown region of experimental values of $\hat{p}_{кр}$, taken from works of different authors. As we see, magnitude $\hat{p}_B = 0.605$ indeed is upper boundary for real critical stresses. From theoretical research it follows that buckling of shells should occur at dimensionless stresses, lying between $\hat{p}_H$ and $\hat{p}_B$. Since final value of $\hat{p}_H$ still has not been found, it is difficult to judge how far this assumption is justified. Significant part of experiments leads to values of $\hat{p}_{кр}$ lying above 0.18. However, certain experimental points lie below this magnitude and in separate cases turn out to be equal to 0.06–0.15. Fig. 11.16 indicates evident tendency of $\hat{p}_{кр}$ to drop during growth** of ratio R/h. Such result, as we have seen, was not obtained in any of works, bases on Ritz method, and came only from research of S. A. Alekseyev. It is necessary to recall that with increase of R/h probability of appearance of initial deflections should increase; this, undoubtedly, should lead to lowering of average magnitude of real critical stresses (see Chapter XX).

---

*These photographs were obtained by S. Kanemitsu and N. H. Nojima.

**Lowering $\hat{p}_{кр}$ with minute R/h is explained by the fact that in this region buckling of shells occurs beyond the elastic limit (see following chapter).

Confirmation of this we find in article [11.33, 1957], containing statistical treatment of a series of experimental data. We, e.g., shall determine lower limit of critical stresses, proceeding from the requirement that probability of experimental point falling in above-situated region constituted 90% or 99%;* then we obtain the following values of $\hat{p}$ depending upon R/h:

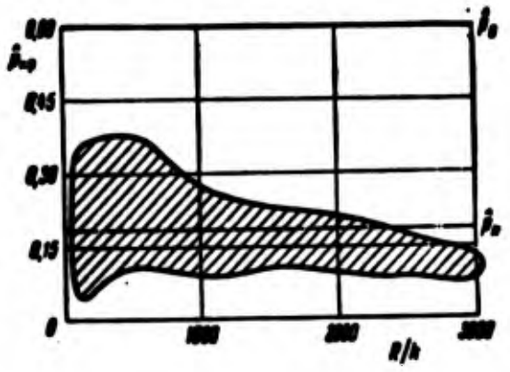

Fig. 11.16. Region of experimental data for critical compressive stress.

R/h	250	500	750	1000	1500	2000	2500
By criterion of 90% probability	0,18	0,16	0,14	0,13	0,11	0,09	0,08
With criterion of 99% probability	0,14	0,12	0,10	0,08	0,07	0,065	0,06

As we see, with increase of R/h values of $\hat{p}$ indeed sharply drop.

What sort of data should be put at base of practical calculations? General requirement, presented in § 118, is that operational load should be determined with significant safety factor with respect to upper critical magnitude $\hat{p}_B$ and, as a rule, lie below $\hat{p}_H$. In case considered by us, upper critical load is so high as compared to experimental values that permissible stress should be determined, by proceeding from lower critical load, found theoretically and also taking into account data of experiments. Such comparison leads to following

*Below-mentioned tables we composed by B. M. Broude on the basis of data in article [11.33] and other works.

table of values of $\hat{p}_{расч}$, which is recommended for use in practice for carefully prepared shells, within elastic limits.

R/h	< 250	500	750	1000	1500
(a) $\hat{p}_{расч}$	0,18	0,14	0,12	0,10	0,09

KEY: (a) $\hat{p}_{расч} = \hat{p}_{calc}$

If, however, shells are prepared insufficiently carefully and initial deflections attain magnitude of order of thickness h, calculated values of $\hat{p}$ should decrease approximately to half. Initial deflections, noticeably exceeding thickness of shell, in general, are impermissible, since rigidity of construction here is sharply decreased.

§ 130. Case of External Pressure. Linear Problem

Let us turn to case when shell is subjected to action of external pressure q evenly distributed on lateral surface (Fig. 11.17). Such form of loading is characteristic for bodies of submarines and shells of aircraft engines. Tanks in chemical industry also frequently experience excess external pressure.

Let us assume that on ends, the shell is fastened by hinge with frames, points of which can obtain certain radial displacements, where frames remain circular.

Let us consider problem of stability of such a shell at first in linear formulation.* If circular shell is subjected to action of

*Linear problem was solved by R. Mises [11.47], and subsequently by Kh. M. Mushtari and A. V. Sachenkov [11.16] and other authors. Other boundary conditions were considered by N. A. Alfutov (Transactions of Yerevan conference on theory of shells, 1962).

external pressure q and bending of shell is absent, then from equations (6) we obtain for $Q_x = Q_y = 0$ stress along arc equal to $\sigma_y = -qR/h$. Thus, action of lateral load q is equivalent to action of compressive stresses $p_y = qR/h$. Therefore, we can use homogeneous equation (17), considering only forces p_y; then we obtain

$$\frac{D}{h}\nabla^4 w + \frac{E}{R^2}\frac{\partial^4 w}{\partial x^4} + \frac{qR}{h}\nabla^4\left(\frac{\partial^2 w}{\partial y^2}\right) = 0. \tag{11.70}$$

We take for w the same expression (36), satisfying boundary conditions, as in case of compression; then instead of (37) we obtain

$$\frac{D}{h}\left(\frac{m^2\pi^2}{L^2} + \frac{n^2}{R^2}\right)^4 + \frac{E}{R^2}\frac{m^4\pi^4}{L^4} - \frac{qR}{h}\left(\frac{m^2\pi^2}{L^2} + \frac{n^2}{R^2}\right)^2\frac{n^2}{R^2} = 0; \tag{11.71}$$

hence

$$q = DR\left(\frac{m^2\pi^2}{L^2 n} + \frac{n}{R^2}\right)^2 + \frac{Eh}{Rn^2}\frac{1}{\left(1 + \frac{n^2L^2}{R^2m^2\pi^2}\right)^2}. \tag{11.72}$$

Obviously, during determination of critical pressure it is necessary to take m = 1. Consequently, in distinction from case of axial compression, during external pressure shell should bulge along generatrix always in one half-wave; this conclusion is confirmed by experiments. We introduce designation

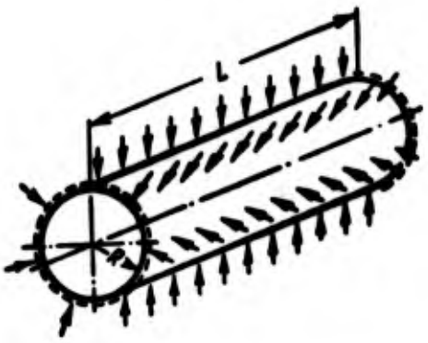

Fig. 11.17. Cylindrical shell subjected to external pressure.

$$\hat{q} = \frac{q}{E}\left(\frac{R}{h}\right)^2; \tag{11.73}$$

instead of (72) we find

$$\hat{q} = \frac{h}{R}\frac{n^2}{12(1-\mu^2)}\left(1 + \frac{\pi^2R^2}{n^2L^2}\right)^2 + \frac{\pi^4R^2}{L^4hn^2}\frac{1}{\left(1 + \frac{\pi^2R^2}{n^2L^2}\right)^2}. \tag{11.74}$$

This formula is simplified, if it is possible to take

$$\left(\frac{\pi R}{nL}\right)^2 \ll 1; \tag{11.75}$$

then we have

$$\hat{q} = \frac{1}{12(1-\mu^2)} \frac{n^2 h}{R} + \frac{\pi^4 R^6}{L^4 h n^6}.$$

Minimizing $\hat{q}$ with respect to n, we obtain

$$n = \sqrt[4]{6\pi^2 \sqrt{1-\mu^2}} \sqrt{\frac{R}{L}} \sqrt[4]{\frac{R}{h}} \qquad (11.76)$$

or, for $\mu = 0.3$,

$$n \approx 2.7 \sqrt{\frac{R}{L}} \sqrt[4]{\frac{R}{h}}. \qquad (11.76a)$$

Putting (76) in expression (74), we determine upper critical value of $\hat{q}_B$:

$$\hat{q}_0 = \frac{\sqrt{6}}{9(1-\mu^2)^{0.75}} \frac{\pi R}{L} \left(\frac{h}{R}\right)^{0.5} \qquad (11.77)$$

or, for $\mu = 0.3$,

$$\hat{q}_0 = 0.92 \frac{R}{L} \sqrt{\frac{h}{R}}. \qquad (11.77a)$$

Corresponding tangential stress is equal to

$$p_1 = 0.92 E \frac{h}{L} \sqrt{\frac{h}{R}}. \qquad (11.77b)$$

Formulas (77) it is possible to use, if condition (75) is met. Otherwise it is necessary to return to full expression (74) and to find value of n, corresponding to minimum $\hat{q}$. In Fig. 11.18 are presented values of $\hat{q}_B$, calculated* by (74) for large range of ratios R/h and L/R.

Expression (74) is valid here on condition that $1/n^2 \ll 1$, pertaining to initial equation (71). As before we consider that this

---

*Calculating graphs of Fig. 11.18 and 11.20 belong to V. A. Nagayev [11.17].

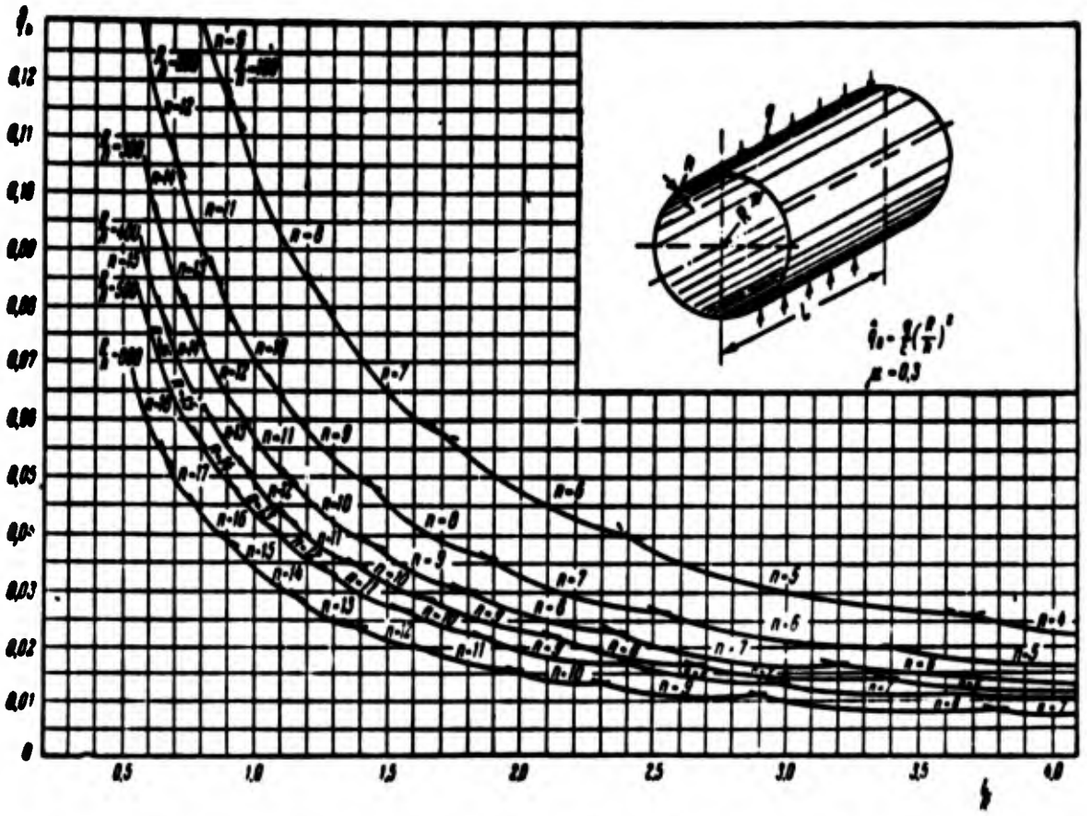

Fig. 11.18. Calculating data for determination of upper critical pressure.

condition is executed if $n \geqslant 4$. Cases $n = 2$ and 3 should be considered, proceeding from definitized expression for curvature of deflection surface along arc. We use expression (4), containing, as compared to (12), additional member $(-w/R^2)$; then instead of (10), we obtain

$$M_1 = -D\left(\frac{\partial^2 w}{\partial y^2} + \frac{w}{R^2} + \mu \frac{\partial^2 w}{\partial x^2}\right).$$

If we introduce thic expression in the third of equations (8), and load q_z for problems of stability we determine by (10.89), then we arrive at following equations:*

$$\frac{D}{h}\left[\nabla^4 w + \frac{1}{R^2}\nabla^4\left(2\mu\frac{\partial^2 w}{\partial x^2} + 2\frac{\partial^2 w}{\partial y^2} + \frac{w}{R^2}\right)\right] + \\ + \frac{E}{R^2}\frac{\partial^4 w}{\partial x^4} + \frac{qR}{h}\nabla^4\left(\frac{\partial^2 w}{\partial y^2} + \frac{w}{R^2}\right) = 0. \qquad (11.78)$$

*This equation was obtained by S. V. Aleksandrovskiy [11.1], and later by Thielemann [11.51] and [11.52] for general case of anisotropic shell.

Substituting here expression (36), we obtain

$$\frac{D}{h}\left(\frac{m^2\pi^2}{L^2}+\frac{n^2}{R^2}\right)^2\left\{\left(\frac{m^2\pi^2}{L^2}+\frac{n^2}{R^2}\right)^2+\frac{1}{R^4}\left[1-2\left(\mu\frac{m^2\pi^2R^2}{L^2}+n^2\right)\right]\right\}+$$
$$+\frac{E}{R}\frac{m^4\pi^4}{L^4}-\frac{q}{Rh}\left(\frac{m^2\pi^2}{L^2}+\frac{n^2}{R^2}\right)^2(n^2-1)=0$$

Hence, when m = 1

$$q_0=\frac{DR}{n^2-1}\left\{\left(\frac{\pi^2}{L^2}+\frac{n^2}{R^2}\right)^2+\frac{1}{R^4}\left[1-2\left(\mu\frac{\pi^2R^2}{L^2}+n^2\right)\right]\right\}+$$
$$+\frac{Eh}{R}\frac{\pi^4}{L^4}\frac{1}{\left(\frac{\pi^2}{L^2}+\frac{n^2}{R^2}\right)^2(n^2-1)}. \qquad (11.79)$$

Let us consider case of very long shell, when L >> R, expression (79) changes into the following:

$$q_0=\frac{(n^2-1)D}{R^3}. \qquad (11.80)$$

Minimum value of q we find when n = 2:

$$q_0=\frac{3D}{R^3}. \qquad (11.81)$$

Let us note that formula (72) gives for L >> R, $q = n^2D/R^3$; when n = 2 we have $q_B = 4D/R^3$, which exceeds (81) by 33%. This example illustrates the fact that region of application of approximate equations of theory of shells of average length is limited and that error of results of calculations in separate cases may be significant.* However, from practical point of view such cases are rather the exceptions.

Since in case of external pressure shell obtains along generatrix to only one hollow, then, in distinction from problem of axial compression, here influence of boundary conditions turns out to be more noticeable. Therefore, we shall consider separately case of shell of average length, clamped on ends.

---

*Using equation of type (79), it is possible to constitute graph for q_B, embracing whole range of ratios L/R, such as in Fig. 11.3; such a graph is given in book of Flügge [10.18].

We take as first approximation the expression for deflection in the form*

$$w = 16f\left(\frac{x}{L}\right)^2\left(1-\frac{x}{L}\right)^2 \sin\frac{ny}{R}. \qquad (11.82)$$

satisfying conditions w = 0, $\frac{\partial w}{\partial x} = 0$ when x = 0, L. We place (82) in the right part of equation (16) and after integration find

$$\Phi = -32\frac{E}{R}\left(\frac{R}{n}\right)^4\frac{f}{L^2}\left\{\left[1+24\left(\frac{R}{nL}\right)^2\right]-6\frac{x}{L}+ \right.$$
$$\left. +6\left(\frac{x}{L}\right)^2\right\}\sin\frac{ny}{R}-\frac{qR}{h}\frac{x^2}{2}. \qquad (11.83)$$

Equation (15a) when $p_x = q = 0$ and $p_y = qR/h$ takes form

$$X \equiv \frac{D}{h}\nabla^4 w - \frac{1}{R}\frac{\partial^2\Phi}{\partial x^2}+\frac{qR}{h}\frac{\partial^2 w}{\partial y^2} = 0.$$

Using Bubnov-Galerkin method, we compose equation

$$\int_0^L\int_0^{2\pi R} X\left(\frac{x}{L}\right)^2\left(1-\frac{x}{L}\right)^2\sin\frac{ny}{R}\,dx\,dy = 0. \qquad (11.84)$$

After integration we obtain

$$\hat{q} = \frac{n^2h}{12R(1-\mu^2)}\left[1+24\left(\frac{R}{nL}\right)^2+504\left(\frac{R}{nL}\right)^4\right]+\frac{504}{n^2}\left(\frac{R}{nL}\right)^4\frac{R}{h}. \qquad (11.85)$$

We determine upper critical pressure $\hat{q}_{B,з}$, minimizing $\hat{q}$ with respect to n (for sufficiently large values of n); it exceeds magnitude $\hat{q}_{B,ш}$ pertaining to hinge-secured edges approximately by 55%.**

If we take for w another approximating expression,***

$$w = f\sin^2\frac{\pi x}{L}\sin\frac{ny}{R}. \qquad (11.86)$$

then analogous path leads to values of $\hat{q}_{B,з}$, lying somewhat below (75) and exceeding $\hat{q}_{B,ш}$ approximately by 40%.

---

*This solution belongs to V. A. Nagayev [11.17].

**Trans. Ed. Note. Subscripts з = clamped, ш = hinged.

***This variant of solution belongs to V. Nash [11.48].

However expression (82) or (86) for w, frequently applied in theory of stability of clamped bars or plates, give for shells of average length values of critical pressure, overstated as compared to experimental data. In Fig. 11.19 is given coefficient $m = q_{в,э}/q_{в,т}$ depending upon parameter L/R when R/h = 100. Curve 1 corresponds to expression (86), curve 2 is built according to work of O. M. Paliy [11.18], in which there is attempt to consider influence of moments of clamping in accordance with theory of boundary effect (see p. 562). As we see, coefficient k for small ratios L/R indeed attains value 1.5–1.6, while in case L/R = 1 it is equal only to 1.08. It is desirable subsequently to investigate this problem in more detail.

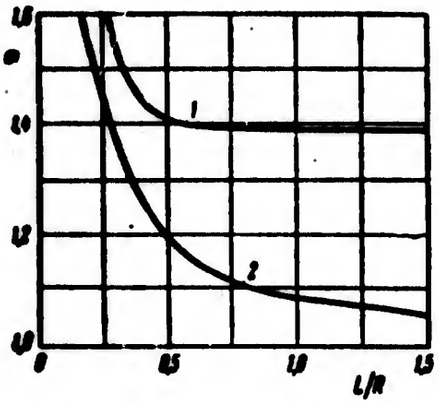

Fig. 11.19. Graph, reflecting influence of clamping of edges on upper critical pressure.

§ 131. Case of External Pressure. Nonlinear Problem

Experiments show that in case of external pressure buckling of shells occurs, as a rule, in the form of a sharply expressed knock. Therefore, we investigate large deflections of a shell.* We preserve scheme of solution, presented in § 127. Approximating expression for deflection is selected in the form

$$w = f_1 \sin\frac{\pi x}{L}\sin\frac{\pi y}{R} + f_2 \sin^2\frac{\pi x}{L} + f_0. \qquad (11.87)$$

*This problem was considered by F. S. Isanbayeva [11.9], V. Nash [11.48], V. A. Nagayev [11.17], N. A. Alfutov [11.4]. Solution of V. A. Nagayev are presented in detail in book [0.3]. Here is given variant of solution belonging to P. G. Burdin.

it coincides with (46), if we take m = 1. Instead of (47) we take designation

$$\theta = \frac{nR}{nL}. \tag{11.88}$$

Equation of type (49) is kept. In expression (49a) for Φ/E there should be introduced magnitude

$$\left(-\frac{qR}{h}\frac{x^2}{2}\right) \text{ in place of } \left(-\frac{py^2}{2}\right).$$

Equation of periodicity (51) takes, in distinction from (55), form

$$\frac{f_0}{R} = \frac{qR}{Eh} + f_1^2\frac{n^2}{8R^2} - \frac{f_2}{2R}. \tag{11.89}$$

Work of normal pressure we calculate by approximate formula

$$W = q\int_0^L\int_0^{2\pi R} w\,dx\,dy; \tag{11.90}$$

we find

$$W = q\pi RL(2f_0 + f_2). \tag{11.91}$$

This magnitude should be introduced in expression for energy (59) in place of last two members.

We preserve designations (61); then equation (62) will remain in force, but with replacement of $\hat{p}$ by $\hat{q}/\$^2$; in equation (63) one should set $\hat{p} = 0$. Putting ζ_1^2 from (63) in equation (62), we obtain (for $\eta = n^2h/R$)

$$\frac{\eta\left[\frac{1}{4\eta} + \frac{\eta\theta^4}{3(1-\mu^2)}\right](1+\theta^2)\zeta_2}{1 - \frac{8\theta^4}{(1+\theta^2)^2} - 8\eta\theta^4\left[\frac{1}{(1+\theta^2)^2} + \frac{1}{(1+9\theta^2)^2}\right]\zeta_2} + \\ + \eta\theta^4\left[\frac{1}{(1+\theta^2)^2} + \frac{1}{(1+9\theta^2)^2}\right]\zeta_2^2 + \frac{\theta^4}{(1+\theta^2)^2\eta} + \\ + \frac{\eta(1+\theta^2)^2}{12(1-\mu^2)} - \frac{1}{4}\left[1 + \frac{8\theta^4}{(1+\theta^2)^2}\right]\zeta_2 = \hat{q}. \tag{11.92}$$

This equation determines $\hat{q}$ as function of parameter ζ_2. Considering $\zeta_2 = 0$, we find

$$\hat{q}=\frac{\eta(1+\theta^2)^2}{12(1-\mu^2)}+\frac{\theta^4}{(1+\theta^2)^2\eta}. \qquad (11.93)$$

which will agree with solution of linear problem by (74).

Further, using dependence (92), one can determine lower critical pressure in first approximation.

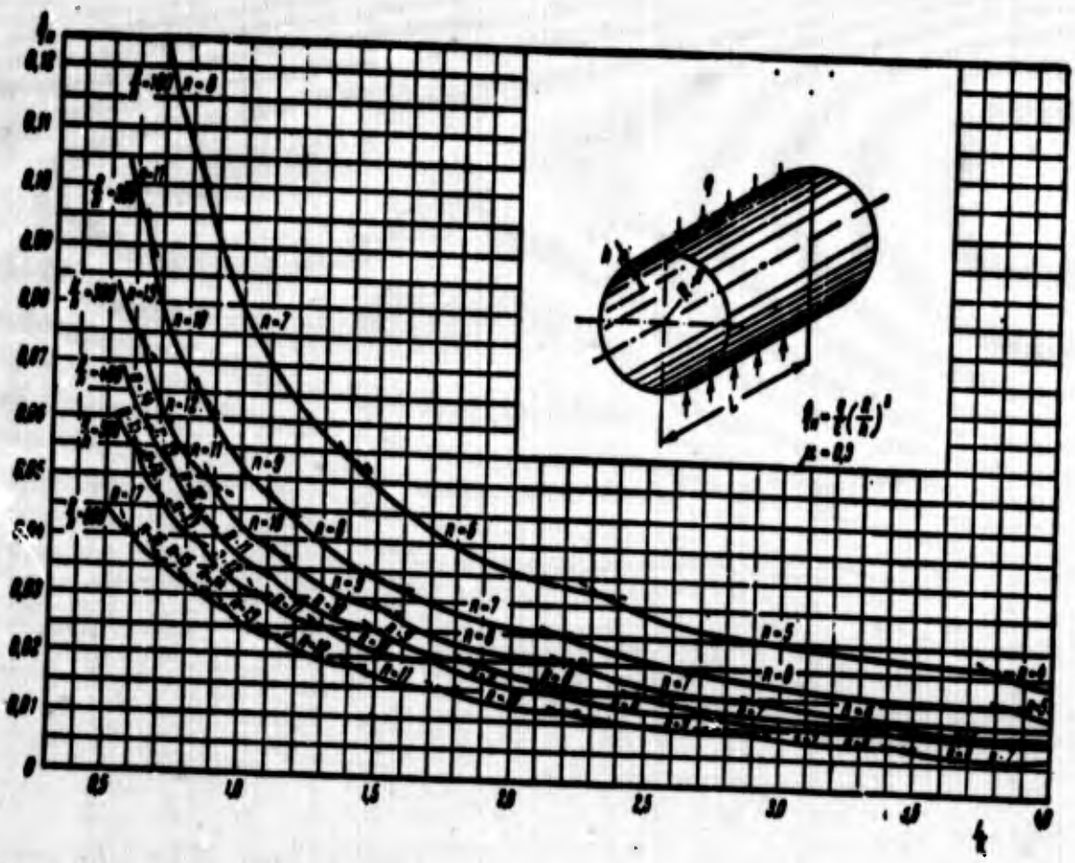

Fig. 11.20. Calculating data for determination of lower critical pressure.

Modifying energy ϑ additionally by n, as in § 127, we arrive at equation

$$\frac{\eta(1+\theta^2)}{6(1-\mu^2)}+\eta\frac{\zeta_1^2}{16}-\frac{2\theta^4}{(1+\theta^2)^2\eta}+2\eta\theta\left[\frac{1}{(1+\theta^2)^2}+\right.$$
$$\left.+\frac{\theta}{(1+3\theta^2)^2}\right]\zeta_2^2-\frac{1}{4}\left[1-\frac{8\theta^4(1-\theta^2)}{(1+\theta^2)^3}\right]\zeta_2=\hat{q}. \qquad (11.94)$$

Combining this equation with (92), we obtain solution of problem in the second approximation.

In Fig. 11.20 are presented final values of lower critical pressure $\hat{q}_н$ for different ratios L/R and R/h. This graph, obtained by

V. A. Nagayev, can be compared with data of Fig. 11.18 for $\hat{q}_B$. If we fix magnitude R/h, then relationship between lower and upper critical pressures will depend on L/R. For very long shells (L/R > 4), and also for short ones (L/R < 0.8) magnitudes $\hat{q}_B$ and $\hat{q}_H$ are close. The sharpest ratio $\nu = \hat{q}_H/\hat{q}_B$ is lower with value L/R lying from 0.8 to 2, as shown in Fig. 11.21. With increase of R/h the minimum shifts in the direction of smaller L/R.

In Fig. 11.22 is depicted dependence of coefficient ν on parameter $\$$, characterizing form of wave formation at lower critical load. Curve $\nu(\$)$ it is possible to consider as not depending on ratio R/h.

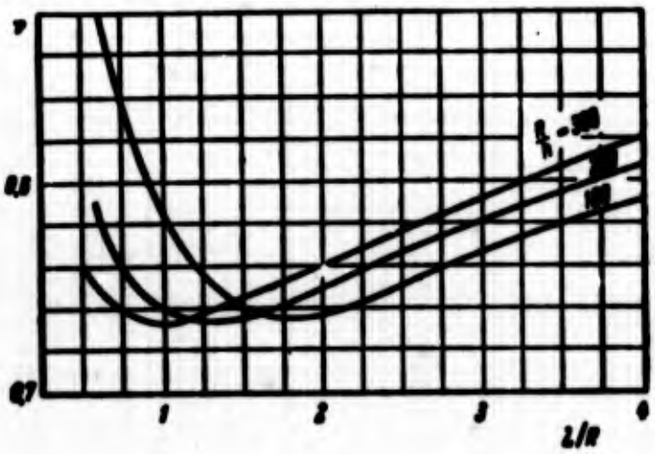

Fig. 11.21. Ratio ν of lower to upper critical pressure depending upon L/R.

Minimum value ν, obtained in second approximation (curve 1), is equal to $\nu_{min} = 0.73$ and pertains to $\$ = 0.3$. Here is given curve (4) of first approximation and there are given dependences, obtained in works of F. S. Isanbayeva [11.9] (curve 2) and N. A. Alfutov [11.4] (curve 3).

As we see, influence of nonlinearity of problem here is significantly less than in case of axial compression; level $\hat{q}_H$ constitutes about 70–75% of $\hat{q}_B$, while compression was lowered to 30–35%. Wave formation also turns out to be different; instead of a series of local hollows, characteristic for case of compression, here there appears a "crystal" with unique elongated faces, embracing the whole length of the test piece.

Such deflection surface also should be close to a surface, isometric with respect to circular cylinder. Therefore, we can in this

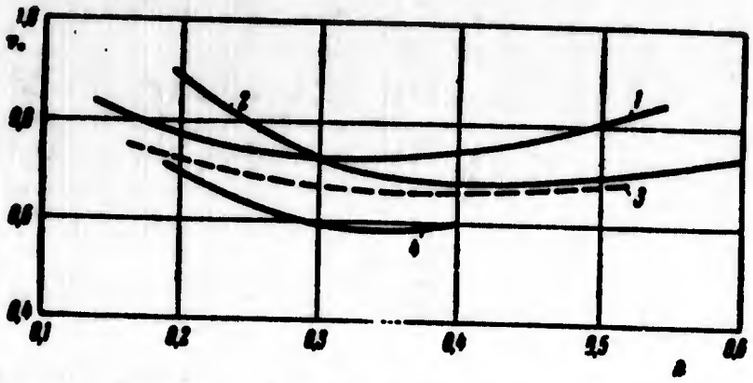

Fig. 11.22. Dependence $\nu = q_H/q_B$ on parameter characterizing form of wave formation in different solutions of problem.

case, also use geometric construction* described in § 128. As lines γ it is possible to take a half-wave of sinusoid, passed through median points of sides of end sections of prism (solid lines in Fig. 11.23a), or rectangular segments, smoothed at middle of face (dotted lines). Again we pass a plane perpendicular to axis of prism and note the polygon connecting points of intersection of plane with lines. During displacement of plane along axis of prism we obtain tubular surfaces shown in Fig. 11.23b for case when as lines γ there are taken sinusoids, and in Fig. 11.23c for case of straight segments. These tubular surfaces of shell well depict character of buckling of a real shell. Consideration of geometric model in Fig. 11.23 allows us comparatively easily to find difference between volume of tube and initial cylinder; but then one can determine work of external pressure by formula (90). Using energy method and disregarding potential strain energy in middle surface, A. V. Pogorelov obtained following expression for coefficient $\nu = \hat{q}_H/\hat{q}_B$:

$$\nu = 2\sqrt[3]{\frac{Rh}{L^2}} + 0.385\sqrt{\frac{Rh}{L^2}}; \qquad (11.95)$$

*See work of A. V. Pogorelov [11.19], Chapter 2 and [11.20], pertaining to case of external pressure.

it pertains to case $Rh/L^2 < 0.016$.

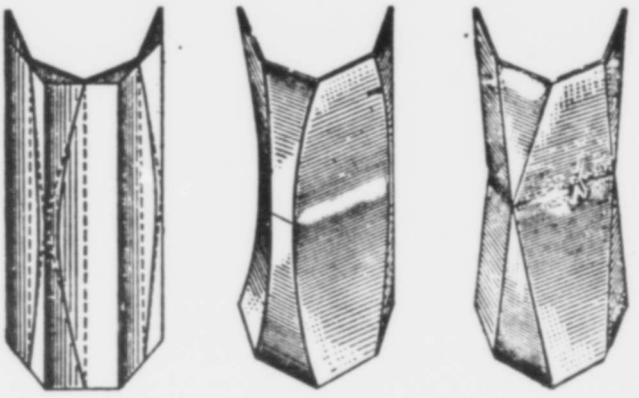

a) b) c)

Fig. 11.23. Construction of surfaces isometric to cylinder in case of buckling under external pressure.

It is desirable to compare subsequently results of calculations by formula (95) with experimental data, pertaining to fairly thin shells.

§ 132. Experiments with Shell, Subjected to External Pressure. Recommendations for Practical Calculations

Let us give data of research on buckling of shells subjected to external pressure. We start from those experiments in which shells were prepared carefully — from pipes on lathe — with observance of rigid tolerances with respect to dimensions. Diagram of one testing unit is shown in Fig. 11.24.* One of ends of testpiece (1) is fastened to piston (2), and the other, to flange (3). Pressure q is transmitted to piece from liquid, forced into chamber (4) by pump (No. 1). In order to exclude extension of shell, in lower chamber (5) from another pump (No. 2) there is fed pressure, depending

*These experiments were conducted by V. A. Nagayev.

on q. Storage battery, containing gas cushion, creates, if necessary, condition of constancy of pressure during knock.

Loss of stability of shells, as a rule, occurs suddenly, with formation of deep, regularly placed hollows, turned toward center of curvature, namely of that form, which was assumed as the basis of solution of the nonlinear problem. If gas pad cushion is disconnected, during first knock there appear only one-to-three waves, and only in process of subsequent knock do remaining waves appear. In Fig. 11.25 are shown photographs of two pieces having identical ratio R/h. Investigated cylindrical part of piece was partially clamped. Let us note that shorter shell (b) buckles with larger number of waves than shell (a); this result ensues from formula (76). Case of hinged support of ends is shown in Fig. 11.26; outline of waves here is close to rectangular. Last, in photographs of Fig. 11.27 are shown piece, having diaphragm, a hard inner ring, dividing shell into two equal parts. For each of these parts internal edge could be considered supported on hinge.

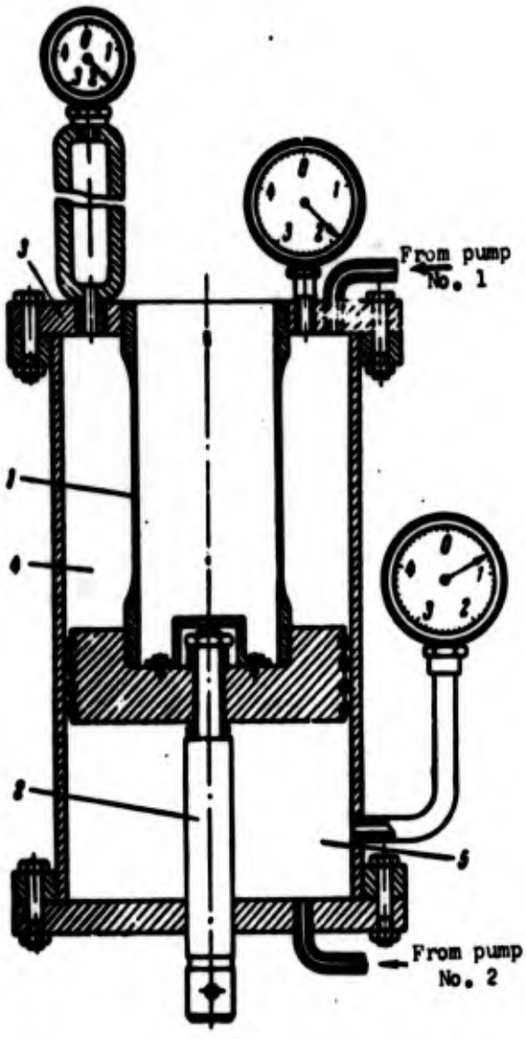

Fig. 11.24. Installation for tests of shells for stability during external pressure.

In Fig. 11.28 are given results of experiments pertaining to form of wave formation. Along the axis of abscissas is plotted magnitude

L/R, along the axis of ordinates — ratio of width l_y of hollow along

a) b)

Fig. 11.25. Form of buckling of shells in case of partial clamping at edges.

Fig. 11.26. With hinged fastening on edges of shell there form "rectangular" waves.

circumference to length L. Solid line corresponds to theoretical calculations of § 130.

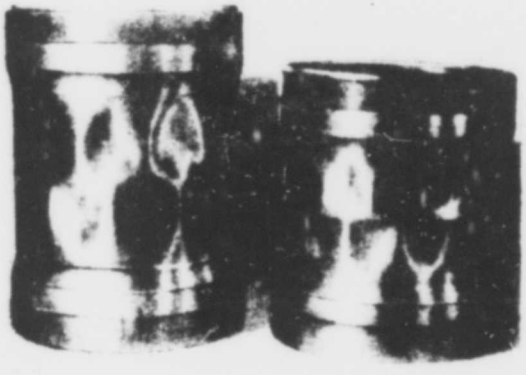

a) b)

Fig. 11.27. Shells, with diaphragm resisting bend, after loss of stability.

We give, further, summary of experimental values of $\nu = q_{кр}/q_в$, obtained by different authors with various conditions of manufacture and test of pieces (Fig. 11.29); by $q_{кр}$ is understood real magnitude of pressure during buckling. In certain series of experiments models were obtained from flat sheets and had significant initial

imperfections; here scattering of experimental points was more significant and level of critical pressure was much lower than in case of carefully prepared shells. For thin shells (R/h from 1000 to 1500) critical pressure drops especially greatly due to large influence of initial imperfections. Analysis of data of experiments shows also that for duralumin pieces values of ν lie on the average somewhat lower than those for steel. Possibly, this is explained by large sensitivity of duralumin shells to thermal effects during treatment, storage, etc.

Dotted line in Fig. 11.29 corresponds, obviously, to q_B; solid line is obtained from data of second approximation for q_H. Overwhelming number of experimental points lies here between these lines. Least value of ν in these series of experiments is 0.68.

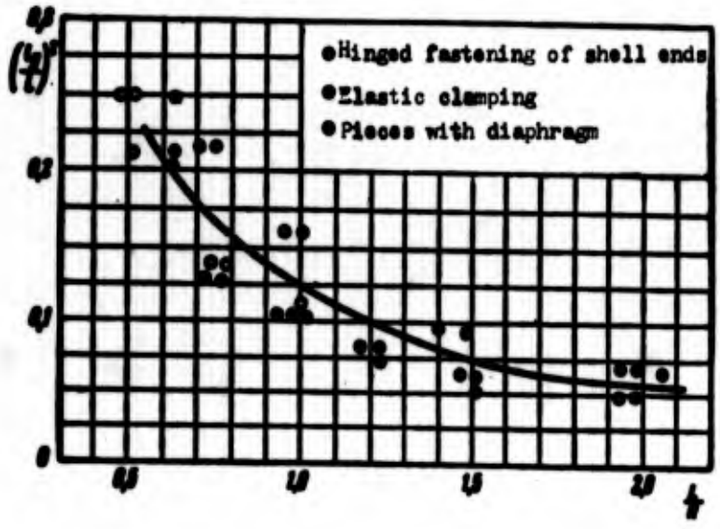

Fig. 11.28. Experimental data, pertaining to form of hollows.

Thus, practical calculations for stability during external pressure must be conducted on upper critical value (see graph of Fig. 11.18 and formula (77), multiplied by coefficient ν; value of ν we shall consider to depend only on ratio R/h.

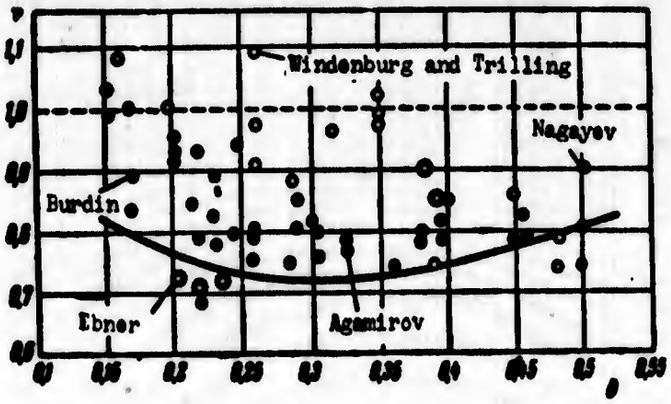

Fig. 11.29. Experimental values of critical pressure according to different authors.

Tentatively recommended are the following values of ν:

R/h	250	500	1000	1500
ν	0,7	0,6	0,5	0,4

These data it is possible to use for hydrostatic stress.

§ 133. Influence of Initial Imperfections During External Pressure

There is every reason to consider that the greatest influence on scattering of experimental values of critical loads is rendered by initial imperfections of the form of the shell. We turn, therefore, to more detailed study of behavior of shells with initial deflection. It is most convenient to do this with respect to shell subjected to external pressure, since configuration of hollows here is more definite than in case of axial compression. Let us consider problem in nonlinear setting and we shall originate from system of equations (29). Let us remember that by w is understood total deflection, under w_0, initial deflection. As before for w we take expression

$$w = f\left(\sin\frac{\pi x}{l}\sin\frac{\pi y}{R} + \phi\sin^2\frac{\pi x}{l} + \varphi\right). \qquad (11.96)$$

We assume that initial deflections are distributed by analogous law:

$$w_0 = f_0\left(\sin\frac{\pi x}{L}\sin\frac{\pi y}{R} + \psi\sin^2\frac{\pi x}{L} + \varphi\right). \tag{11.97}$$

and that quantities ψ and φ in (96) and (97) coincide. In other words, we consider that form of initial wave formation, characterized by parameters ψ and φ, is "in resonance" with wave formation of shell in process of deformation and that the only prescribed parameter is magnitude f_0. Such assumption somewhat increases influence of initial imperfections.*

We place (96) and (97) in the right part of the second of equations (29); integrating equation, we obtain following expression for function of stresses:

$$\begin{aligned}\frac{1}{E}\Phi = &\left(K\frac{f_1^2}{32\beta^2} - \frac{f_1\psi}{8R\alpha^2}\right)\cos 2\alpha x + K\frac{f_1^2}{32}\beta^2\cos^2\beta y + \\ &+ K\frac{\beta^2}{(1+9\beta^2)^2}f_1^2\psi\sin 3\alpha x\sin\beta y - \\ &- \left[K\frac{\beta^2}{(1+\beta^2)^2}f_1^2\psi - \frac{\beta^2}{(1+\beta^2)^2}\frac{f_1}{\beta^2 R}\right]\sin\alpha x\sin\beta y - \frac{qR}{Eh}\frac{x^2}{2}.\end{aligned} \tag{11.98}$$

Here are introduced designations

$$\alpha = \frac{\pi}{L},\quad \beta = \frac{n}{R},\quad f_1 = f - f_0,\quad K = 1 + 2\frac{f_0}{f_1} = \frac{f+f_0}{f-f_0}; \tag{11.99}$$

by f_1 is understood extent of additional (elastic) deflection.

We calculate total energy of system (56), using expressions (10.95) and (90), but with replacement of w by $w - w_0$. If we introduce, furthermore, dimensionless parameters

$$\vartheta = \vartheta\frac{R}{aELh^3},\quad \zeta_1 = \frac{f_1}{h},\quad \xi = \frac{f_1\psi}{h}. \tag{11.100}$$

---

*This assumption, significantly facilitating calculations, is adopted also in work of Loo [11.44], Donnell [11.30], and others. Solution here is given by V. E. Mineyev and the author (see [11.5], articles of 1957).

then we obtain

$$\Im = \frac{1}{2}C_1\zeta_1^2(\zeta_1+2\zeta_0)^2+\frac{1}{2}C_2(\zeta_1+2\zeta_0)^2\xi^2- \\ -C_3(\zeta_1+2\zeta_0)\zeta_1\xi+\frac{1}{2}C_4\zeta_1^2+\frac{1}{2}C_5\xi^2-C_6\hat{q}\zeta_1(\zeta_1+2\zeta_0)+3\hat{q}^2. \qquad (11.101)$$

where

$$C_1=\frac{1+\vartheta^4}{64}\eta^2.\quad C_2=\frac{\vartheta^4}{2}\left[\frac{1}{(1+\vartheta^2)^3}+\frac{1}{(1+9\vartheta^2)^3}\right]\eta^2.$$
$$C_3=\frac{1}{16}\left[1+\frac{8\vartheta^4}{(1+\vartheta^2)^3}\right]\eta.\quad C_4=\frac{\vartheta^4}{2}\left[\frac{1}{(1+\vartheta^2)^3}+\frac{(1+\vartheta^2)^2\eta^2}{12(1-\mu^2)}\right].$$
$$C_5=\frac{1}{4}+\frac{\vartheta^4\eta^2}{3(1-\mu^2)}.\quad C_6=\frac{3}{4}.\quad \eta=\beta^2Rh.$$

Equations of Ritz method in application to parameters ζ and ξ we write in the form

$$\frac{\partial\Im}{\partial\zeta}=0,\quad \frac{\partial\Im}{\partial\xi}=0; \qquad (11.102)$$

disregarding certain immaterial members, we present these equations in the form

$$2C_1\zeta_1(\zeta_1+2\zeta_0)(\zeta_1+\zeta_0)+C_2(\zeta_1+2\zeta_0)\xi^2-2C_3(\zeta_1+\zeta_0)\xi+2C_4\zeta_1- \\ -2C_6\hat{q}(\zeta_1+\zeta_0)=0. \qquad (11.103)$$

$$C_2(\zeta_1+2\zeta_0)^2\xi-C_3\zeta_1(\zeta_1+2\zeta_0)+C_5\xi=0. \qquad (11.104)$$

Let us note also that relationships can be obtained, using Bubnov-Galerkin method in application to the first of equations (29). In Fig. 11.30 are presented results of calculations by equations (103)–(104) for case R/h = 112.5, L/R = 2.2. Along the axis of abscissas is plotted parameter of total deflection ζ, along the axis of ordinates, dimensionless load $\hat{q}$; we take $\mu = 0.3$. Each solid line corresponds to a definite magnitude of ζ_0 and constitutes envelope of a series of curves, built for different values of parameter $\eta = n^2h/R$; in figure there are shown by dotted line similar curves, corresponding to shell of circular form ($\zeta_0 = 0$). Circle on axis of ordinates marks

magnitude $\hat{q}_B$ for ideal shell. As we see, with initial imperfections upper critical load (highest point of loop) is lowered; thus, for example, for $\zeta_0 = 0.1$ lowering constitutes about 12%. Meanwhile lower pressure $\hat{q}_H$ remains almost constant.

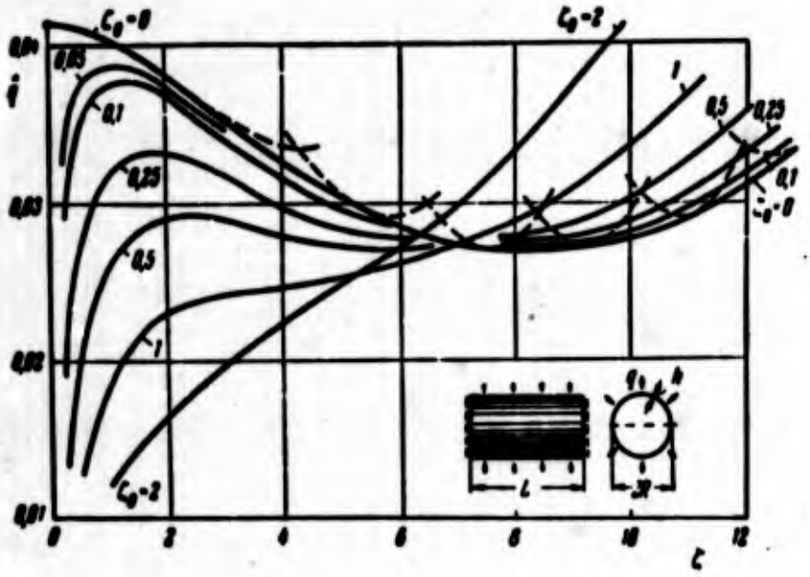

Fig. 11.30. Diagrams "pressure-deflection" for shells with initial deflection.

If extent of initial deflection exceeds thickness of shell, then load changes monotonically. Let us note that on a given stage of loading the characteristic of deformation of shell $\hat{q}(\zeta)$ turns out to be steeper the higher magnitude ζ_0; growth of rigidity is explained by the fact that with significant initial deflections shell becomes as if corrugated. In Fig. 11.31 there is shown dependence of $\hat{q}_B$ on amplitude of initial deflection ζ_0 for various ratios R/h in case of hydrostatic stress; we took $L/R \approx 2.5$.

We will give, further, data of experiments, formulated for research of influence of initial deflection.* Before test duralumin

*These experiments were conducted by V. E. Mineyev.

pieces were dented by a special stamp. Behavior of shells was different depending upon number and location of initial dents. For instance, if piece is given only one dent, there occurs smooth build-up of deflections and stresses in zone adjacent to it, but remaining part of surface of shell remains almost smooth. Then there occurs buckling by a knock (or several knocks) at other points on circum-

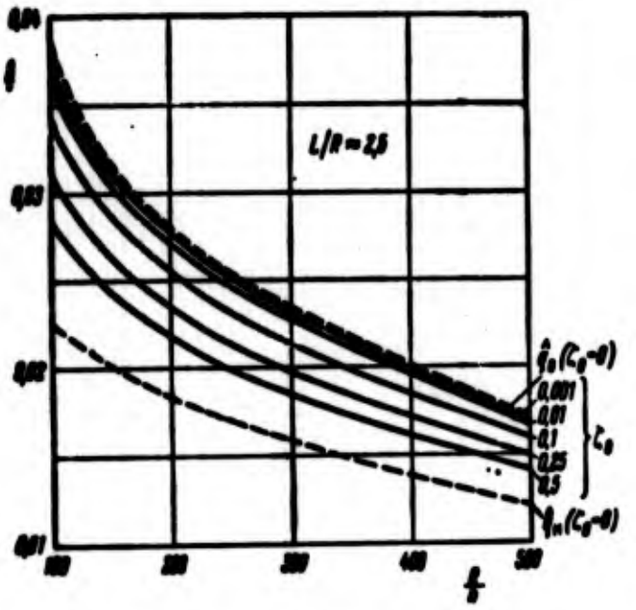

Fig. 11.31. Lowering of upper critical pressure for shells with initial deflection.

ference. This is illustrated by graph of Fig. 11.32 of change of flexural stresses $\hat{\sigma}_{x,и}$ along circumference of average section of shell; by $\hat{\sigma}_{x,и}$ is understood magnitude $\hat{\sigma}_{x,и}b^2/Eh^2$, where $\sigma_{x,и}$ is stress of greatest thickness. At point 1 was disposed initial dent. Stresses were distributed on first stage of loading as per Fig. 11.32a and then by Fig. 11.32b, as shown by solid lines.

It is interesting to compare load, which shell sustains for different numbers of initial dents. Smooth shell of given dimensions buckles in six waves. In Fig. 11.33 are noted loads, corresponding to first knock (lower line) and final wave formation (upper line).

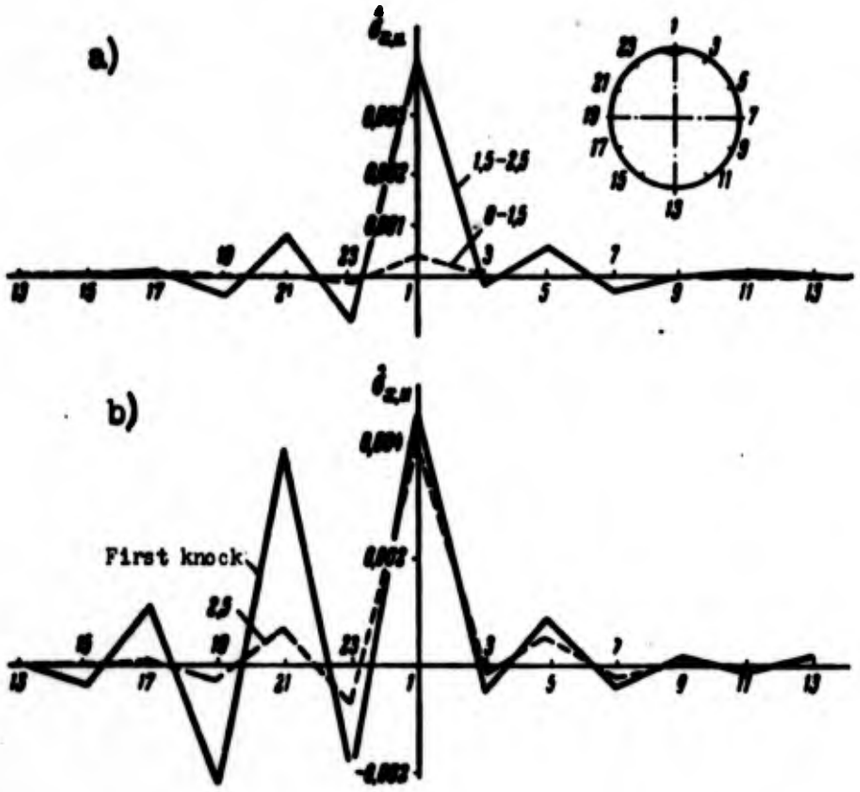

Fig. 11.32. Change of maximum flexural stresses in case of one initial dent.

Depending on number n of identical initial dents, evenly distributed on circumference of shell, from n = 1 to n = 7; value n = 0 pertains to smooth shell. Fig. 11.33a corresponds to maximum initial deflection $\zeta_0 = 1$, Fig. 11.33b, to $\zeta_0 = 2$.

As we see, most dangerous are cases when number of dents corresponds to form of loss of stability of smooth shell (three or six initial dents). If location of initial imperfections does not correspond to form of buckling of ideal shell (n = 4), in process of deformation there occurs reconstruction of wave formation, supporting power of shell can be even higher than in the absence of initial imperfections. In many experiments we managed to observe as if hardening of pieces during significant development of dents, connected with formation of hard ridges of waves. Final destruction of pieces set in upon fracturing of these unique ribs.

In conclusion we compare experimental dependences $\hat{q}(\zeta)$, shown in Fig. 11.34 by solid lines, with theoretical (dotted line) dependences.

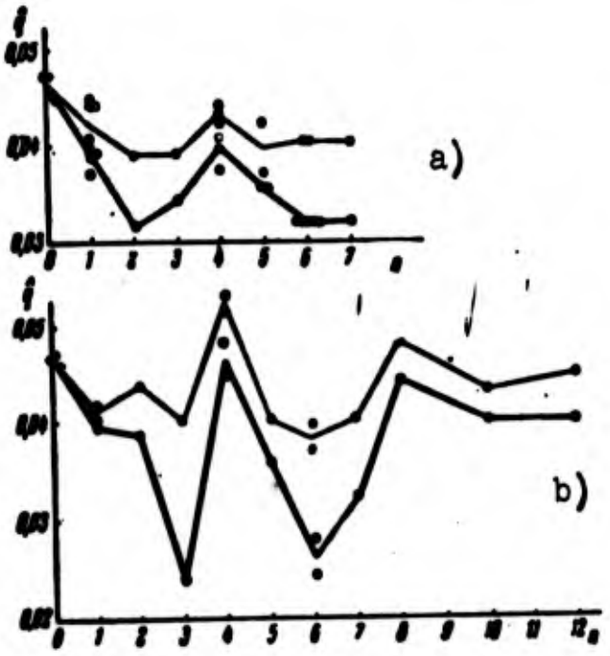

Fig. 11.33. Supporting power of shells with different number of initial dents according to experiments.

Let us note that in experiments faces of shell were partially clamped. Initial branches of curves, pertaining to the same values of ζ_0, turn out to be close to one another; however subsequently curves part. This is explained, apparently, by the fact that in theoretical solution there were made certain limitations, concerning character of buckling; in reality picture of wave formation of shell turns out

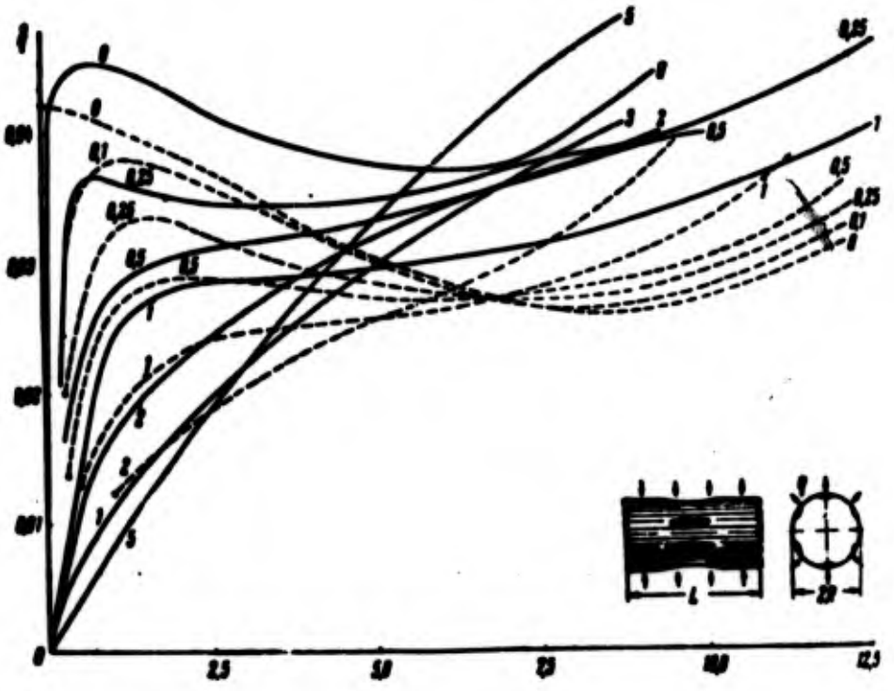

Fig. 11.34. Curves "pressure-deflection" for "ideal" shell ($\zeta_0 = 0$) and shells with initial deflection (ζ_0 from 0.1 to 5).

to be more complicated. It is desirable subsequently to return to this important problem, adopting, in particular, more strict procedure of variation of system energy.

§ 134. Stability of Shell Under Torsion

We turn now to case of torsion of shell by pairs M_K, applied on the ends (Fig. 11.35). Here principal state is determined by tangential stresses; for thin shell they can be considered equal to

$$s = \frac{M_k}{2\pi R^2 h}. \tag{11.105}$$

Buckling during action of such load can take place with known conditions for shells of aircraft and motors.

Fig. 11.35. Shell, subjected to torsion.

Let us consider first linear problem,* considering that shell of average length is supported by hinge on ends. Equation (17) obtains form

$$\frac{D}{h}\nabla^8 w + \frac{E}{R^2}\frac{\partial^4 w}{\partial x^4} + 2s\nabla^4\left(\frac{\partial^2 w}{\partial x\,\partial y}\right) = 0. \tag{11.106}$$

By analogy with problem of stability of plate during shear it is possible to assume that buckling of shell in case of torsion will be accompanied by formation of waves regularly located on circumference, inclined at given angle to generatrix. Therefore, we take for w expression

$$w = f\cos\frac{\pi x}{l}\cos\frac{n}{R}(y + \gamma x). \tag{11.107}$$

---

*This problem was considered by Donnell [11.30], Kh. M. Mushtari [10.9], V. M. Darevskiy [11.7]. The solution below was given by V. A. Mar'in [11.14].

considering that reference point x is located in the middle of length of shell; by n is understood number of full waves on circumference; by γ, the tangent of angle of inclination of wave ridges to generatrix. Expression (107) satisfies condition w = 0 for $x = \pm L/2$. We find, further, that

$$\left.\frac{\partial w}{\partial x}\right|_{x=\pm\frac{L}{2}} = -f\frac{\pi}{L}\cos\frac{n}{R}\left(y \pm \gamma\frac{L}{2}\right).$$

$$\left.\frac{\partial^2 w}{\partial x^2}\right|_{x=\pm\frac{L}{2}} = f\frac{2\pi n\gamma}{LR}\sin\frac{n}{R}\left(y \pm \gamma\frac{L}{2}\right).$$

As we see, expression chosen by us for deflection, strictly speaking, satisfies neither condition of hinged support nor condition of clamping. At the same time we obtain

$$\int_0^{2\pi R}\left(\frac{\partial w}{\partial x}\right)_{x=\pm\frac{L}{2}}dy = \int_0^{2\pi R}\left(\frac{\partial^2 w}{\partial x^2}\right)_{x=\pm\frac{L}{2}}dy = 0.$$

Thus, both these conditions are satisfied simultaneously in integral sense. Expression (107) can be rewritten in the form $w = w_1 + w_2$, where

$$w_1 = \frac{1}{2}f\left(\cos\frac{ny}{R}\cos mx - \sin\frac{ny}{R}\sin mx\right). \tag{11.108}$$

$$w_2 = \frac{1}{2}f\left(\cos\frac{ny}{R}\cos lx - \sin\frac{ny}{R}\sin lx\right). \tag{11.109}$$

whereupon

$$m = \frac{n\gamma}{R} + \frac{\pi}{L}, \quad l = \frac{n\gamma}{R} - \frac{\pi}{L}. \tag{11.110}$$

Putting $w_1 + w_2$ in equation (106), we obtain

$$\left[\left(m^2 + \frac{n^2}{R^2}\right)^4\frac{D}{h} + \frac{E}{R^2}m^4 - 2s\frac{mn}{R}\left(m^2 + \frac{n^2}{R^2}\right)^2\right]w_1 +$$
$$+\left[\left(l^2 + \frac{n^2}{R^2}\right)^4\frac{D}{h} + \frac{E}{R^2}l^4 - 2s\frac{ln}{R}\left(l^2 + \frac{n^2}{R^2}\right)^2\right]w_2 = 0. \tag{11.111}$$

Equating to zero coefficients in w_1 and w_2, we obtain two equations:

$$\frac{2s}{E}=\frac{(m^2R^2+n^2)^2}{12(1-\mu^2)mRn}\left(\frac{h}{R}\right)^2+\frac{m^2R^2}{(m^2R^2+n^2)^2n}. \tag{11.112}$$

$$\frac{2s}{E}=\frac{(l^2R^2+n^2)^2}{12(1-\mu^2)lRn}\left(\frac{h}{R}\right)^2+\frac{l^2R^2}{(l^2R^2+n^2)^2n}. \tag{11.113}$$

Equations (112) and (113) should give the same value of s. Given the number of waves and ratio R/L, we can construct by these equations curves $s = s(n\gamma)$, as shown in Fig. 11.36. These curves are identical in form (since magnitude m and l in (112) and (113) are interchangeable), but are displaced relative to one another along axis of abscissas by a magnitude

$$(m-l)R=\frac{2\pi R}{L}. \tag{11.114}$$

Ordinate of point K of intersection of curves gives critical value of s for adopted conditions. Given different values of n, we look for minimum magnitude s, determining upper critical stress s_B. Let us note that it is sufficient to construct one of curves by (112) or (113) and to inscribe in it parallel to axis of abscissas chord of length $c = 2\pi R/L$. If curve is built by (112), then point K will be on right end of chord. We introduce designations

$$\left.\begin{aligned}\nu&=n\gamma+\frac{\pi R}{L}.\\ p^2&=\frac{1}{12(1-\mu^2)}\left(\frac{h}{R}\right)^2;\end{aligned}\right\} \tag{11.114a}$$

then equation (112) will take form

$$2\frac{s}{E}=\frac{p^2(\nu^2+n^2)^2+\nu^4}{\nu n(\nu^2+n^2)^2}. \tag{11.115}$$

Disregarding ν^2 in comparison to n^2, we obtain

$$2\frac{s}{E}=\frac{n^2p^2+\nu^4}{\nu n^5}. \tag{11.116}$$

Considering that to values of ν and $\nu + \frac{2\pi R}{L}$ there correspond identical

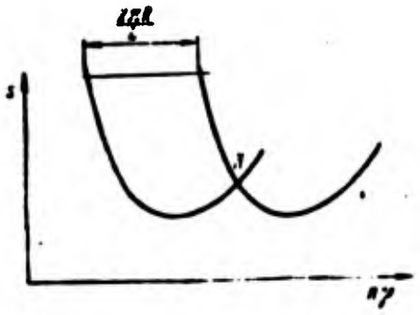

Fig. 11.36. Calculation of upper critical stress under torsion.

magnitudes s, we find

$$\frac{n^2p^2+\nu^4}{\nu n^3}=\frac{n^2p^2+\left(\nu+\frac{2\pi R}{L}\right)^4}{\left(\nu+\frac{2\pi R}{L}\right)n^3}. \qquad (11.117)$$

Hence for given ratio L/R it is necessary to determine n. Solving equation (117), we find*

$$n=4.2\sqrt[8]{1-\mu^2}\sqrt{\frac{R}{L}}\sqrt[4]{\frac{R}{h}}. \qquad (11.118)$$

Using (116), we then determine upper critical stress:

$$s_0=0.74\frac{E}{(1-\mu^2)^{3/4}}\frac{h}{R}\sqrt[4]{\frac{Rh}{L^2}} \qquad (11.119)$$

or, for $\mu = 0.3$.

$$s_0\approx 0.78E\frac{h}{R}\sqrt[4]{\frac{Rh}{L^2}}. \qquad (11.120)$$

We introduce dimensionless parameters

$$\hat{s}=\frac{s}{E}\frac{R}{h},\quad \theta=\frac{\pi R}{nL},\quad \delta=\frac{Rh}{L^2}; \qquad (11.121)$$

then we obtain

$$\hat{s}_0=0.78\sqrt[4]{\delta}. \qquad (11.122)$$

With this value $\hat{s}$ we have

$$\theta=\frac{\pi}{4.2\sqrt[8]{1-\mu^2}}\sqrt[4]{\delta}\approx 0.75\sqrt[4]{\delta},\quad \gamma\approx 1.73\sqrt[4]{\delta}. \qquad (11.123)$$

Judging by (118) and (123), number of waves, forming along arc, drops with increase of relative length of shell L/R and less sharply with increase of relative thickness h/R.

For shells of great length number of waves becomes equal to n = = 2, so that section obtains oval form. If we originate here from

*See work of V. M. Darevskiy [11.7].

more general equations of type (11), then we arrive at following formula for critical stress:*

$$s_* = \frac{1}{3\sqrt{2}} \frac{E}{(1-\mu^2)^{0.75}} \left(\frac{h}{R}\right)^{1.5}; \qquad (11.124)$$

here, considering $\mu = 0.3$, we obtain

$$s_* = 0.254 \sqrt{\frac{h}{R}}. \qquad (11.125)$$

For very long shells s_B does not depend on ration L/R, boundary conditions on faces here become nonessential.

On graph of Fig. 11.37 are united calculating data for shells of different length** for various ratios R/h. Here along the axis of abscissas is plotted ratio L/R, along the axis of ordinates, parameter $s_B = sR^2/Eh^2$; logarithmic scale is applied. Judging by formulas (120) and (125), in case of shell of average length we should obtain on such graph slanted lines, but for very long shell, a horizontal line. Strictly speaking, slanted lines in left part of diagram are envelopes of curves, corresponding to different numbers of waves n; these numbers are shown on graph. Curves n = 2 for significant L/R change into horizontal lines. From graph one can ascertain that the greatest value of ratio L/R at which number of waves constitutes $n \geqslant 4$ corresponds approximately to magnitude $\sqrt{R/h}$; this will agree with inequality (18b), establishing limits of applicability of theory of shells of average length. In Fig. 11.37 is given also magnitude γ, equal to tangent of angle of inclination of wave ridges to generatrix.

Research of influence of clamping of edges on critical stress***

---

*Formula of such type belongs to Schwerin [11.50].

**This graph belongs to Sturm [11.49].

***It was carried out by Donnell [11.30].

showed, as one should have expected, that it is substantial only for comparatively short shells.

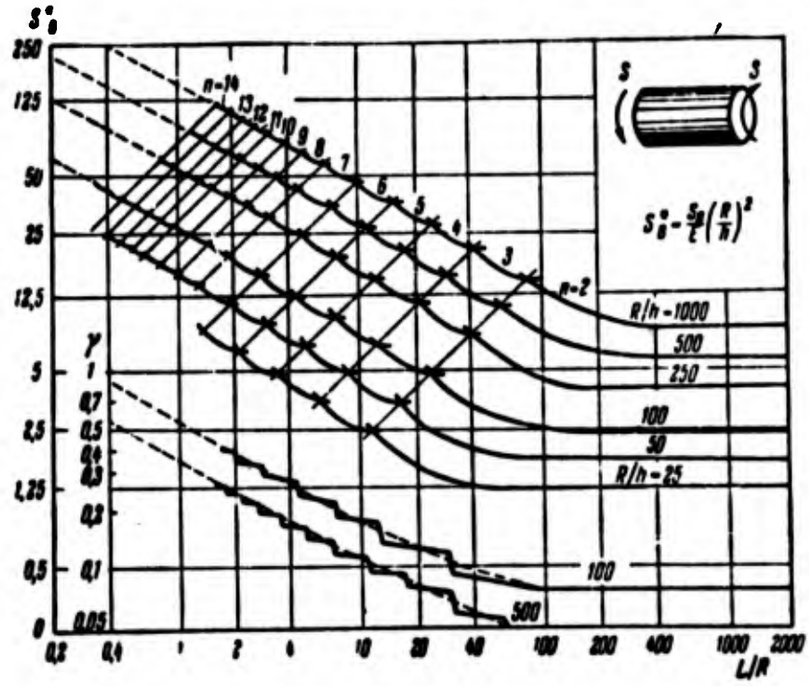

Fig. 11.37. Calculating data for determination of upper critical torsional stress.

As experiments show, real shells buckle during torsion approximately in the same way as in case of external pressure, but buckles are located at a certain angle to generatrix* (Fig. 11.38). Appearance of hollows for shells of average length, as a rule, is accompanied by a knock. Therefore, here, too, it is necessary to turn to solution of nonlinear problem of stability in the large.** We approximate deflection by expression

$$w = f_1 \sin\frac{\pi x}{L} \sin\frac{n}{R}(y - \gamma x) + f_2 \sin^2\frac{\pi x}{L}. \qquad (11.126)$$

First member is analogous to expression (107), pertaining to linear problem. Second member is selected in the same form as in cases of

*Photograph of Fig. 11.38 was obtained by O. I. Terebushko.

**This solution was given by Loo [11.44]; see also work of Yoshimura and Niisawa [11.55].

axial compression and external pressure. After substitution of (126) in the second of equations (29) and integration, we find

$$\frac{\Phi}{E}=\frac{\vartheta^2}{32}\left[\frac{1}{(1+\gamma^2)^2}\cos\frac{2n(y-\gamma x)}{R}+\frac{1}{\vartheta^4}\cos\frac{2\pi x}{L}\right]f_1^2-$$
$$-\frac{\vartheta^2}{2}\left[\frac{1}{(1+a_1^2)^2}\cos\frac{n(y-a_1x)}{R}-\frac{1}{(1+b_1^2)^2}\cos\frac{n(y-b_1x)}{R}-\right.$$
$$\left.-\frac{1}{(1+a_3^2)^2}\cos\frac{n(y-a_3x)}{R}+\frac{1}{(1+b_3^2)^2}\cos\frac{n(y-b_3x)}{R}\right]f_1f_2+$$
$$+\frac{R}{2n^2}\left[\frac{a_1^2}{(1+a_1^2)^2}\cos\frac{n(y-a_1x)}{R}-\frac{b_1^2}{(1+b_1^2)^2}\cos\frac{n(y-b_1x)}{R}\right]f_1-$$
$$-\frac{R}{8n^2\vartheta^2}f_2\cos\frac{2\pi x}{L}+sxy. \qquad (11.127)$$

where

$$a_1=\gamma+\vartheta,\ b_1=\gamma-\vartheta,\ a_3=\gamma+3\vartheta,\ b_3=\gamma-3\vartheta. \qquad (11.128)$$

If we set $\gamma = 0$, we arrive at former expression (49a) for Φ with replacement of $(-py^2/2)$ by sxy.

We determine total energy of system $\mathcal{E}$ by (56). Magnitudes $\mathcal{E}_c$ and $\mathcal{E}_u$ are calculated by formulas (10.95).* Work of external forces is equal to

$$W=M_u\theta=2\pi R^2hs\vartheta, \qquad (11.129)$$

where θ is mutual angle of rotation of ends. By formula (10.99), we have

$$\frac{\partial u}{\partial y}+\frac{\partial v}{\partial x}+\frac{\partial w}{\partial x}\frac{\partial w}{\partial y}=\frac{1}{G}\tau=-\frac{1}{G}\frac{\partial^2\Phi}{\partial x\,\partial y}. \qquad (11.130)$$

Angle θ is equal to $\bar{\gamma}L/R$, where $\bar{\gamma}$ is mean value of that component of shearing deformation which does not depend on w:

$$\bar{\gamma}=-\frac{1}{2\pi RL}\int\int_F\left(\frac{\partial u}{\partial y}+\frac{\partial v}{\partial x}\right)dx\,dy=$$
$$=-\frac{1}{2\pi RL}\int\int_F\left(\frac{1}{G}\frac{\partial^2\Phi}{\partial x\,\partial y}+\frac{\partial w}{\partial x}\frac{\partial w}{\partial y}\right)dx\,dy. \qquad (11.131)$$

---

*Expressions for $\mathcal{E}_c$ and $\mathcal{E}_u$ are given in book [0.3], p.348 .

Using expressions (126) and (127), we find

$$\theta=\left(\frac{s}{G}+\frac{\pi^2}{4}\frac{h}{L^2}\frac{1}{\theta^2}f_1^2\right)\frac{L}{R};$$

hence

$$W=2\pi RLh\left(\frac{s^2}{G}+s\frac{\pi^2}{4}\frac{h^2}{L^2}\frac{1}{\theta^2}f_1^2\right).^{1} \qquad (11.132)$$

Further we compose equations of Ritz method:

$$\frac{\partial\Theta}{\partial f_1}=0,\quad \frac{\partial\Theta}{\partial f_2}=0. \qquad (11.133)$$

We assume in first approximation that in process of postcritical deformation the form of wave formation will be that which corresponds to solution of linear problem of stability in the small, by (123). Then one can determine relationship between parameter s and angle of rotation θ and find lower critical stress $\hat{s}_H$. Relation $\nu = \hat{s}_H/\hat{s}_B$ turns out to depend on parameter $\delta = Rh/L^2$. When $\delta = 1/20$; $1/200$ and $1/2000$ we obtain accordingly $\nu = 0.94$; 0.80 and 0.87. Thus, least value constitutes about 80%. As we see, effect of nonlinearity of problem turns out here to be somewhat less than in the case of external pressure.

Geometric approach to problem (see § 128) allows us also in case of torsion to construct a surface, isometric to initial circular cylinder and reproducing form of buckling of the shell in the large.*

Study of influence of initial imperfections of form for shell** of average length can be conducted the way as in § 133. In Fig. 11.39 is depicted dependence between magnitude $\bar{s} = (s/G)(L/h)^2$ and parameter

---

*See works of A. V. Pogorelov [11.19], Ch. 3 and [11.20].

**It was carried out by Nash [11.48].

of angle torsion of $\overline{\theta} = \theta(L/h)^2$ for shell of ideal form and for shells with initial deflection, when $\delta = 1/200$. Ratio of maximum initial deflection to thickness is designated by φ_0. On graph are marked points, corresponding to upper and lower critical stresses s_B and s_H. General character of these curves is the same as in case of external pressure.

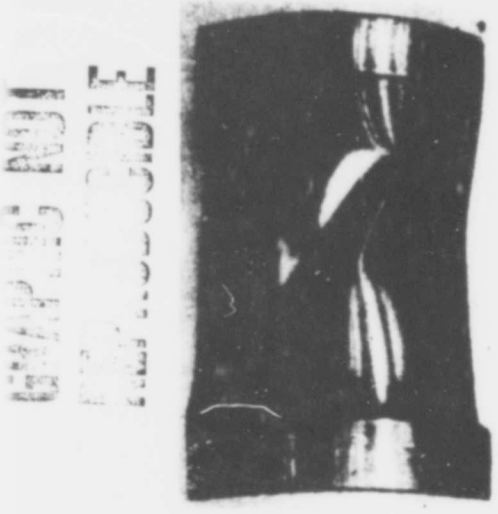

Fig. 11.38. Shell after buckling under torsion.

Judging by data of experiments, experimental values of critical stress lie, as a rule, in fork, constituted by upper and lower critical stresses. Therefore, in practical calculations for determination of s_B it is necessary to use graph of Fig. 11.37 or (for shells of average length) formula (120).

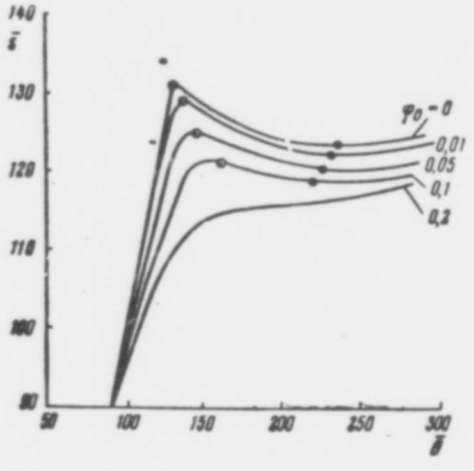

Fig. 11.39. Influence of initial deflection on upper and lower critical torsional stresses.

Calculated value $s_{расч}$ one should take for $R/h \leqslant 250$ equal to νs_B, where $\nu = 0.8$. For larger values of R/h influence of initial deflection will be stronger; therefore, ν should be decreased in approximate accordance with table ν for external pressure (p. 607), where lower limit for $R/h \approx 1500$ is equal to $\nu \approx 0.5$.

§ 135. Stability During Bending

Problem of stability of cylindrical shells during bending arises, for instance, during calculation of long pipelines; buckling can occur here in those zones, where bending moment or transverse force attains a maximum. This problem is met during calculation of many aviation constructions.

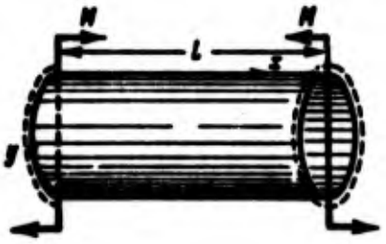

Fig. 11.40. Shell, subjected to pure bending.

Let us consider first the case of pure bending of shell of average length. Let us assume that shell is subjected to action of couples with moments M, applied in plane of diameter (Fig. 11.40). We count off coordinate y from point of intersection of plane of couple with middle surface, located in stretched part of the section. Normal stresses in cross sections are distributed before buckling of shell according to the law

$$p_x = p_1 \cos\frac{y}{R} = \frac{M}{\pi R^2 h}\cos\frac{y}{R}. \qquad (11.134)$$

Corresponding deformations in middle surfaces are equal to

$$\varepsilon_{x,0} = \frac{\partial u}{\partial x} = \frac{p_x}{E}, \quad \varepsilon_{y,0} = \frac{\partial v}{\partial y} - \frac{w}{R} = -\frac{\mu p_x}{E}, \quad \gamma_0 = 0.$$

Considering v = 0 and w = 0 on ends when x = 0 and x = L, we obtain the following expressions for initial displacements:

$$u_0 = \frac{p_1}{E}\left(\frac{L}{2} - x\right)\cos\frac{y}{R},$$

$$v_0 = \frac{p_1}{2ER}x(L-x)\sin\frac{y}{R},$$

$$w_0 = \frac{p_1}{2ER}\left[x(L-x) - 2\mu R^2\right]\cos\frac{y}{R}.$$

As we see, sections of shell do not remain circular; maximum deflections

are equal to $$w_{0,\max} = \frac{p_1 R}{2E}\left(\frac{L^2}{4R^2} - 2\mu\right).$$

However, we will not take into account these displacements, understanding subsequently by w additional deflection; it is easy to show that error of solution will be insignificant.

During research of stability of shell <u>in the small</u> we start from equation (17); it takes form

$$\frac{D}{h}\nabla^4 w + \frac{E}{R^2}\frac{\partial^4 w}{\partial x^4} + p_1\nabla^4\left(\frac{\partial^2 w}{\partial x^2}\cos\frac{y}{R}\right) = 0. \qquad (11.135)$$

Assuming that end sections of shell are supported by hinge, we select solution of equation (135) in the form of the series

$$w = \sin\frac{m\pi x}{L}\sum_{n=1}^{\infty} f_n \sin\frac{ny}{R}. \qquad (11.136)$$

We place this expression in (135) and equate to zero coefficients for uniform members; then we arrive at trinomial equations for parameters f_n of this form:

$$\left[\frac{D}{h}\left(\frac{m^2\pi^2}{L^2} + \frac{n^2}{R^2}\right)^2 + \frac{E}{R^2}\left(\frac{m\pi}{L}\right)^4\right] f_n - \\ - \frac{p_0}{2}\frac{n^2}{R^2}\left(\frac{m^2\pi^2}{L^2} + \frac{n^2}{R^2}\right)(f_{n-1} + f_{n+1}) = 0; \qquad (11.137)$$

here we take into account the fact that

$$\sin\frac{ny}{R}\cos\frac{y}{R} = \frac{1}{2}\left[\sin\frac{(n+1)y}{R} + \sin\frac{(n-1)y}{R}\right].$$

If we limit ourselves to a certain number of parameters f_n and to set determinant of system (137) equal to zero, then it is possible approximately to determine upper critical value p_0. Judging by calculations of A. V. Karmishin, Yu. G. Odinokov* and Flügge [10.18], magnitude $p_{1,в}$ differs by several percent from upper critical stress

*See Transactions of Kazan' Aviation Institute, 1940.

(33) for centrally compressed shell. It is possible to show that by measure of increase of number of parameters this divergence drops.* Such result is easily explained, if we consider that character of loss of stability in both cases is the same. Thus, upper critical value $\hat{p}_{1,в}$ is determined by (33):

$$\hat{p}_{1,в}=\frac{p_{1,в}R}{Eh}=\frac{1}{\sqrt{3(1-\mu^2)}}\approx 0{,}605. \tag{11.138}$$

Experiments show that buckling of shells of average length during pure bending occurs by a knock with formation of comparatively shallow hollows in compressed zone. Therefore, passing to resolution of problem of stability of shell in the large, we assume conditionally that additional deflections take place only in compressed half of section and that linkage of parts of shell by neutral diameter corresponds to conditions of rigid clamping. Approximating expression for deflection in compressed zone we select in the form

$$w=f\left(\cos\frac{\pi x}{l_x}\cos\frac{\pi y}{l_y}+a\cos\frac{2\pi x}{l_x}+b\cos\frac{2\pi y}{l_y}\right)\cos^2\frac{y}{R}, \tag{11.139}$$

where l_x, l_y are length of half-waves in axial and arc directions. This expression is taken by analogy with solution of Kempner, pertaining to case of axial compression (see § 127); there is introduced additionally the factor $\cos^2(y/R)$. If we limit ourselves to first member in parentheses and take for compressed zone

$$w=f\cos\frac{\pi x}{l_x}\cos\frac{\pi y}{l_y}\cos^2\frac{y}{R}, \tag{11.139a}$$

then, solving linear problem by methods of Ritz or Bubnov-Galerkin,

---

*This conclusion was drawn by Yu. A. Shevlyakov and L. I. Manevich. To the same belongs resolution presented below of problem of stability in the large; see Reports of Academy of Sciences of Ukrainian SSR, No. 5 (1960), pp. 605–608.

we obtain upper critical stress, close to (138).

Putting (139) in the right part of equation (16), we find function Φ. Then we determine total energy of system $\mathcal{Э}$. We use parameters $\hat{p}$, $\$$, and η by (38) and (38a) and introduce new designations

$$\mathcal{Э}^{*}=\mathcal{Э}\frac{16R}{3Eh^{3}\pi L},\quad \zeta_{1}=f_{1}\eta/h; \tag{11.140}$$

then we obtain

$$\begin{aligned}\mathcal{Э}^{*}=&\frac{\zeta_{1}^{2}}{\eta^{2}}\Big\{\zeta_{1}^{2}\vartheta^{4}\Big[\frac{(a+b)^{2}+4a^{2}b^{2}}{(1+\vartheta^{2})^{2}}+\frac{a^{2}}{(1+9\vartheta^{2})^{2}}+\\&+\frac{b^{2}}{(9+\vartheta^{2})^{2}}+\frac{1}{128}+\frac{17}{12\cdot256}(1+8a^{2})^{2}\Big]+\frac{1}{4}\frac{\vartheta^{4}}{(1+\vartheta^{2})^{2}}-\\&-\frac{\vartheta^{4}}{(1+\vartheta^{2})^{2}}\zeta_{1}(a+b)+\frac{1}{128}(\zeta_{1}-8a)^{2}\Big\}-\frac{8}{3}\hat{p}_{1}^{2}+\\&+\frac{1}{48(1-\mu^{2})}\zeta_{1}^{2}\left[(1+\vartheta^{2})^{2}+32(a^{2}\vartheta^{4}+b^{2})\right]-0.225\frac{\zeta_{1}^{2}\vartheta^{2}}{\eta}(1+8a^{2}).\end{aligned} \tag{11.141}$$

We minimize total energy for five parameters, assuming

$$\frac{\partial\mathcal{Э}^{*}}{\partial\zeta_{1}}=\frac{\partial\mathcal{Э}^{*}}{\partial\eta}=\frac{\partial\mathcal{Э}^{*}}{\partial a}=\frac{\partial\mathcal{Э}^{*}}{\partial b}=\frac{\partial\mathcal{Э}^{*}}{\partial\vartheta}=0. \tag{11.142}$$

First three equations will be the same as if problem was solved for case of uniform compression (p_1 = const = p). So that other two equations (142) were satisfied for simple compression, parameters $\hat{p}$ and $\hat{p}_1$ should be connected by dependence

$$\hat{p}_{1}=1.1\left[\hat{p}+\frac{17}{384}\frac{\zeta_{1}^{2}\vartheta^{2}}{\eta}(1+8a^{2})\right]. \tag{11.143}$$

Therefore, knowing postcritical forms of shell during pure compression, found in solution of Kempner, it is possible to cross to case of bending. Such transition is made in following table:

$\hat{p}$	0,24	0,22	0,21	0,2	0,19	0,18
ζ_1	1,1	1,2	1,24	1,27	1,35	1,4
$\hat{p}_1$	0,29	0,28	0,27	0,26	0,265	0,27

The smallest parameter of load is equal to $p_{1,н} = 0.26$; remaining parameters will be: $\eta = 0.19$, $\$ = 0.3$, $a = 0.5$.

This problem was solved also on the assumption that along the line of linkage of compressed and stretched zones there is elastic clamping; there was taken a somewhat different expression for w. In compressed zone deflections differed little from (139), and on neutral diameter and in stretched zone they were negligible. Repeating calculations, we arrive at following value of lower critical stress:

$$\bar{p}_{1,н} = 0.24; \qquad (11.144)$$

here we have $\zeta_1 = 1.4$, $\eta = 0.22$, $\$ = 0.36$, $a = 0.18$.

Thus, amplitude of lower critical stress is equal to $p_{1,н} = 0.24Eh/R$, whereas during uniform compression coefficient in this formula was equal to 0.18. Judging by this variant of solution, presence of stretched zone and irregularity of distribution of compressive stresses here has substantial effect; amplitude of lower critical stress exceeds by 33% magnitude $p_н$, pertaining to uniform compression. This, at first glance, contradicts result obtained during solution of linear problem. Final conclusions can be made only later, when this complicated problem has been solved by digital computers.

In practical calculations one should originate, as in case of central compression, from magnitude of lower critical stress taking into account experimental data. Influence of initial imperfections in form of shell in case of bending should be not as great as in axial compression; initial hollows in stretched zone must not substantially affect behavior of shell. Consequently, from statistical point of view probability of clicking of shell in case of bending will be less. On the other hand, during bending of shell there

occurs certain flattening of cross section, which leads to increase of maximum stress as compared to calculated value. Nevertheless, here calculated stresses must be taken somewhat higher than during central compression. Thus, for R/h = 250 one should take $p_{1,\text{расч}}$ = = 0.22 instead of value 0.18 shown for case of central compression.

In general case of <u>eccentric compression</u> one should calculate coefficient $\alpha = 1 - p_2/p_1$, where p_1 is maximum compression stress and p_2 is stress at opposite end of diameter (taking into account sign). Then for calculation it is possible to use data of table for $\hat{p}_{\text{расч}}$ in case of central compression (p.592) (depending upon ratio R/h) and find value of the greatest compressing stress by formula*

$$\hat{p}_{1,\text{расч}} = \hat{p}_{\text{расч}}\left(1 + \frac{\alpha}{2}\right).$$

In case of pure bending we have $\alpha = 2$; hence for $R/h \leqslant 250$ we arrive at magnitude $\hat{p}_{1,\text{расч}} = 1.25 \cdot 0.18$, = 0.225, which corresponds to above-indicated value 0.22.

All above-mentioned data pertained to shell of average length. For thin <u>shells with significant ratio of length to radius</u> we can expect another phenomenon — buckling in <u>long half-waves</u> — like case of uniform compression (p. 570).** Using the same apparatus "semi-membrane" theory of shells, it is possible to solve in linear formulation problem of loss of stability with formation of such long half-waves. Results of approximate solutions are presented in Fig. 11.41. Along the axis of ordinates is plotted parameter $\hat{p}_{1,B}$, along

---

*This formula was offered by B. M. Broude.

**This circumstance was first shown by E. D. Pletnikov in 1949. Subsequently the given problem was investigated in application to different cases of bending of smooth and reinforced shells by K. D. Turkin [11.24]. To him belongs graph of Fig. 11.41 and experimental data shown in it, and also photograph reproduced in Fig. 11.42.

along the axis of abscissas, magnitude $\xi = (L/mR)\sqrt{h/R}$; here m is number of longitudinal half-waves. Least value of $p_{1,B} = 0.38$ occurs for $\xi = 0.58$. For instance, when R/h = 330 this minimum is obtained for shell with ratio L/R = 10, L/R = 20, etc. As can be seen from graph, lowering $p_{1,B}$ as compared to case of bending in short half-waves, when $p_{1,B} \approx 0.605$, occurs, starting from $\xi = 0.35$. During calculations by Fig. 11.41 one should calculate ξ, substituting m = 1, 2, etc., and then select least value of $\hat{p}_{1,B}$. In Fig. 11.42 is shown shell after buckling in long half-waves. Judging by preliminary calculations, calculation of geometric nonlinearity of problem here does not lead to as "catastrophic" a drop of calculated stress, as during buckling in short half-waves. Experimental values of $\hat{p}_1$ shown in Fig. 11.41 by circles bears witness to this; their scattering is comparatively small.

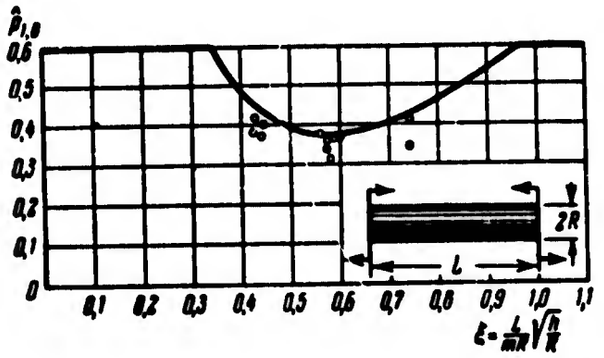

Fig. 11.41. Upper critical stress during pure bending.

If we conduct calculation by value $\hat{p}_{1,\text{расч}} = 0.22$, then, apparently, this will give for long shells a certain additional safety factor. Let us note that all experimental points presented in Fig. 11.41 lie above level $\hat{p}_1 = 0.22$.

Fig. 11.42. Buckling during bending in "long waves."

We analyzed case of pure bending of shell. We turn now to another, practically important case, when shell is subjected to <u>transverse bending</u> under action of concentrated

forces or distributed load. Here two approaches to problem are possible. One of them consists of study of wave formation in zone of greatest normal compression stresses, as during pure bending; it pertains to comparatively long shell ($L > 4R$). Another approach consists in considering zone of the greatest tangential stresses τ_{max}, located at neutral layer. Let us note that in case of shell clamped on one end and loaded with concentrated force on the other, free end, magnitude τ_{max} constitutes $p_1 R/L$.

Influence of tangential stresses will, naturally, increase with decrease of length of shell. Therefore, calculation for stability by τ_{max} has value for short shells when $L < 4R$; it can be conducted, proceeding from data of upper and low critical stresses* during torsion (see § 134). In final calculation there is introduced the least of critical loads, found by p_1 and τ_{max}.

Proceeding from formula (119), we arrive at following final expressions for upper critical transverse force. For shell, clamped at one end and subjected to action of concentrated load at free end, we have (for $\mu = 0.3$)

$$Q_в = 0.78\pi E h^2 \sqrt[4]{\frac{Rh}{L^2}}. \qquad (a)$$

in case of load $Q_в$ distributed the whole length of shell,

$$Q_в = 1.12\pi E h^2 \sqrt[4]{\frac{Rh}{L^2}}. \qquad (b)$$

Example 11.1. Intraplant gas conduit is a cylindrical shell,

---

*Such approach was developed by V. M. Darevskiy [11.7]; to him belong formulas (a), (b); see also book [0.3], p. 351. Judging by calculations of V. V. Serdyukov, upper critical value $\tau_{в,из}$ for transverse bending somewhat differs from $\tau_{в,кр}$ in case of torsion, where divergence depends on ratio L/R. This question should be investigated in more detail.

having a series of supports (Fig. 11.43).* Thickness of wall of gas conduit h = 6 mm, radius of cross section R = 1010 mm, material is low-alloy steel of brand 14KhGS with yield point σ_T = 3500 kg/cm^2.

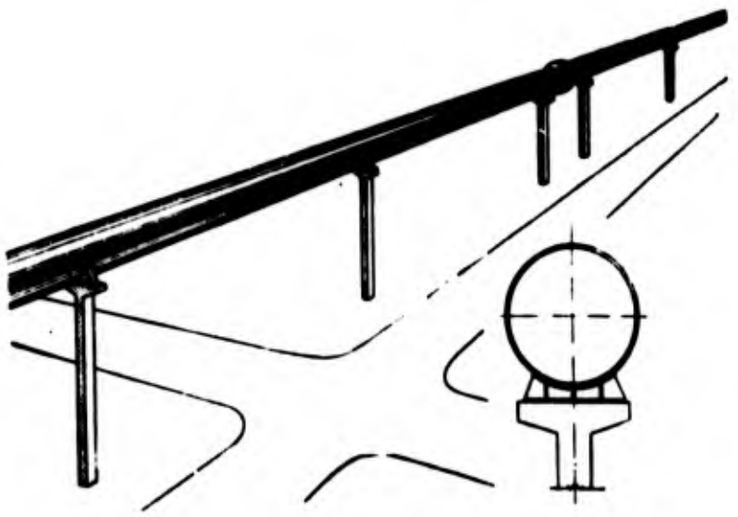

Fig. 11.43. To account calculation of gas conduit on stability during bend.

Linear weight of pipe $d_{тр}$ = 246 kg/m, linear weight of insulation $d_{из}$ = = 600 kg/m, pressure in gas conduit during test by air constitutes q = 3.75 kg/cm^2. Distance between supports, found by norms of strength,** is equal to L = 68 m. Check shell for stability, considering that gas conduit has so-called lens compensators of temperature deformations, shown in Fig. 11.43, and that near one of supports gas conduit may be equipped with a gas valve.

Shell is subjected here to joint action of bending and axial compression. Maximum compressive stress in section above support is

---

*This example was offered by M. N. Ruchimskiy.

**Instructions on determining loads acting on supports of pipelines and tolerable spans between their supports, 1959.

equal to $$p_1 = \frac{(q_{тр} + q_{из}) L^2}{12W} + 1{,}2\frac{qR}{2h} =$$

$$= \frac{(2{,}46 + 6)\,680^2}{12 \cdot 16\,100} + 1{,}2\,\frac{3{,}75 \cdot 101}{2 \cdot 0{,}6} = 2000 + 380 = 2380 \ \text{kg/cm}^2,$$

where W is moment of resistance of section.

First component considers bending stresses caused by weight load in middle spans of pipeline, considered as a continuous beam. Second member corresponds to longitudinal forces from internal pressure; coefficient 1.2 is introduced to account for additional pressure on lens of compensator.

Tensile stress at opposite end of diameter is equal to p_2 = = -2000 + 380 = -1620 kg/cm^2. We calculate coefficient α:

$$\alpha = 1 + \frac{1620}{2380} \approx 1{,}7.$$

For R/h = 1010/6 we find by above-mentioned data (p. 628):

$$\hat{p}_{1,\,расч} = 0{,}18\left(1 + \frac{1{,}7}{6}\right) = 0{,}216.$$

Hence

$$p_{1,\,расч} = 0{,}216 \cdot 2{,}1 \cdot 10^6\,\frac{0{,}6}{101} \approx 2700 \ \text{kg/cm}^2.$$

Taking safety factor of stability equal to 1.5, we find tolerable stress $p_{1,доп}$ = 1800 kg/cm^2. Comparison of this magnitude with calculated stress of 2380 kg/cm^2 shows that construction is not reliable. It is necessary to decrease length of span approximately to 50 m.

In supplement to this we investigate stability of shell in long half-waves (p. 628). According to data of example L/R = 6.7, R/h = = 168; considering m = 1, we obtain ξ = 0.51.

By graph of Fig. 11.41 parameter $\hat{p}_{1,в}$ constitutes 0.38; this magnitude lies higher than the value $\hat{p}_1$ = 0.216 taken by us.

§ 136. Closed Shell Under Combined Loading

In many constructions closed cylindrical shells are subjected simultaneously to action of loads of various type. Let us give data for determination of critical stresses with such combined load.

1. Axial compression or bending and external pressure. Combination of these loads is characteristic, e.g., for high towers of tanks utilized in chemical industry. In lower band of tower there are created compressive stresses from gravity and, at the same time, inside tower there can be a certain vacuum.

Let us consider first the problem of stability of the shell in the small. Combining (30) and (70), we obtain initial equation for shells of average length in the form

$$\frac{D}{h}\nabla^4 w+\frac{E}{R^2}\frac{\partial^4 w}{\partial x^4}+p\nabla^4\left(\frac{\partial^2 w}{\partial x^2}\right)+\frac{qR}{h}\nabla^4\left(\frac{\partial^2 w}{\partial y^2}\right)=0. \qquad (11.145)$$

Substituting solution (36) and using dimensionless parameters (38) and (73), we arrive at following dependences

$$\hat{p}+\frac{\hat{q}}{\beta^2}=\frac{1}{12(1-\mu^2)}\frac{(1+\beta^2)^2}{\beta^4}\eta+\frac{\beta^2}{(1+\beta^2)\eta}. \qquad (11.146)$$

As we see, critical combinations of magnitudes $\hat{p}$ and $\hat{q}$ are interconnected, for definite β and η, by a linear dependence. Graph of $\hat{p}(\hat{q})$ should be a certain broken line ACDB of the type shown in Fig. 11.44. Later (see Chapter XXI) we will confirm the fact that such diagrams of stability under combined loads are always turned with convexity outwards — from origin of coordinates — this ensues from general considerations. Let us note that points A and B in Fig. 11.44 correspond to upper critical loads of axial compression $\hat{p}_{0,B}$ and external pressure $\hat{q}_{0,B}$, applied separately from each other. If we join these points by straight line, then we obtain intermediate values of

$\hat{p}$ and $\hat{q}$, corresponding to equation

$$\frac{\hat{p}}{p_{0.0}}+\frac{\hat{q}}{q_{0.0}}=1$$

or

$$\frac{p}{p_{0.0}}+\frac{q}{q_{0.0}}=1. \qquad (11.147)$$

As it is easy to see, values of $\hat{p}$ and $\hat{q}$ by (147) will always determine upper critical loads with certain safety factor as compared to broken line. Therefore, in practical calculations as a first approximation it is possible to use equation (147).

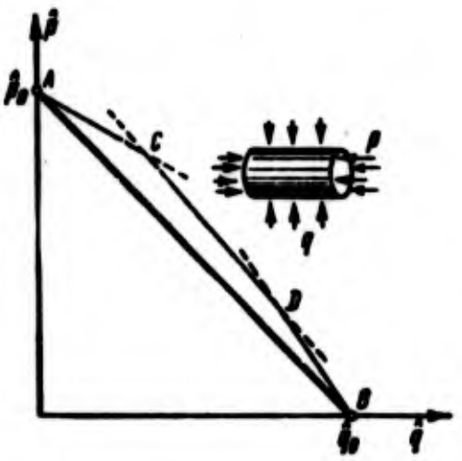

Fig. 11.44. Determination of upper critical stresses under joint action of axial compression and external pressure.

Judging by experimental data, loss of stability of shells <u>in the large</u> under combined loading is accompanied by wave formation of mixed character: hollows turn out to be more drawn out along generatrix than during pure compression,* Solution of nonlinear problem** allows us to determine dependence between lower critical loads. We note that here to diagram $\hat{p}(\hat{q})$ should be outlined with respect to origin of coordinates in the same way as in previous case (see Chapter XXI). Consequently, during calculation of lower critical loads it is possible to use equations of type (147):

---

*These experiments are described in more detail in [0.3], p. 344.

**It was carried out by V. L. Agamirov and O. I. Terebushko.

$$\frac{\hat{p}}{\hat{p}_{\text{н.в}}}+\frac{\hat{q}}{\hat{q}_{\text{н.в}}}=1. \qquad \text{[Subscript н = lower]}. \qquad (11.148)$$

Experimental values of critical loads, obtained for combined load by V. L. Agamirov (see [0.3], p. 344), fill the region lying between lines (147) and (148).

We shall next analyze case of <u>hydrostatic pressure</u>, frequently met in practice. Here we have $\hat{p} = \hat{q}/2$, and formula (146) takes on form*

$$\hat{q}_{\text{в}}=\frac{1}{1+\frac{\vartheta^2}{2}}\left[\frac{(1+\vartheta^2)^2\eta}{12(1-\mu^2)}+\frac{\vartheta^4}{(1+\vartheta^2)^2\eta}\right]. \qquad (11.149)$$

Approximate equation (147) gives

$$\hat{q}_{\text{в}}\left(\frac{1}{2\hat{p}_{\text{н.в}}}+\frac{1}{\hat{q}_{\text{н.в}}}\right)=1.$$

We use formulas (40) and (77a) for $\hat{p}_{0,\text{в}}$ and $\hat{q}_{0,\text{в}}$; then we obtain

$$\hat{q}\left(0.83+1.1\frac{L}{R}\sqrt{\frac{R}{h}}\right)=1.$$

If ratio R/h is great, first member in parentheses will be small as compared to second; therefore, as already mentioned above, critical pressure in case of hydrostatic stress weakly differs from value, corresponding to pure transverse pressure.

2. <u>External pressure and torsion</u>. To such combination of loads is subjected, e.g., the shell of housing of transmission of gas-turbine engine. Excess pressure appears in combustion chamber located on external side, and torque is transmitted from disk, carrier guide vanes.

Solutions of problem of stability of shell in the small and in

---

*Formula of such type was obtained by Mises [11.47].

the large* lead here to approximate formulas of the type in case of plate subjected to simultaneous action of compression and shearing:

$$\frac{\hat{q}_в}{\hat{q}_{в.в}}+\left(\frac{\hat{s}_в}{\hat{s}_{в.в}}\right)^2=1,\quad \frac{\hat{q}_н}{\hat{q}_{в.н}}+\left(\frac{\hat{s}_н}{\hat{s}_{в.н}}\right)^2=1. \tag{11.150}$$

By $\hat{s}$ here is understood parameter (121); to case of independent torsion there corresponds parameter of upper or lower critical stress $\hat{s}_{0,в}$ or $\hat{s}_{0,н}$ (see § 134).

Last, during joint action of axial compression, external pressure and torsion it is possible to use a formula combining (147) and (150):

$$\frac{\hat{p}}{\hat{p}_{в.в}}+\frac{\hat{q}}{\hat{q}_{в.в}}+\left(\frac{\hat{s}}{\hat{s}_{в.в}}\right)^2=1; \tag{11.151}$$

an analogous formula should be recommended for lower critical stresses.

Experiments show that hollows formed during joint action of external pressure and torsion (Fig. 11.45), have more clear boundaries than in case of simple torsion (see Fig. 11.38). If as supplement to external pressure and torsion there is axial compression, edges of hollows are inclined at smaller angle to generatrix (Fig. 11.46).**

3. <u>External pressure, torsion and bending</u>. In preceding item it was shown that housing of transmission of gas-turbine engine is subjected to action of external pressure and torsion. To these efforts it is necessary to add flexural stress, if we consider force of inertia of body of motor during rotary displacements of aircraft.

---

*Solution of linear problem belongs to V. M. Darevskiy [11.7], [11.8], and nonlinear, to O. I. Terebushko [11.22]. Certain authors recommend taking exponent $\hat{s}/\hat{s}_0$ in formula (150) equal to 3.

**Photographs of Figs. 11.45 and 11.46 were obtained by O. I. Terebushko.

From § 135 we know that in case of transverse bending it is necessary to divide shell depending upon relative length. With comparatively great length ($L > 4R$) of principal importance is loss of stability of type of compression with formation of shallow dents in compressed zone. Therefore, here it is appropriate to conduct calculation for combined load, proceeding from formula of type (151), substituting for p_0 the magnitude of maximum stress during bending p_1. In case of shell of small length there should occur buckling of torsion type, with concentration of dents in neutral zone. Then it is necessary to use formula of type (150), understanding by s the sum of tangential forces, caused by torsion, and maximum tangential forces from bending.

Fig. 11.45. Form of wave formation during joint action of torsion and external pressure.

Fig. 11.46. Case of joint action of axial compression, external pressure and torsion.

4. Influence of internal pressure. Question of stability during axial compression or bending and internal pressure appears, for instance, in problem of calculation of supporting shell of aircraft fuel tank. As is known, on starting section in body of aircraft

there appear compressive forces, connected with forces of inertia, on other sections of trajectory body is subjected to bending; at the same time inside the tank there is supported significant pressure. Since for the purpose of economy of weight shell of fuel tank is designed as thin as possible, then this problem has urgent significance.

Let us consider case of joint action of axial compression and internal pressure, not taking into account local stress in zone of linkage of shell with rigid frame, i.e., considering initial state of strain momentless.* If we investigate stability of shell subjected to axial compression by linear theory,** then it will appear that additional internal pressure does not affect magnitude of critical stress, so that value of p_B as before, should be determined by formula (34). We arrive at another conclusion from propositions of nonlinear theory. Actually, buckling of shell in the large is accompanied by formation of deep dents, turned toward center of curvature, but in the presence of internal pressure such clicking of shell will be hampered. Hence it is clear that nature of wave formation here should change. This is confirmed by experiments. With small internal pressure we obtain dent of compression type, but stretched along arc (let us remember that during external pressure they were drawn out along generatrix). This it is possible to see in photographs*** in Fig. 11.47; here there is compared sample (a), tested for simple compression, and samples (b) and (c), subjected to compression in combination with internal pressure. With increase of intensity of

---

*On calculation for this effect see below, in § 141.

**See W. Flügge, Die Stabilität der Kreiszylinderschale, Ing. Archiv 3, No. 5 (1932).

***Photographs of Fig. 11.47 are taken from article [11.33], 1957.

pressure effect of lengthening of dents along arc is increased. With significant internal pressure chain of shallow dents is replaced by solid annular folds, so that loss of stability becomes axisymmetric (Fig. 11.47b).

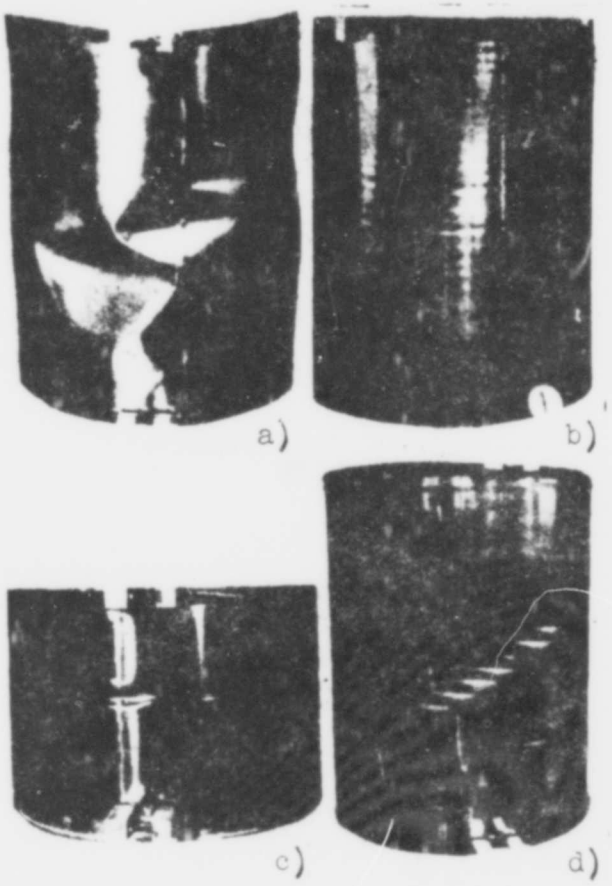

Fig. 11.47. Form of wave formation during action, a) of axial compression, b) and c) of internal pressure combined with axial compression.

But in this case effect of nonlinearity no longer will be essential, and, as one may see from § 126, we again arrive at formula (34) for critical stress.

These conclusions ensue also from theoretical research.* If we generalize solution of Kempner for case when axial compression is combined with internal pressure, then it will appear that lower critical stress $\hat{p}_H$ increases by measure of increase of internal pressure.

On graph of Fig. 11.48 along axis of ordinates is plotted ratio $\hat{p}_H/\hat{p}_{0,B}$ where $\hat{p}_{0,B}$ is parameter of upper critical stress for simple axial compression according to (40), and along the axis of abscissas we plot magnitude $\bar{q} = (q/E)\,(R/h)^2\sqrt{3(1-\mu^2)}$. When $\bar{q} = 0$ we obtain $\hat{p}_H = 0.18$, which corresponds to formula (66). Judging by graph, in region of variation of parameter $0 < \bar{q} < 0.5$ supporting influence of internal pressure sharply increases. When $\bar{q}$ nears $\bar{q} = 2$, magnitude $\hat{p}_H$ practically attains upper limit $\hat{p}_{0,B}$. In Fig. 11.48 are marked also values $\$ = l_y/l_x$, characterizing relative dimensions of dents with stress $\hat{p}_H$; as we see, ratio l_y/l_x rapidly increases by measure of growth of $\bar{q}$. Here, too, is shown region of experimental points.

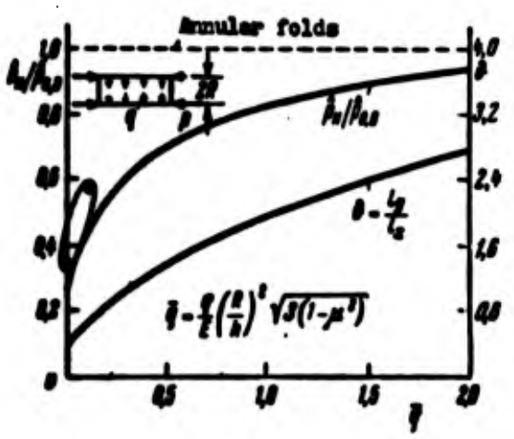

Fig. 11.48. Determination of lower critical loads during joint action of axial compression and internal pressure.

Research of joint action of <u>torsion and internal pressure</u> leads to somewhat different results. Solution, based on <u>linear theory</u>** and pertaining to shell of average length, indicates certain growth

*This solution is contained in article of Thielemann [11.51], [11.52]; see also work of Lo, Crate, and Schwartz [11.43] and Klein [11.40].

**It was given by V. M. Darevskiy [11.7] and V. A. Mar'in [11.14]. See also work of Klein [11.40].

of upper critical stress of torsion $\hat{s}_B$, determined by (121), with increase of parameter of internal pressure $\hat{q}$ according to (73). This one may see from graph of Fig. 11.49. Here along the axis of ordinates is plotted ratio $\hat{s}_B/\hat{s}_{0,B}$, where $\hat{s}_{0,B}$ is from formula (120), and along the axis of abscissas is plotted magnitude $\hat{q}/\hat{q}_{0,B}$, where $\hat{q}_{0,B}$ corresponds to critical value of external pressure for the same shell, calculated by (77) or (77a). The calculated one is the solid line; dotted line corresponds to approximate parabolic line of dependence

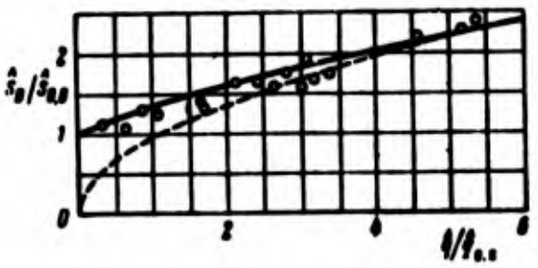

Fig. 11.49. Upper critical loads during joint action of torsion and internal pressure.

$$\left(\frac{\hat{s}_B}{\hat{s}_{0,B}}\right)^2 = 0.907\,\frac{\hat{q}}{\hat{q}_{0,B}},$$

pertaining only to large values of $\hat{q}$. If we consider values of internal pressure usually met in practice, then influence of it on stability during torsion in the small can be little. At the same time, undoubtedly, internally pressure should substantially increase lower critical stress of torsion. It is desirable to give solution of such a nonlinear problem.

In experiments there are marked two different types of wave formation of shell. For small values of internal pressure the hollow appears with a knock, located on helix (Fig. 11.50). With relatively great pressure there are formed short solid waves, developing subsequently at ends. In Fig. 11.51 is shown photograph of such sample, already having undergone plastic deformation flow.*

On graph of Fig. 11.49 are shown experimental points for critical stresses, pertaining to one steel (black circle) and 18 duralumin samples.** Greater part of experimental values of stress lies somewhat

*Photographs of Figs. 11.50 and 11.51 belong to V. A. Mar'in.

**By experiments, carried out by R. I. Kshnyakin, M. V. Nikulin, and V. V. Serdyukov, see [11.11].

below upper critical magnitude; for certain of them lowering constitutes 12–15%. As a result it is possible to recommend conducting practical calculations by graph of Fig. 11.49, introducing correction factor ν somewhat higher than during simple torsion (see § 134), e.g., $\nu = 0.85$ when $R/h \leqslant 250$.

During combined action of internal pressure and bending* it is necessary to use different data depending upon whether during simple bending of given shell normal or tangential stresses are decisive. In first case it is possible to determine lower critical values of maximum flexural stress by graph of Fig. 11.48, increasing $\hat{p}_H$ (for $\hat{q} < 0.5$) approximately by 25%. In second case it is necessary to conduct calculation, using graph of Fig. 11.49, by analogy with problem of torsion.

All given data pertain to elastic region. In the course of calculation it is important to determine

Fig. 11.50. Buckling of shell during simultaneous action of torsion and low internal pressure.

Fig. 11.51. Case of simultaneous action of torsion and significant internal pressure.

*This problem was considered by V. M. Darevskiy [11.7].

whether maximum value of intensity of stresses exceeds limit of proportionality of material. If stresses caused by internal pressure are so great that this requirement is upset, then supporting influence of internal pressure will weaken. Let us turn, e.g., to case of joint action of internal pressure and compression; supplemented graph of Fig. 11.48 will obtain the form shown in Fig. 11.52 (see [11.30a]). Drop of supporting power of shell starts from point A, corresponding to limit of proportionality.

Example 11.2. Body (a) of fuel tank of rocket (Fig. 11.53),* constituting a cylindrical shell, transmits on starting section compressive force P with internal pressure q = 2 technical atmospheres. Length of tank is L = 6.5 m, diameter D = 2.44 m, wall thickness h = = 2 mm. Material is duralumin, $E = 7 \cdot 10^5$ kg/cm^2, $\mu = 0.32$, $\sigma_{пц} =$ = 2400 kg/cm^2. Determine critical compressive load.

We find parameter of internal pressure

$$\hat{q} = \frac{q}{E}\left(\frac{R}{h}\right)^2 = \frac{2}{7 \cdot 10^5}\left(\frac{122}{0{,}2}\right)^2 = 1{,}16;$$

here $\bar{q} = \sqrt{3(1-\mu^2)}\,\hat{q} = 1.91$. By graph of Fig. 11.48 we find, $\nu = 0.92$, $\hat{p}_н = 0.56$. Lower critical load of compression constitutes

$$P_н = 2\pi R h p_н = 2\pi E \hat{p} h^2 = \\ = 2\pi \cdot 7 \cdot 10^5 \cdot 0{,}56 \cdot 0{,}2^2 = 98\,000 \text{ kg}.$$

Tensile stress in arc direction is equal to $\sigma_y = qR/h = 1220$ kg/cm^2, compressive tension from force P constitutes $\sigma_x = -0.56\,Eh/R =$ = -640 kg/cm^2. Intensity of stresses $\sigma_1 = \sqrt{\sigma_x^2 + \sigma_y^2 - \sigma_x\sigma_y} =$ = 2380 kg/cm^2 lies within limits of proportionality.

---

*Figure 11.53 is taken from journal "Weltraumfahrt," No. 3 (1961), p. 75. Dimensions of tank are taken on the basis of data, given in journal "Flight," No. 2, 43 (1959), 507-532.

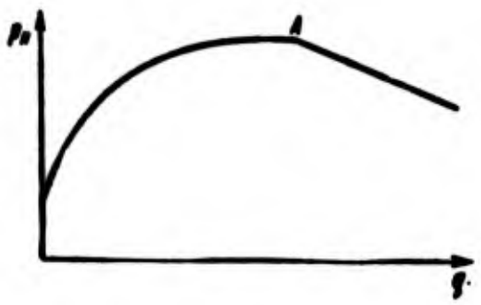

Fig. 11.52. Supporting power of shell during joint action of axial compression and internal pressure drops upon development of plastic deformation.

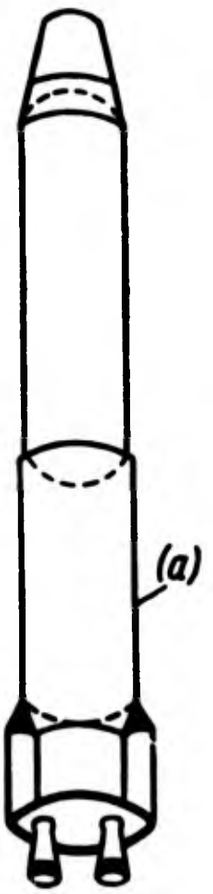

Fig. 11.53. Body of rocket with propellant tank.

If there is no internal pressure, it would be necessary to take $\hat{p}_H = 0.18$; lower critical load here $P_H = 98{,}000 \times (0.18/0.56) = 31{,}500$ kg. Thus, thanks to supporting influence of internal pressure supporting power of tank is increased approximately three times.

Example 11.3. To calculate on stability of body A of transmission shaft and external body B of combustion chambers of gas-turbine engine, having axial-flow compressor.* Diagram of motor is depicted in Fig. 11.54. Shells A and B receive torque M_K from forces S_a and S_b transmitted from vanes of nozzle apparatus a and b. Shell A,

*This example was offered by I. A. Birger.

furthermore, is subjected to action of external pressure q = 8 technical atmospheres. Dimensions of this shell: L = 560 mm, R = 160 mm, h = 1.6 mm. Considering that shell is reinforced by rings, we take reduced thickness equal to $h_{пр}$ = 2.5 mm. External body B experiences

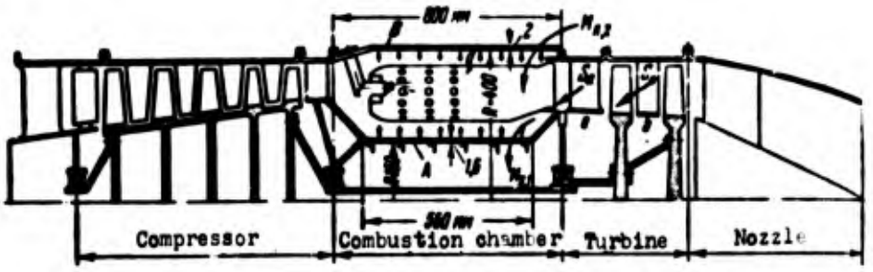

Fig. 11.54. Calculation for stability of shells of gas-turbine engine.

the same pressure, which for it is already internal; dimensions of shell we take: L = 800 mm, R = 400 mm, h = 2 mm. Determine critical value $M_{кр,A}$ and $M_{кр,B}$ for each shell. Material is steel, E = 2.1·$\cdot 10^6$ kg/cm^2, μ = 0.3, $\sigma_{пц}$ = 5000 kg/cm^2.

For shell A we find by graphs of Figs. 11.18 and 11.20 for L/R = = 3.5 and $R/h_{пр}$ = 64 (see also formula (77a))

$$\hat{q}_{0,в} = 0{,}0329, \quad \hat{q}_{0,н} = 0{,}0263.$$

Magnitude $\hat{q}_{0,н}$ we take as the calculated one $\hat{q}_{0,н} = \hat{q}_{0,расч}$. Further, by the formula (122),

$$\hat{s}_{0,в} = 0{,}78\sqrt[4]{\frac{Rh}{L^2}} = 0{,}78\sqrt[4]{\frac{16 \cdot 0{,}25}{56^2}} = 0{,}1475.$$

Taking ν = 0.8, we obtain

$$\hat{s}_{0,расч} = 0{,}8\hat{s}_{0,в} = 0{,}118.$$

Parameter $\hat{q}$, corresponding to q = 8 technical atmosphere, is equal to

$$\hat{q}_{расч} = \frac{8 \cdot 64^3}{2{,}1 \cdot 10^6} = 0{,}0157.$$

For combined load from formula of type (150)

$$\hat{s}_{pacy} = \hat{s}_{0,\,pacy}\sqrt{1-\frac{\hat{q}_{pacy}}{\hat{q}_{0,\,pacy}}} = 0{,}118\sqrt{1-\frac{0{,}0157}{0{,}0263}} = 0{,}075.$$

From this, by (121) and (105),

$$s_{pacy} = \frac{\hat{s}_{pacy}Eh}{R} = 2460 \text{ kg/cm}^2, \qquad M_{kp.\,A} = 2\pi R^2 h\hat{s}_{pacy} = 9{,}88\cdot 10^6 \text{ kg/cm}^2.$$

For shell B when L/R = 2, R/h = 200, analogously, we find

$$\hat{q}_{0,\,B} = 0{,}033, \quad \hat{q}_{0,\,pacy} = 0{,}026, \qquad \hat{s}_{0,\,B} = 0{,}147,$$
$$\hat{s}_{0,\,pacy} = 0{,}118, \quad \hat{q}_{pacy} = 0{,}152, \quad \hat{q}_{pacy}/\hat{q}_{0,\,pacy} = 5{,}86.$$

During joint action of torsion and internal pressure by graph of Fig. 11.49, introducing conditionally calculated critical stresses, we obtain

$$\frac{\hat{s}_{pacy}}{\hat{s}_{0,\,pacy}} = 2{,}3, \quad \hat{s}_{pacy} = 0{,}271$$

and, consequently,

$$s_{pacy} = 2850 \text{ kg/cm}^2, \qquad M_{kr.\,B} = 5{,}72\cdot 10^6 \text{ kg/cm}^2.$$

Thus, outer body of combustion chamber can transmit torque 6 times larger than inner body; this shows partly the influence of direction of lateral load.

§ 137. Reinforced Shells. General Equations

In aircraft and engines, in shipbuilding and engineering constructions there frequently are applied circular cylindrical shells, having longitudinal reinforcing ribs (stringers) and annular ribs (frames). Such reinforced shells are, e.g., fuselage of aircraft and hull of submarine. Similarly to the way it was during investigation of reinforced plates (see Chapter VII), in case of shell two

approaches are possible. If ribs are sufficiently closely spaced, then construction can be considered orthotropic; rigidity of ribs is distributed, or, as it sometimes is expressed, is "spread out" the length of the corresponding section. If, however, ribs are at great distance from each other, then they must be considered discrete members.* Basic attention below will be paid to first approach to problem. Results obtained can be, with certain approximation, applied to shell, prepared from fiberglass.**

We assume that cylindrical shell is orthotropic and that main directions of rigidity coincide with generatrix of cylinder and arc of cross section. We derive basic differential equations of bending of such shell first for case when deflections are small. We shall follow simplified variant of relationships between changes of curvatures and displacements according to (12). Equations of equilibrium according to (8a) and (8) we write in forces N_x, N_y, T and moments M_x, M_y, and H, when $q_z = q$:

$$\left.\begin{aligned} \frac{\partial N_x}{\partial x}+\frac{\partial T}{\partial y}=0, \quad \frac{\partial T}{\partial x}+\frac{\partial N_y}{\partial y}=0. \\ \frac{\partial^2 M_x}{\partial x^2}+2\frac{\partial^2 H}{\partial x\,\partial y}+\frac{\partial^2 M_y}{\partial y^2}+\frac{N_y}{R}+q=0. \end{aligned}\right\} \qquad (11.152)$$

Dependences of Hooke's law, pertaining to deformation in middle surface, will have the same form as for orthotropic plate; we present them in the following form:***

---

*Stability of shells, reinforced by discrete ribs and subjected external pressure, was considered by V. M. Darevskiy and R. I. Kshnyakin [11.8, 1960].

**See below example 11.4.

***See work of Thielemann and other authors [11.51], [11.52].

$$\begin{pmatrix} \varepsilon_x \\ \varepsilon_y \\ \gamma \end{pmatrix} = \begin{pmatrix} \delta_1 & \delta_\mu & 0 \\ \delta_\mu & \delta_2 & 0 \\ 0 & 0 & \delta_0 \end{pmatrix} \begin{pmatrix} N_x \\ N_y \\ T \end{pmatrix}. \qquad (11.15^{*})$$

where in designations § 93 we have

$$\delta_1 = \frac{1}{E_1 h}, \quad \delta_2 = \frac{1}{E_2 h}, \quad \delta_\mu = -\frac{\mu_2}{E_2 h} = -\frac{\mu_1}{E_1 h}, \quad \delta_0 = \frac{1}{Gh}.$$

We expand, for example, matrix (153) for ε_x; then we obtain

$$\varepsilon_x = \delta_1 N_x + \delta_\mu N_y + 0 \cdot T = \frac{N_x}{E_1 h} - \frac{\mu_2 N_y}{E_2 h}.$$

Moments we express in accordance with (7.256):

$$\begin{pmatrix} M_x \\ M_y \\ H \end{pmatrix} = \begin{pmatrix} D_1 & D_\mu & 0 \\ D_\mu & D_2 & 0 \\ 0 & 0 & 2D_0 \end{pmatrix} \begin{pmatrix} \varkappa_x \\ \varkappa_y \\ \chi \end{pmatrix}; \qquad (11.154)$$

here, in designations of § 93 $D_\mu = D_1\mu_2 = D_2\mu_1$.

First two equations of equilibrium (152) are satisfied with introduction of function of stresses by formulas of type (13):

$$N_x = \frac{\partial^2 \varphi}{\partial y^2}, \quad N_y = \frac{\partial^2 \varphi}{\partial x^2}, \quad T = -\frac{\partial^2 \varphi}{\partial x \partial y}.$$

Third equation takes form

$$D_1 \frac{\partial^4 w}{\partial x^4} + 2D_3 \frac{\partial^4 w}{\partial x^2 \partial y^2} + D_2 \frac{\partial^4 w}{\partial y^4} - \frac{1}{R} \frac{\partial^2 \varphi}{\partial x^2} = q. \qquad (11.155)$$

where $D_3 = D_\mu + 2D_0$; it changes into corresponding equation (7.259) for plate when $R \to \infty$. Equation of compatibility (14) changes into the following one:

$$\delta_2 \frac{\partial^4 \varphi}{\partial x^4} + 2\delta_3 \frac{\partial^4 \varphi}{\partial x^2 \partial y^2} + \delta_1 \frac{\partial^4 \varphi}{\partial y^4} + \frac{1}{R} \frac{\partial^2 w}{\partial x^2} = 0. \qquad (11.156)$$

We introduce operators

$$\nabla_1^4 = \delta_2 \frac{\partial^4}{\partial x^4} + 2\delta_3 \frac{\partial^4}{\partial x^2 \partial y^2} + \delta_1 \frac{\partial^4}{\partial y^4}, \quad \nabla_D^4 = D_1 \frac{\partial^4}{\partial x^4} + 2D_3 \frac{\partial^4}{\partial x^2 \partial y^2} + D_2 \frac{\partial^4}{\partial y^4};$$

then equations (155) and (156) can be presented in more compact form:

$$\nabla_D^4 w - \frac{1}{R}\frac{\partial^2 \varphi}{\partial x^2} = q, \quad \nabla_i^4 \varphi + \frac{1}{R}\frac{\partial^2 w}{\partial x^2} = 0. \tag{11.157}$$

For an isotropic shell we have

$$\nabla_D^4 = D\nabla^4, \quad \nabla_i^4 = \frac{1}{Eh}\nabla^4.$$

In problems of stability in the small for q one should substitute intensity of hypothetical load according to (10.89); then the first of equations (157) will take form

$$\nabla_D^4 w - \frac{1}{R}\frac{\partial^2 \varphi}{\partial x^2} + h\left(p_x\frac{\partial^2 w}{\partial x^2} + p_y\frac{\partial^2 w}{\partial y^2} + 2s\frac{\partial^2 w}{\partial x\,\partial y}\right) = 0.$$

We turn to case when deflections are great. Proceeding in this way, as in § 125, we arrive at following equations* (when q = 0):

$$\left.\begin{aligned} \nabla_D^4 w &= L(w, \varphi) + \frac{1}{R}\frac{\partial^2 \varphi}{\partial x^2}, \\ \nabla_i^4 \varphi &= -\frac{1}{2}L(w, w) - \frac{1}{R}\frac{\partial^2 w}{\partial x^2}. \end{aligned}\right\} \tag{11.158}$$

where operator L is expressed by formulas (7.40) and (7.62). If however, we are investigating behavior of shell with initial imperfections, then by (29) we have

$$\left.\begin{aligned} \nabla_D^4 (w - w_0) &= L(w, \varphi) + \frac{1}{R}\frac{\partial^2 \varphi}{\partial x^2}, \\ \nabla_i^4 \varphi &= -\frac{1}{2}|L(w, w) - L(w_0, w_0)| - \frac{1}{R}\frac{\partial^2 (w - w_0)}{\partial x^2}. \end{aligned}\right\} \tag{11.159}$$

By w and w_0 as before there are understood functions of total and initial deflections.

In conclusion we give expression for strain energy in middle surface and energy of bending according to (10.95):

$$U_\varepsilon = \frac{1}{2}\int\int_F (\delta_1 N_x^2 + 2\delta_4 N_x N_y + \delta_2 N_y^2 + \delta_0 T^2)\,dx\,dy. \tag{11.160}$$

---

*Equations of this type were derived by S. V. Aleksandrovskiy [11.1].

$$U_n = \frac{1}{2}\int\int_F \left[D_1\left(\frac{\partial^2 w}{\partial x^2}\right)^2 + 2D_\mu \frac{\partial^2 w}{\partial x^2}\frac{\partial^2 w}{\partial y^2} + D_2\left(\frac{\partial^2 w}{\partial y^2}\right)^2 + \right.$$
$$\left. + 4D_0\left(\frac{\partial^2 w}{\partial x\,\partial y}\right)^2\right] dx\,dy. \qquad (11.161)$$

Let us turn to resolution of certain particular problems.

§ 138. Reinforced Shell During Axial Compression. Simultaneous Action of Axial Compression and Internal Pressure

Let us consider stability of orthotropic shell during axial compression. We solve general problem of stability in the large;* linear problem is a limiting case. We take approximating expression for deflection, selected by Kempner (see p. 625):

$$w = f\left(\cos\frac{\pi x}{l_x}\cos\frac{\pi y}{l_y} + a\cos\frac{2\pi x}{l_x} + b\cos\frac{2\pi y}{l_y} + d\right). \qquad (11.162)$$

Putting, as usual, this expression in the right part of the second of equations (158) and integrating it, we find function of stresses:

$$\varphi = -4\frac{\zeta}{\eta^2}D_2\sqrt{\frac{\delta_2}{\delta_1}}\left\{\frac{\zeta - 8a}{32\vartheta^2}\cos\frac{2\pi x}{l_x} + \right.$$
$$+\frac{\vartheta^2\zeta}{32}\cos\frac{2\pi y}{l_y} + \frac{\vartheta^2}{1+2\nu_c\vartheta^2+\vartheta^4}[2\zeta(a+b)-1]\cos\frac{\pi x}{l_x}\cos\frac{\pi y}{l_y} +$$
$$+2a\zeta\frac{\vartheta^2}{1+2,9\nu_c\vartheta^2+81\vartheta^4}\cos\frac{3\pi x}{l_x}\cos\frac{\pi y}{l_y} +$$
$$+a b\zeta\frac{\vartheta^2}{1+2\nu_c\vartheta^2+\vartheta^4}\cos\frac{2\pi x}{l_x}\cos\frac{2\pi y}{l_y} +$$
$$\left.+2b\frac{\vartheta^2}{81+2,9\nu_c\vartheta^2+\vartheta^4}\cos\frac{\pi x}{l_x}\cos\frac{3\pi y}{l_y}\right\} - N_x\frac{y^2}{2}; \qquad (11.163)$$

here are introduced following parameters:

$$\nu_c = \frac{\delta_0 + \frac{1}{2}\delta_0}{\sqrt{\delta_1\delta_2}},\quad \eta = \frac{2R\pi^2}{l_y^2}\sqrt{\delta_2 D_2},\quad \zeta = \frac{f\eta}{2\sqrt{\delta_2 D_2}},\quad \vartheta = \frac{l_y}{l_x}\sqrt[4]{\frac{\delta_2}{\delta_1}}.$$

For isotropic shell we have $\nu_c = 1$, and magnitudes η and ϑ change into the following:

$$\eta = \frac{\pi^2 R\delta}{l_y^2\sqrt{3(1-\mu^2)}},\quad \vartheta = \frac{l_y}{l_x}. \qquad (11.164)$$

---

*This investigation was conducted by O. I. Terebushko [11.22], and also by W. Thielemann and other authors [11.51], [11.52]. Below is given the solution contained in these last articles.

Analogous designations were introduced above, in § 126; they characterize dimensions and form of hollow.

We determine relative shortening of shell by a formula, analogous to (57):

$$\varepsilon=\frac{\Delta}{L}=-\frac{1}{L}\int_0^L\frac{\partial u}{\partial x}dx=-\frac{1}{L}\int_0^L\left[\left(\delta_{11}\frac{\partial^2\varphi}{\partial y^2}+\delta_{12}\frac{\partial^2\varphi}{\partial x^2}\right)-\frac{1}{2}\left(\frac{\partial w}{\partial x}\right)^2\right]dx. \qquad (11.165)$$

We calculate, then, total dimensionless energy of system $\mathcal{Э}^*$:

$$\mathcal{Э}^*=\frac{\zeta^2}{\eta^2}(\zeta^2A_1-\zeta A_2+A_3+\eta^2A_4+\eta A_5)+\mathcal{Э}_0^*; \qquad (11.166)$$

coefficients $A_1, \ldots, A_5$ depend on a, b, $\$$, ν_c and magnitude $\nu_н = D_3/\sqrt{D_1D_2}$. Minimizing energy for parameters ζ, η, a, b, $\$$, we arrive at system of five nonlinear equations.

Considering $\zeta \to 0$, we find solution of linear problem, determining point of bifurcation of equilibrium states. Here we have a = b = 0, so that for deflection we obtain expression $w = f \sin(\pi x/l_x) \sin(\pi y/l_y)$; buckled surface is divided into rectangular cells. It is necessary to investigate case $\$ \to \infty$ separately, when there are formed axisymmetric annular buckles; here $w = f \sin(\pi x/l_x)$. Upper critical force is obtained in the latter case equal to

$$N_{кр}=\frac{2}{R}\sqrt{\frac{D_1}{\delta_2}}. \qquad (11.167)$$

For isotropic shell from this there follows the classical formula (33). We introduce designations

$$\bar{N}=\frac{NR}{2}\sqrt{\frac{\delta_1}{D_2}}, \quad \gamma=\frac{D_1\delta_1}{D_2\delta_2}. \qquad (11.168)$$

Magnitude $N_в$ corresponds to parameter $\bar{N}_в = \sqrt{\gamma}$; length of half-wave l_x here turns out to be equal to $l_x = \pi\sqrt[4]{R^2D_1\delta_2}$.

Let us return to equations describing large deflection of shell. On following graphs are presented results of their solution obtained by digital computers. The most essential characteristic of tropic shell turns out to be parameter γ; judging by (168), with relatively strong stringers γ is great, and with strong frames, it is small. In Fig. 11.55 is shown, as magnitude of upper critical force N_B and form of diagram depend on γ when $\nu_c = 4$ and $\nu_H = 0.5$. As unit along the axis of ordinates is taken upper critical force of axisymmetric loss of stability $N_{0,B}$, calculated by (167); along the axis of abscissas is plotted ratio $\varepsilon/\varepsilon_{0,B}$, where $\varepsilon_{0,B}$ is critical deformation of annular buckling. As we see, for orthotropic shells points of bifurcations of "cellular" type N_B and "annular" type $N_{0,B}$ do not coincide. Buckling in the small, obviously, should be accompanied by formation of cells, where with growth of γ ratio $N_B/N_{0,B}$ decreases. Postcritical diagrams pertain to buckling "rhomboids;" character of them sharply changes depending upon γ.

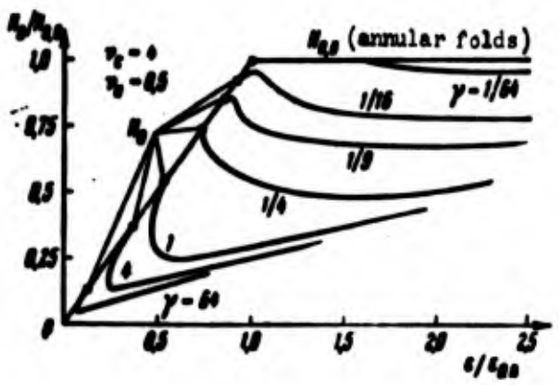

Fig. 11.55. Diagram of equilibrium forms of compressed orthotropic shell during large deflections.

For significant γ, i.e., in case of strengthened stringers, diagram has for point of bifurcation the usual falling section. However, with decrease of γ slope of this section changes, and, starting with $\gamma < 1/9$, we no longer obtain falling, but an ascending curve. True, subsequently, stress anew drops and it turns out to be possible to determine lower critical stress. Apparently, during tests of real

shells we will observe transition from one branch to the other by means of knocks.

In Fig. 11.56 is shown how ratio of lower critical force to upper changes depending upon γ with the same ν_c and $\nu_н$. Judging by these data, effect of nonlinearity turns out to be greatest for isotropic shells. It somewhat weakens in case of shell strengthened in longitudinal direction, and sharply drops for shells having transverse reinforcements. Different, too, is form of wave formation, as it is natural to expect; in case of strong stringers hollows are stretched along generatrix, and with strong frames, along arc.

When reinforced shell is subjected to <u>simultaneous action of axial compression and internal pressure</u>, solution may be conducted analogously. If we use for w former approximation (162), then expression (163) for φ should be supplemented by member $(qRx^2/2)$, where q is intensity of internal pressure.

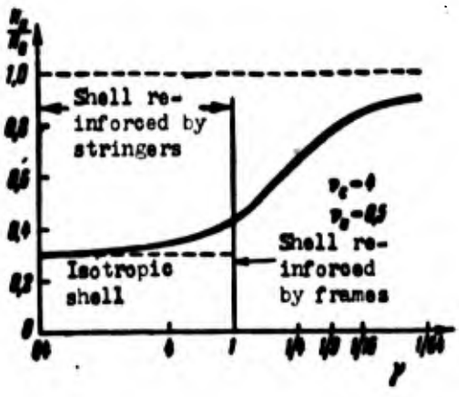

Fig. 11.56. Variation of lower critical compression stress depending upon character of reinforcement of shell.

We introduce parameters

$$\bar{N}=\frac{RN}{2}\sqrt{\frac{b_2}{D_1}},$$
$$\bar{q}=\frac{qR^2}{2}\sqrt{\frac{b_2}{D_1}};$$

in case of isotropic shell they are equal to

$$\bar{N}=\frac{N}{E}\frac{R}{h^2},$$
$$\bar{q}=\frac{q}{E}\left(\frac{R}{h}\right)^2\sqrt{3(1-\mu^2)}.$$

In Fig. 11.57 is depicted dependence between compressive force $\bar{N}$ and magnitude $\bar{\varepsilon}+\delta_u\bar{q}/\sqrt{\delta_1\delta_2}$ for definite values of ν_c and $\nu_н$ (they are shown in figure) for shell reinforced in axial direction (γ = = 8.064). Lower curve pertains to case when internal pressure is

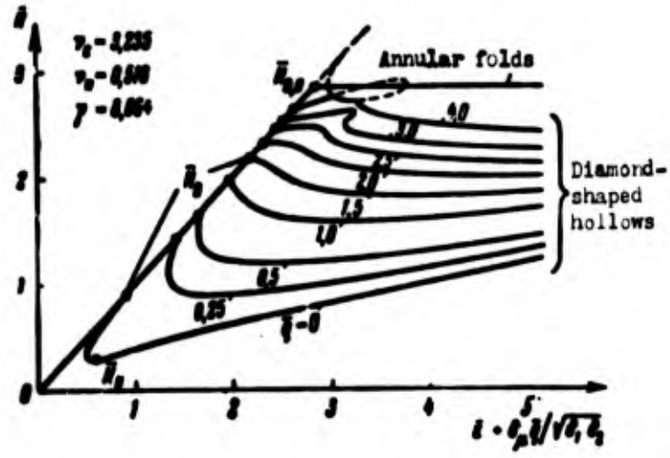

Fig. 11.57. Diagram of "force – reduced deformation" for shell, experiencing axial compression in combination with internal pressure.

absent ($\bar{q} = 0$) and upper curves pertain to successive increasing values of $\bar{q}$. Graph is limited from above by line, corresponding to case of axisymmetric buckling. As we see, with increase of $\bar{q}$ here there increases not only lower, but also upper critical force; in this orthotropic shell differs from isotropic. At the same time, as one may see from figure, on intensity of $\bar{q}$ there depends form of initial section of postcritical diagram; with significant $\bar{q}$ here, too, we obtain ascending sections; for $\bar{q} = 4$ initial section obtains form of a loop.

We can conclude that with significant internal pressure reinforcing of shell in longitudinal direction turns out to be more effective; in this case of magnitudes N_B and N_H turn out to be relatively higher than for shells reinforced in arc direction.

O. I. Terebushko considered nonlinear problem of axial compression of structurally anisotropic shell, using method of Ritz and taking approximation for w in form (68). Solution was conducted also with help of digital computers. Investigating of postcritical behavior of shells for various types of reinforcement, we arrive at conclusion that requirement of least weight corresponds to shell of waffle type

with very closely space longitudinal and annular ribs (Fig. 11.58).

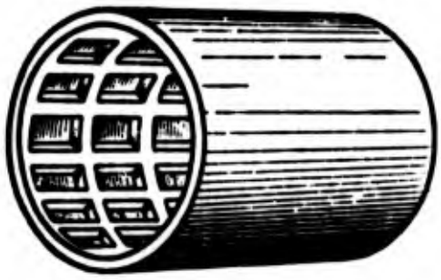

Fig. 11.58. Shell "waffle" type.

Here there was set requirement of equal-stability in the large for closed shell and for separate cylindrical panels, located between reinforcements (see § 139). Such conclusion will become intelligible, if we consider that widely spaced stringers or frames cannot noticeably influence form, so that within limits of every hollow there were located several reinforcing ribs; only then can critical stress significantly grow as compared to case of unreinforced shell. Example of buckling of corrugated shell, satisfying this requirement, is shown in Fig. 11.59.*

Waffle construction depicted in preceding Fig. 11.58 is unusual; there arises question of techniques of its manufacture. Here there can be applied stamping, milling or other methods. However advantage of such construction is evident. As O. I. Terebushko showed, with rational selection of dimensions of ribs and distances between them it is possible to design a reinforced shell which will be 1.5 times lighter than isotropic shell equal in stability to it.

It is important also to note that influence of ribs on upper and lower critical stresses will be different depending upon how ribs are located relative to middle surface. It is possible to show that in case of ribs on the convex side, upper and lower critical stresses will be (other things being equal) higher than in case of ribs located

---

*Tests of such shells were conducted by G. L. Komissarova.

on concave side.

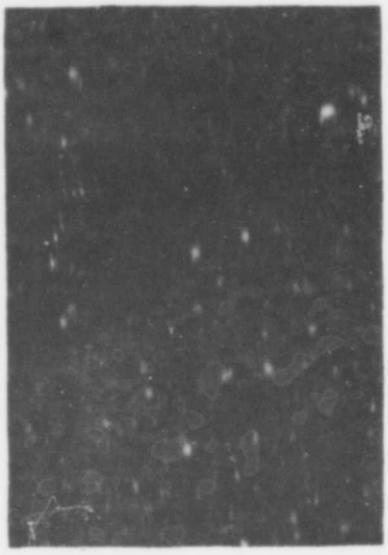

Fig. 11.59. Buckling of corrugated shell subjected to axial compression.

Apparently, investigation of stability in the large for re shells can lead here to model of light construction. We obtain here an example of how improvement of methods of calculation, connected with application of contemporary computer technology, can give impetus to appearance of new types of constructions.

Example 11.4. Determine critical load for closed glass-fiber reinforced shell prepared from glass-fabric of type of cords and polyester resin compressed along axis. Direction of base coincides with generatrix of cylinder. Dimensions: R = 108 mm, h = 1.5 mm. Such type of shell it is possible approximately to consider orthotropic. We are given following values of elastic moduli and Poisson's ratio, $E_1 = 2 \cdot 10^5$ kg/cm^2 (along axis), $E_2 = 1 \cdot 10^5$ kg/cm^2 (in annular direction), $\mu_1 = 0.1$, $\mu_2 = 0.05$.

We find upper critical force by (167) for axisymmetric loss of stability:

$$N_{0,*} = \frac{2}{R}\sqrt{\frac{D_1}{b_2}} = \frac{2}{R}\sqrt{D_1 E_2 h}; \qquad \text{(a)}$$

hence

$$\sigma_{0,*} = \frac{N_{0,*}}{h} = \frac{E_1}{\sqrt{3(1-\mu_1\mu_2)}}\sqrt{\frac{E_2}{E_1}}\frac{h}{R}. \qquad \text{(b)}$$

or

$$\sigma_{0,*} = \frac{2 \cdot 10^6}{\sqrt{3(1-0{,}1 \cdot 0{,}05)}} \sqrt{0{,}5}\,\frac{0{,}15}{10{,}8} = 1120 \quad \text{kg/cm}^2.$$

This magnitude lies within elastic limit of material. Total critical load is equal to

$$P_{0,*} = 2\pi R h \sigma_{0,*} = 11{,}4\ m.$$

Test of such shell in laboratory* showed that in reality buckling occurs in rhombic form, as shown in Fig. 11.60. Critical load constituted 6 m, i.e., about 53% of upper critical magnitude.

Fig. 11.60. Buckling of compressed shell made of fiberglass.

Let us note that glass-plastic shells, reinforced by fabric or braids, are finding ever greater propagation in different regions of technology. It is desirable that there be given definitized methods of calculation for such shells, based on nonlinear theory and considering peculiarities of structure of one or another material.

§ 139. Stability of Cylindrical Panel Under Axial Compression

During designing of reinforced shells it is necessary, as we saw, to calculate for stability separate panels lying between ribs. We turn therefore, to problems of stability of such panels — open circular cylindrical shells — during compression and shear. Conditions of fastening of panel on edges depend on dimensions of

*It was derived by V. V. Ivanov.

reinforcing ribs. Usually ribs have sufficient flexural rigidity in plane perpendicular to middle surface, and therefore, deflection of panel on edges can be taken equal to zero. Depending upon torsional rigidity of ribs we distinguish cases of complete or elastic clamping or hinged support. Furthermore, there must be formulated conditions, concerning displacements of points, belonging to edges of panel in plane tangent to middle surface. In some cases, with ribs flexurally in this plane, one may assume that points of edge shift freely in a direction perpendicular to edge. If however ribs possess great rigidity, there is placed condition of equality to zero of these shifts. Further, there must be considered conditions concerning shifts of points of panel along edges. With welded seam or rivet joint one should consider that shift of points of panel with respect to rib in this direction are absent; this condition in great measure pertains to "homogenous" or "integral" constructions, in which ribs are prepared simultaneously with shell. However, for simplification of problem we most frequently assume that points of panel slip freely along edges.

Let us consider first of all case when circular cylindrical panel is compressed by forces p, evenly distributed along curved edges. We designate by a and b length and width of panel, by θ the central angle embraced by it (Fig. 11.61). Let us consider case of hinged support of panel on all edges. During solution of linear problem* we will originate from equation (17):

---

*This problem was first considered by S. P. Timoshenko; see his "Course on theory of elasticity," Chapter 2, St. Petersburg, 1916, p. 395.

$$\frac{D}{h}\nabla^8 w + \frac{E}{R^2}\frac{\partial^4 w}{\partial x^4} + \\ + p\nabla^4\left(\frac{\partial^2 w}{\partial x^2}\right) = 0. \qquad (11.169)$$

We take

$$w = f \sin\frac{m\pi x}{a}\sin\frac{n\pi y}{b}, \qquad (11.170)$$

where m and n are number of half-waves along the generatrix and along the arc. Putting this expression in (169) we obtain

$$\frac{D}{h}\left(\frac{m^2\pi^2}{a^2}+\frac{n^2\pi^2}{b^2}\right)^2 + \frac{E}{R^2}\frac{m^4\pi^4}{a^4} - p\left(\frac{m^2\pi^2}{a^2}+\frac{n^2\pi^2}{b^2}\right)^2\frac{m^2\pi^2}{a^2} = 0,$$

whence

$$p = \frac{D}{hb^2}\frac{\left(\frac{m^2b}{a}+\frac{n^2}{b}\right)^2\pi^2}{\frac{m^2}{a^2}} + \frac{b^2E}{R^2}\frac{\frac{m^2}{a^2}}{\left(\frac{m^2b}{a^2}+\frac{n^2}{b}\right)^2\pi^2},$$

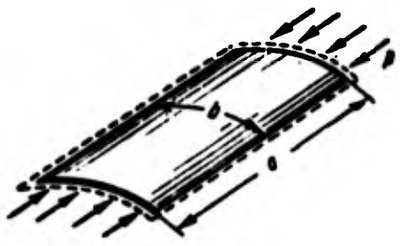

Fig. 11.61. Cylindrical panel under axial compression.

or

$$p = \frac{D}{hb^2}\pi^2\varphi^2 + \frac{E}{R^2}\frac{b^2}{\pi^2\varphi^2}, \qquad (11.171)$$

where

$$\varphi = \left(\frac{m^2b}{a}+\frac{n^2}{b}\right)\frac{a}{m}. \qquad (11.172)$$

Minimizing p with respect to φ, we find

$$\varphi = \frac{1}{\pi}\sqrt[4]{12(1-\mu^2)}\frac{b}{\sqrt{Rh}}. \qquad (11.172a)$$

Upper critical stress turns out to be equal to

$$p_* = \frac{1}{\sqrt{3(1-\mu^2)}}E\frac{h}{R} = 0.605E\frac{h}{R}. \qquad (11.173)$$

We arrived anew at the familiar formula (33), obtained above for closed shell. However this formula is valid only for panel, embracing comparatively great central angle, when operation of differentiation with respect to φ is permissible.

Just as for closed shell, form of wave formation here is not simply determined, we know only magnitude φ, depending on numbers m and n. In case of very shallow panel in (172) we must take n = 1,

m = a/b; then we have $\varphi = 2$. Hence, by (171),

$$p_0 = 4\frac{\pi^2 D}{b^2 h} + \frac{1}{4\pi^2}\left(\frac{b}{R}\right)^2 E. \qquad (11.173)$$

This formula is valid on the condition that

$$\frac{1}{\pi}\sqrt[4]{12(1-\mu^2)}\,\frac{b}{\sqrt{Rh}} \leqslant 2$$

or

$$b < \frac{2\pi}{\sqrt[4]{12(1-\mu^2)}}\sqrt{\frac{h}{R}}.$$

We introduce dimensionless parameters, characterizing compressive effort and curvature of panel:

$$p^* = \frac{p}{E}\left(\frac{b}{h}\right)^2, \quad k = \frac{b^2}{Rh} = \frac{b^2}{Rh}; \qquad (11.174)$$

then from (173) we obtain for panel of great curvature

$$p_0^* = \frac{1}{\sqrt{3(1-\mu^2)}}k \approx 0{,}605k. \qquad (11.175)$$

and for shallow panel when $k < 12$

$$p_0^* = \frac{\pi^2}{3(1-\mu^2)} + \frac{k^2}{4\pi^2} \approx 3{,}6 + \frac{k^2}{39{,}5}. \qquad (11.176)$$

Let us solve the same problem in nonlinear formulation.* We first assume, for simplicity, that we are talking about hinge-supported square panel (b = a) and that unloaded edges approach each other freely, remaining rectilinear. In first approximation we select expression for w as before in the form (170), considering here that in both directions there will be formed only one half-wave (m = n = 1). Putting w in the right part of equation (27) and integrating, we find

---

*Below-mentioned resolution was offered by author [11.5], where condition of rectilinearity of edges is met only approximately. Investigations of stability of panels in the large belong also to W. Koiter, [11.41]. D. Legget, Rep. and Mem., No. 1899 (1942), No. 1972 (1943) and others.

$$\frac{1}{E}\Phi = \frac{1}{32} f^2\left(\cos\frac{2\pi x}{a} + \cos\frac{2\pi y}{a}\right) + \frac{1}{4R} f \frac{a^2}{\pi^2} \sin\frac{\pi x}{a} \sin\frac{\pi y}{a} - \frac{py^2}{2E}.$$

Static boundary conditions on edges: $\sigma_y = 0$, $\tau = 0$ when $y = 0$, b; $\sigma_x = -p$, $\tau = 0$ when $x = 0$; they are satisfied for every edge only on the average.

We use the Bubnov-Galerkin method and compose this equation:

$$\int_0^a \int_0^b \left[\frac{D}{h}\nabla^4 w - L(w, \Phi) - \frac{1}{R}\frac{\partial^2\Phi}{\partial x^2}\right] \sin\frac{\pi x}{a} \sin\frac{\pi y}{a}\, dx\, dy = 0.$$

Substituting expressions for w and Φ and integrating, we arrive at equation

$$\frac{\pi^4}{32a^2} Ef^3 - \frac{5}{6R} Ef + \frac{a^2}{16R^2} E + \frac{\pi^4}{a^2 h} D - \frac{\pi^2}{4} p = 0.$$

Considering $f \to 0$, we find former formula (173) for upper critical stress p_B. Then we find

$$p = p_0 + \frac{\pi^2}{8a^2} Ef^2 - \frac{10}{3R} Ef.$$

Considering $\zeta = f/h$, we obtain

$$p^* = p_0^* + \frac{\pi^2}{8}\zeta^2 - \frac{10}{3\pi^2} k\zeta. \qquad (11.177)$$

Minimizing p* with respect to ζ, we find lower critical stress equal to

$$p_0^* = \frac{\pi^2}{3(1-\mu^2)} - \frac{200}{9\pi^4} k^2 \qquad (11.178)$$

when $\zeta \approx 0.14$ k; it lies somewhat below critical stress for flat panel, equal to $\pi^2/3(1 - \mu^2) \approx 3.6$. Recently this problem for square panel was solved in finite differences with help of digital computer.* In Fig. 11.62 is presented dependence $p^*(\zeta)$, pertaining to case k = = 12; it was assumed that edges of panel remain rectilinear (curve 1)

---

*These results belong to A. Yu. Birkgan. See also article of M. A. Koltunov "Stability of flexible panel of cylindrical shell" in "Herald of Moscow State of university," No. 5 (1962).

or are freely bent (curve 3). Part of curve 1, corresponding to unstable equilibrium states of panel, cannot be obtained by gi n method. Dot-dash line 2 corr to equation (177), obtained at threshold conditions, nearing case of rectilinear edges. As we see, general character of variation of p^* is described by approximate solution satisfactorily, but magnitude $p^*_н$ from (178) lies lower than definitized value.

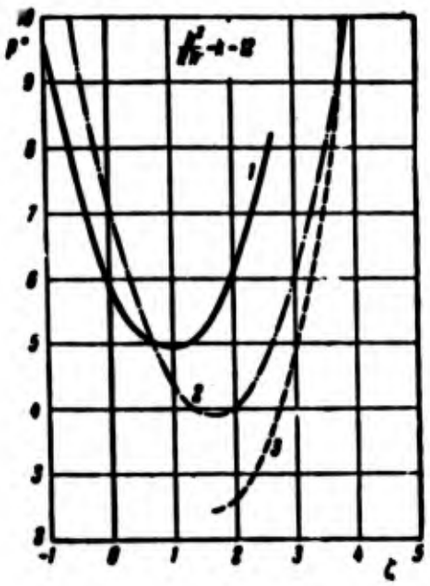

Fig. 11.62. Determining lower critical compression stress for cylindrical panel with different conditions of fastening.

In more general solution* of problem, for panel of arbitrary curvature and $a \neq b$, deflection was given by expression of type (68):

$$w = f_1 \sin\frac{m\pi x}{a}\sin\frac{n\pi y}{b} + f_2 \sin^2\frac{m\pi x}{a}\sin^2\frac{n\pi y}{b}. \qquad (11.179)$$

Lower critical stress turned out to be equal (for $k > 20$) to $p^*_н = 0.26k$. We must assume that in more exact solution of problem theoretical value $p^*_н$ should fall and approach value $0.18k$, obtained for closed cylindrical shell. At the same time for shallow panel (when $k < 20$) magnitude $p^*_н$, as we have seen, differs little from critical stress for flat plate. Therefore, it is possible to recommend conducting practical calculations determining upper critical stress by the formulas (175) and (176), and for lower critical stress taking (in case of carefully prepared shells):

---

*It was given by O. N. Len'ko and author, see [0.3], p. 296.

$$p_{\text{в}}^{*}=3.6 \text{ when } k \leqslant 20; \quad p_{\text{в}}^{*}=0.18k \text{ when } k>20.$$

If however during manufacture and assembly of construction panels receive significant initial deflection, comparable with thickness of shell, one should take $p_{\text{н}}^{*} = 0.12k$ (when $k > 20$).

§ 140. Stability of Panel Under Shear

Cylindrical panels, in construction of aircraft wing, transmit not only normal, but also shearing forces. Let us turn to investigation of stability of panel under shear. Let us assume that panel with sides a and b, secured by hinge on edges, is subjected to action of tangential forces s, evenly distributed on all edges (Fig. 11.63).* Investigating stability of panel in the small, we take as base of equation (15a) and (16)

$$\frac{D}{h}\nabla^4 w=\frac{1}{R}\frac{\partial^2\Phi}{\partial x^2}-2s\frac{\partial^2 w}{\partial x\,\partial y}. \tag{11.180}$$

$$\frac{1}{E}\nabla^4\Phi=-\frac{1}{R}\frac{\partial^2 w}{\partial x^2}. \tag{11.181}$$

Will take expression for w in the form

$$w=\sum_m\sum_n f_{mn}\sin\frac{m\pi x}{a}\sin\frac{n\pi y}{b}.$$

Putting this expression in the right part of equation (171) and integrating, we obtain

$$\Phi=\frac{E}{\pi^2 a^2 R}\sum_m\sum_n f_{mn}\frac{m^2}{\left(\frac{m^2}{a^2}+\frac{n^2}{b^2}\right)^2}\sin\frac{m\pi x}{a}\sin\frac{n\pi y}{b}+sxy.$$

We use Bubnov-Galerkin method and instead of (180) take equation

---

*This problem was first considered by N. V. Zvolinskiy (Transactions of Central Aero-Hydrodynamic Institute, No. 246 (1936)). Solution of problem given here belongs to V. A. Mar'in [11.14].

$$\int_{(F)}\int\left(\frac{D}{h}\nabla^4 w-\frac{1}{R}\frac{\partial^2\Phi}{\partial x^2}+2s\frac{\partial^2 w}{\partial x\,\partial y}\right)\sin\frac{i\pi x}{a}\sin\frac{j\pi y}{b}\,dx\,dy=0.$$

Substituting expressions for w and Φ, after integration, we find

$$f_{mn}\frac{ab}{4}\left[\frac{m^4E}{R^2a^4\left(\frac{m^2}{a^2}+\frac{n^2}{b^2}\right)^2}+\right.$$
$$\left.+\frac{\pi^4D}{h}\left(\frac{m^2}{a^2}+\frac{n^2}{b^2}\right)^2\right]-$$
$$-\sum_i\sum_j f_{ij}8s\frac{mnij}{(m^2-i^2)(n^2-j^2)}=0;$$

here we must consider only those terms for which sum m + i and n + j are odd. This follows from relationships (7.151). Introducing in supplement to (174) designations

$$s^0=s\frac{ab}{Eh^2},\quad \lambda=\frac{a}{b}. \tag{11.182}$$

we arrive at equations of type

$$A_{mn}f_{mn}-\rho\sum_i\sum_j f_{ij}\frac{ij}{(m^2-i^2)(n^2-j^2)}=0, \tag{11.183}$$

where

$$A_{mn}=\frac{\pi^2}{3(1-\mu^2)}\frac{(m^2+n^2\lambda^2)^2}{mn\lambda^2}+\frac{h^2}{\pi^2}\frac{4m^2\lambda^2}{(m^2+n^2\lambda^2)^2n},\quad \rho=\frac{128s^0}{\pi^2}. \tag{11.184}$$

Fig. 11.63. Cylindrical panel under shear.

In <u>first approximation</u> we take numbers m, n, i, j equal to 1, 2. We write corresponding system of equations of type (183):

$$A_{11}f_{11}-\frac{4}{9}\rho f_{22}=0,\quad A_{22}f_{22}-\frac{1}{9}\rho f_{11}=0.$$
$$A_{12}f_{12}+\frac{2}{9}\rho f_{21}=0,\quad A_{21}f_{21}+\frac{2}{9}\rho f_{12}=0.$$

Condition of nontrivial solution of this system has the form

$$\begin{vmatrix} A_{11} & -\frac{4}{9}\rho & 0 & 0 \\ -\frac{1}{9}\rho & A_{22} & 0 & 0 \\ 0 & 0 & A_{12} & \frac{2}{9}\rho \\ 0 & 0 & \frac{2}{9}\rho & A_{21} \end{vmatrix}=0. \tag{11.185}$$

Equation (185) breaks up into two;

$$\begin{vmatrix} A_{11} & -\frac{4}{9}\rho \\ -\frac{1}{9}\rho & A_{22} \end{vmatrix} = 0, \quad \begin{vmatrix} A_{12} & \frac{2}{9}\rho \\ \frac{2}{9}\rho & A_{21} \end{vmatrix} = 0;$$

the first of them corresponds to even sum of indices m + n, the seconds to odd. Hence, we find two roots for ρ:

$$\rho_1 = \frac{9}{2}\sqrt{A_{11}A_{22}}, \quad \rho_2 = \frac{9}{2}\sqrt{A_{12}A_{21}},$$

and values of upper tangential stress:

$$s_1^* = \frac{9\pi^2}{256}\sqrt{A_{11}A_{22}}, \quad s_2^* = \frac{9\pi^2}{256}\sqrt{A_{12}A_{21}}. \qquad (11.186)$$

In case of square panel (λ = 1) we obtain:

$$s_1^* = \frac{3\pi^4}{32(1-\mu^2)}\sqrt{\left[1+\frac{3(1-\mu^2)}{4\pi^4}k^2\right]\left[1+\frac{3(1-\mu^2)}{64\pi^4}k^2\right]}. \qquad (11.187)$$

In <u>second approximation</u> we consider all possible combinations of indices, equal to 1, 2, and 3, where system of equations as before breaks up into systems pertaining to indices with even and odd sums m + n. For case of <u>even</u> sums we obtain equation of form

$$\begin{vmatrix} A_{11} & -\frac{4}{9}\rho & 0 & 0 & 0 \\ -\frac{1}{9}\rho & A_{22} & \frac{1}{5}\rho & \frac{1}{5}\rho & -\frac{9}{25}\rho \\ 0 & \frac{4}{15}\rho & A_{13} & 0 & 0 \\ 0 & \frac{4}{15}\rho & 0 & A_{31} & 0 \\ 0 & -\frac{4}{25}\rho & 0 & 0 & A_{33} \end{vmatrix} = 0.$$

From this

$$s_1^* = \frac{\pi^2}{128}\sqrt{\frac{A_{11}A_{22}A_{13}A_{31}A_{33}}{L_1}},$$

where

$$L_1 = A_{11}A_{13}\left(\frac{36}{625}A_{31} + \frac{4}{75}A_{33}\right) + A_{31}A_{33}\left(\frac{4}{75}A_{11} + \frac{4}{81}A_{13}\right).$$

For odd sums m + n we have

$$s_2^* = \frac{\pi^2}{128}\sqrt{\frac{A_{12}A_{21}A_{23}A_{32}}{L_2}}.$$

where

$$L_2 = \frac{36}{625}A_{12}A_{21} + \frac{4}{81}A_{23}A_{32} + \frac{4}{75}(A_{12}A_{23} + A_{21}A_{32}).$$

Last, in third approximation there are considered all combinations of indices from 1 to 4. It turned out that this approximation gives small corrections to results of second approximation.

Upper critical stress s_B^*, as a rule, is determined by magnitudes pertaining to even sums of indices. An exception is elongated panels ($\lambda \geqslant 3$) of small curvature ($k < 7$).

Will turn to solution of nonlinear problem. We take expression for w in the form

$$w = f_1 \sin\frac{\pi x}{a}\sin\frac{\pi y}{b} + f_2 \sin\frac{2\pi x}{a}\sin\frac{2\pi y}{b}. \qquad (11.188)$$

From equation (27) we find

$$\begin{aligned}\frac{1}{E}\Phi = {} & \frac{1}{32a^2b^2}\left(a^4\cos\frac{2\pi x}{a} + b^4\cos\frac{2\pi y}{b}\right)f_1^2 + \\ & + \frac{1}{32a^2b^2}\left(a^4\cos\frac{4\pi x}{a} + b^4\cos\frac{4\pi y}{b}\right)f_2^2 + \\ & + 4a^2b^2\left[\frac{\cos\frac{\pi x}{a}\cos\frac{3\pi y}{b}}{(b^2+9a^2)^2} + \frac{\cos\frac{3\pi x}{a}\cos\frac{\pi y}{b}}{(a^2+9b^2)^2}\right]f_1f_2 + \\ & + \frac{a^2b^4}{\pi^2(a^2+b^2)^2R}\sin\frac{\pi x}{a}\sin\frac{\pi y}{b}f_1 + \\ & + \frac{a^2b^4}{4\pi^2(a^2+b^2)^2R}\sin\frac{2\pi x}{a}\sin\frac{2\pi y}{b}f_2 + sxy.\end{aligned}$$

We write equations of Bubnov-Galerkin method:

$$\int_F\int X\sin\frac{\pi x}{a}\sin\frac{\pi y}{b}\,dx\,dy = 0, \quad \int_F\int X\sin\frac{2\pi x}{a}\sin\frac{2\pi y}{b}\,dx\,dy = 0,$$

when

$$X = \frac{D}{h}\nabla^4 w - L(w, \Phi) - \frac{1}{R}\frac{\partial^2\Phi}{\partial x^2};$$

then we obtain equations for f_1 and f_2. Introducing additional designations $f_1/h = \zeta$, $f_2/h = \xi$, we give to these equations form

$$C_1\zeta^3 + C_2\zeta\xi^2 - C_3\zeta^2 k - C_4\xi^2 k + C_5\zeta k^2 + \frac{\pi^2}{12(1-\mu^2)}\frac{(\lambda^2+1)^2}{\lambda^2}\zeta + \frac{128}{9\pi^2}s^*\zeta = 0. \quad (11.189)$$

$$16C_1\xi^3 + C_2\xi\zeta^2 - C_4\zeta\xi k + C_5\xi k^2 + \frac{4\pi^2}{3(1-\mu^2)}\frac{(\lambda^2+1)^2}{\lambda^2}\xi + \frac{128}{9\pi^2}s^*\xi = 0. \quad (11.190)$$

where C_1, ..., C_6 are certain functions of λ.

We introduce parameter $\psi = \xi/\zeta$, determining form of wave formation. Excluding s* from equations (189) and (190), we obtain biquadratic equation for ψ:

$$T\psi^4 - R_1\psi^2 - S = 0.$$

where T, R, S are certain functions of λ, k, ζ. Determining ψ from this we then find s*.

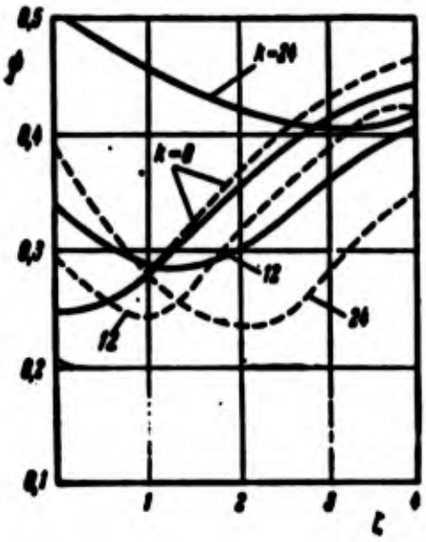

Fig. 11.64. Change of character of wave formation of panel under shear.

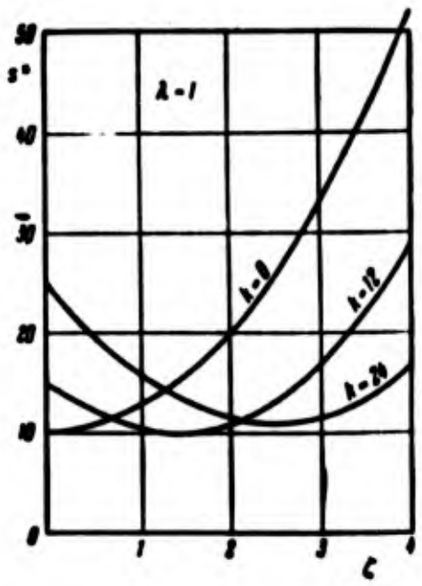

Fig. 11.65. Diagram "force – deflection" for cylindrical panel under shear.

In Fig. 11.64 is shown dependence of ψ on ζ for cases $\lambda = 1$ (solid curves) and $\lambda = 2$ (dotted line). In following Fig. 11.65 are given curves $s^*(\zeta)$ for flat plate ($k = 0$) and cylindrical panel with curvature $k = 12$ and 24 when $\lambda = 1$. Lower critical stress $s^*_н$ is

lowered compared to s_B^* approximately 30% for k = 12 and 50% for k = = 24. One should remember, however, that these results are obtained for binomial approximation of deflection by (188). True, in this case too, calculations are very bulky. More basic data must be found by digital computers.

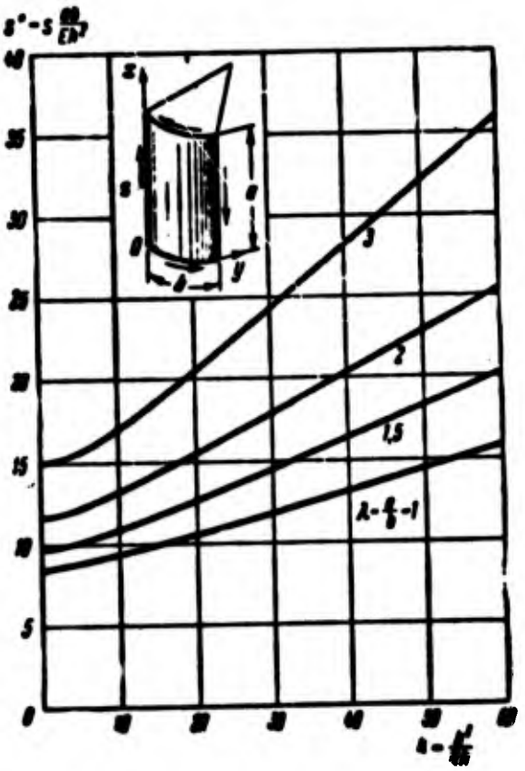

Fig. 11.66. Calculating data for determining lower critical shearing stress in case of cylindrical panel with different ratios of sides.

For practical calculations we recommend graph of Fig. 11.66, composed taking into account experimental data.

§ 141. Stability of Shells in Zone of Application of Concentrated Loads

Till now we considered, as a rule, such problems of stability of shells, in which principal state could be considered zero-moment. However, in practice we find cases, when bending forces in initial state are significant. We already saw this in § 130, when it was necessary to consider influence of clamping of face of shell on stability under action of external pressure. In general we encounter such kinds of problems if to shell there are applied loads, concentrated in a certain narrow region, for instance in region of linkage of shell with bottom or rigid frame. Let us assume that shell is subjected to axial compression and internal pressure or to a internal pressure alone; since the bottom or frame prevent deformation of shell, then

from them to shell are transmitted compressive radial forces. In zone of boundary effect, adjacent to place of linkage, deflection sharply changes; here moments and transverse forces have large amplitude, and consequently, moment stress turns out to be sharply expressed.

Here we encounter, on the one hand, problem of bifurcation of equilibrium states of shell for zone of boundary effect and, on the other hand, determination of supporting power from condition that stresses attain dangerous magnitude. We shall first treat bifurcational problems.

Let us assume that closed shell of length L is subjected to action of external pressure, distributed evenly on strip b, located in the middle of length (Fig. 11.67). Such problem can be met during calculation of shells with frames in different constructions when longitudinal reinforcing ribs are absent. We assume that deformation in middle surface and change of curvatures for initial axisymmetric stress of shell are determined by expressions (2) and (4):

$$\left.\begin{aligned} \varepsilon_x^0 = \frac{\partial u_0}{\partial x} = \mu\frac{w_0}{R}, \quad \varepsilon_y^0 = -\frac{w_0}{R}, \quad \gamma^0 = 0, \\ \varkappa_x^0 = -\frac{\partial^2 w_0}{\partial x^2}, \quad \varkappa_y^0 = -\frac{w_0}{R^2}, \quad \chi^0 = 0. \end{aligned}\right\} \qquad (11.191)$$

where u_0, w_0 are initial shears; we take $\sigma_x^0 = 0$. We consider that loss of stability of shell is accompanied by wave formation both on generatrix and also along the arc. Solving problem of stability in the small by Ritz method,* we present initial and additional deflections by the series

---

*See article of B. O. Almroth, D. O. Brush, Journ. Aerospace Sciences 28, No. 7 (1961), pp. 573–578, 592; these authors obtained the data shown in Figs. 11.68 and 11.69.

$$w_0 = \frac{f}{2} \sum_{m=1,3,5,\ldots} f_{0,m} \sin \frac{m\pi x}{l}, \quad w = \cos \frac{ny}{R} \sum_{p=1,3,5,\ldots} f_p \sin \frac{p\pi x}{l}.$$

Analogous expressions can be written for displacements u, v. Determining total energy of system and minimizing it with respect to parameters f_p, we determine upper critical pressure q_B. In Fig. 11.68 are given values of parameter $\hat{q}_B = q_B R/Eh$ for various b/L with ratio $L/R = \pi/4$, $\pi/2$ and π. Experiments showed that shells lose stability with a knock, where dents are located in zone of band b (Fig. 11.69). It

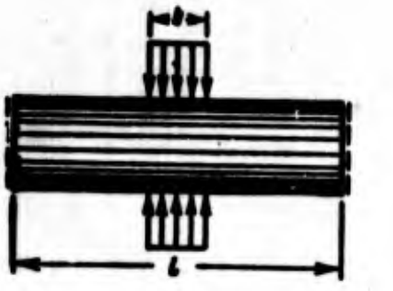

Fig. 11.67. Shell is subjected to external pressure on strip of width b.

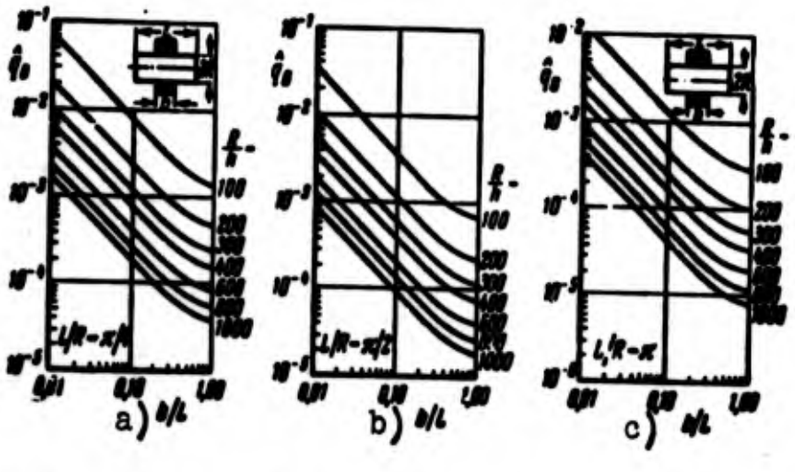

Fig. 11.68. Data for calculation of upper critical pressure with local application of load.

is desirable that subsequently this problem be investigated by nonlinear theory.

Let us consider now, again in linear formulation, the limiting case, when ratio L/R is very great, and width of band b approaches zero, so that pressure turns out to be applied along a line (Fig. 11.70); by N is understood linear intensity of load. Here it is possible to select another approach to problem, connected with composition

of integral equation.* We shall study initial state. In problems of boundary effect type it is possible to disregard magnitude w_0/R^2, appearing in expression (191) for n_y^0. Then we arrive at known simplified variant of resolvent of type (17). Repeating derivation, we are convinced that in axisymmetric problem equation (17) can be replaced by equation of fourth order (when

Fig. 11.69. Character of wave formation during local application of external pressure.

$p_x = p_y = s = 0$)

$$\frac{D}{h}\frac{d^4w_0}{dx^4} + \frac{E}{R^2}w_0 = 0. \qquad (11.192)$$

Fig. 11.70. Calculation for stability of shell in zone of application of concentrated load.

We introduce variable $\alpha = x/R$ and set $\lambda^2 = 3\sqrt{1-\mu^2}\ R/h$; then (17) takes the form

$$\frac{d^4w_0}{d\alpha^4} + 4\lambda^4 w_0 = 0. \qquad (11.192a)$$

On the average section for $\alpha = 0$ we should have

$$Q_x = -\frac{D}{R^3}\frac{d^3w_0}{d\alpha^3} = -\frac{N}{2}, \quad \frac{dw_0}{d\alpha} = 0.$$

---

*This solution of problem was given by L. I. Balabukh and V. M. Marchenko. Variant of derivation given here belongs to A. I. Tyulenev.

Considering these conditions, we use solution of equation (192) in the form

$$w_0 = \frac{NR^2}{8D\lambda^2} e^{-\lambda\alpha}(\cos\lambda\alpha + \sin\lambda\alpha).$$

Forces along arc will be equal to

$$\sigma_y h = -\frac{Eh}{R} w_0 = -\frac{3(1-\mu^2)R^2}{2\lambda^2 h^2} Ne^{-\lambda\alpha}(\cos\lambda\alpha + \sin\lambda\alpha). \qquad (11.193)$$

Let us now turn to consideration of bulged equilibrium state of shell, no longer axisymmetric. We present function of deflection, as in preceding example, in form of trigonometric series for variable $\beta = y/R$:

$$w = \sum_{n=1}^{\infty} w_n(\alpha)\cos n\beta.$$

We use full equation (17), considering $p_y = -\sigma_y$, $p_x = s = 0$; then we obtain equation for amplitudes of deflection w_n:

$$\left[\left(\frac{d^2}{d\alpha^2} - n^2\right)^4 + 4\lambda^4 \frac{d^4}{d\alpha^4}\right] w_n = \frac{4\lambda^4}{E} p_y n^2 \left(\frac{d^2}{d\alpha^2} - n^2\right)^2 w_n. \qquad (11.194)$$

We then apply Fourier transformation.* Considering that stress is symmetric to parallel $\alpha = 0$, we select Fourier cosine transform. In other words, we introduce along with original of function $f(\alpha)$ its image (transform) $F(s)$ by the formula

$$F(s) = \sqrt{\frac{2}{\pi}} \int_0^{\infty} f(\alpha)\cos s\alpha \, d\alpha. \qquad (11.195)$$

Reverse dependence, connecting original $f(\alpha)$ with representation $F(s)$, has the form

$$f(\alpha) = \sqrt{\frac{2}{\pi}} \int_0^{\infty} F(s)\cos s\alpha \, ds. \qquad (11.196)$$

It is necessary to consider that with stress symmetric to zero parallel $\alpha = 0$ odd derivatives of function of deflection are equal to zero

---

*See Sneddon, Fourier transformation, IL, M., 1955, p. 27 et seq.

when $\alpha = 0$.

Applying Fourier cosine transform to equation (194), we obtain following transforming equation:

$$[(s^2+n^2)^4+4\lambda^4 s^4]W(s)=4\sqrt{\frac{2}{\pi}}\frac{\lambda^4}{E}(s^2+n^2)^2 n^2\int_0^\infty p_y w_n \cos s\alpha\, d\alpha. \qquad (11.197)$$

Here W designates Fourier transform of deflection function. Integral in the right part of (197) is Fourier transform of product of functions $p_y(\alpha)$ and $w_n(\alpha)$. In accordance with theorem of convolutions of transforms,* we find

$$\int_0^\infty p_y w_n \cos s\alpha\, d\alpha=\frac{1}{2}\int_0^\infty W(p)[P(|s-p|)+P(s+p)]\,dp. \qquad (11.198)$$

where P is Fourier transform of function $p_y(\alpha)$. Producing Fourier transformation (195) on expression (193), we obtain

$$P(|s-p|)+P(s+p)= =(1-\mu^2)\frac{12}{\sqrt{2\pi}}\frac{R^2}{h^3}N\left[\frac{1}{(s-p)^4+4\lambda^4}+\frac{1}{(s+p)^4+4\lambda^4}\right]. \qquad (11.199)$$

We introduce designation

$$V(s)=\frac{\sqrt{(s^2+n^2)^4+4\lambda^4 s^4}}{s^2+n^2}W(s);$$

then relationships (197)–(199) will give

$$V(s)=N\int_0^\infty K(s,\ p)V(p)\,dp, \qquad (11.200)$$

where

$$K(s,\ p)=\frac{2\lambda^4 n^2}{\pi}\ \frac{12(1-\mu^2)R^2}{Eh^3}\ \frac{s^2+n^2}{\sqrt{(s^2+n^2)^4+4\lambda^4 s^4}}\times \times\frac{p^2+n^2}{\sqrt{(p^2+n^2)^4+4\lambda^4 p^4}}\left[\frac{1}{(s-p)^4+4\lambda^4}+\frac{1}{(s+p)^4+4\lambda^4}\right]. \qquad (11.201)$$

We obtained a uniform Fredholm integral equation (200) of the second type with symmetric nucleus, where external load N can be

---

*Op. cit., p. 35.

considered an independent parameter. Our purpose is to determine upper critical magnitude N_B, i.e., least eigenvalue of equation (200). But we already met such a problem in § 15 in examining stability of compressed bar. As we have seen, N_B is found approximately from relationship

$$\frac{1}{N^2} = \int_0^\infty \int_0^\infty K^2(s, p)\, ds\, dp.$$

For simplification of computations we replace magnitude

$$\frac{1}{(s-p)^4 + 4\lambda^4} + \frac{1}{(s+p)^4 + 4\lambda^4}$$

in expression (201) by a markedly larger one: $1/2\lambda^4$; then we find:

$$\frac{1}{N^2} = \frac{144(1-\mu^2)^2 R^4 n^4}{\pi^2 E^2 h^6} \int_0^\infty \int_0^\infty \frac{(s^2+n^2)^2}{[(s^2+n^2)^4 + 4\lambda^4 s^4]} \frac{(p^2+n^2)^2}{[(p^2+n^2)^4 + 4\lambda^4 p^4]}\, ds\, dp.$$

As it is easy to see, magnitude 1/N is equal to

$$\frac{1}{N} = \frac{12(1-\mu^2) R^2 n^2}{\pi E h^3} \int_0^\infty \frac{(s^2+n^2)^2}{(s^2+n^2)^4 + 4\lambda^4 s^4}\, ds. \qquad (11.202)$$

We introduce designations $z = s/n$, $\nu = \lambda/n$; expression (202) will take the form

$$\frac{1}{N} = \frac{12(1-\mu^2) R^2 \nu}{\pi E h^3 \lambda} \int_0^\infty \frac{(1+z^2)^2}{(1+z^2)^4 + 4\nu^4 z^4}\, dz.$$

Calculating integral here, we find

$$N = \frac{E h^3 \lambda}{3(1-\mu^2) R^2} \cdot \frac{\sqrt{4+\nu^4}}{\nu \sqrt{\sqrt{4+\nu^4}+2}}.$$

Minimizing N with respect to λ, we find

$$\nu^4 - 4 - 2\sqrt{4+\nu^4} = 0;$$

hence $\nu^4 = 12$. Finally

$$N_0 = \frac{E h^3 \lambda}{3(1-\mu^2) R^2} \frac{4}{\sqrt[4]{12}\sqrt{6}} = \frac{\sqrt{12}}{9} \frac{Eh}{(1-\mu^2)^{0.75}} \left(\frac{h}{R}\right)^{1.5}. \qquad (11.203)$$

This formula it is possible to compare with formula (77) for upper critical pressure in case of shell subjected to evenly distributed lateral load.

We turn to problem of determining supporting power of shell in zone of boundary effect. Let us assume that shell of finite length, fastened on ends with frames, is subjected to joint action of internal pressure and axial compression. We investigate stress near frame.* If we limit ourselves to linear formulation of this axisymmetric problem, equation (192) must be supplemented by members, depending on axial force N_x and pressure q:

$$D\frac{d^4w}{dx^4}+N_x\frac{d^2w}{dx^2}+\frac{Eh}{R^2}w=q.$$

During integration of this equation it is necessary to consider condition of linkage of shell with frame. We determine maximum stresses, composed of stresses in middle surface and flexural stresses. Using one or another theory of plasticity, we find combination of efforts N_x and q at which stresses attain dangerous magnitude. Calculating graph for N_x and q obtained thus, are given in article [11.12], from 1960.

---

*This problem was considered by O. N. Len'ko [11.12]. He showed that calculation of nonlinear members in expressions of type (191) in this case little affects result of solution.

Literature

11.1. S. V. Aleksandrovskiy. Stability of cylindrical shell during large deflections, "Design of spatial structures," 3, Stroyizdat (1955), 453-492.

11.2. S. A. Alekseyev. Postcritical deformation of plates and shells, Doct. diss., M., 1958.

11.3. N. A. Alumyae. Critical load of long cylindrical circular shell during torsion, Applied math. and mech., 18, No. 1 (1954), 27-34.

11.4. N. A. Alfutov. Stability of cylindrical and conical reinforced shells, loaded by external pressure, cand, diss., Moscow Higher Tech. school, 1956; On calculation of shells for stability by energy method, Eng. collection, 22 (1955).

11.4a. N. A. Alfutov and V. F. Sokolov. Determining lower critical pressure of elastic cylindrical shell and behavior of the shell after loss of stability, for strength analysis in machine building, Transactions of Moscow Higher Technical School, No. 89 (1959).

11.5. A. S. Vol'mir. Theory of stability and large deformations of a cylindrical shell during compression and shear, "Design of spatial structures," 1, Mashgiz (1950), 285-316; Influence of initial anomalies on stability of cylindrical shells during external pressure, DAN SSSR, 113, No. 2 (1957), 291-293.

11.6. Ye. D. Golitsinskaya. Stability of thin closed cylindrical shells, Transactions of Byelorussian agricultural academy, 31 (1959), 75-82.

11.7. V. M. Darevskiy. Stability of a cylindrical shell during simultaneous action of torque and normal pressure. News of Acad. of Sci. of USSR, OTN, No. 11 (1957), 137-147; Stability of console cylindrical shell during bending by transverse force with torsion and internal pressure, "Strength of cylindrical shells," Oborongiz, 1959, 72-94; "Design of spatial structures," 5 (1959), 431-449.

11.8. V. M. Darevskiy and R. I. Kshnyakin. Stability of a console cylindrical shell with reinforced edge during action of external pressure, DAN SSSR, 131, No. 6 (1960), 1294-1297; Stability of annularly reinforced cylindrical shell during action of external pressure, DAN SSSR, 134, No. 3 (1960), 548-551.

11.9. F. S. Isanbayeva. Determining lower critical load of cylindrical shell with hydrostatic compression, News of Kazan' branch of academy of Sciences of USSR, 7 (1955), 51-59; Theory of stability of a clamped cylindrical shell during hydrostatic pressure, loc. cit., 12, (1958), 149-154.

11.10. N. I. Krivosheyev. Stability of a cylindrical shell under shearing action, News of Kazan' branch of Academy of Sciences of USSR, 12 (1958), 133-142; Stability of a cylindrical shell during joint action of torsion and uniform transverse pressure, loc. cit., 143-148.

11.11. R. I. Kshnyakin. Influence of axial tensile force on stability of cylindrical shells during torsion and during external normal pressure, "Strength of cylindrical shells," Oborongiz, 1959, 55-71.

11.12. O. N. Len'ko. Stability of a circular cylindrical orthothropic shell, Coll. "Design of spatial structures," 4 (1956), 499-524; Influence of edge effect on strength of a cylindrical shell, loaded by internal pressure and axial compression, Structural mechanics and design of structures, No. 1 (1960), 1-6.

11.13. N. N. Leont'yev. Concerning the question of stability of a closed cylindrical shell, Scientific lecture for higher school, Construction, No. 1 (1958), 26-34.

11.13a. P. A. Lukash. On stability of orthotropic cylindrical shells, Scientific lecture for higher school, Construction, No. 2 (1958), 5-13.

11.14. V. A. Mar'in. Stability of a cylindrical shell during torsion and internal pressure, "Design of spatial structures," 5 (1959), 475-484; Stability of a cylindrical panel during shear, loc. cit., 485-501.

11.15. Kh. M. Mushtari. On elastic equilibrium of a cylindrical shell under action of longitudinal compression in the postcritical region, Transactions of Kazan' Aviation Inst., 17 (1946); Approximate determination of reduction factor of skin during axial compression, News of Kazan' branch of Academy of Sciences of USSR, 7 (1955), 23-35.

11.16. Kh. M. Mushtari and A. V. Sachenkov. On stability of cylindrical and conical shells of circular section during joint action of axial compression and external normal pressure, Applied math. and mech., 18, No. 6 (1954), 667-674.

11.17. V. A. Nagayev. Determining lower critical load of cylindrical shell by external transverse pressure, News of higher educational institutions, machine building series, No. 6 (1959), 46-52.

11.18. O. M. Paliy. Stability of a circular cylindrical shell, clamp on curved edges, News of Acad. of Sci. of USSR, OTN, No. 1 (1958), 126-128.

11.19. A. V. Pogorelov. Cylindrical shells during postcritical deformations, Parts 1-3, Khar'kov U. Press, 1962.

11.20. A. V. Pogorelov. On postcritical deformations of compressed cylindrical shells, DAN SSSR, 134, No. 1 (1960), 62-63; Postcritical deformations of cylindrical shells under external pressure, DAN SSSR, 138, No. 6 (1961), 1325-1327; Postcritical deformations of cylindrical shells during torsion, DAN SSSR, 16, No. 2 (1962).

11.21. Yu. N. Rabotnov. Local stability of shells, DAN SSSR, 52. No. 2 (1946).

11.22. O. I. Terebushko. Calculating supporting power of a circular cylindrical panel reinforced with ribs, "Design of spatial structures," 4 (1958), 531-554; Stability of a cylindrical shell during torsion, external pressure and compression, loc. cit., 5 (1959), 502-522; Calculation for stability and designing of cylindrical reinforced shells, loc. cit., 7, (1962), 119-133.

11.23. S. P. Timoshenko. News of Electrical Engineering Inst., 11 (1914).

11.24. K. D. Turkin. Stability of a reinforced cylindrical shell during compression and pure flexure, "Design of spatial structures," 4 (1958), 477-498; General stability of a reinforced cylindrical shell during transverse bending, loc. cit., 5 (1959), 450-474.

11.24a. V. M. Chebanov. Certain problems of research of stability of a shell, Herald of Leningrad State University, Mech. and Math., No. 1, (1959), 79-93.

11.25. L. A. Shapovalov. Applied math. and mech., 20, No. 5 (1956), 669-671

11.26. M. Kozarov. Research of stability of thin elastic orthotropic cylindrical shells by nonlinear theory of V. Z. Vlasov. Annual of Engineering and Building Inst., Sophia, 1957 (in Bulgarian), 93-136.

11.27. H. S. Tsien. A theory for the buckling of thin shells, 9 (1942), 373-384.

11.28. H. Becker and G. Gerard. Torsional buckling of moderate length cylinders. J. Appl. 23, No. 4 (1956), 647-648.

11.29. P. P. Bijlaard. Buckling stress of thin cylindrical clamped shells subject to hydrostatic pressure, J. Aeron. Sci. 21, No. 12 (1954).

11.30. L. H. Donnell. Stability of thin walled tubes under torsion NACA Rep. No. 479 (1933) (translation in collection ed. by A. A. Umanskiy and P. M. Znamenskiy, Publishing House of (ent. Aero-Hydrodynamic Inst., M., 1937, 29-57); Effect of imperfections on the buckling of thin cylinders under external pressure, J. Appl. Mech. 23, No. 4 (1956), 569-575.

11.30a. L. H. Donnell and C. C. Wan. Effect of imperfections on the buckling of thin cylinders and columns under axial compression. J. Appl. Mech. 17, No. 1 (1950), 73-83.

11.31. G. D. Galletly and R. Bart. Effects of boundary conditions and initial out of roundness on the strength of thin-walled cylinders subject to external hydrostatic pressure, Paper Am. Soc. Mech. Eng., NAPM-9, 1956.

11.32. G. Gerard. An evaluation of structural sheet materials in missile application, Jet Propulsion 28, No. 8 (1958), 511-520.

11.33. L. A. Harris, H. S. Suer, W. T. Skene, and R. J. Bendjamine. The stability of thin-walled unstiffened circular cylinders under axial compression including the effects of internal pressure, J. Aeron. Sci. 24, No. 8 (1957), 587-596; The bending stability of thin-walled unstiffened circular cylinders uncluding the effects of internal pressure. J. Aeron. Sci. 25, No. 5 (1958), 281-287.

11.34. H. G. Hopkins and E. H. Brown. The effect of internal pressure on the initial buckling of thin-walled cylinders under torsion, Aer. Res. Com. Rep. and Memo, No. 2423 (1951).

11.35. Th. Kármán and H. S. Tsien. The buckling of thin cylindrical shells under axial compression, J. Aeron. Sci. 8, No. 8 (1941), 303-312.

11.36. J. Kempner. Postbuckling behaviour of axially compressed circular cylindrical shells, J. Aeron. Sci. 21, No. 5 (1954), 329-335, 342 (translations of "Mechanics," IL, Vol. 2, 1955, 105-116).

11.37. J. Kempner, K. Pandalai, S. Patel, and J. Crouze-Pascal. Postbuckling behaviour of circular cylindrical shells under hydrostatic pressure, J. Aeron. Sci. 24, No. 4 (1957), 253-264.

11.38. L. Kirste. Abwickelbare Verformung dünnwandiger Kreiszylinder, Oesterr. Ing. Archiv 8, No. 2-3 (1954), 149-151.

11.39. A. Kirstein and E. Wenk. Observations of snap-through action of thin cylindrical shells under external pressure, Proc. Soc. Exper. Stress Analysis 14, No. 1 (1956), 205-214.

11.40. B. Klein. Interaction equation for the buckling of unstiffened cylinders under combined bending, torsion and internal pressure, J. Aeron. Sci. 22, No. 8 (1955), 583; Buckling of unstiffened thin-walled circular cylindrical shells subjected to various loading conditions with and without internal pressure, Am. Rocket Society, 1958.

11.41. W. T. Koiter. Buckling and postbuckling behaviour of a cylindrical panel under axial compression, Nat. Luchtvaart laborat., Rep. No. 476, Amsterdam, 1956.

11.42. D. Legget and R. Jones. The buckling of a cylindrical shell under axial compression when the buckling load has been exceeded, Rep. and Memo., No. 2190 (1942); Publs. Inst. math. Acad. Serbe Sci. 7 (1954).

11.43. H. Lo, H. Crate, and E. Schwartz. Buckling of thin walled cylinders under axial compression and internal pressure, NACA Rep. No. 1027, 1951.

11.44. Tsu-Tao Loo. Effects of large deflections and imperfections on the elastic buckling of cylinders under torsion and axial compression, Proc. of the 2nd US Nat. Congr. of Appl. Mech., NY, 1954. 345-357.

11.45. R. Lorentz. Zeitschr. d. Ver. deutsche Ing. 52 (1908), 1706; Physik. Zeitschr. 12 (1911), 241.

11.46. H. F. Michielsen. The behaviour of thin cylindrical shells after buckling under axial compression, J. Aeron. Sci. No. 12 (1948), 738-744.

11.47. R. Mises. Der kritische AuBendruck für allseits belastete cylindrischer Rohre. "Festschr. zum. 70 Geburtstag von prof. A. Stodola," Zürich, 1929, 418-432.

11.48. W. Nash. Effect of large deflections and initial imperfections on the buckling of cylindrical shells, J. Aeron. Sci. 22, No. 4 (1955), 264-269; An experimental analysis of the buckling of thin initially imperfect cylindrical shells subject to torsion, Paper of the Soc. Experim. Stress Anal., No. 476 (1957); Buckling of initially imperfect cylindrical shells subjected to torsion, J. Appl. Mech. 24, No. 1 (1957), 125-130.

11.49. R. G. Sturm. Stability of thin cylindrical shells in torsion, Proc. Am. Soc. Civil. Eng. 73, No. 4 (1947), 471-495.

11.50. E. Schwerin. Die Torsionsstabilität des dünnwandigen Rohres, Zeitschr. angew. Math. und Mech., 5, No. 3 (1925), 235-243.

11.51. W. F. Thielemann. New developments in the nonlinear theories of the buckling of thin cylindrical shells, "Aeronautics and Astronautics," Pergamon-Press, 1960, 76-121.

11.52. W. Thielemann, W. Schnell, and G. Fischer. Beul- und Nachbeulverhalten orthotroper Kreiszylinderschalen unter Axial und Innendruck, Zeitschr für Flugwissenschaften 8, No. 10/11 (1960), 284-293.

11.53. E. Wenk, R. S. Scanland, and W. A. Nash. Experimental analysis of the buckling of cylindrical shells subjected to external hydrostatic pressure, Proc. of the Soc. Exper. Stress. Anal. 12, No. 1 (1954).

11.54. D. F. Windenburg and C. Trilling. Collapse by instability of thin cylindrical shells under external pressure, Trans. ASME 56 (1934), 819-825.

11.55. Y. Yoshimura and J. Niisawa. Lower buckling stress of circular cylindrical shells subjected to torsion, J. Aeron. Sci. 24, No. 3 (1957), 211-216.

CHAPTER XII

STABILITY OF CYLINDRICAL SHELLS BEYOND ELASTIC LIMIT

§ 142. Problem of Stability in the Small

Dependences derived in Chapter XI are valid only within elastic limit. Thus, for instance, formula (11.33) for upper critical stress during axial compression of circular cylindrical shell can be used on the condition that $p_в \leqq \sigma_{пц}$;* hence

$$\frac{R}{h} > \frac{1}{\sqrt{3(1-\mu^2)}} \frac{E}{\sigma_{пц}}. \qquad (12.1)$$

For duralumin when $\mu = 0.3$, $\sigma_{пц} = 2 \cdot 10^3$ kg/cm^2, $E = 7 \cdot 10^5$ kg/cm^2, we should have $R/h \geqq 210$. Formula (11.66) for lower critical stress is applicable if $R/h \geqq 70$. However in many cases buckling of shells occurs in plastic region. This pertains, first of all, to engineering constructions, e.g., pipelines. In Chapter VIII it was already said that panels of contemporary heavy aircraft also buckle under stresses, exceeding limit of proportionality. Therefore, research of stability of shells beyond the elastic limit, still weakly presented in literature, is of essential practical value.

As experimental data show (see § 143), during weakly developed plastic deformations it is necessary, just as within elastic limit,

---

*Translation editors note: $p_в$ = upper critical stress; $\sigma_{пц}$ = proportional limit.

to distinguish stability of shells in the small and in the large.

First we approach problem from the point of view of stability in the small. It is natural to extend to solution of this problem those methods which we used during research of stability of plates (Chapter VIII), and to apply deformation theory, or flow theory.

We shall turn in the beginning to deformations theory.* Since, as compared to case of plate, problem here is complicated, we select the simplest variant of solution and will not consider effect of unloading. In other words, we shall consider that middle layer is neutral in the sense that stresses and deformations of natural bending at points of this layer are equal to zero. But for shell it is necessary to consider increase of stresses in middle surface $\delta\sigma_x$, $\delta\sigma_y$, $\delta\tau$ and corresponding deformations $\delta\varepsilon_x$, $\delta\varepsilon_y$, $\delta\gamma$; coordinates x and y we count off as before along the generatrix and along the arc. Using designations (8.33), we rewrite expressions (8.123–8.125) in the form

$$\left.\begin{aligned} \delta s_x &= E_c \delta e_x - (E_c - E_\kappa)\frac{s_x}{\sigma_i}\delta e_i, \\ \delta s_y &= E_c \delta e_y - (E_c - E_\kappa)\frac{s_y}{\sigma_i}\delta e_i, \\ \delta\tau &= \frac{1}{3}E_c\delta\gamma - (E_c - E_\kappa)\frac{\tau}{\sigma_i}\delta e_i. \end{aligned}\right\} \qquad (12.2)$$

[c = secant, κ = tangent]

where $s_x = \sigma_x - 0.5\sigma_y$, $s_y = \sigma_y - 0.5\sigma_x$, and ε_i and σ_i – intensity of deformations and intensity of stresses in middle surface.** We multiply left and right side of equations (2) correspondingly by σ_x, σ_y,

---

*It is necessary to remember that all limitations concerning applications of deformation theory in problems of such type (see § 99) remain in force here.

**In Chapter VIII we used designation s (without index!) for another magnitude – intensity of shearing forces; we will preserve this designation here.

and 3τ and add; taking into account relationship

$$s_x\sigma_x + s_y\sigma_y + 3\tau^2 = \sigma_i^2. \tag{12.3}$$

we obtain

$$\sigma_x\delta s_x + \sigma_y\delta s_y + 3\tau\delta\tau = E_k\sigma_i\delta\varepsilon_i. \tag{12.4}$$

Hence

$$\delta\varepsilon_i = \frac{\sigma_x\delta s_x + \sigma_y\delta s_y + 3\tau\delta\tau}{\sigma_i E_k} = \frac{\Pi(\sigma,\ \delta s)}{\sigma_i E_k}, \tag{12.5}$$

where

$$\Pi(\sigma,\ \delta s) = \Pi(s,\ \delta\sigma) = s_x\delta\sigma_x + s_y\delta\sigma_y + 3\tau\delta\tau.$$

Using (2) we find

$$\left.\begin{aligned}
\delta\varepsilon_x &= \frac{1}{E_c}\left[\delta s_x + \frac{s_x}{\sigma_i^2}\,\frac{E_c - E_k}{E_k}\,\Pi(\sigma,\ \delta s)\right],\\
\delta\varepsilon_y &= \frac{1}{E_c}\left[\delta s_y + \frac{s_y}{\sigma_i^2}\,\frac{E_c - E_k}{E_k}\,\Pi(\sigma,\ \delta s)\right],\\
\delta\gamma &= \frac{1}{E_c}\left[3\delta\tau + \frac{3\tau}{\sigma_i^2}\,\frac{E_c - E_k}{E_k}\,\Pi(\sigma,\ \delta s)\right].
\end{aligned}\right\} \tag{12.6}$$

We write equation of equilibrium of member of shell in projections on directions of generatrix and tangent to arc:

$$\left.\begin{aligned}
\frac{\partial(\delta\sigma_x)}{\partial x} + \frac{\partial(\delta\tau)}{\partial y} &= 0,\\
\frac{\partial(\delta\tau)}{\partial x} + \frac{\partial(\delta\sigma_y)}{\partial y} &= 0.
\end{aligned}\right\} \tag{12.7}$$

These equations will be satisfied, if we introduce function of secondary stresses by the formulas

$$\delta\sigma_x = \frac{\partial^2\Phi}{\partial y^2},\quad \delta\sigma_y = \frac{\partial^2\Phi}{\partial x^2},\quad \delta\tau = -\frac{\partial^2\Phi}{\partial x\,\partial y}. \tag{12.8}$$

Then

$$\Pi(\sigma,\ \delta s) = \Pi(s,\ \Phi) = s_x\frac{\partial^2\Phi}{\partial y^2} + s_y\frac{\partial^2\Phi}{\partial x^2} - 3\tau\frac{\partial^2\Phi}{\partial x\,\partial y}. \tag{12.9}$$

Expressions (6) take form

$$\left.\begin{aligned}
\varepsilon_x &= \frac{1}{E_c}\left[\frac{\partial^2\Phi}{\partial y^2} - \frac{1}{2}\frac{\partial^2\Phi}{\partial x^2} + \frac{s_x}{\sigma_i^2}\frac{E_c - E_\kappa}{E_\kappa}\Pi(\sigma, \Phi)\right].\\
\varepsilon_y &= \frac{1}{E_c}\left[\frac{\partial^2\Phi}{\partial x^2} - \frac{1}{2}\frac{\partial^2\Phi}{\partial y^2} + \frac{s_y}{\sigma_i^2}\frac{E_c - E_\kappa}{E_\kappa}\Pi(\sigma, \Phi)\right].\\
\gamma &= \frac{1}{E_c}\left[-3\frac{\partial^2\Phi}{\partial x\,\partial y} + \frac{3\tau}{\sigma_i^2}\frac{E_c - E_\kappa}{E_\kappa}\Pi(\sigma, \Phi)\right].
\end{aligned}\right\} \qquad (12.10)$$

Projecting forces, acting on member of shell, on direction of normal to middle surface, we obtained earlier the following equation of equilibrium (p. 554):

$$\frac{\partial^2 M_x}{\partial x^2} + 2\frac{\partial^2 H}{\partial x\,\partial y} + \frac{\partial^2 M_y}{\partial y^2} - \left(\sigma_x\frac{\partial^2 w}{\partial x^2} + \sigma_y\frac{\partial^2 w}{\partial y^2} + 2\tau\frac{\partial^2 w}{\partial x\,\partial y} + \frac{q_y}{R}\right)h = 0. \qquad (12.11)$$

Fundamental stresses, corresponding to moment of loss of stability, we designate, as before, by p_x, p_y, and s; magnitudes p_x and p_y are considered positive during compression. Corresponding intensity of stresses is equal to

$$p_i = \sqrt{p_x^2 + p_y^2 - p_x p_y + 3s^2}. \qquad (12.12)$$

Moments M_x, M_y, and H we here, too, determine with help of expressions (8.137)–(8.139). Using, furthermore, relationships (8), we will present equation (11) in the form

$$\begin{aligned}
&\left[1 - \frac{3}{4}\left(1 - \frac{\eta_\kappa}{\eta_c}\right)\frac{p_x^2}{p_i^2}\right]\frac{\partial^4 w}{\partial x^4} + 2\left[1 - \frac{3}{4}\left(1 - \frac{\eta_\kappa}{\eta_c}\right)\frac{p_x p_y + 2s^2}{p_i^2}\right]\frac{\partial^4 w}{\partial x^2\,\partial y^2} +\\
&+\left[1 - \frac{3}{4}\left(1 - \frac{\eta_\kappa}{\eta_c}\right)\frac{p_y^2}{p_i^2}\right]\frac{\partial^4 w}{\partial y^4} - 3\left(1 - \frac{\eta_\kappa}{\eta_c}\right)\frac{s}{p_i^2}\left(p_x\frac{\partial^4 w}{\partial x^3\,\partial y} + p_y\frac{\partial^4 w}{\partial x\,\partial y^3}\right) +\\
&+\frac{h}{D_c}\left(p_x\frac{\partial^2 w}{\partial x^2} + 2s\frac{\partial^2 w}{\partial x\,\partial y} + p_y\frac{\partial^2 w}{\partial y^2} - \frac{1}{R}\frac{\partial^2\Phi}{\partial x^2}\right) = 0;
\end{aligned} \qquad (12.13)$$

equation (8.140), composed earlier for a plate, is augmented here by term containing Φ.

We take equation of compatibility of deformations; in case of small deflections it has form (11.14):

$$\frac{\partial^2\varepsilon_x}{\partial y^2}+\frac{\partial^2\varepsilon_y}{\partial x^2}-\frac{\partial^2\gamma}{\partial x\partial y}=-\frac{1}{R}\frac{\partial^2 w}{\partial x^2}. \qquad (12.14)$$

Substituting expression (10), we arrive at following equation:*

$$\nabla^4\Phi+\frac{\varphi_c-\varphi_K}{\varphi_K B_1^2}\left[\left(p_x-\frac{1}{2}p_y\right)\frac{\partial^2\Pi(p,\Phi)}{\partial y^2}+\left(p_y-\frac{1}{2}p_x\right)\frac{\partial^2\Pi(p,\Phi)}{\partial x^2}-3s\frac{\partial^2\Pi(p,\Phi)}{\partial x\partial y}\right]=-\frac{\varphi_c E}{R}\frac{\partial^2 w}{\partial x^2}. \qquad (12.15)$$

In equations (13) and (15) we take former designations (8.68) and (8.120) for φ_c, φ_K, and D_c'.

We shall use <u>flow theory</u>. As we have seen above (§ 108), relationships of type (6) are preserved also in this case, if we set $E_c = E$. Therefore, we will arrive at the same differential equations (13) and (15), considering $\varphi_c = 1$, $D_c' = D$.

§ 143. Buckling of Closed Shell During Axial Compression

We turn to case of shell supported by hinge on end, compressed along generatrix by forces p. Equation (13) takes form (for $p_x = p_1 = p$, $p_y = s = 0$):

$$\frac{D'\varphi_c}{h}\left[\left(\frac{1}{4}+\frac{3}{4}\frac{\varphi_K}{\varphi_c}\right)\frac{\partial^4 w}{\partial x^4}+2\frac{\partial^4 w}{\partial x^2\partial y^2}+\frac{\partial^4 w}{\partial y^4}\right]+p\frac{\partial^2 w}{\partial x^2}=\frac{1}{R}\frac{\partial^2\Phi}{\partial x^2}. \qquad (12.16)$$

Expression (9) turns out to be equal to

$$\Pi(s,\Phi)=p\left(\frac{\partial^2\Phi}{\partial y^2}-\frac{1}{2}\frac{\partial^2\Phi}{\partial x^2}\right).$$

Equation (15) changes into the following:

$$\left(\frac{3}{4}+\frac{1}{4}\frac{\varphi_c}{\varphi_K}\right)\frac{\partial^4\Phi}{\partial x^4}+\left(3-\frac{\varphi_c}{\varphi_K}\right)\frac{\partial^4\Phi}{\partial x^2\partial y^2}+\frac{\varphi_c}{\varphi_K}\frac{\partial^4\Phi}{\partial y^4}=-\frac{\varphi_c E}{R}\frac{\partial^2 w}{\partial x^2}. \qquad (12.17)$$

---

*Equations (13) and (15) are contained in works of E. I. Grigolyuk [12.4].

We take for w expression

$$w = f \sin \frac{m\pi x}{L} \cos \frac{ny}{R} \tag{12.18}$$

and place it in the right part of equation (17); then we obtain

$$\left(\frac{3}{4} + \frac{1}{4}\frac{\varphi_c}{\varphi_x}\right)\frac{\partial^4 \Phi}{\partial x^4} + \left(3 - \frac{\varphi_c}{\varphi_x}\right)\frac{\partial^4 \Phi}{\partial x^2 \partial y^2} + \frac{\varphi_c}{\varphi_x}\frac{\partial^4 \Phi}{\partial y^4} = \\ = \frac{\varphi_c E}{R} f \left(\frac{m\pi}{L}\right)^2 \sin \frac{m\pi x}{L} \cos \frac{ny}{R}. \tag{12.19}$$

We seek the particular integral of equation (19) in the form

$$\Phi = A \sin \frac{m\pi x}{L} \cos \frac{ny}{R}; \tag{12.20}$$

we find

$$A = E f \frac{\varphi_c}{R\left(\frac{3}{4} + \frac{1}{4}\frac{\varphi_c}{\varphi_x}\right)\left(\frac{m\pi}{L}\right)^4 + \left(3 - \frac{\varphi_c}{\varphi_x}\right)\left(\frac{n}{R}\right)^2 + \frac{\varphi_c}{\varphi_x}\left(\frac{Ln^2}{m\pi R^2}\right)^2};$$

hence

$$\frac{\partial^4 \Phi}{\partial x^4} = -E f \frac{\varphi_c}{R\left(\frac{3}{4} + \frac{1}{4}\frac{\varphi_c}{\varphi_x}\right) + \left(3 - \frac{\varphi_c}{\varphi_x}\right)\left(\frac{Ln}{m\pi R}\right)^2 + \frac{\varphi_c}{\varphi_x}\left(\frac{Ln}{m\pi R}\right)^4} \times \\ \times \sin \frac{m\pi x}{L} \cos \frac{ny}{R}. \tag{12.21}$$

Putting expressions (18) and (21) in (16) and considering $D' = Eh^3/9$, we arrive at the following expression for p:

$$p = E\varphi_c \left\{ \frac{h^2}{9}\left[\left(\frac{1}{4} + \frac{3}{4}\frac{\varphi_x}{\varphi_c}\right)\left(\frac{m\pi}{L}\right)^4 + 2\left(\frac{n}{R}\right)^2 + \left(\frac{n^2 L}{R^2 m\pi}\right)^2\right] + \right. \\ \left. + \frac{1}{\left(\frac{3}{4} + \frac{1}{4}\frac{\varphi_x}{\varphi_c}\right)\left(\frac{m\pi R}{L}\right)^4 + \left(3 - \frac{\varphi_c}{\varphi_x}\right)n^2 + \frac{\varphi_c}{\varphi_x}\left(\frac{Ln^2}{m\pi R}\right)^2} \right\}. \tag{12.22}$$

We introduce dimensionless parameters

$$\hat{p} = \frac{pR}{Eh}, \quad \eta = \frac{n^2 h}{R}, \quad \theta = \frac{m\pi R}{nL}, \quad \lambda = \frac{\varphi_x}{\varphi_c}. \tag{12.23}$$

All these magnitudes, except λ, were met in Chapter XI. Expression (22) obtains form

$$\hat{p} = \varphi_c \left\{ \frac{3}{9}\left(\frac{1 + 3\lambda}{4}\theta^2 + 2 + \frac{1}{\theta^2}\right) + \frac{\lambda}{\eta\left[\frac{1 + 3\lambda}{4}\theta^2 + (3\lambda - 1) + \frac{1}{\theta^2}\right]} \right\}. \tag{12.24}$$

If there is realized <u>axisymmetric</u> form of loss of stability, then n = 0 and from (22) we obtain

$$p = E\varphi_c\left[\frac{h^2}{9}\left(\frac{1}{4}+\frac{3}{4}\frac{\varphi_\kappa}{\varphi_c}\right)\left(\frac{m\pi}{L}\right)^2+\frac{1}{\left(\frac{3}{4}+\frac{1}{4}\frac{\varphi_c}{\varphi_\kappa}\right)\left(\frac{m\pi R}{L}\right)^2}\right].$$

Minimizing obtained expression with respect to $m\pi/L$, we find parameter corresponding to critical stress:*

$$\hat{p}_* = \frac{2}{3}\sqrt{\varphi_\kappa\varphi_c}; \qquad (12.25)$$

here

$$p_* = \frac{2}{3}\sqrt{E_\kappa E_c}\,\frac{h}{R}. \qquad (12.26)$$

In elastic region, when $\varphi_\kappa = \varphi_c = 1$, we have

$$p_* = \frac{2}{3}E\frac{h}{R}. \qquad (12.27)$$

This expression ensues from (11.33) if we take $\mu = 0.5$.

If we use theory of secant modulus [12.10], which we discussed in Chapter VIII (p.450), we would obtain

$$p_* = \frac{2}{3}E_c\frac{h}{R}. \qquad (12.28)$$

Comparison of (26) and (28) shows that solution of problem according to deformation theory without calculation of effect of unloading leads to lower value for p_B.

Based on <u>flow theory</u> and proceeding in the same manner, we arrive at formulas

$$\hat{p}_* = \frac{2}{3}\sqrt{\varphi_\kappa}, \quad p_* = \frac{2}{3}\sqrt{E_\kappa E}\,\frac{h}{R}. \qquad (12.29)$$

If we conditionally take $E_c \approx \sqrt{E_\kappa E}$, these formulas will coincide with (28).

---

*Formula (25) was obtained in works [8.9], [12.3], [12.10] and is generalized for case of compressible material by E. I. Grigolyuk [12.4].

Let us consider now the more general case of asymmetric form of loss of stability of shell. Critical stress by (24) constitutes a function of parameters η and ϑ^2. Minimizing function (24) with respect to η we find

$$\eta = \frac{3\sqrt{\lambda}}{\sqrt{\left(\frac{1+3\lambda}{4}\vartheta^2+2+\frac{1}{\vartheta^2}\right)\left(\frac{1+3\lambda}{4}\vartheta^2+3\lambda-1+\frac{1}{\vartheta^2}\right)}}. \qquad (12.30)$$

Putting this value in (24), we obtain

$$\hat{p}_0 = \frac{2}{3} d_1 \sqrt{\varphi_\lambda \varphi_c}. \qquad (12.31)$$

where

$$d_1 = \sqrt{1+\frac{12(1-\lambda)\vartheta^2}{(1+3\lambda)\vartheta^4+4(3\lambda-1)\vartheta^2+4}}. \qquad (12.32)$$

If we now investigate expression (32), it will appear that it obtains a "local" minimum at

$$\vartheta^2 = \frac{2}{\sqrt{1+3\lambda}}. \qquad (12.33)$$

Since ϑ characterizes ratio of lengths of half-waves in circumferential and longitudinal directions, then from (33) it follows that during transition from elastic region to plastic waves should stretch out along arc; as we shall see later, this is confirmed by experiments.

Finally formula for critical stress during asymmetric buckling of shell will be

$$p_0 = \frac{2}{3} E \varphi_c \sqrt{\lambda} \sqrt{\frac{2+\sqrt{1+3\lambda}}{3\lambda-1+\sqrt{1+3\lambda}}} \frac{h}{R}. \qquad (12.34)$$

For points of yield surface ($\lambda = 0$) formula (31) obtains form $\hat{p}_B = \varphi_c \left(\frac{2}{3}\right)^{1.5}$. From this one can determine critical deformation

$$\varepsilon_{cp} = \left(\frac{2}{3}\right)^{1.5} \frac{h}{R}. \qquad (12.35)$$

Comparison of formulas (25) and (31) shows that when $\lambda \neq 1$ we have $d_1 > 1$ and, consequently, buckling of shells <u>in the small</u> in the presence of plastic deformations should occur in axisymmetric form; therefore, for <u>practical calculations</u> it is necessary to use formula (26). It should be presented in the form

$$\frac{p_B}{E}\frac{1}{\sqrt{\varphi_c\varphi_K}}=\frac{2}{3}\frac{h}{R}. \qquad (12.26a)$$

Knowing dependence of φ_c and φ_K on σ (see § 110), we find critical value of p_B for different ratios R/h. The same method is applied during calculations by formula (29).

We give data of a series of experiments on stability of duralumin shells in elasto-plastic region.* Ratios of length to radius constituted L/R = 2; magnitude R/h changed from 130 to 20. Testpieces were prepared from pipes on a lathe, so that initial imperfections of form were insignificant.

In those cases when loss of stability occurred with weakly developed plastic deformations, it always was accompanied by a knock. Dents appearing had diamond-shaped outline, as in elastic region. With decrease of ratio R/h number of waves on circumference fell. In Fig. 12.1a, b, and c are given photographs of tested pieces with ratio R/h, accordingly equal to 50, 30, and 25. If plastic deformation before loss of stability was significant, effect of knock disappeared, and there was formed solid annular bulge (Fig. 12.1b), as in elastic region with internal pressure. Thus, judging by these experiments, purely plastic buckling of shell indeed is axisymmetric.**

---

*These experiments were conducted by A. N. Bozhinskiy [12.1].

**Analogous results were obtained by V. G. Zubchaninov [12.2].

In Fig. 12.2 sign Δ marks values of parameter $\hat{p}_{кр}$, obtained in experiments depending upon ratio R/h. Solid and dot-dash lines are constructed by formulas (26) and (29), the first of which corresponds to deformation theory, and the second to flow theory. It is interesting to note that graphs $\hat{p}_{в}(R/h)$, constructed by these two theories, differ little from each other, while in case of flat plate diagrams $p_{кр}(b/h)$ sharply differed from one another. Dotted line in Fig. 12.2

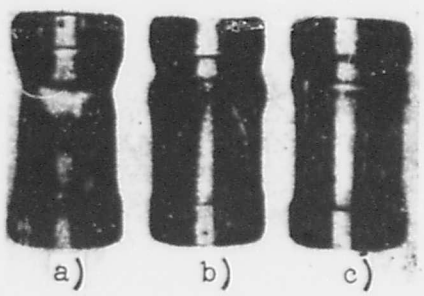

Fig. 12.1. Compression along axis of shell after buckling with plastic deformations; for testpiece c) plastic deformations are the greatest.

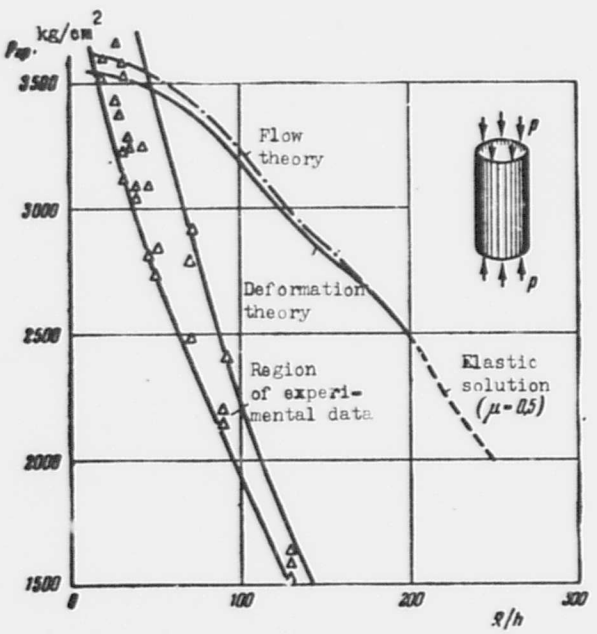

Fig. 12.2. Dependence of upper critical compression stress on ratio R/h by different theories of plasticity in comparison with experimental data.

pertains to elastic region, where we take μ = 0.5. During buckling

within elastic limit real critical stress turned out to be equal to $\hat{p}_{кр} \approx 0.27$ which constitutes about 40% of $\hat{p}_{в} = 0.667$ (for $\mu = 0.5$) and 45% of $p_{в} = 0.606$ (for $\mu = 0.3$). Thus, here we are faced with sharp divergence between real critical stresses and upper value $p_{кр}$. However, as one may see from graph, with increasing plastic deformation this divergence is smoothed out. Thus, for instance, with deformation $\varepsilon_{кр} = 1.4\varepsilon_{пц}$, where $\varepsilon_{пц} = \sigma_{пц}/E$, critical stress constitutes already 80% of $p_{в}$, and when $\varepsilon \geqslant 1.67\varepsilon_{пц}$ magnitudes $\hat{p}_{кр}$ and $\hat{p}_{в}$ turn out to be very close to each other.

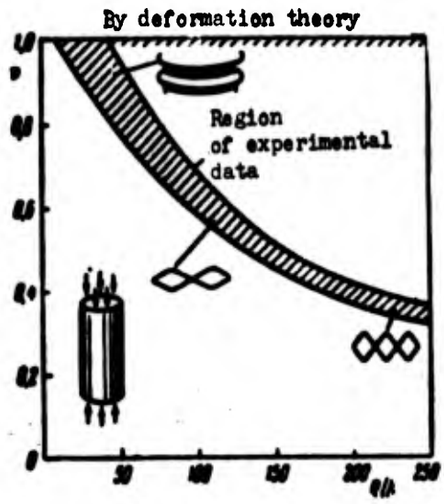

Fig. 12.3. Dependence between dimensionless parameter of compressive force and ratio R/h.

In Fig. 12.3 results of experiments are presented in another form. along the axis of abscissas as before is plotted ratio R/h, but along the axis of ordinates we plot coefficient $\nu = p_{кр}/p_{в}$, where $p_{в}$ is calculated according to deformation theory. Here there is noted the character of wave formation in different cases.

From graphs of Figs. 12.2 and 12.3 there can be drawn the conclusion that for comparatively small values of R/h (for duralumin shells where $R/h < 25$), when plastic deformations are significant, it is possible to conduct practical calculations only for stability in the small. However, with weakly developed plastic deformations, the effect of geometric nonlinearity continues to show; here calculated resolvent stresses should constitute a sizeable fraction of $p_{в}$. Therefore, problem of stability in the large retains its value also for elasto-plastic region. An

attempt at solution of such a problem will be made lower (§ 147) in application to cylindrical panels.

§ 144. Closed Shell Under External Pressure

Let us turn to case when shell of average length is subjected to action of evenly distributed external pressure q.* Considering stability in the small, we originate from equations (13) and (15) of deformation theory. We take $p_x = s = 0$, $p_y = qR/h$; then we obtain

$$\frac{\partial^4 w}{\partial x^4} + 2\frac{\partial^4 w}{\partial x^2 \partial y^2} + \left(\frac{1}{4} + \frac{3}{4}\lambda\right)\frac{\partial^4 w}{\partial y^4} + \frac{h}{\varphi_c D}\left(p_y \frac{\partial^2 w}{\partial y^2} - \frac{1}{R}\frac{\partial^2 \Phi}{\partial y^2}\right) = 0. \qquad (12.36)$$

$$\frac{1}{\lambda}\frac{\partial^4 \Phi}{\partial x^4} + \left(3 - \frac{1}{\lambda}\right)\frac{\partial^4 \Phi}{\partial x^2 \partial y^2} + \left(\frac{3}{4} + \frac{1}{4\lambda}\right)\frac{\partial^4 \Phi}{\partial y^4} = -\frac{\varphi_c E}{R}\frac{\partial^2 w}{\partial x^2}. \qquad (12.37)$$

We take for w expression

$$w = f \sin\frac{m\pi x}{L}\sin\frac{ny}{R}. \qquad (12.38)$$

From equation of compatibility (37) we find function of stresses in the form

$$\Phi = A_1 \sin\frac{m\pi x}{L}\sin\frac{ny}{R}, \qquad (12.39)$$

where

$$A_1 = E\frac{f}{R}\frac{\varphi_c}{\frac{\varphi_c}{\varphi_x}\left(\frac{m\pi}{L}\right)^4 + \left(3 - \frac{\varphi_c}{\varphi_x}\right)\left(\frac{n}{R}\right)^4 + \left(\frac{3}{4} + \frac{1}{4}\frac{\varphi_c}{\varphi_x}\right)\left(\frac{Ln^2}{m\pi R^2}\right)^2}.$$

Putting (38) and (39) in equation (36), we obtain

$$\hat{q} = \frac{1}{\vartheta}\left[\vartheta^4 + 2\vartheta^2 + \left(\frac{1}{4} + \frac{3}{4}\frac{\varphi_x}{\varphi_c}\right)\right] + \frac{\vartheta^4}{\eta\left[\frac{\varphi_c}{\varphi_x}\vartheta^4 + \left(3 - \frac{\varphi_c}{\varphi_x}\right)\vartheta^2 + \left(\frac{3}{4} + \frac{1}{4}\frac{\varphi_c}{\varphi_x}\right)\right]}; \qquad (12.40)$$

here, as before, we designate

$$\hat{q} = \frac{p_y R}{Eh} = \frac{q}{E}\left(\frac{R}{h}\right)^2; \qquad (12.41)$$

magnitudes ϑ and η are determined by (23). As we have seen from

---

*This solution belongs to Gerard [12.10].

consideration of elastic problem, for shells of average length it is possible to take m = 1, $\beta^2 \ll 1$; then we obtain

$$\frac{\hat{q}}{\varphi_c} = \frac{\eta}{9}\left(\frac{1}{4} + \frac{3}{4}\frac{\varphi_\kappa}{\varphi_c}\right) + \frac{\beta^4}{\eta\left(\frac{3}{4} + \frac{1}{4}\frac{\varphi_c}{\varphi_\kappa}\right)},$$

or

$$\frac{\hat{q}}{\varphi_c} = \frac{\varphi_c + 3\varphi_\kappa}{36\varphi_c}\frac{n^2 h}{R} + \frac{4\varphi_\kappa}{3\varphi_\kappa + \varphi_c}\frac{R}{n^2 h}\left(\frac{\pi R}{nL}\right)^4. \qquad (12.42)$$

Finding minimum with respect to n^2, we have

$$n^4_{\text{кр}} = 3^{1,5}\left(\frac{\varphi_\kappa}{\varphi_c}\right)^{0,5}\frac{4\varphi_c}{\varphi_c + 3\varphi_\kappa}\frac{\pi^2 R^2}{hL^2}.$$

Putting this expression in formula (42), we find upper critical pressure:

$$\frac{\hat{q}_0}{\varphi_c} = \frac{4}{3^{3/4}}\left(\frac{\varphi_c + 3\varphi_\kappa}{4\varphi_c}\right)^{1/2}\left(\frac{\varphi_\kappa}{\varphi_c}\right)^{1/4}\frac{\pi R}{L}\left(\frac{h}{R}\right)^{1/2}. \qquad (12.43)$$

If we take $\varphi_K = \varphi_C = 1$, then we find

$$\hat{q}_0 = \frac{4}{3^{3/4}}\frac{\pi R}{L}\left(\frac{h}{R}\right)^{1/2};$$

we arrive at former formula (11.77) for $\mu = 0.5$. And here with weakly developed plastic deformations there can occur buckling of shell in the large. Therefore, in practical calculations one should use formula (43), introducing then correction factor $\nu \approx 0.7$.

§ 145. Torsion of Closed Shell

Let us consider now case of loading of closed shell on ends by torsional couples* with moment

$$M_\kappa = 2\pi R^2 h s. \qquad (12.44)$$

Equations (13) and (15) take form

$$\frac{D'_c}{h}\left[\frac{\partial^4 w}{\partial x^4} + (1+\lambda)\frac{\partial^4 w}{\partial x^2 \partial y^2} + \frac{\partial^4 w}{\partial y^4}\right] + 2s\frac{\partial^2 w}{\partial x \partial y} - \frac{1}{R}\frac{\partial^2 \Phi}{\partial x^2} = 0. \qquad (12.45)$$

---

*This problem was first investigated by Gerard [12.10].

$$\frac{\partial^4\Phi}{\partial x^4}+\left(\frac{3}{\lambda}-1\right)\frac{\partial^4\Phi}{\partial x^2\partial y^2}+\frac{\partial^4\Phi}{\partial y^4}=-\frac{E_c}{R}\frac{\partial^2 w}{\partial x^2}. \qquad (12.46)$$

By analogy with elastic problem we take for w expression

$$w=f\sin\frac{\pi x}{L}\sin\frac{n}{R}(y+\gamma x), \qquad (12.47)$$

where γ is tangent of angle of inclination of wave to generatrix of cylinder.

Particular integral of equation (46) it is possible to seek in the form

$$\Phi=B_1\cos\frac{n}{R}[y+(\gamma+\delta)x]+B_2\cos\frac{n}{R}[y+(\gamma-\delta)x]; \qquad (12.48)$$

here $\delta = \pi R/nL$. We place expression (48) in (46) and find

$$B_1=-\frac{E_cR(\gamma+\delta)^2 f}{2n^2\left[(\gamma+\delta)^4+\left(\frac{3}{\lambda}-1\right)(\gamma+\delta)^2+1\right]},$$

$$B_2=-\frac{E_cR(\gamma-\delta)^2 f}{2n^2\left[(\gamma-\delta)^4+\left(\frac{3}{\lambda}-1\right)(\gamma-\delta)^2+1\right]}.$$

Further, we put w and Φ from (47) and (48) in equation (45) and equate coefficients in $\cos(n/R)[y+(\gamma+\delta)x]$ and $\cos(n/R)[y+(\gamma-\delta)x]$ to zero; then we obtain two relationships between shearing stress s and parameters of shell:

$$\frac{2s}{E_c}=\frac{n^2}{9}\left(\frac{h}{R}\right)^2\frac{(\gamma+\delta)^4+(1+\lambda)(\gamma+\delta)^2+1}{\gamma+\delta}+$$
$$+\frac{(\gamma+\delta)^2}{n^2\left[(\gamma+\delta)^4+\frac{3-\lambda}{\lambda}(\gamma+\delta)^2+1\right]}. \qquad (12.49)$$

$$\frac{2s}{E_c}=\frac{n^2}{9}\left(\frac{h}{R}\right)^2\frac{(\gamma-\delta)^4+(1+\lambda)(\gamma-\delta)^2+1}{\gamma-\delta}+$$
$$+\frac{(\gamma-\delta)^2}{n^2\left[(\gamma-\delta)^4+\frac{3-\lambda}{\lambda}(\gamma-\delta)^2+1\right]}. \qquad (12.50)$$

We introduce designations

$$\gamma+\delta=\frac{R}{n}\left(\frac{\gamma n}{R}+\frac{n}{L}\right)=\frac{R}{n}m_1=\frac{\nu_1}{n}.\quad \nu_1=Rm_1.\quad \rho_1=\frac{h}{3R}. \qquad (12.51)$$

and give equation (49) form

$$\frac{2s}{E_c} = n^2\rho_1^2 \frac{\left(\frac{\nu_1}{n}\right)^4 + (1+\lambda)\left(\frac{\nu_1}{n}\right)^2 + 1}{\frac{\nu_1}{n}} + \frac{\left(\frac{\nu_1}{n}\right)^2}{n^2\left[\left(\frac{\nu_1}{n}\right)^4 + \frac{3-\lambda}{\lambda}\left(\frac{\nu_1}{n}\right)^2 + 1\right]}.$$

For shells of average length it is possible to disregard ν_1^2 as compared to n^2; then we obtain

$$\frac{2s}{E_c} = \frac{n^2\rho_1^2 + \nu_1^4}{\nu_1 n^3}. \qquad (12.52)$$

Comparison of this result with (11.116) shows that right side of equation is the same as during solution of elastic problem. But in § 134 we arrived at expressions (11.118) and (11.119), determining number

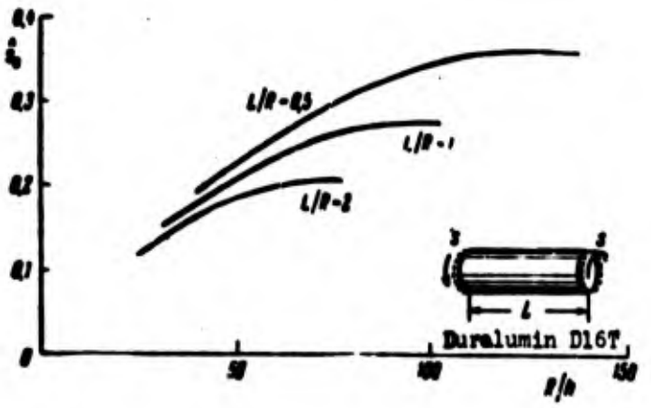

Fig. 12.4. Critical stress of torsion during plastic deformations.

of waves along arc and upper critical stress. Considering in these expressions $\mu = 0.5$ and introducing E_c instead of E, we obtain for our case

$$n = 4.2\,(0.75)^{1/4}\left(\frac{R}{L}\right)^{1/2}\left(\frac{R}{h}\right)^{1/4}. \qquad (12.53)$$

$$s_0 = 0.74\,(0.75)^{-1/4} E_c\left(\frac{R}{L}\right)^{1/2}\left(\frac{h}{R}\right)^{1/4}. \qquad (12.54)$$

Thus, in problem of torsion we arrive directly at calculation by secant modulus, as in certain problems of stability of plates.

Diagrams $\hat{s}_B(R/h)$ for duralumin shells when $L/R = 0.5$, 1 and 2 is presented in Fig. 12.4; here $\hat{s}_B = \hat{s}_B R/Eh$. Considering possibility of buckling of shell in the large, it is recommended in practical calculations to introduce correction factor to magnitude $\hat{s}_B$, equal to $\nu \approx$ ≈ 0.75.

Analogous solution of problem may be given for shells of great length [12.10]; then we arrive at equation, analogous to (11.124):

$$s_0 = 0.272 \cdot 0.75^{-3/4} E_c \left(\frac{h}{R}\right)^{3/4}. \tag{12.55}$$

and here calculation may be conducted by secant modulus.

§ 146. Cylindrical Panel During Axial Compression. Stability in the Small

We investigate case of circular cylindrical panel, secured by hinge on edges and compressed along generatrix. We shall consider first stability of panel in the small with application of deformation theory; then it is necessary to use equations (16) and (17). We take following expression for w:

$$w = f \sin \frac{m\pi x}{a} \sin \frac{n\pi y}{b}. \tag{12.56}$$

Putting (56) in (17), we find

$$\Phi = A_2 \sin \frac{m\pi x}{a} \sin \frac{n\pi y}{b}, \tag{12.57}$$

where

$$A_2 = E \frac{f}{n^2 R} \frac{\varphi_c}{\left(\frac{3}{4} + \frac{1}{4}\frac{\varphi_c}{\varphi_\pi}\right)\left(\frac{m}{a}\right)^4 + \left(3 - \frac{\varphi_c}{\varphi_\pi}\right)\left(\frac{n}{b}\right)^4 + \frac{\varphi_c}{\varphi_\pi}\left(\frac{n^2 a}{mb^2}\right)^2};$$

hence

$$\frac{\partial^2 \Phi}{\partial x^2} = -E \frac{f}{R} \frac{\varphi_c}{\left(\frac{3}{4} + \frac{1}{4}\frac{\varphi_c}{\varphi_\pi}\right) + \left(3 - \frac{\varphi_c}{\varphi_\pi}\right)\left(\frac{an}{bm}\right)^4 + \frac{\varphi_c}{\varphi_\pi}\left(\frac{na}{mb}\right)^4}. \tag{12.58}$$

Using equation (16) and introducing designations

$$\frac{a}{m}=l_x,\quad \frac{b}{n}=l_y,\quad \frac{\varphi_x}{\varphi_c}=\lambda,$$

where l_x and l_y are length of half-waves along sides of panel, we find

$$p=E\varphi_c\left\{\left(\frac{\pi h}{3}\right)^2\left(\frac{1+3\lambda}{4l_x^2}+\frac{2}{l_y^2}+\frac{l_x^2}{l_y^4}\right)+\right.$$
$$\left.+\frac{\lambda}{(\pi R)^2\left[\frac{1+3\lambda}{4l_x^2}+(3\lambda-1)\frac{1}{l_y^2}+\frac{l_x^2}{l_y^4}\right]}\right\}. \qquad (12.59)$$

Study of this expression is significantly simplified if we take in second member $3\lambda - 1 \approx 2$; as it is easy to see, this leads to somewhat minimized value of p. Making such replacement, we find

$$p=E\varphi_c\left(\frac{\pi^2h^2}{9}\nu_1+\frac{\lambda}{\pi^2R^2\nu_1}\right). \qquad (12.60)$$

where

$$\nu_1=\frac{1+3\lambda}{4l_x^2}+\frac{2}{l_y^2}+\frac{l_x^2}{l_y^4}.$$

Considering that for panel of great curvature wave formation is carried out freely, we write condition of minimum of p with respect to ν_1; then for ν_1 we obtain expression

$$\nu_1=\frac{3}{\pi}\sqrt{\frac{\lambda}{Rh}};$$

upper critical stress will be equal to

$$p_*=\frac{2}{3}\sqrt{E_xE_c}\frac{h}{R}. \qquad (12.61)$$

This formula coincides with expression (26), pertaining to closed shell.

In case of <u>panel of small curvature</u> it is necessary to take n = 1; then we obtain expression (59) with replacement of l_y by b. If panel is elongated, then it is necessary to determine minimum value of p_B, varying number of half-waves $m = a/l_x$. For square panel, conditionally

considering m = n = 1, we have

$$p_* = E\varphi_c\left(\frac{h}{b}\right)^2\left[\pi^2\frac{13+3\lambda}{36}+\frac{1}{\pi^2}\left(\frac{b^2}{Rh}\right)^2\frac{4\lambda}{1+15\lambda}\right]. \qquad (12.62)$$

When $R\to\infty$ we arrive at former formula (8.147), pertaining to a plate.

§ 147. Cylindrical Panel During Axial Compression. Stability in the Large

We saw that in case of weakly developed plastic deformations one should approach all problems of given chapter from the point of view of stability in the large. Necessity to consider in such problems simultaneously physical and geometric nonlinearity makes solution exceptionally difficult, primarily from fundamental side. If we talk of deformation theory, then here, when we must investigate large deflections of a shell, the possibility of use of the hypothesis of simple loading becomes especially doubtful. At the same time, application of other theories of plasticity leads to great complication of the problem. Therefore, we conditionally assume that deformation theory may be used, at least, in the first stages of postcritical buckling of a shell. But also then we encounter difficulties, inasmuch as intensity of stresses changes from point to point, both along a specific normal to middle surface, and also for different normals. It is possible to approach research of this field of stresses by double form. One approach consists of solution of problem "head-on," i.e., determination of law of change of intensity of stresses from point to point; during solution of problem according to method of finite differences* we consider definite number of points on normal and along coordinates x and y. The other way, significantly simplifying

*Such method was offered by P. A. Lukashem and V. M. Proskurina for plates; apparently, it may be realized upon the condition of application of digital computers.

solution of problem, is based on assumption that plastic properties of material appear only with respect to fundamental stress in middle surface.* We shall try to use this alternate path for solution of problem of stability in a large shallow cylindrical panel, compressed along generatrix. We shall here consider that physical characteristics of material – secant and tangent moduli – are a function only of average intensity of stresses in middle surface. Obviously, during research of postcritical behavior of shell we must originate from relationships corresponding to theory of shells of large deflection. Therefore, we introduce in equations (16) and (17), describing small deflections of a shell (compressed along generatrix), nonlinear members from equations (11.26) and (11.27). Then we arrive at the following fundamental equations:

$$\frac{D'\eta_c}{h}\left(\frac{1+3\lambda}{4}\frac{\partial^4 w}{\partial x^4}+2\frac{\partial^4 w}{\partial x^2\partial y^2}+\frac{\partial^4 w}{\partial y^4}\right)=L(w,\Phi)+\frac{1}{R}\frac{\partial^2\Phi}{\partial x^2}. \tag{12.63}$$

$$\left(\frac{3}{4}+\frac{1}{4\lambda}\right)\frac{\partial^4\Phi}{\partial x^4}+\left(3-\frac{1}{\lambda}\right)\frac{\partial^4\Phi}{\partial x^2\partial y^2}+\frac{1}{\lambda}\frac{\partial^4\Phi}{\partial y^4}=$$
$$=-E\eta_c\left[\frac{1}{2}L(w,w)+\frac{1}{R}\frac{\partial^2 w}{\partial x^2}\right]. \tag{12.64}$$

Assume for simplicity that panel is square (a = b). We set ourselves the goal of determining equilibrium states of panel when $p \neq p_B$. Considering that shallow panel will bulge in both directions in one half-wave, we take approximating expression for deflection in the form

$$w=f\sin\frac{\pi x}{b}\sin\frac{\pi y}{b}. \tag{12.65}$$

Putting this expression in (64) and integrating, we obtain

---

*This way was shown in first work of Lee and Ades [12.11]. See also [12.12]. Solution given here belongs to A. N. Bozhinskiy.

$$\frac{1}{E_c}\Phi=\left(C_1\cos\frac{2\pi x}{b}+C_2\cos\frac{2\pi y}{b}\right)\frac{f^2}{32}+$$
$$+\frac{C_3}{4}\left(\frac{b}{\pi}\right)^2\frac{f}{R}\sin\frac{\pi x}{b}\sin\frac{\pi y}{b}-\frac{py^2}{2E_c}. \qquad (12.66)$$

where

$$C_1=\frac{4\lambda}{1+3\lambda},\quad C_2=\lambda,\quad C_3=\frac{16\lambda}{1+15\lambda}. \qquad (12.67)$$

Applying, further, Bubnov-Galerkin method for integration of equation (63), we find relationship between load and maximum deflection:

$$\frac{(C_1+C_2)\pi^2}{16}\zeta^2-\frac{4}{3\pi^2}\left(2C_3+\frac{1}{2}C_1\right)k\zeta+$$
$$+\frac{13+3C_2}{36}\pi^2+C_3\frac{k^2}{4\pi^2}-\frac{p^*}{\varphi_c}=0; \qquad (12.68)$$

here are introduced usual parameters

$$p^*=\frac{p}{E}\left(\frac{b}{h}\right)^2,\quad \zeta=\frac{f}{h},\quad k=\frac{b^2}{Rh}.$$

When $\zeta\to 0$ we find upper critical stress by (62). Therefore, (68) can be rewritten in the form

$$p^*=p_B^*+\varphi_c\left[\frac{(C_1+C_2)\pi^2}{16}\zeta^2-\frac{4}{3\pi^2}\left(2C_3+\frac{C_1}{2}\right)k\zeta\right]. \qquad (12.69)$$

Considering $C_i = 1$ ($i = 1, 2, 3$) and $\varphi_c = 1$, we arrive at equation (11.177) pertaining to elastic problem.

Results of calculations by (6.9) in application to duralumin D16T are shown in Fig. 12.5; we take $k = 12$. Curves 1–3 are constructed for different ratios b/h. When $b/h \geq 55$ buckling occurs in elastic region; to this case there corresponds curve 1; let us remember that here we take $\mu = 0.5$. Following curves are built for thicker shells, where $b/h = 40.1$ and 27.4 and pertain to elasto-plastic region. Judging by curves 1–3, in all cases there may be found lower critical stress p_H^*. Ratio p_H^*/p_B^* constitutes in elastic region 59% and for curves 2 and 3 accordingly 74 and 80%. This result is very interesting, since it testifies to gradual smoothing of phenomenon of knock of shell

with development of plastic deformations. Such conclusion will agree with experimental data for closed shells, described in § 143.

Meriting attention is limiting case of flat plate ($k = 0$). In Fig. 12.6 there are constructed by (69) curves $p^*(\zeta)$, characterizing postcritical behavior of plates of different thickness. Curve 1 corresponds to case when critical stress lies within proportional limits and postcritical deformation pertains wholly to elastic region. Curves 3–5 reflect deformation of plate completely in plastic stage for $b/h = 37.5$, 29.5, and 25.2. Curve 2 (for $b/h = 50$) branches off form line 1 at point A, corresponding to limit of proportionality, so that initial stage of deformation of plate is elastic, and the subsequent one is purely plastic. As we see, in case of elastic deformation on curve 1 average stress already for $\zeta = 3$ is more than twice the critical. In plastic region growth of stress above critical value turns out to be significantly smaller, so that <u>supporting power</u> of plate <u>nears the critical load</u>. Thus, during developed plastic deformations chain stresses, appearing during large deflections, do not render essential influence on behavior of plate.

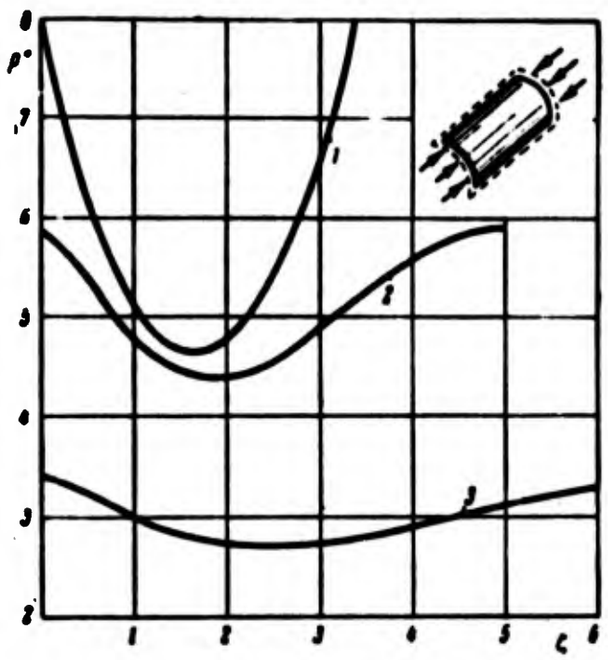

Fig. 12.5. Diagrams "compressive force-deflection" for cylindrical panel depending upon development of plastic deformations.

If by these data we determine reduction factors, then in plastic region they are higher than in elastic. This is natural, since during

developed plastic deformations unevenness of stresses is smoothed. For example in Fig. 12.7 there are given values of reduction factors, pertaining to the same cases as in Fig. 12.6; numeration of curves is maintained. Along the axis of abscissas here are plotted values $n' = \varepsilon/\varepsilon_{кр}$, where ε is deformation of longitudinal fibers near reinforcing ribs, $\varepsilon_{кр}$ is critical deformation; along the axis of ordinates we plot reduction factor φ. It is interesting to compare these data with those which can be obtained by a formula, analogous to Kármán's formula (see [0.3], p. 145). General character of curves $\varphi(n')$ turns out to be in both cases the same; concrete values of φ are somewhat different. Let us note that curve 1 of Fig. 12.7 for elastic region corresponds better to formula of Papkovich, given in Chapter VII.

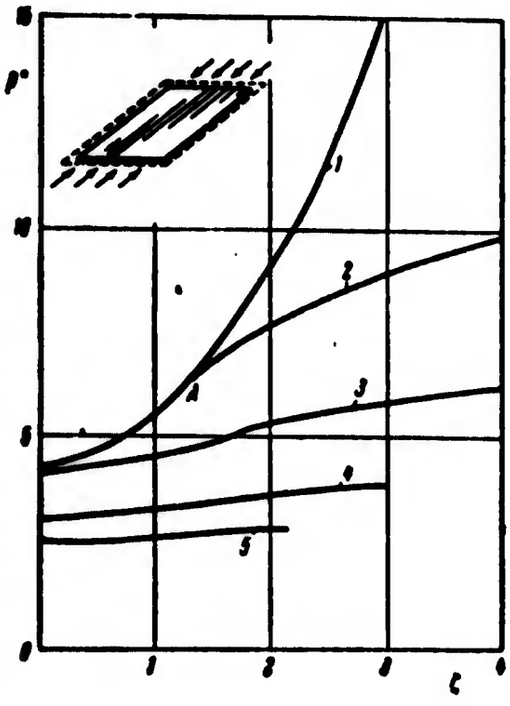

Fig. 12.6. Supporting power of reinforced plate beyond the proportional limit.

An analogous method may be used for research of influence of <u>initial imperfections</u> on behavior of a shell or plate. Initial equations (63)–(64) here obtain form

$$\frac{D'_{\text{red}}}{h}\left(\frac{1+3\lambda}{4}\frac{\partial^4}{\partial x^4}+2\frac{\partial^4}{\partial x^2\partial y^2}+\frac{\partial^4}{\partial y^4}\right)(w-w_0)= =L(w,\Phi)+\frac{1}{R}\frac{\partial^2\Phi}{\partial x^2}. \qquad (12.70)$$

$$\left(\frac{3}{4}+\frac{1}{4\lambda}\right)\frac{\partial^4\Phi}{\partial x^4}+\left(3-\frac{1}{\lambda}\right)\frac{\partial^4\Phi}{\partial x^2\partial y^2}+\frac{1}{\lambda}\frac{\partial^4\Phi}{\partial y^4}= =-E_{\text{red}}\left[\frac{1}{2}L(w,w)-\frac{1}{2}L(w_0,w_0)+\frac{1}{R}\frac{\partial^2 w}{\partial x^2}\right]; \qquad (12.71)$$

by w and w_0 here are implied, as usually, total and initial deflections. Proceeding the same way as before, we arrive at results depicted in Fig. 12.8; here we take k = 12, b/h = 27.4; parameter of initial maximum deflection constitutes $\zeta_0 = f_0/h = 0$; 0.05; 0.1 and 0.25. As we see, initial imperfections render in plastic region significantly smaller influence on behavior of shell than in elastic.

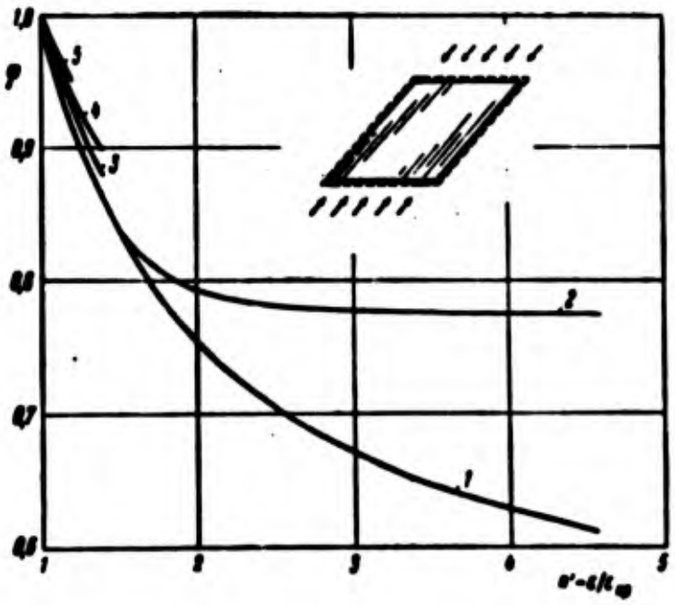

Fig. 12.7. Reduction factors for compressed plate with plastic deformations.

We applied here approximate method, rejecting detailed research of plastic properties of material at different points and concentrating attention on change of plastic properties depending upon basic compressive stress. Apparently, this method allows us to arrive at practically valuable qualitative conclusions.

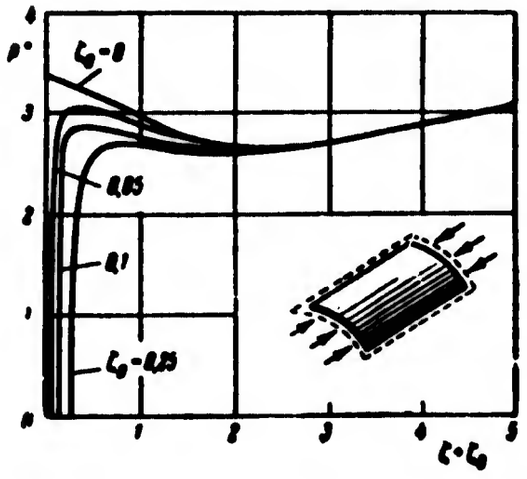

Fig. 12.8. Influence of initial deflection on supporting power of compressed cylindrical panel.

In definitized research one should originate from more general equations, describing large deflections of shell during plastic deformations.* Integration of these equations can be conducted according to method of finite differences, which was discussed above (p.385), or with help of method of successive approximations, proceeding from solution of elastic problem.**

*Such equations for plates were composed by Yu. R. Lepik [12.7].

**Similar research of postcritical deformation of compressed plates was carried out by N. F. Yershov (see collection "Theory of plates and shells," Kiev, 1962, 344-346).

Literature

12.1. A. N. Bozhinskiy and A. S. Vol'mir. Experimental investigation of stability of cylindrical shells beyond the elastic limit, DAN SSSR, 142, No. 2 (1962).

12.2. V. G. Zubchaninov. Axisymmetric inelastic form of loss of stability of a circular cylindrical shell, News of Acad. of Sci. of USSR, mech. and math., No. 5 (1961), 131-132.

12.3. N. S. Ganiyev. Determining critical inelastic load of cylindrical shell during axial compression and external normal pressure, News of Kazan' branch of Academy of Sciences of USSR, series on physical mathematics and technical sciences, 7 (1955).

12.4. E. I. Grigolyuk. On inelastic buckling of thin shells, News of Acad. of Sci. of USSR, OTN, No. 10 (1957), 3-11; Pure plastic loss of stability of thin shells, Applied math. and mech., 21, No. 7 (1957); Calculation of compressibility of material in determination of lower critical loads, News of Acad. of Sci. of USSR, OTN, No. 5 (1958); Tangent modular load of circular cylindrical shells during combined load, Herald of Moscow State University, No. 1 (1958).

12.5. L. M. Kachanov. Concerning the question of stability of elasto-plastic equilibrium, Herald of Leningrad State University, 19, math, mech. and astron. series, No. 4 (1956).

12.6. V. D. Klyushnikov. Stability of plates beyond elastic limit, News of Acad. of Sci. of USSR, OTN, No. 7 (1957).

12.7. Yu. R. Lepik. One possibility of solution of problem of stability of elasto-plastic plates in exact formulation, News of Acad. of Sci. of USSR, OTN, No. 8 (1957); Equilibrium of elasto-plastic plates during large deflections, Eng. collection, 24 (1956), 37-62.

12.8. A. V. Sachenkov. On plastic stability of shells, News of Kazan' branch of Academy of Sciences of USSR, 10 (1956), 81-100.

12.9. L. A. Tolokonnikov. On influence of compressibility of the material on elasto-plastic stability of plates and shells, Herald of Moscow State University, No. 6 (1949), 35-44.

12.10. G. Gerard. Plastic stability theory of thin shells, J. Aeron. Sci. 24, No. 4 (1957), 264-279; J. Aerospace Sci., 29, No. 10 (1962).

12.11. L. Lee and C. Ades. Plastic torsional buckling strength of cylinders including the effects of imperfections, J. Aeron. Sci. 24, No. 4 (1957).

12.12. L. Lee. Inelastic buckling of initially imperfect cylindrical shells subject to axial compression, J. Aerospace Sci. 29, No. 1 (1962), 87-96.

12.13. S. Radhakrishnan. Plastic buckling of circular cylinders, J. Aeron. Sci. 23, No. 9 (1956), 822-894.

C H A P T E R XIII

CONICAL SHELLS

§ 148. Initial Relationships of Linear Theory

Circular conical shell enter in construction of jet engines, aircraft, reservoirs, etc. Solution of problem of stability of conical shells is significantly more difficult than in case of cylindrical shells, since structure of initial equations is more complicated.

We shall give fundamental equations of linear theory of conical shells. We determine first the coefficients of first and second quadratic forms of undeformed middle surface of shell. We locate axis of coordinates as shown in Fig. 13.1a. Let us assume that origin of coordinates coincides with vertex of cone. We determine position of point K of middle surface by radius-vector **r**, passed from vertex of cone O and angle θ between axial plane passing through considered point and a certain fixed axial plane.

Length of vector **r** we designate by s, and angle of inclination of generatrix to base, by α. Projections of **r** on axis of coordinates are equal to

$$x = s\sin\alpha, \quad y = s\cos\alpha\cos\theta, \quad z = s\cos\alpha\sin\theta. \tag{13.1}$$

Vector **r** can be expanded in unit vectors **i**, **j**, and **k**:

$$r = s(i\sin\alpha + j\cos\alpha\cos\theta + k\cos\alpha\sin\theta). \tag{13.2}$$

Magnitudes s and θ we consider as curvilinear coordinates on middle surface $\xi = s$, $\eta = \theta$.

Coefficients of first quadratic form $a_{11} = A_1^2$ and $a_{22} = A_2^2$ will be determined by formulas (10.4):

$$A_1^2 = \left(\frac{\partial r}{\partial s}\right)^2, \quad A_2^2 = \left(\frac{\partial r}{\partial \theta}\right)^2. \tag{13.3}$$

Hence

$$A_1 = 1, \quad A_2 = s\cos\alpha. \tag{13.4}$$

Further we calculate deformation of middle surface and parameters of change of curvatures, considering that radii of curvature of middle surface R_1 and R_2 are equal (see Fig. 13.1b) to

$$R_1 = \infty, \quad R_2 = \frac{s}{\operatorname{tg}\alpha}. \tag{13.5}$$

Elongations and shear in middle surface by formulas (10.52) taking into account (4) and (5) turn out equal to

$$\left.\begin{aligned} \varepsilon_1 &= \frac{\partial u}{\partial s}, \\ \varepsilon_2 &= \frac{1}{s\cos\alpha}\frac{\partial v}{\partial \theta} + \frac{w}{s} - \frac{w\operatorname{tg}\alpha}{s}, \\ \gamma &= \frac{1}{s\cos\alpha}\frac{\partial u}{\partial \theta} + \frac{\partial v}{\partial s} - \frac{v}{s}. \end{aligned}\right\} \tag{13.6}$$

Here u, v, and w are displacements of points of middle surface correspondingly in direction of generatrix, along parallel circle (on circumference, obtained during intersection of middle surface with plane, perpendicular to axis of shell) and on internal normal to surface.

Changes of curvatures and torsion we determine by formulas (10.53):

$$\left.\begin{aligned} \varkappa_1 &= -\frac{\partial^2 w}{\partial s^2}, \\ \varkappa_2 &= -\frac{1}{s^2\cos^2\alpha}\frac{\partial^2 w}{\partial\theta^2} - \frac{\operatorname{tg}\alpha}{s^2\cos\alpha}\frac{\partial v}{\partial\theta} - \frac{1}{s}\frac{\partial w}{\partial s}, \\ \chi &= -\frac{1}{2}\left(\frac{\operatorname{tg}\alpha}{s}\frac{\partial v}{\partial s} - \frac{2\operatorname{tg}\alpha}{s^2}v + \frac{2}{s\cos\alpha}\frac{\partial^2 w}{\partial s\,\partial\theta} - \frac{2}{s^2\cos\alpha}\frac{\partial w}{\partial\theta}\right). \end{aligned}\right\} \qquad (13.7)$$

In simplified variant of solution we disregard in expressions

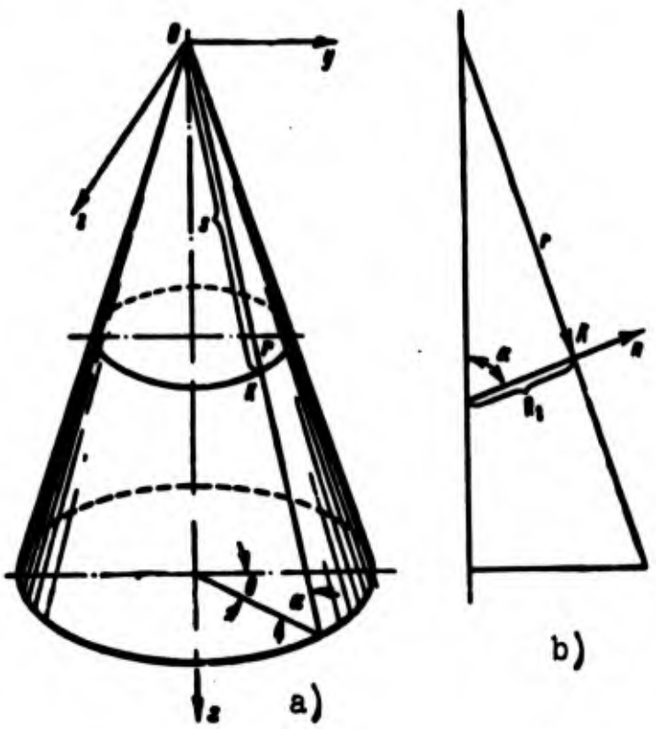

Fig. 13.1. System of coordinates for examining conical shells.

for $\varkappa_2$ and χ members depending on displacement v; then we obtain approximately

$$\left.\begin{aligned} \varkappa_2 &= -\frac{1}{s^2\cos^2\alpha}\frac{\partial^2 w}{\partial\theta^2} - \frac{1}{s}\frac{\partial w}{\partial s}, \\ \chi &= -\frac{1}{s\cos\alpha}\frac{\partial^2 w}{\partial s\,\partial\theta} + \frac{1}{s^2\cos\alpha}\frac{\partial w}{\partial\theta}. \end{aligned}\right\} \qquad (13.8)$$

In § 123 it was shown that equation of equilibrium of a member of a shell and equation of compatibility of deformations during momentless fundamental state (fundamental is state of shell before loss of

stability) can be reduced to system of following simplified equations (10.83) and (10.86):

$$\left.\begin{aligned} D\nabla^4 w - \nabla_k^2 \varphi - q = 0. \\ \nabla^4 \varphi + E\Delta\nabla_k^2 w = 0. \end{aligned}\right\} \qquad (13.9)$$

Under q is implied hypothetical lateral load, equal from (10.89) to

$$q = N_1 \varkappa_1 + N_2 \varkappa_2 + T_{12}\chi; \qquad (13.10)$$

here N_1, N_2, and T_{12} are linear normal and tangential forces in the fundamental state (see Fig. 13.2), φ is function of forces.

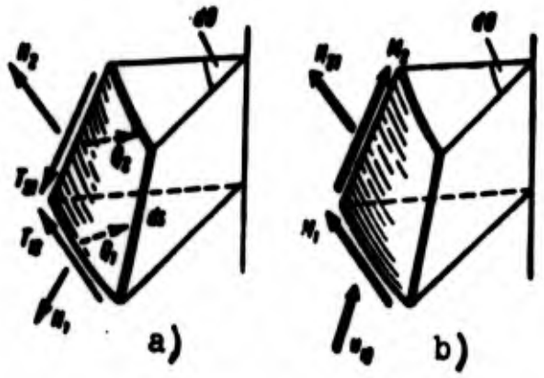

Fig. 13.2. Forces acting on member of shell.

Substituting in (13.10) expressions (13.7) and (13.8) for $\varkappa_1$ and $\varkappa_2$ when $T_{12} = 0$, we obtain

$$q = -N_1 \frac{\partial^2 w}{\partial s^2} - N_2\left(\frac{1}{s\cos\alpha}\frac{\partial^2 w}{\partial\theta^2} + \frac{1}{s}\frac{\partial w}{\partial s}\right). \qquad (13.10a)$$

Operators ∇^2 and ∇_k^2 we find by formulas (10.81) and (10.84):

$$\nabla^2 = \frac{1}{s\cos\alpha}\left[\frac{\partial}{\partial s}\left(s\cos\alpha\frac{\partial}{\partial s}\right) + \frac{\partial}{\partial\theta}\left(\frac{1}{s\cos\alpha}\frac{\partial}{\partial\theta}\right)\right].$$

$$\nabla_k^2 = \frac{\operatorname{tg}\alpha}{s}\frac{\partial^2}{\partial s^2};$$

hence

$$\nabla^2 w = \frac{\partial^2 w}{\partial s^2} + \frac{1}{s}\frac{\partial w}{\partial s} + \frac{1}{s^2\cos^2\alpha}\frac{\partial^2 w}{\partial\theta^2}, \qquad (13.11)$$

$$\nabla_k^2 \varphi = \frac{\operatorname{tg}\alpha}{s}\frac{\partial^2 \varphi}{\partial s^2}. \qquad (13.12)$$

Further we find

$$\nabla^4 w = \nabla^2\left(\frac{\partial^2 w}{\partial s^2} + \frac{1}{s}\frac{\partial w}{\partial s} + \frac{1}{s^2\cos^2\alpha}\frac{\partial^2 w}{\partial\theta^2}\right) =$$

$$= \frac{1}{s\cos\alpha}\left\{\frac{\partial}{\partial s}\left[s\cos\alpha\frac{\partial}{\partial s}\left(\frac{\partial^2 w}{\partial s^2} + \frac{1}{s}\frac{\partial w}{\partial s} + \frac{1}{s^2\cos^2\alpha}\frac{\partial^2 w}{\partial\theta^2}\right)\right] + \right.$$

$$\left. + \frac{\partial}{\partial\theta}\left[\frac{1}{s\cos\alpha}\frac{\partial}{\partial\theta}\left(\frac{\partial^2 w}{\partial s^2} + \frac{1}{s}\frac{\partial w}{\partial s} + \frac{1}{s^2\cos^2\alpha}\frac{\partial^2 w}{\partial\theta}\right)\right]\right\}.$$

or

$$\nabla^4 w = \frac{\partial^4 w}{\partial s^4} + \frac{2}{s}\frac{\partial^3 w}{\partial s^3} - \frac{1}{s^2}\frac{\partial^2 w}{\partial s^2} + \frac{1}{s}\frac{\partial w}{\partial s} + \\ + \frac{2}{s^2\cos^2\alpha}\frac{\partial^4 w}{\partial s^2 \partial\theta^2} - \frac{2}{s^3\cos^2\alpha}\frac{\partial^3 w}{\partial s\,\partial\theta^2} + \\ + \frac{4}{s^4\cos^2\alpha}\frac{\partial^2 w}{\partial\theta^2} + \frac{1}{s^4\cos^4\alpha}\frac{\partial^4 w}{\partial\theta^4}. \tag{13.13}$$

Putting expressions (12) and (13) in equations (9), we arrive at following final equations of linear theory:

$$-D\left(\frac{\partial^4 w}{\partial s^4} + \frac{2}{s^2\cos^2\alpha}\frac{\partial^4 w}{\partial s^2\partial\theta^2} + \frac{1}{s^4\cos^4\alpha}\frac{\partial^4 w}{\partial\theta^4} - \right. \\ - \frac{2}{s^3\cos^2\alpha}\frac{\partial^3 w}{\partial s\,\partial\theta^2} + \frac{4}{s^4\cos^2\alpha}\frac{\partial^2 w}{\partial\theta^2} + \\ \left. + \frac{2}{s}\frac{\partial^3 w}{\partial s^3} - \frac{1}{s^2}\frac{\partial^2 w}{\partial s^2} + \frac{1}{s^3}\frac{\partial w}{\partial s}\right) + \frac{\operatorname{tg}\alpha}{s}\frac{\partial^2\varphi}{\partial s^2} + \\ + N_1\frac{\partial^2 w}{\partial s^2} + N_2\left(\frac{1}{s^2\cos^2\alpha}\frac{\partial^2 w}{\partial\theta^2} + \frac{1}{s}\frac{\partial w}{\partial s}\right) = 0. \tag{13.14}$$

$$\frac{\partial^4\varphi}{\partial s^4} + \frac{2}{s^2\cos^2\alpha}\frac{\partial^4\varphi}{\partial s^2\partial\theta^2} + \frac{1}{s^4\cos^4\alpha}\frac{\partial^4\varphi}{\partial\theta^4} - \\ - \frac{2}{s^3\cos^2\alpha}\frac{\partial^3\varphi}{\partial s\,\partial\theta^2} + \frac{4}{s^4\cos^2\alpha}\frac{\partial^2\varphi}{\partial\theta^2} + \frac{2}{s}\frac{\partial^3\varphi}{\partial s^3} - \\ - \frac{1}{s^2}\frac{\partial^2\varphi}{\partial s^2} + \frac{1}{s^3}\frac{\partial\varphi}{\partial s} + Eh\frac{\operatorname{tg}\alpha}{s}\frac{\partial^2 w}{\partial s^2} = 0. \tag{13.15}$$

We shall use these equations for solution of particular problems.

§ 149. Axial Compression of Conical Shell

Let us consider first of all problem of stability in the small of circular conical truncated shell, compressed along axis. By analogy with solution of problem for cylindrical shell we assume at first that buckling of shell is axisymmetric. Then we have $w = w(s)$, $\varphi = \varphi(s)$ and equations (14) and (15) will be reduced to form

$$-D\left(\frac{d^4 w}{ds^4} + \frac{2}{s}\frac{d^3 w}{ds^3} - \frac{1}{s^2}\frac{d^2 w}{ds^2} + \frac{1}{s^3}\frac{dw}{ds}\right) + \\ + N_1\frac{d^2 w}{ds^2} + \frac{\operatorname{tg}\alpha}{s}\frac{d^2\varphi}{ds^2} = 0. \tag{13.16}$$

$$\frac{d^3\varphi}{ds^3}+\frac{2}{s}\frac{d^2\varphi}{ds^2}-\frac{1}{s^2}\frac{d\varphi}{ds}+\frac{1}{s^2}\frac{d\varphi}{ds}+Eh\frac{\operatorname{tg}\alpha}{s}\frac{d^2w}{ds^2}=0 \qquad (13.17)$$

or, in more compact form,

$$-Ds^{-1}\frac{d}{ds}\left\{s\frac{d}{ds}\left[s^{-1}\frac{d}{ds}\left(s\frac{dw}{ds}\right)\right]\right\}+\frac{\operatorname{tg}\alpha}{s}\frac{d^2\varphi}{ds^2}+N_1\frac{d^2w}{ds^2}=0. \qquad (13.18)$$

$$s^{-1}\frac{d}{ds}\left\{s\frac{d}{ds}\left[s^{-1}\frac{d}{ds}\left(s\frac{d\varphi}{ds}\right)\right]\right\}+Eh\frac{\operatorname{tg}\alpha}{s}\frac{d^2w}{ds^2}=0. \qquad (13.19)$$

We consider that during loss of stability there will be formed a large number of waves; length of each wave will be small, and therefore, magnitudes within one wave it is possible to consider constant.* Let us consider wave, adjoining major base of cone. Putting $s = l_1$, where l_1 is distance on generatrix from vertex to major base, and $N_1 = -N_1^0$, where N_1^0 is compressive force on circumference of major base, according to (18) and (19), we shall obtain

$$\left.\begin{aligned}-D\frac{d^4w}{ds^4}-N_1^0\frac{d^2w}{ds^2}+\frac{\operatorname{tg}\alpha}{l_1}\frac{d^2\varphi}{ds^2}=0.\\ \frac{d^2\varphi}{ds^2}+Eh\frac{\operatorname{tg}\alpha}{l_1}\frac{d^2w}{ds^2}=0.\end{aligned}\right| \qquad (13.20)$$

We seek solution for equations (20) in form

$$\left.\begin{aligned}w=A\sin\frac{\pi}{\lambda}(s-l_1).\\ \varphi=B\sin\frac{\pi}{\lambda}(s-l_1).\end{aligned}\right| \qquad (13.21)$$

where λ is wave length. Putting (21) in (20) we obtain

$$\left.\begin{aligned}A\left[D\left(\frac{\pi}{\lambda}\right)^4-N_1\left(\frac{\pi}{\lambda}\right)^2\right]+B\frac{\operatorname{tg}\alpha}{l_1}\left(\frac{\pi}{\lambda}\right)^2=0.\\ -AEh\frac{\operatorname{tg}\alpha}{l_1}\left(\frac{\pi}{\lambda}\right)^2+B\left(\frac{\pi}{\lambda}\right)^4=0.\end{aligned}\right| \qquad (13.22)$$

Equating to zero the determinant of system (22) and introducing designation $\pi/\lambda = \beta$, we find

$$N_1^0=D\beta^2+\frac{Eh}{\beta^2}\frac{\operatorname{tg}^2\alpha}{l_1^2}. \qquad (13.23)$$

---

*Such assumption was made by I. Ya. Shtayerman [13.11]; formula (25) is his.

Minimizing N_1^0 with respect to β^2, we determine magnitude β^2:

$$\beta^2 = \sqrt{\frac{Eh}{D}\frac{\operatorname{tg}^2\alpha}{l_1^2}}. \tag{13.24}$$

Putting this value in (23), we arrive at following value of upper critical force:

$$N_{k.0} = \frac{Eh^2\operatorname{tg}\alpha}{l_1\sqrt{3(1-\mu^2)}}. \tag{13.25}$$

When $\mu = 0.3$, we obtain

$$N_{k.0} = 0.605\frac{Eh^2}{l_1}\operatorname{tg}\alpha = 0.605\frac{Eh^2}{R_0}, \tag{13.26}$$

where R_0 is radius of curvature of middle surface for major base.

Investigating, then, case when buckling of shell is not axisymmetric, we take

$$w = w_1\cos n\theta, \quad \varphi = \varphi_1\cos n\theta, \tag{13.27}$$

where $w_1 = w_1(s)$, $\varphi_1 = \varphi_1(s)$, n are number of waves on parallel circle.

Putting (27) in (14) and (15) and introducing designation $n = n_1\cos\alpha$, we obtain

$$-D\left[\frac{d^4w_1}{ds^4} + \frac{2}{s}\frac{d^3w_1}{ds^3} - \frac{1+2n_1^2}{s^2}\frac{d^2w_1}{ds^2} + \frac{1+2n_1^2}{s^3}\frac{dw_1}{ds} - \right.$$
$$\left. - \frac{n_1^2(4-n_1^2)}{s^4}w_1 + N_1\frac{d^2w_1}{ds^2} + \frac{\operatorname{tg}\alpha}{s}\frac{d^2\varphi_1}{ds^2}\right] = 0. \tag{13.28}$$

$$\frac{d^4\varphi_1}{ds^4} + \frac{2}{s}\frac{d^3\varphi_1}{ds^3} - \frac{1+2n_1^2}{s^2}\frac{d^2\varphi_1}{ds^2} +$$
$$+ \frac{1+2n_1^2}{s^3}\frac{d\varphi_1}{ds} - \frac{n_1^2(4-n_1^2)}{s^4}\varphi_1 + Eh\frac{\operatorname{tg}\alpha}{s}\frac{d^2w_1}{ds^2} = 0. \tag{13.29}$$

It is easy to see that equations (28) and (29) can be rewritten in the form [13.10]

$$-Ds^{n_1-1}\left[s^{1-2n_1}\frac{d}{ds}\left\{s^{2n_1-1}\frac{d}{ds}\left[s^{1-2n_1}\frac{d}{ds}(s^{n_1}w_1)\right]\right\}\right]+$$
$$+N_1\frac{d^2w_1}{ds^2}+\frac{\operatorname{tg}\alpha}{s}\frac{d^2\varphi_1}{ds^2}=0. \qquad (13.30)$$

$$s^{n_1-1}\frac{d}{ds}\left[s^{1-2n_1}\frac{d}{ds}\left\{s^{2n_1-1}\frac{d}{ds}\left[s^{2n_1-1}\frac{d}{ds}(s^{n_1}\varphi_1)\right]\right\}\right]+$$
$$+Eh\frac{\operatorname{tg}\alpha}{s}\frac{d^2w_1}{ds^2}=0. \qquad (13.31)$$

Replacing in (30) and (31), as in preceding derivation, s by l_1 and N_1 by N_1^0, we arrive at former expression (26) for upper critical force. It is the same as in case of axial compression of cylindrical shell of radius R_0.

As experiments show, real conical shells, compressed along axis, bulge in a knock in rhombic form with formation of two or several strips of bulges in major base. Therefore, here we should take the same approach to problem as in case of cylindrical shell, with consideration of stability in the large. Complete solution of nonlinear problem for compressed conical shell in literature is still absent. We assume therefore, with sufficiently great confidence, that lower critical pressure may be defined by analogy with that taken for cylindrical shell* by the formula

$$N_{l.s}=0.18E\frac{h^2}{R_0}. \qquad (13.32)$$

Formulas (26) and (32) are useful for practical calculations; here it is necessary to consider indications made in § 129 with respect to cylindrical shells. Values of total axial compressive force are here equal to

$$\left.\begin{aligned} P_s&=0.605E\frac{h^2}{R_0}\pi l_1\sin 2\alpha,\\ P_s&=0.18E\frac{h^2}{R_0}\pi l_1\sin 2\alpha=0.18Eh^2\pi\operatorname{tg}\alpha\sin 2\alpha;\end{aligned}\right\} \qquad (13.33)$$

*Validity of such analogy is supported also by theoretical considerations (see [13.9]).

here we take into account relationship $R_0 = l_1/\tan\alpha$.

Formula (26) is valid on the condition that number of waves along generatrix is sufficiently great. Following I. Ya. Shtayerman [13.11], we shall consider that this condition is satisfied if shell is sufficiently steep (angle $\alpha \geq 30^\circ$).

It is desirable so that problem of stability of conical shell during axial compression be developed in more detail, taking into account influence of angle of rise α on character of wave formation. Furthermore, it is interesting to extend to conical shell geometric approach to problem, illuminated in § 131.

Example 13.1. Conical diaphragm of center support (bottom) of air-breathing jet engine, made of steel, is loaded by axial force P = 2500 kg (Fig. 13.3). Check of diaphragm for stability.

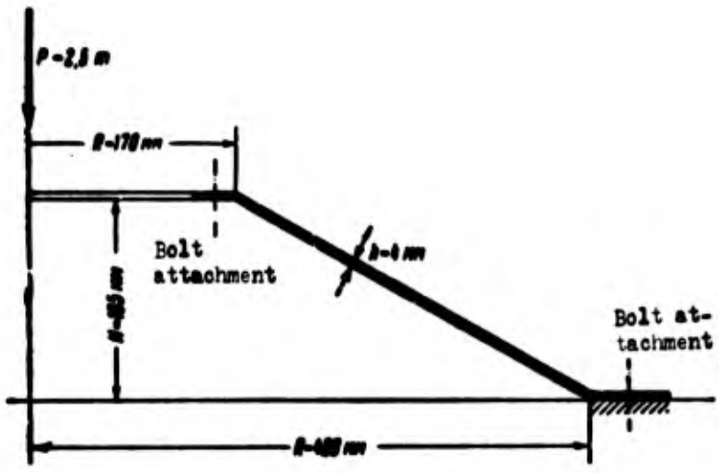

Fig. 13.3. Diaphragm of air-breathing jet engine.

We find $\tan\alpha = \frac{2 \cdot 165}{620} = 0.533$ and $\alpha \approx 28^\circ$. Length of generatrix is equal to $l_1 = \frac{480}{\cos 28^\circ} = 543$ mm, radius of curvature for major base is $R_0 = \frac{543}{0.553} = 980$ mm.

By formula (32) the value of lower critical compressive force will be

$$N_{1,\,\text{в}} = 0{,}18E\frac{h^2}{R_0} = 0{,}18 \cdot 2 \cdot 10^6 \frac{0{,}4^2}{98} = 586 \text{ kg/cm}.$$

Total axial critical force according to (33) is equal to

$$P_{\text{в}} = 0{,}18Eh^2\pi \operatorname{tg}\alpha \sin 2\alpha = 0{,}18 \cdot 2 \cdot 10^6 \cdot 0{,}4^2 \cdot \pi\, 0{,}533 \cdot 0{,}829 = 8 \cdot 10^4 \text{ kg}$$

Critical stress for upper base

$$\sigma_{1,\,\text{в}} = \frac{80\,000}{\pi \cdot 34 \cdot 0{,}4 \cdot \sin 28^\circ} = 4000 \text{ kg/cm}^2.$$

Critical stress does not exceed limit of proportionality. Magnitude P_H turned out to be many times larger than magnitude of given axial force P.

§ 150. Case of External Pressure

In constructions of jet engines, storage tanks, etc., conical shells are subjected to external pressure. Let us turn to consideration of this case, where at first we shall consider shell, closed at top. Preliminarily we simplify initial equations, following N. A. Alumyae [13.1]. We present functions w and φ in the form

$$\left.\begin{aligned} w &= \psi(s) \operatorname{tg}\alpha \cos n\theta, \\ \varphi &= \chi_1(s)\varepsilon^2 Ehl_1 \operatorname{tg}^2\alpha \cos n\theta. \end{aligned}\right\} \qquad (13.34)$$

Here n is number of waves, formed on parallel circumference during loss of stability; by ε is understood magnitude

$$\varepsilon = \sqrt{\frac{\operatorname{ctg}\alpha}{\sqrt{12(1-\mu)^2}}\frac{h}{l_1}}, \qquad (13.35)$$

where l_1 is length of generatrix from top to major base.

Such substitution allows us to isolate in resolvents small members, which can be ignored. Forces of subcritical stress during uniform external pressure q are expressed as follows:

$$N_1 = -\frac{q}{2\operatorname{tg}\alpha}s, \quad N_2 = -\frac{q}{\operatorname{tg}\alpha}s. \qquad (13.36)$$

We introduce dimensionless parameters

$$\nu = \frac{q_1^4}{s^3 E h} \operatorname{ctg}^2 \alpha, \quad p = \frac{\omega^2}{\cos^2 \alpha} \tag{13.37}$$

and dimensionless coordinate

$$x = \frac{s}{l_1}. \tag{13.38}$$

Then expression (36) will take form

$$\left.\begin{aligned} N_1 &= -\frac{x}{2} \nu^2 E h \operatorname{tg}^2 \alpha, \\ N_2 &= -x \nu^2 E h \operatorname{tg}^2 \alpha. \end{aligned}\right\} \tag{13.39}$$

If we consider equalities (34) and (37)–(39), equations (14) and (15) can be given such form:

$$\begin{aligned} &\frac{d^4 \chi_1}{dx^4} + p \psi - \frac{p^2}{x^2} \psi - \varepsilon \left\{ \frac{2p}{x} \left(-\frac{d^3 \psi}{dx^3} - \frac{1}{x} \frac{d^2 \psi}{dx^2} - \frac{2}{x^2} \psi \right) + \right. \\ &\qquad \left. + \nu \left[\left(2 - \frac{x^2}{2} \right) \frac{d^3 \psi}{dx^3} + x \frac{d^2 \psi}{dx^2} \right] \right\} - \\ &\quad - \varepsilon^2 \left(x \frac{d^3 \psi}{dx^3} + 2 \frac{d^2 \psi}{dx^2} - \frac{1}{x} \frac{d^2 \psi}{dx^2} + \frac{1}{x^2} \frac{d \psi}{dx} \right) = 0. \end{aligned} \tag{13.40}$$

$$\begin{aligned} &\frac{d^2 \psi}{dx^2} + \frac{p^2}{x^2} \chi_1 - \varepsilon \frac{2p}{x} \left(\frac{d^2 \chi_1}{dx^2} - \frac{1}{x} \frac{d \chi_1}{dx} + \frac{2 \chi_1}{x^2} \right) + \\ &\quad + \varepsilon^2 \left(x \frac{d^3 \chi_1}{dx^3} + 2 \frac{d^2 \chi_1}{dx^2} - \frac{1}{x} \frac{d^2 \chi_1}{dx^2} + \frac{1}{x^2} \frac{d \chi_1}{dx} \right) = 0. \end{aligned} \tag{13.41}$$

Magnitude ε is small as compared to unity, if only angle α is not close to zero; magnitude p becomes large as compared to unity, if angle α is close to $\pi/2$. If angle α is close neither to zero nor to $\pi/2$, in equations (40) and (41) it is possible to disregard members containing ε and ε^2. Doing this, we obtain

$$\frac{d^4 \chi_1}{dx^4} - \frac{p^2}{x^2} \psi + p \psi = 0. \tag{13.42}$$

$$\frac{d^2 \psi}{dx^2} + \frac{p^2}{x^2} \chi_1 = 0. \tag{13.43}$$

Excluding from these equations function χ_1, we arrive at following resolving equation:

$$\frac{d^2}{dx^2} \left(x^2 \frac{d^2 \psi}{dx^2} \right) + \left(\frac{p^2}{x^2} - p^2 \nu \right) \psi = 0. \tag{13.44}$$

We take this simplified equation as the initial one. During solution of problem we use first the Bubnov-Galerkin method.

For case of hinge-supported shell we are given function ψ in such a form:

$$\psi = Ax^3(1+ax)\sin \pi x, \tag{13.45}$$

where

$$a = -\frac{6+\mu}{8+\mu}. \tag{13.46}$$

For $\mu = 0.3$ we have $a = -0.759$. Function (45) satisfies conditions of hinged support $\psi(1) = 0$ and $\left(\frac{dM_1}{dx}\right)_{x=1} = 0$ (moment M_1 is shown in Fig. 13.2b).

Equation of Bubnov-Galerkin method, corresponding to (44), we write in the form

$$\int_0^1 \frac{d^2}{dx^2}\left(x^3\frac{d^2\psi}{dx^2}\right)\psi\,dx + p^2\int_0^1 \frac{\psi^2}{x^3}\,dx - p^2\nu\int_0^1 \psi^2\,dx = 0. \tag{13.47}$$

Using formula of partial integration, we find

$$\int_0^1 \frac{d^2}{dx^2}\left(x^3\frac{d^2\psi}{dx^2}\right)\psi\,dx = \frac{d}{dx}\left(x^3\frac{d^2\psi}{dx^2}\right)\psi\Big|_0^1 - \int_0^1 \frac{d}{dx}\left(x^3\frac{d^2\psi}{dx^2}\right)\frac{d\psi}{dx}\,dx =$$

$$= -x^3\frac{d^2\psi}{dx^2}\frac{d\psi}{dx}\Big|_0^1 + \int_0^1 x^3\left(\frac{d^2\psi}{dx^2}\right)^2 dx; \tag{13.48}$$

then from (47) we obtain

$$\nu = \frac{\frac{1}{p^2}\left[-x^3\frac{d^2\psi}{dx^2}\frac{d\psi}{dx}\Big|_0^1 + \int_0^1 x^3\left(\frac{d^2\psi}{dx^2}\right)^2 dx + p^2\int_0^1 \frac{\psi^2}{x^3}\,dx\right]}{\int_0^1 \psi^2\,dx}. \tag{13.49}$$

If shell was rigidly clamped on its edge, then boundary condition would have form $\left(\frac{d\psi}{dx}\right)_{x=1} = 0$ and we would arrive at formula*

---

*This formula was obtained by N. A. Alymyae.

$$\nu=\frac{\frac{1}{p^2}\int_0^1 x^3\left(\frac{d^2\psi}{dx^2}\right)^2 dx+p\int_0^1 \frac{\psi^2}{x^3}dx}{\int_0^1 \psi^2 dx}. \qquad (13.50)$$

Putting expression (45) in (49) and determining magnitude p from condition of minimum of ν, we find $\nu_{min} = 20.4$. Using formulas (35), (36) and (39), we obtain following value of upper critical pressure:

$$q_0=3.15E\left(\frac{h}{l_1}\right)^3 \operatorname{tg}\alpha\sqrt{\frac{h}{l_1}\frac{\operatorname{tg}\alpha}{\sqrt{(1-\mu^2)^3}}}=$$
$$=3.15E\left(\frac{h}{l_1}\right)^{7/4}(\operatorname{tg}\alpha)^{3/4}\frac{1}{(1-\mu^2)^{3/4}}. \qquad (13.51)$$

We solve this problem by method of finite differences.* We rewrite equation (44) in the form

$$x^6\frac{d^4\psi}{dx^4}+6x^5\frac{d^3\psi}{dx^3}+6x^4\frac{d^2\psi}{dx^2}+(p^4-p^3\nu x^3)\psi=0. \qquad (13.52)$$

For shell, closed at top, we have $0 \leq x \leq 1$. We divide this interval into n parts. We take following boundary conditions. At peak, when $x = 0$, we set $\psi = 0$, $\frac{d\psi}{dx} = 0$. For points of base, when $x = 1$, we take conditions of hinged support

$$\psi=0,\quad \frac{d^2\psi}{dx^2}+\mu\frac{d\psi}{dx}=0.$$

Expressing in (52) and in boundary conditions derivatives through finite differences by known formulas,** we compose system of algebraic equations for values ψ at nodes. Setting $n = 4$, we come to

---

*This solution was conducted by I. I. Trapezin [13.10]. Formulas (51), (57), (103) and (104) are his.

**See, for instance, E. Kamke, Reference book on ordinary differential equations, IL, 1950, p. 326. It is expedient for points $x = 1/n$ and $x = 1$ to use expressions for derivatives, giving approximation of first order, but for all others of points to use approximations of the second order.

the following equations:

$$\left.\begin{aligned} 7\psi_3 - 16\psi_2 + \left(13 + 16p^4 - \frac{p^3\nu}{4}\right)\psi_1 = 0, \\ -53.48\psi_3 + \left(31.36 + \frac{3}{2}p^4 - \frac{3}{16}p^3\nu\right)\psi_2 = 0, \\ \left(27.83 + \frac{32}{243}p^4 - \frac{p^3}{18}\nu\right)\psi_3 - 12.4\psi_2 - 0.6\psi_1 = 0. \end{aligned}\right\} \qquad (13.53)$$

Equating determinant of this system to zero, we obtain equation from which there may be determined magnitude ν. Minimizing ν with respect to p, we find value $\nu = 17.8$. With smaller step ($n = 5$), we have $\nu_{min} = 18.2$; formula for critical pressure then assumes form

$$q_* = 2.8E\left(\frac{h}{l_1}\right)^{5/2}\frac{(\lg a)^{5/2}}{(1-\mu^2)^{5/4}}. \qquad (13.54)$$

We obtained formula of the same structure as earlier (see expression (51)), but numerical coefficient turned out here to be equal to 2.8, instead of 3.15. Formula (54) is recommended for practical calculations in determining upper critical pressure. Judging by experimental data (see below), values of real critical pressures for carefully made shells lie somewhat above magnitudes obtained by formula (54). Therefore, calculation by formula (54) will be, as a rule, go into safety factor. For shells having initial deflection, one should conduct calculation taking into account lower critical pressure. Corresponding nonlinear problem still has not been solved; therefore, here it is expedient to use the same correction factors as were recommended in § 132 for cylindrical shells.

We turn to case of truncated shell (Fig. 13.4), more frequently encountered in real constructions. Subcritical forces are determined here by formulas

$$N_1 = \frac{q}{2\lg a}\left(\frac{r_0^2}{s} - s\right), \quad N_2 = -\frac{q}{\lg a}s. \qquad (13.55)$$

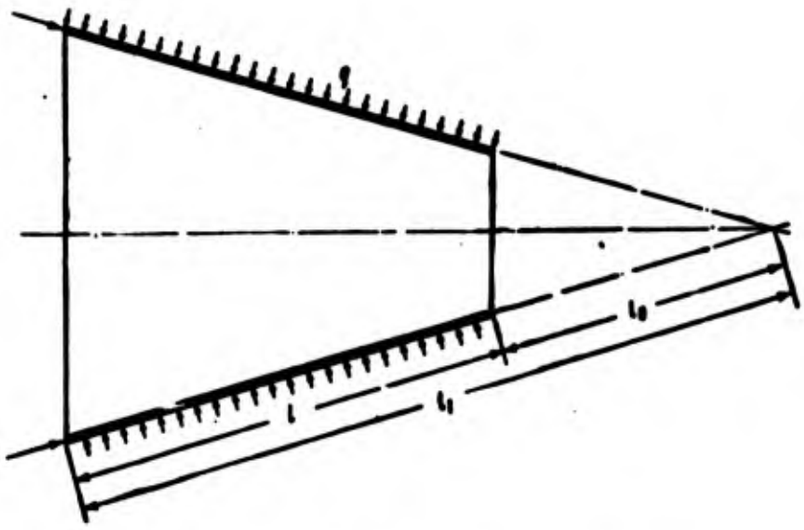

Fig. 13.4. Truncated shell under action of external pressure.

where l_0 is distance on generatrix from vertes to smaller base.

Introducing dimensionless coordinate $x = s/l_1$, we present these expressions in the form

$$N_1 = \frac{x}{2} w^3 Eh \operatorname{tg}^2 \alpha \left(\frac{\beta_0}{x l_1^2} - x \right), \quad N_2 = -x w^3 Eh \operatorname{tg}^2 \alpha. \qquad (13.56)$$

Magnitudes ε and ν are determined as before by (35) and (37). Proceeding just as in case of closed shell, after simplifications we arrive at equation (44). But if in case of shell, closed at vertex, magnitude x varied within limits $0 \leq x \leq 1$, it lies within limits $l_0/l_1 \leq x \leq 1$.

Solving problem of stability of truncated shell by method of finite differences, we obtain for case when shell is clamped on smaller base, and supported by hinge on larger, the following formula:

$$q_0 = C_1 E \left(\frac{h}{l_1} \right)^{5/2} \frac{(\operatorname{tg} \alpha)^{3/2}}{(1-\mu^2)^{1/2}}. \qquad (13.57)$$

Coefficient C_1 is determined by curve of Fig. 13.5.

The obtained formulas are applicable, as already was said, for angle α_1, not close to zero to $\pi/2$. Experiments show that these

formulas can be used with angle, lying within limits $20^\circ \leq \alpha \leq 80^\circ$; at $\alpha > 80^\circ$ it is possible in calculation q_B to replace conical shell with a cylindrical one with a radius, equal to average radius of conical shell.

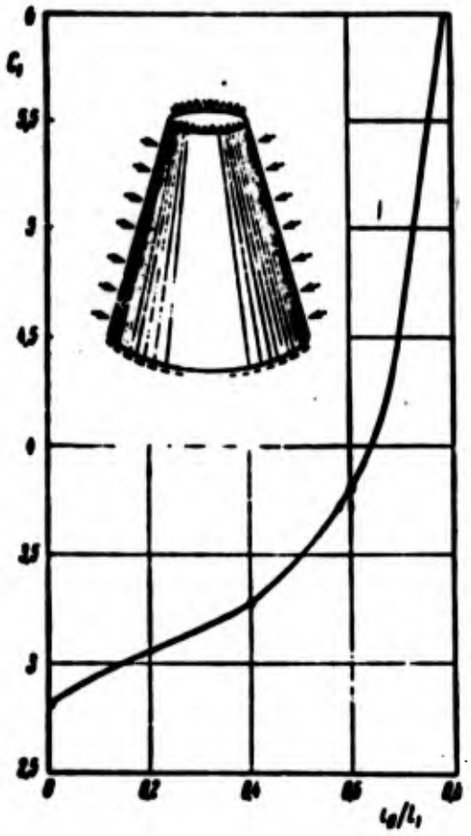

Fig. 13.5. Graph for calculation of truncated shell with smaller end clamped and larger supported by hinge.

Will give data of tests of carefully made closed and truncated conical shell,* subjected to external hydrostatic pressure. Edges of shells were rigidly clamped. Pressure was measured by manometers and sensor; readings of sensor were recorded on tape of oscillograph. Moment of loss of stability was marked by discontinuous decrease of ordinate of pressure curve. In Fig. 13.6 is shown shell, closed at vertex, after buckling. In Fig. 13.7 is depicted truncated conical shell after test; photography was done from side of major base.

Angles α of shells closed at vertex varied from 30 to 75°, and of truncated ones, from 81 to 86°. Ratio h/l_1 varied from $0.235 \cdot 10^{-2}$ to $0.57 \cdot 10^{-2}$. Loss of stability was accompanied by knock, although not sharp. Knock was stronger, if pressure on shell was not from liquid, but from air.

---

*These tests were conducted by I. I. Trapezin [13.10].

For all carefully prepared shells experimental value of critical pressure turned out to be somewhat higher than theoretical, determined by formula (54) (for shells closed at vertex) and (57) (for truncated shells), and lower than pressure from (51). On the average experimental magnitude of critical pressure was approximately 5% higher than value from (54) and P about as much lower than magnitude determined by (51).

In practical calculations it is possible to use formulas (54) and (57) for upper critical pressure; here one should introduce coefficient ν as was recommended for cylindrical shells (see § 132).

Example 13.2. Check for stability of the conical part of inter-

Fig. 13.6. Form of wave formation during buckling of conical shell.

Fig. 13.7. End view of test piece.

nal wall of diffuser, of thickness h = 2.5 mm, located between adjacent reinforcing ribs (Fig. 13.8) and under action of external pressure q = 6.3 kg/cm^2. Dimensions are given on figure; using them, we find

$$\operatorname{tg}\alpha = \frac{2 \cdot 120}{860 - 700} = 1.5, \quad \alpha = 56^\circ 20'$$

$$l_1 = \frac{430}{\cos 56^\circ 20'} = 777 \text{ мм}, \quad l_0 = \frac{350}{\cos 56^\circ 20'} = 632 \text{ мм},$$

$$\frac{h}{l_1} = \frac{2.5}{777} = 3.22 \cdot 10^{-3}, \quad \frac{l_0}{l_1} = \frac{632}{777} = 0.815.$$

Calculation was conducted by formula (57). Values of C_1 in Fig. 13.5 are given for values l_0/l_1, varying from zero to 0.8; in our case $l_0/l_1 = 0.81$. By extrapolation we find $C_1 = 6.2$. Then, by the formula (57), we find

$$q_0 = 6.2 \cdot 2.1 \cdot 10^6 \cdot (3.22 \cdot 10^{-3})^{3/4} \frac{(1.5)^{3/4}}{(1-0.3^2)^{1/4}} = 15.1 \text{ kg/cm}^2$$

Formula (57) was obtained on the assumption that shell is clamped on smaller base and is freely supported on larger. In our case both bases are clamped elastically, but ribs, on which the shell rests, are so powerful that fastening can be considered close to rigid. Calculated critical pressure turns out to be 2.4 times greater than excess external pressure.

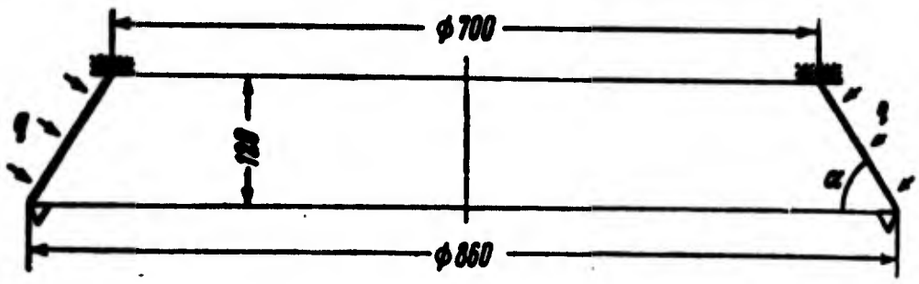

Fig. 13.8. Internal wall of diffuser of gas-turbine engine.

§ 151. Case of Torsion

Let us consider problem of stability of truncated, freely supported conical shell, loaded by shearing forces evenly distributed on end sections.*

Linear force in plane of smaller base ($s = l_0$) we designate by Tl_0, and in plane major base ($s = l_1$) by Tl_1.

*This solution belongs to Kh. M. Mushtari [13.6].

These forces are equal to

$$T_{l_0}=\frac{M_K}{2\pi(l_0\cos\alpha)^2}, \quad T_{l_1}=\frac{M_K}{2\pi(l_1\cos\alpha)^2}. \tag{13.58}$$

where M_K is the torque.

For additional displacements, arising during buckling of shell, we take following expressions, corresponding to helical waves, formed during loss of stability:

$$\left.\begin{aligned} u&=C_1\varepsilon^2\{\sin(\lambda_1 z+n\theta)-\sin(\lambda_2 z+n\theta)\},\\ v&=C_2\varepsilon^2\{\sin(\lambda_1 z+n\theta)-\sin(\lambda_2 z+n\theta)\},\\ w&=-2C_3\varepsilon^2\sin(\lambda z+n\theta)\sin m_1 z. \end{aligned}\right\} \tag{13.59}$$

where

$$z=\ln\frac{s}{l_0}, \quad m_1=\frac{\pi}{\zeta}=\frac{\lambda_1-\lambda_2}{2}, \quad \zeta=\ln\left(1+\frac{l}{l_0}\right), \quad \lambda=\frac{\lambda_1+\lambda_2}{2}.$$

By l there is understood length of shell on generatrix, by C_1, C_2, and C_3 are designated indeterminate constants.

Formulas (59) satisfy kinematic boundary conditions on ends of shell: for $z = 0$ and $z = \zeta$, $u = v = w = 0$.

Using method of Ritz for solution of problems, we arrive at following approximate formula for critical shear force:

$$T_{l_0}=\frac{Eh(\rho^2-1)}{4(\pi^2+\zeta^2)}\varepsilon^{5/2}C_0\operatorname{tg}^2\alpha; \tag{13.60}$$

here are introduced designations

$$\rho=1+\frac{l}{l_0}, \quad \varepsilon^2=\frac{\pi h}{\zeta^{3/2}l_0\operatorname{tg}\alpha\sqrt{1-\mu^2}}\left[\frac{\pi^2+\zeta^2}{6(\rho^2-1)}\right]^{1/2}. \tag{13.61}$$

$$C_0=2{,}61\left(\frac{\nu_1}{\varepsilon}\right)^{1/6}\left[1+0{,}33\left(\frac{\varepsilon}{\nu_1}\right)^{5/6}(1+\nu_1)\right], \quad \nu_1=\frac{1}{2(1+\mu)}. \tag{13.62}$$

Conditions of applicability of given formulas are the following:

$$\varepsilon\leqslant 0{,}1, \quad 0{,}25\leqslant\mu\leqslant 0{,}33.$$

We give table for magnitude C_0 (when $\mu = 0.3$):

ε	0,12	0,10	0,07	0,05	0,03
C_0	3,75	3,87	3,95	4,08	4,31

It is necessary to note that during solution of this problem significant role must be played by nonlinear members; it would be desirable to investigate stability of conical shell during torsion in the large.

§ 152. Reinforced Conical Shell Under Action of External Pressure

In aircraft equipment and motors, shipbuilding and engineering constructions, along with cylindrical shell reinforced by ribs (see § 137), there are applied reinforced conical shells. Furthermore, there are possible cases when material from which conical shell is made, is anisotropic.

Let us consider first problem of stability of conical shell, made from anisotropic material, limited by case of orthotropy. We assume that main directions of rigidity coincide with generatrix of cone and arc of the cross-section.

Dependences of Hooke's law, pertaining to deformation of middle surface, we will assume analogously to those in § 137 (see formula (11.153)):

$$\begin{pmatrix} \varepsilon_1 \\ \varepsilon_2 \\ \tau \end{pmatrix} = \begin{pmatrix} \delta_1 & \delta_2 & 0 \\ \delta_2 & \delta_1 & 0 \\ 0 & 0 & \delta_0 \end{pmatrix} \begin{pmatrix} N_1 \\ N_2 \\ T \end{pmatrix}. \tag{13.63}$$

Here

$$\delta_1 = \frac{1}{E_1 h}, \quad \delta_2 = \frac{1}{E_2 h}, \quad \delta_2 = -\frac{\mu_2}{E_2 h} = -\frac{\mu_1}{E_1 h},$$

$$\delta_0 = \frac{1}{Gh}, \quad T = T_{12} = T_{21}.$$

by E_1, E_2, μ_1, and μ_2 are designated elastic moduli and Poisson's ratios in direction of generatrix and in direction of parallel

circumference (see Fig. 13.2a).

Developing, e.g., matrix for (63), we obtain

$$\varepsilon_1 = \delta_1 N_1 + \delta_0 N_2 + 0 \cdot T = \frac{N_1}{E_1 h} - \frac{\mu_2}{E_2 h} N_2.$$

Moments we express by analogy with (11.154):

$$\begin{pmatrix} M_1 \\ M_2 \\ H \end{pmatrix} = \begin{pmatrix} D_1 & D_0 & 0 \\ D_0 & D_2 & 0 \\ 0 & 0 & D_0 \end{pmatrix} \begin{pmatrix} \varkappa_1 \\ \varkappa_2 \\ \chi \end{pmatrix}. \tag{13.64}$$

Magnitudes $\varkappa_1$, $\varkappa_2$, and χ are determined by equalities (7):

$$D_1 = \frac{E_1 h^3}{12(1-\mu_1\mu_2)}, \quad D_2 = \frac{E_2 h^3}{12(1-\mu_1\mu_2)}, \quad D_0 = G\frac{h^3}{6},$$
$$D_0 = D_1\mu_2 = D_2\mu_1. \tag{13.65}$$

Let us consider now equations of equilibrium from (10.63)—(10.68). They can be written both for fundamental form of equilibrium, and also for a form of neutral equilibrium, differing from fundamental.

We shall call first equations, pertaining to fundamental form of equilibrium, equations (a), and the second, equations (b).

Putting in equations (b) $\xi = s$, $\eta = \theta$, $A_1 = 1$, $A_2 = s\cos\alpha$ and taking into account equations (a), we will reduce these equations to such form:

$$\frac{\partial N_1}{\partial s} s\cos\alpha + N_1\cos\alpha + \frac{\partial T_{21}}{\partial\theta} - N_2\cos\alpha = 0, \tag{13.66}$$

$$\frac{\partial N_2}{\partial\theta} + \frac{\partial T_{12}}{\partial s} s\cos\alpha + T_{12}\cos\alpha + T_{21}\cos\alpha - Q_2\sin\alpha, \tag{13.67}$$

$$\frac{\partial Q_1}{\partial s} s\cos\alpha + Q_1\cos\alpha + \frac{\partial Q_2}{\partial\theta} + N_{10}\frac{\partial^2 w}{\partial s^2} s\cos\alpha +$$
$$+ N_2\sin\alpha + N_{20}\left(\frac{1}{s\cos\alpha}\frac{\partial^2 w}{\partial\theta^2} + \frac{\partial w}{\partial s}\cos\alpha\right) = 0, \tag{13.68}$$

$$\frac{\partial M_1}{\partial s} s\cos\alpha + M_1\cos\alpha + \frac{\partial H_{21}}{\partial\theta} - M_2\cos\alpha - Q_1 s\cos\alpha = 0, \tag{13.69}$$

$$\frac{\partial H_{12}}{\partial s} s\cos\alpha + \frac{\partial M_2}{\partial\theta} + H_{12}\cos\alpha + H_{21}\cos\alpha - Q_2 s\sin\alpha = 0. \tag{13.70}$$

In these equations N_{10} and N_{20} are normal forces, appearing in shell before loss of stability; all remaining forces and moments are additional, i.e., appear during transition of shell from basic axisymmetric form to new form of equilibrium (forces and moments are shown in Figs. 13.2a and 13.2b).

Members, containing N_{10} and N_{20}, are connected with changes of curvatures $(-\varkappa_1)$ and $(-\varkappa_2)$ [see (7) and (8)]. Last of the six equations of equilibrium we did not write, since it, as this was shown in Chapter X is simultaneously satisfied.

If in equation (67) we disregard transverse force, then equations (66) and (67) can be satisfied, setting

$$N_1 = \frac{1}{s^2\cos^2\alpha}\frac{\partial^2\varphi}{\partial\theta^2} + \frac{1}{s}\frac{\partial\varphi}{\partial s}. \tag{13.71}$$

$$N_2 = \frac{\partial^2\varphi}{\partial s^2}. \tag{13.72}$$

$$T_{12} = T_{21} = -\frac{1}{s\cos\alpha}\frac{\partial^2\varphi}{\partial s\,\partial\theta} + \frac{1}{s^2\cos\alpha}\frac{\partial\varphi}{\partial\theta}. \tag{13.73}$$

where φ is function of forces. Excluding from other three equations Q and Q_2, we obtain:

$$\begin{aligned}\frac{\partial^2 M_1}{\partial s^2}s\cos\alpha + 2\frac{\partial M_1}{\partial s}\cos\alpha + \frac{\partial^2 H_{21}}{\partial s\,\partial\theta} + \frac{\partial^2 H_{12}}{\partial s\,\partial\theta} - \frac{\partial M_2}{\partial s}\cos\alpha + \\ + \frac{1}{s}\frac{\partial H_{12}}{\partial\theta} + \frac{1}{s}\frac{\partial H_{21}}{\partial\theta} + \frac{1}{s\cos\alpha}\frac{\partial^2 M_2}{\partial\theta^2} + N_2\sin\alpha + \\ + N_{10}\frac{\partial^2 w}{\partial s^2}\cos\alpha + N_{20}\left(\frac{1}{s\cos\alpha}\frac{\partial^2 w}{\partial\theta^2} + \frac{\partial w}{\partial s}\cos\alpha\right) = 0.\end{aligned} \tag{13.74}$$

Let us turn to equation of compatibility of deformations (10.54); in this case when $\xi = s$, $\eta = \theta$, $A_1 = 1$, $A_2 = s\cos\alpha$ it will take such form:

$$\begin{aligned}-\frac{\varkappa_1}{R_2} - \frac{1}{s\cos\alpha}\frac{\partial^2\gamma}{\partial s\,\partial\theta} - \frac{1}{s^2\cos\alpha}\frac{\partial\gamma}{\partial\theta} + \frac{\partial^2\varepsilon_2}{\partial s^2} + \\ + \frac{1}{s^2\cos^2\alpha}\frac{\partial^2\varepsilon_2}{\partial\theta^2} + \frac{2}{s}\frac{\partial\varepsilon_2}{\partial s} - \frac{1}{s}\frac{\partial\varepsilon_1}{\partial s} = 0.\end{aligned} \tag{13.75}$$

Expressing M_1, M_2, and $H_{12} = H_{21} = H$ by relationship (64) and considering equalities (7) and (8) and (72), we give equation of equilibrium (74) form

$$-D_1\frac{\partial^4 w}{\partial s^4}-D_{\mu}\left(\frac{2}{s^2\cos^2\alpha}\frac{\partial^4 w}{\partial s^2\partial\theta^2}-\frac{2}{s^3\cos^2\alpha}\frac{\partial^3 w}{\partial s\,\partial\theta^2}+\frac{2}{s^4\cos^2\alpha}\frac{\partial^2 w}{\partial\theta^2}\right)-$$
$$-2D_1\frac{1}{s}\frac{\partial^3 w}{\partial s^3}-D_2\left(\frac{1}{s^4\cos^4\alpha}\frac{\partial^4 w}{\partial\theta^4}-\frac{1}{s^2}\frac{\partial^2 w}{\partial s^2}+\frac{1}{s}\frac{\partial w}{\partial s}+\frac{2}{s^4\cos^2\alpha}\frac{\partial^2 w}{\partial\theta^2}\right)-$$
$$-D_0\left(\frac{2}{s^4\cos^2\alpha}\frac{\partial^2 w}{\partial\theta^2}+\frac{2}{s^2\cos^2\alpha}\frac{\partial^4 w}{\partial s^2\partial\theta^2}-\frac{2}{s^3\cos^2\alpha}\frac{\partial^3 w}{\partial s\,\partial\theta^2}\right)+\frac{\operatorname{tg}\alpha}{s}\frac{\partial^2\varphi}{\partial s^2}+$$
$$+N_{10}\frac{\partial^2 w}{\partial s^2}+N_{20}\left(\frac{1}{s^2\cos^2\alpha}\frac{\partial^2 w}{\partial\theta^2}+\frac{1}{s}\frac{\partial w}{\partial s}\right)=0. \qquad (13.76)$$

Using, further, equality (63), taking into account (7) and (8), we reduced equation of compatibility (75) to such form:

$$\delta_1\left(\frac{1}{s^4\cos^4\alpha}\frac{\partial^4\varphi}{\partial\theta^4}+\frac{2}{s^4\cos^2\alpha}\frac{\partial^2\varphi}{\partial\theta^2}-\frac{1}{s^2}\frac{\partial^2\varphi}{\partial s^2}+\frac{1}{s^3}\frac{\partial\varphi}{\partial s}\right)+$$
$$+\delta_2\left(\frac{\partial^4\varphi}{\partial s^4}+\frac{2}{s}\frac{\partial^3\varphi}{\partial s^3}\right)+\delta_{\mu}\left(\frac{2}{s^2\cos^2\alpha}\frac{\partial^4\varphi}{\partial s^2\partial\theta^2}-\right.$$
$$\left.-\frac{2}{s^3\cos^2\alpha}\frac{\partial^3\varphi}{\partial s\,\partial\theta^2}+\frac{2}{s^4\cos^2\alpha}\frac{\partial^2\varphi}{\partial\theta^2}\right)+$$
$$+\delta_0\left(\frac{1}{s^2\cos^2\alpha}\frac{\partial^4\varphi}{\partial s^2\partial\theta^2}-\frac{1}{s^3\cos^2\alpha}\frac{\partial^3\varphi}{\partial s\,\partial\theta^2}+\frac{1}{s^4\cos^2\alpha}\frac{\partial^2\varphi}{\partial\theta^2}+\right.$$
$$\left.+\frac{1}{s^3\cos^2\alpha}\frac{\partial^2\varphi}{\partial s\,\partial\theta}-\frac{1}{s^4\cos^2\alpha}\frac{\partial\varphi}{\partial\theta}\right)\lambda+\frac{tg\alpha}{s}\cdot\frac{\partial^2 w}{\partial s^2}=0.$$

(13.77)

Equations (76) and (77) are initial in the solution of problem of stability of orthotropic shell in the small.

Let us consider case when shell is reinforced by circular and longitudinal ribs, symmetrically located relative to middle surface (Figs. 13.9a and 13.9b). Ribs are considered to be located sufficiently close together so that rigidity of rib can be evenly distributed ("spread out") the length of the interval.

We consider that ribs possess rigidity only in their plane. Under this condition ribs will not influence shearing and torsion of shell. Considering this, we take for $T_{12} = T_{21} = T$ and $H_{12} = H_{21} = H$ the same expressions as for a smooth shell. Remaining forces and moments must be considered separately.

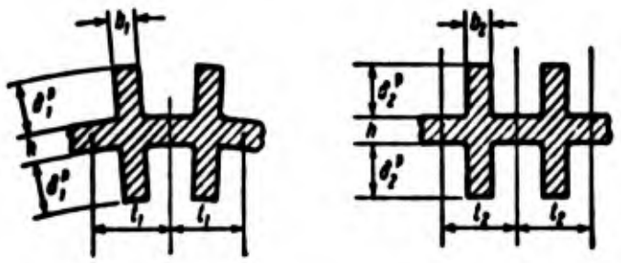

a) b)

Fig. 13.9. Sections of reinforcing ribs.

For fiber, parallel to generatrix and located distance z from middle surface, we obtain such expression for deformation of elongation:

$$\varepsilon_1^z = \varepsilon_1 - \varkappa_1 z. \tag{13.78}$$

For fiber, perpendicular to generatrix, we have

$$\varepsilon_2^z = \varepsilon_2 - \varkappa_2 z. \tag{13.79}$$

For stress σ_1, we obtain

$$\sigma_1^z = \frac{E}{1-\mu^2}(\varepsilon_1^z + \mu\varepsilon_2^z) = \\ = \frac{E}{1-\mu^2}[\varepsilon_1 + \mu\varepsilon_2 - z(\varkappa_1 + \mu\varkappa_2)] \quad \text{when} \quad \left(-\frac{h}{2}\right) \leqslant z \leqslant \frac{h}{2} \tag{13.80}$$

and, further,

when
$$\left.\begin{aligned} &\sigma_1^z = E\varepsilon_1^z = E(\varepsilon_1 - z\varkappa_1) \\ &\left[-\left(\frac{h}{2} + \delta_1^p\right) \leqslant z \leqslant -\frac{h}{2}\right] \text{ and } \left[\frac{h}{2} \leqslant z \leqslant \frac{h}{2} + \delta_1^p\right]. \end{aligned}\right\} \tag{13.81}$$

Here by δ_1^p is understood stress in rib.

Analogously we find

$$\sigma_2^0 = \frac{E}{1-\mu^2}[\varepsilon_2^0 + \mu\varepsilon_1^0] =$$
$$= \frac{E}{1-\mu^2}[\varepsilon_2 + \mu\varepsilon_1 - z(\varkappa_2 + \mu\varkappa_1)] \text{ when } \frac{h}{2} \leqslant z \leqslant \frac{h}{2}. \tag{13.82}$$

when
$$\left.\begin{array}{c} \sigma_2^0 = E\varepsilon_2^0 = E(\varepsilon_2 - z\varkappa_2) \\ \left[-\left(\frac{h}{2}+\delta_2^0\right) < z < -\frac{h}{2}\right] \text{and} \left[\frac{h}{2} < z < \left(\frac{h}{2}+\delta_2^0\right)\right]. \end{array}\right| \tag{13.83}$$

Force N_1 is equal to

$$N_1 = \int_{-\frac{h}{2}}^{\frac{h}{2}} \sigma_1^0\, dz + 2E\frac{b_1}{l_1}\int_{\frac{h}{2}}^{\frac{h}{2}+\delta_1^0} \sigma_1^0\, dz = \frac{Eh}{1-\mu^2}(\varepsilon_1 + \mu\varepsilon_2) + 2E\frac{b_1}{l_1}\delta_1^0\varepsilon_1 =$$
$$= \frac{Eh}{1-\mu^2}\left\{\left[1 + 2\frac{b_1}{l_1 h}\delta_1^0(1-\mu^2)\right]\varepsilon_1 + \mu\varepsilon_2\right\}. \tag{13.84}$$

In this way we obtain

$$N_2 = \frac{Eh}{1-\mu^2}\left\{\left[1 + 2\frac{b_2\delta_2^0}{l_2 h}(1-\mu^2)\right]\varepsilon_2 + \mu\varepsilon_1\right\}. \tag{13.85}$$

Moment M_1 turns out to be equal to

$$M_1 = -\int_{-\frac{h}{2}}^{\frac{h}{2}} z\sigma_1^0\, dz - 2\frac{b_1}{l_1}\int_{\frac{h}{2}}^{\frac{h}{2}+\delta_1^0} z\sigma_1^{(2)}\, dz =$$
$$= \frac{Eh^3}{12(1-\mu^2)}(\varkappa_1 + \mu\varkappa_2) + 2E\frac{b_1}{l_1}I_1^0\varkappa_1.$$

or
$$M_1 = \frac{Eh^3}{12(1-\mu^2)}\left\{\left[1 + 2\frac{12(1-\mu^2)b_1}{h^3 l_1}I_1^0\right]\varkappa_1 + \mu\varkappa_2\right\}. \tag{13.86}$$

For moment M_2 we obtain the same expression:

$$M_2 = \frac{Eh^3}{12(1-\mu^2)}\left\{\left[1 + 2\frac{12(1-\mu^2)b_2}{h^3 l_2}I_2^0\right]\varkappa_2 + \mu\varkappa_1\right\}. \tag{13.87}$$

In equalities (86) and (87) by I_1^0 and I_2^0 are understood moments of inertia of half of section of rib relative to axes, lying in middle surface:

$$I_1^0 = \frac{b_1(\delta_1^0)^3}{12} + \frac{1}{4}b_1\delta_1^0(h+\delta_1^0)^2.$$
$$I_2^0 = \frac{b_2(\delta_2^0)^3}{12} + \frac{1}{4}b_2\delta_2^0(h+\delta_2^0)^2.$$

Introducing designations

$$1+\frac{2b_1\delta_1^2}{l_1h}(1-\mu^2)=\omega_1. \qquad 1+\frac{2b_2\delta_2^2}{l_2h}(1-\mu^2)=\omega_2. \tag{13.88}$$

$$1+\frac{24(1-\mu^2)}{l_1-h^2}f_1^2=\iota_1. \qquad 1+\frac{24(1-\mu^2)}{l_2h^2}f_2^2=\iota_2. \tag{13.89}$$

we present equalities (84)—(87) in form

$$N_1=\frac{Eh}{1-\mu^2}(\omega_1\varepsilon_1+\mu\varepsilon_2). \qquad N_2=\frac{Eh}{1-\mu^2}(\omega_2\varepsilon_2+\mu\varepsilon_1). \tag{13.90}$$

$$M_1=\frac{Eh^3}{12(1-\mu^2)}(\iota_1\varkappa_1+\mu\varkappa_2). \quad M_2=\frac{Eh^3}{12(1-\mu^2)}(\iota_2\varkappa_2+\mu\varkappa_1). \tag{13.91}$$

Expressing ε_1 and ε_2, proceeding from equalities (90), we obtain

$$\left.\begin{aligned}\varepsilon_1&=\frac{1-\mu^2}{Eh(\omega_1\omega_2-\mu^2)}(\omega_2N_1-\mu N_2).\\ \varepsilon_2&=\frac{1-\mu^2}{Eh(\omega_1\omega_2-\mu^2)}(\omega_1N_2-\mu N_1).\end{aligned}\right\} \tag{13.92}$$

Comparing expression for ε_1 and ε_2 in (92) with formulas (63), we obtain following values of δ_1, δ_2, and δ_μ:

$$\delta_1=\frac{\omega_2(1-\mu^2)}{Eh(\omega_1\omega_2-\mu^2)}. \quad \delta_2=\frac{\omega_1(1-\mu^2)}{Eh(\omega_1\omega_2-\mu^2)}. \quad \delta_\mu=\frac{-\mu(1-\mu^2)}{Eh(\omega_1\omega_2-\mu^2)}. \tag{13.93}$$

Comparing, further, equalities (91) with expressions for moments, given by equality (64), we find

$$D_1=\frac{Eh^3\iota_1}{12(1-\mu^2)}. \quad D_2=\frac{Eh^3\iota_2}{12(1-\mu^2)}. \quad D_\mu=\frac{\mu Eh^3}{12(1-\mu^2)}. \quad D_0=G\frac{h^3}{6}. \tag{13.94}$$

Putting (93) and (94) in equations (76) and (77), we find that in case of conical shells, reinforced by longitudinal and transverse ribs, problem is reduced to solution of following equations:

$$\begin{aligned}&\frac{Eh^3}{12(1-\mu^2)}\left[\iota_1\frac{\partial^4w}{\partial s^4}+\frac{2}{s^2\cos^2\alpha}\frac{\partial^4w}{\partial s^2\partial\theta^2}-\frac{2}{s^3\cos^2\alpha}\frac{\partial^3w}{\partial s\,\partial\theta^2}+\frac{\iota_2}{s^4\cos^4\alpha}\frac{\partial^4w}{\partial\theta^4}+\right.\\&\left.+\frac{2(1+\iota_2)}{s^2\cos^2\alpha}\frac{\partial^4w}{\partial\theta^4}+\frac{2\iota_1}{s}\frac{\partial^3w}{\partial s^3}-\frac{\iota_2}{s^2}\frac{\partial^2w}{\partial s^2}+\frac{\iota_2}{s^3}\frac{\partial w}{\partial s}\right]-\\&-\frac{\operatorname{tg}\alpha}{s}\frac{\partial^2\varphi}{\partial s^2}-N_{10}\frac{\partial^2w}{\partial s^2}-N_{20}\left(\frac{1}{s^2\cos^2\alpha}\frac{\partial^2w}{\partial\theta^2}+\frac{1}{s}\frac{\partial w}{\partial s}\right)=0.\end{aligned} \tag{13.95}$$

$$\frac{(1-\mu^2)\omega_1}{\omega_1\omega_2-\mu^2}\frac{\partial^4\varphi}{\partial s^4}+2\left(1+\mu-\frac{1-\mu^2}{\omega_1\omega_2-\mu^2}\mu\right)\frac{1}{s^2\cos^2\alpha}\frac{\partial^4\varphi}{\partial s^2\partial\theta^2}+$$
$$+\frac{(1-\mu^2)\omega_1}{\omega_1\omega_2-\mu^2}\frac{1}{s^4\cos^4\alpha}\frac{\partial^4\varphi}{\partial s^4}+\left[\frac{1-\mu^2}{\omega_1\omega_2-\mu^2}2\mu-2(1+\mu)\right]\frac{1}{s^2\cos^2\alpha}\frac{\partial^4\varphi}{\partial s\,\partial\theta^2}+$$
$$+\frac{2}{s^2\cos^2\alpha}\left[\frac{1-\mu^2}{\omega_1\omega_2-\mu^2}(\omega_2-\mu)+(1-\mu)\right]\frac{\partial^4\varphi}{\partial\theta^4}+$$
$$+\frac{2(1-\mu^2)}{\omega_1\omega_2-\mu^2}\frac{\omega_1}{s}\frac{\partial^3\varphi}{\partial s^3}-\omega_2\frac{1-\mu^2}{\omega_1\omega_2-\mu^2}\frac{1}{s}\frac{\partial^3\varphi}{\partial s^3}+$$
$$+\frac{\omega_2(1-\mu^2)}{\omega_1\omega_2-\mu^2}\frac{1}{s^2}\frac{\partial\varphi}{\partial s}+\frac{\operatorname{tg}\alpha}{s}\frac{\partial^3 w}{\partial s^3}Eh=0. \qquad (13.96)$$

In case of shell equipped with <u>one-sided ribs</u> (Fig. 13.10) expressions for i_1, ω_1 and i_2, ω_2 changes. In this case*

$$\left.\begin{aligned} i_1&=1+\frac{12(1-\mu^2)}{\delta_1 h^3}I_1^p, \quad i_2=1+\frac{12(1-\mu^2)}{\delta_2 h^3}I_2^p.\\ \omega_1&=1+\frac{\delta_1 h_1^2}{\delta_1 h}(1-\mu^2), \quad \omega_2=1+\frac{\delta_2 h_2^2}{\delta_2 h}(1-\mu^2).\end{aligned}\right\} \qquad (13.97)$$

Here I_1^p is moment of inertia of section of longitudinal rib relative

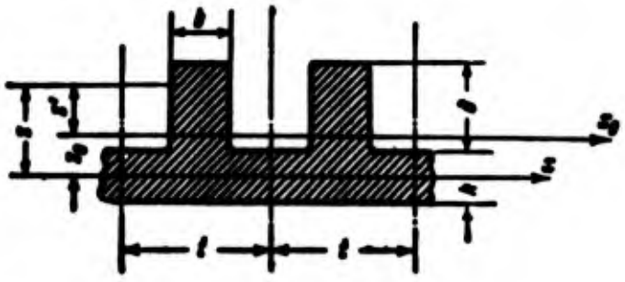

Fig. 13.10. One-sided locating of ribs.

to central axis of profile of circular section of shell, I_2^p is moment of inertia of section of circular rib relative to central axis of profile of axial section of shell. In the absence of longitudinal ribs we have $i_1 = 1$.

Let us consider problem of stability of conical shell, reinforced by ribs, under action of uniform transverse <u>external pressure</u>.

---

*More detailed research of case of one-sided ribs in application to cylindrical shell was given by V. V. Novozhilov, V. I. Korolev, and also O. I. Terebushko [11.22]; see work of 1962.

Equations (95) and (96) can be simplified just as this was done above with respect to relationships (14) and (15) (see § 150); then we obtain equation

$$\frac{d^2}{dx^2}\left(x^3\frac{d^2\psi}{dx^2}\right)+\beta_1\rho^4\frac{\psi}{x^3}-\beta_2\rho^3\nu=0; \tag{13.98}$$

here

$$\beta_1=\frac{(1-\mu^2)\omega_2}{\omega_1\omega_2-\mu^2}l_2, \tag{13.99}$$

$$\beta_2=\frac{(1-\mu^2)\omega_2}{\omega_1\omega_2-\mu^2}. \tag{13.100}$$

Function ψ is connected with function w by equality (34), and magnitudes ν and p come from formulas (37). Solving equation (98) by Bubnov-Galerkin method, we obtain, instead of equality (49),

$$\nu=\frac{\frac{1}{\rho^3}\left[-x^3\frac{d^2\psi}{dx^3}\frac{d\psi}{dx}\Big|_0^1+\int_0^1 x^3\left(\frac{d^2\psi}{dx^2}\right)^2dx+\rho^2\beta_1\int_0^1\frac{\psi^2}{x^3}dx\right]}{\beta_2\int_0^1\psi^2dx}. \tag{13.101}$$

Given, as in case of smooth shell, expression (45) for function ψ, from condition $(M_1)_{x=1}=0$ we find

$$a=-\frac{6i_1+\mu}{8i_1+\mu}. \tag{13.102}$$

Thus, in the presence of not only circular, but also longitudinal ribs magnitude a depends on i_1; change of a turns out to be insignificant: when $i_1=1$ we have $a=-0.759$, and when $i_1=5$, $a=-0.75$. This gives possibility when $\mu=0.3$ to take for a the value, corresponding to $i_1=1$.

As a result, finding p from condition of minimum of ν, we arrive at such formula for critical pressure:

$$q_*=\frac{3{,}15}{\beta_2}\sqrt[4]{\beta_1^3}E\left(\frac{h}{l_1}\right)^{5/4}\frac{(\operatorname{tg}\alpha)^{1/4}}{(1-\mu^2)^{3/4}}. \tag{13.103}$$

We recall here that equation (98), and consequently, equality (103) are obtained on the assumption that angle α is not close to zero or to $\pi/2$. As calculations show, circular ribs essentially increase critical pressure, longitudinal ribs turn out to be significantly less effective. Solving the same problem with help of method of finite differences, we obtain formula (103) with coefficient 2.8 instead of 3.15.

In case of truncated shell we have

$$q_* = \frac{C_1}{\beta_2} \sqrt[4]{\beta_1^3} E \left(\frac{h}{l_1}\right)^{3/4} \frac{(\operatorname{tg}\alpha)^{3/4}}{(1-\mu^2)^{3/4}}. \qquad (13.104)$$

Magnitude of coefficients C_1 one can determine by curve of Fig. 13.5 with the same boundary conditions.

Literature

13.1. N. A. Alumyae. On determination of the state of equilibrium of a circular shell with a axisymmetric load, Applied math. and mech., 17 No. 5 (1958); Determination of critical load of a conical shell of rotation closed at its vertex, under action of external pressure. Transactions of Tallin polytechnic inst., 66 (1955); Asymptotic integration of equations of static stability of a conical shell of rotation, Applied math. and mech., 21, No. 1 (1957).

13.2. N. A. Alfutov. Calculating shells for stability by the energy method, Eng. coll., 21 (1955).

13.3. L. M. Bunich, O. M. Paliy and I. A. Piskovitina. Stability of a truncated conical shell under action of uniform external pressure, Eng. coll., 23 (1956).

13.4. G. N. Geniyev and N. S. Chausov. Certain problems of nonlinear theory of stability of shallow shells, Stroyizdat, 1954.

13.5. E. I. Grigolyuk. On stability of a closed two-ply conical shell under action of uniform normal pressure, Eng. coll., 19 (1954); Nonlinear vibrations and stability of shallow bars and shells, News of Acad. of Sci. of USSR, OTN, No. 3 (1955); Loss of stability during large deflections of a closed sandwich conical shell under action of uniform normal pressure, Eng. collection of mech. inst. of Academy of Sciences of USSR, 22 (1955); Elastic stability of orthotropic and sandwich conical and cylindrical shells, coll. of articles "Design of spatial structures," 3 (1955).

13.6. Kh. M. Mushtari. Certain generalizations of theory of thin shells with application to problem of stability of elastic equilibrium, News of physical-mathematic scientific research institute of math. and mech., at Kazan' university, ser. 3, 11 (1933); Approximate solution of certain problems of stability of thin-walled conical shells of circular section, Applied math. and mech., 7, No. 3 (1943).

13.7. Kh. M. Mushtari and A. V. Sachenkov. On stability of cylindrical and conical shells of circular section during joint action of compression and external normal pressure, Applied math. and mech., 23 No. 6 (1954).

13.8. R. K. Ryayamet. Critical load of a conical shell under action of evenly distributed external pressure, Transactions of Tallin polytechnic inst., 66 (1951); Equilibrium of elastic conical shells in the postcritical stage, Transactions of Tallin polytechnic, inst., series A, No. 82 (1956), Equilibrium of thin-walled elastic conical shells in the postcritical stage, Transactions of Tallin polytechnic inst., series A, No. 82 (1956).

13.9. A. V. Sachenkov. Approximate determination of lower bound of critical load during longitudinal compression of a thin conical shell, News of Kazan' branch of Academy of Sciences of USSR, series of physical-mathematical and technical sciences, 7 (1955); On plastic stability of shells, News of Kazan' branch of Academy of Sciences of USSR, series of phys-math. and tech. sciences, 10 (1956);

Stability of conical shells of circular section under action of uniform external pressure, Ibid., No. 12 (1953).

13.10. I. I. Trapezin. Stability of a thin-walled conical shell of circular section during loads, axisymmetric to its axis. Transactions of Moscow Aviation Inst., No. 17 (1952), Stability of a structurally orthotropic thin-walled conical shell, loaded by uniform external pressure, Transactions of MAI, Issue 69, Oborongiz, (1956); Stability of conical shell, under hydrostatic pressure, "Calculations for strength, rigidity, stability and vibrations," Mashgiz (1956); Stability of a thin-walled conical shell, closed in at vertex, loaded by lateral hydrostatic pressure. "Strength analysis," Mashgiz, 5 (1960); Experimental determination of magnitudes of critical pressure for conical shells, loc. cit.

13.11. I. Ya. Shtayermann. Stability of shells, Transactions of Kiev Aviation Inst., No. 1 (1936).

13.12. J. Fritiof, N. Niordson. Buckling of conical shells subjected to uniform external lateral pressure, Acta Polytechnica Transactions of the Royal Institute of Technology, Stocholm, No. 10 (1947).

13.13. N. Hoff and J. Singer. Buckling of circular conical shells under external pressure, Proc. of the JUTAM Symposium on the theory of thin elastic shells, Delft, 1959.

13.14. A. Pflüger. Stabilitat dünner Kegelschalen, Ing. Archiv 8, No. 3 (1957).

13.15. P. Seide. On the buckling of truncated conical shells under uniform hydrostatic pressure, Proc. of the JUTAM Symposium on the theory of thin elastic shells, Delft. 1959.

13.16. C. E. Taylor. Elastic stability of conical shells loaded by uniform external pressure, Proc of the 3rd midwestern conference on solid mechanics, Michigan, 1957.

CHAPTER XIV

SPHERICAL SHELL

§ 153. Stability in the Small of Spherical Shell Under External Pressure

Shells of revolution, having spherical outline or a form close to spherical, are applied in many areas of technology. Examples are radomes in aircraft, bulkheads of submarines, bottoms of storage tanks, etc. The most important problem of stability of such shells pertains to case when shell is loaded by evenly distributed external pressure. In real constructions we most frequently meet spherical segments, fastened on their edge. We will distinguish segments with large subtended angle, rise H of which is comparable with radius of curvature of middle surface R (Fig. 14.1) and shallow panels, for which $H \ll R$. In given chapter we consider only segments of large rise.* Since buckling of such a segment is accompanied by formation of comparatively shallow dents, critical stresses for it will be the same as for complete spherical shell (Fig. 14.2).

Let us turn, therefore, to determination of critical load for complete spherical shell, subjected to external uniform pressure. As first glance, in view of ultimate simplicity of form of shell and

*Shallow spherical panels are subject of § 161 in the next chapter.

symmetry of load, this problem should not be complicated. And indeed, it does not present special difficulties if we solve it in linear formulation. However, real spherical shell turn out to be just as sensitive to the least initial imperfections, as a cylindrical shell compressed along axis. Buckling of spherical shells, as a rule, is accompanied by a knock, and true values of critical forces lie usually much lower than values found by linear theory. Therefore, problem of stability of spherical shell should be formulated as a nonlinear one. Experimental research of stability of a complete spherical shell or segments of great-rise are more complicated than for cylindrical shells. Peculiarity of process of buckling of real spherical shell is that in some cases it is accompanied by appearance of one rapidly developing dent, and in others by a series of waves, located on circumference. Therefore, construction of approximate solutions, connected with approximation of deflection surface, requires here special case. Thus, the practically important classical problem of buckling of spherical shell is one of the subtlest and most complicated problems of this group both theoretically, and also experimentally.

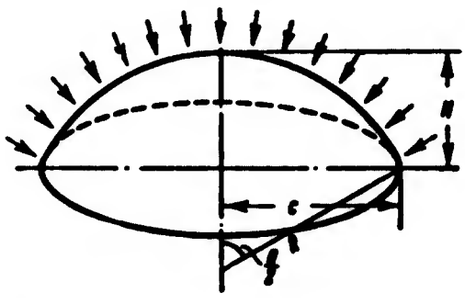

Fig. 14.1. Spherical dome loaded by external pressure.

Let us start with solution of linear problem.* We assume that within limits of zone of primary dent the shell is shallow, and we

*This problem was considered for the first time by R. Zoelly [14.14] and L. S. Leybenzon [14.2] in 1915–17.

use equations (10.83) and (10.86). In our case from (10.88) we have $\nabla_k^2 = (1/R)\nabla^2$, where R is radius by middle of surface; consequently, we arrive at the following system of equations:

$$\left.\begin{aligned} D\nabla^4 w &= \frac{1}{R}\nabla^2\varphi + q_z, \\ \frac{1}{Eh}\nabla^4\varphi &= -\frac{1}{R}\nabla^2 w. \end{aligned}\right\} \qquad (14.1)$$

Excluding φ from those, we obtain finally equation of sixth order for w:

$$D\nabla^6 w + \frac{Eh}{R^2}\nabla^2 w = \nabla^2 q_z. \qquad (14.2)$$

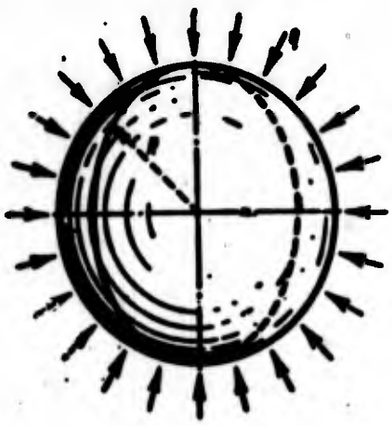

Fig. 14.2. Complete spherical shell under action of external pressure.

where $\nabla^6 = \nabla^2\nabla^2\nabla^2$. During action of external uniform pressure initial forces in all normal sections of shell will be, by (10.65),

$$N_1 = N_2 = -\frac{qR}{2}.$$

If we consider compressive forces N and stresses σ positive, we find

$$N = \frac{qR}{2}, \quad \sigma = \frac{qR}{2h}. \qquad (14.3)$$

We determine radial displacement w_0 of all points of middle surface, corresponding to initial stresses σ. Deformation of elongation along arc of any normal section is equal to $\varepsilon = w_0/R$; on the other hand, $\varepsilon = \sigma(1 - \mu)/E = qR(1 - \mu)/2Eh$, hence

$$w_0 = \frac{qR^2}{2Eh}(1-\mu). \qquad (14.4)$$

Henceforth, by w we shall designate additional deflection taking place during buckling of shell; actual load q will not enter equation (2) directly. Hypothetical load q_z, however, corresponding to stresses σ, we find by (10.89a); $q_z = -h\sigma\nabla^2 w$. Thus, equation (2) obtains form

$$\frac{D}{h}\nabla^4 w + \sigma\nabla^2 w + \frac{E}{R^2}\nabla^2 w = 0. \qquad (14.5)$$

Following V. Z. Vlasov [10.3] we assume that solution of equation (5) should satisfy relationship

$$\nabla^2 w = -\lambda^2 w, \qquad (14.6)$$

where λ is indeterminate variable. Then from (5) we obtain (when $\lambda \neq 0$)

$$\frac{D}{h}\lambda^4 - \sigma\lambda^2 + \frac{E}{R^2} = 0$$

and, further,

$$\sigma = \frac{D}{h}\lambda^2 + \frac{E}{R^2\lambda^2}. \qquad (14.7)$$

Minimizing σ with respect to λ^2, we find

$$\lambda^2 = \sqrt{\frac{hE}{DR^2}} = \frac{1}{Rh}\sqrt{12(1-\mu^2)}. \qquad (14.8)$$

Further by (6) we determine upper critical stress:

$$\sigma_0 = \frac{1}{\sqrt{3(1-\mu^2)}} E\frac{h}{R} \approx 0.605E\frac{h}{R}. \qquad (14.9)$$

Corresponding pressure is equal to

$$q_0 = \frac{2}{\sqrt{3(1-\mu^2)}} E\left(\frac{h}{R}\right)^2 = 1.21E\left(\frac{h}{R}\right)^2. \qquad (14.10)$$

Thus, magnitude of upper critical stress for spherical shell by (9) is exactly the same as for cylindrical shell of radius R, compressed along axis.

§ 154. Case of Axisymmetric Buckling. Linear Problem

Till now we were interested only in value of critical pressure and did not determine form of buckling of shell. We shall now find what the form of deflection surface is if buckling is axisymmetric.

We start first with equation (6), corresponding to theory of shallow shells. We introduce polar coordinates r and φ and assume that deflection is a function only of distance r of given point from pole: $w = w(r)$. Determining $\nabla^2 w$ by formula (9.16), we arrive at equation

$$\frac{d^2w}{dr^2} + \frac{1}{r}\frac{dw}{dr} + \lambda^2 w = 0. \qquad (14.11)$$

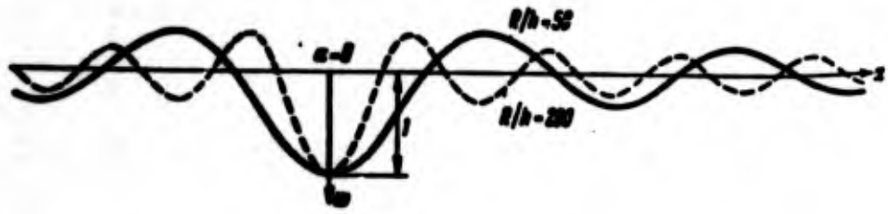

Fig. 14.3. Form of buckling, described by Bessel functions.

We already met an equation of this type above, while examining stability of radially compressed plate. Actually, relationship (9.3) when $\sigma_r = \sigma_\varphi = -p$ can be given form

$$\frac{D}{h}\nabla^4 w + p\nabla^2 w = 0$$

or, when $k^2 = ph/D$,

$$\nabla^2(\nabla^2 w + k^2 w) = 0;$$

from this follows equation (11). As we have seen, such an equation can be integrated in Bessel functions. Considering that at pole $w = f$, we assume

$$w = fJ_0(\lambda r), \qquad (14.12)$$

where $J_0(\lambda r)$ is Bessel function of first kind with index 0. Graph of this function is shown in Fig. 14.3. As we see, axisymmetric buckling of shell should be accompanied by appearance of comparatively deep dent at the pole and a series of annular folds, becoming smaller as we move away from the pole.

If we now use theory of deep shells, then it is natural to pass to geographic coordinates (Fig. 14.4). In general case of asymmetric problem, first quadratic form will be

$$I = R^2 d\alpha^2 + r^2 d\beta^2 = \\ = R^2 (d\alpha^2 + \sin^2\alpha\, d\beta^2). \qquad (14.13)$$

where α and β are angles of latitude and longitude. Form factors I are equal to $a_{11} = A_1^2 = R^2$, $a_{22} = A_2^2 = R^2 \sin^2\alpha$, and $a_{12} = 0$. Laplacian operator of (10.81) obtains form

$$\nabla^2 = \frac{1}{R^2}\left(\frac{\partial^2}{\partial\alpha^2} + \operatorname{ctg}\alpha\frac{\partial}{\partial\alpha} + \right. \\ \left. + \frac{1}{\sin^2\alpha}\frac{\partial^2}{\partial\beta^2}\right). \qquad (14.14)$$

Returning to symmetric problem, we find

$$\nabla^2 = \frac{1}{R^2}\left(\frac{d^2}{d\alpha^2} + \operatorname{ctg}\alpha\frac{d}{d\alpha}\right). \qquad (14.15)$$

We introduce dimensionless operator $\bar{\nabla}^2 = R^2\nabla^2$; then, proceeding from general relationships of Chapter X it is possible to arrive (see [10.3]) at following definitized relationship, replacing (6):

$$(\bar{\nabla}^2 + 2)w = -sw, \qquad (14.16)$$

where s is new indeterminate variable.

Fig. 14.4. Coordinate lines for examining spherical shells.

Substituting value $\bar{\nabla}^2$, we arrive at equation

$$\frac{d^2w}{d\alpha^2} + \frac{dw}{d\alpha}\operatorname{ctg}\alpha + (s+2)w = 0.$$

We take $s + 2 = n(n + 1)$, where $n = 1, 2, 3, \ldots$, then instead of (16) we obtain

$$\frac{d^2w}{d\alpha^2} + \frac{dw}{d\alpha}\operatorname{ctg}\alpha + n(n+1)w = 0. \qquad (14.17)$$

Equation of such type pertains to class of so-called hypergeometric

equations. It is satisfied by harmonious spherical Legendre functions of first kind (Legendre polynomials of first kind). To each index n there corresponds function of definite form. We shall try to c magnitude s with geometric parameters of shell. Comparing equati (6) and (16) we approximately take $s \approx R^2\lambda^2$ or by (8), $s = R\sqrt{12(1-\mu^2)}/h \approx 3.3R/h$.

In Fig. 14.5 is given graph of function $w(\alpha)$, which, proceeding from these approximate dependences, corresponds to ratio $R/h = 50$. As we see, deflection surface here has the same character as in Fig. 14.3. Let us note that number of waves located on given section of meridian increases by measure of growth of ratio R/h; consequently, the thinner the shell, the shorter the wave will be. If amplitude of main dent is taken as 1, the amplitude of adjacent fold will only be equal to 0.4; subsequently, amplitudes gradually decrease with growth of α. During buckling of real shells position of pole of center of basic dent is accidental. In experiments, as we will see below, there may simultaneously appear several focuses of buckling, located in different places of shell. It is necessary to consider that at sufficient distance from pole effect of given focus will not be perceived. If however distance between poles is less than operating range of this effect, then waves belonging to different focuses must overlap.

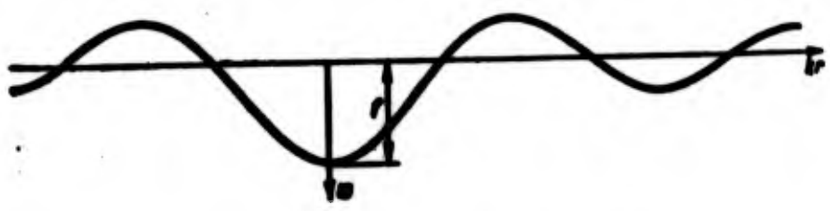

Fig. 14.5. Form of buckling, described by spherical functions.

§ 155. Stability in the Large

Let us turn to research of stability of spherical shell in the large. As we already said, in experiments there is observed either clicking and development of one dent ending in "inversion" of shell, or formation of a group of waves usually united then in one deep dent. In accordance with this two approaches to problem are possible: a) consideration of process of development of single dent occurring in solution of axisymmetric problem, b) research of asymmetric buckling. Up to now we chiefly applied the first of these approaches; it will be explained below.* We consider that on first stage of development of dent, before load reaches lower critical value, behavior of elastic sphere may be described by theory of shallow shells. Fundamental nonlinear equations (10.109) have form (taking into account lateral load q)

$$\left.\begin{aligned} \frac{D}{h}\nabla^4 w &= L(w,\Phi)+\nabla_k^2\Phi+\frac{q}{h}, \\ \frac{1}{E}\nabla^4\Phi &= -\frac{1}{2}L(w,w)-\nabla_k^2 w. \end{aligned}\right\} \qquad (14.18)$$

Considering as before $\nabla_k^2 = (1/R)\nabla^2$, we obtain

$$\left.\begin{aligned} \frac{D}{h}\nabla^4 w &= L(w,\Phi)+\frac{1}{R}\nabla^2\Phi+\frac{q}{h}, \\ \frac{1}{E}\nabla^4\Phi &= -\frac{1}{2}L(w,w)-\frac{1}{R}\nabla^2 w. \end{aligned}\right\} \qquad (14.19)$$

We use polar coordinates r and φ combining origin of radius-vector with center of dent. Considering that functions w and Φ do not depend on φ, we find by (9.16) and (9.29)

$$\left.\begin{aligned} L(w,\Phi) &= \frac{1}{r}\left(\frac{d^2w}{dr^2}\frac{d\Phi}{dr}+\frac{dw}{dr}\frac{d^2\Phi}{dr^2}\right)=\frac{1}{r}\frac{d}{dr}\left(\frac{dw}{dr}\frac{d\Phi}{dr}\right), \\ L(w,w) &= \frac{2}{r}\frac{d^2w}{dr^2}\frac{dw}{dr}, \\ \nabla^2 &= \frac{d^2}{dr^2}+\frac{1}{r}\frac{d}{dr}=\frac{1}{r}\frac{d}{dr}\left(r\frac{d}{dr}\right). \end{aligned}\right\} \qquad (14.20)$$

*Problem of asymmetric buckling of shallow spherical shell was considered by E. I. Grigolyuk (see § 161, p. 788).

Equation (19) it is possible to present in the following manner (after reduction by r):

$$\left.\begin{aligned}\frac{D}{h}\frac{d}{dr}\left[r\frac{d}{dr}(\nabla^2 w)\right]&=\frac{1}{R}\frac{d}{dr}\left(r\frac{d\Phi}{dr}\right)+\frac{d}{dr}\left(\frac{d\Phi}{dr}\frac{dw}{dr}\right)+\frac{qr}{h},\\ \frac{d}{dr}\left[r\frac{d}{dr}(\nabla^2\Phi)\right]&=-E\left[\frac{1}{R}\frac{d}{dr}\left(r\frac{dw}{dr}\right)+\frac{d^2w}{dr^2}\frac{dw}{dr}\right].\end{aligned}\right\} \quad (14.21)$$

We integrate these equations with respect to r; then we obtain (after division by r)

$$\left.\begin{aligned}\frac{D}{h}\frac{d}{dr}(\nabla^2 w)&=\frac{1}{R}\frac{d\Phi}{dr}+\frac{1}{r}\frac{dw}{dr}\frac{d\Phi}{dr}+\frac{1}{h}\Psi,\\ \frac{d}{dr}(\nabla^2\Phi)&=-E\left[\frac{1}{R}\frac{dw}{dr}+\frac{1}{2r}\left(\frac{dw}{dr}\right)^2\right];\end{aligned}\right\} \quad (14.22)$$

by Ψ is implied the function of load:

$$\Psi=\frac{1}{r}\int_0^r qr\,dr. \quad (14.23)$$

Stresses in middle surface are equal (in general case) to

$$\sigma_r=\frac{1}{r}\frac{\partial\Phi}{\partial r}+\frac{1}{r^2}\frac{\partial^2\Phi}{\partial\varphi^2},\quad \sigma_\varphi=\frac{\partial^2\Phi}{\partial r^2},\quad \tau=-\frac{\partial}{\partial r}\left(\frac{1}{r}\frac{\partial\Phi}{\partial\varphi}\right).$$

In axisymmetric problems we have

$$\sigma_r=\frac{1}{r}\frac{d\Phi}{dr},\quad \sigma_\varphi=\frac{d^2\Phi}{dr^2}=\frac{d}{dr}(r\sigma_r),\quad \tau=0. \quad (14.24)$$

Subsequently, we will need expressions for radial displacements u of points of middle surface. We find first deformation of elongation in annular direction:

$$\varepsilon_\varphi=\frac{1}{E}\left(\frac{d^2\Phi}{dr^2}-\frac{\mu}{r}\frac{d\Phi}{dr}\right).$$

On the other hand, magnitude ε_φ is equal to $\varepsilon_\varphi = u/r$; hence

$$u=\frac{r}{E}\left(\frac{d^2\Phi}{dr^2}-\frac{\mu}{r}\frac{d\Phi}{dr}\right). \quad (14.25)$$

We apply these relationships to solution of concrete problem.

We set ourselves the goal of tracing change of maximum deflection of a single dent, forming in a complete spherical shell, depending upon pressure; this should lead to determination of lower critical

load. All solutions of this problem available in literature can be divided into two groups. A significant part of works is based on use of variational methods of Ritz and Bubnov-Galerkin,* and only in the last two works was there conducted numerical integration of differential equations by digital computers.** We stop first on application of variational methods. Difficulty of problem consists here in establishment of boundary conditions on boundary of dent, inasmuch as remaining part of shell also is subjected to deformation. In general, the section of the dent should be considered elastically fastened; however, to approximate deflection surface of dent taking into account deformation of "smooth" zone is difficult. Furthermore, there have appeared a series of methodical questions. In one of first variants of solution [14.10] according to method of Ritz deflection surface was approximated by several variables and then there was produced minimization with respect to one variable of the total energy of the system, and with respect to the other of the magnitude of pressure. Kh.M. Mushtari and R. G. Surkin showed [14.4] that it is more correct to minimize directly with respect to all variables total energy.*** Further, in work [14.9] there were allowed errors in formulation of boundary conditions for forces in middle surface. Regarding application of Bubnov-Galerkin method here it turned out to be essential that we considered change of radius of dent in process of buckling and fundamental equation of method corresponds to principle of virtual

*First work in this region belongs to Kármán and Tsien Hsueh-sêng [14.10]; further research was conducted by Friedrichs [14.9], Kh. M. Mushtari and R. G. Surkin [14.4], [14.6], V. I. Feodos'yev, [14.7], Masuja and Yoshimura [14.12] and other authors.

**These works were carried out in 1961 by A. G. Gabrilyanets, V. I. Feodos'yev [14.1], and also Murray and Wright [14.13].

***Such method was chosen above, in Chapter XI in examining stability of cylindrical shell during axial compression and external pressure.

displacements (see [14.7] and [14.3]).

We give one of the simplest variants of solution of problem with help of Ritz method.* We assume (as first approximation) that boundary of dent (Fig. 14.6) there is met condition of complete clamping:

$$w=0,\quad \frac{dw}{dr}=0 \text{ when } r=c; \tag{14.26}$$

here by c is understood radius of dent. We assume, further, that on edge of dent there are no radial displacements:

$$u=0 \text{ when } r=c; \tag{14.27}$$

by (25) we obtain

$$\frac{d^2\Phi}{dr^2}-\frac{1}{r}\frac{d\Phi}{dr}=0 \text{ when } r=c. \tag{14.28}$$

Fig. 14.6. Form of dent during axisymmetric buckling of spherical shell.

At pole, when $r \to 0$, radial stresses σ_r obviously must be bounded in magnitude. Hence, by (24) there ensues fourth boundary condition:

$$\frac{d\Phi}{dr}=0 \text{ when } r=0. \tag{14.29}$$

Approximating expression for deflection, satisfying conditions (26), we take in the form

$$w=f\left(1-\frac{r^2}{c^2}\right)^2; \tag{14.30}$$

this corresponds to form of deflection surface of circular plate, clamped on its edge and subjected to action of uniform lateral load.

Substituting (30) in the right part of the second of equations (22), we obtain

$$\frac{d}{dr}(\nabla^2\Phi)=-\frac{E}{2r}\frac{16f^2}{c^3}\left(\frac{r}{c}-\frac{r^3}{c^3}\right)^2+\frac{E}{R}\frac{4f}{c}\left(\frac{r}{c}-\frac{r^3}{c^3}\right).$$

---

*This variant was offered by author ([0.3] p. 364) in development of work [14.12].

Integrating this expression, we find

$$\nabla^2\Phi=\frac{1}{r}\frac{d}{dr}\left(r\frac{d\Phi}{dr}\right)=-\frac{8Ef^2}{c^3}\left(\frac{r^3}{2c^3}-\frac{r^5}{2c^5}+\frac{r^7}{6c^7}\right)+$$
$$+\frac{E}{R}\frac{4f}{c}\left(\frac{r^2}{2c}-\frac{r^4}{4c^3}\right)+C_1. \qquad (14.31)$$

New integration gives

$$\frac{d\Phi}{dr}=-\frac{2Ef^2}{c}\left(\frac{r^3}{2c^3}-\frac{r^5}{3c^5}+\frac{r^7}{12c^7}\right)+\frac{Efc}{6R}\left(\frac{3r^3}{c^3}-\frac{r^5}{c^5}\right)+C_1\frac{r}{2}+C_2\frac{1}{r}.$$

Constant C_2 is equal to zero by virtue of condition (29). Determining, further, C_1 from condition (28), we find

$$\frac{d\Phi}{dr}=\frac{Ef^2}{6c}\left(\frac{5-3\mu}{1-\mu}\frac{r}{c}-6\frac{r^3}{c^3}+4\frac{r^5}{c^5}-\frac{r^7}{c^7}\right)-$$
$$-\frac{Efc}{6R}\left[\frac{2(2-\mu)}{1-\mu}\frac{r}{c}-3\frac{r^3}{c^3}+\frac{r^5}{c^5}\right]-\frac{qR}{2h}r. \qquad (14.32)$$

Last member corresponds to fundamental stresses $p_r = p_\varphi = qR/2h$.

We find energy of system. Potential strain energy of middle surface is equal, by (10.95), to

$$U_c=\frac{h}{2E}\int_0^c\left[(\nabla^2\Phi)^2-2(1+\mu)\frac{1}{r}\frac{d\Phi}{dr}\frac{d^2\Phi}{dr^2}\right]2\pi r\,dr. \qquad (14.33)$$

Magnitude $\nabla^2\Phi$ we find, using (31), by expression (32):

$$\nabla^2\Phi=\frac{Ef^2}{3c^3}\left(\frac{5-3\mu}{1-\mu}-12\frac{r^2}{c^2}+12\frac{r^4}{c^4}-4\frac{r^6}{c^6}\right)-$$
$$-\frac{Ef}{3R}\left[\frac{2(2-\mu)}{1-\mu}-6\frac{r^2}{c^2}+3\frac{r^4}{c^4}\right]-\frac{qR}{h}. \qquad (14.34)$$

Expression for U_c by (33) takes form

$$U_c=\frac{(23-9\mu)\pi}{126(1-\mu)}E\frac{h}{c^2}f^4-\frac{(3-\mu)\pi}{9(1-\mu)}\frac{Eh}{R}f^3+$$
$$+\frac{(7-2\mu)\pi}{75(1-\mu)}\frac{Ehc^2}{R^2}f^3-\frac{\pi}{3}qRf^2+\frac{\pi}{3}qc^2f+\frac{1-\mu}{4}\pi q^2\frac{R^2}{E}\frac{c^2}{h}. \qquad (14.35)$$

Potential energy of bending is equal, by (10.95), to

$$U_\sigma=\frac{D}{2}\int_0^c\left[(\nabla^2w)^2-2(1-\mu)\frac{1}{r}\frac{d^2w}{dr^2}\frac{dw}{dr}\right]2\pi r\,dr. \qquad (14.36)$$

Magnitude ∇^2w is equal, by (20) and (30), to

$$\nabla^2w=-\frac{8f}{c^2}\left(1-2\frac{r^2}{c^2}\right). \qquad (14.37)$$

Finally

$$U_c = \frac{32}{3}\pi D\left(\frac{f}{c}\right)^2. \tag{14.38}$$

We determine work of external forces, equal approximately

$$V = \int_0^c q(w + w_0)2\pi r\,dr; \tag{14.39}$$

by w_0 here is understood radial displacement, corresponding to fundamental stresses. Putting in (39) expression (30) and (4) for w and w_0, we find

$$V = \frac{1}{3}qfc^2 + \frac{q^2R^2}{E}(1-\mu)\frac{c^2}{2}. \tag{14.40}$$

Total energy is equal to

$$\Theta = U_c + U_n - V. \tag{14.41}$$

We introduce dimensionless parameters

$$k = \frac{c^2}{Rh} = \frac{R\beta^2}{h}, \quad \hat{\sigma} = \frac{\sigma R}{Eh} = \frac{qR^2}{2Eh^2}, \quad \zeta = \frac{f}{h}, \quad \Theta = \frac{3}{2}\frac{R}{\pi Eh^4}\Theta; \tag{14.42}$$

then we obtain

$$\Theta = \frac{23-9\mu}{84(1-\mu)k}\zeta^4 - \frac{3-\mu}{6(1-\mu)}\zeta^3 + \frac{4}{3(1-\mu^2)k}\zeta^2 + \\ + \frac{7-2\mu}{30(1-\mu)}k\zeta^2 - \hat{\sigma}\zeta^2 - \frac{3(1-\mu)}{2}\hat{\sigma}^2 k. \tag{14.43}$$

We consider variable parameters ζ and k: the first of them characterizes maximum deflection of dent, and the second, its radius. Equations of Ritz method obtain form

$$\frac{\partial\Theta}{\partial\zeta} = 0, \quad \frac{\partial\Theta}{\partial k} = 0. \tag{14.44}$$

Differentiating, we arrive, for $\zeta \neq 0$ at equations

$$\left.\begin{aligned} &\frac{23-9\mu}{21(1-\mu)k}\zeta^2 - \frac{3-\mu}{2(1-\mu)}\zeta + \frac{8}{3(1-\mu^2)k} + \frac{7-2\mu}{15(1-\mu)}k - 2\hat{\sigma} = 0, \\ &\frac{23-9\mu}{84(1-\mu)k^2}\zeta^4 + \left[\frac{4}{3(1-\mu^2)k^2} - \frac{7-2\mu}{30(1-\mu)}\right]\zeta^2 + \frac{3}{2}(1-\mu)\hat{\sigma}^2 = 0. \end{aligned}\right\} \tag{14.45}$$

This system of equations connects magnitudes $\hat{\sigma}$, ζ, and k. We exclude from this k and find dependence $\hat{\sigma}(\zeta)$; then we obtain graph depicted in Fig. 14.7. Lowest point of curve $\hat{\sigma}$ corresponds to value*

*More detailed calculations are given in book [0.3] p. 367.

$$\hat{\sigma}_н = 0.155 \quad \text{when} \quad q_н = 0.155E\frac{h}{R} \tag{14.46}$$

and maximum deflection $\zeta = 9.16$.

Formula (46) determines lower critical stress; to it corresponds pressure

$$q_н = 0.31E\left(\frac{h}{R}\right)^2. \tag{14.47}$$

Value of $\sigma_н$ obtained by us almost is one fourth upper critical stress $\sigma_в$. If we compare formulas (46) and (11.66) for spherical and cylindrical shells, then it turns out that coefficients in them are close to one another, similarly to the way it was in the linear problem.

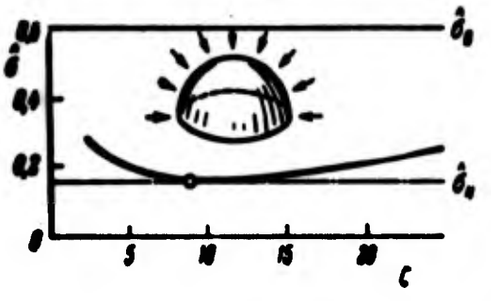

Fig. 14.7. Diagram "stress — deflection" during loss of stability in the large.

Kh. M. Mushtari and R. G. Surkin [14.4] and [14.6] gave definitized solution of problem. They constituted several different approximating expressions for w and, furthermore, for meridional displacement u. In one of variants they took

$$\left.\begin{aligned} w &= f\left(1-\frac{r^2}{c^2}\right)^2\left(1+\frac{1}{2}\frac{r^2}{c^2}\right), \\ u &= u_0\left(1-\frac{r^2}{c^2}\right)\left(1-\frac{6}{5}\frac{r^2}{c^2}\right). \end{aligned}\right\} \tag{a}$$

Further they used Ritz method, and energy of system was minimized with respect to parameters f, c, and u_0. Lower critical stress turned out to be equal to $\hat{\sigma}_н = 0.193/\sqrt{1-\mu^2} \approx 0.203$.

As we already said, threshold condition adopted during derivation of formula (46) do not fully correspond to true character of linkage of zone of dent with other part of shell: clamping on edge of dent must be considered not rigid but elastic. Such assumption was made in work of V. I. Feodos'yev [14.7]; he took following approximating

expression for angle of rotation of normal θ:

$$\theta = A\rho(1-\rho^2)e^{-k\rho}. \qquad (b)$$

where $\theta = -\frac{dw}{dr}$, $\rho = \frac{r}{c}$. Let us note that in preceding solutio ceeding from formula (30), we would obtain $\theta = 2f\rho(1 - \rho^2)$.

Thus, new in (b) is factor $e^{-k\rho}$, considering damping of deflections by measure of removal from dent. If one were to use Bubnov-Galerkin method and in first approximation vary only parameter f, then lower critical pressure turns out to be negative: $\hat{\sigma}_H = -0.13$; this corresponds to pressure directed from center of curvature. If however, in supplement to this we also vary radius of dent r (as this is done in article of Kh. M. Mushtari [14.3]), then we obtain for $\hat{\sigma}_H$ a positive value, $\hat{\sigma}_H = 0.1/\sqrt{1-\mu^2} \approx 0.11$.

If we compare diverse variants of solution of problem, then it will appear that magnitude $\hat{\sigma}_H$ found in them varies in very wide limits. Here is demonstrated that sharp sensitivity of results of application of variational methods to selection of approximating functions which we noted above. Obviously, further precise definition of solution is possible either by increase of number of varied parameters during use of methods of Ritz or Bubnov-Galerkin, or by application of other methods of integration of basic differential equations. In either case, apparently, it is impossible to do without application of digital computers. In connection with this let us turn to results of calculations carried out with help ETsVM (digital computer) in work [14.1] (see also article [14.13]).

A. G. Gabril'yants and V. I. Feodos'yev [14.1] transformed equation (22) introducing new variables; here it was shown that magnitude $\hat{\sigma}_H$ obtained as a result of solutions need not have to depend on ratio

R/h. This important conclusion pertains, of course, only to initial equations of theory of shallow shells. Further, it was assumed that nonlinear dependences extend to certain region with comparatively large deflections, dimensions of which it was possible to change in fairly wide range. Regarding remaining zone of shell, for it fundamental equations were linearized. As we have seen in § 154, solution of such linear equations is expressed in Bessel functions and can be considered known.

The following boundary conditions were taken. For center of dent, when $r = 0$ we considered $\theta = -dw/dr = 0$, and also $d\Phi/dr = 0$ from (29). Furthermore, we wrote four conditions of continuity of functions θ and $\sigma_r = (1/r)(d\Phi/dr)$ along the line of linkage of linear and nonlinear regions; these conditions express equality on this line of angles of rotation of the normal, of bending moments, and also meridional forces and displacements. Machine calculation was applied for numerical integration step by step of equations of type (22) within limits of nonlinear section, from center to boundary. Integration was conducted by trial and error, in order to satisfy above-mentioned conditions of linkage. Results of calculations are shown in Fig. 14.8. Along the axis of abscissas is plotted dimensionless deflection at center $\zeta = w_0/h$, along the axis of ordinates, magnitude $\hat{\sigma}$. Solid line corresponds to fundamental forms of equilibrium, and dotted, to higher forms; these forms are shown in figure. Lowest point of fundamental curve, corresponding to maximum deflection $w \approx 22.5$ h gives magnitude $\hat{\sigma}_H = 0.067$. Thus, judging by this solution of axisymmetric problem, magnitude $\hat{\sigma}_H$ lies significantly lower than it would follow from solutions according to method of Ritz, and at the same time higher

than that value of (-0.13), which was obtained with unvaried radius of dent by Bubnov-Galerkin method. Nevertheless, we must assume that coefficient $\hat{\sigma} = 0.067$ is not yet the final one. First described solution is built on the basis of theory of shallow shells and results can be different if we use definitized equations. Furthermore, problem was considered axisymmetric. Meanwhile, in many experiments discontinuous buckling of shell is expressed in development of

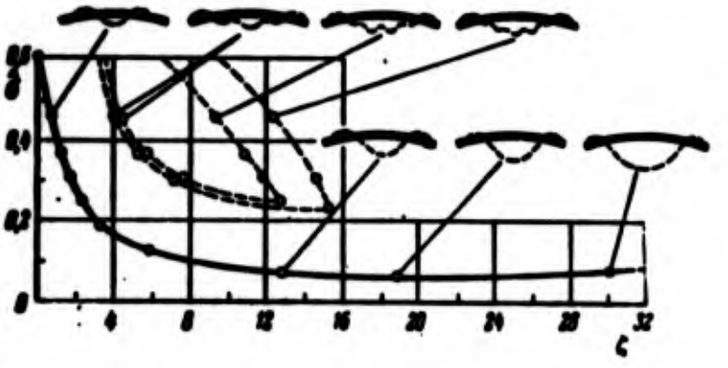

Fig. 14.8. Diagrams of equilibrium states, obtained by digital computers.

series of dents, filling certain region of shell, and is accompanied by mutual influence (interference) of dents, similarly to the way this occurs in case of cylindrical shell. But then problem should be considered asymmetric. Therefore, theoretical research of this important problem must be continued.

Influence of <u>initial imperfections</u> of form on behavior of spherical shells during axisymmetric buckling was studied by R. G. Surkin [14.6] with help of method of Ritz and analogously to how this was described above for cylindrical shells (§ 133). It turned out that, e.g., with maximum initial deflection of dent, equal to thickness of shell, upper critical pressure $\hat{\sigma}_в$ is lowered by 39% as compared to $\hat{\sigma}_в$ for shell of ideal form.

Geometric approach to problem, offered by A. V. Pogorelov [14.5], is based on the fact that buckling of spherical shell (or convex shell of other form) in the large should correspond to isometric transformation of the middle surface. But then, as we saw in § 119, form of dent will correspond to mirror reflection of segment of shell in the plane intersecting it (see Fig. 10.17). Let us consider strain energy formed with such buckling, as this was done for cylindrical shells; it can be composed from energy of bending in zone of dent and strain energy of strip lying between dent and smooth zone. Determining this energy by parameters of dent, it is possible approximately to determine lower critical pressure.

§ 156. Data of Experiments and Recommendations for Practical Calculations

As was already noted above, carrying out of experiments with complete spherical shell is difficult. In article [14.10] are given data of test of spherical segment with aperture angle of 180° with $R/h = 900$. Loss of stability consisted of an abrupt pressing through of a hollow subtending central angle of 16° with maximum deflection $f = 12.5\ h$. Critical stress was equal to $\hat{\sigma} = 0.154$. Numerous experiments with spherical segments were also conducted by R. G. Surkin.* Test pieces were prepared from sheet material (steel, brass, copper, aluminum) by drawing under oil pressure.** Character of buckling of shell depended on form of load. When in internal region there was

*R. G. Surkin, S. G. Stepanov, article in collection "Theory of plates and shells," Kiev., 1962, 311-313.

**We note original method of manufacture of analogous test pieces, offered by L. S. Palatnik and consisting of condensing metal evaporated in vacuum on glass mold (see book of A. V. Pogorelov [14.5] p. 62).

created a vacuum, loss of stability occurred in the process of a sharp knock. During loading by liquid (oil) effect of knock was significantly less. Shell initially lost stability, as a rule, in [illegible] tric form. For shells with high rise, where H/c = 0.6 to 0.75 (see Fig. 14.1) there were observed different pictures of buckling. For certain test pieces there appeared a crescent-shaped dent, adjacent to edge; with subsequent loading this dent continued to expand, embracing whole peripheral part of segment (Fig. 14.9). Another example is shown in Fig. 14.10, from results of high-speed filming. Initially near boundary here there formed one dent, fast deepening; then there appeared adjacent dents. Comparison of separate frames shows that edges of dents changed their outlines in process of buckling. A case of clearly expressed asymmetric loss of stability, occurring in the form of a very strong knock and accompanied by formation of several waves on circumference, is shown in Fig. 14.11. Last, in separate cases there took place pressing through of central zone of shell (Fig. 14.12).

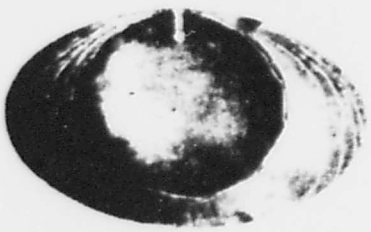

Fig. 14.9. Crescent-shaped dent.

Judging by these experimental data, available theoretical research is far from covering whole range of different forms of loss of stability in the large.

As for experimental values of critical pressure, they turned out to vary greatly and depend on magnitude of angle subtended by segment. We shall characterize curvature of segment by parameter (see Fig. 14.1)

$$\lambda^2 = \sqrt{12(1-\mu^2)}\,\frac{c^2}{Rh}; \qquad (14.48)$$

we assume $\theta \leq 180^\circ$.

In case of steel shells with total subtended angle θ from 9 to 45°, parameter λ^2 from 70 to 350 and ratio R/h from 800 to 3900 tested by creation of a vacuum, there was obtained $\hat{\sigma}$ from 0.606/4.11 to 0.606/2.23; during test by oil pressure magnitude $\hat{\sigma}$ constituted from 0.606/3.8 to 0.606/2.61. We note that tests with constant volume give smaller scattering of experimental points than with constant pressure. For copper shells with subtended angle from 106 to 140°, λ^2 from 1700 to 2350 and R/h from 813 to 860 there were fixed least values of $\hat{\sigma}$, from 0.606/6.14 to 0.606/4.19.

As a result it is necessary to consider that real critical stresses $\hat{\sigma}_{кр}$ of high spherical segments lie between upper critical value $\hat{\sigma}_в = 0.605$ and lower value, which we conditionally will consider equal to $\hat{\sigma}_н = 0.155$. At the same time, calculated values $\hat{\sigma}_{расч}$ should depend on angle, subtended by segment, parameter of curvature λ^2 and ratio R/h. Picture here is obtained approximately the same as for cylindrical shells, although theoretically, lower critical pressure is not connected with ratio R/h; with large values of R/h one should expect significant initial flaws in form of shell, and this leads to lowering of $\hat{\sigma}_{кр}$. Now before accumulation of new theoretical and experimental data in practical calculations one should originate from different values of $\hat{\sigma}_{расч}$ depending upon parameter of curvature of segment. Tentatively it is possible to offer following table for $\hat{\sigma}_{расч}$ and critical pressure $q_{расч}$ pertaining to carefully made shells:

λ^2 by (42)	From 100 to 800	From 800 to 1500	More than 1500
$\hat{\sigma}_{расч}$ by (42) $q_{расч}$	0,15 $0{,}3Eh^2/R^2$	0,12 $0{,}24Eh^2/R^2$	0,09 $0{,}18Eh^2/R^2$

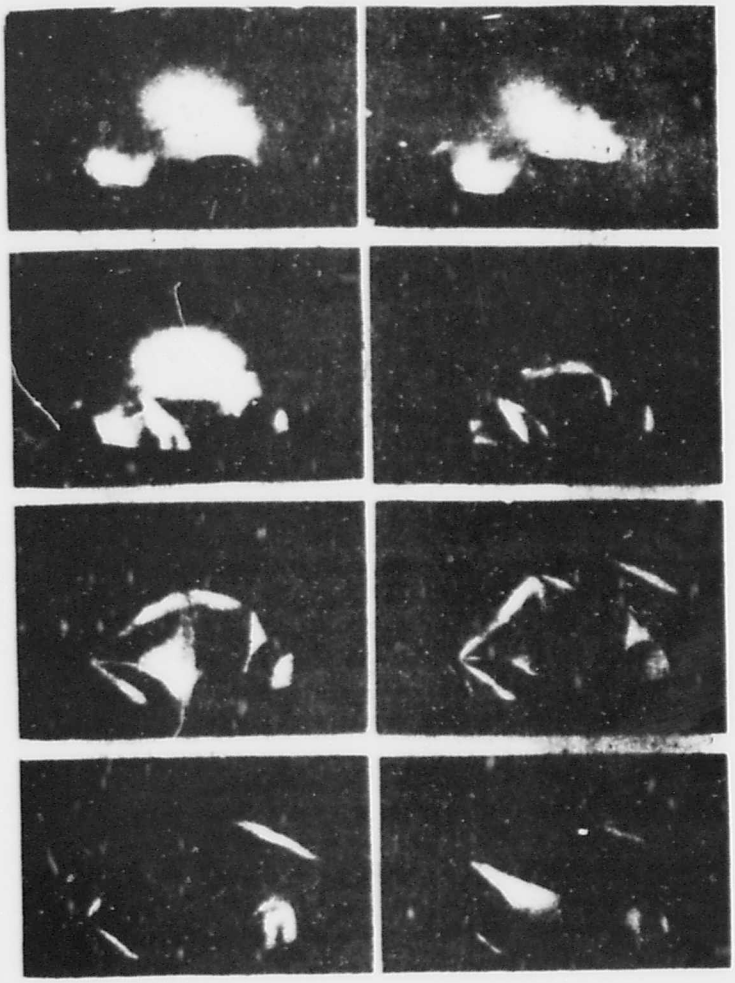

GRAPHIC NOT REPRODUCIBLE

Fig. 14.10. Process of buckling of spherical shell by data of filming.

Fig. 14.11. Asymmetric form of loss of stability.

With initial deflections attaining magnitude of order of thickness of shell these values one should be approximately halved.

We give also experimental formula, recommended in work [14.11] for shells with ratio R/h lying between 400 and 2000, and angle θ from 40 to 120°:

$$q_{\text{расч}} = 0{,}3kE\left(\frac{h}{R}\right)^2;$$

here coefficient k is determined by the formula

$$k = \left(1 - 0{,}175\,\frac{\theta^\circ - 40^\circ}{40^\circ}\right) \times \left(1 - 0{,}07\,\frac{R}{400h}\right).$$

In conclusion let us note that recently during raising of certain constructions they apply domes in the form of shells of revolution with diamond-shaped "dents." Form of these preliminary dents, as it is easily noted, is characteristic for loss of stability of shell in the large. Dependence between lateral load and displacements for such shell should correspond to ascending branch BD of Fig. 10.2, so that shell is as if beforehand in clicked through state. Study of constitution diagrams for shells of different form allows us to make a series of conclusions, pertaining to strength and stability of such domes; it is desirable to analyze this question in more detail.

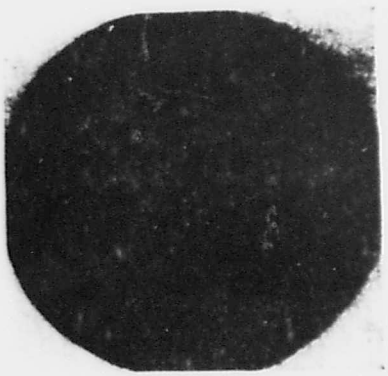

Fig. 14.12. Buckling of shell with pressing through of central part.

§ 157. Ellipsoidal Shells

Let us give, further, data for a calculation of stability of ellipsoidal shells of revolution, encountered in aircraft construction,

chemical industry, instrument-making. It is necessary to distinguish prolate ellipsoids, formed by rotation around axis AB of ellipse with semiaxes a and b where a < b (Fig. 14.13), and oblate (compressed) ellipsoids, where a > b (Fig. 14.14). Let us assume that ellipsoidal shell is subjected to action of external evenly distributed pressure q. Problem of stability of such a shell* is related to analogous problem pertaining to spherical shell, since in both cases we are talking about formation of local dents. For prolate ellipsoidal shell one should expect appearance of such dents in zone of equator, since main radii of curvature of middle surface are the biggest here. Upper critical pressure is equal to

$$q_* = \frac{2E}{\sqrt{3(1-\mu^2)}} \frac{h^2}{2b^2 - a^2} \approx 1{,}21E \frac{h^2}{2b^2 - a^2}. \qquad (14.49)$$

In case of flattened shell, on the contrary, first dents should form

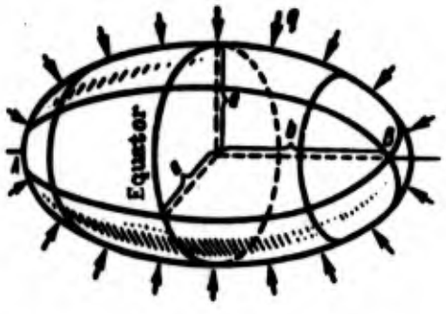

Fig. 14.13. Prolate ellipsoidal shell.

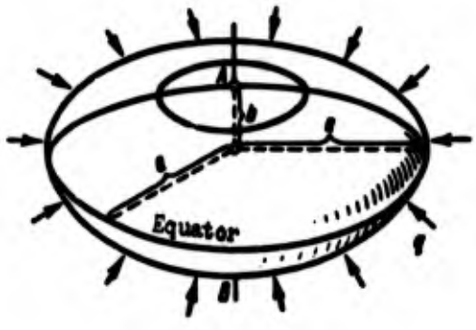

Fig. 14.14. Oblate (compressed) ellipsoidal shell.

in zone of poles A and B. Main curvatures at poles are equal to $R_1 = R_2 = a^2/b$; here known formula (10) for spherical shell turns out to be applicable with replacement of R by a^2/b:

$$q_* = \frac{2E}{\sqrt{3(1-\mu^2)}} \frac{h^2 b^2}{a^4} \approx 1{,}21E \frac{h^2 b^2}{a^4}. \qquad (14.50)$$

*This problem was considered in linear form by Kh. M. Mushtari [10.9] and in nonlinear form by R. G. Surkin [14.6]; see also book [0.6].

We give also experimental formula, recommended in work [14.11] for shells with ratio R/h lying between 400 and 2000, and angle θ from 40 to 120°:

$$q_{\text{расч}} = 0{,}3kE\left(\frac{h}{R}\right)^2;$$

here coefficient k is determined by the formula

$$k = \left(1 - 0{,}175\,\frac{\theta^\circ - 40^\circ}{40^\circ}\right) \times \left(1 - 0{,}07\,\frac{R}{400h}\right).$$

In conclusion let us note that recently during raising of certain constructions they apply domes in the form of shells of revolution with diamond-shaped "dents." Form of these preliminary dents, as it is easily noted, is characteristic for loss of stability of shell in the large. Dependence between lateral load and displacements for such shell should correspond to ascending branch BD of Fig. 10.2, so that shell is as if beforehand in clicked through state. Study of constitution diagrams for shells of different form allows us to make a series of conclusions, pertaining to strength and stability of such domes; it is desirable to analyze this question in more detail.

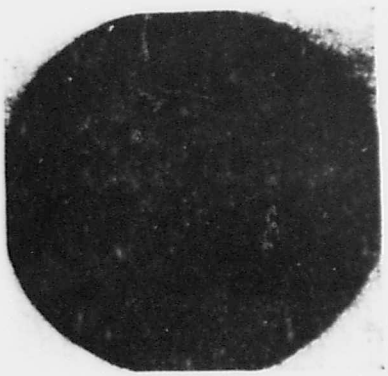

Fig. 14.12. Buckling of shell with pressing through of central part.

§ 157. Ellipsoidal Shells

Let us give, further, data for a calculation of stability of ellipsoidal shells of revolution, encountered in aircraft construction,

Literature

14.1. A. G. Gabril'yants and V. I. Feodos'yev. On axisymmetric forms of equilibrium of an elastic spherical shell, under action of evenly distributed pressure, Applied math. and mech., 25, No. 6 (1961), 1091-1101.

14.2. L. S. Leybenzon. On application of harmonic func[illegible] to problems of stability of spherical and cylindrical shells, Sci. notes of Yuryev University, No. 1 (1917), Collection of works, Vol. 1, Publishing House of Acad. of Sci. of USSR, 50-85.

14.3. Kh. M. Mushtari. To theory of stability of a spherical shell under action of external pressure, Applied math. and mech., 19, No. 2 (1955).

14.4. Kh. M. Mushtari and R. G. Surkin. On the nonlinear theory of stability of elastic equilibrium of a spherical shell during action of evenly distributed external pressure, Applied math. and mech., 14, No. 6 (1950), 573.

14.5. A. V. Pogorelov. To theory of convex elastic shells in the postcritical region, Khar'kov University Press, 1960.

14.6. R. G. Surkin. To theory of stability and strength of spherical and ellipsoidal shells, bottoms and diaphragms, Cand. diss., Kazan' branch of Academy of Sciences of USSR, 1952; Concerning the question of loss of stability of a spherical shell, News of Kazan' branch of Academy of Sciences of USSR, 10 (1956).

14.7. V. I. Feodos'yev. On stability of a spherical shell under the action of external evenly distributed pressure, Applied math. and mech., 18, No. 1 (1954), 35-42.

14.8. W. Z. Chien and H. C. Hu. On the snapping of a thin spherical cap, 9th Congress Int. Mech. Appl. Univ. Bruxelles 6 (1956), 309-320.

14.9. K. O. Friedrichs. On the minimum load for spherical shells, Th. Kármán ann. Volume, 1941, 258-272.

14.10. Th. Kármán and H. S. Tsien. The buckling of spherical shells on external pressure, J. Aeron. Sci. 7 (1949), 43.

14.11. K. Klöppel and O. Jungbluth. Beitrag zum Durchschlags-problem dünnwandiger Kugelschalen, Stahlbau 22, No. 6 (1953), 121-130.

14.12. U. Masuja and Y. Yoshimura. The buckling of spherical shells by external pressure, Proc. 2nd Japan Nat. Congress Appl. Mech., 1953, 145-148.

14.13. F. J. Murray and F. W. Wright. The buckling of thin spherical shells, J. Aerospace Sciences 28, No. 3 (1961).

14.14. R. Zoelly. Ueber ein Knickungsproblem an der Kugelschale, Zürich 1915.

CHAPTER XV

STABILITY OF SHALLOW SHELLS UNDER ACTION OF LATERAL LOAD

§ 158. Initial Dependences

We considered till now shells of various outline, considering that initial curvatures of middle surface can be significant. We separate now especially shallow shells, having small curvatures. In Fig. 15.1 are shown examples of shallow shells, one of which is rectangular in design and the other, circular in design. Let us

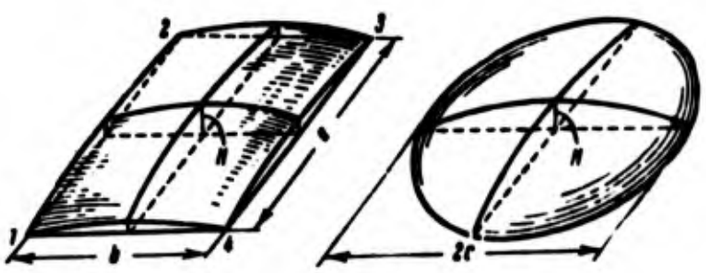

a) b)

Fig. 15.1. Shallow shell, a) rectangular in projection, b) circular in projection.

agree to consider a shell shallow, if rise H does not exceed 1/5 of least dimension in projection.* We assume, further, that shell is

*Such limitation was shown by V. Z. Vlasov (see [10.3], p. 303). E. Reissner in examining shells of revolution assumed that for shallow shell maximum angle of inclination of tangent must not exceed 1/3 (E. Reissner, Journ. Math. and Mech. 7, No. 2, (1958), p. 128).

subjected to action of load, directed on normal to middle surface (pressure of gas or liquid), or load, directed perpendicularly to base plane (weight of shell, weight of snow for roofs, etc.). Shallow shells are applied at present more and more widely in building constructions; they enter also into construction of aircraft, submarines, etc.

During research of shallow shells, under action of transverse forces it is necessary, as a rule, to consider stress to have moment already in first stages of loading. If we limit ourselves determination of stress of shell during small deflections, then it is possible to set it in the frames of linear theory. Distinction between shallow shell and flat plate then show only in the fact that for shell it is necessary to consider secondary stress in middle surface. However, for calculation for stability of shallow shell it is important to study large deflections from propositions of nonlinear theory.

Let us consider diverse variants of diagram "load maximum deflection," which are characteristic of shallow shells of different curvature. In case of very shallow shell parameter of load q monotonically increases with increase of maximum deflection f (Fig. 15.2a); diagram here has point of inflection C, where on first section OC rigidity of shell drops, and on second it increases. If initial

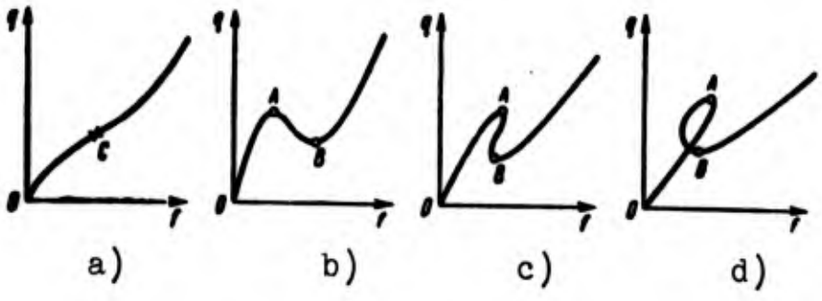

Fig. 15.2. Diverse variants of diagram "load – maximum deflection."

rise of shell is comparable with thickness, diagram obtains limit point A (Fig. 15.2b); here with given conditions – when load is "dead" – loss of stability becomes possible, expressed in clicking of shell to new stable equilibrium state. Further, in Fig. 15.2c there is depicted diagram q(f), corresponding to shell of greater curvature; falling branch AB of unstable states lies near initial branch OA. We analyzed such curves in Chapter XI; clicking becomes possible here with any behavior of load. Last, we meet examples, when deflection in center of shell at a certain stage of load decreases and diagram q(f) becomes loop-shaped (Fig. 15.2d); this is connected with change of form of wave formation.*

In certain cases clicking of shallow shells is a necessary property of them (flapping diaphragms in instruments). On the other hand, for shells, serving as roofs in building constructions, and in many other examples phenomenon of clicking is impermissible. In any case for calculation of shallow shells for stability we must know characteristic points of diagram "load-deflection."

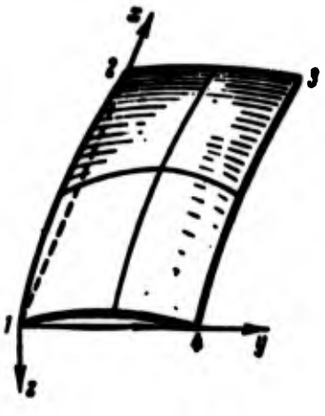

Fig. 15.3. Shallow shell, considered as plate with initial deflection.

In deriving basic dependences of nonlinear theory of shallow shells two approaches are possible. The first of them consists of direct use of equations of Chapter X. We originate from equations (10.111) for shell having initial deflections from ideal form, and introduce in them, instead of total deflection,

*Such type of diagram was obtained by A. Yu. Birkgan for cylindrical panels; see also work of Budyanskiy [15.12].

additional deflection $w_1 = w - w_0$; in expanded form equations will take form

$$\frac{D}{h}\nabla^4 w_1 = \frac{\partial^2 \Phi}{\partial x^2}\left(\frac{\partial^2 w_1}{\partial y^2} + \frac{\partial^2 w_0}{\partial y^2}\right) + \frac{\partial^2 \Phi}{\partial y^2}\left(\frac{\partial^2 w_1}{\partial x^2} + \frac{\partial^2 w_0}{\partial x^2}\right) - \\ - 2\frac{\partial^2 \Phi}{\partial x\,\partial y}\left(\frac{\partial^2 w_1}{\partial x\,\partial y} + \frac{\partial^2 w_0}{\partial x\,\partial y}\right) + k_x \frac{\partial^2 \Phi}{\partial y^2} + k_y \frac{\partial^2 \Phi}{\partial x^2} + \frac{q}{h}. \qquad (15.1)$$

$$\frac{1}{E}\nabla^4 \Phi = \left(\frac{\partial^2 w_1}{\partial x\,\partial y}\right)^2 - \frac{\partial^2 w_1}{\partial x^2}\frac{\partial^2 w_1}{\partial y^2} + 2\frac{\partial^2 w_1}{\partial x\,\partial y}\frac{\partial^2 w_0}{\partial x\,\partial y} - \\ - \frac{\partial^2 w_1}{\partial x^2}\frac{\partial^2 w_0}{\partial y^2} - \frac{\partial^2 w_1}{\partial y^2}\frac{\partial^2 w_0}{\partial x^2} - k_x \frac{\partial^2 w_1}{\partial y^2} - k_y \frac{\partial^2 w_1}{\partial x^2}. \qquad (15.2)$$

Equations (1) and (2) are obtained on the assumption that displacements u, v and w of a point of middle surface are counted off along tangent to lines of curvature x and y on normal to surface; all dimensions of shell also are naturally measured along lines of curvature. By k_x and k_y are implied initial curvatures of lines x and y.

Another approach consists of considering shell as <u>plate with initial deflection</u>. Let us assume that contour of shell in projection is rectangular. Then it is convenient to introduce Cartesian coordinates x and y, laying them in fundamental plane 1-4 along sides of contour (Fig. 15.3). Let us assume that, further, coordinate z determines initial position of points of middle surface.* Deflection w_1 now should be counted off from initial middle surface parallel to axis z. In such treatment in equations (1), (2) we must put $k_x = k_y = 0$ and introduce z in place of w_0; then we have**

$$\frac{D}{h}\nabla^4 w_1 = \frac{\partial^2 \Phi}{\partial x^2}\left(\frac{\partial^2 w_1}{\partial y^2} + \frac{\partial^2 z}{\partial y^2}\right) + \frac{\partial^2 \Phi}{\partial y^2}\left(\frac{\partial^2 w_1}{\partial x^2} + \frac{\partial^2 z}{\partial x^2}\right) - 2\frac{\partial^2 \Phi}{\partial x\,\partial y}\left(\frac{\partial^2 w_1}{\partial x\,\partial y} + \frac{\partial^2 z}{\partial x\,\partial y}\right) + \frac{q}{h}. \qquad (15.3)$$

---

*With location of system of coordinates in Fig. 15.3 values of z will be negative.

**These equations were given by K. Marguerre, Proc. of 5th Internat. Congress of Appl. Mech., 1938.

$$\frac{1}{E}\nabla^4\Phi=\left(\frac{\partial^2 w_1}{\partial x\,\partial y}\right)^2-\frac{\partial^2 w_1}{\partial x^2}\frac{\partial^2 w_1}{\partial y^2}+2\frac{\partial^2 w_1}{\partial x\,\partial y}\frac{\partial^2 z}{\partial x\,\partial y}-$$
$$-\frac{\partial^2 w_1}{\partial x^2}\frac{\partial^2 z}{\partial y^2}-\frac{\partial^2 w_1}{\partial y^2}\frac{\partial^2 z}{\partial x^2} \qquad (15.4)$$

or, in compact notation,

$$\left.\begin{aligned}\frac{D}{h}\nabla^4 w_1&=L(\Phi,\ w_1+z)+\frac{q}{h},\\ \frac{1}{E}\nabla^4\Phi&=-L\left(w_1,\ \frac{1}{2}w_1+z\right).\end{aligned}\right\} \qquad (15.5)$$

If we use this approach, then dimensions of shell should be presented as dimensions in plane xy.

Systems of equations (1)-(2) and (3)-(4) are equivalent* on the condition that central angle 2φ, subtended by the greatest dimension of shell, is sufficiently small, so that it is possible to take $\cos\varphi \approx 1$, $\sin\varphi \approx \varphi$. Let us turn to separate problems, pertaining to shell of different form.

§ 159. Panel, Rectangular in Projection

We start from case when panel with main curvatures k_x and k_y has outline, rectangular in projection (Fig. 15.1a); magnitudes k_x and k_y are assumed constant. Dimensions of sides of support contour we designate by a and b. Let us assume that on edges the shell is fastened by hinge with ribs, absolutely rigid under flexure in direction of normal and at the same time having low flexural rigidity in planes tangent to middle surface. Furthermore, we consider that points belonging to end sections of shell freely slip along ribs. To these assumptions there correspond following boundary conditions for edges $x = 0$, $x = a$:

$$w=0,\quad \frac{\partial^2 w}{\partial x^2}=0;\quad \sigma_x=0,\quad \tau=0. \qquad (15.6)$$

*This question is considered in book of Kh. M. Mushtari and K. Z. Galimov [0.6], p. 181.

and analogous conditions for edges y = 0, y = b. We assume that load of intensity q is evenly distributed over the entire surface and acts on the convex side.*

We use equations (1)-(2); taking $w_0 \equiv 0$, we will present them in the form

$$X \equiv \frac{D}{h}\nabla^4 w_1 - L(\Phi, w_1) - k_x\frac{\partial^2\Phi}{\partial y^2} - k_y\frac{\partial^2\Phi}{\partial x^2} - \frac{q}{h} = 0. \tag{15.7}$$

$$Y \equiv \frac{1}{E}\nabla^4\Phi + \frac{1}{2}L(w_1, w_1) + k_x\frac{\partial^2 w_1}{\partial y^2} + k_y\frac{\partial^2 w_1}{\partial x^2} = 0. \tag{15.8}$$

With boundary conditions given above it is possible to use for integration of system (7)-(8) the Bubnov-Galerkin method, applying it simultaneously to two equations of system.** We approximate function w and Φ in first approximation by expressions

$$w_1 = f_1 \sin\frac{\pi x}{a}\sin\frac{\pi y}{b}, \quad \Phi = A_1 \sin\frac{\pi x}{a}\sin\frac{\pi y}{b}. \tag{15.9}$$

As it is easy to see, first three boundary conditions of type (6) are satisfied on all edges; fourth condition is executed only "on the average," so that, for edges x = 0, x = a we have $\frac{1}{a}\int_0^b \tau dy = 0$. We write Budnov-Galerkin:

$$\int_0^a\int_0^b X \sin\frac{\pi x}{a}\sin\frac{\pi y}{b}\,dx\,dy = 0, \quad \int_0^a\int_0^b Y \sin\frac{\pi x}{a}\sin\frac{\pi y}{b}\,dx\,dy = 0. \tag{15.10}$$

Substituting here (7)-(9) and integrating, we obtain

$$\left.\begin{aligned} &\frac{D}{h}f_1\frac{\pi^6}{16}\left(\frac{1}{a^2}+\frac{1}{b^2}\right)^2 - A_1 f_1\frac{2}{3}\frac{\pi^4}{a^2b^2} + \\ &\qquad + A_1\frac{\pi^4}{16}\left(\frac{k_x}{b^2}+\frac{k_y}{a^2}\right) - \frac{q}{h} = 0. \\ &\frac{A_1}{E} + \frac{16}{3\pi^2\left(\frac{b}{a}+\frac{a}{b}\right)^2}f_1^2 - \left(\frac{k_x}{b^2}+\frac{k_y}{a^2}\right)\frac{1}{\pi^2}\frac{1}{\left(\frac{1}{a^2}+\frac{1}{b^2}\right)^2}f_1 = 0. \end{aligned}\right| \tag{15.11}$$

---

*This pertains to shell of positive and zero Gaussian curvature.

**Such approach was already taken in § 91, see p. 392.

We introduce dimensionless parameters

$$\left.\begin{aligned} k_x^* = \frac{k_x a^2}{h}, \quad k_y^* = \frac{k_y b^2}{h}, \quad k^* = k_x^* + k_y^*, \quad \lambda = \frac{a}{b}, \\ \zeta = \frac{f_1}{h}, \quad q^* = \frac{q}{E}\left(\frac{ab}{h^2}\right)^2; \end{aligned}\right\} \tag{15.12}$$

then by (11) we arrive at following dependence between load and deflection:*

$$q^* = \frac{32\pi^2}{9}\frac{1}{\left(1+\frac{1}{\lambda}\right)^2}\zeta^3 - k^*\frac{\pi^2}{\left(1+\frac{1}{\lambda}\right)^2}\zeta^2 + \left[\frac{\pi^2}{16}k^{*2}\frac{1}{\left(1+\frac{1}{\lambda}\right)^2} + \frac{\pi^4\left(\frac{1}{\lambda}+\lambda\right)^2}{192(1-\mu^2)}\right]\zeta. \tag{15.13}$$

If panel is square (a = b), for $\mu = 0.3$ we have

$$q^* = 8.77\zeta^3 - 2.46k^*\zeta^2 + (0.154k^{*2} + 22)\zeta. \tag{15.14}$$

When shell has <u>cylindrical</u> form and coordinate y is counted off along arcs, we must take $k_x = 0$, $k_y = 1/R$; then we have $k^* = b^2/Rh$. For <u>spherical</u> shell we obtain; $k_x = k_y = 1/R$; when a = b we find $k^* = 2b^2/Rh$. It is interesting to consider case of shell of negative Gaussian curvature. In § 119 there was given example of a pseudosphere, for which $k_x = -k_y$; if we consider a = b, then here we have $k^* = 0$. Equation (14) obtains form

$$q^* = 8.77\zeta^3 + 22\zeta.$$

If we judge by these data, panel of pseudosphere will behave as a flat plate; losses of stability in form, corresponding to (9), cannot occur here.

---

*This dependence was obtained by M. A. Koltunov [15.4]; definitized solution to be mentioned later, carried out with help of digital computers, is his.

On graph of Fig. 15.4 dotted lines depict diagram $q^*(\zeta)$ according to (13) for different values of k^* when $\lambda = 1$. As we see, for small k^* magnitude q^* continuously increases, like case of flat plate; for large k^* diagram has descending section. In order to find value of k^* at which clicking becomes possible it is necessary to investigate derivative $dq^*/d\zeta$. Equating it to zero, we find values of ζ, corresponding to upper and lower critical loads;

$$\zeta = \frac{3}{32}k^* \mp \frac{1}{32}\sqrt{3k^{*2} - \frac{\pi^4\left(\lambda+\frac{1}{\lambda}\right)^4}{2(1-\mu^2)}}. \qquad (15.15)$$

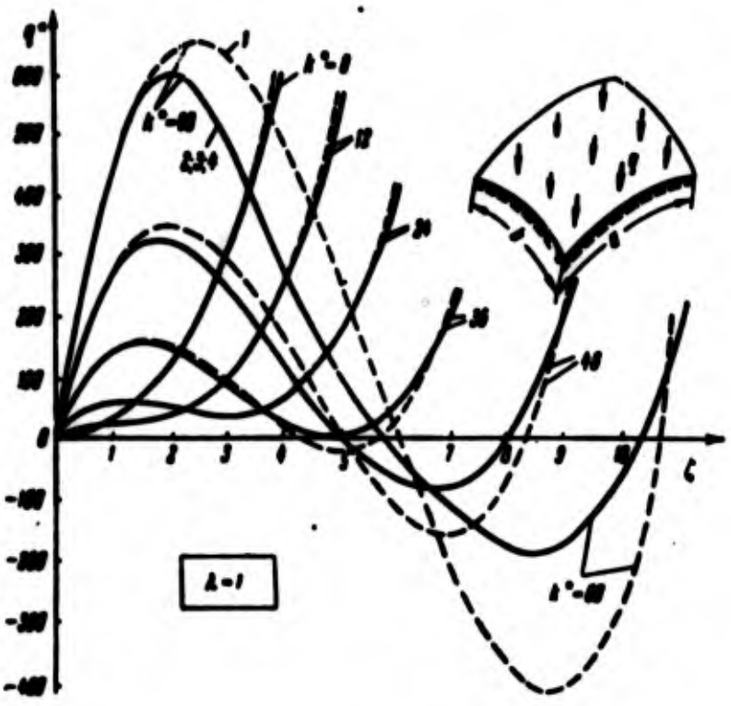

Fig. 15.4. Graph "load-deflection" for square-projection panel.

Boundary of region of clicking corresponds to the case when diagram $q^*(\zeta)$ has point of inflection with horizontal tangent;* here expression under radical in (15) should turn into zero. Thus, limiting value of k^* will be

$$k^* = \frac{\pi^2\left(\lambda+\frac{1}{\lambda}\right)^2}{\sqrt{6(1-\mu^2)}} \quad \text{when} \quad \zeta = \frac{3}{32}k^*.$$

Here we pass from diagram of Fig. 15.2a to diagram of the type depicted in Fig. 15.2b.

At first glance, in the course of designing it is desirable to designate such values of curvatures, at which clicking of shells will be excluded. It is easy to see, however, that here initial section of diagram will have small angle with axis of abscissas, so that rigidity of shell will appear insignificant. Therefore, from practical point of view it is important to determine q_B^* and q_H^* as exactly as possible for shells of relative great curvature. We present, for this, functions w and Φ in the form of series:

$$w = \sum_{i,j} f_{ij} \sin \frac{i\pi x}{a} \sin \frac{j\pi y}{b}, \quad \Phi = \sum_{i,j} A_{ij} \sin \frac{i\pi x}{a} \sin \frac{j\pi y}{b}. \tag{15.16}$$

Solution will be more nearly exact, the larger the number of members of series we take into account during calculations. We give results of such solution, carried out with help of digital computer. If we retain in series (16) members with indices (1, 1) and (2, 2) and then join to them members (3, 3) and (4, 4), we will obtain solid curves of Fig. 15.4, designated correspondingly by 2, 3, 4; on the figure they merge. However, the distinction from data of first approximation turns out to be very perceptible, starting with $k^* \approx 36$. Definitized diagrams give somewhat lower upper critical loads, where peak of curve shifts toward smaller deflections. But lower critical load especially changes, and toward increase; in certain cases it changes sign and becomes positive. Near q_B curve becomes steeper, and near q_H, more gently sloping.* Hence it is clear that when $k^* < 60$ the second approximation gives practically exact results; true, before making final conclusions, one should conduct additionally

---

*V. I. Feodos'yev came to analogous conclusions, investigating by digital computer the clicking of shallow spherical segments (see § 161, p. 784).

calculation for combinations of indices (1, 3), (3, 1), etc., and also consider antisymmetric forms of buckling. On graph of Fig. 15.5 are given values of upper and lower critical loads depending upon k* for plates with various ratios of sides according by data of the fourth approximation ($\lambda = 1$, $\lambda = 1/\sqrt{2}$, $\lambda = 0.5$); we take $\mu = 0.3$. Clicking occurs when $k^* > 18$ for $\lambda = 1$; when $k^* > 20.4$ for $\lambda = 1/\sqrt{2}$ and when $k^* > 30$ for $\lambda = 0.5$. Obviously, with increase of λ rigidity of shell drops.

Let us note that fourth boundary condition of (6) may be satisfied at all points of the edge, if we select approximating expression for Φ in the form $\Phi = U(x)V(y)$, where U and V are "beam" functions, satisfying condition of clamping of a beam on its edges.* If we consider a square panel, then in equation (14) essentially only the coefficient with ζ^3 is essentially changed; it takes value 7.48 instead of 8.77.

Let us turn to other cases of fastening of edges of a panel. Let us assume, e.g., that ribs bordering panel remain rectilinear, and at the same time freely approach one another. Proceeding analogously, we arrive, for a square panel in first approximation, at the equation (for $\mu = 0.3$)

$$q^* = 7.5\zeta^3 - 2.06k^*\zeta^2 + (0.154k^{*2} + 22)\zeta. \qquad (15.17)$$

Coefficient with ζ^2 renders substantial influence on character of diagram, lower critical loads as compared to preceding case greatly increase. Clicking turns out to be possible when $k^* > 25.3$. If,

---

*This solution is given by M. M. Kozarov, cand. disc. MISI [Moscow Construction Engineering Institute], 1955.

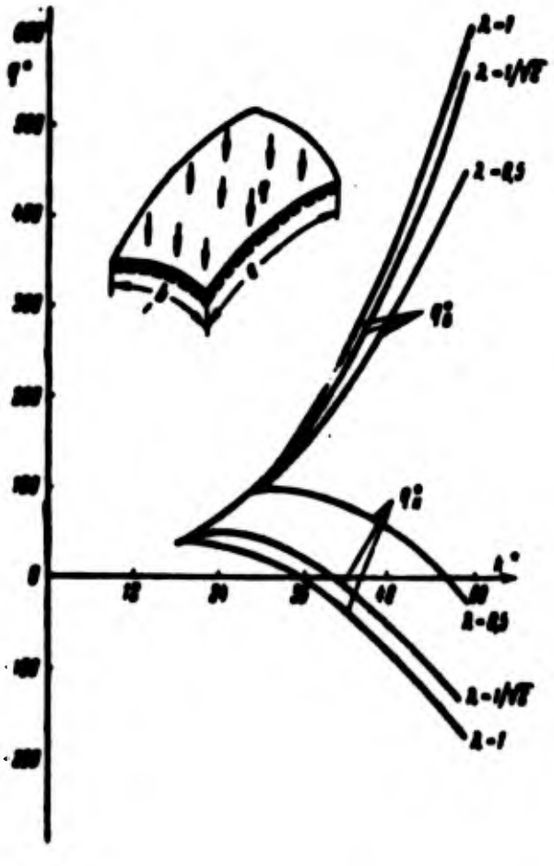

Fig. 15.5. Values of lower and upper critical loads for shallow panels.

however, ribs are not displaceable; dependence (17) obtains form

$$q^* = 28.9\zeta^3 - 6.1\lambda^2\zeta^2 + (0.5\lambda^2 + 22)\zeta. \qquad (15.18)$$

It is desirable that for these cases, important from the point of view of practical applications, there be given definitized solutions.

Let us note that for an elongated cylindrical panel ($a \gg b$) there may be obtained exact solution of the problem;* here we investigate behavior of arch-strip with corresponding conditions of fastening.

§ 160. Conical Panel

We turn to case when outline of panel in projection on a plane

*This solution was given by I. G. Bubnov [0.2] and M. S. Kornishin and Kh. M. Mushatri [15.5].

is not rectangular, but circular. Let us consider at first conical, and then a spherical, panel. Let us assume that shallow shell, with angle of rise $\alpha < 1/5$, is subjected to action of uniform pressure (Fig. 15.6). We shall consider that panel is clamped on its edge and that together with that points of edge shift freely in plane (sliding fixing).* Peculiarities of problem, connected with presence of vertex of cone, we will not consider.

Fig. 15.6. Conical panel under action of lateral load.

Fig. 15.7. System of coordinates for examining conical panel.

We shall use the second of approaches to the problem according to § 158, presenting shell as a distorted plate. From Fig. 15.7 we find $z = Hr/c = \alpha r$, where $\alpha \approx \tan \alpha = H/c$; by c is understood radius of base, by H--initial rise. We take for a base equations (5) and (6) and express operators in polar coordinates r and φ, as in Chapter IX (p. 476). Introducing relative coordinate $\rho = r/c$, we obtain

$$\frac{D}{h}\nabla^4 w = \frac{1}{\rho}\frac{c}{\partial\rho}\left(\frac{\partial\Phi}{\partial\rho}\frac{\partial w}{\partial\rho}\right)+\frac{1}{\rho^2}\left(\frac{\partial^2\Phi}{\partial\varphi^2}\frac{\partial^2 w}{\partial\rho^2}+\frac{\partial^2\Phi}{\partial\rho^2}\frac{\partial^2 w}{\partial\varphi^2}\right)+$$
$$+\frac{2}{\rho^2}\left(\frac{\partial^2\Phi}{\partial\rho\,\partial\varphi}\frac{\partial w}{\partial\varphi}+\frac{\partial\Phi}{\partial\varphi}\frac{\partial^2 w}{\partial\rho\,\partial\varphi}\right)-\frac{2}{\rho^2}\frac{\partial^2\Phi}{\partial\rho\,\partial\varphi}\frac{\partial^2 w}{\partial\rho\,\partial\varphi}-$$
$$-\frac{2}{\rho^2}\frac{\partial\Phi}{\partial\varphi}\frac{\partial w}{\partial\varphi}+\frac{c\alpha}{\rho h}\frac{\partial^2 w}{\partial\rho^2}+\frac{q}{h}c^4. \qquad (15.19)$$

$$\frac{1}{E}\nabla^4\Phi = \frac{1}{\rho^2}\left(\frac{\partial^2 w}{\partial\rho\,\partial\varphi}\right)^2-\frac{2}{\rho^2}\frac{\partial w}{\partial\varphi}\frac{\partial^2 w}{\partial\rho\,\partial\varphi}+\frac{1}{\rho^2}\left(\frac{\partial w}{\partial\varphi}\right)^2-\frac{1}{\rho}\frac{\partial w}{\partial\rho}\frac{\partial^2 w}{\partial\rho^2}-$$
$$-\frac{1}{\rho^2}\frac{\partial^2 w}{\partial\rho^2}\frac{\partial^2 w}{\partial\varphi^2}-\frac{c\alpha}{\rho}\frac{\partial^2 w}{\partial\rho^2}; \qquad (15.20$$

*Similar problem was considered by E. I. Grigolyuk [15.3]. Solution below mentioned belongs to I. I. Trapezin [15.8].

Laplacian operator has the form

$$\nabla^2=\frac{\partial^2}{\partial\rho^2}+\frac{1}{\rho}\frac{\partial}{\partial\rho}+\frac{1}{\rho^2}\frac{\partial^2}{\partial\varphi^2}.$$

Boundary conditions will be

$$w=0,\quad \frac{\partial w}{\partial\rho}=0,\quad \varepsilon_\rho=0,\quad \tau=0 \text{ when } \rho=1. \tag{15.21}$$

We select approximate expression for deflection, satisfying the first two of conditions (21), in the form*

$$w=f_1(1-\rho^2)^2+f_2\rho^4(1-\rho^2)^2\cos n\varphi. \tag{15.22}$$

First member in (22) corresponds, as already indicated in Chapter IX, to solution of axisymmetric linear problem for clamped plate, and the second depicts bending in n waves along arc with equal amplitudes toward and away from center of curvature. In combination these two members characterize formation of a series of dents, chiefly directed toward center of curvature.

Putting (22) in the right part of equation (20), we find

$$\frac{1}{E}\nabla^4\Phi=R_0+R_n\cos n\varphi+R_{2n}\cos 2n\varphi. \tag{15.23}$$

where R_0 and R_n are certain functions of ρ, containing parameters f_1 and f_2. Integrating (23), taking into account the fact that in center of panel, when $\rho = 0$, magnitude σ_r should be bounded, we obtain

$$\frac{1}{E}\Phi=\Phi_0+\Phi_n\cos n\varphi+\Phi_{2n}\cos 2n\varphi. \tag{15.24}$$

where Φ_0, Φ_n, and Φ_{2n} are new functions of ρ, f_1, and f_2. We then integrate equation (19) by Bubnov-Galerkin method, then we arrive at the following two dependences:

$$q^*=C_1\zeta^3+C_2\zeta^2+C_3\zeta+C_4\zeta^2+C_5\zeta, \tag{15.25}$$

$$B_1\zeta^2+B_2\zeta+B_3\zeta+B_4\zeta^2+B_5\zeta^2+B_6\zeta^2=0; \tag{15.26}$$

*This expression was used earlier by V. I. Feodos'yev in examining flexible round plates [15.10].

here there are introduced parameters

$$q^* = \frac{q}{E}\left(\frac{c}{h}\right)^4, \quad \zeta = \frac{f_1}{h}, \quad \xi = \frac{f_2}{h}. \tag{15.27}$$

Coefficients C_1, ..., C_5 and B_1, ..., B_6 depend on number of waves n. Let us note that dimensionless magnitude ζ characterizes according to (27) deflection of panel center. Excluding ξ from system (25)-(26), we find dependence $q^*(\zeta)$, where the case n = 0 corresponds to axisymmetric form of deflection.

In Fig. 15.8 is given diagram $q^*(\zeta)$ for c/h = 100 when $\alpha = 0.1$ and n = 0 (solid line). If we construct curves for $n \neq 0$, then up to value $\zeta = 7.5$ they will go above the curve corresponding to axisymmetric form of equilibrium, and for $\zeta > 7.5$, below this curve. For example in Fig. 15.8 there is given dotted line, pertaining to n = 10. Consequently, asymmetric form of buckling should appear during deflection in center, equal to 7.5 thicknesses of the shell. The envelope of family of curves corresponding to different n, when $\zeta > 7.5$ differs little from curve, corresponding to axisymmetric

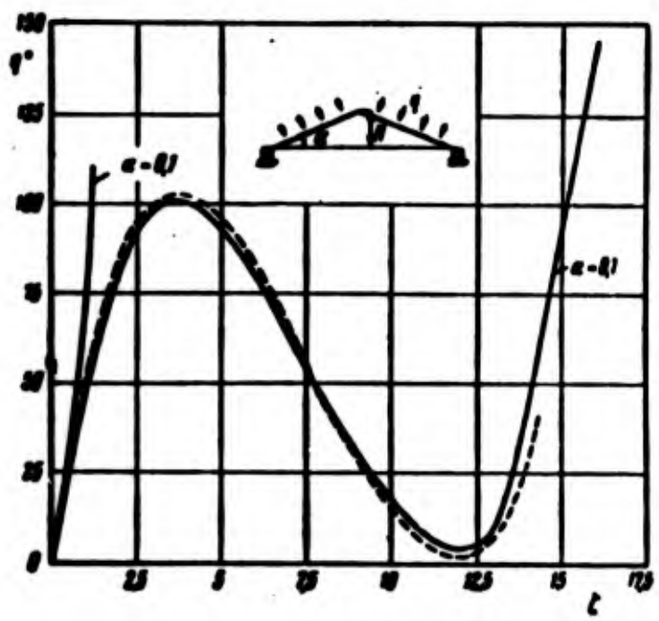

Fig. 15.8. Diagram of equilibrium forms for conical panel.

form.* Lower critical pressure turns out to be close to zero.

If we consider analogously the case of rigid fixing of panel, when points of edge do not shift, then lower critical pressure for c/h = 100 will be negative.

Let us assume, further that conical panel with sliding fixing on the edge is subjected to action of concentrated force P in center, directed along the axis. Research of axisymmetric buckling of panel leads to following dependence between load P and maximum deflection f;

$$P^* = 0.294\zeta^3 - 0.332\frac{ac}{h}\zeta^2 + \left[0.16\left(\frac{ac}{h}\right)^2 + 1.47\right]\zeta,$$

where $P^* = Pc^2/Eh^2$, $\zeta = f/h$.

§ 161. Spherical Panel

Let us turn to problem of the stability of a shallow spherical segment (Fig. 15.9), loaded by evenly distributed external pressure.

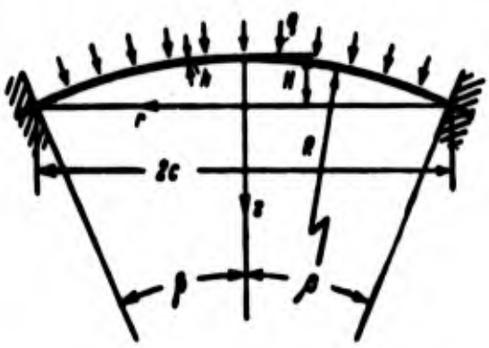

Fig. 15.9. Spherical shallow panel.

This problem has been the subject of numerous studies;** it turned out to be sufficiently difficult, and results of works of different authors frequently appeared contradictory. Study of behavior of shallow panel is intimately connected with research pertaining to complete spherical shell or a high segment, since panel serves as

*This conclusion pertains only to given example. With other parameters of shell result may be different, so that research of asymmetric buckling will be necessary.

**First work in this direction pertained to calculation of flapping diaphragms and belonged to V. I. Feodos'yev [15.9] and [15.10].

a model of the dent, developed during buckling of such shells. At the same time calculation of shallow panels, form of which nears spherical, is itself of great practical value.

We designate by H rise of shell; by c, radius in plane; by R, radius of curvature of middle surface; by β, half of the angle, subtended by panel. As it is easy to see, these magnitudes are connected by relationships*

$$c^2 \approx 2RH, \quad \beta \approx \frac{c}{R}, \quad \frac{R\beta^2}{h} \approx 2\frac{H}{h}. \tag{15.28}$$

Up to now we considered, as a rule, the axisymmetric form of buckling of shallow spherical shell. We originate from equations of type (1) and (2), considering that there is no initial deflection ($w_0 = 0$). Introducing polar coordinates and considering $w = w(r)$ and $\Phi = \Phi(r)$, we can find first integral of these equations, as in Chapter XIV. When q = const by (14.22) we obtain

$$\frac{D}{h} r \frac{d}{dr} \frac{1}{r} \frac{d}{dr} r \frac{dw}{dr} = \left(\frac{d\varphi}{dr} + \frac{r}{R}\right)\frac{d\Phi}{dr} + \frac{qr^2}{2h}, \tag{15.29}$$

$$\frac{1}{E} r \frac{d}{dr} \frac{1}{r} \frac{d}{dr} r \frac{d\Phi}{dr} = -\left(\frac{1}{2}\frac{dw}{dr} + \frac{r}{R}\right)\frac{dw}{dr}. \tag{15.30}$$

We introduce dimensionless parameters**

$$\theta = \frac{r}{c}, \quad \omega = \frac{1}{R\beta^2}\frac{dw}{d\theta} + \theta, \quad \tau = \frac{1}{Eh^3\sqrt{m}}\frac{d\Phi}{dr}, \tag{15.31}$$

$$p' = \frac{1}{\sqrt{m}}\frac{\beta^2 R}{h}, \quad P = \frac{1}{2E\sqrt{m}} q \left(\frac{R}{h}\right)^2, \quad m = \frac{1}{12(1-\mu^2)}; \tag{15.32}$$

---

*If one were to originate from instruction of E. Reissner, shown on p. 763, by (28) spherical shell should be considered shallow when $H/R \leq 1/6$.

**Such parameters are introduced by Reiss, Greenberg and Keller [15.16].

then equations (29) and (30) will change into the following:

$$L'(\alpha)=\rho'(\alpha\gamma+P\theta^2), \tag{15.33}$$

$$L'(\gamma)=\frac{1}{2}\rho'(\theta^2-\alpha^2), \tag{15.34}$$

where by L' is understood linear operator

$$L'=\theta\frac{d}{d\theta}\frac{1}{\theta}\frac{d}{d\theta}\theta. \tag{15.35}$$

Parameters ρ' and P are connected with magnitudes k and $\hat{\sigma}$ introduced by us in Chapter XIV by relationships

$$\rho'=\frac{1}{\sqrt{m}}k, \quad P=\frac{\hat{\sigma}}{\sqrt{m}}. \tag{15.36}$$

We consider that panel is clamped on its edge and that there are no radial displacements of points of edge, as shown in Fig. 15.9. Then boundary conditions obtain form

$$\alpha=0, \quad \gamma=0 \quad \text{when} \quad \theta=0, \tag{15.37}$$

$$\alpha=1, \quad \frac{d\gamma}{d\theta}-\mu\gamma=0 \quad \text{when} \quad \theta=1. \tag{15.38}$$

One variant of solution of problem is the following (15.16). We present magnitudes α and γ in the form of θ-power series:

$$\alpha=\sum_n a_n\theta^{2n-1}, \quad \gamma=\sum_n \gamma_n\theta^{2n-1}. \tag{15.39}$$

The first of expressions (39) constitutes generalization of approximating formula, which we used in § 113, Chapter IX.* Actually, by (9.51), we find

$$\frac{dw}{dr}=-4f\left(\frac{r}{c^2}-\frac{r^3}{c^4}\right)=-\frac{4f}{c}(\theta-\theta^3).$$

---

*See also first member of expression (22), pertaining to conical panel.

Increasing number of members retained in (39) as compared to (9.52), we increase accuracy of solution.

Expressions (39) satisfy boundary conditions (37). By (38) we obtain

$$\left.\begin{aligned}\sum_n a_n - 1 = 0,\\ \sum_n [2n-(1+\mu)]\gamma_n = 0.\end{aligned}\right\} \tag{15.40}$$

Putting (39) in equations (33) and (34), we have

$$a_2 = \frac{\rho'}{8(a_1\gamma_1 + R)}, \quad \gamma_2 = \frac{\rho'}{8(1-a_1^2)} \quad \text{for} \quad n=2 \tag{15.41}$$

and, further,

$$a_n = \frac{\rho'}{4n(n-1)}\sum_{i=1}^{n-1} a_i\gamma_{n-i}, \quad \gamma_n = -\frac{\rho'}{4n(n-1)}\sum_{i=1}^{n-1} a_i a_{n-i} \quad \text{for} \quad n>2 \tag{15.42}$$

These formulas allow us to express all coefficients α_n and γ_n by α_1 and γ_1. Equations (40) then take form

$$F(a_1, \gamma_1) = 0, \quad G(a_1, \gamma_1) = 0. \tag{15.43}$$

where F and G are nonlinear functions of α_1 and γ_1. In work (15.16) determination of roots of equations (43) was conducted by digital computers; there were found points 1, 2, 3, ... on diagram "load P-maximum deflection ζ", as shown in Fig. 15.10. Most favorable was the case when line OAB, connecting these points had a descending branch AB: this gave possibility of finding upper critical load with certain confidence. However, process of calculations did not always lead to required results. Thus, for instance, in individual cases dependence $P(\zeta)$ obtained from depicted in Fig. 15.10 by dotted line; at a certain point C the process of calculations started to part. Such cases in general, we frequently meet during solution of

systems of nonlinear equations in problems of stability; they require additional research, since they can be caused by peculiarities of the given program of calculations. In any case, speculatively take point C for determination of upper critical load. We give comparatively reliable results, pertaining to determination of upper critical load.* In Fig. 15.11 is given dependence of upper critical pressure q_B on geometric parameters of shell for different conditions of fastening: rigid clamping on edge (curve 1), hinged fastening with points of edge not shifting in plane (curve 2) and hinged support with edge freely shifting in plane (curve 3). Along the axis of abscissas is plotted magnitude

Fig. 15.10. Diagrams "load-deflection" according to calculations on digital computers.

$$\rho = \sqrt{2}\rho' = \sqrt{12(1-\mu^2)}\frac{Rp^2}{h} = \sqrt{12(1-\mu^2)}k. \qquad (15.44)$$

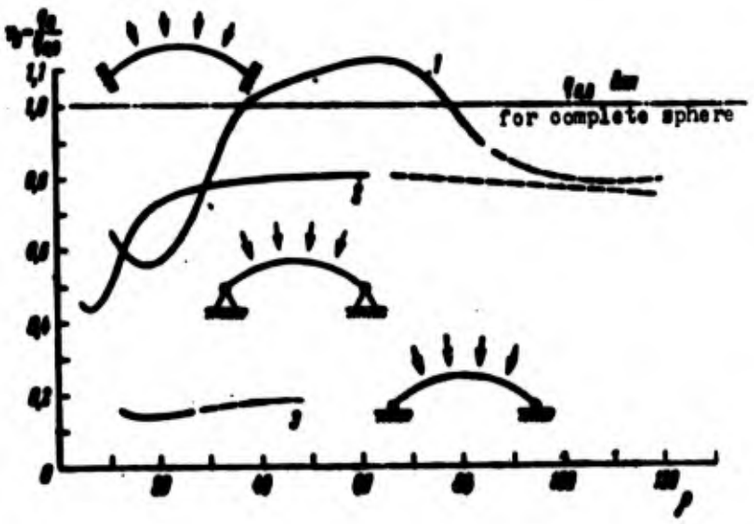

Fig. 15.11. Upper critical load for shallow spherical panel with various conditions of fastening.

*They were obtained by Weinitschke [15.19].

Using relationships (28), we express also parameter ρ by ratio H/h:

$$\rho = 2\sqrt{12(1-\mu^2)}\frac{H}{h} \text{ or, when } \mu = 0.3,\ \rho \approx 6.6\frac{H}{h}. \qquad (15.45)$$

Along the axis of ordinates are plotted values of parameter

$$\nu_B = \frac{p_B}{2\sqrt{2}} = \frac{\sqrt{3(1-\mu^2)}}{2}\frac{q_0}{E}\left(\frac{R}{h}\right)^2. \qquad (15.46)$$

Judging by expression (14.10), in (46) there appears magnitude of upper critical pressure for complete sphere; we designate it $q_{0,B}$. Consequently, magnitude ν_B characterizes upper critical load for shallow panel over $q_{0,B}$; $\nu_B = q_B/q_{0,B}$. When $\rho > 40$ ($k > 12$) process of calculations converged so slowly that results could not be considered final; corresponding sections of curves are shown in Fig. 15.11 by dotted line. We turn first of all to case of panel clamped on its edge. Values ν_B lie for $\rho < 25$ significantly below 1: at the same time for $35 < \rho < 75$ they exceed 1 and, last, when $\rho > 75$ they again lie below 1. Such a form of curve $\nu_B(\rho)$ improbable at first glance, is explained by the fact that depending upon value ρ character of wave formation of shell turns out to be different. This circumstance is confirmed by experiments* conducted on shells made of magnesium alloy and rigidly clamped on their edges. With small ρ deflection was maximum at center and monotonically decreased in the direction of edge (Fig. 15.12a). With large values of ρ middle part of dent became more shallow and at $\rho > 20$ maximum deflection always took place not at the center (Fig. 15.12b). In case of developed

*Number of experiments with shallow spherical segments was conducted by G. N. Geniyev and N. S. Chausov [15.2], and also R. G. Surkin (see § 156). Here are given data obtained by Kaplan and Fung [15.14].

a) b) c)

Fig. 15.12. Forms of wave formation of spherical panels of different curvature.

dent maximum deflection will already be a distance of half the radius from the center. When $\rho > 55$ there appeared a new peak in the center (Fig. 15.12c).

We return to graph of Fig. 15.11. Comparison of curve 2 with curve 1 shows that in a definite region, where $15 < \rho < 30$, magnitude q_B for case of hinged fastening lies higher than during clamping of panel on its edge. This is explained, possibly, by different influence of flexural stresses, formed at the edge. In remaining region of variation of ρ for hinge fastened shell we obtain values of ν_B smaller than for clamped shell. Especially sharply drops ν_B with edge freely displaced in plane.

Let us note that formulation of problem here differs from that taken in § 155. There we conditionally assumed that fundamental state is momentless, and introduced initial deflection w_0. If, though, using equations (14.45), we try to find upper critical pressure for $\zeta \to 0$, we will obtain

$$\hat{\sigma}_B = \frac{8}{3(1-\mu^2)k^2} + \frac{7-2\mu}{15(1-\mu)}k^2.$$

If, then, we construct by this equation curve $\hat{\sigma}_B(k)$, it will remind us of initial section of curve 1 of Fig. 15.11.

All these data pertain to upper critical pressure. Judging by results of experiments (see Fig. 15.15 below), buckling of real shells occurs during load, lying, as a rule, significantly below q_B.

Obviously, here there appear the same peculiarities of the problem as in case of complete sphere. Therefore reliable bases for calculation can be obtained only after study of character of other sections of curve $q(\zeta)$ and determination of lower critical pressure. Such data were obtained very recently also with the help of digital computers.* We give final results of calculations. In Fig. 15.13**

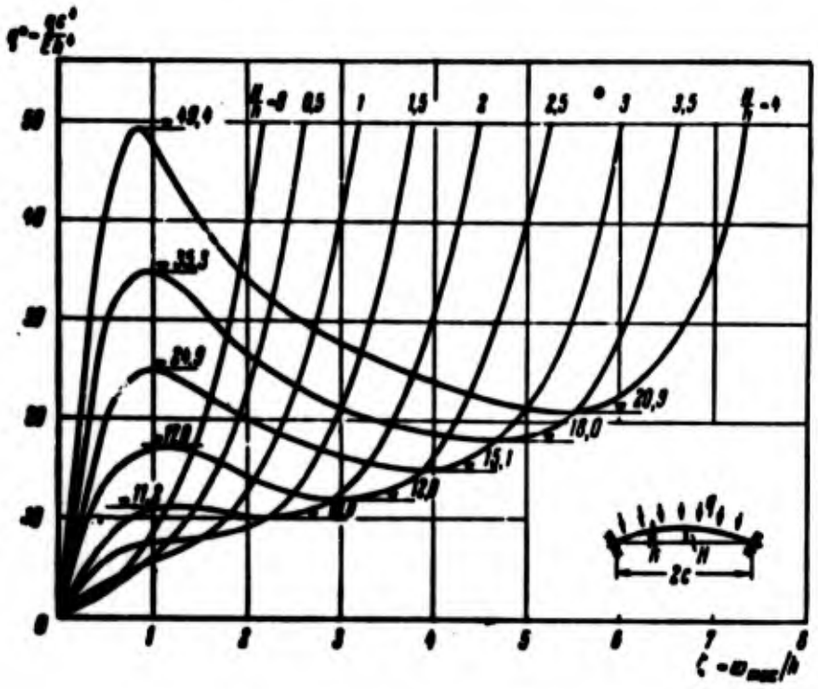

Fig. 15.13. Upper and lower critical loads for spherical panels.

is offered dependence between parameter of load $q^* = qc^4/Eh^4$ and dimensionless maximum deflection in center $\zeta = w_{max}/h$ for panels having different initial curvatures and rigidly clamped their edges. When $H/h = 0$ we obtain case of flat plate. Further, for very shallow

*These studies were carried out almost simultaneously by V. I. Feodos'yev and Thurston [15.18]; let us note that results of these works, obtained by different methods, turned out to be very close.

**Graphs of Figs. 15.13 and 15.16 belong to V. I. Feodos'yev.

panel ($H/h < 1.5$ or $\rho < 11$) load increases with increase of ζ monotonically, which corresponds to Fig. 15.2a. For panels of greater curvature graph $q^*(\zeta)$ obtains form shown in Fig. 15.2b. On graph are marked values of upper and lower critical pressures, where maximum value of H/h here constitutes 4; this corresponds to $\rho \approx 26$.

Fig. 15.14. Branches of equilibrium states of shallow shells of various curvatures.

In case $\rho > 26$ process of calculations is significantly complicated; this is explained by change of character of wave formation in process of buckling of shell. As we have seen from Fig. 15.12, maximum deflection will occur for $\rho > 26$, as a rule, not in center w^0 of panel; on certain sections of loading deflection in center will decrease (see Fig. 15.2d). Nevertheless, we define parameter ζ as deflection in center, over thickness; $\zeta = w^0/h$. In Fig. 15.14* are depicted results of calculations, pertaining to panels of somewhat greater rise, where $36 < \rho < 81$. For values $\rho = 49$ and $\rho = 64$, we obtained several different branches of equilibrium states of shell, not interconnected. Some of these branches correspond, apparently, to stable, and other, to unstable forms of equilibrium. Parameter γ plotted here along the axis of ordinates is equal to

$$\gamma = 6(1-\mu^2)\sqrt{3(1-\mu^2)}q^0 \text{ or, when } \mu = 0.3,\ \gamma \approx 9q^0. \qquad (15.47)$$

*Graphs of Figs. 15.14 and 15.15 were obtained by Thurston [15.18].

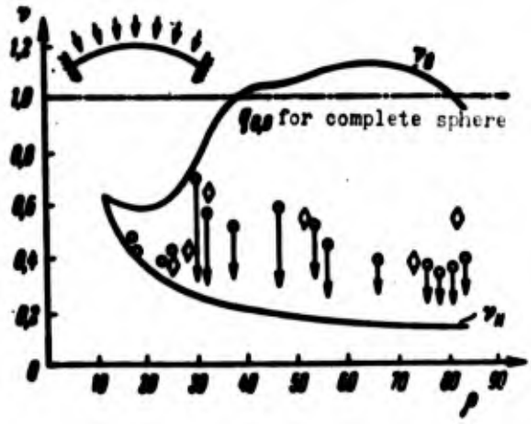

Fig. 15.15. Theoretical values of upper and lower critical loads in comparison with data of experiments.

Study of curves of Figs. 15.13 and 15.14 allowed us to determine upper and lower values of critical pressure q_B and q_H when $0 < \rho < 80$. These final data are shown in Fig. 15.15: along the axis of ordinates are plotted as before parameters ν_B and ν_H, characterizing ratios of q_B and q_H to magnitude $q_{0,B}$ for complete sphere. Curve for ν_B almost coincides with that which was obtained by other methods (see curve 1 of Fig. 15.11); line ν_H is a new one for us. In graph of Fig. 15.15 are also given results of experiments of (15.14); one part of them was obtained with loading of shell by oil (diamonds), and the other part, with loading by air (circles). One may assume that in first case buckling occurred with constant volume, and in second, with constant pressure. Knock appeared the sharpest in the second case; drop of load marked in experiments is shown in Fig. 15.15 by pointers. As we see, experimental values of ν lie in a fork, formed by ν_B and ν_H, and here for $\rho > 40$ nearer to ν_H. In practical calculations one should use graph of Fig. 15.15, determining, for carefully made shells, ν_H directly by curve of graph, but with relatively great initial deflection, with decrease of ν_H by approximately 40%. In

case of hinged fastening of shell there can be obtained tentative calculating data, comparing graphs of Fig. 15.11 and 15.15.

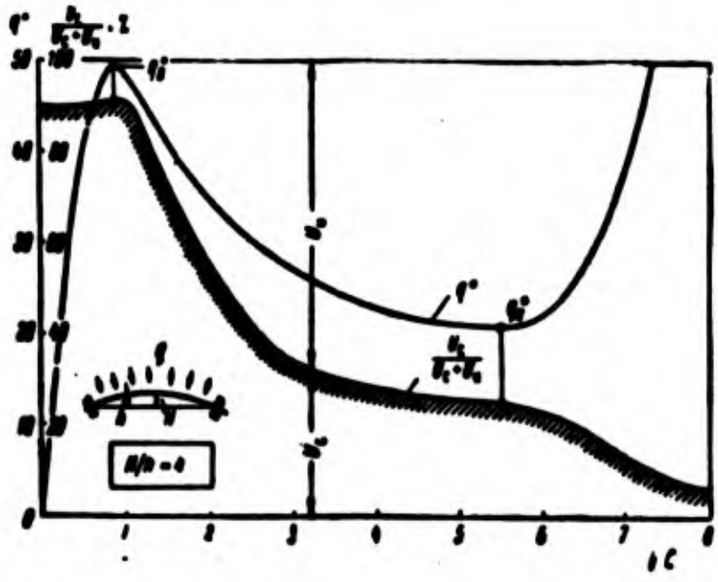

Fig. 15.16. Change of specific weight of strain energy of middle surface during buckling of shell in the large.

In conclusion we give interesting data, allowing us to judge in what relationship potential strain energy of shell is divided into two parts--strain energy of middle surface U_c and energy of bending $U_и$. In Fig. 15.16 is repeated curve $q^*(\zeta)$, pertaining to panel clamped on its edge, with $H/h = 4$. Here it is shown how ratio $U_c/U_c + U_и$, expressed in %, changes in process of buckling. As we see, with small deflections ($\zeta < 1$) basic share--about 90%--of total energy is taken by strain energy of middle surface; this proportion is preserved when $q = q_в$. Then specific weight of U_c rapidly drops, but still at lower critical pressure U_c constitutes approximately 23% of total energy. With subsequent buckling share of U_c drops already to 6%; calculations for values $\zeta > 8$ still remain to be conducted. These data express question of possibility of disregarding magnitudes U_c for $U_в$ during study of different stages of process of

buckling of shell; it is necessary, however, to consider that they pertain only to an individual example.

We considered above only an axisymmetric problem. However, by analogy with case of conical panel it is natural to assume that for certain value of deflection there should occur formation of waves on circumference, where number of waves will depend on intensity of load. As already was noted above, consideration of such problem was started by E. I. Grigolyuk [15.3], taking approximating expression in form, analogous to (22). It is desirable that subsequently these studies be continued both for a shell of ideal form, and also for case of shell with initial deflection with consideration of different conditions of fastening of shell on the edge.

We note unique means of solution of nonlinear problems of theory of shells, offered by N. A. Kilchevskiy (Reports of academy of Sciences of Ukrainian SSR, No. 7, 1962), consisting of use of equivalent linear model with variable elastic characteristics.

Literature

15.1. Ye. F. Burmistrov. Calcualtion of shallow orthotropic shells taking into account ultimate strains, Eng. Collection, 22 (1955), 83-97.

15.2. G. A. Geniyev and N. S. Chausov. Certain questions of nonlinear theory of stability of shallow metal shells, Stroyizdat, M., 1954.

15.3. E. I. Grigolyuk. Nonlinear vibrations and stability of shallow bars and shells, News of Acad. of Sci. of USSR, OTN, No. 3 (1955), 35-68; Applied math. and mech., 19, No. 3 (1955), 376-382; On asymmetric buckling of shells of revolution, News of Acad. of Sci. of USSR, OTN, Mech. and machine building (1960); Proc. IUTAM Symposium on the theory of thin elastic shells, Amsterdam (1960), 112-121.

15.4. M. A. Koltunov. Calculation of finite displacements in the problem of bending and stability of plates and shallow shells, Herald of Moscow State University, No. 5 (1952); Definitized solution of problem of stability of rectangular panels of flexible shallow shells, loc. cit., No. 3 (1961), 37-45.

15.5. M. S. Kornishin and Kh. M. Mushtari. Stability of infinitely long shallow cylindrical panel under action of normal uniform pressure, News of Kazan' branch of Academy of Sciences of USSR, series on phys-math. and tech. sciences, 7 (1955).

15.6. Kh. M. Mushtari and I. V. Svirskiy. Determining large deflections of a cylindrical panel supported on flexible unextensible ribs, under action of external normal pressure, Applied math. and mech., 17, No. 6 (1953), 755-760.

15.7. A. A. Nazarov. On large deflections of shallow shells, Sci. notes of Saratov State University (1956); On large deflections and stability of shallow shell of double curvature with rigidly fastened edges, Reports of Acad. of Sci. of Ukrainian SSR, No. 3 (1956).

15.8. I. I. Trapezin. Finite deformations of a conical shell with small angle of rise, loaded by uniform hydrostatic pressure, "Strength analysis," 3 (1958), Mashgiz, 151-159.

15.9. V. I. Feodos'yev. To calculation of snapping diaphragm, Applied math. and mech., 10, No. 2 (1946), 295-300; Design of snapping diaphragm, Transactions of dept. of structural mech., Moscow Higher Technical School, Mashgiz, M. (1947).

15.10. V. I. Feodos'yev. Elastic elements of exact instrument-making, Oborongiz, M., 1949, 206-337.

15.11. R. R. Archer. Stability limits for a clamped spherical shell segment under uniform pressure, Quart. Appl. Math. 15 (1958), 355.

15.12. B. Budiansky. Buckling of clamped shallow spherical shells, Proc. IUTAM Symposium (see [15.3]), 1960, 64-94.

15.13. B. Budiansky and H. J. Weinitschke. On axisymmetric buckling of clamped shallow spherical shells, J. Aerospace Sci. 27 (1960), 545.

15.14. A. Kaplan and Y. C. Fung. A nonlinear theory of bending and buckling of thin elastic shallow spherical shells NACA TN 3212, 1954.

15.15. H. B. Keller and E. L. Reiss. Spherical cap snapping, J. Aerospace Sci. 26 (1959), 643.

15.16. E. L. Reiss, H. J. Greenberg, and H. B. Keller. Nonlinear deflections of shallow spherical shells, J. Aeron. Sci. 24 (1957), 533.

15.17. E. Reissner. Symmetric bending of shallow shells of revolution, J. Math. and Mech. 7 (1958), 121.

15.18. G. A. Thurston. A numerical solution of the nonlinear equations for axisymmetric bending of shallow spherical shells, J. Appl. Mech. 28, No. 4 (1961), 557-562.

15.19. H. Weinitschke. On the stability problem for shallow spherical shells, J. Math. and Phys. 38 (1960), 209; On the nonlinear theory of shallow spherical shells, J. Soc. Ind and Appl. Math. 6 (1958), 209.

15.20. G. R. Willich. The elastic stability of thin spherical shells, Proc. Am. Soc. Civ. Eng. 185, No. 1 (1959).

C H A P T E R XVI

STABILITY OF SANDWICH PLATES AND SHELLS

§ 162. Fundamental Equations of Linear Theory of Three-Ply Plates and Shells

Sandwich plate or shell consists of two thin outer layers, prepared from strong material (supporting layers), between which there is placed relatively light and low-strength middle layer (filler), ensuring joint work of outer layers. Supporting layers usually are made from such hard materials as metal, plywood or plastic. As filler there can be used foam plastic, balsa wood, porous rubber, or metal in the form of corrugated sheet or honeycomb cells (Fig. 16.1). Sandwich constructions find ever wider application in aircraft building, shipbuilding, industrial construction and in other regions of engineering. Structures whose middle layer is made of a metal corrugated sheet or honeycombs, have begun to be applied at high temperatures.

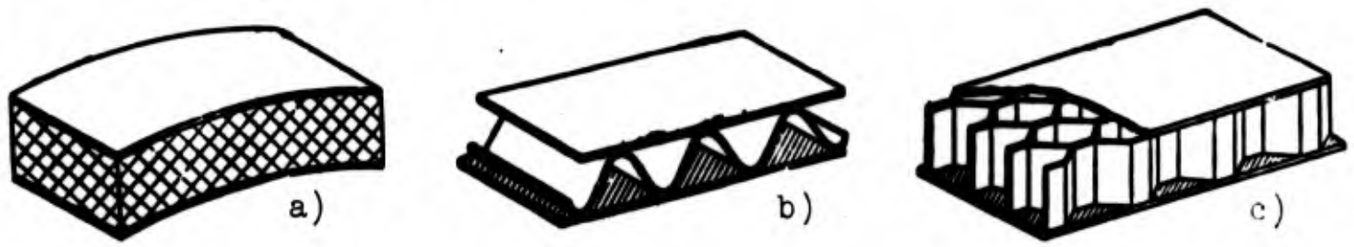

Fig. 16.1. Sandwich panels with fillers of a) solid foam plastic, b) corrugation, c) honeycombs.

Calculation of sandwich constructions for stability should be conducted taking into account different forms of buckling of construction as a whole and of its separate members. Let us assume that sandwich plate or shallow shell with solid filler is loaded symmetrically relative to middle surface. First of all, it is necessary to distinguish two forms of loss of stability: general, caused, basically, by distortion of middle surface of construction (Fig. 16.2a), and local, expressed, mainly, in distortion (wrinkling) of outer layers (Fig. 16.2b) and occurring without distortion of plate or shell as a whole. During local loss of stability of outer layer it may be represented as a plate or shell on an elastic foundation. If middle layer is carried out in the form of corrugated sheet or in the form of honeycomb cells, there is possible, furthermore, local loss of stability of walls of the sheet or plates of the honeycombs.

Research of sandwich constructions for stability of general and local type constitute two independent regions in each of which there are applied different assumptions. Such separation turns out to be possible in light of the fact that for sandwich plates there is absent mutual influence of these forms (16.5), and for sandwich shells mutual influence can be disregarded, if shell is shallow (16.9).

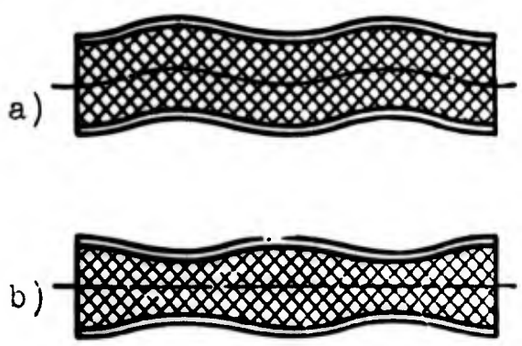

Fig. 16.2. Skew-symmetric and symmetric forms of loss of stability.

In this chapter we will consider only questions of general

stability of sandwich plates and shells.*

Thin supporting layers of sandwich plates and shells are naturally presented as ordinary plates and shells, using in composition of equations for them the hypothesis of straight normals.

Filler of sandwich construction should, generally, be considered a body of three dimensions. In this exact formulation there was carried out a series of studies of stability of sandwich plates.** These studies played a role in establishing effective methods of approximation of calculation of sandwich plates and shells, using certain assumptions about the work of the filler. Approximate theory of stability of sandwich plates and shells within elastic limit will be subject of this chapter.***

We make certain assumptions concerning deformations of filler during general loss of stability of plates and shells. First of all, we shall disregard transverse compressibility of filler, and deflections of outer layers we consider identical. This assumption, as shown in a number of works (16.11) and (16.27), turns out to be acceptable for practical calculations in a very wide range.

---

*Local stability of outer layers in case of solid filler is considered in works of A. P. Voronovich [16.5], V. I. Korolev [16.8], A. L. Rabinovich [16.13], Cox [16.15], March [16.24], and Yussuff [16.37]; local stability in case of filler of corrugation type is considered in work [16.3].

**In this line were works carried out by A. P. Voronovich [16.5], Cox [16.15], Goodier and Neou [16.18], Hunter-Tod [16.21], Neuber [16.26], Legget and Hopkins [16.22] and other authors.

***This theory was developed in works of Neut [16.25], A. L. Rabinovich [16.13], Reissner [16.27], A. P. Prusakov [16.11], and [16.12], Hemp [16.19], Libove and Batdorf [16.23], Stein and Mayers [16.31], Hoff [16.20], E. I. Grigolyuk [16.6], V. F. Karavanov [16.7], L. M. Kurshin [16.9], and [16.10] and other authors.

If filler has rigidity of the same order as support layers, or ratio of dimensions of plate to its thickness is great, then during calculation it is possible to consider valid the hypothesis of straight normals for the whole three ply package. Calculation in this case will not differ from calculation of ordinary single-layer plates and shells, with this difference only, that in it we will use rigidity of compound sections. However, in most cases, from considerations of economy of weight the sandwich construction is executed in such a way that filler turns out to be insufficiently hard, and calculation must be conducted taking into account deformations of transverse shearing of filler. Namely calculation of influence of shear of middle layer of work on outer layers is main distinction of calculation of sandwich constructions from calculation of ordinary single-ply plates and shells.

For calculation of deformations of transverse shift of filler we introduce following assumption. We consider that in filler a straight line, perpendicular to its middle surface before deformation, remains a straight line in process of deformation, but because of shift the perpendicularity is disturbed; in other words, throughout thickness of filler there is a linear law of displacements. To thin outer layers we apply hypothesis of straight normals. Thus, a normal, passed through all three layers, in process of deformation becomes a broken line (Fig. 16.3).

Fig. 16.3. Character of distribution of displacements throughout a sandwich shell.

Such calculating scheme for sandwich plates and shells is very

general and allows us to account for both shearing deformation of filler, so also work of it on longitudinal forces and moments. But calculation of longitudinal forces and moments received by filler by far is not always necessary. If ratio of elastic modulus of supporting layer E to elastic modulus of filler E_3 in plane, parallel to supporting layers, is great, and ratio of thickness of supporting layer t to thickness of filler 2h is not very small ($E_3h/Et < 0.1$), then longitudinal forces are received almost wholly by outer layers. Such fillers by established terminology are called light. Thus, during calculation of sandwich plates and shells with light filler it is possible to disregard on the middle layer normal and tangential stresses, lying in plane parallel to supporting layers. If filler receives noticeable part of longitudinal forces, it is called a rigid filler.

Hypothesis of broken line for displacements allows us to obtain equation of sandwich shells both with light, and also with rigid filler. We will give here derivation of equations for case of light fillers, of the greatest interest for practice. Along the way we will stop briefly to discuss equations for rigid fillers.

Fig. 16.4. Member of a sandwich shell.

Let us consider shallow sandwich shell with identical outer layers and light filler. We designate by R_1 and R_2 principal radii of curvatures of its middle surface (Fig. 16.4). Curvilinear coordinates x, and y on middle surface of shell, let us assume, coincide with lines of principal curvatures.

For displacements of points of upper layer during loss of stability in accordance with hypothesis of straight normals and taking into account shallowness of shell we find (when $(-h-t) \leq z \leq (-h)$):*

$$w_в = w_1,\quad u_в = u_1 - \left(z + h + \frac{t}{2}\right)\frac{\partial w_1}{\partial x},\quad v_в = v_1 - \left(z + h + \frac{t}{2}\right)\frac{\partial w_1}{\partial y}; \tag{16.1}$$

here u_1, v_1, w_1 are displacement of points of <u>middle surface</u> of upper supporting layer.

Analogously for displacements of points of lower layer (when $h \leq z \leq h + t$)

$$w_н = w_2,\quad u_н = u_2 - \left(z - h - \frac{t}{2}\right)\frac{\partial w_2}{\partial x},\quad v_н = v_2 - \left(z - h - \frac{t}{2}\right)\frac{\partial w_2}{\partial y}. \tag{16.2}$$

where u_2, v_2, w_2 are displacement of points of middle surface of lower supporting layer. During research of deformations of general loss of stability of sandwich construction it is possible, as was indicated above, to take

$$w_1 = w_2 = w. \tag{16.3}$$

Displacements of middle layer, in accordance with hypothesis of straight lines in filler, are equal (when $-h \leq z \leq h$) to

$$\left.\begin{aligned} w_с &= w,\\ u_с &= \frac{1}{2}(u_1 + u_2) - \frac{z}{2h}\left(u_1 - u_2 - t\frac{\partial w}{\partial x}\right),\\ v_с &= \frac{1}{2}(v_1 + v_2) - \frac{z}{2h}\left(v_1 - v_2 - t\frac{\partial w}{\partial y}\right). \end{aligned}\right\} \tag{16.4}$$

For deformations of layers we use expressions

$$\left.\begin{aligned} \varepsilon_x &= \frac{\partial u}{\partial x} - \frac{w}{R_1},\quad \varepsilon_y = \frac{\partial v}{\partial y} - \frac{w}{R_2},\\ \gamma_{xy} &= \frac{\partial u}{\partial y} + \frac{\partial v}{\partial x},\quad \gamma_{yz} = \frac{\partial v}{\partial z} + \frac{\partial w}{\partial y},\quad \gamma_{zx} = \frac{\partial u}{\partial z} + \frac{\partial w}{\partial x}. \end{aligned}\right\} \tag{16.5}$$

---

*Indices "в" and "н" here pertain to upper and lower layer, whereas in other sections they correspond to upper and lower critical load.

The last two relationships are necessary only for middle layer, where there occur shearing deformations.

Let us consider sandwich shell with inner and outer layers of isotropic materials. We designate shear modulus of material of filler by G_3. For stresses in outer layers we have expressions

$$\sigma_x=\frac{E}{1-\mu^2}\left(\varepsilon_x+\mu\varepsilon_y\right),\ \sigma_y=\frac{E}{1-\mu^2}\left(\varepsilon_y+\mu\varepsilon_x\right),\ \tau_{xy}=\frac{E}{2(1+\mu)}\gamma_{xy}. \tag{16.6}$$

Tangential stresses τ_{xz} and τ_{yz} in outer layers, as usual when using hypothesis of straight normals, are determined from equations of equilibrium of the member of the outer layer. For tangential stresses in filler we have

$$\tau_{xz}=G_3\gamma_{xz},\ \tau_{yz}=G_3\gamma_{yz} \tag{16.7}$$

We determine force in outer layer. For that we integrate stresses (6) with respect to thickness of outer layer and take into account expressions for deformations (5) and displacements (1). For forces in upper supporting layer we obtain

$$\left.\begin{aligned} N_{x,1}&=B\left(\frac{\partial u_1}{\partial x}+\mu\frac{\partial v_1}{\partial y}-\frac{w}{R_1}-\mu\frac{w}{R_2}\right),\\ N_{y,1}&=B\left(\frac{\partial v_1}{\partial y}+\mu\frac{\partial u_1}{\partial x}-\frac{w}{R_2}-\mu\frac{w}{R_1}\right),\\ T_1&=\frac{1-\mu}{2}B\left(\frac{\partial v_1}{\partial x}+\frac{\partial u_1}{\partial y}\right); \end{aligned}\right\} \tag{16.8}$$

here $B = Et/(1-\mu^2)$ is rigidity of outer layer.

Analogously for forces in lower supporting layer $N_{x,2}$, $N_{y,2}$, and T_2 we obtain the same expressions (8) with replacement in them of u_1 and v_1 by u_2 and v_2 respectively. Positive directions of forces are shown in Fig. 16.5, by analogy with Fig. 10.24.

For bending (M_x, M_y) and torsional (H) moments in outer layers relative to corresponding middle surfaces we obtain, calculating integrals of form

$$\int_{-(h+t)}^{-h}\sigma_x\left(z-h-\frac{t}{2}\right)dz=M_{x,1}.$$

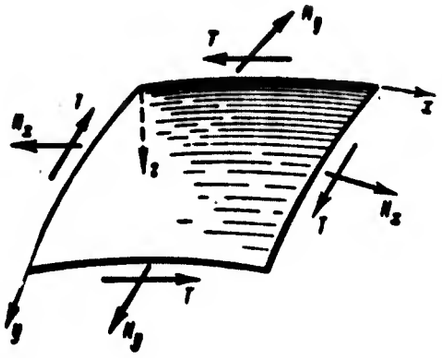

Fig. 16.5. Positive directions of forces in middle surface.

Known expressions:

$$\left.\begin{aligned} M_{x,1} &= M_{x,2} = -D\left(\frac{\partial^2 w}{\partial x^2} + \mu\frac{\partial^2 w}{\partial y^2}\right), \\ M_{y,1} &= M_{y,2} = -D\left(\frac{\partial^2 w}{\partial y^2} + \mu\frac{\partial^2 w}{\partial x^2}\right), \\ H_1 &= H_2 = -(1-\mu)D\frac{\partial^2 w}{\partial x\,\partial y}; \end{aligned}\right\} \qquad (16.9)$$

here D is cylindrical rigidity of outer layer, $D = Et^3/12(1-\mu^2)$. Positive directions of moments are shown in Fig. 16.6.

We determine tangential stresses in filler. From (7), (5) and (4) we have

$$\left.\begin{aligned} \tau_{xz,3} &= G_3\left(\frac{\partial u_c}{\partial z} + \frac{\partial w}{\partial x}\right) = -\frac{G_3}{h}\left[\frac{1}{2}(u_1 - u_2) - \left(h + \frac{t}{2}\right)\frac{\partial w}{\partial x}\right], \\ \tau_{yz,3} &= G_3\left(\frac{\partial v_c}{\partial z} + \frac{\partial w}{\partial x}\right) = -\frac{G_3}{h}\left[\frac{1}{2}(v_1 - v_2) - \left(h + \frac{t}{2}\right)\frac{\partial w}{\partial y}\right]. \end{aligned}\right\} \qquad (16.10)$$

Transverse forces in filler are

$$\left.\begin{aligned} Q_{x,3} &= -2G_3\left[\frac{1}{2}(u_1 - u_2) - \left(h + \frac{t}{2}\right)\frac{\partial w}{\partial x}\right], \\ Q_{y,3} &= -2G_3\left[\frac{1}{2}(v_1 - v_2) - \left(h + \frac{t}{2}\right)\frac{\partial w}{\partial y}\right]. \end{aligned}\right\} \qquad (16.11)$$

We separate from upper outer layer member dx, dy. Let us consider conditions of equilibrium of moments (Fig. 16.7) and longitudinal forces (Fig. 16.8) acting on the member. We designate by $\tau_{xz,\,1}$, and $\tau_{yz,\,1}$ tangential stresses acting at place of linkage of outer

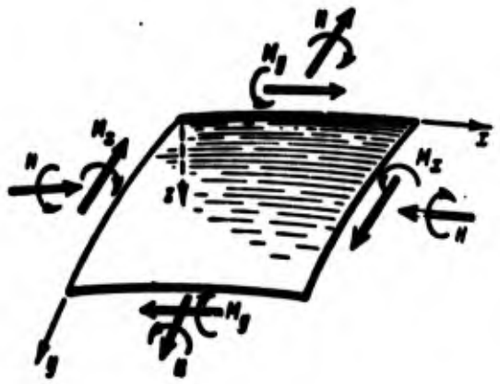

Fig. 16.6. Positive directions of moments.

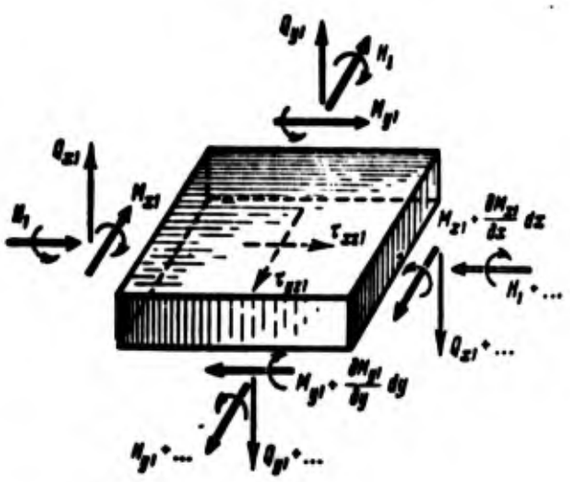

Fig. 16.7. Moments and transverse forces acting on member of external layer.

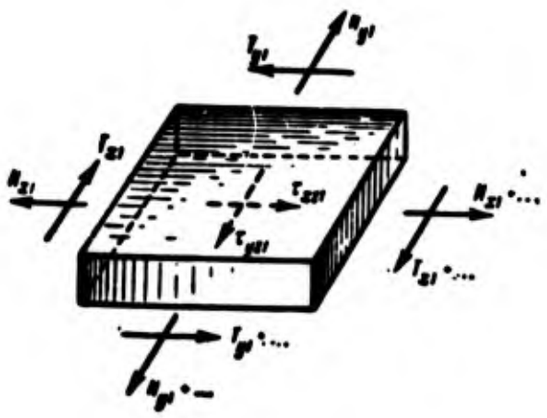

Fig. 16.8. Forces acting on member of outer layer.

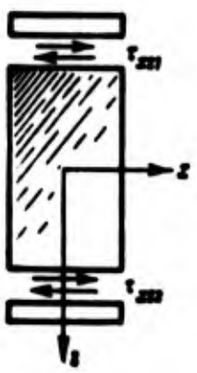

Fig. 16.9. Tangential stresses caused by interaction of outer layer with filler.

layer with filler. From condition of equilibrium of moments we find

$$\left.\begin{aligned} Q_{x,1} &= \frac{\partial M_{x,1}}{\partial x} + \frac{\partial H_1}{\partial y} + \frac{t}{2}\tau_{xz,1}, \\ Q_{y,1} &= \frac{\partial M_{y,1}}{\partial y} + \frac{\partial H_1}{\partial x} + \frac{t}{2}\tau_{yz,1}. \end{aligned}\right\} \qquad (16.12)$$

Conditions of equilibrium of forces give

$$\left.\begin{aligned} \frac{\partial N_{x,1}}{\partial x} + \frac{\partial T_1}{\partial y} + \tau_{xz,1} &= 0, \\ \frac{\partial N_{y,1}}{\partial y} + \frac{\partial T_1}{\partial x} + \tau_{yz,1} &= 0. \end{aligned}\right\} \qquad (16.13)$$

Excluding from (12) stresses $\tau_{xz,\,1}$ and $\tau_{yz,\,1}$, with help of (13) we obtain expressions for transverse forces in outer layer:

$$\left.\begin{aligned} Q_{x,1} &= \frac{\partial M_{x,1}}{\partial x} + \frac{\partial H_1}{\partial y} - \frac{t}{2}\left(\frac{\partial N_{x,1}}{\partial x} + \frac{\partial T_1}{\partial y}\right), \\ Q_{y,1} &= \frac{\partial M_{y,1}}{\partial y} + \frac{\partial H_1}{\partial x} - \frac{t}{2}\left(\frac{\partial N_{y,1}}{\partial y} + \frac{\partial T_1}{\partial x}\right). \end{aligned}\right\} \qquad (16.14)$$

Analogously for lower layer, considering direction of stresses τ_{xz}, and τ_{yz} (Fig. 16.9), from equations of equilibrium of the member we have

$$\left.\begin{aligned} Q_{x,2}&=\frac{\partial M_{x,2}}{\partial x}+\frac{\partial H_2}{\partial y}+\frac{t}{2}\left(\frac{\partial N_{x,2}}{\partial x}+\frac{\partial T_2}{\partial y}\right).\\ Q_{y,2}&=\frac{\partial M_{y,2}}{\partial y}+\frac{\partial H_2}{\partial x}+\frac{t}{2}\left(\frac{\partial N_{y,2}}{\partial y}+\frac{\partial T_2}{\partial x}\right).\end{aligned}\right\} \tag{16.15}$$

Summing transverse forces in filler and outer layers, we obtain for transverse forces in sandwich shell expressions

$$\left.\begin{aligned} Q_x&=Q_{x,3}+\frac{\partial}{\partial x}(M_{x,1}+M_{x,2})+\frac{\partial}{\partial y}(H_1+H_2)-\\ &\quad-\frac{t}{2}\left[\frac{\partial}{\partial x}(N_{x,1}-N_{x,2})+\frac{\partial}{\partial y}(T_1-T_2)\right].\\ Q_y&=Q_{y,3}+\frac{\partial}{\partial y}(M_{y,1}+M_{y,2})+\frac{\partial}{\partial x}(H_1+H_2)-\\ &\quad-\frac{t}{2}\left[\frac{\partial}{\partial y}(N_{y,1}-N_{y,2})+\frac{\partial}{\partial x}(T_1-T_2)\right].\end{aligned}\right\} \tag{16.16}$$

We introduce designations

$$\left.\begin{aligned} u_a&=\frac{1}{2}(u_1+u_2).\quad v_a=\frac{1}{2}(v_1+v_2).\\ u_\beta&=\frac{1}{2}(u_1-u_2).\quad v_\beta=\frac{1}{2}(v_1-v_2).\end{aligned}\right\} \tag{16.17}$$

We express total forces and moments in sandwich shell by displacements of middle surfaces of outer layers. From (8) and (17) we obtain

$$\left.\begin{aligned} N_x&=N_{x,1}+N_{x,2}=2B\left(\frac{\partial u_a}{\partial x}+\mu\frac{\partial v_a}{\partial y}-\frac{w}{R_1}-\mu\frac{w}{R_2}\right).\\ N_y&=N_{y,1}+N_{y,2}=2B\left(\frac{\partial v_a}{\partial y}+\mu\frac{\partial u_a}{\partial x}-\frac{w}{R_2}-\mu\frac{w}{R_1}\right).\\ T&=T_1+T_2=(1-\mu)B\left(\frac{\partial v_a}{\partial x}+\frac{\partial u_a}{\partial y}\right).\end{aligned}\right\} \tag{16.18}$$

Bending moments and torques in a sandwich shell relative to its middle surface will be

$$\begin{aligned} M_x&=M_{x,1}+M_{x,2}-\left(h+\frac{t}{2}\right)(N_{x,1}-N_{x,2}).\\ M_y&=M_{y,1}+M_{y,2}-\left(h+\frac{t}{2}\right)(N_{y,1}-N_{y,2}).\\ H&=H_1+H_2-\left(h+\frac{t}{2}\right)(T_1-T_2).\end{aligned}$$

Using (8), (9) and (17), we obtain

$$\left.\begin{aligned} M_x &= -2D\left(\frac{\partial^2 w}{\partial x^2}+\mu\frac{\partial^2 w}{\partial y^2}\right)-2\left(h+\frac{t}{2}\right)B\left(\frac{\partial u_3}{\partial x}+\mu\frac{\partial v_3}{\partial y}\right).\\ M_y &= -2D\left(\frac{\partial^2 w}{\partial y^2}+\mu\frac{\partial^2 w}{\partial x^2}\right)-2\left(h+\frac{t}{2}\right)B\left(\frac{\partial v_3}{\partial y}+\mu\frac{\partial u_3}{\partial x}\right).\\ H &= -2D(1-\mu)\frac{\partial^2 w}{\partial x\,\partial y}-(1-\mu)\left(h+\frac{t}{2}\right)B\left(\frac{\partial v_3}{\partial x}+\frac{\partial u_3}{\partial y}\right). \end{aligned}\right\} \qquad (16.19)$$

For transverse forces in sandwich shell (16) taking into account (8), (9), (11) and (17) we obtain expressions in displacements:

$$\left.\begin{aligned} Q_x &= -2G_3\left[u_3-\left(h+\frac{t}{2}\right)\frac{\partial w}{\partial x}\right]-2D\frac{\partial}{\partial x}\nabla^2 w-\\ &\quad -Bt\left(\frac{\partial^2 u_3}{\partial x^2}+\frac{1-\mu}{2}\frac{\partial^2 u_3}{\partial y^2}+\frac{1+\mu}{2}\frac{\partial^2 v_3}{\partial x\,\partial y}\right).\\ Q_y &= -2G_3\left[v_3-\left(h+\frac{t}{2}\right)\frac{\partial w}{\partial y}\right]-2D\frac{\partial}{\partial y}\nabla^2 w-\\ &\quad -Bt\left(\frac{\partial^2 v_3}{\partial y^2}+\frac{1-\mu}{2}\frac{\partial^2 v_3}{\partial x^2}+\frac{1+\mu}{2}\frac{\partial^2 u_3}{\partial x\,\partial y}\right). \end{aligned}\right\} \qquad (16.20)$$

We turn to equations of equilibrium of a member of a shallow sandwich shell as a whole. From conditions of equilibrium of forces in directions x and y we obtain (Fig. 16.10)

$$\frac{\partial N_x}{\partial x}+\frac{\partial T}{\partial y}=0, \quad \frac{\partial N_y}{\partial y}+\frac{\partial T}{\partial x}=0. \qquad (16.21)$$

Equations of equilibrium of moments (Fig. 16.11) give

$$\frac{\partial M_x}{\partial x}+\frac{\partial H}{\partial y}=Q_x, \quad \frac{\partial M_y}{\partial y}+\frac{\partial H}{\partial x}=Q_y. \qquad (16.22)$$

Equation of projections of forces on direction of normal taking into account components caused by turn of member (Fig. 16.12), gives

$$\frac{N_x}{R_1}+\frac{N_y}{R_2}+\frac{\partial Q_x}{\partial x}+\frac{\partial Q_y}{\partial y}+\frac{\partial}{\partial x}\left(N_x^0\frac{\partial w}{\partial x}\right)+ +\frac{\partial}{\partial y}\left(N_y^0\frac{\partial w}{\partial y}\right)+\frac{\partial}{\partial x}\left(T^0\frac{\partial w}{\partial y}\right)+\frac{\partial}{\partial y}\left(T^0\frac{\partial w}{\partial x}\right)=0. \qquad (16.23)$$

Here N_x^0, N_y^0, and T^0 are forces in shell before loss of stability.

Considering that forces N_x^0, N_y^0, and T^0 satisfy equations of equilibrium, we write equation (23) in the form

$$\frac{N_x}{R_1}+\frac{N_y}{R_2}+\frac{\partial Q_x}{\partial x}+\frac{\partial Q_y}{\partial y}+N_x^0\frac{\partial^2 w}{\partial x^2}+N_y^0\frac{\partial^2 w}{\partial y^2}+2T^0\frac{\partial^2 w}{\partial x\,\partial y}=0. \qquad (16.24)$$

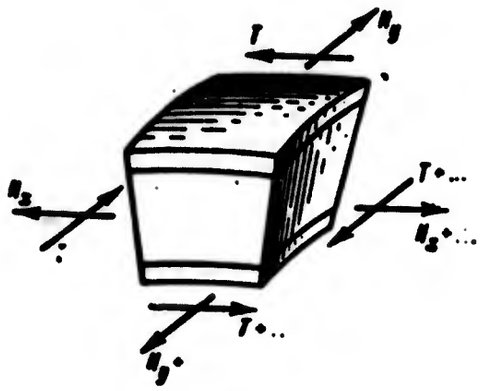

Fig. 16.10. Forces acting on a member of a sandwich shell.

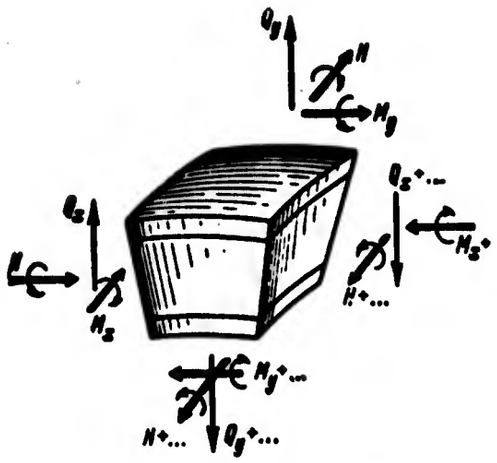

Fig. 16.11. Moments acting on member of sandwich shell.

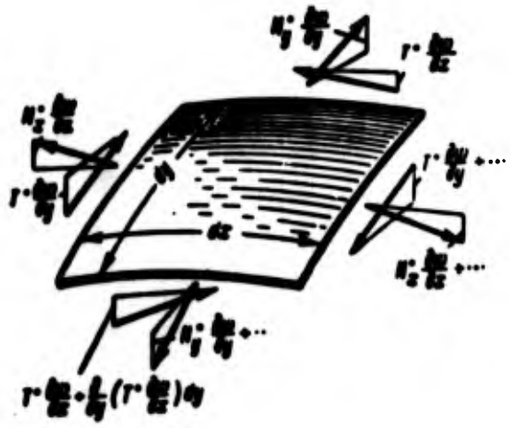

Fig. 16.12. Deriving equation of equilibrium of projections of forces on the normal.

We express in equations (21), (22), and (24) forces and moments by displacements of middle surfaces of outer layers with the help of formulas (18), (19) and (20).

Furthermore, we transform equation (24), adding to it equations (22); differentiating them with respect to x and y and multiplying by $2G_3$, we obtain system of equations of stability of shallow sandwich shell in terms of displacements:

$$\left.\begin{aligned}
&\frac{\partial^2 u_0}{\partial x^2}+\frac{1-\mu}{2}\frac{\partial^2 u_0}{\partial y^2}+\frac{1+\mu}{2}\frac{\partial^2 v_0}{\partial x\,\partial y}-\frac{\partial}{\partial x}\left(\frac{w}{R_1}+\mu\frac{w}{R_2}\right)=0,\\
&\frac{\partial^2 v_0}{\partial y^2}+\frac{1-\mu}{2}\frac{\partial^2 v_0}{\partial x^2}+\frac{1+\mu}{2}\frac{\partial^2 u_0}{\partial x\,\partial y}-\frac{\partial}{\partial y}\left(\frac{w}{R_2}+\mu\frac{w}{R_1}\right)=0,\\
&\frac{Bh}{G_3}\left(\frac{\partial^2 u_3}{\partial x^2}+\frac{1-\mu}{2}\frac{\partial^2 u_3}{\partial y^2}+\frac{1+\mu}{2}\frac{\partial^2 v_3}{\partial x\,\partial y}\right)-\\
&\qquad -u_3+\left(h+\frac{t}{2}\right)\frac{\partial w}{\partial x}=0,\\
&\frac{Bh}{G_3}\left(\frac{\partial^2 v_3}{\partial y^2}+\frac{1-\mu}{2}\frac{\partial^2 v_3}{\partial x^2}+\frac{1+\mu}{2}\frac{\partial^2 u_3}{\partial x\,\partial y}\right)-\\
&\qquad -v_3-\left(h+\frac{t}{2}\right)\frac{\partial w}{\partial y}=0.
\end{aligned}\right\} \qquad (16.25a)$$

$$-2B\left(h+\frac{t}{2}\right)\nabla^2\left(\frac{\partial u_3}{\partial x}+\frac{\partial v_3}{\partial y}\right)-2D\nabla^4 w+$$
$$+\frac{2B}{R_1}\left(\frac{\partial u_0}{\partial x}+\mu\frac{\partial v_0}{\partial y}-\frac{w}{R_1}-\mu\frac{w}{R_2}\right)+$$
$$+\frac{2B}{R_2}\left(\frac{\partial v_0}{\partial y}+\mu\frac{\partial u_0}{\partial x}-\frac{w}{R_2}-\mu\frac{w}{R_1}\right)+$$
$$+N_x^0\frac{\partial^2 w}{\partial x^2}+N_y^0\frac{\partial^2 w}{\partial y^2}+2T^0\frac{\partial^2 w}{\partial x\,\partial y}=0. \qquad (16.25b)$$

System of equations (25) can be reduced to one resolvent. We introduce function of forces φ, considering

$$N_x=\frac{\partial^2\varphi}{\partial y^2},\quad N_y=\frac{\partial^2\varphi}{\partial x^2},\quad T=-\frac{\partial^2\varphi}{\partial x\,\partial y}. \qquad (16.26)$$

Obviously, equations (21), corresponding to first two equations of system (25), here are satisfied.

Excluding from three relationships (18) taking into account (26) functions u_α and v_α, we obtain equation

$$\nabla^4\varphi=-2B(1-\mu^2)\left(\frac{1}{R_2}\frac{\partial^2 w}{\partial x^2}+\frac{1}{R_1}\frac{\partial^2 w}{\partial y^2}\right). \qquad (16.27)$$

Designating

$$F=\frac{\partial u_3}{\partial x}+\frac{\partial v_3}{\partial y}, \qquad (16.28)$$

differentiating third equation of system (25) with respect to x, and the fourth, with respect to y and adding, we obtain

$$Bh\nabla^2 F=G_a\left[F-\left(h+\frac{t}{2}\right)\nabla^2 w\right]. \qquad (16.29)$$

Last equation of system (25) taking into account relationships (26) and (28) will be written in the form

$$-2B\left(h+\frac{t}{2}\right)\nabla^2 F-2D\nabla^4 w+\frac{1}{R_1}\frac{\partial^2\varphi}{\partial y^2}+\frac{1}{R_2}\frac{\partial^2\varphi}{\partial x^2}+$$
$$+N_x^0\frac{\partial^2 w}{\partial x^2}+N_y^0\frac{\partial^2 w}{\partial y^2}+2T^0\frac{\partial^2 w}{\partial x\,\partial y}=0. \qquad (16.30)$$

From equations (29) and (30) it is possible to exclude function F.

We obtain equation

$$2B\left(h+\frac{t}{2}\right)^2\nabla^4 w+\left(1-\frac{Bh}{G_3}\nabla^2\right)\left[2D\nabla^4 w-\frac{1}{R_1}\frac{\partial^2\varphi}{\partial y^2}-\right.$$
$$\left.-\frac{1}{R_2}\frac{\partial^2\varphi}{\partial x^2}-N_x^0\frac{\partial^2 w}{\partial x^2}-N_y^0\frac{\partial^2 w}{\partial y^2}-2T^0\frac{\partial^2 w}{\partial x\,\partial y}\right]=0. \tag{16.31}$$

Thus, for functions of forces φ and deflection w we obtained system of two equations (27) and (31); they can be reduced to one equation in terms of deflection:

$$2B\left(h+\frac{t}{2}\right)^2\nabla^6 w+\left(1-\frac{Bh}{G_3}\nabla^2\right)\left[2D\nabla^6 w+\right.$$
$$\left.+2(1-\mu^2)B\left(\frac{1}{R_2}\frac{\partial^2}{\partial x^2}+\frac{1}{R_1}\frac{\partial^2}{\partial y^2}\right)^2 w\right]-$$
$$-\nabla^4\left(N_x^0\frac{\partial^2 w}{\partial x^2}+N_y^0\frac{\partial^2 w}{\partial y^2}+2T\frac{\partial^2 w}{\partial x\,\partial y}\right)=0. \tag{16.32}$$

Let us note that solution of problem of stability with help of one equation turns out to be possible in those cases when boundary conditions can be expressed in w. Otherwise it is necessary to turn to system of equations (25), allowing us to satisfy boundary conditions, formulated for u_β, v_β, u_α, and v_α.

In case of <u>sandwich plate</u> ($R_1 = \infty$, $R_2 = \infty$) system of equations (25) is broken up into two independent systems: two equations for functions u_α and v_α, having trivial solution, and three equations for functions u_β, v_β, and w. These last three equation will also be equations of stability of sandwich plate with light filler; they have form

$$\left.\begin{aligned}
&\frac{Bh}{G_3}\left(\frac{\partial^2 u_3}{\partial x^2}+\frac{1-\mu}{2}\frac{\partial^2 u_3}{\partial y^2}+\frac{1+\mu}{2}\frac{\partial^2 v_3}{\partial x\,\partial y}\right)-\\
&\qquad-u_3+\left(h+\frac{t}{2}\right)\frac{\partial w}{\partial x}=0.\\
&\frac{Bh}{G_3}\left(\frac{\partial^2 v_3}{\partial y^2}+\frac{1-\mu}{2}\frac{\partial^2 v_3}{\partial x^2}+\frac{1+\mu}{2}\frac{\partial^2 u_3}{\partial x\,\partial y}\right)-\\
&\qquad-v_3+\left(h+\frac{t}{2}\right)\frac{\partial w}{\partial y}=0.\\
&-2B\left(h+\frac{t}{2}\right)\nabla^2\left(\frac{\partial u_3}{\partial x}+\frac{\partial v_3}{\partial y}\right)-2D\nabla^4 w+\\
&\qquad+N_x^0\frac{\partial^2 w}{\partial x^2}+N_y^0\frac{\partial^2 w}{\partial y^2}+2T^0\frac{\partial^2 w}{\partial x\,\partial y}=0.
\end{aligned}\right\} \tag{16.33}$$

It is possible to reduce system (33) to one resolvent for deflection:

$$2B\left(h+\frac{t}{2}\right)^2\nabla^4 w+$$
$$+\left(1-\frac{Bh}{G_3}\nabla^2\right)\left(2D\nabla^4 w-N_x^0\frac{\partial^2 w}{\partial x^2}-N_y^0\frac{\partial^2 w}{\partial y^2}-2T^0\frac{\partial^2 w}{\partial x\,\partial y}\right)=0. \tag{16.34}$$

Let us note that in limiting case, when shear modulus G_3 seeks infinity, equations of sandwich plates and shells are reduced to equations of uniform plates and shallow shells with flexural rigidity $2[D + B\,(h + \frac{t}{2})^2]$, i.e., with rigidity of compound section of two layers, related on height of filler. In other limiting case, when $G_3 \to 0$, there are obtained equations for isolated outer layers.

Thus, proceeding from assumption of linear distribution of displacements the thickness of filler, we obtained equation of stability of shallow sandwich shell with light filler, i.e., without calculation of normal and tangential stresses in filler, parallel to external layers.

In practice of calculation of sandwich plates and shells, as was already said, one can meet cases of more rigid fillers, when in sandwich construction the filler receives noticeable part of longitudinal forces and moments. In this case it is necessary to consider stress in filler, directed parallel to outer layers. Equations can then be obtained, proceeding from linearity of displacements the thickness of filler and disregarding transverse deformation of filler. In principle this conclusion will not differ from the above-mentioned for light fillers; it is necessary only to introduce in expressions for forces and moments components, caused by stresses σ_x, σ_y, and τ_{xy} in filler. Not giving this conclusion, we write final equations of stability of shallow sandwich shell with hard isotropic filler,

$$\frac{\partial N_x}{\partial x}+\frac{\partial T}{\partial y}=0,\quad \frac{\partial N_y}{\partial y}+\frac{\partial T}{\partial x}=0,$$

$$\left.\begin{aligned}\frac{h}{G_c}\left(B+\frac{1}{3}B_c\right)\left(\frac{\partial^2 u_0}{\partial x^2}+\frac{1-\mu}{2}\frac{\partial^2 u_0}{\partial y^2}+\frac{1+\mu}{2}\frac{\partial^2 v_0}{\partial x\partial y}\right)-\\ -\frac{B_c ht}{6G_c}\frac{\partial}{\partial x}\nabla^2 w-u_0+\left(h+\frac{t}{2}\right)\frac{\partial w}{\partial x}=0,\end{aligned}\right\} \tag{16.35a}$$

$$\left.\begin{aligned}\frac{h}{G_c}\left(B+\frac{1}{3}B_c\right)\left(\frac{\partial^2 v_0}{\partial y^2}+\frac{1-\mu}{2}\frac{\partial^2 v_0}{\partial x^2}+\frac{1+\mu}{2}\frac{\partial^2 u_0}{\partial x\partial y}\right)-\\ -\frac{B_c ht}{6G_c}\frac{\partial}{\partial y}\nabla^2 w-v_0+\left(h+\frac{t}{2}\right)\frac{\partial w}{\partial y}=0.\end{aligned}\right\} \tag{16.35b}$$

$$-\left[2B\left(h+\frac{t}{2}\right)+\frac{2}{3}B_c h\right]\nabla^2\left(\frac{\partial u_0}{\partial x}+\frac{\partial v_0}{\partial y}\right)+\left(\frac{1}{3}B_c ht-2D\right)\nabla^4 w+$$
$$+\frac{N_x}{R_1}+\frac{N_y}{R_2}+N_x^0\frac{\partial^2 w}{\partial x^2}+N_y^0\frac{\partial^2 w}{\partial y^2}+2T^0\frac{\partial^2 w}{\partial x\partial y}=0. \tag{16.35c}$$

Forces and displacements are connected by relationships

$$\left.\begin{aligned}N_x=2(B+B_3)\left(\frac{\partial u_0}{\partial x}+\mu\frac{\partial v_0}{\partial y}-\frac{w}{R_1}-\mu\frac{w}{R_2}\right),\\ N_y=2(B+B_3)\left(\frac{\partial v_0}{\partial y}+\mu\frac{\partial u_0}{\partial x}-\frac{w}{R_1}-\mu\frac{w}{R_1}\right),\\ T=(1-\mu)(B+B_3)\left(\frac{\partial v_0}{\partial x}+\frac{\partial u_0}{\partial y}\right).\end{aligned}\right\} \tag{16.36}$$

Here $B_3 = E_3h(1-\mu^2)$; Poisson's ratios μ of filler and outer layers materials are taken identical.

During solution of problems of stability of sandwich plates and shells with middle layer of corrugation, honeycomb or foam plastic-reinforced type it is possible by introduction of reduced rigidity parameters to replace such fillers with a certain equivalent uniform filler.*

Let us note that proposition of linearity of displacements the thickness of filler in case of light fillers used in this paragraph is result of following assumptions: a) equality of zero of stresses σ_x, σ_y, and τ_{xy}, b) inextensionality to filler in transverse direction, $w = w(x, y)$. This directly follows from equations of equilibrium of

*For determination of given elastic moduli of corrugation and honeycombs it is possible to use work [16.2]. Equations of stability of shallow shells with hard orthotropic filler can be found in [16.6].

a member

$$\frac{\partial \tau_{xz}}{\partial z}=0,\quad \frac{\partial \tau_{yz}}{\partial z}=0 \tag{16.37}$$

and relationships

$$\frac{\partial u}{\partial z}+\frac{\partial w}{\partial x}=\frac{\tau_{xz}}{G_3},\quad \frac{\partial v}{\partial z}+\frac{\partial w}{\partial y}=\frac{\tau_{yz}}{G_3}.$$

Nevertheless, method of derivation of equations with assignment of law of change of displacements through the filler is more convenient; it may be almost wholly transfered to more general case of sandwich constructions with hard filler, during examining of which it is necessary to consider stresses σ_x, σ_y, and τ_{xy} in filler; then hypothesis of linear law of displacements will be essential.

§ 163. Variational Equation of Stability. Boundary Conditions

Energy equation of stability of shallow sandwich shell we write in the form

$$U+\frac{1}{2}\int\int\left[N_x^0\left(\frac{\partial w}{\partial x}\right)^2+N_y^0\left(\frac{\partial w}{\partial y}\right)^2+2T^0\frac{\partial w}{\partial x}\frac{\partial w}{\partial y}\right]dx\,dy=0. \tag{16.38}$$

where U is potential energy caused by forces appearing during loss of shell.

For potential energy of upper external layer we have

$$U_1=\frac{1}{2}\int\int_h^{h+t}\int(\sigma_x\varepsilon_x+\sigma_y\varepsilon_y+\tau_{xy}\gamma_{xy})\,dx\,dy\,dz. \tag{16.39}$$

Introducing in (39) expressions (5) for deformations and (1) for displacements and integrating with respect to z, we obtain

$$\begin{aligned}U_1=\frac{1}{2}\int\int\Big\{&N_{x.1}\left(\frac{\partial u_1}{\partial x}-\frac{w}{R_1}\right)+N_{y.1}\left(\frac{\partial v_1}{\partial y}-\frac{w}{R_2}\right)+\\&+T_1\left(\frac{\partial v_1}{\partial x}+\frac{\partial u_1}{\partial y}\right)-M_{x.1}\frac{\partial^2 w}{\partial x^2}-M_{y.1}\frac{\partial^2 w}{\partial y^2}-2H_1\frac{\partial^2 w}{\partial x\,\partial y}\Big\}dx\,dy.\end{aligned} \tag{16.40}$$

Analogously for lower supporting layer we find

$$U_2=\frac{1}{2}\int\int\left\{N_{x.2}\left(\frac{\partial u_2}{\partial x}-\frac{w}{R_1}\right)+N_{y.2}\left(\frac{\partial v_2}{\partial y}-\frac{w}{R_2}\right)+\right.$$
$$\left.+T_2\left(\frac{\partial v_2}{\partial x}+\frac{\partial u_2}{\partial y}\right)-M_{x.2}\frac{\partial^2 w}{\partial x^2}-M_{y.2}\frac{\partial^2 w}{\partial y^2}-2H_2\frac{\partial^2 w}{\partial x\,\partial y}\right\}dx\,dy. \tag{16.41}$$

Potential energy of filler will be

$$U_3=\frac{1}{2}\int_{-h}^{h}\int\int(\tau_{xz}\gamma_{xz}+\tau_{yz}\gamma_{yz})\,dx\,dy\,dz. \tag{16.42}$$

Introducing expressions for deformations (5) and displacements (4) and integrating with respect to z, we have

$$U_3=\frac{1}{2h}\int\int\left\{Q_{x.3}\left[-\frac{1}{2}(u_1-u_2)+\left(h+\frac{t}{2}\right)\frac{\partial w}{\partial x}\right]+\right.$$
$$\left.+Q_{y.3}\left[-\frac{1}{2}(v_1-v_2)+\left(h+\frac{t}{2}\right)\frac{\partial w}{\partial y}\right]\right\}dx\,dy. \tag{16.43}$$

Summing (40), (41), and (42) taking into account designations (17) and formulas (18), (9), and (20) for potential energy, we obtain

$$U=\frac{1}{2}\int\int\left\{N_x\left(\frac{\partial u_3}{\partial x}-\frac{w}{R_1}\right)+N_y\left(\frac{\partial v_3}{\partial y}-\frac{w}{R_2}\right)+T\left(\frac{\partial v_3}{\partial x}+\frac{\partial u_3}{\partial y}\right)+\right.$$
$$+(N_{x.1}-N_{x.2})\frac{\partial u_3}{\partial x}+(N_{y.1}-N_{y.2})\frac{\partial v_3}{\partial y}+$$
$$+(T_1-T_2)\left(\frac{\partial v_3}{\partial x}+\frac{\partial u_3}{\partial y}\right)-M_{x.1}\frac{\partial^2 w}{\partial x^2}-2M_{y.1}\frac{\partial^2 w}{\partial y^2}-$$
$$-4H\frac{\partial^2 w}{\partial x\,\partial y}+\frac{1}{h}Q_{x.3}\left[-u_3+\left(h+\frac{t}{2}\right)\frac{\partial w}{\partial x}\right]+$$
$$\left.+\frac{1}{h}Q_{y.3}\left[-v_3+\left(h+\frac{t}{2}\right)\frac{\partial w}{\partial y}\right]\right\}dx\,dy. \tag{16.44}$$

or

$$U=\frac{1}{2}\int\int\left\{2B\left[\left(\frac{\partial u_3}{\partial x}-\frac{w}{R_1}\right)^2+\left(\frac{\partial v_3}{\partial y}-\frac{w}{R_2}\right)^2+\right.\right.$$
$$+2\mu\left(\frac{\partial u_3}{\partial x}-\frac{w}{R_1}\right)\left(\frac{\partial v_3}{\partial y}-\frac{w}{R_2}\right)+\frac{1-\mu}{2}\left(\frac{\partial u_3}{\partial y}+\frac{\partial v_3}{\partial x}\right)^2+$$
$$\left.+\left(\frac{\partial u_3}{\partial x}\right)^2+\left(\frac{\partial v_3}{\partial y}\right)^2+2\mu\frac{\partial u_3}{\partial x}\frac{\partial v_3}{\partial y}+\frac{1-\mu}{2}\left(\frac{\partial v_3}{\partial x}+\frac{\partial u_3}{\partial y}\right)^2\right]+$$
$$+2D\left[(\nabla^2 w)^2-2(1-\mu)\left(\frac{\partial^2 w}{\partial x^2}\frac{\partial^2 w}{\partial y^2}-\left(\frac{\partial^2 w}{\partial x\,\partial y}\right)^2\right)\right]+$$
$$\left.+\frac{2}{h}G_3\left[u_3-\left(h+\frac{t}{2}\right)\frac{\partial w}{\partial x}\right]^2+\frac{2}{h}G_3\left[v_3-\left(h+\frac{t}{2}\right)\frac{\partial w}{\partial y}\right]^2\right\}dx\,dy. \tag{16.45}$$

Varying in equation (38) displacements, we obtain variational equation

$$\delta W+\frac{1}{2}\int\int\left[N_x^0\delta\left(\frac{\partial w}{\partial x}\right)^2+N_y^0\delta\left(\frac{\partial w}{\partial y}\right)^2+2T^0\delta\left(\frac{\partial w}{\partial x}\frac{\partial w}{\partial y}\right)\right]dx\,dy=0. \tag{16.46}$$

We shall consider, then, a shell bounded by coordinate lines $x = a_1$, $x = a_2$, and $y = b_1$, $y = b_2$. Executing partial integration in equation (46), i.e., performing transformation by the formulas

$$\int_{a_1}^{a_2}\int_{b_1}^{b_2}\left(\frac{\partial u_\alpha}{\partial x}\right)^2 dx\,dy = 2\int_{a_1}^{a_2}\int_{b_1}^{b_2}\frac{\partial u_\alpha}{\partial x}\delta\left(\frac{\partial u_\alpha}{\partial x}\right)dx\,dy =$$

$$= 2\int_{b_1}^{b_2}\left[\frac{\partial u_\alpha}{\partial x}\delta u_\alpha\right]_{a_1}^{a_2}dx\,dy - 2\int_{a_1}^{a_2}\int_{b_1}^{b_2}\frac{\partial^2 u_\alpha}{\partial x^2}\delta u_\alpha\,dx\,dy.$$

we reduce the variational equation to form

$$-\int_{a_1}^{a_2}\int_{b_1}^{b_2}\left\{\left(\frac{\partial N_x}{\partial x}+\frac{\partial T}{\partial y}\right)\delta u_\alpha+\left(\frac{\partial N_y}{\partial y}+\frac{\partial T}{\partial x}\right)\delta v_\alpha+\right.$$
$$+\left[2B\left(\frac{\partial^2 u_\beta}{\partial x^2}+\frac{1-\mu}{2}\frac{\partial^2 u_\beta}{\partial y^2}+\frac{1+\mu}{2}\frac{\partial^2 v_\beta}{\partial x\,\partial y}\right)-\frac{2G_\beta}{h}\left(u_\beta-\left(h+\frac{t}{2}\right)\frac{\partial w}{\partial x}\right)\right]\delta u_\beta+$$
$$+\left[2B\left(\frac{\partial^2 v_\beta}{\partial y^2}+\frac{1-\mu}{2}\frac{\partial^2 v_\beta}{\partial x^2}+\frac{1+\mu}{2}\frac{\partial^2 u_\beta}{\partial x\,\partial y}\right)-\frac{2G_\beta}{h}\left(v_\beta-\left(h+\frac{t}{2}\right)\frac{\partial w}{\partial y}\right)\right]\delta v_\beta+$$
$$+\left[-\frac{2G_\alpha}{h}\left(h+\frac{t}{2}\right)\left(\frac{\partial u_\beta}{\partial x}+\frac{\partial v_\beta}{\partial y}\right)+\frac{2G_\alpha}{h}\left(h+\frac{t}{2}\right)^2\nabla^2 w-2D\nabla^4 w+\right.$$
$$\left.\left.+\frac{N_x}{R_1}+\frac{N_y}{R_2}+N_x^0\frac{\partial^2 w}{\partial x^2}+N_y^0\frac{\partial^2 w}{\partial y^2}+2T^0\frac{\partial^2 w}{\partial x\,\partial y}\right]\delta w\right\}dx\,dy+$$
$$+\int_{a_1}^{a_2}\left\{N_y\delta v_\alpha+T\delta u_\alpha+2B\left(\frac{\partial v_\beta}{\partial y}+\mu\frac{\partial u_\beta}{\partial x}\right)\delta v_\beta+\right.$$
$$+B(1-\mu)\left(\frac{\partial v_\beta}{\partial x}+\frac{\partial u_\beta}{\partial y}\right)\delta u_\beta-2D\left(\frac{\partial^2 w}{\partial y^2}+\mu\frac{\partial^2 w}{\partial x^2}\right)\delta\left(\frac{\partial w}{\partial y}\right)+$$
$$+\left[N_y^0\frac{\partial w}{\partial y}+T^0\frac{\partial w}{\partial x}-2\frac{h+\frac{t}{2}}{h}G_\beta\left(v_\beta-\left(h+\frac{t}{2}\right)\frac{\partial w}{\partial y}\right)-\right.$$
$$\left.\left.-2D\left(\frac{\partial^2 w}{\partial y^2}+(2-\mu)\frac{\partial^2 w}{\partial x^2\,\partial y}\right)\right]\delta w\right|_{b_1}^{b_2}dx+\int_{b_1}^{b_2}\left\{N_x\delta u_\alpha+T\delta v_\alpha+\right.$$
$$+2B\left(\frac{\partial u_\beta}{\partial x}+\mu\frac{\partial v_\beta}{\partial y}\right)\delta u_\beta+B(1-\mu)\left(\frac{\partial v_\beta}{\partial x}+\frac{\partial u_\beta}{\partial y}\right)\delta v_\beta-$$
$$-2D\left(\frac{\partial^2 w}{\partial x^2}+\mu\frac{\partial^2 w}{\partial y^2}\right)\delta\left(\frac{\partial w}{\partial x}\right)+\left[N_x^0\frac{\partial w}{\partial x}+T^0\frac{\partial w}{\partial y}-\right.$$
$$\left.\left.-2\frac{h+\frac{t}{2}}{h}G_\alpha\left(u_\beta-\left(h+\frac{t}{2}\right)\frac{\partial w}{\partial x}\right)-2D\frac{\partial}{\partial x}\left(\frac{\partial^2 w}{\partial x^2}-(2-\mu)\frac{\partial^2 w}{\partial y^2}\right)\right]\delta w\right|_{a_1}^{a_2}dy+$$
$$\left.+4(1-\mu)D\left\{\left[\frac{\partial^2 w}{\partial x\,\partial y}\delta w\right]_{a_1}^{a_2}\right\}_{b_1}^{b_2}=0. \qquad (16.47)$$

Forces N_x, N_y, and T in this equation are connected with displacements by formulas (18).

Inasmuch as variations δu_α, ..., δw are arbitrary, factors in each of variations in first integral must be equal to zero From

this ensues five differential equations of stability. It is easy to see that these equations coincide with equations (25); in order to prove this, one should perform obvious transformations of the last equation by third and fourth equations.

Second and third integrals correspond to homogeneous static boundary conditions on every edge of shell; they are obtained by equating to zero the factors in variations of displacements, arbitrary on the edge. As we see, in distinction from homogeneous shells, where on edge it is possible to assign four conditions, for sandwich shells there should be given six conditions.

Let us turn to edge of shell x = const and write for it the basic boundary conditions.

1. Two boundary conditions are connected with deflections and turns on the edge or, with static boundary conditions, with transverse force and moments. In case of hinged support of external layer or a free edge magnitude $\delta(\partial w/\partial x)$ is arbitrary and boundary condition according to (47) will be

$$2D\left(\frac{\partial^2 w}{\partial x^2}+\mu\frac{\partial^2 w}{\partial y^2}\right)=0. \tag{16.48}$$

With clamping of external layers, instead of (48), we have

$$\frac{\partial w}{\partial x}=0. \tag{16.49}$$

If deflections on edge are arbitrary (edge is free from supports), we have

$$N_x^0\frac{\partial w}{\partial x}+T^0\frac{\partial w}{\partial y}-2\frac{h+\frac{t}{2}}{h}G_c\left[u_1-\left(h+\frac{t}{2}\right)\frac{\partial w}{\partial x}\right]-$$
$$-2D\frac{\partial}{\partial x}\left[\frac{\partial^2 w}{\partial x^2}+(2-\mu)\frac{\partial^2 w}{\partial y^2}\right]=0. \tag{16.50}$$

In the presence of supports, instead of this condition, we have geometric condition

$$w=0. \tag{16.51}$$

2. Two boundary conditions, connected with <u>displacements</u> u_α and v_α or in accordance with <u>forces</u> N_x and T, are determined by character of fastening of edge of shell as a whole relative to <u>displacements</u> in direction perpendicular to edge (u_α), and in direction tangent to edge (v_α).

If supports prevent such displacements, we have

$$u_\alpha = 0. \tag{16.52}$$

$$v_\alpha = 0. \tag{16.53}$$

If displacements u_α and v_α are not constrained, instead of these conditions we have

$$\frac{\partial u_\alpha}{\partial x} + \mu \frac{\partial v_\alpha}{\partial y} - \frac{w}{R_1} - \mu \frac{w}{R_2} = 0, \tag{16.54}$$

$$\frac{\partial v_\alpha}{\partial x} + \frac{\partial u_\alpha}{\partial y} = 0. \tag{16.55}$$

3. Last two boundary conditions are connected with <u>displacements</u> u_β and v_β or corresponding forces and are determined by character of fastening of edge of shell as a whole relative to <u>turns</u> in direction perpendicular to support (u_β), and relative to mutual displacements of external layers in direction tangent to edge (v_β).

If edge of shell is secured as a whole from turning (clamping), then

$$u_\beta = 0. \tag{16.56}$$

With hinged support or free edge

$$\frac{\partial u_\beta}{\partial x} + \mu \frac{\partial v_\beta}{\partial y} = 0. \tag{16.57}$$

If external layers are secured from mutual displacements direction tangent to edge, we have

$$v_\beta = 0. \tag{16.58}$$

In this case external layers in plane of support are united by shear resistant diaphragm. If there is no such diaphragm, then we should have

$$\frac{\partial v_3}{\partial x} + \frac{\partial u_3}{\partial y} = 0. \tag{16.59}$$

Furthermore, as follows from equation (47), in free angles there should be special conditions, having the same form as in theory of uniform plates and shells:

$$\frac{\partial^2 w}{\partial x \partial y} = 0. \tag{16.60}$$

During approximate solution of problems of stability displacements can be sought in a form satisfying not only geometric but also static boundary conditions. In this case it is possible to use the Bubnov-Galerkin method.

For sandwich plates ($R_1 = R_2 = \infty$) during loss of stability we have $u_\alpha = v_\alpha = 0$. In accordance with this the number of boundary conditions is reduced to four, and from equation (47) the first two drop.

Solution of problems of stability of sandwich plates and shells it is possible to simplify, if we disregard irregularity of distribution of stresses in the thickness of external layers, i.e., assume in equations of stability that flexural rigidity of external layers D is equal to zero. This assumption during solution of problems of stability is introduced by most authors. Here the order of system of equations of stability of shells (25) and plates (33) will be lowered. In accordance with this the number of boundary conditions will be reduced. Instead of six conditions for shells we will have five, and for plates instead of four, we have three; there disappears condition (49) for angle of rotation of external layer or

(48) for moment.

Let us turn to consideration of concrete problems, pertaining to sandwich plates and shells.

§ 164. Stability of Infinitely Wide Plate With Light Filler During Compression

Let us start with case when an infinitely wide plate with light filler, having span a, is compressed by evenly distributed forces* N (Fig. 16.13). We shall consider cylindrical form of loss of stability, so that

$$u_0 = u_0(x), \quad v_0 = 0, \quad w = w(x), \quad N_x^0 = -N, \quad N_y^0 = T^0 = 0.$$

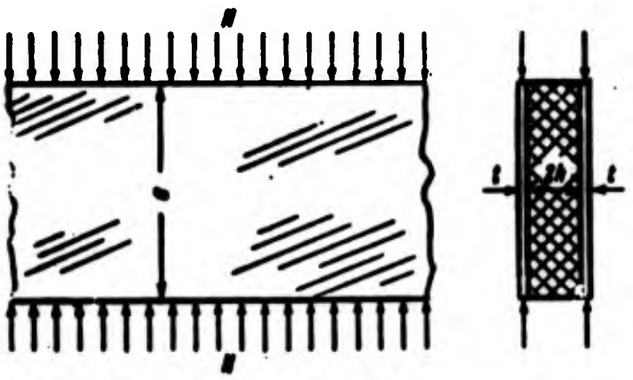

Fig. 16.13. Sandwich plate during compression in conditions of flat deformation.

Equations (33) will be written in the form

$$\left.\begin{aligned} \frac{Bh}{G_3}\frac{d^2u_3}{dx^2} - u_3 + \left(h + \frac{t}{2}\right)\frac{dw}{dx} = 0, \\ -2B\left(h + \frac{t}{2}\right)\frac{d^2u_3}{dx^2} - 2D\frac{d^4w}{dx^4} - N\frac{d^2w}{dx^2} = 0; \end{aligned}\right\} \tag{16.61}$$

here

$$B = \frac{Et}{1-\mu^2}, \quad D = \frac{Et^3}{12(1-\mu^2)}.$$

---

*This problem was considered upon different assumptions in works of A. L. Rabinovich [16.13], A. P. Voronovich [16.5] and many other authors. Different cases of support were considered by A. P. Prusakov [16.11], Bijlaard [16.14]. We gave here results from work [16.11].

We introduce dimensionless magnitudes

$$\xi = \frac{\pi x}{a}, \quad k = \frac{Bh}{G_1}\frac{\pi^2}{a^2}, \quad r = \frac{1}{12}\left(\frac{t}{h+\frac{t}{2}}\right)^3. \tag{16.62}$$

Equations (61) take form

$$\left.\begin{aligned} k\frac{d^2u_1}{d\xi^2} - u_1 + \left(h+\frac{t}{2}\right)\frac{\pi}{a}\frac{dw}{d\xi} = 0. \\ -\frac{a}{\pi\left(h+\frac{t}{2}\right)}\frac{d^2u_1}{d\xi^2} - r\frac{d^4w}{d\xi^4} - \varphi\frac{d^2w}{d\xi^2} = 0. \end{aligned}\right\} \tag{16.63}$$

Here φ is dimensionless parameter of critical load, connected with N by relationship

$$N = \varphi\frac{2\pi^2 B\left(h+\frac{t}{2}\right)^2}{a^2}. \tag{16.64}$$

We find solution of system (63), considering r = 0(D = 0). Characteristic equation of system in this case will be

$$\alpha^2[\alpha^2(1-k\varphi) - \varphi] = 0. \tag{16.65}$$

Solution will be registered in the form

$$\left.\begin{aligned} w &= A_1\sin\alpha\xi + A_2\cos\alpha\xi + A_3\xi + A_4, \\ u_1 &= -\frac{\pi}{a}\left(h+\frac{t}{2}\right)\left[\frac{a}{1+k\alpha^2}(A_2\sin\alpha\xi - A_1\cos\alpha\xi) - A_3\right]. \end{aligned}\right\} \tag{16.66}$$

where

$$\alpha = \sqrt{\frac{\varphi}{1-k\varphi}}.$$

Hence

$$\varphi = \frac{\alpha^2}{1+k\alpha^2}. \tag{16.67}$$

Value of α is determined by conditions of fastening of edges of plate.

Let us turn to boundary conditions. In connection with the fact that in considered case conditions connected with v_β disappear, there must be formulated (taking into account assumption D = 0) two boundary conditions on each of the edges of the plate: for w and u_β

or corresponding forces. With hinged support boundary conditions according to (51) and (57) will be

$$w=0,\ \frac{du_2}{dx}=0 \text{ when } x=0,\ x=a$$

or, in dimensionless form,

$$w=\frac{du_2}{d\xi}=0 \text{ when } \xi=0,\ \xi=\pi. \tag{16.68}$$

Subordinating solution (66) to boundary conditions (68), we obtain

$$\begin{aligned} A_2+A_4&=0, & A_1\sin\alpha\pi+A_2\cos\alpha\pi+A_3\pi+A_4&=0,\\ A_2&=0, & A_3\alpha\cos\alpha\pi+A_3\alpha\sin\alpha\pi&=0. \end{aligned}$$

Nontrivial solution takes place with equality to zero of determinant of the homogeneous system, which gives equation $\alpha\pi = 0$. To least value of critical load there corresponds $\alpha = 1$. Thus, parameter of critical load φ in formula (64) turns out to be, by (67), equal to

$$\varphi=\frac{1}{1+k}. \tag{16.69}$$

If edges of plates are clamped, boundary conditions according to (51) and (56) will be

$$w=s_1=0 \text{ when } \xi=0,\ \xi=\pi. \tag{16.70}$$

Determinant of system, obtained as a result of subordination of solution (66) to conditions (70), is reduced to equation

$$\sin\frac{\alpha\pi}{2}\left[2\sin\frac{\alpha\pi}{2}-\frac{\alpha\pi}{1+e^{2k}}\cos\frac{\alpha\pi}{2}\right]=0,$$

from which least α will be $\alpha = 2$. Then

$$\varphi=\frac{4}{1+4k}. \tag{16.71}$$

If edge x = 0 is clamped, and edge x = a is free (cantilever), boundary conditions for x = 0 according to (51) and (56) will be

$$w=s_1=0; \tag{16.72}$$

when x = a by (57) and (50) we have (taking into account D = 0)

$$\frac{du_0}{dx}=0,\quad -N\frac{dw}{dx}-2\frac{h+\frac{t}{2}}{h}G_0\left[u_0-\left(h+\frac{t}{2}\right)\frac{dw}{dx}\right]=0.$$

Taking into account the first of equations (61) and designations (62) and (64) last conditions will take form

$$\text{for } \xi=\pi\quad \frac{du_0}{d\xi}=0,\quad \frac{d^2u_0}{d\xi^2}+\varphi\left(h+\frac{t}{2}\right)\frac{\pi}{a}\frac{dw}{d\xi}=0. \tag{16.73}$$

By the same means in this case we obtain for α equation $\alpha\pi = 0$, from which $\alpha = 0.5$. Here

$$\varphi=\frac{1}{4+k}. \tag{16.74}$$

When <u>edge x = 0 is clamped</u>, and <u>edge x = a is freely supported</u>, boundary conditions will be

$$\left.\begin{aligned}&\text{for } \xi=0\quad w=u_0=0,\\&\text{for } \xi=\pi\quad w=\frac{du_0}{d\xi}=0.\end{aligned}\right\} \tag{16.75}$$

Equation for determination of α will be

$$\operatorname{tg}\alpha\pi=\frac{\alpha\pi}{1+k\alpha^2}. \tag{16.76}$$

Least of value of φ according to (67) and (76) depending upon k is given in graph of Fig. 16.14.

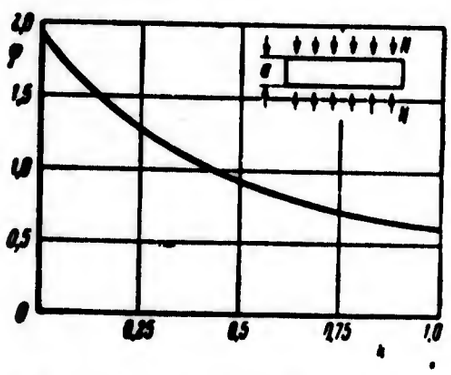

Fig. 16.14. Graph for parameter φ when one edge of plate is clamped, and other is freely supported.

We estimate limits of applicability of obtained solutions on the basis of assumption D = 0(r = 0). Introducing solution (66) in second equation (63), we write condition of acceptability of this assumption in the form

$$kz^2\ll\frac{1}{r}-1\approx\frac{1}{r}; \tag{16.77}$$

considering permissible an error of 5% and considering designation (62), we obtain

$$\frac{Bh}{G_c}\frac{\pi^2}{a^2} \leqslant 0.6\frac{\left(h+\frac{t}{2}\right)^2}{a^2b^2}. \qquad (16.78)$$

where α is determined depending upon boundary conditions ($0.5 < \alpha < 2$). Let us note that case $k = 0$ corresponds to homogeneous plate with flexural rigidity of $2B(h + t/2)^2$.

§ 165. Rectangular Freely Supported Plate During Longitudinal Compression

Let us turn to case of rectangular plate (Fig. 16.15), evenly

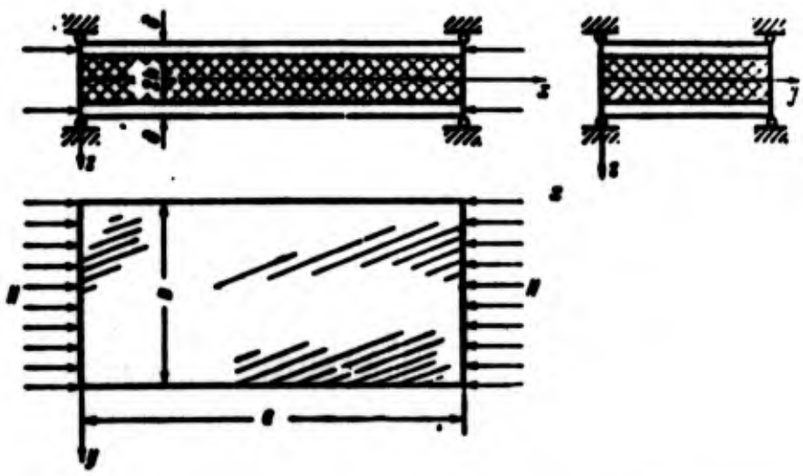

Fig. 16.15. Hinge-supported plate during compression.

compressed by forces* $N_x^0 = -N$. Introducing dimensionless magnitudes

$$\frac{b}{a}=\lambda,\quad \xi=\frac{ax}{a},\quad \eta=\frac{ay}{b},\quad k=\frac{Bh}{G_c}\frac{\pi^2}{b^2},\quad r=\frac{1}{12}\left(\frac{t}{h+\frac{t}{2}}\right)^2 \qquad (16.79)$$

and coefficient φ, equal to

$$\varphi=\frac{Nb^2}{2\pi^2B\left(h+\frac{t}{2}\right)^2}. \qquad (16.80)$$

*This problem was investigated by A. P. Voronovich [16.5], Bijlaard [16.14], Hoff [16.20] and other authors. In works of Bijlaard [16.14], Seide and Stowell [16.30] and A. P. Prusakov [16.11] there is given solution of problem taking into account work of external layers of plate beyond the elastic limits.

we write equation (33) in the form

$$\left.\begin{aligned}
&h\left(\lambda^2\frac{\partial^2 u_3}{\partial\xi^2}+\frac{1-\mu}{2}\frac{\partial^2 u_3}{\partial\eta^2}+\frac{1+\mu}{2}\lambda\frac{\partial^2 v_3}{\partial\xi\,\partial\eta}\right)-u_3+\left(h+\frac{\delta}{2}\right)\frac{\pi}{a}\frac{\partial w}{\partial\xi}=0,\\
&h\left(\frac{\partial^2 v_3}{\partial\eta^2}+\frac{1-\mu}{2}\lambda^2\frac{\partial^2 v_3}{\partial\xi^2}+\frac{1+\mu}{2}\lambda\frac{\partial^2 u_3}{\partial\xi\,\partial\eta}\right)-v_3+\left(h+\frac{\delta}{2}\right)\frac{\pi}{b}\frac{\partial w}{\partial\eta}=0,\\
&-\frac{b}{\pi\left(h+\frac{\delta}{2}\right)}\left(\lambda^2\frac{\partial^2}{\partial\xi^2}+\frac{\partial^2}{\partial\eta^2}\right)\left(\lambda\frac{\partial u_3}{\partial\xi}+\frac{\partial v_3}{\partial\eta}\right)-\\
&\qquad-r\left(\lambda^2\frac{\partial^2}{\partial\xi^2}+\frac{\partial^2}{\partial\eta^2}\right)^2 w-\varphi\lambda^2\frac{\partial^2 w}{\partial\xi^2}=0.
\end{aligned}\right\} \tag{16.81}$$

We obtain, first, a solution, considering r = 0(D = 0). On each of edges of plate there must be set three boundary conditions.

With free support of plate in accordance with (51) and (57) we have condition

$$\left.\begin{aligned}
&\text{when } x=0,\ x=a \quad w=\frac{\partial u_3}{\partial x}+\mu\frac{\partial v_3}{\partial y}=0,\\
&\text{when } y=0,\ y=b \quad w=\frac{\partial v_3}{\partial y}+\mu\frac{\partial u_3}{\partial x}=0.
\end{aligned}\right\} \tag{16.82}$$

Third condition it is possible to formulate differently depending upon presence or absence of shear-resistant diaphragms, connecting external layers on supports. If external layers are united by diaphragms, according to (58) we should have

$$\text{when } x=0,\ x=a \quad v_3=0; \quad \text{when } y=0,\ y=b \quad u_3=0. \tag{16.83}$$

If there are no diaphragms, according to (59) for x = 0, x = a, y = 0, y = b we have

$$\frac{\partial v_3}{\partial x}+\frac{\partial u_3}{\partial y}=0. \tag{16.84}$$

We find solution of problem, assuming that on edge there are diaphragms. Taking into account designations (79) we write boundary conditions in the form,

$$\left.\begin{aligned}
&\text{when } \xi=0,\ \xi=\pi \quad w=\frac{\partial u_3}{\partial\xi}=v_3=0,\\
&\text{when } \eta=0,\ \eta=\pi \quad w=\frac{\partial v_3}{\partial\eta}=u_3=0.
\end{aligned}\right\} \tag{16.85}$$

Boundary conditions (85) and equations (81) it is possible to satisfy, seeking a solution in the form

$$w = A \sin m\xi \sin n\eta, \quad u_1 = B \cos m\xi \sin n\eta, \quad v_1 = C \sin m\xi \cos n\eta. \tag{16.86}$$

where m and n are integers. Equations (81) give homogeneous system, equality to zero of whose determinant leads to equation for parameter of critical load

$$\varphi = \frac{(n^2 + m^2\lambda^2)^2}{m^2\lambda^2[1 + k(n^2 + m^2\lambda^2)]}.$$

Obviously, to least value of φ there corresponds n = 1. Designating $m\lambda = mb/a = \psi$, we obtain

$$\varphi = \frac{(1 + \psi^2)^2}{\psi^2[1 + k(1 + \psi^2)]}. \tag{16.87}$$

Integer m in formula (87) is selected in such a way that value of φ is the smallest. Critical load is determined by the formula

$$N = \varphi \frac{2\pi^2 B\left(k + \frac{1}{2}\right)^2}{b^2}.$$

On graph of Fig. 16.16 there are given values of φ depending upon ratio a/b for a series of values of parameter k. If ratio a/b is great (a/b > 2.5), value of φ in formula (87) can be found from condition of minimum

$$\frac{d\varphi}{d\psi} = 0. \tag{16.88}$$

Equation (88) will be written in the form

$$\frac{(1 + \psi^2)[\psi^2(1 - k) - (1 + k)]}{\psi^3[1 + k(1 + \psi^2)]^2} = 0. \tag{16.89}$$

When k < 1, we have

$$\psi^2 = \frac{1 + k}{1 - k}, \quad \varphi = \frac{4}{(1 + k)^2}. \tag{16.90}$$

When k > 1, the only positive root of equation (89) is equal to $\psi^2 = \infty$, consequently

$$\varphi = \frac{1}{k}. \tag{16.91}$$

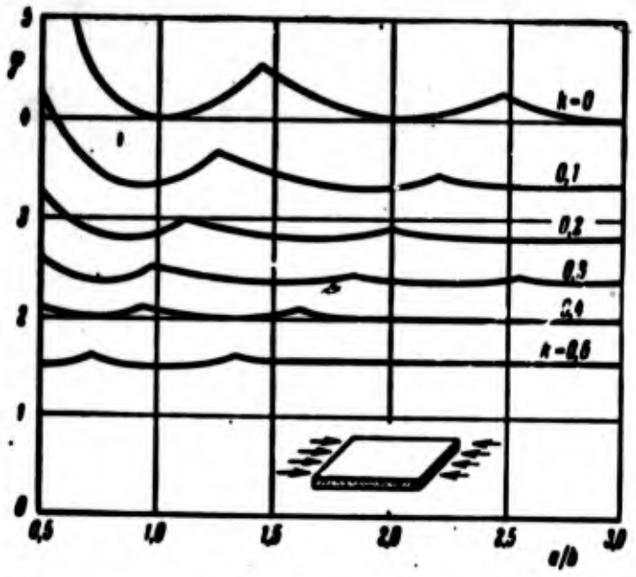

Fig. 16.16. Graph for parameter φ in case of freely supported plate.

Let us note that when $k \to 1$, in longitudinal direction by our conclusions there should appear waves, length of which $a/m \to 0$. It is not difficult to see that this finding is result of assumption of $r = 0$ for $D = 0$. In connection with this it is possible to write solution of problem taking into account flexural rigidity of external layers and to try to estimate limits of applicability of assumption $D = 0$.

As a result it turns out to be expedient to limit applicability of assumption $D = 0$ to conditions $k < 1$. When $k > 1$ assumption $D = 0$ leads to essential distortion of true character of wave formation.

Inequality $k < 1$ it is possible to take as criterion of acceptability of assumption $D = 0$ also with other conditions of fastening and other forms of load. Such conclusion is confirmed by comparison with more exact solutions, obtained without this assumption.

§ 166. Other Conditions of Fastening of Edges. Method of Split Rigidities

During solution of problems of stability of rectangular plates,

two opposite edges of which are freely supported and on the two others there are given different conditions, it is possible to use method of Levy known in theory of homogeneous plates. Let us consider case of rectangular plate, compressed uniformly by forces $N_x^0 = -N$, unloaded edges of which are clamped, and loaded edges are freely supported* (Fig. 16.17). Assuming that on edges of plate there are diaphragms, we write boundary conditions taking into account designations (79) in the form

$$\left.\begin{aligned} \xi=0,\ \xi=\pi,\quad & w=\frac{\partial u_3}{\partial \xi}=v_3=0,\\ \eta=0,\ \eta=\pi,\quad & w=v_3=u_3=0. \end{aligned}\right\} \tag{16.92}$$

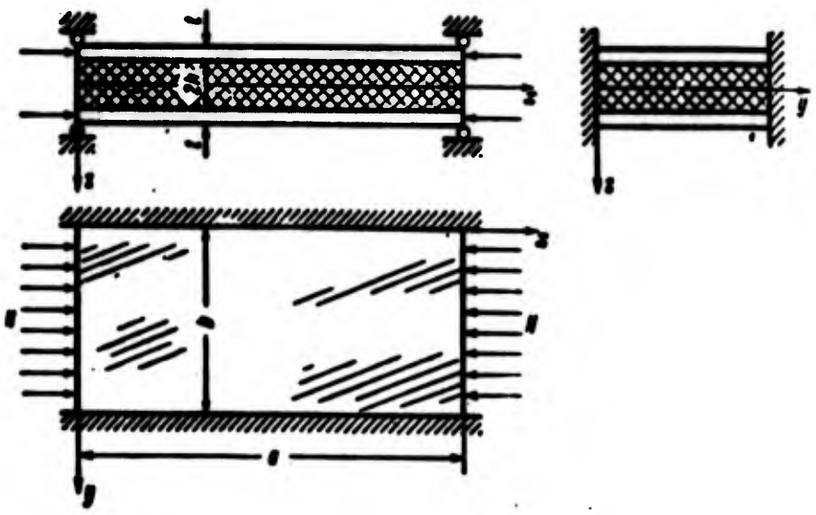

Fig. 16.17. Compressed plate with clamped longitudinal edges.

*Solution of this problem was obtained in works of Seide [16.29], Yen, Salerno and Hoff [16.36], A. P. Prusakov [16.11]. Other boundary conditions are considered by Thurston [16.32] and A. P. Prusakov [16.11]. Problem of stability of long freely supported plate during shear was considered by Seide [16.29]; of a rectangular freely supported plate during shear, by A. P. Voronovich [16.5]; during shear together with compression, by A. P. Prusakov [16.11]; during compression in two directions, by Reissner [16.27]. Stability of sandwich plates with filler of corrugation type was considered by Seide [16.29].

Solution of equations (81) for r = 0 we shall seek in the form

$$w = f_1(\eta)\sin m\xi, \quad u_2 = f_2(\eta)\cos m\xi, \quad v_3 = f_3(\eta)\sin m\xi. \tag{16.93}$$

where m is an integer. Boundary conditions on edges $\xi = 0$, $\xi = \pi$, obviously, are satisfied. Introducing expressions (93) in equations (81), we obtain system of ordinary differential equations for functions $f(\eta)$:

$$\left.\begin{aligned} -k\psi^2 f_2 + \frac{1-\mu}{2}kf_2'' + \frac{1+\mu}{2}k\psi f_3' - f_2 + \left(h+\frac{t}{2}\right)\frac{\pi}{b}\psi f_1 = 0, \\ kf_3'' - \frac{1-\mu}{2}k\psi^2 f_3 - \frac{1+\mu}{2}k\psi f_2' - f_3 + \left(h+\frac{t}{2}\right)\frac{\pi}{b}f_1' = 0, \\ -\psi^2 f_2 + \psi f_2'' + \psi^2 f_3' - f_3''' + \varphi\left(h+\frac{t}{2}\right)\frac{\pi}{b}\psi^2 f_1 = 0. \end{aligned}\right\} \tag{16.94}$$

where

$$\psi = \frac{bm}{a} = \lambda m, \quad \varphi = \frac{Nb^2}{2\pi^2 B\left(h+\frac{t}{2}\right)^2}.$$

Characteristic equation of system will be

$$\left[1 - \frac{1-\mu}{2}k(\gamma^2-\psi^2)\right]\left[(\gamma^2-\psi^2)^2 - \varphi\psi^2\left[1-k(\gamma^2-\psi^2)\right]\right] = 0. \tag{16.95}$$

Designating

$$\gamma_{1,2} = \psi\sqrt{1-\frac{k\varphi}{2} \pm \sqrt{\frac{k^2\varphi^2}{4} + \frac{\varphi}{\psi^2}}}, \quad \gamma_3 = \sqrt{\psi^2 + \frac{2}{(1-\mu)k}} \tag{16.96}$$

we write solution of system (94) in the form

$$\left.\begin{aligned} f_2 &= \sum_{i=1}^{3}(A_i \operatorname{ch}\gamma_i\eta + C_i \operatorname{sh}\gamma_i\eta), \\ f_3 &= \sum_{i=1}^{2}\frac{\gamma_i}{\psi}(C_i \operatorname{ch}\gamma_i\eta + A_i \operatorname{sh}\gamma_i\eta) + \frac{\psi}{\gamma_3}(C_3 \operatorname{ch}\gamma_3\eta + A_3 \operatorname{sh}\gamma_3\eta), \\ f_1 &= -\frac{b}{\left(h+\frac{t}{2}\right)\pi\psi}\sum_{i=1}^{2}[k(\gamma_i^2-\psi^2)-1](A_i \operatorname{ch}\gamma_i\eta + C_i \operatorname{sh}\gamma_i\eta). \end{aligned}\right\} \tag{16.97}$$

Subordinating solution (97) to boundary conditions, which according to (92) and (93) have form

$$f_1 = f_2 = f_3 = 0 \quad \text{when} \quad \eta = 0, \ \eta = \pi,$$

we will obtain system of homogeneous equations for arbitrary constant A_i and C_i. Equating determinant of this system to zero, we obtain equation which is split into two equations. The first of them has the form

$$\gamma_1\left[k\left(\gamma_2^2-\psi^2\right)-1\right]\operatorname{th}\frac{\gamma_1\pi}{2}-\gamma_2\left[k\left(\gamma_1^2-\psi^2\right)-1\right]\operatorname{th}\frac{\gamma_2\pi}{2}+$$
$$+\frac{\psi^2k\left(\gamma_1^2-\gamma_2^2\right)}{\gamma_3}\operatorname{th}\frac{\gamma_3\pi}{2}=0. \qquad (16.98)$$

Second equation is obtained from equation (98) by replacement everywhere of function th by cth. Calculations show that least value of φ gives equation (98). During calculations by equation (98) number of half-waves m should be selected from condition of minimum φ. On graph of Fig. 16.18 are given values of φ, obtained by equation (98), for a series of values of k as a function of ratio of sides a/b.

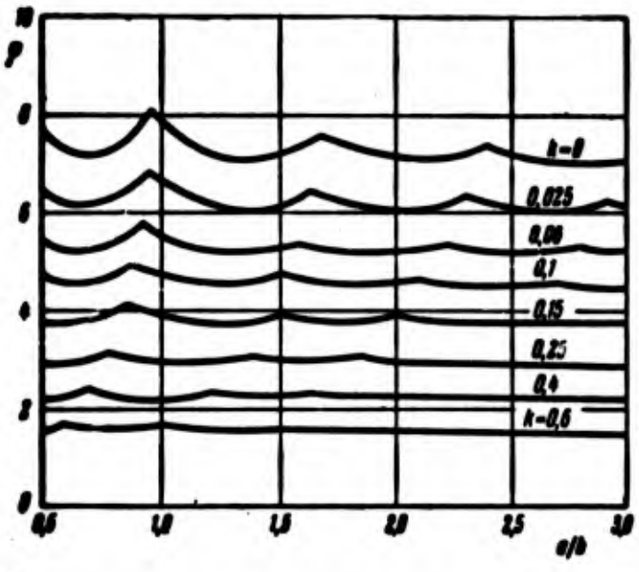

Fig. 16.18. Values of parameter φ for rectangular plate with clamped longitudinal edges.

We will specially consider case of compressed long plate with clamped longitudinal edges (Fig. 16.19). We turn for solution of this problem to method of approximation of split rigidities,*

*This method was offered by Bijlaard [16.14], who solved with its help a great number of different problems.

consisting of the following. In equation of stability of a sandwich plate (34)

$$2B\left(h+\frac{t}{2}\right)^2\nabla^4 w+\left(1-\frac{Bh}{G_3}\nabla^2\right)\left[2D\nabla^4 w-\right.$$
$$\left.-N_x^0\frac{\partial^2 w}{\partial x^2}-N_y^0\frac{\partial^2 w}{\partial y^2}-2T^0\frac{\partial^2 w}{\partial x\,\partial y}\right]=0$$

we assume $N_x^0 = -Nn_x$, $N_y^0 = -Nn_y$, $T^0 = -Nn_{x,y}$; here N is sought critical parameter with given character of loading of plate by forces n_x, n_y, $n_{x,y}$. Equation will take form

$$2B\left(h+\frac{t}{2}\right)^2\nabla^4 w+\left(1-\frac{Bh}{G_3}\nabla^2\right)[2D\nabla^4 w+NP(w)]=0. \qquad (16.99)$$

where

$$P(w)=n_x\frac{\partial^2 w}{\partial x^2}+n_y\frac{\partial^2 w}{\partial y^2}+2n_{xy}\frac{\partial^2 w}{\partial x\,\partial y}.$$

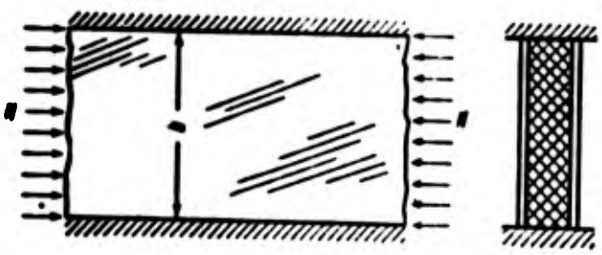

Fig. 16.19. Compressed infinitely long plate.

Then we consider three problems of stability.

Let us assume, first of all, that shear strength of middle layer is infinitely great ($G_3 \to \infty$), and that flexural rigidity of external layers is equal to zero. Equation (99) will take form

$$2B\left(h+\frac{t}{2}\right)^2\nabla^4 w+NP(w)=0. \qquad (16.100)$$

Further, we will assume that plate basically works on shearing ($G_c \to 0$), and, furthermore, as in first case, we take D = 0. Equation of this problem will be

$$2B\left(h+\frac{t}{2}\right)^2\nabla^4 w-\frac{Bh}{G_c}N\nabla^2 P(w)=0. \qquad (16.101)$$

Last, we shall consider extensional rigidity of external layer equal to zero (B = 0); then equation (99) will change into the following:

$$2D\nabla^4 w + NP(w) = 0. \tag{16.102}$$

Let us assume that in all cases forms of loss of stability w are identical. If we designate by N_1, N_2, N_0 critical loads correspondingly for each of three problems, then we obtain

$$2B\left(h+\frac{t}{2}\right)^2\nabla^4 w = -N_1 P(w),$$
$$\frac{Bh}{G_c}\nabla^2 P(w) = -\frac{N_1}{N_2}P(w),$$
$$2D\nabla^4 w = -\frac{N_2}{N_0}P(w).$$

Introducing these expressions in fundamental equation (99), we find

$$-N_1 P(w) + \left(1+\frac{N_1}{N_2}\right)(N-N_0)P(w) = 0,$$

hence

$$N = N_0 + \frac{1}{\frac{1}{N_1}+\frac{1}{N_2}}. \tag{16.103}$$

This formula is the principal one in method of split rigidities. Length of half-wave of buckling for N_0, N_1, N_2 is taken as the same; it is determined from condition of a minimum N.

We shall illustrate method of split rigidities by the example of the problem in Fig. 16.19. Finding N_1, we, essentially, consider case of a homogeneous plate. Considering

$$w = \sin\frac{\pi x}{l}\left(1-\cos\frac{2\pi y}{b}\right)$$

and integrating according to Bubnov-Galerkin method an equation of type (100):

$$2B\left(h+\frac{t}{2}\right)^2\nabla^4 w + N_1\frac{\partial^2 w}{\partial x^2} = 0,$$

we obtain

$$N_1 = \frac{2\pi^2 B\left(h+\frac{t}{2}\right)^2}{b^2}\cdot\frac{[2+(1+4\beta^2)^2]}{3\beta^2}, \quad \beta = \frac{l}{b}; \tag{16.104}$$

here L is half of wave length during buckling.

For determination of N_2 we present equation (101) in the form

$$2\frac{G_c\left(h+\frac{t}{2}\right)^2}{h}\nabla^2 w - N_2\frac{\partial^2 w}{\partial x^2}=0.$$

Considering

$$w = F(y)\sin\frac{\pi x}{L},$$

we obtain equation

$$2\frac{G_c\left(h+\frac{t}{2}\right)^2}{h}\left(\frac{\partial^2 F}{\partial y^2}-\frac{\pi^2}{L^2}F\right)+N_2\frac{\pi^2}{L^2}F=0.$$

Integral of this equation will be

$$F(y) = C_1\sin\varkappa y + C_2\cos\varkappa y,$$

where

$$\varkappa^2 = \frac{\pi^2}{L^2}\left[\frac{N_2}{2G_c\left(h+\frac{t}{2}\right)^2}-1\right].$$

We use boundary conditions F(0) = F(b) = 0; then we find $bx = \pi$; hence

$$N_2 = 2G_c\frac{\left(h+\frac{t}{2}\right)^2}{h}(1+\beta^2). \qquad (16.105)$$

Turning to formula (103) and disregarding in it flexural rigidity of external layers ($N_0 = 0$), we obtain finally

$$N = \frac{2\pi^2 B\left(h+\frac{t}{2}\right)^2}{b^2}\frac{[2+(1+4\beta^2)^2]}{3\beta^2}\frac{1}{1+\frac{\pi^2 Bh}{G_c b^2}\frac{[2+(1+4\beta^2)^2]}{3\beta^2(1+\beta^2)}}.$$

Parameter φ in formula

$$N = \varphi\frac{2\pi^2 B\left(h+\frac{t}{2}\right)^2}{b^2}$$

will be equal to

$$\varphi = \frac{[2+(1+4\beta^2)^2](1+\beta^2)}{3\beta^2(1+\beta^2)+k[2+(1+4\beta^2)^2]},$$

where $k = \pi^2 Bh/G_3 b^2$. Parameter β is determined here from condition of minimum φ. Dependence of φ on parameter k is presented in Fig. 16.20.

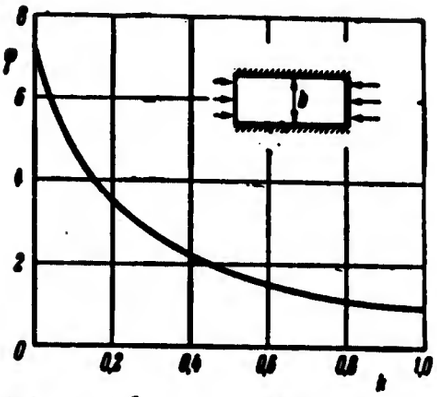

Fig. 16.20. Values of φ for infinitely long plate with clamped edges.

In conclusion let us note that method of split rigidities gives for real sandwich plates fully acceptable results.

§ 167. Stability of Cylindrical Sandwich Panel During Compression

Let us turn to problems pertaining to sandwich shells.

Let us consider stability in the small of a freely supported cylindrical panel, compressed by longitudinal evenly distributed forces* (Fig. 16.21). Equations of stability (25) on the assumption D = 0 will be written in the form

$$\left.\begin{aligned}\frac{\partial^2 u_0}{\partial x^2}+\frac{1-\mu}{2}\frac{\partial^2 u_0}{\partial y^2}+\frac{1+\mu}{2}\frac{\partial^2 v_0}{\partial x\,\partial y}-\frac{\mu}{R}\frac{\partial w}{\partial x}=0,\\ \frac{\partial^2 v_0}{\partial y^2}+\frac{1-\mu}{2}\frac{\partial^2 v_0}{\partial x^2}+\frac{1+\mu}{2}\frac{\partial^2 u_0}{\partial x\,\partial y}-\frac{1}{R}\frac{\partial w}{\partial y}=0.\end{aligned}\right\} \tag{16.106a}$$

$$\left.\begin{aligned}\frac{Bh}{G_3}\left(\frac{\partial^2 u_3}{\partial x^2}+\frac{1-\mu}{2}\frac{\partial^2 u_3}{\partial y^2}+\frac{1+\mu}{2}\frac{\partial^2 v_3}{\partial x\,\partial y}\right)-u_3+\left(h+\frac{t}{2}\right)\frac{\partial w}{\partial x}=0,\\ \frac{Bh}{G_3}\left(\frac{\partial^2 v_3}{\partial y^2}+\frac{1-\mu}{2}\frac{\partial^2 v_3}{\partial x^2}+\frac{1+\mu}{2}\frac{\partial^2 u_3}{\partial x\,\partial y}\right)-v_3+\left(h+\frac{t}{2}\right)\frac{\partial w}{\partial y}=0.\end{aligned}\right\} \tag{16.106b}$$

$$-2B\left(h+\frac{t}{2}\right)\nabla^2\left(\frac{\partial u_3}{\partial x}+\frac{\partial v_3}{\partial y}\right)+ +\frac{2B}{R}\left(\frac{\partial v_0}{\partial y}+\mu\frac{\partial u_0}{\partial x}-\frac{w}{R}\right)-N\frac{\partial^2 w}{\partial x^2}=0. \tag{16.106c}$$

Assuming that on edges of plate there are diaphragms, boundary conditions for case of free support we write in the form (see § 163)

$$\left.\begin{aligned}&\text{when } x=0,\ x=a \quad w=\frac{\partial u_\beta}{\partial x}=v_\beta=v_\alpha=\frac{\partial u_\alpha}{\partial x}=0,\\ &\text{when } y=0,\ y=b \quad w=\frac{\partial v_\alpha}{\partial y}=u_\alpha=u_\beta=\frac{\partial u_3}{\partial y}=0.\end{aligned}\right\} \tag{16.107}$$

*Solution of problem of stability of cylindrical freely supported panel with light filler is obtained in work of Stein and Mayers [16.31] and in work [16.9]. Other boundary conditions are considered by V. F. Karavanov [16.7]. Number of problems is solved in work [16.9] of L. M. Krushin; he also investigated problem about stability during shearing and of stability during compression beyond the elastic limit.

We seek the solution of equations (106) in the form

$$\left.\begin{aligned} w &= A_1 \sin m\xi \sin n\eta, \\ u_\alpha &= A_2 \cos m\xi \sin n\eta, \quad u_\beta = A_3 \cos m\xi \sin n\eta, \\ v_\alpha &= A_4 \sin m\xi \cos n\eta, \quad v_\beta = A_5 \sin m\xi \cos n\eta; \end{aligned}\right\} \tag{16.108}$$

here m and n are integers; $\xi = \pi x/a$, $\eta = \pi y/b$.

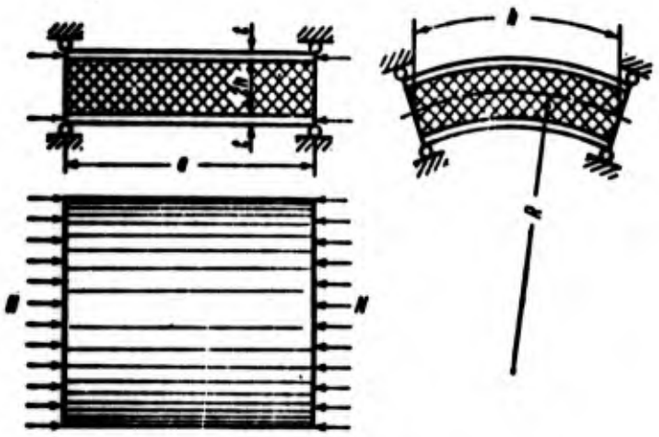

Fig. 16.21. Cylindrical freely supported panel during compression.

Introducing displacements (108) in equations (106), from condition of equality to zero of determinant of the system we find for parameter of critical load expression

$$\varphi = \frac{(n^2 + m^2\lambda^2)^2}{m^2\lambda^2[1 + k(m^2\lambda^2 + n^2)]} + \alpha^2 \frac{m^2\lambda^2}{(m^2\lambda^2 + n^2)^2}; \tag{16.109}$$

here

$$\varphi = \frac{Nb^2}{2\pi^2 B\left(h + \frac{t}{2}\right)^2}, \quad k = \frac{\pi^2 Bh}{G_c b^2}, \quad \alpha^2 = \frac{b^4(1-\mu^2)}{\pi^4 R^2\left(h + \frac{t}{2}\right)^2}, \quad \lambda = \frac{b}{a}.$$

Values of integers m and n in formula (109) are determined in such a way as to obtain least value of φ. In Figs. 16.22 and 16.23 are given minimum magnitudes of φ for certain values of α and k. Obtained results are applicable, as is shown in work [16.10], when $\alpha^2 < (1 - k)/k^2$. In case $\alpha^2 > (1 - k)/k^2$ it is necessary to take into account rigidity of external layers (see [16.10]). Results without calculation for D give in this case somewhat decreased value of critical load.

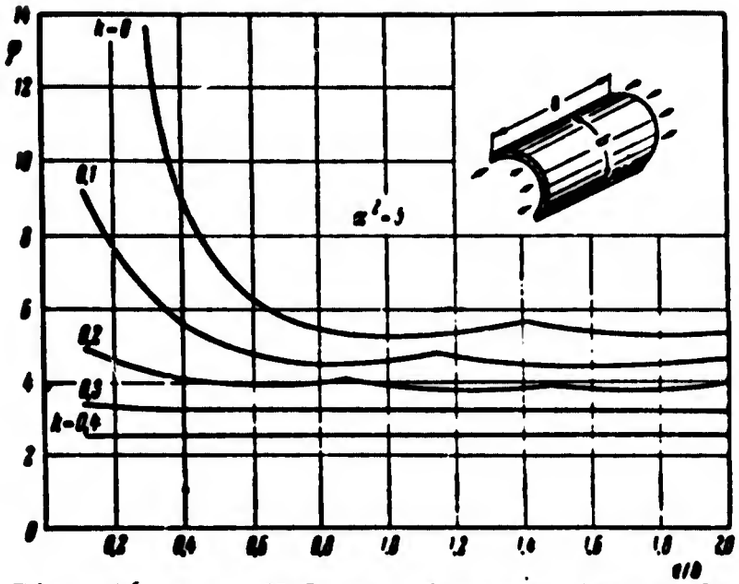

Fig. 16.22. Values of parameter φ for cylindrical panel when $\alpha^2 = 5$.

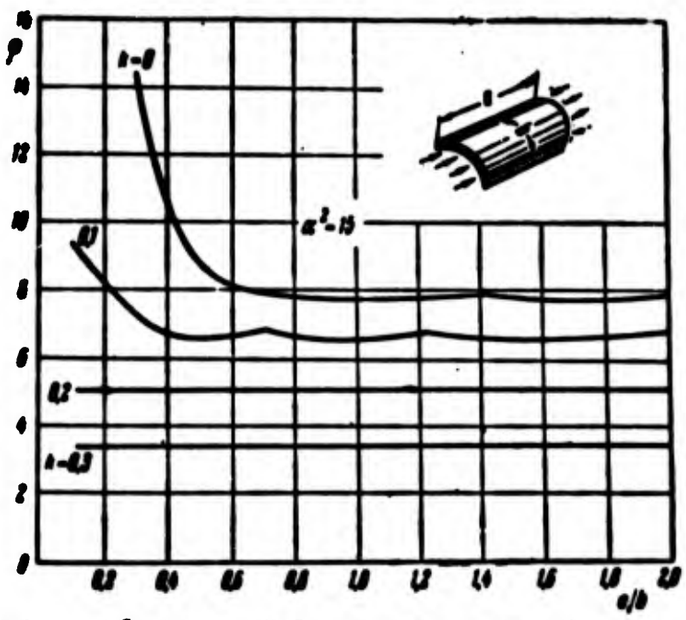

Fig. 16.23. Values of parameter φ for cylindrical panel when $\alpha^2 = 15$.

Certain research of stability of sandwich panels in the large [16.10] leads to preliminary conclusion that effect of nonlinearity of problem is not so evident here, as in case of homogeneous shell. Consideration of this question should be pursued.

§ 168. Stability of Sandwich Cylinder During Longitudinal Compression and External Pressure

Let us consider long sandwich cylinder with light filler, loaded by uniform compressive longitudinal load* $N_x^0 = -N$ (Fig. 16.24). Here, too, we shall originate from linear equations.

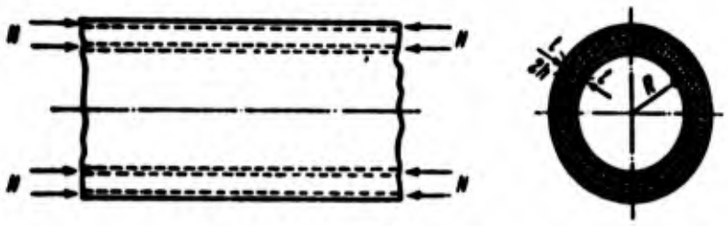

Fig. 16.24. Sandwich cylinder, compressed along generatrix.

Equation of stability (32) for deflection on the condition that $D = 0$ we write in the form

$$2B\left(h+\frac{t}{2}\right)^2\nabla^2 w+\left(1-\frac{Bh}{G_c}\nabla^2\right)\left[\frac{2(1-\mu^2)}{R^2}\frac{\partial^4 w}{\partial x^4}+\nabla^2\left(N\frac{\partial^2 w}{\partial x^2}\right)\right]=0. \qquad (16.110)$$

If loss of stability is axisymmetric, equation (110) will take form

$$2B\left(h+\frac{t}{2}\right)^2\frac{d^4 w}{dx^4}+\left(1-\frac{Bh}{G_c}\frac{d^2}{dx^2}\right)\left[\frac{2(1-\mu^2)B}{R^2}\frac{d^4 w}{dx^4}+N\frac{d^6 w}{dx^6}\right]=0. \qquad (16.111)$$

Considering $w = A \sin(\pi x/L)$, where L is length of half-wave in longitudinal direction, from (111) we find

$$\varphi=\frac{\beta^2}{\gamma^2}+\frac{\gamma^2}{1+k_B\gamma^2}. \qquad (16.112)$$

---

*Linear problems of stability of sandwich cylindrical shells with light filler during compression were considered in works of Legget and Hopkins [16.22], Stein and Mayers [16.31], and Gerard [16.17]. Case of filler of corrugation type is considered in works [16.31] and [16.9]. Stability of sandwich cylinder during compression beyond the elastic limit is considered by E. I. Grigolyuk [16.6]. Problem of stability of long sandwich cylinder with light filler during torsion was solved in works of Gerard [16.17] and L. M. Kurshin [16.9].

where

$$\varphi=\frac{2NR^2}{B\left(h+\frac{t}{2}\right)^2},\quad k_R=\frac{Bh}{G_c R^2},\quad \beta^2=\frac{R^2(1-\mu^2)}{\left(h+\frac{t}{2}\right)^2},\quad \gamma=\frac{\pi R}{L}.$$

From condition of minimum (112) we obtain

$$\text{when } k_R\beta<1\ \ \gamma=\frac{\beta}{\sqrt{1-k_R\beta}};\quad \text{when } k_R\beta>1\ \ \gamma^2=\infty.$$

Thus, in first case,

$$\varphi=\beta(2-k_R\beta) \tag{16.113}$$

and in second,

$$\varphi=\frac{1}{k_R}. \tag{16.114}$$

Research, conducted for general case of loss of stability [16.9], shows that for sandwich cylinders when $R/(h + t/2) > 100$ least value of critical load is given by symmetric form. Let us note that formula (114), obtained without calculation of flexural rigidity of external layers, gives decreased value of load.

It would be desirable to consider problem of stability of cylindrical sandwich shell from positions of nonlinear theory and to conduct experimental research, which would allow us to estimate practical value of above mentioned formulas.

In conclusion we give without derivation the formula for calculation for stability in the small of a long sandwich cylinder with light filler, loaded by evenly distributed external pressure. Critical pressure is determined by the formula

$$q=\frac{6B\left(h+\frac{t}{2}\right)^2}{R^3(1+4k_R)}. \tag{16.115}$$

Loss of stability here, as in case of long single-layer cylinder, occurs with formation of two waves in circumferential direction.

Literature

16.1. A. Ya. Aleksandrov, L. E. Bryukker, L. M. Kurshin, and A. P. Prusakov. Design of sandwich panels, Oborongiz, 1960.

16.2. A. Ya. Aleksandrov. Elastic parameters of ribbed fillers of sandwich panels, "Problems of design of elements of aviation constructions," Oborongiz, 1 (1959); Determining reduced elastic parameters of honey comb fillers of sandwich panels (jointly with E. P. Trofimovoy), loc. cit., 2.

16.3. A. Ya. Aleksandrov, G. S. Savvina, and G. M. Talanova. Local stability of sandwich panels with ribbed filler during compression, "Problems of design of elements of aviation constructions," coll. of articles 2, Oborongiz (1959).

16.4. L. E. Bryukker and L. M. Kurshin. On derivation by static means of equations of bending of a sandwich plate with rigid filler, News of Acad. of Sci. of USSR, OTN, Mech. and machine building, No. 3 (1959).

16.5. A. P. Voronovich. Stability of a skin with filler during compression and shear, Cand. diss., 1948.

16.6. E. I. Grigolyuk. Equations of sandwich shells with light filler, News of Acad. of Sci. of USSR, OTN, No. 1 (1957), Final deflections of sandwich shells with rigid filler, News of Acad. of Sci. of USSR, OTN, No. 1 (1958); On plastic stability of sandwich shells and plates, loc. cit., No. 6 (1958).

16.7. V. F. Karavanov. Equations of shallow sandwich shells with light filler during final displacements, News of Higher Educational Institutions, "Aviation technology," No. 1 (1958); Axisymmetric sandwich shell with light filler; News of Higher Educational Institutions, "Machine building," No. 6 (1958); Stability of shallow sandwich cylindrical panel with light filler with clamped longitudinal edges during axial compression, News of Higher Educational Institutions, "Aviation technology," No. 2 (1960); Equations of axisymmetric sandwich shells with light filler, "Strength of aircraft structures," Transactions MAI, No. 130 (1960), 110-132.

16.8. V. I. Korolev. Symmetric form of loss of stability of sandwich plates and shells, Herald of Moscow State University, series of phys-math. sciences, No. 5 (1956).

16.9. L. M. Kurshin. Certain questions of bending and stability of sandwich cylindrical shells, diss., Inst. of Mechanics of Academy of Sciences of USSR, 1958.

16.10. L. M. Kurshin. Equations of sandwich cylindrical shells, News of Acad. of Sci. of USSR, OTN, No. 3 (1958); On stability of a shallow cylindrical sandwich shell during compression, loc. cit., No. 8 (1958); On calculation of flexural rigidity of a curved sandwich panel, working on longitudinal compression, "Problems of design of elements of aviation constructions," coll. articles, 1, Oborongiz (1959); Stability during compression of a curved cylindrical

sandwich panels, longitudinal edges of which are freely supported, and transverse ones are clamped, loc. cit.; Stability during compression of cylindrical freely supported sandwich panel and a cylinder with corrugated filler, loc. cit.; Plastic stability of sandwich cylindrical shell, loc. cit., 2, Oborongiz (1959); On stability of sandwich plate during bending, News of Higher Educational Institutions, series "Construction and archt," No. 9 (1959).

16.11. A. P. Prusakov. Stability and free vibrations of sandwich plates with light filler, Doct. diss., Inst. of Mech of Acad. of Sci. of Ukrainian SSR, 1958.

16.12. A. P. Prusakov. Fundamental equations of bending and stability of sandwich plates with light filler, Applied math. and mech., 15, No. 1 (1951), Stability and free vibrations of sandwich plates with light filler, Combined works of Dnieperpetrovsk engineering and construction inst., No. 4 (1958).

16.13. A. L. Rabinovich. Stability of a skin with filler during compression, Oborongiz, 1946.

16.14. P. P. Bijlaard. Stability of sandwich plates, J. Aeron. Sci. 16, No. 9 (1949); Stability of sandwich plates in combined shear and compression, op. cit., 17, No. 1 (1950); Analysis of the elastic and plastic stability of sandwich plates by the method of split rigities. J. Aeron. Sci. 18, No. 5, No. 12 (1951); 19, No. 7 (1952); Buckling of sandwich cylinders under combined compression, torsion and bending loads, J. Appl. Mech. 23, No. 1 (1956).

16.15. H. L. Cox and J. R. Riddel. Sandwich construction and core materials, part 3, Instability of sandwich struts and beams, ARC Rep. and Memo., No. 2125, 1945.

16.16. A. C. Eringen. Bending and buckling of rectangular sandwich plates, Proc. of the 1st US Nat. Congr. of Appl. Mech., 1952.

16.17. G. Gerard. Buckling of a sandwich cylinder under uniform axial compressive load, J. Appl. Mech. 18, No. 4 (1951); Compressive and torsional instability of sandwich cylinders, Symp. of Struct. Sandwich Constr., ASTM, Spec. Techn. Publ., 118, 1951; Torsional instability of a long sandwich cylinder, Proc. of the 1st US Nat. Congr. of Appl. Mech., NY, 1952.

16.18. J. N. Goodier and J. M. Neou. The evaluation of theoretical critical compression in sandwich plates, J. Aeron. Sci. 18, No. 10 (1951).

16.19. W. S. Hemp. On a theory of sandwich construction, ARC Rep. and Memo., No. 2672, 1952; Proc. 7th Intern. Congr. Appl. Mech. 1, 1948.

16.20. N. J. Hoff. Bending and buckling of rectangular sandwich plates, NACA TN No. 2225, 1950.

16.21. J. H. Hunter-Tod. The elastic stability of sandwich plates, ARC Rep. and Memo, No. 2778, 1953.

16.22. D. Legget and H. Hopkins. Sandwich panels and cylinders under compressive end loads, ARC Rep. and Memo. No. 2262, 1942.

16.23. C. Libove and S. Batdorf. A general small deflection theory for flat sandwich plates, NACA Rep. No. 899, 1948; NACA TN No. 1526, 1948.

16.24. H. W. March. Sandwich construction in the elastic range, Symp. Struct. Sand. Constr., ASTM, Spec. Tech. Publ. No. 118, 1952; Elastic stability of the facings of sandwich columns, Proc. Symp. Appl. Math. 3 (1950).

16.25. A. Neut. Die Stabilität geschichteter Streifen, Netherlands Nat. Luchtvaartlabor., Amsterdam, Bericht No. 284 (1943).

16.26. H. Neuber. Theorie der Druckstabilität der Sandwich Platte, Teil 1, Zeit, für angv. Math. und Mech., No. 11/12 (1952); Teil 2, No. 1/2 (1953).

16.27. E. Reissner. Finite deflections of sandwich plates, J. Aeron. Sci. 15, No. 7 (1948); 17, No. 2 (1950); Small bending and stretching of sandwich-type shells, NACA TN No. 1832, 1949; NACA Rep. No. 975, 1950.

16.28. J. R. Robinson. The buckling and bending of orthotropic sandwich panels with all edges simply-supported, the Aeron. Quart. 6, No. 2 (1955).

16.29. P. Seide. The stability under longitudinal compression of flat symmetric corrugated-core sandwich plates with simply-supported loaded edges and simply supported or clamped unloaded edges, NACA TN No. 2679, 1952; Compressive buckling of flat rectangular metalite type sandwich plates with simply supported loaded edges and clamped unloaded edges, NACA TN No. 1886, 1949; No. 2637, 1952; Shear buckling of infinitely long simply supported metalite type sandwich plates, NACA TN No. 1910, 1949; On the torsion of rectangular sandwich plates, J. Appl. Mech. 23, No. 2 (1956), 191-194.

16.30. P. Seide and E. Stowell. Elastic and plastic buckling of simply supported metalite type sandwich plates in compression, NACA TN No. 1822, 1949; NACA Rep. No. 967, 1950.

16.31. M. Stein and J. Mayers. A small deflection theory for curved sandwich plates, NACA TN No. 2017, 1950; NACA Rep. No. 1008, 1951; Compressive buckling of simply supported curved plates and cylinders of sandwich construction, NACA TN No. 2601, 1952.

16.32. G. A. Thurston. Bending and buckling of clamped sandwich plates, J. Aeron. Sci. 24, No. 6 (1957), 407-412.

16.33. C. T. Wang. Principle and applications of complementary energy method for thin homogeneous and sandwich plates and shells with finite deflections, NACA TN No. 2620, 1952.

16.34. C. T. Wang and G. V. Rao. A study of an analogues model giving the nonlinear characterictics in the buckling theory of sandwich cylinder, J. Aeron. Sci. 19, No. 2 (1952).

16.35. C. T. Wang, R. J. Vaccaro, and D. F. deSanto. Buckling of sandwich cylinders under combined compression, torsion and bending loads, J. Appl. Mech. 22, No. 3 (1955).

16.36. K. T. Yen, V. G. Salerno, and N. J. Hoff. Buckling of rectangular sandwich plates subjected to edgewise compression with loaded edges simply supported and unloaded edges clamped, NACA TN No. 2556, 1952.

16.37. S. Yussuff. Theory of wrinkling in sandwich construction, J. Roy. Aeron. Soc. 59, No. 529 (1955).

C H A P T E R XVII

PLATES AND SHELLS AT HIGH TEMPERATURES

§ 169. General Equations

In this chapter we will return to the question of influence of high temperatures on stability of elastic systems, which partly was considered in Chapter V. As was already said in § 56, problems pertaining to this are urgent for aviation constructions: design of skin of aircraft having supersonic speed of flight is conducted taking into account aerodynamic heating. Question of influence of high temperatures is important also for design of shells in constructions of engines. But buckling of shells under the influence of thermal effects can occur also in constructions pertaining to other areas of engineering, e.g., in shells of towers or tanks which experience uneven heating in various directions.

We shall supplement fundamental equations of theory of flexible shallow shells (given in Chapter X) on the assumption that temperature changes both in middle surface and also throughout thickness of shell. We write expression for deformation ε_x^z along line of curvature x at distance z from middle surface

$$\varepsilon_x^z = \frac{1}{E^z}(\sigma_x^z - \mu^z \sigma_y^z) + \alpha t^{0,z}; \qquad (a)$$

by σ_x^z and σ_y^z here are understood stresses in the same layer of shell; by $t^{0,z}$ the temperature in degrees C in given layer; by E^z and μ^2; the elastic modulus and Poisson's ratio, depending, in general, on temperature; and by α, the coefficient of linear expansion of the material. Subsequently we shall consider magnitude $E^z = E$ and $\mu^z = \mu$ constants throughout thickness and corresponding to temperature of middle layer.

Magnitude ε_x^z, on the other hand, is equal to

$$\varepsilon_x^z = \varepsilon_x - z\frac{\partial^2 w}{\partial x^2}. \qquad (b)$$

where by ε_x is understood deformation in middle surface. Thus, we find,

$$\varepsilon_x - z\frac{\partial^2 w}{\partial x^2} = \frac{1}{E}(\sigma_x^z - \mu\sigma_y^z) + \alpha t^{0,z} \qquad (17.1)$$

and, analogously,

$$\varepsilon_y - z\frac{\partial^2 w}{\partial y^2} = \frac{1}{E}(\sigma_y^z - \mu\sigma_x^z) + \alpha t^{0,z}. \qquad (17.2)$$

We multiply all members of expressions (1) and (2) by z and integrate over thickness of plate, then we obtain

$$\left.\begin{aligned} -\frac{h^2}{12}\frac{\partial^2 w}{\partial x^2} &= \frac{1}{E}(M_x - \mu M_y) - \frac{h^2}{12}\alpha\theta, \\ -\frac{h^2}{12}\frac{\partial^2 w}{\partial y^2} &= \frac{1}{E}(M_y - \mu M_x) - \frac{h^2}{12}\alpha\theta; \end{aligned}\right\} \qquad (17.3)$$

here M_x, and M_y are bending momenty, and θ is reduced magnitude of "temperature moment:"

$$\theta = -\frac{12}{h^3}\int_{-\frac{h}{2}}^{\frac{h}{2}} t^{0,z} z\, dz. \qquad (17.4)$$

We find moments by (3):

$$\left.\begin{aligned} M_x &= -D\left(\frac{\partial^2 w}{\partial x^2} + \mu\frac{\partial^2 w}{\partial y^2}\right) + E\frac{h^2}{12}\frac{1}{1-\mu}\alpha\theta, \\ M_y &= -D\left(\frac{\partial^2 w}{\partial y^2} + \mu\frac{\partial^2 w}{\partial x^2}\right) + E\frac{h^2}{12}\frac{1}{1-\mu}\alpha\theta. \end{aligned}\right\} \qquad (17.5)$$

Putting these expressions in equation of equilibrium of a member of the shell (10.105), we arrive at following final equation,* replacing (10.107):

$$\frac{D}{h}\nabla^4 w = L(w, \Phi) + k_x\frac{\partial^2\Phi}{\partial y^2} + k_y\frac{\partial^2\Phi}{\partial x^2} + \frac{q}{h} - \frac{Eh}{12(1-\mu)}\nabla^2\theta. \qquad (17.6)$$

Further, we write by (1) and (2) expressions for deformations in the middle surface:

$$\left.\begin{aligned} \varepsilon_x &= \frac{1}{E}(\sigma_x - \mu\sigma_y) + \alpha T, \\ \varepsilon_y &= \frac{1}{E}(\sigma_y - \mu\sigma_x) + \alpha T; \end{aligned}\right\} \qquad (17.7)$$

here by T is understood magnitude

$$T = \frac{1}{h}\int_{-\frac{h}{2}}^{\frac{h}{2}} t^{0,z}\,dz. \qquad (17.8)$$

σ_x, σ_y are stresses in the middle surface. Putting (7) in equation of compatibility of deformations (10.93), we obtain in exchange for (10.109) this equation:

$$\frac{1}{E}\nabla^4\Phi = -\frac{1}{2}L(w, w) - k_x\frac{\partial^2 w}{\partial y^2} - k_y\frac{\partial^2 w}{\partial x^2} - \alpha\nabla^2 T. \qquad (17.9)$$

Consideration of equations (6) and (9) shows that temperature effect shows in them only through Laplacians $\nabla^2 T$ and $\nabla^2\theta$. Consequently, if magnitude T and θ remain constant along lines x and y or change by linear law, basic differential equations will be the same as for "cold" constructions. However, influence of temperature can nevertheless be seen in boundary conditions. Such case is characteristic for reinforced constructions. If skin is heated faster than reinforcing ribs, then temperature deformation of skin will be constrained

---

*Equations (6) and (9) are found in book of Kh. M. Mushtari and K. Z. Galimov [0.6]. General linear equations are given in book of W. Nowacki, "Questions of thermoelasticity," see Russian translation, 1962.

and in sheathing there can appear significant compressive stresses, causing buckling.

If we investigate small deflections of shell taking into account given forces in middle surface, then equations (6) and (9) will change into the following:

$$\left.\begin{aligned}\frac{D}{h}\nabla^4 w &= -p_x\frac{\partial^2 w}{\partial x^2}-p_y\frac{\partial^2 w}{\partial y^2}-2s\frac{\partial^2 w}{\partial x\,\partial y}+\\ &\quad+\frac{q}{h}+k_x\frac{\partial^2\Phi}{\partial y^2}+k_y\frac{\partial^2\Phi}{\partial x^2}-\frac{Eh\alpha}{12(1-\mu)}\nabla^2\Theta,\\ \frac{1}{E}\nabla^4\Phi &= -k_x\frac{\partial^2 w}{\partial y^2}-k_y\frac{\partial^2 w}{\partial x^2}-\alpha\nabla^2 T;\end{aligned}\right\} \qquad (17.10)$$

by p_x and p_y as before are understood given normal efforts (positive during compression); by s, tangential forces.

Excluding from this Φ, we obtain following resolvent with respect to w (with constant k_x and k_y),

$$\begin{aligned}&\frac{D}{Eh}\nabla^8 w+k_x^2\frac{\partial^4 w}{\partial y^4}+2k_xk_y\frac{\partial^4 w}{\partial x^2\partial y^2}+k_y^2\frac{\partial^4 w}{\partial x^4}+\\ &\quad+\frac{1}{E}\nabla^4\left(p_x\frac{\partial^2 w}{\partial x^2}\right)+\frac{2}{E}\nabla^4\left(s\frac{\partial^2 w}{\partial x\,\partial y}\right)+\frac{1}{E}\nabla^4\left(p_y\frac{\partial^2 w}{\partial y^2}\right)-\\ &-\frac{1}{Eh}\nabla^4 q-\frac{h\alpha}{12(1-\mu)}\nabla^6\Theta-\alpha k_x\frac{\partial^6}{\partial y^6}\nabla^2 T-\alpha k_y\frac{\partial^6}{\partial x^6}\nabla^2 T=0.\end{aligned} \qquad (17.11)$$

For circular cylindrical shell we will have

$$\begin{aligned}&\frac{D}{Eh}\nabla^8 w+\frac{1}{R^2}\frac{\partial^4 w}{\partial x^4}+\frac{1}{E}\nabla^4\left(p_x\frac{\partial^2 w}{\partial x^2}\right)+\\ &\quad+\frac{2}{E}\nabla^4\left(s\frac{\partial^2 w}{\partial x\,\partial y}\right)+\frac{1}{E}\nabla^4\left(p_y\frac{\partial^2 w}{\partial y^2}\right)-\frac{1}{Eh}\nabla^4 q-\\ &\quad-\frac{h\alpha}{12(1-\mu)}\nabla^6\Theta-\frac{\alpha}{R}\frac{\partial^6}{\partial x^6}\nabla^2 T=0.\end{aligned} \qquad (17.12)$$

For thin shells one may assume that temperature $t^{0,z}$ changes through thickness by linear law. With such assumption we find

$$T=t^{\circ}_{\text{сред.}},\quad \Theta=-\Delta t^{\circ}. \qquad (17.13)$$

Here Δt° characterizes temperatures differential $t_{\text{внеш}}$ and $t_{\text{внутр}}$

between external ($z = -h/2$) and internal ($z = h/2$) surfaces, and $t^\circ_{\text{сред}}$ is average temperature:

$$\Delta t^\circ = \frac{t^\circ_{\text{внеш}} - t^\circ_{\text{внутр}}}{2}, \quad t^\circ_{\text{сред}} = \frac{t^\circ_{\text{внеш}} + t^\circ_{\text{внутр}}}{2}. \tag{17.14}$$

If we consider $w \equiv 0$, then by (9) we obtain known equation of flat problem of thermoelasticity:*

$$\frac{1}{E}\nabla^4\Phi = -\alpha\nabla^2 T. \tag{17.15}$$

If however, we take $\Phi \equiv 0$, then we arrive at initial equation of problem of bending of plates in a nonuniform temperature field:

$$D\nabla^4 w = -\frac{Eh^3\alpha}{12(1-\mu)}\nabla^2\theta. \tag{17.16}$$

During research of stability of shells in the small one should write equations in "variations," which can be obtained from (10)-(12), if by w and Φ we understand deflection and function of stresses, connected with buckling, and set $q = 0$; temperature members here disappear.

§ 170. Flat Reinforced Panel

Let us consider case when flat rectangular panel of sheeting is fastened by hinge on its edges with bend-resistant ribs, so that points of all edges of panel are not displaced either in plane of plate or in transverse direction. We assume that temperature changes along axes x and y (Fig. 17.1) by parabolic law

$$T = T_0 + T_1\left[1 - \left(\frac{2x-a}{a}\right)^2\right]\left[1 - \left(\frac{2y-b}{b}\right)^2\right],$$

and is constant with thickness. We determine critical value of parameters T_0 and T_1, at which there will occur buckling of the plate.**

*Here is considered case of plane stress.

**This problem was considered by Klosner and Forray [17.15].

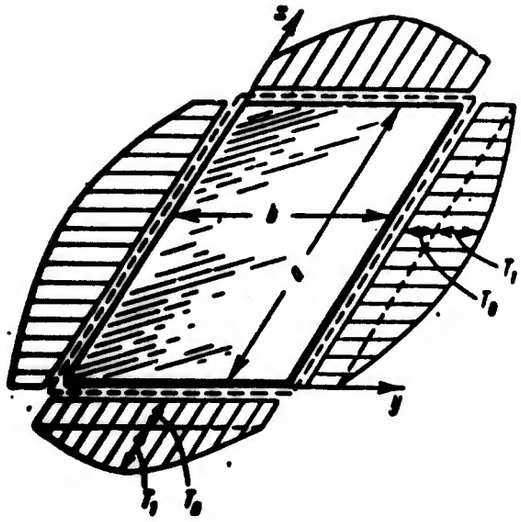

Fig. 17.1. Reinforced plate during nonuniform heating.

Stresses of fundamental state are determined from equation (15). Integral of this equation we write in the form

$$\Phi = \sum_m A_m \cos\frac{2m\pi x}{a} + \sum_n B_n \cos\frac{2n\pi y}{b} + \sum_m \sum_n C_{mn} \cos\frac{2m\pi x}{a} \cos\frac{2n\pi y}{b} - \frac{p_x y^2}{2} - \frac{p_y x^2}{2}. \tag{a}$$

where p_x, and p_y are average compressive stresses along x and y. Constants here are determined from boundary conditions, corresponding to fixed edges. Then we apply Ritz method. We select approximating expression for deflection in the form

$$w = \sum_m \sum_n f_{mn} \sin\frac{m\pi x}{a} \sin\frac{n\pi y}{b}. \tag{b}$$

Minimizing total energy of system with respect to f_{mn}, we arrive at system of linear equations for f_{mn}. Equating, as usual, the determinant of this system to zero, we find critical stress. Results of calculations by [17.15], conducted with retention of four members of series (b), are given by solid lines in Fig. 17.2 (we took $\mu = 0.32$). Along the axis of abscissas is plotted ratio a/b; along

the axis of ordinates, value of coefficient k_T, determining critical drop of temperatures $T_{1,kp}$ by the formula

$$T_{1,kp}^{\circ} = \frac{k_T}{1-\mu^2}\frac{1}{a}\left(\frac{h}{b}\right)^2.$$

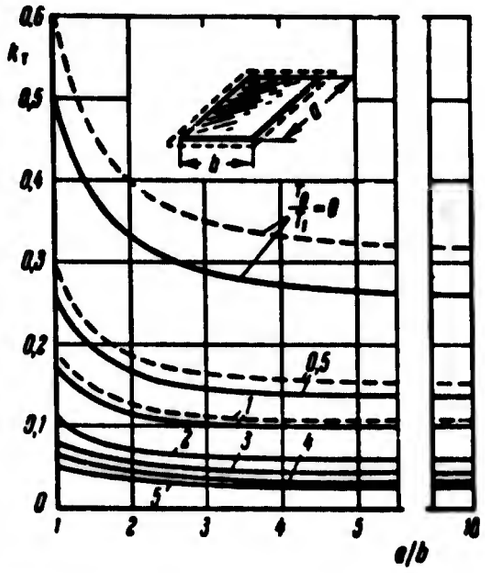

Fig. 17.2. Determining critical temperatures in case of reinforced plate.

Curves are constructed for various ratios T_0/T_1, characterizing temperature field. Dotted lines give results of approximate solution, in which temperature is taken uniform and corresponding to certain mean value between T_0 and T_1. When $T_0/T_1 \geqslant 2$ results of definitized and approximate solutions can be considered to coincide, while in case $T_0/T_1 < 2$ effect of irregularity of temperature field turns out to be substantial.

When one considers case, where reinforcing ribs are elastic and deformation of plate is less constrained, the irregularity of distribution of temperature will be even greater.

Question of postcritical deformation of plates in the presence of uniform or nonuniform distribution of temperatures is important, first of all, for calculation of aircraft skins. As already was said in Chapter VII, aerodynamic properties of construction depend on amplitudes of local buckles. On the one hand, wave formation of skin leads to increase of drag, and on the other, to increase of turbulence of flow, which, in turn, is connected with appearance of dangerous oscillations and development of fatigue cracks.* Last, it is

*This is indicated, in particular, in article of van der Neut [17.18].

necessary to determine influence of high temperatures on reduction factors. Problems of postcritical thermal buckling of plates must be solved with help of equations (6) and (9). Certain results in this region were obtained by van der Neut [17.18], and also V. V. Bolotin and Yu. N. Novichkov [19.5].

Case of cylindrical panel with nonuniform distribution of temperature throughout thickness was considered with help of equations (6) and (9) by M. S. Ganeyeva [17.3]. Problems, pertaining to stability of circular plates with nonuniform distribution of temperatures along radius, were investigated by S. G. Vinokurov [17.1] and E. I. Grigolyuk [17.4].

§ 171. Reinforced Cylindrical Shell

We turn to problems about stability of shells with high temperatures. These problems are of special interest for designing thin-walled constructions: thermal buckling of shell, frequently accompanied by knocks, leads to appearance of permanent deformations and lowering of rigidity of construction; such a phenomenon, as a rule, is impermissible. Furthermore, thermal stresses, even if they are themselves insignificant, can be that disturbing factor, which in connection with fundamental forces causes loss of stability of a shell in the large.

We shall consider first the case of an evenly heated circular cylindrical shell, fastened on ends with "cold" frames (Fig. 17.3), under the condition that ends freely are displaced in axial direction relative to each other. We assume that difference of temperatures of shell and frames constitutes T. "Cold" frame greatly blocks thermal lengthening of shell in circumferential direction, therefore in

shell there appear ring compressive stresses. Magnitude of them drops by measure of removal of considered point from frame, we obtain here stress of boundary effect type. At that moment, when compressive stresses attain critical level, near frame there appear buckling, axial symmetry of bending of shell is disturbed. We shall determine critical temperature at which such buckling of shell in the small occurs.* This problem is very close to those problems of stability of shells in zone of boundary effect, which were considered in § 141.

Fig. 17.3. Shell in case of nonuniform distribution of temperatures along generatrix.

We consider that in axial direction shell is deformed freely and that on ends there is clamping. In order to find stress in subcritical state, we use the first of equations (10). For axisymmetric problem with uniform distribution of temperatures we have

$$\frac{D}{h}\frac{d^4w}{dx^4}=\frac{\sigma_y}{R}=\frac{E}{R}\varepsilon_y. \tag{17.17}$$

or

$$\frac{D}{h}\frac{d^4w}{dx^4}-\frac{E}{R}\left(\alpha T-\frac{w}{R}\right)=0.$$

From this follows this equation:

$$\frac{Rh^2}{12(1-\mu^2)}\frac{d^4w}{dx^4}+\frac{w}{R}=\alpha T; \tag{17.18}$$

when T = 0 it changes into equation (11.192). Integrating (18) taking

*Similar problem was considered by Zuk [17.22], Johns [17.11], Hoff [17.14], L. M. Kurshin.

into account boundary conditions

$$w = 0, \quad \frac{dw}{dx} = 0 \text{ when } x = 0, \quad x = L,$$

we find

$$w = aRT\left[1 - e^{-2\beta\bar{x}}(A_1 \cos 2\beta\bar{x} + A_2 \sin 2\beta\bar{x}) - \right.$$
$$\left. - e^{-2\beta(1-\bar{x})}[A_1 \cos 2\beta(1-\bar{x}) + A_2 \sin 2\beta(1-\bar{x})]\right]. \qquad (17.19)$$

where

$$\bar{x} = \frac{x}{L}, \quad \beta = \frac{1}{2}\sqrt[4]{3(1-\mu^2)}\sqrt{\frac{L^2}{Rh}}.$$

By A_1 and A_2 we designate certain functions of magnitude β, characterizing relative length of shell. Using (17), we determine by (19) ring stresses σ_y. In Fig. 17.4 solid lines show dependence of magnitude $\sigma_y/E\alpha T$ on $\bar{x}$ for different values of β. Dotted line depicts function

$$\frac{\sigma_y}{E\alpha T} = \cos^2 \pi\bar{x}. \qquad (17.20)$$

As can be seen from graph, it approximately corresponds to parameter $\beta = 2$.

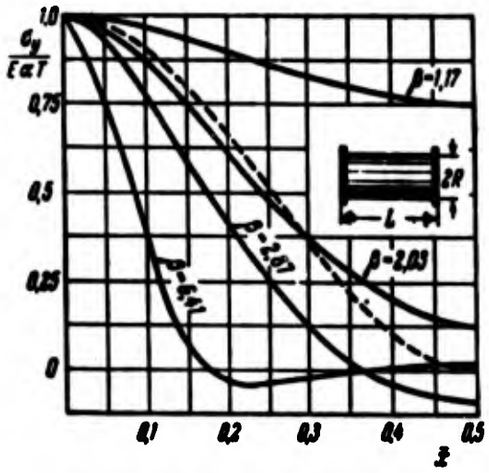

Fig. 17.4. Calculating stability of shell with nonuniform distribution of temperatures.

We take for example dependence (20) as initial* and determine critical temperature drop. We originate from equation (12); in our case it takes form

$$\frac{D}{Eh}\nabla^4 w + \frac{1}{R^2}\frac{\partial^4 w}{\partial x^4} - \frac{1}{E}\nabla^4\left(\sigma_y \frac{\partial^2 w}{\partial y^2}\right) = 0;$$

here by w is understood additional deflection. Approximating w with help of expression

$$w = f \sin^2 \frac{\pi x}{L} \sin \frac{ny}{R},$$

*Such assumption was made by Zuk [17.22].

as done in § 131 (p. 597), and using Bobnov-Galerkin method, we arrive at following expression for critical temperature:*

$$T_{кр} = \frac{1}{\sqrt{3(1-\mu^2)}} \frac{h}{R\alpha} \left\{ \frac{\pi^2}{4\psi^2} \left[1 + \frac{(1+4\psi^2)^2}{2} \right] + 128 \frac{\psi^4 n^2}{\pi^2} \right\}. \qquad (17.21)$$

where $\psi = \pi R/nL$. The number of waves n here should be determined from condition of minimum $T_{кр}$.

Let us give calculating formulas obtained by other means, pertaining to long shell, when $\beta > 5$. With clamping on end, the critical temperature is equal to

$$T_{кр} = \frac{6{,}41}{\sqrt{3(1-\mu^2)}} \frac{h}{\alpha R}, \qquad (17.22)$$

and with hinged support on end,

$$T_{кр} = \frac{12{,}21}{\sqrt{3(1-\mu^2)}} \frac{h}{\alpha R}. \qquad (17.23)$$

Corresponding ring stress near frames is equal in first case to $\sigma_{кр} = 3.88Eh/R$, and in second, $\sigma_{кр} = 7.4Eh/R$. The circumstance that magnitude $T_{кр}$ was higher for hinge-supported shell than for clamped is explained by great pliability of hinge-supported shell during heating. Judging by resulting expressions for $\sigma_{кр}$, thermal buckling of duralumin shells clamped on ends with $R/h < 1500$ will occur already beyond the elastic limit.

If ends of the shell cannot shift relative to each other during temperature increase in shell there will appear axial compressive stresses. Here one should expect buckling as in Fig. 17.5a within elastic limit and as in Fig. 17.5b, in elastoplastic region.

Of significant interest also are problems of buckling of cylindrical shells at a temperature, varying along circumference. Example

---

*This expression was obtained by L. M. Kurshin; formulas (22) and (23) are also his.

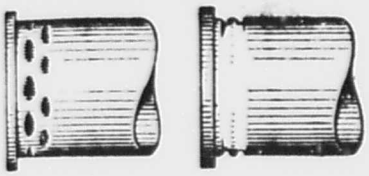

a) b)

Fig. 17.5. Thermal buckling of shell, a) with formation of diamond-shaped dents, b) axisymmetric.

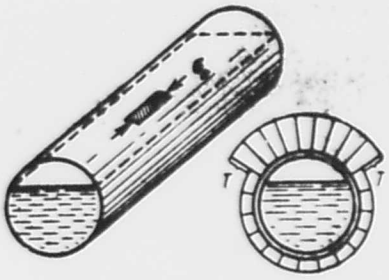

a) b)

Fig. 17.6. Shell in case of temperature, varying along circumference.

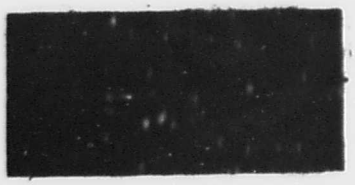

Fig. 17.7. Buckling of shell with nonuniform distribution of temperatures along circumference.

can be a shell, partially filled by liquid* (Fig. 17.6a). Let us assume that zone of shell, touching the liquid, has temperature lower than remaining zone, and difference of temperatures constitutes T (Fig. 17.6b). Then in region of heightened temperatures there will appear sections with compressive stresses (Fig. 17.6a) and here buckling can occur. Such conclusion is confirmed by experiments. Dents have form of diamonds and are located in middle part of shell by length (Fig. 17.7): appearance of dents usually is accompanied by a knock.

The method of solution of such a problem consists of the following. We determine diagram of distribution of initial stresses; of decisive value here are axial stresses σ_x. The diagram has various forms depending upon relationship between dimensions of

*This problem was considered by V. I. Usyukin; he also conducted experiments described here.

heated and cold zones. Further, for solution of problem of stability in the small we use equation (12). Detailed research shows that it is possible to produce practical calculations, as in case of buckling of shell during bending, by the greatest compression stress, comparing it with magnitude 0.605Eh/R. It is desirable to consider such problem in nonlinear formulation; apparently, here too one should compare the greatest compression stress with lower critical magnitude (see § 135).

§ 172. Buckling of Plates and Shells During Creep

Let us turn to problems of buckling of plates and shells during creep. They are more complicated than analogous problems, pertaining to bars (see Chapter V), since here in every layer of plate or shell there will be formed not uniaxial, but biaxial stress. Meanwhile laws of creep in complicated stress by themselves still have not been explained. Furthermore, peculiarity of phenomenon of buckling of plates and shells during creep consists of the fact that during deflections, comparable with their thickness, there appears effect of chain stresses. As we will see, for plates this influence is reduced to the fact that the process of buckling of the plate is "braked" and build-up of deflections fades.

At the same time for shells, subjected to creep, characteristic is buckling in the course of a knock. Therefore, research of this phenomenon will be sufficiently full only when it is conducted from propositions of stability in large. In Fig. 17.8 are compared characteristic diagrams "maximum deflection ζ-time t" for bars, plates and shells. Here we consider members of constructions, approximating real ones and having some initial deflection. In case

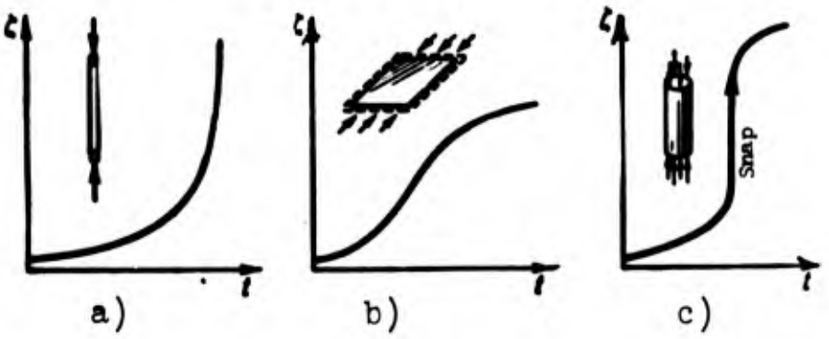

Fig. 17.8. Characteristic diagrams "deflection-time" for bar, plate and shell during creep.

of bar deflections monotonically grow in time (Fig. 17.8a). Deflections of plate at first increase in accelerated manner, then speed of growth of deflections gradually drops (Fig. 17.8b). Finally, in case of shell monotonic increase of deflections ends in a knock (Fig. 17.8c). These diagrams intentionally are simplified in separate experiments there can appear influence of such factors as non-correspondence of form of initial deflection and form of buckling, relationship between transient and steady-state creep, etc. What sort of form will "Deflection-time" diagram have for ideal member of construction not having initial imperfections? Is it possible to obtain such dependence as limiting one for diagrams of type of Fig. 17.8, driving initial deflections to zero? Apparently, to this question at present it is still impossible to give a final answer. Nevertheless in a number of works there are offered criteria of buckling of ideal constructions, presented in § 61. For plates and shells they frequently apply criterion of critical strain.* For instance, for elongated plate of width b compressed in one direction,

---

*See work of Gerard and Gilbert [17.10]. A somewhat different approach is offered in another article by Gerard (J. Aerospace Sci., 29, No. 9, 1962).

critical deformation in elastic region is equal to

$$\varepsilon_{кр} \approx 3{,}62\left(\frac{h}{b}\right)^2. \qquad (a)$$

We assume that creep buckling will set in when approach of loaded edges attains this magnitude. For compressed circular cylindrical shell analogous approach leads to formula

$$\varepsilon_{кр.ц} = 0{,}605\,\frac{h}{R}. \qquad (b)$$

if as the basis we take upper critical load. But, as we will see later, calculation by (b) gives sharply overstated values of critical time, calculation by lower critical deformation will agree better with experiments

$$\varepsilon_{кр.ц} \approx 0{,}18\,\frac{h}{R}. \qquad (c)$$

A dynamic criterion of stability of plates during creep was developed by Yu. N. Rabotnov and S. A. Shesterikov [5.6]. V. M. Panferov offered method of determination of critical time during transient creep on the basis of a series of experiments in extension of samples with given speeds of change of deformation.

Subsequently we in detail will discuss criterion of initial imperfections; we shall consider that initial and additional deflections are comparable to thickness of plate or shell.

§ 173. Buckling of Plate, Having Initial Deflection

We shall investigate case of rectangular plate with sides a and b, supported on edges and compressed along edges a (Fig. 17.9); we assume that edges of plate remain rectilinear and that unloaded edges freely approach one another.*

*The problem was considered in such form by author in 1959.

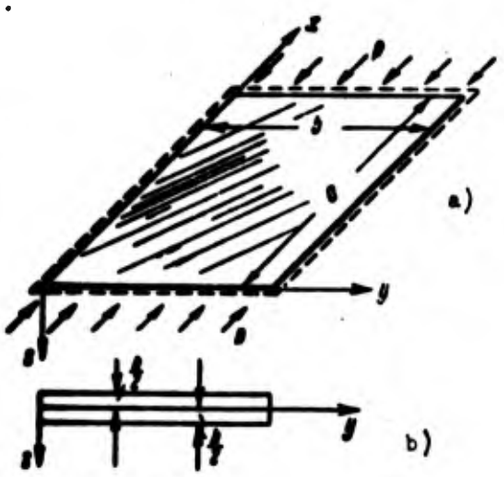

Fig. 17.9. Square flat panel, compressed along one of its sides.

Fundamental equations we write according to (10.111);

$$\left.\begin{aligned} \frac{D}{h}\nabla^4(w-w_0) &= L(w,\Phi),\\ \frac{1}{E}\nabla^4\Phi &= \frac{1}{2}[L(w_0,w_0)-L(w,w)]. \end{aligned}\right\} \tag{17.24}$$

where w and w_0 are total and initial deflections.

Solving problem in first approximation, we take for deflections the approximating expressions

$$w = f\sin\frac{\pi x}{a}\sin\frac{\pi y}{b},\quad w_0 = f_0\sin\frac{\pi x}{a}\sin\frac{\pi y}{b}. \tag{17.25}$$

Putting (25) in the right part of the second of equations (24), we find

$$\Phi = \frac{E}{32}(f^2-f_0^2)\left[\left(\frac{a}{b}\right)^2\cos\frac{2\pi x}{a}+\left(\frac{b}{a}\right)^2\cos\frac{2\pi y}{b}\right]-\frac{py^2}{2}; \tag{17.26}$$

by p is understood intensity of forces of compression. Stresses in middle surface will be

$$\sigma_x = \frac{\partial^2\Phi}{\partial y^2},\quad \sigma_y = \frac{\partial^2\Phi}{\partial x^2},\quad \tau = -\frac{\partial^2\Phi}{\partial x\,\partial y}. \tag{17.27}$$

Flexural stresses, the greatest by thickness of plate, are equal to

$$\left.\begin{aligned} \sigma_{x,u} &= \mp\frac{Eh}{2(1-\mu^2)}\left[\frac{\partial^2(w-w_0)}{\partial x^2}+\mu\frac{\partial^2(w-w_0)}{\partial y^2}\right].\\ \sigma_{y,u} &= \mp\frac{Eh}{2(1-\mu^2)}\left[\frac{\partial^2(w-w_0)}{\partial y^2}+\mu\frac{\partial^2(w-w_0)}{\partial x^2}\right].\\ \tau_u &= \mp\frac{Eh}{2(1+\mu)}\frac{\partial^2(w-w_0)}{\partial x\,\partial y}. \end{aligned}\right\} \tag{17.28}$$

Minus sign pertains to points of plate (Fig. 17.9b), lying on lower surface (z = h/2); plus sign, to points on upper surface (z = -h/2). We determine total stresses for center of plate (x = = a/2, y = b/2):

$$\left.\begin{aligned} \sigma_{x,\pi} &= \frac{E\pi^2}{b^2}(f^2 - f_0^2) \pm \frac{\pi^2 Eh}{2(1-\mu^2)}(f - f_0)\left(\frac{1}{a^2} + \frac{\mu}{b^2}\right) - p, \\ \sigma_{y,\pi} &= \frac{E\pi^2}{b^2}(f^2 - f_0^2) \pm \frac{\pi^2 Eh}{2(1-\mu^2)}(f - f_0)\left(\frac{1}{b^2} + \frac{\mu}{a^2}\right), \\ \tau_{\pi} &= 0. \end{aligned}\right\} \qquad (17.29)$$

Intensity of stresses in each of the points with coordinates z = $\pm$h/2 is equal to

$$\sigma_i = \sqrt{\sigma_{x,\pi}^2 + \sigma_{y,\pi}^2 - \sigma_{x,\pi}\sigma_{y,\pi}};$$

this magnitude corresponds to intensity of deformations $\varepsilon_i = \sigma_i/E$; in all cases by E is understood elastic modulus of material at corresponding temperature; we assume that during whole process of deformation of plate stresses lie within proportional limit.

Let us turn to dimensionless parameters

$$\sigma_i^* = \sigma_i = \frac{\sigma_i b^2}{h^2} = \frac{\sigma_i b^2}{Eh^2}, \quad \sigma_x^* = \frac{\sigma_{x,\pi}}{E}\left(\frac{b}{h}\right)^2, \quad \sigma_y^* = \frac{\sigma_{y,\pi}}{E}\left(\frac{a}{h}\right)^2. \qquad (17.30)$$

$$\zeta = \frac{f}{h}, \quad \zeta_0 = \frac{f_0}{h}, \quad \lambda = \frac{a}{b}, \quad p^* = \frac{p}{E}\left(\frac{b}{h}\right)^2. \qquad (17.31)$$

Let us agree henceforth to consider compressive stresses positive. Then we obtain

$$\sigma_x^* = -\frac{\pi^2}{\lambda^2}(\zeta^2 - \zeta_0^2) \mp \frac{\pi^2(1+\mu\lambda^2)}{2(1-\mu^2)\lambda^2}(\zeta - \zeta_0) + p^*. \qquad (17.32)$$

$$\sigma_y^* = -\frac{\pi^2\lambda^2}{b}(\zeta^2 - \zeta_0^2) \mp \frac{\pi^2(\lambda^2+\mu)}{2(1-\mu^2)}(\zeta - \zeta_0). \qquad (17.33)$$

$$\sigma_i^* = \sqrt{(\sigma_x^*)^2 + \left(\frac{1}{\lambda^2}\sigma_y^*\right)^2 - \frac{1}{\lambda^2}\sigma_x^*\sigma_y^*}. \qquad (17.34)$$

Let us assume that in initial moment plate experiences compression by forces p. In supplement to initial deflections it immediately obtains elastic deflections. For determination of

additional deflection it is necessary to turn to the first of equations (24). If we place in this equation expressions for w, w_0 and Φ and use Bubnov-Galerkin method, then we arrive at following dependence (see book [0.3], p. 286):

$$p^* = \left[p^*_{кр} + \frac{\pi^2}{16}\frac{1+\lambda^2}{\lambda^2}(\zeta^2 + \zeta_0)\right]\frac{\zeta - \zeta_0}{\zeta}. \qquad (17.35)$$

Here by $p^*_{кр}$ is understood parameter of critical compressive stress:

$$p^*_{кр} = \frac{\pi^2}{12(1-\mu^2)}\left(\lambda + \frac{1}{\lambda}\right)^2. \qquad (17.36)$$

With given parameter of compressive force p* from (35) we can find total deflection ζ. Knowing ζ, we can determine intensity of deformations at any point of plate. For simplification we shall limit ourselves to determination of intensity of deformations at two points of normal $z = \pm h/2$ for center of plate where $x = a/2$, $y = b/2$.

For characteristic of process of creep during complicated stress we shall use dependences of theory of elasto-plastic flows. We introduce concept of intensity of creep deformations:

$$\bar{\varepsilon}_i = \frac{2}{\sqrt{3}}\sqrt{\bar{\varepsilon}_x^2 + \bar{\varepsilon}_y^2 - \bar{\varepsilon}_x\bar{\varepsilon}_y}. \qquad (17.37)$$

We use <u>theory of aging</u> and assume, e.g., that during steady-state creep magnitude $\bar{\varepsilon}_i$ is a function of intensity of stresses σ_i and time t:

$$\bar{\varepsilon}_i = A\sigma_i^m t. \qquad (17.38)$$

It is assumed that this law takes place, in particular, during uniaxial extension and compression with constant parameters A and m for given material. For determination of components of creep we use relationships

$$\bar{\varepsilon}_x = \frac{\bar{\varepsilon}_i\left(\sigma_x - \frac{\sigma_y}{2}\right)}{\sigma_i}, \quad \bar{\varepsilon}_y = \frac{\bar{\varepsilon}_i\left(\sigma_y - \frac{\sigma_x}{2}\right)}{\sigma_i}. \qquad (17.39)$$

We introduce designation:

$$\bar{\sigma}_i^\circ = \frac{\bar{\sigma}_i h^2}{b^2}, \quad \bar{\sigma}_x^\circ = \frac{\bar{\sigma}_x h^2}{b^2}, \quad \bar{\sigma}_y^\circ = \frac{\bar{\sigma}_y h^2}{b^2}, \quad A^\circ = AE^m \left(\frac{h}{b}\right)^{2m-2}; \tag{17.40}$$

then relationship (38) and (39) will take form

$$\bar{\varepsilon}_i^\circ = A^\circ (\sigma_i^\circ)^m t, \tag{17.41}$$

$$\bar{\varepsilon}_x^\circ = \frac{\bar{\sigma}_i^\circ \left(\sigma_x^\circ - \frac{\sigma_y^\circ}{2\lambda^2}\right)}{\sigma_i^\circ}, \quad \bar{\varepsilon}_y^\circ = \frac{\bar{\sigma}_i^\circ \left(\sigma_y^\circ - \frac{\lambda^2 \sigma_x^\circ}{2}\right)}{\sigma_i^\circ}. \tag{17.42}$$

We take following order of calculation. Let us assume that plate is subjected to action of forces p constant in magnitude. Let us consider certain interval of time Δt, counting from beginning of process of creep. We calculate intensity of stresses at points $z = \pm h/2$ at center of plate. Further by expression (41) we establish intensity of creeps and by (42), components $\bar{\varepsilon}_x^*$ and $\bar{\varepsilon}_y^*$. Following step should consist of determination of additional deflections $\Delta\bar{w}$ of plate, caused by creep. For that we use relationship, pertaining to point $z = h/2$:

$$(\varepsilon_{x,n})_{h/2} = -\frac{h}{2} \frac{\partial^2 \Delta \bar{w}}{\partial x^2}. \tag{17.43}$$

Taking

$$\Delta\bar{w} = \Delta f \sin \frac{\pi x}{a} \sin \frac{\pi y}{b}, \quad \Delta\zeta = \frac{\Delta f}{h}, \tag{17.44}$$

for center of plate we obtain

$$(\varepsilon_{x,n}^\circ)_{h/2} = \frac{\pi^2}{2} \Delta\zeta. \tag{17.45}$$

When $z = -h/2$ we have

$$(\varepsilon_{x,n}^\circ)_{-h/2} = -\frac{\pi^2}{2} \Delta\zeta. \tag{17.46}$$

We write expression for $\Delta\zeta$ in the form

$$\Delta\zeta = \frac{1}{\pi^2} [(\varepsilon_{x,n}^\circ)_{h/2} - (\varepsilon_{x,n}^\circ)_{-h/2}]. \tag{17.47}$$

From bending strains it is possible to pass to total deformations, since deformations in middle surface will be eliminated during subtraction. We obtain

$$\Delta\zeta = \frac{1}{a^2}\left[(\varepsilon^{\circ}_{x,a})_{\Delta t} - (\varepsilon^{\circ}_{x,a})_{-\Delta t}\right]. \qquad (17.48)$$

Adding increment of deflection $\Delta\zeta$ to initial ζ_0, we find new deflection ζ_0':

$$\zeta_0' = \zeta_0 + \Delta\zeta. \qquad (17.49)$$

Magnitude ζ_0' we consider initial deflection for following interval of time Δt. Repeating this procedure, it is possible to trace development of plastic and elastic deformations of plate.

Example 17.1. Let us consider case of square duralumin plate, for which ratio a/h constitutes 60. Forces of compression we take equal to 80% of critical magnitude:

$$p^{\circ} = 0{,}8\,p^{\circ}_{cp} = 0{,}8 \cdot 3{,}6 = 2{,}88. \qquad (a)$$

We constitute relationship (35). Introducing designation $k = \zeta/\zeta_0$, we obtain

$$p^{\circ} = 3{,}6\left(1 - \frac{1}{k}\right) + 1{,}23\,(k^2 - 1)\,\zeta_0^2 \qquad (b)$$

In given example we have

$$\zeta_0^2 = \frac{5 - k}{1{,}7k\,(k^2 - 1)}. \qquad (c)$$

Using expression (b), we compose table or graph for dependence $\zeta_0(k)$. Such a graph is depicted in Fig. 17.10.

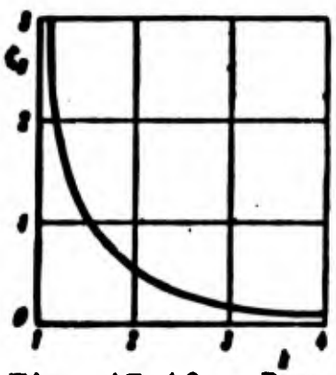

Fig. 17.10. Dependence between total and initial deflections for plate.

Let us assume that ambient temperature constitutes 300°C. Elastic modulus of duralumin at this temperature we take equal to $E = 4 \times 10^5$ kg/cm^2. Law of creep we give in the form

$$\bar{\varepsilon}_t = 9 \cdot 10^{-12}\sigma_i^3 t. \qquad (d)$$

where σ_i is expressed in kg/cm^2; t, in hours. When m = 3 by expression (40)

$$A^* = 9 \cdot 10^{-12} (4 \cdot 10^3)^3 \frac{1}{60^2} = 0{,}0445, \qquad (e)$$

and, further,

$$\bar{\varepsilon}_i^* = 0{,}0445 (\sigma_i^*)^3 t. \qquad (f)$$

We take initial deflection equal to $f_0 = 0.1h$ or $\zeta_0 = 0.1$. Using graph of Fig. 17.10, we find corresponding value k = 4; dimensionless total deflection constitutes $\zeta = 0.4$.

By expressions (32)-(33) for $\mu = 0.3$ we find

$$\sigma_x^* = -1{,}23 \cdot 0{,}15 + 7{,}05 \cdot 0{,}3 + 2{,}88 = -0{,}19 - 2{,}12 + 2{,}88 = 4{,}81 \text{ when } z = -h/2,$$
$$\sigma_x^* = -0{,}19 - 2{,}12 + 2{,}88 = 0{,}57 \text{ when } z = h/2,$$
$$\sigma_y^* = -0{,}19 + 2{,}12 = 1{,}93 \text{ when } z = -h/2,$$
$$\sigma_y^* = -0{,}19 - 2{,}12 = -2{,}31 \text{ when } z = h/2.$$

Intensity of stresses by (34) is equal to

$$\sigma_i^* = \sqrt{4{,}81^2 + 1{,}93^2 - 4{,}81 \cdot 1{,}93} = 4{,}17 \text{ when } z = -h/2,$$
$$\sigma_i^* = \sqrt{0{,}57^2 + 2{,}31^2 + 0{,}57 \cdot 2{,}31} = 2{,}64 \text{ when } z = h/2.$$

We select interval of time t = 0.5 hour. By expression (41) we determine intensity of creep deformations:

$$\bar{\varepsilon}_i^* = 0{,}0445 \cdot 0{,}5 \cdot 4{,}17^3 = 1{,}62 \text{ when } z = -h/2,$$
$$\bar{\varepsilon}_i^* = 0{,}0445 \cdot 0{,}5 \cdot 2{,}64^3 = 0{,}42 \text{ when } z = h/2.$$

Component deformations along axis by expression (42) will be

$$\bar{\varepsilon}_x^* = \frac{1{,}62 (4{,}81 - 0{,}5 \cdot 1{,}93)}{4{,}17} = 1{,}5$$
when $z = -h/2$,
$$\bar{\varepsilon}_x^* = \frac{0{,}42 (0{,}57 + 0{,}5 \cdot 2{,}31)}{2{,}64} = 0{,}27$$
when $z = h/2$.

Increment of deflection constitutes

$$\Delta\zeta = \frac{1{,}5 - 0{,}27}{\pi^3} = 0{,}13.$$

We would obtain somewhat different result if we conducted calculation by deformations $\bar{\varepsilon}_y^*$. More consequential would be to correct

obtained values $\bar{\varepsilon}_x^*$ and $\bar{\varepsilon}_y^*$ so that magnitude $\Delta\zeta$ turned out to be the same. However, we shall continue calculations, using values $\bar{\varepsilon}_x^*$.

Considering interval of time from 30 to 60 min, we must consider initial deflection equal to

$$\zeta_0' = \zeta_0 + \Delta\zeta = 0{,}23.$$

Using Fig. 17.10, we find k = 3 and $\zeta' = 3 \times 0.23 = 0.69$. Then we repeat calculation by the same scheme. Below are given results of calculations, pertaining to first nine intervals of time (of 30 min); here are given dimensionless total deflection ζ at beginning of interval and increase of deflection $\Delta\zeta$, taking place during the given interval due to creep.

Number of step	1	2	3	4	5	6	7	8	9
ζ	0,4	0,69	0,92	1,14	1,38	1,51	1,67	1,79	1,92
$\Delta\zeta$	0,13	0,17	0,20	0,21	0,20	0,17	0,11	0,11	0,05

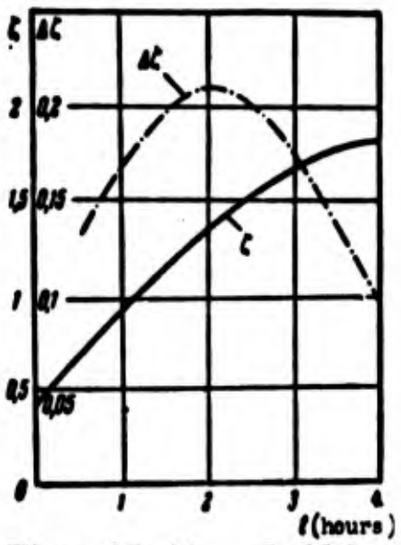

Fig. 17.11. Build-up of deflection of a plate in time (t in hours).

Graph of dependence $\zeta(t)$ is shown in Fig. 17.11 (solid line).

As we see, speed of build-up of deflections connected with creep at first increases, and then starts to drop; dot-dash line in Fig. 17.11 corresponds to increments $\Delta\zeta$. Apparently, in case of reinforced plate in general, it is impossible to determine critical period of time upon the expiration of which speed of build-up of deflections becomes infinitely great. As we already said, in this

we see the effect of chain stresses, appearing during deflections of plate, comparable with thickness.

Solution of problem was given here only in first approximation. However, obtained results are interesting from qualitative aspect; they testify to uniqueness in behavior of plate, expressed in increase of its supporting power as compared to case of compressed bar.

§ 174. Buckling in Large Cylindrical Panel

We shall clarify now peculiarity of behavior of shells during creep from example of shallow circular cylindrical panel, compressed along generatrix (Fig. 17.12).* Fundamental equations obtain such a form from (10.111):

$$\frac{D}{h}\nabla^4(w-w_0)=L(w,\Phi)+\frac{1}{R}\frac{\partial^2\Phi}{\partial x^2}, \tag{17.50}$$

$$\frac{1}{E}\nabla^4\Phi=\frac{1}{2}[L(w_0,w_0)-L(w,w)]-\frac{1}{R}\frac{\partial^2(w-w_0)}{\partial x^2}. \tag{17.51}$$

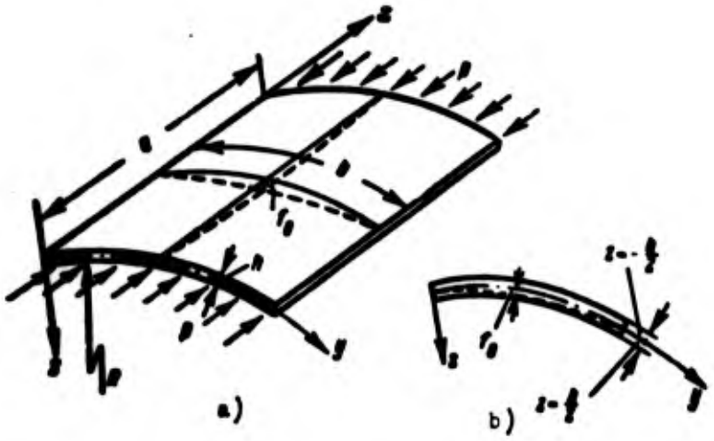

Fig. 17.12. a) Cylindrical panel, compressed along generatrix, b) section of panel.

Taking former expressions for deflection (25) and putting them in equation (51), we find, instead of (26)

$$\Phi=-\frac{1}{32}E(f^2-f_0^2)\left[\left(\frac{a}{b}\right)^2\cos\frac{2\pi x}{a}+\left(\frac{b}{a}\right)^2\cos\frac{2\pi y}{b}\right]+\frac{E}{\pi^2R}\frac{a^2b^2}{(a^2+b^2)^2}(f-f_0)\sin\frac{\pi x}{a}\sin\frac{\pi y}{b}-\frac{py^2}{2}. \tag{17.52}$$

*This problem is considered by P. G. Zykin; he also conducted the experiments described in § 175.

Stresses in middle surface are determined as before by (27), and flexural stress, by (23). Using dimensionless parameters (30) and (31), we find total stresses in center of plate (considering their positive during compression):

$$\sigma_x^* = -\frac{\pi^2}{8\lambda^2}(\zeta^2 - \zeta_0^2) + k\frac{\lambda^2}{(1+\lambda^2)^2}(\zeta - \zeta_0) \mp \frac{\pi^2(1+\mu\lambda^2)}{2(1-\mu^2)\lambda^2}(\zeta - \zeta_0) + p^*. \qquad (17.53)$$

$$\sigma_y^* = -\frac{\pi^2\lambda^2}{8}(\zeta^2 - \zeta_0^2) + k\frac{\lambda^2}{1+\lambda^2}(\zeta - \zeta_0) \mp \frac{\pi^2}{2(1-\mu^2)}(\lambda^2 + \mu)(\zeta - \zeta_0). \qquad (17.54)$$

where $k = b^2/Rh$. Integrating equation (50) according to Bubnov-Galerkin method, we obtain, instead of (35),

$$p^* = \left(p_B^* + \frac{\pi^2}{16}\frac{1+\lambda^4}{\lambda^2}(\zeta^2 + \zeta\zeta_0) - \frac{2\lambda^2}{3\pi^2}k\left\{\left[\frac{16}{(1+\lambda^2)^2} + 1\right]\zeta + \zeta_0\right\}\right)\frac{\zeta - \zeta_0}{\zeta}, \qquad (17.55)$$

where p_B^* is parameter of upper critical stress. We consider that parameter of curvature of panel k lies within limits $k < 24$ and that buckling of panel occurs in one half-wave along sides a and b.

We try to introduce here, instead of (38), a more general law of creep in order to describe not only steady-state, but also transient phase. We take

$$\dot{\bar{\varepsilon}}_i = K\bar{\sigma}_i^B t^\gamma. \qquad (17.56)$$

where K, B and γ are constants for given material at a definite temperature. We use former relationships (40) and introduce designation:

$$K^* = K\left(\frac{b}{h}\right)^B, \quad B^* = BE\left(\frac{h}{b}\right)^2, \quad \bar{\sigma}_i^* = \bar{\sigma}_i\left(\frac{b}{h}\right)^2. \qquad (17.57)$$

then we have

$$\dot{\bar{\varepsilon}}_i^* = K^*\bar{\sigma}_i^{B^*}t^\gamma. \qquad (17.58)$$

We preserve the same order of calculations as in § 173. Expressions (45)-(49) remain unchanged.

Example 17.2. We perform calculation for duralumin panel with following data: $\lambda = 1$, a = b = 200 mm, R = 615 mm, h = 1.9 mm,

$\zeta_0 = 0.3$. Parameters in formula (56) we take for material D16ATV at a temperature of 250°C equal to, $K = 4.51 \times 10^{-5}$; $B = 327 \times 10^{-5}$; $\gamma = 0.63$; σ is expressed in kg/cm^2; t, in hours. We consider, furthermore, that $E = 5.38 \times 10^5$ kg/cm^2, $\mu = 0.42$.

By formulas (57) we have

$$K^* = 0{,}503, \quad B^* = 0{,}159.$$

If we construct by (55) dependence $p^*(\zeta)$ for different values of ζ_0, then we obtain graph of Fig. 17.13. Parameters of upper and

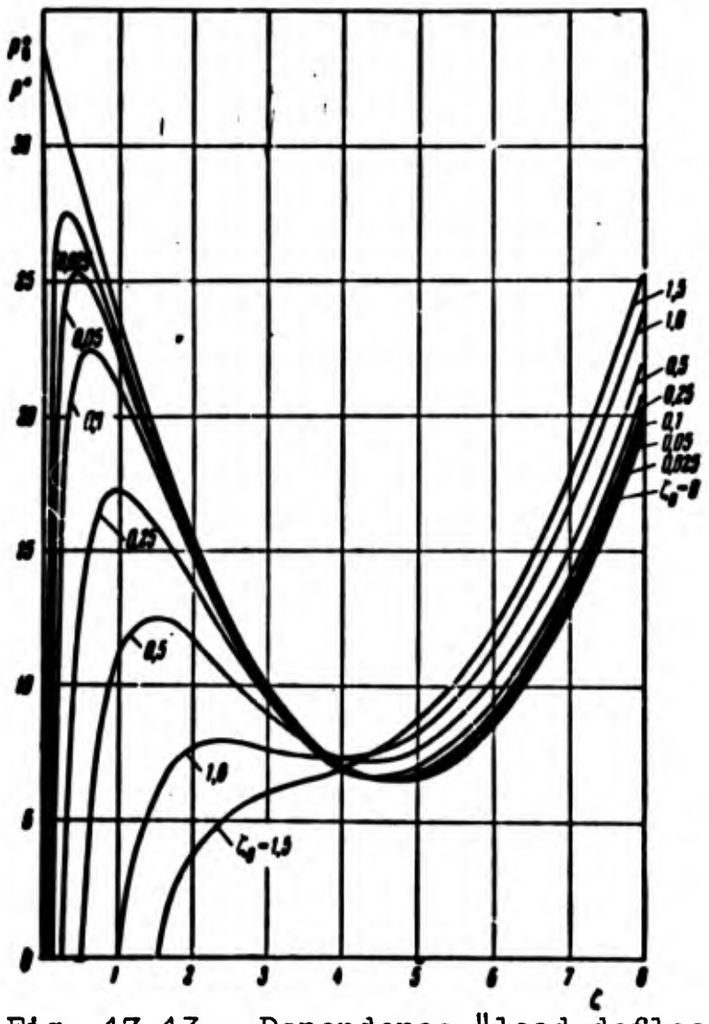

Fig. 17.13. Dependence "load-deflection" for cylindrical panel with initial deflection.

lower critical stress for $\zeta_0 = 0$ are equal to $p^*_{\text{в}} = 33.6$, $p^*_{\text{н}} = 6.6$. Using curves of Fig. 17.13, it is possible to pass to dependence

$\zeta(\zeta_0)$ with given forces of compression p*, determined depending upon parameter p^*_B by ratio $\alpha = p^*/p^*_B$. Graph of $\zeta(\zeta_0)$ is depicted in Fig. 17.14. For values $\alpha > 2$, there occurs a jump from one stable equilibrium state to the other.

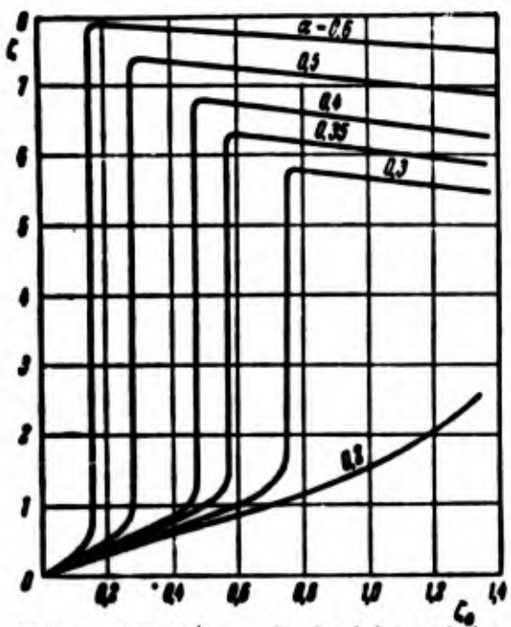

Fig. 17.14. Relationship between total and initial deflections for cylindrical panel.

We take for example $\alpha = 0.35$, which corresponds to average compressive stress $p = 570$ kg/cm^2. As first step of calcualtions we find by (53)-(54),

$$\varepsilon_x^* = 15{,}36, \quad \varepsilon_y^* = 3{,}61 \quad \text{when} \quad z = -h/2;$$
$$\varepsilon_x^* = 11{,}53, \quad \varepsilon_y^* = -0{,}22 \quad \text{when} \quad z = h/2$$

and, further,

$$\varepsilon_i^* = 14{,}6 \text{ when } z = -h/2, \quad \varepsilon_i^* = 11{,}63 \text{ when } z = h/2.$$

Interval of time we take equal to 0.2 hour. From (58) intensity of creeps is equal to

$$\bar{\varepsilon}_i^* = 1{,}86 \text{ when } z = -h/2, \quad \bar{\varepsilon}_i^* = 1{,}16 \text{ when } z = h/2.$$

Hence

$$\bar{\varepsilon}_x^* = 1{,}72 \text{ when } z = -h/2, \quad \bar{\varepsilon}_x^* = 1{,}16 \text{ when } z = h/2.$$

Increment of deflection constitutes

$$\Delta\zeta = \frac{1{,}72 - 1{,}16}{\pi^3} = 0{,}057.$$

For following interval, from 0.2 to 0.4 hour, initial deflection is equal to $\zeta_0' = \zeta_0 + \Delta\zeta = 0.357$. Using graph of Fig. 17.14, we find $\zeta = 0.634$. Continuing calculation, we compose the following table:

Number of step	1	2	3	4	5	6	7
Interval of time in hours	0,2	0,2	0,2	0,2	0,2	0,2	0,1
ζ	0,525	0,634	0,710	0,785	0,880	1,050	1,430
$\Delta\zeta$	0,057	0,039	0,031	0,034	0,039	0,058	0,054

In Fig. 17.15 are depicted graphs $\zeta(t)$ and $\Delta\zeta(t)$. Decrease of increment of deflection on first steps is explained by drop of speed of creep in first phase. With increase of deflections creep deformations accumulate ever faster; this leads, in turn, to accelerated growth of elastic deflections. At the end of the 7-th interval of time deflection attains such a magnitude that there should occur a knock with sharp increase of deflection. As we will see later, such knocks are observed also in experiments.

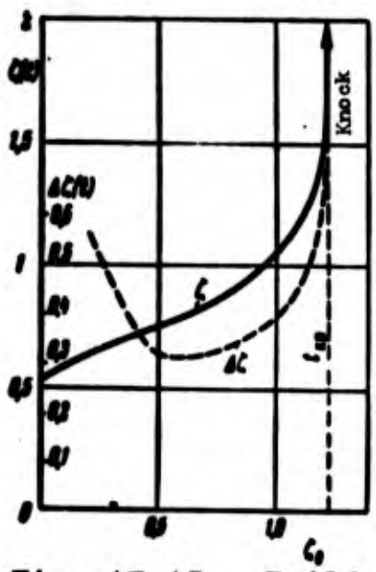

Fig. 17.15. Build-up of deflections of panel in time, ending in a knock.

Knock of shell is accompanied, as a rule, by appearance of significant plastic flows. Therefore, we again return to idea of critical time, understanding by it the period of accumulation of deflections, ending in a knock. If we turn to graph $p^*(\zeta)$ in

Fig. 17.13, for given value of forces of compression p* = 0.9 p_1 we gradually pass from one curve to the other; after we attain "jump" of curve $\zeta_0 = 0.5$, there takes place a jump.

§ 175. Data of Experiments and Recommendation for Practical Calculations

Let us give data of a series of experiments on stability of flat and cylindrical panels in conditions of creep. Samples were prepared from duralumin D16ATV. Panels were loaded by a special attachment, allowing us to carry out different conditions of fastening of edges. Deflections were measured by indicators of dial type. Stress was investigated by electrical heat resistant resistance pick-ups.

Preliminary tests on stability at normal temperature gave possibility of establishing order of error in determination of critical stresses; for flat panels it constituted not more than 5% of theoretical values. Further we conducted brief tests on stability of plates at heightened temperatures (up to 250°C); they showed that in this case usual calculating formulas with modified modulus E are applicable. For cylindrical panels real critical stresses (during knock) constituted (0.65-0.7) of upper theoretical values; experimental values of $p_{кр}$ could be approximated by formula $p_{кр} \approx 0.41Eh/R$.

Tests for creep were conducted at a temperature of 250°C; compressive forces p constituted such fractions of critical pressure:

$$\alpha = \frac{p}{p_{кр}} = 0.65;\ 0.8;\ 0.94.$$

Combined graph of dependence of deflection on time (dotted lines) for three flat panels is given in Fig. 17.16; by α is understood ratio of compressive stress to static critical value. As we see, here there occurs monotonic change of deflections with decreasing speed. Creep does not lead, thus, to stormy growth of deflection; this is

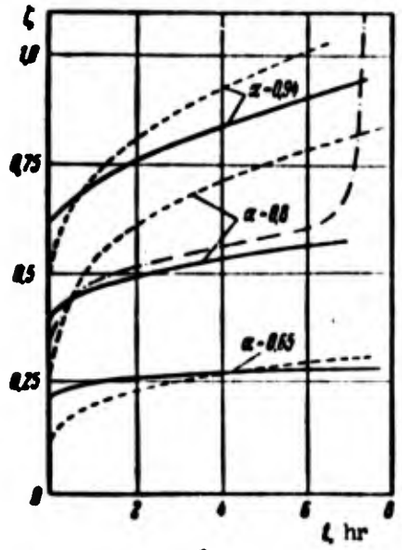

Fig. 17.16. Diagrams "deflection-time" for flat panels (t, in hours).

confirmed by results obtained above in § 173; theoretical data are shown by solid lines. To check we conducted experiment with plate, longitudinal edges of which shifted freely; in other words, we investigated case of beam-strip. Curve $\zeta(t)$ obtained here is depicted in Fig. 17.16 by dot-dash line; it corresponds to usual diagrams pertaining to bars, and allows us to determine critical time $t_{кр}$.

Data of tests of ten cylindrical panels are shown in Fig. 17.17 and 17.18. Solid curves here depict dependence $\zeta(t)$, obtained in

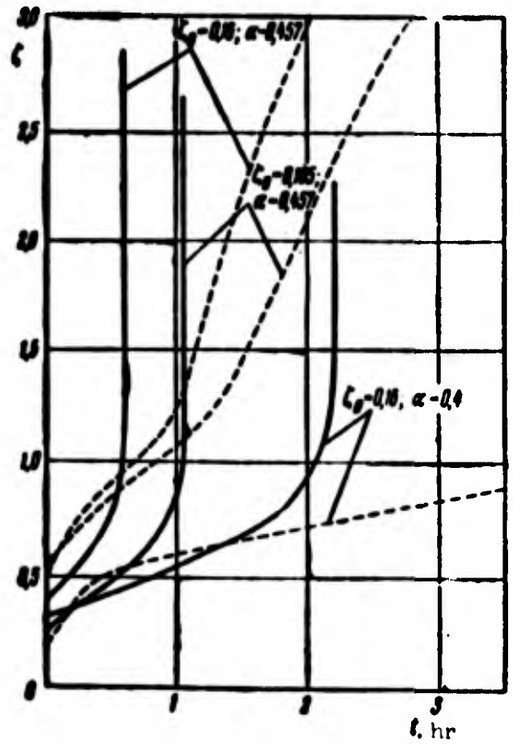

Fig. 17.17. Diagrams "deflection-time" for cylindrical panels of first series in comparison with data of experiments.

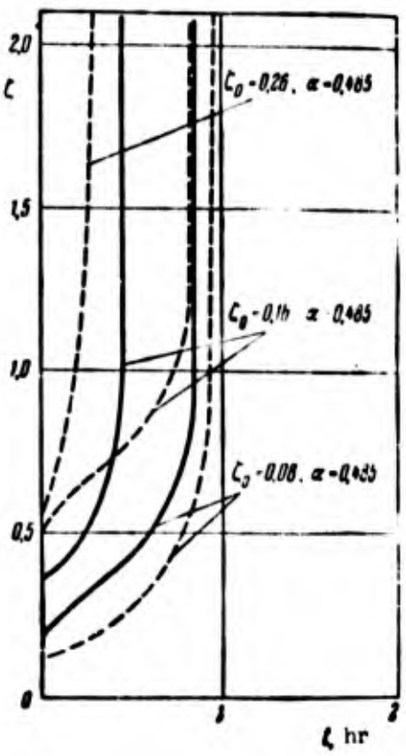

Fig. 17.18. Diagrams "deflection-time" for cylindrical panels of second series.

experiments; dotted lines are constructed according to approximate solution presented in § 174; ζ_0 designates parameter of initial deflection; α shows ratio of compressive stress to upper critical magnitude. If average stress is equal to lower critical value ($\sigma = p_н$, $\alpha = 0.3$), shell behaved similarly to a flat panel. If however, stress lay within limits $p_н < \sigma < p_в$, buckling of shell in all cases ended in a knock.

With help of graphs of Figs. 17.17 and 17.18 we established critical time $t_{кр}$, upon the expiration of which there occurred buckling in the large. These data are depicted in Fig. 17.19.

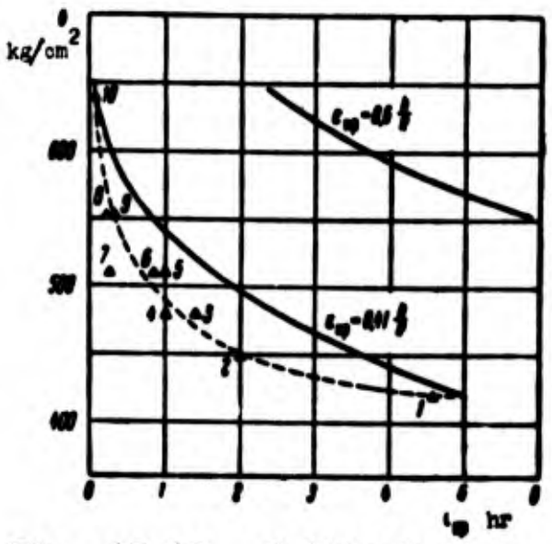

Fig. 17.19. Critical time for cylindrical panels at different levels of compressive stress.

If we conditionally take magnitude of initial deflection for all tested samples as approximately identical, then it is possible, using experimental data (triangles), to construct graph of dependence of critical time $t_{кр}$ on average compression stress (dotted line in Fig. 17.19). As we see, critical time sharply drops with increase of compressive stress. At loads, constituting 90-95% of $p_в$, critical time in a number of cases was calculated in seconds.

Thus, data of a calculation by criterion of initial imperfections sufficiently well agree with experiments.

In Fig. 17.19 by solid lines there are also plotted values of $t_{кр}$, obtained by criterion of critical deformation $\varepsilon_{кр}$, if we consider it equal to 0.605h/R or 0.41h/R. As we see, results of calculation

by these formulas greatly deviate from experimental data. As already was said, it is more correct as base of calculation to take lower critical deformation 0.18h/R.

As a result it is possible to recommend for rough calculations of buckling of plates and shells during creep use of criterion of critical deformation. For plates here there will be determined, apparently, that time interval, upon the expiration of which speed of build-up of deflection is the greatest. As for shells, here, thus, there will be found moment of time, corresponding to phenomenon of knock. Moreover, as initial strain it is necessary to take deformation, corresponding to lower critical stress, found for elastic region (see Chapters XI-XV). This pertains not only to case of compression, but also to other loads.

More reliable data about behavior of plates and shells during creep can be obtained by using criterion of initial imperfections, as this described in §§ 173 and 174. But here it is necessary to have information about approximate values of initial deflections for constructions of one or another type. And in this case the most valid is statistical approach to problem.

We did not touch here upon important question of decrease of torsional rigidity and possible loss of stability of a thin-walled construction of the type of an aircraft wing, connected with thermal stresses; this question is illuminated in articles of B. Budiansky, J. Mayers, J. Aeron. Sci., 23, No. 12, 1956, van der Heut [17.18] and other authors; see book of A. A. Umanskiy [4.12] 1961.

Literature

17.1. S. G. Vinokurov. Thermal stresses in plates and shells, News of Kazan' branch of Academy of Sciences of USSR, series of phys-math. and tech. sciences, No. 3 (1953).

17.2. A. S. Vol'mir and P. G. Zykin. Stability in large cylindrical shells during creep, Transactions of 2nd conference on thermal stresses, Kiev, 1962.

17.3. M. S. Ganeyeva. Stability of rectangular cylindrical panel, rigidly fixed on its edges and in a nonuniform temperature field, Sci. notes of Kazan' University, 116 No. 1 (1956), 41-44.

17.4. E. I. Grigolyuk. Certain problem of stability of round plates during nonuniform heating; Eng. coll., 6 (1950).

17.5. L. M. Kurshin. Stability of wing panels during heating, Reports of Academy of Sciences of USSR, 136, No. 2 (1960).

17.6. L. A. Shapovalov. Thermal stability of plates and shells, "Strength and deformation in nonuniform temperature field," M (1961), 241-255.

17.7. S. A. Shesterikov. Stability of rectangular plates during creep, Journal of applied mech. and tech. physics, No. 3 (1961), 93-100; Stability of plates during creep according to flow theory, loc. cit., No. 5 (1961), 100-108.

17.8. P. P. Bijlaard. Differential equations for cylindrical shells with arbitrary temperature distribution, J. Aeron. Sci. 25, No. 9 (1958), 594-595.

17.9. C. C. Chang and J. K. Ebcioglu. Thermoelastic behavior of a simply supported sandwich panel under large temperature gradient and edge compression, J. Aerospace Sci. 28, No. 6 (1961), 480-492.

17.10. G. Gerard and A. Gilbert. A critical strain approach to creep buckling of plates and shells, J. Aerospace Sci. 25, No. 7 (1958), 429-438; 458 (coll. of translation, "Mechanics," IL, No. 2, 1959).

17.11. D. J. Johns. Comments on "Thermal buckling of clamped cylindrical shells," J. Aeron. Sci. 26, No. 1 (1959), 59.

17.12. L. A. Harris. Axial compression buckling of a pressurized cylinder with a thermally induced ring compression, J. Aeron. Sci. 23, No. 12 (1956), 1120-1121.

17.13. W. S. Hemp. Fundamental principles and theorems of thermoelasticity, Aeron. Quarterly 7, No. 3 (1956), 184-192.

17.14. N. J. Hoff. Thermal buckling of supersonic wing panels, J. Aeron. Sci. 23, No. 11 (1956), 1019-1028; Buckling of thin cylindrical shell under hoop stresses varying in axial direction, J. Appl. Mech. 24, No. 3 (1957), 405-412; Buckling at high temperature, J. Roy. Aeron. Soc. 61, No. 563 (1957), 756-774 (coll. of translation,

"Mechanics," IL, No. 5, 1958).

17.15. J. Klosner and M. Forray. Buckling of simply supported plates under arbitrary symmetrical temperature distributions, J. Aeron. Sci. 25, No. 3 (1958), 181-184.

17.16. T. H. Lin. Creep deflection of wiscoelastic plate under uniform edge compression, J. Aeron. Sci. 23, No. 9 (1956), 883-887.

17.17. K. Miura. Thermal buckling of rectangular plates, J. Aerospace Sci. 28, No. 4 (1961), 341-343.

17.18. A. van der Neut. Buckling caused by thermal stresses, "High temperature effects in aircraft structures" (1958), 215-247 (trans. in book "Problems of high temperatures in aircraft structures," M., 1961).

17.19. J. S. Przemieniecki. Transient temperature distributions and thermal stresses in fuselage shells with bulkheads of frames, J. Roy. Aeron. Soc. 60, No. 552 (1956), 799-804.

17.20. J. Singer. Thermal buckling of solid wings of arbitrary aspect ratio, J. Aeron. Sci. 25, No. 9 (1958), 573-580.

17.21. T. Wan and R. K. Gregory. Creep collapse of long cylindrical shells under high temperature and external pressure, J. Aerospace Sci. 28, No. 3 (1961), 177-188, 208.

17.22. W. Zuk. Thermal buckling of clamped cylindrical shells, J. Aeron. Sci. 24, No. 5 (1957), 389.

C H A P T E R XVIII

STABILITY OF PLATES AND SHELLS UNDER DYNAMIC LOADING

§ 176. Formulation of Problem

In Chapter VI we met certain problems pertaining to stability of bars under dynamic loading. We turn now to analogous questions of stability of plates and shells. If we consider various problems in linear formulation, then between them there will be no fundamental distinction. However, if we investigate deflections, comparable with thickness of plates or shells, then problem will be nonlinear and will obtain a series of peculiarities. We recall case of loading of bar with compressive force rapidly growing in time under the condition that bar has initial deflection and is considered as a system with one degree of freedom. Diagram "deflection-load" has the form shown in Fig. 18.1a by the solid line, in distinction from static diagram depicted by dotted line.*

We turn to the same problem for shell with initial deflection, subjected to buckling under action of certain load. Here too we

---

*When we are given law of mutual displacement of ends of bar in time, problem also becomes nonlinear (see Chapter VI).

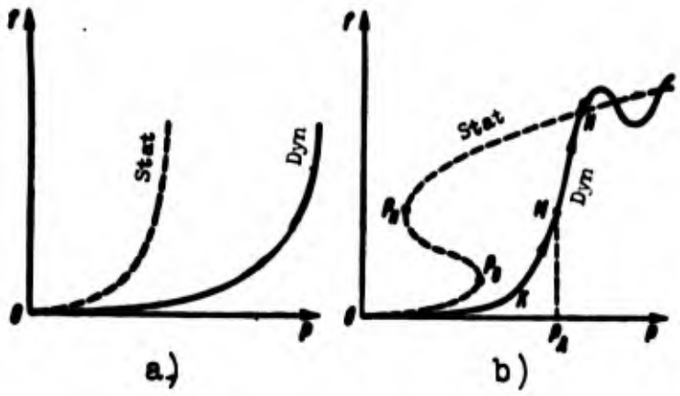

Fig. 18.1. Build-up of static and dynamic deflections in case, a) of a plate, b) of a shell.

conditionally consider shell a system with one degree of freedom. Let us assume that, investigating equilibrium forms during static loading, we obtain on diagram "load-deflection" a line with upper and lower critical points P_B and P_H (Fig. 18.1b). If load rapidly increases in time, then parameter of external forces can "pass" levels of both lower and upper critical loads (section of solid line OK in Fig. 18.1b), whereupon in initial section (where $P < P_B$) there will occur oscillations about equilibrium positions, characterized by "small" deflections.

At a certain moment, approach of which is determined by program of loading and different perturbing factors, there occurs a sudden displacement of shell to equilibrium positions with great deflections (line KN in Fig. 18.1b); after that there will start oscillations about new equilibrium forms, having a clearly expressed nonlinear character. Subsequently this process of knock of a shell with rapidly increasing load we shall conditionally call dynamic buckling or dynamic loss of stability. We introduce also concept of dynamic critical load $P_д$, corresponding to moment of knock. We will find it conditionally by diagram of type 18.1b, determining abscissa of point M of bend of curve P(f), i.e., point, corresponding to greatest

"speed of buckling" of shell. It is possible also to conditionally determine $P_д$ with help of other magnitudes, characterizing section of knock KN.

Till now we assumed that load applied to shell increases in time and that snapping of the shell occurs on this ascending path of load. Let us assume now that load increases only to a certain magnitude $P_д' < P_д$ (Fig. 18.2) (where snapping of shell is not carried out) and that then load starts to decrease in time by given law. If drop of load is accomplished sufficiently intensely, then shell will obtain oscillation around initial position of equilibrium and after damping of vibrations will return to this position. In that same case, if load drops comparatively slowly, snapping of panel, nevertheless, can take place on descending branch of load. Approximate curve, characterizing change of f during drop of P, is shown in Fig. 18.2 by heavy line. We will conditionally consider that snapping of shell was accomplished, if the greatest deflection $f_д$ attains value $f_{ст}$; by $f_{ст}$ is understood static deflection corresponding to load $P_д'$. Such comparison is necessary in order to find whether during dynamic loading, accomplished by complicated program, there will appear noticeable permanent deformations.

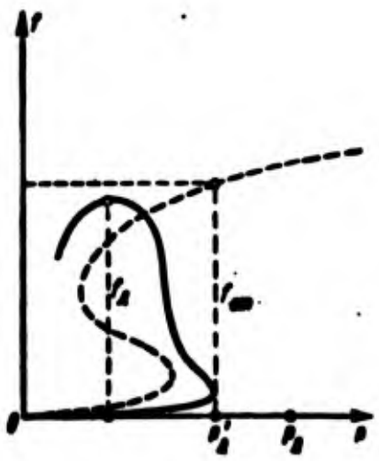

Fig. 18.2. Dynamic deflections on descending branch of loading.

Problems described here are important for aircraft construction and other fields of engineering. For instance, hull of aircraft is subjected to dynamic loading on starting section. Fast change of

load in time is experienced also by certain engine shells.

We write basic dynamic equations of nonlinear theory of shallow shells taking into account initial incorrectnesses of form of shell. We originate from equations (10.111) and supplement them with an inertial member, corresponding to normal displacement (deflection of shell) w. Inertial loads, corresponding to displacements u and v in middle surface, we shall not consider. Thus, we here refuse to research process of propagation of elastic waves in middle surface; limitations with respect to character of application of loads, given in Chapter VI for bars, remain in force.* Finally we obtain equations in the form

$$\frac{D}{h}\nabla^4(w-w_0)=L(w,\Phi)+k_x\frac{\partial^2\Phi}{\partial y^2}+k_y\frac{\partial^2\Phi}{\partial x^2}+\frac{q}{h}-\frac{\gamma}{g}\frac{\partial^2 w}{\partial t^2}. \tag{18.1}$$

$$\frac{1}{E}\nabla^4\Phi=\frac{1}{2}[L(w_0,w_0)-L(w,w)]-k_x\frac{\partial^2(w-w_0)}{\partial y^2}-k_y\frac{\partial^2(w-w_0)}{\partial x^2}; \tag{18.2}$$

under γ is understood specific gravity of shell material.

§ 177. Stability of Plates and Cylindrical Panels During Action of Compressing Load

Let us consider shallow cylindrical panel, secured by hinge on its edges (see Fig. 11.61). Let us assume that panel is subjected to dynamic compression along generatrix; we investigate its behavior in time under the condition that shell has initial deflections. Equations (1) and (2) take form

$$X\equiv\frac{D}{h}\nabla^4(w-w_0)-L(w,\Phi)-\frac{1}{R}\frac{\partial^2\Phi}{\partial x^2}-\frac{q}{h}=0, \tag{18.3}$$

$$\frac{1}{E}\nabla^4\Phi=-\frac{1}{2}[L(w,w)-L(w_0,w_0)]-\frac{1}{R}\frac{\partial^2(w-w_0)}{\partial x^2}. \tag{18.4}$$

*More general problems were considered by N. A. Alumyae [18.2] and V. L. Agamirov.

We shall analyze first the case when <u>force of compression p increases in time</u> according to the law p = ct. We take for total and initial deflections the expressions

$$w = f \sin \frac{\pi x}{a} \sin \frac{\pi y}{b}, \quad w_0 = f_0 \sin \frac{\pi x}{a} \sin \frac{\pi y}{b}. \tag{18.5}$$

Substituting these expressions in equation (4), we find, as usual, function of Φ (see p. 858):

$$\frac{1}{E}\Phi = \frac{h^2}{32}(\zeta^2 - \zeta_0^2)\left(\frac{a^2}{b^2}\cos\frac{2\pi x}{a} + \frac{b^2}{a^2}\cos\frac{2\pi y}{b}\right) + \\ + \frac{h}{a^2 R\pi^2}(\zeta - \zeta_0)\frac{1}{\left(\frac{1}{a^2}+\frac{1}{b^2}\right)^2}\sin\frac{\pi x}{a}\sin\frac{\pi y}{b} - \frac{py^2}{2E}. \tag{18.6}$$

where p is intensity of average compressive force, depending on time $\zeta = f/h$, $\zeta_0 = f_0/h$. Further, we use Bubnov-Galerkin in application to equation (1). Integrating, we arrive for <u>square</u> panel (a = b) at following dependence:

$$\left[p^* - \frac{\pi^2}{8}(\zeta^2 - \zeta_0^2)\right]\zeta + \frac{2k}{3\pi^2}(\zeta^2 - 4\zeta\zeta_0 - \zeta_0^2) - \\ - \left[\frac{\pi^2}{3(1-\mu^2)} + \frac{k^2}{4\pi^2}\right](\zeta - \zeta_0) - \frac{16a^4}{\pi^2 E g h^2}\frac{d^2\zeta}{dt^2} = 0; \tag{18.7}$$

here there are introduced former dimensionless parameters $p^* = pa^2/Eh^2$, $k = a^2/Rh$.

Dropping in (7) inertial member, we obtain solution of static problem of stability in the large. Considering $\zeta_0 \equiv 0$ and $\zeta \to 0$, we find parameter of <u>upper</u> critical stress for panel which does not have initial deflection:

$$p_0^* = \frac{p_0 a^2}{Eh^2} = \frac{\pi^2}{3(1-\mu^2)} + \frac{k^2}{4\pi^2}.$$

On the other hand, rejecting nonlinear members and considering $p^* = 0$, $\zeta_0 = 0$, we arrive at equation of small oscillations of unloaded panel without initial deflection:

$$p_0^*\zeta + \frac{16a^4}{\pi^2 E g h^2}\frac{d^2\zeta}{dt^2} = 0.$$

Square of principal frequency of oscillations turns out to be equal to

$$\omega^2 = \frac{\pi^2 E g h^2}{\gamma a^4 p_0^*}.$$

We divide each member of equation (7) by p_p and introduce designation t_1^* for parameter of time:

$$t_1^* = \frac{at}{p_0} = \frac{p^*}{p_0}; \tag{18.8}$$

then we obtain ordinary differential equation for deflection:

$$\frac{1}{S_1}\frac{d^2\zeta}{dt_1^{*2}} - \left\{\left[t_1^* - \frac{\pi^2}{8p_0^*}(\zeta^2 - \zeta_0^2)\right]\zeta + \right. \\ \left. + \frac{2k}{3\pi^3 p_0^*}(5\zeta^2 - 4\zeta\zeta_0 - \zeta_0^2) - (\zeta - \zeta_0)\right\} = 0. \tag{18.9}$$

By S_1 is understood magnitude

$$S_1 = p_0^{*2}\left(\frac{\pi V E h^2}{ca^4}\right)^2.$$

where V is speed of sound in material of shell. Comparing expressions for ω^2 and S_1, we find: $\sqrt{S_1} = \omega(p_p/c)$. In distinction from equation (6.31), composed above for compressed bar, equation (9) is nonlinear; integrating it, we find dependence $\zeta(t_1^*)$.

Let us turn to other case, when we are given <u>law of mutual displacement of curvilinear edges of panel</u>.* Deformation in middle surface along generatrix is equal to

$$\varepsilon_x = \frac{1}{E}\left(\frac{\partial^2\Phi}{\partial y^2} - \mu\frac{\partial^2\Phi}{\partial x^2}\right).$$

On the other hand

$$\varepsilon_x = \frac{\partial u}{\partial x} + \frac{1}{2}\left[\left(\frac{\partial w}{\partial x}\right)^2 - \left(\frac{\partial w_0}{\partial x}\right)^2\right].$$

where u is displacement of point of middle surface along generatrix. Shortening of a certain fiber, parallel to generatrix, is equal to $e_x = -\int_0^a \frac{\partial u}{\partial x}\,dx$. We designate by e mean value of e_x with respect to arc edge: $e = \frac{1}{b}\int_0^b e_x\,dy$; then we obtain

$$e = -\frac{1}{b}\int_0^a\int_0^b \frac{1}{E}\left(\frac{\partial^2\Phi}{\partial y^2} - \mu\frac{\partial^2\Phi}{\partial x^2}\right) - \frac{1}{2}\left[\left(\frac{\partial w}{\partial x}\right)^2 - \left(\frac{\partial w_0}{\partial x}\right)^2\right]dx\,dy.$$

*This problem was considered by author [18.11].

We take e = st. In case of square panel in former designations we obtain

$$\frac{\sigma_{kp}}{h^2} = p + \frac{\pi^2}{8}(\zeta^2 - \zeta_0^2) + \frac{h(1-\mu)}{\pi^2}(\zeta - \zeta_0).$$

or

$$\frac{p^*}{p_0^*} = t_2^* - \frac{\pi^2}{8p_0^*}(\zeta^2 - \zeta_0^2) - \frac{h(1-\mu)}{\pi^2 p_0^*}(\zeta - \zeta_0). \qquad (18.9a)$$

Here is introduced new parameter of time

$$t_2^* = \frac{\sigma_{kp}}{h^2 p_0^*}. \qquad (18.10)$$

We place p* if (9a) in equation (7) and express t by (10); then we arrive at dependence

$$\frac{d^2\zeta}{dt_2^{*2}} - S_2\left\{\left[p^* - \frac{\pi^2}{4p_0^*}(\zeta^2 - \zeta_0^2) - \frac{h(1-\mu)}{\pi^2 p_0^*}(\zeta - \zeta_0)\right]\zeta + \right.$$
$$\left. + \frac{2h}{3\pi^2 p_0^*}(3\zeta^2 - 4\zeta\zeta_0 - \zeta_0^2) - (\zeta - \zeta_0)\right\} = 0; \qquad (18.11)$$

by S_2 here is understood new magnitude

$$S_2 = p_0^{*3}\left(\frac{\pi V h^3}{8D}\right)^2.$$

Equation (11) was integrated by numerical method, and also with help of analog computer for different values of ζ_0 and S_2. We took initial conditions

$$\zeta = \zeta_0, \quad \frac{d\zeta}{dt_2^*} = 0 \text{ when } t_2^* = 0.$$

Results of integration for case k = 0 (flat panel) with ζ_0 = 0.001 and S_2 = 1.000 are presented in Fig. 18.3a. Along the axis of abscissas is plotted parameter t_2^*; along the axis of ordinates, magnitude ζ and ratio of compressive force to critical p^*/p_{kp}^*. To static dependences there correspond: for deflection--sections OB and BLF, and for load--sections OA and AC. With dynamic loading there occurs pulling of initial section to point M (or K); then deflections sharply grow, and there appear steady nonlinear oscillations. These results are

very close to those which were obtained in Chapter VI for a bar, but postcritical diagram for load AC here is ascending. In Fig. 18.3b

Fig. 18.3. Diagrams "load--time" for, a) plate and b) shell during static and dynamic loading.

are depicted analogous graphs for square cylindrical panel with k = = 12; values ζ_0 and S_2 remain as before. To static problem there correspond curves OBLF and OAC; to dynamic, lines OBM and OAK. In dynamic application load attains, as for plate, approximately 165% of upper static magnitude. Then there occurs a sharp drop of p*, where magnitude p* becomes negative, which corresponds to extension of the panel.

§ 178. Application of Digital Computers

In the preceding section we reduced plate or shell to system with one degree of freedom and determined dependence of deflection on time. Here we did not manage to trace change of character of deflection surface of plate or shell in process of loading. More exact solution of problem can be given if we approximate deflection surface by means of several parameters or present the initial equations in finite differences. In both cases calculations are greatly complicated and for their fulfillment there must be called in electronic digital computers.

Solution of problem with help of method of finite differences is set forth below.* Let us consider general case of shallow panel with sides (in plane) a and b, having certain initial deflections. We use dimensionless parameters

$$\bar{x}=\frac{x}{a},\quad \bar{y}=\frac{y}{b},\quad \bar{t}=\frac{th}{ab}V,\quad \bar{w}=\frac{w}{h},\quad \bar{\Phi}=\frac{\Phi}{Eh^2}; \tag{18.12}$$

then it is possible to present initial equations (1) and (2) in the form

$$\begin{aligned}\frac{\partial^2\bar{w}}{\partial\bar{t}^2}=&\frac{\partial^2\bar{w}}{\partial\bar{x}^2}\left(\frac{\partial^2\bar{\Phi}}{\partial\bar{y}^2}-\bar{p}_x\right)+\frac{\partial^2\bar{w}}{\partial\bar{y}^2}\left(\frac{\partial^2\bar{\Phi}}{\partial\bar{x}^2}-\bar{p}_y\right)-\\&-2\frac{\partial^2\bar{w}}{\partial\bar{x}\,\partial\bar{y}}\frac{\partial^2\bar{\Phi}}{\partial\bar{x}\,\partial\bar{y}}-\frac{1}{12(1-\mu^2)}\bar{\nabla}^4(\bar{w}-\bar{w}_0)+\\&+\frac{\bar{k}_y}{\lambda^2}\left(\frac{\partial^2\bar{\Phi}}{\partial\bar{x}^2}-p_y\right)+\bar{k}_x\lambda^2\left(\frac{\partial^2\bar{\Phi}}{\partial\bar{y}^2}-\bar{p}_x\right)+\bar{q};\end{aligned} \tag{18.13}$$

$$\begin{aligned}\bar{\nabla}^4\bar{\Phi}=&\left(\frac{\partial^2\bar{w}}{\partial\bar{x}\,\partial\bar{y}}\right)^2-\frac{\partial^2\bar{w}}{\partial\bar{x}^2}\frac{\partial^2\bar{w}}{\partial\bar{y}^2}-\left(\frac{\partial^2\bar{w}_0}{\partial\bar{x}\,\partial\bar{y}}\right)^2+\\&+\frac{\partial^2\bar{w}_0}{\partial\bar{x}^2}\frac{\partial^2\bar{w}_0}{\partial\bar{y}^2}-\frac{\bar{k}_y}{\lambda^2}\frac{\partial^2(\bar{w}-\bar{w}_0)}{\partial\bar{x}^2}-\bar{k}_x\lambda^2\frac{\partial^2(\bar{w}-\bar{w}_0)}{\partial\bar{y}^2}.\end{aligned} \tag{18.14}$$

Here are introduced relationships

$$\left.\begin{aligned}&\lambda=\frac{a}{b},\quad \bar{k}_x=\frac{b^2k_x}{h},\quad \bar{k}_y=\frac{a^2k_y}{h},\\&\bar{p}_x=\frac{p_x}{E}\left(\frac{b}{h}\right)^2,\quad \bar{p}_y=\frac{p_y}{E}\left(\frac{a}{h}\right)^2,\quad \bar{q}=\frac{q}{E}\left(\frac{ab}{h^2}\right)^2.\end{aligned}\right\} \tag{18.15}$$

Operator $\bar{\nabla}^4$ has the form

$$\bar{\nabla}^4=\frac{1}{\lambda^4}\frac{\partial^4}{\partial\bar{x}^4}+2\frac{\partial^4}{\partial\bar{x}^2\,\partial\bar{y}^2}+\lambda^4\frac{\partial^4}{\partial\bar{y}^4}. \tag{18.16}$$

Let us note that during selection of dimensionless parameters by (12) and (15) a panel rectangular in projection will be converted in a square with a side, equal to one.

Boundary conditions, given in the form of linear uniform dependences we shall consider constant in time. Initial conditions can, e.g., have form $\bar{w} = \bar{w}_0$, $\partial\bar{w}/\partial\bar{t} = 0$ for $\bar{t} = 0$. Henceforth, the dash above designations w, x, y, t, etc., will be omitted.

---

*This resolution was given by A. Yu. Birkgan and the author [18.6].

In space of variables x, y, t, bounded by plane t = 0 and planes x = 0, x = 1 and y = 0, y = 1, we construct system of planes t = 0, t = Δt, t = $2\Delta t$, ..., t = $m\Delta t$, ..., covered by net of straight lines x = 0, x = s, x = 2s, ..., x = 1, y = 0, y = s, ..., y = 1. Here Δt is step in time, s is step in space coordinates x and y (Fig. 18.4).

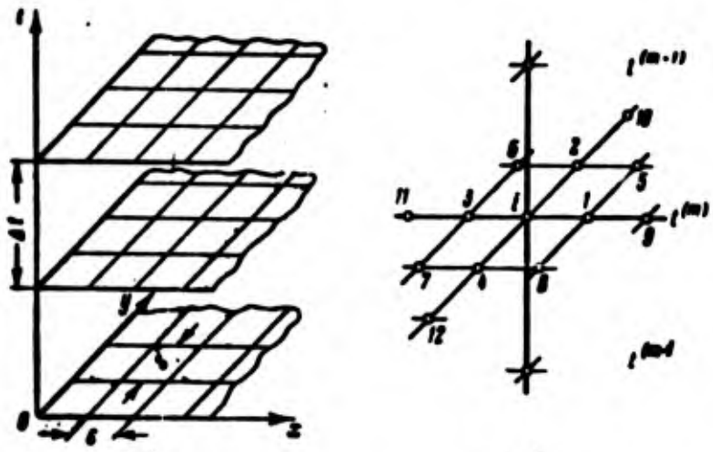

a) b)

Fig. 18.4. Three-dimensional net region.

At nodes three-dimensional grid region net constructed thus, there must be satisfied equations in finite differences, approximating system of differential equations. Furthermore, for expression of boundary conditions with help of symmetric finite differences we introduce necessary quantity of extra-contour nodes, located on planes

$$x=-2s,\quad x=-s,\quad x=1+s,\quad x=1+2s,$$
$$y=-2s,\quad y=-s,\quad y=1+s,\quad y=1+2s.$$

Derivatives with respect to space coordinates we replace by differential operators from formulas of type (7.238) and (7.239):

$$\frac{\partial^2 w}{\partial x^2}=\frac{w_1-2w_0+w_3}{s^2},$$
$$\frac{\partial^2 w}{\partial x\,\partial y}=\frac{w_2-w_5+w_7-w_8}{4s^2},$$
$$\frac{\partial^4 w}{\partial x^4}=\frac{w_9-4w_1+6w_0-4w_3+w_{11}}{s^4},$$
$$\frac{\partial^4 w}{\partial x^2\partial y^2}=\frac{4w_0-2(w_1+w_2+w_3+w_4)+w_5+w_6+w_7+w_8}{s^4}.$$

with error, having order of the square of the step. Numbering of nodes of computing cell is given in Fig. 18.4. Time derivative we replace by relationship

$$\frac{\partial^2 w}{\partial t^2} = \frac{w_0^{(m+1)} - 2w_0^{(m)} + w_0^{(m-1)}}{(\Delta t)^2}.$$

Placing these expressions in equations (13) and (14) and dropping members of order of square of the step, we obtain at current (zero) point of layer $t^{(m)}$ two equations in finite differences. Transition from m-th to (m + 1)-th layer in time is produced by a formula, in the right part of which are known values of functions (such differential scheme is called explicit):

$$\begin{aligned} w_0^{(m+1)} = {} & 2w_0^{(m)} - w_0^{(m-1)} + \frac{(\Delta t)^2}{s^4}\Big[\left(w_1'^{(m)} - 2w_0'^{(m)} + w_3'^{(m)}\right)\left(\Phi_2^{(m)} - \right. \\ & - 2\Phi_0^{(m)} + \Phi_4^{(m)} - p_x^{(m)}s^2\Big) + \left(w_2^{(m)} - 2w_0^{(m)} + w_4^{(m)}\right)\left(\Phi_1^{(m)} - \right. \\ & - 2\Phi_0^{(m)} + \Phi_3^{(m)} - p_y^{(m)}s^2\Big) - \frac{1}{6}\left(w_5'^{(m)} - w_6'^{(m)} + w_7'^{(m)} - w_8'^{(m)}\right)\left(\Phi_5^{(m)} - \right. \\ & - \Phi_6^{(m)} + \Phi_7^{(m)} - \Phi_8^{(m)} + rs^2\Big)\Big] + \frac{(\Delta t)^2}{s^2}\Big[\frac{k_y}{\lambda^2}\left(\Phi_1^{(m)} - \right. \\ & - 2\Phi_0^{(m)} + \Phi_3^{(m)} - p_y^{(m)}s^2\Big) + k_x\lambda^2\left(\Phi_2^{(m)} - 2\Phi_0^{(m)} + \Phi_4^{(m)} - \right. \\ & - p_x^{(m)}s^2\Big)\Big] - \frac{c(\Delta t)^2}{s^4}\Big[\left(\frac{6}{\lambda^2} + 8 + 6\lambda^2\right)w_0^{(m)} - \\ & - 4\left(1 + \frac{1}{\lambda^2}\right)\left(w_1^{(m)} + w_3^{(m)}\right) - 4\left(1 + \lambda^2\right)\left(w_2^{(m)} + w_4^{(m)}\right) + \\ & + 2\left(w_5^{(m)} + w_6^{(m)} + w_7^{(m)} + w_8^{(m)}\right) + \frac{1}{\lambda^2}\left(w_9^{(m)} + w_{11}^{(m)}\right) + \lambda^2\left(w_{10}^{(m)} + w_{12}^{(m)}\right)\Big] + \\ & + (\Delta t)^2\left(L_0 + q_0^{(m)}\right). \end{aligned} \tag{18.17}$$

For determination of function of stresses at moment $t^{(m+1)}$ it is necessary to solve jointly system of differential equations of such type:

$$\begin{aligned} \Phi_0^{(m+1)} = {} & \frac{1}{\frac{6}{\lambda^2} + 8 + 6\lambda^2}\Big\{\frac{1}{16}\left(w_5^{(m+1)} - w_6^{(m+1)} + w_7^{(m+1)} - \right. \\ & - w_8^{(m+1)}\Big)^2 - \left(w_1^{(m+1)} - 2w_0^{(m+1)} + w_3^{(m+1)}\right)\left(w_2^{(m+1)} - 2w_0^{(m+1)} + \right. \\ & + w_4^{(m+1)}\Big) + 4\left(1 + \frac{1}{\lambda^2}\right)\left(\Phi_1^{(m+1)} + \Phi_3^{(m+1)}\right) + \\ & + 4\left(1 + \lambda^2\right)\left(\Phi_2^{(m+1)} + \Phi_4^{(m+1)}\right) - \frac{1}{\lambda^2}\left(\Phi_9^{(m+1)} + \Phi_{11}^{(m+1)}\right) - \\ & - \lambda^2\left(\Phi_{10}^{(m+1)} + \Phi_{12}^{(m+1)}\right) - 2\left(\Phi_5^{(m+1)} + \Phi_6^{(m+1)} + \Phi_7^{(m+1)} + \Phi_8^{(m+1)}\right) - \\ & - s^2\Big[\frac{k_y}{\lambda^2}\left(w_1^{(m+1)} - 2w_0^{(m+1)} + w_3^{(m+1)}\right) + k_x\lambda^2\left(w_2^{(m+1)} - \right. \\ & \left. - 2w_0^{(m+1)} + w_4^{(m+1)}\right)\Big] + H_0 s^4\Big\}. \end{aligned} \tag{18.18}$$

Here L_0 and H_0 are functions, depending on initial deflection, $c = 1/12(1 - \mu^2)$.

Process of calculations starts with consecutive passing around nodes of grid to determine deflection $w^{(2)}(x, y, 2\Delta t)$ by formula (17). Then we find function of stresses $\Phi^{(2)}(x, y, 2\Delta t)$ by solving by method of successive approximations the system of differential equations according to formula (18). Essentially, on a given stage there is solved a linear problem, since values of deflection $w^{(m+1)}$ in the right part of equation (18) already were calculated at preceding point. As initial approximation of function of stresses there can be taken its values on preceding step in time, if they are not equal to zero, or values of function Hs^4. Iterations are finished after we attain required degree of accuracy.

A step in time is completed by recount of extra-contour values of w and Φ in accordance with taken boundary conditions. Then calculations are repeated: we find values of $w^{(3)}(x, y, 3\Delta t)$ and $\Phi^{(3)}(x, y, 3\Delta t)$, determine functions in extra-contour nodes knots, etc. After every step in time or after definite intervals it is possible to determine value of stresses.

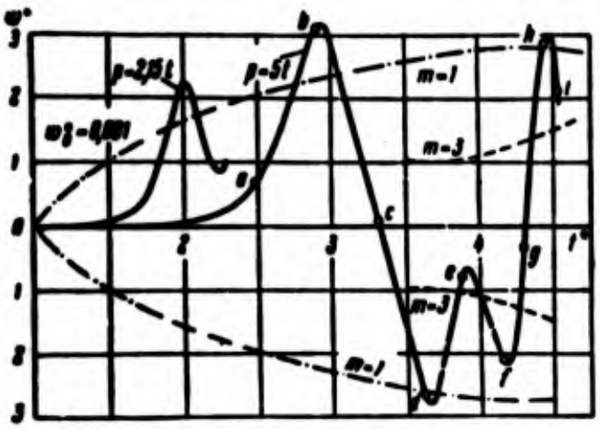

Fig. 18.5. Change of deflection of plate during dynamic loading with different speeds (according to calculations on digital computer).

Concrete calculations were conducted on computer for square flat plate with step s = 1/8. Step in time was selected in such a way that stability of differential equations was ensured. Preliminarily we determined static equilibrium forms of plate during postcritical deformations, corresponding to different "generating" deflection forms. The latter corresponded to values of linear problem with the number of half-waves m = 1 and m = 3 in direction x and one half-wave along y. In Fig. 18.5 dotted lines represent static dependence of deflection in center of plate w* on parameter $t^* = p/p_{кр}$ with initial deflection $w_0^* = 0.001$; by $p_{кр} = \pi^2/3(1 - \mu^2)$ is understood parameter of static critical stress. Deflections directed in the direction of initial deflection are plotted upwards. Further, solid lines show results of solution of dynamic problem with load increasing in proportion to time. When speed of loading is relatively small (p/t = 2.15), intense build-up of deflections occurs with load $p \approx 1.8p_{кр}$; then there occur nonlinear oscillations about positions of static equilibrium. With high speed of loading (p = 5t) deflection sharply increases, where $p \approx 2.6p_{кр}$; after that in the course of every period of oscillations the plate jumps from one equilibrium form to the other, so that

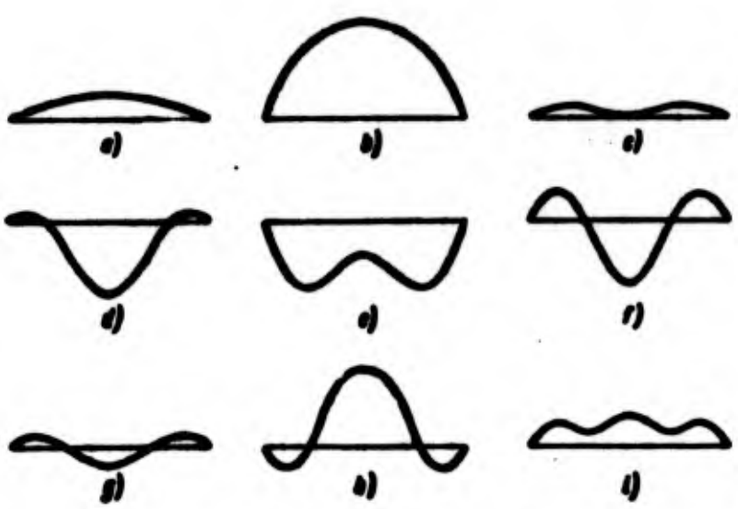

Fig. 18.6. Deflection forms of plate at different moments of time.

deflection changes sign. With sharp build-up of deflections and subsequent oscillations the form of deflection surface greatly changes. This is possible to see from Fig. 18.6; here are presented deflection forms of plate in middle section, parallel to x. Each of these forms corresponds to points of curve in Fig. 18.5, designated by the same letter (a, b, c, etc).

Let us note that for solution of dynamic problem by described method it is necessary to execute about 50 million operations.

§ 179. Buckling of Closed Cylindrical Shells During Hydrostatic Pressure

Let us turn to case of closed circular cylindrical shell, subjected to dynamic application of hydrostatic pressure. We assume that on ends the shell is fastened with frames (see Fig. 10.17), remaining circular during deformation of shell. For total and initial deflections by analogy with solution of static problem (§ 133) we select following approximating expressions (see work [18.1]),

$$\left.\begin{aligned} w &= f(\sin\alpha x \sin\beta y + \psi \sin^2 \alpha x + \varphi),\\ w_0 &= f_0(\sin\alpha x \sin\beta y + \psi \sin^2 \alpha x + \varphi), \end{aligned}\right\} \tag{18.19}$$

where $\alpha = \pi/L$, $\beta = n/R$.

We place expressions (19) in the right part of equation (2). Then integral of this equation may be presented in the form

$$\Phi = E(K_1 \cos 2\alpha x + K_2 \cos 2\beta y + K_3 \sin\alpha x \sin\beta y + K_4 \sin 3\alpha x \sin\beta y) - \frac{qR}{2h} x^2 - \frac{qR}{4h} y^2. \tag{18.20}$$

Here

$$\left.\begin{aligned} K_1 &= \frac{1}{16\alpha^2}\left[\frac{(f-f_0)^2\beta^2}{2} + (f-f_0)f_0\beta^2 - \frac{2(f-f_0)\psi}{R}\right],\\ K_2 &= \frac{\alpha^2}{32\beta^2}(f^2 - f_0^2), \quad K_4 = \frac{\alpha^2\beta^2}{(9\alpha^2+\beta^2)^2}(f^2 - f_0^2)\psi,\\ K_3 &= \frac{\alpha^2(f-f_0)}{R(\alpha^2+\beta^2)^2} - \frac{\alpha^2\beta^2(f^2-f_0^2)}{(\alpha^2+\beta^2)^2}\psi. \end{aligned}\right\} \tag{18.21}$$

The last two members in expression (20) correspond to stresses in middle surface, determined by membrane theory.

Comparing expression for ε_y in terms of deflection and function of stresses, similarly to the way this was done in § 127, we find

$$\frac{\partial v}{\partial y} = \frac{1}{E}\left(\frac{\partial^2 \Phi}{\partial x^2} - \mu \frac{\partial^2 \Phi}{\partial y^2}\right) - \frac{1}{2}\left(\frac{\partial w}{\partial y}\right)^2 + \frac{1}{2}\left(\frac{\partial w_0}{\partial y}\right)^2 + \frac{w}{R}. \qquad (18.22)$$

We write condition of closure which we already used during solution of static problem (p. 574):

$$\int_0^b \frac{\partial v}{\partial y}\, dy = 0.$$

Substituting (22), taking into account preceding relationships, we find

$$\varphi = \frac{E}{8(1-\mu^2)}\left(1 - \frac{f}{\delta}\right) - \frac{f}{\delta} + \frac{f}{\delta}(U + f_0)^2. \qquad (18.23)$$

Thus, magnitude φ turns out to be expressed through ψ and f. It remains to compose equation for determination of these parameters. We use Bubnov-Galerkin method and write equations

$$\left.\begin{aligned} \int_0^a \int_0^b X \sin \alpha x \sin \beta y\, dx\, dy = 0, \\ \int_0^a \int_0^b X \sin^2 \alpha x\, dx\, dy = 0; \end{aligned}\right| \qquad (18.24)$$

here X is determined by (3). We place under integral sign the above-described expressions for w, w_0 and Φ. Integrating, we arrive at following equation, connecting parameters of deflection with load varying in time:

$$\dot{\psi} = C_0\left(1 - \frac{\psi}{\delta}\right) + C_1(\delta^2 - \psi) + C_2(\delta^2 - \psi)\psi^2 - C_3'\left(1 - \frac{\psi}{\delta}\right)\psi\varphi - C_3(\delta - \psi)\varphi + C_4 \frac{1}{\delta}\frac{dU}{dt}. \qquad (18.25)$$

where

$$C_0=\frac{1}{1+\frac{1}{2}\varepsilon^2}\left[\frac{\varepsilon^2}{\pi^2(1+\varepsilon^2)^2\delta}+\frac{\pi^2}{12(1-\mu^2)}\frac{(1+\varepsilon^2)^2}{\varepsilon^2}\delta\right].$$

$$C_1=\frac{\pi^2}{16\left(1+\frac{1}{2}\varepsilon^2\right)}\frac{1+\varepsilon^2}{\varepsilon^2}\delta. \quad C_2=\frac{\pi^2\varepsilon^2}{1+\frac{1}{2}\varepsilon^2}\left[\frac{1}{(1+\varepsilon^2)^2}+\frac{1}{(1+2\varepsilon^2)^2}\right]\delta.$$

$$C_2'=\frac{\varepsilon^2}{(1+\varepsilon^2)^2\left(1+\frac{1}{2}\varepsilon^2\right)}. \quad C_3=\frac{1}{4\left(1+\frac{1}{2}\varepsilon^2\right)}\left[1+\frac{8\varepsilon^2}{(1+\varepsilon^2)^2}\right].$$

$$C_4=\frac{\gamma R^2}{\left(1+\frac{1}{2}\varepsilon^2\right)gE\eta}.$$

In the above equations there were introduced dimensionless parameters

$$\left.\begin{aligned}\hat{q}&=\frac{q}{E}\left(\frac{R}{h}\right)^3. \quad \zeta=\frac{f}{h}. \quad \zeta_0=\frac{f_0}{h}.\\ \varepsilon&=\frac{\pi R}{nL}=\frac{a}{b}. \quad \eta=n^2\frac{h}{R}. \quad \delta=\frac{Rh}{L^2}.\end{aligned}\right\} \tag{18.26}$$

Second equation of system (24) we shall not develop here, and, in order to simplify calculations, we take for parameter ψ that expression, which ensues from solution of static problem:

$$\psi=\frac{N_2\zeta_1}{2(N_1\zeta_1^2+N_2)}. \tag{18.25a}$$

where

$$N_1=\frac{\pi^4}{8(1-\mu^2)}\delta^2+\frac{1}{8}. \quad N_2=C_2\frac{\pi^2}{4}\frac{1+\frac{1}{2}\varepsilon^2}{\varepsilon^2}\delta. \quad N_3=\frac{C_{23}}{4}\left(1+\frac{\varepsilon^2}{2}\right).$$

This means that for a given value of ζ the form of wave formation is considered in case of rapid loading the same as and during slow loading.

Limited in (25) to first member and considering $\zeta_0 = 0$, we find parameter of upper critical pressure for given value of η equal to $\hat{q}_B = C_0$ or

$$\hat{q}_0=\frac{1}{1+\frac{1}{2}\varepsilon^2}\left[\frac{\varepsilon^2}{(1+\varepsilon^2)^2\eta}+\frac{(1+\varepsilon^2)^2}{12(1-\mu^2)}\eta\right]. \tag{18.27}$$

This expression corresponds to formulas (11.74) and (11.93) taking into account $\xi = 1$. In order to obtain calculating upper critical value $\hat{q}_B$, we should find such magnitude η (or such number of waves n),

at which expression for $\hat{q}_в$ will be minimum.

We assume that intensity of pressure increases according to the law q = ct, and we introduce parameter of time

$$\hat{t} = \frac{cR^2}{Eh^2 q_0} = \frac{\hat{q}}{q_0} = \frac{q}{q_0}; \tag{18.28}$$

then it is possible to give equation (25) form

$$\frac{d^2\zeta}{d\hat{t}^2} - S\left[\left(\hat{t} - \frac{\zeta - \zeta_0}{\zeta}\right)\zeta - B_1(\zeta^2 - \zeta_0^2)\zeta - B_2\frac{(\zeta^2 - \zeta_0^2)\zeta^2}{(N_2^2 + N_3)^2} + B_3\frac{(\zeta - \zeta_0)\zeta^2}{N_2^2 + N_1} + B_4\frac{(\zeta - \zeta_0)\zeta\zeta_0}{N_2^2 + N_1}\right] = 0; \tag{18.29}$$

here

$$B_1 = C_1\frac{R^2}{h^2}\frac{1}{4q_0}, \quad B_2 = C_2\frac{4N_3^2}{4q_0}, \quad B_3 = \frac{C_2N_3}{2q_0}, \quad B_4 = \frac{C_2'C_3\eta\left(1 + \frac{1}{2}\eta^2\right)}{4q_0},$$

$$S = \left(1 + \frac{\mu}{2}\right)\hat{q}^2\left(\frac{VR}{cR}\right)^2\left(\frac{h}{R}\right)^4\eta.$$

Equation (29) for dimensionless deflection ζ was integrated by numerical method, and also with help of analog and digital computers with following initial data:

$$\zeta = \zeta_0, \quad \frac{d\zeta}{d\hat{t}} = 0 \text{ when } \hat{t} = 0.$$

During calculations we assumed in application to duralumin shell $V = 5 \times 10^5$ cm/sec, $\mu = 0.3$, $E = 7.75 \times 10^5$ kg/cm^2. Furthermore, we took $R/L = 0.45$, $R/h = 112$, $\delta = 1.8 \times 10^{-3}$.

In Fig. 18.7 is presented graph of $\zeta(\hat{t})$, reflecting dependence between total deflection and time of loading (or load) for case $\zeta_0 = 0.001$. First curve on the left corresponds to solution of static problem for $c \to 0$; this solution can be obtained according to method shown in § 133. On graph is depicted envelope of different curves, corresponding to various numbers of waves n. Upper critical pressure takes place at n = 6; lower, at n = 5. In the same Fig. 18.7 are plotted curves, found for case of dynamic loading with speeds of

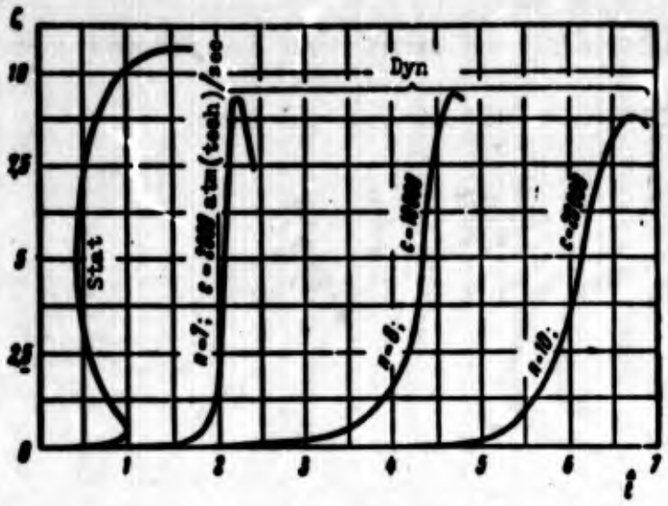

Fig. 18.7. Diagrams "deflection-load" with initial deflection of 0.001 the thickness of the shell.

$c = 0.2 \times 10^4$, $c = 1 \times 10^4$, $c = 2 \times 10^4$ atm(tech)/sec. All curves are reconstructed in such a way that as a base there is taken least upper critical pressure $\hat{q}_B$. On figure are given curves for those numbers of waves n, at which rapid growth of deflections corresponds to least parameter $\hat{t}$.

As we see, dynamic effect here too appears in consecutive growth of number of waves and significant increase of critical pressure.

Graph of Fig. 18.8 contains the same curves for case of large initial deflection ($\zeta_0 = 0.1$). As one should have been led to expect, with comparable values of speed c here there appear less high forms of loss of stability with respect to case $\zeta_0 = 0.001$; smaller (approximately by factor of 1.5) are critical values of pressure. General form of curves of also somewhat different;

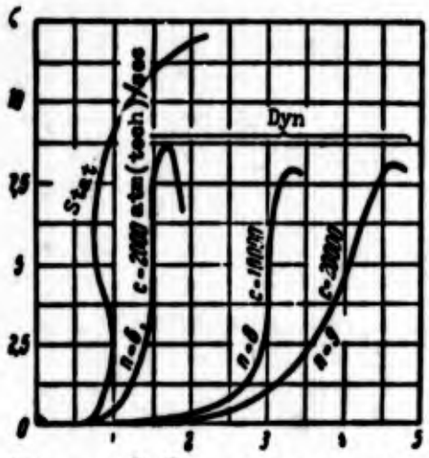

Fig. 18.8. Case, when initial deflection constitutes 0.1 of thickness of shell.

build-up of deflections is less sharp than for $\zeta_0 = 0.001$.

Given scheme of solution of problem was used by V. L. Atamirov* for determination of critical parameter $\hat{t}$ with the most diverse values of R/L, R/h and c. As an example we shall show the results of unique study, carried out by digital computer. In Fig. 18.9 is depicted dependence between <u>coefficient of dynamic overload</u> $k_д$, equal to ratio of conditional dynamic critical load to upper static value, and initial deflection for L/R = 2 and R/h = 100. Here we intentionally selected vanishing minute dimensionless initial deflections from 10^{-4} to 10^{-20}.

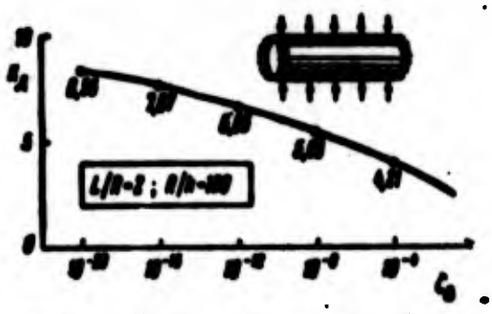

Fig. 18.9. Dynamic "critical" load depending upon initial deflection.

Magnitude $k_д$ monotonically increased from 4.21 to 8.56. There arises the natural question whether it is possible to find a finite value of $k_д$ for limiting case of ideal shell (when $\zeta_0 \to 0$). This question is important from theoretical aspect, and it should be considered in greater detail. However, one may assume that case of vanishing small magnitudes of ζ_0 (of the order 10^{-20}) may be practically investigated.

Let us consider a <u>more complicated program of loading of a shell</u>. Let us assume that shell is subjected to pressure, growing with speed c = 2000 atm/sec, and attaining value, equal to 80% of dynamic critical load. As we have seen, here in process of loading shell does not obtain noticeable deflections. Let us assume that

---

*Another solution of problem was given by Yu. I. Kadashevich and A. K. Pertsev [18.15], taking into account inertness of axisymmetric "compression" of a shell.

subsequently load changes by different laws, as shown in Fig. 18.10b.

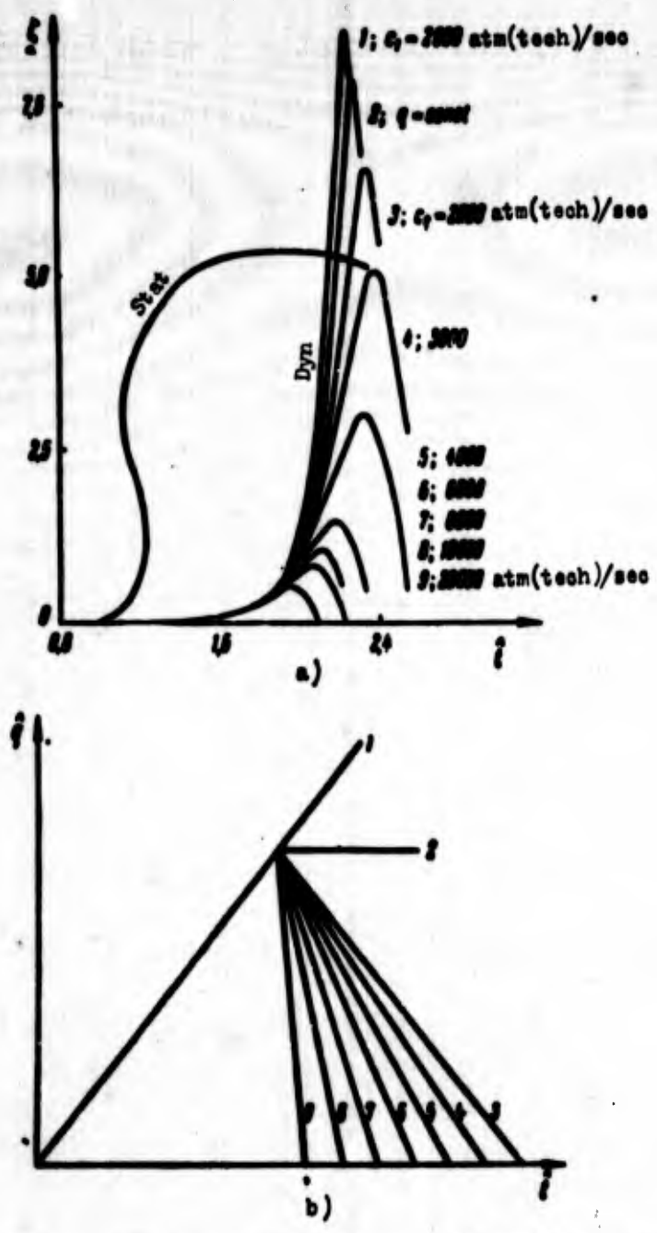

Fig. 18.10. Build-up of deflections of a shell during more complicated program of loading.

Variant 1 coincides with that which was analyzed earlier; here load continues to grow with former speed. In variant 2 load on second stage remains constant. In remaining variants (3-9) load drops by linear law; rate of drop of load is designated by c_2 and changes from 2×10^3 to 2×10^4 atm(tech)/sec. In Fig. 18.10a are shown graphs of change of deflection in time. In spite of the fact that in variants

3-9 load drops, deflection grows to a certain limit, after which it starts to decrease. Behavior of shell on wave of unloading is characterized by magnitude of maximum deflection. In § 176 we agreed to consider that shell buckles in period of unloading if maximum deflection exceeds static deflection, corresponding to the biggest value of pressure; static curve is shown in Fig. 18.10a on the left. If we agree with this assumption, then dangerous speeds of unloading will be all speeds c_2, smaller than 3,000 atm/sec.

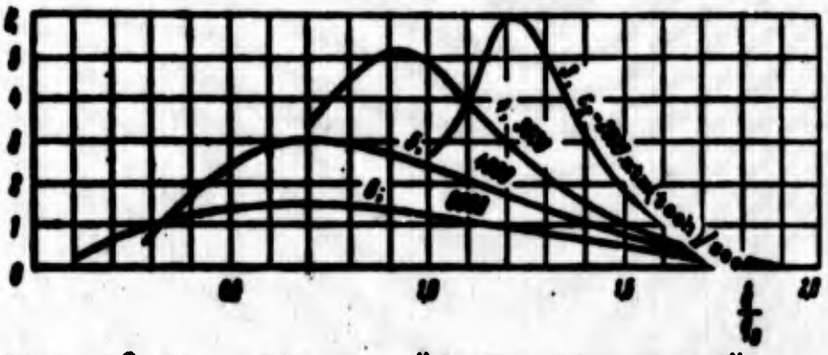

Fig. 18.11. Diagram "deflection-load" during fast unloading.

In Fig. 18.11 these curves are presented in other coordinates. Along the axis of abscissas is plotted magnitude of load, and along the axis of ordinates, deflection.

It is possible to take other criteria of loss of stability or exhausting of supporting power of a shell in period of unloading. For instance, there are grounds to take as limiting parameter the deflection related to thickness of shell. Most important here is to establish, with what deflection the shell does not obtain noticeable permanent deformations.

§ 180. Solution with Help of Analog Computers

Along with digital computers for research of dynamic stability

there can also be applied analog computers,* basic elements of which were briefly described in § 24. Considered problem preliminarily should be reduced to integration of system of ordinary differential equations.

We give scheme of solution on machine MN-7 of the problem, analyzed in § 179, for case when load increases in proportional to time. We rewrite equation of type (29) in form

$$\zeta = A\zeta + B\zeta\hat{t} + C + D\zeta^2 + E\zeta^3 + F\zeta^5$$

or in the form of system of equations

$$\dot{x}_1 = x_2(A + B\hat{t} + Dx_2 + Ex_2^2 + Fx_2^4) + C, \quad \dot{x}_2 = x_1. \tag{18.30}$$

where $x_2 = \zeta$, $\dot{x}_2 = d\zeta/d\hat{t}$. Let us consider shell with former parameters, taking h = 0.8 mm, R = 90 mm, L = 200 mm, $\zeta_0 = 0.001$, n = 6, $\hat{q}_p = 0.0402$, c = 6,000 atm (tech)/sec.

In this case system (30) will take form

$$\dot{x}_1 = x_2(\hat{t} - 1 - 0.508 \cdot 10^{-3}x_2 + 0.02x_2^2 - 0.234 \cdot 10^{-3}x_2^4)6.9 + 6.9 \cdot 10^{-3}; \quad \dot{x}_2 = x_1. \tag{18.31}$$

We select maximum value of functions $x_1 = 100$, $x_2 = 20$.

So that process in circuit did not go so very fast that it is inconvenient to remove indications of instruments and observe functions on the beam indicator, we multiply machine time by 10 times. Then we have

$$T = 10\hat{t}, \quad \bar{x}_1 = \frac{100}{100}x_1, \quad \bar{x}_2 = \frac{20}{100}x_2.$$

Now it is possible to record system (31) in machine form:

$$\dot{\bar{x}}_1 = \bar{x}_2(0.138 \cdot 100 + 1.38T + 1.1\bar{x}_2^2 - 5.3\bar{x}_2^4) + 6.9 \cdot 10^{-4}, \quad \dot{\bar{x}}_2 = 0.5x_1. \tag{18.32}$$

---

*Analog computers for solution of such problems were applied by V. V. Bolotin, G. A. Boychenko and other authors [18.9], [18.10]. Solution of problem given here belongs to Yu. I. Kadshevich and A. K. Pertsev.

Here it is considered that during multiplication of two functions the block of products divides product by 100.

For setting up problem on machine there is composed a block-diagram. In this case load linearly depends on time, and on nonlinearity unit there was set up function $F(T) = T$. Since nonlinearity unit allows us to set up a function of any form, then on machine it is easily possible to investigate more complicated cases of loading. Block-diagram for system (32) is shown in Fig. 18.12.

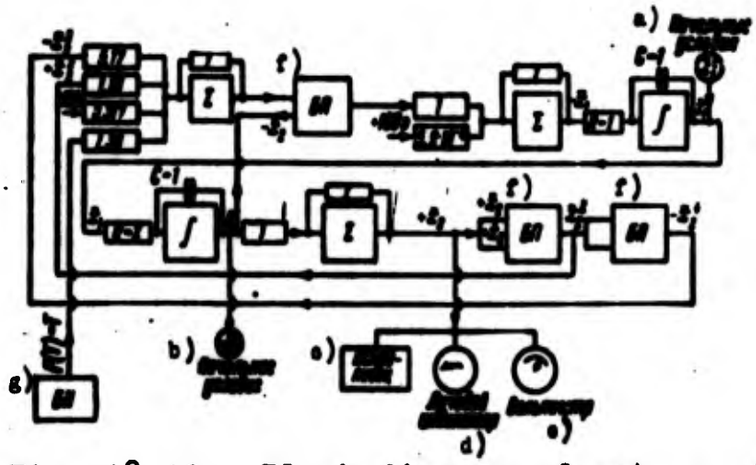

Fig. 18.12. Block-diagram of set-up of problem on analog computer.
KEY: (a) Initial conditions; (b) Initial condition; (c) Spark recorder; (d) Beam indicator; (e) Voltmeter; (f) бп = Product unit; (g) бн = Nonlinearity unit.

Let us note that machine practically works well with increase of initial values of function by 30-50 times. A specific condition of problems of research of questions of loss of stability of shells is the requirement to obtain increment of a function of several thousand times. Therefore, such problems must be solved, either by calculating initial section of curve numerically (what is facilitated by the fact that with small deflections equations become linear), or by solving problem by stages on machine, reconstructing on each stage the block-diagram.

Given example was solved on machine MN-7, starting with time $\hat{t} = 3.3$. Values of function ζ and its derivative at this instant were obtained by numerical integration. System of equations (32) is converted to new machine time; $T_1 = T - 33$. Solution of problem is recorded on spark recorder and is shown in Fig. 18.13 (solid curve). Here dotted line shows section of curve, obtained by numerical integration. As can be seen from graph, accuracy of solution on machine turned out to be sufficiently high.

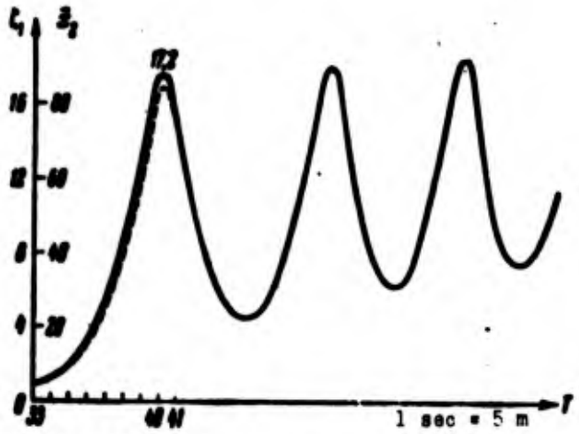

Fig. 18.13. Diagrams "deflection-load," obtained on analog computer (solid line) and by human calculation (dotted line).

§ 181. Experimental Research of Buckling of Shells Under Hydrostatic Pressure

Let us give results of experimental research, conducted on a series of carefully prepared (machined) duralumin pieces,* with $R/h = 220$ and $L/R = 2.2$. Specially designed installation consisted of two tanks, inserted one in the other and filled with oil (Fig. 18.14). The test piece, consisting of circular cylindrical shell, was in the inner tank and upper end of piece remained open. Hole in

*Experiments were conducted by V. Ye. Mineyev with participation of V. S. Smirnov. Data of these experiments were given in part in article [18.12].

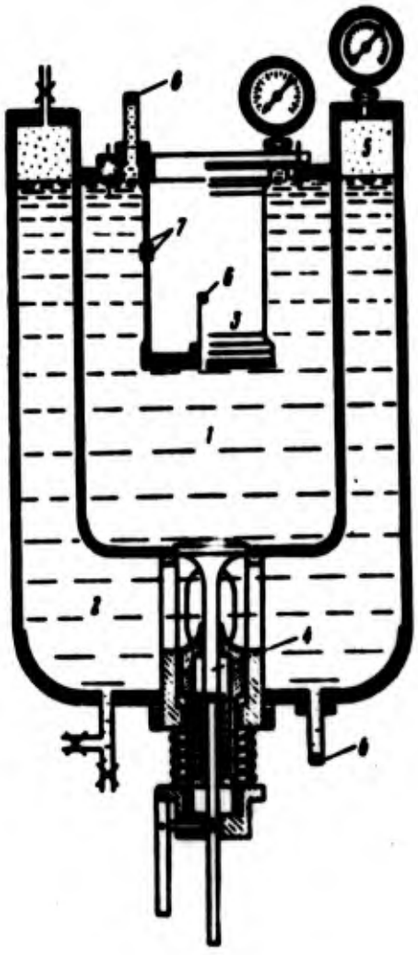

Fig. 18.14. Installation for experiments: test piece (3), inner (1) and outer (2) tanks, pickups (6, 7).

bottom of inner tank was closed by valve, connected with system of springs. In outer tank there was created heightened pressure of 5 to 50 atm(tech); here gas "pad" in upper part of tank was compressed. With sudden opening of valve in inner reservoir there occurred a hydraulic shock, transmitted to test piece; with known approximation it was possible to consider that piece was subjected here to dynamic loading by hydrostatic external pressure. Change in time of pressure at several points of tank was measured by special pickups, signals from which were fixed on tape of loop oscillograph. Pickups of ohmic resistance, fastened to outer and inner surface of test piece, allowed us to determine deformation of elongation at corresponding points; indications of pickups also were transmitted to oscillograph (lines 1-3 in Fig. 18.15). During tests we varied pressure gradients in outer and inner tanks, and also time of opening of valve, which allowed us to obtain different speeds of build-up of pressure from 2×10^3 to 6.5×10^3 atm(tech)/sec.

In Fig. 18.16 are given photographs of pieces, subjected to static loading (Fig. 18.16a) and dynamic loading with speed of build-up of pressure of 4,700 and 5,000 atm(tech)/sec (Fig. 18.16b and c).

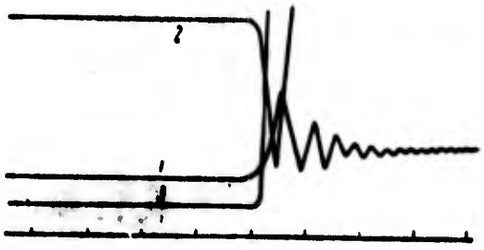

Fig. 18.15. Oscillogram of dynamic loading of shell.

a) b) c)

Fig. 18.16. Shells after buckling; a) with static loading, b) with loading at speed of 4,700 atm(tech)/sec, c) at speed of 5,000 atm(tech)/sec.

General character of deep dents, turned, mainly, toward center of curvature, in all cases was the same; however, configuration of dents changes somewhat; with dynamic application of pressure they have outline close to a rectangle. As we see, with increase of speed of loading form of wave formation changes, as follows from the theoretical solution. At the same time supporting power of shell is sharply increased in stage of loading.

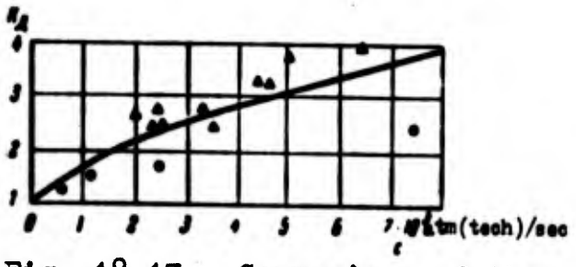

Fig. 18.17. Comparison of theotical data for case $\zeta = 0.001$ (solid line) with experimental.

In Graph of Fig. 18.17 experimental data are compared with results obtained in § 179 for shells with the same dimensions. Along the axis of abscissas is plotted speed c in atm(tech)/sec, and on axis of ordinates, coefficient of dynamic overloading $k_д$. Solid line connects points obtained from graphs of Fig. 18.7 for $\zeta_0 = 0.001$. Triangles mark experimental data for initially "smooth" shells;

circles show same for shells with initial deflection, where initial deflection constituted 2h. Judging by graph, experiments confirmed theoretical conclusions, at least, qualitatively. Certain deviation cf experimental values of critical pressure for shells of "ideal form" upwards from theoretical curve can be explained by the fact that in experiments edges of shells were clamped and what to forces of inertia of mass of shell were joined forces of inertia of adjacent layer of liquid. Furthermore, theoretical solution cannot be considered final; it is desirable, in particular, to clarify in greater detail nature of change cf parameter ψ.

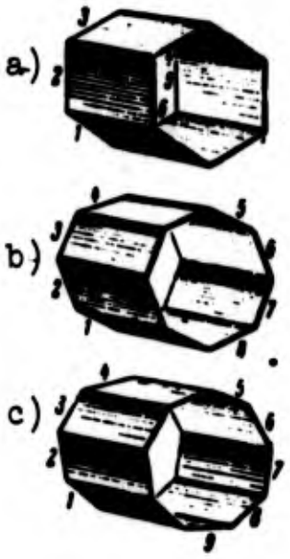

Fig. 18.18. Form of buckling of shells during shock loading.

Another series of experiments was conducted on steel shells,* parameters of which were, R/h = = 200, L/R = 2.9. Shells with insertable bottoms were placed in tank filled with liquid. On free surface of liquid there was produced a shock by a falling load. Change of height of drop of load allowed us to vary speed of build-up of hydrostatic pressure transmitted to shell. In Fig. 18.18 are depicted test pieces after buckling (bottoms were removed). During static loading the shell received six dents on its circumference (a); during dynamic loading with different speeds; it received eight (b) and nine dents (c).

*This research was carried out by V. V. Sorokin.

§ 182. Closed Cylindrical Shells Under Axial Compression

Let us turn to case when circular cylindrical shell is subjected to dynamic impact of axial compression (see Fig. 11.2).*

Total and initial deflection we approximate by analogy with (19) in the following manner:

$$w = f(\sin \alpha_m x \sin \beta y + \psi \sin^2 \alpha_m x + \varphi),$$
$$w_0 = f_0(\sin \alpha_m x \sin \beta y + \psi \sin^2 \alpha_m x + \varphi).$$

In these expressions there enters new coefficient α_m, equal to $\alpha_m = m\pi/L$, where m is the number of half-waves the length of the shell, whereas in § 179 the corresponding coefficient was taken in the form $\alpha = \pi/L$. Let us remember that during axial compression, in distinction from case of hydrostatic pressure, loss of stability of shell in the large is expressed by appearance of diamond-shaped dents, located in checkerboard order and generating several strips along length L. Substituting w and w_0 in equation (6) and integrating, we find

$$\Phi = E(K_1' \cos 2\alpha_m x + K_2' \cos 2\beta y + K_3' \sin \alpha_m x \sin \beta y + K_4' \sin 3\alpha_m x \sin \beta y) - \frac{py^2}{2}.$$

Coefficients K_1', ..., K_4' are determined by former expressions (21) with replacement of α by α_m; by p is understood average intensity of compressive forces, applied to ends of shell.

Applying Bubnov-Galerkin method, we use equation (3). After integration we arrive at following relationship:

$$\tilde{p} = C_0'\left(1 - \frac{\zeta_0}{\zeta}\right) + C_1'(\zeta^2 - \zeta_0^2) + C_2'(\zeta^2 - \zeta_0^2)\psi^2 - C_3'(\zeta - \zeta_0)\psi + C_4'\frac{1}{\zeta}\frac{d^2\zeta}{dt^2} - C_5'\frac{\zeta^2 - \zeta_0^2}{\zeta}\psi. \qquad (18.33)$$

---

*Here there is offered solution of problem, obtained by S. N. Kiryushina. Other works on this question are those of V. L. Agamirov and the author [18.1], and O. I. Terebushko [18.19]. Detailed research of linear axisymmetric problem is conducted by A. I. Blokhina [18.7].

where

$$C_0' = \frac{\xi_m^2}{(1+\xi_m^2)\eta} + \frac{1}{12(1-\mu^2)} \frac{(1+\xi_m^2)^2}{\xi_m^2} \eta,$$

$$C_1' = \frac{1}{16} \frac{1+\xi_m^2}{\xi_m^2} \eta, \quad C_2' = \xi_m^2 \left[\frac{1}{(1+\xi_m^2)^2} + \frac{1}{(1+9\xi_m^2)^2} \right] \eta;$$

$$C_3' = \frac{1}{4\xi_m^2} \left[1 + \frac{4\xi_m^4}{(1+\xi_m^2)^2} \right], \quad C_4' = \frac{\gamma R^2}{E\delta\eta} \frac{1}{\xi_m^2}, \quad C_5' = \frac{\xi_m^2}{(1+\xi_m^2)^2}.$$

In supplement to (26) here there are introduced dimensionless parameters

$$\hat{p} = \frac{p}{E} \frac{R}{h}, \quad \zeta_0 = \frac{w_0 R}{hL} = \frac{c_0}{\beta}.$$

If from equation (33) we exclude inertial member and set $\zeta_0 = 0$, we arrive at solution of static problem for shell of ideal form. Upper critical stress for certain given form of buckling will be equal to

$$\hat{p}_0 = C_0' = \frac{1}{12(1-\mu^2)} \frac{(1+\xi_m^2)^2}{\xi_m^2} \eta + \frac{\xi_m^2}{(1+\xi_m^2)^2 \eta},$$

which corresponds to formula (11.39). Minimizing $\hat{p}$, we find certain value of $\hat{p}_B = 0.605$. As for lower critical stress, given variant of solution leads to parameter* $\hat{p}_H = 0.15 p_B = 0.09$; it corresponds to value $\xi_m = 0.6$.

Let us return to dynamic problem. We assume that external forces increase according to the law p = ct, and we introduce dimensionless parameter

$$\tau = \frac{ct}{Eh\beta_0} = \frac{t}{t_0};$$

then equation (33) will take form (indices m are dropped):

$$\frac{1}{s} \frac{d^2\zeta}{d\tau^2} - \left\{ \left(r - \frac{\zeta - \zeta_0}{\zeta} \right) \zeta - \frac{1}{16\hat{p}_0} \eta \frac{1+\xi^2}{\xi^2} (\zeta^2 - \zeta_0^2) - \frac{\xi^2 \eta}{\hat{p}_0} \left[\frac{1}{(1+\xi^2)^2} + \frac{1}{(1+9\xi^2)^2} \right] (\zeta^2 - \zeta_0^2) \psi^2 + \right.$$

$$\left. + \frac{1}{4\xi^2 \hat{p}_0} \left[1 + \frac{4\xi^4}{(1+\xi^2)^2} \right] \psi (\zeta - \zeta_0) \zeta + \frac{\xi^2}{(1+\xi^2)^2} \frac{1}{\hat{p}_0} (\zeta^2 - \zeta_0^2) \psi \right\} = 0. \qquad (18.34)$$

*Above (see § 127) in this approximation there was obtained somewhat different magnitude (0.124). In § 126 magnitude ξ_m is designated ϑ.

Equation (34) was integrated by numerical method and with help of digital computer. Here we took form of dents, which corresponds to least upper critical stress. Parameter ψ was taken the same as in corresponding static problem for shell of ideal form (see § 127). Furthermore, we took R/h = 180, L/R = 2.2. Results of calculations are presented in Fig. 18.19. Along the axis of abscissas are plotted values of

$$r = \frac{p}{p_*} = \frac{\dot{p}}{\dot{p}_*};$$

here in denominator is least upper critical stress. Along the axis of ordinates in Fig. 18.19 are laid values of deflection ζ. Different series of curves pertain to dynamic loading with speeds $c = 1 \times 10^6$; 2×10^6; and 5×10^6 kg/cm^2 sec. Every curve corresponds to certain number of waves n, shown on graph. As we see, violent growth of deflections occurs in first case at n = 11; in second, at n = 12; in third, at n = 13.

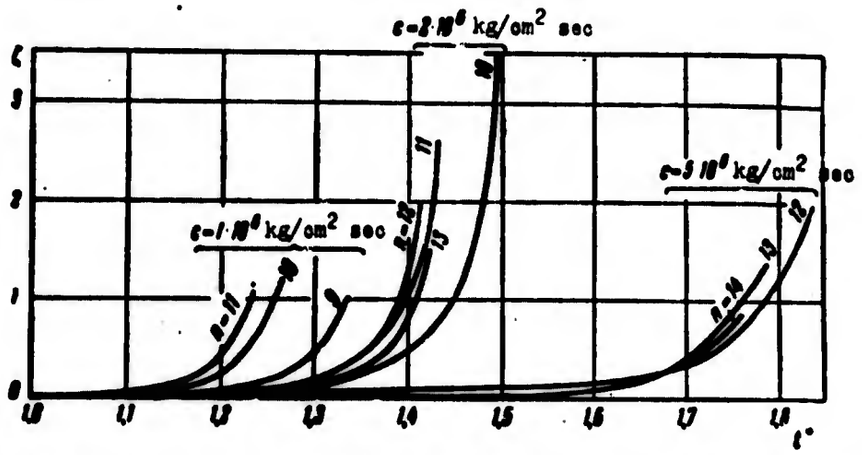

Fig. 18.19. Curves "deflection-load" during dynamic compression along generatrix.

In another variant of solution of the problem (see [18.1] and [18.19]) deflection was approximated by expression

$$w = f\left(\sin\frac{m\pi x}{L}\sin\frac{ny}{R} + \psi\sin^2\frac{m\pi x}{L}\sin^2\frac{ny}{R}\right).$$

In calculations conducted in the same way we assumed that waves are square: $\xi_m = m\pi R/nL = 1$. Integration of equation of type (34) was carried out with help of digital machine "Ural-2" and by numerical method; data turned out to be very close. Results of calculations are given in work of O. I. Terebushko [18.19].

Theoretical conclusions can be compared with data of a series of experiments on duralumin shells,* conducted on the same installation as was described in § 181. In Fig. 18.20 are shown experimental values of coefficient of dynamic overloading; it was obtained by division of magnitude of load, at which dynamic buckling occurred, by static critical value of load, also found from experiments. Solid line is passed through points obtained by integration of equation (34). Let us note that experimental points have here larger scattering than in case of hydrostatic compression (see Fig. 18.17). Effect of dynamicness in case of axial compression turns out to be smaller.

Fig. 18.20. Comparison of theoretical curve with data of experiments (triangles).

In case of compression buckling is expressed in formation of shallow dents, occupying usually only part of surface of shell; therefore, force of inertia here does not render such an influence

*These experiments belong to S. N. Kiryushina.

as during lateral loading, when, as a rule, the whole mass of the shell is set in motion.

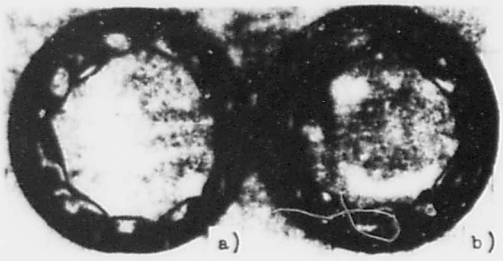

Fig. 18.21. Photographs of test pieces (end view) after buckling.

In Fig. 18.21 are depicted photographs (end view) of shells 0.5 mm thick, one of which was tested statically (Fig. 18.21a) and the other, during dynamic loading with speed $c = 0.65 \times 10^6$ kg/cm^2 (Fig. 18.21b).

A series of interesting experiments on dynamic buckling of shells during axial compression was conducted also by Smitt [18.23] and Coppa [18.22]. It is true, experiments of these authors pertained more to purely shock loading of shell than to the case of moderate speed of growth of load, which was considered above. Nonetheless, qualitative results of experiments correspond to theoretical conclusions obtained by us. It seemed that during dynamic loading size of dents was less and number of dents in cross section was greater than during static application of force. In work [18.22] special attention was allotted to form of buckling of shell under a blow. It turned out that here the same geometric approach to the problem may be applied, as was offered for static problems (see § 128).

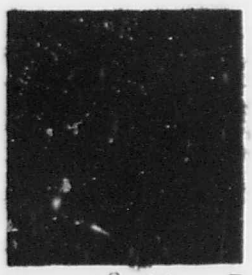

Fig. 18.22. Buckling of shell under sharp blow.

In Fig. 18.22 is shown form of wave formation of real shell, approximating isometric. In the following figure isometric form obtained by construction (Fig. 18.23a) is comparable with actual configuration of dents (Fig. 18.23b).

a) b)

Fig. 18.23. Shell bulges under blow (b) in a form, very close to isometric (a).

§ 183. Spherical Shell Under External Pressure

We shall consider now spherical shell, subjected to dynamic action of evenly distributed external pressure. We are talking both about a closed spherical shell and also about a spherical segment enveloping a sufficiently great central angle (see Figs. 14.1 and 14.2). Up to loss of stability of shell compressive stresses in wall are equal to $\sigma = qR/2h$.

We shall limit ourselves to solving problem of dynamic stability of the shell in linear formulation. Considering in (1) and (2) $k_x = k_y = 1/R$ and rejecting nonlinear members, we arrive at equations

$$\frac{D}{h}\nabla^4(w - w_0) = \frac{1}{R}\nabla^2\Phi - \frac{qR}{2h}\nabla^2 w - \frac{\gamma}{g}\frac{\partial^2 w}{\partial t^2}, \tag{18.35}$$

$$\frac{1}{E}\nabla^4\Phi = -\frac{1}{R}\nabla^2(w - w_0). \tag{18.36}$$

Uniting these two equations, we obtain following resolvent deflection

$$\frac{D}{h}\nabla^4(w-w_0)+\frac{E}{R^2}\nabla^2(w-w_0)+\frac{qR}{2h}\nabla^4 w+\frac{1}{g}\frac{\partial^2}{\partial t^2}(\nabla^2 w)=0. \qquad (18.37)$$

Proceeding the same way as in § 153, we shall not write for functions w and w_0 concrete expressions, but will take following dependence, ensuing from periodic character of these functions:

$$\nabla^2 w=-\lambda^2 w,\quad \nabla^2 w_0=-\lambda^2 w_0;$$

then equation (37) will take form

$$\frac{D}{h}\lambda^4(w-w_0)+\frac{E}{R^2}(w-w_0)-\frac{qR}{2h}\lambda^2 w+\frac{1}{g}\frac{\partial^2 w}{\partial t^2}=0. \qquad (18.38)$$

We introduce designations

$$\frac{w}{h}=\zeta,\quad \lambda^2 Rh=\eta^2,\quad \frac{qR^2}{Eh^2}=\hat{q},\quad \frac{\sigma R}{Eh}=\hat{\sigma};$$

then after simple transformations we obtain

$$\left[\frac{\eta^4}{12(1-\mu^2)}+1\right](\zeta-\zeta_0)-\frac{\hat{q}}{2}\eta^2\zeta+\frac{1}{g}\frac{\partial^2 w}{\partial t^2}=0. \qquad (18.39)$$

If in this equation we drop inertial member, then when $\zeta_0 \to 0$, we find static critical pressure, corresponding to given parameter η:

$$\hat{q}_1=2\left[\frac{\eta^2}{12(1-\mu^2)}+\frac{1}{\eta^2}\right].$$

Minimizing this magnitude with respect to η, we find certain value of upper critical pressure $\hat{q}_B = 1.21$. Corresponding dimensionless membrane stress is equal to $\hat{\sigma}_B = 0.605$.

Dynamic equation (39) it is possible now to rewrite in the form

$$\frac{\gamma R^2}{gE\eta^2}\frac{d^2\zeta}{dt^2}+\frac{\hat{q}_{\eta=0}}{2}(\zeta-\zeta_0)-\frac{\hat{q}}{2}\zeta=0$$

or

$$\frac{\gamma R^2}{gE\eta^2\hat{q}_{\eta=0}}\frac{d^2\zeta}{dt^2}+\frac{1}{2}(\zeta-\zeta_0)-\frac{\hat{q}}{2\hat{q}_{\eta=0}}\zeta=0. \qquad (18.40)$$

We assume that pressure changes according to the law q = ct, and

we introduce dimensionless parameter of time

$$\tau = \frac{t}{t_1} = \frac{t R^2}{E h^2 t_1}.$$

Then equation (40) will change into the following,

$$\frac{1}{S}\frac{d^2\zeta}{d\tau^2} = (\zeta - 1)\zeta + \zeta_0 \qquad (18.41)$$

where

$$S = \frac{1}{3}\eta^2 \left(\frac{\nu z_0 R}{h^2}\right)^2 \tau^2. \qquad (18.42)$$

Integrating equation (41), we find dependence $\zeta(t^*)$ for given S. Then one should change to "unitary" time

$$\zeta_1 = \frac{t}{t_0} = \tau \frac{t_1}{t_0}$$

and compare curves $\zeta(t_1^*)$, corresponding to different values of η. Finding curve, to which there corresponds the most violent growth of deflections, we determine dynamic critical pressure.

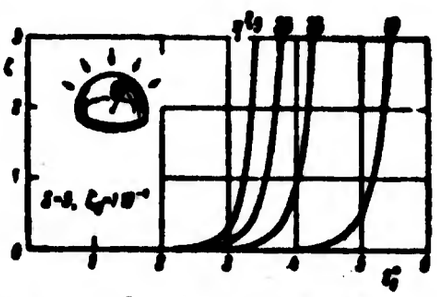

Fig. 18.24. Diagram "deflection-load" for spherical shell.

In Fig. 18.24 are depicted curves of $\zeta(t_1^*)$, obtained with help of digital computer "Ural-1". They pertain to values S = 5, $\zeta_0 = 10^{-4}$ and different η^2. As we see, rapid growth of deflections occurs first of all in case $\eta^2 = 5$.

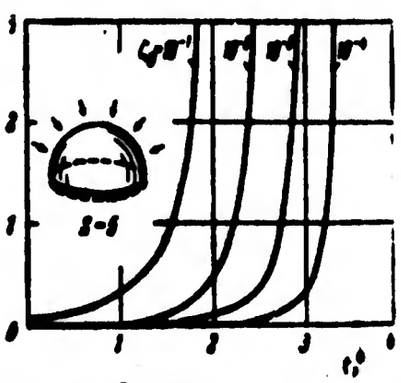

Fig. 18.25. Curves of dynamic buckling of spherical shell with various initial deflection.

On following figure, Fig. 18.25, are compared curves $\zeta(t_1^*)$, pertaining to parameter S = 5 and different ζ_0; here we selected only curves, lying nearest of axis of ordinates.

§ 184. Practical Conclusions. Other Dynamic Problems

In this chapter we considered in detail different approaches to solution of dynamic problem, which from practical point of view is the most urgent--the behavior of plates and shells of different form during rapid monotonic growth of load. We outlined also ways of research of more complicated programs of loading. General conclusion is that character of buckling of plates and shell during dynamic loading is different than during static, and that in first case there appear higher forms of loss of stability. This allows us to design lightened thin-walled constructions, anticipating in advance their overloading in short period of application of forces.

Given data are interesting also from theoretical point of view, since they open a new region in problem of stability of plates and shells. They indicate, in particular, importance of study not only of first form of loss of stability, but also higher forms. Furthermore, certain properties of shells, as, for instance, transition to almost isometric surface during buckling, are more distinct in dynamic process.

We considered behavior of shells, as a rule, from propositions of nonlinear theory. We note, however, that integration of linear equations (see § 183) also allows us, although with certain error, to judge initial stage of rapid growth of deflections.

We considered only forces of inertia, corresponding to normal displacement. More complete equations include inertial members for displacements u and v. Preliminary calculations* show that in a

---

*They were carried out by V. L. Agamirov; see also above-indicated works of N. A. Alumyae [18.2] and Coppa [18.22].

number of cases it is possible to separate study of influence of inertia in direction of normal from consideration of influence of inertia in middle surface. This question should be investigated additionally.

We turn now to other dynamic problems, considered in Chapter VI in application to bars. Most attention in literature was paid to problem of parametric oscillations of plates and shells* And here full picture of behavior of plates and shells may be obtained only with use of nonlinear theory. This is of especially great value for shells, since process of oscillations can be accompanied by their snapping. Let us consider for example case of closed cylindrical shell under action of pulsating normal pressure. We use scheme of solution of problem, adopted in § 179 in application to ideal shell, i.e., considering $\zeta_0 \equiv 0$. It is possible to give equations (25) and (25a) form

$$\left.\begin{aligned} C_4\frac{d^2\zeta}{dt^2}+[C_0-q(t)]\zeta-C_3\psi\zeta^2+(C_1+C_2\psi)\zeta^3=0,\\ \psi=\frac{N_3\zeta}{2(N_1\zeta+N_1)}. \end{aligned}\right\} \qquad (18.43)$$

We take $q(t) = q^0 \cos \theta t$ and assume approximately $\psi = (N_3/2N_1)\zeta$; then the first of equations will take form

$$\frac{d^2\zeta}{dt^2}+\omega^2(1-2\mu\cos\theta t)\zeta-\alpha\zeta^2+\beta\zeta^3=0. \qquad (18.44)$$

where

$$\omega^2=\frac{C_0}{C_4},\quad \mu=\frac{q^0}{2C_0},\quad \alpha=\frac{C_2N_3}{2C_4N_1}-\frac{C_1}{C_4},\quad \beta=\frac{C_2N_3^2}{4C_4N_1^2}.$$

---

*These problems were first considered by V. V. Bolotin [18.8], and subsequently, by S. A. Ambartsumyan, Zh. Ye. Bagdasaryan and others [18.3]-[18.5], and [18.13]. Below are described data, obtained by V. Ts. Gnuni.

If we exclude from (44) nonlinear members, then we arrive a known Mathiev equation (6.118). Results of research of such a linear equation coincide with those which were presented in § 77. Meanwhile solution of nonlinear problem has essential peculiarities. If we consider linear damping, then for $\pi R/nL < 2.66$ we will obtain dependence between square of amplitude of steady-state oscillations c^2 and square of frequency of excitation force θ^2 in region of smooth (first) parametric resonance, depited in Fig. 18.26. As we see, curves $c^2(\theta^2)$ have characteristic loop-like form; this indicates possibility of realization of knock from some stable steady positions to other.*

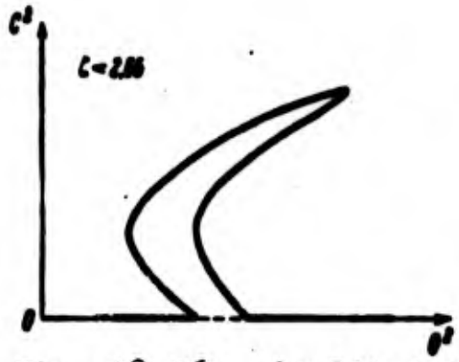

Fig. 18.26. Amplitudes of shell in zone of parametric resonance.

Investigating behavior of shells during dynamic application of load, we became acquainted already with natural nonlinear oscillations of shell around stable equilibrium states. Interesting peculiarities of such oscillations were studied by E. I. Grigolyuk [18.14] and O. D. Oniashvili [18.18]. Specific traits of forced oscillations of shells were considered in works of S. A. Ambartsumyan and V. Ts. Gnuni [18.3], G. V. Mishenkov [18.17] and other authors.

In conclusion let us note that above-mentioned research is only a first step in development of theory of stability of shells and plates during dynamic loading, including description of phenomenon of snapping shell. The "vulnerable" point of solutions by Ritz and Bubnov-Galerkin methods, especially in application to a closed

---

*V. V. Bolotin turned attention to this circumstance in his work [18.8] 1958.

cylindrical shell, is the assumptions, concerning character of wave formation of shell in process of buckling. It is desirable to continue more precise definition of solutions of different problems with application of digital computers (see § 178), and also to conduct new series of experiments. Other directions of possible research in this regions are outlined in § 204 (p.1020).

Literature

18.1. V. L. Agamirov and A. S. Vol'mir. Behavior of cylindrical shells during dynamic application of hydrostatic pressure and axial compression, News of Acad. of Sci. of USSR, OTN, Mech. and machine building, No. 3 (1959), 78-83.

18.2. N. A. Alumyae. On application of method of dismemberment of stresses during solution of axisymmetric problem of the dynamics of closed cylindrical shell, News of Acad. of Sci. of Estonian SSR, 10, No. 3 (1961).

18.3. S. A. Ambartsumyan and V. Ts. Gnuni. On dynamic stability of nonlinearly elastic sandwich plates, Applied math. and mech., 25, No. 4 (1961); On forced vibrations and dynamic stability of orthotropic sandwich plates, News of Acad. of Sci. of USSR, OTN, Mech. and math., No. 3 (1961).

18.4. S. A. Ambartsumyan and A. A. Khachatryan. On stability and vibrations of anisotropic plates, News of Acad. of Sci. of USSR, OTN, Mech. and machine building, No. 1 (1960); On stability and vibrations of a shallow orthotropic cylindrical panel, Reports of Acad. of Sci. of Armenian SSR, 30, No. 1 (1960).

18.5. Zh. Ye. Bagdasaryan and V. Ts. Gnuni. To theory of dynamic stability of anisotropic sandwich shells of revolution, News of Acad. of Sci. of Armenian SSR, series on phys-math. sciences, 13, No. 5 (1960).

18.6. A. Yu. Birkgan and A. S. Vol'mir. Application of digital computers to problem of dynamic stability of shells, DAN SSSR, 135, No. 5 (1960).

18.7. A. I. Blokhina. Dynamic stability of a cylindrical shell with initial bend at given rate of approach of ends, Eng. coll., 31 (1961).

18.8. V. V. Bolotin. Certain nonlinear problems of dynamic stability of plates, News of Acad. of Sci. of USSR, OTN, No. 10 (1954), 48-59; Dynamic stability of plates, Transactions MEI, State Power Engineering Publishing House, No. 7 (1955), 22-46; Stability of a thin-walled spherical shell under action of periodic forces, "Strength analysis," Mashgiz, 2 (1958), 284-299.

18.9. V. V. Bolotin and G. A. Boychenko. Research of snapping-through of thin elastic shells under action of dynamic loads, "Strength analysis," Mashgiz, 5 (1960), 259-282.

18.10. V. V. Bolotin, G. A. Boychenko, B. P. Makarov, N. I. Sudakov, and Yu. Yu. Shveyko. On loss of stability of thin elastic shells under action of impulsive load, "Structural mechanics and design of structures," No. 2 (1959).

18.11. A. S. Vol'mir. On stability of cylindrical shells during dynamic loading, DAN SSSR, 123, No. 5 (1958), 806-808.

18.12. A. S. Vol'mir and V. Ye. Mineyev. Experimental research of process of buckling of a shell during dynamic loading, DAN SSSR, 125, No. 5 (1959).

18.13. V. Ts. Gnuni. To theory of dynamic stability of shells, News of Acad. of Sci. of Armenian SSR, series of phys-math. sciences, 13, No. 1 (1960); News of Acad. of Sci. of USSR, OTN, Mech. and machine building, No. 1 (1961), 181-182; On bounds of dynamic instability of shells, Transactions on theory of shells, Kazan' 1960; On parametrically excited vibrations of anisotropic sandwich shells, News of Acad. of Sci. of Armenian SSR, series of phys-math. sciences, 15, No. 3 (1962).

18.14. E. I. Grigolyuk. On vibrations of a shallow circular cylindrical panel experiencing finite deflections, Applied math. and mech., 19, No. 3 (1955).

18.15. Yu. I. Kadashevich and A. K. Pertsev. On buckling of a cylindrical shell, News of Acad. of Sci. of USSR, OTN, Mech. and machine building, No. 3 (1960).

18.16. L. A. Movsisyan. On one dynamic problem for a cylindrical shell, Reports of Acad. of Sci. of Armenian SSR, 32, No. 5 (1961).

18.17. G. V. Mishenkov. On forced nonlinear vibrations of elastic panels, News of Acad. of Sci. of USSR, OTN, Mech. and machine building, No. 4 (1961), 97-103.

18.18. O. D. Oniashvili. Certain dynamic problems of theory of shells, Publishing House of Academy of Sciences of USSR, 1951.

18.19. O. I. Terebushko. Stability of a cylindrical shell during rapid loading of axial force, "Structural mechanics and design of structures," No. 1 (1960).

18.19a. U. R. Upmanis. Survey of research in dynamic buckling, Sci. notes of Riga polytechnic inst., 1 (1959), 171-186.

18.20. A. A. Khachatryan. On stability and vibrations of round transverse-isotropic plates, News of Acad. of Sci. of Armenian SSR, series of phys-math. sciences, 13, No. 1 (1960), On stability and vibrations of a transverse-isotropic spherical shell, loc. cit., 13, No. 4 (1960).

18.21. V. N. Chelomey. On possibility of increasing stability of elastic systems by vibrations, DAN SSSR, 110, No. 3 (1956).

18.22. A. P. Coppa. On the mechanism of buckling of a circular cylindrical shell under longitudinal impact, Space Sciences Laboratory, General Electric, 1960.

18.23. A. F. Smitt. Dynamic buckling tests of aluminum shells, Aeronaut. Eng. Review, Sept. 1956, 54-58.

C H A P T E R XIX

CERTAIN PROBLEMS OF AEROELASTICITY

§ 185. Divergence and Flutter of a Panel in a Gas Flux

We turn to problems of stability of plates and shells, pertaining to region of aeroelasticity, when behavior of plate or shell is intimately connected with influence of a gas flux flowing past them. Consideration of these problems is important, inasmuch as question of elastic stability inevitably appears during calculation of the construction of any aircraft. These studies are no less interesting from theoretical point of view, since they allow us to find different forms of loss of stability. One of them consists of monotonic buckling; for instance, with onset of certain conditions not the plane form of panel, but the bent form becomes stable. In aviation literature such a process of static loss of stability usually is called divergence. Another, oscillatory form of onset of instability is expressed by appearance of undamped vibrations of a construction. We already met this second type of instability during the study of parametric oscillations. Peculiarity of that oscillatory motion, which we meet in this chapter, consists of the fact that it is maintained by energies furnished by gas flux, where speed and direction of flux can remain constant. Such kinds of vibration are called

natural oscillations or oscillations of flutter type. We shall here be concerned only with static buckling and natural oscillations of reinforced plates or shells which are panels of the skin of the wing, fuselage or empennage of an aircraft; such oscillations obtained name of panel flutter.

Let us assume that elongated panel, secured on edges, is flowed past by gas flow along line AB (Fig. 19.1); velocity of flow is equal to U. If panel deviates from plane AB, then it will be subjected to transverse pressure, depending at every given point on angle between normal to middle surface and direction of flow. When bent outline of panel is symmetric with respect to middle section, normal pressure turns out to be in first approximation antisymmetric, as shown in Fig. 19.1. Panel obtains unique deformed configuration, combining symmetric and antisymmetric deflections. Behavior of panel here depends on character of fastening of edges and on whether there, are initial forces in middle surface. If plate in initial position is flat and is subjected to action of compressive forces then at certain velocity of flow this initial form can become unstable, while bent forms will be stable; in this case there sets in static buckling of panel (divergence). On the other hand, with a certain combination of compressive forces and velocity of flow there can appear oscillation of panel flutter type. Since oscillation cause accelerated development of fatigue cracks in the skin,* then they are undesirable, even if their amplitude is limited.

Fig. 19.1. Panel under influence of flow of gas; distribution of normal pressure.

*In the literature there is information that influence of gas flow caused in its time destruction of certain panels of the skin of the German V-2 rocket.

For aircraft, having supersonic or hypersonic speed, initial forces in skin can be caused by increase of temperature, connected with influence of the same gas flow. Therefore, fundamental equations describing behavior of plates and shells in flow of gas must take into account the influence of temperature field, and they should be referred to region of aerothermoelasticity.

Determination of aerodynamic pressure at great supersonic speeds is facilitated by possibility of application of so-called piston theory. We shall subsequently have to use basic relationships of this theory; therefore, will give a brief derivation of them.

§ 186. Determining Normal Pressure by Piston Theory

Let us consider one-dimensional problem of transient isentropic motion of an ideal gas inclosed in a cylindrical tube and on the right of piston A (Fig. 19.2). Piston shifts to the right with velocity u, small as compared to speed of sound in an undisturbed gas medium; obviously, particle of gas adjacent to piston possess this velocity. Speed of propagation of small perturbations (velocity of sound) in gas medium we designate by c; pressure, by p; density, by ρ. All these magnitudes changed with distance from piston. At a sufficiently great distance from piston points of gas are at rest, so that velocity u = 0; remaining characteristic magnitudes correspondingly are equal to c_0, p_0, and ρ_0.

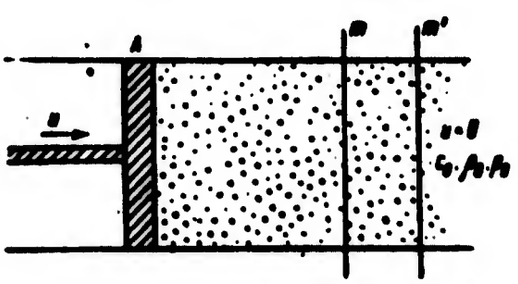

Fig. 19.2. Deviation of equation of motion of gas with movement of piston.

We select at a certain distance from piston two infinitely close sections m and m' in such a way that small perturbation is transmitted from m to m' with velocity of sound c during the time dt; distance

between sections will be dx = c dt. Let us assume that in section m pressure is equal to p, and in section m' it is equal to p—dp.

We compose momental equation for elementary mass of gas ρ dx, included between sections with unit area, considering that under the influence of perturbation this mass during time dt obtains additional velocity du:

$$\rho dx\, du = p\, dt - (p - dp)\, dt.$$

Hence

$$du = \frac{1}{\rho c} dp. \tag{19.1}$$

Assuming that during time dt inside the element through the section there flows mass of gas ρ du dt, we determine new value of density in that same volume;

$$\rho + d\rho = \frac{\rho dx + \rho\, du\, dt}{dx},$$

consequently,

$$du = \frac{c}{\rho} d\rho. \tag{19.2}$$

Another derivation of obtained dependences consists of the following. We write equations of motion of elementary mass of gas and continuity known in aerodynamics:

$$\left.\begin{aligned} \rho\left(\frac{\partial u}{\partial t} + u\frac{\partial u}{\partial x}\right) + \frac{\partial p}{\partial x} = 0. \\ \frac{\partial \rho}{\partial t} + u\frac{\partial \rho}{\partial x} + \rho\frac{\partial u}{\partial x} = 0. \end{aligned}\right| \tag{19.3}$$

Considering that velocity u and increments of u and ρ are small, we disregard their products; then equations (3) take form

$$\left.\begin{aligned} \rho\frac{\partial u}{\partial t} = -\frac{\partial p}{\partial x}. \\ \frac{\partial \rho}{\partial t} = -\rho\frac{\partial u}{\partial x}. \end{aligned}\right| \tag{19.4}$$

For perturbation, transmitted through gas to the right of piston, all

characteristic magnitudes will depend on one variable* x' = x - ct. For certain function f we have

$$\frac{\partial f(x')}{\partial x} = \frac{df}{dx'}, \quad \frac{\partial f(x')}{\partial t} = -c\frac{df}{dx'}. \tag{19.5}$$

Replacing partial derivatives in (4) with total derivatives with respect to x', we arrive at relationships (1) and (2).

Comparing (1) and (2), we obtain known formula for speed of sound:

$$c = \sqrt{\frac{dp}{d\rho}}. \tag{19.6}$$

On the other hand, for isentropic process there is dependence

$$p = C\rho^{\varkappa},$$

where C is a constant, $\varkappa$ is relation of heat capacity of gas at constant pressure to heat capacity at constant volume. Considering $\varkappa$ = const, we find

$$\frac{dp}{d\rho} = C\varkappa\rho^{\varkappa-1} = \varkappa\frac{p}{\rho} \tag{19.7}$$

and

$$c = \sqrt{\varkappa\frac{p}{\rho}}. \tag{19.8}$$

Equalities (1) and (8) give

$$du = \frac{c}{\varkappa p}dp. \tag{19.9}$$

Using (7) and (8), we express velocity of sound c in an arbitrary section in terms of velocity of sound c_0 at infinity:

$$\frac{c}{c_0} = \sqrt{\frac{p\rho}{p_0\rho_0}} = \left(\frac{p}{p_0}\right)^{\frac{\varkappa-1}{2\varkappa}}. \tag{19.10}$$

---

*This proposition implicitly figured in preceding derivation, when we took dx = c dt.

Relationship (9) takes form

$$du = \frac{c_0}{\varkappa}\left(\frac{p}{p_0}\right)^{\frac{\varkappa-1}{2\varkappa}}\frac{dp}{p}. \tag{19.11}$$

Integrating (11), we have

$$u - u_0 = \int_1^{p/p_0} \frac{c_0}{\varkappa}\left(\frac{p}{p_0}\right)^{\frac{\varkappa-1}{2\varkappa}-1} d\left(\frac{p}{p_0}\right).$$

Hence for $u_0 = 0$

$$u = \frac{2c_0}{\varkappa-1}\left[\left(\frac{p}{p_0}\right)^{\frac{\varkappa-1}{2\varkappa}} - 1\right]. \tag{19.12}$$

Further we obtain

$$\frac{p}{p_0} = \left(1 + \frac{\varkappa-1}{2}\frac{u}{c_0}\right)^{\frac{2\varkappa}{\varkappa-1}}; \tag{19.13}$$

here u should be taken with a plus sign during ejection of gas by piston (Fig. 19.2) and minus during suction into the tube.

For air when $\varkappa = 1.4$, we have $\frac{p}{p_0} = (1 + 0.2\,\frac{u}{c_0})^7$.

Considering $u \leq c_0$, we expand expression (13) into a series by Newton's binomial theorem:

$$\frac{p}{p_0} = 1 + \varkappa\frac{u}{c_0} + \frac{\varkappa(\varkappa+1)}{4}\left(\frac{u}{c_0}\right)^2 + \frac{\varkappa(\varkappa+1)}{12}\left(\frac{u}{c_0}\right)^3 + \\ + \frac{\varkappa(\varkappa+1)(3-\varkappa)}{96}\left(\frac{u}{c_0}\right)^4 + \ldots \tag{19.14}$$

Hence

$$p - p_0 = p_0\varkappa\left[\frac{u}{c_0} + \frac{\varkappa+1}{4}\left(\frac{u}{c_0}\right)^2 + \frac{\varkappa+1}{12}\left(\frac{u}{c_0}\right)^3 + \right. \\ \left. + \frac{(\varkappa+1)(3-\varkappa)}{96}\left(\frac{u}{c_0}\right)^4 + \ldots\right]. \tag{19.15}$$

Using (8), we find, $p_0 = c_0^2\rho_0/\varkappa$; consequently, it is possible to record factor before brackets in (15) in the form $(c_0^2\rho_0)$.

For small perturbations in first approximation we have

$$p - p_0 = \frac{p_0\varkappa}{c_0}u = \rho_0 c_0 u. \tag{19.16}$$

We obtained linear relationships, connecting increase of pressure with the velocity of flow. Let us note that (16) also directly ensues from (2). Retaining in expression (15) two or three members of the series, we obtain correspondingly nonlinear dependences of the second or third approximation.

Let us consider the case when elongated slightly distorted panel is subjected to action of a supersonic or hypersonic flow (see Fig. 19.1). We designate velocity of undisturbed flow by U, velocity of sound in undisturbed flow by c_0, and corresponding Mach number by $M = U/c_0$. We consider that this number lies above value $M = 2$.

If length of panel b is significantly greater than width a, for research of deformation of panel it is sufficiently to consider line of width, equal to 1 (Fig. 19.3), and consider all sought magnitudes to be functions of coordinate x and time t. We designate by $\theta(x, t)$

Fig. 19.3. Case of elongated panel: problem becomes one-dimensional.

total angle of inclination of normal to middle surface with respect to a plane perpendicular to vector U; magnitude θ, expressed in radians, we consider small: $\theta^2 \ll 1$.

Let us assume that to left of panel (Fig. 19.4) is a hard barrier, so that panel is flowed past by flow only from below. We assume first

Fig. 19.4. Different cases of distortion of a panel, a) convexity upwards, b) convexity downwards.

that panel is bent with convexity upwards (Fig. 19.4a). Then directly after point A there will lie a zone of rarefaction of the flow. In this zone flow is isentropic; let us note that if it was one-dimensional, then it would be described by exactly the same equations (2) and (4), as for subsonic flow; we should consider that piston depicted in Fig. 19.2 moves to the left. However, considered problem is much more complicated, since it is two-dimensional. Let us assume now that panel is distorted with convexity downwards (Fig. 19.4b). Then in the zone nearest point A there will take place compression of gas; from A the front of a compression shock takes its beginning. Possible outline of this shock is depicted in the figure. Perturbed zone of the flow (shaded in Fig. 19.4b) is between surface of plate and front of the shock. Here already the one-dimensional problem should be formulated in a new fashion, since between layer of gas adjacent to piston and the other region there is located a shock wave; within perturbed zone entropy of gas changes.

Thus, as compared to above-described one-dimensional problem of subsonic motion of piston we encounter here two basic difficulties: (a) problem turns out to be two-dimensional, and (b) there are compression shocks in compressed zone, where entropy of gas cannot be considered constant.

The first of these difficulties may be surmounted by introduction of so-called hypothesis of plane sections. As more detailed research shows, with sufficiently great **M** numbers the front of the compression shock lies comparatively close to surface of plate. During passage through the shock the velocity of a particle of gas changes insignificantly; after contact with plate particle of gas continues to move with almost constant tangential velocity. This tangential velocity U_1 with small angles θ can be considered equal to velocity of undisturbed flow U. Perturbation of flow, caused by contact with plate, consists, mainly, in transverse displacements of particles of gas. The picture of flow is the same as if the particle of gas continued to move with constant speed U, deviating in the direction of the normal to the surface of the plate. Let us reverse motion, i.e., assume that plate moves with speed U in a quiescent gas medium (Fig. 19.5).

Fig. 19.5. Formulation of hypothesis of plane sections.

Then we find that plate "cuts" the medium, imparting to particles transverse motions. We separate layer of particles of gas by two planes mn and m_1n_1, normal to vector U. One may assume that with great supersonic speeds of motion of plate particles of a layer are displaced only within limits of given layer; planes mn and m_1n_1 turn out to be as it were "impenetrable walls."* This constitutes the hypothesis of plane sections.

Such formulation of hypothesis of plane sections is given in work of A. A. Ilyushin [19.6]. Research in this region belong, furthermore, to Hayes [19.19], Lighthill [19.25], Ashley and Zartarian [19.14] and other authors.

If we return to initial flow past of panel and consider that panel is motionless, then transverse component of velocity (Fig. 19.6) will be equal to $U\theta$; for plate accomplishing oscillations it is necessary to consider also transport velocity dz/dt, which a point of middle surface with coordinate z possesses. In other words, problem of determining pressure on a plate is reduced to consideration of transient motion of particles of gas in the presence of a hard wall, travelling with velocity

$$w = U\theta + \frac{dz}{dt}. \qquad (19.16a)$$

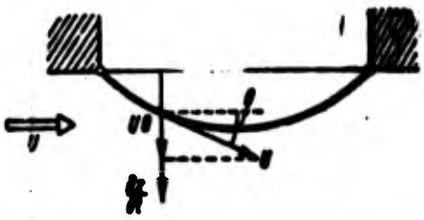

Fig. 19.6. Transverse component of velocity of flow and transport velocity.

If this perturbed motion of gas was isentropic, then for solution of problem we could use results obtained in examining one-dimensional propagation of perturbations in gas, displaced by piston; velocity of piston should, obviously, be determined by formula (16a). For zone of rarefaction we can do this without any new assumptions. However, for zone of compression of gas additional hypotheses are necessary.

It is possible to show that with use of nonlinear expression (15), in which there is retained cubic power (u/c_0), we obtain values of pressure, very close to "exact" ones, even if the latter are found taking into account the strongest adjoint shock wave. Thus, here too process of propagation of perturbations in gas it is possible to assume approximately isentropic.

Piston theory gives satisfactory results, if M number of flow satisfies requirement $M^2 \gg 1$; in practice it may be applied even when $M > 2$. We note, further, that during derivation of relationships

pertaining to one-dimensional problem about motion of a piston we considered that velocity of piston is small as compared to velocity of sound c_0. Consequently, we should have $u < c_0$ or

$$\left(U\theta + \frac{\partial z}{\partial t}\right)_{max} < c_0. \qquad (a)$$

Let us assume that investigated process is oscillatory and that magnitude z changes according to the law $z = A \sin \omega t$, where A and ω are the amplitude and frequency of oscillations, then $(\partial z/\partial t)_{max} = A\omega$. Here condition (a) will be rewritten in the form

$$\frac{U}{c_0}\theta_{max} + \frac{A\omega}{c_0} < 1,$$

where θ_{max} is the biggest value of θ, or

$$M\left(\theta_{max} + \frac{A\omega}{U}\right) < 1. \qquad (b)$$

We put amplitude A over width of panel b; then instead of (b) we find

$$M\left(\theta_{max} + \frac{A}{b}\frac{b\omega}{U}\right) < 1. \qquad (c)$$

Additional research showed that formulas of piston theories are applicable also when basic flow is non-stationary, i.e., when $U = U(t)$; here there must be maintained certain conditions with respect to character of change U.

In many cases it is possible to disregard the second component in expression (16a) as compared to the first and to set

$$w = U\theta = Mc_0\theta. \qquad (19.16b)$$

Such formulation of problem carries name of quasi-static; we conditionally consider that at every given moment of time pressure on surface of vibrating plate is distributed just as for motionless plate of the same configuration.

In courses of aerodynamics there is given known expression for

excess pressure:

$$p - p_0 = \frac{2q_д}{\sqrt{M^2-1}}\theta.$$

where $q_д$ is dynamic pressure, equal to $q_д = \rho_0 U^2/2$. Taking $U = Mc_0$, we find

$$p - p_0 = p_0 c_0^2 \frac{M^2}{\sqrt{M^2-1}}\theta.$$

When $M^2 \gg 1$ it is possible to consider $\sqrt{M^2 - 1} \approx M$. Then we arrive at linear dependence*

$$p - p_0 = p_0 c_0^2 M\theta;$$

it coincides with formula (16), derived by piston theory if we determine u by (16b).

Let us turn to case, when sides a and b of panel are comparable. Here deflections of plate depend both on coordinate x, and also on y. Hypothesis of plane sections remains in force; transverse movement of particle of gas must here be considered to occur along normal to deformed surface of plate. If direction of velocity of flow coincides with direction x, then by angle θ we must understand rotation of the normal in plane xz:

$$\theta = \theta_x = -\frac{\partial w}{\partial x};$$

all remaining relationships remain in force. Reasoning thus, we disregard effect of deflection of vector of velocity of flow from plane xz.

§ 187. Initial Equations for Shallow Shell Past Which a Supersonic Flow Flows

We shall henceforth consider a shallow shell as a slightly

*Introducing instead of M factor $M^2/\sqrt{M^2 - 1}$, it is possible to move lower bound of applicability of piston theory approximately to $M = \sqrt{2}$; see book of V. V. Bolotin [0.1], 1961.

distorted plate, considering initial and additional deflections comparable to thickness. As initial dependences we take the dynamic nonlinear equations given in the preceding chapter (p. 872):

$$\left.\begin{aligned} &\frac{D}{h}\nabla^4(w-w_0)=L(\Phi, w)-\frac{1}{g}\frac{\partial^2 w}{\partial t^2}+\frac{q}{h},\\ &\frac{1}{E}\nabla^4\Phi=-\frac{1}{2}[L(w, w)-L(w_0, w_0)]; \end{aligned}\right\} \qquad (19.17)$$

here as before w and w_0 are total and initial deflections.

Intensity of lateral load q we determine, using (13):

$$q=-(p-p_0)=p_0\left[1-\left(1+\frac{\varkappa-1}{2}\frac{u}{c_0}\right)^{\frac{2\varkappa}{\varkappa-1}}\right]. \qquad (19.18)$$

Minus sign before $(p - p_0)$ is explained by the fact that with positive value of θ load turns out to be directed upwards, i.e., in a direction the reverse of axis z; with negative θ load will act downwards (see Fig. 19.1).

Considering from (16b)

$$\frac{u}{c_0}=M\frac{\partial w}{\partial x},$$

we introduce (18) in equations (17) and supplement them by temperature members from (17.6) and (17.9). Furthermore, we take into account linear damping, as this is usually done in theory of oscillations. Then we obtain following <u>dynamic equations of aerothermoelasticity for a shallow shell of great deflection</u>,* past which there flows a supersonic flow of gas in direction x:

$$\left.\begin{aligned} &\frac{D}{h}\nabla^4(w-w_0)=L(\Phi, w)-\frac{1}{g}\frac{\partial^2 w}{\partial t^2}-\varepsilon\frac{\partial w}{\partial t}+\\ &+\frac{1}{h}p_0\left[1-\left(1+\frac{\varkappa-1}{2}M\frac{\partial w}{\partial x}\right)^{\frac{2\varkappa}{\varkappa-1}}\right]-\frac{Eh^2}{12(1-\mu)}\nabla^2\Theta,\\ &\frac{1}{E}\nabla^4\Phi=-\frac{1}{2}[L(w, w)-L(w_0, w_0)]-\alpha\nabla^2 T. \end{aligned}\right\} \qquad (19.19)$$

*Equations of such type were composed by V. V. Bolotin (see "Strength Calculations" 6, 1960).

If we present q by formulas of third approximation (15) in the form

$$q = -p_0\left[M\frac{\partial w}{\partial x} + \frac{\varkappa+1}{4}M^2\left(\frac{\partial w}{\partial x}\right)^2 + \frac{\varkappa+1}{12}M^3\left(\frac{\partial w}{\partial x}\right)^3\right].$$

the first of equations (19) will take form

$$\frac{D}{h}\nabla^4(w-w_0) = L(\Phi, w) - \frac{1}{g}\frac{\partial^2 w}{\partial t^2} - \varepsilon\frac{\partial w}{\partial t} - \\ -\frac{1}{h}p_0 M\frac{\partial w}{\partial x}\left[1 + \frac{\varkappa+1}{4}M\frac{\partial w}{\partial x}\left(1 + \frac{1}{3}M\frac{\partial w}{\partial x}\right)\right] - \frac{Eh^3}{12(1-\mu)}\nabla^2\theta. \qquad (19.20)$$

Equations (19) and (20) are nonlinear from two points of view: on the one hand, they consider geometric nonlinearity in accordance with basic assumptions of theory of flexible plates and, on the other, they account for aerodynamic nonlinearity of dependence of normal pressure on velocity of flow. If we assume <u>aerodynamic relationsphips linear</u>, we obtain equation (20) in the form

$$\frac{D}{h}\nabla^4(w-w_0) = L(\Phi, w) - \frac{1}{g}\frac{\partial^2 w}{\partial t^2} - \varepsilon\frac{\partial w}{\partial t} - \\ -\frac{p_0}{h}M\frac{\partial w}{\partial x} - \frac{Eh^3}{12(1-\mu)}\nabla^2\theta. \qquad (19.20a)$$

Let us turn to particular case of <u>elongated</u> plate, experiencing cylindrical bending. Deflection w will here depend only on x and t, i.e., $w = w(x, t)$. Of the stresses in the middle surface it is necessary to consider only $\sigma_x = \sigma_0$, where this magnitude should be considered constant the width of the plate. The second of equations (19) drops, and the first obtains by (20) the form

$$\frac{D}{h}\frac{\partial^4(w-w_0)}{\partial x^4} = \sigma_0\frac{\partial^2 w}{\partial x^2} - \frac{1}{g}\frac{\partial^2 w}{\partial t^2} - \varepsilon\frac{\partial w}{\partial t} - \\ -\frac{1}{h}p_0 M\frac{\partial w}{\partial x}\left[1 + \frac{\varkappa+1}{4}M\frac{\partial w}{\partial x}\left(1 + \frac{1}{3}M\frac{\partial w}{\partial x}\right)\right] - \frac{Eh^3}{12(1-\mu)}\frac{d^2\theta}{dx^2}. \qquad (19.21)$$

Instead of equation (20a) we have (compressive stresses are considered positive here):

$$\frac{D}{h}\frac{\partial^4(w-w_0)}{\partial x^4} = -\sigma_0\frac{\partial^2 w}{\partial x^2} - \frac{1}{g}\frac{\partial^2 w}{\partial t^2} - \varepsilon\frac{\partial w}{\partial t} - \frac{1}{h}p_0 M\frac{\partial w}{\partial x} - \frac{Eh^3}{12(1-\mu)}\frac{\partial^2\theta}{\partial x^2}. \qquad (19.21a)$$

If long edges of plate do not shift, then magnitude σ is connected with initial and total deflection according to (7.44) and (7.207) by relationship

$$\sigma = \frac{E}{2b(1-\mu^2)} \int_0^b \left[\left(\frac{\partial w_0}{\partial x} \right)^2 - \left(\frac{\partial w}{\partial x} \right)^2 \right] dx. \qquad (19.22)$$

Let us turn to solution of certain concrete problems.

§ 188. Equilibrium Forms of Plate with Shifting Edges

Let us consider at first an elongated plate, past which there flows from one side a gas flow under the condition that long edges are supported by hinge and can freely approach one another in plane of plate. Let us assume that plate in initial state is flat and what it is subjected to action of constant compressive forces σ_0 along axis x (Fig. 19.7).

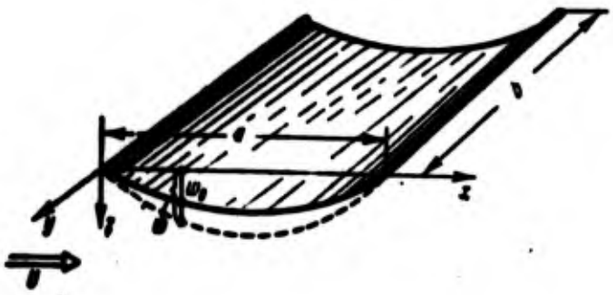

Fig. 19.7. Initial and total deflections of plate.

Compressive forces can be caused by general bending of the construction and, furthermore, by thermal strain of the skin. True, thermal stresses are determined by various conditions of joining of skin with reinforcing members; meanwhile we consider edges of panel free-moving. However, study of case of constant compressive forces allows us to find basic peculiarities of problem.

We assume, further, that deflections are small as compared to thickness of plate, and we solve problem as linear both geometrically,

and aerodynamically. We rewrite equation (21a) in the form ($\sigma = \sigma_0$):

$$X = \frac{D}{h}\frac{d^4w}{dx^4} + \sigma_0\frac{d^2w}{dx^2} + \frac{1}{h}p_0 xM\frac{dw}{dx} = 0; \qquad (19.23)$$

here we take $\varepsilon = 0$ and $\theta = \text{const}$. We noted already that uniqueness of problem consists in combination of symmetric and antisymmetric forms of bending of the plate. Therefore, the expression approximating deflection will be selected in the following form:

$$w = f_1 \sin\frac{\pi x}{a} + f_2 \sin\frac{2\pi x}{a}. \qquad (19.24)$$

Applying Bubnov-Galerkin method, we write equations

$$\int_0^a X \sin\frac{\pi x}{a}\,dx = 0, \quad \int_0^a X \sin\frac{2\pi x}{a}\,dx = 0. \qquad (19.25)$$

Substituting here (24) and integrating, we obtain

$$\left.\begin{aligned} \frac{D}{h}\frac{\pi^4}{2a^3}f_1 - \sigma_0\frac{\pi^2}{2a}f_1 - \frac{4}{3h}p_0 xMf_2 = 0, \\ \frac{D}{h}\frac{8\pi^4}{a^3}f_2 - \sigma_0\frac{2\pi^2}{a}f_2 + \frac{4}{3h}p_0 xMf_1 = 0. \end{aligned}\right| \qquad (19.26)$$

We introduce dimensionless parameters

$$\zeta_1 = \frac{f_1}{h}, \quad \zeta_2 = \frac{f_2}{h}, \quad \sigma_0^* = \frac{\sigma_0}{\sigma_э} = \frac{\sigma_0 a^2 h}{\pi^2 D}, \quad q^* = \frac{p_0 xMa^3}{\pi^4 D}; \qquad (19.27)$$

by $\sigma_э$ is understood is Euler's critical stress: $\sigma_э = \pi^2 D/a^2 h$. Equations (26) take form

$$\left.\begin{aligned} (1-\sigma_0^*)\zeta_1 - \frac{8}{3}q^*\zeta_2 = 0, \\ \frac{8}{3}q^*\zeta_1 + (16-4\sigma_0^*)\zeta_2 = 0. \end{aligned}\right| \qquad (19.28)$$

Considering parameters of deflection ζ_1 and ζ_2 different from zero, we equate determinant of this system to zero; then we find

$$q^* = \frac{3}{4}\sqrt{(\sigma_0^*-1)(4-\sigma_0^*)}. \qquad (19.29)$$

This solution, obviously, has meaning when $1 \leq \sigma_0^* \leq 4$, so that magnitude σ_0^* lies between critical values, corresponding to buckling of plate in one and two half-waves. It is interesting to note that in

a certain zone of values M critical compression stress for plate, past which there flows a gas flow, turns out to be larger than in the absence of flow. Thus, here the gas flow has a stabilizing effect, "straightening" the plate. Certainly, research of postcritical deformation of plate, when deflections become comparable to its thickness, should be conducted by general nonlinear equations.

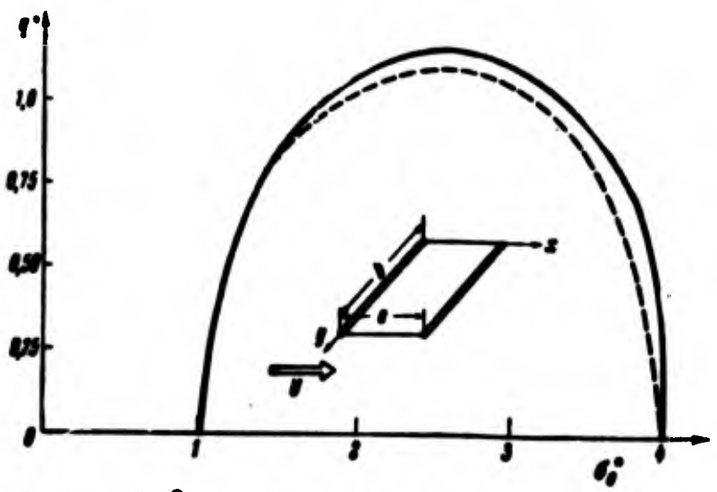

Fig. 19.8. Dependence between pressure and compressive forces for elongated plate by exact solution (solid line) and approximate solution of problem (dotted line).

On graph of Fig. 19.8 dotted line is depicted dependence $q^*(\sigma_0^*)$ by (29); curve has the form of loop. To every value of q* there correspond two equilibrium forms* with different relationship of ζ_1 and ζ_2. At a certain limiting value of q* these forms merge; obviously, for large values of q* in general there exist no equilibrium forms combining one and two half-waves of sinusoid. Minimizing q* with respect to σ_0^*, we find values of σ_0^* and q* for limit point: $\sigma_0^* = 5/2$, $q^* = 9/8$. If we select form of deflection in the form of combination of three and four half-waves, then we obtain on the graph of $q^*(\sigma_0^*)$ the following loop, included between values

*Obviously, only the form pertaining to left part of loop is stable.

$\sigma_0^* = 9$ and $\sigma_0^* = 16$. Corresponding maximum q* lies much higher than the first; therefore, here from practical point of view it is sufficient to consider the first loop.

We pass to case of plate supported by hinge at its edges with sides a and b, comparable to one another, and we assume that direction of flow is parallel to side a. Let us assume that plate is compressed in the same direction by forces σ_0. Solving problem in the same formulation as in preceding case, we write equation (20a) in the form

$$Y = \frac{D}{h}\nabla^4 w + \sigma_0 \frac{\partial^2 w}{\partial x^2} + \frac{p_0}{4h} \varkappa M \frac{\partial w}{\partial x} = 0.$$

We approximate deflection by expression

$$w = f_1 \sin\frac{\pi x}{a} \sin\frac{\pi y}{b} + f_2 \sin\frac{2\pi x}{a} \sin\frac{\pi y}{b}. \qquad (19.30)$$

introducing, in addition to form of bending in one half-wave along both sides, an antisymmetric form along direction of flow.

We write usual equations of Bubnov-Galerkin method; after integration we find

$$\left.\begin{aligned} \frac{D}{h}\frac{\pi^4}{4}\left(\frac{1}{a^2}+\frac{1}{b^2}\right)^2 f_1 - \sigma_0 \frac{\pi^2}{4a^2} f_1 - \frac{2}{3\pi h} p_0 \varkappa M f_2 = 0, \\ \frac{D}{h}\frac{\pi^4}{4}\left(\frac{4}{a^2}+\frac{1}{b^2}\right)^2 f_2 - \sigma_0 \frac{\pi^2}{a^2} f_2 + \frac{2}{3\pi h} p_0 \varkappa M f_1 = 0. \end{aligned}\right\} \qquad (19.31)$$

If we take in first equation $p_0 = 0$, we find magnitude of critical stress;

$$\sigma_0 = \frac{\pi^2 D}{h}\pi^2\left(\frac{1}{a^2}+\frac{1}{b^2}\right)^2. \qquad (19.31a)$$

This expression is valid under the condition that sides of plate differ little from one another: $a \leq b\sqrt{2}$. We introduce in supplement to (27) dimensionless parameters $\hat{\sigma}_0 = \sigma_0/\sigma_э$, $\alpha = a/b$; then equation (31) will take form

$$\left.\begin{aligned} (1-\hat{\sigma}_0)\zeta_1 - \varepsilon^2 \frac{8}{3(1+\alpha^2)^2}\zeta_2 = 0, \\ \varepsilon^2 \frac{8}{3(1+\alpha^2)^2}\zeta_1 + \left[\frac{(4+\alpha^2)^2}{(1+\alpha^2)^2} - 4\hat{\sigma}_0\right]\zeta_2 = 0. \end{aligned}\right\} \qquad (19.32)$$

Equating to zero the determinant of the system, we find

$$q^* = \frac{3(1+\alpha^2)^2}{8}\sqrt{(\hat{\sigma}_0 - 1)\left[\frac{(4+\alpha^2)^2}{(1+\alpha^2)^2} - 4\hat{\sigma}_0\right]}. \qquad (19.33)$$

Magnitude q* turns into zero when $\hat{\sigma}_0 = 1$, $\hat{\sigma}_0 = \frac{1}{4}\frac{(4+\alpha^2)^2}{(1+\alpha^2)^2}$. Second value of $\hat{\sigma}_0$ corresponds to highest critical force for the second of the forms of buckling taken by us (two half-waves in direction x and one along y).

In case of square plate we obtain

$$q^* = \frac{3}{2}\sqrt{(\hat{\sigma}_0 - 1)\left(\frac{25}{4} - 4\hat{\sigma}_0\right)}. \qquad (19.34)$$

Limiting value of q* is at $\sigma_0 = 41/32$ and is equal to $q^* = 27/32$.

We met solution of problems, pertaining to an elongated plate, and also a plate of finite dimensions, in first approximation. However, for these problems there can also be obtained an exact solution. We return to initial equation (23) for an elongated plate and rewrite it in the form

$$\frac{d^4w}{dx^4} + \frac{\sigma_0 h}{D}\frac{d^2w}{dx^2} + \frac{p_0 \varkappa M}{D}\frac{dw}{dx} = 0. \qquad (19.35)$$

We introduce designations

$$\bar{x} = \frac{x}{a}, \quad \bar{\sigma}_0 = \frac{\sigma_0 h a^2}{D} = \pi^2\sigma_0^*, \quad \bar{q} = \frac{p_0 \varkappa M a^3}{D} = \pi^4 q^*; \qquad (19.36)$$

instead of (35) we obtain

$$w^{IV} + \bar{\sigma}_0 w'' + \bar{q}w' = 0; \qquad (19.37)$$

dashes designate derivatives with respect to $\bar{x}$. Corresponding characteristic equation will be

$$r^4 + \bar{\sigma}_0 r^2 + \bar{q}r = 0. \qquad (19.38)$$

One of its roots is equal to $r_1 = 0$; the others we find from cubic equation

$$r^3 + \bar{\sigma}_0 r + \bar{q} = 0. \qquad (19.39)$$

Discriminant of this equation is positive; consequently, one of roots is real, and the other two are complex. We designate them $r_2 = \alpha$, $r_{3,4} = \gamma \pm i\delta$. Roots of equations are connected with its coefficients by following dependences:

$$r_2 r_3 r_4 = -\bar{q}. \quad r_2 + r_3 + r_4 = 0. \quad r_2 r_3 + r_1 r_2 + r_1 r_3 = \bar{\sigma}_0.$$

From this we find

$$\alpha = -2\gamma. \quad \delta = \sqrt{3\gamma^2 + \bar{\sigma}_0}. \quad \bar{q} = 2\gamma(4\gamma^2 + \bar{\sigma}_0). \tag{19.40}$$

Roots $r_1, \ldots, r_4$ corresponds to solution of equation (37):

$$w = A + Be^{\alpha x} + C_1 e^{(\gamma + i\delta)x} + D_1 e^{(\gamma - i\delta)x}.$$

or

$$w = A + Be^{-2\gamma x} + Ce^{\gamma x}\cos\delta x + De^{\gamma x}\sin\delta x. \tag{19.41}$$

Boundary conditions we write in the form

$$w = 0. \quad \frac{d^2 w}{dx^2} = 0 \quad \text{when} \quad x = 0;\ 1.$$

Substituting here (41), we obtain four equations, connecting constants A, ..., D. The first of them has the form A + B + C = 0. Expressing hence A in B and C, we equate to zero the determinant of remaining three equations:

$$\begin{vmatrix} 1 - e^{-2\gamma} & 1 - e^{\gamma}\cos\delta & -e^{\gamma}\sin\delta \\ 4\gamma^2 & \gamma^2 - \delta^2 & 2\gamma\delta \\ 4\gamma^2 e^{-2\gamma} & e^{\gamma}(\gamma^2\cos\delta - 2\gamma\delta\sin\delta - \delta^2\cos\delta) & e^{\gamma}(\gamma^2\sin\delta + 2\gamma\delta\cos\delta - \delta^2\sin\delta) \end{vmatrix} = 0.$$

Expanding this determinant, we arrive at equation*

$$[(\gamma^2 + \delta^2)^2 + 4\gamma^2(\delta^2 - \gamma^2)]\sin\delta(e^{\gamma} - e^{-\gamma}) - 8\gamma^{3/2}\cos\delta(e^{\gamma} + e^{-\gamma}) + 8\gamma^{3/2}(e^{2\gamma} + e^{-2\gamma}) = 0$$

or

$$[(\gamma^2 + \delta^2)^2 + 4\gamma^2(\delta^2 - \gamma^2)]\operatorname{sh}\gamma\sin\delta = 8\gamma^{3/2}(\operatorname{ch}\gamma\cos\delta - \operatorname{ch}2\gamma). \tag{19.42}$$

---

*A similar equation for more general dynamic problem was obtained by A. A. Movchan [19.9], and also Hedgepeth [19.22].

Using (40) and (42), one can find dependence between $\bar{\sigma}_0$ and $\bar{q}$, or, in other words, between σ_0^* and q^*. In case $\bar{q} = 0$ we obtain by (42) $\gamma = 0$; here we have $\sin\delta = 0$, $\delta = \pi, 2\pi, \ldots$ or $\bar{\sigma}_0 = \pi^2, 4\pi^2, \ldots$, which corresponds to values $\sigma_0^* = 1, 4, \ldots$ When $\gamma \neq 0$ and $1 < \sigma_0^* < 4$ we obtain solid curve $q^*(\sigma_0^*)$ in Fig. 19.8; it slightly deviates from dotted curve of first approximation. Limiting value of q^* by exact solution turns out to be equal to 1.17, which is very close to approximate value 9/8 = 1.12.

Analogous solution can be obtained for plate with finite ratio of sides [19.3], if we originate from equation (20a) and present w in the form $w = X(x) \sin(\pi y/b)$. Let us turn to study of second type of loss of stability, oscillatory.

§ 189. Dynamic Problem for Plate with Shifting Edges

We start from equations (21) and (21a), describing process of motion of elongated plate in time. Again we consider case when plate does not have initial deflection and edges shift freely; we shall consider deflections small as compared to thickness. Taking linear expression for pressure and not considering damping and influence of irregularity of temperature, we obtain the following initial equation from (21a), where $\sigma = \sigma_0$:

$$\frac{D}{h}\frac{\partial^4 w}{\partial x^4} = -\sigma_0\frac{\partial^2 w}{\partial x^2} - \frac{1}{g}\frac{\partial^2 w}{\partial t^2} - \frac{1}{h}p_0 xM\frac{\partial w}{\partial x}. \qquad (19.43)$$

Let us assume that as a result of certain perturbations panel begins to accomplish small harmonious oscillations of frequency ω near position of equilibrium. Then deflection w can be presented in the form

$$w = \bar{w}(x)\sin(\omega t + \alpha).$$

Putting this expression in (43), we arrive at equation

$$X(x) = \frac{D}{h}\frac{d^4\bar{w}}{dx^4} + \sigma_0\frac{d^2\bar{w}}{dx^2} + \frac{1}{h}p_0 xM\frac{d\bar{w}}{dx} - \frac{1}{g}\omega^2\bar{w} = 0. \qquad (19.44)$$

We take for $\overline{w}$, as before, approximating expression (24) and we write Bubnov-Galerkin equation of type (25). After integration we obtain equations, analogous to (26), but in the first of them there will enter additional member $(-a\gamma/2g)\omega^2 f_1$, and in second $(-a\gamma/2g)\omega^2 f_2$. If we assume in these equations that $\sigma = 0$ and $p_0 = 0$, then will arrive at certain values of first two frequencies of free vibrations of an elongated plate:

$$\omega_1 = \frac{\pi^2}{a^2}\sqrt{\frac{Dg}{\gamma h}}, \quad \omega_2 = \frac{4\pi^2}{a^2}\sqrt{\frac{Dg}{\gamma h}}.$$

We introduce supplementing (27) parameter $\omega^* = \sqrt{\omega/\omega_1}$; then system of equations of type (28) will take form

$$\left.\begin{aligned}(1-\sigma_0^*-\omega^{*4})\zeta_1-\tfrac{8}{3}q^*\zeta_2=0.\\ \tfrac{8}{3}q^*\zeta_1+(16-4\sigma_0^*-\omega^{*4})\zeta_2=0.\end{aligned}\right\} \qquad (19.45)$$

Equating to zero the determinant of this system, we find

$$q^* = \frac{3}{8}\sqrt{(\omega^{*4}+\sigma_0^*-1)(16-4\sigma_0^*-\omega^{*4})}. \qquad (19.46)$$

We obtained dependence between reduced velocity of flow q^* and frequency of steady-state vibrations of plate ω^*, if we consider given the value of initial compressive force σ_0^*. We assume at first that $\sigma_0^* = 0$; then we have

$$q^* = \frac{3}{8}\sqrt{(\omega^{*4}-1)(16-\omega^{*4})}.$$

This dependence is depicted in graph of Fig. 19.9 by dotted line; along the axis of ordinates are laid off values of ω^{*4}. And here curve $q^*(\omega^{*4})$ has the form of a loop. For every value of q^* we obtain within this loop two different types of vibrations, with frequencies ω_a^* and ω_b^*. During vibrations with frequency ω_a^*, obviously, symmetric form of deflection predominates, and at frequency ω_b^*, the antisymmetric predominates. At certain limiting value $q^* = q_\Phi^*$ these frequencies

merge, and in case $q^* > q^*_\Phi$ steady-state vibrations of plate become impossible. Obviously, in this case there should appear unsteady motion of flutter type, accompanied (in the absence of damping) by growth of amplitude. Magnitude q^*_Φ is dimensionless critical velocity

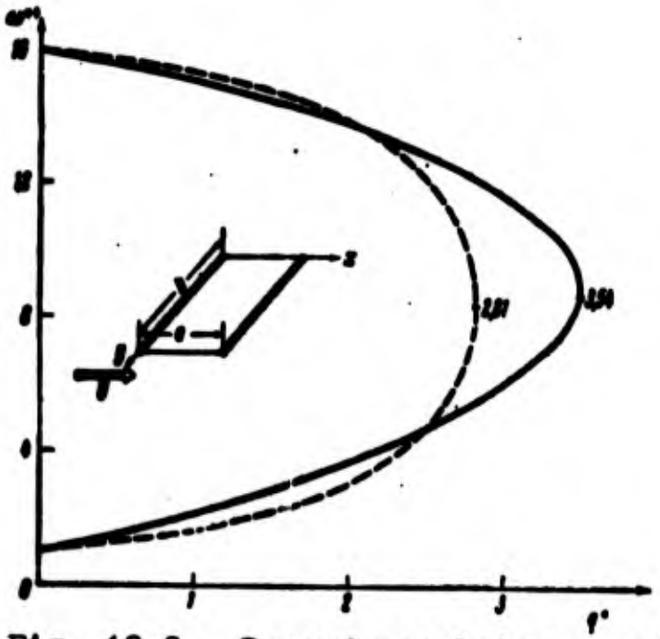

Fig. 19.9. Dependence between velocity of flow and frequency of vibrations of plate in the absence of compressive forces.

of flow. For determination of this magnitude we write condition $dq^*/d\omega^{*4} = 0$, whence $\omega^{*4} = 17/2$. Corresponding value of q^*_Φ will be $45/16 \approx 2.81$. We used Bubnov-Galerkin method, where approximating expression for deflection contained two parameters. If we consider three parameters, corresponding to three first natural modes of vibration, then we find $q^*_\Phi = 3.68$.

We turn now to general case $\sigma^*_0 \neq 0$. In Fig. 19.10 is given three-dimensional graph* depicting dependence of q^* on σ^*_0 and ω^{*4} by (46). Here is shown surface, including loops $q^*(\omega^*)$ for different σ^*_0, and also loop $q^*(\sigma_0)$, corresponding to static buckling.

---

*Graphs of Figs. 19.10 and 19.12 were built by E. D. Skurlatov. Graph, analogous to the one depicted in Fig. 19.11, was offered by V. V. Bolotin, see book [0.1], 1961, p. 268.

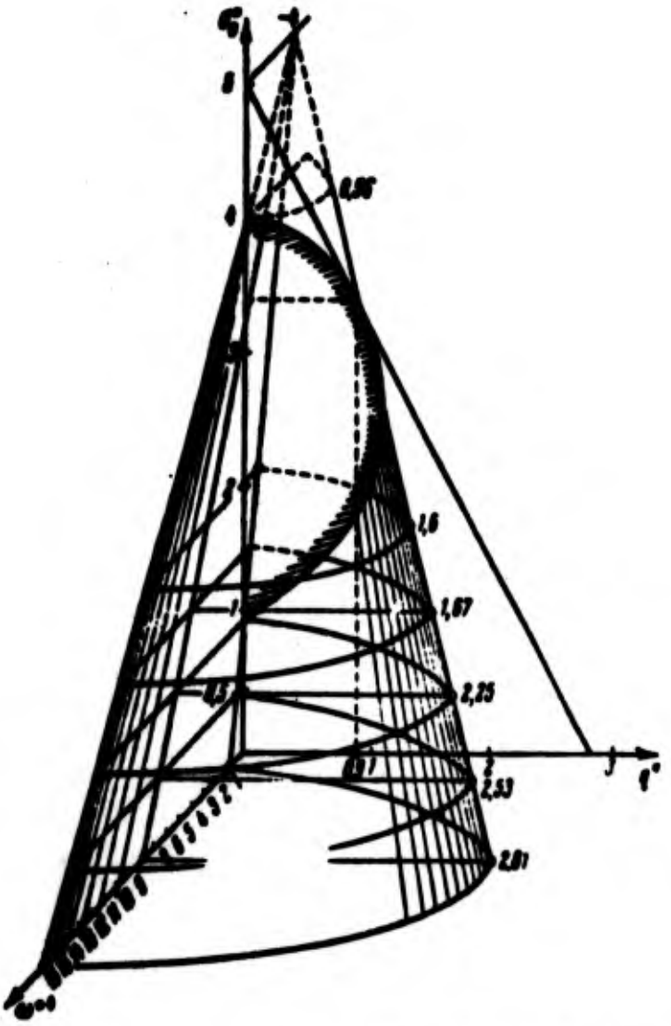

Fig. 19.10. Loops of static and vibrational instability of elongated panel.

In Fig. 19.11 is shown final curve of $q^*(\sigma_0^*)$ according to first approximation. Slanted straight line, determining boundary of flutter, touches loop of static buckling at point $q^* = 0.9$, $\sigma_0^* = 3.4$. Analysis of this curve lead to interesting conclusions concerning behavior of panel during increase of flow velocity. Let us assume that compressive forces are small and lie below σ_3. With growth of q^* and $\sigma_0^* = \text{const}$ we will move on graph on the level of a certain line mn. Plate will remain flat up to moment, corresponding to point n; here there should appear flutter. Let us assume now that magnitude q^* remains constant and in skin there appear compressive forces. Then, going along the

line lp, we approach point p, corresponding to divergence of the panel.

Consequently, shifting on graph from region of plane equilibrium forms, we may in one case intersect boundary of monotonic, and in the other, the boundary of vibrational instability.

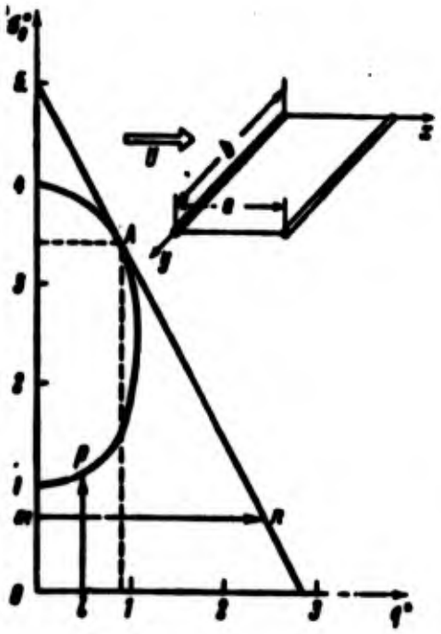

Fig. 19.11. Graph of critical velocity of flow for elongated panel.

It is possible to give exact solution of linear problem similarly to how this was done in § 188. Using designations

$$\bar{x}=\frac{x}{a},\ \bar{\sigma}_0=\frac{\sigma_0 a^2 h}{D},\ k=\frac{\gamma h a^3}{Dg}\omega^2,$$

we rewrite equation (44) in the form

$$w^{IV}+\bar{\sigma}_0 w''+\bar{q}w'-kw=0.$$

Instead of characteristic equation (39) we obtain here equation

$$r^4+\bar{\sigma}_0 r^2+\bar{q}r-k=0. \qquad (19.47)$$

Study of its roots* leads to curve shown in Fig. 19.9 by solid line, where magnitude q^*_{Φ} turns out to be equal to 3.54, i.e., 26% above q^*_{Ψ} of the first approximation and 4% below q^*_{Φ} of the second approximation. Will note, however, that during study of equilibrium forms of panel in postcritical region and, especially, in zone, lying on curve of Fig. 19.11 above point of tangency A, one should use nonlinear dependences (see § 190).

---

*It was conducted by A. A. Movchan [19.9] and Hedgepeth [19.22]; study of case of plate with finite ratio of sides is also his. Here account is constructed from [19.22].

Let us turn to case of plate with finite ratio of sides. Solving problem in that same formulation as above, we assume that plate is compressed along axis x by forces σ_0. Equation (20a) takes form

$$\frac{D}{h}\nabla^4 w = -\sigma_0 \frac{\partial^2 w}{\partial x^2} - \frac{1}{g}\frac{\partial^2 w}{\partial t^2} - \frac{p_0 \pi M}{h}\frac{\partial w}{\partial x} \qquad (19.48)$$

Considering $w = \bar{w} \sin(\omega t + \alpha)$, we arrive at equation for function $\bar{w} = \bar{w}(x, y)$:

$$X = \frac{D}{h}\nabla^4 \bar{w} + \sigma_0 \frac{\partial^2 \bar{w}}{\partial x^2} + \frac{p_0 \pi M}{h}\frac{\partial \bar{w}}{\partial x} - \frac{1}{g}\omega^2 \bar{w} = 0. \qquad (19.49)$$

Using as before an approximating expression for deflection of type (30), we write Bubnov-Galerkin equation; then arrive at equations

$$\left.\begin{aligned} \left[\frac{D}{h}\frac{\pi^4}{4}\left(\frac{1}{a^2}+\frac{1}{b^2}\right)^2 - \sigma_0\frac{\pi^2}{4a^2} - \frac{\pi^2}{4g}\right] f_1 - \frac{2}{3\pi h} p_0 \pi M f_2 = 0. \\ \frac{2}{3\pi h} p_0 \pi M f_1 + \left[\frac{D}{h}\frac{\pi^4}{4}\left(\frac{4}{a^2}+\frac{1}{b^2}\right)^2 - \sigma_0\frac{\pi^2}{a^2} - \frac{\pi^2}{4g}\right] f_2 = 0. \end{aligned}\right| \qquad (19.50)$$

Considering in first equation $\omega = p_0 = 0$, we again find static value of critical stress (31a). On the other hand, considering in both equations $\sigma_0 = p_0 = 0$, we obtain two frequencies of free vibrations:

$$\omega_1 = \pi^2\left(\frac{1}{a^2}+\frac{1}{b^2}\right)\sqrt{\frac{Dg}{\gamma h}}, \quad \omega_2 = \pi^2\left(\frac{4}{a^2}+\frac{1}{b^2}\right)\sqrt{\frac{Dg}{\gamma h}}; \qquad (19.51)$$

they correspond to forms of deflection appearing in (30).

Subsequent calculations we conduct for square plate (a = b); then we have

$$\sigma_0 = \frac{4\pi^2 D}{b^2 h}, \quad \omega_1 = \frac{5\pi^2}{b^2}\sqrt{\frac{Dg}{\gamma h}}, \quad \omega_2 = \frac{8\pi^2}{b^2}\sqrt{\frac{Dg}{\gamma h}}.$$

We introduce dimensionless parameters

$$\bar{\sigma}_0 = \frac{\sigma_0 b^2 h}{4\pi^2 D} = \frac{\sigma_0}{\sigma_0}, \quad \bar{\omega} = \sqrt{\frac{\omega}{\omega_0}}, \quad \bar{q} = \frac{p_0 \pi M b^3}{D\pi^4}; \qquad (19.52)$$

equations (50) will take form

$$\left.\begin{aligned} (1 - \bar{\sigma}_0 - \bar{\omega}^2)\zeta_1 - \frac{2}{3}\bar{q}\zeta_2 = 0. \\ \frac{2}{3}\bar{q}\zeta_1 + \left(\frac{25}{4} - 4\bar{\sigma}_0 - \bar{\omega}^2\right)\zeta_2 = 0 \end{aligned}\right| \qquad (19.53)$$

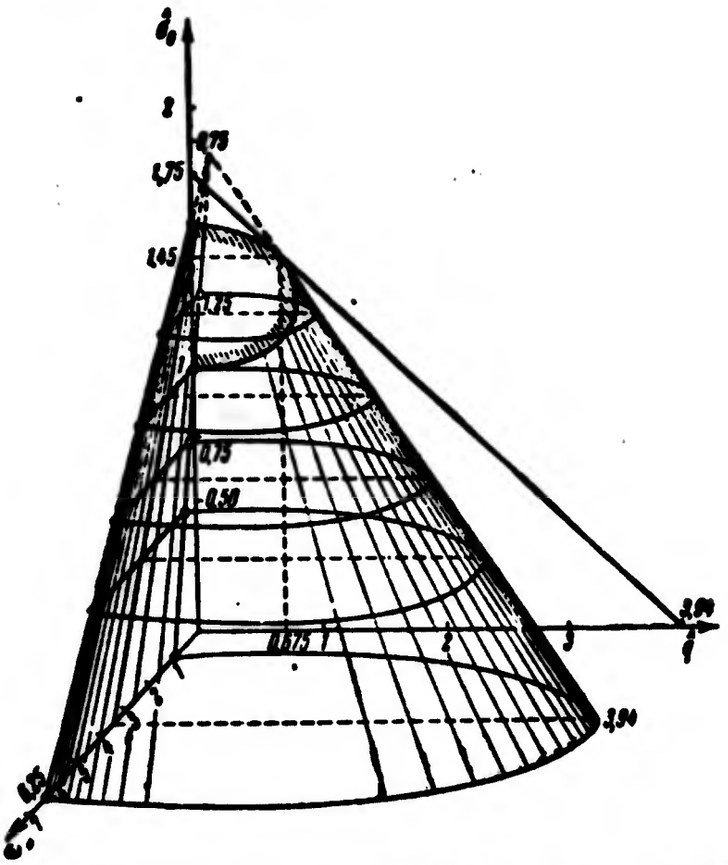

Fig. 19.12. Loops of static and vibrational instability of square panel.

Equating to zero the determinant of this system, we find

$$\hat{q} = \frac{3}{2}\sqrt{(\hat{\omega}^4 + \hat{\sigma}_0 - 1)\left(\frac{25}{4} - 4\hat{\sigma}_0 - \hat{\omega}^4\right)}. \quad (19.54)$$

From condition $\partial\hat{q}/\partial\hat{\omega} = 0$ we find $\hat{\omega}^4 = \frac{29}{8} - \frac{5}{2}\hat{\sigma}_0$. Maximum value of $\hat{q}$, which we consider critical, is equal to

$$\hat{q}_* = \frac{9}{4}\left(\frac{7}{4} - \hat{\sigma}_0\right). \quad (19.55)$$

In the absence of compressive force we have $\hat{q}_* = 63/13$. In Fig. 19.12 is curve change of $\hat{q}$ depending upon $\hat{\sigma}_0$ and ω^4, analogous to curve of Fig. 19.10. In Fig. 19.13 is shown loop of static equilibrium

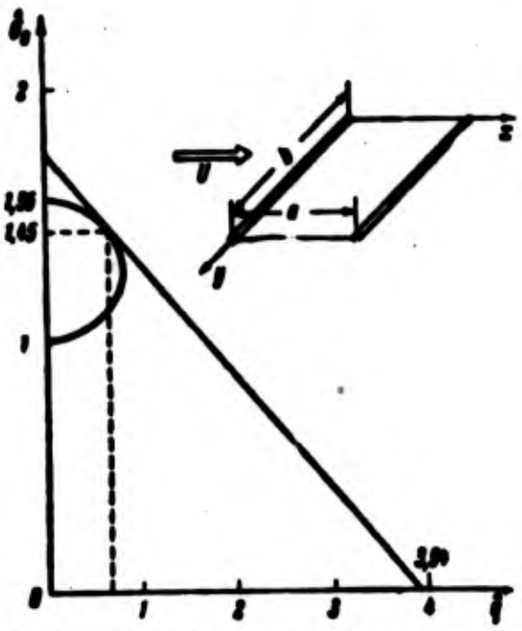

Fig. 19.13. Graph of critical flow velocity for square panel.

forms and straight line (55); point of tangency corresponds to values $\hat{q} = 0.675$ and $\hat{\sigma}_0 = 1.45$.

§ 190. Plate with Fixed Edges

In all preceding examples we assumed that compressive force σ_0 is assigned and that edges of plate shift freely. In real constructions, however, panel of skin is connected to reinforcing ribs. Therefore, for practical calculations it is important to determine behavior of panel in interaction with other members of a construction. We assume, e.g., that along lines $x = 0$, $x = a$ an elongated plate is fastened by hinge with ribs so rigid that these edges must be considered fixed. We investigate equilibirum positions of plate, assuming that in initial state plate is distorted in a half-wave of a sinusoid $w_0 = f_0 \sin(\pi x/a)$ and that initial deflection f_0 is comparable with thickness of the plate.* Thus, here we consider problem from propositions of geometrically nonlinear theory. At the same time we consider aerodynamics in the first variant to be linear. Consequently, we have to start from equation (21a):

$$\chi = \frac{D}{h}\frac{d^4(w-w_0)}{dx^4} + \sigma\frac{d^2w}{dx^2} + \frac{1}{h}p_0 M\frac{dw}{dx} = 0.$$

Magnitude σ here is not given, but is connected with deflection by relationship (22).

Taking from w approximating expression (24), we find

$$\sigma = -\frac{\pi^2 E}{4a^2}(f_1^2 - f_1 - 4f_2)\frac{1}{1-\mu^2}. \qquad (19.56)$$

We write Bubnov-Galerkin equation (25). After integration we arrive

*A similar problem was solved by Fung [19.16] taking into account initial forces in the middle surface.

at following equations:

$$\left.\begin{aligned}\frac{D}{h}\frac{\pi^4}{2a^3}(f_1-f_0)-\sigma\frac{\pi^2}{2a}f_1-\frac{4}{3h}p_0\varkappa M f_2=0.\\ \frac{D}{h}\frac{8\pi^4}{a^3}f_2-\sigma\frac{2\pi^2}{a^2}f_2+\frac{4}{3h}p_0\varkappa M f_1=0.\end{aligned}\right\} \qquad (19.57)$$

We introduce in supplement to (27) designation $\zeta_0 = f_0/h$ and substitute expression σ from (56); then equation (57) will take form

$$\left.\begin{aligned}3(\zeta_1^2+4\zeta_1\zeta_2^2-\zeta_0^2\zeta_1)+(\zeta_1-\zeta_0)-\frac{8}{3}q^*\zeta_2=0.\\ 3(4\zeta_2^2+\zeta_1^2\zeta_2-\zeta_0^2\zeta_2)+4\zeta_2+\frac{2}{3}q^*\zeta_1=0.\end{aligned}\right\} \qquad (19.58)$$

Using this system of cubic equations for parameters of deflection ζ_1, and ζ_2, for given values of q* and ζ_0 we can determine equilibrium forms of panel.

More exact solution (taking into account aerodynamic nonlinearity) leads to very complicated calculations; therefore, it was carried out on digital computers.* We will introduce dimensionless parameters

$$\left.\begin{aligned}\bar{x}=\frac{x}{a},\quad \bar{w}=\frac{w}{h},\quad \zeta_0=\frac{f_0}{h},\quad \bar{\sigma}=\sigma\frac{12a^2}{Eh^2},\\ \bar{q}=p_0\frac{12(1-\mu^2)\varkappa Ma^3}{Eh^3},\qquad \eta=M\frac{h}{a}.\end{aligned}\right\} \qquad (19.59)$$

If we consider $\varkappa$ = 1.4, then fundamental equation (21), containing three members of the series in the expression for q, will take form (dashes above dimensionless magnitudes are omitted)

$$\frac{d^4(w-w_0)}{dx^4}+\sigma\frac{d^2w}{dx^2}+q\frac{dw}{dx}\left[1+\frac{3}{5}\eta\frac{dw}{dx}\left(1+\frac{1}{3}\eta\frac{dw}{dx}\right)\right]=0. \qquad (19.60)$$

Expression (22) is reduced to the following form:

$$\sigma=6\int_0^1\left[\left(\frac{dw_0}{dx}\right)^2-\left(\frac{dw}{dx}\right)^2\right]dx; \qquad (19.61)$$

---

*This solution for elongated plate and panel with finite ratio of sides (see below) belongs to A. Yu. Birkgan.

coefficient $(1-\mu^2)$ here is omitted. As can be seen from (60), parameter η allows us here to consider higher members of expansion of aerodynamic load in a series according to (15). We present (60) and (61) in finite differences, using symmetric operators of the second order of accuracy from (7.238) and (7.239). In the i-th node equation has the form

$$w_{i-2} - Aw_{i-1} + Bw_i - Aw_{i+1} + w_{i+2} = C_i. \qquad (19.62)$$

where $A = 4 + \sigma s^2$, $B = 6 + 2\sigma s^2$. By s is understood step of integation; C_i depends on aerodynamic load and initial deflection. Magnitude σ is determined by numerical integration, e.g., by Simpson's formula. Thus, we arrive at system of nonlinear algebraic equations, which is solved by successive approximations.

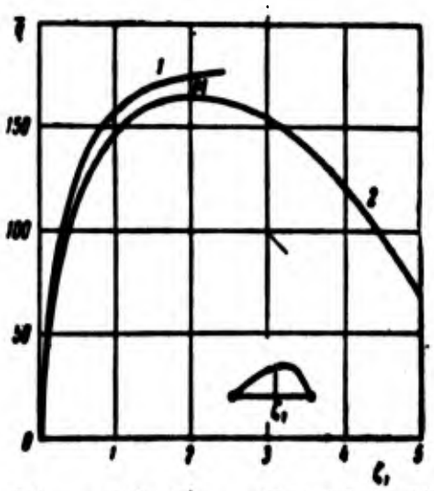

Fig. 19.14. Equilibrium forms of panel with fixed edges.

In Fig. 19.14 is shown dependence between magnitude $\bar{q}$ and deflection in center of panel $\zeta_1 = f_1/h$ for $\zeta_0 = 5$ and $\eta = 0$. Curve 1 corresponds to results of machine calculation; curve 2 is obtained by Bubnov-Galerkin method by (58). As we have seen, magnitude η accounts here for aerodynamic nonlinearity; case $\eta = 0$ corresponds to linear aerodynamics. Points of right section of branch we could not determine by machine calculation; apparently, for this there must be found special methods (see footnote on p. 926).

In Fig. 19.15 is shown dependence $\bar{q}(\sigma)$ for different values of η. Let us remember that compressive stress σ here is the result of bending of the panel. As we see, inclusion of aerodynamic nonlinearity

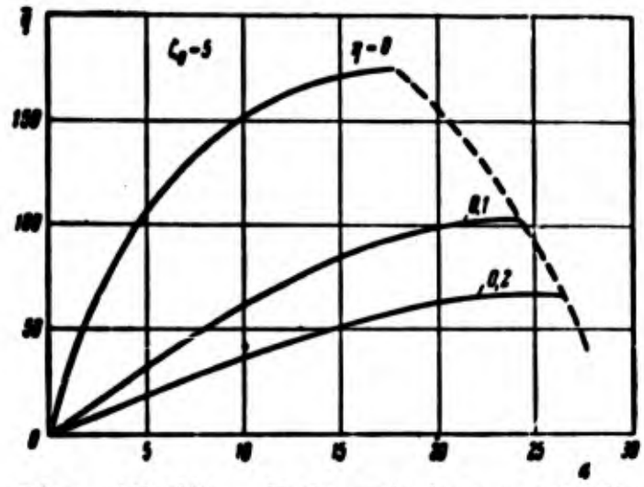

Fig. 19.15. Determining equilibrium forms of panel taking into account aerodynamic nonlinearity.

here leads to lowering of limit point.* Forms of deflection surfaces, corresponding to different values of $\bar{q}$ when $\eta = 0.2$ are presented in Fig. 19.16.

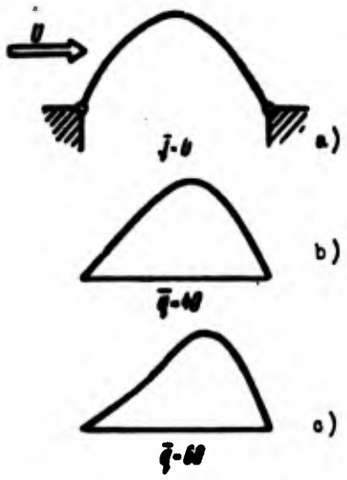

Fig. 19.16. Forms of deflection surface of panel for different $\bar{q}$.

Let us turn to case of panel of finite dimensions. Let us consider square hinge-supported panel with side a, having initial deflection $w_0 = f_0 \sin(\pi x/a)\sin(\pi y/a)$ and past which there flows on the convex side a flow with parameters M, p_0. We assume that edges of panel can be displaced, remaining rectilinear. We solve this problem, accounting simultaneously for geometric and aerodynamic nonlinearity, without expansion of

*This circumstance was shown by V. V. Bolotin (Scientific reports of the higher schools of machines and instruments, No. 3, 1958).

magnitude $(p-p_0)$ in a series; then we have (for $\varkappa = 1.4$)

$$q = p_0\left[1-\left(1-\frac{1}{5}\eta\frac{dw}{dx}\right)^7\right].$$

where, as before,* $\eta = Mh/a$. Taking dimensionless parameters

$$\left.\begin{aligned} \bar{x} &= \frac{x}{a},\ \bar{y} = \frac{y}{a},\ \bar{w} = \frac{w}{h},\ \zeta = \frac{f_0}{h}, \\ \bar{\sigma} &= \frac{\sigma}{E\beta^2},\ p = \frac{pa^4}{Eh^4},\ c = \frac{1}{12(1-\mu^2)}. \end{aligned}\right\} \tag{19.63}$$

we bring system of equations (19) to form (dashes above w, Φ, etc. are omitted

$$c\nabla^4 w = L(w, \Phi) + p\left[1-\left(1-\frac{1}{5}\eta\frac{\partial w}{\partial x}\right)^7\right] + \psi, \tag{19.64}$$

$$\nabla^2\Phi = -\frac{1}{2}L(w, w) - \varphi; \tag{19.65}$$

here ψ and φ are functions of initial deflection. Equations (64) and (65) can be presented in finite differences and calculation conducted on digital computers, as in § 90.

Resolution of <u>dynamic</u> problem for elongated panel and a panel with finite ratio of sides may also be carried out on digital computers. For that we use method described in preceding chapter (§ 178). If we turn for example to equation (60), then it will be transformed to

$$\begin{aligned} &\frac{\partial^4(w-w_0)}{\partial x^4} + c\frac{\partial^2 w}{\partial x^2} + \\ &+ p\frac{\partial w}{\partial x}\left[1+\frac{3}{5}\eta\frac{\partial w}{\partial x}\left(1+\frac{1}{3}\eta\frac{\partial w}{\partial x}\right)\right] + \\ &+ \frac{\partial^2 w}{\partial t^2} + \varepsilon\frac{\partial w}{\partial t} = 0. \end{aligned} \tag{19.66}$$

Here in supplement to expressions (59) are introduced parameters

$$\left.\begin{aligned} \bar{t} &= t\frac{h}{a^2}\sqrt{\frac{Eg}{12(1-\mu^2)\gamma}}, \\ \bar{\varepsilon} &= \varepsilon\frac{a^2}{h}\sqrt{\frac{12(1-\mu^2)g}{E\gamma}}; \end{aligned}\right\} \tag{19.67}$$

---

*Here parameter η is the only magnitude corresponding to velocity of flow.

magnitude ε accounts for damping of vibrations.* Net region is constructed in general in space x, y, t. Step in time is selected from condition of stability of solution of differential equations. As a result of calculations we obtained the following results. Let us assume that panel with initial deflection is placed in flow with parameters η and p. Behavior of panel to significant extent depends on values of η and p and coefficient of damping. With relatively small η and p vibrations are quickly damped. When parameters η and p attain certain critical magnitude, peak values of deflections and stresses have a tendency to grow, or, at least, do not decrease, in spite of presence of damping; this corresponds to phenomenon of flutter. Especially interesting is the picture with compressive forces significantly exceeding critical magnitude. In the course of every period of vibrations deflection changes sign, so that panel should accomplish one knock after another. Similar process of vibrations with large amplitudes it is possible to characterize as violent flutter.** If we trace any nodal point of panel, then it will appear that it shifts in time along a path. Thus, here distinctly is observed phenomenon of so-called traveling waves. It is desirable subsequently to conduct fuller solution of dynamic problem for panels of different outlines and different conditions of fastening, and also to carry out additional experimental research.

Here we touched on only certain problems, pertaining to flutter of flat and slightly distorted plates, with determination of aerodynamic forces by piston theory. A survey of literature concerning this

---

*In equation (66) dashes above t and ε are omitted.

**It was observed in experiments, described by Fung [10.16], and also in experiments of V. L. Agamirov.

question, and also about limits of application of piston theory, is contained in works of Goodman and Rattaya [19.18] 1960, and V. V. Bolotin ([0.1] 1961, and [21.1] 1962). Boundary layer effect on critical speed of flutter is discussed in article of Miles [19.26] 1959; influence of magnetic field, in article of A. D. Lisunov (Journal of applied mechanics and technical physics No. 4, 1960).

Concept of panel flutter extends also to free vibrations of closed cylindrical shells, accompanied by formation of local dents. This problem was investigated by V. V. Bolotin [19.3], Miles [19.26], R. D. Stepanov [19.11], A. A. Movchan [19.9], Yu. Yu. Shveyko [19.12] and others.

Calculations and experiments show that in practice phenomenon of panel flutter is dangerous for relatively thin plates and shells (see experimental data of G. N. Mikishev [19.8] and E. I. Grigolyuk, R. Ye. Lamper and L. G. Shandarov, Transactions of Yerevan conf. on theory of shells, 1962); therefore, research, based on geometrically nonlinear theory, is of special interest. This pertains, especially, to case of closed cylindrical shells.

Literature

19.1. S. A. Ambartsumyan and Zh. Ye. Bagdasaryan. On stability of orthotropic plates past which there flows a supersonic flow of gas, News of Acad. of Sci. of USSR, OTN, Mech. and machine building, No. 4 (1961), 91; On stability nonlinearly-elastic sandwich plates, past which there flows a supersonic flow of gas, loc. cit., No. 5 (1961), 96.

19.2. Zh. Ye. Bagdasaryan. On stability of an orthotropic sandwich plate in a supersonic flow of gas, News of Academy of Sciences of Armenian SSR, series on phys-math. sciences, 14 No. 5 (1961).

19.3. V. V. Bolotin. Vibrations and stability of an elastic cylindrical shell in a flow of compressible fluid, Eng. coll., 24 (1956), 3-16; Concerning the question of stability of plates in a flow of compressible gas, "Problems of strength of materials and structures," Publishing House of Academy of Sciences of USSR; Certain new problems of theory of shells, "Strength analysis," 4 (1959); On application of Galerkin's method to problems of flutter of elastic panels, News of higher educational inst., series "Machine building," No. 12 (1959), 25-32; Nonlinear flutter of plates and shells, Eng. coll., 28 (1960), 55-75; Application of "law of plane sections" for determination of aerodynamic pressure on a fluctuating shell, News of Academy of Sciences of USSR, OTN, Mech. and machine building, No. 1 (1961).

19.4. V. V. Bolotin, Yu. V. Gavrilov, B. P. Makarov, and Yu. Yu. Shveyko. Nonlinear problems of stability of flat panels at high supersonic speeds, News of Acad. of Sci. of USSR, OTN, Mech. and machine building, No. 3 (1959), 59-64.

19.5. V. V. Bolotin and Yu. N. Novichkov. Buckling and steady flutter of thermally compressed panels in a supersonic flow, Eng. Journal, 1, No. 2 (1961), 82-96.

19.6. A. A. Il'yushin. Law of plane sections in aerodynamics of high supersonic speeds, Applied math. and mech., 20, No. 6 (1956), 733-755.

19.7. B. P. Makarov. On stability of clamped plates in flow of compressible gas, News of higher educational institutions, series "Machine building," No. 1 (1961); On amplitudes of steady flutter of clamped panels, loc. cit., No. 5 (1961).

19.8. G. N. Mikishev. Experimental research of free vibrations of a square plate in supersonic flow, News of Acad. of Sci. of USSR, OTN, Mech. and machine building, No. 1 (1959), 154-157.

19.9. A. A. Movchan. On vibrations of a plate moving in gas, Applied math. and mech., 20, No. 2 (1956), 211-222; Stability of a panel, moving in a gas, op. cit., 21, No. 2 (1957), 211-243; Stability of a blade moving in gas, op. cit., 21, No. 5 (1957), 700-706.

19.10. P. M. Ogibalov. To formulation of problem of flutter of shells and panels, Herald of Moscow State University, Math., Mech.,

No. 5 (1961), 60-66.

19.11. R. D. Stepanov. On flutter of cylindrical shells and panels moving in a flow of gas, Applied math. and mech., 21, No. 5 (1957), 644-657; News of higher educational institutions, Machine building and instrument-making, No. 8 (1960).

19.12. Yu. Yu. Shveyko. Stability of a circular cylindrical shell in a flow of gas, News of Acad. of Sci. of USSR, OTN, Mech. and machine building, No. 6 (1960), 71-79; On influence of supersonic flow of gas on lower critical force for a cylindrical panel, loc. cit., No. 4 (1961), 14-19.

19.13. Tung Ming-tieh. On stability of elastic plate in a supersonic flow, DAN SSSR, 120, No. 4 (1958), 726-729.

19.14. H. Ashley and G. Zartarian. Piston theory--a new aerodynamic tool for the aeroelastician, J. Aeron. Sci. 23, No. 12 (1956), 1109-1118.

19.15. J. P. Chawla. Aeroelastic instability at high Mach numbers, J. Aerospace Sci., 25, No. 4 (1958), 246-258.

19.16. Y. Fung. An introduction to the theory of aeroelasticity, NY, 1955, 260-261 (trans: Fizmatgiz, M., 1960); The static stability of a two-dimensional curved panel in a supersonic flow, with an application to panel flutter, J. Aeron. Sci. 21, No. 8 (1954); Flutter of curved plates with edge compression in a supersonic flow, Proc. of the 3th midwestern conf. on solid mech., Ann Arbor, 1957, 221-245; On two-dimensional panel flutter, J. Aeron. Sci. 25, No. 3 (1958) (trans: "Mechanics," IL, No. 1, 1959, 75-106).

19.17. M. Goland and Y. L. Luke. An exact solution for two-dimensional linear panel flutter at supersonic speeds, J. Aeron. Sci. No. 4 (1954), 275-276.

19.18. L. E. Goodman and J. V. Rattaya. Review of panel flutter, Applied Mech. Reviews 13, No. 1 (1960), 2-1 (trans: "Mechanics," IL, No. 5, 1960).

19.19. W. H. Hayes. Quart. Appl. Math. 5, N 1 (1947), 105-106.

19.20. D. J. Johns. Some panel-flutter studies using piston theory, J. Aeron. Sci. 25, No. 11 (1958), 679-684.

19.21. P. F. Jordan. The physical nature of panel flutter, Aero-Digest, No. 2 (1956), 34-38.

19.22. J. M. Hedgepeth. On the flutter of panels at high Mach numbers, J. Aeron. Sci. 23, No. 6 (1956), 609-610; Flutter of rectangular simply supported panels at high supersonic speeds, op. cit., 24, No. 8, 1957, 563-573 (trans: "Mechanics," IL, No. 2, 1958, 103-126).

19.23. J. M. Hedgepeth, B. Budiansky, and R. W. Leonard. Analysis of flutter in compressible flow of a panel on many supports,

J. Aeron. Sci. 21, No. 7 (1954), 475-486.

19.24. F. D. Hains. Flutter of a thin membrane in hypersonic flow, J. Aeron. Sci. 25, No. 9 (1958).

19.25. M. J. Lighthill. Oscillating airfoils at high Mach number, J. Aeron. Sci. 20, No. 6 (1953), 402-406.

19.26. J. W. Miles. On panel flutter in the presence of a boundary layer, J. Aerospace Sci. 26, No. 2 (1959), 81-93 (see coll. of translations "Mechanics," IL, No. 4, 1959, 97-122); On the aerodynamic stability of thin panels, J. Aeron. Sci. 23, No. 8 (1956); 24, No. 2 (1957); 25, No. 5 (1958).

19.27. J. W. Miles and W. P. Rodden. On the supersonic flutter of two-dimensional infinite panels, J. Aerospace Oci. 26, No. 3 (1959).

19.28. S. F. Shen. Remarks on "An exact solution for two-dimensional linear flutter," J. Aeron. Sci., No. 9 (1955), 656-657; An approximate analysis of nonlinear flutter problems, J. Aerospace Sci. 26, No. 1 (1959) (trans: "Mechanics," IL, No. 4, 1959, 79-96).

CHAPTER XX

APPLICATION OF STATISTICAL METHODS

§ 191. Fundamental Concepts

In preceding section of this book we considered, essentially, certain models of concrete constructions, reflecting in some approximation physical properties of material, geometric characteristics of members, conditions of loading. In certain cases we tried to bring the model selected by us close to real constructions, considering transition of elastic deformations of material to elasto-plastic, initial incorrectnesses of form of a member or character of change of load in process of buckling, studying stability in the large, etc. Nonetheless, here too we remained in the frames of definite schemes. We encountered individual constructions only when we gave final data of separate experiments, although certain characteristics of experiments remained for us unknown or were not noted.

All this is completely natural: characteristics of material of a given member of constructions, initial imperfections, reaction of other parts of constructions, applied loads are random variables. Having certain theoretical results or data of a series of experiments, we can judge the behavior of any construction new to us only with a certain probability. In certain cases we can consider our judgements

practically reliable, in others, not so. Therefore, it is very important to use statistical methods and to try to establish probability of realization of one or another conclusion obtained by us for concrete constructions.

Let us give certain propositions and formulas of probability theory, which we will need subsequently.* An event, the occurrence or nonoccurrence of which it is impossible to definitely predict, is called random. Such a random event we can consider the result of a single trial. Let us assume that after n trials, conducted under certain conditions, random event A appeared m times. Ratio

$$\nu = \frac{m}{n} \tag{20.1}$$

is called relative frequency of appearance of event A. It was determined that this frequency, with sufficiently large number of trials, is stabilized near a certain magnitude, which is called probability of event under the given conditions. We designate probability by Φ. Obviously, frequency of event and its probability must satisfy inequalities

$$0 \leqslant \nu \leqslant 1, \quad 0 \leqslant \Phi \leqslant 1. \tag{20.2}$$

Probability of a reliable event is equal to one; of an impossible one, to zero. Random events are called incompatible, if they cannot occur simultaneously; and independent, if probability of one of them does not depend on whether the second happens.

If events A_1, A_2, ..., A_n are incompatible, then probability of appearance of one of them is equal to the sum of probabilities of

*See Ye. S. Venttsel', Probability theory, 2nd edition, Fizmatgiz, M., 1962, V. S. Pugachev, Theory of random functions, 2nd edition, Fizmatgiz , M., 1960, and others. In this section the account is basically from book of B. R. Levin, Theory of random processes and its application in radio engineering, 2nd edition, "Soviet radio," M., 1960.

every event separately:

$$\Phi(A_1 \text{ or } A_2 \text{ or } \ldots \text{ or } A_n) = \Phi(A_1) + \Phi(A_2) + \ldots + \Phi(A_n). \qquad (20.3)$$

If events B_1, B_2, ..., B_n are compatible, but independent, then probability of their simultaneous occurrence is equal to product of probabilities of every event:

$$\Phi(B_1 \text{ and } B_2 \text{ and } \ldots \text{ and } B_n) = \Phi(B_1) \times \Phi(B_2) \times \ldots \times \Phi(B_n). \qquad (20.4)$$

Result of a single trial is also presented by a certain <u>random variable</u> ξ; thus, instead of qualitative characteristic of trial there is introduced its quantitative estimate. In certain cases possible values of random variable can be renumbered beforehand with help of a natural series of numbers: such a magnitude is discrete. In other cases the random variable can take <u>any value</u> in certain interval; then probability that the magnitude will take a given value, is equal to zero. It is possible, however, to determine the probability that such a random variable will be in a certain interval of possible values.

Let us assume that random variable ξ can take any real values from $-\infty$ to $+\infty$. Then it is important to establish probability that ξ <u>does not exceed</u> certain given level x, i.e., to establish probability of fulfillment of inequality $\xi < x$. This probability carries name of <u>integral distribution function</u> of random variable ξ and depends on value of x. We designate distribution function by F(x):

$$F(x) = \Phi(\xi < x). \qquad (20.5)$$

Probability that magnitude ξ will be in interval between values x_1 and x_2 is equal to

$$\Phi(x_1 < \xi < x_2) = F(x_2) - F(x_1); \qquad (20.6)$$

we always should have $F(x_2) \geq F(x_1)$ when $x_2 > x_1$.

We assume that random variable is changed continuously and that integral distribution function also is continuous and is differentiable. Then it is possible to introduce new important characteristic of random variable, called probability density or differential distribution function, equal to

$$f(x)=\frac{dF(x)}{dx}; \tag{20.7}$$

since function F(x) is nondecreasing with growth x, then we always have $f(x) \geq 0$.

From preceding relationships there ensues

$$\Phi(\xi < x)=F(x)=\int_{-\infty}^{x} f(x)\,dx. \tag{20.8}$$

$$\Phi(x_1 < \xi < x_2)=\int_{x_1}^{x_2} f(x)\,dx. \tag{20.9}$$

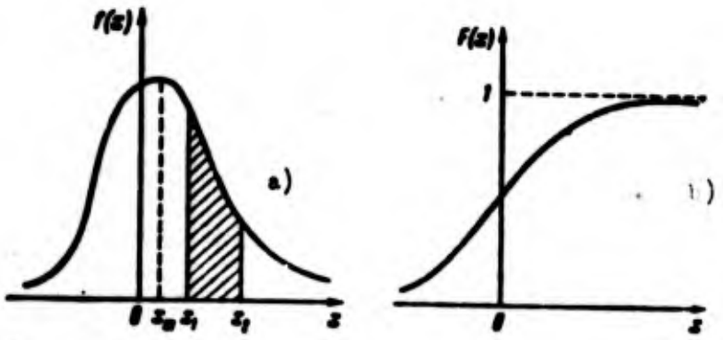

Fig. 20.1. Curves (a) of probability density and (b) integral distribution function.

In Fig. 20.1 is depicted form of differential and integral distribution functions f(x) and F(x). Probability that ξ lies between values x_1 and x_2 (by (9)) graphically corresponds to shaded area on Figure 20.1a located in these limits. Since probability that magnitude ξ will take any value from $-\infty$ to $+\infty$ is equal to one, then total area under density curve of probability is equal to

$$\int_{-\infty}^{\infty} f(x)\,dx=1. \tag{20.10}$$

Correspondingly integral curve in Fig. 20.1b is located between axis of abscissas and line F = 1. Value $\xi = x$ at which probability density is maximum, is called the mode.

In practice we frequently meet random variables having so-called normal distributive law:

$$f(x) = ce^{-\frac{(x-a)^2}{2s^2}}. \qquad (20.11)$$

Coefficient c is found from condition (10); it is equal to

$$c = \frac{1}{\sqrt{2\pi}s}. \qquad (20.12)$$

Mode of normal distributive law is equal to a; in Fig. 20.2 are plotted values of f(x) depending upon (x - a)/s. As it is easy to see, second derivative of $d^2f(x)/dx^2$ turns into zero at $x = a \pm s$; consequently, with these values of x curve f(x) has point of inflection. Maximum value of f(x) is equal to

$$f(a) = f_{max} = \frac{1}{\sqrt{2\pi}s} = c. \qquad (20.13)$$

In Fig. 20.2 is shown what percent of total area under distribution curve is occupied by area of band between lines $a \pm s$, $a \pm 2s$,

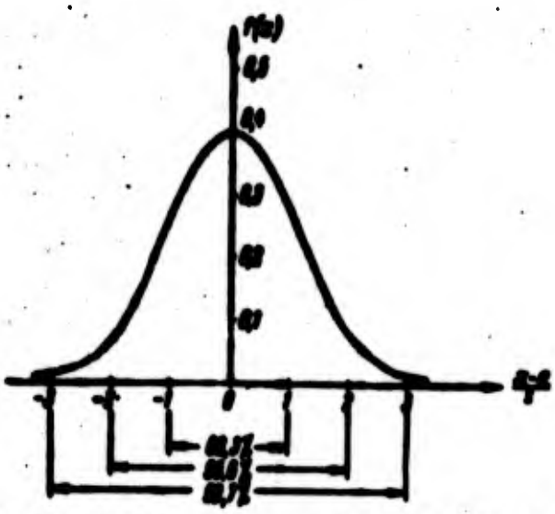

Fig. 20.2. Normal distributive law.

$a \pm 3s$. Judging by these data, it is possible in practice to consider

that any random variable, distributed by normal law, lies within a $\pm 3s$. Probability of such an event is equal to 0.997, and it therefore, can be assumed practically reliable. The larger parameter s, the more gentle be curves f(x) and the more significant the scattering of the random variable. In Fig. 20.3 are depicted curves of f(x) and F(x) for different parameters s.

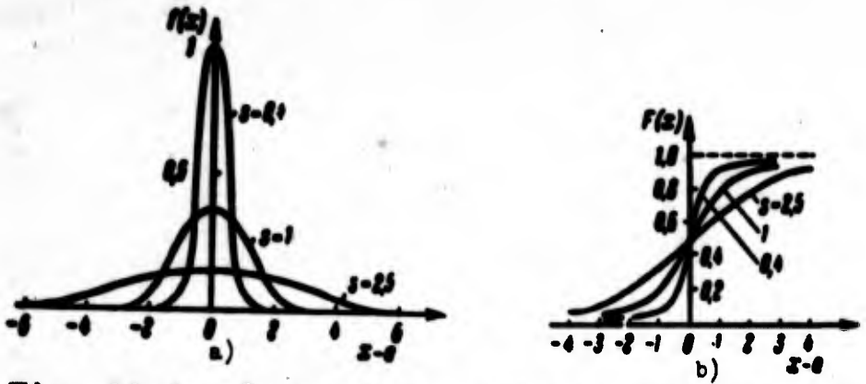

Fig. 20.3. Probability density (a) and integral function (b) for normal law for different parameters s.

One of the characteristics of distribution of a random variable is the so-called mathematical expectation or mean value, equal to

$$m(\xi) = \int_{-\infty}^{\infty} x f(x)\,dx. \qquad (20.14)$$

Magnitude $m(\xi)$ is numerically equal to static moment of area, lying between line f(x) and axis of abscissas, around the axis of ordinates. But since actual area is equal to one, then expression (14) simultaneously determines abscissa of center of gravity of the area. Deviation of random variable from mathematical expectation is equal to $[\xi - m(\xi)]$.

Expression

$$D(\xi) = \int_{-\infty}^{\infty} (x - m(\xi))^2 f(x)\,dx \qquad (20.15)$$

is mathematical expectation or mean value of the square of the deviation and bea s the name of dispersion of magnitude ξ.

Calculating square root of dispersion, i.e., $\sqrt{D(\xi)}$, we find root mean square deviation or so-called standard of the distributive law.

For normal distributive law after simple calculations we find

$$m = a, \quad D = s^2. \tag{20.16}$$

Consequently, by a it is necessary to understand mathematical expectation (and at the same time the mode), and by s, the root mean square deviation or the standard of the normal distributive law. For distribution, symmetric with respect to axis of ordinates, mathematical expectation is equal to zero.

Subsequently we shall need to determine probability density $\varphi(y)$ of random variable η, if we know dependence of $\eta = U(\xi)$ on another random variable ξ and probability density $f(x)$ of this second magnitude is given (Fig. 20.4). Let us assume that there is a one-to-one

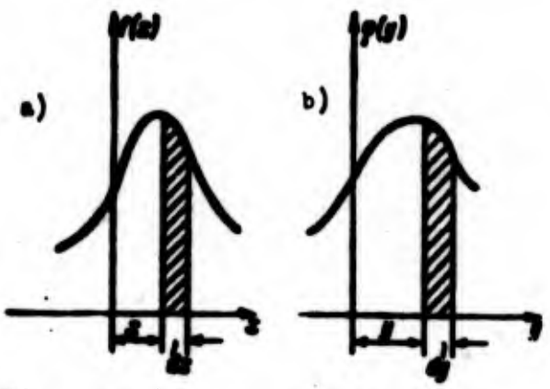

Fig. 20.4. Probability densities of f and φ for magnitudes ξ and $\eta = \eta(\xi)$.

correspondence between ξ and η. If ξ lies within $x < \xi < x + dx$, then from this follows inequality $y < \eta < y + dy$ when $y = U(x)$. Probabilities of fulfillment of these inequalities are equal to one another. But since these probabilities correspond to shaded areas of $f(x)dx$ and $\varphi(y)dy$ in Fig. 20.4a and b, then it is possible to

record equality

$$f(x)dx = \varphi(y)dy. \qquad (20.17)$$

From this we find the simplest formula for transformation of probabilities:

$$\varphi(y) = \frac{f(x)}{\left|\frac{dy}{dx}\right|}. \qquad (20.18)$$

We recall that here the presence of simple inverse function $x = V(y)$ is assumed. Since we always know $\varphi(y) \geq 0$ and $f(x) \geq 0$, then in (18) we should set substitute absolute value of dy/dx.

Let us assume that magnitude ξ is distributed by normal law (11)

$$f(x) = \frac{1}{\sqrt{2\pi s^2}} e^{-\frac{(x-a)^2}{2s^2}}. \qquad (20.19)$$

If second random variable η linearly depends on the first,

$$\eta = k\xi, \quad y = kx, \qquad (20.20)$$

that from (18) we obtain

$$\varphi(y) = \frac{1}{\sqrt{2\pi (sk)^2}} e^{-\frac{(y-ka)^2}{2(ks)^2}}. \qquad (20.21)$$

Thus, mathematical expectation, the standard and dispersion for new magnitude η are equal to

$$a_1 = ka, \quad s_1 = ks, \quad D_1 = k^2 D. \qquad (20.22)$$

Transformation is reduced to change of scales along coordinate axes by k times.

Let us turn to consideration of two-dimensional problem, when probability of simultaneous fulfillment of inequalities $\xi < x$, $\eta < y$ for two dependent, generally, random variables ξ and η is determined. We designate integral function $F(x, y)$:

$$\Phi(\xi < x, \eta < y) = F(x, y). \qquad (20.23)$$

On graph of Fig. 20.5 is given geometric interpretation of inequalities in (23): coordinates (ξ, η) of a point on a plane must

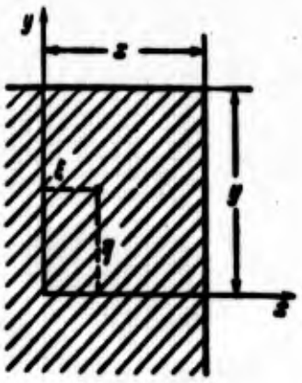

Fig. 20.5. Determining two-dimensional distribution function.

not exceed levels x and y, i.e., must be within limits of shaded area.

Two-dimensional probability density of f(x, y) is defined as mixed second derivative of F(x, y):

$$f(x, y)=\frac{\partial^2 F(x, y)}{\partial x\,\partial y}. \qquad (20.24)$$

Two-dimensional probability density can be geometrically depicted in the form of a surface, located above plane x, y.

Probability of F(x, y) by (23) is equal to

$$F(x, y)=\int_{-\infty}^{x}\int_{-\infty}^{y} f(x, y)\,dx\,dy. \qquad (20.25)$$

Considering upper limits $x \to \infty$ and $y \to \infty$, we arrive at formula

$$\int_{-\infty}^{\infty}\int_{-\infty}^{\infty} f(x, y)\,dx\,dy=1. \qquad (20.26)$$

Consequently, volume under surface of distribution is equal to one. Let us assume, further, that in (25) the second of limits $y \to \infty$; then two-dimensional density changes into one-dimensional, pertaining to magnitude ξ:

$$F(x, +\infty)=\int_{-\infty}^{x}\int_{-\infty}^{\infty} f(x, y)\,dx\,dy=F_1(x). \qquad (20.27)$$

Derivative of this magnitude is equal to probability density of $f_1(x)$:

$$f_1(x)=\int_{-\infty}^{\infty} f(x, y)\,dy. \qquad (20.28)$$

If random variables ξ and η are independent, then by rule of multiplication of probabilities we obtain

$$F(x, y)=P(\xi<x, \eta<y)=F_1(x)F_2(y). \qquad (20.29)$$

where $F_1(x)$, $F_2(y)$ are integral distribution functions for each of magnitudes ξ and η. The same relationship takes place for probability densities:

$$f(x, y) = f_1(x) f_2(y). \tag{20.30}$$

Let us assume that we know mathematical expectations a and b of two random variables ξ and η:

$$a = \int_{-\infty}^{\infty} x f_1(x)\,dx, \quad b = \int_{-\infty}^{\infty} y f_2(y)\,dy. \tag{20.31}$$

We find mathematical expectation for the sum of these magnitudes $\zeta = \xi + \eta$:

$$c = \int_{-\infty}^{\infty}\int_{-\infty}^{\infty} (x+y) f(x, y)\,dx\,dy. \tag{20.32}$$

Comparing (28) and (31), we have

$$a = \int_{-\infty}^{\infty}\int_{-\infty}^{\infty} x f(x, y)\,dx\,dy, \quad b = \int_{-\infty}^{\infty}\int_{-\infty}^{\infty} y f(x, y)\,dx\,dy. \tag{20.33}$$

Consequently, magnitude c is equal to the sum of mathematical expectations:

$$c = a + b. \tag{20.34}$$

Let us assume that, further, we are given dispersions D_1 and D_2 of independent random variables ξ and η:

$$D_1 = \int_{-\infty}^{\infty} (x-a)^2 f_1(x)\,dx, \quad D_2 = \int_{-\infty}^{\infty} (y-b)^2 f_2(y)\,dy. \tag{20.35}$$

We define dispersion of sum $\zeta = \xi + \eta$ as mathematical expectation of magnitude $(\zeta - c)^2$ or $(\xi + \eta - a - b)^2$. From (34) we have

$$D(\zeta) = m[(\xi-a)+(\eta-b)]^2. \tag{20.36}$$

or

$$D(\zeta) = m(\xi-a)^2 + m(\eta-b)^2 + 2m(\xi-a)(\eta-b). \tag{20.37}$$

For independent magnitudes the last component turns into zero, since for each of factors $(\xi - a)$ and $(\eta - b)$ the corresponding integral is equal to zero; e.g.,

$$\int_{-\infty}^{\infty}\int_{-\infty}^{\infty}(x-a)f(x,\ y)\,dx\,dy=\int_{-\infty}^{\infty}(x-a)f_1(x)\,dx=0. \qquad (20.38)$$

Finally we find that magnitude D is equal to sum of dispersions:

$$D(\xi)=D(\xi)+D(\eta). \qquad (20.39)$$

Let us assume that magnitudes ξ and η are independent and that each of them is distributed by normal law:

$$f_1(x)=\frac{1}{\sqrt{2\pi}\sigma_1}e^{-\frac{(x-a)^2}{2\sigma_1^2}},\quad f_2(y)=\frac{1}{\sqrt{2\pi}\sigma_2}e^{-\frac{(y-b)^2}{2\sigma_2^2}}; \qquad (20.40)$$

then two-dimensional probability density by (30) is equal to

$$f(x,\ y)=\frac{1}{2\pi\sigma_1\sigma_2}e^{-\frac{1}{2}\left[\frac{(x-a)^2}{\sigma_1^2}+\frac{(y-b)^2}{\sigma_2^2}\right]}; \qquad (20.41)$$

surface corresponding to f(x, y) with sections, parallel to coordinate planes, is shown in Fig. 20.6.

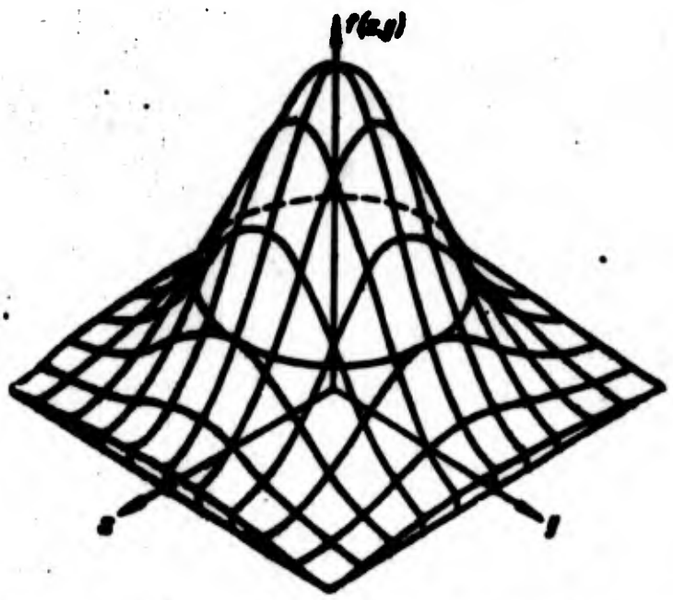

Fig. 20.6. Section of surface, corresponding to two-dimensional normal distributive law.

Probability density for sum of magnitudes x + y = z by (39) and (34) will be equal to*

*For direct derivation of formula (42) and (41) see book of S. N. Bernstein "Probability theory," M., 1946, p. 270.

$$f(z)=\frac{1}{2\pi s^2}e^{-\frac{1}{2}\frac{(z-cp)^2}{s^2}}. \tag{20.42}$$

where

$$c=a+b,\quad s^2=s_1^2+s_2^2. \tag{20.43}$$

Let us assume that it is required, by two-dimensional distribution function $f(x_1, x_2)$ of random variables ξ_1 and ξ_2, to determine two-dimensional distribution function of $\varphi(y_1, y_2)$ of random variables η_1 and η_2 which are functions of first variables: $\eta_1 = U_1(\xi_1, \xi_2)$, $\eta_2 = U_2(\xi_1, \xi_2)$; if functions of ξ and η are identical, we have

$$\varphi(y_1, y_2)=f(x_1, x_2)|V|; \tag{20.44}$$

by V is understood determinant, composed from the derivatives:

$$V=\begin{vmatrix}\frac{\partial x_1}{\partial y_1} & \frac{\partial x_1}{\partial y_2}\\ \frac{\partial x_2}{\partial y_1} & \frac{\partial x_2}{\partial y_2}\end{vmatrix}=\frac{\partial(x_1, x_2)}{\partial(y_1, y_2)}. \tag{20.45}$$

If we transform n random variables, then we have

$$\varphi(y_1, y_2, \ldots, y_n)=f(x_1, x_2, \ldots, x_n)|V|; \tag{20.46}$$

determinant V is composed by analogy to (45):

$$V=\frac{\partial(x_1, x_2, \ldots, x_n)}{\partial(y_1, y_2, \ldots, y_n)}. \tag{20.47}$$

Let us turn to application of statistical methods for determination of supporting power of real bars, plates and shells.

§ 192. Supporting Power of Compressed Rods

As we have seen, supporting power of compressed bars greatly depends on initial incorrectnesses in form of bar, eccentricity in application of load, conditions of fastening, etc. These factors are random, and for them there can be fixed certain distributive laws. For function of these magnitudes—supporting power—it is possible also to find a certain distributive law and, thus, establish

probability of exhausting the supporting power in different conditions.

In work of A. R. Rzhanitsyn [20.5] there was offered the following approach to this problem. Let us assume that axis of hinge-supported bar has initial deflection, varying according to the law $w_0 = f_0 \sin(\pi x/l)$. Composing differential equation of bending line

$$EI\left(\frac{d^2w}{dx^2} - \frac{d^2w_0}{dx^2}\right) = -Pw,$$

where w and w_0 are total and initial deflections (Fig. 20.7), and considering $w = f \sin(\pi x/l)$, we arrive at known formula (1.182):

$$f = \frac{f_0}{1 - \frac{P}{\pi^2 EI}}. \qquad (20.48)$$

Fig. 20.7. Bar with initial deflection, subjected to eccentric compression.

We determine stress σ_1 in edge fiber for an average section;

$$\sigma_1 = \frac{P}{F} + \frac{Pf}{W}, \qquad (20.49)$$

where F and W are the area of section and moment of resistance of section. Introducing designations for average stress $\sigma_0 = P/F$ and for radius of the kernel of the section $\rho = W/F$, we find

$$\sigma_1 = \sigma_0\left(1 + \frac{m}{1 - \frac{\sigma_0 F}{\pi^2 EI}}\right), \qquad (20.50)$$

where $m = f_0/\rho$. If force is applied with eccentricity e_0, increasing initial curvature, it is possible to set $m = (f_0 + e_0)/\rho$.

Analysis of experimental data shows that magnitude m is higher,

the greater the slenderness ratio of the bar. We use formula*

$$m = \alpha + \beta\left(\frac{l}{\rho}\right)^2. \tag{20.51}$$

and assume that values of l and ρ, and also the load are given and quantities α and β are random and that they are distributed by normal law with center (mode) at the origin of coordinates. Then magnitude σ_1 will also be random. We shall consider that material obeys the Hooke's law up to the yield surface. Then supporting power of the bar can be determined by the stress σ_0, at which in extreme fibers the yield point is attained.**

We determine difference between "absolute" supporting power of bar, corresponding to yield point σ_T, and the actual supporting power:

$$R = \sigma_T - \sigma_0 - \sigma_0 \frac{\left(\alpha + \beta \frac{F}{\rho^2}\right)\pi^2 E}{\pi^2 E - \sigma_0 l^2}. \tag{20.52}$$

Magnitude R characterizes, as it were, the unused part of the absolute supporting power of the bar.

We set ourselves the goal of determining distributive law of R. It will be normal when R is expressed by α and β linearly. Therefore, we will take R approximately in the form

$$R = \sigma_T - \sigma_0 + A\alpha + B\beta \tag{20.53}$$

and determine A and B as partial derivatives of R with respect to α and β:

$$A = -\frac{\pi^2 E \sigma_0}{\pi^2 E - \sigma_0 l^2}, \quad B = \left(\frac{l}{\rho}\right)^2 A. \tag{20.54}$$

---

*Such dependence was offered by A. R. Rzhanitsyn [20.5]; a formula close to this is recommended also by Donnell and Wan [11.30a].

**In more precise solution of problem one should also consider that load P and yield point of material σ_T are random variables, and, furthermore, consider possible changes in method of fastening of ends of the bar [20.5].

Center of distribution of R will be

$$e_R = e_\tau - e_\varphi \tag{20.55}$$

and standard from (22) and (43) is equal to

$$s_R = \frac{n^2 E \varepsilon_0}{n^2 E - \sigma_0 \lambda^2} \sqrt{s_\sigma^2 + \left(\frac{1}{\rho}\right)^4 s_\varphi^2}. \tag{20.56}$$

where s_α and s_β are standards of distributions of magnitudes α and β.

We introduce designations

$$\psi = \frac{e_\varphi}{e_\tau}, \quad \gamma = \frac{e_R}{s_R} = \frac{e_\tau - e_\varphi}{s_R}, \quad \lambda_\tau^2 = \frac{n^2 E}{\sigma_\tau}, \quad \xi = \frac{i}{\rho}. \tag{20.57}$$

By ψ is understood coefficient of lowering of supporting power of a bar as compared to yield point, or, in other words, coefficient of lowering of tolerable stress. Magnitude γ determines scattering of deviations of limiting stresses from yield point with respect to mean deviation; the higher the γ, the less this scattering. A. R. Rzhanitsyn recommends to taking tentative values of γ for bars of asymmetric section equal to 3, and for bars of symmetric section equal to 3.2. This means that point of inflection of distribution curve will lie, in the case of asymmetric section, distances from point R = 0 equal to $2/3(\sigma_T - \sigma_0)$ and $4/3(\sigma_T - \sigma_0)$. With a symmetric section probability of reaching the yield point in extreme fibers is larger; this is explained by increase of γ. By λ_T is understood slenderness ratio of an ideal bar, corresponding to critical stress, equal to yield point σ_T. Finally, parameter ξ is equal to ratio of radius of gyration to radius of the kernel of the section; for a rectangular section we have $\xi = \sqrt{3}$, for I-beam section during bending in plane of web $\xi \approx 1$. Using (57), we reduce expression (56) to form

$$\frac{1-\psi}{\gamma} = \frac{\lambda_\tau^2 \psi}{\lambda_\tau^2 - \lambda^2 \psi} \sqrt{D_\sigma + (\lambda\xi)^4 D_\varphi} \tag{20.58}$$

where $D_\alpha = s_\alpha^2$, $D_\beta = s_\beta^2$ are dispersions of distributions of α and β.

Given values of D_α, D_β, λ_T and γ, we determine from (58) dependence between coefficient ψ and slenderness ratio of the bar λ when $\gamma = 3$, $\xi = \sqrt{3}$. $\lambda_T \approx 90$. In Figs. 20.8 and 20.9 are given curves* of $\psi(\lambda)$ for steel St 3 for different values of D_α; we take $D_\beta = 0$ and $D_\beta = 25 \cdot 10^{-12}$. When $D_\alpha = D_\beta = 0$ by equation (58) we obtain $\psi = 1$. However, by graph of Fig. 20.8 for $D_\alpha = D_\beta = 0$ we find $\psi = 0.7$. This is explained by the fact that during construction of curves of Figs. 20.8 and 20.9 we also considered possible scattering of values of yield point of steel by normal law. We assumed that ratio of dispersion of distribution of σ_T to the mean value was equal to 0.1. If we take $D_\alpha = D_\beta = 0$, then we find $(1 - \psi)/\gamma = 0.1$; when $\gamma = 3$ we have $\psi = 0.7$.

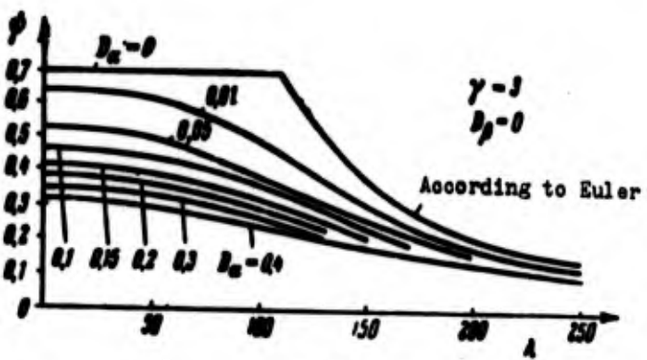

Fig. 20.8. Coefficient of lowering of supporting power ψ for bars of different slenderness ratio λ with dispersion $D_\beta = 0$.

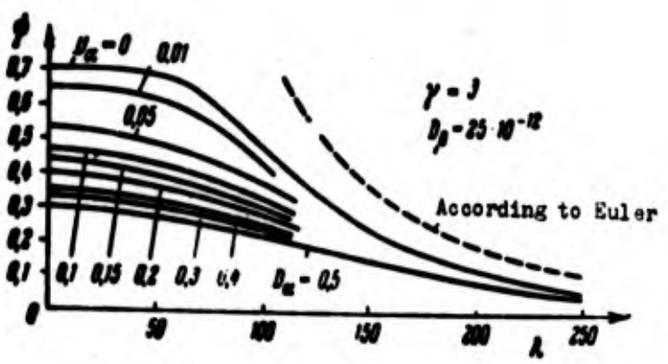

Fig. 20.9. Coefficient ψ with dispersion $D_\beta = 25 \cdot 10^{-12}$.

Taking a definite value of γ, we thereby fix distributive law for magnitude R. Now we can determine probability Φ of exhausting of supporting power of a bar from condition that magnitude R turns into zero. In Fig. 20.10 is shown approximate distribution curve of magnitude

$$x = m\frac{\pi^2 E\varepsilon_0}{\pi^2 E - \sigma_0\lambda^2} = R - (\sigma_T - \sigma_0). \qquad (20.59)$$

*These graphs are taken from work [20.5].

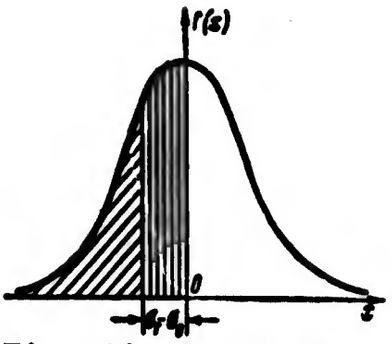

Fig. 20.10. Determining of probability of exhausting of supporting power of a bar.

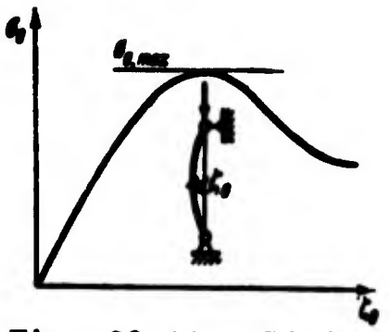

Fig. 20.11. Limit point for eccentrically compressed bar in elasto-plastic stage.

If this magnitude becomes equal to $[-(\sigma_T - \sigma_0)]$; then supporting power of bar must be considered exhausted. Corresponding probability is equal to area, shaded by slanting lines in Fig. 20.10, or, in other words, difference between half-area under the total distribution curve, equal to 1/2, and area, shaded by vertical lines. We find

$$\Phi = \frac{1}{2} - \frac{1}{\sqrt{2\pi s_R^2}} \int_{-(\sigma_T - \sigma_0)}^{0} e^{-\frac{x^2}{2}} dx. \qquad (20.60)$$

or

$$\Phi = \frac{1}{2} - \frac{1}{\sqrt{2\pi}} \int_{0}^{\gamma} e^{-\frac{y^2}{2}} dy = \frac{1}{2} - \Phi(\gamma). \qquad (20.61)$$

where $y = x/s_R$. Determining integral $\Phi(\gamma)$ by tables, we find that to value $\gamma = 3$ there corresponds probability $\Phi = 0.135\%$ and to $\gamma = 3.2$, probability of 0.067%. As we see, value $\gamma = 3.2$ was obtained taking into account the fact that with symmetric section probability of appearance of yield should be twice as large as from preceding derivations.

We originated in the given derivation from the fact that supporting power of a bar is exhausted by the greatest stress reaching the yield point. It would be more valid to originate from data of Chapter II, pertaining to eccentricity of compression of bars in the

elasto-plastic stage. As we have seen, to each value of eccentricity (and consequently, each magnitude of initial deflection ζ_0) on diagram $\sigma_0(\zeta_0)$ there corresponds a certain limit point, determining true supporting power (Fig. 20.11). Let us assume that for given material dependence of maximum average stress $\sigma_{0,max}$ from disturbing factors—eccentricity and initial incorrectnesses of form of the bar—is determined. Then, using some distributive law for perturbing factors, it is possible to establish distributive law of the magnitude of true supporting power and to compare it, e.g., with supporting power, corresponding to the yield point σ_T. Pravda, distributive law of supporting power no longer will be normal, since dependence of $\sigma_{0,max}$ on eccentricity and initial deflection cannot be assumed linear. Problem becomes here more complicated and may be solved by the means shown below in application to a shell. It is desirable that namely such an approach to problem be taken in further investigations.

§ 193. Influence of Initial Incorrectnesses on Behavior of Shells. Cylindrical Panel

Application of statistical methods is especially important in examining stability of elastic systems in the large. As we have seen from examples of shells subjected to various kinds to loads, influence of perturbing factors on their behavior and supporting power is very great. Shells, and also certain other systems, inclined to snap, are sensitive to the slightest flaws in form of the middle surface, eccentricities in application of load, errors in manufacturing technique, etc. This explains great divergence in critical loads for real constructions and in experiments. Valid analysis of such experimental data and an attempt to predict behavior of members of

real constructions, obviously, are impossible without the probability approach.

We subsequently shall conditionally consider, that buckling in the large is a dangerous event for a shell.* Obviously, probability of this event with a load below lower critical magnitude is equal to zero, but with a load attaining upper critical magnitude, it is equal to one. Let us assume that upper and lower loads are determined for shell of ideal form and for shells, having different initial imperfections, and at the same time with various boundary conditions. Then statistical approach can consist of determining from given probability characteristics of initial incorrectnesses and conditions of fastening of shells the probability characteristics of critical load. Problem leads, thus, to transformation of probabilities. It is very important here to agree on how a shell behaves during change of load. One of the approaches to solution of the problem consists of the following. We shall consider here that load changes comparatively slowly and that deformation of shell continuously follows the load. Obviously, such a system is noninertial, and behavior of shell completely is determined by nonlinear diagram of equilibrium states p(f) of the type depicted in Fig. 20.12a. Such an approach to the problem can be characterized as static.** It is necessary, further,

---

*This corresponds to above-mentioned theoretical and experimental data. More general formulation of problem consists considering possibility of occurrence of other dangerous states, for instance transition from elastic region to plastic, etc.

**Or, better, as quasi-static; with its help we can also solve certain dynamic problems. This approach belongs to V. V. Bolotin [20.1].

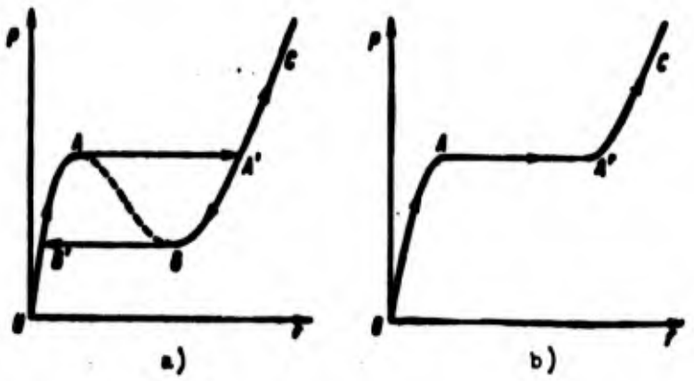

Fig. 20.12. Diagrams of equilibrium states of a shell.

to establish which of the branches of the diagram of Fig. 20.12a is used during solution of the problem so that dependence p(f) is unambiguous. We assume that during growth of load from $p < p_H$ equilibrium states of shell correspond to branch OA; when load reaches value p_B there occurs a knock.* If, however, load drops from value $p > p_B$ then it is necessary to use branch CB; when $p = p_H$ there is a reverse knock. Unstable states, corresponding to branches AB, in general, are not realized. Thus, strictly speaking, state of shell depends on the history of loading. Subsequently for simplicity we shall consider that load always is increasing and that, consequently, states of the shell are unambiguously determined by the diagram in Fig. 20.12b.

We apply such approach to solution of the problem primarily to the case of a square cylindrical panel, by hinge supported its edges and compressed along generatrix by forces p (see Fig. 11.61). We assume that all important perturbing factors are reduced to equivalent initial anomalies in form of the middle surface. We shall consider the panel a system with one degree of freedom; here formulas of

---

*Translation Editor's Note: H = lower critical, B = upper critical.

transformation of probabilities are significantly simplified. If we approximate total and initial deflections by expressions (17.25) and introduce dimensionless parameters from (17.31), then dependence between compressive force $p^* = pb^2/Eh^2$ and deflection ζ will take form (17.55). For square plate ($\lambda = 1$) we obtain

$$p^* = \left[p^*_{в,\,ид} + \frac{\pi^2}{8}(\zeta + \zeta_0)\zeta - \frac{2k}{3\pi^2}(3\zeta + \zeta_0)\right]\frac{\zeta - \zeta_0}{\zeta}, \qquad (20.62)$$

where $k = b^2/Rh$; by $p^*_{в,\,ид}$ is understood upper critical force for shell of ideal form; by ζ_0, the initial deflection. We take $k = 12$. Curves $p^*(\zeta)$, constructed by (62) for different values of ζ_0 with such magnitude k, are given in book [0.3], p. 288; they have the same character as curves of Fig. 17.13. We determine with help of this graph values of upper critical forces $p^*_{в,\,нач}$ for shells with different initial deflections ζ_0. In Fig. 20.13 is depicted curve of $\zeta_0(p^*)$; magnitudes $p^*_{в,\,нач}$ lie between load $p^*_{в,\,нач} = 3.3$, corresponding to $\zeta_0 = 0.25$, and upper critical load $p^*_{в,\,ид} = 7.2$ for ideal shell. When $\zeta_0 > 0.25$ snapping of shell does not occur. In Fig. 20.13 are given also absolute values of derivative $d\zeta_0/dp^*$.

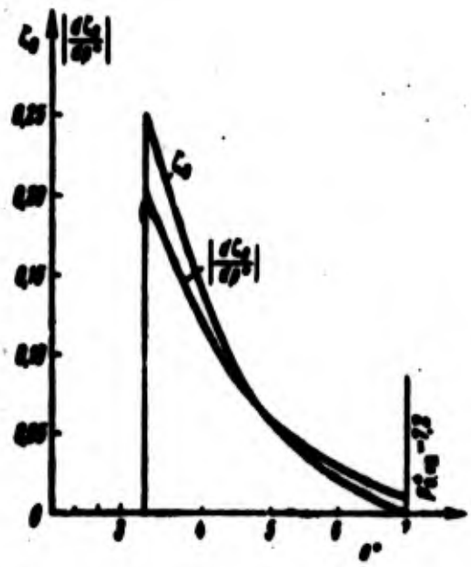

Fig. 20.13. Data for transformation of distribution function in case of compressed cylindrical panel.

Thus, we established dependence between upper critical forces and initial deflection for that region, where snapping of the shell occurs. Problem is now posed thus; by given probability curves

for ζ_0, establish probability curves for $p_в^*$. The most difficult part of the solution of the problem consists in determination of probability parameters for initial deflection. At present there is still little data for selection of these parameters. We assume as a first approximation that magnitude ζ_0 is distributed by normal law with its center at the origin of coordinates:

$$f(\zeta_0) = \frac{1}{\sqrt{2\pi\sigma_{\zeta_0}^2}} e^{-\frac{\zeta_0^2}{2\sigma_{\zeta_0}^2}}. \tag{20.63}$$

We use, then, formula (18) for transformation of probabilities. But one should keep in mind that, by our assumption, ζ_0 takes any value from $-\infty$ to $+\infty$, while phenomenon of a knock occurs only at $0 \leq \leq \zeta_0 \leq \bar{\zeta}_0$, where $\bar{\zeta}_0 = 0.25$. Therefore, during transformation of probabilities one should introduce normalizing factor (see [20.1]). We shall determine the probability that ζ_0 lies in the shown limits:

$$\bar{F} = \int_0^{\bar{\zeta}_0} f(\zeta_0)\, d\zeta_0. \tag{20.64}$$

By this magnitude, smaller than one, it is necessary to divide density (63); then from curve 1 of Fig. 20.14 we turn to curve 2, where area

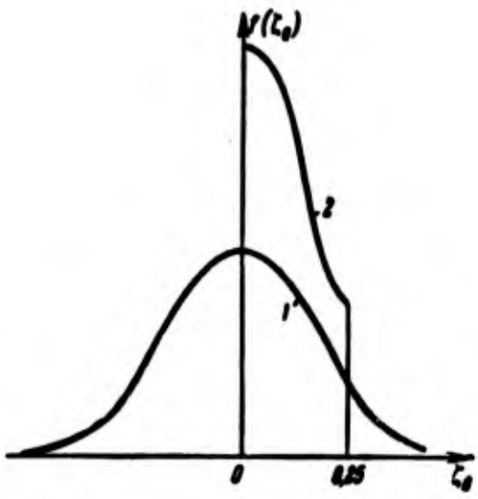

Fig. 20.14. "Normalization" of distribution curve of initial deflections.

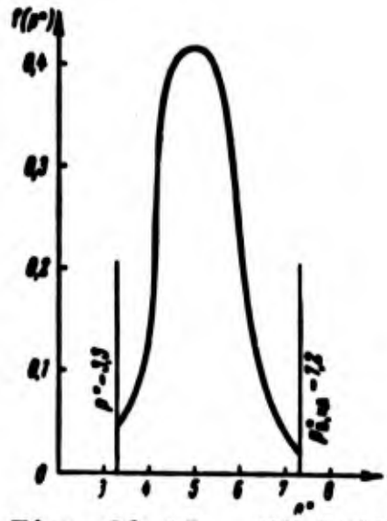

Fig. 20.15. Distribution function of critical load for compressed panel.

under this curve will remain equal to one. Finally probability density of f(p*) turns out to be equal to

$$f(p^*) = \frac{1}{F} f(\zeta_0) \left| \frac{d\zeta_0}{dp^*} \right|. \qquad (20.65)$$

In Fig. 20.15 is depicted curve f(p*), obtained in work [20.1] for case $s_{\zeta_0} = 0.1$. As a result of transformation the density is especially increased for those values of p* where absolute values of derivative $d\zeta_0/dp^*$ are great, i.e., for the zone closest to the lower critical load. Mathematical expectation m(p*) and dispersion D(p*) of new distributive law are determined by formulas (14) and (15) taking into account factor $1/F$:

$$m(p^*) = \frac{1}{F} \int_0^{\zeta_0} p^*(\zeta_0) f(\zeta_0) d\zeta_0 \qquad (20.66)$$

$$D(p^*) = \frac{1}{F} \int_0^{\zeta_0} [p^*(\zeta_0) - m(p^*)]^2 f(\zeta_0) d\zeta_0 \qquad (20.67)$$

According to work of V. V. Bolotin [20.1, 1958], in case $s(\zeta_0) = 0.1$ mathematical expectation is equal to 4.84, or 67% of $p^*_{р,\text{ид}}$; and 146% of $p^*_{н,\text{ид}}$; when $s(\zeta_0) = 0.25$ it is equal to 4.5, or accordingly 62% and 136%. As we see, magnitude m(p*) with given distributive law depends little on dispersion of initial deflections.

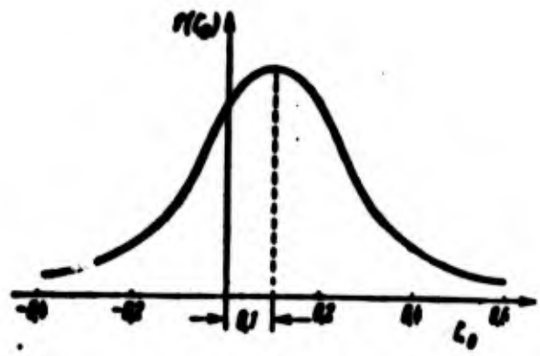

Fig. 20.16. Probability density of initial deflections, chiefly directed toward center of curvature.

It is necessary, however, to consider that initial anomalies in form of shell appear as a result of industrial working, various kinds of blows during transportation and assembling of constructions; one should consider that reaction of shell to these perturbations has the same character as during action of working load; more likely will there appear initial dents, directed toward the center of curvature. Therefore, center of distribution of initial deflections is selected appropriately at a point located a certain distance from the origin of coordinates--in the direction of positive deflections turned toward the center of curvature. In Fig. 20.16 is depicted such a distributive law of probability density with center, equal to $\bar{\zeta}_0$ = = 0.1, and standard s_{ζ_0} = 0.1. In Fig. 20.17a is shown corresponding

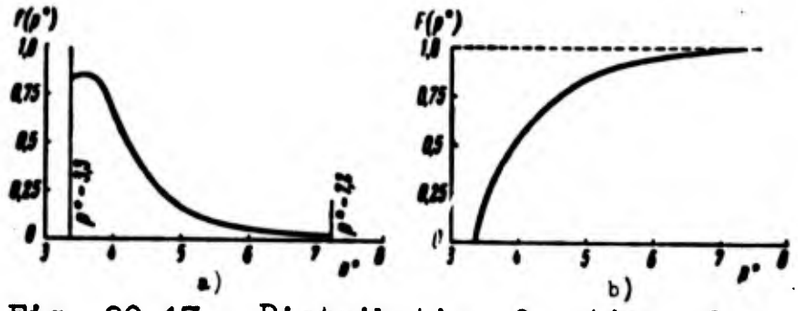

Fig. 20.17. Distribution functions for panel with initial deflections by Fig. 20.16.

probability distribution of f(p*), calculated by (65). Mathematical expectation turned out to be equal to 4.14 or 57% of $p^*_{в,ид}$ and 107% of $p^*_{н,ид}$. In Fig. 20.17b is depicted corresponding integral distributive law. Let us note that mathematical expectation of p* for shells with initial anomalies here almost coincides with lower critical load $p^*_н$ for a smooth shell. This conclusion has essential practical value, since it shows that in calculations for real panels it is necessary to start first from magnitude $p^*_н$.

Analogously we take into account probability curves of conditions

of fastening of shell at its edges.

§ 194. Influence of Initial Anomalies on Behavior of Closed Cylindrical Shells

We turn to case of closed cylindrical shell,* supported by hinge on its edges, subjected to external evenly distributed pressure (Fig. 11.17). In Fig. 11.30 is depicted dependence of parameter of load $\hat{q} = qR^2/Eh^2$ on deflection for during different values of dimensionless initial deflection ζ_0. Leaving for ζ_0 the distributive law of probability density of Fig. 20.16 when $s_{\zeta_0} = 0.1$ and using formula (65), we find distribution of probability density of critical load, shown in Fig. 20.18. Mathematical expection by (66) turns out

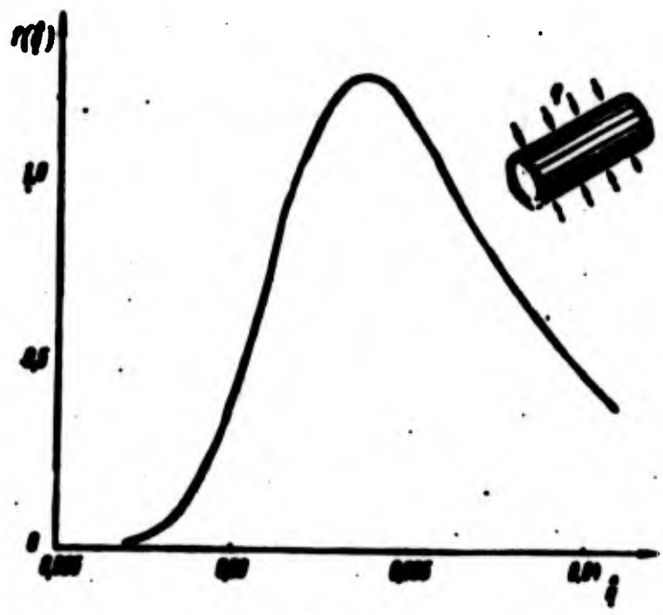

Fig. 20.18. Distribution function for critical load in case of a closed shell subjected to external pressure.

to be equal to 0.035 and constitutes 85% of $\hat{q}_{в, нд}$. As we saw, such a result comparatively well reflects experimental data (see § 132).

*A number of problems, pertaining to closed shell, are considered more specifically in the first of works of B. P. Makarov [20.4].

Let us consider analogous problem for closed shell under action of axial compression. Parameter of external load we select as before in the form $\hat{p} = pR/Eh$. Dependence $\zeta_0(\hat{p})$, found according to work [11.30a] for R/h = 1000, is depicted in Fig. 20.19. Preserving former distributive law of Fig. 20.16, we arrive at distribution of probability density of load (Fig. 20.20a) and integral distribution function (Fig. 20.20b). Mathematical expectation of $\hat{p}$ is equal to 0.369, or 61% of upper critical tension $\hat{p}_{в, ид}$.

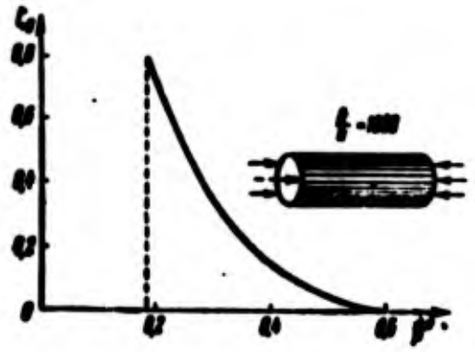

Fig. 20.19. Dependence "initial deflection-upper critical load" for case of axial compression.

Till now we consider given distributive law unrelated to dimensions of shell. In reality,

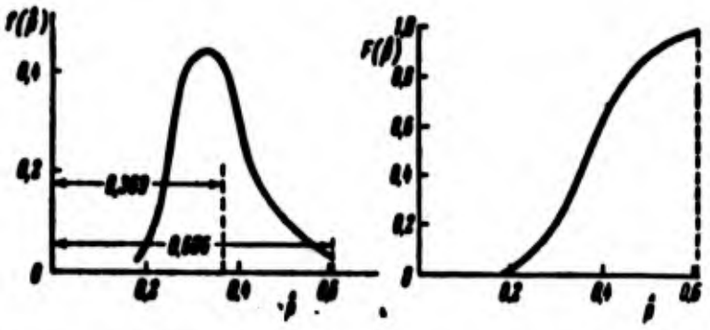

Fig. 20.20. Distribution functions for critical load in case of closed shell during axial compression.

however, amplitude and form of initial deflection depend on geometric parameters of shell. For bar above we assumed that dimensionless initial deflection is proportional to square of the ratio of the length of the bar or, better, the length of the half-wave of the deflection line to the characteristic transverse dimension. For shells it is possible to introduce an analogous assumption, but here

the amplitude of the dent should depend on dimensions of the dent not in one, but in at least two directions. In case of cylindrical shell we naturally connect possible initial deflection with lengths of half-waves of the deflection surface in two directions (Fig. 20.21a)— along generatrix (l_x) and along the arc (l_y). In works [11.30], [11.30a] there was offered formula for dimensionless initial deflection (ratio of deflection to thickness) of such a structure:

$$\zeta = \frac{C}{\delta^2}\left(\frac{l_x l_y}{l_x + l_y}\frac{1}{100k}\right)^2. \qquad (20.68)$$

where C, δ are empirical coefficients.

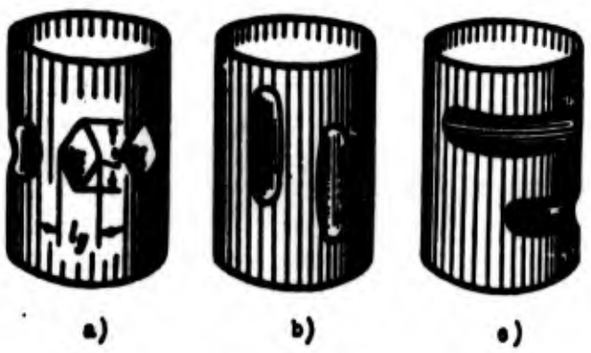

Fig. 20.21. Possible outlines of initial anomalies.

Judging by certain empirical data, parameter δ varies from 1.5 to 3. By analogy with the case of a bar it is possible to select a mean value δ = 2.

Donnell and Wan [11.30a] consider that when δ = 2 coefficient C will be equal to: for shells made from pipes, C = 1.5-3; for cylinders carefully prepared from specially treated flat sheets C = 3-5; and, last, for shells obtained from sheet without special requirements on manufacture, C = 5-10. In one of Nash's article [11.48] magnitude C was taken significantly larger, C = 30. Thus, at present there are no definite data on coefficient C; obviously,

it will sharply change depending upon technique of manufacture of shells and conditions of storage, transportation, tests, etc.

Attention was also turned [11.30a] to the fact that during manufacture of hollowed shells, stretched along generatrix (Fig. 20.21b) are more frequent than ones along the arc (Fig. 20.21c). Therefore, they offered a formula of type

$$\zeta_0 = \frac{C_1}{\pi^2} \frac{l_x^{1+\lambda} l_y^{1-\lambda}}{(100h)^2}. \tag{20.69}$$

where $\lambda < 1$. Taking $\lambda = 0.5$, we obtain

$$\zeta_0 = \frac{C_1}{\pi^2} \frac{l_x^{1.5} l_y^{0.5}}{(100h)^2}. \tag{20.70}$$

The value of C_1, judging by structure of the formula, should be approximately one fourth of C.

If we take $l_x = L/m$ and $l_y = \pi R/n$, where m is number of half-waves along the generatrix of the shell and n is the number of waves in a cross-section, then we obtain

$$\zeta_0 = \frac{C_1}{\pi^2} \left(\frac{L}{100mh}\right)^{1.5} \left(\frac{\pi R}{100nh}\right)^{0.5}. \tag{20.71}$$

Introducing former parameter (11.38)

$$\theta = \frac{mn\pi R}{nL}, \tag{20.72}$$

we give (71) the form

$$\zeta_0 = C_1 \frac{1}{\theta^{1.5} n^2} \left(\frac{R}{100h}\right)^2. \tag{20.73}$$

Magnitudes C and C_1 depend, mainly, on technique of manufacture of test pieces. If we conditionally consider that C and C_1 do not depend on R/h, then by (73) it will appear that deflection of initial dents is proportional to $(R/h)^2$. It is possible to outline the following way of determining dependence of mathematical expectation of $\hat{p}$ on R/h. Taking for C_1 a certain distributive law and using formulas of transformation of probabilities, we find mathematical

expectation of $\hat{p}$ for different ratios R/h. As a result we should conclude that average critical stress for real shells should be lowered with increase R/h. Meanwhile by classical linear theory upper dimensionless critical stress $\hat{p}_{в, ид} = 0.606$ does not depend on R/h. Analogous conclusion ensues from nonlinear solutions according to Ritz method with respect to lower critical stress, equal to $\hat{p}_{н, ид} = 0.18$. Consequently, from statistical point of view we should get consecutive lowering of mathematical expecation of $\hat{p}_{в}$ from the level $\hat{p}_{в, ид}$ to the level $\hat{p}_{н, ид}$, and possibly further to the level of lower critical stress for given initial deflection $\hat{p}_{н, нач}$ as shown in Fig. 20.22. Such a conclusion, as we have seen in Chapter XI, will agree with experimental data; it is the basis of recommendations of § 129 for practical calculations.*

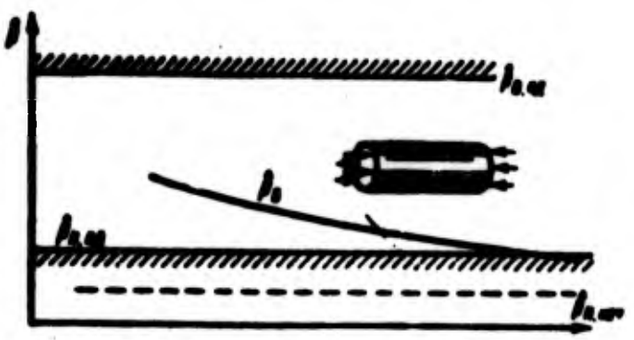

Fig. 20.22. Lowering of level of upper critical stress with increase of R/h.

We assumed in examples, for simplicity, that initial deflections are distributed by normal law. However, this assumption is not fully founded. Really, during manufacture of members of real constructions we usually originate from definite specifications. If these specifications regulate the maximum deflections from a given

*This concerns only that case when stresses in a shell lie within the elastic limit.

form of a shell, then pieces which do not correspond to them are rejected and are eliminated from the lot. Therefore, distributive law of initial deflections must be selected specially for every investigated lot of pieces. It is possible to expect that for a limited lot the probability density of initial deflection ζ_0 will be more or less evenly distributed on a limited section $\zeta_1 < \zeta \leq \zeta_2$.

Further, during consideration of influence of various other perturbing factors by far it will not always be convenient to transform them to equivalent initial deflections. Then one must pass to the solution of a more complicated problem, transforming probability by formulas (44) or (46).

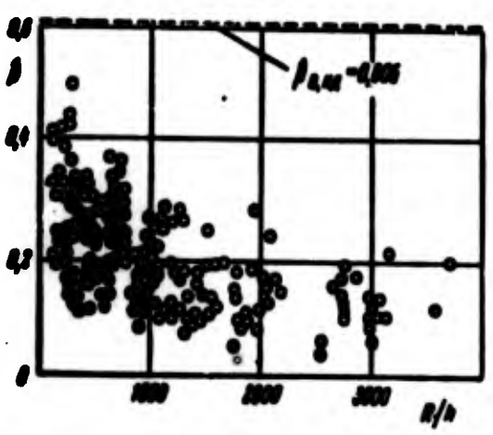

Fig. 20.23. Critical compression stresses by experimental data.

Since distributive laws of initial imperfections have not yet been studied much, it is interesting to formula the reverse problem; by final data of results of experiments on real shells to determine probability characteristics of initial deflections. Let us consider the same case of axial compression* and use experimental data of article [11.33]. In Fig. 20.23 are given values of dimensionless critical stress $\hat{p}$ for different ratios R/h. By these data it is possible for different R/h to construct histogram of magnitude $\nu = \hat{p}/\hat{p}_{в, \text{эд}}$, i.e., diagrams, consisting of rectangles and indicating, what number of experiments

*This case was investigated by B. P. Makarov in his second work [20.4], the data mentioned below are his.

corresponds to given interval of change of ratio ν of real critical stress to magnitude $\hat{p}_{в,ид} = 0.605$. Such histograms are depicted in Fig. 20.24. Let us note that with growth of ratio R/h the spectrum

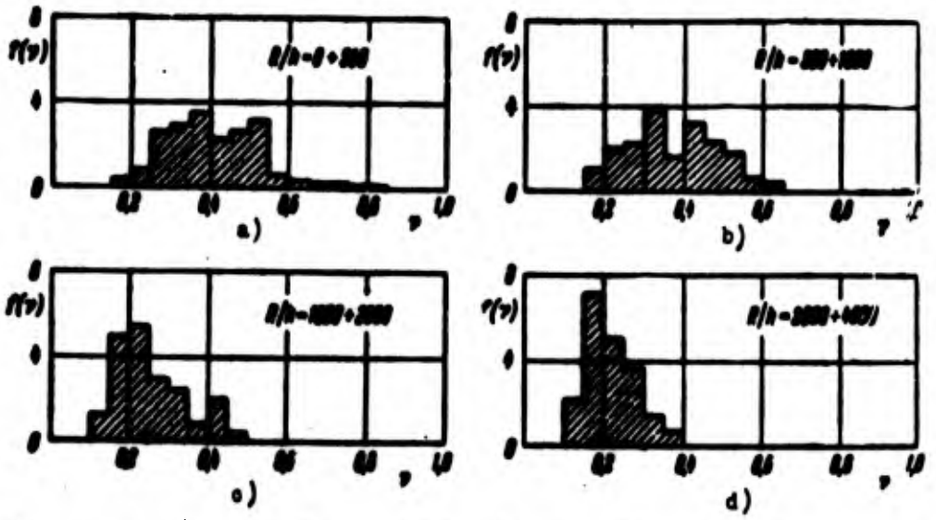

Fig. 20.24. Histograms of values of real critical stresses.

of real values of $\hat{p}$ narrows and shifts to zone of smaller ν. Furthermore, it is interesting that two first histograms have two maxima of probability density, so that distributive law turns out to be "double-humped."* If, further, we transform probabilities by graph of Fig. 20.19 and use formula of type (73), then we can find histogram for parameter u, corresponding to C_1. Such a final diagram is shown in Fig. 20.25. Solid line corresponds to normal distributive law u with center u = 0.1 and standard s = 0.06. We find here confirmation of assumption made above that center of

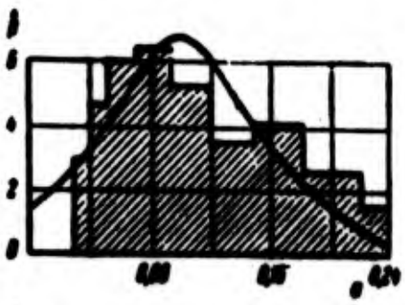

Fig. 20.25. Determining distributive law of initial deflections according to real critical stresses.

*Analogous double-humped distributive law was obtained by V. M. Goncharenko in another problems: see the second of works [20.3]. Whether such a result is regular still remains vague.

distributive law of initial deflections should be displaced in the direction of positive ζ_0.

§ 195. Influence of Random Loads on Behavior on Shells

Till now we paid our main attention to the influence of initial imperfections of form, and also boundary conditions on behavior of shell. But a very important role in phenomenon of snapping of a shell is also played by character of change of load. By far not always does load change in time so slowly that it is possible to be limited to consideration of equilibrium diagrams of "load-deflection." Thus, for instance, shells of aircraft, located near jet engines, are subjected to acoustic pressure, the spectral representation of which is almost constantly in a very wide region of frequencies. Another example is influence on shell on aircraft shells of turbulence of the atmosphere.

We consider that load applied to shell consists of two parts: fundamental, which is a systematic nonrandom magnitude, and additional, having character of random actions. We assume that these random load variations are independent of factors characterizing scattering of initial anomalies and other parameters of the shell. Further, we assume that random actions have character of white noise, i.e., evenly distributed in wide range of frequencies. Term "white noise" corresponds to white light, characterized by uniform spectrum.

During the study of influence of variable load on phenomenon of knock of a shell we naturally first of all use the energy approach.* In Chapter X we talked about the fact that "spontaneous" knock for an

*Such an approach to problem belongs to I. I. Vorovich [20.2].

ideal shell occurs only at upper critical load $p_{в, ид}$. But since real shells buckle, as a rule, at a lower load, then here there should be surmounted a certain energy barrier. This barrier is higher, the lower the load. Certainly, we are talking here only about such loads at which there is the possibility of loss of stability in the large. Whether there will occur a knock of the shell at load p, lying within limits $p_{н, ид} \leq p \leq p_{в, ид}$, depends on presence of random perturbing factors, allowing us to surmount energy barrier. Here there is a certain analogy with problems of passage through a potential barrier, met in other fields of physics, for instance in examining Brownian movement, where statistical methods are also used.

Obviously, probability of system surmounting the potential barrier depends on level of total energy of system at given load and its possible variations in process of tests or operation of the construction. It is possible to try to establish probability of a shock, using expression for total energy in terms of generalized coordinates, not passing—as in preceding paragraphs—to direct dependence between these coordinates and perturbing factors. We designate dimensionless total potential energy of system by ϑ and introduce parameter δ, determining scattering of random dynamic loads which construction can experience, so that level of random load can attain magnitude ϑ/δ. Conditions of tests or utilization of construction will be especially "restless" for low values of δ.

At the same we shall consider different geometric and elastic imperfections of system with help of equivalent initial anomalies of form; for simplicity we assume as before that these anomalies can be determined by the one parameter ζ_0. As a result of application of random loads the system may receive deformations of one or another

scale. We shall describe these deformations conditionally also with help of one parameter ζ (dimensionless deflection).

Let us assume that we are given initial imperfections of shell and we determine steady-state probability density of $f_1(\zeta)$ for times, great as compared to so-called relaxation time ($t \gg t_p$). We use for that Gibbs distribution known from statistical physics. For fixed ζ_0 the sought probability density will be equal to

$$f_1(\zeta)=\frac{1}{J}e^{-\frac{\alpha}{T}\vartheta(\zeta)}. \tag{20.74}$$

where α is a certain coefficient, depending on character of construction;* by 1/J is understood "normalizing" factor, where

$$J=\int_{-\infty}^{\infty}e^{-\frac{\alpha}{T}\vartheta(\zeta)}d\zeta. \tag{20.75}$$

Let us note that probability density of one or another value of ζ depends here on magnitude of energy of the system; density is greater, the lower the energy level. This is natural, since most frequently there must be realized more stable states of a system with minimum energy.

We take into account, further, scattering of initial deflections, considering that here we account for other deflections from the calculating model of a shell. Designating probability density ζ_0 through $\varphi(\zeta_0)$, on the basis of theorem of multiplication of probabilities we obtain

$$f(\zeta)=f_1(\zeta)\varphi(\zeta_0); \tag{20.76}$$

here we assume that parameters, determining scattering of values of load and initial imperfections, are independent. Probability that

---

*In work [20.2] this coefficient is expressed through parameters, characterizing oscillations of a construction taking into account damping.

deflection ζ will lie in interval $\zeta_1 < \zeta \leq \zeta_2$, is equal to

$$F = \int_{\zeta_1}^{\zeta_2} \int_{-\infty}^{\infty} f_1(\zeta) \varphi(\zeta_0) d\zeta_0 d\zeta. \qquad (20.77)$$

As an example we consider the same shallow cylindrical panel as § 193. Dimensionless energy of system is equal to*

$$\Theta = (\zeta^4 + 4\zeta^2\zeta_0 + 4\zeta^2) - \frac{64k}{\pi^4}\left(\frac{8}{3}\zeta^3 + 2\zeta\zeta_0\right) + \\ + \frac{16}{\pi^2}\zeta^2(p^*_{в,ид} - p^*) - \frac{32}{\pi^2}p^*\zeta_0. \qquad (20.78)$$

where $p^*_{в,ид}$ is parameter of upper critical load, p* is parameter of given static load, and k is paremeter of curvature.

Behavior of the system during random actions depends on relative level of static load $\nu = p^*/p^*_{в,ид}$, distribution of initial imperfections ζ_0 and parameter α/δ.

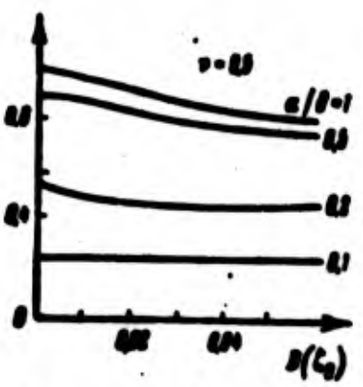

Fig. 20.26. Probability F, pertaining to total deflection of panel at level of average load $\hat{p} = 0.5$.

In Fig. 20.26 and the following are given results of calculations contained in work of I. I. Vorovich [20.2]. In Fig. 20.26 along the axis of ordinates is plotted probability F that dimensionless deflection ζ in modulus will not attain one, and along the axis of abscissas is plotted dispersion D of initial deflection ζ_0 on the assumption that for ζ_0 we select symmetric triangular distributive law. We take k = 12 and $\nu = 0.5$. Graph shows, as one should have expected, that the greater α/δ and consequently scattering of dynamic loads, the greater will the probability of obtaining maximum deflection

*See book [0.3], p. 282-286 and work [20.2].

will become. We note, that for small α/δ dispersion of initial deflections almost does not affect probability F.

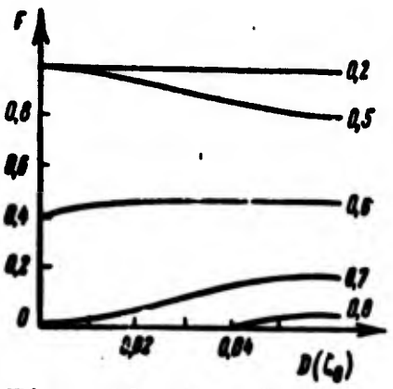

Fig. 20.27. Probability F for total deflection of panel at different levels of average load.

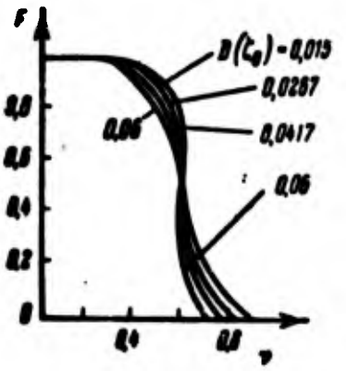

Fig. 20.28. Probability F for magnitude of total deflection of panel depending upon load.

In Fig. 20.27 it is shown how probability F depends on dispersion of ζ_0 and level of load ν when $\alpha/\delta = 1$. The higher the ν, the less the probability that deflection will remain within limits $(-1) \leq \zeta \leq 1$. In Fig. 20.28 the same dependence is given in coordinates of F and ν. Let us note that level of lower critical load is characterized by $\nu = 0.544$. As we see, when $\nu > 0.544$ probability of appearance of dangerous deflections sharply increases.

We determine now the probability F_* that at any random selected moment of time $t >> t_p$ shell will be in the neighborhood of a snapped state; subsequently we shall conditionally call F_* the probability of a knock. By (77) this probability will be equal to

$$F_* = \int_{\zeta}^{\infty} \int_{-\infty}^{\infty} f_1(\zeta) \varphi(\zeta_0) \, d\zeta_0 \, d\zeta. \tag{20.79}$$

As we have seen, knock can occur only under the condition that ζ_0 does not exceed known magnitude ζ_0 (for k = 12 the value ζ_0 was equal to 0.25). Thus, we obtain

$$F_* = \int_{\zeta}^{\infty} \int_{-\infty}^{\bar{\zeta}} f_1(\zeta) \varphi(\zeta_0) \, d\zeta_0 \, d\zeta. \tag{20.80}$$

In distinction from § 193, here we consider not only positive, but also negative initial deflections, i.e., directed both toward and also from the center of curvature; knocks take place in real tests also with negative deflections (see Fig. 20.29), although for an infinitely slow process here it is impossible to obtain a diagram of gradual transition from one form of equilibrium to another.

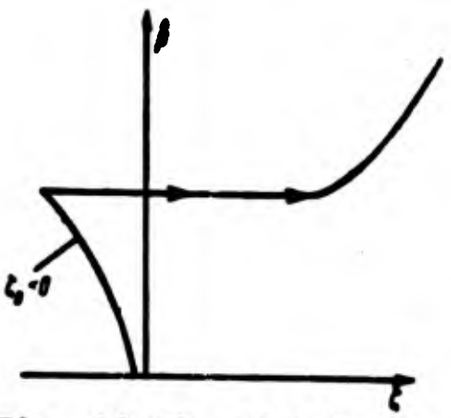

Fig. 20.29. Knock of a shell with transition from "negative" deflections to "positive."

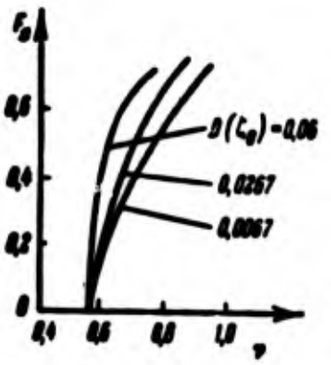

Fig. 20.30. Probability of snap of a cylindrical panel depending upon level of load.

In Fig. 20.30 is shown how probability of a snap F_* depends on level of load ν and dispersion of magnitude ζ_0. With increase of ν near lower critical value probability of a knock rapidly increases.

Let us note that energy approach allows us to establish certain statistical dependences and to arrive at definite qualitative conclusions without direct use of equilibrium diagrams for a shell; it is necessary only to have expression for the total potential energy of the system.

§ 196. Other Problems of Statistical Theory

Approach described above leads to characteristics of behavior of shells, established during the comparatively large interval of time. It is possible to set another problem—to determine probability

characteristics of behavior of shells in a fairly small time interval. In first case it was possible to consider shell as an elastic system with slight inertia or with strong damping. In second case we must consider system inertial, i.e., use as it were a dynamic approach.*

Thus, e.g., the following problem can be solved; to establish probability that the shell will be in the environment of a snapped state at moment of time t where $t \ll t_p$. This probability turns out to depend on height of potential barrier dividing stable forms of equilibrium of shell, and the damping decrement, which here plays an essential role. Another problem is formulated as follows: to determine probability that during certain interval of time the shell will appear at least once in a snapped state. In work [20.3], 1961, there is considered, e.g., the case when an elongated shallow cylindrical panel is under action of a normal pressure, whose characteristics correspond to acoustic pressure on an aircraft fuselage. Especially important is problem of determination of probability characteristics of process of consecutive forward and backward snaps of the shell, leading to development of fatigue cracks in the material.

In general, investigation of influence of a random action, having character of white noise, is connected with application of theory of so-called Markov processes. Solution of problem of probability characteristics of behavior of the system boils down to integration of a Fokker-Planck-Kolmogorov equation;** in general it is possible to conduct such integration only numerically. Therefore, it is necessary to look for a way of effective solution of different partial problems.

---

*V. M. Goncharenko indicated this [20.3].

**See R. L. Stratonovich, Selected problems of theory of fluctuations in radio engineering, M., 1961, p. 59.

We assumed till now that "basic" part of load is a nonrandom given function of time. But the problem should be formulated otherwise e.g., if we discuss behavior of shells during dynamic loading (see Chapter XVIII). In Fig. 20.31 is given for an example the diagram "deflection-time" for a load, whose main part is also a random function of time. Although character of process remains, as a rule, the same, concrete outlines of diagram change from case to case. Therefore, in experiments for test pieces of the same series we obtain different dynamic "critical" loads $q_д$, different "peaks" of deflection ζ_1 and etc.

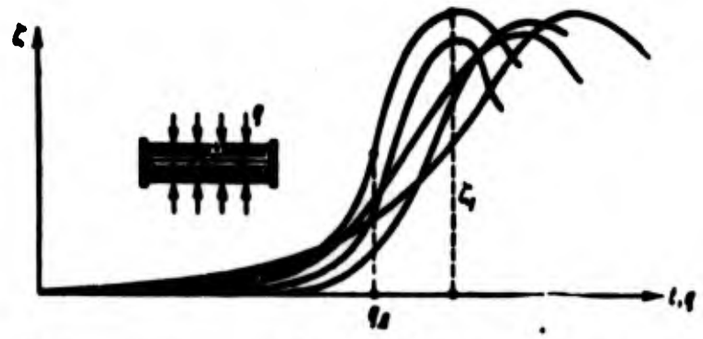

Fig. 20.31. Random dynamic processes for shells.

The important case of high-frequency changes of load, leading to increase of lower and upper critical forces is also investigated (see work of V. N. Chelomey [18.21] and V. M. Goncharenko, DAN Ukrainian SSR, No. 7, 1962).

Thus, statistical approach to problems of stability of shells should consider, on the one hand, dispersion of parameters of shell and boundary conditions and, on the other, influence on behavior of shells of different groups of loads: a) random loads of white noise type; b) loads, whose variation may be described by a finite number of random variables with a certain distributive law.

In conclusion let us note that application of probability methods

in theory of stability of elastic systems will be effective only after we have gathered more detailed data about initial imperfections of constructions and obtained characteristic of random loads, etc. It would be desirable, if subsequently experiments, on fairly large lots of pieces always were accompanied by statistical treatment of results.

Literature

20.1. V. V. Bolotin. Statistical methods in nonlinear theory of elastic shells, News of Acad. of Sci. of USSR, OTN, No. 3 (1958), Statistical methods in structural mechanics, Gosstroyizdat, M., 1961.

20.2. I. I. Vorovich. Statistical method of theory of stability of thin elastic shells, Applied math. and mech., 23, No. 5 (1959), 885-892.

20.3. V. M. Goncharenko. Research of stability of shells by methods of probability theory, Cand. diss., Kiev, 1961; To determination of probability of loss of stability by a shell, News of Acad. of Sci. of USSR, OTN, Mech. and machine building, No. 1 (1962), 159-160.

20.4. B. P. Makarov. Application of statistical method for analysis of nonlinear problems of stability of shells, Transactions of L'vov conference on theory of shells, Kiev, 1962; Application of statistical method for analysis of experimental data on stability of shells, News of Acad. of Sci. of USSR, OTN, Mech. and machine building, No. 1 (1962), 157-158.

20.5. A. R. Rzhanitsyn. Statistical method of determination of tolerable stresses during buckling, Gosstroyizdat, M., 1951.

CHAPTER XXI

GENERAL CRITERIA OF STABILITY OF ELASTIC SYSTEMS

§ 197. Dynamic Criterion of Stability in the Small

In preceding sections of this book we analysed a number of problems pertaining to buckling of bars, plates and shells. We met different methods of solution of problems, at the basis of which lay static, energy and dynamic criteria of stability. In this chapter we will consider these criteria from a more general point of view, connecting them with those approaches to concept of stability which are taken in analytical mechanics and nonlinear theory of elasticity.

Even in § 1, introducing the concept of stability of a compressed bar, we, as it were, intuitively used a simple dynamic model. And here we will start with the dynamic criterion, applying it first of all to stability in the small. Here we naturally turn to those concepts of stability and instability of mechanical systems with a finite number of degrees of freedom, which were in their time introduced by Lagrange.* He spoke of stable equilibrium "in the sense that if at first a system was in a state of equilibrium, and then

---

*J. L. Lagrange, Analytical mechanics, Vol. 1, Gostekhizdat, 1950, p. 97.

was somewhat removed from it, by itself it seeks rushes to return to this state, accomplishing near it infinitesimal oscillations." Further, with unstable equilibrium "the system, once removed from this state, can accomplish oscillations, which will no longer be very small and which can more and more deflect the system from its initial state."

A strict definition of stability of equilibrium, as a particular case of motion, was first given by A. M. Lyapunov.** Let us assume that position of system is determined by n generalized coordinates q_i ($i = 1, 2, \ldots, n$), where in equilibrium state we have $q_i = 0$ with the same i.

We assume that in initial moment $t = 0$ absolute values of coordinates and velocities lie within limits

$$|q_i^0| < \delta, \quad |\dot{q}_i^0| < \delta$$

and that in any subsequent moment of time $t > 0$ we compare coordinates $q_i(t)$ and velocities $\dot{q}_i(t)$ with certain magnitude ε. Stable equilibrium state is characterized by the fact that for any $\varepsilon > 0$ it is possible to select corresponding magnitude $\delta(\varepsilon) > 0$ at which for whole period of time $t > 0$ magnitudes $|q_i|$ and $|\dot{q}_i|$ will be within limits

$$|q_i| < \varepsilon, \quad |\dot{q}_i| < \varepsilon.$$

In other words, in case of stable equilibrium of a system we always can select such initial conditions that generalized coordinates and velocities will not go beyond certain prescribed bounds, lying in the neighborhood of the base state. If we approach this determination

---

*A. M. Lyapunov, General problem of stability of motion, Gostekhizdat, 1950, pp 17-21. See also N. G. Chetayev, Stability of motion, Gostekhizdat, 1955.

from geometric point of view, then it is necessary to imagine a certain tube in a $(2n + 1)$-dimensional space. Let us assume that magnitudes q_i and $\dot{q}_i$ are plotted in an imaginary section of such a tube, having $2n$ dimensions, and time t, along its axis. Stable equilibrium is characterized by the fact that if one were to select properly initial values of q_i^o and $\dot{q}_i^o$, then magnitudes q_i and $\dot{q}_i$ for any t will lie inside a tube with the given section.

A. M. Lyapunov also introduced concept of asymptotic stability; this form of stability pertains to case when system with unlimited growth of t returns to base state, i.e., $q_i(t)$, $\dot{q}_i(t) \to 0$, if $t \to \infty$.

We assume, further, that a mechanical system with given parameters has not one, but several stable equilibrium states; a series of examples were encountered above. Then the definition of stability in the small, given here, should be related to the vicinity of each of these equilibrium states.

The criterion of stability and instability mentioned above can be generalized for a deformed construction which is a system with an infinitely great number of degrees of freedom. Circle of magnitudes, characterizing behavior of such a system in time, is expanded; here there can be introduced, along with displacements of points of the system and velocities, such magnitudes as components of additional deformations and stresses. Emerging from frames of mechanics itself, we can consider also change of temperature in different points of the system, etc.

Magnitudes, which are selected in this or that problem for description of the behavior of a construction, will henceforth (for brevity) be called characteristics.

§ 198. Static Criterion of Stability in the Small. Investigation of Neighboring Equilibrium Forms for Three-Dimensional Problem.

Let us turn to static criterion which we repeatedly used during investigation of stability in the small. Let us assume that the load received by a construction is proportional to a certain parameter and that to small values of the parameter there corresponds only in a considered range of characteristics a stable state of the system. We increase parameter of load, investigating here the state of constructions, close to the base state. That value of the parameter at which at least one of the adjacent states of the construction for the first time becomes an equilibrium state we call critical value. With a load exceeding the critical magnitude, the base state, as a rule, ceased to be stable.*

We studied by investigation the neighborhood of the basic equilibrium state in many particular problems, when it was uniaxial (bar) biaxial (plate, shell); in practical applications namely these problems are essential. But in order to establish common features in the formulation of different problems, we shall consider the case of a triaxial stress.**

We relate the deformed and stressed state of an elastic body to the Cartesian system of coordinates. We designate, as before, by u, v and w shift of points of the body along axes x, y and z; by ε_x, γ_{xy},

---

*For certain mechanical systems exceptions are possible; see A. Yu. Ishlinskiy, S. I. Malashenko and M. Ye. Temchenko, News of Academy of Sciences of the USSR, Dept. of Tech. Sciences, No. 8 (1958), 53-61.

**In the subsequent account we follow V. V. Novozhilov [21.8].

etc., deformation of lengthening and shear; by σ_x, τ_{xy}, etc., normal and tangential stresses. Subsequently components of deformations and stresses, corresponding to the base state, we designate ε_x^0, γ_{xy}^0, σ_x^0, τ_{xy}^0, etc. With growth of parameter of load magnitudes ε_x^0, σ_x^0, ... change at every point of the body monotonically. Formulation and solution of problems are significantly facilitated in case of simple loading, when main deformations and stresses at any point preserve their direction, or, in other words, when all components of deformations and stresses change proportionally to the same parameter of load. This requirement is satisfied, e.g., for shells if the base state is momentless. However, we also met cases of complex loading,* when direction of main deformations and stresses for various points changes in process of loading (moment base state for shells).

In one way or another we can express deformation by shifts by certain formulas of the linear theory of elasticity:**

$$\left.\begin{aligned} \varepsilon_x &= \frac{\partial u}{\partial x}, \quad \varepsilon_y = \frac{\partial v}{\partial y}, \quad \varepsilon_z = \frac{\partial w}{\partial z}, \\ \gamma_{xy} &= \frac{\partial u}{\partial y} + \frac{\partial v}{\partial x}, \quad \gamma_{yz} = \frac{\partial v}{\partial z} + \frac{\partial w}{\partial y}, \quad \gamma_{zx} = \frac{\partial w}{\partial x} + \frac{\partial u}{\partial z}. \end{aligned}\right\} \qquad (21.1)$$

We consider here that magnitudes ε_x^0, γ_{xy}^0, ... are small in comparison to 1. We compose, then, the equation of equilibrium of a member having dimensions dx, dy and dz. If we do not consider mass forces (for instance, force of gravity), then these equations in projections on axis of coordinates will take form***

---

*Terms "simple loading" and "complex loading" are often applied in literature on the theory of plasticity.

**See, e.g., P. F. Pankovich, Theory of elasticity, Oborongiz, 1939, pp. 44-48.

***See above-indicated book of P. F. Pankovich. pp. 19 and 31.

$$\left.\begin{aligned}\frac{\partial \sigma_x^\circ}{\partial x}+\frac{\partial \tau_{xy}^\circ}{\partial y}+\frac{\partial \tau_{xz}^\circ}{\partial z}=0,\\ \frac{\partial \tau_{yx}^\circ}{\partial x}+\frac{\partial \sigma_y^\circ}{\partial y}+\frac{\partial \tau_{yz}^\circ}{\partial z}=0,\\ \frac{\partial \tau_{zx}^\circ}{\partial x}+\frac{\partial \tau_{zy}^\circ}{\partial y}+\frac{\partial \sigma_z^\circ}{\partial z}=0.\end{aligned}\right\} \qquad (21.2)$$

and equation of moments lead to equalities

$$\tau_{xy}^\circ=\tau_{yx}^\circ,\quad \tau_{xz}^\circ=\tau_{zx}^\circ,\quad \tau_{yz}^\circ=\tau_{zy}^\circ. \qquad (21.3)$$

Then we write dependence of Hooke's law,

$$\varepsilon_x=\frac{1}{E}(\sigma_x-\mu\sigma_y-\mu\sigma_z),\quad \gamma_{xy}=\frac{2(1+\mu)}{E}\tau_{xy}^\circ \text{ etc.} \qquad (21.4a)$$

Using (4a), it is possible to express stresses by deformations; then we obtain formulas of type

$$\sigma_x=\frac{E}{1+\mu}\left(\varepsilon_x+\frac{\mu}{1-2\mu}\theta\right),\quad \tau_{xy}^\circ=\frac{E}{2(1+\mu)}\gamma_{xy} \text{ etc.} \qquad (21.4b)$$

where $\theta = \varepsilon_x + \varepsilon_y + \varepsilon_z^\circ$ is volumetric strain.

If we place these expressions in equations of equilibrium (2) and use relationship (1), then we obtain linear equations for shifts u°, v° and w°. Solution of these equations should satisfy <u>boundary conditions</u>. Let us assume that on the surface of a body there are given components of external load p_x°, p_y°, p_z°. Then from condition of equilibrium of a boundary member we obtain

$$\left.\begin{aligned}\sigma_x^\circ l+\tau_{xy}^\circ m+\tau_{xz}^\circ n=p_x^\circ,\\ \tau_{yx}^\circ l+\sigma_y^\circ m+\tau_{yz}^\circ n=p_y^\circ,\\ \tau_{zx}^\circ l+\tau_{zy}^\circ m+\sigma_z^\circ n=p_z^\circ.\end{aligned}\right\} \qquad (21.5)$$

where l, m, n are cosines of angles formed, by a normal to the given area of the surface with the x, y and z axes.

From known <u>theorem of Kirchhoff</u> it follows that with given boundary conditions <u>the solution of linear static equations of theory</u>

of elasticity is unique.* Consequently, the possibility of determining of the neighboring equilibrium state by usual linear equations is excluded. If we turn to the example of a plate experiencing force in its plane, then in this case it is impossible to investigate stability of the plate using linear equations of a plane problem and corresponding boundary conditions.

A peculiarity of problems of stability in the small is that during investigation of a neighboring equilibrium state it is necessary to consider change of orientation of the faces of an element of the body, while in composing usual equations of classical theory of elasticity of type (2) this change is not considered. In other words, in problems of stability there must be introduced into consideration rotation of the element about the coordinate axes.

Let us consider transition from the base state of body to a neighboring state. We designate additional shifts of any point of the body, appearing with such transition, by u', v', w', and correspondingly additional deformations and stresses by ε_x', σ_x', etc. For deformations we write expressions of type (1):

$$\left.\begin{aligned} \varepsilon_x' &= \frac{\partial u'}{\partial x}, \quad \varepsilon_y' = \frac{\partial v'}{\partial y}, \quad \varepsilon_z' = \frac{\partial w'}{\partial z}, \\ \gamma_{xy}' &= \frac{\partial u'}{\partial y} + \frac{\partial v'}{\partial x}, \quad \gamma_{yz}' = \frac{\partial v'}{\partial z} + \frac{\partial w'}{\partial y}, \quad \gamma_{zx}' = \frac{\partial w'}{\partial x} + \frac{\partial u'}{\partial z}. \end{aligned}\right\} \qquad (21.6)$$

We set ourselves the goal of characterizing the turns of an element about the coordinate axes. In Fig. 21.1 is presented the face of a body's element, perpendicular to axis z. Turn of unit vector of axis x in plane xy is equal to $\partial v'/\partial x$, and turn of unit vector of axis y

*See, e.g., A. Lyav, Mathematical theory of elasticity, ONTI, 1935, p. 181.

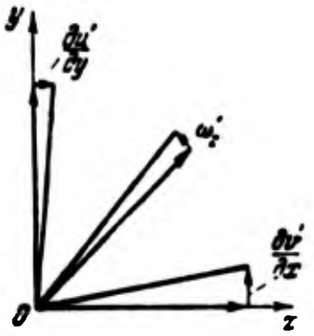

Fig. 21.1. Determination of rotation of an element about the z-axis.

in that same plane is equal to $\partial u'/\partial y$, where it will be positive, if it occurs in the direction of positive u', i.e., in a direction the reverse of the first turn. By turn ω_z' of face xy about axis z we will understand the halfsum of magnitudes $\partial v'/\partial x$ and $-\partial u'/\partial y$, determining as it were the "average" value of turns about z of various straight lines passing through point 0 and lying on face xy. Analogous reasonings lead to the following formulas for turns of the element about axes x, y and z:

$$\left.\begin{aligned} \omega_x' &= \frac{1}{2}\left(\frac{\partial w'}{\partial y} - \frac{\partial v'}{\partial z}\right), \\ \omega_y' &= \frac{1}{2}\left(\frac{\partial u'}{\partial z} - \frac{\partial w'}{\partial x}\right), \\ \omega_z' &= \frac{1}{2}\left(\frac{\partial v'}{\partial x} - \frac{\partial u'}{\partial y}\right). \end{aligned}\right\} \qquad (21.7)$$

We shall consider that deformations of elongation and shearing, occurring in plane of every face, according to (6) are small as compared to "average" turns of the face ω_z', ω_x', ω_y', and, in turn, these magnitudes are small with respect to 1. But then during determination of new position of unit vectors of coordinate axes one should consider, e.g., that the face of the element xy is a <u>rigid disk</u>, turning about axis z an angle equal to ω_z'. This gives possibility of writing a table of approximate values of cosines of angles, which rotated unit vectors **i'**, **j'** and **k'** of axes x, y and z will constitute with their initial directions (Fig. 21.2).

We now write equation of equilibrium of the element of a body in a neighboring state, considering fundamental stresses after rotation, secondary stresses and mass forces. Considering secondary

stresses small as compared to fundamental ones, we will not consider their rotation.

	i'	j'	k'
x	1	$-\omega_z'$	ω_y'
y	ω_z'	1	$-\omega_x'$
z	$-\omega_y'$	ω_x'	1

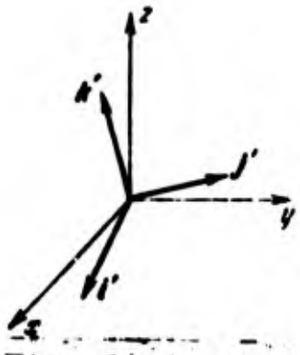

Fig. 21.2. Turns of unit vectors of coordinate axes.

Equation of type (1) in projections on axis x will have form*

$$\frac{\partial}{\partial x}(\sigma_x' - \tau_{xy}'\omega_z' + \tau_{xz}'\omega_y' + \sigma_x') + \frac{\partial}{\partial y}(\tau_{yx}' - \sigma_y'\omega_z' + \\ + \tau_{yz}'\omega_y' + \tau_{yx}') + \frac{\partial}{\partial z}(\tau_{zx}' - \tau_{zy}'\omega_z' + \sigma_z'\omega_y' + \tau_{zx}') = 0. \quad (21.8)$$

Here increments of forces in planes with normals i', j', k' consecutively are projected on axis x taking into account first line of table of cosines. Subtracting (2) from (8), we obtain finally

$$\frac{\partial}{\partial x}(\sigma_x' - \tau_{xy}'\omega_z' + \tau_{xz}'\omega_y') + \frac{\partial}{\partial y}(\tau_{yx}' - \sigma_y'\omega_z' + \\ + \tau_{yz}'\omega_y') + \frac{\partial}{\partial z}(\tau_{zx}' - \tau_{zy}'\omega_z' + \sigma_z'\omega_y') = 0. \quad (21.9)$$

By analogy we write two other equations:

$$\frac{\partial}{\partial x}(\tau_{xy}' + \sigma_x'\omega_z' - \tau_{xz}'\omega_x') + \frac{\partial}{\partial y}(\sigma_y' + \tau_{yx}'\omega_z' - \tau_{yz}'\omega_x') + \\ + \frac{\partial}{\partial z}(\tau_{zy}' + \tau_{zx}'\omega_z' - \sigma_z'\omega_x') = 0. \quad (21.10)$$

$$\frac{\partial}{\partial x}(\tau_{xz}' - \sigma_x'\omega_y' + \tau_{xy}'\omega_x') + \frac{\partial}{\partial y}(\tau_{yz}' - \tau_{yx}'\omega_y' + \sigma_y'\omega_x') + \\ + \frac{\partial}{\partial z}(\sigma_z' - \tau_{zx}'\omega_y' + \tau_{zy}'\omega_x') = 0. \quad (21.11)$$

It is possible to present these equations in somewhat different form. Since we agreed to disregard deformations as compared to rotations, then during calculation of ω_x', ω_y', ω_z' will set

$$\left.\begin{aligned} \gamma_{xy}' = \frac{\partial u'}{\partial y} + \frac{\partial v'}{\partial x} \approx 0, \quad \gamma_{yz}' = \frac{\partial v'}{\partial z} + \frac{\partial w'}{\partial y} \approx 0, \\ \gamma_{zx}' = \frac{\partial w'}{\partial x} + \frac{\partial u'}{\partial z} \approx 0. \end{aligned}\right\} \quad (21.12)$$

*Equations of this type were composed in work of Biezeno and Hencky [21.9].

Then, by (7) we find

$$\omega_x' \approx \frac{\partial w'}{\partial y} \approx -\frac{\partial v'}{\partial z}, \quad \omega_y' \approx \frac{\partial u'}{\partial z} \approx -\frac{\partial w'}{\partial x}, \quad \omega_z' \approx \frac{\partial v'}{\partial x} \approx -\frac{\partial u'}{\partial y}. \tag{21.13}$$

If we turn, for example, to equation (11), then, using (13), we can give it form

$$\frac{\partial}{\partial x}\left(\tau_{xz}' + \sigma_x^{\circ}\frac{\partial w'}{\partial x} + \tau_{xy}^{\circ}\frac{\partial w'}{\partial y}\right) + \frac{\partial}{\partial y}\left(\tau_{yz}' + \tau_{yx}^{\circ}\frac{\partial w'}{\partial x} + \sigma_y^{\circ}\frac{\partial w'}{\partial y}\right) + \frac{\partial}{\partial z}\left(\sigma_z' + \tau_{zx}^{\circ}\frac{\partial w'}{\partial x} + \tau_{zy}^{\circ}\frac{\partial w'}{\partial y}\right) = 0. \tag{21.14}$$

In equations of type (9) or (14) stresses, as before, can be expressed by deformations by the formulas

$$\sigma_x' = \frac{E}{1+\mu}\left(\varepsilon_x' + \frac{\mu}{1-2\mu}\theta'\right), \quad \tau_{xy}' = \frac{E}{2(1+\mu)}\gamma_{xy}' \text{ etc.} \tag{21.15}$$

where $\theta' = \varepsilon_x' + \varepsilon_y' + \varepsilon_z'$, and then deformation and rotations are expressed in shifts according to (6) and (7). Then we obtain three homogeneous equations for u', v' and w'.

Let us turn to boundary conditions for a neighboring state of the body. Let us assume here that during transition from base state to a neighboring one the external load remains constant in magnitude and direction. Then for the new position we have

$$(\sigma_x - \tau_{xy}^{\circ}\omega_z' + \tau_{xz}^{\circ}\omega_y' + \sigma_x')l + (\tau_{xy}' - \sigma_y^{\circ}\omega_z' + \tau_{yz}^{\circ}\omega_y' + \tau_{yx}')m + (\tau_{zx}' - \tau_{zy}^{\circ}\omega_z' + \sigma_z^{\circ}\omega_y' + \tau_{zx}')n = p_x. \tag{21.16}$$

Substracting first equality (5) from (16), we obtain

$$(\sigma_x' - \tau_{xy}^{\circ}\omega_z' + \tau_{xz}^{\circ}\omega_y')l + (\tau_{yx}' - \sigma_y^{\circ}\omega_z' + \tau_{yz}^{\circ}\omega_y')m + (\tau_{zx}' - \tau_{zy}^{\circ}\omega_z' + \sigma_z^{\circ}\omega_y')n = 0. \tag{21.17}$$

The other two conditions it is possible to write by analogy.

Thus, problem is reduced to investigation of a system of homogeneous equations, containing shifts u', v', w' (or equations, equivalent to them), where fundamental stresses σ_z°, τ_{xy}°, ... in (17) are considered certain given functions of coordinates. If fundamental stresses are proportional to a certain parameter λ, then, finding

magnitude of λ, at which these equations have a nontrivial solution, we obtain the so-called eigenvalues of the problem about stability in the small; they correspond to branching points (bifurcation) of equilibrium forms (when examining problem in linear formulation). As a rule, in elastic systems to every eigenvalue of a problem there corresponds one natural form, i.e., one definite form of loss of stability. It is possible, however, to imagine that in certain cases (for instance, for plates or shells) to some eigenvalue there will correspond two, three, etc., forms of loss of stability (different buckled states); then we will obtain eigenvalues of second, third, etc., multiplicity. If we compare consecutive eigenvalues of a problem of stability of a system, then it appear that the least of them has direct practical meaning, since it corresponds to loss of stability of the base state; this value also determines first Euler critical load or, in terminology adopted by us, upper critical load. As for the following of points of bifurcation, then to them only unstable branches converge, and equilibrium states corresponding to all these branches are not realized.

We compare equations obtained by us with those, which we used for plates. We take, for instance, equation (14). Considering σ_x^0, σ_y^0, and τ_{xy}^0 as not depending on coordinates and, furthermore, taking $\tau_{zx}^0 = \tau_{zy}^0 = 0$ and $\sigma_z' = 0$, we obtain

$$\frac{\partial \tau_{xz}'}{\partial x} + \frac{\partial \tau_{yz}'}{\partial y} + \sigma_x \frac{\partial^2 w'}{\partial x^2} + 2\tau_{xy} \frac{\partial^2 w'}{\partial x \partial y} + \sigma_y \frac{\partial^2 w'}{\partial y^2} = 0.$$

After integration with respect to thickness of plate we easily obtain those equations which lay at the base of solution of linear problems of stability. In order to obtain analogous dependences of the theory of stability of shells, one should express basic dependences in

curvilinear coordinates [see § 120].

We compare equations of equilibrium of type (2), pertaining to base state, and equations (14), corresponding to transition from base state to a neighboring one. Both groups of equations are linear, but they have different meaning. Equations of second type must be considered equations obtained by linearization of certain nonlinear dependences, describing large shifts of the system (see § 201), since these equations of second type are derived taking into account rotation of an element of the body. Therefore, it is possible to say that ultimately every stability problem is nonlinear. There arises the question: are points of bifurcation, found with help of linearized equations, the same, as if they were obtained proceeding from nonlinear dependences? This question was considered with help of methods of functional analysis.* It turned out that for practically important cases, when to critical values of parameter λ there corresponds only one definite form of buckling (or, in general, an odd number of such forms, i.e., when eigenvalues have odd multiplicity), all eigenvalues of linearized equations are points of bifurcation of a nonlinear problem. Meanwhile, if eigenvalues have even multiplicity, such coincidence cannot take place.

§ 199. Energy Criterion for Stability in the Small. Lagrange-Dirichlet Theorem.

Let us turn to the energy criterion of stability in the small. This criterion in application to a conservative system with a finite number of degrees of freedom is based on known Lagrange-Dirichlet

*See M. A. Krasnoselskiy, Topological methods in theory of nonlinear integral equations, Gostekhizdat, 1956; I. I. Vorovich, Reports of Acad. of Sci., USSR, 122, No. 1 (1958).

theorem,* which is formulated as follows. If in a certain (base) state of a conservative system the potential energy is minimum with respect to values of energy for all adjacent (deflected) states of the system, then base position is a position of stable equilibrium. For proof we assume that in the base position generalized coordinates $q_1, q_2, \ldots, q_n$ are equal to zero, potential energy $\Im$ for that position we also take equal to zero. For adjacent positions of the system, where $|q_i| < \varepsilon$ and $|\dot{q}_i| < \varepsilon$ and condition $\Im(0, 0, \ldots, 0) = \min = 0$ will be $\Im > 0$. But then total energy E, consisting of kinetic T and potential $\Im$, will be for these positions $E = T + \Im > 0$, since always $T > 0$. We note values of E for different states on the boundary of the region ε and establish the least from these values E^*. We assume that magnitude E changes continuously inside region ε; here there can be found such a narrow region δ inside ε, for which we have $|q_i| < \delta$, $|\dot{q}_i| < \delta$, and energy will be $E < E^*$. We select coordinates q_i and velocity $\dot{q}_i$, satisfying this condition, as initial, and then initial energy E^0 (for $t = 0$) will be $E^0 < E^*$. But since, for conservative system, total energy remains constant, then for all the subsequent time energy of the system will be $E = E^0 < E^*$. Here the system will appear stable, since for any $t > 0$ coordinates and velocity will leave the bounds of ε.

Judging by given proof, Lagrange-Dirichlet theorem may be extended to systems, on which there act, in addition to potential forces, also dissipative forces; for such systems $E < E^0 < E^*$, i.e.,

---

*This theorem was formulated first by J. Lagrange (see his "Analytical mechanics," Vol. 1, 1950, p. 97); proof belongs to P. G. Lejeune-Dirichlet (see the same book of Lagrange, p. 537). Here we follow F. R. Gantmakher; see his "Lecture on analytical mechanics," 1960.

motion will be accompanied by energy dissipation.

A. M. Lyapunov gave for two important cases a conversion of the Lagrange-Dirichlet theorem. In one case there is considered a certain (base) equilibrium position of the system, in which potential energy is maximum with respect to energy of adjacent positions, where this maximum corresponds to members of lowest (not necessarily the second) order in the expansion of potential energy on coordinates q_i; in this case base position is unstable. In another theorem we talk about the case when we know only that energy in the basic equilibrium position is not minimum; such a position will be unstable, if absence of minimum is determined by members of the second order in the expansion of potential energy.

All the given theorems pertained to systems with a finite number of degrees of freedom. Generalization of them for case of a system with an infinitely great number of degrees of freedom is the subject of a number of investigations* and has not yet been completed. But, as was already said during solution of many problems an elastic construction is considered as a system with a finite number of degrees of freedom, and then the fundamental theorems can be directly applied.

The theorems of Lagrange-Dirichlet and Lyapunov indicate a way of finding critical load. Considering small deflections of a system from its base state, we will present increase of total potential energy in the form

$$\Delta\Theta = \lambda\Theta + \frac{1}{2}\delta^2\Theta;$$

*See, e.g., A. A. Movchan, Applied mathematics and physics, 24 (1960), 988-1001.

in linear problems the following members of the expansion will be absent, since energy is quadratic form of generalized coordinates. For any equilibrium state $\delta\Im = 0$; therefore, the character of equilibrium must be judged by the sign of the second variation. Equilibrium will be stable when $\delta^2\Im > 0$ and unstable when $\delta^2\Im < 0$. But first upper critical load corresponds to transition from stable equilibrium positions to unstable ones; consequently, for that the value of load should be $\delta^2\Im = 0$. If system has n degrees of freedom and deflections from the base state are determined by generalized coordinates q_1, q_2, ..., q_n, then the second variation can be presented in the form

$$\delta^2\Im = \frac{\partial^2\Im}{\partial q_1^2}\delta q_1^2 + \frac{\partial^2\Im}{\partial q_2^2}\delta q_2^2 + \ldots + 2\frac{\partial^2\Im}{\partial q_1\,\partial q_2}\delta q_1\,\delta q_2 + \ldots$$

Condition $\delta^2\Im = 0$ is equivalent here to the following equation, containing coefficients of the given series:*

$$\begin{vmatrix} \frac{\partial^2\Im}{\partial q_1^2} & \frac{\partial^2\Im}{\partial q_1\,\partial q_2}\cdots \\ \frac{\partial^2\Im}{\partial q_2\,\partial q_1} & \frac{\partial^2\Im}{\partial q_2^2}\cdots \\ \cdots\cdots\cdots & \end{vmatrix} = 0. \qquad (21.18)$$

Roots of this equation determine all critical loads, including the least of them.

We did not distinguish here "classical" problems of stability, in which subcritical loading is simple, and upper critical load is a point of bifurcation, and problems with complex loading, when critical load constitutes a limit point. In both cases the branch of stable solutions is linked at the first point with the branch of unstable solutions. Question of to what branch the critical point itself

---

*See N. G. Chetayev, Stability of motion, Gostekhizdat, 1955, p. 52.

pertains remains vague here; it may be considered only during solution of nonlinear problem taking into account highest members of expansion of $\Delta\Im$ (see § 202).

A number of examples of application of the energy criterion were given in sections pertaining to bars and plates.

§ 200. Dynamic Criterion of Stability in the Large.

Till now we considered criterion of stability of the basic equilibrium state of an elastic system as compared to adjacent states. As we know, in many problems, pertaining, first of all, to a shell, more important is the study of stability in the large. Loss of stability practically is accomplished for such systems not by means of continuous shift of equilibrium forms, but suddenly. Since new states of equilibrium turn out to be remote from the initial, then problems of stability in the large are essentially nonlinear. Application of a dynamic criterion consists in investigating character of nonlinear oscillations of system about its equilibrium positions.

Of special interest here is case when construction may be reduced to a conservative system with one degree of freedom. Then character of equilibrium is determined by curves on the so-called phase plane.* These curves express dependence between generalized coordinate ζ and generalized velocity $\dot{\zeta}$ ensuing from law of conservation of energy $E = T + \Im = \text{const}$, on the condition of invariability of level of load. By E here is understood total reserve of energy obtained by system at the initial moment of time. In Fig. 21.3a is shown curve of $\dot{\zeta}(\zeta)$ for case, when load does not reach lower critical value. System here

*See, e.g., I. M. Babakov, Theory of oscillations, 1958, Gostekhizdat, p. 510 et seq.

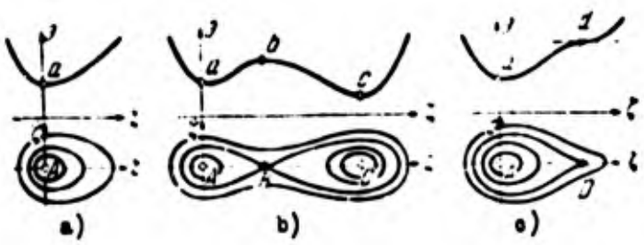

Fig. 21.3. Curves on the phase plane.

has a single stable equilibrium position, corresponding to point A. This singular point carries the name of the center; it is surrounded by closed nonintersecting lines (phase trajectories), each of which corresponds to a definite reserve of energy E. Above in the same figure is depicted dependence $\Theta(\zeta)$. As we see, to center A there corresponds a minimum value of Θ.

The following curve, Fig. 21.3b, contains phase trajectories for case when load exceeds lower critical value. Here there are two centers, A and C, between which there lies another singular point B, called the saddle; it corresponds to the unstable equilibrium state. Depending upon which initial values ζ_0 and $\dot{\zeta}_0$ are given to the system, we will obtain oscillation around one of the stable positions or oscillations, embracing both these positions. As can be seen from upper graph, to the saddle there corresponds the maximum value of Θ.

Finally, curve in Fig. 21.3c corresponds to case when load is exactly equal to lower critical magnitude. At point D one of centers coincides with the saddle. On graph of energy to position D there corresponds a point of inflection from the horizontal tangent.

Examples of phase trajectories for shells, considered as a system with one degree of freedom, were given by E. I. Grigolyuk*

*See News of Acad. of Sci., USSR, Dept. of Tech. Sci., No. 3 (1955), 35-68.

and the author [0.3, p. 294]. Above, in Chapter XVIII, we also gave an example pertaining to cylindrical panel, when oscillations embraced different stable equilibrium states; here the panel was presented as a system with several degrees of freedom.

§ 201. Static Criterion of Stability in the Large.

As we have seen, for a system with one degree of freedom, analysis of character of nonlinear oscillations of construction is relatively simple, but for system with large number of degrees of freedom it is fairly complicated. Therefore, research on stability in the large, is based, as a rule, on a static criterion. Equations, describing different equilibrium states removed from each other, remain here nonlinear. We shall become acquainted with the structure of such static equations, pertaining to a three-dimensional problem.* We will not give here general relationships of the nonlinear theory of elasticity, but will immediately introduce those assumptions, which are appropriate during investigation of stability of a flexible construction. They are the fact that it is possible to disregard components of deformations, if they enter in equations along with rotations, and that both deformations and rotations are small as compared to 1.

Henceforth we shall reject separate consideration of deformation of a body in the base state and during transition to the new state, as in § 198, and we shall consider an undeformed position of the body as the initial state.

---

*This question was investigated by V. V. Novozhilov [21.8], V. V. Bolotin [21.1] and others. Survey of literature on general relationships of nonlinear theory of elasticity is given by K. Z. Galimov [21.4]. Following presentation is built basically from book of V. V. Novozhilov [21.8].

We designate by u, v and w shift of points of the body along axes of Cartesian system of coordinates x, y and z. Deformations of elongation turns out to be equal to*

$$\left.\begin{aligned}\varepsilon_x &= \frac{\partial u}{\partial x} + \frac{1}{2}\left[\left(\frac{\partial u}{\partial x}\right)^2 + \left(\frac{\partial v}{\partial x}\right)^2 + \left(\frac{\partial w}{\partial x}\right)^2\right],\\ \varepsilon_y &= \frac{\partial v}{\partial y} + \frac{1}{2}\left[\left(\frac{\partial u}{\partial y}\right)^2 + \left(\frac{\partial v}{\partial y}\right)^2 + \left(\frac{\partial w}{\partial y}\right)^2\right],\\ \varepsilon_z &= \frac{\partial w}{\partial z} + \frac{1}{2}\left[\left(\frac{\partial u}{\partial z}\right)^2 + \left(\frac{\partial v}{\partial z}\right)^2 + \left(\frac{\partial w}{\partial z}\right)^2\right].\end{aligned}\right\} \qquad (21.19)$$

and deformations of shearing are equal to

$$\left.\begin{aligned}\gamma_{xy} &= \frac{\partial u}{\partial y} + \frac{\partial v}{\partial x} + \frac{\partial u}{\partial x}\frac{\partial u}{\partial y} + \frac{\partial v}{\partial x}\frac{\partial v}{\partial y} + \frac{\partial w}{\partial x}\frac{\partial w}{\partial y},\\ \gamma_{yz} &= \frac{\partial v}{\partial z} + \frac{\partial w}{\partial y} + \frac{\partial u}{\partial y}\frac{\partial u}{\partial z} + \frac{\partial v}{\partial y}\frac{\partial v}{\partial z} + \frac{\partial w}{\partial y}\frac{\partial w}{\partial z},\\ \gamma_{zx} &= \frac{\partial w}{\partial x} + \frac{\partial u}{\partial z} + \frac{\partial u}{\partial z}\frac{\partial u}{\partial x} + \frac{\partial v}{\partial z}\frac{\partial v}{\partial x} + \frac{\partial w}{\partial z}\frac{\partial w}{\partial x}.\end{aligned}\right\} \qquad (21.20)$$

If we consider shifts u and v small as compared to w and disregard in (19) and (20) nonlinear members containing u and v, then we obtain the formulas for ε_x, ε_y, and γ_{xy}, which were derived in Chapter VII for flexible plates.

We use, further, approximate dependences of type (13):

$$\frac{\partial w}{\partial y} \approx -\frac{\partial v}{\partial z} \approx \omega_x, \quad \frac{\partial u}{\partial z} \approx -\frac{\partial w}{\partial x} \approx \omega_y, \quad \frac{\partial v}{\partial x} \approx -\frac{\partial u}{\partial y} \approx \omega_z, \qquad (21.21)$$

and designate linear components ε_x, γ_{xy}, etc., by $\varepsilon_{x,л}$, $\gamma_{xy,л}$, ...; disregarding squares of these magnitudes as compared to squares of rotations, we obtain

$$\left.\begin{aligned}\varepsilon_x &= \varepsilon_{x,л} + \frac{1}{2}(\omega_y^2 + \omega_z^2), \quad \gamma_{xy} = \gamma_{xy,л} - \omega_x\omega_y,\\ \varepsilon_y &= \varepsilon_{y,л} + \frac{1}{2}(\omega_z^2 + \omega_x^2), \quad \gamma_{yz} = \gamma_{yz,л} - \omega_y\omega_z,\\ \varepsilon_z &= \varepsilon_{z,л} + \frac{1}{2}(\omega_x^2 + \omega_y^2), \quad \gamma_{zx} = \gamma_{zx,л} - \omega_z\omega_x.\end{aligned}\right\} \qquad (21.22)$$

---

*See book of P. F. Papkovich, indicated in § 198, p. 69.

Equations of equilibrium of an element of a body we compose using former assumptions about relative magnitude of deformations and rotations. Then cosines of angles, constituted by unit vectors of rotated axes of coordinates with fixed axes x, y and z, are determined the same table as on p. 996, but replacement of ω_x' on ω_x, etc. Reasoning just as in § 198, we obtain equation of equilibrium in the form (mass forces, as before, we ignore)

$$\left.\begin{aligned}
&\frac{\partial}{\partial x}(\sigma_x - \tau_{xy}\omega_z + \tau_{xz}\omega_y) + \frac{\partial}{\partial y}(\tau_{yx} - \sigma_y\omega_z + \tau_{yz}\omega_y) + \\
&\qquad + \frac{\partial}{\partial z}(\tau_{zx} - \tau_{zy}\omega_z + \sigma_z\omega_y) = 0,\\
&\frac{\partial}{\partial x}(\tau_{xy} + \sigma_x\omega_z - \tau_{xz}\omega_x) + \frac{\partial}{\partial y}(\sigma_y + \tau_{yx}\omega_z - \tau_{yz}\omega_x) + \\
&\qquad + \frac{\partial}{\partial z}(\tau_{yz} + \tau_{xz}\omega_z - \sigma_z\omega_x) = 0,\\
&\frac{\partial}{\partial x}(\tau_{xz} - \sigma_x\omega_y + \tau_{xy}\omega_x) + \frac{\partial}{\partial y}(\tau_{yz} - \tau_{yx}\omega_y + \sigma_y\omega_x) + \\
&\qquad + \frac{\partial}{\partial z}(\sigma_z - \tau_{zx}\omega_y + \tau_{zy}\omega_x) = 0.
\end{aligned}\right\} \qquad (21.23)$$

Let us consider again as an example a flexible plate. We take rotations in the plane of plate to be negligible [$\omega_z = 0$] and do not consider in the first two equations members depending on tangential stresses τ_{xy}, τ_{yz}. If, furthermore, we take relationship (21), then system (23) will take on form

$$\frac{\partial \sigma_x}{\partial x} + \frac{\partial \tau_{yx}}{\partial y} = 0, \quad \frac{\partial \tau_{xy}}{\partial x} + \frac{\partial \sigma_y}{\partial y} = 0,$$

$$\frac{\partial \tau_{xz}}{\partial x} + \frac{\partial \tau_{yz}}{\partial y} + \sigma_x \frac{\partial^2 w}{\partial x^2} + 2\tau_{xy}\frac{\partial^2 w}{\partial x\,\partial y} + \sigma_y \frac{\partial^2 w}{\partial y^2} = 0;$$

these equations also lie at the base of the nonlinear theory of plates (see Chapter VII).

Boundary conditions in general preserve the same form as in § 198; the first condition is composed by (16):

$$(\sigma_x - \tau_{xy}\omega_z + \tau_{xz}\omega_y)l + (\tau_{yx} - \sigma_y\omega_z + \tau_{yz}\omega_y)m + (\tau_{zx} - \tau_{zy}\omega_z + \sigma_z\omega_y)n = -p_x. \qquad (21.24)$$

where p_x is component of external load; we assume that external forces do not change their magnitude and direction.

We write, then, relationships between stresses and deformations of type (15):

$$\sigma_x = \frac{E}{1+\mu}\left(\varepsilon_x + \frac{\mu}{1-2\mu}\theta\right), \quad \tau_{xy} = \frac{E}{2(1+\mu)}\gamma_{xy} \text{ etc.} \tag{21.25}$$

If we substitute in (23) values of σ_x, τ_{xy}, ... from (25) and use dependences (19) and (20), then we arrive at equations for shifts u, v and w. In distinction from the equations composed in § 198, they will now be nonlinear, and this is explained by the structure of formulas (19) and (20) or (22) for components of deformations. Thus, nonlinearity here has a geometric sense and is caused by the fact that shifts are considered not small, but terminal. If it is necessary to consider also physical nonlinearity, then relationships (25) must be replaced by corresponding dependences pertaining to the considered system. In all preceding calculations we considered deformations and rotations small as compared to 1, otherwise we had to consider not only change of orientation of faces of the element, but also change of area of faces; furthermore, table of cosines, shown on p.996 , would have a different form (see [21.8]).

System of equations for u, v and w may be replaced by an equivalent system, containing, e.g., one of shifts and, furthermore a function of stresses, as we did in examining a flexible plate; but, then we must write dependences, ensuing from (19) and (20) and expressing the condition of compatibility of deformations.

Solution of the final system of equations determines dependence between parameter of load λ and magnitudes characterizing deformed state of body. In a number of problems we sought to establish the value of lower critical load. We try now to give a more strict

definition of this concept. We recall, first, that course of reasoning which led us to the concept of an upper critical load. We considered the fundamental stable stress. Then we increased parameter λ and determined point of branching of solutions, considering that at this point where $\lambda = \lambda_B$ the fundamental state ceases to be stable.

Now we approach the problem from the other direction. We assume that with sufficiently large value of λ in a given region of characteristics there occurs stable secondary equilibrium states, differing from the base state (for instance, moment states for shell, when base state is momentless). We decrease parameter λ and trace the character of solutions, determining secondary states. That value of parameter λ, at which secondary states of body cease to be stable, we call lower critical value λ_H. We assume at the same time that for values of λ, smaller than λ_H, there can take place secondary states (for instance, moment states for a shell), but they already are unstable.* If construction is ideal, i.e., it completely corresponds to given model, then with a load corresponding to λ_H, there can occur a sudden transition of construction from a secondary state to the base state.

From given definitions it follows that "first" lower critical load must not lie above the "first" upper critical load. Actually, when $\lambda = \lambda_B$ in the neighborhood of the base state there appear certain secondary states, which we consider stable. Consequently, we should have relationship $\lambda_H \leq \lambda_B$.**

---

*Such states are found, for instance, for an elongated cylindrical panel, subject to lateral load (see [0.3], p. 244).

**It is possible, indeed, to imagine that interval of fundamental stable states is broken at a certain point $\lambda = \lambda_B$, and secondary stable states appear only at higher value of λ, but such case is hypothetical.

In preceding chapters we understood by lower critical load that load at which basic form of equilibrium ceases to be unique. For system with one degree of freedom both approaches lead to the same result. But in case of system with two or more degrees of freedom together with growth of number of points of bifurcation (values of linearized) the number of lower points of branches of diagram "load—characteristic of deformation" is increased.*

But of these lower points only that which corresponds to loss of stability of secondary forms of equilibrium has practical value. The following point corresponds to shift from one form of instability to another. Consequently, during determination of lower critical parameter of load, which is the basis for practical calculations, we should study namely those solutions of the initial equations which correspond to stable secondary positions. This circumstance must be taken into account when using different approximate methods of integration of the initial equations. Method of Ritz gives possibility to directly investigate energy of system and to derive solutions, corresponding to stable states. Method of Bubnov-Galerkin, applied to equations formally, can lead to unstable solutions.** If we use method of finite differences and calculations are conducted with help of digital computers, here it is necessary to deal with results cautiously. However, experience shows that unstable solutions can be obtained in the process of machine computation only as an exception.

---

*In above-indicated example with a cylindrical panel, reduced to a system with two degrees of freedom, we found two upper and two lower points of diagram.

**This signifies solutions corresponding to unstable forms of equilibrium.

Thus, theory of stability of elastic system in the large is closely tied with qualitative theory of nonlinear differential equations. A number of results, pertaining to shallow flexible shells, were obtained in this direction by I. I. Vorovich [21.3]. By methods of functional analysis he showed that in those cases when initial state of shell is momentless, there always exists a number $\lambda_* > -\infty$ such that for $\lambda < \lambda_*$ there is possible a unique form of equilibrium and at the same time, in the interval of values of parameter $\lambda_* \leq \leq \lambda < \lambda_* + \varepsilon$ (where ε is any arbitrarily small positive number) there exist such λ to which, besides momentless, there corresponds at least one moment form of equilibrium of the shell. These values of λ_* satisfy relationship $\lambda_* \leq \lambda_B$, where λ_B is lowest eigenvalue of linearized problem, corresponding to point of bifurcation of the initial equations. Thus, for the most important class of nonlinear problems there is strictly proven possibility of obtaining no unique solution of initial equations for loads, lying lower than Eulerian.

§ 202. Energy Criterion of Stability in the Large.

As we have seen, in seeking practically valuable branches of solutions of nonlinear problem it is important to determine character of corresponding forms of equilibrium; an essential role here is played by the energy criterion. Using it, we are able, first of all, to definitize our ideas about equilibrium forms of a conservative system near the point of bifurcation, i.e., at loads, differing little from upper critical value.

Let us consider the case of a system with one degree of freedom.*

*Investigation of this case belongs to W. T. Koiter [21.14].

We designate parameter of load by p and parameter of characteristic shift (e.g., deflection of the shell) by ζ. In distinction from linear problem (§ 199), we can now present energy taking into account higher powers of ζ. Let us assume that in expression for dimensionless total energy $\Im^*$ there are retained powers of ζ up to and including the fourth and this expression has the form

$$\Im^* = C_2(p_в - p)\zeta^2 - C_3\zeta^3 + C_4\zeta^4. \qquad (21.26)$$

where $p_в$ is the parameter of upper critical load, C_i are certain constants. We met examples of expressions of such type for energy in problems pertaining to flexible plates and shells.

Let us consider first of all the critical state and set $p = p_в$. Let us assume at first that $C_3 \neq 0$; then the member containing C_4 can be rejected, so that we have $\Im^* = -C_3\zeta^3$. When $C_3 > 0$ and $\zeta > 0$ or $C_3 < 0$ and $\zeta < 0$ transition to adjacent state will be accompanied by a drop of total energy; therefore, here the equilibrium state corresponding to $p_в$ will be unstable; this conclusion ensues also from Lyapunov's first theorem (p. 1001). If however, $C_3 = 0$, then we should study expression $\Im^* = C_4\zeta^4$. When $C_4 > 0$ deflection of system from base state will be connected with increase of the energy level, and critical state will be stable. Conversely, when $C_4 < 0$ it will be unstable.

We turn now to equilibrium forms for levels of load lying somewhat above or below critical. If we consider only members of the second power, we obtain, $\Im^* = C_2(p_в - p)\zeta^2$. Considering the base state to be stable when $p < p_в$, will obtain $C_2 > 0$. When $C_3 \neq 0$ we reject again the member with ζ^4. Considering that adjacent state is an equilibrium state, we write equality $\partial\Im^*/\partial\zeta = 0$ where $\zeta \neq 0$; then

we obtain

$$\zeta=\frac{2}{3}(p_*-p)\frac{C_3}{C_4},\quad \frac{\partial^2\vartheta^*}{\partial\zeta^2}=2(p-p_*)C_2.$$

If $C_3 > 0$, then with a load exceeding p_B, i.e., when $p > p_B$, we have $\zeta < 0$, $\partial^2\vartheta^*/\partial\zeta^2 > 0$, so that deflected states will be stable; when $p < p_B$ we obtain $\zeta > 0$, $\partial^2\vartheta^*/\partial\zeta^2 < 0$, which indicates instability. In Fig. 21.4 is depicted diagram $p(\zeta)$ for $C_3 > 0$ and $C_4 = 0$ pertaining to $\zeta_0 = 0$ (absence of initial deflections); branches of stable states are depicted by solid lines, of unstable, by dotted line. At upper critical point A there occurs exchange of stability between branches,* where actual critical point belongs, as we saw, to the unstable branch (black circle).

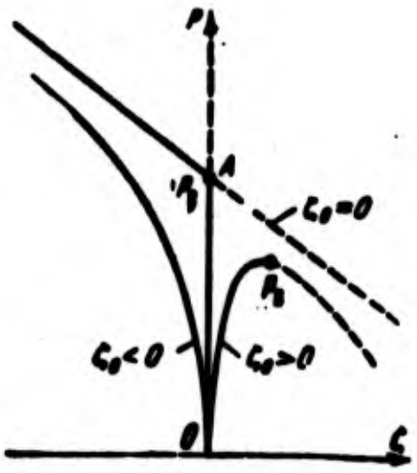

Fig. 21.4. Diagram "load-deflection" for $C_3 > 0$; point of branching belongs to unstable branch.

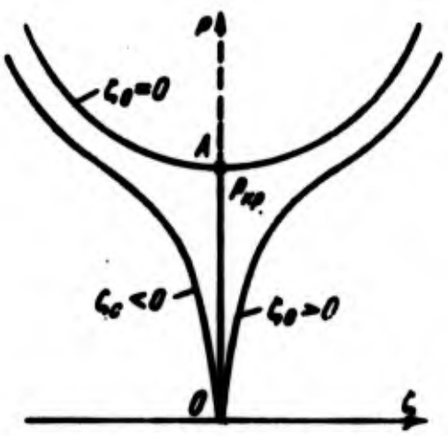

Fig. 21.5. Diagram "load-deflection" when $C_3 = 0$, $C_4 > 0$; point of branching belongs to stable branch.

We shall next analyze the cases $C_3 = 0$ and $C_4 \neq 0$. When $C_4 > 0$

*Properties of such diagrams, containing points of bifurcation, were first investigated by Poincaré (Acta mathematica 7 (1885), 259-380) in connection with study of figures of equilibrium of celestial bodies; in problems of elastic stability these diagrams were investigated by G. Yu. Dzhanelidze [21.5], V. V. Bolotin [21.1] and other authors.

we have

$$\zeta^2 = \frac{1}{2}\frac{C_3}{C_4}(p - p_в), \quad \frac{\partial^2 \Im^*}{\partial \zeta^2} = 4C_2(p - p_в).$$

Hence we conclude that when $p > p_в$ adjacent equilibrium states will be stable as shown in Fig. 21.5, where point A for $p_в = p_{кр}$ should belong to the stable branch (light circle). Conversely, when $C_4 < 0$ curves for $p(\zeta)$ will be turned with convexity upwards (Fig. 21.6) and point A will belong to branch of instability.

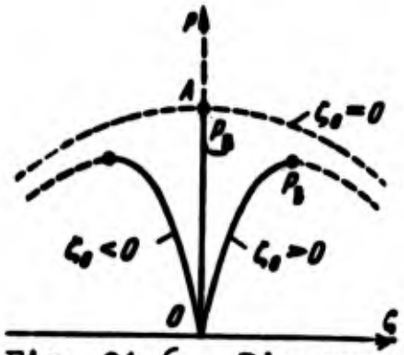

Fig. 21.6. Diagram "load-deflection" when $C_3 = 0$, $C_4 < 0$.

Let us consider, further, influence of initial perturbations (for instance, initial deflection in the case of a shell) on behavior of a system. We write augmented expression for energy in the form

$$\Im^* = C_2(p_{в,\,ид} - p)\zeta^2 - C_3\zeta^3 + C_4\zeta^4 - C_0 p \zeta_0 \zeta. \tag{21.27}$$

where ζ_0 is parameter of initial perturbation, $p_{в,\,ид}$ is upper critical load for an ideal system. Analysis of expressions for $\partial\Im^*/\partial\zeta$ and $\partial^2\Im^*/\partial\zeta^2$ leads to following conclusions. In case $C_3 > 0$, $\zeta > 0$ or $C_3 = 0$, $C_4 < 0$ diagrams of $p(\zeta)$ have boundary points as shown in Figs. 21.4 and 21.6, where these points belong to unstable branches. When $C_3 = 0$, $C_4 > 0$ all equilibriums form turn out to be stable (Fig. 21.5).

As an example, corresponding to Fig. 21.4, we can use a cylindrical panel, compressed along its generatrix (§ 139), and for Fig. 21.5, a compressed reinforced plate (§ 88). An example of a construction corresponding to diagram of Fig. 21.6 is given in article of B. L. Nikolai [21.7].

Analogously we can investigate equilibrium states adjacent to lower critical point $p_н$. This point, as we have seen, divides region of instability and stability. Consequently, when $p = p_н$ the second variation of total energy should turn into zero: $\delta^2 Э^* = 0$.

Finally, the power criterion can to a certain extent serve for determination of load at which we should expect snapping of real constructions. Certain authors offered to take as the basis of calculation for stability in the large not the lower critical load, but such load $p_э$, at which energy of base state is equal to energy of snapped state. It should be noted, however, that in those concrete problems which have been solved till now magnitude $p_э$ exceeds $p_н$ slightly (within 10%); therefore, this proposal does not have essential practical value. At the same time during the presence of sufficient perturbations snapping to a stable state with higher energy levels can occur. Obviously, question of realization of various equilibrium forms may be solved only by probability methods.

We discussed above only criterion of stability of equilibrium of deformed bodies in application to conservative and partly to dissipative systems, these criteria lie at the base of all methods of solution of particular problems for such systems familiar to us. Criterion of stability of systems having an influx of energy from without must be considered specially (see, e.g., § 21).

We turn now to the case when a conservative system is subjected to combined loading.

§ 203. Criterion of Stability with a Combined Load.

Let us assume that loss of stability of an elastic system may occur during action of loads of different form. For instance, for a

reinforced rectangular plate such loads may be compressive forces in several directions or shearing forces.

Let us assume that we have found critical value of loads during their separate application, and we consider case when they act jointly in some combination.*

We assume that a system having one degree of freedom is subjected to action of two loads of different type and that we are investigating stability of the system in the small.

Fig. 21.7. Transition from region of stability to region of instability during combined load.

In Fig. 21.7 on the axes are laid off parameters of loads P and Q; critical values of them in separate application we shall designate by P_* and Q_*, and in combined action, by P_B and Q_B. Point A noted in Fig. 21.7 has coordinates P_0, Q_0, lying within limits $0 < P_0 < P_B$, $0 < Q_0 < Q_B$. Obviously, point A is in region of stability belonging to the base state.

Total energy corresponding point A we will present in the form

$$\mathcal{E}_0 = \frac{1}{2}(a - \beta P_0 - \gamma Q_0) q^2 = \frac{1}{2} b_0 q^2. \qquad (21.28)$$

where q is generalized coordinate, varying during transition from the base state to a neighboring one. Derivative $\partial \mathcal{E}_0 / \partial q$ turns into zero only when $q = 0$; proceeding from the criterion of stability of the base state, we find

$$\frac{\partial^2 \mathcal{E}}{\partial q^2} = b_0 > 0.$$

---

*In general form the problem of stability under combined load was first solved by P. F. Papkovich [0.7].

Further, we vary the loads, applied to system, considering

$$P=P_0+Xk,\quad Q=Q_0+Xl.$$

In Fig. 21.7 magnitude X is plotted along ray An; parameters k and l represent directing cosines of the ray, $k = \cos(\widehat{x, n})$, $l = \cos(\widehat{y, n})$. Since work of external loads is subtracted from total energy of the system, then for the new state we have

$$\Im=\frac{1}{2}(\alpha-\beta P-\gamma Q)q^2=\frac{1}{2}[\delta_0-X(\beta k+\gamma l)]q^2. \tag{21.29}$$

Designating $(\beta k + \gamma l)$ by $\$$, we obtain

$$\Im=\frac{1}{2}(\delta_0-\$X)q^2,\quad \frac{\partial^2\Im}{\partial q^2}=\delta_0-\$X. \tag{21.30}$$

If parameters k and l are positive, then we always have $\$ > 0$; with negative k and l we have $\$ < 0$. If one of parameter k and l are positive, and the other negative (ray A'n' depicted in Fig. 21.7) it may be that $\$ > 0$ or $\$ < 0$. Depending upon sign of $\$$ system will behave differently with increase of X.

Let us assume that $\$ > 0$. Then for a certain value of X we obtain

$$\frac{\partial^2\Im}{\partial q^2}=\delta_0-\$X=0, \tag{21.31}$$

which corresponds to the criterion of loss of stability; consequently, we will find the first pair of critical loads P_B, Q_B. With further growth of X we always will have

$$\frac{\partial^2\Im}{\partial q^2}=\delta_0-\$X<0, \tag{21.32}$$

so that equilibrium will be <u>unstable</u>.

Let us assume that Fig. 21.7 equality (31) is satisfied for points B and B'; these points will lie on the <u>boundary line</u> separating stable region from the unstable. If we move along ray An from point A, after we pass point B, we no longer can return to region of stability; the same pertains to transition from A' to B' along A'n'.

When $\Delta < 0$, magnitude $\partial^2 \Im / \partial q^2$ cannot turn into zero, and consequently, we always will be in the region of stability.

Thus, passing a ray from any point of the region of stability in an arbitrary direction, we can either intersect a boundary line, and only once, or not intersect it at all. It is easy to see that the boundary line satisfying such requirement cannot be turned with its convexity facing the region of stability. This means that boundary line should consist of sections of straight lines or sections of curves, turned with their convexity toward the region of instability (Fig. 21.8). Here the angle of inclination of straight sections, tangent to curved sections, should change monotonically.

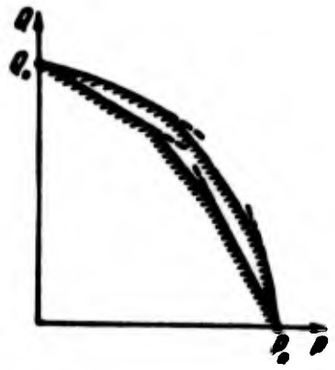

Fig. 21.8. Boundary lines, separating stable region from unstable.

This conclusion gives us the possibility of establishing approximate values of critical forces during combined load. Actually, points P_* and Q_* are connectable by a straight line (Fig. 21.9); obviously, its points give critical combinations of forces P and Q either exactly, or approximately, but in the second case always with a certain margin of stability.

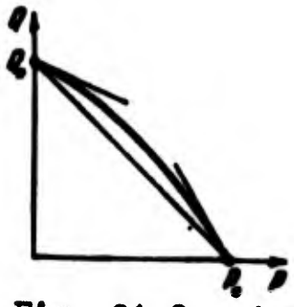

Fig. 21.9. Approximate determination of boundary line for zone of stability.

Let us assume that we know the position of the tangent to boundary lines at points $P = P_*$ and $Q = Q_*$ (Fig. 21.9); then the sought boundary curves must lie between line P_*Q_* and these tangents. Equation of the "safe" line

has the form

$$\frac{P_2}{P_*}+\frac{Q_2}{Q_*}=1. \qquad (21.33)$$

These results are simple to spread to case when system is subjected to action of three loads of different type, P, Q, R; instead of a two dimensional picture we obtain a three-dimensional one; instead of a boundary line, a surface; instead of straight sections, planes. With a number of loads greater than three we must pass to a multi-dimensional space.

Analogous conclusions may be obtained also in the more complex case, when system has n degrees of freedom [0.7]. B. M. Broude extended these conclusions to nonlinear problems pertaining to stability in the large. It turned out that the given criteria of stability during combined loading can in certain cases serve for determination of not only the upper, but also the lower critical loads. This question requires additional investigation.

§ 204. Certain Problems for Further Investigation

In conclusion we shall enumerate certain urgent problems of the theory of stability of elastic systems, which we already discussed in part above. Most important from the practical point of view—especially for aviation—are, at present, problems pertaining to stability of shells. It is necessary, using digital computers, to find reliable data for calculation of shells for stability in the large. The basic purpose here is determination of definitized values of lower critical loads. It is desirable to consider anew cases of a circular cylindrical shell, subjected to axial compression, external pressure and torsion, spherical and ellipsoidal shells under external pressure, shallow shells of different outline in plane during action of

lateral load. It is desirable to investigate different cases of combined loading of circular cylindrical shells; special attention should be given to problem of joint action of internal pressure and axial compression or torsion.

Of essential practical value are problems of stability of reinforced shells. It is necessary to consider more specifically different models of such constructions—the anisotropic shell with dispersed rigidity of ribs and a smooth shell with discrete ribs--and to establish limits of application of such models. It is important to find methods for rational designing of reinforced shells of minimum weight.

Shell prepared from glass-fiber plastics enjoy ever wider application in different regions of technology, however, data for calculation of such shells is extremely scarce. Here it is important to establish what models must be taken as the basis of investigations for shells of one or another structure, and depending upon this to compose initial equations, originating from the theory of orthotropic shells from the general theory of anisotropic shells. Further, it is necessary to clarify for what circle of such shells we should consider stability in the large. It is necessary experimentally to establish basic elastic characteristics for shells of different structure.

The number of works devoted to sandwich shells is sufficiently great, but at present there is not yet reliable data for calculation for stability sandwich shells of average length experiencing external pressure and torsion, and also these forms of load in combination with axial compression. These problems must be solved not only in linear, but also in nonlinear formulation. Little experimental data has been accumulated for such shells.

Question of stability of shells in the small and in the large beyond the elastic limit requires significant attention. It is desirable to find how appropriate it is to use here one or another theory of plasticity, especially with finite shifts, and to obtain practically accessible methods of solution of concrete problems. Further, it is necessary to determine upper and lower critical loads for shells of different outline.

Question of thermal buckling of shells and plates awaits further development. Here it is important to consider reinforced shells with one or another distributive law of temperatures by section of skin and reinforcing ribs, and also on the surface of the skin, and to determine values of critical temperatures. The question of buckling of plates and shells during a thermal shock has still been little developed.

Problem of stability of shells, plates and bars during creep also needs development. It is necessary to analyze anew available criteria and methods of determination of critical time, comparing them with experimental data for different materials. Essential is the question about stability of shells in the large during creep. Criterion of stability in temperature problems must be generalized proceeding from thermodynamic relationships for reversible and irreversible processes.

Urgent are problems pertaining to stability of shells, plates and bars during dynamic loading. It is desirable to investigate stability of shells and plates during very fast (shock) loading, taking into account propagation of waves in the middle surface. In available works there are considered, as a rule, elements of constructions with "equally-possible" initial imperfections of different

types. For real constructions various forms of initial imperfections can predominate; in this case it is necessary to expect jumps from some forms of buckling to others in the process of dynamic loading. There arises the question; is it possible to realize passage to the limit from a problem for a construction with initial imperfections to the problem of behavior of an ideal construction? Solution of this question will give possibility of more strictly approaching the concept of dynamic critical load. For practical calculations it is also important to determine magnitude of work which may be absorbed by a construction up to moment of buckling. It is desirable to investigate the problem of dynamic stability of closed shells, containing a fluid, taking into account the reduced mass of the fluid.

It is desirable to continue solving problems of stability of shells for that case when the fundamental stress is a moment one. This pertains to a short cylindrical shell subjected to external pressure or joint action of axial compression and internal pressure, to shallow shells supporting a normal load, etc. Here it is useful to consider bifurcational problems, when initial form of shell is replaced successively by forms of different type and there appear various numbers of shallow dents. In certain problems (for instance, with internal pressure in a closed shell) it is necessary to consider development of plastic flows in the base state.

Especially important are studies in the application of statistical methods for calculation of constructions for stability. This pertains, first of all, to stability of shells in the large. All available statistical approaches to the problem should be intensely developed. It is necessary to study distributive laws of initial imperfections for real shells with different techniques of manufacture and

probability characterisitics of loads experienced by elements of various constructions. Application of statistical methods should explain experimental data with respect to scattering of critical loads and at the same time introduce a more reliable basis for designing real constructions. In examining dynamic stability of constructions it is necessary to apply statistical methods pertaining to random processes.

Various methods of solution of particular problems of stability must be examined, proceeding from possibilities of digital computer techniques. It is desirable to apply digital computers to the preliminary stages of solution of problems by the Ritz method, starting from determination of the energy. It is necessary to learn to separate stable branches of solutions from unstable ones during application of method of finite differences or method of collocation. It would be useful to develop a special program for determination of lower critical loads without investigation of the whole region of buckling of shells.

For many constructions calculation for stability is decisive. Till now during determination of dimensions of designed constructions they originate usually from comparison with analogous already realized constructions or from "intuitive" considerations, and then conduct a check for stability. Meanwhile application of computers should allow us to compare a large number of variants of a construction and find the most advantageous of them. This pertains, e.g., to constructions of glass-fiber plastic, for which there may be established the most profitable combination of different layers with one or another direction of the fibers. Thus there would be found a basis for determination not only of dimensions, but also desirable

techniques of manufacture of the construction.

It is necessary to return to initial equations of nonlinear theory of shells and to constitute a system of equations which could describe buckling of shells in long waves. Methods of functional analysis for qualitative investigation of nonlinear equations of theory of shells and, especially, for clarification of properties of solutions near lower critical points await further development.

General linear theory of stability of shells also has not yet been perfected. Here it is especially important to definitize limits of applicability of equations of different types and to clarify to what extent of boundary point-by-point fulfillment conditions on edges of the shell affects solution of problems of stability.

Literature

21.1. V. V. Bolotin. Questions of general theory of elastic stability, Applied math. and mech., 20, No. 5 (1956), 561-577; Nonlinear theory of elastic stability in the large "Strength analysis," 3 (1958), 310-354; Contemporary trends in area of dynamics of plates and shells, "Theory of plates and shells," Kiev, 1962, 16-32.

21.2. A. S. Vol'mir. Contemporary problems of theory of stability of shells, Report on L'vov conference on theory of plates and shells, 1961.

21.3. I. I. Vorovich. On existence of solutions in nonlinear theory of shells, News of Acad. of Sci. of USSR, math. series, 19 (1955); On certain approximate methods in the nonlinear theory of sloping shells, DAN SSSR, 105, No. 1, (1955); Applied mathematics and mechanics, 20, No. 4, (1956); On the existence of solutions in nonlinear theory of shells, DAN SSSR, 117, No. 2 (1957); Certain mathematical problems of nonlinear theory of shells, Doct. diss., 1958.

21.4. K. Z. Galimov. Equation of equilibrium of theory of elasticity during finite displacements and their application to theory of shells, News of Kazan' branch of Academy of Sciences of USSR, series on phys-math. and tech. sciences, No. 1 (1948), 25-45.

21.5. G. Yu. Dzhanelidze. Stability of equilibrium of nonlinearly deformed systems, Transactions Leningrad polytechnic inst., 178 (1955).

21.5a. G. V. Ivanov. On stability of equilibrium during inelastic deformations, Journal applied mech. and tech. physics, No. 1 (1961), 47-55; No. 3 (1961), 74-84.

21.6. A. Yu. Ishlinskiy. Consideration of questions of stability of equilibrium of elastic bodies from the point of view of mathematical theory of elasticity, Ukr. math. journal, 6, No. 2 (1954), 140-146.

21.7. B. L. Nikolai. On criterion of stability of elastic systems, Trans. Odessa inst. of eng. of civic and municipal construction 1 (1939), 191-208.

21.8. V. V. Novozhilov. Principles of nonlinear theory of elasticity, Gostekhizdat, 1948.

21.8a. Yu. N. Rabotnov. Theory of creep and its application, in collection "Plasticity" Pergamon-Press, 1960, 338-346.

21.9. C. B. Biezeno and H. Hencky. On the general theory of elastic stability, Proc. Roy. Neth. Acad. Sci., Amsterdam 31 (1928), 569-592; 32 (1929), 444.

21.10. G. H. Bryan. On the stability of elastic systems, Proc. of the Cambridge Phil. Soc. 6 (1888), 199.

21.11. D. C. Drucker and E. T. Onat. On the concept of stability of inelastic systems, J. Aeron. Sci. 21, No. 8 (1954).

21.12. R. Hill. On uniqueness and stability in the theory of finite elastic strain, J. Mech. Phys. Solids 5, No. 4 (1957), 229-241; Stability of rigid-plastic solids, 6, No. 1 (1957), 1-8.

21.12a. R. Hill and M. Sewell. A general theory of inelastic column failure, J. Mech. Phys. 8, No. 2 (1960), 105-118.

21.13. R. Kappus. Zur Elastizitätstheorie endlischer Verschiebungen, Zeitschr. angew. Math. und Mech. 19, No. 5 (1939), 271-285; No. 6, 344-361.

21.14. W. T. Koiter. Over de stabiliteit van het elastisch evenwicht, Amsterdam, 1945; Elastic stability and postbuckling behaviour, 1960 (Trans. "Mechanics," IL, No. 5, 1960).

21.15. F. Murnaghan. Finite deformation of an elastic solid, NY, 1951.

21.16. C. E. Pearson. General theory of elastic stability, Quart. Appl. Math. 14 (1956), 133.

21.17. W. Prager. The general variational principle of the theory of structural stability, Quart, Appl. Math. 4 (1957), 378.

21.18. R. V. Southwell. On the general theory of elastic stability, Phil. Trans. Roy. Soc. London A213 (1913), 187.

21.19. M. Skaloud. Poktriticka pevnost sten ocelových nosniku, Praha, 1962.

21.20. E. Trefftz. Ueber die Ableitung des Stabilitätskriterien des elastischen Gleichgewichts, Verhandl. III Intern. Kongr. techn. Mech. 3 (1930), 44-50.

21.21. Chi-The Wang. Applied elasticity, NY, 1953 (Trans., M., 1959).

21.22. O. Zanaboni. Premesse allo studio della stabilitá del d'equilibrio elastico, G. Genio civile 99, No. 6 (1961), 457-473.

21.23. H. Ziegler. Die Stabilitätskriterien der Elastomechanik, Ing. Arch. 20, No. 1 (1952); Advances in applied mechanics 4 (1956) (Trans. in "Problems of Mechanics," 2, IL, 1959, 116-160).

Literature for the Whole Book

0.1. V. V. Bolotin. Dynamic stability of elastic systems, Gostekhizdat, M., 1956; Nonconservative problems of the theory of elastic stability, Fizmatgiz, M., 1961.

0.2. I. G. Bubnov. Structural mechanics of a ship, Part I, 1912; Part II, 1914.

0.3. A. S. Vol'mir. Flexible plates and shells, Gostekhizdat, M., 1956.

0.4. A. N. Dinnik. Stability of elastic systems, ONTI, 1935; Buckling, ONTI, M., 1936.

0.5. N. V. Kornoukhov. Strength and stability of bar systems, Stroyizdat, M., 1949.

0.6. Kh. M. Mushtari and K. Z. Galimov. Nonlinear theory of elastic shells, Tatknigoizdat, Kazan', 1957.

0.7. P. F. Papkovich. Structural mechanics of a ship, Part II, Sudpromgiz, L., 1939.

0.8. S. D. Ponomarev, V. L. Biderman, K. K. Likharev, V. M. Makushin, N. N. Malinin, and V. I. Feodos'yev. Calculations for strength in machine building, 1st edition, Vol. II, Mashgiz, M., 1952; 2nd edition, Vol. III, 1959.

0.9. A. R. Rzhanitsyn. Certain questions of mechanics of systems, deformed in time, Gostekhizdat, M., 1949.

0.10. A. R. Rzhanitsyn. Stability of equilibrium of elastic systems, Gostekhizdat, M., 1955.

0.11. A. F. Smirnov. Static and dynamic stability of constructions, 1947, Stability and vibrations of constructions, 1958.

0.12. V. G. Chudnovskiy. Methods of calculating vibrations and stability of elastic systems, Publishing House of the Academy of Sciences of the Ukrainian SSR, Kiev, 1952.

0.13. I. Ya. Shtayerman and A. A. Pikovskiy. Principles of the theory of stability of building constructions, Gosstroyizdat, M., 1939.

0.14. C. B. Biezeno and R. Grammel. Technische Dynamik, Berlin, 1939 (in translation, Technical dynamics, Part I, Gostekhizdat, L., 1950).

0.15. F. Bleich. Buckling strength of metal structures, NY, 1952 (in translation, Fizmatgiz, M., 1959).

0.16. G. Bürgermeister and H. Steup. Stabilitätstheorie, Ak. Verlag, Berlin, Teil 1, 1957.

0.17. G. Gerard. Weight analysis of compression structures, NY, University Press, 1956; Introduction to structural stability, 1962.

0.18. F. Hartmann, Knickung, Kippung, and Beulung (in translation, F. Hartmann, Stability of engineering constructions, Gosstroyizdat, M., 1939).

0.19. C. F. Kollbrunner and M. Meister. Knicken, Springer-V, Berlin, 1955; Ausbeulen, 1958.

0.20. R. Mayer. Die Knickfestigkeit, Springer-V., Berlin, 1921.

0.21. A. Pflüger. Stabilitätsprobleme der Elastostatik, Springer-V., Berlin, 1950.

0.22. F. R. Shanley. Weight-strength analysis of aircraft structures. NY, 1952 (in the translation: Shanley, Analysis of weight and strength of aircraft structures, Oborongiz, M., 1957).

0.23. S. P. Timoshenko. Theory of elastic stability NY, 1936 (in translation, S. P. Timoshenko, Stability of elastic systems, Gostekhizdat, M., 1st ed., 1946, 2nd ed, 1955), S. Timoshenko and J. Gere. Theory of elastic stability, NY, 1961.